

# ADVANCED **WELL** COMPLETION ENGINEERING

Wan Renpu



G | P  
P | 

ADVANCED  
**WELL**  
COMPLETION  
ENGINEERING

This page intentionally left blank

# ADVANCED **WELL** COMPLETION ENGINEERING

Third Edition

Wan Renpu



AMSTERDAM • BOSTON • HEIDELBERG • LONDON  
NEW YORK • OXFORD • PARIS • SAN DIEGO  
SAN FRANCISCO • SINGAPORE • SYDNEY • TOKYO  
Gulf Professional Publishing is an imprint of Elsevier



Gulf Professional Publishing is an imprint of Elsevier  
225 Wyman Street Waltham, MA 02451, USA  
The Boulevard, Langford Lane, Kidlington, Oxford, OX5 1GB, UK

First Printed in Chinese.  
Chinese edition © 2008 Petroleum Industry Press

The Chinese version of *Advanced Well Completion Engineering* by Wan Renpu was published by Petroleum Industry Press in June, 2008.

English translation © 2011, Elsevier Inc. All rights reserved.

This English translation of *Advanced Well Completion Engineering* by Wan Renpu is published by arrangement with Petroleum Industry Press, which undertook the translation.

No part of this publication may be reproduced or transmitted in any form or by any means, electronic or mechanical, including photocopying, recording, or any information storage and retrieval system, without permission in writing from the Publisher. Details on how to seek permission, further information about the Publisher's permissions policies and our arrangements with organizations such as the Copyright Clearance Center and the Copyright Licensing Agency, can be found at our website: [www.elsevier.com/permissions](http://www.elsevier.com/permissions)

This book and the individual contributions contained in it are protected under copyright by the Publisher (other than as may be noted herein).

#### Notices

Knowledge and best practice in this field are constantly changing. As new research and experience broaden our understanding, changes in research methods, professional practices, or medical treatment may become necessary.

Practitioners and researchers must always rely on their own experience and knowledge in evaluating and using any information, methods, compounds, or experiments described herein. In using such information or methods they should be mindful of their own safety and the safety of others, including parties for whom they have a professional responsibility.

To the fullest extent of the law, neither the Publisher nor the authors, contributors, or editors, assume any liability for any injury and/or damage to persons or property as a matter of products liability, negligence or otherwise, or from any use or operation of any methods, products, instructions, or ideas contained in the material herein.

#### Library of Congress Cataloging-in-Publication Data

Renpu, Wan.

Advanced well completion engineering / by Wan Renpu. – 3rd ed.

p. cm.

Includes bibliographical references and index.

ISBN 978-0-12-385868-9 (alk. paper)

1. Oil well completion. I. Title.

TN871.2.R384 2011

6220'.3381–dc22

2011004087

#### British Library Cataloguing-in-Publication Data

A catalogue record for this book is available from the British Library.

Chinese Edition ISBN: 978-7-5021-6364-8

English Translation ISBN: 978-0-12-385868-9

For information on all Gulf Professional Publishing publications visit our website at [www.elsevierdirect.com](http://www.elsevierdirect.com)

11 12 13 14 10 9 8 7 6 5 4 3 2 1  
Printed in the United States of America

Working together to grow  
libraries in developing countries

[www.elsevier.com](http://www.elsevier.com) | [www.bookaid.org](http://www.bookaid.org) | [www.sabre.org](http://www.sabre.org)

ELSEVIER

BOOK AID  
International

Sabre Foundation

# CONTENTS

Foreword, ix

Preface to the Third Edition, xi

About the Author, xiii

Introduction, xv

## **1 Basis of Well Completion Engineering, 1**

- 1.1 Grounds of Reservoir Geology and Reservoir Engineering, 3
- 1.2 Core Analysis Techniques, 13
- 1.3 Reservoir Sensitivity to Fluid and Working Fluid Damage Evaluation, 22
- 1.4 Reservoir Stress Sensitivity Analysis, 41
- 1.5 In Situ Stress and Mechanical Parameters of Rock, 54
- 1.6 Technological Grounds of Petroleum Production Engineering, 67

## **2 Well Completion Mode Selection, 75**

- 2.1 Vertical, Slant, and Directional Well Completion, 76

## **3 Selection and Determination of Tubing and Production Casing Sizes, 117**

- 3.1 Overview, 118
- 3.2 Overview of Nodal Analysis, 119
- 3.3 Selection and Determination of Tubing and Production Casing Sizes for Flowing Wells, 121
- 3.4 Selection and Determination of Tubing and Production Casing Sizes for Gas Wells, 130
- 3.5 Selection and Determination of Tubing and Production Casing Sizes for Artificial Lift Wells, 136
- 3.6 Effects of Stimulation on Tubing and Production Casing Size Selection, 156
- 3.7 Selection and Determination of Tubing and Production Casing Sizes for Heavy Oil and High Pour-Point Oil Production Wells, 161

## **4 Completion and Perforating Fluids, 171**

- 4.1 Functions of Drilling and Completion Fluid and Basic Requirements, 172
- 4.2 Drilling and Completion Fluid Systems and Application, 175
- 4.3 Shield-Type Temporary Plugging Technique, 185
- 4.4 Drilling and Completion Fluid for a Complicated Reservoir, 203
- 4.5 Perforating Fluid, 210

## **5 Production Casing and Cementing, 221**

- 5.1 Basic Requirements for Production Casing Design and Integrity Management of Production Casing, 223

- 5.2 Hole Structure and Types of Casing, 231
- 5.3 Strength of Casing and Strength Design of Casing String, 242
- 5.4 Cementing, 256
- 5.5 Production Casing and Cementing for Complex Type Wells, 272

## **6 Perforating, 295**

- 6.1 Perforating Technology, 297
- 6.2 Perforated Well Productivity Influencing Rule Analysis, 315
- 6.3 Perforating Differential Pressure Design, 337
- 6.4 Optimizing the Perforation Design, 346

## **7 Well Completion Formation Damage Evaluation, 364**

- 7.1 Overview, 365
- 7.2 Principle of Formation Damage Evaluation by Well Testing, 369
- 7.3 Formation Damage Diagnosis of Homogeneous Reservoir by Graphic Characteristics, 373
- 7.4 Graphic Characteristics of a Dual Porosity Reservoir and a Reservoir with a Hydraulically Created Fracture, 383
- 7.5 Distinguishing Effectiveness of Stimulation by Graphic Characteristics, 397
- 7.6 Quantitative Interpretation of Degree of Formation Damage, 403
- 7.7 Well Logging Evaluation of Formation Damage Depth, 413

## **8 Measures for Putting a Well into Production, 417**

- 8.1 Preparations before Putting a Well into Production, 418
- 8.2 Main Measures for Putting the Well into Production, 423
- 8.3 Physical and Chemical Blocking Removal, 425
- 8.4 Hydraulic Fracturing for Putting a Well into Production, 445
- 8.5 Acidizing for Putting a Well into Production, 470
- 8.6 High-Energy Gas Fracturing for Putting a Well into Production, 495
- 8.7 Flowing Back, 512

## **9 Well Completion Tubing String, 524**

- 9.1 Oil Well Completion Tubing String, 525
- 9.2 Gas Well Completion Tubing String, 537
- 9.3 Separate-Layer Water Injection String, 544
- 9.4 Heavy Oil Production Tubing String, 547
- 9.5 Completion Tubing String Safety System, 553
- 9.6 Tubing String Mechanics, 562

## **10 Wellhead Assembly, 572**

- 10.1 Oil-Well Christmas Tree and Tubinghead, 574
- 10.2 Gas-Well Christmas Tree and Tubinghead, 587
- 10.3 Water Injection and Thermal Production Wellhead Assembly, 596
- 10.4 Common Components of a Wellhead Assembly, 601

- 
- 11 Oil and Gas Well Corrosion and Corrosion Prevention, 617**
- 11.1 Related Calculation of Oil and Gas Well Corrosion, 619
  - 11.2 Oil and Gas Well Corrosion Mechanisms and Classification, 624
  - 11.3 Material Selection for Corrosive Environment of Oil and Gas Wells, 640
  - 11.4 Oil and Gas Well Corrosion Prevention Design, 655
  - 11.5 Tubing and Casing Corrosion Prevention for Sour Gas Reservoirs, 672
- Index, 701**

This page intentionally left blank

# FOREWORD

Well completion is an important link in oil field development. The designing level and implementation quality play a key role in the expected production target and economic effectiveness of an oil field.

As early as the initial development period of the Yumen oil field in Gansu province, our engineers kept improving well completion technology, and completed a great amount of probing work on many aspects, such as wellbore configuration design, cementing, openhole completion, liner completion, packer setting, and bullet perforating, all of which set up a relatively sound basis for well completion technology for our infant petroleum industry.

In the early 1960s (the years of developing the Daqing oil field), a wide utilization of package explosive perforating completion technology promoted the technical progress of jet perforating, perforating with carrier and non-carrier, and magnetic locating. The technical requirements of separate-layer production and injection impelled the development of packer technology. Then, during the development of oil fields around the Bohai Gulf, the types of formations encountered by drilling and reservoirs became more and more complex. A sand production problem was found in several oil fields, which propelled the progress of sand control technology, including chemical sand control, wire-wrapped screen gravel pack, and sand screen methods. In order to avoid formation damage in the tight layer of the Changqing oil field in northwest China, core analysis and sensitivity tests were carried out. Effective well completion methods have also been put into use in sour gas wells in the Sichuan gas field. In the meantime, a great amount of work was done in casing design, cementing, perforating gun, detection of perforating cartridge quality, surface detection while downhole perforating, as well as research on

the perforating process by the use of high-speed photographs. All of this work accomplished in formation protection and enhancement of the well completion quality helped to advance well completion technology.

Nevertheless, we found this technology too simple. The fundamental requirements of well completion, that is, “liberating oil formation,” were not completely realized; only the simple reservoir was dealt with effectively, not the complex.

As ideas about reform and open policy in China developed, and the principle of “science-technology is first” was established and carried out, science and technology have been greatly pushed forward, and so has well completion engineering. The study of formation damage and sensitivity causes the attention of well completion engineering to go up to the drilling period. This requires reasonable design of drilling, completion, and perforating fluids according to the reservoir mineral composition, and pore pressure. The study of in-situ formation stress takes the attention of completion engineering forward to the selection of development well pattern orientation, thereby giving consideration to oil recovery caused by water injection, gas injection, and the orientation of hydraulic fracture. In order to liberate oil formation and gain reasonable gas and oil production rates under the minimum pressure difference, we have reinforced the research work on perforating technology and developed various software for designing perforating and establishing a perforator quality guarantee system and detection center. Perforating penetration has reached as far as 700 cm. Modern well-testing technology has been a commonplace method in evaluating the completeness ratio of an oil well. The application of the nodal analysis method, the selection of tubing and production casing sizes, and the

research into artificial lift all consider the flow from the reservoir to the wellhead as a whole, not only from the initial stage but also to the later production stage. The aforementioned techniques have achieved great progress in both vertical and directional wells, and also have been used in the development of the four oil fields in the central Talimu basin, in which completion technology for horizontal wells has made great contributions to the stable oil production of 1,000 t/d. Today, well completion technology has become a form of system engineering. The entire period of an oil field development requires putting emphasis not only on the development plan, but also on each engineering design, and operational links, which must be considered seriously in the management of an oil field development project.

During the “battle for oil” in the Daqing oil field, one good conventional practice was to gather various materials and data precisely, completely, and integrally while drilling a well. With respect to well completion engineering, the requirement is the same in the appraisal well so as to guarantee the success of oil field development. Therefore, a successful exploration project must be one in which enough exploration investment is done to obtain high-quality, complete materials, and data for the next step, that is, oil field development (including well

completion engineering) from the period of drilling an appraisal well. Otherwise, this exploration project cannot be thought of as a successful one. By these means, the appraisal well-drilling period in exploration must consider the requirements of exploration and development in coordination. The economic benefit of exploration and development can only be obtained in this way. Each participant in these two areas must learn to work with each other.

This book summarizes the theory and practical experiences of well completion, describes the well completion engineering system, and reflects well completion technology and its development level in China.

One possible inadequacy of this book is that it only mentions the corrosion problem in sour gas wells, but does not deal with the casing problems that occur in many oil fields in China. Casing corrosion problems caused by formation water and bacteria can be solved by water treatment during oil production operation, but those caused by geocurrent can only be solved effectively during well completion procedures. The further consideration of this problem can perfect our knowledge in practice.

**Li Tianxiang**

Former Vice Minister of China National  
Petroleum Industry Ministry

# PREFACE TO THE THIRD EDITION

The first edition of the book *Advanced Well Completion Engineering* of 1996 was revised in the second edition of 1999. During the 12 years from the first to this third edition, new breakthroughs in petroleum exploration and new improvements in field development have taken place. At the same time, a new challenge has been met, and a new requirement for well completion engineering is raised. The third edition aims to meet the demand in exploration and field development.

Well completion engineering is an important component part of oil and gas well construction and a basis of field development implementation. It has a goal of ensuring regular and safe production and prolonging the production life of oil and gas wells. The traditional mode of well completion engineering, which had been adopted in China for a long time, cannot meet the requirements of developing circumstances; thus, reform is needed. After summing up domestic and foreign experience and lessons, the new *Advanced Well Completion* concept has been presented. Based on field geology and reservoir engineering, it adopts the nodal analysis method, and drilling, well completion, and production are organically integrated, thus forming an integrated well completion engineering system. The book develops what is correct and proper in classic well completion engineering and discards what is not, and initiates new concepts and ideas. The book *Advanced Well Completion Engineering* has been used not only for solving theoretical problems, but also as a guide to oil and gas well completion, an important basis for formulation of a well completion program, and a textbook in petroleum institutes and universities. Practice has proven that this book conforms to objective practice and has scientific rationality, practicality, and operability. It is the first worldwide systematic monograph in well completion engineering.

In recent years, many new oil and gas field domains have been constantly found by exploration in China, and field development has made obvious progress. However, in the current field development, deep and ultra-deep wells appear more and more, and high-pressure and high-production-rate gas wells are put into production. The gas in some wells contains high-concentration corrosive gas, such as  $H_2S$  and  $CO_2$ . Also, pressure-sensitive formations, sloughing formations, and fine silt-producing formations have been continuously met. Horizontal wells have been extensively adopted. Well completion for horizontal branched wells, extended reach wells, MRC wells, deep and ultra-deep wells with heavy oil, gravity drainage wells, underbalance wells, coal-bed gas wells, and gas storage wells is realistic. However, it is difficult to adapt to the new development and requirements by using existing well completion techniques, equipment, and tools.

The third edition not only adds new techniques developed in recent years, but introduces the current development tendency of well completion engineering, thus extending the field of vision of well completion engineering. This is conducive to the technical development and advances and field application of well completion engineering in China. The main points revised by the third edition include adding gas well completion relative to the previous editions, which emphasized oil well completion; adding well completion modes for various types of wells, such as horizontal branched wells, extended reach wells, MRC wells, coal-bed gas wells, and underbalance wells; separating the topic of completion tubing string into a separate chapter, which aims to emphasize the importance and practice of well completion tubing string; and adding a chapter about corrosion and corrosion inhibition for oil and gas wells,

which stresses that corrosion prevention is an important component part of well completion engineering.

The specialists made the mass investigation and data collection and wrote the articles for the book, which have passed preexamination and final examination. Many units and individuals provided valuable data. The leaders of CNPC, Exploration and Production Division of CNPC, Southwest Petroleum University, Langfang Division, and Production Institute of China Petroleum Exploration & Development Research Institute, and Petroleum Industry Press have provided energetic support and help. We hereby express our most heartfelt thanks.

Oil and gas exploration and development are becoming more prosperous and changing with

each passing day. Science and technology are advancing, and similarly, well completion engineering is developing and bringing forth new ideas. This is the third edition of the book *Advanced Well Completion Engineering*, and we hope that from now on it will be further revised and developed. Many of the authors are growing older. It seems that younger researchers will be obliged to bear the task of future revision.

The authors of this book are conscientious and earnest and have made great efforts, but still some blemishes are hard to avoid. We hope that our readers will oblige us by giving us their valuable comments.

**Wan Renpu**

# ABOUT THE AUTHOR

Mr. Wan Renpu, a native of Nanchang, Jiangxi, China, graduated from the Petroleum Department of Tsinghua University in 1953. After that he worked in the Shanbei, Yumen, Sichuan, Daqing, and Shengli oil fields for 25 years. In 1978, he was transferred to the Development & Production Department of the Ministry of Petroleum Industry and later to the Development & Production Bureau of CNPC and appointed to be chief engineer and deputy director. He was engaged in drilling for the first 10 years and has since been active in production and research work in petroleum production engineering, workover, servicing operations, and well completion engineering. He has authored numerous technical papers in Chinese oil and gas

journals and in *JPT*, *World Oil*, *SPE*, and so on, and also authored more than ten books in petroleum production engineering and other readings in science and technology as well. Mr. Wan was awarded the titles of professor and specialist with outstanding contribution by the Ministry of Personnel of PRC in 1983 and 1989, respectively, and enjoys the special allowance for specialist at state level. He is a chief founder in the Chinese petroleum production engineering system. At present, he also is one of the distinguished specialists in production engineering in China and a professor of China Petroleum University, Southwestern Petroleum University, Xi'an Petroleum University, and Jiangnan Petroleum Institute.

This page intentionally left blank

# INTRODUCTION

The concept of well completion engineering has been gradually enriched, perfected, and updated by the progress of science and technology. Both exploration and development wells have well completion procedures and are concerned with well completion engineering problems. This book focuses on the development of well completion engineering, which can also act as the reference for exploration wells.

The outdated concept in the USA, USSR, and China is that well completion engineering is the final procedure of drilling engineering, which includes casing setting, cementing, and perforating after drilling through the target formation. During recent years, with the wide use of new techniques and technology in many areas, petroleum engineers have acquired a deeper understanding of the microscopic characteristics of oil and gas reservoirs and taken some measures to protect reservoirs from damage. In the meantime, with the application of different well completion methods, the productivity of gas and oil wells has been enhanced. Due to the progress of technology in these two aspects, the individual-well production rate is augmented. Well completion engineering not only includes casing setting and cementing, but also is closely bound up with enhancing the productivities of oil and gas wells. This is the new concept of advanced well completion engineering, which widens the range of well completion. However, until now, the definitions of what advanced well completion engineering is, what contents it contains, and what the relations with drilling engineering and production engineering are have not yet been clearly and systematically presented. This book is prepared to answer all of these questions systematically and to make well completion engineering more scientific, systematic, practical, and operable.

1. Definition of well completion engineering  
Well completion engineering not only links up drilling and production engineering, but also is relatively independent; it is a form of system engineering including drilling in, production casing setting, cementing, perforating, tubing string running, flowing back, and putting the well into production.
2. Fundamental theory of well completion engineering
  - a. In accordance with oil and gas reservoir research and potential formation damage evaluation, reservoir protection measures should be taken during each operational procedure from drilling to production in order to reduce formation damage as far as possible, maintain good communication between reservoir and wellbore, and maximize reservoir productivity.
  - b. By means of nodal analysis, the oil and gas reservoir energy is perfectly utilized and the pressure system is optimized. In light of reservoir engineering characteristics, the whole process of field development, and the measures taken in oil field development, well completion method and casing size are selected. Tubing string size is first selected and determined, and then the production casing size is selected and determined. After that the casing program is calculated. Thus the necessary conditions for scientific field development are provided.
3. Contents of well completion engineering
  - a. Core analysis and sensitivity analysis  
Core analysis and sensitivity analysis are systematically carried out on the core samples of exploratory and appraisal wells. In accordance with the test results, the basic requirements for drilling in,

perforating, fracturing, acidizing, well killing, and workover fluids are presented.

The terms of core analysis and sensitivity analysis are as follows.

- (1) Core analysis: conventional core analysis, thin section analysis, X-ray diffraction (XRD), scanning electron microscope (SEM).
  - (2) Sensitivity analysis: water sensitivity, rate sensitivity, acid sensitivity, alkali sensitivity, salt sensitivity, and stress sensitivity.
- b. Drilling-in fluid selection
- For selection of drilling fluid, preventing formation damage caused by the invasion of filtrate and solids into formation should be considered, and safety problems during drilling of high-pressure, low-pressure, lost circulation, halite, halite gypsum, and fractured formations should also be considered. The type, formula, and additives of drilling fluid should be designed on the basis of well log data, core analysis, sensitivity analysis data, and empirical practice.
- c. Well completion mode and method selection
- The well completion modes should be selected in accordance with field geology characteristics, field development practices, and types of wells of different rock formations such as sandstone, carbonatite, igneous rock, and metamorphic rock. The well completion modes are basically divided into two categories, openhole completion and perforated completion. The openhole completion mode has several different methods such as open hole, slotted liner, and wire-wrapped screen gravel pack, while the perforated completion mode includes casing perforation, liner (including casing tie-back) perforation, and inside casing wire-wrapped screen gravel pack.
- d. Selection of tubing and production casing sizes

The nodal analysis or pressure system analysis is used for reservoir–wellbore–surface pipeline sensitivity analysis. The tubing sensitivity analysis is based on the composite analysis of reservoir pressure, production rate, liquid production rate, fluid viscosity, stimulation method, and development practices. The tubing size is selected first, and then the production casing size is designed on the basis of the tubing size. Formerly, it was necessary to choose the production casing size before selecting the tubing size. Advanced well completion engineering disregards this outdated method and has developed a system in which production casing size is determined on the basis of the tubing size.

The casing system design was originally composed of surface casing, intermediate casing, and production casing. Here we focus on the design of production casing rather than the other two, which have a special design that should match the requirements of drilling engineering.

e. Production casing design

The fundamental production casing design data, including category of well, type of well, well depth, physical properties of reservoir, fluid properties, in-situ stress, and engineering measures are listed as follows.

- (1) Category of well: oil well, gas well, thermal production well, water injection well, gas injection well, or steam injection well.
- (2) Type of well: straight well, horizontal well, or horizontal branch hole.
- (3) Well depth: shallow well, medium depth well, deep well, or ultra-deep well.
- (4) Reservoir pressure and temperature.
- (5) Ground water properties: pH value, salinity, and the degree of corrosion to casing.

- (6) Water and corrosive gas contents in natural gas.
- (7) Formation fracture pressure gradient, peak pressure in hydraulic and acid fracturing.
- (8) Trend and orientation of in-situ stress and its value.
- (9) Pressure and temperature for steam injection.
- (10) Halite bed creeping.
- (11) Pressure changes and interzonal communication after waterflooding.
- (12) Situation of sand production and sand grain size.

On the basis of the well completion method determined and the aforementioned influence factors, the casing steel grade, strength, wall thickness, types of thread and thread sealer, make-up torque, and so on are selected. For liner completion, the hanging depth and fashion should be designed. For a steam injection well, the tension borne by casing thread and the sealing property of thread under thermal conditions should be considered, and the well should be completed under prestress. For directional and horizontal wells, the problems of casing bending, tension borne by casing thread, and casing thread sealing property should also be considered.

#### f. Cementing design

One-step, staged, or outside casing packer cementing and its cement slurry formulation are selected in accordance with the following conditions:

- (1) The requirements of different types of wells (such as oil well, gas well, water injection well, gas injection well, and steam injection well) for properties and return height of cement slurry.
- (2) The pressure conditions in oil and gas reservoirs, such as high pressure zone, low pressure zone, leakage zone, and in-situ fracture distribution.
- (3) The pressure change in adjustment wells in waterflooding oil fields.

- (4) The flow condition of reservoir fluid.
- (5) The required heat-resisting cement property in steam injection wells.
- (6) The cement corrosion problem caused by corrosive gas (such as  $H_2S$  and  $CO_2$ ) and high-salinity underground water.
- (7) When cementing gas wells, gas injection wells, and steam injection wells, the cement slurry is required to be returned to the surface, that is, long well section cementing is required.

#### g. Cementing quality evaluation

Here, the cementing quality evaluation refers to inspecting the cementing sealing condition outside the casing, finding the channel and mixed mud-slurry segment, and determining the cement slurry return height. At present, acoustic amplitude logging is commonly used for detecting the first sealing interface. The ultrasonic logging tool (UCT-1) developed by the Jiangnan Log Institute is a good cement job quality assessment instrument due to high penetrance of ultrasonic wave with high sensitivity to the change of propagation medium. The acoustic variable density log, which detects the second sealing surface of displacement, has not widely been used.

#### h. Perforating and completion fluid selection

The perforation density, perforation diameter, and phase are designed on the basis of perforating sensitivity analysis. The perforator is selected according to reservoir permeability, oil property, and formation damage. The perforating methods, including cable perforating, tubing conveyed perforating (TCP), modular perforating, and underbalance perforating, are determined by the reservoir pressure, reservoir permeability, and oil and gas properties. In the meantime, the perforating and completion fluids should be designed to match the reservoir clay minerals and reservoir fluid.

#### i. Evaluation of well completion damage by well testing

After well completion and putting the well into production, the standard method of determining the degree of formation damage

is to calculate skin factor by well testing. By analyzing skin factor, the causes of formation damage can be found in order to remove or reduce the damage.

j. Well completion tubing string

The production tubing string in gas and oil wells and special tubing string developed in China can be divided into the following types:

(1) Permanent tubing string

The permanent packer is set on the top of the reservoir before putting the well into production. Each functional tool can be inserted into the mandrel below the packer, such as tools for separate zone injection, separate zone production, and separate zone testing.

This tubing string can be used for sand washing, injecting cement plugs, and carrying out small-scale acidizing operations.

(2) Gas lift tubing string

If it is expected that the well will soon be changed from flowing production to gas lift production, the gas lift tubing string and downhole tools (single-string or dual-string) should be set by running once before putting the well into production. The well can be converted into gas lift production if the flowing production rate decreases. However, this string is only adopted when the flowing period before gas lift is short because the gas lift valve is easily corroded during long idle times in the well and it has malfunctioned by the time of use.

(3) Anti-corrosion, paraffin controlling, anti-scale, and salt deposit-resisting tubing strings

If the natural gas or dissolved gas contains  $H_2S$ , or  $CO_2$ , and if the salinity in reservoir water, edge water, or bottom water is high, the tubing string is generally installed with the packer at the top of the reservoir to seal the annulus between the casing and tubing, which can be filled with protection liquid or anti-corrosive fluid periodically to protect the casing from corrosion. The

paraffin controlling, anti-scale, and salt deposit-resisting tubing strings are the same as the anti-corrosion tubing string, but the paraffin controlling, anti-scale, or salt deposit-resisting chemicals are injected. All of the preceding types of tubing strings should have circulation passage between the tubing and annulus.

In addition, offshore wells, deep wells, ultra-deep wells, natural gas wells, high-productivity wells, and wells in special geographic environments (such as flood discharge and earthquake regions) must be installed with downhole safety valve at about 100–200 m below the wellhead (100 m below the sea level for offshore well) in order to avoid blowout.

k. Wellhead assembly

The wellhead assembly is a main restrictor at the surface for the oil and gas flow from downhole. It is used for opening or shutting the well and controlling the direction and rate of oil and gas flow from downhole. In addition, it should be able to bear high pressure and resist corrosion, and ensure safety. This is more important for oil wells with high pressure and productivity and especially gas wells with high pressure and productivity (or  $H_2S$ -containing natural gas well), for which the packaged cast-steel wellhead assembly is inappropriate and the integral forged block wellhead assembly should be used.

l. Measures for putting a well into production

Different measures should be taken in accordance with the degree of formation damage and the type of oil and gas reservoir. The measures usually include swabbing, gas lift ( $N_2$ ), gassy water, and foam to aid flowing back, and sometimes hydrochloric acid or mud acid soak or high-energy gas fracture is used for plugging removal if necessary. In some wells, the acidizing and hydraulic fracturing must be taken before putting into production.

The aforementioned definition, theory foundation, content, and operation procedures of well completion engineering form

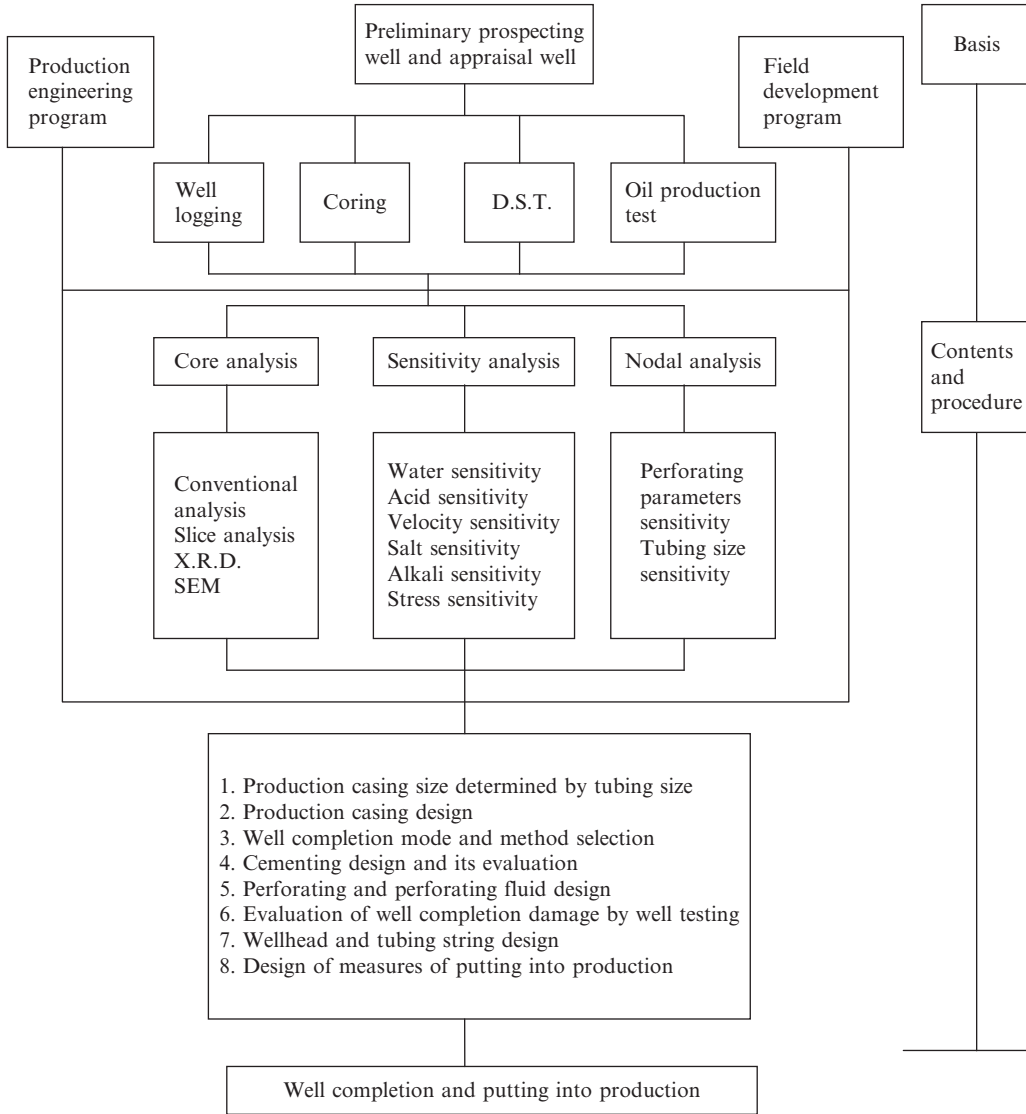
the well completion engineering system. Although well completion engineering combines drilling engineering and production engineering and remains a relatively independent domain, this engineering (engineering system) is not a work system but an inherent connection among drilling, well completion, and production engineering that considers the current and future macroscopic condition of the oil field development. Well completion engineering is incapable of replacing drilling and production engineering; drilling, well completion, and production engineering must each do its own work well. In this era of advanced technology, they are mutually infiltrated, and all achieve a common progress. The goals of the proposed well completion engineering concept and well completion engineering system are:

- (1) To reduce formation damage as far as possible and to allow the natural potential of the reservoir at its best;
- (2) To provide the necessary conditions for adjusting the producing pressure

difference, enlarging the drainage area, and increasing the flow conductivity, thus resulting in the augmentation of the individual-well production rate;

- (3) To put the reservoir reserves into effective use;
  - (4) To provide the necessary conditions for the application of different oil production techniques and technologies;
  - (5) To protect tubing and casing, retard tubing and casing corrosion, reduce downhole servicing operations, and prolong the well's production life;
  - (6) To combine current and future targets to improve the composite economic effectiveness;
  - (7) To design and operate at the minimum cost and the maximum economic benefit.
4. Design procedure for well completion engineering

The system design procedure of well completion engineering is as follows.



# Basis of Well Completion Engineering

## OUTLINE

### 1.1 Grounds of Reservoir Geology and Reservoir Engineering

Types of Oil and Gas Reservoirs

*Classification of Reservoirs on the Basis of Storage and Flow*

*Characteristics of Reservoirs*

*Classification of Reservoirs on the Basis of Reservoir Geometry*

*Classification of Reservoirs on the Basis of Properties of Reservoir Fluids*

*Classification of Reservoirs on the Basis of Main Characteristics of Development Geology*

Reservoir Fluid Properties

*Crude Oil*

*Natural Gas*

*Formation Water*

Reservoir Characteristics and Interlayer Differences

*Reservoir Lithology*

*Physical Properties of Reservoir*

*Reservoir Pressure and Interlayer Pressure Difference*  
*Fluid Properties and Interlayer Differences*

### 1.2 Core Analysis Techniques

Requirements of Well Completion Engineering for Core Analysis

Contents and Applications of Core Analysis

*Petrographic Analysis Techniques*

*Pore Configuration Analysis*

*Clay Mineral Analysis*

*Grain Size Analysis*

### 1.3 Reservoir Sensitivity to

**Fluid and Working Fluid**

**Damage Evaluation**

Overview of Formation Damage

Rate Sensitivity Evaluation Experiment

*Concept of Rate Sensitivity and*

*Experimental Goals Experimental Procedure and Result Analysis*

Water Sensitivity Evaluation

Experiment

*Concept of Water Sensitivity and Experimental Goals Experimental Procedure and Result Analysis*

Salt Sensitivity Evaluation Experiment

*Concept of Salt Sensitivity and*

*Experimental Goals Experimental Procedure and Result Analysis*

Alkali Sensitivity Evaluation Experiment

*Concept of Alkali Sensitivity and*

*Experimental Goals Experimental Procedure and Result Analysis*

Acid Sensitivity Evaluation Experiment

*Concept of Acid Sensitivity and*

*Experimental Goals Experimental Procedure and Result Analysis*

Experiments of Drilling and Completion Fluid Damage Evaluation

*Static Damage*

*Experiment of Drilling and Completion Fluid*

<i>Dynamic Damage Experiment of Drilling and Completion Fluid Evaluation Experiment of Drilling and Completion Fluid Invasion Depth and Degree of Damage Experimental Result Analysis and Evaluation Standard</i>	<i>Sands Gas Reservoir in Eerduosi Basin Stress Sensitivity of Tight Sands Gas Reservoir in Rook Mountains</i>	<i>Completion Engineering Design Fracture Configurations Generated by Hydraulic Fracturing and Acid Fracturing Depend on in Situ Stress State</i>
<i>Other Evaluation Experiments</i>	<i>Stress Sensitivity of Carbonatite Reservoir Stress Sensitivity of Carbonatite Reservoir of Zhanaruoer Oil Field in Kazakstan</i>	<b>1.6 Technological Grounds of Petroleum Production Engineering</b>
<b>1.4 Reservoir Stress Sensitivity Analysis</b>	<i>Stress Sensitivity of Carbonatite Gas Reservoir of Northeastern Sichuan Basin</i>	<i>Water Injection Fracturing and Acidizing Control of Gas Cap, Bottom Water, or Edge Water Management Adjustment Well Thermal Recovery by Steam Injection Sand Control Corrosion Prevention and Scale Control Injection of Natural Gas and Other Gases Stratified Oil Reservoir with Vertical or Composite Fractures and High Dip Angle Stratified Oil Reservoir Massive Oil Reservoir Fractured Oil Reservoir Multiple-Zone Commingled Production in Well with Great Interzone Pressure Difference Horizontal Well</i>
<i>Stress Sensitivity Experiment Evaluation Experimental Goals and Procedure Stress Sensitivity Evaluation Indices Contrast between Different Stress Sensitivity Evaluation Methods</i>	<i>Variation Rules of Stress Sensitivity of Carbonatite Reservoir</i>	<i>References</i>
<i>Stress Sensitivity of Low-Permeability Sandstone Oil Reservoir</i>	<b>1.5 In Situ Stress and Mechanical Parameters of Rock</b>	
<i>Stress Sensitivity of Tight Sands Gas Reservoir Stress Sensitivity of Conventional to Tight Sands Gas Reservoirs in Sichuan Basin</i>	<i>Basic Conception of in Situ Stress Stress State of Borehole Wall Rock Firmness of Borehole Wall Rock Mechanical Stability of Borehole</i>	
<i>Stress Sensitivity of Upper Paleozoic Tight</i>	<i>Relationship between in Situ Stress and Well Completion Engineering Grounds Are Provided by in Situ Stress State for Completion Mode Optimization and</i>	

Well completion engineering is system engineering that includes drilling-in reservoir, well cementing, well completing, and putting the well into production. The basis of well completion engineering is a theory composed of the parts in reservoir geology, reservoir engineering, and petroleum production engineering, which are related to well completion. The parts in reservoir geology and reservoir engineering include types, configuration, lithology, fluid properties, pore configuration, and fluid flow

characteristics of oil and gas reservoirs, which are the theoretical grounds for selecting well completion mode and avoiding formation damage, while the part in petroleum production engineering includes the requirements of different types of wells (such as oil well, gas well, water injection well, gas injection well, steam injection well, and horizontal well), production modes (such as multizone commingled production in a well, separate zone production, artificial lift after flowing

production, and production with steam treatment), and technical measures necessary during oil and gas field development (such as fracturing, acidizing, sand control, water shutoff, and gas well dewatering and gas production) for well completion mode selection, casing size and strength selections, cement slurry return height and high-temperature resistance of cement, and life prolongation of production and injection wells, etc.

## 1.1 GROUNDS OF RESERVOIR GEOLOGY AND RESERVOIR ENGINEERING

### Types of Oil and Gas Reservoirs

An oil and gas reservoir is the oil and gas accumulation in an independent trap with a single pressure system and the unitary gas–oil interface and oil–water interface. In the light of development geology, an oil and gas reservoir has its geometric configuration and boundary conditions, storage and flow characteristics, and fluid properties.

**Classification of Reservoirs on the Basis of Storage and Flow Characteristics of Reservoirs.** In accordance with different storage spaces and main flow channels of formation

fluids, oil and gas reservoirs can be divided into the following types, shown in Table 1-1.

1. *Porous reservoir.* The storage space and percolation channels are the intergranular pores. Therefore, the flow is called flow in porous media such as sandstone, conglomerate, bioclastic limestone, and oolitic limestone reservoirs.
2. *Fractured reservoir.* Natural fractures are not only the main storage space, but also the flow channels. There may be no primary pores or be disconnected pores. Generally, the fracture porosity is not more than 6%. Tight carbonatite and metamorphic rock reservoirs, and mud shale gas reservoirs, are of this type of reservoir.
3. *Fracture porosity reservoir.* Intergranular pores are the main storage space, whereas fractures are the main flow channels. The flow is called flow in dual-porosity single-permeability media. Usually, the fractures extend for a long distance, but the pore permeability is very low. The Renqiu carbonatite oil field of China and the Spraberry Trend oil field of the United States are of this type of reservoir.
4. *Porous fractured reservoir.* Both intergranular pores and fractures are the storage space and the flow channels. The flow is called flow in dual-porosity dual-permeability media. Fractures grow fine, but extend for a short distance. The matrix porosity is low.

TABLE 1-1 Types of Reservoirs and Classification of Storage and Flow Space System

No.	Type	Growth Degree of Storage Space (%)			Relative Porosity of Fractures (%)			Fracture-Matrix Permeability Ratio
		Pore	Vug	Fracture	Macro-Fracture	Medium Fracture	Crackle	
1	Pore	>75	<25	<5	0	0	100	≤1
2	Fracture-pore	>50	<25	>5	25	25	50	≥10
3	Microfracture-pore	50~95	<25	<25	0	0	90	≥3
4	Fracture	<25	<25	>50	30	30	40	∞
5	Pore-fracture	25~75	<25	25~75	40	40	20	≥10
6	Vug-fracture	<25	25~75	25~75	50	40	10	∞
7	Vug, fracture-vug	<25	>75	5~25	50	40	10	∞
8	Fracture-vug-pore	25~75	25~75	5~50	33	30	40	≥10
9	Para pore	>50	<1	≈50	0	0	100	1

5. *Combined fracture–vug–pore reservoir.* Fractures, vugs, and pores are both the storage space and the flow channels. All reservoirs of this type are soluble salinestone. The secondary pores are the main. This type of reservoir is also called a triple-porosity reservoir.

**Classification of Reservoirs on the Basis of Reservoir Geometry.** Reservoirs can be divided into massive, stratified, fault block, and lenticular reservoirs in accordance with the geometry.

1. Massive reservoir

The reservoir has a large effective thickness (more than 10 m). The oil reservoir may have a gas cap and bottom water while the gas reservoir may have bottom water. The reservoir has a unitized hydrodynamic system and good connectivity. The bottom water has rechargeability. When choosing completion modes, whether gas cap and bottom water exist for oil reservoir and whether bottom water is active for gas reservoir should be considered. Generally, perforating or open hole completion is selected.

2. Stratified reservoir

Most reservoirs of this type belong to an anticlinal trap with a complete structure and a unitized oil–water interface. It has good stratification and a number of beds along a vertical section. Every individual bed has a small thickness. A bed with a thickness of 5–10, 1–5, and less than 1 m is called thick, medium thick, and thin, respectively. These beds differ greatly in permeability. The drive energy of edge water is weaker. Separate zone water injection, separate zone fracturing, and separate zone water shutoff should be applied during waterflooding in order to control injection and production profiles and increase flooding efficiency, thus the perforated completion mode is generally adopted. Reservoirs in the Daqing Shaertu, Shengli Shengtuo, and Changqing Malin oil fields in China are of this type of reservoir.

3. Fault block reservoir

Fractures well developed in reservoirs of this type. The structure is cut into many fault

blocks of different sizes. The areas of some fault blocks are less than 0.5 km<sup>2</sup>. Vertically, there are many oil-bearing series of strata with a long total oil-bearing section. In each fault block or even various reservoir groups in the same fault block, different oil–water interfaces and obvious differences in degrees of oil and gas enrichment, physical property of reservoir, and natural drive energy exist. For a seal-type fault block, elastic energy is used in the early stage, whereas selective scattered flooding is used in the late stage. Peripheral or outer edge waterflooding is applicable to the open-type fault block. Generally, the perforated completion mode is adopted for this type of reservoir due to their numerous oil-bearing series of strata and the great interlayer differences. The Shengli Dongxin and Zhongyuan Wenminzhai oil fields are of this type of reservoir.

4. Lenticular reservoir

The geologic description of geometry for a sand body depends on the length-to-width ratio. A sand body with a ratio less than or equal to 3 is called lens. Lenses are scattered, and the major area is occupied by the pinchout region. When lenses alternately overlap each other, multiple reservoirs may appear on the vertical oil- and gas-bearing well section.

**Classification of Reservoirs on the Basis of Properties of Reservoir Fluids.** Reservoirs can be divided into gas, condensate gas, volatile oil, conventional oil, high pour-point oil, and heavy oil reservoirs in accordance with the properties of reservoir fluids.

**Classification of Reservoirs on the Basis of Main Characteristics of Development Geology.** The continental reservoirs in China are divided into multilayer sandstone oil reservoirs, gas cap sandstone oil reservoir, low-permeability sandstone oil reservoirs, complex fault-block sandstone oil reservoirs, glutenite oil reservoirs, fractured buried-hill basement rock reservoirs, conventional heavy oil reservoirs, high pour-point oil reservoirs, and condensate gas reservoirs in accordance with the main characteristics of development geology and the development mode of the continental reservoirs in China.

## Reservoir Fluid Properties

**Crude Oil.** Crude oil is composed of various hydrocarbons, porphyrin complex, asphalt, a small amount of sulfur, and other nonhydrocarbon materials, thus its physical and chemical properties vary considerably. The important physical properties of crude oil include density, viscosity, pour point, and so on under both surface and subsurface conditions.

### 1. Density

Density is the mass of substance per unit volume and is expressed by  $\rho$  in such units as  $\text{g}/\text{m}^3$  or  $\text{kg}/\text{m}^3$  (SI system). The density under pressure of 0.101 MPa at a temperature of 20°C is stipulated as the standard density of petroleum and liquid petroleum products and is expressed by  $\rho^{20}$ .

The standard condition for engineering in China is a temperature of 20°C and the pressure is 0.101 MPa. The property at the surface is namely the property under the standard condition.

API gravity is usually used to reflect the density of petroleum in the United States. The conversion formula is as follows:

(1-1)

$$^{\circ}\text{API} = \frac{141.5}{\text{Density at } 60^{\circ}\text{F (15.6}^{\circ}\text{C)}} - 131.5$$

The number of API degree decreases as the density increases.

### 2. Viscosity

Viscosity is the friction resistance produced by relative motion between molecules of liquid (or gas). The unit of viscosity in the SI system is  $\text{Pa}\cdot\text{s}$ , while  $\text{mPa}\cdot\text{s}$  is normally used in reservoir engineering. The viscosity of crude oil changes in a wide range. Crude oil is divided into conventional oil and heavy oil in accordance with their viscosities in China. The former has a degassed oil viscosity of less than 50  $\text{mPa}\cdot\text{s}$  at reservoir temperature, whereas the latter has a viscosity more than 50  $\text{mPa}\cdot\text{s}$ . Heavy oil can be further divided in accordance with its own standard.

Heavy oil is asphalt-based crude oil. It is generally called viscous oil in China on the basis of viscosity. Heavy oil is the international general term on the basis of specific gravity. Viscosity is used as the main index, and specific gravity as the auxiliary index internationally or in China. Practically viscous oil is namely heavy oil. The standards of division in various countries are different slightly due to slight differences in the genesis of heavy oil. The standards of division in China and the heavy oil and asphalt classification standards recommended by UNITAR are shown in Tables 1-2 and 1-3, respectively.

Class I-1 oil of common heavy oil, such as oil in the Shengli Gudao, Gudong, Chengdong, and Shengtuo oil fields, can be mostly developed by waterflooding, whereas Class I-2 oil should be developed using steam injection.

TABLE 1-2 Classification of Heavy Oil in China

Classification of Heavy Oil		Main Index Viscosity, $\text{mPa}\cdot\text{s}$	Auxiliary Index Specific Gravity	Production Mode
Name	Class			
Common heavy oil	I I-1	50~150 <sup>a</sup>	>0.9200	Conventional production or steam injection
	I-2	150 <sup>a</sup> ~10,000	>0.9200	Steam injection
Extra-heavy oil	II	10,000~50,000	>0.9500	Steam injection
Ultraheavy oil (natural asphalt)	III	>50,000	>0.9800	Steam injection

<sup>a</sup>It means viscosity under standard condition, while others mean the viscosity of degassed oil at reservoir temperature.

TABLE 1-3 Heavy Oil and Asphalt Classification Standards Recommended by UNTAR

Classification	First Index	Second Index	
	Viscosity <sup>a</sup> (mPa·s)	Density (60°F) (g/cm <sup>3</sup> )	Density (60°F) (°API)
Heavy oil	100~10,000	0.934~1.0	20~10
Asphalt	>10,000	>1.0	<10

<sup>a</sup>Viscosity of degassed oil at reservoir temperature.

Extra-heavy oil (Class II) and ultraheavy oil (Class III), such as the oil in the Liaohe Gaosheng, Shuguang, and Huangxiling oil fields, Jiu-6,7,8 regions of the Xinjiang Kelamayi oil field, Shengli Shanjiashi and Lean oil fields, and the Henan Jinglou oil field, should be developed using steam injection.

Heavy oil reservoir rock is mostly midcoarse grain sandstone and glutenite with loose argillaceous cementation, which are easy of sand production.

### 3. Pour point

Pour point is the highest temperature at which crude oil, chilled under test conditions with a flow plane inclination angle of 45°, will not flow after 1 min. Crude oil with a high pour point is rich in paraffin.

About 90% of Chinese crude oils have a pour point above 25°C, in which 15% is above 30°C. A few reservoirs have crude oil with a pour point above 40°C. Crude oil of the Liaohe Shenyang oil field has a pour point average of 55°C and the highest of 67°C. China refers the reservoir of crude oil with a pour point above 40°C to the high pour-point oil reservoir. The high pour-point oil of the Liaohe Shenyang oil field is rare worldwide. The key to high pour-point oil field development is that the flowing temperature of the crude oil must be above the pour point in order to keep normal production.

**Natural Gas.** The natural gas in oil and gas fields includes dissolved gas and gas cap gas in oil reservoir, free gas in gas reservoir, and dissolved gas in formation water.

The main component in natural gas is methane; in addition, ethane, propane, butane, and pentane

plus are contained. Nonhydrocarbon gas in natural gas includes N<sub>2</sub>, CO<sub>2</sub>, H<sub>2</sub>S, and H<sub>2</sub>.

If formation water contains dissolved CO<sub>2</sub>, the decrease in pressure may lead to a decrease in the partial pressure of CO<sub>2</sub>, thus causing the formation of CaCO<sub>3</sub> scale.

H<sub>2</sub>S is the common component in natural gas. Particularly, the natural gas in a carbonate reservoir generally contains various amounts of H<sub>2</sub>S gas. The gas reservoir classification in accordance with the type and content of nonhydrocarbon gas is shown in Table 1-4. Gas of the Luojiashai gas reservoir and Puguangte reservoir in the northeastern Sichuan of China is high sulfur gas with a sulfur content of 150.0–264 g/m<sup>3</sup>. When the natural gas contains some amount of sour gas (H<sub>2</sub>S and CO<sub>2</sub>), it may endanger the operator's life; therefore, the specific requirements for drilling and well completion, anticorrosion design of tubing and casing, wellhead, natural gas treatment, and transportation should be met.

**Formation Water.** Formation water exists naturally in the rock all along, before drilling. It is water associated with the oil and gas reservoir and has some outstanding chemical characteristics. Connate water is fossil water that was out of contact with the atmosphere during most part of the geologic age at least. The physical properties of formation water include mainly density, viscosity, and compressibility. These properties may be determined using charts due to fewer changes of these properties of formation water with pressure and temperature than that of crude oil. Thus, the chemical properties of formation water become more important. The salts contained are mainly composed of K<sup>+</sup>, Na<sup>+</sup>, Ca<sup>2+</sup>, Mg<sup>2+</sup>, Cl<sup>-</sup>, SO<sub>4</sub><sup>2-</sup>, CO<sub>3</sub><sup>2-</sup>, and HCO<sub>3</sub><sup>-</sup>.

TABLE 1-4 Gas Reservoir Classification in Accordance with Nonhydrocarbon Gas Content

Type	Subtype	Subtype/Classification Index					
		Slight-Sulfur Gas Reservoir	Low-Sulfur Gas Reservoir	Mid-Sulfur Gas reservoir	High-Sulfur Gas Reservoir	Extra-Sulfur Gas Reservoir	Hydrogen Sulfide Gas Reservoir
H <sub>2</sub> S-bearing gas reservoir	H <sub>2</sub> S, g/cm <sup>3</sup>	<0.02	0.02~5.0	5.0~30.0	30.0~150.0	150.0~770.0	≥770.0
	H <sub>2</sub> S, %	<0.0013	0.0013~0.3	0.3~2.0	2.0~10.0	10.0~50.0	≥50.0
CO <sub>2</sub> -bearing gas reservoir	Subtype	Slight-CO <sub>2</sub> gas reservoir	Low-CO <sub>2</sub> gas reservoir	Mid-CO <sub>2</sub> gas reservoir	High-CO <sub>2</sub> gas reservoir	Extra-CO <sub>2</sub> gas reservoir	CO <sub>2</sub> gas reservoir
	CO <sub>2</sub> , %	<0.01	0.01~2.0	2.0~10.0	10.0~50.0	50.0~70.0	≥70.0
N <sub>2</sub> -bearing gas reservoir	Subtype	Slight-N <sub>2</sub> gas reservoir	Low-N <sub>2</sub> gas reservoir	Mid-N <sub>2</sub> gas reservoir	High-N <sub>2</sub> gas reservoir	Extra-N <sub>2</sub> gas reservoir	N <sub>2</sub> gas reservoir
	NO <sub>2</sub> , %	<2.0	2.0~5.0	5.0~10.0	10.0~50.0	50.0~70.0	≥70.0

The unit mg/liter is generally used as the unit of total salinity (or TDS).

#### 1. Composition and properties of formation water

Field water contains various soluble inorganic and organic compounds. Main elements include K, Na, Ca, Mg, and Cl. In addition, CO<sub>3</sub><sup>2-</sup>, HCO<sub>3</sub><sup>-</sup>, and SO<sub>4</sub><sup>2-</sup> also exist in field water. Generally, the concentrations of ions in field water are as follows:

10 <sup>3</sup> –10 <sup>5</sup> mg/liter	K <sup>+</sup> +Na <sup>+</sup> , Cl <sup>-</sup>
10 <sup>3</sup> –10 <sup>4</sup> mg/liter	Ca <sup>2+</sup> , Mg <sup>2+</sup> , SO <sub>4</sub> <sup>2-</sup> , CO <sub>3</sub> <sup>2-</sup> , HCO <sub>3</sub> <sup>-</sup>
10 <sup>1</sup> –10 <sup>3</sup> mg/liter	K <sup>+</sup> , Na <sup>+</sup> , Sr <sup>2+</sup>
10 <sup>0</sup> –10 <sup>2</sup> mg/liter	Al <sup>3+</sup> , B, Fe <sup>2+</sup> , Li <sup>+</sup>
10 <sup>-3</sup> mg/liter (most field water)	Cr, Cu, Mn, Ni, Sn, Ti, Zr
10 <sup>-3</sup> mg/liter (some field water)	Be, Co, Ga, Ge, Pb, V, W, Zn

Ca<sup>2+</sup> may form scale of CaCO<sub>3</sub> or CaSO<sub>4</sub>; Ba<sup>2+</sup> and Sr<sup>2+</sup> may also form scale of sulfate, such as the scale in tubing in the Changqing Maling oil field and the scale of barium sulfate in tubing of the production well during polymer flooding in the Daqing oil field. A high Cl<sup>-</sup> content means high corrosiveness. Scale prevention and corrosion prevention of completion tubing string should be considered.

The properties of formation water, which are related to well completion engineering,

include mainly the pH value and total salinity.

##### a. pH value

The pH value of formation water is controlled by the bicarbonate system. The solubilities of carbonate and ionic compounds depend substantially on the pH value. A high pH value leads to a strong tendency of scaling. A low pH value leads to a weak tendency of scaling, but leads to high corrosiveness. The pH value of most field water is between 4 and 9. During preservation in the laboratory, the pH value of most field water rises due to the dissociation of HCO<sub>3</sub><sup>-</sup> into CO<sub>3</sub><sup>2-</sup>.

##### b. Total salinity

Total salinity can be calculated using the summation of cationic and anionic concentrations. Water with high salinity (e.g., formation water of the Zhongyuan oil field with 30 × 10<sup>4</sup> mg/liter) has high corrosiveness and serious damage to casing. Salt precipitation in the tubing during production often plugs up the tubing.

Formation water can be divided into four basic types and further divided into group, subgroup, and class in accordance with the different combinations of salts dissolved in the water. In general, the types are only referred to. The characteristic coefficient or division standard for each type is listed in Table 1-5.

**TABLE 1-5 Characteristic Coefficient of Connate Water Type and Formation Water Classification**

Type of Water	Concentration Ratio Expressed by Milligrammequivalent Percentage		
	$\frac{\text{Na}^+}{\text{Cl}^-}$	$\frac{\text{Na}^+ - \text{Cl}^-}{\text{SO}_4^{2-}}$	$\frac{\text{Cl}^- - \text{Na}^+}{\text{Mg}^{2+}}$
Calcium chloride	<1	<0	>1
Magnesium chloride	<1	<0	<1
Sodium bicarbonate	>1	>1	<0
Sodium sulfate	>1	<1	<0

## 2. Application of formation water analysis

Formation water is syngenetic with oil, gas, and rock. They had the same or similar evolutionary history. Therefore, water analysis data have important value in well completion engineering. The application of these data is as follows.

- (1) The chemical composition analysis of formation water can help us determine the source of water and possible water production rate. This is important for the drilling design for drilling-in target using gas base fluid.
- (2) Experimental fluid can be prepared, and reservoir sensitivity and degree of working fluid damage can be evaluated using formation water property data.
- (3) Oil and gas saturations can be determined, and oil and gas reservoirs can be identified using logging data of formation water resistivity,  $R_w$ .
- (4) The type and tendency of scale, as well as the compatibility with drilling and completion, perforating, killing, fracturing, and acidizing fluids, can be identified using formation water analysis data.
- (5) The completion fluid required for reservoir protection can be formulated on the basis of formation water analysis data.

## Reservoir Characteristics and Interlayer Differences

The types of reservoirs are without doubt the main grounds for determining the completion mode.

In addition, it will still be necessary to consider reservoir characteristics, such as reservoir lithology, permeability, interlayer difference in permeability, reservoir pressure and interlayer difference in pressure, spatial fluid distribution and interlayer difference in fluid property, and whether the gas cap, edge water, and bottom water exist or not.

**Reservoir Lithology.** At present, the most important and extensive reservoir rocks include sandstone, conglomerate, limestone, and dolomite. In addition, less volcanic rock, metamorphic rock, mudstone, and coal rock exist as reservoir rock. In order to produce oil and gas from productive reservoirs effectively, the reservoir characteristics should be studied, thus the drilling and well completion technologies can fully play the reservoir potential.

### 1. Clastic rock

Clastic rock includes principally sandstone, glutenite, conglomerate, siltstone, and argillaceous siltstone. These are presently the most important types of reservoirs in China. Clastic rock is mainly composed of grains and cement. Cement is chiefly siliceous and calcareous cement and clay minerals—sometimes crude oil or asphalt. During the various operations, formation damage is caused due primarily to the many types and wide content variation range (3–25%) of clay minerals, as well as the ease with which their properties are influenced by foreign fluids. In China, sandstone reservoirs are mostly stratified with a wide variation range of formation pressure coefficient and

are predominantly medium-low permeable. Commingled production, separated-zone water injection, and stimulation are applied to the development of these reservoirs. Therefore, casing or tailpipe perforation completion is generally used, while open hole or slotted liner completion is seldom adopted.

## 2. Carbonatite

Carbonatite includes mainly limestone and dolomitite. Carbonatite accounts for about 55% of the total area of sedimentary rock and developed well in southwestern and central-southern China in particular. The older the geologic era, the more carbonatite accounts for. About half of the total world oil reserves are in carbonatite. Apart from the buried hill oil reservoirs of carbonatite in northern China, carbonatite is used mostly as a gas reservoir, such as Jurassic Daanzhai shell limestone gas reservoirs in the Sichuan basin, Carboniferous oolitic limestone gas reservoirs in eastern Sichuan, and weathering crust carbonatite gas reservoirs in the central Shanganning basin.

Carbonatite differs from sandstone in many aspects. Carbonatite is chiefly composed of the remains of animals and plants (algae) that existed and grew almost at the same place. Because the carbonate mineral is dissolved easily by water, it was commonly dissolved and recrystallized during the diagenesis process after deposition. Carbonatite is much more brittle than sandstone, and fractures and vugs develop well, which are relatively important for storage and flow.

Carbonatite is mostly hard and tight with pores, fractures, and vugs as the storage and flow space, and it is possible that bottom water and a gas cap exist in the carbonatite reservoir. Most of the wells need stimulation, such as acidizing, acid fracturing, and fracturing. For the porous carbonatite (such as the Muxileiyi gas reservoir in the central Sichuan basin with a permeability of  $0.88 \times 10^{-3} \mu\text{m}^2$  and a porosity of 8.35%), the completion mode is similar to that of sandstone, and acidizing, prepad acid fracturing, or sandfrac can be adopted. Open hole completion can

be used for fractured buried hill carbonatite reservoirs (such as the Renqiu buried hill oil reservoir in North China); however, in recent years, casing perforated completion has been adopted in China and overseas in order to control bottom water and to conduct stimulation. In recent years, it is a tendency that a horizontal well is used for carbonatite reservoir development. Good results have been obtained using a horizontal well in the Muxileiyi gas reservoir development. A horizontal well is being used extensively for development of the reservoir of the Talimu Tahe oil field in the Talimu basin and the Kenjijak undersalt reservoirs in Kazakstan.

## 3. Other types of rock

In addition to clastic rock and carbonatite, other types of reservoir rocks include volcanic rock, metamorphic rock, mud shale, and coal rock, of which reservoirs have been found in China and other countries, and research on them should not be ignored. The reservoirs of volcanic and metamorphic rocks are mostly buried hill reservoirs. These types of rocks themselves are tight and contain fractures and vugs. Open hole completion is carried out for these reservoirs after the weathering crust at the unconformity surface is drilled. The plagioclase amphibolite and hybrid granite of the Liaohe Dongshengbu oil field, the greiss of the Shengli and Liaohe oil fields, the slate of the Kelamayi oil field, the basalt of the Jiangsu oil field, and the andesite of the Liaohe oil field are examples of these types of rocks. Certainly, perforated completion can also be used for these types of rocks.

**Physical Properties of Reservoir.** The physical properties of a reservoir are basic parameters for evaluating the storage and flow capacities related closely to the types of pores and throats and the pore-throat matching relations. Pores and throats are important components of porous media (reservoir rock). Studies of physical properties and pore configuration are highly important for drilling and completion fluid design, completion mode selection, and development program formulation.

## 1. Porosity

The porosity of rock is a measure of the fluid storage capacity of porous media (reservoir rock). For clastic rock, porosity is closely related to permeability with obvious correlativity. The porosity of clastic rock depends mainly on sedimentation and diagenesis, including clastic grain size and degree of sorting, compaction and pressure solution, cementation, dissolution, and cataclasis. A good reservoir sandstone in China includes medium- and fine-grained sandstones. Generally, porosity decreases as the cement content increases. The porosity of sandstone with argillaceous cement is greater than that with carbonate mineral cement. The pore abundance of granular carbonatite, different from the organic framework of carbonatite, is similar to that of sandstone and is influenced easily by grain size, sorting, shape, and cement content. The porosity of dolomitite does not obviously correlate with these properties.

The fissure (or fracture) porosity is normally low (0.01–6%, rarely >6%). For carbonatite, pores are still the oil and gas storage space, whereas fractures are principally flow channels.

Recommended reservoir classification standards for clastic rock oil reservoir development in China are listed in Table 1-6.

## 2. Permeability and interlayer permeability differences

Geologic factors affecting porosity also affect directly the absolute permeability of the pore system. Permeability relates closely to porosity, grain size, sorting, spread pattern,

type of cement, and in situ stress value and orientation.

Reservoirs in China have been classified as superhigh, high, medium, low, and superlow permeability. In recent years, a large amount of petroleum reserves that were difficult to produce in the low permeability reservoirs, have been found. As the development techniques progress, the upper limit of low permeability has been adjusted from 100 to  $50 \times 10^{-3} \mu\text{m}^2$ . The nonconventional reservoir classification programs required by the exploration and development of the tight sandstone and carbonatite reservoirs in the Sichuan and Erduosi basins are given in Tables 1-7 and 1-8, which have been obtained from the foreign experience and through the domestic gas field development practice.

Permeability is an important index for well completion mode selection. Permeability is roughly divided into high and low permeabilities abroad; 10 and  $100 \times 10^{-3} \mu\text{m}^2$  are used as the distinguishing standards between high and low permeabilities for porous and fractured reservoirs, respectively. Gas reservoirs with air permeability less than  $0.1 \times 10^{-3} \mu\text{m}^2$  under in situ conditions are known as tight gas reservoirs. The oil and gas wells of high permeability reservoirs have a high production rate and inflow velocity. This should be considered when selecting the well completion mode. Permeability coefficient of variation, permeability contrast, and coefficient of heterogeneity (or breakthrough coefficient) are used for describing the degrees of in-layer and interlayer permeability heterogeneities:

**TABLE 1-6 Recommended Reservoir Classification Standards for Clastic Rock Oil Reservoir Development**

Name	Porosity (%)	Name	Permeability ( $10^{-3} \mu\text{m}^2$ )
Superhigh porosity	>30	Superhigh permeability	>2000
High porosity	25~30	High permeability	500~2000
Medium porosity	15~25	Medium permeability	50~500
Low porosity	10~15	Low permeability	10~50
Superlow porosity	<10	Superlow permeability	≤10

**TABLE 1-7 Gas Reservoir Classification in Accordance with Physical Properties of Reservoirs (SY/T6168-1995)**

Name	Effective Permeability <sup>a</sup> (10 <sup>-3</sup> μm <sup>2</sup> )	Absolute Permeability <sup>a</sup> (10 <sup>-3</sup> μm <sup>2</sup> )	Porosity (%)
High-permeability gas reservoir	>50	>300	>20
Medium-permeability gas reservoir	10~50	20~300	15~20
Low-permeability gas reservoir	0.1~10	1~20	10~15
Tight gas reservoir	≤0.1	≤1	≤10

<sup>a</sup>Effective and absolute permeabilities are obtained by the well test and core analysis data, respectively.

**TABLE 1-8 Gas Reservoir Classification in Accordance with Reservoir Matrix Permeability (Elkins, 1980)**

Type	Name	Permeability (10 <sup>-3</sup> μm <sup>2</sup> ) <sup>a</sup>
Conventional gas reservoir		>1.0
Nonconventional gas reservoir	Subtight	0.1~1.0
	Tight	0.005~0.1
	Very tight	0.001~0.005
	Ultratight	<0.001

<sup>a</sup>Air permeability measured by modeling in situ conditions. Types of reservoirs are divided by the median of the cumulative rock sample permeability distribution curve.

Permeability variation coefficient:  $K_v = \sigma / K_a$ .  $K_v$  varies between 0 and 1. The closer to 1 the  $K_v$  is, the more serious heterogeneity is.

Permeability contrast:  $K_b = K_{\max} / K_{\min}$ . The greater the  $K_b$  is, the more serious heterogeneity is.

Coefficient of heterogeneity:  $K_k = K_{\max} / K_a$ . The greater the  $K_k$  is, the more serious heterogeneity is.

$\sigma$  is mean square deviation of permeability (weighted value of thickness should be considered),  $K_a$  is average permeability of single zone or series of strata (weighted value of thickness should be considered),  $K_{\max}$  is maximum permeability of single zone or series of strata (weighted value of thickness should be considered), and  $K_{\min}$  is minimum permeability of single zone or series of strata (weighted value of thickness should be considered).

The interlayer permeability difference is very common for stratified sandstone reservoirs. Interlayer permeability differences for some stratified reservoirs in China may be up to several dozen times, even a hundred times. The following interlayer permeability difference ranges are used abroad for division of the difference:

- (1)  $K > 1 \mu\text{m}^2$ ;
- (2)  $K = 0.5 \sim 1 \mu\text{m}^2$ ;
- (3)  $K = 0.1 \sim 0.5 \mu\text{m}^2$ ;
- (4)  $K = 0.05 \sim 0.1 \mu\text{m}^2$ ;
- (5)  $K = 0.01 \sim 0.05 \mu\text{m}^2$ ; and
- (6)  $K < 0.01 \mu\text{m}^2$ .

If the permeability change among layers does not exceed one of these ranges, the interlayer permeability difference is not considered obvious, thus commingled production in a well can be adopted. Otherwise, two layer series of development are required. The permeability contrast for same layer

series of development in the Daqin oil field is not more than 5. Generally, the measure taken for interlayer permeability difference is stimulation (fracturing or acidizing) of the relatively low permeability reservoirs after well completion, which is followed by commingled production in a well. If the interlayer permeability difference is too great to adjust by fracturing, two layer series of development have to be applied.

### 3. Saturation

Well logging and core analysis methods can be used to determine reservoir fluid saturations. It is impossible, however, to substitute the well logging method, by which the fluid saturations can be obtained, for the core analysis method. During coring, the fluid (oil, gas, and water) may invade the core. After the core is taken to the surface, its original saturation conditions may be changed due to changes in temperature and pressure. It is generally recognized that the water saturation of the core only changes a little using the sealed coring with the oil base drilling fluid.

In recent years, a new understanding of fluid saturation analysis has been acquired. The water saturation of the tight sandstone gas reservoir in the Eerduosi basin, which was determined by coring with water base drilling fluid, is up to 40–70%. However, the water saturation determined by the sealed coring with oil base drilling fluid is only 15–25%. Minimum and average water saturations determined by the analysis of 156 core samples obtained by sealed coring from the gas reservoir of the Feixianguan formation gas reservoir of the Fuguang gas field in northeastern Sichuan are only 1.4 and 8.09%, respectively. More than 20% of the core samples have water saturation  $S_{wi}$  equal to or less than 5%.

**Reservoir Pressure and Interlayer Pressure Difference.** Reservoir pressure means the pressure of the fluid in pores and fractures, which reflects the energy of the reservoir and is the power pushing the fluid to move in the reservoir. The correct well completion design, effective utilization of

reservoir energy, and rational development of field presuppose clarifying the pressures of various reservoirs and distinguishing the different pressure systems.

The reservoir pressure can be determined by measurement using bottomhole pressure gauge, well testing, or graphics.

Generally, formation pressure is assessed by the pressure gradient and the pressure coefficient. The pressure gradient (MPa/100 m) is the pressure variation value corresponding to the sea level elevation difference in the same reservoir. There may be multiple pressure systems in an oil and gas field. A reservoir must be in a same pressure system. After a reservoir is put into development, pressures in adjacent reservoirs may change due to differences of permeability, energy recharge, and engineering measures.

The ratio of the original reservoir pressure to the hydrostatic column pressure is known as pressure coefficient  $\alpha$ . In practice,  $1.0 \text{ g/cm}^3$  may be taken as the density of formation water for calculating hydrostatic column pressure. The reservoirs are divided abroad into abnormal high pressure ( $\alpha > 1.0$ ), normal pressure ( $\alpha = 1.0$ ), and abnormal low pressure ( $\alpha < 1.0$ ). In China, reservoirs with  $\alpha = 0.9$ – $1.2$ ,  $\alpha > 1.2$ , and  $\alpha < 0.9$  are divided into normal pressure, abnormal high pressure, and abnormal low pressure, respectively. The following interlayer pressure difference ranges are used abroad for division of the difference: (1)  $\alpha < 0.9$ , (2)  $\alpha = 0.9$ – $1.1$ , (3)  $\alpha = 1.1$ – $1.3$ , (4)  $\alpha = 1.3$ – $1.8$ , and (5)  $\alpha > 1.8$ . If the pressure change range among layers does not exceed one of these ranges, the interlayer pressure difference is not considered obvious.

At present, there is no quantitative standard of interlayer pressure difference in China. The following three methods are generally used: (1) dual-string separate-layer production in a well; (2) single-string separate-layer production with packer; and (3) for continuous production using flowing, gas lift, electric submersible pump, or screw pump, installation of a bottomhole choke at the high pressure reservoir to decrease its flowing pressure so that it might be close to the flowing pressure of the low pressure reservoir. If the interlayer

contradictions cannot be adjusted using these methods, the wells have to be placed in accordance with two layer series of development. The main interlayer contradiction is still at the interlayer pressure difference.

#### **Fluid Properties and Interlayer Differences.**

Crude oil properties are mainly considered due to fewer effects of the solutes, temperature, and pressure on the physicochemical properties of water. The viscosity, density, and pour point of crude oil are related to gum, asphaltine, and paraffin contents and are also affected by temperature and pressure. As mentioned earlier, oil reservoirs have been classified by reservoir geology in accordance with oil viscosity, density, and pour point. If the oil property of layers is of the same type, the interlayer oil property difference is not considered obvious. Otherwise, reservoirs should be divided into different oil-bearing series, and zonation should be adopted when completing or the reservoirs are developed in accordance with different layer series of development.

## **1.2 CORE ANALYSIS TECHNIQUES**

### **Requirements of Well Completion Engineering for Core Analysis**

Core is the subsurface rock sample taken by drilling. Core analysis is a very important means of acquiring information on subsurface rock by reason that a core is representative of the subsurface rock. The sample for core analysis can be a regular cylinder, a sidewall coring plunger, or drill cuttings, depending on the content of the analyzed item. Experience has shown that drill cuttings are poorly representative. The regular core plunger is generally used, and a complete set of tests for multiple items can be done, thus favoring finding the internal relations among the various properties of rock.

Core analysis in well completion engineering mainly includes conventional physical property analysis, petrographic analysis, pore configuration analysis, sensitivity analysis, and compatibility evaluation, as given in Table 1-9.

A sampling density of 3–10 pieces/m is required for the necessary item of physical property analysis, whereas the sampling interval for optional items may be longer. Physical property analysis is the basic content of reservoir physics and is not introduced specially in this book.

Petrographic analysis is necessary and based on understanding of the macroscopic description and conventional physical property of core and observation of the common thin section. The cast thin section sample should include the extreme conditions of all rock properties in the reservoir. The average sampling density is 1–2 pieces/m and can be greater if necessary. Sample densities for X-ray diffraction (XRD) and scanning electron microscope (SEM) analyses are about one-third to one-half of that for cast thin section analysis. Oil and gas reservoir sampling should be densified, whereas only controlling analyses are needed by an aquifer. In addition, XRD and SEM analyses should be done for interbeds with an interval of 5–20 m per sample.

Samples for pore configuration analysis, particularly for the capillary pressure curve measurement, should be selected after physical property analysis and thin section observation. For a reservoir group, each permeability class should have at least three to five capillary pressure curves. Finally, the average capillary pressure curve of the reservoir group is obtained in accordance with the physical property distribution.

Sensitivity and compatibility evaluation tests are necessary. For each reservoir group, a permeability class should have at least three samples in order to understand each sensitivity. The analysis item selection depends on the contents of study.

The compositions of mud shale and unstable interbed and their property changes after action with working fluid should be studied for well completion design and hole stability. The means of study are basically the same as shown in Table 1-9. For mud shale, physical and chemical property analysis items should be further added.

For a fractured reservoir, core fractures should be described in detail, and comprehensive studies, including fracture distribution and development and the effects on future oil and

TABLE 1-9 Contents of Core Analysis in Well Completion Engineering

Analysis Item	Total Number of Items	Necessary Item		Optional Item	
		Item	Analysis Item	Item	Analysis Item
Conventional physical property	12	4	Air permeability Porosity Saturation Grain size		Oil, gas and water saturation (sealed coring) Carbonate content Apparent density of rock Relative permeability Vertical permeability In situ permeability and porosity Physical property analysis of full-scale core Wettability
Petrography	10	4	Thin section XRD SEM Electronic probe or energy spectrum		Heavy mineral analysis and identification Cathodeluminescence Infrared spectrum Thermoanalysis Fluorescence analysis
Pore configuration	5	3	Cast thin section image Mercury injection capillary pressure curve SEM		1. X-ray CT scanning 2. NMR technique
Sensitivity and compatibility	18	8	Kerosene velocity sensitivity Formation water velocity sensitivity Water sensitivity Salt sensitivity Alkali sensitivity Acid sensitivity Fluid compatibility Stress sensitivity		Damage evaluation of drilling fluid Two-way flow test Volumetric flow rate evaluation test Sequential contact fluid evaluation test Cation-exchange capacity test Clay swelling test Acid solubility test Acid soak test Capillary imbibition test Temperature sensitivity test

gas production, should be done in combination with conventional logging, rock strength logging, well testing, and production testing.

### Contents and Applications of Core Analysis

As mentioned earlier, core analysis chiefly includes conventional physical property analysis, petrographic analysis, pore configuration analysis,

sensitivity analysis, and compatibility evaluation. Conventional physical property analysis items are basic necessary contents and are not described in this book. Sensitivity analysis and compatibility evaluation are described in detail later. Petrographic and pore configuration analyses are described in this section.

**Petrographic Analysis Techniques.** In petrographic analysis techniques, cast thin section, X-ray diffraction, and scanning electron microscope

are most widely used; electronic probe analysis is also sometimes used.

#### 1. Cast thin section

Rock pore configuration, area–volume ratio, fracture index, fracture density and width, pore throat coordination number, and so on can be measured accurately by cast thin section. Combined with ordinary polaroid, cathodoluminescence thin section, fluorescence thin section, thin section staining techniques, and so on, the cast thin section can be used for determining the types and occurrences of frame grains, matrix, cement, and other sensitive minerals, describing type and origin of pores, and estimating strength and structural stability of rock. This is very important for reservoir protection, sand control, and acidization designs during well completion.

#### 2. X-ray diffraction

X-ray diffraction is the most widely used, effective technique of identifying crystalline minerals and is especially useful for fine dispersed clay mineral and its inner structure analyses. An X-ray diffraction instrument can be used to determine the various types of clay minerals, which also include the interlayer clay minerals forming during diagenesis. XRD can also be used for determining the proportion of montmorillonite in interlayer minerals (e.g., illite–montmorillonite interlayer minerals). In addition, the structural type of clay minerals can be further determined. In general, the XRD analysis technique is very important for determining the absolute content, type, and relative content of clay minerals, which are the basic parameters necessary for the performance of reservoir protection from damage in well completion process and also are helpful in the analysis of type of scales in tubing and perforations and in the analysis of corrosion products.

#### 3. Scanning electron microscope

The type of sensitivity and the degree of damage are closely related to the composition, content, and occurrence distributions

of sensitive minerals. The aforementioned XRD is particularly suitable for identifying the composition and content of sensitive minerals, whereas SEM is especially applicable to visually identifying mineral grain size and occurrence, pore configuration, throat size, and grain surface and pore throat wall configuration fast and effectively (Table 1-10). In addition, SEM can also be used for observation of the pore throat plugging status after contact between the rock and the foreign fluids. Combined with the energy spectrometer, SEM can be further used for conducting element analysis, such as ferric ion identification related to formation damage. Therefore, the results of SEM analysis are also important data needed by performing the reservoir protection in the well completion process.

In recent years, an environment scanning electron microscope (ESEM) has been used for studying the formation damage and observing the swelling process of clay minerals and the microscopic structure of polymer in pore throats. Samples can be observed in the wet state by using ESEM. This is its most outstanding superiority.

#### 4. Electron probe analysis

Electron probe X-ray microanalysis is such a spectral analysis that high-speed minute electron beams are used as a fluorescent X-ray exciting source. The electron beams, which are as minute as a needle, can perform analysis of the microscopic area in a sample and penetrate into a sample by 1–3  $\mu\text{m}$  without disrupting the chemical composition of the measured microscopic area. The information provided by this analysis includes fine mineral composition, crystal structure, diagenetic environment, and type and degree of formation damage.

**Pore Configuration Analysis.** Based on the aforementioned cast thin section and pore cast analyses, pore configuration analysis can be used for determining the type and diameter, throat size, and distribution rule in combination with measuring the core capillary pressure curve.

TABLE 1-10 Main Clay Minerals and Their Characteristics under SEM

Structural Type	Family	Mineral	Chemical Formula	$D_{001} \text{ } 10^{-1} \text{ nm}$	Shape of Monomer	
1:1	Kaolinite	Kaolinite, dickite	$\text{Al}_4(\text{SiO}_4\text{O}_{10})(\text{OH})_8$	7.1~7.2,3,58	Pseudo-hexagonal tablet, scale, batten shaped	Page, worm, accordion shaped, step crystal
	Halloysite	Halloysite	$\text{Al}_4(\text{SiO}_4\text{O}_{10})(\text{OH})_8$	10.05	Injection pipe shaped	Fine stick, nest shaped
2:1	Smectite	Smectite, smegmatite	$\text{R}_x(\text{AlMg})_2(\text{Si}_4\text{O}_{10})(\text{OH})_2 \cdot 4\text{H}_2\text{O}$	Na~12.99 Ca~15.50	Bend flake, wrinkle scale shaped	Honeycomb, wad ball shaped
	Illite	Illite, glauconite, vermiculite	$\text{KAl}((\text{AlSi}_3)\text{O}_{10})(\text{OH})_2 \cdot m\text{H}_2\text{O}$	10	Scale, chip, hair shaped	Honeycomb, silk thread shaped
2:1:1	Chlorite	Various types of chlorite	FeMgAl layer shaped silicate (common isomorphous replacement)	14,7,14,4,72, 3.55	Flake, scale conifer leaf shaped	Rose, down ball, stacked flake shaped
2:1:1 layer-chain shaped	Sepiolite	Attapulgite	$\text{Mg}_2\text{Al}_2(\text{Si}_8\text{O}_{20})(\text{OH})_2(\text{OH}_2)_4 \cdot m(\text{H}_2\text{O})_4$	10.40,3.14, 2.59	Palm fiber shaped	Silk, fiber shaped

This is very important for studying the rule of formation fines migration in rock pores, the mechanism of reservoir plugging by foreign solids, the completion, perforating, and killing fluids for temporary plugging during drilling-in reservoir, the fluid loss control agent during

hydraulic fracturing, the solids control agent during water injection, and the water-plugging agent for profile control.

As mentioned earlier, well completion engineering is closely related to oil and gas field development, as listed in Table 1-11.

**TABLE 1-11 Information and Application of Conventional Physical Property and Petrographic Analyses**

Main Analysis Item	Main Information Acquired	Main Applications
1. Conventional physical property analysis (porosity, permeability, and saturation measurement, grain size distribution)	Porosity, permeability, grain size distribution of clastic rock	<ol style="list-style-type: none"> <li>1. Reservoir evaluation, reserves calculation, development program design</li> <li>2. Well completion method selection, completion fluid design, perforated completion optimization, optimal gravel size selection of gravel packing</li> </ol>
2. Pore throat configuration analysis (cast thin section and pore cast analysis, capillary pressure curve measurement, nuclear magnetic resonance analysis)	Types of pores, geometric parameters and distribution of pore configuration; types of throats, geometric parameters and distribution of throats, etc.	<ol style="list-style-type: none"> <li>1. Reservoir evaluation, reserves calculation, development performance analysis</li> <li>2. Potential damage evaluation, reservoir protection program formulation</li> <li>3. Designing drilling and completion, perforating, killing, and workover fluids of temporary plugging</li> </ol>
3. Thin section analysis (ordinary polaroid, cast thin section, fluorescence thin section, and cathodeluminescence thin section)	Rock texture and frame; grain composition; matrix composition and distribution; type and distribution of cement; pore characteristics; types, concentrations, and occurrences of sensitive minerals	<ol style="list-style-type: none"> <li>1. Reservoir evaluation, petrological properties, potential damage evaluation</li> <li>2. Reservoir protection program formulation</li> <li>3. Completion fluid design</li> <li>4. Appraisal of degree of consolidation and strength of rock</li> </ol>
4. Scanning electron microscope analysis (including environment scanning electron microscope analysis)	Pore throat characteristics analysis; rock texture analysis; occurrence and type analyses of clay minerals	<ol style="list-style-type: none"> <li>1. Reservoir evaluation, petrological properties, potential damage evaluation</li> <li>2. Completion fluid and reservoir protection program designs</li> </ol>
5. X-ray diffraction analysis	Absolute concentrations, types, and relative concentrations of clay minerals, interlayer ratio, degree of order	<ol style="list-style-type: none"> <li>1. Potential damage evaluation</li> <li>2. Completion fluid and reservoir protection program designs</li> </ol>
6. Electron probe analysis (electron probe wave and energy spectra)	Mineral composition identification, crystal structure analysis	<ol style="list-style-type: none"> <li>1. Potential damage evaluation</li> <li>2. Completion fluid and reservoir protection program designs</li> </ol>

**Clay Mineral Analysis.** The composition, content, occurrence, and distribution characteristics of clay minerals in the reservoir not only have a direct effect on storage capacity and productivity, but also are the most important factors in deciding sensitivities of the reservoir. The features of clay minerals in the reservoir should be considered in the designs of completion mode, completion fluid, and putting into production in order to avoid or decrease formation damage. When analyzing the potential damage of clay minerals, we should put emphasis on the occurrences and types of clay minerals. The different occurrences and compositions will generate different effects on the reservoir.

#### 1. Potential damage of various types of clay minerals

In various physicochemical properties of clay minerals, the particulate properties, including specific surface area, cation-exchange capacity, and hydrophilicity, are of great importance to potential formation damage and protection measures. The types and degrees of damage resulting from the different clay minerals reflect substantially the differences of physicochemical properties between the clay minerals. Common types of clay minerals are as follows.

- (a) **Smectite** occurs commonly in reservoirs with shallower depth and adheres to the clastic grain surface in the form of thin film or forms the bridging consolidation in the pore throats. If its content is higher, it will pack the pores in the form of aggregates with various configurations. Its strong water wettability and high cation exchange capacity lead to its strong water sensitivity. In particular, the volume of Na-rich smectite may be increased by 600–1000% due to swelling after meeting water, which can cause serious pore throat plugging and stratal configuration disrupting.
- (b) Kaolinite, as the most common clay mineral, can be transformed into other clay minerals in different physicochemical environments. Kaolinite, which is packed in

the pores, is often leafy and wormy. The kaolinite aggregate, in which the binding force between crystal wafers is weak, has a weak force of adhesion to the clastic grain surface and is easy to migrate with pore fluids and plug the pore throats under the shearing stress of a high-rate fluid. Therefore, kaolinite is strongly rate sensitive.

- (c) **Illite** is a clay mineral with many different shapes. Its content increases as the depth of the reservoir increases. The common scaly illite occurs in the form of thin film adhering to frame grains, whereas hairy and fibery illites grow by bridging in pores. They are distributed alternately. The former will possibly form plugging at pore throats, whereas the latter will mainly increase the tortuosity of pore channels and decrease reservoir permeability.
- (d) **Chlorite** occurs commonly in deep reservoirs, grows in the direction perpendicular to frame grain surface in the form of a willow leaf and forms a jacket, or packs the pores in the form of down ball- and rose-shaped aggregates. Fe-rich chlorite has a stronger acid sensitivity. During the reservoir acidizing operation, chlorite may be dissolved by acid and ferric ions are released. The ferric ions may combine with other components under the oxygen-rich condition, thus generating a ferric hydroxide precipitant, of which the grain size is larger than the pore throats.

In addition, there still are common illite-smectite and chlorite-smectite interlayer minerals, of which the characteristics and the degree of damage are dependent on their contents and interlayer ratio.

#### 2. Effects of occurrences of clay minerals on formation damage

The original clay minerals deposited at the same time as the frame grains often exist in sandstone in the forms of thin bed vein and glomerate. Its formation damage is weak due to the small contact area between these clay minerals and the pore fluids. However, because of the entire exposure to the pore fluids, the

authigenic clay minerals formed by chemical precipitation and early clay mineral evolution in the diagenetic process react predominantly on the fluids entering the formation physico-chemically, thus causing serious formation damage. A large amount of studies indicate that in many cases the effect of the occurrences of clay minerals on formation damage is greater than that of composition.

Diagenesis of clay minerals of the sandstone reservoir includes clastogene and authigenesis. The clay of clastogene was deposited at the same time as the grains or was introduced by the biological activities after deposition. Common occurrences of clastic clay in sandstone are shown in Figure 1-1. If the buried depth is shallower, the degree of consolidation of the rock is poor and fine particle migration and sand production are easy to generate. If dissolution is serious when acidizing, rock texture is destroyed and sand production is induced. When clay contacts fresh water, the clay lamina swells, thus resulting in the shrinkage of pores and the closure of microfractures.

Authigenic clay minerals are the most common clay minerals in sandstone reservoirs. The occurrences of authigenic clay minerals

can be divided into seven types in accordance with the spatial relation between clay mineral aggregate and grain/pore and the effects on physical properties of reservoir and sensitivity, as shown in Figure 1-2.

- (1) *Comb shell type*. This can be divided further into pore lining side and jacket types. The clay mineral leaves grow in a direction perpendicular to the grain surface with a large surface area and are in the fluid channel position. This type of occurrence belongs mainly to smectite and chlorite. The fluid suffers a large resistance when flowing through them, and they suffer the shock of the high-rate fluid. Then they split, form fine particles, and migrate with the fluid. If they are etched by acid,  $\text{Fe}(\text{OH})_3$  and  $\text{SiO}_2$  precipitants will form, thus plugging the pore throats.
- (2) *Thin film type*. The clay minerals arrange parallel to the frame grain surface with the grains wrapped partially or fully. This type of occurrence belongs mainly to smectite and illite. The fluid suffers a weak resistance when flowing through them. Generally, fine particle migration is not easy to generate. However, this type of clay mineral easily generates hydration

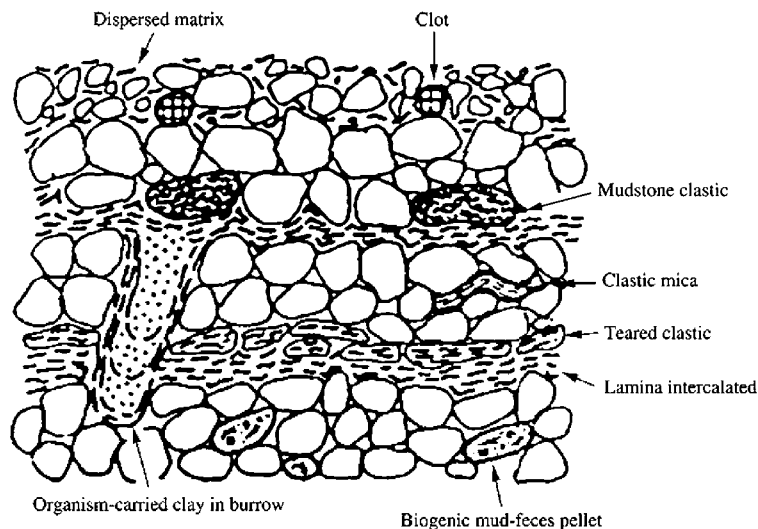
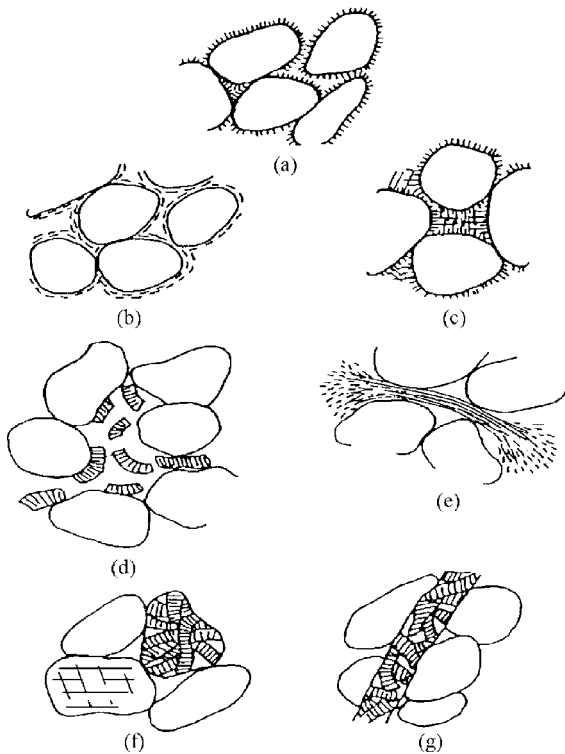


FIGURE 1-1 Occurrences of clastic clay in sandstone.



**FIGURE 1-2** Occurrences of authigenic clay minerals in sandstone. (a) Comb shell type, (b) thin film type, (c) bridging type, (d) dispersed particle type, (e) broomy scattered type, (f) particle metasomatic type, and (g) fracture packing type.

and swelling, which may narrow the pore throats. If micropores are well developed, the damage of water blocking may even be caused.

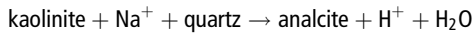
- (3) *Bridging type*. The hairy or fibery minerals (such as illite) are bridged between the grains and are broken easily by shock of the fluid and cause fine particle migration. In addition, the comb shell-type smectite, illite-smectite interlayer minerals, and chlorite-smectite interlayer minerals sometimes overlap mutually at the pore throats narrowed with a high potential of hydration, swelling, and water blocking.
- (4) *Dispersed particle type*. The clay is packed in the pores between the frame grains in the dispersive state. Micropores between the

clay particles are well developed. Kaolinite and chlorite often have this type of occurrence and very easily generate fine particle migration under the action of high-rate fluid.

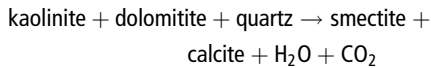
- (5) *Broomly scattered type*. Hydration, swelling, dissolution, and dispersion of black mica and white mica may lead to forming kaolinite, chlorite, illite, illite-smectite interlayer minerals, and vermiculite at the ends. These fines are easy to release, enter the flow system in pores, and generate fine particle migration and the damage of swelling.
  - (6) *Particle metasomatic type*. In the diagenesis process, feldspar or unstable detritus transforms to clay minerals (such as kaolinization of feldspar, chloritization of black mica, and smectization of detritus of extrusive rock). The sensitivity damage is much weaker than that of the aforementioned occurrences, only it is slightly obvious for acidizing.
  - (7) *Fracture packing type*. In fractured sandstone, metamorphic rock, and magmatic rock reservoirs, the fractures are packed partially or fully by the clay minerals, such as smectite, kaolinite, chlorite, and illite, which may cause the various types of sensitivity damage related to clay minerals.
3. Artificial diagenetic reaction of clay minerals at high temperature
 

During heating, clay minerals may be dehydrated, decomposed, oxidized, reduced, and phase changed. To study these chemical and physicochemical changes is of great significance for avoiding the formation damage of the heavy oil reservoirs in the thermal recovery operations, during which the surface temperature of the steam for injection is up to 360°C. When arriving at the reservoir, the steam condenses and mixes with the formation water. Then, the various changes of the clay minerals in the reservoir will take place under participation of the other minerals. The following potential formation damage is mainly dependent on formation mineral

properties, fluid composition, and formation temperature. For a heavy oil reservoir with a shallow depth, the main result of the water–rock reaction at temperature 200–250°C is the dissolution of quartz and kaolinite and the generation of analcite and smectite. When the pH value of the fluid mixture is high enough, the following reaction will take place:



For the lower pH value:



Generally, analcite does not plug the pore throats due to not belonging to clay minerals and the smaller surface area. Therefore, the first reaction is favorable for avoiding formation damage in the thermal recovery process.

Composition ranges of the produced water of the heavy oil and stone reservoirs and the boiler water (containing saturated steam) for steam injection in Albert, Canada, are shown in Figure 1-3. Coordinates in the phase diagram are the ionic concentration ratios in the water phase at 200°C. The requirement for the mineral-stabilized region is that the quartz is fully on the saturation conditions. The contents of  $\text{Na}^+$  and  $\text{K}^+$  in the produced water are higher than that in the boiler water, whereas the change of the formation water toward acidity is faster than that of the boiler water. Therefore, the produced water of the steam-assisted recovery tends toward the kaolinite region, whereas the boiler water falls in the feldspar and analcite-stabilized regions. Obviously, the composition of the produced water is in the three-phase region of the common clay mineral aggregate (kaolinite, illite, and smectite). This indicates that despite the very high pH value of the injected steam favorable for the formation of analcite, the dilution of condensate water by formation water and the reaction between the condensate water and the minerals may cause the formation of smectite with the most serious potential formation damage. Therefore, the

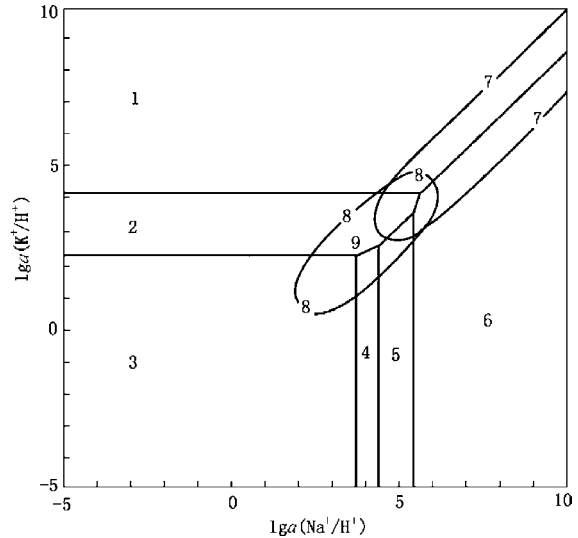


**FIGURE 1-3** Relationship between chemical properties of formation water and the stability of clay minerals at 200°C. 1, potash feldspar; 2, illite; 3, kaolinite; 4, sodium smectite; 5, paragonite; 6, analcite; 7, boiler water; 8, produced water; 9, preservoir minerals; and  $\alpha$ , ionic molar concentration ratio.

detailed core analysis and the reaction product appraisal before steam injection are of great significance for the prediction and prevention or reduction of formation damage.

**Grain Size Analysis.** Grain size analysis means determining the contents of the grains of different sizes in the rock. Not only is grain size analysis applied broadly to studies of the genesis and sedimentary environment of sedimentary rocks and the classification and evaluation of reservoir rocks, but the parameter of grain size is also an important engineering parameter of gravel pack completion design of unconsolidated and weakly consolidated reservoirs and important ground for identifying reservoir heterogeneity in field development.

The laboratory methods of measuring rock grain size include mainly sieve analysis, settling, thin-section image statistics, and laser diffraction. Each method has advantages and limitations. In practice, the choice of methods depends on the range of grain sizes of the analyzed sample and the technical level of the laboratory.

Sieve analysis is the most common grain size analysis measurement method. Before sieve analysis, the sample is cleaned and oven-dried, and grain disintegration is carried out. Then, it is placed into the sieves of different sizes. These sieves are placed on an acoustic or mechanical sieve shaker. After vibrating and sieving, the grain mass in each sieve is weighed, thus obtaining grain size analysis data of the sample. The analysis range of the sieve analysis method is generally from 4 mm (gravel fine) to 0.0372 mm (silt).

Figure 1-4 shows results of grain size analysis of the tertiary reservoir in the Liaohe oil field. The used grades of screen grids include 50, 60, 70, 80, 100, 120, 140, 170, 230, 325, and 400 meshes. The main grain size distribution of the rock sample is in the range of 0.3 to 0.06 mm. The sample is determined as medium-grained sandstone in accordance with the interval of main peak of the grain size distribution.

Parameters required by the gravel pack completion design may be obtained from Figure 1-4. In accordance with the cumulative mass percentage curve,  $D_{40}$ ,  $D_{50}$ , and  $D_{90}$  of the grain size values, to which 40, 50, and 90% of the

cumulative mass correspond, are 0.31, 0.26, and 0.061 mm, respectively. The median grain diameter  $D_{50}$  represents the concentrated trend of the grain size distribution. The uniformity coefficient  $C$ , that is,  $D_{40}/D_{90}$ , is equal to 5.080.

### 1.3 RESERVOIR SENSITIVITY TO FLUID AND WORKING FLUID DAMAGE EVALUATION

The reservoir sensitivity evaluation investigates mainly the degrees of effects of the physicochemical actions generated between the reservoir core and the foreign fluids after contacting on the rock properties (mainly permeability) on the basis of the core flow tests. The physicochemical properties of rock minerals related closely to reservoir sensitivities have to be measured by other methods in order to optimize the working fluid compatible with reservoirs by the laboratory damage evaluation tests after comprehensive and full understanding of the reservoir properties and to provide the necessary parameters and grounds for the well completion engineering design and its implementation.

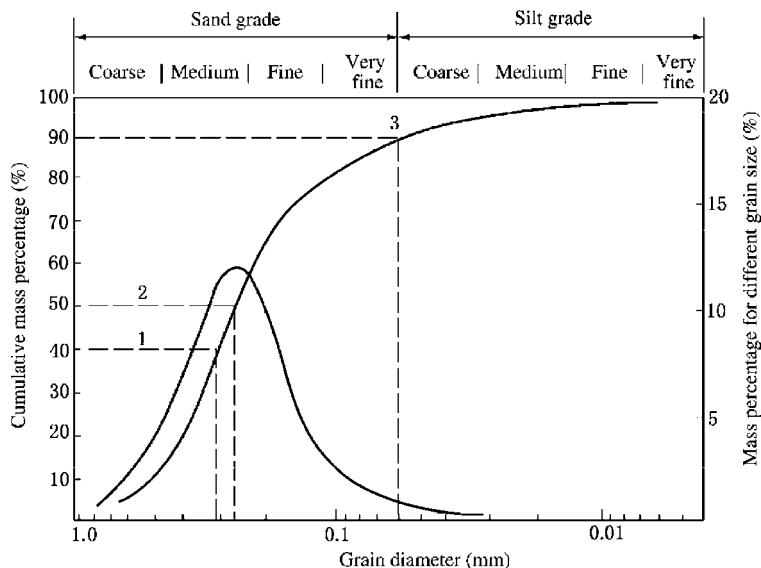


**FIGURE 1-4** Grain-size distribution curve by the sieve analysis method: 1,  $D_{40}$ ; 2,  $D_{50}$ ; and 3,  $D_{90}$ .

## Overview of Formation Damage

Most reservoirs contain sensitive minerals in varying degrees. Generally, these minerals have a very small grain diameter ( $<20 \mu\text{m}$ ) and distribute over the pore surfaces and throats where they may predominantly contact the foreign fluids. During the completion operations, the various foreign fluids interact easily with the fluids and minerals contained in the reservoir after invading, thus reducing the natural productivity or injectivity of the reservoir, that is, generating formation damage, of which the degree is indicated by the extent of reduction of the reservoir permeability.

Types of formation damage include physical, chemical, biological, and thermal. Each type can be divided into some subtypes. The practice indicates that during drilling, completion, stimulation, workover, water injection, and oil production operations, different types and degrees of formation damage may be caused, as listed in Table 1-12. Furthermore, most formation damages are permanent and irreversible. Therefore, once formation damage is caused, it is difficult to remove. The principle “prevention first, remedy second” should be taken to approach the problem of formation damage. The conditions under which the reservoir becomes sensitive and the degree of formation damage can be found by reservoir sensitivity evaluation, thus providing scientific grounds for optimizing the completion fluid design and engineering parameters.

## Rate Sensitivity Evaluation Experiment

**Concept of Rate Sensitivity and Experimental Goals.** The rate sensitivity of reservoirs means the phenomenon of reservoir permeability reduction caused by fine particle migration and throat blocking due to fluid flow in the reservoir during drilling, production, stimulation, and water injection. For a specific reservoir, formation damage caused by fine particle migration is mainly related to the flow rate of fluid in the reservoir. Therefore, the experimental goals of the rate sensitivity evaluation experiment are as follows.

- (1) To find the critical flow rate at which formation damage caused by fine particle migration due to the action of flow rate will occur and to find the degree of formation damage induced by rate sensitivity.
- (2) To provide a basis for determining the rational experimental flow rates of the after experiments, including water, salt, alkali, and acid sensitivities, and the other various evaluation experiments. Generally, after the critical flow rate is obtained by the rate sensitivity evaluation experiment, the experimental flow rate used for other evaluation experiments, which equals 0.8 times the critical flow rate, can be determined. Therefore, the rate sensitivity evaluation experiment should be completed before the other evaluation experiments.
- (3) To provide a scientific basis for determining the rational flooding rate.

### Experimental Procedure and Result Analysis.

With reference to the “The methods of flow test evaluation of reservoir sensitivity” (SY/T5358-2002), the core permeability at various injection rates is measured during injection of the experimental fluid (kerosene or formation water) at different injection rates. In accordance with the relationship between the injection rate and the permeability, the flow rate sensitivity of the reservoir core is identified, and the critical flow rate, at which the permeability will be obviously reduced, is determined. Sensitivity to the flow rate has occurred if permeability  $K_{i-1}$  at flow rate  $Q_{i-1}$  and permeability  $K_i$  at flow rate  $Q_i$  satisfy the following formula:

$$(1-2) \quad D_k = \frac{K_{i-1} - K_i}{-1} \times 100\% \geq 5\%$$

Flow rate  $Q_{i-1}$  is now the critical flow rate. Evaluation indices of the degree of rate sensitivity are listed in Table 1-13.

The degree of rate sensitivity damage can be determined in accordance with Table 1-13 and the following formula:

$$(1-3) \quad D_k = \frac{K_{\max} - K_{\min}}{K_{\max}} \times 100\%$$

where  $D_k$  is rate of permeability damage caused by rate sensitivity;  $K_{\max}$  is maximum value between

**TABLE 1-12** Types and Degrees of Formation Damage during Well Construction and Oil and Gas Production

	Well Construction Phase		Oil and Gas Production Phase				
	Drilling and Cementing	Well Completion	Downhole Operation	Stimulation	Well Testing	Natural Recovery	Supplementary Recovery
Drilling fluid solids invading	****	**	***	—	*	—	—
Fine particle migration	***	****	***	****	****	***	****
Clay mineral swelling	****	**	***	—	—	—	**
Emulsification plugging/water phase trap damage	***	****	**	****	*	****	****
Wettability reversal	**	***	***	****	—	—	****
Relative permeability reduction	***	***	****	***	—	**	—
Organic scale	*	*	***	****	—	****	—
Inorganic scale	**	***	****	*	—	***	**
Foreign fluid solids invading	—	****	***	***	—	—	****
Secondary mineral precipitation	—	—	—	****	—	—	***
Bacteria invasion damage	**	**	**	—	—	**	****
Sand production	—	***	*	****	—	***	**

Note: “\*” represents the degree of severeness, whereas “—” represents “no damage.”

**TABLE 1-13 Evaluation Indices of Degree of Rate Sensitivity Damage**

Rate of permeability damage (%)	$D_k \leq 5$	$5 < D_k \leq 30$	$30 < D_k \leq 50$	$50 < D_k \leq 70$	$D_k > 70$
Degree of damage	None	Weak	Medium to weak	Medium to strong	Strong

core sample permeability points before critical flow rate,  $10^{-3} \mu\text{m}^2$ ; and  $K_{\min}$  is minimum value between core sample permeability points after critical flow rate,  $10^{-3} \mu\text{m}^2$ .

The rate sensitivity curves of kerosene and salt water, which are obtained by the tertiary reservoir cores of the Nanyang Xiaermen oil field, are shown in Figures 1-5 and 1-6, respectively.  $K_{\infty}$  is the original air permeability. Critical flow

rates of kerosene and formation water are 3.0 and 0.4 ml/min, respectively.

Evaluation results of the 10 samples of this horizon are listed in Table 1-14. The critical flow rates of kerosene and formation salt water are 0.5–3.5 and 0.1–0.5 ml/min, respectively. The degree of rate sensitivity damage of kerosene is obviously weaker than that of salt water. The reason is that reservoir rock is of weak water wettability to water

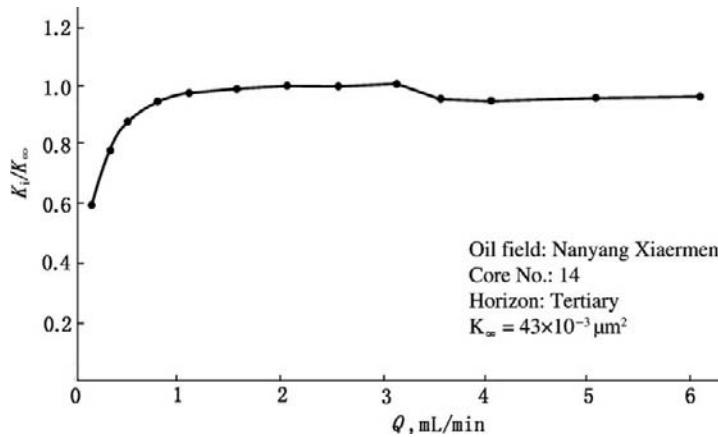


**FIGURE 1-5** Experimental curve of rate sensitivity of kerosene.

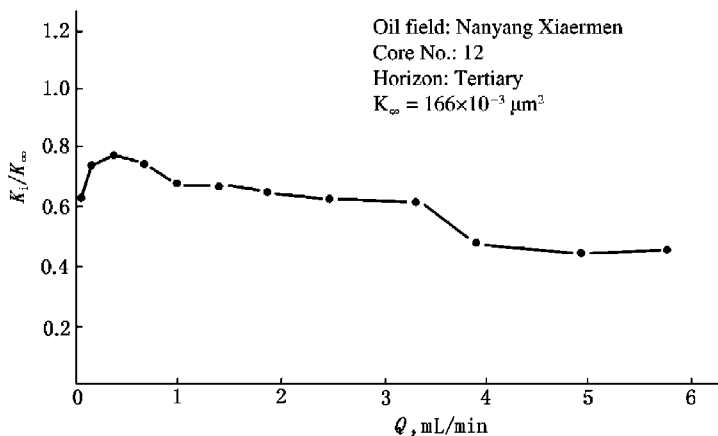


**FIGURE 1-6** Experimental curve of rate sensitivity of salt water (formation water).

TABLE 1-14 Rate Sensitivity Evaluation Results of Kerosene Obtained by Cores of the Nanyang Xiaermen Oil Field

Serial Number of Well	Core No.	Horizon	$K_{\infty}$ ( $10^{-3} \mu\text{m}^2$ )	$K_{\max}$ ( $10^{-3} \mu\text{m}^2$ )	$K_{\min}$ ( $10^{-3} \mu\text{m}^2$ )	Critical Flow Rate		$D_k$ (%)	Degree of Rate Sensitivity
						Linear Flow (ml/min)	Radial Flow ( $\text{m}^3/\text{day}\cdot\text{m}$ )		
1	11	H <sub>3</sub> VI	176.0	158.0	70.5	1.5	5.50	55	Medium by strong
	14	H <sub>3</sub> VI	43.0	43.3	40.8	3.0	10.9	6	Weak
	20	H <sub>3</sub> VI	5.40	6.19	3.88	2.5	9.10	37	Medium by weak
2	81	H <sub>3</sub> VII	14.0	13.5	9.97	3.5	12.7	26	Weak
	115	H <sub>3</sub> VII	100.0	100.0	50.9	0.5	1.80	49	Medium by weak
3	12	H <sub>3</sub> VI	166.0	136.0	73.8	0.4	1.80	46	Medium by weak
	15	H <sub>3</sub> VI	93.0	93.0	62.7	0.1	0.36	33	Medium by weak
	20	H <sub>3</sub> VII	4.55	3.82	1.62	0.1	0.36	58	Medium by strong
4	82	H <sub>3</sub> VI	44.0	42.3	14.9	0.25	0.91	65	Medium by strong
5	150	H <sub>3</sub> VII	80.9	77.5	39.9	0.25	0.91	49	Medium by weak

wettability. When the fluid is salt water, formation fines are easily carried by the wetting phase (salt water), and fine particle migration is generated, thus leading to permeability damage. When the fluid is kerosene, which is the nonwetting phase, fine particle migration will not be generated if only the flow rate of kerosene does not rise to a higher value and does not generate a mechanical shear failure. This leads to the different results of kerosene and salt water rate sensitivity experiments and also indicates that the allowable flow rate of oil in the production process can be higher than that of water in the water injection operation.

The critical flow rate of the radial flow in Table 1-14 is obtained by conversion of the critical flow rate obtained by the linear flow test of core and can be directly used in field production. The conversion formula is as follows:

$$(1-4) \quad \frac{Q}{h} = \frac{1.152r_w Q_c}{D^2},$$

where  $Q$  is critical production or injection rate,  $m^3/day$ ;  $h$  is effective thickness of reservoir, m;  $r_w$  is radius of wellbore (distance from the end of perforation to the center of the well for perforated well), cm;  $Q_c$  is critical volume flow rate obtained by rate sensitivity experiment of core,  $cm^3/min$ ; and  $D$  is diameter of experimental core, cm.

Note that for a production well, kerosene used as the experimental fluid should be dried and treated by clay to remove the polar substance and then filtered using the G5 funnel with sand; for an injection well, the filtered formation water (or simulated formation water) should be used as the experimental fluid.

## Water Sensitivity Evaluation Experiment

**Concept of Water Sensitivity and Experimental Goals.** Under original reservoir conditions, the clay minerals in the reservoir contact the

water with some salinity. When fresh water enters the reservoir, some clay minerals may swell, disperse, and migrate and then the reservoir pores and throats are contracted or plugged, thus causing a decrease in permeability. The reservoir permeability is decreased after the reservoir contacts fresh water. This phenomenon is termed water sensitivity. The water sensitivity experiment is used to understand the processes of swell, dispersal, and migration and to determine the conditions generating water sensitivity and the degree of formation damage caused by the water sensitivity, thus providing a basis for the designs of various completion fluids.

### Experimental Procedure and Result Analysis.

With reference to the “Methods of flow test evaluation of reservoir sensitivity” (SY/T5358-2002), the following experimental procedure is adopted: (1) measuring core permeability  $K_f$  using formation water; (2) measuring core permeability using subformation water (experimental fluid with a salinity equal to 50% of the formation water salinity); (3) measuring core permeability  $K_w$  using distilled water (deionized water); (4) measuring the permeability of forward formation water; and (5) measuring the permeability of backward formation water. The swell due to hydration of clay minerals in core when contacting fresh water and the degree of damage caused are determined. Also, the rates of restoration of forward and backward formation water action are understood. Evaluation indices of the degree of water sensitivity are shown in Table 1-15. The calculation formula is as follows:

$$(1-5) \quad I_w = \frac{K_f - K_w}{K_f} \times 100\%,$$

where  $I_w$  is water sensitivity index;  $K_f$  is core permeability average measured by formation water,  $10^{-3} \mu m^2$ ; and  $K_w$  is core permeability measured by distilled water,  $10^{-3} \mu m^2$ .

TABLE 1-15 Evaluation Indices of Degree of Water Sensitivity

Water sensitivity index (%)	$I_w \leq 5$	$5 < I_w \leq 30$	$30 < I_w \leq 50$	$50 < I_w \leq 70$	$70 < I_w \leq 90$	$I_w > 90$
Degree of water sensitivity	None	Weak	Medium by weak	Medium by strong	Strong	Very strong

TABLE 1-16 Water Sensitivity Evaluation Results of Oil Field in Southern Songliao Basin

Sample No.	Well No.	Horizon	$K_f$ ( $10^{-3}$ $\mu\text{m}^2$ )	$K_{sf}$ ( $10^{-3}$ $\mu\text{m}^2$ )	$K_w$ ( $10^{-3}$ $\mu\text{m}^2$ )	$I_w$ (%)	Degree of Water Sensitivity
DB15-10B	DB15	Qing 2 member	7.750	7.003	5.459	29.6	Weak
DB16-3	DB16	Qing 2 member	1.839	1.904	1.764	4.1	None
DB18-2B	DB18	Qing 1 member	0.423	0.399	0.41	3.1	None
DB20-3A	DB20	Qing 1 member	2.524	2.497	2.231	11.6	Weak
DB16-28B	DB16	Quan 4 member	0.210	0.161	0.14	33.3	Medium by weak
DB17-24B	DB17	Quan 4 member	0.074	0.065	0.025	66.2	Medium by strong

Table 1-16 shows results of a water sensitivity experiment of the Cretaceous reservoir core of a low-permeability oil field in the southern Songliao basin. Figure 1-7 shows a typical experimental curve with a weak-to-medium water sensitivity. After separate soaking for 20–24 hours, the forward and backward formation water permeabilities are partially restored only. This indicates that formation damage due to fine particle dispersal and migration is generated.

## Salt Sensitivity Evaluation Experiment

**Concept of Salt Sensitivity and Experimental Goals.** In drilling, well completion, and other operations, various working fluids have different salinities, of which some are lower than the salinity of formation water and some are higher. The entering of a filtrate of working fluid with salinity higher than that of formation water may induce

contraction, destabilization, and shedding of clay minerals, whereas the entering of a filtrate of working fluid with a salinity lower than that of formation water may cause swelling and dispersal of the clay minerals. These will lead to contracting and plugging of pore spaces and throats and to a reduction in permeability. Therefore, the salt sensitivity evaluation experiment is used to determine the critical salinity generating salt sensitivity and the degree of formation damage caused by salt sensitivity, thus providing a basis for the designs of various working fluids.

### Experimental Procedure and Result Analysis.

Salt water with a different salinity, formulated in accordance with the chemical composition of formation water, is injected into the core, and the core permeability for salt water under different salinity is measured. The degree of salt sensitivity damage is evaluated, and the conditions generating salt sensitivity are determined in accordance with the change in permeability with

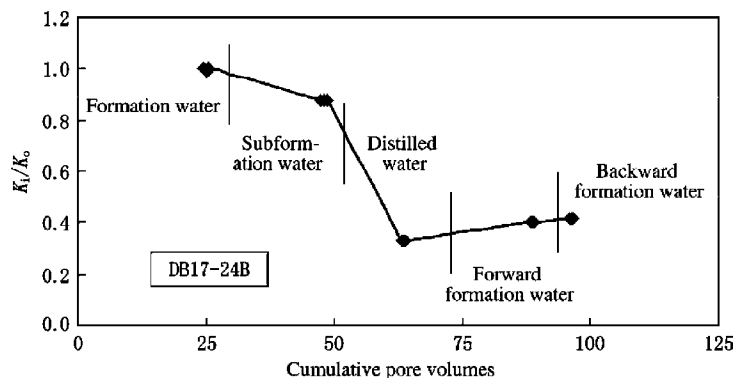


FIGURE 1-7 Water sensitivity experiment curve of core.

salinity. In light of practical conditions, two types of salt sensitivity evaluation experiments (increasing and decreasing salinity) should be done. In the salt sensitivity evaluation experiment of increasing salinity, the first stage of salt water is formation water, and salt water salinity is increased in stages in accordance with a specific concentration difference, until the critical salinity  $C_{c2}$  is determined or the maximum salinity of working fluid is reached. In the salt sensitivity evaluation experiment of decreasing salinity, the first stage of salt water is still formation water, and the salt water salinity is decreased in stages in accordance with a specific concentration difference until the salinity of the injected fluid approaches zero and then the critical salinity  $C_{c1}$  is obtained.

Salt sensitivity has been generated and the salinity  $C_{i-1}$  is just the critical salinity  $C_c$  if the permeability  $K_{i-1}$  corresponding to salinity  $C_{i-1}$  and the permeability  $K_i$  corresponding to salinity  $C_i$  meet the following relation:

(1-6)

$$\frac{K_{i-1} - K_i}{K_{i-1}} \times 100\% \geq 5\%.$$

In accordance with this standard, critical maximum salinity  $C_{c2}$  and critical minimum salinity  $C_{c1}$  can be determined by experiments of increasing and decreasing salinity, respectively, thus

determining the effective salinity interval of completion fluid, in which salt sensitivity damage is avoided. The calculation formula of degree of damage is the same as Equation (1-3). The evaluation indices are the same as those in Table 1-15.

Results of the salt sensitivity experiment of decreasing salinity of the representative core of the Jurassic oil reservoir in the Tuha Hill oil field are shown in Figure 1-8 and Table 1-17. It is obvious that core permeability decreases gradually as the salt water salinity decreases in stages. The reason is that the clay minerals swell due to contacting the fresh water, thus leading to the contraction of pore throats, the dispersal and shedding of the clay minerals, and the plugging of small throats. After the salinity decreases to the distilled water, the core permeability when the salinity is restored to the formation water salinity is then measured. The permeability value is much lower than the core permeability of the initial formation water. This indicates that the salt sensitivity damage is decreasing.

Results of the salt sensitivity experiment of increasing salinity for the Tuha Hill oil field are shown in Figure 1-9 and Table 1-18. It is obvious that the core permeability decreases gradually as the salt water salinity increases in stages. The reason is that the contraction and dispersal of the clay minerals result in plugging the throats. After the salinity increases to the

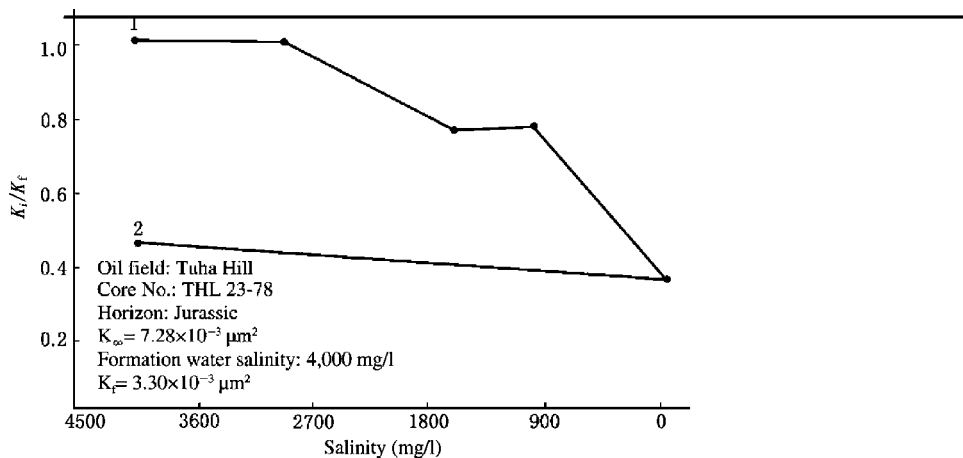
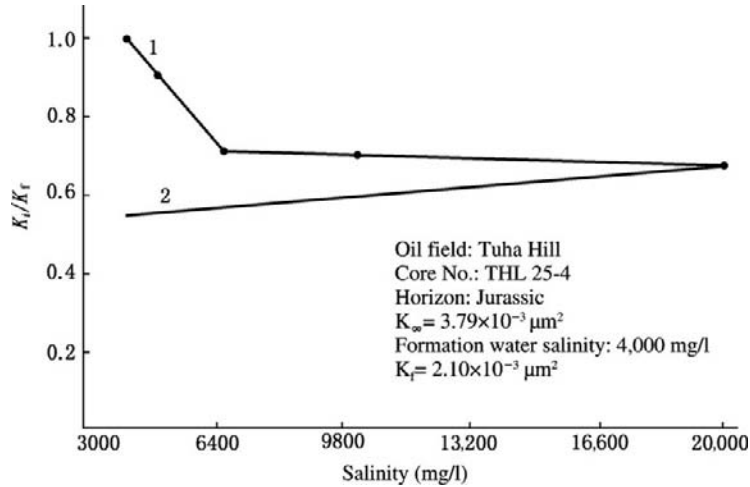


FIGURE 1-8 Salt sensitivity experiment curve of decreasing salinity for the Tuha Hill oil field: 1, decreasing salinity in stages; and 2, restoring formation water salinity.

**TABLE 1-17 Results of Salt Sensitivity Experiment of Decreasing Salinity for Tuha Hill Oil Field**

Well No.	Sample No.	Horizon	$K_{\infty}$ ( $10^{-3} \mu\text{m}^2$ )	Salinity ( $10^4$ mg/liter)	0.4	0.3	0.15	0.1	0	0.4
Ling 23	23-18	E <sub>s1</sub>	16.2	$K_i$ ( $10^{-3} \mu\text{m}^2$ )	3.77	3.44	2.89	2.04	1.01	1.43
				Degree of damage (%)	—	8.75	23.34	45.89	73.21	62.07
Ling 22	22-30	E <sub>s2</sub>	2.36	$K_i$ ( $10^{-3} \mu\text{m}^2$ )	0.75	0.68	0.66	0.62	0.35	0.46
				Degree of damage (%)	—	9.60	11.60	18.00	53.47	38.93
Ling 7	7-27	E <sub>s3</sub>	9.34	$K_i$ ( $10^{-3} \mu\text{m}^2$ )	2.32	2.28	1.95	1.85	0.39	0.78
				Degree of damage (%)	—	2.15	16.31	20.60	84.16	66.59
Ling 23	23-78	E <sub>s2</sub>	7.28	$K_i$ ( $10^{-3} \mu\text{m}^2$ )	3.30	3.37	2.47	2.66	1.26	1.51
				Degree of damage (%)	—	-2.12	25.15	19.39	61.82	54.24
Ling 12	12-16	E <sub>s2</sub>	2.07	$K_i$ ( $10^{-3} \mu\text{m}^2$ )	0.47	0.40	0.32	0.32	0.13	0.16
				Degree of damage (%)	—	16.25	33.12	33.33	73.21	85.61
Ling 12	12-9	E <sub>s2</sub>	3.73	$K_i$ ( $10^{-3} \mu\text{m}^2$ )	1.19	0.98	0.75	0.47	0.21	0.36
				Degree of damage (%)	17.48	36.98	60.67	82.77		69.66



**FIGURE 1-9** Salt sensitivity experiment curve of increasing salinity for the Tuha Hill oil field: 1, increasing salinity in stages; and 2, restoring formation water salinity.

maximum value of the experiment, the core permeability when the salinity is restored to the formation water salinity is then measured. The permeability value not only cannot be restored, but has a trend of retaining reduction. This indicates that the salt sensitivity damage of wrecking clay microstructure stability is irreversible. In the salt sensitivity evaluation method, the salt sensitivity evaluation process of increasing salinity is included, thus this method is applicable to most oil and gas reservoirs. However, for some reservoirs with high salinity formation water, the salt sensitivity evaluation experiment of increasing salinity will not be selected in accordance with the practical conditions due to the working fluid salinity not exceeding generally the formation water salinity.

## Alkali Sensitivity Evaluation Experiment

**Concept of Alkali Sensitivity and Experimental Goals.** The pH value of formation water is generally 4–9, whereas the pH values of most drilling and completion fluids and cement slurry are between 8 and 12. After the fluid with a high pH value enters the reservoir, the texture of clay minerals and siliceous cement in the

reservoir is destroyed due to the dissolution of clay minerals and cement and the release of fine particles produced, thus causing reservoir plugging. In addition, the insoluble substance generated by binding of a large number of hydroxide radicals with bivalent cations also causes reservoir plugging. Therefore, the alkali sensitivity evaluation experiment is to determine the conditions generating alkali sensitivity, mainly the critical pH value, and the degree of formation damage caused by alkali sensitivity, hence providing a basis for the designs of various working fluids.

### Experimental Procedure and Result Analysis.

Permeability is measured by injecting formation water with different pH values, and the degree of alkali sensitivity damage is evaluated by the variation in permeability, thus determining the conditions generating alkali sensitivity damage. The experimental procedure includes (1) salt water with different pH values being prepared. Beginning from the pH value of formation water, the pH value is increased in stages; the pH value for the final stage may be determined as 12–13. (2) The core selected is vacuum pumped and saturated by the salt water of the first stage and then soaked for 20–24 hr. Under the flow rate lower than the critical flow rate,

**TABLE 1-18 Results of Salt Sensitivity Experiment of Increasing Salinity for Tuha Hill Oil Field**

Well No.	Sample No.	Horizon	$K_{\infty}$ ( $10^{-3} \mu\text{m}^2$ )	Salinity ( $10^4$ mg/liter)	0.4	0.5	0.7	1	2	0.4
Ling 25	25-4	$E_{s1}$	3.79	$K_i$ ( $10^{-3} \mu\text{m}^2$ )	2.1	1.92	1.50	1.48	1.43	1.11
				Degree of damage (%)	—	8.57	28.57	29.52	31.90	47.14
Ling 23	23-101	$E_{s2}$	1.87	$K_i$ ( $10^{-3} \mu\text{m}^2$ )	0.56	0.44	0.40	0.42	0.40	0.25
				Degree of damage (%)	—	20.50	28.59	24.64	27.87	54.50
Ling 22	22-51	$E_{s3}$	0.92	$K_i$ ( $10^{-3} \mu\text{m}^2$ )	0.22	0.19	0.13	0.12	0.14	0.10
				Degree of damage (%)	—	11.47	42.66	44.49	37.62	54.17
Ling 7	7-21	$E_{s2}$	15.3	$K_i$ ( $10^{-3} \mu\text{m}^2$ )	3.52	2.49	2.04	1.89	1.84	1.62
				Degree of damage (%)	—	29.26	42.05	46.31	47.73	53.98
Ling 23	23-65	$E_{s2}$	6.63	$K_i$ ( $10^{-3} \mu\text{m}^2$ )	2.84	2.38	1.88	1.88	2.01	1.52
				Degree of damage (%)	—	16.19	33.80	33.80	21.32	46.48
Ling 12	12-13	$E_{s3}$	2.96	$K_i$ ( $10^{-3} \mu\text{m}^2$ )	2.07	0.62	0.48	0.54	0.53	0.48
				Degree of damage (%)	—	69.90	29.81	74.16	74.49	77.05

the stable core permeability  $k_1$  is measured using the first-stage salt water. (3) Ten pore volumes of second-stage salt water are injected and then the core is soaked for 20–24 hr. Under the flow rate lower than the critical flow rate, the stable core permeability  $K_2$  is measured using second-stage salt water. (4) Repeat step 3 by changing the stages of salt water injected until the stable core permeability  $K_n$  of the core being treated with the final-stage salt water is measured.

The alkali sensitivity has been generated and the pH value of stage  $i-1$  is just the critical pH value if the permeability  $K_{i-1}$  of the salt water with the pH value of stage  $i-1$  and the permeability  $K_i$  of the salt water with the pH value of stage  $i$  meet Equation (1-6). The calculation formula of degree of damage is the same as Equation (1-3). Evaluation indices are the same as those in Table 1-13.

The alkali sensitivity evaluation curve of the core of the Talimu East Pond oil field is shown in Figure 1-10. Evaluation results of three cores of the reservoir are shown in Table 1-19. It is obvious that the core permeability decreases as the pH value increases. After the pH value is restored to 8.55 of the pH value of formation water, the core permeability is basically constant, but some have a further decrease. This indicates that the alkali sensitivity damage is similarly irreversible.

### Acid Sensitivity Evaluation Experiment

**Concept of Acid Sensitivity and Experimental Goals.** Acidizing and acid fracturing are the blocking removing and stimulation measures widely adopted in oil and gas fields. After entering the reservoir, acid liquor improves reservoir

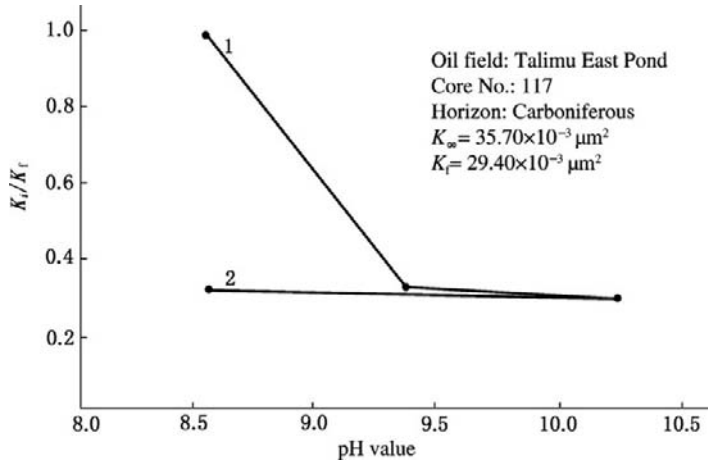


FIGURE 1-10 Alkali sensitivity experiment curve of the core of the Talimu East oil field: 1, increasing pH value; and 2, restoring pH value.

TABLE 1-19

Alkali Sensitivity Experiment Results of Carboniferous Sandstone Reservoir in Talimu East Pond Oil Field

Well No.	Core No.	Horizon	$K_{\infty}$ ( $10^{-3} \mu\text{m}^2$ )	$K_i$ ( $10^{-3} \mu\text{m}^2$ ) (Degree of Damage)			
				pH 8.55	pH 9.41	pH 10.24	pH 10.55
Hedong 1	117	C	35.70	29.40	9.58 (67.4%)	8.68 (70.5%)	9.47 (67.8%)
	123	C	21.20	11.30	7.99 (29.3%)	6.90 (38.9%)	5.22 (53.8%)
	171	C	22.30	15.10	12.90 (14.6%)	10.30 (31.8%)	10.30 (31.8%)

permeability; however, it reacts with the minerals and formation fluids and generates precipitation plugging the pore throats of the reservoir. The acid sensitivity of the reservoir means that the phenomenon of permeability reduction was induced after the acid acted on the reservoir. Therefore, the acid sensitivity experiment studies the degree of rock permeability damage caused by the acid liquor, and intrinsically studies the compatibility of the acid liquor with the reservoir. This will provide grounds for determining the rational formulation of acid liquor when matrix acidizing the reservoir.

#### Experimental Procedure and Result Analysis.

The acid liquor used for acid sensitivity experiments includes raw acid (hydrochloric acid, hydrofluoric acid, mud acid with some concentration) and spent acid (prepared by reaction of the raw acid with another core). The experimental procedure includes (1) forward injecting formation water and measuring the basic permeability  $K_1$ ; (2) backward injecting 0.5–1.0 pore volumes of acid liquor and then closing the valve for reaction for 1–3 hr; and (3) forward injecting formation water and measuring the restored permeability  $K_2$ .

The improved experimental procedure includes (1) forward injecting formation water and measuring the basic permeability and then forward injecting kerosene and measuring the

permeability  $K_1$  before acting of acid; (2) backward injecting 0.5–1.0 pore volumes of acid liquor; and (3) forward injecting kerosene and measuring the restored permeability  $K_2$  and then calculating the rate of damage (i.e., acid sensitivity index  $I_a$ ) to evaluate the degree of acid sensitivity (see Table 1-20). Results of acid sensitivity evaluation of the Triassic sandstone reservoir in the Jilake oil field are shown in Table 1-21.

To sum up, experimentation of the five types of sensitivities is one of the important means of evaluation and diagnosis of formation damage. In general, experimentation of the five types of sensitivities should be done for each block, and the technical program for protecting the reservoir from damage in well completion operations is formulated with reference to Table 1-22 and is used for guiding the operations.

### Experiments of Drilling and Completion Fluid Damage Evaluation

When drilling-in reservoir under overbalance pressure conditions, the drilling and completion fluid will be sure to enter the reservoir. If the completion fluid is incompatible with the reservoir, the invasion of solids and liquid phase must cause formation damage. Therefore, in well completion engineering, in addition to evaluation of the five types of reservoir sensitivities mentioned earlier,

**TABLE 1-20 Evaluation Indices of Degree of Acid Sensitivity**

Acid sensitivity index (%)	$I_a \approx 0$	$0 < I_a \leq 15$	$15 < I_a \leq 30$	$30 < I_a \leq 50$	$I_a > 50$
Degree of acid sensitivity	Weak	Medium to weak	Medium to strong	Strong	Very strong

**TABLE 1-21 Results of Acid Sensitivity Evaluation of Triassic Sandstone Reservoir in Jilake Oil Field**

Well No.	Sample No.	Horizon	Type of Acid Liquor	$K_1$ Before Experiment ( $10^{-3} \mu\text{m}^2$ )	$K_2$ After Experiment ( $10^{-3} \mu\text{m}^2$ )	$K_2/K_1$	$I_a$ (%)	Degree of Acid Sensitivity
Lunnan 55	118	T	Hydrochloric acid	200.57	126.78	0.63	37	Strong
	179			242.49	240.04	0.99	1	Medium to weak
Lunnan 57	96	T	Mud acid	82.62	43.64	0.53	47	Strong
	104			103.83	67.68	0.65	35	Strong

TABLE 1-22 Application of Experimental Results of Five Types of Reservoir Sensitivities

Type of experiment	Application of experimental results
Rate sensitivity experiment (including oil and water)	<ol style="list-style-type: none"> <li>(1) Determining the experimental flow rate of other sensitivity experiments (water, salt, acid, and alkali sensitivity experiments)</li> <li>(2) Determining the critical production rate <math>Q_{\infty}</math> without rate sensitivity damage of oil and gas wells</li> <li>(3) Determining the critical injection rate <math>Q_{cw}</math> without rate sensitivity damage of injection well. If <math>Q_{cw}</math> is too small to meet the requirements of injection allocation, stimulation of the injection well should be considered or the clay-stabilizing agent and antishwelling agent should be added.</li> <li>(4) Determining the admissible maximum density <math>\rho_{max}</math> of various working fluids</li> </ol>
Water sensitivity experiment	<ol style="list-style-type: none"> <li>(1) If no water sensitivity, the salinity of working fluids entering the reservoir, which is lower than formation water, is only required without other strict demands</li> <li>(2) If any water sensitivity, the salinity of working fluids entering the reservoir should be constantly higher than <math>C_{c1}</math></li> <li>(3) If water sensitivity is strong, the clay-stabilizing agent and antishwelling agent should be used in the working fluids</li> </ol>
Salt sensitivity experiment (including increasing and decreasing salinity)	<ol style="list-style-type: none"> <li>(1) The salinity of various working fluids should be constantly between the two critical salinities, i.e., <math>C_{c1} &lt; \text{salinity of working fluids} &lt; C_{c2}</math></li> <li>(2) If the salinity of the injected water used for waterflooding is lower than <math>C_{c1}</math>, a suitable clay-stabilizing agent must be added to the injected water or the injection well treated periodically using a clay-stabilizing agent in order to avoid generating water sensitivity damage</li> </ol>
Alkali sensitivity experiment	<ol style="list-style-type: none"> <li>(1) The pH value of various working fluids entering the reservoir should be constantly lower than the critical pH value</li> <li>(2) If the reservoir is strongly alkali sensitive, the shielding-type temporary blocking technique is recommended due to being unable to keep the pH value of cement slurry lower than the critical pH value in order to avoid formation damage</li> <li>(3) For a reservoir with alkali sensitivity, avoid using strong alkaline working fluids</li> </ol>
Acid sensitivity experiment	<ol style="list-style-type: none"> <li>(1) Providing scientific grounds for the formulation design of acid liquor used for matrix acidizing</li> <li>(2) Providing grounds for determining the rational block removing method and stimulation</li> </ol>

formation damage caused by working fluids should be studied. This is particularly important for drilling and completion operations. Hence, completion fluid evaluation experiments are used to understand the degree of formation damage resulting from the completion fluid used for field after contacting core and then to evaluate the completion fluid and optimize formulation. If necessary, the treating agent in the completion fluid and the formation damage caused by the filtrate of drilling fluid are specially evaluated.

**Static Damage Experiment of Drilling and Completion Fluid.** Before and after the core is contacted with drilling and completion fluid some time under constant pressure, permeability

values are measured and then the degree of drilling and completion fluid damage may be evaluated. A hollow stainless steel cylinder is attached to the upstream end face of the core for this experiment. In fact, the static damage experiment of drilling and completion fluid is mainly used to simulate the effect of drilling and completion fluid on formation soak. The experimental procedure includes (1) forward measuring formation water permeability  $K_f$  of the core; (2) forward driving water by oil (gas) and forward measuring the oil (gas) phase permeability  $K_o$  ( $K_g$ ) of the core under the irreducible water condition; (3) backward completion fluid filtering with a constant differential

pressure of 3.5 MPa until the filtrate flows out from the upstream end; (4) forward displacing the completion fluid until the discharged fluid of the downstream end is fully oil (gas); and (5) forward measuring the oil (gas) phase permeability  $K_{op}$  ( $K_{gp}$ ) of the core after damage. In the experimental process, a fluid flow rate not higher than the critical flow rate is required.

**Dynamic Damage Experiment of Drilling and Completion Fluid.** The main purpose of the dynamic damage experiment of drilling and completion fluid is to simulate the static and dynamic wellbore fluid filtering in the wellbore annulus and the solid and liquid phase damage of shearing effect in reservoir rock. A typical device for evaluating the dynamic damage is shown in Figure 1-11. The device consists mainly of a plunger pump, core holder, heating and pressurized systems, and a metering system.

The experimental procedure consists of (1) forward measuring formation water permeability  $K_f$  of the core; (2) forward driving water by oil (gas) and forward measuring the oil (gas)

phase permeability  $K_o$  ( $K_g$ ) of the core under the irreducible water condition; and (3) backward injecting completion fluid to contact the core under dynamic conditions. The dynamic conditions for simulating include a differential pressure of 3.5 MPa, the temperature equal to practical formation pressure, the flow rate at the end face of the core, which is constantly retained at 50% of the critical flow rate for 1–2 hr; (4) forward displacing the completion fluid until the discharged fluid at the downstream end is fully oil (gas); and (5) forward measuring the oil (gas) phase permeability of the core after damage. In the experimental process, a fluid flow rate not higher than the critical flow rate is required.

**Evaluation Experiment of Drilling and Completion Fluid Invasion Depth and Degree of Damage.** The aforementioned static and dynamic damage experiments only evaluate the degree of damage of drilling and completion fluid. However, the invasion of completion fluid during drilling is a progressive process, and the

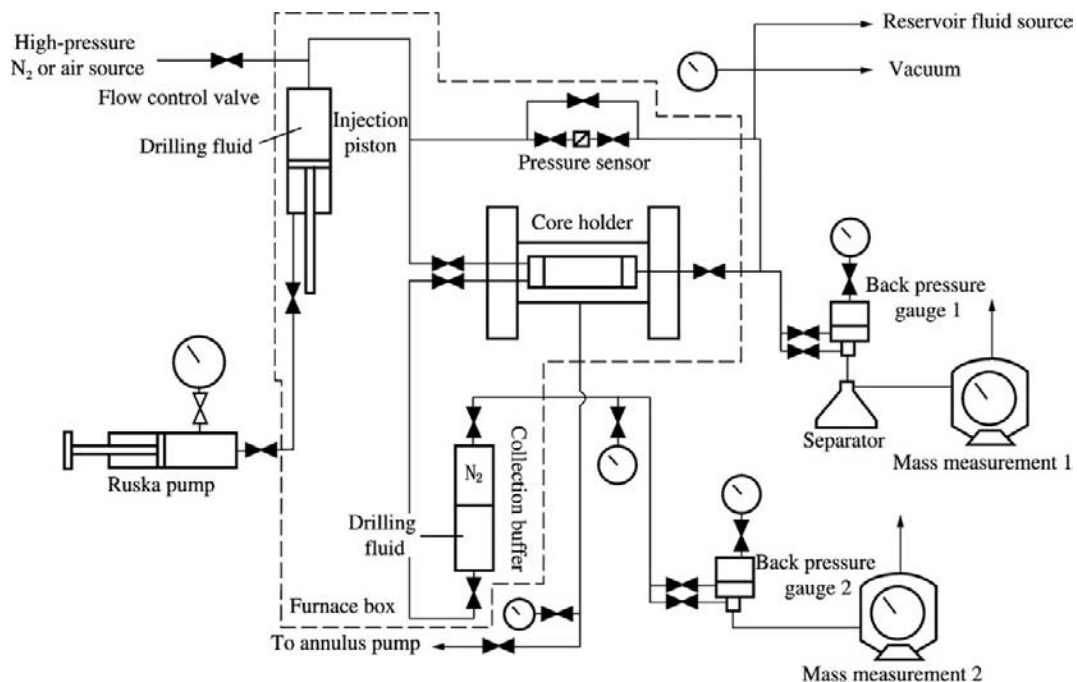


FIGURE 1-11 Dynamic damage evaluation instrumentation system of drilling and completion fluid.

invaded zone is irregular. Due to completion fluid invasion, from wellbore to in-depth reservoir, flushed, transitional, diffusional, and virgin zones appear. Because each zone has a different invasion volume, the invasion depth of solid and liquid phases is different and the degree of damage is also different. Therefore, the evaluation experiment of drilling and completion fluid invasion depth and degree of damage on the one hand investigates the relationship between the degree of damage and invasion depth and provides grounds for optimizing the penetration depth design or evaluation during perforating, and on the other hand lays a foundation for establishing the mutual conversion relationship between field logging and well testing evaluation and laboratory evaluation.

The high-temperature, high-pressure, long core, multipoint damage evaluation system developed and manufactured by Southwest Petroleum University is shown in Figure 1-12. The highest working temperature is 150°C, and the highest confining pressure is 50 MPa. The core used for the experiment has a maximum length of 100 cm and a diameter of 2.45 cm. There are altogether 16 points for measuring the pressure and resistivity at intervals of 3–6 cm along the core axis. The invasion depth of the filtrate and the change in original reservoir fluid saturation may be determined accurately by measuring the core resistivity. The change in permeability may be obtained accurately by measuring the pressure, thus evaluating the degree of damage. This evaluation system, which adopts two formats of data acquisition, processing, and output, including real-time monitoring and display by

computer and data playback, may simulate not only the dynamic damage but the static soak or the composite effects of both. The experimental procedure is basically similar to the two types mentioned earlier.

The completion fluid invasion depth, damage depth, degree of damage, and their mutual relations can be obtained by this experiment, and the average core permeability after damage can be further obtained in accordance with Equation (1-7). By consideration of the macroscopic scale of formation fluid flow before and after damage, when the measurement conditions coincide with downhole conditions, this measurement value can be compared with the permeability value obtained by the well test evaluation.

(1-7)

$$\bar{k} = \frac{1}{\frac{L_1}{L} \cdot \frac{1}{k_1} + \frac{L_2}{L} \cdot \frac{1}{k_2} + \dots + \frac{L_i}{L} \cdot \frac{1}{k_i}}$$

It is worth noting that this evaluation system can also be widely applied to the experimental evaluations of waterflooding and tertiary recovery.

**Experimental Result Analysis and Evaluation Standard.** The static and dynamic damage experiment results of four cores of the tertiary sandstone oil reservoir of the Nanyang Xiaermen oil field are shown in Table 1-23. Formulation of the working fluid system is similar to that of field completion fluid.

The degree of damage may be determined in accordance with the oil phase permeabilities before and after damage (see Table 1-24). It is

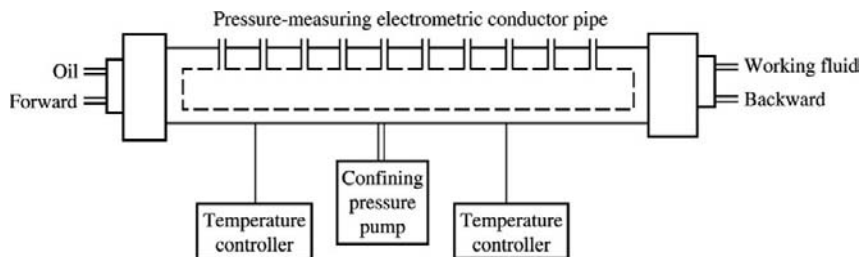


**FIGURE 1-12** High-temperature, high-pressure, long core, multipoint damage evaluation experiment device.

**TABLE 1-23 Static and Dynamic Damage Experiment Results of Nanyang Xiaermen Oil Field**

Well No.	Core No.	Horizon	Initial Permeability $K_o$ ( $10^{-3} \mu\text{m}^2$ )	Permeability After Damage $K_{op}$ ( $10^{-3} \mu\text{m}^2$ )	Rate of Damage (%)	Experimental Conditions				Filtrate (ml)
						Differential Pressure (MPa)	Rate of Shear ( $S^{-1}$ )	Time (hr)	Temperature ( $^{\circ}C$ )	
Mi 118	147	H <sub>3</sub> V	1.66	0.58	65.1	3.5	180	1	90	6.7
Mi 191	377	H <sub>3</sub> IV	11.5	2.43	78.9	3.5	180	1	90	4.2
Xia 16	265	H <sub>3</sub> VI	6.93	4.95	28.6	3.5	0	1	90	0.5
Xia 16	262	H <sub>3</sub> VI	36.4	27.7	27.7	3.5	0	1	90	0.8

**TABLE 1-24 Completion Fluid Damage Experiment Evaluation Indices**

Rate of damage $D_k$ (%)	$D_k \leq 5$	$5 < F_k \leq 30$	$30 < F_k \leq 50$	$50 < F_k \leq 70$	$D_k > 70$
Degree of damage	None	Weak	Medium by weak	Medium by strong	Strong

**TABLE 1-25 Completion Fluid Filtrate Damage Experiment Results of Nanyang Xiaermen Oil Field**

Well No.	Core No.	Horizon	Initial Permeability $K_o$ ( $10^{-3} \mu\text{m}^2$ )	Permeability After Damage $K_{op}$ ( $10^{-3} \mu\text{m}^2$ )	Rate of Damage (%)	Soak Temperature ( $^{\circ}\text{C}$ )	Soak Time (hr)
Xia 16	313	H <sub>3</sub> VII	42.86	35.24	17.8	90	24
Mi 118	152	H <sub>3</sub> VII	21.63	17.54	18.9	90	24
Mi 191	328	H <sub>3</sub> IV	10.50	8.39	20.1	90	24
Mi 118	119		4.38	3.32	24.2	90	24

shown that the damage to this oil reservoir, which is caused by completion fluid, is obvious; static damage is medium by a weak degree; and dynamic damage is medium by a strong degree. This damage is a composite effect consisting of solids invasion, water sensitivity due to water base completion fluid, and treating agents. In order to investigate completion fluid filtrate damage, the static filtrate damage experiment of four cores has been done. Results are shown in Table 1-25. Obviously, in this region, the degree of damage due to completion fluid solids invasion is higher than the degree of filtrate damage; the dynamic damage is higher than the static damage. In general, this system is not suitable for drilling-in reservoir, unless special measures such as the shielding-type temporary blocking technique or the underbalanced drilling-in technique are taken.

Experimental results of drilling fluid filtrate invasion depth and degree of damage for the core of the Jurassic oil reservoir in the Tuha Shanshan oil field in China are listed in Table 1-26. Data processing results are shown in Figures 1-13 and 1-14.

The following knowledge can be obtained from the aforementioned data: (1) the filtrate invasion

depth is 24 cm, and the damage depth is 27 cm. The ratio between them is 0.89. The reason that the damage depth is larger than the invasion depth is ionic diffusion, which generates salt sensitivity damage of the core, that is, permeability is decreased when the filtrate with high salinity invades the core containing formation water with a low salinity. (2) The filtrate invasion is a tonguing process. The total filtrate invasion volume is about one-third of the total core pore volume, whereas the invasion depth is up to two-thirds of total core length. In addition, the shorter the distance to the upstream end of the core, the larger the amplitude of resistivity reduction is and the larger the filtrate invasion volume is. (3) The degree of filtrate damage is obviously related to the damage depth. The larger the filtrate invasion volume, the higher the degree of damage. The rate of permeability restoration increases gradually with the invasion depth. (4) A power function relationship exists between filtrate invasion depth and invasion volume and between filtrate damage depth and degree of damage. In combination with field logging and well test evaluation, the range and degree of downhole formation damage can be further determined, thus guiding well completion operations.

**TABLE 1-26** Experimental Data of Drilling Fluid Filtrate Invasion Depth and Degree of Damage for Tuha Shanshan Oil Field

Measurement Point	1	2	3	4	5	6	7	8	9	10	11
Distance (cm)	3	6	9	12	15	18	21	24	27	30	33
$\varphi$ , %	10.28	10.54	10.68	10.38	11.76	11.92	9.72	9.24	10.00	11.86	11.77
$S_{wi}$ , %	28.15	29.33	28.17	26.64	25.77	25.01	29.81	30.55	22.37	23.05	34.76
$K_{o1}$ , $10^{-3} \mu\text{m}^2$	5.52	5.58	5.29	5.50	6.03	6.35	6.18	6.06	5.95	6.26	6.38
$R_{t1}$ , $\Omega \cdot \text{m}$	272.3	258.4	277.7	286.0	294.9	301.3	264.1	236.7	331.5	319.4	310.8
$R_{t2}$ , $\Omega \cdot \text{m}$	25.60	33.59	52.76	70.79	132.3	205.5	239.0	236.7	331.5	319.4	310.8
$K_{o2}$ , $10^{-3} \mu\text{m}^2$	1.126	1.534	1.793	2.393	3.401	4.731	5.500	5.866	5.95	6.26	6.38
$R_{t2}/R_{t1}$	0.094	0.130	0.190	0.279	0.450	0.682	0.905	1.00	1.00	1.00	1.00
$K_{o2}/K_{o1}$	0.204	0.275	0.339	0.435	0.564	0.745	0.890	0.968	1.00	1.00	1.00

Note: Repeated measurement errors of resistivity, permeability, and porosity are 3, 1, and 0.3%, respectively.

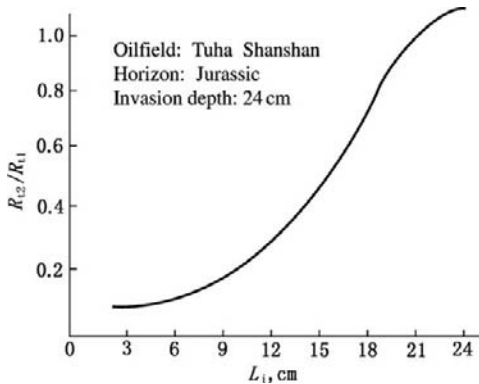


**FIGURE 1-13** Drilling fluid filtrate invasion depth vs. resistivity.

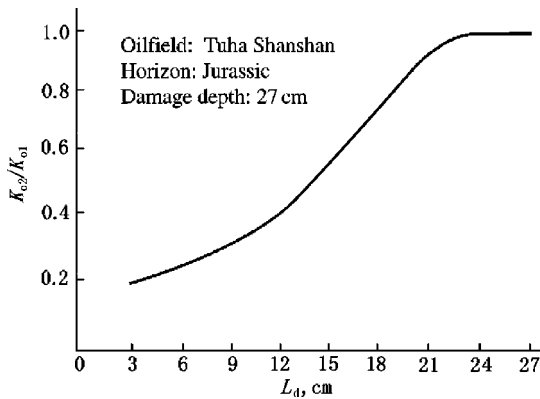


**FIGURE 1-14** Drilling fluid filtrate damage depth vs. permeability.

## Other Evaluation Experiments

Other damage evaluation methods include volume flow rate evaluation, series fluid evaluation, fast evaluation of working fluid by capillary pressure measured using the centrifugal method, forward and backward flow, wettability evaluation, and relative permeability curve experiments. The goals and uses of these experiments are shown in Table 1-27.

To sum up, laboratory formation damage evaluation results can provide grounds for formulating the technical programs of reservoir protection at the links in the operational chain, that is, these evaluation results are necessary

for determining the technical programs of reservoir protection at all operational links in whole process from drilling-in to field development.

Laboratory formation damage evaluation techniques are developing further with continuous technical progress. At present, the following development directions have formed: (1) full modeling experiment simulating the practical downhole status, such as temperature, pressure (backpressure, formation pressure), anisotropy, and formation damage evaluation; (2) application of a multi-point permeameter and development toward long core from short core; (3) core size developing toward full diameter from small diameter; (4) experimental automation, widely introducing computerized data acquisition; and (5) combination of computerized mathematical simulation with laboratory physical simulation.

## 1.4 RESERVOIR STRESS SENSITIVITY ANALYSIS

In general, reservoir sensitivity evaluation means the results of action of fluids on reservoir minerals, whereas stress sensitivity investigates the performance, which is the change of the parameters of physical properties of rock samples under the effective stress exerted. Stress sensitivity reflects the response of rock pore geometry, fracture face configuration, and mechanical properties of rock to the change in stress. Stress sensitivity is closely related to drilling and completion fluid filtration loss and circulation loss, fracturing fluid loss, and fracture closure during testing and production. Stress sensitivity is generally stacked on other factors of damage. For example, the drillstem test and well completion test may contain both rate sensitivity damage and stress sensitivity damage problems.

### Stress Sensitivity Experiment Evaluation

Stress sensitivity has the two following meanings: (1) the difference between measured values of physical properties under standard and in situ conditions and (2) the performance of change

TABLE 1-27 Other Formation Damage Evaluation Methods

Experiment Item	Experimental Goals and Uses
Forward and backward flow experiments	Observing the effects of fluid flow direction on fine particle migration and formation damage caused by migration.
Volume flow rate evaluation experiment	Investigating the core cementation stability when flowing of working fluid of large volume through the core under a flow rate lower than the critical flow rate. Evaluating the water injection rate sensitivity of reservoir rock when water injecting.
Series fluid evaluation experiment	Understanding the total damage and its degree caused by contact of foreign working fluids with core in accordance with the practical operating procedure.
Cation exchange experiment	Determining the relative degree of seriousness of clay mineral hydration and swell by measuring the cation-exchange capacity of reservoir rock, thus providing grounds for formation damage mechanism study and well completion measures avoiding formation damage.
Acid liquor evaluation experiment	Evaluating and selecting acid liquor formulation, which can avoid formation damage caused by injecting acid liquor into core in accordance with the practical acidizing operation procedure.
Wettability evaluation experiment	Determining the change in reservoir rock wettability, caused by the working fluid, by measuring reservoir rock wettability before and after injecting the working fluid.
Relative permeability curve evaluation experiment	Determining the degree of water phase trap damage by measuring the relative permeability curve of reservoir rock. Determining the change in relative permeability of reservoir rock, caused by the working fluid, and the degree of damage by measuring relative permeability curves before and after injecting working fluid.
Capillary imbibition experiment	Evaluating the degree of potential water phase trap damage and presenting preventive measures by measuring the dynamic rule of imbibition of working fluid filtrate and experimental fluid under different initial water saturation.
Expansion ratio evaluation experiment	Evaluating working fluid compatibility with reservoir rock (particularly clay minerals) by measuring the expansion ratio after working fluid enters the core.
Fast evaluation experiment of capillary pressure using centrifuge	Fast evaluating formation damage by measuring the change in capillary pressure using the centrifugal method before and after working fluid enters reservoir rock.

in physical property (including fracture width) with stress when in situ stress changes. Porous-type, high-permeability unconsolidated reservoirs and tight reservoirs with very poor physical properties have obvious stress sensitivity, whereas fractured reservoirs are highly sensitive to changes in stress.

**Experimental Goals and Procedure.** Experimental goals include (1) converting the conventional porosity value into the in situ value to

be used for reserves calculation by measuring the porosity under simulated in situ conditions in order to evaluate the reservoirs accurately; (2) obtaining the core permeability value under in situ conditions, establishing the relationship between the core permeability  $K_c$  and the tested effective permeability  $K_e$ , and helping understand the relationship between  $K_e$  and formation resistivity; and (3) determining the rational producing pressure drawdown.

The maximum confining pressure of the core holder used for measuring stress sensitivity should not be lower than 60 MPa. The dry core sample is generally used for the air permeability experiment. The diameter of the standard core sample is 25.4 or 38.1 mm. The relationship between effective stress and parameters of physical properties for matrix and fractured rock samples are determined respectively. The evaluation procedure consists of the following: (1) selecting the experimental core and measuring its length and diameter; (2) selecting the experimental points of effective stress 2.5, 5.0, 10, ...40, and 60 MPa; and (3) measuring the values of permeability and porosity under various experimental stress values using the fully automatic core testing device (or other high-pressure permeameter).

**Stress Sensitivity Evaluation Indices.** At present, there are three common types of experimental methods (and evaluation indices) of stress sensitivity in China: (1) petroleum industry standards method (SY/T5358-2002), (2) stress sensitivity factor method, and (3) rate of permeability damage method based on in situ effective stress.

#### 1. Petroleum industry standards method

In "The flow test evaluation methods of reservoir sensitivity" (SY/T5358-2002), the experimental method and evaluation indices of stress sensitivity are given. This method describes systematically the experimental conditions, procedure, and data processing evaluation.

In petroleum industry standards, the clear definition of the permeability damage coefficient is given. The calculation formula is as follows:

(1-8)

$$D_{kp} = (K_i - K_{i+1}) / (K_i | p_{i+1} - p_i |),$$

where  $D_{kp}$  is the permeability damage coefficient,  $\text{MPa}^{-1}$ ;  $K_i, K_{i+1}$  is core sample permeability under effective stress No.  $i, i+1$ ,  $10^{-3} \mu\text{m}^2$ ;  $p_{i+1}, p_i$  is effective stress No.  $i, i+1$ , MPa; and  $D_{kp}$  indicates the reduction rate of core sample permeability per unit effective stress increase.

The rate of permeability damage is calculated using the following formula:

(1-9)

$$D_k = (K_1 - K_{\min}) / K_1 \times 100\%,$$

where  $D_k$  is rate of permeability damage;  $K_1$  is core sample permeability corresponding to the first stress point,  $10^{-3} \mu\text{m}^2$ ; and  $K_{\min}$  is minimum permeability of the core sample after reaching critical stress,  $10^{-3} \mu\text{m}^2$ .

The petroleum industry standards method has the following shortcomings: (1) the maximum effective stress value for set measurement points is 20 MPa. This value is generally lower than in situ effective stress. In the drilling, well completion, and field development process, engineers pay close attention to the change in reservoir permeability when effective stress fluctuates near in situ effective stress. (2) The stress value corresponding to the permeability damage coefficient maximum is taken as critical stress (Figure 1-15). However, in practice, the effective stress of the reservoir is generally much higher than the critical stress, thus causing that definition of the critical stress is of no obvious engineering significance for the practical application. (3) Selection of the measurement point of the highest effective stress is restricted by the subjective choice of experimental personnel and the pressure rating of the experimental instrument, thus obtaining a different value of rate of permeability damage for the same core and causing unnecessary trouble for practical engineering application.

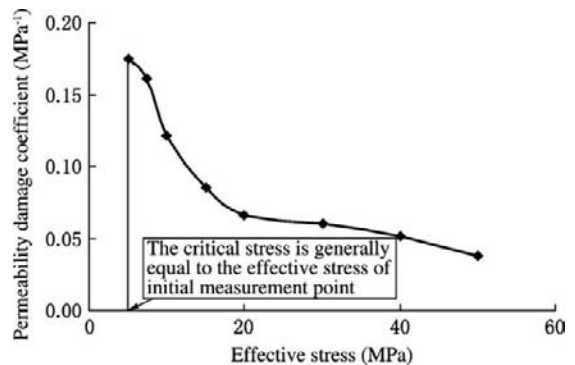


FIGURE 1-15 Permeability damage coefficient vs. effective stress.

## 2. Stress sensitivity factor method

The stress sensitivity factor method (Jones and Owens, 1980; Kang Yili, 1998) uses Equation (1-10) for processing experimental data obtained, thus obtaining the stress sensitivity coefficient of the core sample and evaluating the degree of stress sensitivity of the core sample.

(1-10)

$$S_s = \left[ 1 - \left( \frac{K}{K_o} \right)^{1/3} \right] / \lg \frac{\sigma}{\sigma_o}$$

where  $S_s$  is stress sensitivity factor;  $\sigma$  is effective stress, MPa;  $K$  is permeability corresponding to effective stress point,  $10^{-3} \mu\text{m}^2$ ;  $\sigma_o$  is effective stress of initial measurement point, MPa; and  $K_o$  is permeability of initial measurement point,  $10^{-3} \mu\text{m}^2$ .

Equation (1-10) is mathematically converted into Equation (1-11). If  $\left( \frac{K}{K_o} \right)^{1/3}$  is the ordinate and  $\lg \frac{\sigma}{\sigma_o}$  is the abscissa, the experimental points should theoretically form a straight line and its slope is the stress sensitivity factor  $S_s$ . The linear regression is needed by compilation of data measured, then they are matched into a straight line, and the absolute value of slope is the stress sensitivity factor, as shown in Figure 1-16.

(1-11)

$$\left[ \frac{K}{K_o} \right]^{1/3} = 1 - S_s \lg \frac{\sigma}{\sigma_o}$$

The measurement points of effective stress, which are used for straight line match,

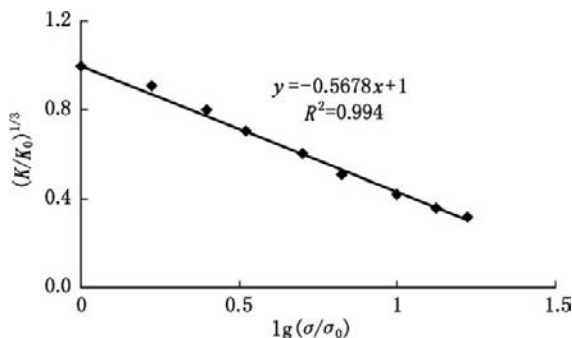


FIGURE 1-16 Match diagram of stress sensitivity factor.

include points both lower and higher than in situ stress, thus meeting the requirements for data processing. The stress sensitivity factor is obtained by matching all data obtained by the experiment. Each core sample corresponds to a stress sensitivity factor with uniqueness. However, it is inferior to the rate of permeability damage in physical visualization and ease of understanding.

## 3. Stress sensitivity evaluation based on in situ effective stress

Selection of the measurement points of effective stress is concentrated in the vicinity of in situ effective stress, and the measurement points of effective stress are determined by increasing and decreasing the reservoir pore pressure percentage. For example, for an average overburden density of  $2.50 \text{ g/cm}^2$ ,  $1.50 \text{ MPa/100 m}$  is taken as the formation pressure gradient, thus the formation pressure at a depth of  $2000 \text{ m}$  is  $30 \text{ MPa}$  with an in situ effective stress of  $20 \text{ MPa}$ , and the measurement points of effective stress can be determined by  $20 \pm 30 \times \beta\%$ . Then, the effective stress measurement points of effective stress  $5, 12.5, 15.5, 17, 18.5, 20, 21.5, 23, 24.5, 27.5, 35,$  and  $42.5 \text{ MPa}$  are obtained by taking  $\beta = 5, 10, 15, 25, 50,$  and  $75$ . The stress sensitivity evaluation formula based on in situ effective stress is as follows. The evaluation index in petroleum industry standards is continued to be used for the evaluation of rate of permeability damage.

(1-12)

$$R_1 = |(K_{\text{in situ}} - K_1)| / K_{\text{in situ}} \times 100\%,$$

where  $R_1$  is rate of permeability damage with effective stress of  $1 \text{ MPa}$  (the negative value indicates that permeability increases as the effective pore pressure increases);  $K_1$  is permeability with effective stress of  $1 \text{ MPa}$ ,  $10^{-3} \mu\text{m}^2$ ; and  $K_{\text{in situ}}$  is core permeability corresponding to in situ effective stress,  $10^{-3} \mu\text{m}^2$ .

The calculation of change in permeability on the basis of in situ effective stress is done by dividing into two sections (Figure 1-17).

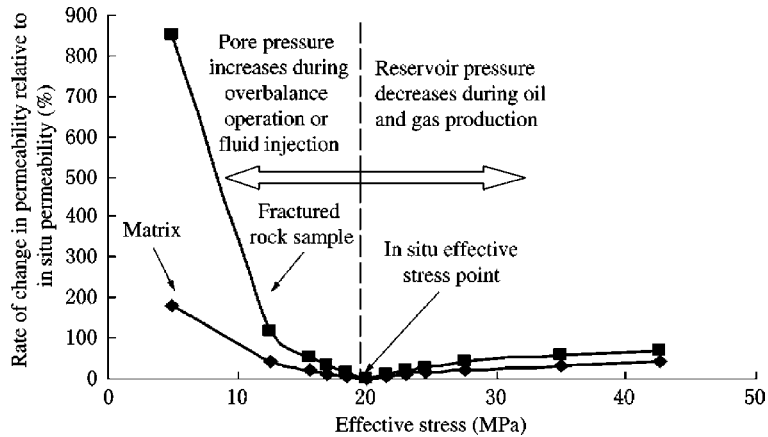


FIGURE 1-17 Rate of change in permeability vs. effective stress.

As effective stress is decreased gradually from in situ stress (e.g., overbalance operating or injecting the fluid, during which the pore pressure is increased and the effective stress of reservoir is decreased), the permeability increases. As effective stress is increased gradually from in situ stress (i.e., oil and gas are produced), the pore pressure is decreased, thus leading to an increase in the effective stress of the reservoir. The combination of the stress sensitivity evaluation with the oil and gas production evaluation practice is favorable to the correct evaluation of the degree of stress damage and the practical engineering application.

**Contrast between Different Stress Sensitivity Evaluation Methods.** The results of permeability damage evaluation for a core sample, which are obtained in accordance with the different evaluation indices, are shown in Table 1-28. Permeability damage evaluations obtained in accordance with the initial point of 3 MPa and in situ stress indicate strong and medium grades, respectively. Therefore, the permeability damage caused by effective stress is overestimated by the evaluation results obtained using the petroleum industry standards.

The rate of permeability damage and grade of damage determined by Equations (1-9) and (1-12) are shown in Table 1-29. Results indicate

TABLE 1-28 Permeability Damage Evaluation Results of Different Evaluation Indices

Evaluation Method	Stress Sensibility Factor Method $S_s$	Rate of Damage Method of Petroleum Industry Standards $(K_3 - K_{20})/K_3$	Rate of Damage Method of Petroleum Industry Standards $(K_3 - K_{35})/K_3$	Rate of Damage Method Based on In Situ Stress $(K_{20} - K_{35})/K_{20}$
Calculation example	0.54	0.83	0.92	0.55
Evaluation grade	Medium by strong	Strong	Strong	Medium by strong
Evaluation standards	$D_k \leq 0.30$ , weak; $0.30 < D_k \leq 0.50$ , medium by weak; $0.50 < D_k \leq 0.70$ , medium by strong; $D_k > 0.70$ , strong $S_s \leq 0.30$ , weak; $0.30 < S_s \leq 0.50$ , medium by weak; $0.50 < S_s \leq 0.70$ , medium by strong; $0.70 < S_s \leq 1.0$ , strong; $S_s > 1.0$ , very strong			

Note:  $K_i$  is the core sample permeability at  $i$ MPa. In situ effective stress is 20 MPa. The effective stress increases to 35 MPa after reservoir pressure decreases by 50%.

**TABLE 1-29 Correlation of Degree of Stress Sensitivity Damage of Some Core Samples by Different Evaluation Index**

$20 + 30 \times \beta\%$ (MPa)	20.0	21.5	23.0	24.5	27.5	35.0	42.5
$D_k$ calculated by initial measurement point (3 MPa)(%)	64.5	66.3	68.0	69.0	72.0	76.6	79.7
Grade of damage	Medium by strong	Medium by strong	Medium by strong	Medium by strong	Strong	Strong	Strong
$R_1$ calculated by in situ stress (20 MPa)(%)	—	5.3	10.0	14.1	21.1	34.1	43.0
Grade of damage	—	Weak	Weak	Weak	Weak	Medium by weak	Medium by weak

Note: The average in situ effective stress of this reservoir is 20 MPa and the reservoir pressure is 30 MPa.

that the permeability damage calculated on the basis of the initial measurement point is of medium by strong to strong grade, whereas the permeability damage calculated on the basis of in situ effective stress is of weak to medium by weak grade. Analyses of more than 70 core samples taken from the tight oil and gas sandstone reservoirs in central Sichuan and the low-permeability oil reservoirs in the Songliao basin in China indicate that the stress sensitivity factor is linear with the rate permeability damage based on in situ stress when the reservoir pressure decreases by 50%, and the values of the former are very close to the values of the latter (Figure 1-18). Thus the stress sensitivity factor can be used for characterizing the stress sensitivity of the core sample, and obtaining the average

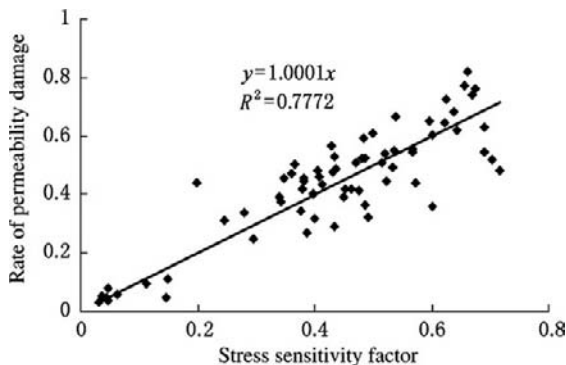


**FIGURE 1-18** Linear relationship between stress sensitivity factor and rate of permeability damage based on in situ stress.

values of horizon and region for correlation just as porosity and permeability. Therefore, it is recommended that the stress sensitivity factor method be used for evaluating the stress sensitivity of the reservoir. Evaluation results are shown in Table 1-30.

### Stress Sensitivity of Low-Permeability Sandstone Oil Reservoir

The low-permeability oil reservoir in the southern Songliao basin is fine- to medium-grained lithic arkose with an average porosity of 10.73%. The permeability is  $0.04\text{--}434 \times 10^{-3} \mu\text{m}^2$  and its average is  $8.55 \times 10^{-3} \mu\text{m}^2$ . Fractures in the core well develop. Thus the stress sensitivities of both matrix and fractured core samples should be studied. The experimental results of stress sensitivity of the matrix are shown in Table 1-31 and Figure 1-19. The stress sensitivity factor of the matrix is 0.03–0.30. Experimental results indicate none to weak stress sensitivity. The weak stress sensitivity of the Quan 4 member coincides with the higher hardness of particular cores.

The experimental results of stress sensitivity of fracture are shown in Table 1-32, Figure 1-20, and Figure 1-21. The degree of stress sensitivity of the naturally fractured core is medium by strong degree, whereas the degree of stress sensitivity of the artificially fractured core is medium by strong to strong. The degree of stress sensitivity

**TABLE 1-30 Evaluation Results of Degree of Stress Sensitivity by Stress Sensitivity Factor**

Stress sensitivity factor $S_s$	$S_s \leq 0.05$	$0.05 < S_s \leq 0.30$	$0.30 < S_s \leq 0.50$	$0.50 < S_s \leq 0.70$	$0.70 < S_s \leq 1.0$	$S_s > 1.0$
Degree of stress sensitivity	None	Weak	Medium by weak	Medium by strong	Strong	Very strong

**TABLE 1-31 Stress Sensitivity Evaluation of Matrix in Southern Songliao Basin**

No.	Sample No.	Horizon	Depth (m)	Permeability ( $10^{-3} \mu\text{m}^2$ )			$S_s$	Evaluation
1	D5-6A	Yaojia formation	1638.38	94.60	87.00	82.80	0.05	None
2	D15-17A	Qing 2 member	2035.34	0.622	0.559	0.540	0.05	None
3	D6-14	Qing 2 member	2035.00	0.604	0.544	0.529	0.05	None
4	D6-4A	Qing 2 member	2033.82	3.180	2.960	2.880	0.03	None
5	D8-3A	Qing 1 member	2181.68	0.437	0.392	0.378	0.05	None
6	D8-3C	Qing 1 member	2181.68	0.504	0.434	0.414	0.06	Weak
7	D2-3C	Qing 1 member	1953.62	2.320	2.060	2.010	0.05	None
8	D2-4A	Qing 1 member	1953.80	2.290	2.130	2.050	0.04	None
9	D20-7C	Qing 1 member	1955.14	32.400	28.10	22.80	0.20	Weak
10	D6-23E	Qing 4 member	2249.10	0.065	0.032	0.023	0.28	Weak
11	D16-43B	Qing 4 member	2261.66	0.105	0.045	0.037	0.30	Weak
12	D7-18B	Qing 4 member	2027.78	1.800	1.350	1.250	0.11	Weak
13	D17-30B	Qing 4 member	2031.58	0.533	0.370	0.339	0.15	Weak

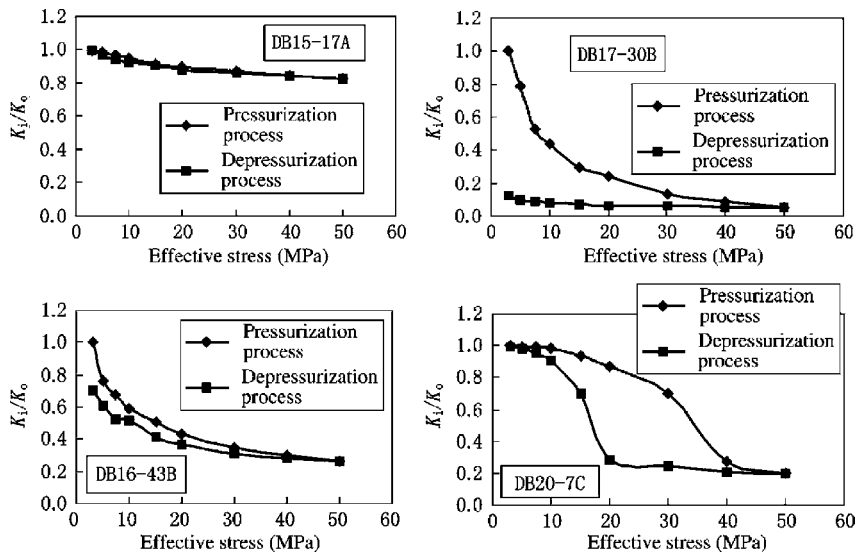


**FIGURE 1-19** Stress sensitivity evaluation experiment curves of a matrix in southern Songliao basin.

TABLE 1-32 Stress Sensitivity Evaluation of Fracture in Southern Songliao Basin

No.	Sample No.	Horizon	Depth (m)	Permeability ( $10^{-3} \mu\text{m}^2$ )	$S_s$	$S_r$	Evaluation	Remarks	
1	DB2-1	Qing 1 member	2065.34	63.50	2.960	1.640	0.69	Medium by strong	Natural fracture
2	DB22-5C	Qing 1 member	2066.04	7.840	1.320	0.794	0.53	Medium by strong	
3	DB17-15A	Qing 4 member	2027.28	28.70	3.780	2.500	0.52	Medium by strong	
4	D5-17A	Qing 2 member	2035.34	1340.0	255.0	153.0	0.52	Medium by strong	Artificial fracture
5	DB16-14	Qing 2 member	2035.00	103.00	3.820	2.310	0.72	Strong	
6	D8-3C	Qing 1 member	2181.68	166.00	19.30	4.080	0.66	Medium by strong	
7	DB16-23E	Qing 4 member	2249.10	879.00	185.00	80.300	0.54	Medium by strong	

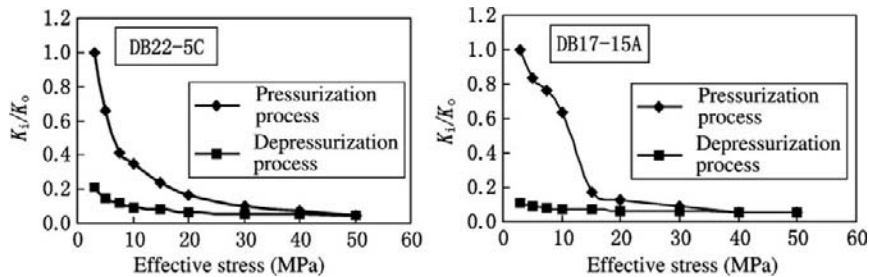


FIGURE 1-20 Stress sensitivity evaluation experiment curves of a natural fracture in southern Songliao basin.

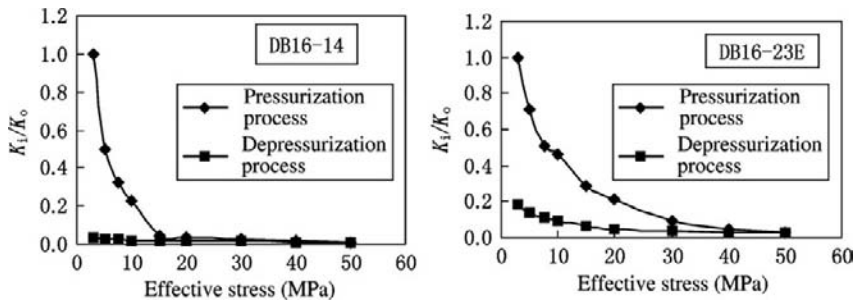


FIGURE 1-21 Stress sensitivity evaluation experiment curves of an artificial fracture in southern Songliao basin.

of the artificially fractured core is slightly stronger than the degree of stress sensitivity of the naturally fractured core. The stress sensitivity of the fractured core is obviously stronger than the stress sensitivity of the matrix core.

The tight sands oil reservoirs of the Shaximiao and Lianggaoshan formations of the Gongshanmiao oil field in the central Sichuan basin have a range of porosity of 0.25–5.16% and a range of permeability of

$0.0012\text{--}0.1340 \times 10^{-3} \mu\text{m}^2$ . The reservoir rocks are fine-grained lithic quartzose sandstone and lithic feldspathic quartzose sandstone. The stress sensitivity evaluation indicates that the stress sensitivity of the matrix core sample has medium by weak degree with a stress sensitivity factor of 0.35–0.49, whereas the stress sensitivity of the fractured core sample is medium by strong to strong with a stress sensitivity factor of 0.57–0.88. Similarly, in the oil fields of Tuha, Qinghai, Nanyang, Zhongyuan, and Changqing, the stress sensitivity increases as the matrix permeability of the low-permeability sandstone oil reservoir decreases with a weak to medium by weak degree overall, and the stress sensitivity of the fractured core sample has medium by strong to strong degree.

### Stress Sensitivity of Tight Sands Gas Reservoir

The sandstone gas reservoir with an air permeability lower than  $0.1 \times 10^{-3} \mu\text{m}^2$  under the in situ condition is known as a tight sands gas reservoir. The tightness of rock is caused by the two following factors: (1) large buried depth and strong compaction and cementation and (2) fine grains of rock and a large amount of interstitial matter. The former forms low-porosity tight sands, whereas the latter forms porous tight sands such as siltstone. The sand bodies can be divided further into lenticular and sheet sand bodies in accordance with the geometry of sand body in consideration of the effects of stimulation. Worldwide tight sands gas development activities are mainly conducted in the Rocky Mountains and Texas basins of the United States, Alberta basin of Canada, and Sichuan and Eerduosi basins of China. The stress sensitivity of tight sands gas reservoirs may be illustrated by examples of the Sichuan, Eerduosi, and Rocky Mountain basins.

**Stress Sensitivity of Conventional to Tight Sands Gas Reservoirs in Sichuan Basin.** The gas reservoirs of the Jurassic Penglaizhen, Shaximiao, and Qianfuya formations and the upper Triassic Xujiahe formation have a buried

depth of 250–5500 m. Most of the reservoirs have an abnormal high pressure, and multiple pressure systems exist with a pressure gradient of 1.15–2.05 MPa/100 m. Fine- and medium-grained sandstones predominate. Conventional reservoirs exist in the upper part of the Penglaizhen formation, the nearly tight reservoirs in the middle, and the tight reservoirs in the lower part. Most reservoirs of the Shaximiao and Xujiahe formations are tight to very tight and quite a bit are ultratight. The median capillary pressures of conventional, nearly tight, tight, and very tight reservoirs are <1.5, 1.5–3.0, 10–20, and 30–50 MPa, respectively. Regardless of occurrence, nonsealing fractures have a width  $b < 0.1$  mm to 0.1–0.5 mm, mostly  $b < 0.1$  mm. Sealing fractures have a larger width. Some sealing fractures filled with calcite have a width up to several millimeters. Fracture development has an obvious heterogeneity. Microfractures provide main permeability for the tight sands. The average content of clay minerals, including kaolinite, chlorite, illite, illite–smectite interlayer, chlorite–smectite interlayer, and smectite, is 3.7–7.3%.

The permeability of a conventional to nearly tight reservoir decreases slowly as the stress increases, whereas the permeability of a tight reservoir obviously decreases. The stress sensitivity of a conventional to nearly tight fractured core sample is stronger than that of a matrix core sample. The buried depths of reservoirs of the Penglaizhen formation are shallower, the original effective stress is 6.9–13.8 MPa, and the process of increasing stress is actually a simulation of compaction action. When reservoir pressure decreases, the matrix permeability is basically constant, whereas the permeability of the fractured reservoir obviously decreases (Figure 1-22).

Reservoirs of the Xu 4 member are buried deeply with an original effective in situ stress of about 25.5 MPa. When the effective stress is lower than 25.5 MPa, the permeability decreases steeply as the stress increases; after crossing the point of 25.5 MPa, the permeability slowly decreases as the stress increases (Figures 1-23 and 1-24). Experiments indicate that when the effective stress condition is simulated, the matrix

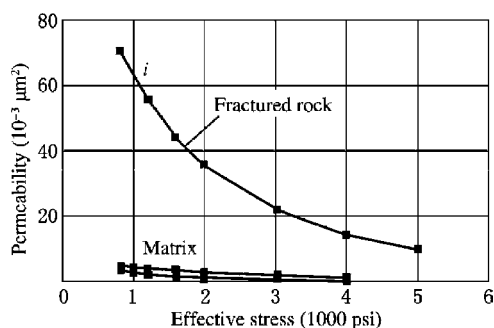


**FIGURE 1-22** Stress sensitivity of a fractured core sample of Penglaizhen formation.

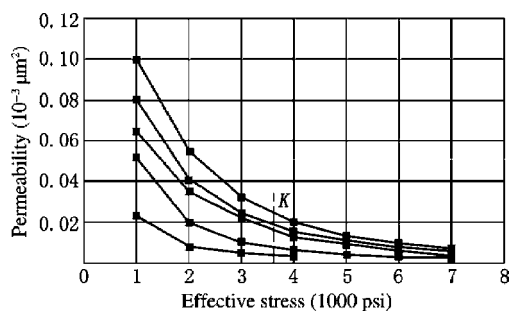


**FIGURE 1-23** Stress sensitivity of matrix core sample of tight sands of Xu 4 member.

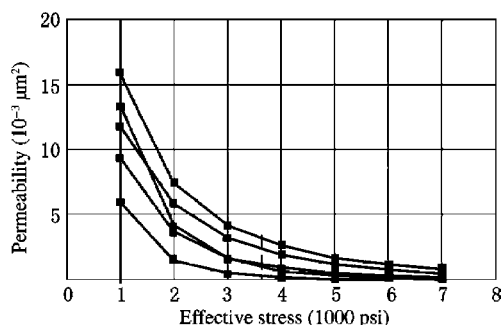


**FIGURE 1-24** Stress sensitivity of matrix core sample of tight sands of Xu 4 member.

core sample permeability of a conventional to nearly tight reservoir is four-fifths to one-third of the conventional value, whereas the permeability of a tight reservoir is one-fifth to one-twentieth of the conventional value. The change in porosity is relatively small. After they are corrected to original reservoir conditions, the porosity of a conventional reservoir decreases

by about 10%, while the porosity of tight sands decreases by 10–25%.

Table 1-33 shows that the stress sensitivity factor of the matrix of a conventional to nearly tight sands gas reservoir is 0.03–0.33 and the degree of stress sensitivity is generally weak, while the stress sensitivity factor of a fractured reservoir increases to 0.40–0.52 and the degree of stress sensitivity is generally medium by weak. The stress sensitivity factor of the matrix of typical tight sands of the Xu 4 member is 0.70–0.85, whereas the stress sensitivity factor of a fractured reservoir is 0.74–1.16 and the degree of stress sensitivity increases from strong to very strong with an increase by 100%.

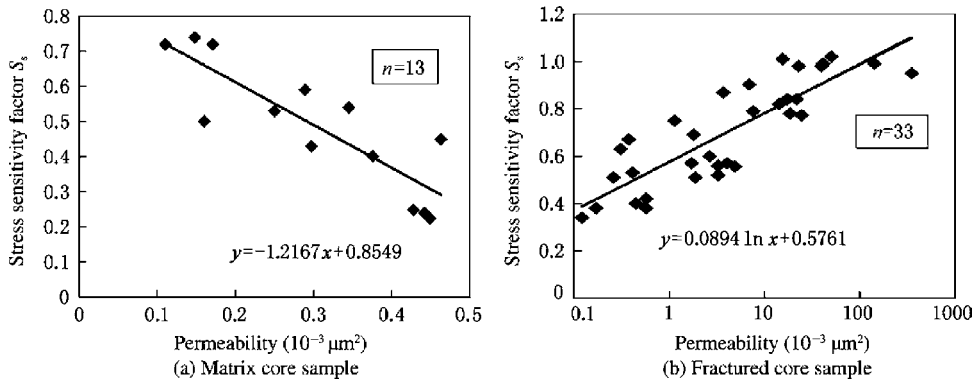
Analyses of more than 40 tight sands gas reservoir core samples of the Xiangxi group (corresponding to the Xujiache formation in the western Sichuan basin) in the central Sichuan basin indicate that the stress sensitivity factor of the matrix core sample is 0.37–0.69 with an average of 0.48, and the stress sensitivity factor of the fractured core sample is 0.381–0.704 with an average of 0.65. The degree of stress sensitivity of the former is medium by weak, whereas the degree of stress sensitivity of the latter is medium by strong. The lower the permeability of the matrix of tight sands, the stronger the stress sensitivity.

The very strong stress sensitivity of fractured tight sands is the basic reason for the ease of generating blowout and circulation loss during drilling. When the positive differential pressure increases, the effective stress decreases and the fracture width of rock increases, thus leading to circulation loss. A reasonable differential pressure should be retained during the tight gas reservoir test, and the effect of change in pressure on effective permeability should be considered when test data are interpreted.

**Stress Sensitivity of Upper Paleozoic Tight Sands Gas Reservoir in Eerduosi Basin.** The stress sensitivity factor of the matrix core sample of the upper Paleozoic tight sands gas reservoir in the Eerduosi basin is 0.22–0.74, whereas the stress sensitivity factor of the fractured core sample is 0.37–1.02. The stress sensitivity of the matrix core sample decreases as the permeability increases, whereas the stress sensitivity

**TABLE 1-33 Stress Sensitivity Evaluation of Low Permeability to Tight Clastic Rock Reservoir in Western Sichuan Basin**

No.	Sample No.	Permeability ( $10^{-3} \mu\text{m}^2$ )				$S_s$	Evaluation	Remarks
		5.52 MPa	6.9 MPa	13.8 MPa	27.6 MPa			
1	0-12	5.150		4.990		0.03	None	
2	2-23	6.080		3.970		0.33	Medium by weak	
3	2-28	32.00		25.20		0.19	Weak	$J^{3p}$ Matrix
4	2-36	0.618		0.519		0.14	Weak	
5	2-37	0.705		0.564		0.18	Weak	
6	2-38	12.10		11.15		0.07	Weak	
7	2-36	69.66		34.73		0.52	Medium by strong	
8	2-37	4.402		2.618		0.40	Medium by weak	$J^{3p}$ artificial fracture
9	5-7		$5.11 \times 10^{-2}$		$5.84 \times 10^{-3}$	0.85	Strong	$T^{3 \times 4}$ matrix
10	5-36		$2.25 \times 10^{-2}$		$3.17 \times 10^{-2}$	0.80	Strong	
11	5-53		$8.09 \times 10^{-2}$		$1.47 \times 10^{-2}$	0.72	Strong	
12	5-54		$7.99 \times 10^{-2}$		$1.51 \times 10^{-2}$	0.71	Strong	
13	5-65		$1.01 \times 10^{-1}$		$1.59 \times 10^{-2}$	0.76	Strong	
14	5-69		$6.42 \times 10^{-2}$		$1.23 \times 10^{-2}$	0.70	Strong	
15	5-7		6.0500		0.170	1.16	Very strong	
16	5-53		13.469		0.681	1.02	Very strong	
17	5-54		16.010		2.552	0.74	Strong	$T_{3 \times 4}$ artificial fracture
18	5-65		12.023		1.896	0.76	Strong	
19	5-69		9.5630		0.879	0.91	Strong	

**FIGURE 1-25** Stress sensitivity factor of tight sands vs. air permeability.

of the fractured core sample increases contrarily as the permeability increases (Figure 1-25). These analysis results coincide with those of the western and central Sichuan basin.

The core is pressurized and depressurized repeatedly, and the permeability corresponding to the effective stress point is measured. Results indicate that the primary pressurization process

has a higher degree of stress sensitivity, and the subsequent pressurization and depressurization processes decrease the degree of stress sensitivity gradually (Figure 1-26). As the times of pressurization and depressurization increase, plastic deformation of the core tends to perfection; the fracture closing and opening and the pore throat shrinkage and diastolization coincide

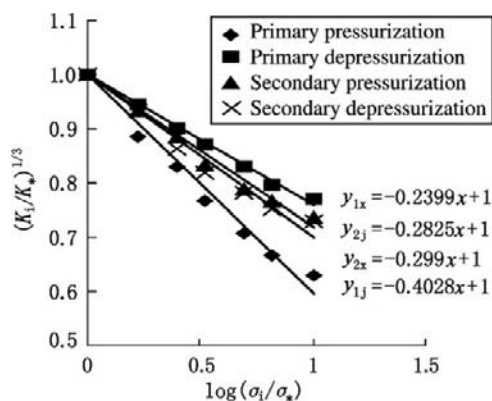


**FIGURE 1-26** Stress sensitivity of core sample pressurized and depressurized repeatedly.

gradually with the change in effective stress, thus the degree of stress sensitivity decreases macroscopically. The change in effective stress certainly leads to closing of pore throat and fracture, thus obviously decreasing gas reservoir permeability. It is very important for the gas well production rate to retain the rational pressure drawdown and pressure stabilization.

The stress sensitivity factor of a water-bearing core sample is almost larger than 0.5. This indicates that the existence of water aggravates the degree of stress sensitivity of the core sample (Table 1-34). The higher the water saturation of the group core sample (close physical properties), the stronger the stress sensitivity. The reason is that as the water saturation of the core sample increases, the actual channels of gas flow decrease, or the physicochemical change of rock, which is generated under pressure due to the existence of water, decreases the compressive strength of rock, thus increasing the stress sensitivity of the core sample. The combined effects of water saturation and effective stress may further aggravate the degree of damage.

**Stress Sensitivity of Tight Sands Gas Reservoir in Rook Mountains.** The tight sands gas reservoirs are mainly Cretaceous low-porosity tight sands with a porosity of 5–16% and a permeability of  $0.05\text{--}2.0 \times 10^{-3} \mu\text{m}^2$ . The stress sensitivity factor decreases as matrix permeability increases. Average stress sensitivity factors of the Frontier, Mesaverde, and Cotton Valley groups are 0.50, 0.30, and 0.30, respectively.

The average stress sensitivity factor of the tight sands of the Spirit River group in Canada is 0.30–0.50 (see Figures 1-27 and 1-28).

## Stress Sensitivity of Carbonate Reservoir

**Stress Sensitivity of Carbonate Reservoir of Zhanaruoer Oil Field in Kazakstan.** The Palaeozoic lower Carboniferous to Quaternary strata deposit widely in the range of the Zhanaruoer oil field. The reservoirs are Carboniferous carbonate consisting of two oil-bearing series of strata, that is, KT-I and KT-II. Limestone predominates in the thick neritic carbonate intercalated with a little dolomite. Secondary dissolution pores are the main storage space, and some microfractures developed. KT-I is a saturated reservoir with a condensate gas cap. The northern region of KT-II is a nonsaturated reservoir with a condensate gas cap, whereas the southern region of KT-II is a nonsaturated oil reservoir. The oil and gas reservoir has unified oil–gas and oil–water interfaces with weak edge and bottom waters. The average porosity of the reservoir is 10.6–13.7%, and the average permeability is  $13.1\text{--}138 \times 10^{-3} \mu\text{m}^2$ . Experiments indicate that the degree of stress sensitivity of the matrix is none to weak and can be negligible; the degree of stress sensitivity of the naturally fractured core sample is medium; and the degree of stress sensitivity of the artificially fractured core sample is medium by strong to strong and the stress sensitivity factor is generally not larger than 0.80 (Table 1-35).

**Stress Sensitivity of Carbonate Gas Reservoir of Northeastern Sichuan Basin.** The grey limy dolomite, dark grey limy dolomite, grey dolomite, and grey dissolved pore dolomite are predominant. Porosity is generally 0.1–15%. The porosity and permeability of the reservoir of the Feixianguan formation are unusually good, with a maximum porosity of 22.59% and permeability of up to  $1640 \times 10^{-3} \mu\text{m}^2$ . Stress sensitivity experiment evaluation results are shown in Tables 1-36 and 1-37. The degree of stress sensitivity of matrix is none to weak with a little

TABLE 1-34 Stress Sensitivity Evaluation Results of Water-Bearing Tight Sands

Core Sample No.	Horizon	$S_w$ Before Measurement (%)	Air Permeability ( $10^{-3} \mu\text{m}^2$ )					$S_w$ After Measurement (%)	Stress Sensitivity Factor $S_s$	Evaluation
			2.5 MPa <sup>a</sup>	3 MPa	10 MPa	30 MPa	40 MPa			
D16-6B	He 2+3	14.98	0.205	0.139	0.0755	0.0307	0.0235	14.61	0.38	Medium by weak
D16-6C		21.43	0.427	0.284	0.113	0.0400	0.0296	21.43	0.48	Medium by weak
D16-6A		53.24	0.360	0.109	0.0469	0.0124	0.009	50.93	0.51	Medium by strong
D1-17-2	He 1	15.45	0.414	0.340	0.161	0.0456	0.0342	15.45	0.53	Medium by strong
D1-17-3		28.04	0.440	0.364	0.150	0.0378	0.0283	27.63	0.57	Medium by strong
D1-18-2		46.44	0.440	0.354	0.137	0.0338	0.0260	46.18	0.59	Medium by strong
D15-47B	Shan 2	9.30	0.344	0.135	0.0532	0.0073	0.0036	9.30	0.56	Medium by strong
D15-47C		20.10	0.236	0.115	0.0405	0.0055	0.0032	20.09	0.62	Medium by strong
D15-47A		43.46	0.319	0.105	0.0399	0.0032	0.0025	43.13	0.64	Medium by strong
D15-69A	Shan 1	13.50	0.329	0.112	0.0394	0.0066	0.0030	13.50	0.61	Medium by strong
D15-68A		26.98	0.633	0.211	0.0659	0.0083	0.0043	26.89	0.65	Medium by strong
D15-69B		45.41	0.207	0.046	0.0037	0.0001	0.00008	45.34	0.92	Strong

<sup>a</sup>Air permeability of dry core sample ( $S_w = 0$ ) under the confining pressure of 2.5 MPa.

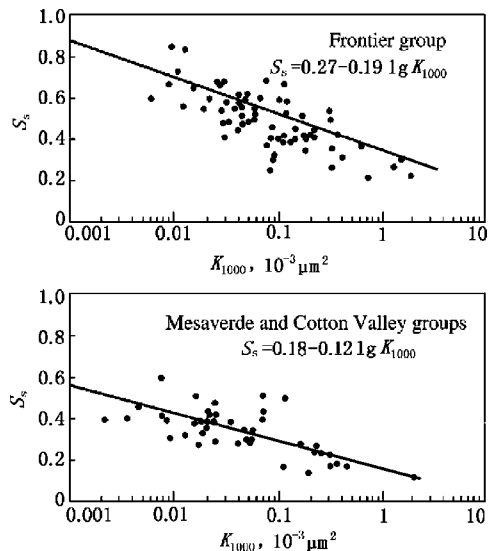


FIGURE 1-27 Stress sensitivity factor vs. permeability of typical tight sands in North America.

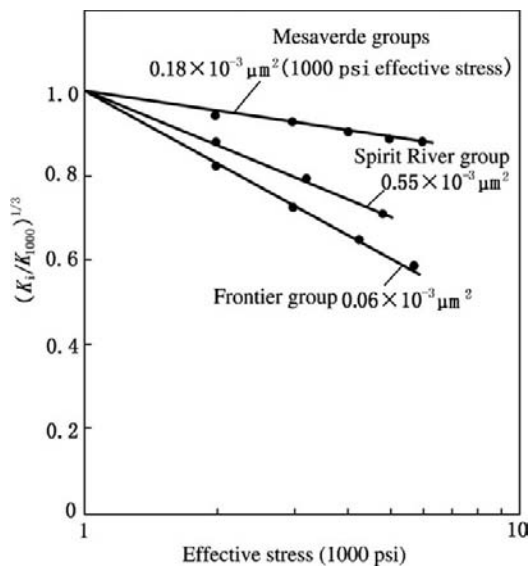


FIGURE 1-28 Cube root of permeability vs. logarithm of effective stress.

part medium by weak degree. The degree of stress sensitivity of naturally and artificially fractured cores is mostly medium by weak to medium by strong with a stress sensitivity factor of 0.41–0.75. Only the degree of stress sensitivity of some artificially fractured cores is

strong. Integrally, the degree of stress sensitivity of an artificially fractured core is slightly stronger than that of a naturally fractured core. The degree of stress sensitivity of a fractured core is stronger than that of a matrix core.

**Variation Rules of Stress Sensitivity of Carbonatite Reservoir.** The stress sensitivity factor is affected by differences of physical parameters (permeability and porosity) of the matrix core sample of the carbonatite reservoir between the two regions to some extent. Integrally, the stress sensitivity factor (average  $S_s = 0.056$ ) of the high-porosity, high-permeability matrix core sample is slightly lower than the stress sensitivity factor (average  $S_s = 0.219$ ) of the low-porosity, low-permeability matrix core sample. The average stress sensitivity factor of the matrix core sample is 0.145, and the average degree of stress sensitivity is weak (Figure 1-29).

There is an obvious difference of the stress sensitivity factor between naturally fractured and artificially fractured core samples. The stress sensitivity factor of an artificially fractured core sample is mostly more than 0.61, whereas the stress sensitivity factor of a naturally fractured core sample is concentrated on about 0.40. Artificially fractured core samples have an average stress sensitivity factor of 0.669 and medium by strong degree of stress sensitivity, whereas naturally fractured core samples have an average stress sensitivity factor of 0.471 and medium by weak degree of stress sensitivity (Figure 1-30). The reason is that natural fractures may be filled, contorted, dissolved, and deformed during the long years after forming, and their surfaces are not straight and regular like artificial fractures. Therefore, the degree of damage of a natural fracture is weaker than that of an artificial fracture when the stress changes.

## 1.5 IN SITU STRESS AND MECHANICAL PARAMETERS OF ROCK

The stress state around a wellbore and the mechanical properties of rock after drilling a well are closely related to well completion engineering.

TABLE 1-35 Stress Sensitivity Factors of Reservoirs of Zhanaruoer Oil Field

No.	Sample No.	Horizon	Permeability ( $10^{-3} \mu\text{m}^2$ )				$S_s$	Evaluation	Remarks
			2.5 MPa <sup>a</sup>	10 MPa	20 MPa	40 MPa			
1	9-2B	Γ	46.219	44.033	43.099	41.275	0.026	None	Matrix
2	9-6B	Γ	26.490	25.6077	22.271	23.392	0.034	None	
3	9-9C	Γ	308.80	316.04	302.74	285.84	0.013	None	
4	9-12A	Γ	7.531	7.3436	7.051	6.9336	0.022	None	
5	9-17B	Γ	0.328	0.2945	0.2824	0.2643	0.060	Weak	
6	2-13A	B	19.260	9.726	4.130	1.553	0.435	Medium by weak	Natural fracture
7	2-15	B	15.638	3.200	1.122	0.433	0.613	Medium by strong	
8	2-4B	B	16864.1	3903.5	917.1	318.06	0.627	Medium by strong	Artificial fracture
9	2-10B	B	185.697	76.432	42.465	18.875	0.434	Medium by weak	
10	9-5B	Γ	760.817	113.91	34.24	—	0.723	Strong	
11	9-15B	Γ	3729.02	1052.70	311.13	58.72	0.633	Medium by strong	
12	9-21C	Γ	1830.03	145.34	34.290	5.375	0.789	Strong	
13	2-19B	Д	1623.20	435.56	102.90	12.949	0.633	Medium by strong	
14	2-20A	Д	312.560	62.660	18.743	3.158	0.666	Medium by strong	
15	2-21A	Д	1871.24	225.99	41.501	4.841	0.764	Strong	
16	2-22A	Д	654.724	93.049	24.540	2.891	0.721	Strong	
17	2-22D	Д	887.367	135.20	39.326	8.593	0.674	Medium by strong	
18	2-26B	Д	78.184	17.251	6.835	1.392	0.619	Medium by strong	
19	2-29A	Д	604.274	122.914	37.832	—	0.691	Medium by strong	
20	2-29C	Д	812.752	85.388	18.503	1.818	0.773	Strong	

<sup>a</sup>Effective stress.

**TABLE 1-36 Stress Sensitivity Evaluation of Matrix Core Sample of Carbonatite of Northeastern Sichuan Basin**

Sample No.	Sample No.	Horizon	Depth (m)	Permeability ( $10^{-3} \mu\text{m}^2$ )			$S_g$	Evaluation
1	S1-6A	T <sub>2</sub> l	2742.06~2749.4	0.135	0.033	0.0197	0.467	Medium by weak
2	H1-01A	T <sub>1</sub> j	4483.61	0.0279	0.0205	0.0190	0.117	Weak
3	H1-02A	T <sub>1</sub> j	4484.11	0.5210	0.4830	0.4650	0.035	None
4	H1-02C	T <sub>1</sub> j	4484.11	0.5620	0.5460	0.5360	0.015	None
5	H1-12C	T <sub>1</sub> j	4519.69	0.0697	0.0402	0.0327	0.230	Weak
6	P1-10A1	T <sub>1</sub> f	5298.50	3.9700	1.2100	0.6380	0.437	Medium by weak
7	P1-10A2	T <sub>1</sub> f	5298.50	2.0600	0.5120	0.2920	0.468	Medium by weak
8	P1-16A	T <sub>1</sub> f	5422.05	0.5450	0.1150	0.0712	0.481	Medium by weak
9	P1-17C	T <sub>1</sub> f	5422.65	6.1000	2.5500	1.7500	0.342	Medium by weak
10	P1-23B1	T <sub>1</sub> f	5427.55	1.3000	0.9020	0.7840	0.154	Weak
11	P1-24A2	T <sub>1</sub> f	5427.90	0.6430	0.6430	0.2470	0.269	Weak
12	P2-2	T <sub>1</sub> f	5090.86~5094.63	427.0	360.0	353.0	0.065	Weak
13	P2-3	T <sub>1</sub> f		587.0	407.0	357.0	0.157	Weak
14	P2-6	T <sub>1</sub> f		487.0	454.0	445.0	0.029	None
15	P2-7	T <sub>1</sub> f		208.0	181.0	170.0	0.0638	Weak
16	P2-8	T <sub>1</sub> f		1.770	1.440	1.380	0.0782	Weak
17	P2-18A	T <sub>1</sub> f		1020.0	913.0	875.0	0.0534	Weak
18	P2-19	T <sub>1</sub> f		1090.0	1040.0	1010.0	0.0270	None
19	P2-20	T <sub>1</sub> f		428.0	366.0	342.0	0.0753	Weak
20	P2-24B	T <sub>1</sub> f		840.0	711.0	654.0	0.0843	Weak
21	P2-29	T <sub>1</sub> f		597.0	578.0	566.0	0.0236	None
22	P2-37A	P <sub>2</sub> ch	5094.63~5104.43	0.0519	0.0195	0.00959	0.3769	Medium by weak

This has a bearing not only on the completion mode to be adopted, but on the design and implementation of certain engineering measures after well completion. Therefore, it becomes very important to study in situ stress, particularly the change of the stress state of rock around the wellbore due to stress concentration after drilling.

In this section, the stress state of rock around wellbore, including firmness of borehole wall and mechanical stability of borehole, is chiefly discussed from the basic conception of in situ stress, and the relationship between in situ stress and well completion engineering is briefly mentioned.

### Basic Conception of in Situ Stress

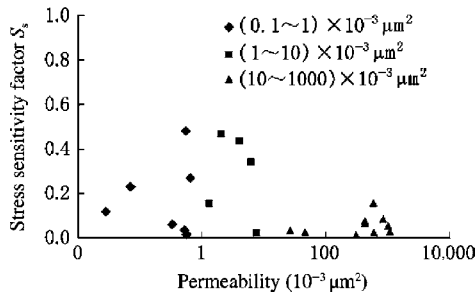
Internal stress is generated within the rock mass by the external forces exerted on the rock mass in the earth crust under the mutual balance

condition, thus leading to a deformation of rock mass. This internal stress is exactly the in situ stress. It is a mutual acting force per unit area between adjacent particles within the rock mass along the interface. In situ stress can be decomposed into two components, that is, the normal stress  $\sigma$  acting along the normal line of interface and the shear stress  $\tau$  acting along the interface, as shown in Figure 1-31.

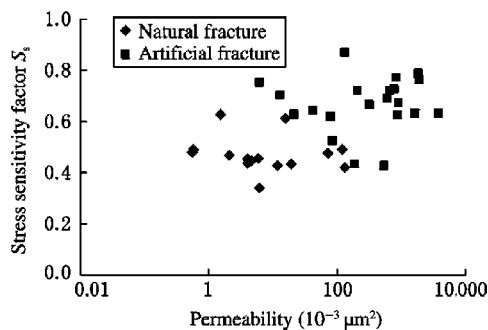
The study of in situ stress should include both normal stress and shear stress, otherwise it is incomplete with many phenomena unable to be understood. Normal stress toward the interface is compressive stress, whereas normal stress departing from the interface is tensile stress. Whereas compressive stress within the earth crust is absolutely predominant, in order to be convenient, the compressive stress in geomechanics is defined as a positive value, contrary to that

TABLE 1-37 Stress Sensitivity Evaluation of Fractured Core Sample of Carbonatite of Northeastern Sichuan Basin

No.	Sample No.	Horizon	Depth (m)	Permeability ( $10^{-3} \mu\text{m}^2$ )			$S_g$	Evaluation	Remarks
				3 MPa	20 MPa	30 MPa			
1	S1-1B	T <sub>2</sub> l		532	157	90.6	0.428	Medium by weak	Artificial fracture
2	S1-4A	T <sub>2</sub> l	2742.06~2749.40	84	13.2	7.48	0.526	Medium by strong	Artificial fracture
3	S1-9A	T <sub>2</sub> l		1030	357	179	0.414	Medium by weak	Artificial fracture
4	H1-06A	T <sub>1</sub> j	4500.57	1.5200	0.1480	0.0771	0.628	Medium by strong	Natural fracture
5	H1-10C	T <sub>1</sub> j	4514.12	0.5740	0.1200	0.0726	0.491	Medium by weak	Natural fracture
6	H1-07A	T <sub>1</sub> j	4505.82	277.00	58.1000	33.5000	0.512	Medium by strong	Artificial fracture
7	H1-08C	T <sub>1</sub> j	4507.22	41.500	3.6600	2.0100	0.645	Medium by strong	Artificial fracture
8	H1-11C	T <sub>1</sub> j	4517.02	12.800	0.7760	0.3460	0.705	Strong	Artificial fracture
9	H1-16C	T <sub>1</sub> j	4525.02	6.0700	0.2360	0.1000	0.755	Strong	Artificial fracture
10	P1-11A	T <sub>1</sub> f	5300.90	3.9800	0.9950	0.6630	0.455	Medium by weak	Natural fracture
11	P1-12C	T <sub>1</sub> f	5292.90	11.7000	3.7300	2.1100	0.429	Medium by weak	Natural fracture
12	P1-14B	T <sub>1</sub> f	5304.22	132.0000	35.1000	27.0000	0.421	Medium by weak	Natural fracture
13	P1-18C	T <sub>1</sub> f	5423.15	120.0000	31.2000	11.9000	0.491	Medium by weak	Natural fracture
14	P1-19B	T <sub>1</sub> f	5425.10	5.8800	1.5800	0.9950	0.457	Medium by weak	Natural fracture
15	P1-19C	T <sub>1</sub> f	5425.10	72.0000	12.3000	8.2500	0.477	Medium by weak	Natural fracture
16	P1-20B	T <sub>1</sub> f	5426.55	4.5800	1.2000	0.7120	0.447	Medium by weak	Natural fracture



**FIGURE 1-29** Stress sensitivity factor  $S_s$  of matrix core sample of carbonatite reservoir vs. permeability.



**FIGURE 1-30** Stress sensitivity factor  $S_s$  of fractured core sample of carbonatite reservoir vs. permeability.

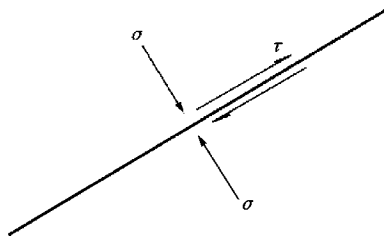


**FIGURE 1-31** Normal stress  $\sigma$  and shear stress  $\tau$ .

in mechanics of materials and engineering mechanics.

When the rock mass is exerted by external forces under the mutual balance condition, in situ stress is generated at arbitrary points within the rock mass. These in situ stresses occur or disappear simultaneously. The stresses, including normal and shear stresses, are different in different spatial orientations. As shown in Figure 1-32,  $\sigma_a \neq \sigma_b$ ,  $\tau_a \neq \tau_b$ ,  $\sigma_a$ , and  $\tau_a$  are normal stress

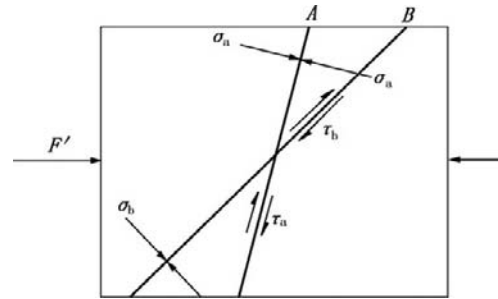


**FIGURE 1-32** Differences of stress values of interfaces with different directions.

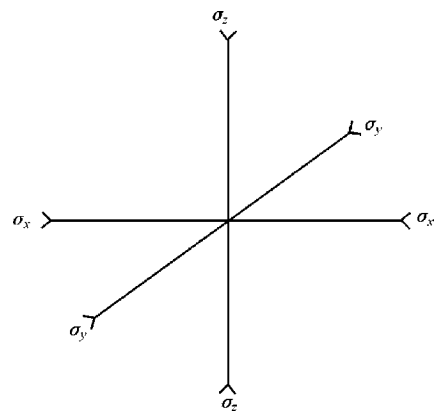


**FIGURE 1-33** The three principal stresses of in situ stress tensor.

and shear stress on interface A and  $\sigma_b$  and  $\tau_b$  are normal stress and shear stress on interface B, respectively. However, a certain relationship exists between stress values on interfaces in different directions at the same point, which make up an entity by the name of the in situ stress tensor, commonly known as the in situ stress state. There always are three orthogonal planes within the in situ stress tensor, on which there are only normal stresses and no shear stress. These three planes are named for principal planes, the directions of their normal lines are named for principal directions, and the normal stresses borne by them are called principal stresses. The three principal stresses of an in situ stress tensor, as shown in Figure 1-33, are mutually perpendicular.

Customarily, principal stresses with the highest, intermediate, and lowest values are

known as maximum principal stress  $\sigma_1$ , intermediate principal stress  $\sigma_2$ , and minimum principal stress  $\sigma_3$ , respectively. The in situ stress tensor can be described briefly by three principal stresses with three principal directions as the coordinates. When three principal stress values are known, normal stress and shear stress on an interface in an arbitrary direction are definite and can be calculated.

In situ stress on a specific interface is different from the in situ stress tensor. They are of different levels and have different characters. The in situ stress tensor is often abbreviated to in situ stress, hence the two different types of things are easily mixed up under the same name, and misunderstanding will be generated. Therefore, it is necessary to determine exactly whether the word “in situ stress” means the in situ stress tensor or in situ stress on a specific interface when we see “in situ stress.” The in situ stress tensor reflects comprehensively the in situ stress state of a rock mass.

The rock mass in the earth crust bears multiple pairs of mutually balanced acting forces. Each pair of mutually balanced acting forces (i.e., external forces) will generate a stress tensor in the rock mass, which consists of six substresses of which the most important, widespread substresses, include gravitative stress, tectonic stress, and fluid pressure. Sometimes the thermal stress caused by the change in temperature is also important. Some other substresses are important locally or in a short time.

Gravitative stress is stress caused within the rock mass by a pair of mutually balanced external forces consisting of the overburden weight and the counteracting force of underlying formation. Gravitative stress within the earth crust, which is different from that at the surface, has a high value and is difficult to simulate in a laboratory. The vertical principal stress  $\sigma_{gz}$  of gravitative stress is as follows:

(1-13)

$$\sigma_{gz} = \rho_r g h,$$

where  $\rho_r$  is average density of overburden,  $h$  is buried depth, and  $g$  is gravitational acceleration.

Due to the horizontal confinement of formation, the following relation exists between horizontal principal stress  $\sigma_{gh}$  and vertical stress  $\sigma_{gz}$ :

(1-14)

$$\sigma_{gh} = \sigma_{gx} = \sigma_{gy} = \sigma_{gz} = \left( \frac{\nu}{1-\nu} \right)^{1/n},$$

where  $\nu$  is Poisson's ratio of rock.

A creep correction should be made for the Poisson's ratio obtained from the laboratory by reason that the bearing time of the rock mass is counted by geologic age. “ $n$ ” in the equation is a coefficient related to the nonlinear compression of rock and is generally 0.67. The nonlinearity of the compressive effect should be considered due to great pressure borne by the subsurface rock.

Tectonic stress is stress caused within the rock mass by a pair of mutually balanced external forces consisting of tectonic force and resistance to the movement of the rock mass. The vertical component of tectonic stress is generally zero, that is, no change in vertical principal stress occurs around acting of the tectonic force. The other two principal stresses are in the horizontal direction. One horizontal principal stress is along the acting direction of compressive tectonic force  $S_c$  or tensional tectonic force  $S_t$  and has the same values as tectonic forces, which are, respectively,

(1-15)

$$\begin{aligned} \sigma_{\alpha} &= S_c \\ \sigma_{\alpha} &= S_t \end{aligned}$$

The other horizontal principal stress is the following:

(1-16)

$$\begin{aligned} \sigma_{\alpha} &= \sigma_{\alpha} \nu^{1/n} \\ \sigma_{\beta} &= \sigma_{\beta} \nu^{1/n} \end{aligned}$$

Sometimes tectonic force appears in the form of a couple of force, which is balanced by the counteracting couple of force resisting rotation of the rock mass. The result of a combined action of both is tectonic stress generated within the rock mass. At this time the signs of the two horizontal principal stresses of the tectonic stress tensor are mutually contrary, that is, one is positive and the other is negative. It is shown that the types of tectonic stress tensors are

divided in accordance with the signs of horizontal principal stresses.

There always is fluid in the oil-bearing rock formation, and the fluid always has a certain pressure. The fluid pressure is substantially stress caused by the action of the gravity on the fluid, which is spheric stress, that is, stress with the same normal stress value in any direction. There is no shear stress within static fluid. Therefore, arbitrary coordinates can be taken and the three principal stress values are equal. The fluid pressure  $p$  in the normal hydrostatic pressure system is

(1-17)

$$p = \rho_f \cdot h \cdot g,$$

where  $\rho_f$  is average fluid density from shallow to deep.

In an enclosed environment, the fluid pressure may be higher than this value, and in a few instances it may be lower than this value. When deviating obviously from this value, the pressure is known as abnormal pressure.

The fluid pressure acts on the rock matrix and tends to open the pores and fractures, thus compensating the compressive stress borne by the rock mass. Permanent deformation of the rock mass is dependent on the difference between the rock matrix stress and the fluid pressure. This difference is commonly known as effective stress. For convenience, the in situ stress mentioned later means effective in situ stress unless otherwise specified. During field development, the change in in situ stress is not considerable, whereas the fluid pressure often changes quickly, thus leading to a subsequent change in effective in situ stress.

The change in temperature may generate thermal stress in the rock mass. Thermal stress can be conducted out and disappeared gradually during the very long geologic period. However, in a petroleum engineering operation, there is not enough time to conduct the thermal stress out. If the temperature changes obviously, thermal stress can play an important role in well completion engineering. Thermal stress is also a stress tensor. It depends on the change in temperature and the thermodynamic behavior and is further related to the free and nonfree directions of the environment where it is located at.

In situ stress is an algebraic sum of the aforementioned various substresses. One of the basic characteristics of in situ stress is that there always is a principal stress located in the vertical (or nearly vertical) direction. The other two principal stresses are in the horizontal direction, and their directions coincide with that of the two principal stresses of tectonic stress.

In the near-surface environment, the free and nonfree directions located by the rock mass may be changed with topography. This may affect the horizontal principal stress value of gravity and cause a deviation of tectonic principal stresses from vertical or horizontal directions, thus affecting the earth stress value and causing slightly deviating principal stresses of in situ stress from vertical and horizontal directions. Under near-surface and severe topographic relief conditions, this affection is obvious and gradually decreases toward deep. Because of the deeper burying of most oil reservoirs, the effect of topography on in situ stress is weak.

Other basic characteristics of in situ stress are that the three principal stresses under most conditions are compressive stresses (positive values) and their values may be great; only under a few conditions may one principal stress be negative (tensile stress). This is also different from conditions in normal engineering mechanics.

The types of in situ stress are divided by the azimuths of the maximum, intermediate, and minimum principal stresses, that is, by that which among the maximum, intermediate, and minimum principal stresses locate in the vertical direction. In situ stress with the maximum principal stress locating in the vertical direction is of type I. It can be further divided into two subtypes. In situ stress with positive minimum principal stress (compressive stress) is of type I<sub>a</sub> (Figure 1-34), and under its control the normal fault with a big dip angle develops. In situ stress with negative minimum principal stress is of type I<sub>b</sub>, and under its control a tensile fracture or normal fault develops. In situ stress with minimum principal stress locating in the vertical direction is of type II, and under its control a reverse fault with a small dip angle develops. In situ stress with intermediate principal stress

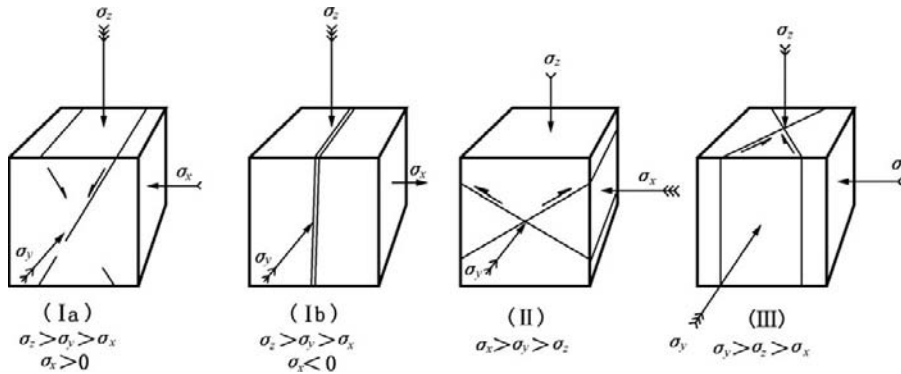


FIGURE 1-34 Types of in situ stress.

locating in the vertical direction is of type III, and under its control the nearly vertical strike-slip fault or shear fracture with the same character as a strike-slip fault develops.

Spatial change in the in situ stress tensor is known as the distribution of in situ stress. From the constitution of in situ stress, distribution of the in situ stress tensor is complicated. Any change in any principal stress of any substress tensor will result in a change in the in situ stress tensor. The vertical principal stress of gravitative stress increases with depth, whereas the horizontal principal stress is related not only to depth but to Poisson's ratio. The signs (positive and negative) and values of the two horizontal principal stresses are different for different types of tectonic stress and change laterally with attenuation of tectonic force during propagation. Generally, tectonic stress has some increase with depth and is also related to the rock properties to some extent. In addition, fluid pressure also has some change spatially. In general, one or several principal stress values rapidly or slowly change longitudinally or laterally. For instance, in two adjacent formations of interbedding with different lithology, the horizontal principal stresses of in situ stress may make a greater difference if the difference of the Poisson's ratio is greater. Therefore, in situ stress values measured at minority spatial points in a basin cannot be representative simply of the whole area.

Each type of substress may cause an elastic deformation of rock. However, whether a permanent deformation may be caused and what

type of permanent deformation may be caused depend on total stress (effective stress). Permanent deformation, including ruptural and plastic deformations, cannot be restored after the stress disappears. The relationship between permanent deformation of rock and in situ stress should be studied at the two levels, that is, interface in situ stress and in situ stress tensor.

At the level of interface in situ stress, permanent deformation is generated on the interface, on which in situ stress exceeds resistance to deformation. This resistance includes two parts related to cohesive force and internal friction. The resistance related to cohesive force is reflected by the following three strengths.

### 1. Tensile strength

When tensile stress on an interface exceeds this value, tension fracture of rock along this interface occurs. This point corresponds to the intersection of the rupture envelope and the abscissa, that is, point A in Figure 1-35.

### 2. Shear strength

If shear stress exceeds this value when normal stress is equal to zero on an interface, the shear fracture of rock may occur. This point corresponds to the intersection of the rupture envelope and the ordinate, that is, point B in Figure 1-35.

### 3. Yield strength

After shear stress on an interface exceeds this value, a microscopic shift occurs but the cohesive force is not affected, thus generating plastic deformation.

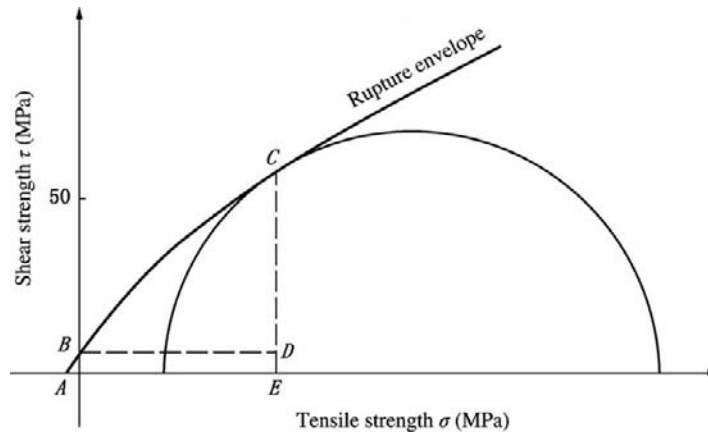


FIGURE 1-35 Mohr's circle and failure envelope.

This resistance, which increases with the normal stress of the interface, corresponds to frictional force known as internal friction, which is shown by rising of the rupture envelope toward the upper right (see Figure 1-35). However, the yield condition is affected slightly by normal stress.

The just-described strengths are inherent permanent deformation conditions. Data obtained can be used directly for solving the problems of subsurface and downhole rock deformation. Certainly the effects of conditions, including temperature on the physical properties of rock, should be considered.

However, at this level, the reason for generating permanent deformation on one interface but not another and the reason for a rock easily fracturing under one condition but not fracturing under another condition until the greater shear stress is available are not known. These problems should be considered at the level of the in situ stress tensor in order to find conditions of generating permanent deformation of the in situ stress tensor. In addition, it should be found which interface first attains the conditions of permanent deformation and which type of permanent deformation condition is attained under the specific in situ stress tensor.

The problem at this level may be studied thoroughly using the Mohr diagram. The

rupture conditions of rock are reflected comprehensively by the rupture envelope, on which each point represents the shear stress and normal stress values (as values at point C in Figure 1-35) on this interface when the rupture conditions are attained. Interfaces with values of greater shear stress and smaller normal stress in a specific stress tensor are shown by Mohr's circle, including minimum and maximum principal stresses. The combination of a rupture envelope and Mohr's circle clearly show whether the rupture may be generated under a specific stress state; to which extent when the maximum principal stress increases and the minimum principal stress decreases, the rupture is generated; on which interface the rupture should be generated; and how much the stress value on the rupture face is.

In a material test, rock strength is often characterized by the external force exerted. This is not the internal deformation condition mentioned earlier. Substantially, the deformation condition is characterized by the stress tensor during deformation. For example, in a uniaxial compression (or tension) test, rock strength is characterized by axial compression (or tension) when fracturing occurs. At this time, an axial principal stress in the  $x$  direction is exerted, whereas the other two stresses in the  $y$  and  $z$  directions are zero.

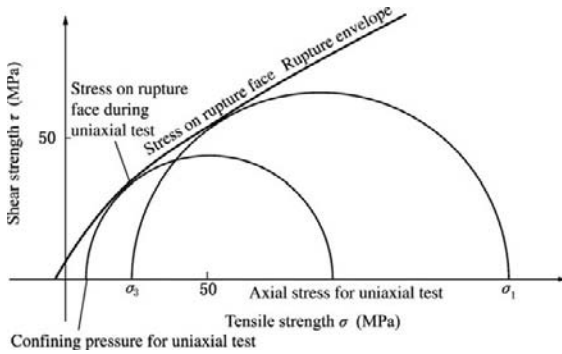


**FIGURE 1-36** Difference of rupture conditions between uniaxial test and subsurface rock.

During the uniaxial loading test under certain confining pressures, principal stresses in the  $y$  and  $z$  directions are the confining pressures, and rock strength obtained is different from that under no confining pressure. This rock strength obtained is the deformation condition under the aforementioned stress tensor (see the smaller circle in Figure 1-36).

The stress tensor borne by the subsurface rock mass is very different from that under the test condition. The principal stresses in the  $y$  and  $z$  directions are far higher than that under the test condition, and certainly the compression able to be borne in the  $x$  direction is further higher than that under the test condition. Full attention to the difference in stress tensor should be paid when laboratory rock strength test data are applied to the subsurface condition.

## Stress State of Borehole Wall Rock

After drilling, the stress state of borehole wall rock is changed greatly due to the effect of stress concentration.

As a result of stress concentration, stress borne by the borehole wall and the near-wellbore rock depends not only on in situ stress, but is affected by the wellbore. One of the principal stresses of stress tensor for the borehole wall and a near-wellbore rock mass is in the vertical direction, and its value is equal to the

vertical principal stress value of in situ stress. That is, the vertical principal stress is not affected by the wellbore, whereas the two horizontal principal stresses are obviously affected by the wellbore. This is similar to the stress state around the round hole on a flat plate. The two horizontal principal stresses are respectively in normal and tangential directions. The former is known as normal principal stress  $\sigma_r$ , whereas the latter is known as tangential principal stress  $\sigma_t$ . Their values are related to the two horizontal principal stresses  $\sigma_x$  and  $\sigma_y$  of in situ stress and also to the wellbore radius  $a$ , the distance between the rock mass and the center of wellbore  $r$ , and the location of rock mass on the borehole wall. Suppose the direction of  $\sigma_x$  is the zero azimuth; the included angle  $\theta$  between  $r$  and  $\sigma_x$  can characterize the location of rock mass on the borehole wall. The values of  $\sigma_r$  and  $\sigma_t$  are as follows:

(1-18)

$$\sigma_r = \frac{1}{2}(\sigma_x + \sigma_y) \left(1 - \frac{a^2}{r^2}\right) + \frac{1}{2}(\sigma_x - \sigma_y) \left(1 - \frac{a^2}{r^2}\right) \left(1 - \frac{3a^4}{r^4}\right) \cos 2\theta$$

(1-19)

$$\sigma_t = \frac{1}{2}(\sigma_x + \sigma_y) \left(1 + \frac{a^2}{r^2}\right) - \frac{1}{2}(\sigma_x - \sigma_y) \left(1 + \frac{3a^4}{r^4}\right) \cos 2\theta$$

For any point on the wellbore  $r = a$ , then  $\sigma_r = 0$

$$\sigma_t = (\sigma_x + \sigma_y) - 2(\sigma_x - \sigma_y) \cos 2\theta$$

When  $r = a$  and  $\theta = 0$

$$\sigma_t = 3\sigma_y - \sigma_x$$

When  $r = a$  and  $\theta = \pi/2$

$$\sigma_t = 3\sigma_x - \sigma_y$$

When  $r$  is more than  $3a$  or  $4a$ ,  $\frac{a^2}{r} \approx 0$  and  $\frac{a^4}{r^4} \approx 0$ , thus

$$\sigma_r \approx \frac{1}{2}[(\sigma_x + \sigma_y) + (\sigma_x - \sigma_y) \cos 2\theta]$$

$$\sigma_t \approx \frac{1}{2} [(\sigma_x + \sigma_y) - (\sigma_x - \sigma_y) \cos 2\theta]$$

At  $\theta = 0$

$$\sigma_r \approx \sigma_x \quad \sigma_t \approx \sigma_y$$

At  $\theta = \pi/2$

$$\sigma_r \approx \sigma_y \quad \sigma_t \approx \sigma_x$$

It is shown that at a distance more than  $4a$  from the center of the wellbore, the stress borne by the rock has approached the in situ stress state.

Whether the borehole wall and the near-wellbore rock mass are in a stable state depends on whether the permanent deformation condition (plastic deformation or rupture condition) of rock has been attained by the stress tensor borne by the rock mass.

As mentioned earlier, if the maximum tensile stress borne by the borehole wall rock exceeds the tensile strength of rock, tension fracture or tensile failure may occur. This is specifically reflected by causing the borehole wall rock to be infirm and resulting in sand production from the reservoir. If the maximum shear stress borne by the borehole wall rock exceeds the shear strength of rock, shear failure may occur. This is specifically reflected by causing the borehole to be unstable.

**Firmness of Borehole Wall Rock.** Sand production from the reservoir is caused by the structural failure of borehole wall rock. The internal causes of sand production from the reservoir are the stress state of borehole wall rock and the tensile strength of rock (affected chiefly by consolidation strength of rock), whereas external causes are the producing pressure drawdown value and the change in reservoir fluid pressure. In addition, the properties of reservoir fluid (oil) and the water cut are also factors affecting sand production from the reservoir.

In the thermal recovery process, thermal stress may be superimposed on the stress of borehole wall rock. However, due to no ripe theory and method at present, the thermal effect has not been considered during discussions of the firmness of borehole wall rock. In addition,

the effects of oil properties and water cut on the firmness of borehole wall rock are being pursued and are not considered here.

In accordance with research results [57], the maximum tangential stress borne by the borehole wall rock of a vertical well is shown by the following formula:

(1-20)

$$\sigma_t = 2 \left[ \frac{\nu}{1-\nu} (10^{-6} \rho g H - p_s) + (p_s - p_{wf}) \right].$$

On the basis of the rock failure theory, when the compressive strength of rock is lower than the maximum tangential stress  $\sigma_t$ , the borehole wall rock is infirm, thus leading to the structural failure of rock and rock matrix sand production. The discriminant for determining whether the borehole wall rock of a vertical well is firm is as follows:

(1-21)

$$C \geq 2 \left[ \frac{\nu}{1-\nu} (10^{-6} \rho g H - p_s) + (p_s - p_{wf}) \right],$$

where  $\sigma_t$  is maximum tangential stress of borehole wall rock, MPa;  $C$  is compressive strength of formation rock, MPa;  $\nu$  is Poisson's ratio of rock, decimal number;  $\rho$  is average density of overburden,  $\text{kg/cm}^3$ ;  $g$  is gravitational acceleration,  $\text{m/s}^2$ ;  $H$  is reservoir depth, m;  $p_s$  is reservoir fluid pressure, MPa; and  $p_{wf}$  is flowing bottomhole pressure during production, MPa.

If Equation (1-21) is satisfied, that is,  $C \geq \sigma_t$ , under the aforementioned producing pressure drawdown ( $p_s - p_{wf}$ ), the borehole wall rock is firm and the structural failure of rock will not be caused, the rock matrix sand production will not be generated, then the sand control completion mode will not be selected. However, when the reservoir has low consolidation strength and the maximum tangential stress of borehole wall rock exceeds the compressive strength of rock, the structural failure of rock may be induced and the rock matrix sand production from the reservoir may be generated, then the sand control completion mode should be adopted.

The maximum tangential stress  $\sigma_t$  borne by the borehole wall rock of a horizontal well is shown by the following formula:

(1-22)

$$\sigma_t = \frac{3-4\nu}{1-\nu}(10^{-6}\rho gH - p_s) + 2(p_s - p)$$

The meanings of the parameter signs are the same as described earlier. By comparing Equation (1-21) with Equation (1-22), it is shown that due to the Poisson's ratio of rock, which is generally between 0.15 and 0.4,  $(3-4\nu)/(1-\nu) > 2\nu(1-\nu)$ . Then, at the same buried depth, the tangential stress borne by the borehole wall rock of a horizontal well will be higher than that of a vertical well. Therefore, at the same buried depth, for the formation, from which sand production will not be generated in a vertical well, sand production is still possible in a horizontal well. Similarly, the discriminant for determining the firmness of borehole wall rock of a horizontal well is as follows:

(1-23)

$$C \geq \frac{3-4\nu}{1-\nu}(10^{-6}\rho gH - p_s) + 2(p_s - p_{wf})$$

For the directional wells of other angles, refer to reference [57] about evaluating the firmness of borehole wall rock.

**Mechanical Stability of Borehole.** Borehole stability is affected by the combined mechanical and chemical stabilities. Chemical stability means whether the reservoir contains interbedded clay, which is strongly swellable and ease of collapse, gypsum bed, and salt bed. These interbeds are very easy of swell and plastic creep when meeting water during production, thus leading the reservoir to losing support and collapsing. The chemical stability problem will not be discussed here due to generation only in special formations and its complexity and variability. In this section, the mechanical stability of wellbore during production will be chiefly discussed, the relationship between the shear stress borne by borehole wall rock and the shear strength of rock during production will be studied, and then grounds are provided for determining whether the well completion mode of supporting borehole wall is selected.

Without consideration of the effect of thermal stress, in accordance with Mohr-Coulomb's shear failure theory, in which the intermediate

principal stress is neglected, shear stress and effective normal stress acting on the maximum shear stress plane of borehole wall rock are:

(1-24)

$$\begin{aligned} \tau_{\max} &= (\sigma_1 - \sigma_3)/2 \\ \bar{\sigma}_N &= (\sigma_1 + \sigma_3)/2 - p_s \end{aligned}$$

where  $\tau_{\max}$  is maximum shear stress, MPa;  $\bar{\sigma}_N$  is effective normal stress acting on maximum shear stress plane, MPa;  $\sigma_1$  is maximum principal stress acting on borehole wall rock, MPa;  $\sigma_3$  is minimum principal stress acting on borehole wall rock, MPa; and  $p_s$  is formation pore pressure, MPa.

In accordance with von Mises's shear failure theory, in which intermediate principal stress is considered, the shear stress root mean square (the generalized shear stress) and effective normal stress acting on the borehole wall rock are as follows:

(1-25)

$$J_2^{0.5} = \sqrt{1/6[(\sigma_1 - \sigma_2)^2 + (\sigma_2 - \sigma_3)^2 + (\sigma_3 - \sigma_1)^2]}$$

$$\bar{J}_1 = \frac{1}{3}(\sigma_1 + \sigma_2 + \sigma_3) - p_s$$

where  $J_2^{0.5}$  is shear stress root mean square, MPa;  $\bar{J}_1$  is effective normal stress, MPa; and  $\sigma_2$  is intermediate principal stress, MPa.

The meanings of the other signs in the formulae are the same as given earlier. The two types of criteria of stability are discussed briefly later.

Bradley's method of calculating the stress around a borehole is as follows.

- (1) In situ stress is converted into the three normal stresses and three shear stresses in the rectangular coordinate system of the borehole axis on the basis of the original horizontal in situ stresses  $\sigma_{T1}$  and  $\sigma_{T2}$  and original vertical in situ stress  $\sigma_0$ , inclination angle  $\gamma$  of the borehole, and azimuth angle  $\varphi$  of the borehole.

$$\sigma_x = (\sigma_{T1} \cos^2 \varphi + \sigma_{T2} \sin^2 \varphi) \cos^2 \gamma + \sigma_0 \sin^2 \gamma$$

$$\sigma_y = (\sigma_{T1} \sin^2 \varphi + \sigma_{T2} \cos^2 \varphi)$$

$$\sigma_{zz} = (\sigma_{T1} \cos^2 \varphi + \sigma_{T2} \sin^2 \varphi) \sin^2 \gamma + \sigma_0 \cos^2 \gamma$$

$$\tau_{yz} = 0.5(\sigma_{T2} - \sigma_{T1}) \sin^2(2\varphi) \sin \gamma$$

$$\tau_{xz} = 0.5(\sigma_{T1} \cos^2 \varphi + \sigma_{T2} \sin^2 \varphi - \sigma_0) \sin(2\gamma)$$

$$\tau_{xy} = 0.5(\sigma_{T2} - \sigma_{T1}) \sin(2\varphi) \cos \gamma$$

- (2) The three normal stresses and the three shear stresses in the rectangular coordinate system of the borehole axis are changed into the three normal stresses  $\sigma_r$ ,  $\sigma_\theta$ , and  $\sigma_z$  and the three shear stresses  $\tau_{r\theta}$ ,  $\tau_{rz}$ , and  $\tau_{\theta z}$  in the circular cylindrical coordinate system of a borehole.

$$\begin{aligned}\sigma_r &= p_w \\ \sigma_\theta &= (\sigma_x + \sigma_y - p_w) - 2(\sigma_x - \sigma_y) \cos(2\theta) - 4\tau_{xy} \sin(2\theta) \\ \sigma_z &= \sigma_z - 2\mu(\sigma_x - \sigma_y) \cos(2\theta) - 4\mu\tau_{xy} \sin(2\theta) \\ \tau_{r\theta} &= \tau_{rz} = 0 \\ \tau_{\theta z} &= 2(\tau_{yz} \cos\theta - \tau_{xy} \sin\theta)\end{aligned}$$

- (3) The principal stresses are calculated on the basis of normal stresses and shear stresses in the circular cylindrical coordinate system of a borehole.

$$\begin{aligned}\sigma_1 &= \sigma_r = p_w \\ \sigma_{2,3} &= \frac{1}{2}(\sigma_\theta + \sigma_z) \pm \frac{1}{2}[(\sigma_\theta - \sigma_z)^2 + 4\tau_{\theta z}^2]^{1/2}\end{aligned}$$

After calculating, the subscripts are rearranged. The signs  $\sigma_1$ ,  $\sigma_3$ , and  $\sigma_2$  represent maximum, minimum, and intermediate principal stresses, respectively.

Finally, the shear strength of borehole wall rock is calculated in accordance with the linear shear strength formula, that is,

(1-26)

$$[\tau] = C_h + \bar{\sigma}_N \tan \Phi$$

$$C_h = \frac{1}{2} \sqrt{\sigma_c \sigma_t}$$

$$\Phi = 90^\circ - \arccos \frac{\sigma_c - \sigma_t}{\sigma_c + \sigma_t}$$

where  $[\tau]$  is shear strength of oil reservoir rock, MPa;  $C_h$  is cohesive force of oil reservoir rock, MPa;  $\Phi$  is internal friction angle of oil reservoir rock, °C;  $\sigma_c$  is uniaxial compressive strength of oil reservoir rock, MPa;  $\sigma_t$  is uniaxial tensile strength of oil reservoir rock, MPa; and  $\bar{\sigma}_N$  is effective normal stress calculated by Equation (1-24), MPa.

Equation (1-26) shows that the shear strength  $[\tau]$  of oil reservoir rock can be calculated provided the uniaxial compressive strength  $\sigma_c$

and tensile strength  $\sigma_t$  of oil reservoir rock are known. If the shear strength of oil reservoir rock, which is obtained by Equation (1-26), is greater than the maximum shear stress of borehole wall rock, which is calculated by Equation (1-24), that is,  $[\tau] > \tau_{\max}$ , it is indicated that the mechanical instability of the borehole will not be generated. However, the mechanical instability of a borehole will be generated, that is, borehole collapse is possible, thus the open hole completion mode should not be adopted.

If the stress state of borehole wall rock is calculated in accordance with von Mises's shear failure theory, the shear strength root mean square of borehole wall rock can be calculated in accordance with the linear formula of shear strength root mean square, that is,

(1-27)

$$[J_2^{0.5}] = \alpha + J_1 \tan \beta$$

$$\alpha = \frac{3C_h}{(9 + 12 \tan^2 \Phi)^{0.5}}$$

$$\tan \beta = \frac{3 \tan \Phi}{(9 + 12 \tan^2 \Phi)^{0.5}}$$

where  $[J_2^{0.5}]$  is shear strength root mean square of oil reservoir rock, MPa;  $\alpha$  is rock material constant, MPa;  $\beta$  is rock material constant; and  $J$  is effective normal stress calculated by Equation (1-25).

If the shear strength root mean square  $[J_2^{0.5}]$  calculated by Equation (1-27) is greater than the shear stress root mean square  $J_2^{0.5}$  calculated by Equation (1-25), mechanical instability will not be generated. However, the mechanical instability of the borehole will be generated.

## Relationship between In Situ Stress and Well Completion Engineering

The in situ stress state in the long-term production process should be considered in advance for completion mode selection and completion engineering design. The relationship between in situ stress

distribution (particularly the stress state around a borehole) and well completion engineering is chiefly reflected in the following aspects.

**Grounds Are Provided by In Situ Stress State for Completion Mode Optimization and Completion Engineering Design.** After drilling, due to the effect of stress concentration around the borehole, the stress state around the borehole is changed greatly and completely different from in situ stress. In particular, maximum tangential stress and maximum shear stress borne by borehole wall rock during production are directly related to the failure of borehole wall rock. In general, whether the failure of borehole wall rock is generated is related to the borehole stability and then whether the completion mode of the supporting borehole wall is adopted is determined, while whether the tensile failure of borehole wall rock is generated is related to the firmness of borehole wall rock and then whether the completion method of sand control for sandstone reservoir is adopted is determined. Thus the selection and determination of completion mode and method (as detailed in Chapter 2) are directly affected by the stress state around the borehole. In addition, the production casing design (see Chapter 5) and the hydraulic fracturing and acid fracturing designs (see Chapter 8) may also be affected directly by the stress state around the borehole.

**Fracture Configurations Generated by Hydraulic Fracturing and Acid Fracturing Depend on In Situ Stress State.** For the formation of type I of in situ stress, vertical stress is the maximum principal stress, the fracture generated by hydraulic fracturing is perpendicular to minimum principal stress, and this type of fracture generated by hydraulic fracturing or acid fracturing is always a vertical fracture. However, for the formation of type II of in situ stress, vertical stress is the minimum principal stress, the fracture generated by hydraulic fracturing is perpendicular to minimum principal stress, and this type of fracture generated by hydraulic fracturing or acid fracturing is always a horizontal fracture. Therefore, the fracture configurations generated by hydraulic

fracturing or acid fracturing depend on the state and type of in situ stress, which then influences directly the fracturing design.

## 1.6 TECHNOLOGICAL GROUNDS OF PETROLEUM PRODUCTION ENGINEERING

---

### Water Injection

The sandstone oil fields in China are formed chiefly by continental sedimentation. They are characterized by a series of strata, multiple thin interbeds, notable proportion of low-permeability oil reservoirs, and reservoir pressure commonly on the low side. Thus the oil fields are mostly developed using early waterflooding, and multiple-zone production in a well is commonly adopted. Therefore, separate-zone waterflooding technology is mostly applied. Seeing that water injection is applied in the whole process of oil field development and the water injection pressure is approaching the breakdown pressure of the oil reservoir, in particular the water injection pressure of the low-permeability oil reservoir in a deep well is especially high, thus the rational water injection pressure should be determined in accordance with the nodal analyses of the oil well and water injection well, the casing perforation completion should be adopted, and the well should have good cement job quality. In addition, a good isolation between the oil reservoirs and between oil reservoir and interbed without seeping and crossflow is required. Not only should the water injection beds be mutually isolated, but also the strength of production casing and its thread-sealing property should be considered, thus ensuring the normal work of the injection well under long-term, high-pressure conditions.

### Fracturing and Acidizing

Waterflooding and fracturing stimulation are mostly necessary to the low-permeability sandstone reservoirs in China, and separate-zone

fracturing is required due to the multiple series of strata. When fracturing fluid is injected through tubing, the operation pressure is high due to the high pumping rate and the high frictional resistance. Sometimes the means of increasing the tubing size is adopted to decrease the frictional resistance of tubing, thus decreasing the operation pressure. The casing perforation completion should be applied to the oil and gas production well and water injection well to be treated by fracturing. If the operation pressure is high and increasing tubing size is required, matching between tubing and casing sizes should be considered. The conventional acidizing treatment is mostly necessary to the carbonatite reservoir whether fractured or porous. In the well for this type of reservoir, open hole completion is sometimes applied. If the interval of the oil reservoir is very long or bottom water and a gas cap exist and acid fracturing treatment is required, casing perforation completion should be applied. For the oil or gas well in which acid fracturing is necessary, high pressure during the operation should be considered in the casing strength calculation of the casing design, in which the sealing property of thread should also be considered.

### **Control of Gas Cap, Bottom Water, or Edge Water Management**

Control of the gas cap, bottom water, or edge water is generally required whether for the massive oil and gas reservoirs of sandstone or carbonatite. Some oil reservoirs may have a gas cap, bottom water, and edge water simultaneously, while some only have a gas cap, bottom water, or edge water. When a well is completed, not only how to play a favorable role of gas cap, bottom water, and edge water should be fully considered, but also unfavorable factors should be controlled effectively.

Open hole completion is unsuitable, and only casing perforation completion should be applied. At the same time, the location of perforating should be suitably selected in order to control

the invasion of gas cap gas, bottom water, or edge water into the oil well.

### **Adjustment Well**

An adjustment well is such an oil well or water injection well, which is redrilled during the middle and late field development period to adjust the well pattern or to perfect the well pattern if the oil well or water injection well cannot be used due to failure. This type of well is considerably different from the development wells drilled originally. The pressure system of an oil well and water injection well, interlayer pressure, and oil saturation have changed to a great extent. Some interbeds or oil reservoirs have collapsed. It is more important that the downhole fluid is in a flow state, thus causing great difficulty in well cementing. Therefore, when an adjustment well is cemented, water injection of the surrounding injection wells should be stopped, the surrounding oil wells should be shut in, or adding of external casing packer on casing string is necessary in order to isolate the high-pressure flow bed.

### **Thermal Recovery by Steam Injection**

Heavy crude oil, particularly extra-heavy and superheavy crude oil, is almost impossible of flow due to high underground viscosity and cannot be produced using conventional methods, thus thermal recovery should be adopted. At present, thermal recovery by steam injection is broadly applied worldwide. The steam injection pressure and temperature depend on the depth of the oil reservoir. Due to the high viscosity and flow resistance of heavy crude oil, a large-diameter ( $\geq 7$  in.) casing and large-diameter ( $\geq 3$  in.) tubing are suitable. At the same time, prestressed casing should be used due to elongation of the casing under the high temperature, and the sealing property of casing threads should be considered. In addition, high-temperature-resistant cement should be used for well cementing and should be returned to the surface. If necessary, the gravity drainage of a horizontal well may also be used.

## Sand Control

On the basis of the firmness of borehole wall rock and formation test data, if it is determined that sand production from an oil reservoir will occur, sand control completion should be selected. In general, if the oil reservoir is thick without a gas cap and bottom water, open hole or casing perforation sand control completion may be adopted. For thin beds or interbeds, the casing perforation completion mode with sand control should be applied. The different sand control methods will be selected in accordance with the degree of sand production and sand grain diameter. A casing with a diameter larger than 178 mm (7 in.) is suitable for a sand-controlled well by reason that the oil inflow velocity can be decreased and the sand control thickness of the gravel pack can be increased to enhance the effectiveness of sand control.

## Corrosion Prevention and Scale Control

Hydrogen sulfide ( $H_2S$ ) and carbon dioxide ( $CO_2$ ) are corrosive gases and have a very strong effect of corrosion and hydrogen embrittlement on casing, tubing, and downhole tools. The natural gas in a gas well and the associated gas in an oil well contain commonly  $H_2S$  or  $CO_2$  gas. The casing, tubing, and downhole tools of anticorrosive steel should be used for the well completion of these oil and gas wells. At the same time, permanent packer and matching string are set above the top of the reservoir in order to prevent corrosive gas from entering the tubing-casing annulus. If necessary, a protective fluid is displaced into the tubing-casing annulus or anticorrosive fluid is injected into the annulus in order to protect the tubing, casing, and downhole tools.

In some oil fields, formation water has a very high salinity. For example, the salinity of formation water in the Zhongyuan oil field is up to  $20\text{--}30 \times 10^4$  mg/liter, whereas that in the Talimu Donghetan oil field is up to

$20\text{--}26 \times 10^4$  mg/liter. Tubing and casing may be seriously corroded by formation water with a high salinity. Sometimes scale and salt will deposit at the inner wall of tubing. In addition to the aforementioned measures of corrosion prevention, chemicals, including an antiscaling additive, are mostly injected into the tubing from the annulus during well completion.

## Injection of Natural Gas and Other Gases

Gas injection means mainly cyclic gas injection in a condensate gas field or injection of  $N_2$ ,  $CO_2$ , or other gases during tertiary recovery. No matter what gas is injected, the gas injection pressure is high due to the low density and gas column pressure. Because the casing will work over a long period under high pressure, casing perforation completion should only be selected. The casing strength and gas tightness of the casing thread should also be considered. The gas channeling inhibitor should be added in the cement during the cementing job of the gas injection well and the cement slurry should be returned to the surface. The permanent packer is set above the top of the reservoir in order to protect the casing. Tubing string with snubbing downhole tools is required. Thus the tubing string can be pulled up to a place above the reservoir under snubbing conditions for well killing in order to prevent killing fluid from damaging the reservoir.

## Stratified Oil Reservoir with Vertical or Composite Fractures and High Dip Angle

The oil reservoirs of the Kelamayi Dongjiang Huosaoshan, Shixi, and Xiaoguai oil fields are mostly vertically or compositely fractured reservoirs with a formation pressure coefficient commonly on the low side. If the conventional completion mode is adopted, a large amount of cement slurry is leaked off during cementing, thus not only is the reservoir not sealed off, but also serious damage is caused in reservoir deeps.

During well completion of this type of reservoir, the intermediate casing should be run to the top of the reservoir and the well is cemented, then the reservoir is drilled in and a slotted liner is run in for completion or else the reservoir is separated into several intervals using an external casing packer. Putting into production with fracturing is unsuitable for wells of a fractured oil reservoir due to the very high fluid loss into fractures and the difficulty of forming a pressure field to open up fractures. Even if a high pumping rate and high proppant concentration are applied, it is difficult to form long fractures linking up other fractures. This has been proven by the practice of some oil fields. For this type of fractured oil reservoirs, horizontal well completion is mostly applied. The fractures are cut through by the horizontal section, which will be much longer than fractures formed by fracturing. Horizontal wells are applied to cutting through multiple fractures in the Cretaceous vertically fractured formation in Austin, Texas, and the obvious results of development have been obtained.

Straight well completion is unsuitable for stratified oil reservoirs with a high dip angle by reason that only a few oil reservoirs (sometimes only one or two reservoirs) can be met by drilling a straight well. If directional well completion is adopted, multiple oil reservoirs with a great total thickness can be drilled through. If horizontal well completion is adopted, results are better than that of directional and straight wells. In the Shengli Chengdong oil field, directional and horizontal well completions are applied to multiple sets of Carboniferous and Permian stratified fractured oil reservoirs with a high dip angle ( $60^\circ$  unconformity surface), thus increasing the individual-well production rate greatly.

### Stratified Oil Reservoir

A stratified oil reservoir is formed by continental deposit, that is, the deposit forming sandstone is followed by the deposit forming mudstone, thus forming the stratified oil reservoir with a certain thickness or some thin interbeds. For a stratified oil reservoir, a straight well is commonly applied.

A horizontal well may also be applied if the conditions of horizontal well production are met. However, the thin intercalated oil reservoirs can only adopt straight well completion. Casing perforation completion should be adopted whether for the stratified oil reservoir or for the thin intercalated oil reservoir by reason that mudstone interbeds are easily collapsible (particularly in the waterflooding reservoir) and clay swelling or sliding may be caused if the water injected enters mudstone, thus aggravating the collapse of mudstone. Under casing perforation completion conditions, only oil reservoirs are perforated, and multiple-zone commingled production or separate-zone production in a well and separated-zone water injection can be applied to waterflooding of an oil field.

### Massive Oil Reservoir

A massive oil reservoir is a thick oil reservoir with a large area in which there is almost no restraining barrier of mudstone. A massive oil reservoir not only can be a sandstone oil reservoir (such as region III of the Liaohe Gaosheng oil field), but also can be a carbonatite oil reservoir (such as the Renqiu oil field in north China). A massive oil reservoir contains thin oil or heavy oil, and straight well completion may be applied. If a gas cap and bottom water exist, casing perforation completion should be adopted. In the Renqiu carbonatite oil field in north China, to which open hole completion is applied, bottom water coning is generated after producing for a time, and water cut of the fluid produced increases rapidly. Horizontal well completion may also be applied to a massive oil reservoir. In accordance with the specific conditions, casing perforation or open-hole slotted liner completion (particularly slotted liner plus external casing packer) is selected.

### Fractured Oil Reservoir

Buried hill oil reservoirs, including carbonatite, metamorphic rock, and igneous rock oil reservoirs, are mostly massive oil reservoirs, and

sometimes are stratified oil reservoirs. These oil reservoirs are generally fractured or fracture porosity reservoirs, and sometimes bottom water and a gas cap exist. For a stratified oil reservoir, the whole reservoir should be drilled through and casing perforation completion should be applied. For a massive oil reservoir, the intermediate casing may be run to the top of the oil reservoir and then open hole completion is applied after drilling the weathering crust. However, many problems regarding open hole completion, such as bottom water or gas cap management, acidizing, and water shutoff, are difficult to solve. Therefore, casing perforation completion is also applied to most of the massive oil reservoirs at present.

### Multiple-Zone Commingled Production in Well with Great Interzone Pressure Difference

When multiple-zone commingled production in a well is required, the well completion mode should be seriously considered. The pressure and production rate differences between various series of strata should first be considered. If the differences are not obvious, commingled production in a well is suitable. If the differences (particularly interzone pressure difference) are obvious, the oil in a single series of strata is only produced in a well, as otherwise the oil in the high-pressure reservoir will flow into the low-pressure reservoir due to the obvious interlayer interference, and the production rate of multiple series of strata is contrarily lower than that of single series of strata. If the reserve of single series of strata is too low to be produced alone, only two-string production can be applied with each string used for production from one series of strata in order to avoid the interlayer interference and ensure normal production to the two series of strata (Figure 1-37).

Two-string production has some limitations, although the interlayer interference problem can be solved by reason that the two series of strata corresponding to the two strings may have different flowing production periods, that is,

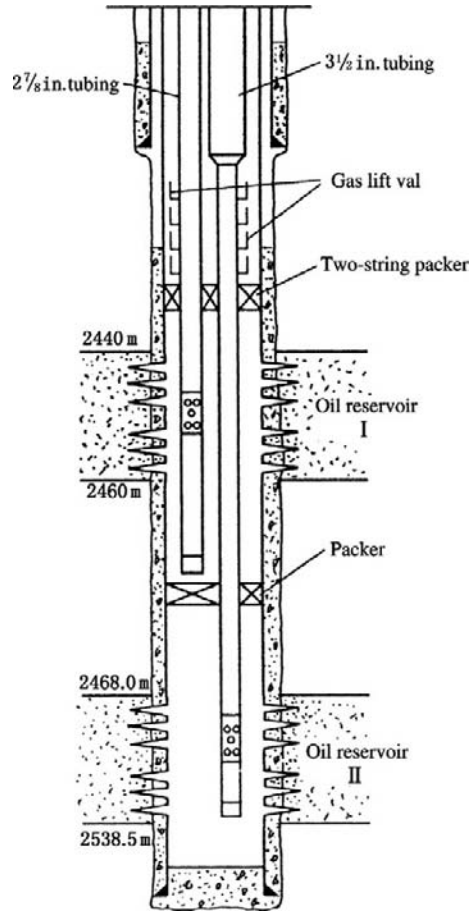


FIGURE 1-37 Two-string gas lift production diagram.

flow from one of the two series of strata may possibly stop first. In order to maintain the production rate of two-string production, a gas lift valve is attached to the lower end of each string. Once flow from one of the two series of strata becomes irregular or stops, the production from this series will be converted into gas-lift production at once. Other artificial lifting modes are unsuitable for two-string production. Despite the advantages of gas-lift production, the gas-lift production mode is limited to some extent due to the complicated downhole tools, the need for a two-string Christmas tree at the wellhead, and particularly the requirement of the natural gas source used for gas-lift production and the gas supply flowsheet and equipment. If these

conditions cannot be provided, only production from one series of strata by a single-string well can be applied.

## Horizontal Well

The term horizontal well has been broadly applied to the development of oil reservoirs of various types under various conditions since the 1990s. It is applied not only to individual-well production and finding remaining oil, but to whole oil field development. As for horizontal well completion, open hole, open-hole liner, or casing perforation completion can be selected in accordance with the specific reservoir conditions and the requirements of oil field development. At present, the whole completion process of a horizontal well mostly includes intermediate casing completion, drilling horizontal section and completion, and final production casing tie-back completion in order to ensure safe production.

At present, the horizontal well is no longer the single-hole horizontal well, but has multiple forms, including a horizontal branched well and multibore well. For example, horizontal branches are further separated from the horizontal or vertical section of a horizontal well in order to produce oil and gas from several series of strata, to increase the individual-well production rate, and to decrease the well construction cost. Multibranch well completion is relatively difficult. It is possible that casing-perforated completion is applied to one branch, whereas liner completion is applied to another one or two branches. As for the rest, only open hole completion can be applied.

## REFERENCES

- [1] M.И. Максимуб, *Oilfield Development Geology Basis*, second ed. (Wei Zhi, He Qingsen, Trans.), Petroleum Industry Press, Beijing, 1980 (In Russian).
- [2] P.A. Dickey, *Petroleum Development Geology*, second ed. (Wu Zhenxin, Min Yu, et al., Trans.), Petroleum Industry Press, Beijing, 1984.
- [3] Qiu Yinan, Cheng Ziqi, et al., *Reservoir Description*, Petroleum Industry Press, Beijing, 1996 (In Chinese).
- [4] Jin Yusun, et al., *Petroleum Production Geology Engineering*, second ed., Petroleum Industry Press, Beijing, 2003 (In Chinese).
- [5] Tang Zeyao, et al., *Gasfield Development Geology*, Petroleum Industry Press, Beijing, 1997 (In Chinese).
- [6] Wu Yuanyan, Xu Long, Zhan Changming, et al., *Oil and Gas Reservoir Geology*, Petroleum Industry Press, Beijing, 1996 (In Chinese).
- [7] Wang Yuncheng, *Oil and Gas Reservoir Evaluation*, Petroleum Industry Press, Beijing, 1999 (In Chinese).
- [8] Chen Yong, Huang Tingfang, *Petrophysics*, Beijing University Press, Beijing, 2001 (In Chinese).
- [9] D. Tiab, E.C. Donaldson, *Petrophysics*, Gulf Publishing Company, Houston, TX, 1996.
- [10] Bai Mao, Liu Tianquan, *Pore and Fissure Elasticity Theory and Application Guide*, Petroleum Industry Press, Beijing, 1999 (In Chinese).
- [11] Jiali Ge, Ning zhengfu, Liu Yuetian, et al., *Modern Oil Reservoir Flow Mechanics Principle*, Petroleum Industry Press, Beijing, 2001 (In Chinese).
- [12] R.F. Krueger, *An Overview of Formation Damage and Well Productivity in Oil Field Operations*, J. Petroleum Tech. Feb. (1986).
- [13] J.O. Amaefule, D.G. Kersey, D.K. Norman, P.M. Shannon, *Advances in Formation Damage Assessment and Control Strategies*, CIM 88-39-65, 1988.
- [14] K.E. Porter, *An overview of formation damage*, J. Petroleum Tech. Aug. (1989).
- [15] M.G. Read, *Formation Damage Prevention during Drilling and Completion*, NMT 890006, Oct. 1989, 33–38.
- [16] A.W. Layne, A.B. Yost, *Development of Advanced Drilling, Completion, and Stimulation System for Minimum Formation Damage and Improved Efficiency: A Program Overview*, SPE 27353, 1994.
- [17] D.B. Bennion, F.B. Thomas, *Underbalanced Drilling of Horizontal Wells: Does It Really Eliminate Formation Damage?* SPE 27352, 1994.
- [18] D.B. Bennion, F.B. Thomas, R.F. Bietz, *Low Permeability Gas Reservoirs: Problems, Opportunities and Solutions for Drilling, Completion, Stimulation and Production*, SPE 35577, May 1996.
- [19] D.B. Bennion, *Screening criteria help select formations for underbalanced drilling*, Oil Gas J. Jan. 8, 1996.
- [20] A. Ghalambor, M.J. Economides, *Formation Damage Abatement: A Quarter-Century Perspective*, SPE 58744, 2000.
- [21] Luo Pingya, *CNPC Academician Literature Collection (Luo Pingya's Collection)*, China Encyclopedia Press, Beijing, 1997 (In Chinese).
- [22] Zhang Shaohuai, Luo Pingya, et al., *Reservoir Protecting Techniques*, Petroleum Industry Press, Beijing, 1993 (In Chinese).

- [23] Wan Renpu, et al., *Advanced Well Completion Engineering*, second ed., Petroleum Industry Press, Beijing, 2000 (In Chinese).
- [24] Kexiang Li, et al., *Drilling and Completion Techniques of Oil and Gas Reservoir Protection*, Petroleum Industry Press, Beijing, 1993 (In Chinese).
- [25] Xu Tongtai, Hong Peiyun, Pan Shikui, et al., *Drilling and Completion Fluids of Horizontal Well*, Petroleum Industry Press, Beijing, 1999 (In Chinese).
- [26] Fan Shizhong, *Drilling and Completion Fluids and Oil and Gas Reservoir Protection Techniques*, China Mining University Press, Xuzhou, 2002 (In Chinese).
- [27] Luo Yingjun, et al., *Oil and Gas Reservoir Protection Techniques in Development Production Process*, Petroleum Industry Press, Beijing, 1996 (In Chinese).
- [28] Xu Tongtai, Zhao Ming, Xiong Youming, et al., *Oil and Gas Reservoir Protecting Techniques*, second ed., Petroleum Industry Press, Beijing, 2003 (In Chinese).
- [29] Luo Pingya, Kang Yili, Meng Yingfeng, Crossing development of reservoir protection in China, *Nat. Gas. Ind.* 26 (1) (2006) 84–87 (In Chinese).
- [30] Kang Yili, Luo Pingya, Effects of clay minerals on sandstone formation damage: Review and prospect, *Drilling Completion Fluids* 17 (5) (2000) 36–40 (In Chinese).
- [31] Kang Yili, Luo Pingya, Jiao Di, et al., The clay minerals of tight gas-bearing sands in western Sichuan and the potential formation damage, *J. Southwest Petroleum Institute* 20 (4) (1998) 1–5 (In Chinese).
- [32] Kang Yili, Luo Pingya, Yang yong, et al., The engineering geological characteristics and protection game of tight sands gas reservoir in western Sichuan, *J. Southwest Petroleum Institute* 21 (1) (1999) 1–5 (In Chinese).
- [33] Kang Yili, Luo Pingya, Jiao Di, et al., Controlling strategy of tight gas-bearing sands formation damage due to drilling and completion, *Nat. Gas. Ind.* 19 (4) (1999) 46–50 (In Chinese).
- [34] Kang Yili, Luo Pingya, Xu Jin, et al., The protection techniques of tight sands gas reservoir in western Sichuan: Progress and challenge, *J. Southwest Petroleum Institute* 22 (3) (2000) 1–5 (In Chinese).
- [35] Kang Yili, Luo Pingya, Xu Jin, Xu Xinghua, Employing Both Damage Control and Stimulation: A Way to Successful Development for Tight Gas Sandstone Reservoirs, Paper SPE 64707 presented at the SPE International Oil and Gas Conference and Exhibition in China, held in Beijing, China, 7–10 November 2000.
- [36] Kang Yili, Zhang Hao, et al., Comprehensive studies of stress sensitivity of tight sands reservoir of Daniudi gas field, *Natural Gas Geosci.* 17 (3) (2006) 335–338 (In Chinese).
- [37] Zhang Hao, Kang Yili, et al., Effects of rock components and fractures on tight sands stress sensitivity, *Nat. Gas. Ind.* 24 (7) (2004) 55–57 (In Chinese).
- [38] Zhang Hao, Kang Yili, et al., Effects of effective stress and temperature on tight sands permeability, *Nat. Gas. Ind.* 24 (Suppl. issue) (2004) (In Chinese).
- [39] Zhang Hao, Kang Yili, et al., Deformation theory and stress sensitivity of oil and gas reservoir rock of tight sands, *Natural Gas Geosci.* 15 (5) (2004) 482–486 (In Chinese).
- [40] Zhang Hao, Kang Yili, et al., Experimental evaluation of stress sensitivity of tight sands gas reservoir in northern Eerduosi basin, *Low Permeability Oil Gas Field* 10 (1) (2005) 17–20 (In Chinese).
- [41] Zhang Hao, Kang Yili, et al., Microstructure and fluid sensitivity of tight sands clay in northern Eerduosi basin, *Drilling Completion Fluids* 22 (6) (2005) 22–25 (In Chinese).
- [42] Lan Lin, Kang Yili, et al., Inquisition into method of evaluating low permeability-tight sands reservoir stress sensitivity, *Drilling Completion Fluids* 22 (3) (2005) 1–4 (In Chinese).
- [43] Lan Lin, Kang Yili, et al., Reservoir stress sensitivity evaluation based on in-situ effective stress, *Nat. Gas. Ind.* 26 (Suppl. issue) (2006) 125–127 (In Chinese).
- [44] Jian He, Kang Yili, et al., Stress sensitivity studies of porous and fracture porosity carbonatite reservoirs, *Drilling Production Technol.* 28 (2) (2005) 84–86, 93 (In Chinese).
- [45] Jian He, Kang Yili, et al., Experimental studies of alkali sensitivity of carbonatite gas reservoir during drilling in Chongqing area of Sichuan, *Nat. Gas. Ind.* 25 (8) (2005) 60–61 (In Chinese).
- [46] Yang Jian, Kang Yili, et al., Intensifying effects of formation damage due to drilling and completion fluid on stress sensitivity of tight sands, *Nat. Gas. Ind.* 26 (8) (2006) 60–62 (In Chinese).
- [47] Yang Jian, Kang Yili, et al., Evaluation of acid sensitivity of iron-rich tight sands reservoir: Gas reservoir of Upper Triassic Xujiahe formation in central Sichuan, *Oil Gas Geology Recovery Factor* 13 (6) (2006) 70–72 (In Chinese).
- [48] Yang Jian, Kang Yili, et al., Effects of pH value of fluid on tight sands reservoir permeability, *Nat. Gas. Ind.* 25 (10) (2005) 33–35 (In Chinese).
- [49] Gao Bo, Kang Yili, et al., Salt sensitivity experiments and applications of ultra-low permeability sandstone reservoir, *Drilling Completion Fluids* 22 (4) (2005) 49–51 (In Chinese).
- [50] Gao Bo, Kang Yili, et al., Experimental studies of rate sensitivity characteristics of ultra-low permeability sandstone reservoir, *Low Permeability Oil Gas Field* 9 (3) (2004) 13–16 (In Chinese).

- [51] You Lijun, Kang Yili, et al., Effects of water saturation and effective stress on effective permeability of tight sands, *Nat. Gas. Ind.* 24 (12) (2004) 105–107 (In Chinese).
- [52] You Lijun, Kang Yili, et al., Stress sensitivity of tight sands in consideration of fractures and water saturation, *J. China Petroleum Univ.* 30 (2) (2006) 59–63 (In Chinese).
- [53] You Lijun, Kang Yili, et al., Experimental studies and applications of water phase trap damage of tight sands gas reservoir, *Drilling Completion Fluids* 23 (2) (2006) 4–7 (In Chinese).
- [54] You Lijun, Kang Yili, et al., New method of establishing water saturation of tight sands: Capillary imbibition method, *J. Southwest Petroleum Institute* 26 (6) (2004) 28–31 (In Chinese).
- [55] You Lijun, Kang Yili, et al., The study of capillary imbibition of tight sands gas reservoir, *Nat. Gas. Ind.* 24 (Suppl. issue) (2004) 90–92 (In Chinese).
- [56] Wang Yongheng, Kang Yili, et al., New progress of experimental evaluation technique of formation damage due to drilling and completion fluid of horizontal well, *Drilling Completion Fluids* 23 (1) (2006) 72–75 (In Chinese).
- [57] Xiong Youming, et al., The formula for diagnostic index C of firmness of reservoir rock and its application, *J. Southwest Petroleum Institute* (1994) (In Chinese).

# CHAPTER 2

## Well Completion Mode Selection

### OUTLINE

2.1 Vertical, Slant, and Directional Well Completion	<i>Wire-Wrapped Screen Gap Size Selection</i>	Fiber Complex Fine Silt Control Completion
Perforated Completion	<i>Multiple Gravel Pack Technology</i>	<i>Fiber Complex Fine Silt Control Principle</i>
Casing Perforation Completion	<i>Diverter Pipe Gravel Pack Technique</i>	<i>Fiber Complex Silt Control Stimulation Principle</i>
Liner Perforation Completion	<i>Hydraulic Fracturing Gravel Pack Technique</i>	<i>Fiber Complex Silt Control Application</i>
Liner Tieback Perforation Completion	Other Sand Control	Intelligent Well Completion Overview
Open Hole Completion	Screen Completions	<i>Functions of Intelligent Well Completion System</i>
Slotted Liner Completion	<i>Precision Millipore Composite Sand Control Screen</i>	Monobore Well Completion
Shape of Slot	<i>Precision Punched Screen</i>	<i>Good Results Obtained in Gulf of Thailand</i>
Width of Slot Opening	STARS Star Pore Screen	<i>Main Features of Monobore Well Completion</i>
Arrangement of Slots	STARS Composite Screen	Underground Natural Gas Storage Well Completion
Size of Slotted Liner	Prepacked Gravel Wire-Wrapped Screen	<i>Depleted Oil and Gas Reservoir and Aquifer Gas Storage Well Completion</i>
Length of Slot	Metallic Fiber Sand Control Screen	
Quantity of Slots	External Guide	
Slot Cutting of Liner	Housing Sand Filtering Screen	
Gravel Pack Completion	Chemical Sand	
Open Hole Gravel Pack Completion	Consolidation Well	
Casing Gravel Pack Completion	Completion	
Gravel Quality Requirements		

Well completion mode selection is an important component of well completion engineering. At present, there are multiple types of well completion modes and their own applicable conditions and limitations. Only the most

suitable well completion mode is selected in accordance with the type and properties of an oil and gas reservoir—can the oil and gas field be developed effectively, the life of the oil and gas well be prolonged, and the economic

benefit be enhanced? The potential of oil reservoir intervals should be fully played by applying the reasonable completion mode in accordance with requirements of the oil field development program. The tubing string design should not only meet the requirements of flowing production of an oil well, but consider the requirements of artificial lift production in the later stage, and also create favorable conditions of necessary downhole operations and measures. A well completion mode should meet the following requirements:

- (1) The optimum condition of communication between reservoir and wellbore should be retained to reduce formation damage to the full extent.
- (2) The flow area between reservoir and wellbore should be provided as fully as possible in order to decrease the resistance to oil and gas flow into the well as far as possible.
- (3) The oil and gas reservoirs and aquifer should be effectively isolated in order to avoid gas and water channeling and inter-layer interference.
- (4) Sand production should be effectively controlled in order to prevent the borehole wall from sloughing and ensure long-term production of the oil well.
- (5) The oil well, which is run in after the well is completed, should not only meet the requirements of flowing production, but suit the need of artificial lift production in the later stage.
- (6) The conditions of downhole operations and measures, including separate-zone water injection and gas injection, separate-zone fracturing and acidizing, and water shutoff and profile control, should be provided.
- (7) The requirements of steam injection should be met during the thermal recovery of heavy oil.
- (8) The conditions of side-tracking should be provided in the later stage of oil field development.
- (9) The conditions of drilling horizontal branch holes of a horizontal well should be provided.
- (10) The corrosion caused by  $H_2S$ ,  $CO_2$ , and salt water with a high salinity should be effectively prevented.
- (11) The creeping of salt rock bed and salt paste bed should be resisted.
- (12) Simple and convenient operations and good economic benefits should be provided.

## **2.1 VERTICAL, SLANT, AND DIRECTIONAL WELL COMPLETION**

At present, the most common well completion modes include casing (or liner) perforation completion, open hole completion, and slotted liner completion, which can be further subdivided into completion with a slotted liner at the bottom of the casing and completion with a slotted liner run in the open hole.

It is important to understand the distinguishing features of various completion modes due to their different applicable conditions and limitations.

### **Perforated Completion**

Perforated completion is the most important and widely applied completion mode in China and abroad and includes casing perforation completion, liner perforation completion, and tieback liner perforation completion.

**Casing Perforation Completion.** Casing perforation completion includes drilling through the reservoir to the design depth, running-in production casing to the bottom of the reservoir and cementing, and perforating with perforator to perforate through the production casing and cement sheath, and penetrate into a certain depth in the reservoir in order to make channels to allow the oil and gas to flow into the well (Figure 2-1).

Casing perforation completion can achieve selective perforating oil reservoir with different pressure and physical properties in order to avoid interlayer interference, can keep clear of interbedded water, bottom water, and gas cap,

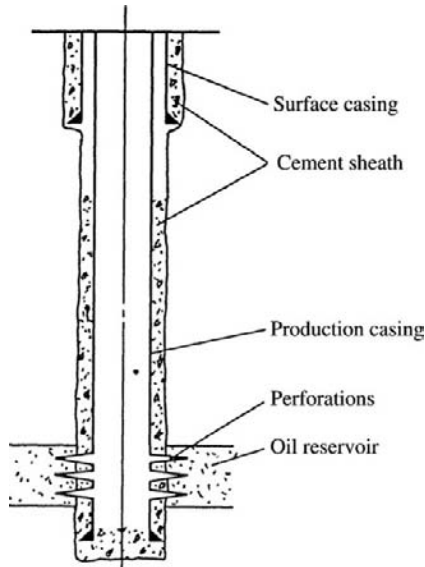


FIGURE 2-1 Casing perforation completion.

keep away from collapse of interbed, and provide the conditions of separate-zone operations, including separate-zone injection and production and selective fracturing and acidizing.

**Liner Perforation Completion.** Liner perforation completion includes running-in intermediate casing and cementing after drilling to the top of the reservoir, drilling through the reservoir to the design depth using a smaller size bit, running in a liner using drilling tools and hanging the liner on the intermediate casing (with an overlap section of the liner with the intermediate casing not less than 50 m), and then cementing and perforating (Figure 2-2).

During liner perforation completion, by reason that the upper formations have been sealed by the intermediate casing, drilling fluid compatible with the oil reservoir can be used to drill in the oil reservoir under a balanced or underbalanced pressure, thus providing favorable protection of the reservoir. In addition, perforated liner perforation completion can decrease the weight of casing string and the cement slurry volume, thus decreasing the completion cost. At present, oil and gas wells with a greater depth are mostly completed by this method.

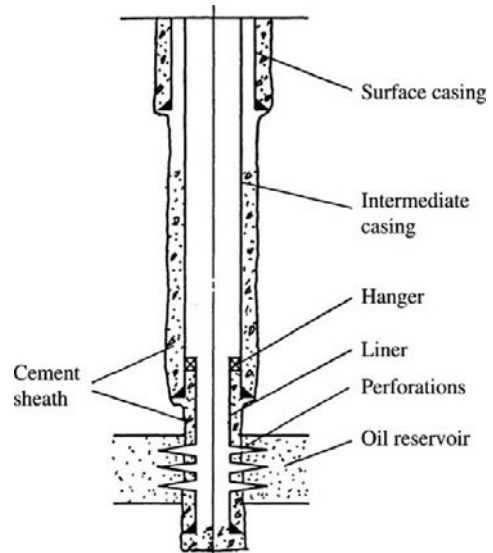


FIGURE 2-2 Liner perforation completion.

### Liner Tieback Perforation Completion

Liner perforation completion mentioned earlier is only suitable for oil and gas wells with a medium or low pressure. Under the conditions of no packer or malfunctioning of packer on the tubing string, the intermediate casing functions practically as a production casing and has difficulty withstanding high pressure of oil and gas.

Currently, liner tieback perforation completion is commonly applied to deep and ultradeep oil and gas wells and to high-pressure and superhigh pressure oil and gas wells and includes generally running liner in, cementing, running in production casing to tie back liner, cementing into intermediate casing-production casing annulus under atmospheric pressure and returning cement slurry to the surface, and then perforating at the liner, thus ensuring the cementing quality at the oil reservoir and throughout the whole wellbore above the oil reservoir and achieving safe production of the oil and gas well. If the liner is a screen pipe, the procedure is the same as just mentioned, but perforating is unnecessary. Liner tieback perforation completion is shown in Figure 2-3.

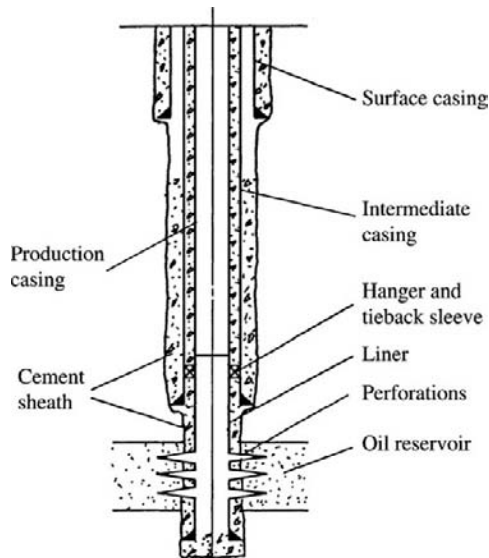


FIGURE 2-3 Liner tieback perforation completion.

Perforated completion is applicable to most oil reservoirs. The specific service conditions are listed in Table 2-13 later on in this chapter.

## Open Hole Completion

Open hole completion means that the oil reservoir is completely exposed during completion of a straight or horizontal well. There are two types of procedures for open hole completion.

1. After drilling to the top of the oil reservoir, the intermediate casing is run in and the well is cemented. After the cement slurry is returned to the predetermined design height, a bit with a smaller diameter is run through the intermediate casing, and the cement plug is drilled through. Then the oil reservoir is drilled in to the design depth and the well is completed (Figure 2-4).

Open hole completion is also suitable for some thick oil reservoirs. If a gas cap on the top or a water-bearing bed near the top boundary exists, the intermediate casing may be run across the oil–gas interface and the upper part of the oil reservoir is sealed and then open hole completion follows. If necessary,

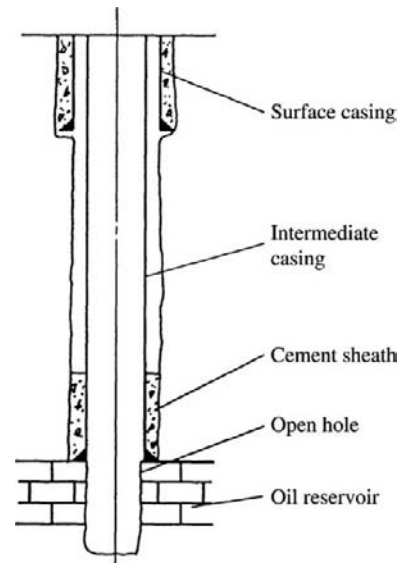


FIGURE 2-4 Initial open hole completion.

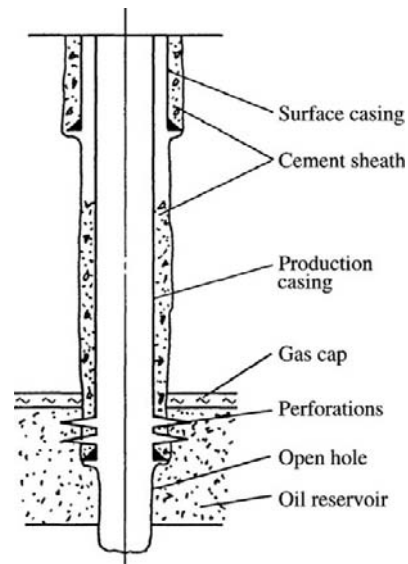


FIGURE 2-5 Composite well completion.

the oil-bearing interval is perforated. This type of well completion is known as composite well completion (Figure 2-5).

2. The bit is not changed. The oil reservoir is drilled directly through to the design depth, the intermediate casing is run to the top of

the oil reservoir, and the well is cemented. During cementing, the oil reservoir is padded with sand in order to prevent the oil reservoir below the casing shoe from damaging by cement slurry; the drilling fluid with low fluid loss and high viscosity is displaced in order to prevent the cement slurry from settling; or an external casing packer and cement stinger are set at the lower part of the casing in order to retain the cement slurry in the annulus and prevent the cement slurry from settling. During well completion using this procedure, the target can be drilled through using a set of drilling tools. However, after the target is drilled through, the intermediate casing should be further run in and the well should be cemented, the cement plug should be drilled, and then the well should be redrilled. Under normal conditions, this procedure is not applied due to the complicated operating sequence, long duration, serious formation damage, and possible formation collapse (see Figure 2-6).

Because complete exposure of the oil reservoir is the most important characteristic of open hole completion, the oil reservoir has the maximum percolation area. This type of well is known as a hydrodynamically

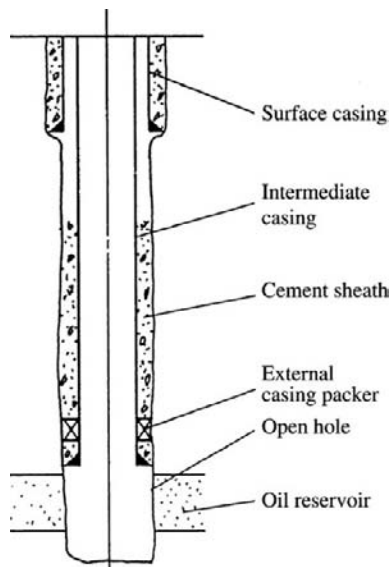


FIGURE 2-6 Final open hole completion.

completely penetrating well and has a higher productivity. Despite a high degree of completeness, open hole completion has a great limitation. The fracturing stimulation is mostly required by medium and low permeability sandstone oil and gas reservoirs. Open hole completion cannot meet these requirements. At the same time, sandstone contains mostly mud shale interbeds, which easily collapse when meeting water, thus plugging the wellbore. Open hole completion has been applied to the carbonatite oil and gas reservoirs (including fractured oil and gas reservoirs), such as many oil fields of the Middle East in the 1970s, the buried hill oil reservoirs of Wumishan of Renqiu oil field in north China, and the Sichuan gas field. At present, most of these oil and gas reservoirs adopt casing perforation completion due to difficulties in conducting stimulation, controlling bottom water coning, and plugging water and advances in the perforating technique. In the initial application period of horizontal wells in the early 1980s, open hole completion was applied to most of the horizontal wells of Cretaceous vertically fractured carbonatite reservoirs in Austin, Texas, and also to some horizontal wells in other countries. However, late in the 1980s, open hole completion was mostly replaced by the completion mode of a slotted liner or a slotted liner with an external casing packer. In particular, along with the extending of horizontal sections or drilling of horizontal branch holes, open hole completion is rarely applied because the wellbore collapse problem induced by open hole completion is difficult to solve. Thus, a slotted liner or perforated pipe is run in the open hole wellbore during well completion. The geological conditions suitable for open hole completion are listed in Table 2-3 later in this chapter.

In general, in the same oil and gas reservoirs, the daily production rate of the open hole completion well is higher in the initial period; however, after a time, the daily production rate of the casing perforation completion well is basically the same as that of the

open hole completion well, and finally cumulative production of the casing perforation completion well is yet higher than that of the open hole completion well. Casing perforation completion is favorable to conducting stimulation and various downhole operations and helpful in stabilized production of the oil and gas field.

### Slotted Liner Completion

Slotted liner completion also has two types of procedures. In the first procedure, after drilling through the oil reservoir using the same size bit, a liner at the bottom of the casing string is run to the position of the oil reservoir and then the well is cemented using an external casing packer and cement stinger to isolate the annulus above the top boundary of the oil reservoir (Figure 2-7). Under this procedure, the downhole liner damage cannot be repaired or changed. Therefore, this type of procedure is generally not applied.

In the second procedure, after drilling to the top boundary of the oil reservoir, the intermediate casing is run in and the well is cemented, then a bit with a smaller diameter is run through the intermediate casing and the oil reservoir is drilled through

to the design depth, and finally a liner slotted in advance is run to the position of the oil reservoir. The liner is hung on the wall of the intermediate casing by using the liner hanger on the top of the liner and the liner hanger seals the liner-casing annulus, thus the oil and gas may flow into the wellbore through the slots of the liner (Figure 2-8). This procedure is commonly adopted.

When this procedure is adopted, the oil reservoir will not be damaged by the cement slurry during cementing. The oil reservoir can be drilled in using drilling fluid compatible with the oil reservoir or other drilling techniques of protecting the oil reservoir. The slotted liner that is worn or failed may be pulled out to be repaired or changed.

The mechanism of sand control of the slotted liner is that the fine sand grains of a certain size, which can be carried to the surface by crude oil, are permitted to pass through the slots, whereas larger sand grains are retained out of the liner to form a sand bridge, thus achieving sand control (Figure 2-9).

The small sand grains cannot remain in the sand bridge due to the higher flow velocity at the sand bridge. This natural sorting of sand grains provides a good throughput capacity for

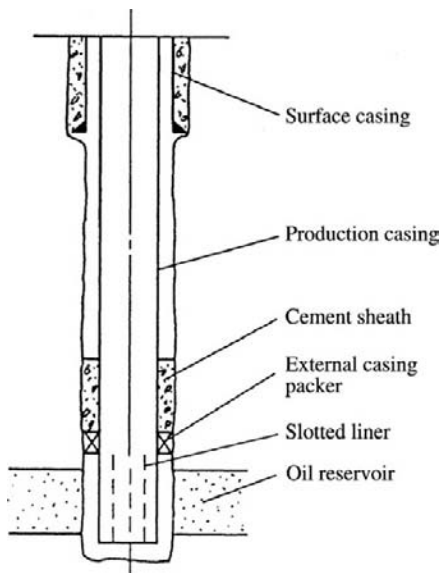


FIGURE 2-7 Slotted liner completion.

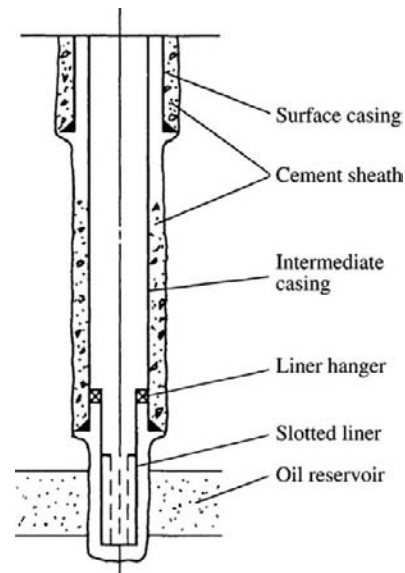
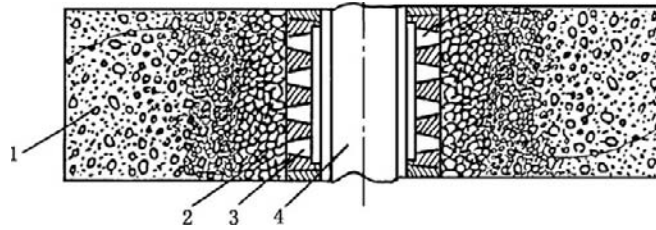


FIGURE 2-8 Hook-wall slotted liner completion.



**FIGURE 2-9** Sand bridge formed by natural sorting outside liner: 1, oil reservoir; 2, sand bridge; 3, slot; and 4, wellbore.

the sand bridge, which also acts as a protector of the borehole wall matrix sand. The shape and size of the slots should be determined by the grain size of the matrix sand.

**Shape of Slot.** The shape of the slot should be trapezoid, as shown in Figure 2-10. The included angle of the two hypotenuses of the trapezoid is related to the pressure borne by the liner and the throughput and is generally about  $12^\circ$ . The large bottom of the trapezoid should be the internal surface of the liner, while the small bottom should be the external bottom of the liner. This shape of slot may prevent sand grains from sticking in the slot and plugging the liner.

**Width of Slot Opening.** The width of the small bottom of a trapezoid slot is known as the width of the slot opening. The sand control efficiency of a slotted liner depends on the width of the slot opening. In accordance with experimental studies, the condition of forming a sand bridge outside the slot is that the width of the slot opening is not larger than two times the sand grain diameter, that is,

(2-1)

$$e \leq 2D_{10}$$

where  $e$  is the width of the slot opening and  $D_{10}$  is the sand grain diameter corresponding to 10% of the accumulative quality on the cumulative

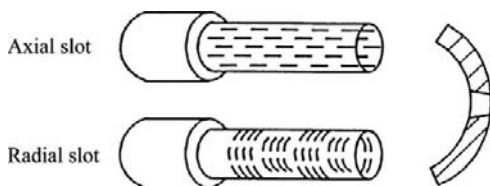


**FIGURE 2-10** Shape of slot.

curve of the reservoir sand grain size composition. This indicates that fine sand grains, which are 90% of the total sand sample quality, can pass through the slots, whereas large-diameter, load-bearing matrix sand grains cannot pass but are retained out of the liner and form a sand bridge with a higher permeability.

**Arrangement of Slots.** There are two arrangement patterns of slots: arranged parallel or perpendicular to the axis of the liner (see Figure 2-10).

The former is commonly applied by reason that the strength of the liner of the latter is lower than that of the former. In addition, the arrangement of staggered slots is appropriate in order to retain the maximum original strength of the liner and ensure an open slot area of 2–3%, as shown in Figure 2-11.

Suppose the length of a slot is  $l$  (mm), and the longitudinal distance between the slots is  $1.3l$  (or other appropriate multiple optimized). Suppose  $n$  is slots per meter liner, and a generatrix of slots is distributed per  $\left(360^\circ / \frac{n}{1000/2.3l}\right)$  (degree) along the circumference of the liner.

If the slots are distributed staggeringly in twinning form on the liner, the liner may have the optimum drainage area, as shown in Figure 2-12.

**Size of Slotted Liner.** The diameter of the slotted liner can be determined by the intermediate

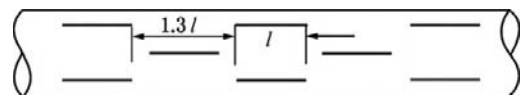


**FIGURE 2-11** Arrangement of staggered slots.

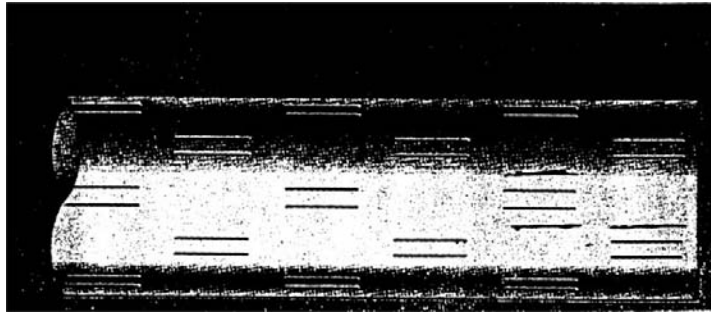


FIGURE 2-12 Staggered multislot sets.

casing size and the bit diameter of the open hole section, as shown in Table 2-1.

**Length of Slot.** The length of the slot depends on the liner diameter and the arrangement of slots and is normally 20–300 mm. The length of the slot perpendicular to the axis of the liner is shorter and is normally 20–50 mm due to the lower strength of the slotted liner, while the length of the slot parallel to the axis of the liner is normally 50–300 mm. A high value is taken for the liner with a small diameter and high strength, whereas a low value is taken for the liner with a large diameter and low strength.

**Quantity of Slots.** The quantity of slots is dependent on the flow area of the slotted liner. When the flow area of the slotted liner is determined, both the liquid production requirement and the strength of the slotted liner should be considered. Under the premise of ensuring the strength of the liner, the flow area of the liner should be increased to the full extent. Generally, 2–3% of the total external surface area of the liner is taken

as the total area of slots. The quantity of slots may be determined by the following formula:

(2-2)

$$n = \frac{\alpha F}{el}$$

where  $n$  is quantity of slots,  $m^{-1}$ ;  $\alpha$  is total slot area percentage of total external surface area of liner, normally 2–3%;  $F$  is external surface area per meter liner,  $mm^2/m$ ;  $e$  is width of slot opening, mm; and  $l$  is length of slot, mm.

Slotted liner completion is presently one of the important completion methods. It can act as open hole completion, can prevent open hole completion from borehole wall sloughing and wellbore plugging, can also control sand production to some extent. Slotted liner completion is commonly applied to medium and coarse sand oil reservoirs without serious sand production due to simple technology, convenient operation, and low cost, in particular to horizontal wells (including horizontal branched wells). Specific

TABLE 2-1 Matching of Casing, Bit, and Liner for Slotted Liner Completion

Intermediate Casing		Bit of Open Hole Section		Slotted Liner	
Nominal Size (in.)	Casing OD (mm)	Nominal Size (in.)	Bit Diameter (mm)	Nominal Size (in.)	Liner OD (mm)
7	177.8	6	152	5~5 <sup>1</sup> / <sub>2</sub>	127~140
8 <sup>5</sup> / <sub>8</sub>	219.1	7 <sup>1</sup> / <sub>2</sub>	190	5 <sup>1</sup> / <sub>2</sub> ~6 <sup>5</sup> / <sub>8</sub>	140~168
9 <sup>5</sup> / <sub>8</sub>	244.5	8 <sup>1</sup> / <sub>2</sub>	216	6 <sup>5</sup> / <sub>8</sub> ~7 <sup>5</sup> / <sub>8</sub>	168~194
10 <sup>3</sup> / <sub>4</sub>	273.1	9 <sup>5</sup> / <sub>8</sub>	244.5	7 <sup>5</sup> / <sub>8</sub> ~8 <sup>5</sup> / <sub>8</sub>	194~219

use conditions are listed in Table 2-13 later in this chapter.

**Slot Cutting of Liner.** In order to ensure a high precision and constant flow rate of the slotted liner, multidisc mechanical equipment, a special digital calculating system, and a hydraulic holding device should be adopted during slot cutting. This equipment with good stability and firmness can stabilize the liner firmly. The liner after slotted has an accurate allowable tolerance, clean slots, and a constant slot width along the slot length. Under the condition of the exposed open area of 3%, the liner still has maximum strength.

## Gravel Pack Completion

Generally, gravel pack completion should be adopted toward unconsolidated formations with serious sand production. First, a wire-wrapped screen is run to the position of the oil reservoir and then gravel selected at the surface in advance is pumped to the annulus between the wire-wrapped screen and the borehole or between the wire-wrapped screen and the casing using packing fluid, thus forming a gravel pack bed in order to retain reservoir sand to prevent sand from entering into the wellbore and protect the borehole wall.

During gravel pack completion, the stainless steel wire-wrapped screen is generally used, but not the slotted liner. The reasons are as follows.

- (1) The minimum width of the slot opening of the slotted liner is 0.5 mm due to the limitation of cutter strength. Thus, the slotted liner is only suitable for medium-coarse grain reservoirs. However, because the minimum gap width of the wire-wrapped screen is 0.12 mm, its applicable range is much larger.
- (2) The wire-wrapped screen has a continuous gap formed by the wrapping wire, as shown in Figure 2-13(a). There almost is no pressure drop when fluid flows through the screen. The flow cross section of the wire-wrapped screen is trapezoid with a narrow outside and a wide inside, thus providing a certain self-cleaning action so that slight plugging can be dredged by the produced fluid, as shown in Figure 2-13(b and c). The wire-wrapped screen without self-cleaning action is shown in Figure 2-13(d). Their flow areas are much larger than that of the slotted liner (see Figure 2-14).
- (3) The wire used for the wire-wrapped screen is a stainless steel wire with strong corrosion resistance, long service life, and high economic benefits.

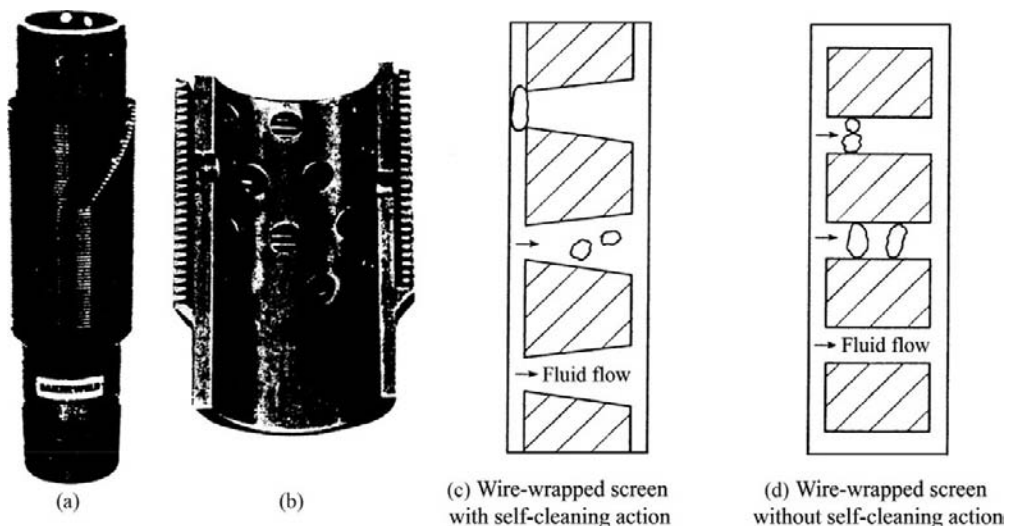
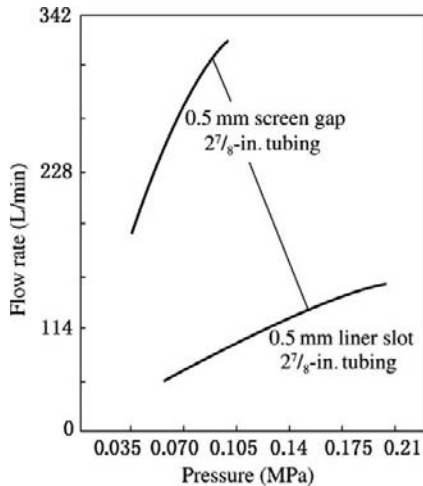


FIGURE 2-13 Wire-wrapped screen cross section.



**FIGURE 2-14** Screen liner throughput capacity comparison diagram.

In order to suit the needs of different oil reservoir characters, open hole gravel pack or casing gravel pack may be selected.

**Open Hole Gravel Pack Completion.** If the geological conditions allow adopting open hole and sand control is needed, open hole gravel pack completion should be applied. The procedure includes drilling to 3 m above the top boundary of the oil reservoir, running intermediate casing, cementing, drilling through the cement plug with a smaller bit, drilling-in the oil reservoir to design depth, changing into the underreaming expansion bit, enlarging the borehole diameter up to 1.5–3.0 times the outside diameter of the intermediate casing in order to ensure a larger annulus during gravel packing, an increased thickness of the sand control bed and an enhanced effectiveness of sand control, and then packing gravel (see Figure 2-15). Generally, the thickness of the gravel bed is not less than 50 mm. Size matching of open hole underreaming is shown in Table 2-2.

Conditions adaptable to open hole gravel pack completion are listed in Table 2-13 later in this chapter.

**Casing Gravel Pack Completion.** The casing gravel pack completion procedure includes drilling through the oil reservoir to design depth, running

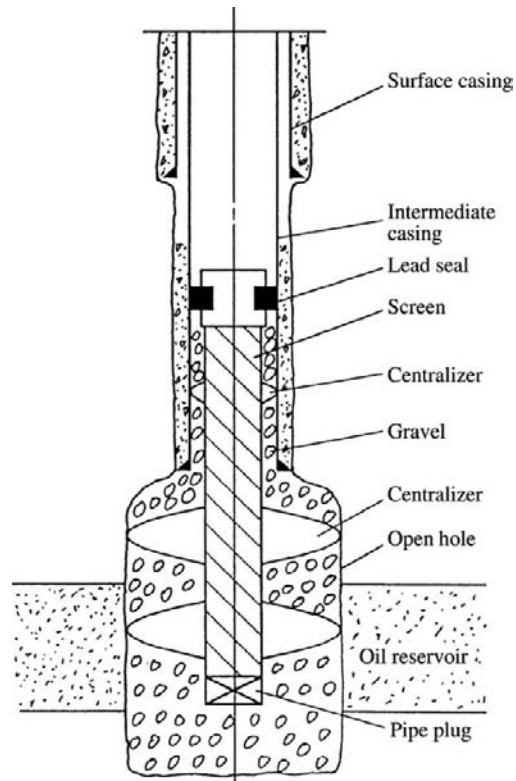


**FIGURE 2-15** Open hole gravel pack completion.

production casing to the bottom of the oil reservoir, cementing, and then perforating the oil reservoir. During perforating, a high perforation density (30–40 perforations/m) and a large perforation diameter (20–25.4 mm) are required in order to increase flow area. Sometimes the reservoir sand outside the casing may be washed out in order to pack gravel into the location of the oil reservoir outside the perforations to avoid mixing of gravel with formation sand and increasing flow resistance. There are two types of packing fluid. One is hydroxyethyl cellulose or polymer. High-density packing is adopted with a gravel-carrying volume ratio up to 96% (12 lb/gal), that is, 1 m<sup>3</sup> fluid should pack 0.96 m<sup>3</sup> gravel. The other is low-viscosity salt water with a gravel-carrying volume ratio of 8–15% (1–2 lb/gal), which can avoid the possible formation damage induced by the high-viscosity, gravel-carrying fluid.

TABLE 2-2 Size Matching of Underreaming for Open Hole Gravel Pack

Casing Size		Small Hole Size		Size of Hole Enlarged		Outside Diameter of Screen	
in.	mm	in.	mm	in.	mm	in.	mm
5 <sup>1</sup> / <sub>2</sub>	139.7	4 <sup>3</sup> / <sub>4</sub>	120.6	12	305	2 <sup>7</sup> / <sub>8</sub>	87
6 <sup>5</sup> / <sub>8</sub> ~7	168.3~177.8	5 <sup>7</sup> / <sub>8</sub> ~6 <sup>1</sup> / <sub>8</sub>	149.2~155.5	12~16	305~407	4~5	117~142
7 <sup>5</sup> / <sub>8</sub> ~8 <sup>5</sup> / <sub>8</sub>	193.7~219.1	6 <sup>1</sup> / <sub>2</sub> ~7 <sup>7</sup> / <sub>8</sub>	165.1~200	14~18	355.6~457.2	5 <sup>1</sup> / <sub>2</sub>	155
9 <sup>5</sup> / <sub>8</sub>	244.5	8 <sup>3</sup> / <sub>4</sub>	222.2	16~20	407~508	6 <sup>5</sup> / <sub>8</sub>	184
10 <sup>3</sup> / <sub>4</sub>	273.1	9 <sup>1</sup> / <sub>2</sub>	241.3	18~20	457.2~508	7	194

Casing gravel pack completion is shown in Figure 2-16. Matching of production casing with a wire-wrapped screen is listed in Table 2-3. Conditions appropriate to casing gravel pack completion are shown in Table 2-13 later in this chapter.

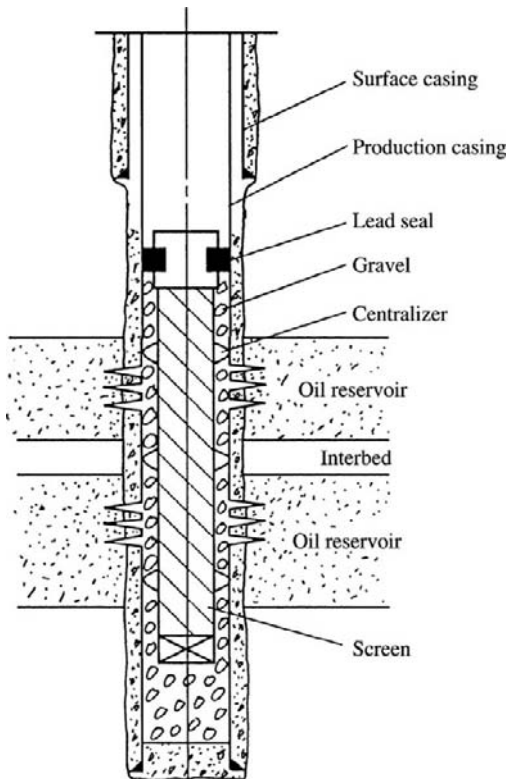


FIGURE 2-16 Casing gravel pack completion.

Both open hole and casing gravel pack completions have the same mechanism of sand control.

Under open hole gravel pack completion, the gravel bed at the bottom of the borehole acts as a sand filter—it only allows fluid to pass through, not formation sand. Under the casing gravel pack completion condition, the wire-wrapped screen matching the grain size of sand produced and the gravel size matching the reservoir rock grain composition should be selected. The selection principle is that not only can reservoir sand be retained, but also the gravel pack bed has a higher permeable property. Therefore, the sizes of wire-wrapped screen and gravel, quality of gravel, performance of packing fluid, packing with gravel ratio (gravel-fluid volume ratio of 0.8–1:1), and operational quality are important successful factors of sand control by gravel pack completion.

TABLE 2-3 Screen Matching with Casing for Gravel Pack Completion

Production Casing Diameter		Outside Diameter of Screen	
mm	in.	mm	in.
139.7	5 <sup>1</sup> / <sub>2</sub>	74	2 <sup>3</sup> / <sub>8</sub>
168.3	6 <sup>5</sup> / <sub>8</sub>	87	2 <sup>7</sup> / <sub>8</sub>
177.8	7	87	2 <sup>7</sup> / <sub>8</sub>
193.7	7 <sup>5</sup> / <sub>8</sub>	104	3 <sup>1</sup> / <sub>2</sub>
219.1	8 <sup>5</sup> / <sub>8</sub>	117	4
244.5	9 <sup>5</sup> / <sub>8</sub>	130	4 <sup>1</sup> / <sub>2</sub>
273.1	10 <sup>3</sup> / <sub>4</sub>	142	5

**Gravel Quality Requirements.** The quality of gravel packed may directly affect the effect of sand control and the productivity after completion. Hence the quality control of gravel is very important. The quality of gravel includes gravel grain diameter selection, qualified degree of gravel size, sphericity and psephicity of gravel, acid solubility of gravel, and strength of gravel.

- (1) Gravel grain diameter selection: The recommended grain diameter of gravel in China and abroad is five to six times the median grain diameter of reservoir sand.
- (2) Qualified degree of gravel size: The API standard of the qualified degree of gravel size is that the content of gravel larger than the required size in the gravel sample should not exceed 0.1%, whereas the content of gravel smaller than the required size should not exceed 2%.
- (3) Strength of gravel: The API standard of the strength of gravel is that the content of crushed gravel measured in the crushing test should not exceed the value shown in Table 2-4.
- (4) Sphericity and psephicity of gravel: The API standard of sphericity and psephicity of gravel is that mean sphericity and psephicity should be greater than 0.6. The visual chart used for appraising sphericity and psephicity is shown in Figure 2-17.
- (5) Acid solubility of gravel: The API standard of acid solubility of gravel is that the weight percentage of gravel dissolved in standard

**TABLE 2-4 Recommended Standard of Crushing Strength of Gravel**

Pack Grain Size (Mesh)	Weight Percentage of Crushed Gravel (%)	Pack Grain Size (Mesh)	Weight Percentage of Crushed Gravel (%)
8~16	8	20~40	2
12~20	4	30~50	2
16~30	2	40~60	2

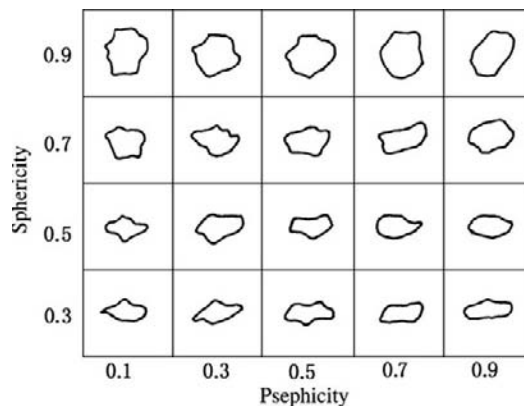


**FIGURE 2-17** Visual chart of sphericity and psephicity.

mud acid (3% HF + 12% HCl) should not exceed 1%.

- (6) Conglomeration of gravel: The API standard stipulates that the gravel should be composed of single quartz sand grain, and the gravel sample should not be used if the gravel sample contains conglomerate gravel grains of 1%.

#### **Wire-Wrapped Screen Gap Size Selection.**

The wire-wrapped screen should ensure the integrity of the gravel pack bed. Thus the wire-wrapped screen gap size should be less than the smallest gravel size in the gravel pack bed, and is normally one-half to two-thirds of the smallest gravel size. For instance, if it is determined that the gravel grain size is 16–30 meshes and the range of gravel size is 0.58–1.19 mm in accordance with the median reservoir sand grain size, the wire-wrapped screen gap size selected should be 0.3–0.38 mm, or taken from Table 2-5.

**Multiple Gravel Pack Technology.** During sand control operation in a well of multiple reservoirs, the reservoir is separated into several intervals in accordance with the requirements of oil reservoir development. The advantage is that the separate-zone control and measure can be achieved by wire and downhole operations during oil well production, thus favoring the water-cut control and the increase in oil well production rate, that is, increasing the recovery factor of the oil field. The segregated sand control methods are as follows.

**TABLE 2-5** Recommended Size Matching of Gravel with Screen Gap

Standard Sieve Mesh	Gravel Size mm	Screen Gap Size	
		mm	in.
40~60	0.419~0.249	0.15	0.006
20~40	0.834~0.419	0.30	0.012
16~30	1.190~0.595	0.35	0.014
10~20	2.010~0.834	0.50	0.020
10~16	2.010~1.190	0.50	0.020
8~12	2.380~1.680	0.75	0.030

### 1. Zone-by-zone gravel packing method

Gravel packing is conducted zone by zone from bottom to top. The operational procedure for each zone is the same as that for a single zone, except that a corresponding plug is set in every packer between zones. The configuration of the plug is shown in Figure 2-18. The plug acts as a temporary bridge plug in order to avoid damage to the lower reservoir, thus operations including pressure testing, perforating, and washing can be conducted above the packer. After perforating of the upper zone, the plug should be pulled out and then a sand control screen is run in. The same operational procedure is conducted zone by zone from bottom to top.

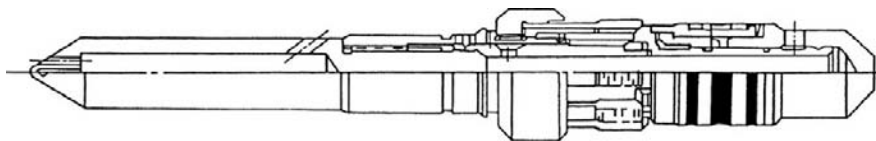
### 2. Once multizone gravel packing method

Once two-zone gravel packing is conducted by one or two trips of string. There are two to eight intervals of oil reservoirs in some oil fields in the South China Sea. Each interval needs sand control. In order to decrease the duration of the packing operation, the sand control method of once two-zone packing by two trips of string is adopted.

The two trips of string mean that the screen and the packer setting tool assembly are run in by the first trip of string and the string is pulled out after all packers are set and checked for sealing; then the second trip of string (gravel packing string) is conducted for sand control of two separate zones (see Figures 2-19 and 2-20). After the lower two zones are packed, packing of the upper interval of the oil reservoir follows.

Fixed downhole tools, setting tool assembly, packing tool assembly, and packing technology are as follows.

- (1) Fixed downhole tools for once two-trip multizone packing include bottom packer and insertion seal assembly, lower zone wire-wrapped screen, blind pipe, isolation packer assembly (location indicating sub, packoff nipple, sliding sleeve, and isolation packer), wire-wrapped screen, blind pipe, and top sand control packer assembly (location indicating sub, packoff nipple, sliding sleeve, packoff nipple, inner seal sleeve, and top sand control packer).
- (2) The setting tool assembly for once two-trip multizone packing includes blind plug, elastic claw indicator, washing pipe, packoff nipple, ported nipple, packoff nipple, washing pipe, and hydraulic setting tool assembly.
- (3) The packing tool assembly for once two-trip multizone packing includes packoff nipple, ported nipple, washing pipe, sliding sleeve switch, washing pipe, elastic claw indicator, washing pipe, adjustable seat with one-way ball, seal elements, circulating nipple, seal elements, washing pipe, limit sub, washing pipe, inner seal sleeve running tool and seal sleeve, and top operation tool.
- (4) Packing technology includes running fixed downhole tools for sand control and setting

**FIGURE 2-18** Plug.

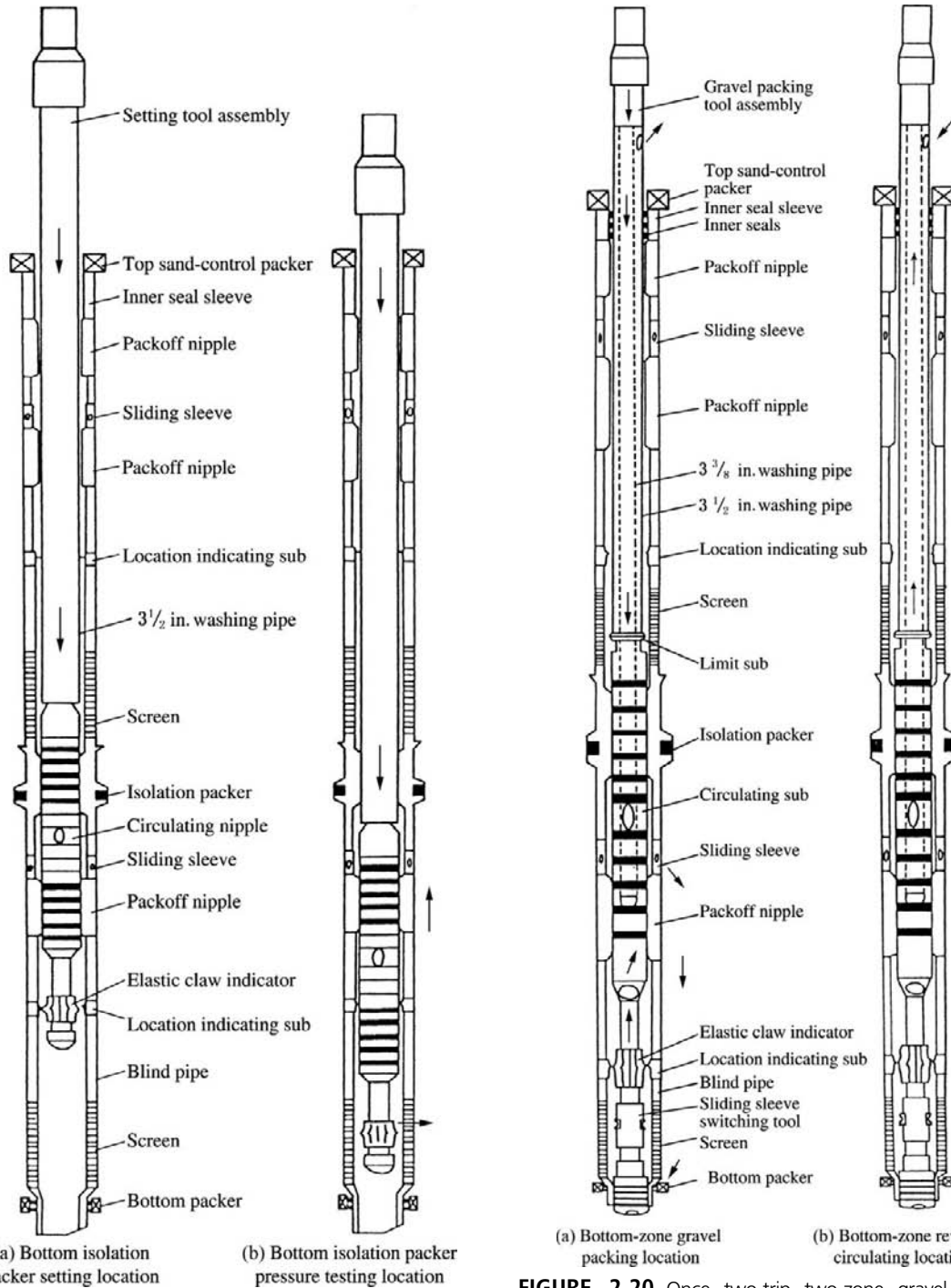


FIGURE 2-19 Once two-trip two-zone packer setting.

FIGURE 2-20 Once two-trip two-zone gravel packing technology.

tool assembly to the predetermined location, dropping the ball, pressurizing and setting the top packer, turning right and pulling up after checked for sealing to release the operation tools, further pulling up to the reverse circulation location, reverse circulating the setting ball out, and then pulling out the setting tool assembly and running in the packing string for separate zone sand control.

Advantages of once one- or two-trip multizone gravel packing include decreasing times of trips, saving operational duration, and favoring economic benefits, especially for a multizone sand control well.

A hydraulic packer without slip is used for interzone isolation. Almost all downhole tools do not need rotating in addition to the only right rotating for releasing after setting of the packer, thus operations in a slant well are safe and reliable.

Case 1. Three-zone sand control completion is applied to the oil reservoirs of some oil fields in the Bohai Sea. The oil reservoirs are Dongying formation sandstones. The reservoir depth is 1450–1700 m. The relative density of crude oil is 0.95–0.96, and the in situ oil viscosity is 70 mPa·s. The length of the oil-bearing section is up to 100–200 m with a low flowing capability of oil wells. During the formation test, an electric submersible pump had been used for determining the production rate. The sand production of the oil well is serious with a sand column height up to more than 20 m in casing. Inside the casing, wire-wrapped screen gravel pack completion is adopted by reason of the long oil-bearing section, multiple oil reservoirs, and serious sand production. The production casing size is 9 5/8 or 7 in. The perforation density is 30 perforations/m. The wire-wrapped screen with an outside diameter of 6.05 in. and an inside diameter of 4.95 in. is run in the 9 5/8-in. casing, while the wire-wrapped screen with an outside diameter of 4.62 in. and an inside diameter of 3.94 in. is run in the 7-in. casing. In accordance with division of the bed set, three zones are packed separately with gravel. A sliding

sleeve is attached for each of the upper two zones. A mandrel for the plug is attached for the lowest zone. If necessary, any zone may be shut in. The tubing diameter is 3 1/2-in. After gravel is packed, an electric submersible pump is run to a depth of 1000 m. The field was put into production in 1993. The initial average individual-well daily production is 100–130 tons/day. The producing pressure differential is 4 MPa. No sand production problems have occurred since the field was put into production more than 10 years ago. The electric submersible pump string with a Y-shaped sub for sand-control separate zone production is shown in Figure 2-21.

Case 2. Multizone sand control string is applied to well completion of some oil fields in the South China Sea. The oil field is located in the water area of the mouth of the Zhujiang River. The water depth is 99 m. The Tertiary Hanjiang and Zhujiang formation oil-bearing series include 27 subzones and are divided into five reservoir groups with a buried depth of 1607–2843.2 m and a length of oil-bearing section of more than 1200 m. The marine sandstone reservoirs have good pore connectivity and an effective permeability up to  $1700\text{--}1800 \times 10^{-3} \mu\text{m}^2$ . The relative density of crude oil is 0.87–0.91. The reservoirs have sand production, whereas the production rate of the oil well is high. In order to develop the oil field effectively, the oil reservoirs are divided into four series of strata. Sand control is applied to each well of every series. Some include up to 11 subzones. Its reservoirs have a total effective thickness of 30.5 m with an individual-layer effective thickness of 1.5–5.4 m and an effective permeability of  $522\text{--}1761.7 \times 10^{-3} \mu\text{m}^2$ . The oil–water interfaces of subzones are not coincident completely. In order to achieve the productivity of each subzone and control the high water cut of the subzone, the 11 subzones of this series of strata are divided into eight sand control zones with packers between sand control zones and with sliding sleeves between packers. Once two-trip multizone gravel pack completion is applied. After that, a high-duty electric submersible pump is run in. Because the oil wells

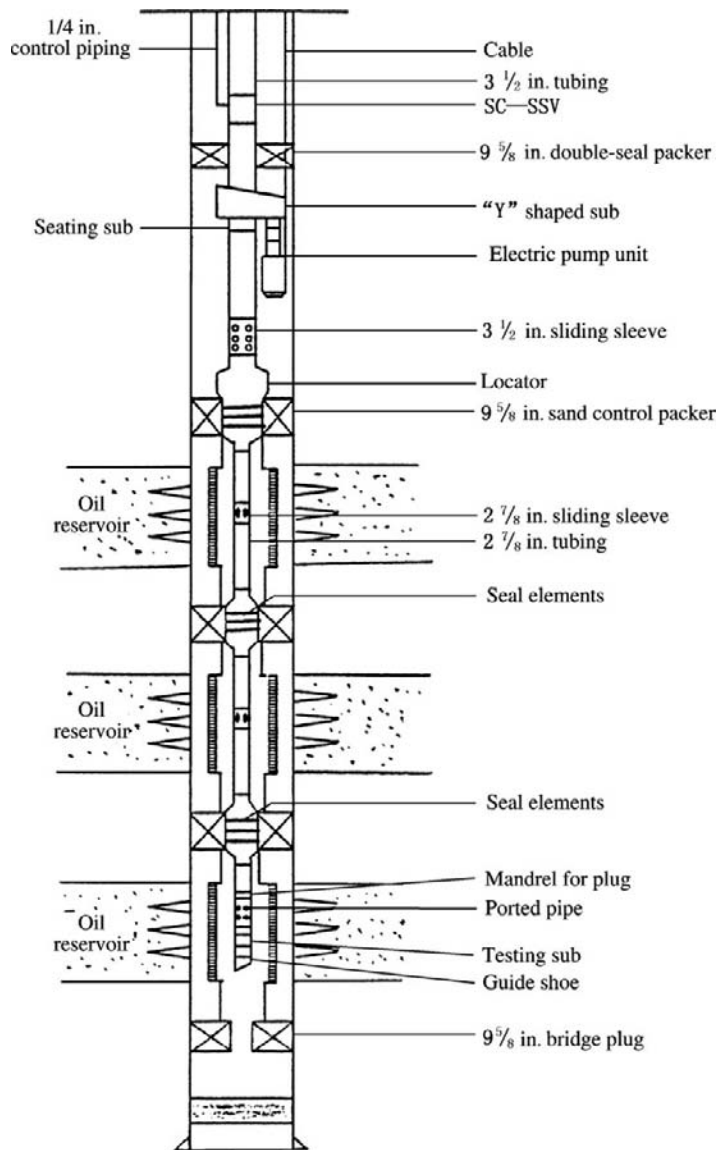


**FIGURE 2-21** Electric submersible pump string with Y-shaped sub for sand control separate-zone production of an oil field in the Bohai Sea.

have flowing capability, the initial flowing daily production is more than  $600 \text{ m}^3/\text{day}$ . After producing for 6 months, using an electric submersible pump, wells produce a daily oil production of  $800\text{--}1000 \text{ m}^3/\text{day}$ . No sand production problems have occurred since the field was put into production about 10 years ago. This proves the good effect of multizone gravel pack sand control. In addition to the function of sand control, this string can be

used for separate-zone production logging to grasp the conditions of production rate, pressure and water cut of each subzone, and for shutting off the sliding sleeve to control and decrease the interference effect of water production interval on oil well production. The multizone sand control string is shown in Figure 2-22.

**Diverter Pipe Gravel Pack Technique.** Diverter pipe gravel pack means changing the path of

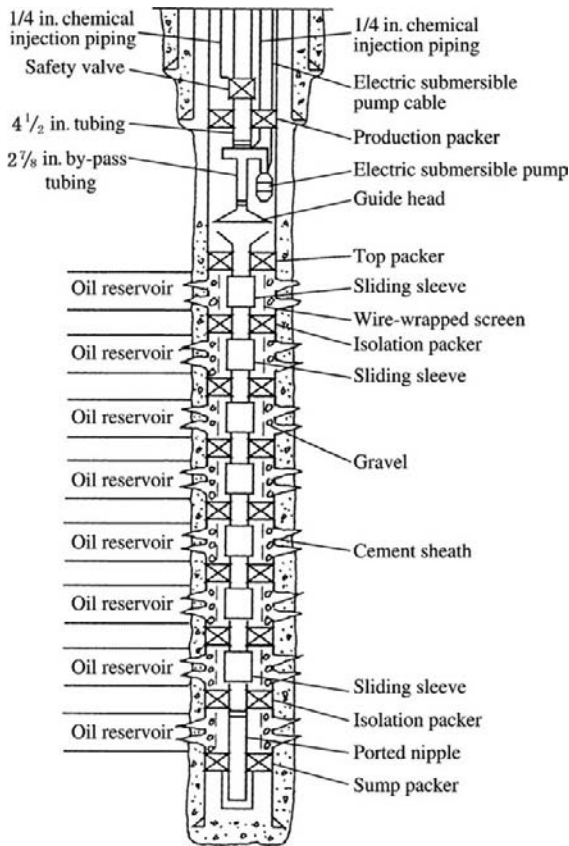


**FIGURE 2-22** Multizone sand control string of some oil field in the South China Sea.

gravel slurry in the gravel pack process using diverter pipes (with nozzles) outside the packing screen so that under the condition of premature sand bridge formation in annulus the caves below the sand bridge can be further packed by the gravel slurry through the nozzles of the diverter pipe. Initially, gravel packing is conducted in accordance with the standard packing mode until screenout of gravel slurry; after that the packing pressure is increased in order to pack the left caves with gravel slurry through the nozzles of the diverter pipes until all the caves are filled. Finally, screenout is generated and tight gravel pack is achieved. The packing operations are finished.

One, two, or three diverter pipes with a rectangular cross section are installed outside the screen. The sizes of diverter pipes are  $1 \times 0.5$  in. (used for gravel packing) or  $1.5 \times 0.75$  in. (used for fracturing). They are connected concentrically or eccentrically to the screen joint. There is a  $1/4$ - or  $3/8$ -in. nozzle in each 6-in. well section on each diverter pipe. These nozzles can be used as paths for further packing the caves below the sand bridge once the sand bridge is prematurely formed in the screen-casing annulus. The cross sections of eccentric and concentric diverter pipes are shown in Figure 2-23. The outside shapes of the screens with diverter pipes are shown in Figure 2-24.

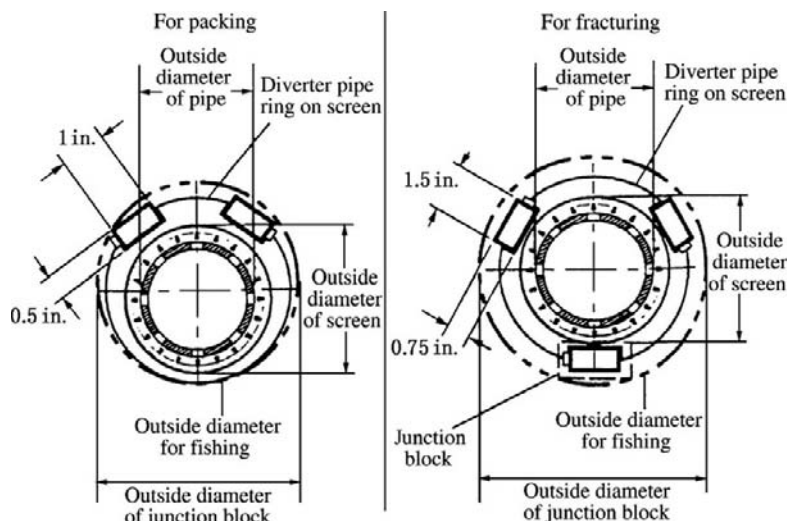


**FIGURE 2-23** Cross sections of eccentric and concentric diverter pipes within casing.

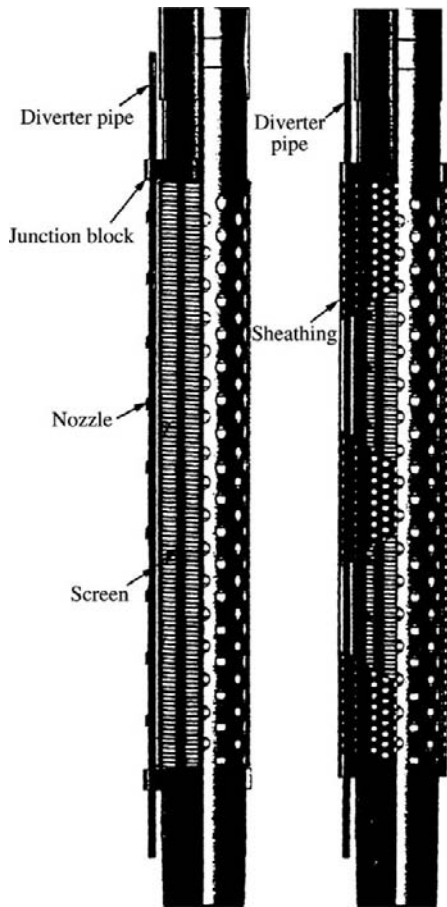


**FIGURE 2-24** Outside shapes of screens with diverter pipes.

The matching unit of the screen with the diverter pipe also includes packers that can pass through the diverter pipe and be used for multizone isolation. This technique, combined with matching downhole tools, can be used for the separate-zone gravel packing and fracturing operations of straight and directional wells and the gravel packing completion operations of a horizontal well, thus achieving a high-quality gravel pack. The investigation indicates that the average quantity of gravel packed outside the casing using this technique is 42 lb/ft, whereas it is only 15 lb/ft using conventional packing technology. The diverter pipe gravel pack technique can achieve a complete pack of perforations and less caves left in the

screen-casing annulus, thus obviously increasing oil well production and prolonging the sand control life of the oil well. In recent years, the diverter pipe gravel pack technique has been applied to sand control of the horizontal well in China and abroad and good results have been achieved.

#### **Hydraulic Fracturing Gravel Pack Technique.**

In recent years, the following two hydraulic fracturing gravel pack techniques have been developed by Baker Hughes: high-rate water gravel pack (HRWP) and tip screenout prepack (TSO-Prepack).

The two techniques use sea water or salt water to fracture oil reservoirs and form short fractures for the gravel pack; which of the two techniques is adopted depends on the type of oil reservoir. Common characters include fracturing the formation damage zone, packing the near-wellbore zone with gravel, and forming a high flow conductivity area. The formation of caves during transporting gravel to long fractures by high-viscosity polymeric carrying fluid and the decrease in fracture conductivity due to incomplete breaking of polymeric carrying fluid are both avoided, and the operation costs are also reduced.

#### 1. Tip screenout fracturing design

The fracture propagation process of tip screenout fracturing includes a normal three-dimensional extension stage before fracture screenout and a one-dimensional fracture width extension stage after screenout. After fracture screenout, the three-dimensional fracture extension becomes the extension in the fracture width direction; at this time the rate of fluid loss from fractures to formation through fractures is obviously decreased, thus leading to an increase in pressure inside fractures and an increase in fracture width growth rate. The calculation procedure of fracturing screenout design is as follows.

- (1) Changes of fracture sizes, fracture generation efficiency, and bottomhole pressure with time are determined by normal three-dimensional fracture simulation before screenout, and discharge capacity and fluid viscosity are optimized.

- (2) The relational fracture length  $L_f$  is selected, and the duration required to achieve this length and the fluid efficiency  $e_{so}$  at this time are determined using the conventional method.
- (3) The starting time of pumping the carrying fluid with low proppant concentration is calculated:

$$t_{fp} = t_{so}[(1 - e_{so})^2 + 5F],$$

where SF is safety factor. The formula also indicates the filtration time of prepad fluid.

- (4) The proppant input ending time  $t_{eoj}$  is determined, and the fluid efficiency  $e_{eoj}$  at this time is calculated.

$$\begin{aligned} \Delta V_f &= q(t_{eoj} - t_{so}) - \Delta V_L \\ e_{eoj} &= (qt_{so}e_{so} + \Delta V_f)/(qt_{eoj}) \end{aligned}$$

where  $\Delta V_f$  is fracture volume increment after screenout and  $\Delta V_L$  is fluid loss after screenout.

- (5) The starting time of pumping the carrying fluid with a high proppant concentration is calculated using  $t_{eoj}$  and  $e_{eoj}$ :

$$t_{ms} = t_{eoj}[(1 - e_{eoj})^2 + 5F]$$

This formula also indicates the ending time of pumping carrying fluid with a low proppant concentration.

- (6) The proppant pack concentration cross section and total proppant weight from  $t_{ms}$  to  $t_{eoj}$  are calculated:

$$C_d(\zeta) = C_{dmax}\zeta^a$$

- (7) The proppant pack concentration in fractures is calculated.
  - (8) The increase in pump pressure during proppant packing is estimated.
  - (9) Design parameters are adjusted and recalculated, and the optimization design is conducted.
2. High-rate water gravel pack

This method is appropriate for oil wells of stratified reservoirs for which sand control is necessary. Before operation, formation pressure is tested in order to prove that formation can be

fractured by sea water or salt water. Then the water is pumped with a high pumping rate of  $1.59 \text{ m}^3/\text{min}$  to fracture the first interval with a fracture length of 1.5–3 m; after that it is followed by pumping a thin gravel slurry with a concentration of  $120\text{--}240 \text{ kg/m}^3$  until tip screenout, thus the pressure increases and the second interval is fractured and packed by self-diversion until the whole perforation section is packed.

By reason of the self-diversion characteristic, a good treatment result of a long well section up to 137 m has been obtained using high-rate water gravel pack. The HRWP process is shown in Figure 2-25.

Case 3. High-rate water gravel pack. The treated well depth is 1188–1322 m, and the bottomhole pressure is 13.098 MPa. Before gravel packing, reservoirs are treated by the acidizing fluid of  $5.7 \text{ m}^3$  (10% hydrochloric acid and 5% acetic acid). The pumping rate is  $1.59 \text{ m}^3/\text{min}$ , the surface pressure is 18.9585 MPa, and 5818 kg of thin gravel slurry with gravel of 40/60 mesh are used. The thickness of production casing is 10.36 mm. Completion fluid of  $\text{CaCl}_2$  type with a density of  $1282 \text{ kg/m}^3$  is used.

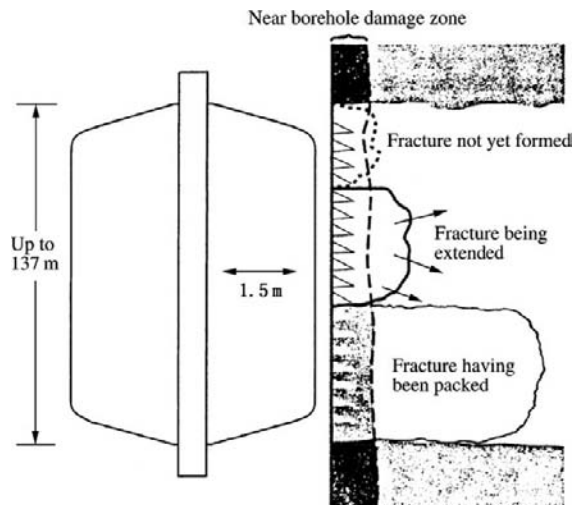


FIGURE 2-25 High-rate water gravel pack process.

After being treated, the oil well has a flowing production rate of 202.2 m<sup>3</sup>/day. The skin factor is  $-2.7$ , and permeability is  $50 \times 10^{-3} \mu\text{m}^2$  in accordance with well test data. The net oil reservoir thickness is 76 m.

### 3. TSO-Prepack

This technique is applicable to oil wells with serious formation damage and a circulation loss, for which HRWP is unsuitable. This method adopts a prepad fluid used for washing the perforations. The calcium carbonate particles and polymeric bridging particles that match the formation pore size are added into the prepad fluid in order to control the fluid loss by reason that a cake can be formed rapidly on the fracture face and fluid loss on the fracture face for fracturing formation is minimized. After a pressure field is established by the prepad fluid, fracture the formation and pump water with a low pumping rate of 0.8 m<sup>3</sup>/min. Then packing with a low proppant concentration of 59.9–287.5 kg/m<sup>3</sup> is applied, and tip screenout is generated, thus forming a propped fracture of 3–6 m. The pack thickness should be less than 30 m. The thicknesses of upper and

lower restraining barriers should not be less than 3 m. During tip screenout of hydraulic fracturing, resin can be added into the tail proppant for wrapping the proppant in order to avoid disgoring proppant after fracturing. Sometimes this technique may be combined with acidizing. This technique is mainly used as pretreatment. After that, the gravel pack is further conducted inside the casing or the well may be put into production after tip screenout. Tip screenout prepack is illustrated in Figure 2-26.

Case 4. Tip screenout prepack. The treated well depth is 516–542 m (vertical depth 445–453 m). The borehole deviation is 73°. The pumping rate is 0.8 m<sup>3</sup>/min. The prepad fluid volume is 11.4 m<sup>3</sup>. The carrying fluid volume is 20.8 m<sup>3</sup>. The carrying fluid concentration is 59.9–287.5 kg/m<sup>3</sup>. The quantity of proppant is 3311 kg. The flowing production rate of the oil well after treating is 159–318 m<sup>3</sup>/day, and the pumping production rate by an electric submersible pump is 127 m<sup>3</sup>/day. Oil well test analysis indicates that the permeability is  $2200 \times 10^{-3} \mu\text{m}^2$ , and the skin factor is 0–6.

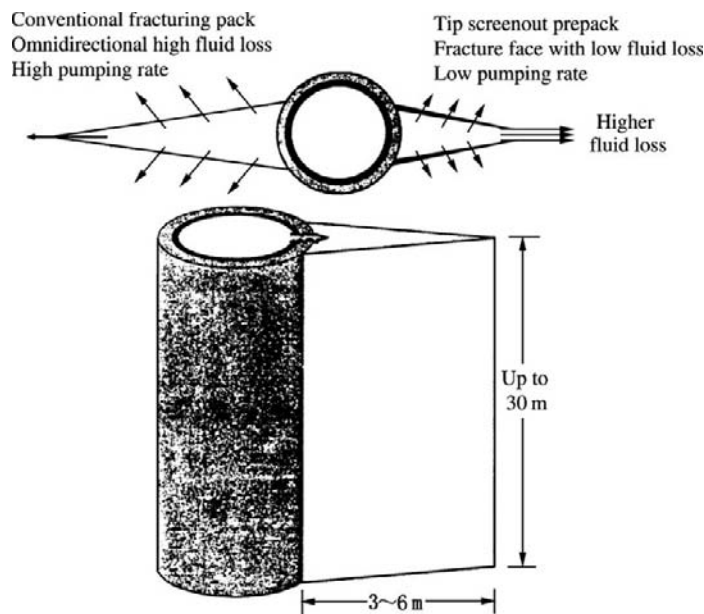


FIGURE 2-26 Tip screenout prepack.

## Other Sand Control Screen Completions

**Precision Millipore Composite Sand Control Screen.** The base pipe is API standard casing or tubing. The sand control filter layer is stainless steel precision Millipore composite filtering material of all-welded construction. This type of screen has good operating performance due to the high permeability, high strength, high deformation resistance, and high corrosion resistance of the composite filtering bed. The precision Millipore composite sand control screen is shown in Figure 2-27. The Millipore composite sand control screen cross section is shown in Figure 2-28.

The precision Millipore screen grid of the multilayer composite sand control filter layer is woven with 316L stainless steel material. This Millipore screen grid is known as a filtering layer. The screen grid with a larger pore, which is woven with the same material, is known as the diffusion layer. A screen grid of a diffusion layer and a screen grid of a filtering layer are overlapped, thus forming a single filtering layer. Then a diffusion layer and a filtering layer are overlapped on the formed single filtering layer. There are four layers of Millipore screen grids altogether. They are welded on the base pipe, thus forming a multilayer composite sand control filter layer.

Features of composite sand control filter layer:

- Large filtrating area (10 times that of slotted screen or wire-wrapped screen), small resistance to flow

- Stable filtering pores with high deformation resistance (the sand control capability is still constant under the condition of radial deformation of 40%), which can meet the servicing requirements of a horizontal well

- Uniform filtering pores, high permeability, high resistance to plugging (the plugging period is two to three times that of common screen); convenience of reverse flushing

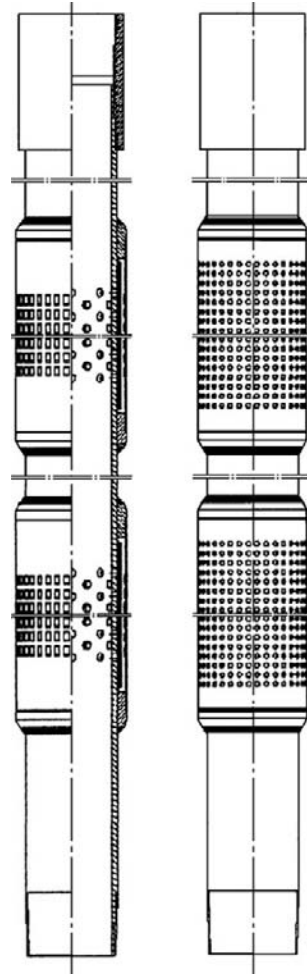


**FIGURE 2-27** Precision Millipore composite sand control screen.

- Small outside diameter, light-weight convenient to be pushed along long-distance horizontal section

Material and anticorrosion performance:

The base pipe of J55 and N80 grade of steel is used for common oil and gas wells. For oil and gas wells with  $H_2S$ ,  $CO_2$ , and high  $Cl^-$  content, anticorrosion casing, tubing or stainless steel pipe is used as the base pipe, and acid-, alkali-, and salt-resistant quality stainless steel material is used for the sand control filter layer and outside protective sleeve.

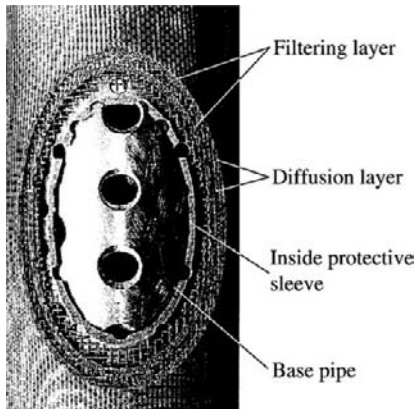


**FIGURE 2-28** Millipore composite sand control screen cross section.

Filtration accuracy and technical parameters of sand control screen:

The filtration accuracy can be determined by the composition of formation sand or user's requirement (see Table 2-6). The

technical parameters of sand control screen are shown in Table 2-7.

**Precision Punched Screen.** This screen is composed of the base pipe, stainless steel punched filtering screen, and support ring. The base pipe is a perforated API standard casing or tubing. The high-density spatial slots on the quality stainless steel punched filtering screen are formed using computerized precision punching technology. The punched filtering screen and the base pipe are welded into a hole through the bearing ring. During production, formation sand is retained outside the punched filtering screen, whereas formation fluid enters the screen through the punched slot clearance, thus achieving sand control. In accordance with practical requirements, an outside protective sleeve can also be added outside the punched filtering screen in order to strengthen protection of the punched filtering screen. The punched screen structure is shown in Figure 2-29.

**TABLE 2-6** Filtration Accuracy

Sand control media	WF60	WF80	WF100	WF120	WF160	WF200	WF250	WF300	WF350
Filtration precision ( $\mu\text{m}$ )	60	80	100	120	160	200	250	300	350

**TABLE 2-7** Technical Parameters of Sand Control Screen

Base Pipe	Precision Millipore Composite Filter Layer		Stainless Steel Fiber Composite Filter Layer	
	Weight per Meter (kg/m)	Outside Diameter	Weight per Meter (kg/m)	Outside Diameter
Size				
2 <sup>3</sup> / <sub>4</sub> in.	6.85	3 in. (76 mm)	12	3.5 in. (89 mm)
2 <sup>7</sup> / <sub>8</sub> in.	9.54	3.5 in. (89 mm)	15	4 in. (102 mm)
3 <sup>1</sup> / <sub>2</sub> in.	13.7	4.3 in. (108 mm)	20	4.9 in. (124 mm)
4 in.	14.2	4.9 in. (124 mm)	22	5.4 in. (138 mm)
4 <sup>1</sup> / <sub>2</sub> in.	17.3	5.3 in. (135 mm)	25	5.9 in. (150 mm)
5 in.	22.4	5.9 in. (150 mm)	30	6.4 in. (162 mm)
5 <sup>1</sup> / <sub>2</sub> in.	25.3	6.3 in. (159 mm)	35	6.9 in. (175 mm)
6 <sup>5</sup> / <sub>8</sub> in.	35.8	7.3 in. (188 mm)	46	8 in. (203 mm)
7 in.	38.7	7.7 in. (196 mm)	50	
Length (m)	5~5.3	Filtration section length 4 m × 1		
	9.3~9.6	Filtration section length 4 m × 2		

Note: The base pipe length can be determined by user's requirement.



**FIGURE 2-29** Punched screen structure.

Features of the punched screen are as follows.

- (1) Precision controllable gap. The gap width can be controlled precisely in the range of 0.15–0.8 mm. The precision of gap width is  $\pm 0.02$  mm. It can match well with the formation sand of different grain size composition, thus meeting sand control requirements.
- (2) High corrosion resistance. The stainless steel punched filtering screen can be resistant to acid, alkali, and salt corrosions and can meet the special requirements of oil and gas wells with  $H_2S$ ,  $CO_2$ , and high  $Cl^-$  content. The gap will not widen due to corrosion under the long-term use condition.
- (3) High integral strength and deformation resistance. The punched filtering screen is sustained by the base pipe inside. In accordance with requirements, an outside protective sleeve can be added. The integral strength of the perforated base pipe is decreased by only a matter of 2–3% as compared with that of standard casing and tubing. It has enough strength for the compressive deformation of formation.

- (4) High-density gaps and low resistance to flow. The gap density is three to five times that of a common slotted screen. The low resistance to flow is favorable for increasing oil and gas well production. The filtration precision of the punched screen is shown in Table 2-8. The technical parameters of the punched screen are listed in Table 2-9.

Sand control performance comparison among wire-wrapped screen, slotted screen, metallic fiber screen, precision Millipore composite screen, and precision punched screen is shown in Table 2-10.

**STARS Star Pore Screen.** This screen has been applied to horizontal branch holes of the Suizhong 36-1 oil field in the Bohai Sea, directional wells of the Luda 10-1 and Penglai 19-3 oil fields, and horizontal wells of the Wei 11-4 oil field in the western South China Sea, and good results have been achieved.

#### 1. Features of STARS star pore screen

Technical features of the STARS star pore screen include unique structured design, simple operation, operational safety and reliability, broad applicable range, and good sand control results. Outside configuration of the STARS star pore screen is shown in Figure 2-30.

- (1) Structure is similar to that of tubing or casing. No welding seam. High strength and deformation resistance.
- (2) Filter medium units sink into the surface of the base pipe and are not easily damaged with safety and reliability.
- (3) There is no sandwich space in the whole screen, and sand accumulation is avoided within the screen.
- (4) Because the flow filter units are distributed uniformly on the whole screen, a blind pipe end will not be reserved, thus the tripping operations are not influenced.

**TABLE 2-8** Filtration Precision of Punched Screen

Gap width of filtering screen (mm)	0.15	0.20	0.25	0.30	0.35	0.40	0.45	0.50	0.60	0.70	0.80
Filtration precision (mm)	150	200	250	300	350	400	450	500	600	700	800

Note: Filtration precision can be determined by formation sand grain size composition or user's requirement.

TABLE 2-9 Technical Parameters of Punched Screen

Base Pipe			Precision Punched Screen		
Size		Weight per Meter (kg/m)	Maximum Outside Diameter	Weight per Meter (kg/m)	Filtration Precision
2 <sup>3</sup> / <sub>8</sub> in.	60.3 mm	6.85	66 mm	7.90	150~800 μm
2 <sup>7</sup> / <sub>8</sub> in.	73 mm	9.54	80 mm	10.9	150~800 μm
3 <sup>1</sup> / <sub>2</sub> in.	88.9 mm	13.7	96 mm	15.5	150~800 μm
4 in.	101.6 mm	14.2	109 mm	16.3	150~800 μm
4 <sup>1</sup> / <sub>2</sub> in.	114.3 mm	17.3	121 mm	19.9	150~800 μm
5 in.	127 mm	22.4	134 mm	25.8	150~800 μm
5 <sup>1</sup> / <sub>2</sub> in.	139.7 mm	25.3	147 mm	29.1	150~800 μm
6 <sup>5</sup> / <sub>8</sub> in.	168.3 mm	35.8	175 mm	41.2	150~800 μm
7 in.	177.8 mm	38.7	185 mm	44.5	150~800 μm
Base pipe length, m		4.8~5.0		Filtration section length 4 m × 1	
		9.3~9.6		Filtration section length 4 m × 2	

Note: The base pipe length and filtration precision can be determined in accordance with user's requirement.

- (5) It is applicable to vertical, directional, horizontal, side-tracked, and multibore wells due to being light weight, ease of running in, and wide sand control range. In addition, its features also include small frictional resistance to flow, high unit permeability, small pressure loss, and erosion resistance due to buffering flow.
- (6) Pores can be distributed with gradation or variable density, thus maximizing the oil and gas well capacity of horizontal sections.
- (7) Good sand controllability due to self-removal of blocking under varying pressure differentials.
- (8) Short operation period and low integrated costs.

## 2. STARS star pore screen structure

Single-layer, thick-walled quality stainless steel pipe, tubing, or casing can be used as the base pipe of a STARS star pore screen. There are step-type pores on the base pipe. The filter units are made of SS304 or SS316 and threaded into the pipe pores. The integral structure is similar to tubing or casing, as shown in Figure 2-31.

The filter units of a STARS star pore screen are relatively independent. They consist of housing, inside and outside support nets, filtering net, and gasket. There are various types of filter units dependent on filtering material. Presently, widely used filter units include metallic fiber and woven filter units. The minimum filtration precision is 60 μm.

## STARS Composite Screen

### 1. Features of STARS composite screen

The STARS composite screen has high permeability, strength, deformation resistance, and corrosion resistance and can be applied to sand control of open hole or perforated oil and gas wells and water injection wells.

- (1) The STARS composite screen is convenient for downhole operations due to being light weight and having good permeability.
- (2) The STARS composite screen is not inferior to steel pipe in pliability. The radial deformation during running in can be up to 65%, while the torsional and bending deformations are less than 1°/m.
- (3) The integral tensile and compressive strengths of sand control pipe are not less than 90% of that of base pipe.

<b>Performance Index</b>	<b>Wire-Wrapped Screen</b>	<b>Slotted Screen</b>	<b>Metallic Fiber Screen</b>	<b>Precision Millipore Composite Screen</b>	<b>Precision Punched Screen</b>
Filtration area percentage	≈3%	2~3%	80~85%	80~85%	4~6%
Filtering pore size precision	Excellent error ±30 μm	Medium error ±50–100 μm	Poor error >200 μm	Excellent error ±7 μm	Excellent error ±30 μm
Filtering pore instability	Stable	Unstable, slot width increased due to corrosion	Unstable, filtering pore deformed due to compression	Stable	Stable
Filtration precision controllability	Difficult to control when <200 μm	Difficult to control when <200 μm	Uncontrollable	Precise control when 60–400 μm	Controllable when >500 μm
Collapse resistance	Poor	Poor	Medium	Excellent	Excellent
Slot corrosion resistance	Good	Poor	Good	Excellent	Excellent
Sand control reliability	Good	Poor	Poor	Good	Good
Resistance to plugging	Medium	Medium	Good	Excellent	Medium
Adaptability to horizontal well	Unadaptable to horizontal well, variable slot width during pushing along horizontal section	Basically adaptable to horizontal well, mostly applicable to formation with slight sand production	Unadaptable to horizontal well due to large outside diameter	Adaptable to horizontal well, easy to be run in and pushed due to outside protective sleeve	Adaptable to horizontal well, easy to be run in due to compact structure and light weight
Sand control life	Long	Short	Shorter	Long	Long
Economy	Excellent	Excellent	Good	Excellent	Excellent

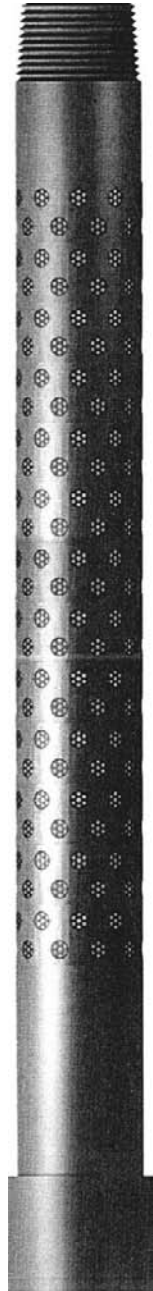


**FIGURE 2-30** Outside configuration of a STARS pore screen.

- (4) Good corrosion resistance, including resistances to acid, alkali, and salt. For oil and gas wells and water injection wells containing corrosive fluid, anticorrosive and

hydrogen sulfide resisting casing or tubing can be used for the base pipe of the screen, and the whole screen and its components can be made of stainless steel.

- (5) Each layer of the filtering net of the composite screen is welded, and the weld strength of the soldering point is equal to or even higher than the strength of each layer.
- (6) The STARS composite screen has a large flow area, and coverage of the filtering net on the base pipe is up to 70%, thus it decreases producing pressure differential and friction loss and is applicable to heavy oil reservoirs.
- (7) The composite screen adopts a multilayer filtering net. Even if one of the layers is damaged, the other layers can still maintain the filtering effect and normal production.
- (8) The shoulder and base pipe should be connected by socket head bolts and then surface welded in order to avoid slippage at welds due to corrosion, thus application of the screen in wells containing  $H_2S$ ,  $CO_2$ , or a high content of  $Cl^-$  is safer and more reliable. Especially for 13 Cr or other materials with a higher content of alloy, the strength at the connection of the shoulder with the base pipe is further ensured by fastening with a socket head bolt and further surface welding.

The outside drawing of a STAR composite screen is shown in Figure 2-32.

## 2. STAR composite screen structure

A STAR composite screen consists mainly of a base pipe, inner and outer support nets, a filtering net, and an outside protection pipe. The materials of the inner and outer support nets and filtering net are SS304 or SS316 stainless steel. The outside protection pipe material is stainless steel. The STAR composite screen structure is shown in Figure 2-33. The outside protection pipe is used for protecting the inner and outer support nets and filtering net during installing and bearing negative pressure. The outer support net provides

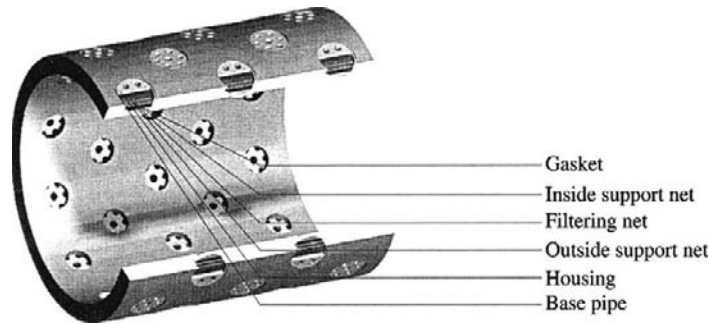


FIGURE 2-31 STARS star pore screen structure.

uniformly distributed fluid flow. The filtering net can meet the requirements of controlling sand of coarse, medium, and fine sizes. The inner support net is wrapped on the base pipe and the seam is welded longitudinally. The filtering net provides uniformly distributed fluid flow for the base pipe. The base pipe is made of API standard casing or tubing, and the holes are distributed evenly in accordance with a specific rule. The minimum degree of precision is 60  $\mu\text{m}$ .

**Prepacked Gravel Wire-Wrapped Screen.** The prepacked gravel wire-wrapped screen is a sand control screen in which gravel conformable to reservoir properties is prepacked into the annulus between inner and outer wire-wrapped screens. The screen is run to the sand production horizon. Oil well productivity using this sand control method is lower than that of downhole gravel pack, and the valid period is not as long as that of the gravel pack method by reason that the prepacked gravel wire-wrapped screen sand control method can only prevent the reservoir sand after entering the wellbore from further entering the tubing. (The gravel pack sand control method can prevent reservoir sand from entering the wellbore.) However, due to convenient technology and low cost, it is still an effective method for wells in which the gravel pack sand control method cannot be adopted. Therefore, it is commonly used abroad, especially in horizontal wells. The structure is shown in Figure 2-34.

The selections of the prepack gravel grain size and the gap between inner and outer wire-wrapped

screens are the same as those of downhole gravel pack. The difference between the outside diameter of the outer screen and the internal diameter of the casing should be small to the full extent and is normally about 10 mm in order to increase the thickness of the prepacked gravel layer, thus enhancing the sand control effectiveness. A prepacked gravel layer thickness of about 25 mm should be ensured. The inside diameter of the inner screen should be more than 2 mm larger than the outside diameter of the central pipe in order to be installed smoothly on the central pipe.

**Metallic Fiber Sand Control Screen.** There are two types of metallic fiber sand control screens: the sand control screen of roll-formed metallic fiber and the sand control screen of sintered metallic fiber.

#### 1. Sand control screen of roll-formed metallic fiber

The basic structure is shown in Figure 2-35. The main sand control material is the wire-cut and mixed stainless steel fiber, which is then rolled, carded, and formed. The sand control principle is that when bulk fibers accumulate together, some gaps form in between and the formation sand grains are retained. The gap size is related to the compactedness of the cumulated fiber. The sand control of different diameter reservoir sand grains is achieved by controlling the metallic fiber gap size, that is, the fiber compactedness. However, the metallic fiber has elasticity and the small sand grains can pass through the gaps under some driving force, thus avoiding plugging up.

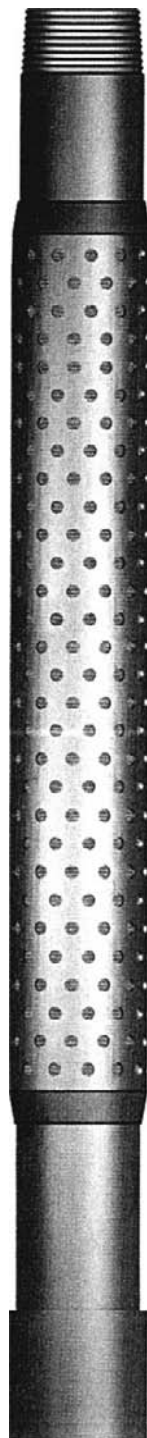


FIGURE 2-32 STARS composite screen.

The fiber can resume to its former state and the self-cleaning effect can be achieved.

Under steam injection oil production, the high temperature (360°C), high pressure (18.9 MPa) and corrosion (pK 8–12)-resistant sand control tools are required and stainless steel fiber can meet these requirements.

In the Liaohe oil field, the wire diameter of the stainless steel fiber that is used is 50–120  $\mu\text{m}$ , the fiber filtering layer thickness is 15–25 mm, and the compressibility is 22–28  $\text{MPa}^{-1}$ . The fiber filtering layer permeability is greater than 1000  $\mu\text{m}^2$ , the porosity is greater than 90%, and the sand production is not greater than 0.01%. The screen is applicable to sand control of open hole, casing, vertical, and horizontal wells.

## 2. Sintered metallic fiber sand control screen

Tubing or casing may be used as the base pipe of a sintered metallic fiber sand control screen. The base pipe is perforated in accordance with a specific rule, and the metallic fiber is sintered on the perforated base pipe, thus forming a spatial cellular filtering shield. Crude oil and fine silt smaller than 0.07 mm can pass through the metallic fiber. The fine silt is carried away from the wellbore by the oil flow, whereas the coarse sand grains with a larger diameter are retained outside the screen, thus forming a sand-retaining barrier and achieving the sand control goal. The technical characteristic indices of sintered metallic fiber screen are listed in Table 2-11.

This sand control string is not only applicable to the sand control of various oil and gas wells and water injection wells, which are casing completed vertical, directional, side-tracking, or horizontal wells, but also applicable to the sand control of various open hole wells.

## External Guide Housing Sand Filtering Screen.

The external guide housing sand filtering screen is a combination of a wire-wrapped screen and a sand screen. It has not only the performance of a wire-wrapped prepack screen, but the performance of a sand screen, thus surpassing the

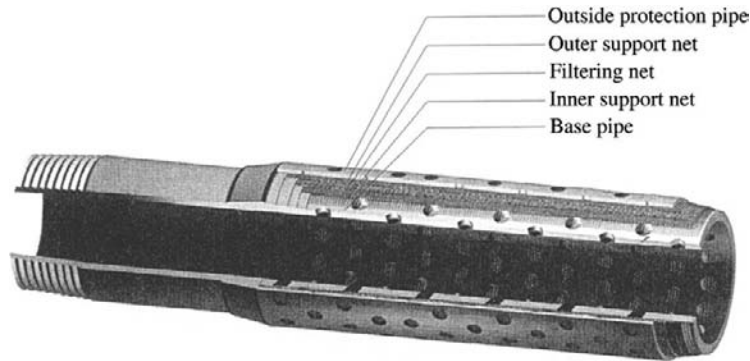


FIGURE 2-33 STARS composite screen structure.

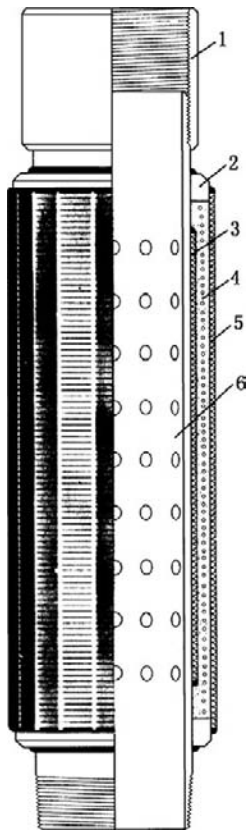


FIGURE 2-34 Prepacked gravel wire-wrapped screen: 1, collar; 2, gland; 3, inner wire-wrapped screen; 4, gravel; 5, outer wire-wrapped screen; and 6, central pipe.

performance of each. From inside to outside the sand filtering screen consists of a perforated base pipe, wire-wrapped screen, net sleeve woven with thin steel wire, and external guide housing

used for protecting the sand filtering screen. This structure provides optional productivity and prolongs the life of the screen. It is applicable to the vertical and horizontal wells of casing perforation or open hole completion. The external guide housing the sand filtering screen is shown in Figure 2-36.

#### 1. External guide housing

The external guide housing protects the screen and guiding. It can prevent borehole debris and casing burr from damaging the screen. When the well is put into production, the guide housing inflow structure can change the flow direction of the produced formation fluid with sand, thus mitigating screen erosion and prolonging the screen life. The external guide housing structure is shown in Figure 2-37.

#### 2. Sand filtering net sleeve woven with thin steel wire

The inflow area of the sand filtering net sleeve woven with thin steel wire is 11 times as large as that of the prepack screen. It provides the maximum inflow area and uniform pore throats, which help form permeable cake. In addition, the changing of the sand carrying fluid flow direction once more decreases screen erosion. Furthermore, this sand filtering net sleeve can be backwashed in order to remove the fine sand and cake adsorbed on the sand filtering net sleeve. The sand filtering net sleeve woven with thin steel wire and the wire-wrapped screen are shown in Figure 2-38.

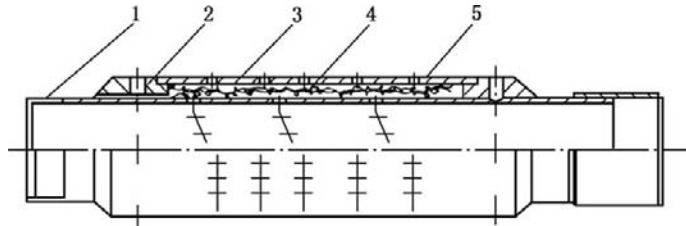


**FIGURE 2-35** Roll-formed metallic fiber sand control screen structure: 1, base pipe; 2, bulkhead; 3, protection pipe; 4, metallic fiber; and 5, metallic net.

**TABLE 2-11** Technical Characteristic Indices of Sintered Metallic Fiber Screen

Type	Minimum Bore Diameter (mm)	Permeability ( $\mu\text{m}^2$ )	Sand Retaining Grain Size (mm)	Internal Pressure Strength (MPa)	External Pressure Strength (MPa)	Flow Area ( $\text{cm}^2/\text{m}$ )	Temperature Resistance ( $^{\circ}\text{C}$ )	Remarks
$\phi 168$ mm	$\phi 140$	38~120	Over 0.07	22	35	286	350	Horizontal well
$\phi 148$ mm	$\phi 120$	32~120	Over 0.07	22	35	267	350	7-in. well
$\phi 108$ mm	$\phi 82$	28~65	Over 0.07	20	32	260	350	5 1/2 in.
$\phi 102$ mm	$\phi 78$	38~80	Over 0.07	20	32	254	350	Side-tracked hole
$\phi 102$ mm	$\phi 82$	38~65	Over 0.07	18	28	254	350	Sand anchor
$\phi 89$ mm	$\phi 68$	24~52	Over 0.07	18	32	205	350	Sand anchor

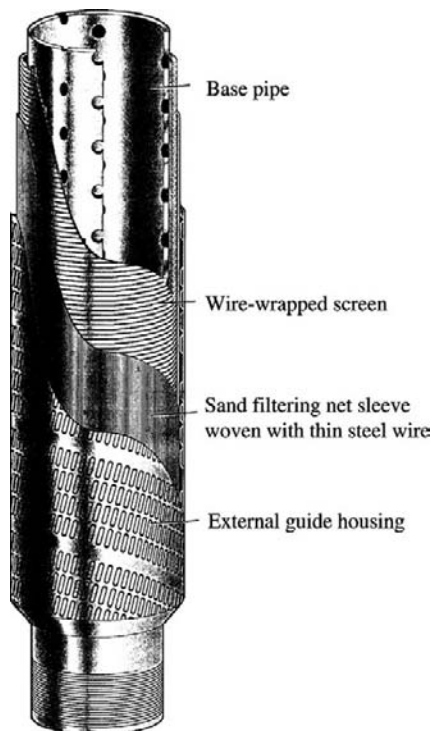


**FIGURE 2-36** External guide housing sand filtering screen.

### 3. Wire-wrapped screen

The formation fluid first enters the internal guide housing, passes through the sand filtering net sleeve woven with thin steel wire, and finally passes through the wire-wrapped screen. The sand carried by the formation fluid is retained outside the sand control screen. The fluid enters the central pipe of the screen through the holes, then enters tubing, and finally flows to the surface. The wire-wrapped screen is also welded to the frame the same as the former wire-wrapped screen. However, the cross section of the wire is circular but not trapezoidal. Therefore, the whole circular surface area can be fully used and the fluid flow is diverted, thus mitigating erosion and prolonging the service life.

The technical specifications are the following: wire spacing 25  $\mu\text{m}$ ; destructive strength up to 41.4 MPa; tensile elongation 2%; crush diameter up to 60% of original diameter; torque test torsion 3.3 $^{\circ}/\text{m}$ .

This screen, which improves the structure, material, and manufacturing technology, can be used for controlling coarse, medium, and

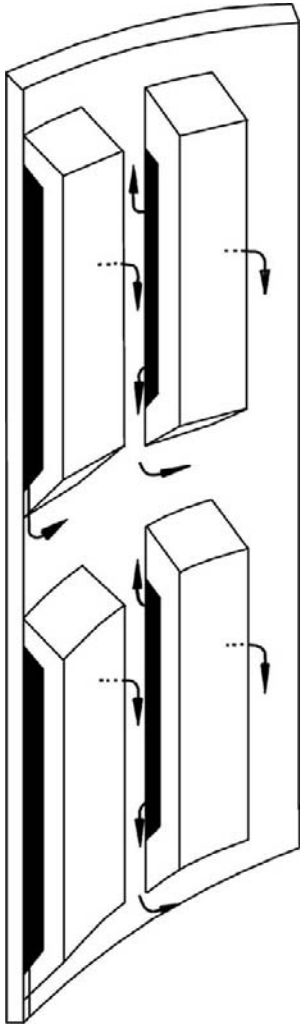


**FIGURE 2-37** External guide housing.

fine sand, and the sand control effectiveness and service life are improved.

The directional well completion mode is basically the same as that of the straight well by reason that the deviation angle of the directional well is generally about  $50^\circ$ .

### Chemical Sand Consolidation Well Completion

The chemical sand consolidation process includes mixing the binding agent (cement slurry or phenolaldehyde resin, etc.), pore retaining agent



**FIGURE 2-38** A sand filtering net sleeve woven with thin steel wire and a wire-wrapped screen.

(light oil), and supporting agent (rigid grains, such as quartz sand, walnut hull) uniformly in a specific proportion, squeezing the mixture outside the casing, and accumulating it at the sand production horizon. After setting, the mixture forms an artificial borehole wall with a specific strength and permeability, thus preventing the reservoir from producing sand, or the supporting agent is not added, the binding agent is squeezed directly into the sand producing reservoir outside the casing, and the unconsolidated sandstone is firmly consolidated, thus preventing the reservoir from producing sand. In accordance with the features of a thermal production well of heavy oil, a high-strength sand consolidating agent (Liaohe No.5) and high-temperature foam resin for controlling fine silt are obtained by testing and the artificial borehole wall sand control of the thermal

production well is achieved and broadly applied in the Liaohe oil field, and good results have been obtained. In addition, the subsurface-synthesized phenolaldehyde resin sand control technique developed at the Shengli oil field and the fine silt control technique using the chemical sand consolidating agent formulated with polymer, etc., by the Canadian Alberta Research Center (ARC) have been applied successfully to sand control in oil fields.

Despite a sand control method, chemical sand consolidation has limitations of use. It is only applicable to the sand control of a single and thin bed of about 5 m thick and is not applicable to sand control of a thick bed and long well section. The applicable range and advantages and disadvantages are listed in Table 2-12. The applicable conditions of various well completion methods are listed in Table 2-13.

### Fiber Complex Fine Silt Control Completion

The fiber complex fine silt control technique has been applied in the Sebei gas field in Qinghai, the Shengli Gudao oil field, and the heavy oil thermal production wells in the Liaohe oil field since 2001 and good results have been obtained.

Reservoirs of the Sebei gas field in Qinghai are mainly quaternary siltstone and argillaceous siltstone with loose consolidation, low diagenetic grade, high clay content, high shale content, high salinity, strong sensitivity, and serious silt production. The produced fine silt has a grain size of 0.04–0.07 mm. Conventional sand control techniques have no effect or only very poor results, thus restricting seriously the highly effective development of this gas field. Laboratory tests and field applications of the fiber complex fine silt technique have obtained obvious effects.

**Fiber Complex Fine Silt Control Principle.** The fiber complex fine silt control technique uses two types of fiber. One is the soft fiber used for stabilizing silt, which changes fine silt to larger aggregates of fine silt. The other is the hard fiber used for retaining silt. The hard fiber and the resin-wrapped sand form a complex retaining silt and preventing silt from entering the wellbore.

The soft fiber is a long-chain cationic polymer with a branched chain. The branched chain has a cationic gene. This soft fiber may expand naturally due to the electrical behavior effect in aqueous solution. When the soft fiber enters the reservoir, the branched chain with a positive charge in soft fiber will adsorb the fine silt in the reservoir to become a larger fine silt aggregate similar to large grain, thus decreasing the starting speed of fine silt and increasing the critical flow velocity of fine silt, which will stabilize and consolidate the silt to some extent and achieve fine silt control.

The hard fiber is a special silt control fiber, which is woven by using crook, crimp, and spiral intersection of the tailored hard fiber to form a stable three-dimensional reticulated structure and bind up the sand grains in it, thus forming a firm filtration body with a specific permeability and achieving silt control. The hard fiber silt control principle is shown in Figure 2-39.

The reservoir of the Sebei gas field is ooze sandstone with poor consolidation and serious fine silt production. When the reservoir is being fractured along the maximum principal stress, the fiber mixture is packed around the borehole, a pack ring is formed, all perforations in the borehole are plugged, and a quasi-screen is formed, thus achieving the effects similar to that of a pack screen and the goal of fine silt control. The pack ring around the borehole and the man-made fracture are shown in Figure 2-40.

### Fiber Complex Silt Control Stimulation Principle

#### 1. Removing original formation damage

It is unavoidable that the reservoir may be damaged to some extent during drilling, well completion, formation testing, and well workover, thus impairing well productivity. Therefore, two procedures should be considered for removing formation damage during the fiber complex sand control application. First, the reservoir is treated with organic acid to dissolve the acid-soluble minerals in the reservoir and the foreign invasion material, thus the reservoir permeability is improved and near-wellbore formation damage is removed.

TABLE 2-12 Chemical Sand Consolidation Method Selection Reference

Method	Binding Agent	Supporting Agent	Formulation (Weight Ratio)	Applicable Range	Advantages and Disadvantages
Sand-cement slurry artificial borehole wall	Cement slurry	Quartz sand	Cement:water:quartz sand = 1:0.5:4	Later sand control of oil production and water injection wells Sand control of low pressure and shallow wells	Wide material source, low strength, short valid period
Water-cement-sand artificial borehole wall	Cement	Quartz sand	Cement:quartz sand = 1:2–2.5	Later sand control of high water cut oil well and water injection well Low pressure oil production and water injection wells	Wide material source, low cost, serious plug
Diesel oil-cement slurry emulsion artificial borehole wall	Diesel oil-cement slurry emulsion		Diesel oil:cement:water = 1:1:0.5	Initial sand control of oil production and water injection wells Less sand production	Wide material source, low cost, serious plug
Phenol aldehyde resin artificial borehole wall	Phenol aldehyde resin solution		Phenol:formaldehyde:ammonia water = 1:1.5:0.05	Initial and early sand control of oil production and water injection wells Sand control of medium and coarse sandstone reservoirs	Strong adaptability, high cost, short resin storage life
Resin walnut hull artificial borehole wall	Phenol aldehyde resin	Walnut hull	Resin:walnut hull = 1:1.5	Early and later sand control of oil production and water injection wells Less sand production	High binding strength, high permeability, good sand control effectiveness, difficult material source, complicated operation
Sand-resin slurry artificial borehole wall	Phenol aldehyde resin	Quartz sand	Resin:quartz sand = 1:4	Later sand control of oil production and water injection wells	High binding strength, strong adaptability, complicated operation
Phenol aldehyde solution subsurface synthesis	Phenol aldehyde solution		Phenol:formaldehyde:hardening agent = 1:2:0.3–0.36	Initial and early sand control of oil production and water injection wells with reservoir temperature above 60°C	Low solution viscosity, easy to be squeezed into reservoir, able to be used for separate-layer sand control
Resin coating gravel artificial borehole wall	Epoxy resin	Quartz sand	Resin:gravel = 1:10–20	Early and later sand control of oil production and water injection wells with reservoir temperature above 60°C	High permeability, high strength, simple operation

**TABLE 2-13 Geological Conditions Suitable for Various Well Completion Modes (vertical well)**

<b>Completion Mode</b>	<b>Suitable Geological Condition</b>
Perforated completion	<ol style="list-style-type: none"> <li>1. Reservoir required to be separated into intervals due to complicated geological conditions, such as gas cap, bottom water, water-bearing interbed, or sloughing interbed</li> <li>2. Reservoir that needs separate-zone testing, production, water injection, and treatments due to differences in pressure and lithology between separate zones</li> <li>3. Low-permeability reservoir that needs massive hydraulic fracturing</li> <li>4. Sandstone reservoir and fractured carbonatite reservoir</li> </ol>
Open hole completion	<ol style="list-style-type: none"> <li>1. Competent carbonatite reservoir</li> <li>2. Reservoir without gas cap, bottom water, water-bearing interbed, and sloughing interbed</li> <li>3. Single thick reservoir or the multizone reservoir with basically same pressure and lithology</li> <li>4. Reservoir not required to be separated into intervals and treated selectively</li> </ol>
Slotted liner completion	<ol style="list-style-type: none"> <li>1. Reservoir without gas cap, bottom water, water-bearing interbed, and sloughing interbed</li> <li>2. Single thick reservoir or the multizone reservoir with basically same pressure and lithology</li> <li>3. Reservoir not required to be separated into intervals and treated selectively</li> <li>4. Unconsolidated medium and coarse sand grain reservoir</li> </ol>
Open hole gravel pack completion	<ol style="list-style-type: none"> <li>1. Reservoir without gas cap, bottom water, and water-bearing interbed</li> <li>2. Single thick reservoir or multizone reservoir with basically same pressure and physical properties</li> <li>3. Reservoir not required to be separated into intervals and treated selectively</li> <li>4. Unconsolidated, seriously sand-producing, coarse, medium, and fine sand grain reservoir</li> </ol>
Casing gravel pack completion	<ol style="list-style-type: none"> <li>1. Reservoir required to be separated into intervals due to complicated geological conditions, such as gas cap, bottom water, water-bearing interbed, or sloughing interbed</li> <li>2. Reservoir required to be treated selectively due to differences in pressure and lithology between separate zones</li> <li>3. Unconsolidated, seriously sand-producing, coarse, medium, and fine sand grain reservoir</li> </ol>
Complex-type completion	<ol style="list-style-type: none"> <li>1. Competent reservoir</li> <li>2. Reservoir without water-bearing and sloughing interbeds in the open hole section</li> <li>3. Single thick reservoir or multizone reservoir with basically same pressure and lithology</li> <li>4. Reservoir not required to be separated into intervals and treated selectively</li> <li>5. Reservoir with gas cap and a high-pressure water-bearing formation near the top boundary of the reservoir and without bottom water</li> </ol>

Second, the tip screenout fracturing technique is used to widen the fracture at the fractured end, pack the mixture of fiber and proppant, and form a high flow conductivity fracture zone. Formation damage is in the near-wellbore zone. For high permeability formation, the formation damage zone is generally in a range of 3 m. The length of the

short fracture generated by tip screenout fracturing may far exceed the damage radius, and the original formation damage can be removed (see Figure 2-40).

## 2. Improving original flow conditions

The fracture generated using the tip screenout fracturing technique used in the fiber complex silt control technology system

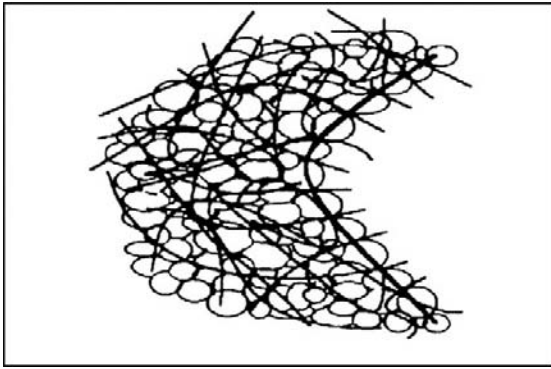


**FIGURE 2-39** Hard fiber sand control principle.

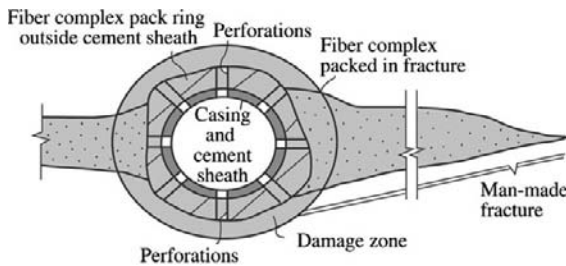


**FIGURE 2-40** The pack ring around a borehole and the man-made fracture.

increases flow area, the original radial flow is changed to quasi-liner flow, the producing pressure drawdown is apportioned in a larger range of formation deep, the pressure drop in the near-wellbore zone is decreased, and the gas flow velocity around the borehole is reduced greatly, thus mitigating or avoiding the failure of the rock matrix, decreasing the degree of reservoir silt production, increasing the well production rate, and achieving silt control.

Furthermore, the fiber complex ring formed by packing around the borehole has a higher permeability, which is much higher than the original reservoir permeability, thus also improving the flow conditions around the borehole in the nonfracture zone (see Figure 2-40).

**Fiber Complex Silt Control Application.** The argillaceous siltstone reservoir of the Sebei gas field in Qinghai has a shale content of 40–60%.

The clay minerals include mainly illite (45–67%), chlorite (18–29%), kaolinite (12–17%), a mixed illite–smectite layer (0–14%), and a small amount of smectite. The median grain diameter of reservoir silt is 0.03–0.07 mm. Reservoir silt with a grain size smaller than 0.01 mm accounts for 28%.

The degrees of formation damages of water, salt, acid, and alkali sensitivities are strong. The average degrees of damages of water and salt sensitivities are 94 and 97%, respectively, whereas the average degrees of damages of acid and alkali sensitivities are 76%. The critical salinity is 80,000 mg/liter. The critical pH value is about 7.5. In order to protect the reservoir, enhance the flow conductivity of the proppant zone, and favor fracturing tip screenout, in accordance with the strong salt sensitivity of the reservoir, a clean fracturing fluid has been developed and used as the carrying fluid of fiber complex silt control operation.

In 2002–2005, fiber was used for stabilizing and retaining silt in 23 wells of the Sebei gas field. The glass fiber was used as hard fiber, which is 1–1.5% of the resin-wrapped sand volume weight ratio. The fiber had a diameter of 10–13  $\mu\text{m}$  and a length of 10–15 mm. The resin-wrapped sand was used for preventing the proppant from flowback. The clean fracturing fluid was used as the carrying fluid to conduct tip screenout fracturing as a measure of fine silt control. Obvious results were obtained. No silt has been produced since the measure was taken. The gas production rate averages 1.7–2.3 times the original production rate.

The Guantao and Minghuazhen formation reservoirs of the Shengli Gudao oil field have a buried depth of 1120–1350 m. With production extended, serious fine silt production is generated. Good results have been obtained in the laboratory and on-site experimental studies of fiber complex silt control. The long-chain cationic polymer with a branched chain is used as soft fiber. In accordance with the reservoir features, both ceramic and glass fibers may be used as the hard fiber. The cost of glass fiber is much lower than that of ceramic fiber. Laboratory experiments of acid-, alkali-, salt-, and temperature-resistant properties

have proven that glass fiber has good chemical stability and can meet the requirements of the reservoir silt control, thus glass fiber was selected and used. An on-site case history is the following: The N7 N6 well of the Gudao oil field is located in the polymer injection oil production area. The reservoir is the Guantao formation  $N_6^{5^{4-5}}$ . It has an average porosity of 30%, permeability of  $1.61 \mu\text{m}^2$ , median grain size of 0.103 mm, shale content of 9.6%, surface crude oil viscosity of 4655 mPa, formation water salinity of 8000 mg/liter, reservoir temperature of  $71^\circ\text{C}$ , and perforated thickness of 7.5 m. A large amount of fine silt was produced in this well due to polymer injection. The well was shut down on July 6, 2004, due to silting. A fiber complex silt control operation was conducted on December 20, 2005. The pumping rate was 900–1000 liter/min, the mean sand carrying ratio was 29.5%, the fiber complex sand body of 12 tons was actually squeezed, and the pumping pressure was increased from 6 to 15 MPa. The well was opened on December 23, 2005. The silt production problem was fully solved.

Furthermore, good results of fine silt control in the steam injection well of the heavy oil reservoir in the Liaohe oil field have been obtained. High-temperature resin plus glass fiber was pumped into the oil reservoir to prevent fine silt from producing. After hardening, it can be temperature resistant to above  $350^\circ\text{C}$  and has been applied extensively.

## Intelligent Well Completion

In the late 1980s, the first intelligent well appeared and a downhole pressure-temperature meter was run in, thus achieving reading out data at the surface and real-time monitoring of the downhole pressure and temperature of an oil well. After the 1990s, the intelligent well, which is able to control the downhole flow rate, appeared. Data of downhole temperature, pressure, and flow rate can be acquired at the surface using a hydraulic or electric control system. By 2004, there were more than 130 intelligent wells worldwide. In addition, more than 200 wells had downhole remote control devices by which

downhole tools and gauges can be controlled remotely at the surface and more data of reservoir production parameters can be acquired.

**Overview.** The intelligent well completion system is a computerized automatic control system for controlling oil and gas production. It can be used for real-time monitoring and controlling the oil and gas production of production horizons in oil and gas wells or branch holes of a multibore well. It can measure and monitor downhole oil and gas production at the surface remotely, thus optimizing production rates of production horizons in accordance with theoretical calculation results and actual measurement data, enabling producing of production horizons in the optimum working state. Hence, the recovery factor of oil and gas reservoirs may be enhanced, the times of downhole operations may be decreased, and the operating management of oil field production may be optimized.

The intelligent well completion system includes the following subsystems: downhole information sensing system, downhole production control system, downhole data transmission system, and surface data acquisition, analysis, and feedback control system. The downhole production control system includes various removable downhole tools and downhole sensors. These devices have good flexibility and can meet various requirements of well completion in accordance with oil reservoir production features. The intelligent well completion system consists mainly of the following components:

1. Surface SCADA (supervisory control, alarm, and data acquisition) system interface
2. Underwater control network
3. Downhole control network
4. Separate-zone packers with bypass
5. Removable, switchable, and open degree adjustable downhole tools
6. Downhole sensors of pressure, temperature, flow rate, water cut, and density

All of the downhole devices, including sensors and removable tools, are connected with the downhole control network. The system uses permanently installed cable for supplying power

and provides bidirectional digital communication between the surface and the downhole sensors. The hydraulic or electromagnetic drive can be adopted. If the hydraulic drive is adopted, hydraulic power is supplied through a hydraulic line connected with the surface hydraulic power installation. If the electromagnetic drive is adopted, the electric driver is selectively indicated to provide mechanical power for various mechanical devices.

**Functions of Intelligent Well Completion System.** The intelligent well completion system has the following advantages and functions in reservoir management and behavior monitoring aspects.

- (1) Multilayer reservoirs can be selectively produced, and the optimum working mode can be selected on the basis of the surveyed inflow and working environment parameter data of each layer in wells. The injection performance of the injection well and the production performance of the oil well can be improved, the choke of the high water-cut
- layer or high gas–oil ratio layer can be timely shut, more oil and gas can be produced from the reservoir, and the recovery factor of the oil field can be increased.
- (2) Pressure build-up and drop tests can be conducted with no need for well shut-in, and production rate, pressure, and temperature can be measured at any time. Material balance calculation of the reservoir can be conducted accurately. The reservoir performance can be kept informed. The oil and gas well management quality and efficiency can be enhanced by effectively analyzing and processing the flow parameter data of each layer.
- (3) Downhole horizons can be treated with no need for downhole operations, thus decreasing times of downhole operations, decreasing production downtime, decreasing production operation costs, and enhancing the competitive power of oil field production.

The hole structures of conventional and intelligent well completions are shown in Figure 2-41.

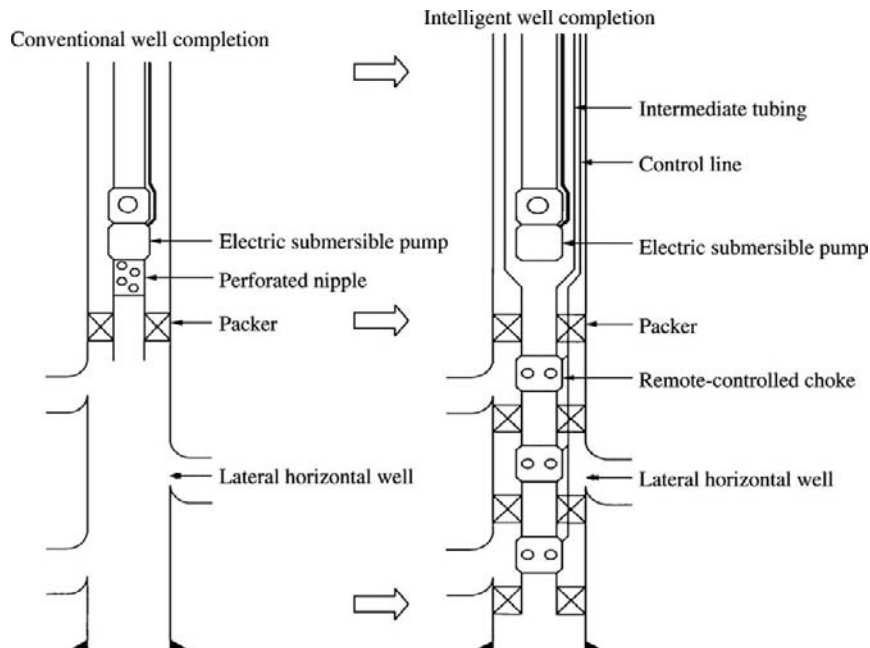


FIGURE 2-41 Hole structures of conventional and intelligent well completions.

By reason of the high investment of downhole completion devices, the intelligent well completion system is chiefly used for the subsea satellite wells, horizontal wells, and extended reach wells in offshore deep water areas and the unattended oil wells, multilayer injection and production wells, and electric submersible pump wells in frontier areas at present. It is mostly used in oil fields with high productivity and downhole operation costs. The intelligent well completion system can achieve real-time production optimization of various production horizons, thus achieving a higher recovery factor and economic benefits. Presently, oil fields adopting the intelligent well completion system are located in the North Sea, Adriatic Sea, Gulf of Mexico, West Africa, Indonesia, and Venezuela. The intelligent well completion is a completion method with development prospects; however, it is unsuitable for low-productivity wells, shallow wells, and wells with a single series of strata due to diseconomy and no need.

The Suizong oil field in the Bohai Gulf, China, has an oil-bearing area of 43 km<sup>2</sup> with oil reserves of  $2.6 \times 10^8$  tons and an initial individual-well daily production rate of 70–100 tons per day with sand production. In the early 1990s during development of the pilot area, there was a packer between two reservoirs in addition to a gravel pack in the well. There is a sliding sleeve for each, thus water cut may be controlled by shutting the sliding sleeve if the water cut of some reservoirs is high. Also, a batch of electronic pressure gauges was selected, thus keeping informed on downhole pressure conditions in time. In the late 1990s–early 2000s, a new capillary pressure gauge was adopted and located at 100 m below the electric submersible pump. Thus, downhole pressure data can be read out on the platform at any time. The oil reservoir permeability, skin factor, downhole flowing pressure, and reservoir pressure can be calculated by interpreting and analyzing these pressure data. An excessive skin factor and a lower production rate in an oil well indicate that some plugging of the reservoir in the well exists, and a plugging removal measure may be taken. Until 2005, the downhole capillary pressure gauge had been applied in 39 wells,

which accounted for 20% of more than 200 production wells in the whole oil field. Thus, by using downhole pressure and production data, the oil well and field production conditions can be analyzed in time and corresponding adjustments can be made, thus optimizing oil field production.

## Monobore Well Completion

The hole structure of a traditional oil and gas well includes two flow channels: the tubing used for oil and gas production and the tubing–casing annulus used for circulation and well killing [see Figure 2-42(a)]. The hole structure of a monobore well has only a flow channel, that is, tubing [see Figure 2-42(b)]. This hole structure can save the drilling and completion equipment and tools, such as casing, packer, and circulating valve, and the operating procedures of running these equipment and tools. In addition, the perforated completion operation of monobore well completion does not take up rig time, thus reducing drilling and completion costs greatly. However, the problems of well killing, lifting, induced flow, and plugging will occur when the monobore hole structure is used; as a result, the monobore well completion application is restricted to some extent. The monobore well completion technique is mainly applicable to oil

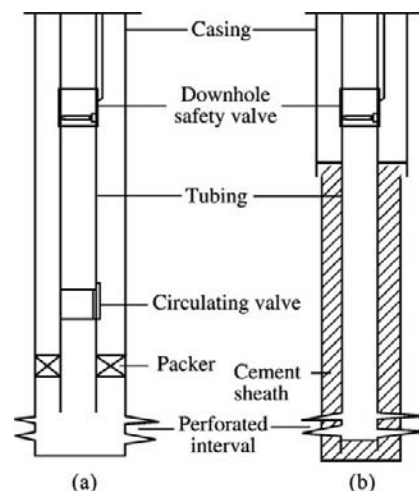


**FIGURE 2.42** Hole structures of a traditional oil and gas well (a) and monobore oil and gas well (b).

wells flowing in whole production life, especially to gas wells. For gas fields with low reserves, low permeability, a low individual-well production rate, and no sand production, the investment can be reduced greatly by using this completion technique, thus achieving better economic benefit.

#### Good Results Obtained in Gulf of Thailand.

The geological features of the Gulf of Thailand include continental deposit, cataclastic structure, more faults, low oil and gas reserves, and lower individual-well production rate. By adhering to the low-cost strategy and uninterrupted technical innovation, Unocal has implemented a series of measures with the monobore well completion technique as the kernel and has acquired great success in oil and gas exploration and development.

More than 80 wellhead platforms have been built, and more than 1600 wells have been drilled by Unocal in the Gulf of Thailand (Figure 2-43). In 1983–2002, the hole structure of the wells drilled in the Gulf of Thailand had been improved many times and well completion with  $\Phi 73$ -mm tubing had been achieved. The borehole size changed from large to small, and the hole structure decreased from four to three layers. Using the monobore well completion technique, the well construction period of the oil and gas fields in the Gulf of Thailand was shortened and well construction costs were decreased, as shown in Figure 2-44. The further significance of reducing drilling and completion costs is that the saved costs increased the

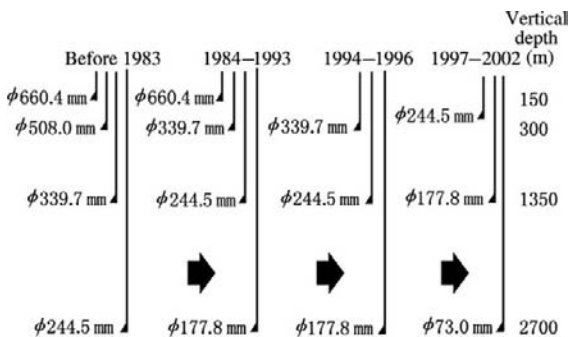


**FIGURE 2.43** The hole structure improvements of wells drilled by Unocal in the Gulf of Thailand.

quantity of wells drilled and completed, and more oil and gas reserves were found.

#### Main Features of Monobore Well Completion.

- (1) The monobore well completion technique decreases borehole size. Production casing size is decreased from  $\Phi 177.8$  mm (7 in.) to  $\Phi 73$  mm (2 7/8 in.). The matching techniques and tools have been had.
- (2) When the monobore well completion technique is used for development well drilling and completion, tubing may be run in and the well cemented after drilling. Then the drilling rig and drill vessel can be evacuated from the site and the through-tubing wireline perforating can be conducted on the well site or platform, thus the rental of a drilling rig or drill vessel can be decreased.
- (3) The monobore well completion technique can also be used for drilling exploration wells. For conventional well completion, during a drillstem test [Figure 2-45(a)], a series of downhole tools, including packer, circulating valve, jar, and killing valve, should be run in, long running-in and pulling-out time and a large amount of materials will be consumed, and high costs are required. Under monobore well completion [Figure 2-45(b)], after tubing running-in, cementing, and wireline perforating, testing may be conducted. When testing of the lowest zone is ended, a bridge plug is set at its top to

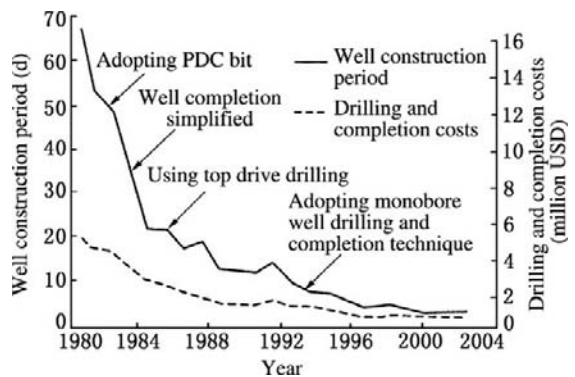


**FIGURE 2.44** The operation technique improvements and corresponding well construction period and drilling and completion cost changes of Unocal in the Gulf of Thailand in 1980–2002.

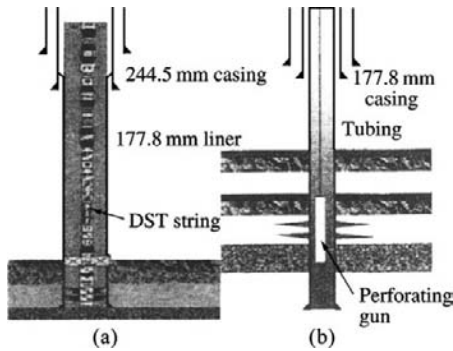


**FIGURE 2.45** Conventional DST (a) and monobore structure tubing (b) testing diagram.

conduct testing at the next zone. After the testing task is finished, a bridge plug is set at the uppermost zone and the upper tubing is cut using cutting bullets. After the cement plug is set using tubing string, the exploration well operations may be finished. By comparison with the string operations, the wireline operations are quite timesaving.

- (4) The monobore well completion technique changes operation mode from the traditional bibore operation mode able to conduct circulating well killing to the monobore operation mode able only to conduct squeezing well killing. In order to solve the difficulty of induced flow of oil and gas in the production well, in addition to coiled tubing for induced flow, diesel oil can also be used as the tail slurry for cementing. The underbalance condition may be formed by diesel oil in the wellbore, thus the well can be put into production just after perforating.
- (5) If monobore well completion is adopted, the downhole safety valve is run in before the cementing operation and may be affected negatively by the cementing fluid. Therefore, the downhole safety valve should be moved many times in the cementing operation process in order to prevent the safety valve from being stuck by the cementing fluid.
- (6) For wells completed using the monobore well completion technique, operations including perforating, setting bridge plug, induced flow operation, and downhole safety valve servicing

operation may only be conducted using wire, wireline, and coiled tubing, and because the well servicing operations of running or pulling string cannot be conducted, higher quality wire and wireline operations are required.

- (7) The monobore hole structure has no traditional circulating and killing channel, thus generating oil and gas well operation risk to some extent. However, the experiences of a large number of applications in the Gulf of Thailand indicate that this risk may be controlled by installing a downhole safety valve and taking other risk-controlling measures so that the operations are also safe.
- (8) The monobore hole structure is simple and the operational measures are limited. If downhole problems occur and repair is needed, the side-tracking method may often be used but not traditional repair measures. Hence, the requirement of side-tracking should be considered when the cement return height is designed in the cementing design.

During the monobore well completion operations, the matching technology and management concept optimization, including large-scale, three-dimensional seismic survey and interpretation for enhancing the accuracy of reservoir interpretation, integrally completed well-site design for batch drilling and centralized drilling wells with the same borehole size, using more logging while drilling for decreasing wireline logging, drilling two monobore wells within the same marine riser for reducing surface engineering and riser building costs, and optimizing the drilling rig evacuation and emplacement and the drilling fluid properties, for enhancing integral benefit of the monobore well completion technique, is required. Drilling two monobore wells within the same marine riser and the monobore well drilling and completion technique are shown in Figure 2-46.

In general, monobore (2 7/8-in. tubing) well completion is relatively suitable for gas wells of gas fields that have low reserves, low permeability, low individual-well production rates, no sand production, and no need of dewatering gas production for the following reasons.

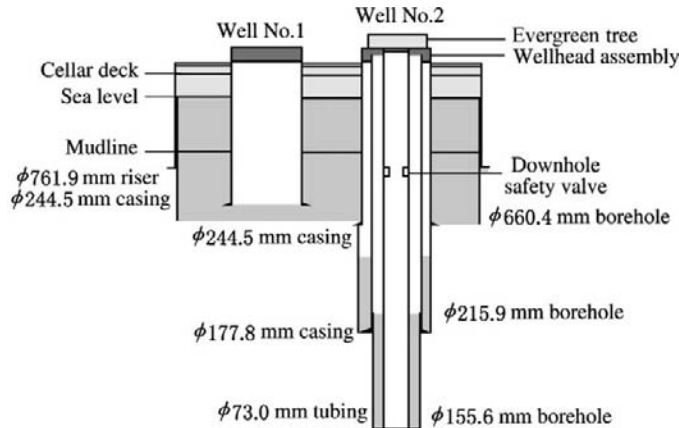


**FIGURE 2.46** Drilling two monobore wells within the same marine riser and the monobore well drilling and completion technique.

1. The gas production of gas wells is generally flowing production.
2. The downhole operation workload is relatively low during the gas production of gas wells.
3. The downhole technology and tools, including perforating and separate-zone testing, have been matched for 2 7/8-in. tubing well completion.
4. When the 2 7/8-in. tubing well completion is adopted, a 7-in. intermediate casing is needed to be run to some depth in order to produce the remaining natural gas by late side-tracking if necessary.

A large amount of investment can be saved and better economic benefits of gas field production can be achieved by adopting monobore well completion. However, for the oil fields of pumping production, small-hole oil production is limited by reservoir depth and has to solve downhole production technology and tool problems; therefore, specific studies and economic benefit analysis should be conducted in accordance with the practical conditions of the field and then a strategic decision can be prudently made.

### Underground Natural Gas Storage Well Completion

Underground natural gas storages are underground facilities for storing natural gas. At present, there

are three types of underground natural gas storages worldwide, which include depleted oil and gas reservoir gas storages, salt-cave gas storages, and aquifer gas storages. They are distributed mostly in the United States, Canada, the former USSR, and Germany, and 10–30% of the yearly consumption is supplied by underground natural gas storages. According to statistics in 2000, about 200 underground natural gas storages had been built worldwide and the total effective working gas volume was up to  $3003.5 \times 10^8 \text{ m}^3$ . In the United States and Europe, over 20% of commercial gases were from underground natural gas storages. The working gas volume of the 23 underground natural gas storages operated just by Russia Natural Gas Industry Co., Ltd. had reached  $600 \times 10^8 \text{ m}^3$  and the average daily gas supply in winter had reached about  $50 \times 10^8 \text{ m}^3$ . In recent years, three large underground natural gas storages with a total peak adjusting gas volume of several hundred million cubic meters have been built in the North China area. Also, underground salt-cave natural gas storages with a total peak adjusting gas volume of several hundred million cubic meters, are being built in the Changjiang delta area. In addition, a series of larger underground natural gas storages are being planned in northern, northeastern, and southwestern China.

Natural gas is generally injected into the natural gas storages in the slack season of gas usage and is produced from storages in the busy season

(generally winter) or security period. A high flow rate is adopted for injection or production, and the individual-well productivity should be generally up to  $100\text{--}300 \times 10^4 \text{ m}^3/\text{day}$ . A well of the underground salt-cave natural gas storage of the American Duke Energy Co. in northern Texas has a diameter of 20 in. (508 mm) and the maximum gas productivity is up to  $1870 \times 10^4 \text{ m}^3/\text{day}$ .

Underground natural gas storages suffer breathing of higher gas injection and production rates during working and the wellbore bears intermittently the repeated alternating load from low to high and from high to low. Furthermore, in order to achieve the maximization of benefit, the service life of an underground natural gas storage well should be prolonged to the full extent. Therefore, well completion technology, injection and production string, downhole tools, cementing quality, and integral wellbore leakproofness should fulfill higher requirements. In addition, in the depleted oil and gas reservoir and aquifer gas storages, some reservoirs have a decreased pore pressure coefficient lower than 0.5 and attention to the protection of reservoir properties should be paid, as otherwise the gas injection pressure and the injection and production rates will be reduced greatly and the operation loads of the surface equipment will be increased, thus increasing the operation costs of gas storage greatly.

In order to meet the requirements of operation safety and strong injection and production, the injection and production strings, perforating and completion strings, wellhead facilities, cementing, and wellbore leakproofness detection should be optimized, thus achieving optimum injection and production results and prolonging wellbore service life.

## Depleted Oil and Gas Reservoir and Aquifer Gas Storage Well Completion

### 1. Gas storage well completion string selection

Gas storage gas injection and production well completion string should meet the requirements of the working environment of gas storage. The high-pressure gas flow under abnormal conditions should be controlled rapidly, and casing and tubing corrosion by downhole fluids in the gas injection and production process and the strong injection and production should be considered. In addition, a long service life of completion string is also required. The selection principles of gas storage well completion string include the following.

- (1) Meeting the requirement of injection and production scales of gas storage
- (2) Suiting the corrosive environment
- (3) Ensuring long-term safe operation of injection and production wells
- (4) Matching of cost control with technological measures

In the gas storage injection and production well string design, a packer and downhole safety valve are generally adopted. The packer is normally set at the bottom of string, thus preventing reservoir fluid from corroding the upper string and prolonging wellbore service life. The downhole safety valve is set between 80 and 100 m above the bottom of string and is used for cutting off the channel between downhole and surface rapidly and safely when high-pressure gas flow in the wellbore gets out of control, thus ensuring the safety of people at the surface and surrounding area.

## Selection and Determination of Tubing and Production Casing Sizes

### OUTLINE

- 3.1 Overview
- 3.2 Overview of Nodal Analysis
- 3.3 Selection and Determination of Tubing and Production Casing Sizes for Flowing Wells
  - Importance of Sensitivity
  - Analysis of Tubing Size
  - Sensitivity Analysis and Optimization of Tubing Size of Flowing Well
    - Optimization Method Based on Surface Tubing Pressure Derived by Given Separator Pressure*
    - Optimization Method Based on the Given Wellhead Tubing Pressure  $p_{wh}$*
    - Case 1
    - Solving Process*
    - Case 2
    - Solving Process*
    - Case 3
    - Solving Process*
    - Tubing Size Optimization Method of Ensuring Longer Flowing Period*
    - Case 4
    - Solving Process*
    - Method of Analyzing Tubing Size Sensitivity Affected by Inflow Performance*
    - Case 5
    - Solving Process*
  - Production Casing Size
  - Determination of Flowing Well
- 3.4 Selection and Determination of Tubing and Production Casing Sizes for Gas Wells
  - Selection and Determination of Tubing Size of Natural Gas Well
    - Selection and Determination Method of Tubing Size with Minimum Energy Consumption of Lifting under Rational Production Rate*
    - Case 6
    - Solving Process*
    - Case 7
    - Solving Process*
    - Case 8
    - Solving Process*
  - Method of Selecting and Determining Maximum Tubing Size under Condition of Meeting Carrying Liquid in Gas Well*
  - Case 9
  - Solving Process*
  - Selection and Determination Method of Minimum Tubing Size Avoiding Erosion due to Excessive Flow Velocity in Gas Well*
  - Case 10
  - Solving Process*
- 3.5 Selection and Determination of Tubing and Production Casing Sizes for Artificial Lift Wells
  - Prediction of Daily Liquid Production Rate Level in the High Water Cut Period Artificial Lift Mode
  - Determination
    - Preliminary Selection of Artificial Lift Mode*
  - Production Casing Size
  - Determination of Natural Gas Well



field development and the specific lifting mode. Therefore, the nodal analysis is briefly described at first, and the selection and determination of tubing and production casing sizes are then described in detail.

The tubing and production casing sizes of oil and gas wells should be selected and determined before well completion. The tubing size can be changed, but the production casing cannot be changed after well completion. Therefore, the type of well, production mode, stimulation, oil properties, and requirements of production engineering in the entire production process should be considered when a production casing size is selected and determined; that is, natural gas wells, flowing wells, artificial lift wells, stimulation, and heavy oil production have different requirements for selecting tubing and production casing sizes. Thus, for a specific well, the aforementioned factors should be considered when the rational tubing and production casing sizes are determined.

For a natural gas well, both production optimization and stimulation should be considered. Therefore, the tubing and production casing sizes should be computed as shown in Equation (3-1):

$$(3-1) \quad \text{Tubing and production casing sizes of natural gas well} = \max \{T_1, T_2, T_3\}$$

where  $T_1$  = tubing and production casing sizes by production optimization;  $T_2$  = tubing and production casing sizes by stimulation;  $T_3$  = tubing and production casing sizes by other special technological requirements; max = maximum value function.

For a conventional oil production well, the tubing and production casing sizes should be calculated as shown in Equation (3-2):

$$(3-2) \quad \text{Tubing and production casing sizes of conventional oil production well} = \max \{t_1, t_2, t_3, t_4\}$$

where  $t_1$  = tubing and production casing sizes at flowing stage by production optimization;  $t_2$  = tubing and production casing sizes by artificial lift selected;  $t_3$  = tubing and production casing sizes by stimulation;  $t_4$  = tubing and production

casing sizes by other special technological requirements; and max = maximum value function.

For a heavy oil production well, the tubing and production casing sizes should be calculated as shown in Equation (3-3):

$$(3-3) \quad \text{Tubing and production casing sizes of heavy oil production well} = \max \{T_{t1}, T_{t2}, T_{t3}\}$$

where  $T_{t1}$  = tubing and production casing sizes by artificial lift selected;  $T_{t2}$  = tubing and production casing sizes by heavy oil production;  $T_{t3}$  = tubing and production casing sizes by other special technological requirements; max = maximum value function.

After the tubing and production casing sizes are determined, the casing program of a specific well is determined in accordance with well depth, technical requirements of drilling technology, complexity of oil and gas reservoir, and characteristics of overburden.

The slim hole (hole size  $\leq 5$  in.) completion mode includes open hole, slotted liner, and liner cementing perforated completions. In addition, the monobore well completion technique has been used by Shell. The slim hole completion is basically the same as the conventional wellbore completion, except that the matching techniques of the slim hole, including perforating, stimulation, artificial lift, downhole tools, and fishing tools, should be considered in order to ensure the normal production from a slim hole.

## 3.2 OVERVIEW OF NODAL ANALYSIS

The oil and gas flow from reservoir to surface separator is shown in Figure 3-1.

The total fluid pressure loss from reservoir deep to surface separator is composed of several sections of pressure loss caused by resistance: pressure loss through porous media (first pressure subsystem), pressure loss through well completion section (second pressure subsystem), total pressure loss through tubing string (third pressure subsystem), and total pressure loss through flowline (fourth pressure subsystem).

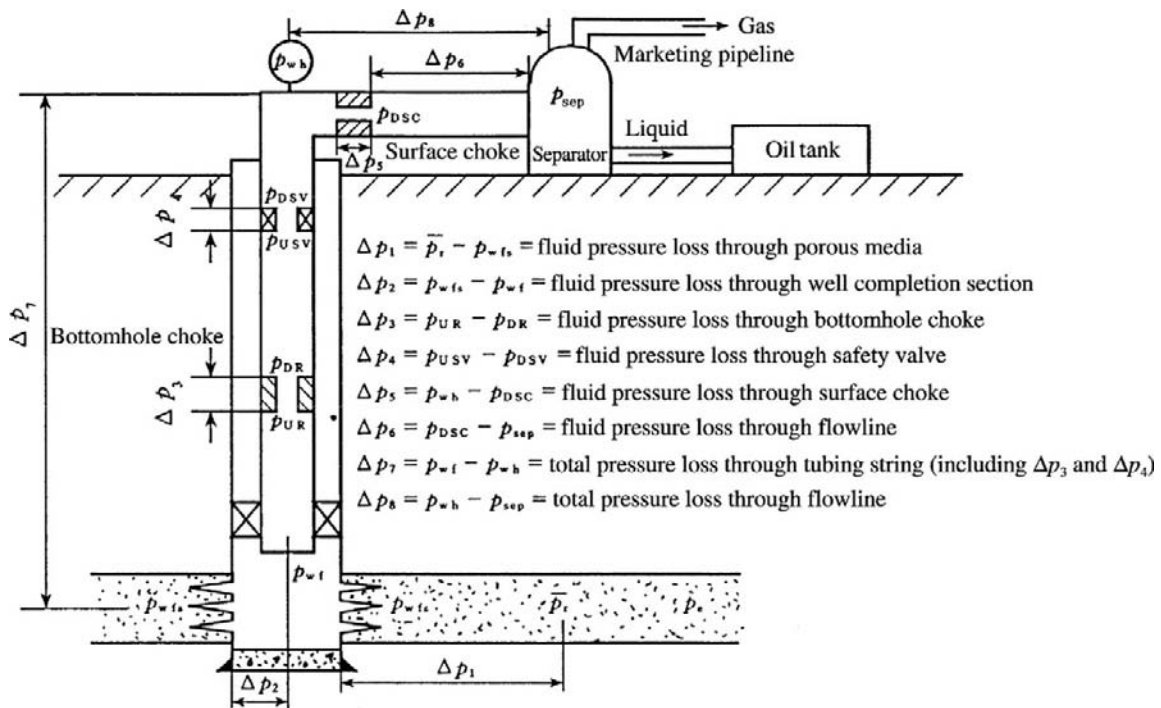


FIGURE 3-1 Various pressure losses in the production system.

1. Fluid pressure loss through porous media

In accordance with the relation between reservoir pressure, bottomhole flowing pressure, oil saturation pressure, and the theory of mechanics of fluid through porous media, the pressure distribution relations of single-phase liquid flow, single-phase gas flow, two-phase flow of oil and gas, three-phase flow of oil, gas, and water, and dissolved gas drive and the oil and gas inflow performance relationship can be derived; thus the total fluid pressure loss through porous media can be determined.

2. Fluid pressure loss through well completion section

The fluid pressure loss through well completion section is closely related to the well completion mode and can be calculated by calculating the total skin factor  $S$  under a different completion mode.

3. Total fluid pressure loss through tubing string

This pressure loss can be determined by the calculation under the multiphase flow condition in tubing string. At present, there are various methods to calculate multiphase flow in pipe.

4. Total fluid pressure loss through flowline

The same calculation method as that of multiphase flow in pipe is used.

The oil and gas production passes through the four subsystems in the preceding list, which can be joined together into a unity by setting up nodes. If the analog calculation of each subsystem is conducted, the whole production system can be mathematically simulated. The nodal analysis method uses just such an analogy calculation process to analyze and optimize the production system of an oil and gas well. When a specific problem is to be solved by using the nodal analysis method, it is usual to take aim at some node (known as the solution node) in the system. The production system of an oil

and gas well can be simplified into two large parts (that is, inflow and outflow parts) by selecting the solution node. For instance, when the solution node is selected at  $p_{wf}$  of the bottomhole of the oil well, the inflow part includes the two subsystems, that is, the fluid flow through porous media and the fluid flow through completion section, while the outflow part includes the other two subsystems, that is, the fluid flow through tubing string and the fluid flow through surface flowline. Thus, the following two major problems can be solved.

1. Under the condition of constant parameter values of the outflow part, the completion section can be optimized using the nodal systems analysis method. For instance, for a perforated well, the parameters of perforated completion, including perforation density, perforation diameter, perforation length, and phase angle, can be optimized using this analysis method.
2. However, under the conditions of constant completion mode and completion parameter values, the tubing size and choke can be optimized. The sensitivity analysis of tubing size, which is described later, is just a worsening of this problem.

Nodal analysis of an oil and gas well not only can be used for solving the problem mentioned earlier, but also can be used for solving others, including determining the dynamic performance of an oil and gas well under current production conditions, optimizing the production restriction factor of an oil and gas well and presenting adaptable stimulation and adjustment measures of an oil and gas well, determining the production state when flowing stops or is turned to pumping and analyzing the reason, determining the optimum moment of turning to an artificial lift and its optimum mode, and finding a way to enhance the production rate.

To sum up, for a new well, the maximum daily fluid production and the minimum flowing pressure in the future for the entire production process of the oil well should be predicted using the numerical simulation method or the method

of predicting the future inflow-performance relationship (IPR) curve in order to optimize completion parameters and tubing size using the nodal analysis method. This is what well completion engineering pays the most attention to. For an oil and gas well that has been put into production, the nodal analysis method is helpful for scientific production management.

The theory and practice of nodal analysis have been described in detail in the related literature.

### **3.3 SELECTION AND DETERMINATION OF TUBING AND PRODUCTION CASING SIZES FOR FLOWING WELLS**

Tubing is one of the important component parts in the production system of a flowing well and is the main channel for oil and gas field development. The pressure drop for fluid lifting from the bottomhole to the surface can be up to 80% of the total pressure drop of the oil and gas well system. Any oil well system has an optimum tubing size. Undersized tubing will limit the production rate due to the increased friction resistance caused by excessive flow velocity. Contrarily, oversized tubing may lead to an excessive liquid phase loss due to slippage effect or an excessive downhole liquid loading during lifting. Therefore, sensitivity analysis of tubing size should be carried out using the nodal analysis method. On the basis of the sensitivity analysis of tubing size, the tubing and production casing sizes required during the flowing period can be determined. However, the production casing size of the well cannot be determined yet. The reason is that the tubing and production casing sizes of the oil and gas well should meet the requirements of the well during the entire production life, whereas the flowing period of the oil and gas well is limited, and the tubing and production casing sizes are often on the small side. After the flowing period, the oil and gas well may turn to artificial lift production. The tubing and production casing sizes in the flowing production period of an oil and gas well cannot meet the requirements of stable production in the

artificial lift production period. For a waterflooding oil field, after entering the high water cut period of the oil well, the large-size pump with a high pumping rate should often be used in order to ensure stable oil production and rational producing pressure drawdown. For a different lifting mode, different tubing and production casing sizes should be adopted. The pump diameter should be determined in accordance with the daily fluid production rate during the whole development period of the oil field, and the corresponding tubing and production casing sizes are then selected. In addition, different tubing and production casing sizes are required by stimulation and sand control technology. Therefore, the tubing and production casing sizes can only be finally determined after all of the aforementioned factors are taken into consideration.

By comparison with other production modes, under flowing and gas lift production modes, a certain production rate and a certain tubing shoe pressure (flowing bottomhole pressure if the tubing shoe is in the middle of the oil reservoir) should be maintained. Under the other production modes, the flowing bottomhole pressure can be reduced to the full extent if that is allowed by reservoir pressure and casing condition.

### Importance of Sensitivity Analysis of Tubing Size

The tubing size should be optimized in order to ensure the lowest energy consumption for lifting and the longest flowing time, that is, to utilize rationally the energy of the oil and gas reservoir.

The inflow performance relationship (IPR) curve indicates the relationship in a well between the flowing bottomhole pressure at a stabilized production rate and the liquid production rate, which can be obtained on the basis of reservoir pressure, flowing bottomhole pressure, liquid production rate, and open flow rate under zero flowing bottomhole pressure. The tubing performance relationship (TPR) curve, which is obtained on the basis of the tubing shoe pressure (flowing bottomhole pressure if the tubing shoe is

in the middle of the oil reservoir) calculated in accordance with the flow rule (single- or two-phase flow) in tubing under the given gas-liquid ratio, water cut, well depth, and wellhead pressure for different production rates, reflects the lifting capability of lifting tubing, which is only dependent on tubing flow parameters, such as wellhead pressure, well depth, tubing diameter, and gas-liquid ratio, and is independent of reservoir productivity.

Many methods of calculating the IPR can be used, and the Vogel formula shown in Equation (3-4) is generally adopted:

$$(3-4) \quad \frac{q_o}{q_{oma}} = 1 - 0.2 \frac{p_{wf}}{p_r} - 0.8 \left( \frac{p_{wf}}{p_r} \right)^2$$

where  $q_o$  is the surface production rate of the oil well at  $p_{wf}$ ,  $m^3/d$ ;  $q_{oma}$  is the surface production rate of the oil well at  $p_{wf} = 0$ ,  $m^3/d$ ;  $p_{wf}$  is the flowing bottomhole pressure, MPa; and  $p_r$  is the average reservoir pressure in the oil drainage area, MPa.

Many methods of calculating the TPR can be used, and the Orkiszewski and Hagedorn Brown method is generally adopted in practice.

The coordination between inflow and outflow performances should be studied using the IPR and TPR curves in accordance with the nodal analysis method in order to ensure the optimum utilization of natural energy.

The tubing performance relationship is shown in Figure 3-2. This figure indicates when a

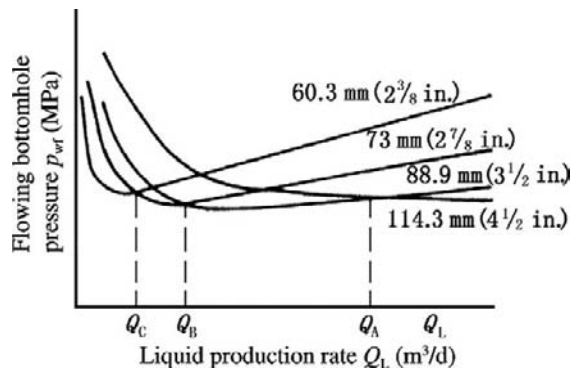


FIGURE 3-2 The effect of tubing size on lifting capability of tubing in a flowing well.

high production rate  $Q_L > Q_A$ , 114.3-mm (4 ½ in.) tubing has the highest lifting efficiency; when  $Q_A > Q_L > Q_B$ , 73-mm (2 ⅞ in.) tubing is more economic; and when  $Q_L < Q_C$ , 60.3-mm (2 ⅜ in.) tubing is most appropriate.

### Sensitivity Analysis and Optimization of Tubing Size of Flowing Well

The fluid flow in tubing during flowing production can be analyzed in accordance with the aforementioned vertical flow rule in tubing. The most sensitive factors affecting the pressure gradient distribution of multiphase vertical flow in tubing include tubing size, production rate, gas-liquid ratio, viscosity, and water cut. For a well design, the gas-liquid ratio, viscosity, and water cut are basically in a range, whereas the production rate can be controlled and changed. In accordance with the theory of multiphase flow in tubing, each production rate value corresponds to the optimum tubing size so that the pressure gradient (or pressure depletion) in tubing can be the minimum. For a given production rate, an undersized tubing may have an excessive flow velocity so that the friction resistance may be increased, whereas an oversized tubing may have a flow velocity on the low side so that a serious gas slippage effect may be caused. Therefore, only by selecting an appropriate tubing size can the friction resistance and liquid phase loss due to slippage effect be in the optimum state and the maximum energy utilization efficiency be achieved.

Because the production rate is an important parameter for optimizing and selecting the tubing size and the optimum tubing size is different under different production rates, the production rate acts as a variable in all analyses. In the flow process from the reservoir to the surface, the production rate is closely related to the pressure, thus the pressure acts as the other variable. The effect of change in tubing size is often analyzed using the coordinate diagram of pressure  $p$  and production rate  $Q$ . The optimum tubing size is generally determined using the nodal analysis method.

There are two methods of analyzing the optimum tubing size. (1) Under given surface conditions (such as separator pressure, wellhead pressure, or surface flowline size), the tubing size capable of maximizing the production rate is the optimum tubing size. (2) Under a specific production rate, the tubing size capable of minimizing the producing gas-oil ratio, maximizing gas expansion energy utilization efficiency, and ensuring the longest flowing production time is the optimum tubing size; that is, there are two methods of optimizing and selecting the tubing size or two different objective functions. In accordance with the specific conditions of an oil field, one of these methods can be selected or the two methods can be used for determining the optimum tubing size; the optimum tubing size is finally determined by composite consideration. The methods generally used include the optimization method based on the surface tubing pressure derived by a given separator pressure; the optimization method on the basis of a given surface tubing pressure; and the optimization method of ensuring a relatively long flowing period.

#### Optimization Method Based on Surface Tubing Pressure Derived by Given Separator Pressure.

In order to ensure the flow from wellhead to separator for the produced fluid, the minimum wellhead tubing pressure  $p_{wh}$  should be achieved on the basis of the surface pipe network design and the specific well location. In general, the minimum entering pressure is required by entering the separator. Thus the wellhead tubing pressure can be derived in accordance with the entering pressure, surface flowline size, path of surface flowline, and flow rate in the pipeline. If a choke is needed by controlling the flowing well production, the choke pressure differential  $\Delta p_{choke}$  through the choke should be added. Thus, the wellhead tubing pressure  $p_{wh}$  under the minimum separator pressure can be obtained. Obviously, the  $p_{wh}$  is related to the production rate  $Q$ . The higher the production rate, the higher the minimum wellhead tubing pressure  $p_{wh}$  required. In Figure 3-3, curve 1 is the surface flowline and wellhead tubing pressure curve (no choke); curve 2 is the combined

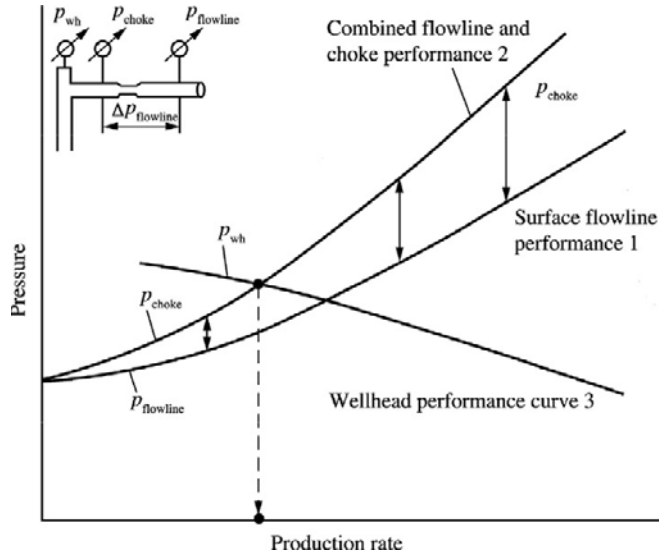


**FIGURE 3-3** The pressure system analysis using wellhead as node under a given separator pressure.

flowline, choke, and wellhead tubing pressure curve; and curve 3 is the remaining wellhead pressure  $p_{wh}$  of flow from reservoir to wellhead vs. production rate curve (OPR curve), as shown in Figure 3-4.

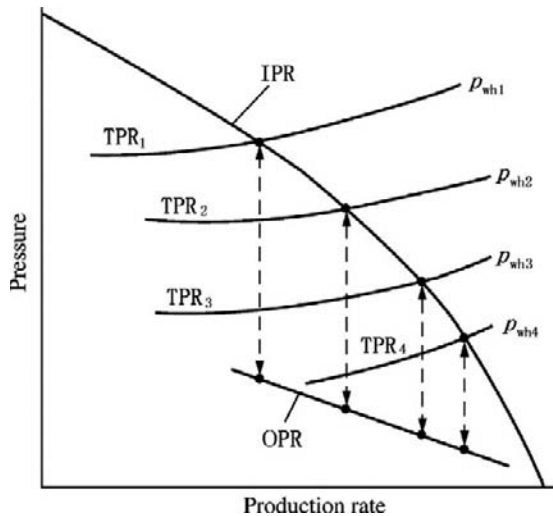


**FIGURE 3-4** Wellhead pressure relationship curve (OPR curve) taking reservoir flow and tubing flow as oil well flow system.

Obviously, the changes in surface parameters (including choke size, surface flowline, and separator pressure) will change the TPR curve as shown in Figure 3-4. The changes of reservoir condition, completion mode, and tubing size (such as reservoir pressure reduction with time, different perforating parameters, and change in tubing diameter) will also affect the OPR curve.

Under uncertain wellhead tubing pressure  $p_{wh}$ , the change in tubing size is displayed by the OPR curve. The wellhead inflow performance curves under the three tubing sizes and the wellhead outflow performance curves under the two choke sizes are shown in Figure 3-5. Obviously, when the choke size is  $d_{ch1}$ , the tubing with diameter  $d_{t1}$  is the optimum production tubing; and when the choke size is  $d_{ch2}$ , the tubing with diameter  $d_{t3}$  is the optimum production tubing.

**Optimization Method Based on the Given Wellhead Tubing Pressure  $p_{wh}$ .** In many circumstances, the conditions of surface flowline cannot be determined in advance and the first method cannot be used for the sensitivity analysis of tubing size. Thus, the tubing size is optimized by setting wellhead tubing pressure  $p_{wh}$ .

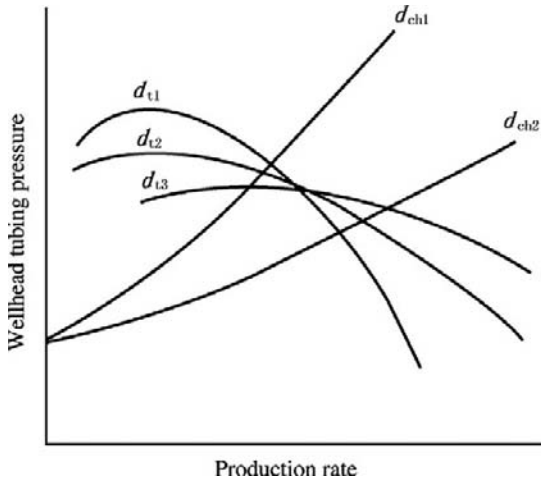


**FIGURE 3-5** Sensitivity analysis of tubing size under uncertain wellhead tubing pressure.

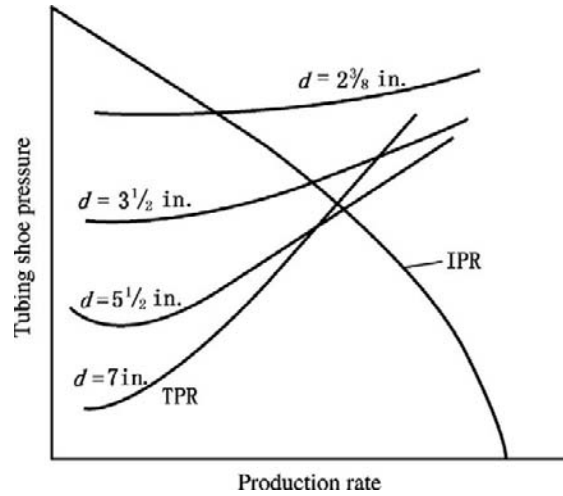


**FIGURE 3-6** Sensitivity analysis of tubing size under given wellhead tubing pressure.

The inflow performance relationship (IPR) curve is first obtained. Then, in accordance with the given wellhead tubing pressure  $p_{wh}$  and the various production rates supposed, the tubing shoe pressures are calculated under different tubing sizes. (The tubing shoe pressure is equal to the flowing bottomhole pressure  $p_{wf}$  if the tubing shoe is in the middle of the oil reservoir.) The production rate vs. tubing shoe pressure  $p_{wf}$  relationship (TPR, that is, tubing performance relationship) curves under the different tubing sizes can be obtained. Figure 3-6 shows the TPR curves under various tubing sizes. The intersections of the TPR curves and the IPR curve are just the production points under the various tubing sizes.

In general, increasing the tubing size will increase the production rate of a flowing well. However, when the tubing size exceeds the critical tubing size, the increase in tubing size may lead to a decrease in production rate, as shown in Figure 3-6.

**Case 1.** The Shen 77 well of the Liaohe Shenyang oil field has the following known parameter values: mean reservoir pressure  $p_r = 16.3$  MPa, depth in middle of reservoir  $H = 1673.1$  m, producing gas-liquid ratio  $GLR = 108.7$  m<sup>3</sup>/m<sup>3</sup>, saturation pressure  $p_b = 18.89$  MPa, relative

density of oil  $\gamma_o = 0.856$ , relative density of gas  $\gamma_g = 0.73$ , and water cut  $f_w = 0$ . The IPR curve obtained with the measured production data is shown in Figure 3-7. The wellhead tubing pressure  $p_{wh} = 4.4$  MPa, the wellhead temperature  $T_{wh} = 20^\circ\text{C}$ , and the bottomhole temperature  $T_{wb} = 68^\circ\text{C}$ . Try determining the optimum tubing size under flowing production mode.

**Solving Process.** The outflow performances of the various tubing sizes are calculated using the Orkiszewski method, and it is found that when the tubing size  $d_t$  exceeds 60.3 mm ( $2\frac{3}{8}$  in.), the well will stop flowing. Figure 3-8 shows the tubing outflow curve of the well. Figure 3-9 shows

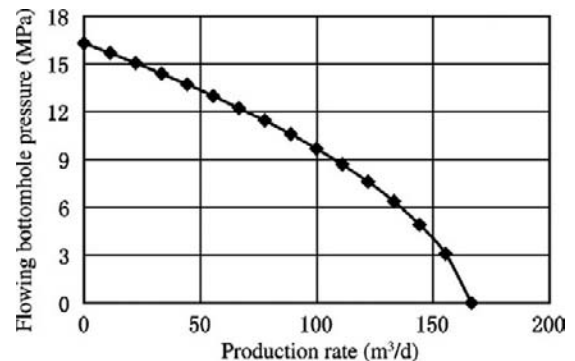


**FIGURE 3-7** IPR curve of Shen 77 well.

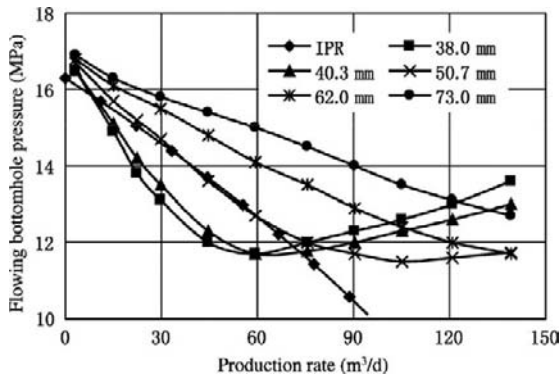


**FIGURE 3-8** Outflow curves of Shen 77 well (obtained by matching the measured data) under various tubing sizes (tubing sizes in figure are inside diameters).

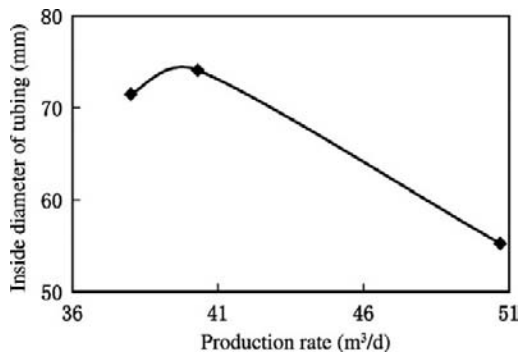


**FIGURE 3-9** Production rate vs. tubing size for Shen 77 well.

the production rate vs. tubing size relationship obtained by the values of the intersections of the IPR curve and the TPR curves. Obviously, the production rate is very sensitive to the tubing size. When the tubing size is increased from 42.2 mm (1.660 in., inside diameter 35.1 mm) to 48.3 mm (1.900 in., inside diameter 40.3 mm), the production rate is obviously increased. When the tubing size is further increased to 60.3 mm (2 3/8 in., inside diameter 50.7 mm), the production rate may be greatly decreased. Thus, the optimum tubing size is 48.3 mm (1.900 in., inside diameter 40.3 mm).

**Case 2.** The Tazhong 402 well of the Talimu oil field has the following known parameter values: mean reservoir pressure  $p_r = 42.49$  MPa, depth in

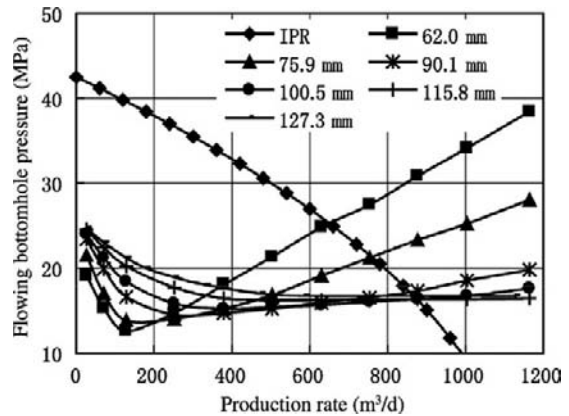


**FIGURE 3-10** Tazhong 402 well system analysis curves (tubing sizes in figure are inside diameters).

middle of reservoir  $H = 3695$  m, producing gas-liquid ratio  $GLR = 220 \text{ m}^3/\text{m}^3$ , oil saturation pressure  $p_b = 42.49$  MPa, relative density of oil  $\gamma_o = 0.8331$ , relative density of gas  $\gamma_g = 0.7851$ , and water cut  $f_w = 0$ . The IPR curves obtained by matching the data of step-rate testing are shown in Figure 3-10 and indicate a high-productivity oil well. The wellhead tubing pressure  $p_{wh} = 2.0$  MPa. The wellhead temperature  $T_{wh} = 30^\circ\text{C}$ , while the bottomhole temperature  $T_{wb} = 85^\circ\text{C}$ . Try determining the optimum tubing size under flowing production mode.

**Solving Process.** The outflow performance relationship curves under various tubing sizes are obtained by analyzing and calculating. These tubing sizes include 73.0 mm (2 7/8 in., internal diameter 62 mm), 88.9 mm (3 1/2 in., inside diameter 75.9 mm), 101.6 mm (4 in., inside diameter 90.1 mm), 114.3 mm (4 1/2 in., inside diameter 100.5 mm), 127 mm (5 in., inside diameter 115.8 mm), and 139.7 mm (5 1/2 in., inside diameter 127.3 mm). The  $Q - d_t$  curve and the  $p_{wf} - d_t$  curve, which are obtained by the values of intersections of the IPR curve and the TPR curves, are shown in Figure 3-11 and Figure 3-12, respectively. The production rate increases with the increase of tubing size when the tubing size is smaller than 114.3 mm (4 in.), whereas the production rate will start reducing when the tubing size is increased to 127 mm (5 in.). Thus, the optimum tubing size is 114.3 mm (4 1/2 in.).

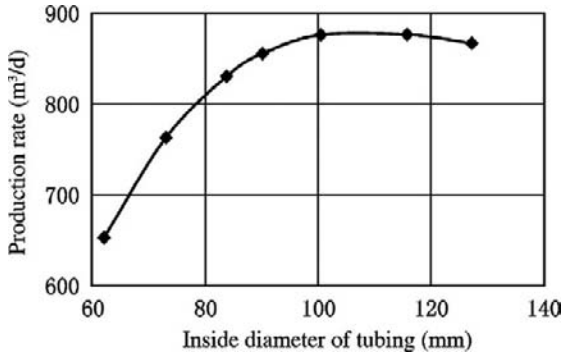


**FIGURE 3-11** Production rate vs. inside diameter of tubing for Tazhong 402 well.

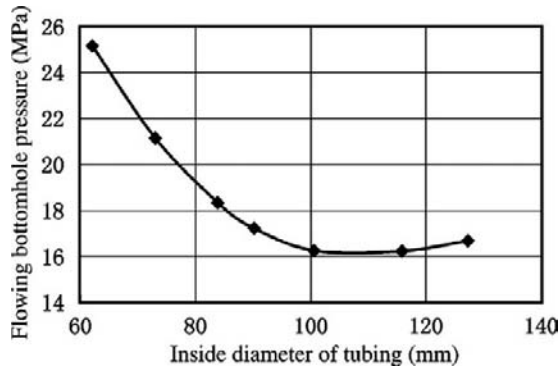


**FIGURE 3-12** Flowing bottomhole pressure vs. inside diameter of tubing for Tazhong 402 well.

This example shows that a larger tubing should be used in a high-productivity well, but an oversized tubing may reduce the production rate by reason of slippage and increase the well construction cost.

**Case 3.** The offshore Oudna oil field in Tunisia has the following known parameter values: original reservoir pressure  $p_r = 16$  MPa, depth in middle of reservoir  $H = 1600$  m, producing gas-liquid ratio  $GLR = 4.5$  m<sup>3</sup>/m<sup>3</sup>, oil saturation pressure  $p_b = 1.56$  MPa, relative density of oil  $\gamma_o = 0.82$ , relative density of gas  $\gamma_g = 0.76$ , relative density of reservoir water  $\gamma_w = 1.05$ , and water cut  $f_w = 2\%$ . The wellhead temperature  $T_{wh} = 40^\circ\text{C}$  and the bottomhole temperature  $T_{wb} = 77.4^\circ\text{C}$ . The fluid productivity index of 764.6 m<sup>3</sup>/(d · MPa) is obtained by well-testing

analysis. Try determining the optimum tubing size to achieve the production rate of 3000 m<sup>3</sup>/d under gas lift mode when the reservoir pressure is reduced to 13 MPa. (The tubing pressure value of 0.6 MPa is necessary for transport.)

**Solving Process.** The gas lift performance curve under various tubing sizes is obtained by analyzing and calculating as shown in Figure 3-13. When the tubing size is smaller than 168.27 mm (6 5/8 in., inside diameter 153.6 mm), the production rate increases with the increase of tubing size under constant gas lift gas injection rate; and when the tubing size is larger than 168.27 mm (6 5/8 in., inside diameter 153.6 mm), the production rate decreases with the increase of tubing size. The gas lift gas injection rate under production rate of 3000 m<sup>3</sup>/d (on gas lift performance curve) vs. corresponding inside diameter of tubing is shown in Figure 3-14. In order to obtain the production rate of 3000 m<sup>3</sup>/d, the tubing size of 168.27 mm (6 5/8 in., inside diameter 153.6 mm) needs the minimum gas lift gas injection rate and has the highest efficiency. Thus, the optimum tubing size is 168.27 mm (6 5/8 in., inside diameter 153.6 mm).

**Tubing Size Optimization Method of Ensuring Longer Flowing Period.** Flowing oil production is the most economic production method and the flowing period of the oil well should be prolonged to the full extent. The key to that lies in economically and rationally utilizing the energy

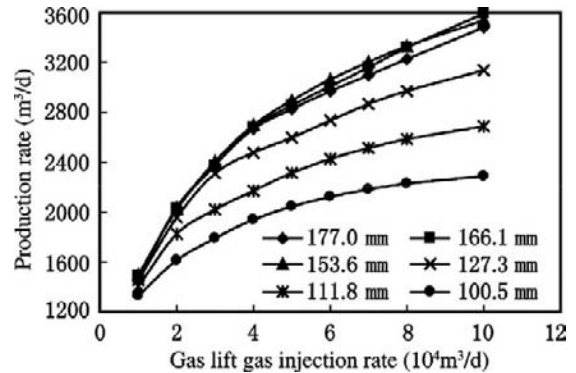


**FIGURE 3-13** Gas lift performance curves of oil well in Oudna oil field under various tubing sizes (tubing sizes in figure are inside diameters).

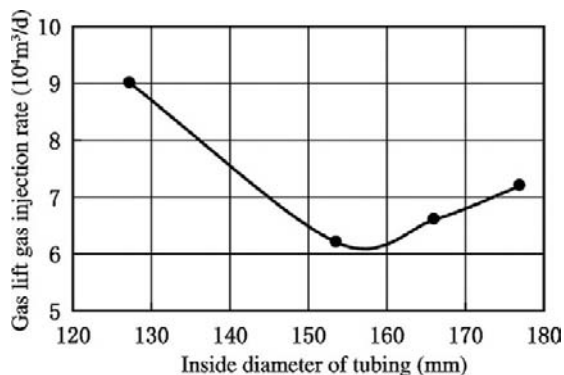


**FIGURE 3-14** Inside diameter of tubing to achieve the production rate required vs. gas lift gas injection rate.

of reservoir fluids, including the pressure energy of fluid and expansion energy of gas. When the flowing wellhead tubing pressure is lower than the saturation pressure or even when the flowing bottomhole pressure is lower than the saturation pressure, the reservoir energy is mainly released in the form of gas expansion energy. When the gas-liquid ratio of the fluid produced from the reservoir is not enough, the oil well may stop flowing.

The production rate and the bottomhole pressure will gradually decrease in the whole flowing production process. The decrease in flowing bottomhole pressure will lead to the increase in producing gas-oil ratio, which will first rapidly increase on the basis of the lower initial value and then gradually decrease to a point lower than the initial point. Thus, the problem of prolonging the flowing period of the oil well changes into the problem of rationally utilizing gas expansion energy.

It has been believed that the tubing size selected should still ensure producing under the maximum lifting efficiency at the end of the flowing period. The formula of selecting tubing diameter is shown in Equation (3-5).

(3-5)

$$d = 0.074 \left( \frac{\gamma_1 L}{p_{wf} - p_{wh}} \right)^{0.5} \left[ \frac{Q_1 L}{\gamma_1 L - 10(p_{wf} - p_{wh})} \right]^{1/3} \times 25.4$$

where  $d$  = internal diameter of tubing, mm;  $\gamma_1$  = relative density of liquid;  $Q_1$  = production rate at the end of the flowing period, t/d;

$L$  = tubing length, m;  $p_{wf}$  = flowing bottomhole pressure at the end of the flowing period,  $10^5$ Pa;  $p_{wh}$  = flowing tubing pressure at the end of the flowing period,  $10^5$ Pa.

The production rate at the end of the flowing period can be determined by the intersections of the future inflow performance IPR curve and tubing TPR curve. The tubing size, which can maximize the current production rate, can be used for obtaining the tubing IPR curve. The intersections of the IPR curve and TPR curve at different stages of drop in reservoir pressure are drawn. The tangential point of the IPR curve and TPR curve is just the quit flowing point. The production rate and the bottomhole pressure at this time are respectively the quit flowing production rate and the quit flowing bottomhole pressure. In practice, the tubing performance curve may also gradually change. With continuous production, the water cut and viscosity may gradually increase and the gas-liquid ratio may gradually decrease; thus the TPR curve also changes. When the wellhead tubing pressure is constant, the TPR curve may gradually move up, whereas the IPR curve may move down, as shown in Figure 3-15.

After the quit flowing production rate and bottomhole pressure are predicted, the tubing size that can maximize the flowing period can be selected using Equation (3-5).

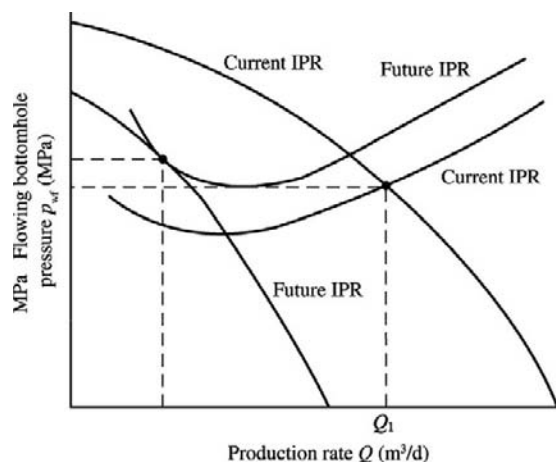


**FIGURE 3-15** The change of production point with decrease of reservoir pressure and the prediction of quit flowing point.

**Case 4.** A certain well has predictive  $Q_1 = 75 \times 10^3 \text{ kg/d}$ , minimum wellhead tubing pressure  $p_{wh} = 2 \times 10^5 \text{ Pa}$ , flowing bottomhole pressure  $p_d = 23 \times 10^5 \text{ Pa}$ , well depth  $L = 1000 \text{ m}$ , and relative density of produced fluid  $\gamma_1 = 0.9$ . Try selecting the tubing size with the longest flowing period.

**Solving Process.** The inside diameter of the tubing is calculated using Equation (3-5).

$$d = 0.074 \left( \frac{0.9 \times 1000}{23 - 2} \right)^{0.5} \left[ \frac{75 \times 1000}{0.9 \times 1000 - 10(23 - 2)} \right]^{1/3} \\ \times 25.4 = 58.7 \text{ mm}$$

Tubing with an inside diameter closer to this value, such as 2  $\frac{7}{8}$ -in. (inside diameter 62.0 mm) tubing, can be used.

**Method of Analyzing Tubing Size Sensitivity Affected by Inflow Performance.** The principles and methods of optimizing tubing size for flowing wells have been briefly described in the preceding sections. The inflow performance and outflow performance of a production well are influenced and conditioned by each other. The inflow performance is the internal factor of conditioning the system, whereas the tubing itself is only an external factor. Therefore, the effect of inflow performance change on tubing size should be analyzed.

The reservoir pressure may reduce with the production time, and that may lead to inflow performance change and gradual fluid property change, thus changing the tubing outflow performance and possibly changing the optimum tubing size. In order to simplify the analysis, the effect of inflow performance change on the optimum tubing size is only discussed here.

**Case 5.** The Tuha Wenxi 1 well has the following data: mean reservoir pressure 24.6 MPa, depth in middle of reservoir 2513 m, producing gas-liquid ratio  $116 \text{ m}^3/\text{m}^3$ , oil saturation pressure 18.89 MPa, relative density of oil 0.8147, relative density of water 1.05, relative density of gas 0.824, water cut 30%, fluid productivity index under the flowing bottomhole pressure higher than saturation pressure  $5 \text{ m}^3/(\text{d} \cdot \text{MPa})$ , given wellhead tubing pressure 1.5 MPa, bottomhole temperature  $79^\circ\text{C}$ , and wellhead temperature

$20^\circ\text{C}$ . Try analyzing the change of the optimum tubing size when the reservoir pressure reduces from 20.6 MPa to 18.6 MPa.

**Solving Process.** The inflow performance relationships on the basis of the given data and three different reservoir pressures are shown in Figure 3-16. The production rate vs. tubing size under the different reservoir pressures is obtained on the basis of the intersections of the inflow performance curves and the tubing performance curves, as shown in Figure 3-17. When the reservoir pressure is 24.6 MPa, the optimum tubing size is 48.3 mm (1.900 in.) or 60.3 mm (2  $\frac{3}{8}$  in.). When  $p_r$  is reduced to 20.6 MPa, the production rate is obviously reduced, the tubing larger than 60.3 mm (2  $\frac{3}{8}$  in.) may stop the flowing of the oil well, and the optimum tubing size is changed to 48.3 mm (1.900 in.). When the reservoir pressure is reduced to 18.6 MPa, the optimum tubing size is 42.2 mm (1.660 in.).

If flowing production can only be achieved using such a small tubing, a series of problems of production technology will certainly result (such as difficulty of paraffin removal). Thus it is better to use a larger tubing for turning to artificial lift, and the economic benefit may be much better. Therefore, this method can be used for predicting the time of turning to pumping.

## Production Casing Size Determination of Flowing Well

The tubing size should first be optimized and determined on the basis of oil field development mode (waterflooding and flowing or artificial lifting production), oil production rate, liquid production rate, recovery rate, reservoir pressure, rule of water cut rising, water cut, ultimate recovery factor, timing of turning to artificial lift from flowing production, oil properties (thin oil, heavy oil, high pour-point oil, and condensate oil), sand production situation of oil well, and stimulation. After that, the maximum size of the matching downhole tools (such as the maximum outside diameter of downhole safety valves of different specifications) should also be considered and the production casing size should be finally determined.

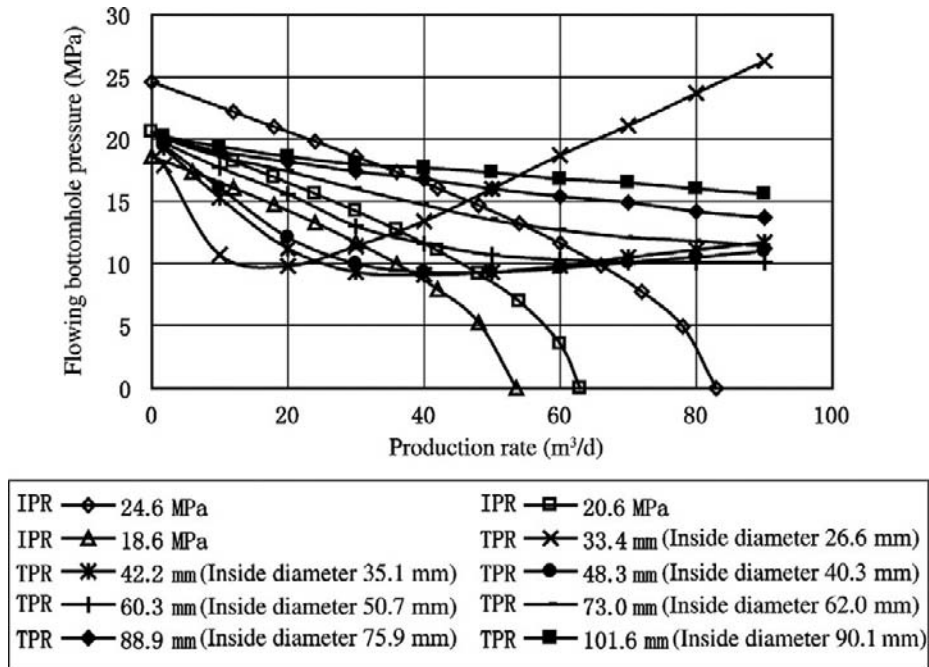


FIGURE 3-16 Tubing sensitivity analysis under changing reservoir pressure.

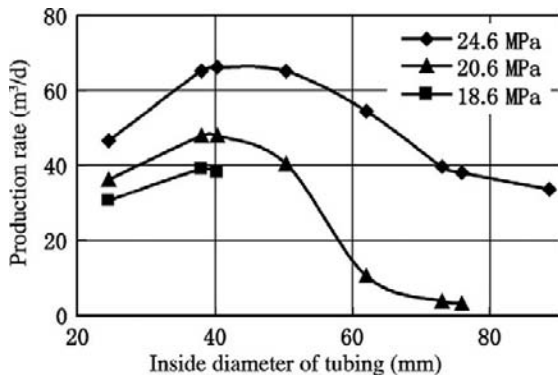


FIGURE 3-17 Tubing size vs. production rate under different reservoir pressures.

### 3.4 SELECTION AND DETERMINATION OF TUBING AND PRODUCTION CASING SIZES FOR GAS WELLS

Tubing size optimization of a natural gas well should ensure the minimum energy consumption of lifting under rational production rate of the

gas well, and should consider the maximum tubing size meeting the requirement of carrying liquid and the minimum tubing size meeting the requirement of avoiding erosion.

#### Selection and Determination of Tubing Size of Natural Gas Well

**Selection and Determination Method of Tubing Size with Minimum Energy Consumption of Lifting under Rational Production Rate.** The tubing size of the gas well should avoid excessive pressure loss in tubing and should ensure a certain tubing pressure for a longer period in order to meet the requirement of the surface engineering. The pressure loss is generally calculated using the gas phase conduit flow pressure drop calculation method under different production rates, flowing bottomhole pressures, and tubing sizes.

The inflow performance curve of a gas well is generally obtained using the exponential deliverability equation or the binomial deliverability equation.

The exponential deliverability equation is as follows

(3-6)

$$q_g = C \times (p_r^2 - p_{wf}^2)^n$$

where  $q_g$  = daily gas production rate,  $10^4 \text{ m}^3/\text{d}$ ;  $p_r$  = mean reservoir pressure, MPa;  $p_{wf}$  = flowing bottomhole pressure, MPa;  $C$  = gas productivity index (related to gas reservoir permeability and thickness, gas viscosity, and bottomhole cleanliness)  $10^4 \text{ m}^3/\text{d}(\text{MPa})^{-n}$ ;  $n$  = filtrate index depending on gas flow mode ( $n = 1$  for linear flow;  $n < 1$  for high flow velocity or multiphase flow).

The binomial deliverability equation is shown in Equation (3-7).

(3-7)

$$\frac{p_r^2 - p_{wf}^2}{q_g} = A + Bq_g$$

where  $A$  = laminar coefficient;  $B$  = turbulence coefficient.

The  $A$  means the pressure loss induced by viscosity and the  $Bq_g$  means the pressure loss induced by inertia. The sum of both form the total pressure drop of inflow. When the flow velocity is low and the flow is linear, the  $Bq_g$  can be negligible and the  $(p_r^2 - p_{wf}^2)$  vs.  $q_g$  relationship is linear. When the flow velocity increases or the flow is multiphase flow, the inertia resistance (that is,  $Bq_g$ ) should be considered.

**Case 6.** A certain gas well has the following data: well depth  $H = 3000$  m, mean gas reservoir temperature  $T = 50^\circ\text{C}$ , relative density of gas  $\gamma_g = 0.65$ , tubing wall roughness  $e = 0.016$  mm, and wellhead tubing pressure = 2 MPa. Try determining the tubing performance curves for the inside diameters of tubing, that is,  $d = 40.8$  mm, 50.7 mm, 62.0 mm, and 101.6 mm.

**Solving Process.** The flowing bottomhole pressures are calculated under the various tubing sizes and the various gas production rates  $Q_{sc} = 1, 10, 20, 40, 60, 80 \times 10^4 \text{ m}^3/\text{d}$  in accordance with the flowing bottomhole pressure calculation formula. The tubing performance curves are shown in Figure 3-18. It is shown that with the increase in gas production rate the TPR curves of smaller tubings are getting steeper

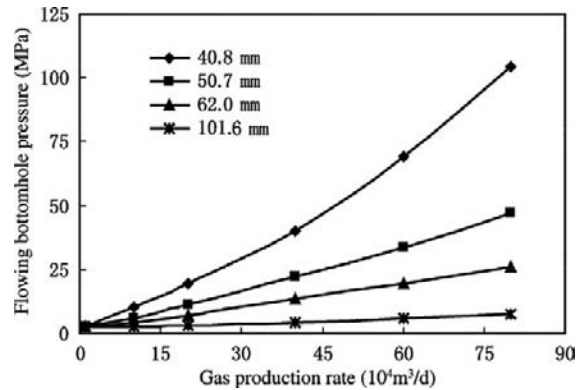


**FIGURE 3-18** Tubing performance curves of pure gas well (tubing sizes in figure are inside diameters).

while the TPR curves of larger tubings are more gentle. The gas flow velocity and friction resistance increase as the tubing size decreases.

**Case 7.** A certain water-bearing gas well has the following data: well depth  $H = 3000$  m, tubing size =  $\Phi 73$  mm ( $2 \frac{7}{8}$  in.), relative density of gas  $\gamma_g = 0.65$ , relative density of reservoir water  $\gamma_w = 1.05$ , reservoir water viscosity  $\mu_w = 0.8$  MPa  $\cdot$  s, and wellhead tubing pressure  $p_{wh} = 2$  MPa. Calculate and draw the tubing performance curve under the various water production rates  $Q_w = 1, 10, 20, 50, 100 \text{ m}^3/\text{d}$ .

**Solving Process.** The flowing bottomhole pressures are calculated using the Hagedorn-Brown two-phase flow calculation method with progressive increase by  $10 \times 10^4 \text{ m}^3$  under different water production rate ( $Q_w$ ) values, and the tubing performance curves of the gas well under different water production rates are obtained (Figure 3-19).

Figure 3-19 shows that when the gas production rate is very low, the effective density of the mixture in tubing is high and the flowing bottomhole pressure is relatively high; with an increase in gas production rate, the mixture density decreases and the flowing bottomhole pressure decreases to some extent; and with a continuous increase in gas production rate, the flow velocity increases, the friction resistance increases, and the flowing bottomhole pressure contrarily increases. When the water production rate is very low, the effective density of the mixture is slightly

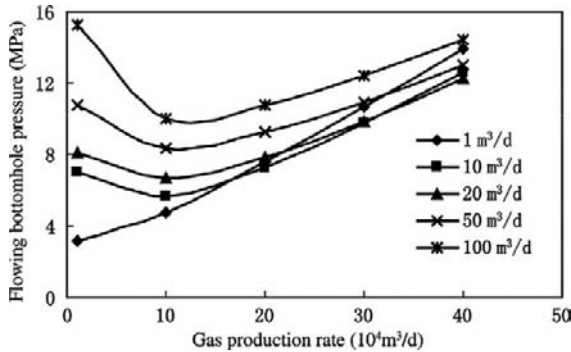


**FIGURE 3-19** Tubing performance curves of a water-bearing gas well (the different curves in the figure correspond to the different water production rates).

affected by water and the flowing bottomhole pressure has no decreasing stage, and the flowing bottomhole pressure increases with the increase in gas production rate.

The TPR curves mentioned earlier are obtained by giving tubing pressure and changing production rate. If a constant tubing pressure is sometimes not needed, the change in tubing pressure under the coordinated condition of reservoir pressure and tubing flow should be determined (Figure 3-20). In the figure, the ordinate represents pressure including reservoir pressure, flowing bottomhole pressure, and tubing pressure. The outflow performance relationship

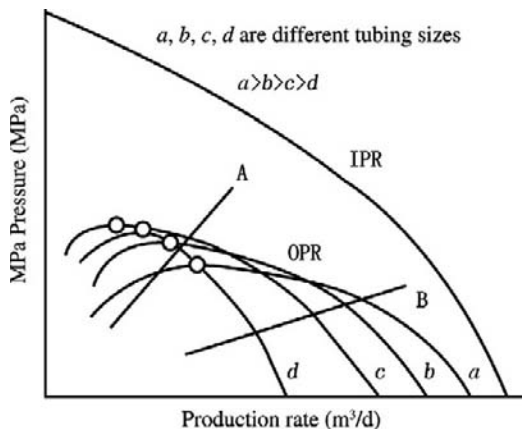


**FIGURE 3-20** Effect of tubing size on gas-well deliverability.

(OPR) curve, known as the gas well outflow curve, is derived on the basis of the inflow performance relationship (IPR) curve and the well-head tubing pressure is obtained using the given flowing bottomhole pressure and the tubing flow formula.

The IPR curve of a water-bearing gas well and the OPR curves of different tubing sizes shown in Figure 3-20 indicate that the production of the gas well is controlled by choke, and the two straight lines A and B represent respectively the choke performance relationships (CPR) of two chokes of different sizes. In accordance with the stability analysis, the gas well production should be conducted on the right side of the peak value for each OPR curve; otherwise, a pressure surge and production stoppage may be caused. When the daily gas production rate is low, a larger diameter tubing may cause gas well production to stop, whereas a smaller diameter tubing can maintain gas well production. Contrarily, in a higher gas production rate range, a larger diameter tubing has a higher flow efficiency. Therefore, a large diameter tubing is used in the initial gas field development period while a small diameter tubing is adopted in the late gas field development period in order to utilize rationally the gas reservoir energy and prolong the gas production period.

Figure 3-20 also shows that the lifting pressure drop of a gas well is not certain to increase with the increase in production rate, and it has a lower value at a certain critical production rate. Different tubing sizes have different gas well production rates, different lifting pressure drops, and different tubing pressures. Therefore, the tubing size should be rationally selected in order to meet the requirement of optimizing production.

**Case 8.** The results of calculation of the Kelaz 2 gas well are shown in Table 3-1.

**Solving Process.** Taking the flowing bottomhole pressure of 70 MPa as an example, the curves can be drawn (Figure 3-21). It can be shown that when the flowing bottomhole pressure is lower, the pressure loss is low and the requirement of high production rate can still be met.

TABLE 3-1 Pressure Loss in Tubing

Tubing Size [in (ID mm)]	Daily Production Rate (10 <sup>4</sup> m <sup>3</sup> )	Flowing Bottom Pressure (MPa)					
		70	60	50	40	30	20
7 (157.07)	200	10.41	9.68	8.80	7.72	6.40	4.88
	300	10.79	10.10	9.27	8.27	7.11	6.01
	400	11.40	10.75	9.99	9.12	8.21	7.83
	500	12.20	11.63	10.97	9.73	9.73	10.71
	600	13.22	12.72	12.20	11.76	11.76	17.02
	700	14.43	14.05	13.70	14.46	14.46	—
5 <sup>1</sup> / <sub>2</sub> (121.36)	200	11.39	10.74	9.97	9.08	8.12	7.61
	300	13.10	12.59	12.04	11.53	11.42	15.27
	400	15.58	15.30	15.13	15.32	17.39	—
	500	18.80	18.95	19.39	21.08	—	—
	600	23.06	23.70	25.30	32.30	—	—
	700	28.29	29.89	34.38	—	—	—
5 (108.61)	200	12.47	11.90	11.27	15.33	10.12	11.45
	300	15.60	15.32	15.14	23.74	17.37	—
	400	20.18	20.41	21.14	—	—	—
	500	26.43	27.63	30.74	—	—	—
	600	34.85	34.48	—	—	—	—
	700	47.08	—	—	—	—	—

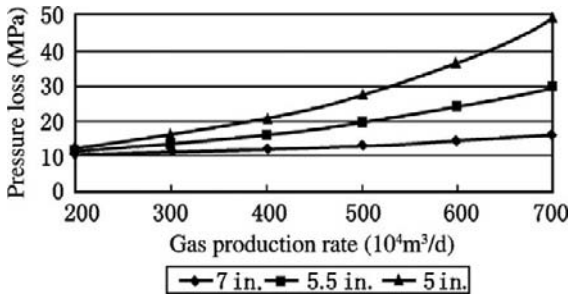


FIGURE 3-21 Pressure losses of different inside diameters of tubing under flowing bottomhole pressure of 70 MPa.

**Method of Selecting and Determining Maximum Tubing Size under Condition of Meeting Carrying Liquid in Gas Well.**

The tubing size of the gas well should meet the requirement of carrying liquid in order to avoid the downhole liquid accumulation due to slippage and the increase in flowing bottom pressure that may cause a decrease in production rate. Thus the maximum tubing size limit should be

determined. Generally, the following Jones Pork formula is used for calculation:

(3-8)

$$Q_{min} = 35.119D^{2.5} \sqrt{p_{wf}/(M_tTZ)^2}$$

where  $Q_{min}$  = minimum allowable production rate, 10<sup>4</sup>m<sup>3</sup>/d; D = inside diameter of tubing, cm;  $p_{wf}$  = flowing bottomhole pressure, MPa;  $M_t$  = relative molecular mass of downhole fluid; T = flowing bottomhole temperature, K; Z = gas deviation factor under bottomhole condition, dimensionless.

The maximum inside diameter of tubing vs. daily production rate curves of a gas well under the different flowing bottomhole pressures are shown in Figure 3-22.

The maximum allowable tubing size under different flowing bottomhole pressures and different daily gas production rates can be determined as shown in Figure 3-22. When the tubing size selected does not exceed the maximum allowable size, the downhole liquid accumulation may be avoided.

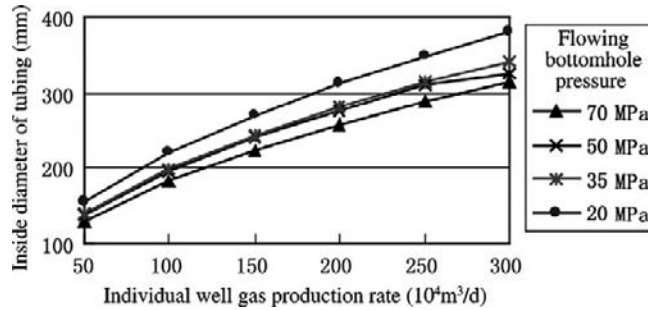


FIGURE 3-22 Maximum allowable tubing size meeting requirement of carrying liquid.

**Case 9.** A certain gas well has the following inflow performance:  $Q_g = 0.3246 (13.495^2 - p_{wf}^2)^{0.8294}$  ( $Q_g$ :  $10^4 \text{ m}^3/\text{d}$ ,  $p$ : MPa). Relative density of gas  $\gamma_g = 0.6$ . Depth in middle of reservoir  $H = 2100$  m. Reservoir temperature is  $80^\circ\text{C}$  and wellhead temperature  $T_{wh}$  is  $25^\circ\text{C}$ . The given wellhead tubing pressure  $p_{wh}$  is 6 MPa. Try analyzing the effects of tubing sizes of 2  $\frac{3}{8}$  in. (60.3 mm, inside diameter 50.7 mm) and 3  $\frac{1}{2}$  in. (88.9 mm, inside diameter 75.9 mm) on the deliverability of the system.

**Solving Process.** First the inflow performance relationship (IPR) curves of a gas well are drawn (Figure 3-23). Then the outflow performance relationship (TPR) curves (TPR1 and TPR2) of the two tubing sizes are drawn, using the calculation method of vertical tubing flow of a pure gas

well. The following results are obtained by the intersections of the IPR curve and the two TPR curves: production rate  $Q_{g1} = 15.1 \times 10^4 \text{ m}^3/\text{d}$  ( $p_{wf} = 8.97$  MPa) when  $d_{t1} = 60.3$  mm (2  $\frac{3}{8}$  in.); and production rate  $Q_{t2} = 18.27 \times 10^4 \text{ m}^3/\text{d}$  ( $p_{wf} = 7.37$  MPa) when  $d_{t2} = 88.9$  mm (3  $\frac{1}{2}$  in.). In this case history, the production rate of the system can be increased by 21.0% when the tubing size is increased from 2  $\frac{3}{8}$  in. to 3  $\frac{1}{2}$  in.

The maximum allowable tubing sizes under the different daily production rates and flowing bottomhole pressures can be calculated using Equation (3-8) and are listed in Table 3-2.

**Selection and Determination Method of Minimum Tubing Size Avoiding Erosion due to Excessive Flow Velocity in Gas Well.** A serious erosion may occur in the tubing of a gas well

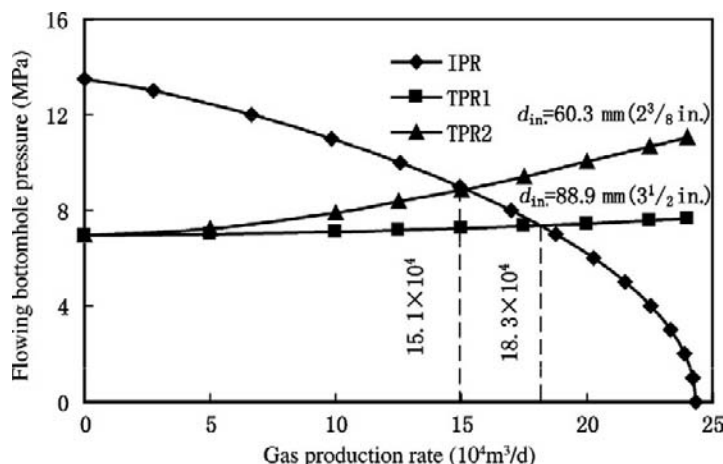


FIGURE 3-23 Effects of different tubing sizes on production rates.

**TABLE 3-2 Maximum Allowable Tubing Sizes Required by Carrying Liquid**

Flowing Pressure (MPa)	Daily Gas Production Rate (10 <sup>4</sup> m <sup>3</sup> /d)					
	50	100	150	200	250	300
70	128.9	182.3	223.3	257.8	288.3	314.2
50	138.7	196.2	240.3	277.4	310.2	325.9
35	140.5	198.7	243.7	281.0	314.1	342.8
20	155.9	220.5	270.1	311.8	348.6	381.9

due to excessive flow velocity, thus leading to premature failure of the tubing. The Beggs formula is generally used for calculation.

1. Beggs erosion velocity formula, as shown in Equation (3-9):

(3-9)

$$V_e = \frac{C}{\rho_g^{0.5}}$$

where  $V_e$  = erosion velocity, m/s;  $\rho_g$  = gas density, kg/m<sup>3</sup>; C = constant, dimensionless (generally 1.22; 1.5 or so under favorable corrosion conditions).

2. Anti-erosion production rate formula, as shown in Equation (3-10):

(3-10)

$$Q_{max} = 55.164 \times 10^4 A \sqrt{\frac{p}{ZT\gamma_g}}$$

where:  $Q_{max}$  = limiting anti-erosion production rate, 10<sup>4</sup>m<sup>3</sup>/d; A = internal cross-sectional area, m<sup>2</sup>; p = mean pressure in tubing, MPa; T = mean temperature in tubing, K; Z = gas

deviation factor under bottomhole condition, dimensionless;  $\gamma_g$  = relative density of gas.

The minimum anti-erosion tubing sizes can be calculated using Equation (3-10) under different flowing bottomhole pressures and gas production rates as listed in Table 3-3.

The daily gas production rate vs. minimum anti-erosion tubing size can be drawn under the different flowing bottomhole pressures (see Figure 3-24). The minimum anti-erosion tubing sizes under different flowing bottomhole pressures and gas production rates are shown.

**Case 10.** The erosion failure of tubing wall and downhole tools may be caused during high-velocity gas flowing in tubing. In consideration of the effect of erosion on the tubing size selection for the Kela 2 gas well, the binomial deliverability equation is shown in Equation (3-11).

(3-11)

$$\frac{73.89^2 - p_{wf}^2}{q} = 2.4033 + 0.0034q$$

where q = gas flow rate, 10<sup>4</sup>m<sup>3</sup>/d; p<sub>wf</sub> = flowing bottomhole pressure, MPa.

**TABLE 3-3 Minimum Anti-Erosion Tubing Sizes**

Flowing Bottomhole Pressure (MPa)	Daily Gas Production Rate (10 <sup>4</sup> m <sup>3</sup> /d)					
	200	300	400	500	600	700
70	83.54	102.42	118.34	132.37	145.05	156.72
60	85.33	104.62	120.89	135.23	148.20	160.12
50	87.83	107.67	124.43	139.17	152.53	164.81
40	91.52	112.17	129.58	144.95	158.84	171.62
30	97.46	119.40	137.87	154.19	168.93	182.50
20	108.00	132.11	152.46	170.42	186.65	201.59

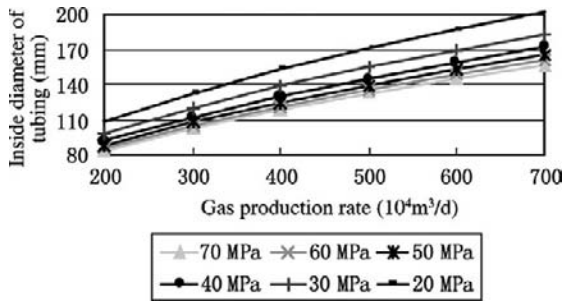


FIGURE 3-24 Minimum anti-erosion tubing sizes.

The relative density of gas ( $\gamma_g$ ) is 0.578. The relative density of gas condensate ( $\gamma_o$ ) is 0.843. The relative density of reservoir water is 1.01. The water cut is 80%. The gas-liquid ratio is  $145,000 \text{ m}^3/\text{m}^3$ . The depth in the middle of the reservoir is 3670 m. The reservoir temperature is  $103.5^\circ\text{C}$ . The wellhead temperature is  $76.2^\circ\text{C}$ . The tubing pressure is 55 MPa. Try selecting the rational tubing size.

**Solving Process.** The erosion may be caused by high-rate gas flowing in tubing and will be very obvious when the flow rate exceeds a certain flow rate (erosive flow rate). Thus the throughput capacity of the gas well tubing is constrained by the erosive flow rate. The critical anti-erosion production rate can be calculated in accordance with the daily throughput capacity determined by erosive flow rate and Equation (3-10).

The sensitivity analyses of tubing sizes of 193.7 mm (7  $\frac{7}{8}$  in.), 177.8 mm (7 in.), 168.2 mm (6  $\frac{5}{8}$  in.), 139.7 mm (5  $\frac{1}{2}$  in.), and 127 mm (5 in.), corresponding to which the inside diameters are respectively 177.0 mm, 154.0 mm, 147.2 mm, 124.2 mm, and 112.0 mm, are made and the corresponding gas production rates are obtained. The corresponding erosive flow rates are calculated by substituting inside diameters of tubing into Equation (3-10). The gas production rate and erosive flow rate vs. tubing size curves are obtained (Figure 3-25). It is shown that the erosion will be generated under smaller tubing. In order to avoid erosion and reduce cost to the full extent, a tubing between 168.2 mm (6  $\frac{5}{8}$  in.) and 177.8 mm (7 in.) is selected.

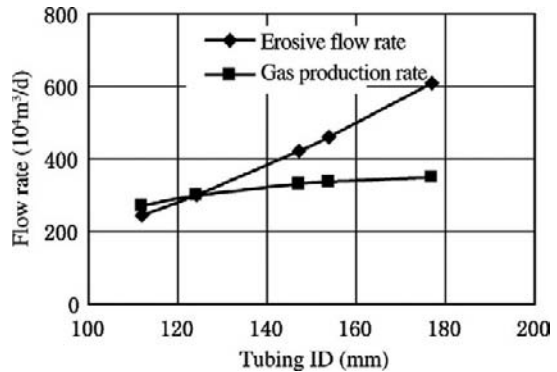


FIGURE 3-25 Effect of tubing ID on flow rate.

### Production Casing Size Determination of Natural Gas Well

The production casing size selection of a natural gas well should ensure minimum lifting friction resistance or energy consumption under the rational natural gas production rate, maximum tubing size meeting the requirement of carrying liquid, and minimum tubing size decreasing erosion force. In addition, the maximum size of the matching downhole tools (such as the maximum outside diameter of downhole safety valve), the stimulations in the process of putting the well into production, and the measures of dewatering gas production in the late producing period should also be considered in order to select the rational tubing size. Finally, the production casing size is determined (see Table 3-4).

The outdated nominal tubing diameter is the inside diameter, while the updated or international nominal tubing diameter is the outside diameter (see Tables 3.5 and 3.6).

### 3.5 SELECTION AND DETERMINATION OF TUBING AND PRODUCTION CASING SIZES FOR ARTIFICIAL LIFT WELLS

When the reservoir energy is insufficient or the water cut is higher despite sufficient reservoir energy, the artificial lift method should be used in order to maintain oil well production under rational producing pressure drawdown.

**TABLE 3-4 Matching Tubing Size with Production Casing Size for Oil and Gas Wells**

Outside Diameter of Tubing [mm (in.)]	Production Casing Size [mm (in.)]	Outside Diameter of Tubing [mm (in.)]	Production Casing Size [mm (in.)]
≤60.3(2 <sup>3</sup> / <sub>8</sub> )	127(5)	127.5(5)	177.8~193.7(7~7 <sup>5</sup> / <sub>8</sub> )
73.0(2 <sup>7</sup> / <sub>8</sub> )	139.7(5 <sup>1</sup> / <sub>2</sub> )	139.7(5 <sup>1</sup> / <sub>2</sub> )	193.7(7 <sup>5</sup> / <sub>8</sub> )~244.5(9 <sup>5</sup> / <sub>8</sub> )
88.9(3 <sup>1</sup> / <sub>2</sub> )	168.3~177.8(6 <sup>5</sup> / <sub>8</sub> ~7)	177.8(7)	244.5(9 <sup>5</sup> / <sub>8</sub> )
101.6(4)	177.8(7)	193.7(7 <sup>5</sup> / <sub>8</sub> )	273.1(10 <sup>3</sup> / <sub>4</sub> )
114.3(4 <sup>1</sup> / <sub>2</sub> )	177.8(7)	244.5(9 <sup>5</sup> / <sub>8</sub> )	339.7(13 <sup>3</sup> / <sub>8</sub> )

Note: When the downhole safety valve is set, the production casing above the safety valve should be enlarged by one grade (generally 100–200 m from the surface).

**TABLE 3-5 Comparison of Updated Nominal Tubing Sizes and Outdated Nominal Tubing Sizes**

Nominal Diameter [mm (in.)]	Inside Diameter of Tubing (mm)	Outside Diameter of Tubing (mm)	Outdated Standard (in.)
33.4(1.315)	26.4	33.4	1
42.2(1.660)	35.2	42.2	1 <sup>1</sup> / <sub>4</sub>
48.3(1.900)	40.3	48.3	1 <sup>1</sup> / <sub>2</sub>
60.3(2 <sup>3</sup> / <sub>8</sub> )	50.7	60.3	2
73.0(2 <sup>7</sup> / <sub>8</sub> )	62.0	73.0	2 <sup>1</sup> / <sub>2</sub>
88.9(3 <sup>1</sup> / <sub>2</sub> )	75.9	88.9	3
101.6(4)	90.1	101.6	3 <sup>1</sup> / <sub>2</sub>

**TABLE 3-6 Common Production Casing Sizes**

Nominal Diameter (in.)	Outside Diameter of Casing (mm)	Casing Wall Thickness (mm)
4 <sup>1</sup> / <sub>2</sub>	114.3	5.21, 6.35, 7.37, 8.56
5	127.0	5.59, 6.43, 7.52, 9.20
5 <sup>1</sup> / <sub>2</sub>	139.7	6.20, 6.98, 7.72, 9.17, 10.54
6 <sup>5</sup> / <sub>8</sub>	168.3	7.32, 8.94, 10.59, 12.07
7	177.8	5.87, 6.91, 8.05, 9.20, 10.36, 11.51, 12.65, 13.72
7 <sup>5</sup> / <sub>8</sub>	193.7	7.62, 8.33, 9.93, 10.92, 12.70
8 <sup>5</sup> / <sub>8</sub>	219.2	6.71, 7.72, 8.94, 10.16, 11.43, 12.70, 14.15
9 <sup>5</sup> / <sub>8</sub>	244.5	7.93, 8.94, 10.03, 11.05, 11.99, 13.84
10 <sup>3</sup> / <sub>4</sub>	273.0	7.09, 8.89, 10.16, 11.43, 12.57, 13.84, 15.11, 16.51, 17.78
11 <sup>3</sup> / <sub>4</sub>	298.9	8.46, 9.52, 11.05, 12.42
13 <sup>3</sup> / <sub>8</sub>	339.7	8.38, 9.65, 10.92, 12.19, 13.06

Different artificial lift methods require different matching tubing sizes and different corresponding production casing sizes due to different lifting devices and equipment and different well conditions. For instance, when the conventional tubing pump of  $\Phi 56$  mm is used for oil pumping, the matching tubing size should be  $\Phi 73$  mm ( $2 \frac{7}{8}$  in.) and the maximum outside diameter of the pump is 89.5 mm, and then the production casing of  $\Phi 139.7$  mm ( $5 \frac{1}{2}$  in.) can be selected under the single-string production with no sand control. If the inside casing gravel pack sand control method should be used and the pump is required to be set at reservoir position (this factor should be considered when a wire-wrapped screen size is selected), the production casing should be larger than  $\Phi 177.8$  mm (7 in.). When the conventional tubing pump of  $\Phi 110$  mm is used for oil pumping, the matching tubing size should be  $\Phi 114.3$  mm ( $4 \frac{1}{2}$  in.), and the maximum outside diameter of the pump is 146 mm, then the production casing size should be at least  $\Phi 177.8$  mm (7 in.) even if the single-string production with no sand control is adopted. If the inside casing gravel pack sand control method is required, the production casing of  $\Phi 244.5$  mm ( $9 \frac{5}{8}$  in.) is more adaptable.

When the tubing and production casing sizes of the artificial lift well are determined, the mode of lift should be emphatically considered. The common artificial lift production modes include sucker rod pump, electric submersible pump, hydraulic piston pump, hydraulic jet pump, screw pump, and gas lift production. Sucker rod pumping accounts for more than 90% in China. The other key to determination of the type of pump and the tubing and production casing sizes is the daily fluid production rate level in the middle and late periods of waterflooding.

### Prediction of Daily Liquid Production Rate Level in the High Water Cut Period

For a new well with adequate energy, flowing production can be initially adopted, but the daily liquid production rate is relatively low because a

certain tubing shoe pressure should be maintained. After oil well production is turned to artificial lift production during oil field waterflooding, in order to adjust the producing pressure drawdown, utilize reservoir potential, and achieve stable oil production, the daily fluid production rate should be gradually increased with the increase in water cut and flowing bottom-hole pressure, thus maintaining the rational producing pressure drawdown.

The well completion design should be completed before drilling. Thus, leadership and foresight should be provided for selection and determination of tubing and production casing sizes. The daily liquid production rate during the whole oil field development, especially in the high water cut period, and the requirements for tubing and production casing sizes should be considered.

In general, the daily liquid production rate in the flowing period is relatively low and the corresponding tubing and production casing sizes are also relatively small. After turning to artificial lift production, especially in the high water cut period, larger tubing and production casing sizes are required in order to adapt production under the condition of a large pump. After the lift mode of the oil well is determined, the possible daily liquid production rate in the future should be predicted and the tubing and production casing sizes are then selected and determined; otherwise, the production rate may be limited due to the unreasonable strings in many oil wells. For instance, a certain well selects sucker rod pumping and the conventional tubing pump is selected. The initial daily oil production rate is 50t/d. The water cut is 10%. The daily liquid production rate is 55.6 t. If the mean pump efficiency is 60% and a tubing pump of  $\Phi 56$  mm is selected, the matching tubing size is  $\Phi 73$  mm ( $2 \frac{7}{8}$  in.), the outside diameter of the pump is 89.5 mm, and the production casing of  $\Phi 139.7$  mm ( $5 \frac{1}{2}$  in.) is possible. However, when the water cut of this well  $f_w = 90\%$ , the stable oil production rate of 40t/d is required, and the daily liquid production rate level should be at least 400 t/d. If the mean pump efficiency is still 60%, the tubing

pump of  $\Phi 110$  mm should be selected. At this time, the tubing size matching with the pump is  $\Phi 114.3$  mm (4 in.) and the outside diameter of the pump barrel is 146 mm; thus, the production casing should be at least  $\Phi 177.8$  mm (7 in.). If this well is in the high water cut period and sand control is required, the production casing of 7 in. cannot meet the requirement. The daily oil production rate of 40t/d cannot be reached, and the oil production rate has to be reduced.

Therefore, the selection and determination of tubing and production casing sizes in consideration of the future daily production rate level are scientific and realistic practices. After a well is completed, the tubing size is changeable, whereas the production casing size is unchangeable. In order to discharge liquid by a large pump in the high water cut period, a larger production casing size is better. Therefore, in the initial flowing and artificial lift period, rational tubing size is adopted on the basis of production optimization (nodal systems analysis), whereas in the high water cut period during which a large pump is needed for discharging the liquid, the tubing size can be changed to a larger tubing size.

The daily liquid production rate in the high water cut period can be predicted in accordance with the requirement of stable oil production design. In the development program, the daily oil production rate level (allocating oil production rate) is formulated on the basis of the reservoir oil properties, reservoir parameters, and requirement of allocation of oil field development. In the waterflooding oil field, the daily liquid production rate of the oil well should be increased after entering into the high water cut period of the oil well in order to meet the requirement of stable oil production. The empirical method shown in Equation (3-12) is commonly used in the field:

(3-12)

$$Q_L = \frac{Q_{po}}{1 - f_w}$$

where  $Q_{po}$  = daily allocating oil production rate of oil well in development design,  $m^3/d$ ;

$Q_L$  = daily liquid production rate predicted,  $m^3/d$ ;  $f_w$  = water cut.

The numerical simulation method or the method of predicting the future IPR curve should be used for calculating accurately the daily liquid production rate in the high water cut period.

## Artificial Lift Mode Determination

On the basis of the maximum tubing diameter or the minimum production casing diameter, in accordance with the predicted highest daily liquid production rate level in the high water cut period and the theoretical discharge capacity and discharge head calculated by supposing pump efficiency of 60%, with reference to down-hole conditions, surface environment, operation condition, maintenance and management, and economic benefit, artificial lift mode is optimized and selected. In general, artificial lift mode is selected and determined using the methods described in the following sections.

**Preliminary Selection of Artificial Lift Mode.** Artificial lift mode is preliminarily selected in accordance with adaptability to production conditions, as shown in Table 3-7.

**Production Mode Optimization Using the Grade Weighted Method.** The evaluation parameters related to the feasibility and complexity of various artificial lift modes are digitized, compared, and graded. The first type parameter (X) is the parameter related to the feasibility of successful use of artificial lift mode and is divided into five grades (Grades 4, 3, 2, 1, and 0 represent respectively excellent feasibility, good feasibility, moderate feasibility, poor feasibility, and infeasible). The second type parameter (Y) is the parameter related to the method complexity, investment, and steel product consumption and is divided into three grades (Grades 3, 2, and 1 represent respectively favorable complexity, moderate complexity, and unfavorable complexity). X, Y, and Z are respectively calculated using Equations (3-13), (3-14), and (3-15), with reference to Table 3-8 and Table 3-9 under the specific conditions of the oil well. The artificial lift methods with higher Z values are selected as

TABLE 3-7 Adaptability Comparison between Artificial Lift Systems

Item	Adaptability Condition	Sucker Rod Pump	Screw Pump	Electric Submersible Pump	Hydraulic Piston Pump	Hydraulic Jet Pump	Gas Lift	Plunger Lift
Basic conditions of system	Degree of complexity	Simple	Simple	Complex bottomhole	Complex surface	Complex surface	Complex surface	Complex surface
	One investment Operation cost	Low Low	Low Low	High High	High Low; High in high water cut period	High Low	Highest Low; High for small oil field	Highest Low; High for small oil field
Discharge capacity m <sup>3</sup> /d	Normal range	1~100	10~200	80~700	300~600	10~500	30~3180	20~32
	Maximum	410	(1000)	1400 (3170)	(1293)	1590 (4769)	(7945)	63
Pump depth m	Normal range	3000	1500	2000	4000	2000	3000	3000
	Maximum	4421	3000	3084	5486	3500	3658	3658
Downhole conditions	Slim hole	Appropriate	Appropriate	Inappropriate	Appropriate	Appropriate	Appropriate	Appropriate
	Separate-zone production	Inappropriate	Inappropriate	Appropriate	Appropriate	Inappropriate	Appropriate	Appropriate
	Directional well Degree of cavitation	General wear Strong	Serious wear Strong	Appropriate Strong	Appropriate Strong	Appropriate Strong	Appropriate Strong	Appropriate Strong
Surface environment	Offshore and city Harsh climate	Inappropriate General	Appropriate General	Appropriate Appropriate	Appropriate Appropriate	Appropriate Appropriate	Appropriate Appropriate	Appropriate Appropriate

Operation problems	High gas-oil ratio	Adaptable	General	Inadaptable	General	Adaptable	Very adaptable	Very adaptable
	Heavy oil and high pour-point oil	Good	Good	Inadaptable	Very good	Very good	Inadaptable	Inadaptable
	Sand production	Good	Adaptable	Inadaptable	General	General	Very adaptable	Very adaptable
	Corrosion	Adaptable	Adaptable	Adaptable	Adaptable	Adaptable	Adaptable	Adaptable
	Scaling	Adaptable	Inadaptable	Inappropriate	Adaptable	Adaptable	General	General
	Working system adjustment	Convenient	Convenient	Lack of flexibility	Lack of flexibility	Convenient	Convenient	Convenient
	Power source	Electricity, natural gas, oil	Electricity, natural gas, oil	Electricity	Electricity, natural gas, oil	Electricity, natural gas, oil	Electricity, natural gas, oil	Electricity, natural gas, oil
Requirement for power media	None	None	None	Special power fluid	Water power fluid	Avoiding hydrate	Avoiding hydrate	
Maintenance and management	Pump inspection	Pulling out tubing for tubing pump	Pulling out tubing	Pulling out tubing	Hydraulic or wire pulling and running	Hydraulic or wire pulling and running	Wire pulling and running	Wire pulling and running
	Mean repair-free period (a)	2	1	1.5	0.5	0.5	3	3
	Auto-control	Appropriate	General	Appropriate	Appropriate	Appropriate	General	General
Production test	Basically matching	Unmatching	Basically matching	Basically matching	Unmatching	Completely matching	Basically matching	

Notes: 1. The discharge capacity values in parentheses ( ) mean the discharge capacity values achievable when the external diameter of production casing is larger than 177.8 mm.

2. If a frequency converter is used, the working system adjustment for various artificial lift modes is convenient, but the cost is high.

3. For the various artificial lift modes, the flowing bottomhole pressures can be reduced to zero under sufficient production casing strength except gas lift mode, under which a certain tubing shoe pressure (that is, flowing bottomhole pressure when tubing is set in the middle of reservoir) is required in order to lift the well liquid.

TABLE 3-8 Local Feasibility Parameter Assessment Values (X)

No.	Related Contents of Local Parameter	Symbol	Sucker Rod Pump	Electric Submersible Pump	Hydraulic Piston Pump	Hydraulic Jet Pump	Gas Lift	Surface-Driven Screw Pump
1	High production rate (>100 m <sup>3</sup> /d)	X <sub>1</sub>	2	4	2	2	4	2
2	Medium production rate (5–100 m <sup>3</sup> /d)	X <sub>2</sub>	3	4	3	3	4	3
3	Low production rate (<5 m <sup>3</sup> /d)	X <sub>3</sub>	4	1	4	4	0	4
4	High discharge head (>1350 m)	X <sub>4</sub>	1	3	4	4	4	0
5	Medium discharge head (450–1350 m)	X <sub>5</sub>	3	4	4	4	4	2
6	Low discharge head (<450 m)	X <sub>6</sub>	4	4	4	4	4	4
7	Failure-free time, rate of well utilization	X <sub>7</sub>	2	3	3	3	3	3
8	Well test, production test	X <sub>8</sub>	3	2	2	2	4	2
9	Automated oil production, parameter adjustment	X <sub>9</sub>	2	4	3	3	3	3
10	Integrity of production technology	X <sub>10</sub>	2	2	3	3	3	3
11	Oil production method efficiency	X <sub>11</sub>	1	3	3	2	2	3
12	Ability of separate production in a well	X <sub>12</sub>	2	2	2	2	3	2
13	Adaptability to slant and directional well	X <sub>13</sub>	1	3	4	4	4	3
14	Adaptability to 70°C well temperature	X <sub>14</sub>	3	3	3	3	4	3
15	Adaptability to well temperature higher than 70°C	X <sub>15</sub>	2	0	3	3	4	2
16	Mechanical admixture in produced liquid ≤1%	X <sub>16</sub>	2	3	2	2	4	4
17	Mechanical admixture in produced liquid >1%	X <sub>17</sub>	0	0	0	0	3	4
18	Scaling and corrosion	X <sub>18</sub>	1	1	1	1	2	2
19	Water cut	X <sub>19</sub>	2	3	2	3	2	3
20	Enhanced oil recovery ability	X <sub>20</sub>	1	4	1	1	2	2
21	High gas-oil ratio	X <sub>21</sub>	2	2	2	2	4	3
22	High paraffin content	X <sub>22</sub>	2	3	2	2	1	4
23	Heavy oil (<100)	X <sub>23</sub>	2	1	4	4	2	4
24	High wellhead tubing pressure	X <sub>24</sub>	1	2	3	3	2	2
25	Harsh climate, offshore	X <sub>25</sub>	1	2	3	3	2	2
26	Adaptability to slim hole	X <sub>26</sub>	2	2	1	3	4	2

TABLE 3-9 Local Complexity Parameter Assessment Values (Y)

No.	Related Contents of Local Parameter	Symbol	Sucker Rod Pump	Electric Submersible Pump	Hydraulic Piston Pump	Hydraulic Jet Pump	Gas Lift	Surface-Driven Screw Pump
1	Serviceability	$Y_1$	3	3	3	3	2	2
2	Simplicity and convenience of equipment	$Y_2$	2	3	2	2	2	3
3	Energy utilization efficiency	$Y_3$	2	3	2	1	1	2
4	Mobility of equipment	$Y_4$	1	3	2	2	2	3
5	Demulsification ability	$Y_5$	2	1	2	1	1	3
6	Degree of simplicity and ease of oil well equipment	$Y_6$	1	3	1	2	1	3
7	Initial investment efficiency	$Y_7$	2	1	2	2	2	3
8	Utilization rate of metal	$Y_8$	1	3	1	1	1	3

the preliminary results, and the technical and economic demonstration is then conducted in accordance with the technical design of a typical well, and the artificial lift mode meeting the requirements is finally determined.

(3-13)

$$X = n \sqrt{\prod_{i=1}^n X_i}$$

(3-14)

$$Y = n \sqrt{\prod_{i=1}^n Y_i}$$

(3-15)

$$Z = \sqrt{XY}$$

**Chart Method of Selecting Oil Production Mode.** The two methods of selecting the oil production mode are as follows:

1. A rational usable range chart of sucker rod pump, electric submersible pump, and

hydraulic piston pump, which was obtained by reference to the related charts in the late 1980s and in combination with the oil field conditions and use experience in China, is shown in Figure 3-26. The artificial lift mode can be determined by the location of the predicted coordinate point of discharge head and liquid production rate.

2. The optimum usable range charts of gas lift, plunger lift, sucker rod pump, electric

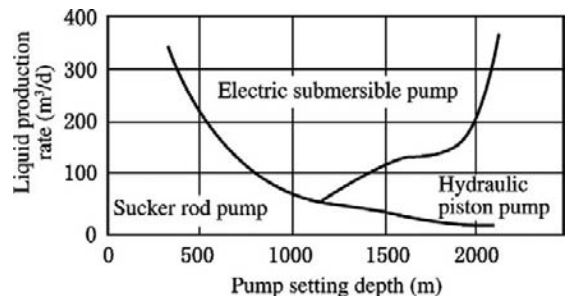


FIGURE 3-26 Rational usable ranges of sucker rod pump, electric submersible pump, and hydraulic piston pump.

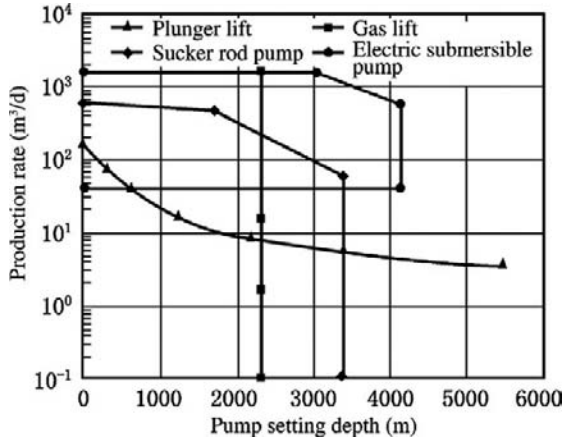


FIGURE 3-27 Optimum usable ranges of plunger lift, sucker rod pump, gas lift, and electric submersible pump.

submersible pump, hydraulic piston pump, and jet pump, which were presented by Blais et al. in 1986, are shown in Figures 3-27 and 3-28. The artificial lift mode can be determined by the location of the coordinate point of the predicted discharge lead and liquid production rate.

After artificial lift modes are determined using these methods, the tubing and production casing sizes are selected and determined on the basis of the artificial lift modes.

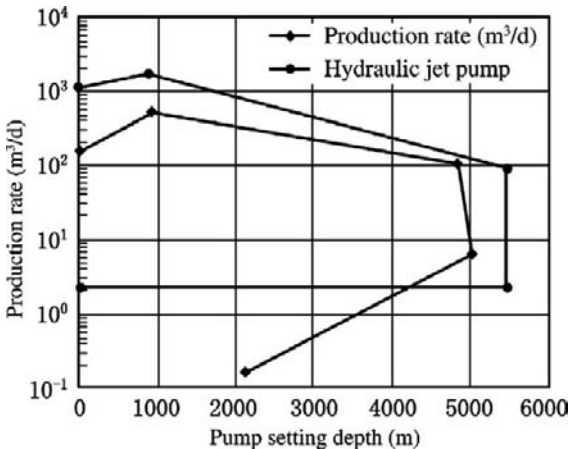
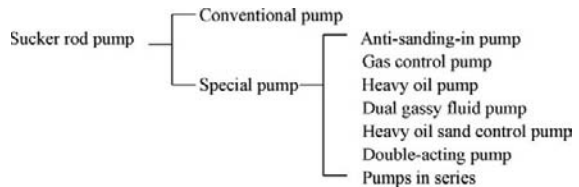


FIGURE 3-28 Optimum usable ranges of hydraulic piston pump and hydraulic jet pump.

## Selection and Determination of Tubing and Production Casing Sizes for Sucker Rod Pump Well

Sucker rod pumping has played a leading role in artificial lift production mode worldwide all along. At present, sucker rod pumping has been adopted by more than 90% of artificial lift production wells in China. Sucker rod pumps are divided into two categories: conventional and special pumps. Special pumps include anti-sanding-in pumps, gas control pumps, heavy oil pumps, dual gassy fluid pumps, heavy oil sand control pumps, double-acting pumps, and pumps in series.



The procedure for selecting the tubing and production casing sizes of sucker rod pumping wells is as follows.

1. Predicting daily liquid production rate level in the high water cut period of an oil well.
2. Selecting theoretical discharge capacity. The theoretical pump discharge capacity  $Q_{tL}$  vs. daily liquid production rate  $Q_L$  relationship is shown in Equation (3-16):

(3-16)

$$Q_{tL} = \frac{Q_L}{\eta_p}$$

where  $Q_{tL}$  = theoretical pump discharge capacity,  $m^3/d$ ;  $Q_L$  = daily liquid production rate predicted,  $m^3/d$ ;  $\eta_p$  = actual pump efficiency, % (generally 60% selected preliminary).

3. Selecting the nominal diameter of the pump on the basis of theoretical discharge capacity of the pump.
4. Determining production casing size. The tubing size and the maximum outside diameter of the pump can be obtained on the basis of the nominal diameter of the pump. The production casing size matching the pump size is determined under the condition of gravel

pack sand control well or non-sand control well and the condition of single-string or dual-string production.

The pump barrel of the tubing pump is at the lower end of the tubing string and the sucker rod is run in the pump barrel with the plunger. The tubing pump has mainly a pump barrel and plunger. Thus a relatively large pump size with a theoretical discharge capacity can be chosen. It can be used in shallow and moderately deep pumping wells with high productivity (Table 3-10).

The rod-insert pump has inside and outside working barrels and has relatively small pump size and discharge capacity. It is used in deep wells with low liquid levels and low production rates (see Table 3-11).

In practice, the pumping unit cannot operate under the maximum stroke, maximum strokes per minute, and maximum load; the fullness coefficient cannot be equal to 1; and the pump efficiency cannot be equal to 100%. When the pump size is selected, pump efficiency of 50%

to 80% and (stroke) × (strokes per minute) value ≤ 36 can be preliminarily selected.

The special pumps, such as the anti-sanding-in pump, gas control pump, hydraulic feedback heavy oil pump, circulation flow heavy oil pump, and dual gassy fluid pump, will not be discussed in detail because they are rarely used. However, the methods of selecting production casing size are the same as that of the conventional tubing pump and conventional rod-insert pump.

**Case 11.** The allocating oil production rate of a certain well on the basis of development design is 15 m<sup>3</sup>/d. The underground oil viscosity is 14.5 MPa · s. The oil well has no sand production. The oil field adopts waterflooding. Try selecting the production casing size.

**Solving Process.** (1) The daily liquid production rate in the high water cut period is predicted using Equation (3-12). When the water cut  $f_w = 80%$ ,  $Q_{L1} = 75 \text{ m}^3/\text{d}$ ; when  $f_w = 90%$ ,  $Q_{L2} = 150 \text{ m}^3/\text{d}$ ; and when  $f_w = 95%$ ,  $Q_{L3} = 300 \text{ m}^3/\text{d}$ . (2) The conventional tubing pump is selected.

TABLE 3-10 Matching Conventional Tubing Pump (Integral Pump Barrel) with Tubing and Production Casing

Nominal Diameter of Pump (mm)	Outside Diameter of Connecting Tubing (mm)	Theoretical Discharge Capacity (m <sup>3</sup> /d)	Maximum Outside Diameter (mm)	Casing Size Recommended (in.)	
				Non-Sand Control Well	Gravel-Pack Sand-Control Well
32	73.0	14~35	89.5	5~5 <sup>1</sup> / <sub>2</sub>	7
38	73.0	20~44	89.5	5~5 <sup>1</sup> / <sub>2</sub>	7
44	73.0	26~66	89.5	5~5 <sup>1</sup> / <sub>2</sub>	7
57	73.0	40~110	89.5	5~5 <sup>1</sup> / <sub>2</sub>	7
70	88.9	67~166	107	5 <sup>1</sup> / <sub>2</sub>	7
83	101.6	94~234	114	7	7
95	114.3	122~306	132.5	7	7
110	114.3	164~410	146	7~9 <sup>5</sup> / <sub>8</sub>	9 <sup>5</sup> / <sub>8</sub>

Plunger stroke length range: 1.2–5.0 m

Notes: 1. Under theoretical discharge capacity, lower limit strokes per minute = 10/min, stroke = 1.2 m; upper limit strokes per minute = 6/min, stroke = 5 m.  
 2. For an inside casing gravel pack sand control well, the production casing size should be increased by one grade and a production casing size larger than 7 in. should be selected in order to ensure sand control effectiveness and increase thickness of gravel pack zone. For an outside gravel pack sand control well, the production casing size should be decreased by one grade. If the pump is required to be set below the top of a perforated interval, the production casing size should be increased by one grade. Generally, the distance between pump and perforation should not be less than 80 m in order to protect the reservoir from surges.

**TABLE 3-11 Matching of Conventional Rod-Insert Pump with Tubing And Production Casing**

Nominal Diameter of Pump (mm)	Outside Diameter of Connecting Tubing [mm (in.)]	Theoretical Discharge Capacity (m <sup>3</sup> /d)	Maximum Outside Diameter (mm)	Casing Size Recommended (in)	
				Sand Control Well	Non-Sand Control Well with Gravel Pack
32	60.3(2 <sup>3</sup> / <sub>8</sub> )	14~35	89.5	5~5 <sup>1</sup> / <sub>2</sub>	7
38	73.0(2 <sup>7</sup> / <sub>8</sub> )	20~49	89.5	5~5 <sup>1</sup> / <sub>2</sub>	7
44	73.0(2 <sup>7</sup> / <sub>8</sub> )	26~66	89.5	5~5 <sup>1</sup> / <sub>2</sub>	7
51	73.0(2 <sup>7</sup> / <sub>8</sub> )	35~88	107	5 <sup>1</sup> / <sub>2</sub>	7
56	88.9(3 <sup>1</sup> / <sub>2</sub> )	43~106	107	5 <sup>1</sup> / <sub>2</sub>	7
57	88.9(3 <sup>1</sup> / <sub>2</sub> )	44~110	107	5 <sup>1</sup> / <sub>2</sub>	7
63	88.9(3 <sup>1</sup> / <sub>2</sub> )	54~135	114	7	7

Plunger stroke length range: 1.2–5.0 m

Notes: 1. Under theoretical discharge capacity, lower limit strokes per minute = 10/min, stroke = 1.2 m; upper limit strokes per minute = 6/min, stroke = 5 m.

2. For an inside casing gravel pack sand control well, the production casing size should be increased by one grade and a production casing size larger than 7 in. should be selected in order to ensure sand control effectiveness and increase thickness of gravel pack zone. For an outside gravel pack sand control well, the production casing size should be decreased by one grade. If the pump is required to be set below the top of a perforated interval, the production casing size should be increased by one grade. Generally, the distance between pump and perforation should not be less than 80 m in order to protect the reservoir from surges.

Suppose the pump efficiency  $\eta_p$  is 80% when the water cut is high. The theoretical discharge capacities of the pump under the water cuts of 80%, 90%, and 95% are 93.8 m<sup>3</sup>/d, 187.5 m<sup>3</sup>/d, and 375 m<sup>3</sup>/d, respectively, in accordance with Equation (3-16). In order to ensure the stable oil production rate of 15 m<sup>3</sup>/d in the high water cut period, the pump of  $\Phi 110$  mm with a theoretical discharge capacity of 164–410 m<sup>3</sup>/d can be selected using Table 3-10. The tubing of  $\Phi 114.3$  mm (4 1/2 in.) and the maximum pump OD of 146 mm can also be selected. The production casing of  $\Phi 177.8$  mm (7 in.) should be selected. The calculation results show the pump size required when the ultimate liquid production rate is reached. Thus the tubing and production casing sizes can be derived. When the well is completed, whether the sucker rod pump or electric submersible pump is adopted should be considered, and then the tubing and production casing sizes are selected and the economization and effectiveness of both types of pumps are compared.

### Selection and Determination of Tubing and Production Casing Sizes for Hydraulic Piston Pump Well

A hydraulic piston pump has a wide discharge capacity range (30–1274 m<sup>3</sup>/d) and is adaptable to mid-viscosity oil, high pour-point oil, and deep pumping conditions; thus it has become an important component part of artificial lift production technology in China. The adaptability and the technological conditions are shown in Table 3-12.

The common hydraulic piston pumps include a single-acting pump with variable pressure ratio, balanced single-acting pump, long-stroke double-acting pump, and dual hydraulic motor double-acting pump. The power fluid circulation and tubing string assembly are shown in Table 3-13.

The selection procedures of tubing and production casing sizes of a hydraulic piston pump are similar to that of a sucker rod pump and are as follows.

**TABLE 3-12 Adaptability and Technological Conditions of Hydraulic Piston Pump**

Item	Adaptability	Application Ranges or Technological Conditions
Lift height	Strong	Normal range 3500 m, up to 5486 m
Liquid production rate	Wide range	Up to more than 600 m <sup>3</sup> /d for oil well with casing of $\Phi$ 140 mm (5 1/2 in.); up to more than 1000 m <sup>3</sup> /d for oil well with casing of $\Phi$ 178 mm (7 in.)
High gas-liquid ratio	Conditional adaptation	No limitation if gas flows out through separate passage. A certain submergence is required if gas is produced through pump.
Borehole deviation or bending	Strong	Deviation angle of about 45°
Scaling	Moderately strong	Anti-scaling additive is carried by power fluid, or magnetic anti-scaler is used.
Sand production	Poor	Sand content of power fluid should be lower than 0.01%.
High pour-point oil well	Strong	Flow rate and temperature of power fluid should be ensured.
Heavy oil well	Moderately strong	Thin crude oil or water base power fluid should be used and flow rate and temperature should be ensured.
Corrosion	Moderately strong	Corrosion inhibitor should be carried by power fluid.
Selective zone production	Strong	Pump and tubing string appropriate to selective zone production are used.

**TABLE 3-13 Power Fluid Circulation and Tubing String Assembly**

Outside Diameter of Production Casing [mm (in.)]	Outside Diameters of Tubing Strings Assembled [mm (in.)]		
	Open Single String	Dual Parallel String	Dual Concentric String
127(5)	60.3(2 <sup>3</sup> / <sub>8</sub> ) 73.0(2 <sup>7</sup> / <sub>8</sub> )	—	—
140(5 <sup>1</sup> / <sub>2</sub> )	60.3(2 <sup>3</sup> / <sub>8</sub> ) 73.0(2 <sup>7</sup> / <sub>8</sub> ) 88.9(3 <sup>1</sup> / <sub>2</sub> )	60.3×33.4 (2 <sup>3</sup> / <sub>8</sub> ×1.315)	73.0×48.3 (2 <sup>7</sup> / <sub>8</sub> ×1.900) 88.9×48.3 (3 <sup>1</sup> / <sub>2</sub> ×1.900)
178(7)	60.3(2 <sup>3</sup> / <sub>8</sub> ) 73.0(2 <sup>7</sup> / <sub>8</sub> ) 88.9(3 <sup>1</sup> / <sub>2</sub> ) 101.6(4) 114.3(4 <sup>1</sup> / <sub>2</sub> )	60.3×60.3 (2 <sup>3</sup> / <sub>8</sub> ×2 <sup>3</sup> / <sub>8</sub> ) 73.0×40.3 (2 <sup>7</sup> / <sub>8</sub> ×1.900)	73.0×48.3 (2 <sup>7</sup> / <sub>8</sub> ×1.900) 88.9×48.3 (3 <sup>1</sup> / <sub>2</sub> ×1.900) 101.6×60.3 (4×2 <sup>3</sup> / <sub>8</sub> ) 114.3×73.0 (4 <sup>1</sup> / <sub>2</sub> ×2 <sup>7</sup> / <sub>8</sub> )

1. Predict the daily liquid production rate in the late development period.
2. Select and determine the theoretical discharge capacity  $Q_{TL}$  of the pump.
3. Find the matching tubing size and maximum outside diameter of the pump in the technical parameter table of a hydraulic piston pump.

Then determine the production casing size in accordance with single-string production or dual-string production.

The long-stroke double-acting hydraulic piston pump is the most common hydraulic piston pump and is appropriate to the oil pumping of

**TABLE 3-14 Matching of Long-Stroke Double-Acting Hydraulic Piston Pump with Tubing and Production Casing**

Model Number of Pump		SHB2.5×10/20	SHB2.5×20/20	SHB2.5×30/20	SHB3.0×50/20
Tubing size [mm (in.)]		73.0(2 <sup>7</sup> / <sub>8</sub> )	73.0(2 <sup>7</sup> / <sub>8</sub> )	73.0(2 <sup>7</sup> / <sub>8</sub> )	88.9(3 <sup>1</sup> / <sub>2</sub> )
Discharge capacity (m <sup>3</sup> /d)		100	200	300	500
Maximum outside diameter (mm)		114(102)	114(102)	114	114
Recommended nominal diameter of production casing	Single-string production	139.7 mm, 127 mm (5 <sup>1</sup> / <sub>2</sub> , 5 in.)	139.7 mm, 127 mm (5 <sup>1</sup> / <sub>2</sub> , 5 in.)	139.7 mm (5 <sup>1</sup> / <sub>2</sub> in.)	139.7 mm (5 <sup>1</sup> / <sub>2</sub> in.)
	Dual-string production	177.8 mm (7 in.)	177.8 mm (7 in.)	177.8 mm (7 in.)	193.7~244.5 mm (7 <sup>3</sup> / <sub>8</sub> ~9 <sup>5</sup> / <sub>8</sub> in.)

the oil well with high productivity and a high liquid production rate. Matching the pump with tubing and production casing is shown in Table 3-14.

**Case 12.** On the basis of the parameters of Case 11, try selecting the tubing and production casing sizes of a hydraulic piston pump well.

**Solving Process.** By calculating as Case 11, when the water cut is 95%, the daily liquid production rate is up to 300 m<sup>3</sup>/d in order to ensure the stable oil production rate of 15 m<sup>3</sup>/d. When the long-stroke double-acting hydraulic piston pump is adopted, at least the ×HB 3.0 × 50/20 pump should be selected. Its theoretical discharge capacity is 500 m<sup>3</sup>/d (by taking the pump efficiency of 80%, the actual discharge capacity can be up to 400 m<sup>3</sup>/d). The outside diameter of tubing is 76.2 mm (3 in.) and the production casing size is Φ139.7 mm (5 ½ in.).

### Selection and Determination of Tubing and Production Casing Sizes for Hydraulic Jet Pump Well

A main feature of a hydraulic jet pump is that there is no moving component and water can be used as the power fluid. The other surface equipment and downhole working barrel are the same as that of a hydraulic piston pump. The discharge capacity can be up to 4769 m<sup>3</sup>/d and is second only to that of gas lift. The discharge head can be up to 3500 m and is second

only to that of a hydraulic piston pump. However, the pump efficiency is relatively low and the maximum pump efficiency is only up to 32%. The hydraulic jet pump can be used for oil pumping production and is appropriate especially to the high pour-point oil production and the oil production in the high water cut period, during which the hydraulic piston pump can be replaced by the hydraulic jet pump. The hydraulic jet pump is also appropriate for formation tests, drillstem tests, blocking removal, spent acid removal, and scavenging, due to its simple structure and strong adaptability.

The selection procedures of tubing and production casing sizes of hydraulic jet pump wells are as follows.

1. The maximum daily liquid production rate in the high water cut period is predicted using the aforementioned method of predicting the daily liquid production rate level in the high water cut period.
2. The lifting rate H is calculated as shown in Equation (3-17).

(3-17)

$$H = \frac{p_3 - p_4}{p_1 - p_3}$$

where H = lifting rate; p<sub>1</sub> = working pressure at nozzle inlet, MPa (pump depth multiplied by power fluid pressure gradient plus well-head pressure of the system); p<sub>3</sub> = discharge pressure of mixed liquid, MPa (pump depth

**TABLE 3-15 Empirical Values of Key Parameters**

Lifting Rate H	Jetting Rate M	Area Ratio R
<>0.15	>1.5	0.17
0.15~0.25	1.5~1.0	0.21
0.25~0.3	1.0~0.7	0.26
0.3~0.45	0.7~0.5	0.33
0.45~0.8	0.5~0.1	0.41

multiplied by mixed liquid pressure gradient plus wellhead backpressure);  $p_4$  = suction pressure, MPa (submergence multiplied by crude oil pressure gradient).

- The jetting rate and area ratio are determined in accordance with the empirical values in Table 3-15.
- The maximum power fluid flow rate is obtained by the theoretical pump discharge capacity divided by the jetting rate minimum.
- The nozzle diameter is estimated using Equation (3-18):

(3-18)

$$d_1 = \sqrt{\frac{Q_e}{9.6 \times 10^7 \alpha \sqrt{\frac{p_1 - p_4}{\rho}}}}$$

where  $d_1$  = nozzle diameter, m;  $Q_e$  = power fluid flow rate,  $m^3/d$ ;  $\alpha$  = flow rate coefficient determined by testing results ( $\alpha = 3.1$  when power fluid is water and  $\alpha = 8.5$  when power

fluid is heavy oil);  $\rho$  = power fluid density,  $kg/m^3$ .

- Throat diameter is predicted using the following formula:

(3-19)

$$d_2 = \sqrt{\frac{d_1^2}{R}}$$

where  $d_2$  = throat diameter, mm;  $R$  = area rate (see Table 3-15).

- The tubing and production casing sizes are determined on the basis of nozzle diameter and throat diameter in accordance with Table 3-16 and the type of pump selected.

**Case 13.** In accordance with the development program of a certain well, the allocating oil production rate in the late period is  $7 m^3/d$ , the working pressure at the nozzle inlet is 26.7 MPa, the suction pressure is 12.1 MPa, and the discharge pressure of mixed liquid is 17.0 MPa. The water base power fluid is adopted. Try selecting the production casing size.

**Solving Process**

- On the basis of the allocating oil production rate of  $7 m^3/d$  and the predicted water cut of 95%, the maximum daily liquid production rate of  $139 m^3/d$  is predicted in accordance with Equation (3-12).
- The lifting rate  $H$  is calculated as follows.

$$H = \frac{17.0 - 12.1}{26.7 - 17.0} = 0.51$$

**TABLE 3-16 Matching of Conventional Jet Pump with Tubing and Production Casing**

Index	Type of Jet Pump			
	SPB 2.5 Series	Casing-Type Jet Pump	Up-Jet-Type Jet Pump	Φ62 mm Short-Type Jet Pump
Nozzle diameter	1.9~6.0	2.1~3.9	1.8~6.8	1.8~6.8
Throat diameter	4.5~9.8	3.3~6.2	2.9~11.0	2.9~11.0
Tubing OD	73	73	60.3	73
Maximum OD of pump	114	114	89	114
Minimum ID of casing	127(5 <sup>1</sup> / <sub>2</sub> in.)	127(5 <sup>1</sup> / <sub>2</sub> in.)	100(4 <sup>1</sup> / <sub>2</sub> in.)	127(5 <sup>1</sup> / <sub>2</sub> in.)

Note: The power fluid of a casing-type jet pump flows in from casing and the mixed liquid flows out through tubing.

- The jetting rate of 0.5 and the area ratio of 0.41 are obtained using Table 3-15.
- The power fluid flow rate  $Q_e$  is predicted as follows.

$$Q_e = \frac{139}{0.5} = 278 \text{ m}^3/\text{d}$$

- The nozzle diameter is predicted using Equation (3-18).

$$d_1 = \sqrt{\frac{278}{9.6 \times 10^7 \times 3.1 \sqrt{\frac{26.7 - 12.1}{1000}}} - 0.0028} \text{ m}$$

$$= 2.8 \text{ mm}$$

- The throat diameter is predicted using Equation (3-19).

$$d_2 = \sqrt{\frac{2.8^2}{0.41}} = 4.4 \text{ mm}$$

- On the basis of the nozzle diameter and the throat diameter, the short-type jet pump of  $\Phi 62$  mm is selected, and the maximum pump OD of 114 mm and the minimum production casing ID of 127 mm are obtained. Thus the production casing of  $\Phi 139.7$  mm ( $5 \frac{1}{2}$  in.) or  $\Phi 177.8$  mm (7 in.) should be selected.

### Selection and Determination of Tubing and Production Casing Sizes for Electric Submersible Pump Well

The electric submersible pump is adaptable to oil wells (including directional wells) of high discharge capacity, low and medium viscosity oil, low sand content, and pump depth less than 2500 m. The electric submersible pump can also be used in the gravel pack sand control well under the conventional production condition of heavy oil. At present, the theoretical discharge capacity of the electric submersible pump adaptable to the production casing of  $\Phi 139.7$  mm ( $5 \frac{1}{2}$  in.) can be up to  $550 \text{ m}^3/\text{d}$ . Therefore, the selection procedures of tubing and production casing sizes of electric submersible pump wells are same as that of a hydraulic piston pump. Matching the electric

submersible pump with tubing and production casing is shown in Table 3-17.

Matching the TRW Reda Pumps electric submersible pump with tubing and production casing is shown in Table 3-18.

**Case 14.** On the basis of the parameters of Case 12, try selecting the production casing size of the electric piston pump well.

**Solving Process.** By calculation similar to Case 11, in order to ensure the daily oil production rate of  $15 \text{ m}^3/\text{d}$  under the water cut of 95%, the daily liquid production rate of  $300 \text{ m}^3/\text{d}$  is required. In accordance with Table 3-17, the QYB120-425 pump with theoretical discharge capacity of  $425 \text{ m}^3/\text{d}$  can be used. By taking the pump efficiency of 80%, the actual discharge capacity can be up to  $340 \text{ m}^3/\text{d}$ , which can meet the requirement of daily liquid production rate of  $300 \text{ m}^3/\text{d}$ . The corresponding tubing size of  $\Phi 73$  mm ( $2 \frac{7}{8}$  in.) can be selected. For a conventional well with no sand control, the production casing size of  $\Phi 139.7$  mm ( $5 \frac{1}{2}$  in.) is selected. For the gravel pack sand control well, the production casing of  $\Phi 177.8$  mm (7 in.) can be selected in order to ensure sand control effectiveness by increasing the thickness of the gravel pack sand control zone. If a larger discharge capacity is required in the late production period, a larger production casing, that is, the production casing of  $\Phi 177.8$  mm (7 in.) for conventional wells and the production casing of  $\Phi 244.5$  mm ( $9 \frac{3}{8}$  in.) for sand control wells, can be adopted in order to leave some selection margin for adopting the electric submersible pump with larger discharge capacity in the future. For instance, a higher daily liquid production rate can be obtained by selecting the G-160 or G-225 type of pump in Table 3-18.

### Selection and Determination of Tubing and Production Casing Sizes for Gas Lift Oil Production Well

Gas lift production is especially adaptable to sand production wells, medium and low viscosity oil wells, high gas-oil ratio wells, deep wells, and directional wells, and is an important artificial lift production mode. The advantages and

**TABLE 3-17 Matching Partial Chinese Electric Submersible Pumps with Tubing and Production Casing**

Manufacturer	Model Number	Tubing Size (mm)	Rated Discharge Capacity (t/d)	Outside Diameter (mm)	Casing Size Recommended (in.)	
					Conventional Well	Gravel Pack Well
Tianjing Electric Motor	A10	60.3, 73.0	100	95	5½	7
	A15	60.3, 73.0	150	95	5½	7
	A20	60.3, 73.0	200	95	5½	7
	A42	60.3, 73.0	425	95	5½	7
	A53	60.3, 73.0	500	95	5½	7
Zibo Submerged Electric Pump Manufacturer	5.5QD100	60.3, 73.0	100	100, 98	5½	7
	5.5QD160	60.3, 73.0	160	100, 98	5½	7
	5.5QD200	60.3, 73.0	200	100, 98	5½	7
	5.5QD250	60.3, 73.0	250	100, 98	5½	7
	5.5QD320	60.3, 73.0	320	100, 98	5½	7
	5.5QD425	60.3, 73.0	425	100, 98	5½	7
Huxi Electric Motor Manufacturer	QYB120-75	60.3, 73.0	75	100, 98	5½	7
	QYB120-100	60.3, 73.0	100	100, 98	5½	7
	QYB120-150	60.3, 73.0	150	100, 98	5½	7
	QYB120-200	60.3, 73.0	200	100, 98	5½	7
	QYB120-250	60.3, 73.0	250	100, 98	5½	7
	QYB120-320	60.3, 73.0	320	100, 98	5½	7
	QYB120-425	60.3, 73.0	425	100, 98	5½	7
	QYB120-550	60.3, 73.0	550	100, 98	5½	7

Note: The electric submersible pump in this table should be used in the production casing of 5 1/2 in. The tubing sizes include 60.3 mm (2 3/8 in.) and 73.0 mm (2 7/8 in.).

limitations of gas lift production are listed in Table 3-19.

The modes of gas lift include continuous gas-lift and intermittent gas-lift. The intermittent gas-lift can be further divided into conventional intermittent gas-lift, chamber gas-lift, and plunger gas-lift. The continuous gas-lift is only discussed because the daily liquid production rate of intermittent gas-lift is much lower than that of continuous gas-lift.

The selection procedures of tubing and production casing sizes for a gas lift well are as follows:

1. Predict the daily liquid production rate level  $Q_L$ .
2. Determine the tubing and production casing sizes meeting the requirement of daily liquid

production rate  $Q_L$  for a single-string gas-lift well using Tables 3-20 and 3-21.

The tubing and production casing sizes of the gas lift well with a high production rate under the condition of tubing-casing annulus production (known as reverse lift, that is, gas injection into tubing and oil production from annulus) are selected and determined using the following recommended procedure:

1. On the basis of the possibly provided gas injection rate, gas injection pressure, and gas properties, the tubing with sufficiently small frictional pressure drop is selected.
2. A sensitivity analysis of production casing size is made and the optimum production casing size is selected and determined.

**TABLE 3-18 Matching TRW Reda Pumps Electric Submersible Pump with Tubing and Production Casing**

Model Number	Outside Diameter (mm)	Type of Pump	Maximum Power (kw)	Theoretical Discharge Capacity (t/d)	Casing Size Recommended (in.)	
					Conventional Well	Gravel Pack Well
338	85.9	A—10	62	33~66	127 mm (5)	177.8 mm (7)
		A—14E	62	58~86		
		A—25E	62	90~140		
		A—30E	62	115~195		
		A—45E	79	160~240		
400	101.6	D—9	62	26~53	139.7 mm (5 <sup>1</sup> / <sub>2</sub> )	177.8 mm (7)
		D—12	62	33~66		
		D—13	62	53~80		
		D—20E	62	75~115		
		D—26	78	106~146		
		D—40	78	125~240		
		D—51	78	180~260		
		D—55E	78	190~320		
		D—82	161	280~480		
450	117.35	E—35E	99	135~200	139.7 mm (5 <sup>1</sup> / <sub>2</sub> )	177.8 mm (7)
		E—41E	99	140~235		
		E—100	161	380~560		
540	130.3	G—52E	161	210~310	177.8 mm (7)	244.5 mm (9 <sup>5</sup> / <sub>8</sub> )
		G—62E	161	240~360		
		G—90E	161	320~480		
		G—110	224	420~600		
		G—160	224	580~840		
		G—180	224	660~960		
		G—225	224	636~1140		

**TABLE 3-19 Advantages and Limitations of Gas Lift Production**

Method	Advantages	Limitations
Gas lift	<p>Low deep well investment cost and lift cost.</p> <p>Most effective for high gas-liquid ratio well.</p> <p>Low lift operation cost for sand production well.</p> <p>Easy to change production conditions, wide adaptive range.</p> <p>Adaptable to slant well and crooked well.</p> <p>Appropriate to high liquid production rate well.</p> <p>Convenient for production test.</p>	<p>Sufficient gas source adjacent to the oil field is required.</p> <p>High cost required by purchasing the gas lift gas.</p> <p>High lift cost when corrosive gas exists.</p> <p>Difficult to maintain low downhole liquid level when perforation interval is long.</p> <p>Unsafe high-pressure gas.</p> <p>Production casing is required to be able to bear pressure.</p>

TABLE 3-20 Matching of Tubing with Production Casing for Single-String Gas-Lift Well

Minimum Liquid Production Rate (t/d)	Maximum Liquid Production Rate (t/d)	Tubing ID mm (OD in.)	Casing Size Recommended (in.)	
			Conventional Well	Gravel Pack Well
4~8	55	26.6(1.315)	5~5 <sup>1</sup> / <sub>2</sub>	7
8~12	96	35.1(1.660)	5~5 <sup>1</sup> / <sub>2</sub>	7
12~20	159	40.3(1.990)	5~5 <sup>1</sup> / <sub>2</sub>	7
31~40	397	50.3(2 <sup>3</sup> / <sub>8</sub> )	5 <sup>1</sup> / <sub>2</sub>	7
50~80	476	62.0(2 <sup>7</sup> / <sub>8</sub> )	5 <sup>1</sup> / <sub>2</sub>	7
30~120	636	75.9(3 <sup>1</sup> / <sub>2</sub> )	5 <sup>1</sup> / <sub>2</sub>	7
159~240	1590	100.5(4 <sup>1</sup> / <sub>2</sub> )	5 <sup>1</sup> / <sub>2</sub> ~7	7

TABLE 3-21 Matching Tubing with Production Casing for Tubing-Casing Annulus Gas-Lift Well (Medium Production Rate)

Minimum Liquid Production Rate (t/d)	Maximum Liquid Production Rate (t/d)	Tubing Size (in.)	Production Casing Size (in.)
476	1270	2 <sup>3</sup> / <sub>8</sub>	5 <sup>1</sup> / <sub>2</sub>
795	2380	2 <sup>3</sup> / <sub>8</sub>	7.0
636	1900	2 <sup>7</sup> / <sub>8</sub>	7.0
500	1590	3 <sup>1</sup> / <sub>2</sub>	7.0

**Case 15.** On the basis of the given data in Case 5, the production technology of tubing-casing annulus gas lift is adopted. Try analyzing the optimum tubing and production casing sizes for the production rate of 3200 m<sup>3</sup>/d under the gas lift production mode when the reservoir pressure is reduced to 13 MPa. In order to be convenient for transporting, the wellhead tubing pressure of 0.6 MPa is necessary. The maximum gas injection flow rate of 10 × 10<sup>4</sup> m<sup>3</sup>/d can be provided and the gas injection pressure is 15 MPa.

**Solving Process.** Under the condition of tubing-casing annulus gas lift, the gas flow in tubing should be studied in order to determine the tubing size. If the tubing size is too small, the frictional resistance may be high due to the reverse direction of frictional resistance against the gas flow. However a tubing that is too large may increase the cost. The tubing sensitivity analysis is conducted and the gas injection point pressure vs. the inside diameter of the tubing curve is obtained (Figure 3-29). The 3 1/2-in., 4-in., and

4 1/2-in. ID tubings have close gas injection point pressures (that is, close frictional resistances). In consideration of decreasing the cost and because the gas injection rate of 10 × 10<sup>4</sup> m<sup>3</sup>/d is not necessarily required, the 3 1/2-in. ID tubing is selected. The 3-in. ID tubing has a relatively large effect on gas injection point pressure; thus it is inappropriate.

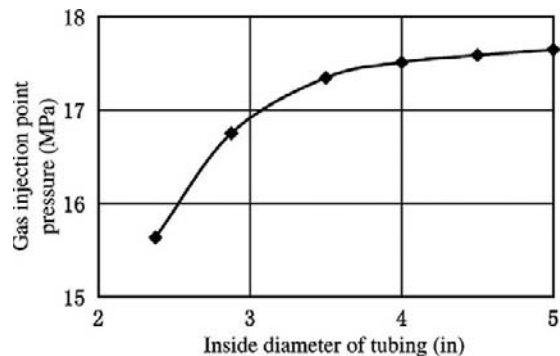
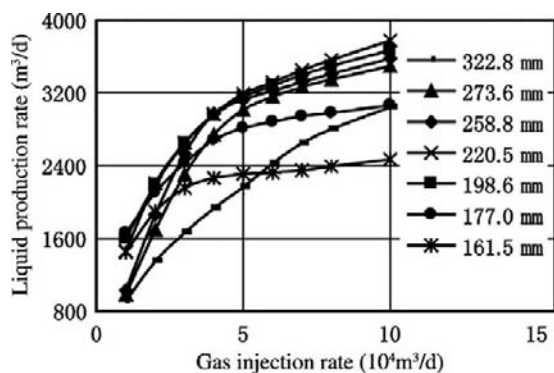
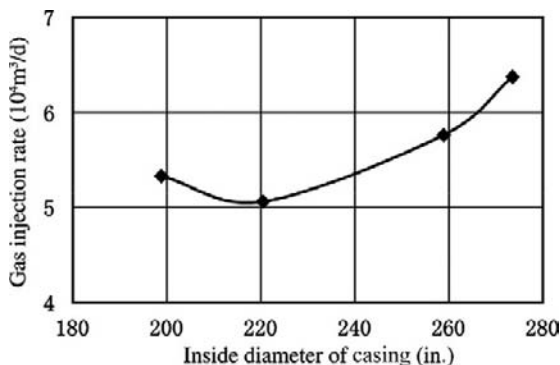


FIGURE 3-29 Frictional pressure drop analysis of tubing.



**FIGURE 3-30** Effect of casing size on gas lift performance curve (the curves are obtained by calculating under various tubing IDs).

The casing size sensitivity analysis is conducted. Figure 3-30 shows that under the gas injection rate lower than  $10 \times 10^4 \text{ m}^3/\text{d}$ , the 12.71-in., 6.97-in., and 6.36-in. ID casings cannot meet the production requirement due to the too large annulus of the former (high slippage loss) and the too small annulus of the latter two (high friction loss). The production casing size vs. gas injection rate curve is obtained by using the four casing sizes meeting the requirement and the corresponding gas injection rate under the liquid production rate of  $3200 \text{ m}^3/\text{d}$  (Figure 3-31). In order to achieve the required production rate of  $3200 \text{ m}^3/\text{d}$ , the production casing size of  $9 \frac{5}{8}$  in. (222.4 mm ID) has the minimum necessary gas injection rate and the highest efficiency; thus, it is the optimum production casing size.



**FIGURE 3-31** The casing size required by necessary production rate vs. gas injection rate.

## Selection and Determination of Tubing and Production Casing Sizes for a Screw Pump Production Well

This type of pump is appropriate to the production well with crude oil viscosity lower than  $2000 \text{ MPa} \cdot \text{s}$ , sand content lower than 5%, discharge head of 1400–1600 m, discharge capacity lower than  $200 \text{ m}^3/\text{d}$ , and working temperature lower than  $120^\circ\text{C}$ . With the increase of high-viscosity crude oil production and high-viscosity polymer gas production by tertiary recovery in recent years, oil production using a screw pump has been widely used. In the late 20th century, with the advance in synthetic rubber technology and vulcanizing binding technology, the screw pump has been greatly improved in France. At present, the screw pump has been adapted to the production of oil with viscosity lower than  $15,000 \text{ MPa} \cdot \text{s}$ , sand content lower than 60%, and temperature not exceeding  $120^\circ\text{C}$ , and it has a discharge head up to 3000 m and discharge capacity up to  $1050 \text{ m}^3/\text{d}$ . A screw pump has a large discharge capacity and a slightly large outside diameter. The tubing and production casing sizes for a screw pump well can be determined by reference to Table 3-22 on the basis of the late liquid production rate (water cut of 95%) predicted by the development program.

## Selection and Determination of Production Casing Size for Dual-String Production Well

**Selection and Determination of Production Casing for Dual-String Gas Lift Well.** The selection procedure of production casing size for a dual-string gas lift production well is as follows.

1. The daily liquid production rates  $Q_{L1}$  and  $Q_{L2}$  of upper and lower oil reservoirs are respectively predicted.
2. The tubing sizes corresponding to  $Q_{L1}$  and  $Q_{L2}$  are obtained using Table 3-20.
3. The recommended production casing size is obtained using Table 3-23 on the basis of the tubing sizes obtained.

**TABLE 3-22** Relation between Theoretical Discharge Capacity and Maximum Outside Diameter of Screw Pump

Producing Area	Connecting Tubing [mm (in.)]	Theoretical Discharge Capacity (mm)	Maximum Outside Diameter of Pump (mm)	Adaptable Minimum Casing Diameter [mm (in.)]
China	60.3(2 <sup>3</sup> / <sub>8</sub> )	4~17	73	127(5)
	73.0(2 <sup>7</sup> / <sub>8</sub> )	32~180	90	139.7(5 <sup>1</sup> / <sub>2</sub> )
	88.0(3 <sup>1</sup> / <sub>2</sub> )	35~108	114	139.7~177.8(5 <sup>1</sup> / <sub>2</sub> ~7)
	101.6(4)	64~500	114	139.7~177.8(5 <sup>1</sup> / <sub>2</sub> ~7)
Other countries	60.3(2 <sup>3</sup> / <sub>8</sub> )	15~80	78	127(5)
	73.0(2 <sup>7</sup> / <sub>8</sub> )	60~240	94	139.7~(5 <sup>1</sup> / <sub>2</sub> )
	88.0(3 <sup>1</sup> / <sub>2</sub> )	120~300	108	139.7~177.8(5 <sup>1</sup> / <sub>2</sub> ~7)
	101.6(4)	180~840	120	139.8(7)
	127.0(5)	430~1000	138	139.8(7)

**TABLE 3-23** Matching of Tubing Size\* with Production Casing Size\* for Dual-String Gas-Lift Well

Upper-Reservoir (or Lower-Reservoir) Gas-Lift Tubing (1) Size (in.)	Upper-Reservoir (or Lower-Reservoir) Gas-Lift Tubing (2) Size (in.)	Minimum Casing Size Recommended (in.)
1.315	1.315~2 <sup>7</sup> / <sub>8</sub>	5 <sup>1</sup> / <sub>2</sub>
1.660	1.315~2 <sup>7</sup> / <sub>8</sub>	5 <sup>1</sup> / <sub>2</sub>
1.990	1.315~2 <sup>7</sup> / <sub>8</sub>	5 <sup>1</sup> / <sub>2</sub> ~7
2 <sup>3</sup> / <sub>8</sub>	1.315~2 <sup>7</sup> / <sub>8</sub>	5 <sup>1</sup> / <sub>2</sub> ~7
2 <sup>7</sup> / <sub>8</sub>	1.315~2 <sup>7</sup> / <sub>8</sub>	5 <sup>1</sup> / <sub>2</sub> ~7
3 <sup>1</sup> / <sub>2</sub>	1.315~2 <sup>7</sup> / <sub>8</sub>	7~9 <sup>5</sup> / <sub>8</sub>
4 <sup>1</sup> / <sub>2</sub>	1.315~2 <sup>7</sup> / <sub>8</sub>	7~9 <sup>5</sup> / <sub>8</sub>
	1.315~2 <sup>7</sup> / <sub>8</sub>	9 <sup>5</sup> / <sub>8</sub> ~11 <sup>3</sup> / <sub>4</sub>
3 <sup>1</sup> / <sub>2</sub>	3 <sup>1</sup> / <sub>2</sub>	9 <sup>5</sup> / <sub>8</sub>
4 <sup>1</sup> / <sub>2</sub>	3 <sup>1</sup> / <sub>2</sub>	10 <sup>3</sup> / <sub>4</sub>

Note: If a large value is taken as the tubing (2) size, the casing size enlarged by one grade is taken.

\*Tubing and casing sizes mean outside diameter.

**Case 16.** A certain oil well includes two oil reservoirs, that is, upper and lower oil reservoirs, and dual-string separate-zone production in a well under gas lift is designed. The daily liquid production rate  $Q_{L1}$  of 450 m<sup>3</sup>/d for the upper reservoir and the daily liquid production rate  $Q_{L2}$  of 1000 m<sup>3</sup>/d for the lower reservoir are predicted. Try selecting the production casing size.

**Solving Process.** Using Table 3-24, the tubing of  $\Phi 73$  mm (2 <sup>7</sup>/<sub>8</sub> in.) with a collar of 89.5 mm

OD is appropriate for the upper reservoir, while the  $\Phi 101.6$  mm (4-in.) tubing with a collar of 121 mm OD is appropriate for the lower reservoir. The sum of the two collar ODs has reached 210.5 mm (8 <sup>1</sup>/<sub>4</sub> in.). In consideration of the clearances between the tubings and between tubing and casing, in which the packer should be set, at least a  $\Phi 244.5$  mm (9 <sup>5</sup>/<sub>8</sub>-in.) production casing should be selected (see Table 3-24).

TABLE 3-24 Recommended Production Casing Size for Dual-String Production Well

Tubing Size Required by Upper (or Lower) Reservoir (in.)	Tubing Size Required by Lower (or Upper) Reservoir (in.)	Minimum Casing Size Recommended (in.)
1.315	1.315~3 <sup>1</sup> / <sub>2</sub>	5 <sup>1</sup> / <sub>2</sub>
1.315	1.315~3 <sup>1</sup> / <sub>2</sub>	5 <sup>1</sup> / <sub>2</sub>
1.990	1.315~2 <sup>7</sup> / <sub>8</sub>	5 <sup>1</sup> / <sub>2</sub>
2 <sup>3</sup> / <sub>8</sub>	1.315~2 <sup>7</sup> / <sub>8</sub>	5 <sup>1</sup> / <sub>2</sub> ~7 <sup>1</sup>
2 <sup>3</sup> / <sub>8</sub>	3 <sup>1</sup> / <sub>2</sub> ~4	7
2 <sup>7</sup> / <sub>8</sub>	1 <sup>9</sup> / <sub>32</sub> ~2 <sup>7</sup> / <sub>8</sub>	5 <sup>1</sup> / <sub>2</sub> ~7 <sup>1</sup>
2 <sup>7</sup> / <sub>8</sub>	2 <sup>3</sup> / <sub>8</sub> ~2 <sup>7</sup> / <sub>8</sub>	7
3 <sup>1</sup> / <sub>2</sub>	2~2 <sup>7</sup> / <sub>8</sub>	7
3 <sup>1</sup> / <sub>2</sub>	3 <sup>1</sup> / <sub>2</sub>	9 <sup>5</sup> / <sub>8</sub>
4 <sup>1</sup> / <sub>2</sub>	3 <sup>9</sup> / <sub>32</sub> ~2	7
4 <sup>1</sup> / <sub>2</sub>	2 <sup>3</sup> / <sub>8</sub> ~3 <sup>1</sup> / <sub>2</sub>	9 <sup>5</sup> / <sub>8</sub>
4 <sup>1</sup> / <sub>2</sub>	4 <sup>1</sup> / <sub>2</sub>	10 <sup>3</sup> / <sub>4</sub>

<sup>1</sup>Tubing and casing sizes mean outside diameters.

### Selection and Determination of Production Casing Size for Other Dual-String Production Well.

For the oil well with great interzone difference, dual-string production can adjust the interzone contradiction. The production casing size for a dual-string production well is much larger than that of a single-string production well. The tubing size required by each zone is selected using the previously mentioned method, while the production casing size corresponding to a dual-string production well can be selected in accordance with Table 3-24.

### Selection and Determination of Production Casing Size for Oil Production Well of Electric Submersible Pump with Y-Shaped Adapter.

An electric submersible pump with a Y-shaped adapter can be used for oil wells (especially offshore oil wells) in which multizone production, production logging, through-tubing perforation, and coiled tubing operation will be conducted.

The production casing size under this condition can be selected in accordance with the thinking and method of selecting and determining production casing size for a dual-string production well (Table 3-24). At present, it is common that a tubing of 2 <sup>7</sup>/<sub>8</sub> in. and a bypass of 2 <sup>3</sup>/<sub>8</sub>-2 <sup>7</sup>/<sub>8</sub> in. are run in the production casing of  $\Phi 244.5$  mm (9 <sup>5</sup>/<sub>8</sub> in.).

## 3.6 EFFECTS OF STIMULATION ON TUBING AND PRODUCTION CASING SIZE SELECTION

Stimulation mainly includes hydraulic fracturing and acidizing and is used for both the measure of putting into production and the measure of blocking removal and increasing production rate. No special requirement for tubing size should be met during matrix acidizing due to the lower displacement. However, the hydraulic sand fracturing of the sandstone reservoir and the hydraulic sand fracturing and acid fracturing of the carbonate reservoir (especially for deep wells and high breakdown pressure wells) may affect the selection of tubing and production casing sizes.

Hydraulic fracturing and acidizing are high-pressure high-displacement operations. The higher hydraulic friction resistance can be caused by a high pumping rate in the wellbore, thus leading to the excessive wellhead pressure and the unavailable power loss of the fracturing unit. Thus the reservoir cannot be fractured. The relationship among wellbore friction loss, wellhead pressure, and reservoir breakdown pressure is shown in Equation (3-20).

(3-20)

$$p_{wh} = \alpha H + \Delta p_f - 10^{-6} \rho g H + \Delta p_b$$

where  $p_{wh}$  = wellhead pressure during fracturing, MPa;  $\alpha$  = reservoir breakdown pressure gradient, MPa/m;  $H$  = depth in middle of reservoir, m;  $\Delta p_f$  = friction loss of fracturing fluid in wellbore, MPa;  $\rho$  = fracturing fluid density, kg/m<sup>3</sup>;  $g$  = gravitational acceleration, m/s<sup>2</sup>;  $\Delta p_h$  = total friction resistance of fracturing fluid through perforations, MPa.

It is shown that when the reservoir breakdown pressure  $\alpha H$  is high (breakdown pressure gradient  $\alpha$  is great or well is deep),  $p_{wh}$  can only be reduced by decreasing  $\Delta p_f$  and  $\Delta p_h$ . In general,  $\Delta p_f$  is much greater than  $\Delta p_h$ . Thus the key lies in decreasing the wellbore friction loss  $\Delta p_f$ .

The fracturing fluids used in the field include Newtonian and non-Newtonian fluids. The fracturing fluid of Newtonian fluid has the wellbore friction resistance pressure drop described in Equation (3-21):

(3-21)

$$\Delta p_f = f \frac{Hv^2}{2Dg} \times 10^{-2}$$

where  $f$  = friction resistance coefficient, dimensionless;  $H$  = well depth, m;  $D$  = inside diameter of tubing, m;  $v$  = fracturing fluid flow velocity in wellbore, m/s;  $\Delta p_f$  = friction resistance pressure drop, MPa;  $g$  = gravitational acceleration, m/s<sup>2</sup>.

The relationship between the displacement  $Q$  and the flow velocity  $v$  during fracturing is shown in Equation (3-22).

(3-22)

$$v = \frac{Q}{15\pi D^2}$$

where  $Q$  = fracturing fluid pumping rate, m<sup>3</sup>/min;  $D$  = inside diameter of tubing, m;  $V$  = fracturing fluid flow velocity, m/s.

By substituting Equation (3-22) into Equation (3-21), the formula in Equation (3-23) is obtained:

(3-23)

$$\Delta p_f = 2.29 \times 10^{-7} f \frac{HQ^2}{D^5}$$

where  $\Delta p_f$  = friction resistance pressure drop, MPa;  $Q$  = fracturing fluid, m<sup>3</sup>/min;  $D$  = inside diameter of tubing, m.

The other symbols are as explained earlier.

It is shown that the  $\Delta p_f$  is directly proportional to the well depth  $H$  and the square of the pumping rate and is inversely proportional to the fifth power of the tubing ID. The pumping rate of hydraulic fracturing is generally 2–6.0 m<sup>3</sup>/min and will be up to about 6 m<sup>3</sup>/min during the limited entry fracturing.

For low-permeability tight sand, the scale of hydraulic fracturing has been greatly increased and the massive hydraulic fracturing (MHF) technique has been developed. The hydraulic fluid volume is up to several thousand cubic meters, the proppant volume is up to several hundred to several thousand tons, and the fracture length is up to several hundred to several thousand meters. In the medium and late stage of the MHF operation, the fracture length has been great and the fluid loss into formation through the fracture wall face may be great. In order to continue to extend and spread the fracture, a high pumping rate is required. This can be explained using the formula in Equation (3-24):

(3-24)

$$Q \times \Delta t = V_w + \Delta V_f$$

where  $Q$  = fracturing fluid pumping rate, m<sup>3</sup>/min;  $\Delta t$  = unit time, min;  $V_w$  = fluid loss into formation through fracture wall face per unit time, m<sup>3</sup>;  $\Delta V_f$  = fracture volume increment per unit time, m<sup>3</sup>.

It is shown that in order to maintain the fracture volume increment  $\Delta V_f$  per unit time as a positive value (that is, to increase continuously the fracture volume), a high pumping rate of fracturing fluid is necessary because the fluid loss into formation through the fracture wall face per unit time increases with the increase in fracture length. The fracture extension and spreading cannot be achieved by a fracturing fluid volume lower than the fluid loss. The massive hydraulic fracturing is a fracturing operation with a very high pumping rate, which is even higher than that of limited entry fracturing and up to 6–10 m<sup>3</sup>/min.

The deep well and high pumping rate operation has a large wellbore friction resistance pressure

**TABLE 3-25** Calculated Values of Friction Resistance Pressure Drop in Tubing During Fracturing and Wellhead Pressure

Tubing Size [ID mm (OD in.)]	Tubing Friction Loss (MPa)		Wellhead Pressure (MPa)	
	Pumping Rate 3 m <sup>3</sup> /min	Pumping Rate 6 m <sup>3</sup> /min	Pumping Rate 3 m <sup>3</sup> /min	Pumping Rate 6 m <sup>3</sup> /min
50.3(2 <sup>3</sup> / <sub>8</sub> )	107.99	430.81	152.95	475.77
62.0(2 <sup>7</sup> / <sub>8</sub> )	33.48	133.37	78.44	178.33
75.9(3 <sup>1</sup> / <sub>2</sub> )	12.89	51.26	57.85	96.22
88.6(4)	5.76	22.87	50.72	67.83
100.3(4 <sup>1</sup> / <sub>2</sub> )	2.87	11.38	47.84	56.34
114.1(5)	1.56	6.16	46.52	51.11

Note: Clear water viscosity is 1 MPa · s. Well depth H = 4000 m. Breakdown pressure  $p_f = 92$  MPa. Relative density of fracturing fluid is 1.2.

drop  $\Delta p_f$ . The methods of reducing friction resistance pressure drop include the method of reducing effective viscosity of fracturing fluid or adding a friction-reducing agent into fracturing fluid (which can only reduce friction resistance to 40% to 60% of clear water friction resistance) and the method of increasing tubing size, which is the most effective. This can be shown in Table 3-25 on the basis of Equation (3-23).

Table 3-25 indicates that the reservoir cannot be fractured by using the tubing of 50.7 mm ID (2 <sup>3</sup>/<sub>8</sub> in.) and 1000-type fracturing unit under the pumping rate of 3 m<sup>3</sup>/min. However, the reservoir has begun to be fractured by using a tubing of slightly larger ID to 62.0 mm ID (2 <sup>7</sup>/<sub>8</sub> in.) and the wellhead pressure of 78.44 MPa. The reservoir can be easily fractured when the tubing ID increases and is above 75.9 mm (3 <sup>1</sup>/<sub>2</sub> in.). Under the pumping rate of 6 m<sup>3</sup>/min, the reservoir cannot be fractured by using a tubing of smaller ID than 75.9 mm (3 <sup>1</sup>/<sub>2</sub> in.). However, the reservoir can be easily fractured when the tubing ID is above 88.6 mm (4 in.).

Figures 3-32 and 3-33 show the pumping rate vs. friction loss relationships obtained by Halliburton under various tubing and casing IDs.

When a non-Newtonian fluid is used as fracturing fluid or acidizing fluid, the relation between shear stress and shear rate can be considered as a power law model:

$$\tau = K' \gamma^{n'}$$

where  $\tau$  = shear stress;  $\gamma$  = shear rate;  $K'$  = liquid consistency coefficient;  $n'$  = liquid flow regime index.

$K'$  and  $n'$  are determined by experiment. The friction loss can still be calculated using the one-way resistance pressure drop and Equation (3-21). The friction resistance coefficient is also obtained by experiment and is related to the Reynolds number and  $n'$  values. It should be indicated that the water-base gel fracturing fluid used presently is basically a viscoelastic fluid, so the actual situation cannot be accurately reflected by calculation in accordance with the power-law model. The friction resistance pressure drop value is obtained by using the instant pumping off in the fracturing operation. The value obtained is compared with the clear water friction resistance pressure drop value and the percentage is obtained. The water-base plant gel fracturing fluid friction loss in tubing is generally lower than the friction loss of clear water and is related to fracturing fluid, material, formulation, and shear rate. The water-base plant gel fracturing fluid friction loss is generally about 60% of clear water fracturing fluid friction loss. The friction resistance pressure drop of hydroxypropylguar (HPG) gum titanium gel fracturing fluid has been lower than 45% of that of clear water under some conditions. Because the long-chain linear molecules may restrain the turbulence of water and reduce the friction resistance, the high molecular polymer can reduce the friction resistance pressure drop. However, it should still be

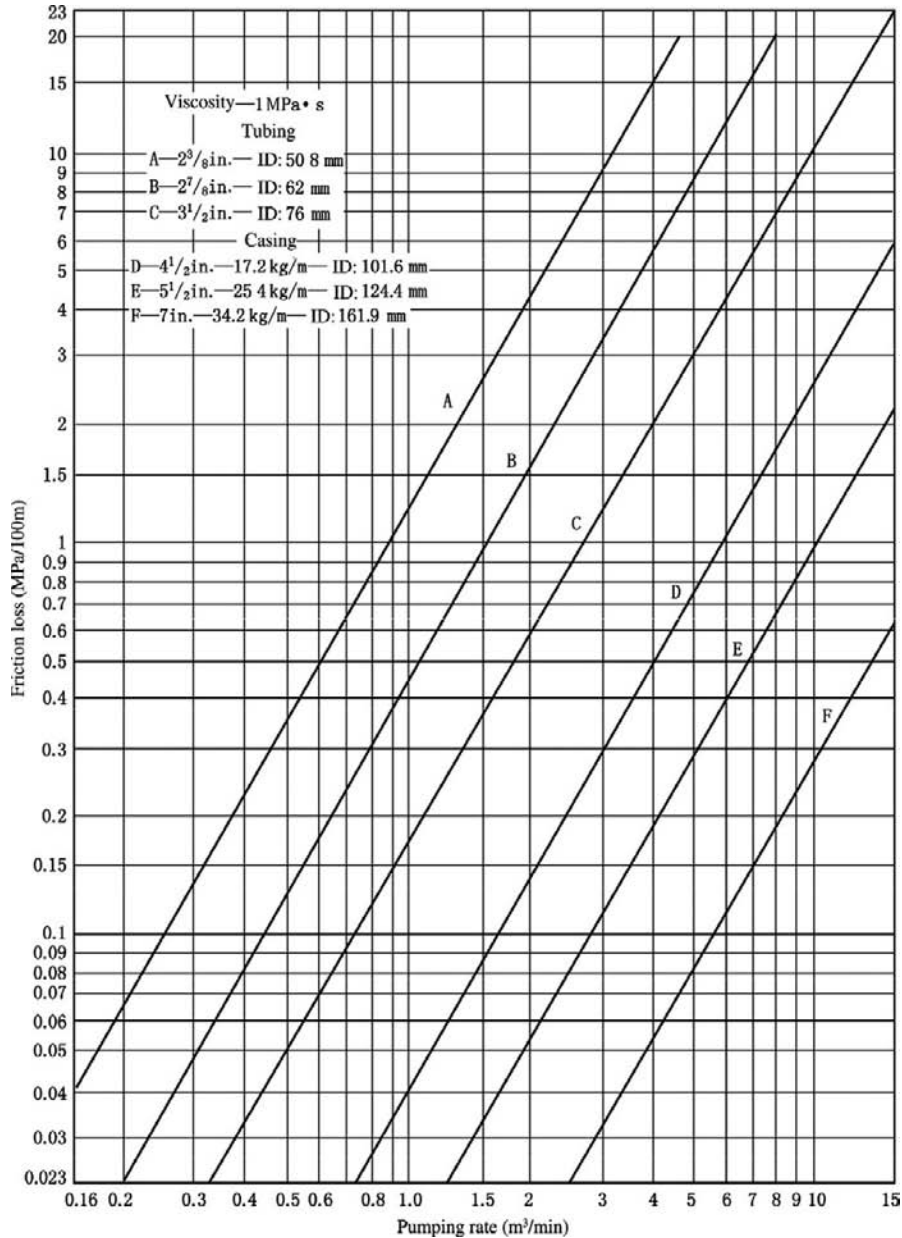


FIGURE 3-32 Friction loss vs. pumping rate for clear water fracturing fluid.

indicated that the friction loss sensitivity is greatly affected by the tubing size. For instance, during hydraulic fracturing in a certain area a small tubing of 2 7/8 in. was first used, the friction resistance pressure drop exceeded 30 MPa under the pumping rate of 2 m<sup>3</sup>/min and the tubing length of

3000 m, the operating wellhead pressure exceeded 70 MPa, and the reservoir could not be fractured under a high breakdown pressure. When the tubing size was changed to 3 1/2 in., the operating wellhead pressure was reduced to about 50 MPa and the reservoir could be fractured. Under the

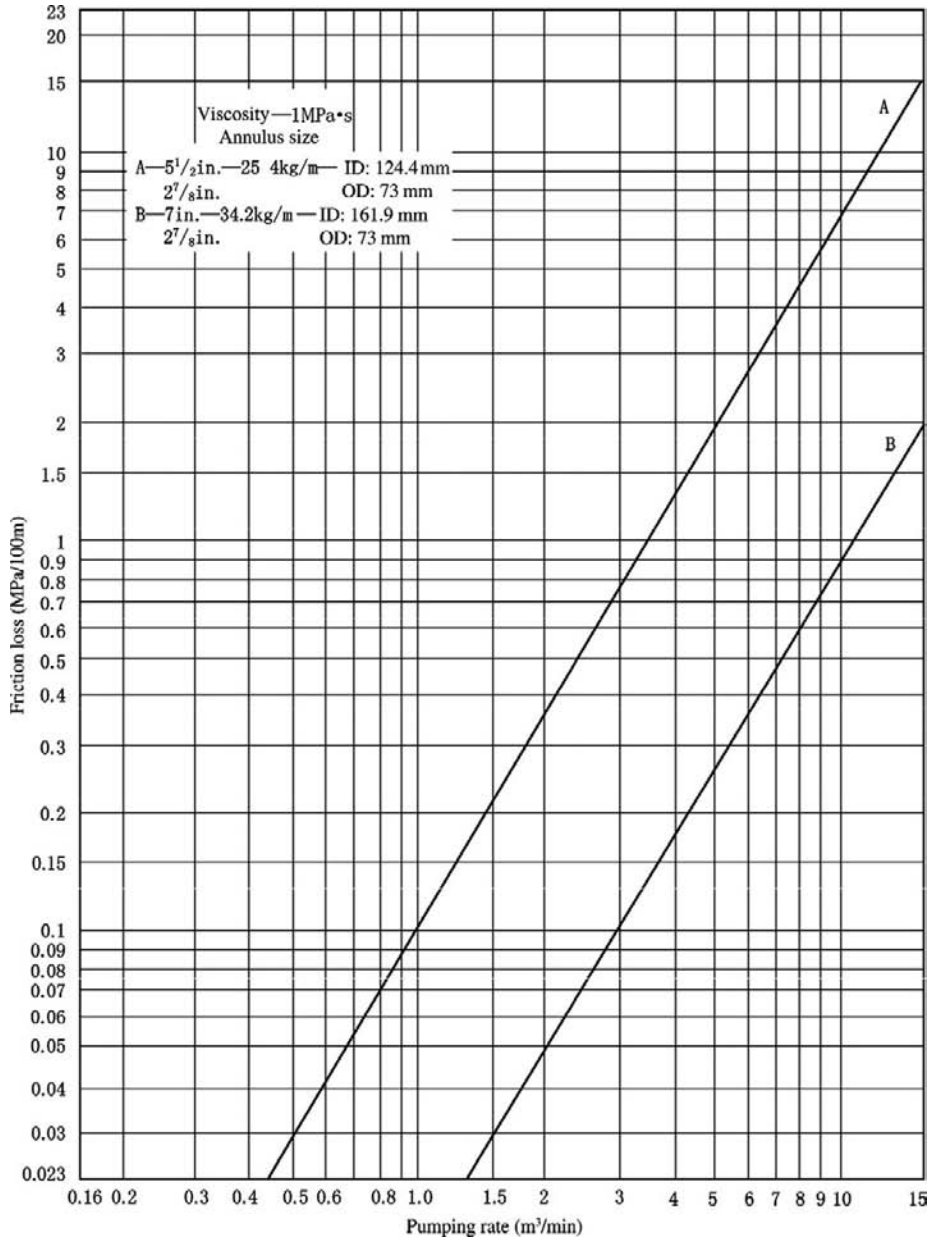


FIGURE 3-33 Friction loss vs. pumping rate for fracturing fluid.

aforementioned conditions, the clear water friction resistance pressure drop is 46.5 MPa (Figure 3-32) and the friction resistance pressure drop of fracturing fluid is 63.5% of that of clear water. Despite the fact that the friction-reducing effect of polymer

has been achieved, the friction resistance pressure drop value is still high. When the tubing size is increased from 2 7/8 in. to 3 1/2 in., the friction resistance pressure drop of clear water is changed into only 17.6 MPa, that is, 40% of that of 2 7/8-in.

tubing. When the friction-reducing effect of fracturing fluid is also considered, the pumping rate is possibly increased (for example, to  $3 \text{ m}^3/\text{min}$ ), the friction resistance pressure drop is only 35 MPa, and the wellhead pressure can be decreased to a value below 54 MPa, thus improving the fracturing operation condition.

With the increase in tubing size, the friction resistance pressure drop in tubing decreases rapidly. Therefore, for a high breakdown pressure well or deep well, a relatively large tubing size and corresponding large production casing size should be designed.

The tubing friction resistance pressure drop and the operating wellhead pressure are predicted under the different tubing sizes on the basis of reservoir breakdown pressure gradient and well depth in accordance with Equation (3-20) and Equation (3-21) or Figures 3-32 and 3-33. The minimum tubing size can be selected by the criterion of operating wellhead pressure  $\leq 80\% \times$  working pressure of the fracturing unit. The corresponding minimum

production casing size is selected in accordance with the matching relation between tubing and production casing sizes, as shown in Table 3-4. On this basis, by reference to the preselected tubing and production casing sizes for the artificial lift well, appropriate tubing and production casing sizes are selected and determined.

### 3.7 SELECTION AND DETERMINATION OF TUBING AND PRODUCTION CASING SIZES FOR HEAVY OIL AND HIGH POUR-POINT OIL PRODUCTION WELLS

Heavy oil is asphalt-based crude oil and has low or no flowability due to the high content of colloid and asphaltene and the high viscosity. The heavy oil viscosity is sensitive to change in temperature (Figure 3-34). With the increase in temperature the heavy oil viscosity may rapidly decrease and vice versa. This inherent feature of heavy oil makes the recovery methods

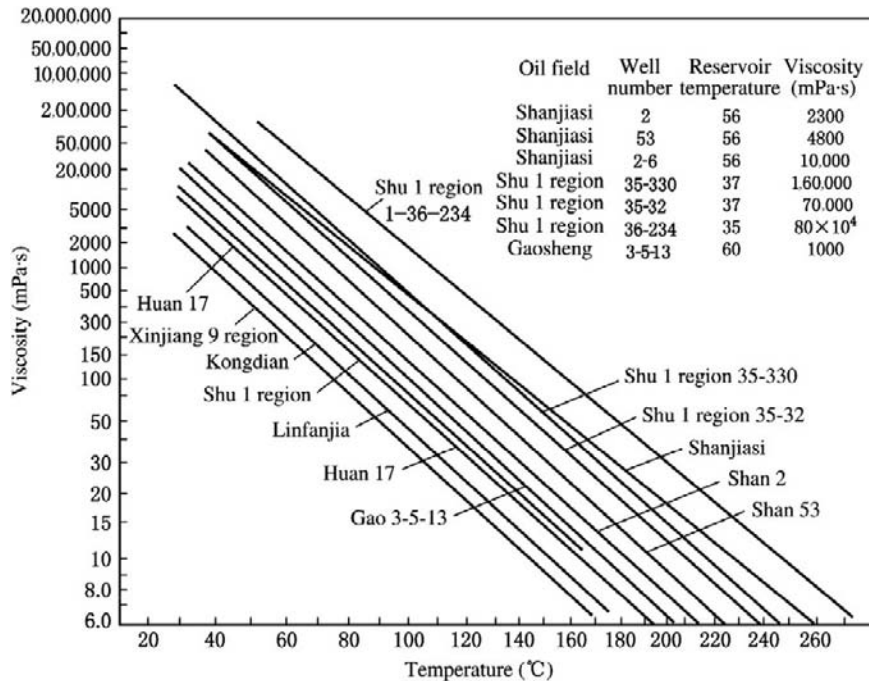


FIGURE 3-34 Heavy oil viscosity vs. temperature.

different from that of conventional light oil and makes the recovery process complicated. At present in China the ordinary heavy oil with a viscosity lower than  $150 \text{ MPa} \cdot \text{s}$  under reservoir conditions is recovered by waterflooding, while the ordinary and extra-heavy oils with a viscosity higher than  $150 \text{ MPa} \cdot \text{s}$  are recovered by steam injection.

### Heavy Oil Recovery by Waterflooding

The heavy oil with a viscosity lower than  $150 \text{ MPa} \cdot \text{s}$  under reservoir conditions is commonly recovered by waterflooding because this heavy oil generally contains a higher dissolved-gas content and has a certain flowability under reservoir conditions, despite the fact that the surface crude oil viscosity may be up to several thousand millipoises. The features of waterflooding include mature technique, simple technology, relatively low investment, and good economic benefit. Therefore, waterflooding is the first selected recovery method. For instance, the conventional waterflooding has been adopted in the Gudao, Gudong, Chengdong, and Shengtuo oil fields of the Shengli oil region and the Jing 99 block, Niuxintuo, and Haiwaihe oil fields of the Liaohe oil region, and good development results have been achieved through continuous adjustment.

**Flowing Production.** The flowability of heavy oil is low due to the high intermolecular friction resistances of colloid and asphaltene. The friction head loss of fluid flow in tubing can be calculated using the hydraulics formula in Equation (3-25):

(3-25)

$$H_f = f \frac{L}{D} \cdot \frac{v^2}{2g}$$

where  $H_f$  = friction head loss, m;  $f$  = friction resistance coefficient, dimensionless;  $L$  = tubing setting depth, m;  $D$  = tubing diameter, m;  $v$  = liquid flow velocity, m/s.

The friction head loss vs. tubing setting depth relationships under a certain heavy oil viscosity

and the different tubing diameters are calculated using Equation (3-25) and are shown in Figure 3-35.

It is well known that the higher the crude oil viscosity, the greater the friction head loss. As shown in Figure 3-35(a), under the same crude oil viscosity, the friction head loss increases with the increase of fluid flow velocity in

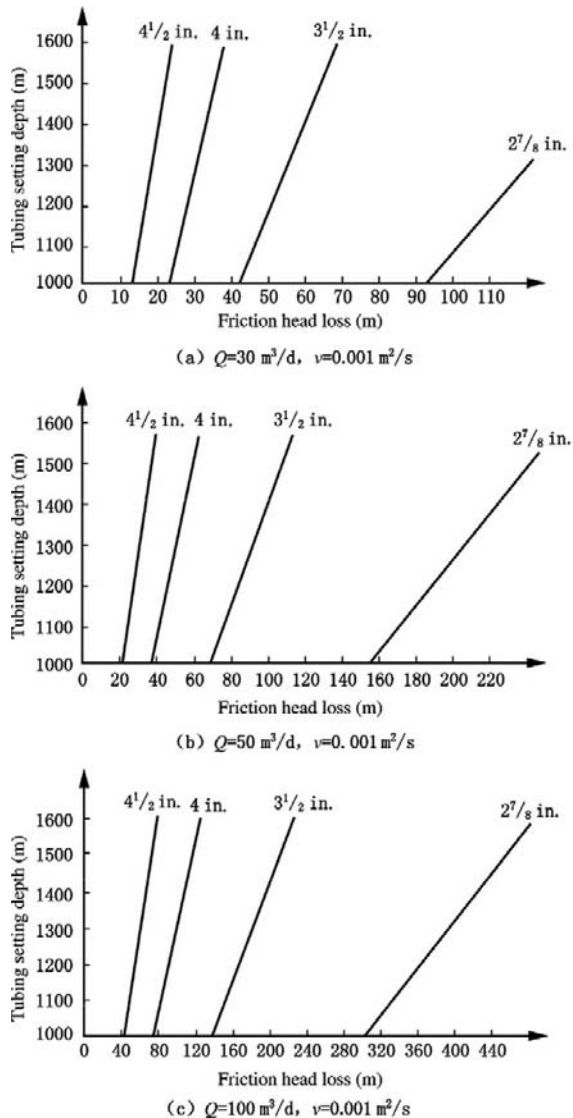


**FIGURE 3-35** Effect of tubing diameter on friction head loss.

tubing and decreases with the increase of tubing diameter. For heavy oil with high viscosity, tubing with a relatively large diameter should be adopted in order to maintain flowing production, and the corresponding production casing with a larger diameter should also be selected.

**Oil Production by Pumping Unit and Deep Well Pump.** Because of the limitations of traditional ideas, small size tubing was set in most heavy oil wells in the early development period. On the downstroke of the sucker rod, the dropping velocity of the sucker rod is reduced by the great friction resistance of heavy oil to the sucker rod, and the movement of the sucker rod lags behind the movement of the hanging point of the horsehead. When the hanging point is rising, the sucker rod is still dropping. Not only the normal movement of sucker rod may be affected, but also the impact of the horsehead on the sucker rod may be caused. Thus the impact load may be generated, the service life is reduced, and even mechanical failure may result (see Figure 3-36).

In view of this, when the pumping unit and deep well pump are used for producing heavy oil, the upstroke friction resistance and the downstroke resistance should first be reduced. The friction resistance of the wellbore liquid column to the sucker rod can be calculated using the formula shown in Equation (3-26):

(3-26)

$$F_r = \frac{2\pi\mu Lv}{10^3} \left( \frac{1}{\ln m} + \frac{4b^2}{a} + \frac{4b}{a} \right)$$

$$v = \frac{S_n}{30}$$

$$m = \frac{d_t}{d_r}$$

$$a = m^4 - 1 - \frac{(m^2 - 1)^2}{\ln m}$$

$$b = \frac{m^2 - 1}{2 \ln m} - 1$$

where  $F_r$  = friction resistance of wellbore liquid column to sucker rod, N;  $\mu$  = liquid viscosity, MPa · s;  $L$  = pump setting depth, m;  $v$  = sucker rod movement velocity, m/s;  $S$  = length of stroke, m;  $n$  = strokes per minute,  $\text{min}^{-1}$ ;  $d_t$  = tubing diameter, m;  $d_r$  = sucker rod diameter, m.

It is shown that the friction resistance is related to the wellbore liquid viscosity, flow velocity, and tubing diameter. The friction resistance curves under the different tubing diameters and the different crude oil viscosities (Figure 3-37) indicate that the friction resistance increases with the increase in viscosity and the decrease in tubing diameter. Therefore, the large-diameter tubing of 101.6–114.3 (3 1/2–4 1/2 in.) should be used in order to reduce the friction resistance and reduce the sucker rod flotation and impact on the horsehead.

When heavy oil is produced by large-diameter tubing and pumps, the friction resistance and sucker rod flotation can be reduced, and the pump stroke efficiency and pumping rate can be increased. Under the conventional waterflooding of heavy oil, the oil-water viscosity ratio is high, the early water breakthrough occurs, the water cut rapidly increases, most oil should be produced in the high water cut period, the water-free recovery factor is only 2% to 5%, and the yearly average water cut increases by about 3%. When the water cut is higher than 50%, the liquid production rate should be increased by 2 to 20 times in order to maintain a stable oil production rate (see Table 3-26).

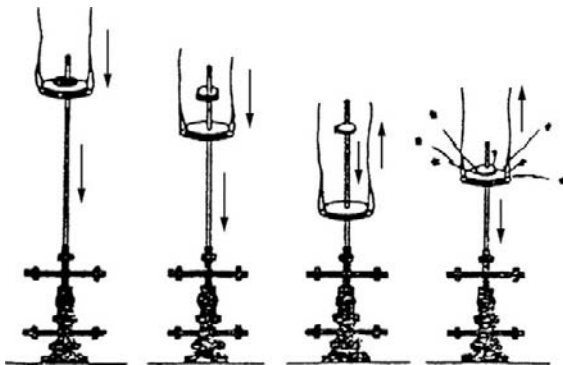


**FIGURE 3-36** Crude oil viscosity effect during heavy oil pumping (sucker rod flotation).

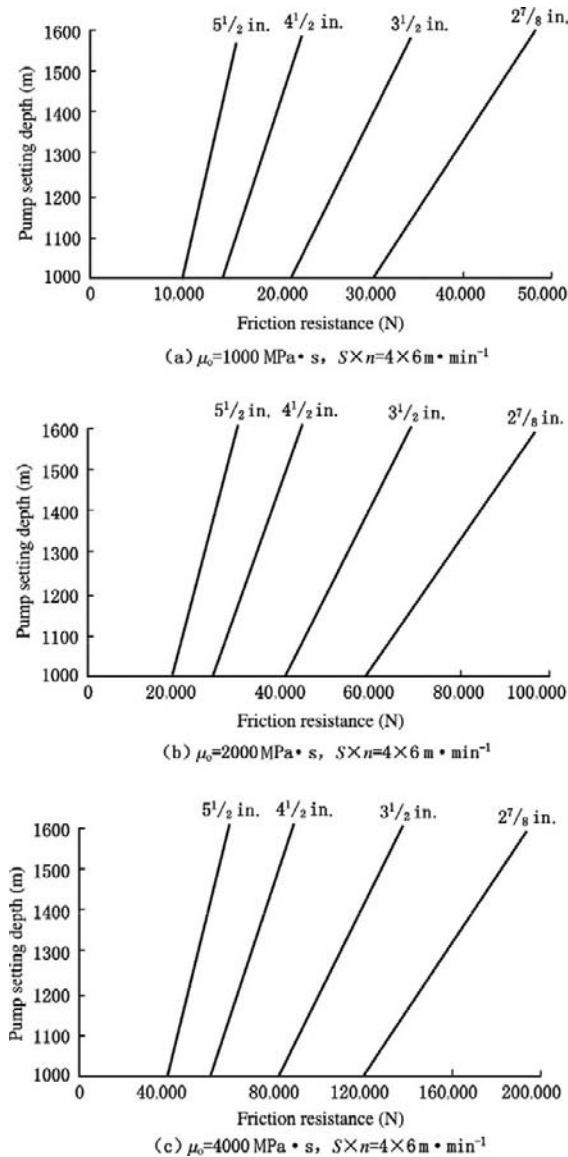


FIGURE 3-37 Effects of tubing diameter on friction resistance of liquid to sucker rod.

Therefore, in order to increase the liquid production rate and maintain a stable oil production rate, the tubing diameter should also be increased.

In the Gudao oil field of the Shengli oil region, the surface stock tank oil viscosity is 250–5700  $\text{MPa} \cdot \text{s}$ , the reservoir oil viscosity is 20–130  $\text{MPa} \cdot \text{s}$ , and the oil-water viscosity ratio is 80–350. This oil field was put into production in 1973 and started waterflooding in April 1974. The water cut increased rapidly due to the high oil viscosity, and a large amount of crude oil would be produced in the high water cut period. In order to maintain a stable oil production rate and increase the liquid production rate, the original pumps of  $\Phi 43$ –56 mm have been changed into pumps of  $\Phi 70$  mm and  $\Phi 83$  mm. When pumps of  $\Phi 43$ –56 mm were used, the individual-well daily oil production rate was 20 t/d, and the tubing diameter of  $2 \frac{7}{8}$  in. could meet the requirement. When the water cut increases to 80%, the liquid production rate of 100 t/d is required by retaining the stable oil production rate. Thus the oil well pumps of  $\Phi 70$  mm and  $\Phi 83$  mm are required, the corresponding tubing diameter should be above  $3 \frac{1}{2}$  in., and the relatively large production casing diameter should be selected in the well completion design.

## Heavy Oil Recovery by Steam Injection

**Huff and Puff.** Huff and puff is a commonly used method of producing heavy oil. In China most heavy oil is produced using huff and puff. At the steam injection stage, the injected steam heats the reservoir, the crude oil viscosity is decreased, and the flowability of crude oil is increased. When a well is put on, the heated crude oil flows into the well under the effects

TABLE 3-26 Water Cut vs. Liquid Production Rate

Water cut (%)	0	10	20	30	40	50	60	70	80	90	95
Liquid production rate (t/d)	15.0	16.6	18.8	21.4	25.0	30.0	37.5	50.0	75.0	150	300

of elastic energy and gravity. In the wellbore, with the flow of crude oil toward the wellhead, the fluid temperature gradually decreases due to heat conduction, and the oil viscosity gradually increases. Therefore, both the oil pumping condition during production and the wellbore heat loss condition during steam injection should be considered in the huff and puff well tubing string design.

The heat-insulated tubing string should be set in the well in order to decrease wellbore heat loss and improve steam quality at the steam injection stage. This string consists of tubing, insulating layer, and outside pipe. The different string sizes have different overall heat transfer coefficients, and the insulating layer thickness and annulus size will play important roles. The overall heat transfer coefficients for different sizes of wellbore string configuration (Table 3-27) indicate that the small heat-insulated string has great overall heat transfer coefficient and great wellbore heat loss. In the production casing of 7 in., the insulating effectiveness of the heat-insulated string of  $2\frac{3}{8}$  in.  $\times$  4 in. is higher than that of the heat-insulated string of  $2\frac{7}{8}$  in.  $\times$  4 in. due to the larger insulating layer thickness. However, the mechanical strength (in a deep well) and safety load of the former are lower than that of the latter. Moreover, the low bottomhole steam pressure and high wellbore steam pressure are caused by the former due to the high flow velocity, high friction resistance, and great wellbore pressure drop of the small tubing size (Figure 3-38). Therefore,

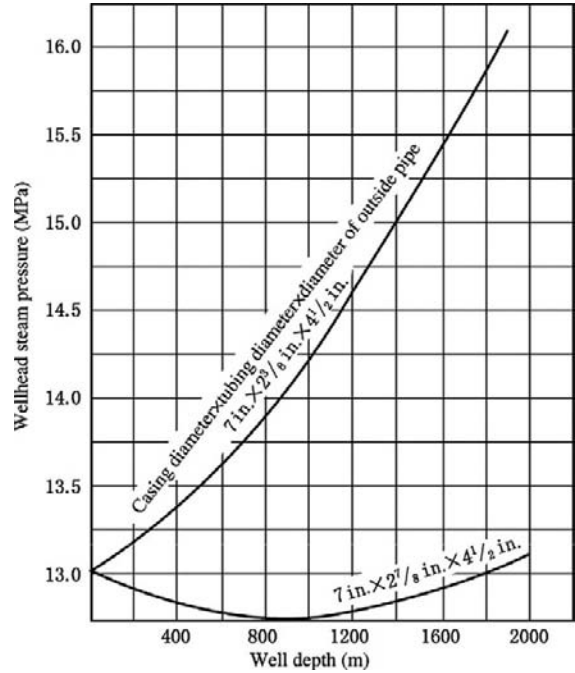


FIGURE 3-38 Wellhead steam pressure under different tubing sizes.

on the premise of ensuring good insulating effectiveness, a larger diameter string should be used to the full extent for steam injection and later pumping.

The liquid production rate of huff and puff is high. The condensate water of injected steam should be rapidly produced, and the crude oil should be produced as much as possible, thus the huff and puff production effectiveness may

TABLE 3-27 Overall Heat Transfer Coefficient  $U_{\infty}$  [W/(M<sup>2</sup> · K)] under Different Sizes of Wellbore String Configuration

No.	Sizes of Wellbore String Configuration (in.)	Insulating Layer Thickness (mm)	Annulus Clearance (mm)	Steam Injection Temperature (°C)		
				250	300	350
1	$7 \times 2\frac{3}{8} \times 4$	17	28.7	1.91	2.52	2.67
2	$7 \times 2\frac{7}{8} \times 4$	10.5	28.7	4.13	4.48	4.78
3	$7 \times 2\frac{7}{8} \times 4\frac{1}{2}$	16	22.5	3.58	3.79	4.02
4	$5\frac{1}{2} \times 2\frac{3}{8} \times 3\frac{1}{2}$	10.4	17.7	4.18	4.85	5.41
5	$5\frac{1}{2} \times 2\frac{3}{8} \times 4$	16.8	11.1	3.99	4.01	4.33

be increased. As a result, the tubing size should meet the requirement of the liquid production rate. If a small size tubing is used, the fluid flow velocity may be very high under a high production rate. Under the same tubing size, with the increase in flow rate or (stroke  $\times$  strokes per minute) value, the friction resistance of liquid to sucker rod will increase (Figure 3-39), and the friction resistance will increase with the increase in oil viscosity (Figure 3-40). Thus the problems (including sucker rod flotation, impact of the horsehead on the sucker rod, and decrease in stroke efficiency) that may be generated under the conventional water-flooding of heavy oil will occur.

In order to reduce friction resistance during the movement of the sucker rod in the tubing liquid, a larger diameter tubing should be selected. For instance, when the liquid viscosity is  $1000 \text{ MPa} \cdot \text{s}$ , and the working parameter  $S \times n$  is  $3.3 \text{ m} \times 6 \text{ min}^{-1}$ , the friction resistance of  $2 \frac{7}{8}$ -in. tubing is 1.4 times that of  $3 \frac{1}{2}$ -in. tubing and 2.2 times that of  $4 \frac{1}{2}$ -in. tubing (Table 3-28). Obviously, the friction resistance can be effectively reduced by using the tubing of  $3 \frac{1}{2}$  to  $4 \frac{1}{2}$  in. Correspondingly, a larger production casing should be adopted.

It is shown that a large diameter string is required by the huff and puff during both the

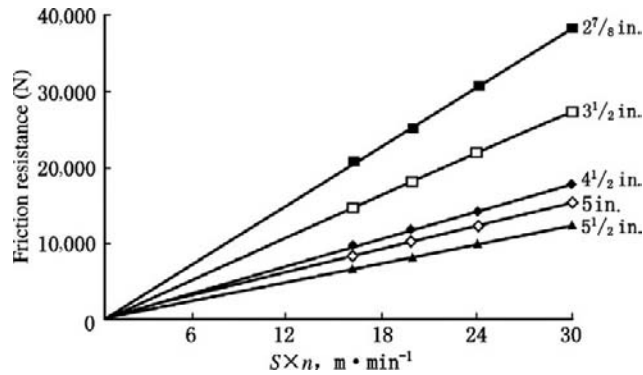


FIGURE 3-39 Flow velocity vs. friction resistance to sucker rod under different tubing sizes.

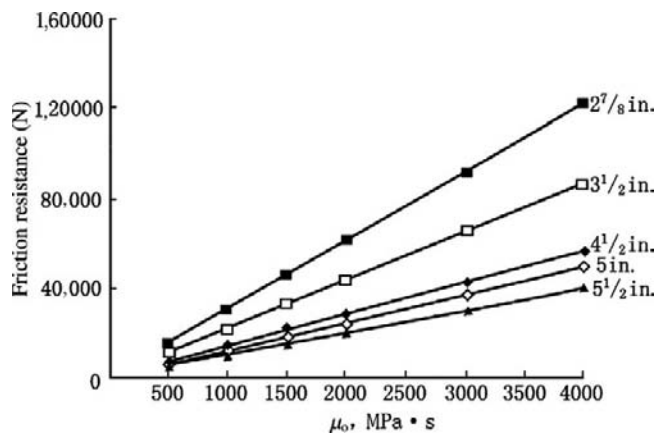


FIGURE 3-40 Oil viscosity vs. friction resistance to sucker rod under different tubing sizes.

**TABLE 3-28 Friction Resistances to Sucker Rod under Different Tubing Sizes and Different  $S \times n$  Values**

Tubing Diameter (in)		2 <sup>7</sup> / <sub>8</sub>	3 <sup>1</sup> / <sub>2</sub>	4 <sup>1</sup> / <sub>2</sub>	5 <sup>1</sup> / <sub>2</sub>
Friction resistance under different $S \times n$ value (N)	$2.7 \times 6 \cdot \text{min}^{-1}$	20,500	14,500	9500	6600
	$3.3 \times 6 \cdot \text{min}^{-1}$	25,000	17,800	11,600	8100
	$4.0 \times 6 \cdot \text{min}^{-1}$	30,400	21,600	14,000	9800
	$5.0 \times 6 \cdot \text{min}^{-1}$	38,000	27,000	17,600	12,300

Note: The results are obtained by calculating under viscosity of 1000 MPa · s and sucker rod diameter of 25 mm.

steam injection and the liquid production in order to increase the production effectiveness of the huff and puff.

#### Heavy Oil Recovery by Steam-Flooding.

Steam-flooding is an important method of heavy oil recovery. When heavy oil is produced by huff and puff to some extent, with the decrease in reservoir pressure and the increase in water saturation, the effectiveness will decrease gradually. In order to further enhance the crude oil recovery factor, the huff and puff should be substituted by steam-flooding. Laboratory studies and field practice indicate that the liquid productivity of the production well will greatly affect the recovery effectiveness of steam-flooding, and the liquid production rate should be higher than the steam injection rate; that is, the production-injection ratio should be up to 1.2–2.0 in order to achieve good recovery effectiveness. For instance, in the steam-flooding pilot test area of the Du 66 block of the Shuguang oil field in the Liaohe oil region, the optimized steam

injection rate is 135 t/d. Under this steam injection rate, the steam-flooding production effectiveness of the different liquid production rates of the production well indicate that when the liquid production rate of the production well is lower than or equal to the steam injection rate, that is, the production-injection ratio is lower than or equal to 1, the production effectiveness of steam-flooding is low (the oil-steam ratio and recovery factor are low); when the liquid production rate of the production well is higher than the steam injection rate, that is, the production-injection ratio is higher than 1, the production effectiveness of steam-flooding is improved (Table 3-29).

The Tangleflags oil field in Canada has stock tank oil viscosity of 13,000 MPa · s, reservoir thickness of 27 m, and reservoir depth of 450 m. The combined steam-flooding tests of vertical and horizontal wells were conducted by Sceptre in 1988 and met with success. The main experience and practice include:

**TABLE 3-29 Effects of Liquid Production Rate of Production Well on Steam-Flooding Effectiveness**

Liquid Production Rate (t/d)	Production Time (d)	Cumulative Steam Injection (t)	Cumulative Oil Production (t)	Average Oil Production Rate (t/d)	Oil-Steam Ratio	Recovery Factor (%)	Production-Injection Ratio	Net Oil Production Increment (t)
80	126	17,010	2410	19.1	0.142	4.1	0.59	992
100	147	19,845	2860	19.5	0.144	4.8	0.74	1206
120	218	29,430	3870	17.8	0.132	6.5	0.89	1417
140	304	41,040	5190	17.1	0.126	8.7	1.04	1770
160	1341	1,81,035	23,050	17.2	0.127	38.8	1.18	7963
180	788	1,06,380	16,390	20.8	0.154	27.6	1.33	7525
200	751	1,01,385	16,010	21.3	0.158	26.8	1.48	7561
220	706	95,310	15,150	21.5	0.159	25.5	1.63	7207

1. The productivity of the oil reservoir should be fully understood. The drainage radius predicted initially by numerical simulation in this region is 50 m. The practical production data indicate that the drainage radius should be up to 80 m. The predicted maximum liquid production rate is  $650 \text{ m}^3/\text{d}$ , while the actual liquid production rate has been up to  $1200 \text{ m}^3/\text{d}$ . Due to the initial underestimation of the liquid production rate, a pump of  $3 \frac{3}{4}$  in., which was initially set, has been inappropriate for production and was changed later from  $4 \frac{3}{4}$  in. through  $5 \frac{3}{4}$  in. to  $7 \frac{3}{4}$  in. The corresponding liquid production rate was also increased. Be that as it may, the high production period was missed. Later a pump of  $7 \frac{3}{8}$  in. was used. The tubing diameter is  $7 \frac{5}{8}$  in. and the production casing diameter is  $10 \frac{3}{4}$  in. (Figure 3-41). During oil pumping, slow downstroke movement and quick upstroke movement are adopted in

order to increase the fullness coefficient. The actual liquid production rate is up to  $1200 \text{ m}^3/\text{d}$  and the daily oil production rate is  $480 \text{ m}^3/\text{d}$  under the water cut of 60%. If the maximum liquid production rate had initially been predicted accurately, the effectiveness would be better.

2. The period after steam breakthrough is an important production period. Before steam breakthrough the production rate of a production well is relatively low. Only after steam breakthrough can the liquid production rate be increased and most of the crude oil will be produced in the period with a water cut of up to 60% to 80%. In this period a sufficiently high liquid production rate of the production well and a production-injection ratio higher than 2 should be ensured. Thus a sufficiently large string and the matching large diameter production casing should be set in a production well.

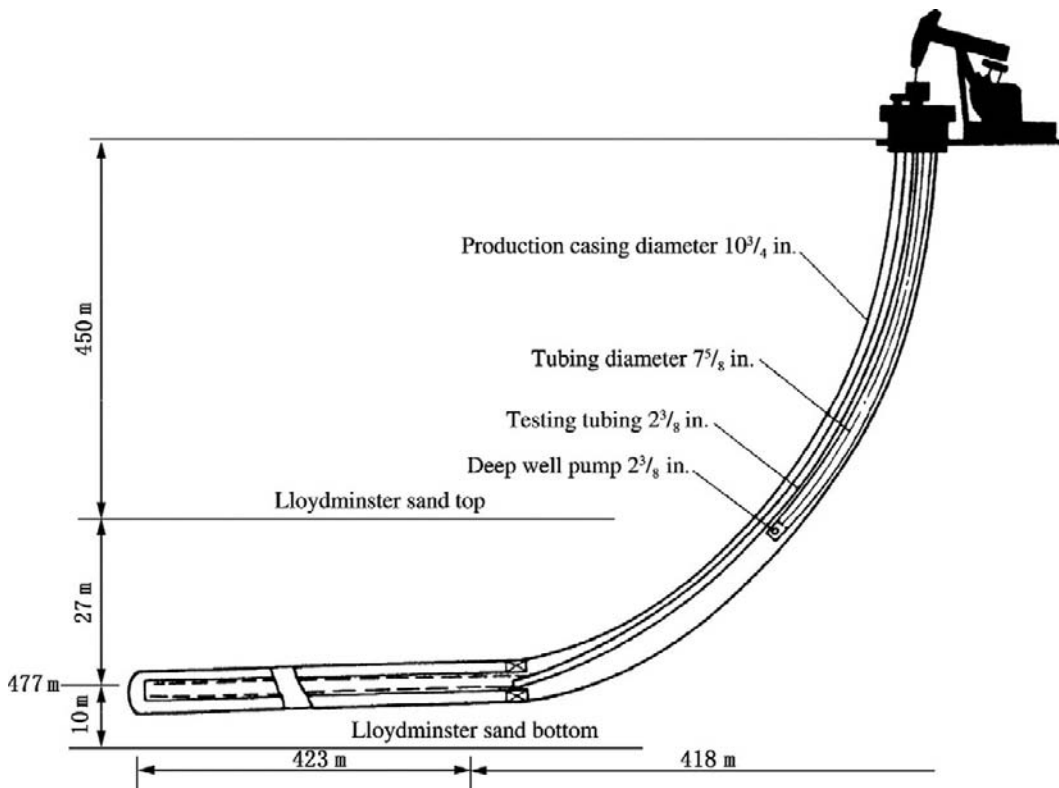


FIGURE 3-41 Typical production well completion in Tangleflags oil field.

### High Pour-Point Crude Production

High pour-point crude is a paraffin-based crude oil and has a high pour point and low viscosity. Crude oil viscosity is highly sensitive to the change in temperature (Figure 3-42). When the temperature is higher than the pour point, the crude oil is a Newtonian fluid and the viscosity can be reduced to several to several dozen MPa · s. However, when the temperature is lower than the wax precipitation point, the fluid configuration may change and become non-Newtonian. The crude oil viscosity is not only

related to temperature, but to shear rate. The flow performance reduces obviously with the decrease in temperature. Therefore, when the temperature is higher than the pour point of oil, the oil viscosity is low, the flowability is good, and the oil flows easily from reservoir to bottomhole. However, when the crude oil flows from bottomhole to wellhead, with the decrease in temperature, the wax precipitates from the crude oil. When the temperature is lower than the wax precipitation point, the crude oil viscosity increases, the flowability decreases, and even the crude oil cannot flow due to the

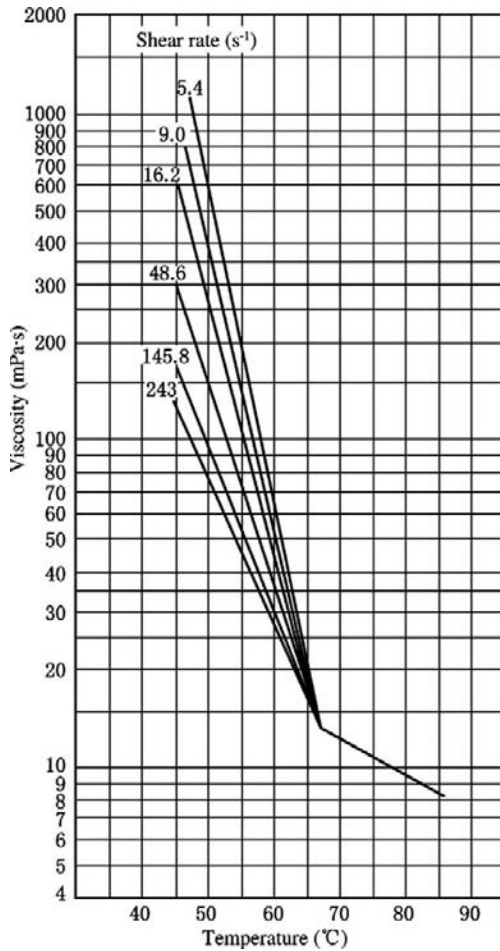


FIGURE 3-42 Rheological curves of high pour-point crude of Shenbei oil field in Liaohe oil region.

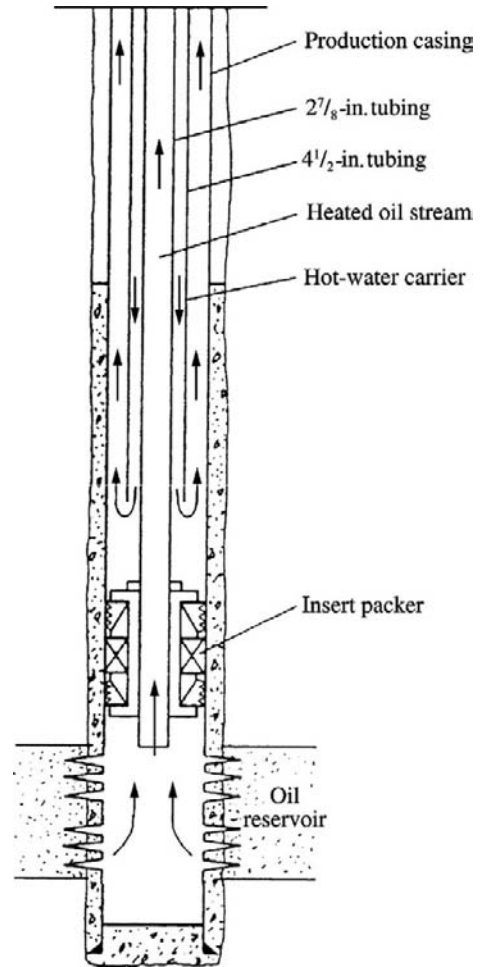


FIGURE 3-43 Concentric string hot-water circulation production.

solidification of wax. Thus the key to high pour-point oil production lies in keeping a higher oil temperature than the pour point. The crude oil flow in the near-wellbore zone and in the wellbore should be ensured and the precipitation of wax should be prevented.

At present, the following approaches can be taken in order to ensure the normal production of high pour-point crude:

1. Self-controlled electric heating cable
2. Hollow sucker rod (electric heating and hot-water circulation)
3. Hydraulic piston pump
4. Electric submersible pump
5. Concentric string hot-water circulation (Figure 3-43)

The former four selections are mainly dependent on the liquid production rate and the technological conditions, and no special requirement for production casing size. In the fifth selection, the concentric tubing string configuration requires that the outer tubing should be larger than the inner tubing. In general, the outer tubing of 4 ½ in. and the inner tubing of 2 ⅞ in. are set in the production casing of 7 in., thus forming a hot-water circulation path.

As mentioned earlier, the selection of tubing and production casing sizes may be affected by natural gas wells, flowing wells, artificial lift wells, stimulation, heavy oil, or high pour-point oil production. Therefore, these aspects should

be considered when rational tubing and production casing sizes are determined.

## REFERENCES

- [1] K.E. Brown, et al., *Petroleum Production Technology of Lifting Methods*, vol. 4, Petroleum Industry Press, Beijing, 1990.
- [2] J. Mach, E. Proano, K.E. Brown, A Nodal Approach for Applying Systems Analysis to the Flowing and Artificial Lift Oil or Gas Well. SPE 8025.
- [3] H. Duns Jr., N.C.J. Ros, *Vertical Flow of Gas and Liquid Mixtures in Wells*, 6th World Petroleum Congress, Frankfurt, Germany, 1984.
- [4] J. Orkiszewski, Predicting Two-phase Pressure Drop in Vertical Pipe, JPT (6) (1967).
- [5] H.D. Beggs, J.P. Brill, A Study of Two Phase Flow in Inclined Pipes, JPT (5) (1973).
- [6] Wang Deyou, *Case History of Nodal Analysis of Oil and Gas Wells*, Petroleum Industry Press, Beijing, 1991 (in Chinese).
- [7] Wan Renpu, Luo Yingjun, et al., *Petroleum Production Technology Handbook*, vol. 4, Petroleum Industry Press, Beijing, 1991 (in Chinese).
- [8] *Drilling Handbook (Party A)*, Petroleum Industry Press, Beijing, 1990 (in Chinese).
- [9] Wan Renpu, The 7-in. Production Casing Selection Proof, *Petroleum Drilling and Production Technology* (1) (1981) (in Chinese).
- [10] Shilun Li, et al., *Natural Gas Engineering*, Petroleum Industry Press, Beijing, 2000 (in Chinese).
- [11] Yingchuan Li, et al., *Petroleum Production Engineering*, Petroleum Industry Press, Beijing, 2001 (in Chinese).
- [12] Wan Renpu, et al., *Petroleum Production Engineering Handbook*, Petroleum Industry Press, Beijing, 2000 (in Chinese).

## Completion and Perforating Fluids

### OUTLINE

#### 4.1 Functions of Drilling and Completion Fluid and Basic Requirements

- Functions of Drilling and Completion Fluid
  - Features of Formation Damage of Drilling and Completion Fluid
  - Solids Content and Solid Particle Grading in Drilling and Completion Fluid*
  - Clay-Hydration-Inhibiting Property of Drilling and Completion Fluid*
  - Compatibility between the Drilling and Completion Fluid Filtrate and the Reservoir Fluid*
  - Formation Damage Caused by Treating Agents in Drilling and Completion Fluid*
  - Requirements of Reservoir Protection for Drilling and Completion Fluid
- #### 4.2 Drilling and Completion Fluid Systems and Application
- Aero-Based Drilling and Completion Fluid
  - Aero-Fluid*

- Fog Fluid*
- Aerated Drilling and Completion Fluid*
- Foam Fluid*

#### Water-Based Type Drilling and Completion Fluid

- Solid-Free Clean Salt Drilling and Completion Fluid*
- Clay-Free Drilling and Completion Fluid with Solids*

#### Oil-Based Type Drilling and Completion Fluid

- Formation Damage Mechanism of Oil-Based Type Drilling and Completion Fluid*
- Formulation of Oil-Based Drilling and Completion Fluid*

#### 4.3 Shield-Type Temporary Plugging Technique

- Overview
- Theoretical Basis of Shield-Type Temporary Plugging Technique of Modified Drilling Fluid
- Reasons for Developing Shield-Type Temporary Plugging Technique*
- Mechanism and Experimental Results of*

- Shield-Type Temporary Plugging Technique*

- Reservoir Protecting Shield Type Temporary Plugging Technique Program and Application Results
- Development of Shield-Type Temporary Plugging Technique

- New Theory and Method of Optimizing Temporary Plugging Agent Particle Size Distribution in Drilling and Completion Fluid*
- Drilling and Completion Fluid for Protecting a Fractured Reservoir*

#### 4.4 Drilling and Completion Fluid for a Complicated Reservoir

- Drilling and Completion Fluid for Wells Prone to Lost Circulation and Borehole Sloughing
- Drilling and Completion Fluid for Adjustment Wells
- Drilling and Completion Fluid for Deep and Ultra-Deep Wells

Drilling and Completion Fluid for Directional and Horizontal Wells	<i>Formation Damage of Solid Particles in Perforating Fluid</i>	<i>Solid-Free Clean Salt-Water Perforating Fluid</i>
Drilling and Completion Fluid for Tight Sand Gas Reservoir Protection	<i>Formation Damage Caused by Perforating Fluid Filtration</i>	<i>Polymer-Type Perforating Fluid</i>
<i>Features of Formation Damage of Tight Sand Gas Reservoir Completion Fluid for Protecting a Tight Sand Gas Reservoir</i>	<i>Formation Damage of a Rate-Sensitive Reservoir by Perforating Fluid</i>	<i>Oil-Based Perforating Fluid</i>
<b>4.5 Perforating Fluid</b>	Design Principle of a Perforating Fluid System	<i>Acid-Based Perforating Fluid</i>
Formation Damage Mechanism of the Perforating Fluid	Common Perforating Fluid Systems and Their Features	<i>Gas-Based Perforating Fluid</i>
		Requirements of Perforating Technology for Perforating Fluid
		<b>References</b>

The drilling fluid used during drilling-in the oil and gas reservoir belongs to the category of completion fluid and is known as drilling and completion fluid. The drilling and completion fluid should serve the function of protecting the reservoir and ensuring downhole safety and smooth drilling work, thus combining the drilling fluid technique with the reservoir-protecting technique and forming a drilling and completion fluid technique that enables protection of the reservoir. Perforating fluid is a working fluid used for perforating operations in the well completion process and should be able to protect the reservoir and meet the requirements of the perforating operation.

#### **4.1 FUNCTIONS OF DRILLING AND COMPLETION FLUID AND BASIC REQUIREMENTS**

##### **Functions of Drilling and Completion Fluid**

Different types and properties of drilling and completion fluid are required by different oil and gas reservoirs and different drilling engineering requirements. However, the basic requirements are similar; that is, the drilling fluid should have the required functions, and the

requirements of protecting the reservoir should be met. In general, a drilling and completion fluid should have the following functions:

1. Controlling the formation fluid pressure and ensuring normal drilling. The drilling fluid density can be regulated in accordance with actual downhole conditions and the technological requirements of drilling in order to effectively control the reservoir fluid.
2. Meeting the requirements of rheological properties necessary for drilling engineering. The rheological parameters of drilling and completion fluid should be optimized in order to maximize the hydraulic horsepower. Furthermore, drilling and completion fluid should have the corresponding rheological properties in order to clean the bottomhole, carry cuttings, and suspend weighting material. In addition, enhancing displacement efficiency during cementing should be considered when the rheological property of drilling and completion fluid is determined.
3. Stabilizing the borehole wall. Drilling and completion fluid should have appropriate density, inhibitive property, filtration and wall-building properties, and shut-off capacity, which are required by the formations to be drilled in order to keep the borehole wall stable.

4. Improving the wall-building property, enhancing cake quality, stabilizing the borehole wall, and preventing differential pressure sticking. Improving the wall-building property is an important requirement for drilling and completion fluid. It can stabilize the borehole wall, can prevent differential pressure sticking during drilling-in a reservoir with higher permeability, and also is necessary to protect the reservoir. It is an important drilling and completion technique.
5. Other functions that are required of drilling fluid.

In addition, drilling and completion fluid should avoid formation damage as much as possible.

Different formation damage occurs when different reservoirs contact different types of completion fluid. The location of the damage is dependent on reservoir characteristics and completion fluid properties. Therefore, studies of formation damage mechanisms and the reasons for generating formation damage, selection of the adaptive completion fluid system, and determination of the corresponding application technology are the main contents in the reservoir-protecting completion fluid technique.

Drilling-in upsets the original balanced state of the reservoir. The reservoir is brought into contact with the foreign working fluids (drilling fluid, cement slurry, and so on) and formation damage may be caused. Therefore, when the reservoir is drilled in, the problem of preventing formation damage is the first link in the system engineering of the reservoir protection technique, to which attention should be fully paid.

Because drilling-in upsets the original balanced state of the reservoir and the working fluid (drilling and completion fluid, cement slurry, and so on) contacts the reservoir for a longer time, various problems of formation damage may be generated. These include formation damage caused by the entrance of solid particles in the working fluid into the reservoir, and also formation damages caused by the hydration of formation grains (clay minerals and water-wet secondary minerals),

reservoir surface wettability reversal, phase trap damage, blocking by emulsification, inorganic scale deposition formed by contacting formation water, fine migration, blowout, lost circulation, and borehole collapse, after the liquid phase of the working fluid enters the reservoir.

Therefore, during drilling and completion the reasons for formation damage should be accurately analyzed on the basis of reservoir characteristics and potential problems, and the corresponding measures of drilling operation should be taken, thus ensuring the effectiveness of reservoir protection, finding the reservoir in time, and the original productivity of the reservoir, and thus achieving the desired results of the first link in the system engineering of reservoir protection.

### Features of Formation Damage of Drilling and Completion Fluid

Formation damage exists at several links in the whole process from drilling-in to the end of cementing. During this period of time, the formation damage is related to differential pressure, soak time, and annular return velocity. The factors affecting formation damage by drilling and completion fluid are discussed in the following sections.

**Solids Content and Solid Particle Grading in Drilling and Completion Fluid.** During drilling-in, blocking may be caused by solid particles in drilling and completion fluid to some extent. The higher the solids content in drilling and completion fluid, the greater the formation damage (see Figure 4-1).

The formation damage caused by solids depends on the shape, size, property, and grading of solid particles. In the drilling and completion process, particles with diameters larger than the reservoir throat diameter may not cause formation damage, whereas particles with diameters smaller than the reservoir throat diameter may cause formation damage after entering formation. The smaller the particle, the greater the invasion depth. When there are fine or ultra-fine particles in drilling and completion fluid,

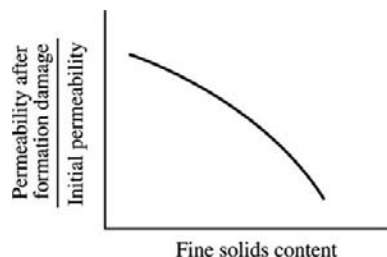


**FIGURE 4-1** Effect of solids content in drilling and completion fluid on reservoir permeability.

the invasion depth and formation damage may be greater. When there are various diameter particles in drilling and completion fluid, the invasion depth of fine and ultrafine particles will be reduced, but the degree of damage in the damage zone will not be reduced.

Formation damage caused by solid particles will be more remarkable for a fractured oil and gas reservoir. In order to reduce the formation damage caused by solid particles in drilling and completion fluid, the solid particles should be well controlled, the solids content (especially fine and ultrafine solids content) in drilling and completion fluid should be reduced, and a rational solid particle grading in drilling and completion fluid should be maintained. Furthermore, the increase of solids content in drilling and completion fluid, which is caused by shale sloughing (due to unstable borehole wall during drilling), borehole diameter enlargement, mud yielding of mud shale, and so on, will aggravate the formation damage caused by solids.

**Clay-Hydration-Inhibiting Property of Drilling and Completion Fluid.** The basic reasons for generating water-sensitive formation damage include hydration and swelling and dispersion and migration of the clay minerals in the reservoir. The higher the clay-hydration-inhibiting ability of the drilling and completion fluid, the lower the degree of water-sensitive formation damage. Therefore, on the basis of the types and properties of clay minerals in the reservoir, enhancing the inhibiting property is also an important aspect of the reservoir-protecting drilling and completion technique.

**Compatibility between the Drilling and Completion Fluid Filtrate and the Reservoir Fluid.** The precipitation or emulsion generated by the chemical action between the drilling and completion fluid filtrate and the reservoir fluid may plug the reservoir. Incompatibility between the water-based drilling and completion fluid filtrate and the formation water may generate various types of precipitation (or scaling), which commonly cause formation damage.

**Formation Damage Caused by Treating Agents in Drilling and Completion Fluid.** The various treating agents in the drilling and completion fluid will react on the reservoir when entering the reservoir with the drilling and completion fluid filtrate. Despite the fact that the different types of treating agents and different reservoir compositions and textures have different types and mechanisms of reaction, formation damage may be generated to varying extents. Because the treating agents are the requisite components, the selection of appropriate treating agents on the basis of oil and gas reservoir characteristics is also an important aspect of the reservoir-protecting drilling and completion technique.

## Requirements of Reservoir Protection for Drilling and Completion Fluid

In order to achieve reservoir protection, the following requirements for drilling and completion fluid should be met:

1. Maintaining compatibility between the liquid phase of drilling and completion fluid and the reservoir.
  - Compatibility with the liquid phase in the reservoir, including no precipitation caused by contact with formation water, no emulsification caused by contact with oil, and no bubble generated.
  - Compatibility with the reservoir. More attention should be paid to reservoirs with a serious water, salt, or alkali sensitivity.
  - Effect on reservoir wettability. The completion fluid composition, including treating agents, inorganic salts, and

surfactants, should be appropriately selected in consideration of the aforementioned compatibilities and should be determined after being checked and evaluated using an effective evaluation method.

2. The content of solids (especially clay and barite) and solid particle grading should be strictly controlled on the basis of the features of reservoir throat distribution in order to reduce the formation damage caused by solid particles in the drilling and completion fluid.
3. Attention should be paid to preventing completion fluid from corroding drill tools and casing. The drill tool and casing corrosion caused by the various inorganic salts (including NaCl, KCl, and CaCl<sub>2</sub>) in completion fluid may be more obvious. Not only may the corrosion reduce drill tool life and oil and gas well life, but also the corrosion products may cause formation damage.
4. No environmental pollution will be generated or the pollution can be eliminated.
5. The system should have stable performance, and downhole safety can be ensured. For a deep well, the thermal stability problem should also be considered.
6. Low cost and simple technology.

Practical experience indicates that drilling and completion fluid with good effectiveness has generally high cost and complicated technology (including preparation, usage, and purification and maintenance treatment). Therefore, drilling and completion fluid with good effectiveness, low cost, and simple technology should be researched and developed.

## 4.2 DRILLING AND COMPLETION FLUID SYSTEMS AND APPLICATION

The different types of drilling and completion fluids with different compositions and properties should be selected under different reservoir pressures as well as different compositions, textures, and properties of rock and reservoir fluids.

At present, there are three categories of drilling and completion fluid in accordance with composition and working principles. These are: aero-based drilling and completion fluid, including aero-fluid, fog fluid, foam fluid, and aeration drilling and completion fluid; water-based drilling and completion fluid, including solid free clean salt water completion fluid, clay-free solids-laden completion fluid (temporarily blocking-type system), and modified completion fluid; and oil-based drilling and completion fluid, including oil-based completion fluid and water-in-oil emulsion drilling and completion fluid.

### Aero-Based Drilling and Completion Fluid

Conventional water-based or oil-based drilling fluid cannot be used during drilling-in a low-pressure reservoir with a pressure coefficient less than 1 in order to avoid generating excessive overbalance pressure and formation damage, and the aero-based drilling and completion fluid should be adopted with the permission of reservoir conditions. The so-called aero-based drilling and completion fluid is not always such a system taking gas as a dispersed medium but is just to achieve a drilling and completion fluid system density lower than 1 g/cm<sup>3</sup> by using gas, thus favoring drilling-in a low-pressure reservoir.

**Aero-Fluid.** Aero-fluid means the circulation fluid composed of air or natural gas, corrosion inhibitor, and drying agent. Aero-fluid is often used for drilling of lost-circulation zones, strongly sensitive reservoirs, vuggy low-pressure zones, and low-pressure payzones, due to low aero-fluid density. The penetration rate can be increased by three to four times in comparison with the conventional drilling fluid. The aero-fluid has the features of high penetration rate, short drilling time, and low drilling cost. Special equipment, such as air compressors, is needed on the well site when an aero-fluid is used for drilling. In general, aero-fluid drilling can be effectively conducted under a surface injection pressure of 0.7–1.4 MPa and an annular velocity of 762–914 m/min. The usage of aero-fluid is often

limited by well depth, formation water production, and an unstable borehole wall.

**Fog Fluid.** Fog fluid means the circulation fluid composed by air, foaming agent, corrosion inhibitor, and a small amount of water, and it is a transitional technology. The low-pressure oil and gas reservoir can be drilled-in by using fog fluid when the formation liquid production rate is lower than  $24 \text{ m}^3/\text{h}$ , whereas the reservoir can only be drilled-in by using foam fluid when the formation liquid production rate is higher than  $24 \text{ m}^3/\text{h}$ . In the fog fluid, air is the continuous phase while liquid is the discontinuous phase. The air requirement of fog fluid drilling is 30% (sometimes 50%) higher than that of aero-fluid drilling. Twenty to 50 liters of foam liquid (99% water and 1% foaming agent) are generally required to be injected into the well depending on the liquid production rate.

In order to effectively carry the cuttings out of the wellhead, the surface injection pressure should be generally higher than 2.50 MPa; thus, the annular velocity can be higher than 914 m/min. The payzone is only affected by aero-fluid or fog fluid in a small degree due to the low annular pressure and underbalanced drilling.

**Aerated Drilling and Completion Fluid.** Air is injected into the drilling fluid to reduce the fluid column pressure. The aerated drilling and completion fluid density can be minimized to  $0.5 \text{ g}/\text{m}^3$ . The drilling fluid-to-air ratio is generally 10:1. An annular velocity of 50–500 m/min is required during drilling using aerated drilling and completion fluid, and a surface normal working pressure of 3.5–8 MPa is required. Attention should be paid to the problems of gas separation, corrosion prevention, and anti-erosion during drilling.

**Foam Fluid.** At present, the foam fluid is a commonly used effective completion fluid for drilling a low-pressure payzone. It can also be used as a workover fluid, and good results have been obtained. The most common foam used for drilling is stable foam. It is formed at the surface and then pumped into the well for use, hence it is also known as prepared stable foam.

1. Application features of stable foam completion fluid
  - a. Foam has low density (generally  $0.032\text{--}0.065 \text{ g}/\text{cm}^3$ ) and low hydrostatic column pressure in a well (only 2% to 5% of the water column pressure). The underbalance as a consequence will generate very low formation damage. However, foam is unsuitable for a formation with an unstable borehole wall, for mechanical reasons.
  - b. Stable foam has a strong cuttings-carrying capacity. It is a gas-water-dispersed system with dense fine bubbles that are covered by liquid film with a higher strength. The stable foam has a lower density and a higher strength and has a certain texture, thus generating a higher apparent viscosity under a lower velocity gradient and forming a plunger moving up. The plunger has a strong cuttings-lifting ability due to its high viscosity and strength. In addition, foam has a high compressibility and has a tendency to expand during rising, thus favoring cuttings lifting. The cuttings-carrying capacity of stable foam is up to 10 times that of water and up to 4 to 5 times that of common drilling and completion fluid and can fully meet the requirements of bottomhole cleaning and cuttings-carrying during drilling. Obviously, the cuttings-carrying capacity of foam is directly related to the foam's stability and strength.
  - c. Low liquid content. The water phase content in foam cannot be higher than 25%. The possibility of water phase contacting and entering the reservoir is greatly reduced due to low water phase content and binding by liquid film.
  - d. No solids in liquid. It is possible that there are no other solids (that is, no special solid foam-stabilizing agent is selected) except cuttings in foam, thus reducing the formation damage caused by solids.
  - e. The stable foam cannot be reclaimed and cyclically utilized. The prepared foam is difficult to reclaim after circulating in the

well and returning to the surface. The reclaimer should meet the higher requirements. Therefore, the foam fluid is only to be used once in a well. Obviously, a practical effective foam reclaimer should be researched and developed.

## 2. Foam composition and preparation

The foam used for drilling and completion and workover consists mainly of the following components:

- a. Fresh or salt water. The salinity and the type of ion depend on reservoir conditions. The water content is 3% to 25% (volumetric ratio).
- b. Foaming agent. There are many types of foaming agents, which are film-forming surfactants, and mainly include alkyl sulfate, alkyl sulfonate, alkyl benzene sulfonate, alkyl polyoxyethylene ether, and alkyl benzene polyoxyethylene ether.
- c. Aqueous-phase viscosifying agent. In general, it is a water-soluble high-molecular polymer (such as CMC). Its volume is dependent on the appropriate water-phase viscosity.
- d. Gas phase. Air or nitrogen. It is supplied by air compressor and special gas supply equipment.
- e. Others. The special components used for increasing foam stability.

An appropriate foam composition (formulation) should have good compatibility with the reservoir and high stability. A high-stability foam has a long foam life period.

After foam composition is selected and determined, whether the foam fluid that is applicable under downhole conditions can be formed depends mainly on the special preparation equipment that has been approved and supplied for field use.

## 3. Determination of gas-liquid ratio of foam

The gas-liquid ratio of foam is a complicated application technology. In general, a liquid phase content of 3% to 25% (volumetric ratio) can form a foam with a high cuttings-carrying capacity. When the liquid phase content is lower than 3% (volumetric

ratio) and the foam is known as dry foam, the foam stability may be reduced and the bubbles will merge and even form a gas bag, thus losing the cuttings-carrying capacity of foam. When the liquid phase content is higher than 25% (volumetric ratio) and the foam is known as wet foam, the foam texture tends to fail, the foam becomes gassy fluid (water foam) of which the flow performance is similar to that of an aqueous solution, and the cuttings-carrying capacity is similar to that of water, thus losing the function of foam. The water-gas ratio in foam can be regulated and controlled by the gas injection rate and water injection rate. In general, when the gas injection rate is 12–30 m<sup>3</sup>/min, and the water injection rate is 40–200 l/min, an annular return velocity of 2.5–10 m/s can be kept under a surface working pressure of 1.5–3.5 MPa, thus keeping the borehole clean.

However, the gas-liquid ratio of the stable foam formed in the use process of foam will change greatly with the temperature and pressure borne by foam because the effects of temperature and pressure on gas volume are much greater than the effects on water volume. Therefore, in order to maintain stable foam in the whole well section, the gas-liquid ratio appropriate to temperatures and pressures in various well sections must be correctly designed, and then the total injection rate and the total ratio are determined. The gas-liquid ratio of foam is a complicated problem, related to basic borehole parameters, air injection rate, foam injection rate, penetration rate, and so on, and is generally controlled by using a special computer program.

## 4. Annular backpressure control

In order to adapt to formation conditions and ensure smooth drilling and downhole safety, the fluid pressure on formation should be controlled and regulated, and the annular backpressure control method can generally be used. The annular backpressure control method can also be used for understanding the change in downhole pressure and

controlling the gas-liquid ratio of downhole foam in time. Therefore, the annular backpressure control is a necessary component part of the foam drilling and completion technique. The annular backpressure is generally controlled by using a backpressure value between the wellhead outlet and the cuttings discharge pipeline, and the expected results can be obtained.

#### 5. Rheological characteristics of foam fluid

Because of the strongly compressible gas in foam, the rheological characteristics of foam and the research approach are different from those of ordinary fluid.

To sum up, foam drilling and completion is one of the best low-pressure reservoir drilling and completion methods when the reservoir and downhole conditions permit. Foam fluid has been successfully used as the drilling and completion fluid and the workover fluid of low-pressure reservoirs in the Xinjiang and Changqing oil fields in China, and an obvious effectiveness has been obtained.

## Water-Based Type Drilling and Completion Fluid

Water-based type is a main category of drilling and completion fluid, which is most widely used at present. It is a dispersed system in which water is the dispersed medium.

### Solid-Free Clean Salt Water Drilling and Completion Fluid

#### 1. Basic thinking

The formation damage caused by solids can be avoided by having no solids in the completion fluid. As a result, the requirements of reservoir protection and drilling technology can be met.

- a. The system is a clean salt water with no solids. The cleanliness of salt water can be ensured by precise filtration.
- b. The completion fluid density can be adjusted by the type, concentration, and formulation of inorganic salts in order to meet the downhole requirements.

- c. Water-sensitive minerals can be highly inhibited by the high salinity and various ions of the system, thus preventing formation damage due to water sensitivity.
- d. The viscosity can be increased by using a polymer with no or low formation damage.
- e. The fluid loss can be reduced by using a polymer with no or low formation damage.
- f. Surfactant and corrosion inhibitor can be used if necessary.

#### 2. Density control of clean salt water

Clean salt water is formulated with clean water and various inorganic salts. Its density is determined by the salt concentration and the proportions of various salts. The density range is 1.00–2.30 g/cm<sup>3</sup>. When the various salt water solutions are under saturation conditions, their densities are different from each other, as shown in Table 4-1.

The water solutions of the same type of salt under different concentrations have different densities, and the density can be changed by changing the concentration. The water solutions of the same type of salt with the same concentration have different densities under different temperatures. The effect of temperature should be considered during formulating.

**TABLE 4-1** Maximum Densities of Various Salt Water Solutions

Type of Salt Water	Mass Concentration of Salt (%)	Density at 21° (g/cm <sup>3</sup> )
NH <sub>4</sub> Cl	24	1.0
KCl	26	1.07
NaCl	26	1.17
KBr	39	1.20
CaCl <sub>2</sub>	38	1.37
NaBr	45	1.39
NaCl/NaBr		1.49
CaCl <sub>2</sub> /CaBr <sub>2</sub>	60	1.50
CaBr <sub>2</sub>	62	1.81
ZnBr <sub>2</sub> /CaBr <sub>2</sub>		1.82
CaCl <sub>2</sub> /CaBr <sub>2</sub> /ZnBr <sub>2</sub>	77	2.30

3. Formulation of common solid-free salt water solutions
  - a. Potassium chloride salt water. The potassium chloride salt water is the best drilling and completion fluid for a water-sensitive reservoir. The salt water solution of  $1.003\text{--}1.17\text{ g/cm}^3$  can be formulated at the surface. The density is determined by the KCl concentration.
  - b. Sodium chloride salt water. Sodium chloride salt water is most commonly used. Its density range is  $1.003\text{--}1.20\text{ g/cm}^3$ . In order to prevent clay minerals from hydrating, KCl of 1% to 3% can be added during formulating. KCl does not act as a weighting agent but just acts as a formation damage inhibitor. The density is determined by the NaCl concentration.
  - c. Calcium chloride salt water. A drilling and completion fluid density higher than  $1.20\text{ g/cm}^3$  is required by drilling and completion of a deep well and abnormally high-pressure reservoir. The formulating range of calcium chloride salt water density is  $1.008\text{--}1.39\text{ g/cm}^3$ . There are two types of calcium chloride: granular calcium chloride (purity 94% to 97%, water content 5%, soluble fast in water) and sheet calcium chloride (purity 77% to 82%, water content 20%). If the latter is used, more should be added. Combined usage can reduce cost to some extent. The density is determined by the  $\text{CaCl}_2$  concentration.
  - d. Calcium chloride and calcium bromide salt water. When a working density of  $1.40\text{--}1.80\text{ g/cm}^3$  is required by the borehole, calcium chloride and calcium bromide salt water should be used. When the salt water is formulated, calcium bromide solution with a density of  $1.82\text{ g/cm}^3$  is used as the base solution, and calcium chloride solution with a density of  $1.38\text{ g/cm}^3$  is added to the base solution to reduce and adjust the system density. The density is determined by  $\text{CaCl}_2$  and  $\text{CaBr}_2$  concentrations.
  - e. Calcium chloride, calcium bromide, and zinc bromide salt water. Completion fluid with a density of  $1.81\text{--}2.31\text{ g/cm}^3$  can be formulated by the calcium chloride, calcium bromide, and zinc bromide salt water and can be specially used for some high-temperature high-pressure wells. When the calcium chloride, calcium bromide, and zinc bromide salt water is formulated, the mutual effects (density, crystallization point, corrosion, and so on) should be considered in the light of specific well conditions and environment. An increase of density and a reduction of crystallization point can be achieved by increasing the densities of calcium bromide and zinc bromide. The highest crystallization point of the highest density is  $-9^\circ\text{C}$ . Increasing calcium chloride concentration can reduce the density, raise the crystallization point to  $18^\circ\text{C}$ , and have the best compositional economy. The density is determined by the concentrations of  $\text{CaCl}_2$ ,  $\text{CaBr}_2$ , and  $\text{ZnBr}_2$ .
4. Fluid loss control and viscosifying
 

There are no solids in clean salt water, and no cake will be formed on the borehole wall; thus, a higher fluid loss may be generated, and a leakage into a high-permeability reservoir can easily form. In order to reduce the leakage of costly completion fluid and reduce the formation damage, the fluid loss should be controlled. Some special water-soluble polymer can be used to increase water phase viscosity and reduce the filtration rate. The special polymer should have the following features:

  - a. Capable of dissolving in high-salinity salt water, and incapable of precipitating by high-valence metallic ion
  - b. Higher viscosifying action in salt water
  - c. No obvious formation damage
  - d. Highly stable, not easy to degrade, and remaining effective at a temperature above  $100^\circ\text{C}$

Hydroxyethyl cellulose (HEC), Xanthomonas Campestris polymer (XC), hydroxythylated starches, and so on are commonly used for controlling the fluid loss of clean

salt water. When the fluid loss is measured, a core instead of filter paper is used as a filtering medium.

Drilling and completion fluid should have a certain viscosity in order to meet the requirement of borehole cleaning. A water-soluble polymer should be added due to no solids in the clean salt water in order to increase the system viscosity. It is known that the increase of viscosity is similar to the decrease of fluid loss for clean salt water drilling and completion fluid. HEC and XC (used alone or jointly) not only can increase the clean salt water viscosity up to 40–50 MPa · s (apparent viscosity), but also can reduce the system fluid loss to below 10 ml, thus meeting the requirements of drilling and completion technology and reservoir protection.

#### 5. Effects of temperature

The effects of temperature on the properties of a clean salt water completion fluid system are as follows (especially the effect on density).

a. Crystallization temperature of saturated salt water. High-salinity salt water close to a saturation condition under a higher temperature will be able to reach a saturation or supersaturated condition when the temperature is reduced to a certain value. Salt crystallization will occur, the pipeline will be plugged, the salt concentration in the solution will be reduced, liquid phase density will be greatly reduced, drilling and completion fluid density will not meet the design requirement, and the drilling and completion fluid cannot be used. Therefore, the crystallization temperature of this type of completion fluid used in an area should be higher than the lowest atmospheric temperature in this area. The crystallization temperature is related to the types of salt and the proportions of different salts. As a result, when the mixed salt is selected to adjust and control completion fluid density, the system should have a higher crystallization temperature. For instance, there are several formulations for clean salt water

with a density of 1.40 g/cm<sup>3</sup>, and the saturated CaCl<sub>2</sub> solution and the mixed CaCl<sub>2</sub> and CaBr<sub>2</sub> solution may meet the requirement. However, the former starts crystallizing at 18°C, and the latter's crystallization temperature may reduce to -35°C as the proportion of CaBr<sub>2</sub> increases. CaBr<sub>2</sub> has a high cost. In order to meet the requirement of density, raise the system crystallization temperature to a temperature higher than the lowest temperature in use, and to reduce the cost, it is important to rationally select the mixed salt and the proportion.

b. Effects of temperature on system density. The change in temperature will induce a change of solution volume; thus, the system density will change. As a result, the bottomhole temperature is an important factor affecting the design and maintenance of the completion fluid. The completion fluid temperature change from the surface to the bottomhole may affect the mean density of the completion fluid. When the temperature increases, the density will decrease. Therefore, the mean working temperature of the completion fluid in the borehole should be known in advance before preparing the completion fluid in order to determine the density under surface conditions. Figure 4-2 shows the relations between the temperature and the density, which are obtained by experimental data of several types of salt water at 21–43°C (70–110°F). The salt water density at the surface, which can balance the reservoir pressure at the bottomhole temperature, can be calculated in accordance with the correction factors shown in Figure 4-2, and as shown in the following equation.

#### (4-1)

$$\rho_{21}^{\circ\text{C}} = \rho_1 + 1.8K_x (t - 21)$$

where:

$\rho_{21}^{\circ\text{C}}$  = density at 21°C, g/cm<sup>3</sup>;

$\rho_1$  = salt water density necessary for balancing reservoir pressure, g/cm<sup>3</sup>;

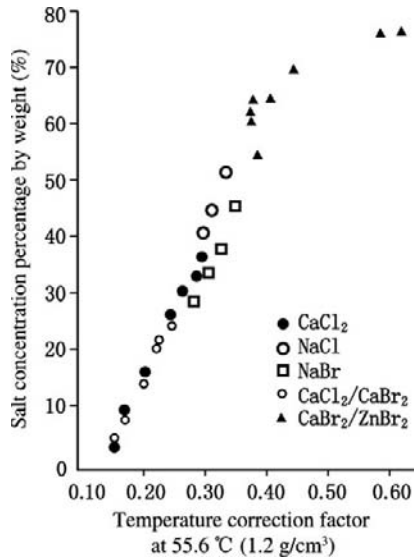


**FIGURE 4-2** Temperature correction factors for several salt water solutions.

$t$  = mean temperature in borehole [ $t$  = (bottomhole temperature + surface temperature)/2], °C;

$K_x$  = temperature correction factor at 55.6°C, g/cm<sup>3</sup>.

In general, the effects of temperature on the salt water densities of KCl, NaCl, and CaCl<sub>2</sub> are small, in the density range of 1.02–1.40 g/cm<sup>3</sup>, while the effects of temperature on heavy salt water (such as CaBr<sub>2</sub> and ZnBr<sub>2</sub>) densities are greater. For some salt water, the higher the density, the smaller the effect of temperature on density change.

#### 6. Keeping the completion fluid system clean

The basic advantage of solid-free clean salt water is that it can avoid the formation damage caused by solids. Removing various solids and keeping the system clean are important for applying this kind of system. The system must be kept clean during preparation, transportation, and reservation. Therefore, precision filtering equipment as well as clean preparation, transportation, and reservation equipment are required.

#### 7. Corrosion prevention

Salt water solutions may seriously corrode the surface equipment, pipeline, and downhole tubulars, and corrosion inhibition should be considered. There are quite a few corrosion inhibitors. However, the corrosion inhibitors used by the system should not cause formation damage, thus increasing the degree of technological difficulty.

#### 8. Reclamation

Clean salt water completion fluid should be reclaimed after use due to its high cost and should be used repeatedly. Solid-free clean salt water completion fluid has been used, and good results have been obtained. For instance, in the US block 573, Gulf of Mexico, the individual-well average oil production rate and gas production rate are respectively 31.8 m<sup>3</sup>/d and 56,634 m<sup>3</sup>/d before using clean salt water completion fluid, whereas the individual-well average oil production rate and gas production rate are respectively 270.3 m<sup>3</sup>/d and 566,343 m<sup>3</sup>/d after using clean salt water completion fluid. However, there are quite a few problems, and wide application has been obstructed. These problems include:

- High cost. The high-density clean salt water fluid has a high cost due to the high cost of bromide and the high costs of viscosifying agent and fluid loss additives. The unit price per cubic meter of high-density clean salt water fluid is several to several dozen times that of common drilling and completion fluid.
- Complicated technology with high requirements. Special equipment and technology are required in order to keep the system clean during use and a special design for keeping the system density stable is also required, thus complicated application technology with high requirements is needed.
- The viscosifying agent, such as HEC or XC, may cause formation damage, and serious formation damage may be caused under a higher density.

- d. A large fluid loss may cause aqueous trap formation damage.
- e. The high-salinity water phase entering the salt-sensitive reservoir will cause serious formation damage; that is, this system is inappropriate for a salt-sensitive reservoir.

To sum up, the advantages and disadvantages of a clean salt water completion fluid system result from no solids in the system to a great extent. Thus a completion fluid with solids causing formation damage that can be eliminated later has been developed. This type of completion fluid system is just a temporary plugging-type completion fluid system.

**Clay-Free Drilling and Completion Fluid with Solids.** The highly dispersed clay particles in drilling and completion fluid may cause permanent formation damage that cannot be eliminated after invading the reservoir and should be removed from the drilling and completion fluid as much as possible. Solid-free clean salt water has no solids and can avoid the formation damage caused by solids, but it is difficult to control density and fluid loss and will generate a series of complicated problems and high costs. If the solid particles that can weight drilling and completion fluid and favor forming cake and controlling fluid loss are added into the salt water, weighting the system and controlling the fluid loss will become easier. Despite the fact that these solid particles will certainly plug the reservoir during drilling, these solid particles can later be eliminated by using special measures and may not generate formation damage. Thus this type of special solid particle is known as a temporary plugging agent, and this technique is known as a temporary plugging technique. This type of drilling and completion fluid system is just the clay-free drilling and completion fluid with solids and is known as a temporary plugging type completion fluid system.

This type of system consists of water phase and solid particles used as a temporary plugging agent. The water phase is generally the water solution that contains various inorganic salts and inhibitors and is compatible with the reservoir,

and obviously may not be fresh water. In addition, it is not required to consider the density of the aqueous phase of the system. The solid phase (that is, temporary plugging agent) can weight the system and form inner and outer cakes on the borehole wall (which can be removed later) to reduce fluid loss. These fine solids are highly dispersed and the dispersion degree should be adaptable to reservoir throats. They should be at a multigrade dispersion state and have a rational grading. They can form an outer tight cake on the reservoir borehole wall surface, form bridging at reservoir throats, and form an inner tight cake. These solids can dissolve themselves in acid, oil, or water. Therefore, they can be divided into acid-soluble, oil-soluble, and water-soluble temporary plugging agents in accordance with density and solubility. In general, the particles of a temporary plugging agent can be divided into bridging particles and packing particles.

#### 1. Acid-soluble system

All components in this system should be soluble in strong acid. Polymer-CaCO<sub>3</sub> drilling and completion fluid is a commonly used acid-soluble system. This system consists mainly of salt water, polymer, calcium carbonate fines (2500 mesh), weighting agent, and other necessary treating agents, and the density range is 1.03–1.56 g/cm<sup>3</sup>.

After operating, the inner and outer solids or cake on the reservoir borehole wall can be removed by acidizing.

#### 2. Water-soluble system

A water-soluble system consists mainly of saturated salt water, polymer, salt particles, and corresponding additives, and the density range is 1.0–1.56 g/cm<sup>3</sup>. The salt solids of a certain size are added into the saturated salt water, and the polymer is also added. The salt solids cannot be further dissolved in the saturated salt water. They suspend in viscous solution and act as inert solids. Thus the salt solids and colloidal component can have the effects of bridging, weighting, and controlling fluid loss. The salt particles and

cake plugging temporarily on the reservoir can be removed by soaking and washing with fresh water or nonsaturated salt water. There is no need for acidizing.

### 3. Oil-soluble system

The oil-soluble system consists of oil-soluble resin, salt water, polymer, and additives. Oil-soluble resin is used as bridging material. HEC polymer is used for increasing viscosity. Water-wet surfactant is added in order to wet the resin. The oil-soluble resin can be dissolved by the crude oil or the gas condensate produced from the reservoir, and can also be dissolved by injecting diesel oil and oil-wet surfactant.

Despite the fact that this type of system has many advantages, it has not been widely used yet because the oil-soluble temporary plugging agent is difficult to suspend, cannot form texture, and is difficult to prepare. The drilling and completion fluid system can be modified using temporary plugging agents by means of the following actions:

- a. Adjusting the kinds of inorganic ions in drilling fluid to make them similar to the kinds of ions in formation water, and increasing drilling fluid salinity to exceed the critical salinity of the reservoir; or adjusting the drilling fluid salinity in accordance with the activity equilibrium principle to meet the requirements and to ensure compatibility of the liquid phase of drilling fluid with formation water.
- b. Reducing the solids content in drilling fluid.
- c. Adjusting the solids grading in drilling fluid. The solids size corresponding to reservoir throat diameter is selected as the bridging particle size. Furthermore, the amount of submicron particles smaller than 1  $\mu$  should be reduced as much as possible.
- d. Adopting an acid-soluble or oil-soluble temporary plugging agent.
- e. Improving cake quality and reducing the fluid loss of drilling fluid under high temperature and high pressure.
- f. Adopting a drilling fluid treating agent with low formation damage.

At present, modified drilling fluid has been widely used as completion fluid for drilling-in reservoirs due to its low cost (much lower than that of special completion fluid), simple application technology, and no special requirement for hole structure and drilling technology. Practice indicates that the formation damage of this type of drilling and completion fluid can be reduced to a value below 10%, and the skin factor can be close to zero.

Furthermore, special completion fluid systems, including clean salt water and clay-free temporary plugging systems, cannot be used under practical conditions. For instance, if there is an uncased cavey formation above the reservoir, the drilling fluid should have a higher density in order to keep the borehole at this section stable, thus generating a greater overbalance pressure during drilling-in. If the reservoir to be drilled is in itself a cavey formation, the drilling and completion fluid should have a good antisloughing property. The high temperature at a deep reservoir in a deep well is difficult to deal with using special completion fluid. In practice, multiple oil-bearing series may often be drilled-in, and there is a clay-rich mud shale interbed between reservoir groups. Thus the special completion fluid makes it difficult to keep the original composition and properties in use and still become the clay-particle-containing drilling fluid system. As a result, the predominance of special completion fluid will be lost.

To sum up, the special completion fluid cannot be adopted and kept in practice due to complicated downhole conditions, multiple oil and gas reservoirs, and limitations of the casing program. Thus a modified drilling fluid that can deal with the complicated downhole situations should be adopted in order to minimize the formation damage. It is the most valuable part of the reservoir-protecting drilling and completion fluid technique. At present, the modified drilling fluid is mostly used as a completion fluid on the basis of minimizing formation damage caused by drilling fluid in China and abroad. The shield-type temporary plugging technique is a new type of modified drilling fluid technique.

## Oil-Based Type Drilling and Completion Fluid

The oil-based type drilling and completion fluids include water-in-oil emulsion (such as invert emulsion drilling and completion fluid) and the dispersed system in which oil is the dispersed phase and solids are in oil (such as oil-based drilling and completion fluid). They have good thermal stability and a large density range with rheological properties that are easily adjustable. They can resist the pollution of various salts, inhibit mud shale, stabilize the borehole wall, and control corrosion. The water-sensitive effect of the reservoir can be avoided due to the filtrate, which is oil phase. Thus the formation damage that may be caused by oil-based type drilling and completion fluid is generally considered to be low, and this type of drilling and completion fluid can be considered as a completion fluid that not only can meet the various operation requirements but also has a good effect of protecting the reservoir. It can be widely used for drilling-in, reaming, perforating, workover, and so on, and also can be used as a gravel packing fluid. Good results have been obtained in practice; however, economy and safety should also be considered.

**Formation Damage Mechanism of Oil-Based Type Drilling and Completion Fluid.** Practical experience indicates that formation damage can still be generated by oil-based type drilling and completion fluid. The formation damage mechanisms of any oil-based completion fluids are similar and include:

- Reversing the reservoir wettability and reducing the relative permeability of the oil phase
- Forming an emulsion with reservoir water and plugging the reservoir
- Fine particle migration of oil-wet particles
- Completion fluid solids that may invade the reservoir
- Formation damage due to other components

### 1. Reservoir wettability reversal

A change in reservoir wettability may lead to a change in relative permeability. When the

reservoir surface changes from water wettability into oil wettability, the relative permeability of the oil phase may be reduced by 40% and above. The action of the surfactant on the rock surface will certainly change the wettability of the rock surface. The surfactants, such as the main emulsifying agent, supplementary emulsifying agent, and wettability reversing agent (from water wettability to oil wettability), are unavoidably used in the oil-based drilling and completion fluid in large amounts. When the adsorption of amphiphilic textures of the various emulsifying agents is generated on the hydrophilic rock surface, the hydrophilic group will certainly combine with the hydrophilic rock surface, and the lipophilic group is directed to outside, thus causing the oil-wetted rock surface. The cationic surfactant has the most obvious effect.

### 2. Forming an emulsion and plugging reservoir

In an oil-based drilling and completion fluid, there is always an emulsifying agent. Excessive emulsifying agent enters the reservoir with the filtrated oil and meets the reservoir water. The emulsifying agent containing oil may form an emulsion when meeting the reservoir water under flow conditions. The emulsion formed may be water-in-oil emulsion or oil-in-water emulsion. The liquid droplets of emulsion may reduce reservoir permeability due to the Jamin effect during moving. If the water-in-oil emulsion is formed, the formation damage is more serious due to the high viscosity.

### 3. Formation damage due to solids

First, formation damage will occur when the solids in drilling and completion fluid invade the reservoir. An oil-based completion fluid contains unavoidable solids. Some completion fluids need adding dispersible solids (such as organic clay and oxidized asphalt) into oil. All of these will cause formation damage. Second, formation damage will be caused if the oil phase contains a wettability reversing agent that may change the clay in the reservoir into oil-wet solids. These solids

may swell, disperse, and migrate, and formation damage may be caused. Third, the water-wet solids bound by the water layer, which is adsorbed on the water-wet surface, may be released due to surface wettability reversal and changed into movable solids, thus generating formation damage.

**Formulation of Oil-Based Drilling and Completion Fluid.** The formulation of oil-based drilling and completion fluid can be changed with the usage and the reservoir properties; however, the basic composition and application rule are basically constant. The formulation of oil-based drilling and completion fluid should be optimized by using reservoir evaluation experiments of the various components of the drilling and completion fluid under specific reservoir conditions, thus meeting the requirements of the drilling and completion and protecting reservoir.

### 4.3 SHIELD-TYPE TEMPORARY PLUGGING TECHNIQUE

#### Overview

In order to ensure drilling safety, reduce drilling cost, and simplify application technology, taking the modified drilling fluid as a drilling and completion fluid is an effective measure. The factors of formation damage, including high solids content and multistage dispersion of solids in drilling fluid and high pressure difference and long-time soak in reservoir, always exist when the reservoir is drilled-in. The shield-type temporary plugging technique of modified drilling fluid is adaptable to high pressure difference and long-time soak in reservoir and can achieve reservoir protection when the reservoir is drilled-in by using drilling fluid with a high solids content.

On the basis of reservoir properties and a full understanding of the rock mineral composition, the sensitive mineral components, contents and occurrences, and the reservoir pore texture, porosity, permeability, temperature, and reservoir water composition, the shield-type temporary plugging technique becomes a reservoir protection

technique with no special requirements for drilling operation and drilling fluid. In accordance with the rule of plugging the reservoir by the solids in drilling fluid, some bridging particles, packing particles, and deformable plugging particles that match the mechanism of plugging reservoir throats are artificially added to the drilling fluid; thus, these particles can rapidly (in several to a dozen minutes) form an effective impermeable shield ring within 10 cm around the borehole wall and prevent the solids and liquid phase in drilling fluid from further invading the reservoir, thus eliminating formation damage possibly caused by drilling and completion fluid and cement slurry during drilling, completion, and cementing and also eliminating the formation damage possibly caused by excessive soak. Then the shield ring is perforated. Thus there is no or slight formation damage generated. The breakthrough in the reservoir protection idea of this technique is at full-plugging the reservoir in the vicinity of the wellbore in order to prevent the foreign material from invading the reservoir. This reservoir protection idea is completely different from the traditional reservoir protection idea.

The features of the shield-type temporary plugging technique include:

1. This technique is appropriate for various sandstone oil and gas reservoirs. It has low cost, simple technology, and no special requirements for drilling fluid and drilling technology, and is easy to deploy. When this technique is applied, it is only necessary to reform slightly the drilling fluid used for drilling and add some temporary plugging materials to the drilling fluid, and it is unnecessary to formulate any new drilling fluid or completion fluid, thus greatly reducing cost and simplifying operation technology (it is only necessary to add evenly to the drilling fluid the temporary plugging agent within a certain time with no need for adding any equipment). Therefore, it has been widely adopted in the field.
2. The unfavorable condition of overbalance pressure difference, which may cause formation damage during drilling, is converted into an

essential condition favoring reservoir protection. In order to ensure forming a very low-permeability shield ring in the vicinity of the wellbore within a dozen minutes, a greater pressure difference is necessary. Furthermore, with the increase of pressure difference, shield ring permeability will reduce more rapidly, and formation damage will decrease.

This feature of the shield-type temporary plugging technique is very important for drilling an adjustment well or reservoirs with multiple pressure systems in a borehole. In general, drilling technology requires a high-density drilling fluid to protect upper borehole stability. However, the high-density drilling fluid may enter the reservoir and cause serious formation damage. This will violate the reservoir protection principle. The shield-type temporary plugging technique can successfully solve this contradiction and combine technically the objectives of drilling and production.

3. The reservoir permeability can be resumed by up to 80% during flowback. This feature is very important to a drillstem test. Because of the thin shield ring (thickness less than 10 cm), which is close to the borehole, the deformable particles are first flowed back during flowback, and then the packing particles and bridging particles are flowed back, thus ensuring that the drillstem test can accurately reflect the original physical parameters and the productivity of the reservoir.
4. The formation damage that can be caused by cement slurry during cementing can be eliminated, thus enhancing the cement job quality. Because the shield ring that is formed in the oil and gas interval during drilling has a very low permeability, the solids and the high pH value filtrate have difficulty invading the reservoir during cementing, thus eliminating the formation damage that can be caused by the cement slurry. Furthermore, forming of the shield ring makes the borehole diameter regular, thus enhancing the displacement efficiency of drilling and completion fluid by cement slurry and the consolidation strength of cement sheath with formation.

To sum up, the key to the shield-type temporary plugging technique lies in rapidly forming an effective thin shield ring in the reservoir near the borehole wall. Thus the physical properties of the reservoir should be fully understood, and some temporary plugging particles can be artificially added to the drilling fluid. The shield-type temporary plugging technique is a new technique on the basis of physical properties of the reservoir after a breakthrough in the idea of reservoir protection has been made.

### Theoretical Basis of Shield-Type Temporary Plugging Technique of Modified Drilling Fluid

**Reasons for Developing Shield-Type Temporary Plugging Technique.** As is well known, reservoir protection is just to avoid formation damage, that is, to prevent the oil and gas passage in the reservoir from plugging. Formation damage is certainly generated during drilling and completion, and the formation damage of cement slurry during cementing is further superposed on the formation damage of drilling and completion. The related data indicate that the formation damage during drilling and completion operations can be from 10% to 100%, while formation damage during cementing is generally higher than the formation damage of drilling and completion by 20% or above. Therefore, an effective reservoir protection technique should be adopted during drilling and completion.

Studies indicate that the formation damage during drilling and completion is mainly caused by entering of the solids and liquid phase of drilling and completion fluid into the reservoir under pressure difference. The solids will plug up the throats, and formation damage may be caused from 10% to 100%. The liquid phase may cause formation damage due to water-, alkali-, and salt-sensitivity and formation damage due to Jamin effect, water phase trap, and incompatible treating agents. The influence factors include potential reservoir problems (rock minerals) and drilling and completion fluid (drilling and completion fluid properties) as well

as the external conditions such as overbalance pressure difference  $\Delta p$  (the greater the  $\Delta p$ , the greater the formation damage), soak time  $t$  of the drilling and completion fluid (the longer the  $t$ , the greater the formation damage), and annular velocity (irrational annular velocity will aggravate formation damage of drilling and completion fluid). Formation damage during cementing is mainly caused by the entrance of cement slurry filtrate into the reservoir.

Therefore, the main approaches to preventing formation damage during drilling and completion are as follows.

1. In drilling and completion engineering, the near balanced drilling-in is adopted to the full extent, and the pressure difference  $\Delta p$  is minimized. Measures including meticulously organizing the operations, preventing failure, decreasing nonproducing time, optimizing hydraulic parameters, increasing penetration rate, and controlling appropriately annular velocity are taken in order to decrease the soak time of the reservoir.
2. The special completion fluid is used for drilling-in. (1) No solids or minimized solids content (especially the high-dispersity clay content) in drilling and completion fluid, or contained solids, which can be removed later. (2) Liquid phase compatible with the reservoir: Liquid phase compatible with reservoir fluids (oil, gas, and water); increasing compatibility between liquid phase and reservoir rock (no water-sensitivity damage, no salt-sensitivity damage, no alkali-sensitivity damage, no incompatibility with reservoir pore surface property, and so on).
3. Preventing drilling and completion fluid from entering the reservoir.

Thus it can be seen that the reservoir-protecting drilling and completion fluid technique embodies the two aspects: preventing drilling and completion fluid from entering the reservoir as much as possible; and preventing the components that enter the reservoir from plugging the reservoir as much as possible. The former should first be fully considered.

### Mechanism and Experimental Results of Shield-Type Temporary Plugging Technique.

The key to the shield-type temporary plugging technique lies in whether the solid particles can plug up the reservoir throats, how they can plug up the reservoir throats, and how they can be artificially controlled and can fully plug up the throats at a circular shallow part of the reservoir.

1. Physical model of plugging reservoir throats by solid fines
  - a. Deposition and plugging (bridging) of fine particles during migration. Studies indicate that the solid fines that migrate with fluid flow in reservoir pores may be caught and stop moving in pores. The deposition is mostly generated at the places of large diameter in pores while the throat plugging is generated at the throats. The solid fines deposited can remigrate when flow conditions are changed (flow rate or pressure difference is increased). The solid fines that plug throats stick firmly in throats and will not remigrate. Both the deposition and plugging of solid fines will reduce reservoir permeability, but the latter will reduce permeability more greatly. For the original modified drilling fluid, both (especially the latter) should be prevented. However, the shield-type temporary plugging technique has to utilize generating the latter to take the effect of bridging. This technique is known as bridge plug-type bridging.
  - b. Single-particle staged plugging model. When the reservoir is drilled-in, the drilling and completion fluid contacts the reservoir and starts filtrating into the reservoir under pressure difference.

A particle larger than the reservoir pore will deposit on the reservoir surface and form a cake (outer cake). A particle smaller than the reservoir pore will enter the reservoir with liquid phase and migrate to the throat. A particle larger than the throat diameter  $D_t$  will deposit on the borehole wall. A particle with particle diameter  $D_f$  much smaller than the throat diameter ( $D_t$

$>D_f > 7$ ) will pass through the throat and enter the deep reservoir. Only a particle with size and shape similar to the diameter and type of throat will stick firmly in the throat. A smaller new throat will be formed by bridging the original throat by bridging particles. At this new throat, solid fine particles will repeat the aforementioned migration process, except that the diameter of fine-particle-generating deposition, passing, and sticking will be much smaller than that for the first time. Then the fine particle of which the diameter and shape are similar to that of the new throat will stick to the new throat. This type of particle is known as a packing particle. Obviously, a packing particle is a particle of the stage next to the bridging particle. After packing, a new throat of smaller diameter will be generated, and only the further smaller particle will act as a packing particle of the next stage, on the analogy of this until the smallest particle in the fluid is packed to the corresponding new throat. At this time the process of packing the throat by solid particles is ended. Serious formation damage is caused by throat packing. Because the final packing of the smallest fine particle in the throat cannot fully seal the throat, there certainly is a further smaller throat left behind. Obviously, the new throat left finally decides the degree of formation damage or plugging degree. Generally, deformable particles should be added in order to further plug the throat and to plug it entirely. The plugging and packing of this throat at a time are the single-particle action in stages from large to small particle diameter; that is, at any time only a single fine particle migrates and passes through the throat section. Therefore, this process of throat plugging is known as single-particle staged plugging model.

- c. Double-particle (or multiparticle) bridging model. When the liquid phase, which has a higher solid particle concentration, passes through any cross-section of the throat at

any time, two or more solid particles exist at the same time. Despite the fact that the diameter of each fine particle is not enough to generate bridging or packing, two or more fine particles put together in the throat simultaneously will generate bridging or packing when the sum of the diameters of two or more particles almost equals the throat size. This process of throat plugging is known as the double-particle or multiparticle bridging model.

Studies indicate that these two throat-plugging models cannot be absolutely divided and that they will not conflict. The gradual single-particle plugging in combination with the simultaneous multiparticle plugging will generate better results.

2. Mechanism of plugging the throat by fine particles (single-particle staged plugging model)
  - a. Studies of bridging particle and bridging effect. In accordance with the single-particle staged plugging model, plugging effectiveness is based on the existence and effect of a bridging particle. The bridging particle is required to be stuck firmly in the throat. It can greatly decrease the throat diameter and will still not migrate under the long-term shock of fluid flow; that is, it will be firmly stuck in the throat and become a cornerstone of plugging.
    - (1) Relation between bridging particle diameter and throat size. The principle of particle-to-throat diameter ratio of  $1/3$  has been widely accepted since it was presented by Abram. This principle is based on formation damage and has been examined by experiments. However, whether this principle can meet our bridging requirements needs to be proved by experimental studies.

After the core throat diameter is determined, the suspension of solid particles with particle diameter  $D_f = D_t/n$  is injected into the core on a flow device, the plugging is conducted (the plugging conditions depend on requirements of study), and the permeability  $K$

is measured by using salt water under the same conditions.

The bridging experiments are done when  $n = 3, 2,$  and  $3/2$ , that is, a particle-to-throat diameter ratio of  $1/3, 1/2,$  and  $2/3$  under  $\Delta p = 3.5 \text{ MPa}$ ,  $t = 15 \text{ min}$ , and room temperature. The solid particle size distribution of some drilling and completion fluid in the experiments is shown in Figure 4-3. The experimental results under the particle-to-throat diameter ratio of  $1/3$  indicate that when the particle-to-throat diameter ratio is  $1/3$ , the reservoir can be plugged, and formation damage of 50% to 80% is caused regardless of core throat size (Figure 4-4). However, the experimental curve also shows that the fine particles still migrate continuously, and the core permeability  $K$  is obviously reduced. The clay fines that do not belong to the original core are observed in the filtrate flowing out of the core, and the core permeability will increase, thus proving that these particles can still migrate and cannot be firmly stuck, although the throat can be plugged under a particle-to-throat diameter ratio of  $1/3$ , and that this type of particle is not enough to be used as a bridging particle.

Under the particle-to-throat diameter ratio of  $1/2$ , the plugging is more serious, and the core permeability is reduced by

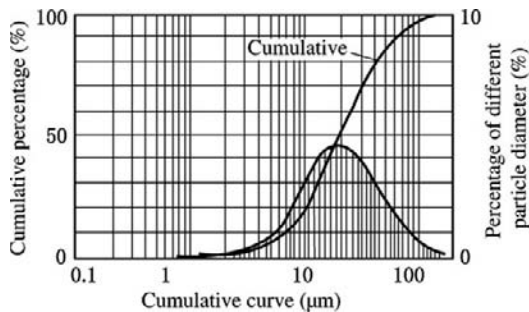


FIGURE 4-3 Particle size distribution of some drilling and completion fluids.

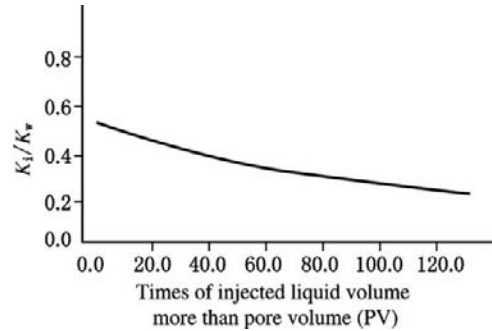


FIGURE 4-4 Bridging by using particles with a particle-to-throat diameter ratio of  $1/3$  in a reservoir.

more than 80%. The decreasing trend of the curve is much gentler, but the curve still shows a tendency to drop. This indicates that this type of particle with a particle-to-throat diameter ratio of  $1/2$  is still not enough to be used as a bridging particle (Figure 4-5).

Under the particle-to-throat diameter ratio of  $2/3$ , the plugging is more serious, and the core permeability is reduced by more than 90% (Figure 4-6). When the injected liquid volume is up to more than 10 times pore volume (PV), the curve is basically parallel to the abscissa axis. This indicates that no fine particle migrates, and this type of particle can be firmly stuck in the throat and taken as a bridging particle.

(2) Stability of the bridging particle. On the cores that are respectively plugged

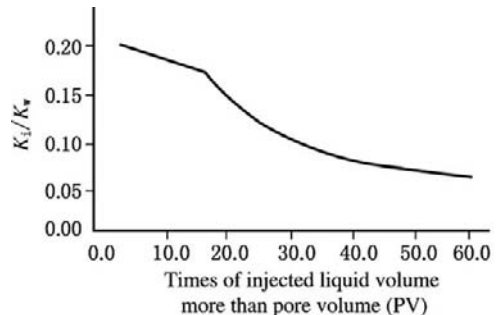
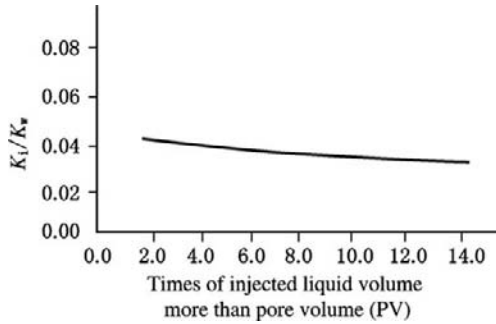
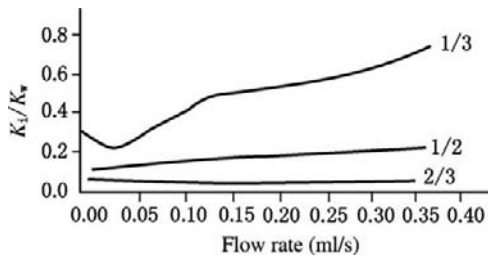


FIGURE 4-5 Bridging by using particles with a particle-to-throat diameter ratio of  $1/2$  in a reservoir.



**FIGURE 4-6** Bridging by using particles with a particle-to-throat diameter ratio of  $2/3$  in a reservoir.



**FIGURE 4-7** Effects of flow rate on permeability.

by particles with particle-to-throat diameter ratios of  $1/3$ ,  $1/2$ , and  $2/3$ , permeability is measured under different flow rates, and the  $K_i/K_w$  ( $K_w$  is original salt water permeability) vs. flow rate curves are obtained (Figure 4-7). The results indicate that only the bridging particle that meets the principle of particle-to-throat diameter ratio of  $2/3$  is stable.

- (3) Effect of bridging particle concentration. Whether the bridging particle can form bridging and can be stable after bridging also depends greatly on bridging particle concentration. Too low a concentration will form bridging of part of the throats by bridging particles and bridging of other parts of the throats by the particles with particle-to-throat diameter ratio smaller than  $2/3$ , thus leading to a bridging strength too low to meet

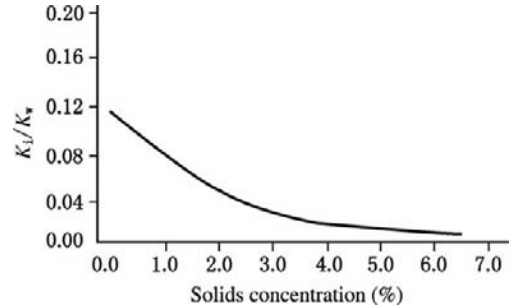


**FIGURE 4-8** Effects of bridging particle concentrations.

the requirements of shield and temporary plugging for pressure-bearing ability and permeability of shield ring. Too high a concentration will cause waste. Figure 4-8 shows the plugging results of bridging agents with different concentrations.

The concentration curve indicates that  $K_i/K_w$  value decreases with the increase in concentration. When the concentration is higher than 2%,  $K_i/K_w$  value is relatively stable. When the concentration is higher than 3%,  $K_i/K_w$  value is basically constant, which indicates that the bridging effectiveness is basically constant. Thus the concentration value of 3% can be taken as critical concentration. Obviously, the critical concentration is related to the development situation of reservoir pores. The larger the porosity, the higher the critical concentration value, or vice versa.

The relation between the bridging depth of plugging particle and the concentration of plugging particle is as follows. In accordance with the single-particle staged plugging model, the plugging depth of the bridging particle decides the plugging depth of fine particles of drilling and completion fluid in the reservoir. Thus the key to meeting the requirement of shallow zone plugging of the shield-type temporary plugging technique lies in the bridging depth of bridging particles. In the

**TABLE 4-2 Physical Properties of Core and Bridging Particle Size and Concentration**

Core No.	Original $K_w$ ( $10^{-3}\mu\text{m}^2$ )	Mean Throat Dia. ( $\mu\text{m}$ )	Solid Particle Dia. ( $\mu\text{m}$ )	Bridging Particle Concentration (%)
M-16	2003.2	6.60	4.0~5.0	2.5
M-60	3738.6	9.41	6.0~7.0	0.5
L-4-22	1516.0	5.30	3.0~4.0	1.5
M-25	1996.5	6.77	4.0~5.0	3.5
M-29	2011.1	7.06	4.0~5.0	5.0

laboratory, the cores are respectively plugged by using the different bridging particle concentrations, and the invasion depths are measured by using the cutting method. The experimental results are shown in Tables 4-2 and 4-3.

It has been proven in practice that the entering depth of the bridging particles is only 2 to 3 cm regardless of particle density.

- (4) Effect of time. In this technique, the duration of the bridging operation is of great significance. A short plugging time can ensure that the plugging is only generated in a shallow zone of the reservoir. The plugging results of different plugging durations are shown in Table 4-4.

The experiments indicate that the bridging effect of bridging particles can be rapidly achieved within 10 minutes.

- b. Study of the packing rule. In accordance with the single-particle staged packing model, the process of fine particle packing by stages will be conducted after bridging of the bridging particles.

As mentioned earlier, bridging by using particles with a particle-to-throat diameter ratio of  $\geq 3$  is characterized by speed, shallow zone, and effectiveness, and this type of particle can be used as the bridging particle of the shield-type temporary plugging technique. Notwithstanding the low  $K_i/K_w$  value after bridging, the throats have not been entirely plugged, and there is a passage through which the fluid enters. In accordance with the plugging mechanism, after bridging by using particles with a particle-to-throat diameter ratio of  $\geq 3$ , the smaller throats should be packed by smaller particles, and so forth. The staged packing will reduce the permeability to the full extent. It would be best if  $K_i \rightarrow 0$ .

- (1) Staged bridging. Select a core. After bridging by using particles with a

**TABLE 4-3 Experimental Results**

Core No.	Section Permeability $K_w$ and $K_i/K_w$		
	Section Length (cm)	$K_i$ ( $10^{-3}\mu\text{m}^2$ )	$K_i/K_w$
M-60	0.0~1.8	19.1	0.051
	1.9~3.7	3540.0	0.95
	3.8~6.6	3740.2	1.00
	6.7~7.5	3742.7	1.00
L-4-22	0.0~1.6	69.5	0.046
	1.7~3.2	1322.6	0.87
	3.3~4.9	1500.8	0.99
	5.0~6.6	1517.2	1.00
M-16	0.0~1.4	76.4	0.038
	1.5~2.8	1707.0	0.85
	2.9~4.3	2011.5	1.0
	4.4~5.8	2010.4	1.0
M-25	0.0~1.9	39.8	0.020
	2.0~3.5	1805.1	0.90
	3.6~5.3	2002.7	1.00
	5.4~7.1	2011.5	1.00
M-29	0.0~2.0	39.1	0.019
	2.1~3.7	1984.0	0.99
	3.8~5.6	2041.0	1.01
	5.7~7.3	2024.8	1.00

TABLE 4-4 Effect of Plugging Time

Core No.	$K_{\infty}$ ( $10^{-3}\mu\text{m}^2$ )	$K_w$ ( $10^{-3}\mu\text{m}^2$ )	$K_1$ ( $10^{-3}\mu\text{m}^2$ )	Temporary Plugging Condition (Dynamic)		
				$\Delta p$ (MPa)	Time (min)	Filtrate (ml)
1-2	63.14	60.40	0.43	3.5	10	1.0
2-3	74.80	50.07	0.48	3.5	30	1.5
3-5	60.55	41.08	0.32	3.5	60	3.3

Note: Temporary plugging liquid: composite clay slurry (3% clay) + 1%QS-2 + 2%HL-2 (QS = superfine  $\text{CaCO}_3$  powder, HL = sulfonated asphalt).

$K_1$ : permeability measured with 1% KCl solution under 0.12 MPa after temporary plugging.

particle-to-throat diameter ratio of  $2/3$ , the core is respectively plugged by particles with ratios of  $1/2$  and  $1/4$ . The experimental results are shown in Figure 4-9 and Table 4-5.

The bridging experiments indicate that  $K_i/K_w$  has been reduced to a value less than 0.1 after bridging by particles with a particle-to-throat diameter ratio of  $2/3$ . Thus this bridging is effective and crucial. The following two packings further reduce permeability respectively, thus indicating their effectiveness and necessity. The flat curve indicates that bridging and packing are stable with no fine particle migration. In addition, the packing particle concentration has no decisive effect, and it is all right so long as packing particles exist. Generally, the packing particle concentration should be lower than 1%.

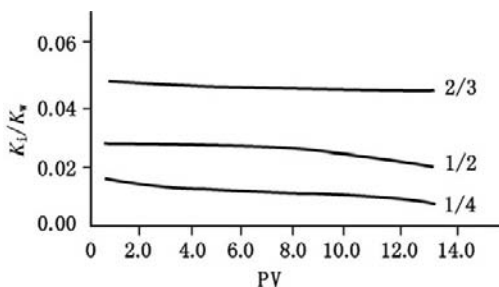


FIGURE 4-9 Experimental studies of the staged packing effect.

Figures 4-3, 4-4, and 4-7 show that if there is no bridging particle, the obvious migration of fine particles with particle-to-throat diameter ratios of  $1/2$  and  $1/3$  will be generated in the core. However, after bridging by the bridging particle, these fine particles cannot move, thus indicating that there are staged packing and plugging effects.

- (2) Plugging effect of mixed particles of different grades. In practice, it is impossible to plug different reservoirs by using particles of different grades. In a drilling and completion fluid system, particles of various particle diameters act simultaneously on reservoir throats. Under the condition of adequate bridging particles, the packing particles are added in a proper proportion to form a shield-type temporary plugging drilling and completion fluid system, thus achieving temporary plugging. The experimental results of the drilling and completion fluid that contains a bridging agent and packing agent are shown in Table 4-6.

The experimental results show that the plugging effectiveness of mixed particles of different grades ( $K_i/K_w = 0.017$ ) and the effectiveness of staged plugging ( $K_i/K_w = 0.010$ ) are about the same. This indicates that this plugging

**TABLE 4-5 Experimental Results of Staged Packing**

PV	4.4	6.1	7.9	10.7	14.5	16.5	Note: Bridging by using $\frac{2}{3}$ particle		
$K_i, 10^{-3} \mu\text{m}^2$	198.2	211.6	211.3	204.3	196.9	169.6			
$K_i/K_w$	0.047	0.050	0.050	0.048	0.047	0.040			
PV	2.4	3.2	4.3	6.9	9.2	11.45	Note: Bridging by using $\frac{1}{2}$ particle after bridging by $\frac{2}{3}$ particle		
$K_i, 10^{-3} \mu\text{m}^2$	100.7	104.0	103.0	100.2	94.4	91.2			
$K_i/K_w$	0.024	0.025	0.024	0.024	0.022	0.022			
PV	0.9	0.7	3.9	5.0	5.9	7.0	7.9	8.8	Note: Bridging by using $\frac{1}{4}$ particle after bridging by $\frac{2}{3}$ particle
$K_i, 10^{-3} \mu\text{m}^2$	52.5	57.4	56.2	54.0	52.6	50.1	49.3	46.9	
$K_i/K_w$	0.012	0.014	0.013	0.013	0.012	0.012	0.012	0.011	

**TABLE 4-6 Plugging Effectiveness of Mixed Particles of Different Grades**

PV	0.0	1.2	3.4	5.7	6.9	8.1	9.7	10.5	12.0
$K_i, 10^{-3} \mu\text{m}^2$	2060.9	36.48	35.27	36.25	35.07	35.85	35.65	35.47	35.55
$K_i/K_w$	1.0	0.018	0.018	0.018	0.018	0.017	0.017	0.017	0.017

model and mechanism are appropriate for drilling and completion fluid.

- (3) Effect of deformable particles. Under the aforementioned conditions, a seriously plugged zone can be formed in a shallow place of the reservoir at the borehole wall, and its permeability can be reduced by 99.9% but cannot be zero, so that the continuous liquid phase invasion cannot be fully arrested, and the requirement conceived by the shield-type temporary plugging technique cannot be met. The plugging model analysis indicates that this plugging cannot achieve zero permeability because there is always a minute throat left to be packed by even smaller fine particles, and this throat is much larger than water molecules despite the fact that it is small. The minute throat should be fully sealed with the aid of the plugging mechanism of deformable fine particles.

After packing the minute throat by highly dispersed fine particles, the

smaller throat has not been fully packed. If the fine particle is rigid, the smaller throat may be conserved unless it is packed with further smaller fine particles. If this fine particle is deformable under pressure difference, it will deform toward the unfilled space. If the size of this space is about the same as the size and deformation of deformable fine particles, this space can be fully plugged by deformation, and there is no smaller throat left over. At this time the plugged zone has zero permeability. In accordance with this mechanism, these deformable particles should meet the following two requirements: First, they can disperse themselves highly into the fine particles of micron grade or even smaller in water; second, they can soften and deform but cannot become fluid at reservoir temperature. The use of this type of particle is closely related to temperature.

Theoretical analysis and experimental studies have proven that the

envisioning of the shield-type temporary plugging technique is feasible. Whether the plugging will meet with success depends first on the ratio of the size of fine particles in drilling and completion fluid to reservoir throat diameter (whether the  $2/3$  principle is met, that is, the bridging particles exist) and the necessary concentration; next, on the existence of packing particles of various grades and the necessary concentration; and then on the existence of soft fine particles and the necessary concentration regardless of the reservoir characteristics and the type of drilling and completion fluid.

Despite the fact that the various types of particles need their lowest concentration, the concentration value is not high (generally 1% to 3%) and is easy to achieve in drilling and completion fluid. Even if the solid particle concentration in drilling and completion fluid is excessive, there is no unfavorable effect.

c. Effects of external environment

- (1) Effect of pressure difference. The pressure difference  $\Delta p$  is an essential condition of forming the shield ring.

Three cores are selected for experiments on the effect of pressure difference on a temporary plugging result. The experimental results are shown in Table 4-7.

The experiments indicate that the greater the pressure difference, the better the plugging effectiveness of the shield ring. In order to ensure the quality of the shield ring, it should be ensured that  $\Delta p \geq 1.0$  MPa. Generally, under the condition of 3.5 MPa, an effective shield ring can be formed. And the technically difficult problems that will be generated during drilling-in under high pressure difference can be solved by using this technique. The

aforementioned plugging mechanism indicates that the plugged zone has a compressibility, and this effect of pressure difference can be considered as an inevitable expression of compressibility of the plugged zone.

- (2) Effect of time. Three cores are selected for experiments on the effect of time on temporary plugging effectiveness (Table 4-8).

The experiments show that this shield ring can be formed within 10 minutes, and there is no obvious effect when time is prolonged. Thus the requirement of a fast-forming shield ring can be met, further formation damage of drilling and completion fluid can be prevented, and the unfavorable effect of soak time can also be eliminated.

- (3) Effect of temperature. The effect of temperature is mainly the effect of temperature on softening and deformation of deformable particles, which this technique includes. The experimental results are shown in Table 4-9.

The experiments indicate that the effect of temperature depends mainly on the softening point of deformable particles. If the temperature is lower than the softening point, plugging effectiveness increases as the temperature increases. If the temperature is higher than the softening point, plugging effectiveness decreases as the temperature increases. Therefore, for different reservoir temperatures, deformable particles with different softening points should be selected.

- (4) Effect of cement slurry after forming a shield ring. The experimental results are shown in Table 4-10.

The experiments show that the reservoir, which has been damaged by drilling and completion fluid, may still be damaged by cement slurry. The formation damage due to cement slurry is

TABLE 4-7 Effect of Pressure Difference on Forming the Shield Ring

Core No.	$K_{\infty}$ ( $10^{-3}\mu\text{m}^2$ )	$\Phi$ (%)	R ( $\mu\text{m}$ )	$K_w$ ( $10^{-3}\mu\text{m}^2$ )	$K_1$ under 0.15 MPa ( $10^{-3}\mu\text{m}^2$ )	$K_2$ under 0.15 MPa ( $10^{-3}\mu\text{m}^2$ )	$K_3$ under 0.15 MPa ( $10^{-3}\mu\text{m}^2$ )	$K_4$ under 0.15 MPa ( $10^{-3}\mu\text{m}^2$ )	Temporary Plugging Condition (Dynamic)		
									$\Delta p$ (MPa)	Time (min)	Filtrate (ml)
3-2	307.19	33.07	2.3	228.05	6.35				1.0	10	1.2
8-1	316.87	33.15	2.4	252.09	0.94	0.88		0.67	3.0	10	1.2
5-2	310.93	32.80	2.3	238.16	0.86	0.75	0.51	0.43	3.50	10	1.2

Note: R is mean pore throat radius obtained by calculating. Temporary plugging liquid: composite clay slurry (3% clay) + 1%QS-2 + 2%HL-2 (QS = superfine  $\text{CaCO}_3$  powder, HL = sulfonated asphalt).  $K_1$ ,  $K_2$ ,  $K_3$ , and  $K_4$  are permeabilities measured with 1% KCl solution after temporary plugging.

TABLE 4-8 Effect of Time on Temporary Plugging Effectiveness

Core No.	$K_{\infty}$ ( $10^{-3}\mu\text{m}^2$ )	$\Phi$ (%)	R ( $\mu\text{m}$ )	Temporary Plugging Condition (Dynamic)				
				$K_w$ ( $10^{-3}\mu\text{m}^2$ )	$K_1$ ( $10^{-3}\mu\text{m}^2$ )	$\Delta p$ (MPa)	Time (min)	Filtrate (ml)
8-1	316.87	33.15	2.4	252.09	0.94	3.0	10	1.2
8-2	519.39	34.56	2.9	442.68	0.87	3.0	30	2
8-3	451.92	34.23	2.8	337.86	0.93	3.0	60	3

Note: Temporary plugging liquid: composite clay slurry (3% clay) + 1%QS-2 + 2%HL-2.  $K_1$ : permeability measured with 1% KCl solution under 0.15 MPa after temporary plugging.

TABLE 4-9 Effect of Temperature on Shield Ring

Temperature	$K_i$ after Plugging ( $\mu\text{m}^2$ )	$K_i/K_o$
15	12.98	0.015
32	9.01	0.1
45	4.93	0.0057
50	0.64	0.00074
60	2.34	0.0027

Note: Core permeability  $K_o = 865.29 \mu\text{m}^2$ ,  $\Phi = 37.77\%$ ,  $R = 6.44 \mu\text{m}$ , injected volume = 1050 ml.  
Particle system: D (diameter) = 1.0–8.0  $\mu\text{m}$ , concentration = 4.1%, soft particle content = 1%, softening point of soft particle = 52°C.

generally added to the formation damage by 20% to 40% or above. However, the reservoir that is protected by using the shield-type temporary plugging technique with an ideal result is only damaged by cement slurry within a damage depth range of 2–3 cm, thus indicating that the components of cement slurry cannot pass through the shield ring, and formation damage due to cement slurry can be effectively prevented.

- (5) Flowback effect under underbalance pressure. For the shield ring formed under overbalance pressure, the greater the overbalance pressure, the better the effectiveness. Under an underbalance pressure, a backflow may be generated,

the shield ring may be broken, and the permeability can be recovered with a recovery rate of 70% to 80% or higher depending on plugging depth (Table 4-11), thus indicating that the plugging of the shield ring, which is formed under overbalance pressure, may be removed by flowback under an underbalance pressure. Therefore, an underbalance pressure should be strictly prevented from generating in the process of using the shield-type temporary plugging technique, whereas the removal of plugging by flowback can be adopted if necessary.

### Reservoir Protecting Shield-Type Temporary Plugging Technique Program and Application Results

The feasibility of the shield-type temporary plugging technique has been proven, and the following technical program for performing this technique has been obtained on the basis of the study results:

1. Measuring the reservoir throat distribution curve and mean throat diameter  $D_t$  by using the mercury injection method or other method that can be used for measuring the reservoir throat diameter.
2. Measuring the solid particle grade distribution of drilling fluid by using a hondrometer or the settling analysis method, and measuring the solids content of various grades and total solids content.

TABLE 4-10 Results of Dynamic Experiment of Formation Damage by Cement Slurry after Forming the Shield Ring

Core No.	$K_{\infty}$ ( $10^{-3}\mu\text{m}^2$ )	$K_{w1}$ ( $10^{-3}\mu\text{m}^2$ )	$K_{w2}$ ( $10^{-3}\mu\text{m}^2$ )	Length of Section (cm)	K ( $10^{-3}\mu\text{m}^2$ )	Temporary Plugging				System
						$\Delta p$ (MPa)	Shear Rate ( $\text{s}^{-1}$ )	Time (min)	Filtrate (ml)	
143	1265.38	410.84	0	2.02	406.72	3.5	180	1	0.9	1. Raw mud + 2%QS-1 + 2%QS-2 + 2% 250 mesh CaCO <sub>3</sub> + 1.5% 320 mesh CaCO <sub>3</sub> ; 2. Cement slurry
70	119.95	57.17	0	1.96	56.35	3.5	100	1	0.4	

TABLE 4-11 Permeability Recovery by Flowback

Core No.	$K_{\infty}$ ( $10^{-3}\mu\text{m}^2$ )	$\Phi$ (%)	R ( $\mu\text{m}$ )	$K_w$ ( $10^{-3}\mu\text{m}^2$ )	$K_1$ ( $10^{-3}\mu\text{m}^2$ )	Flowback Pressure (MPa)	$K_2$ ( $10^{-3}\mu\text{m}^2$ )	Recovery Rate (%)	Temporary Plug Condition (Dynamic)		
									$\Delta p$ (MPa)	Time (min)	Filtrate (ml)
8-3	519.39	34.57	2.9	442.68	0.87	0.295	427.33	96.6	3.0	30	2.0
8-2	310.93	32.8	2.3	238.16	0.86	0.713	227.39	99.9	1.0	10	1.2

Note: Temporary plugging liquid: composite clay slurry (3% clay) + 1%QS-2 + 2%HL-2.

$K_1$ : permeability measured with 1% KCl solution under 0.15 MPa after temporary plugging.

$K_2$ : permeability measured with distilled water after flowback.

3. Ensuring that particles with a median particle diameter of  $(\frac{1}{2} \text{ to } \frac{2}{3}) D_t$  in drilling and completion fluid account for 2% to 3% (weight percent) of drilling and completion fluid.
4. Ensuring that the content of particles of various grades smaller than bridging particles in drilling and completion fluid is 1% to 2% (weight percent).
5. Adding deformable fine particles (such as sulfonated asphalt with a higher degree of sulfonation and deformable resin) by 1% (weight percent). The softening point of the deformable fine particle to be used should be adaptable to reservoir temperature.
 

After completing these five steps, determine the program of drilling fluid reformation for the shield-type temporary plugging technique.
6. System evaluation. The modified drilling and completion fluid that has been determined is evaluated as follows.
  - a. Plugging rate of shield. Zero permeability after plugging is required. No fine particle migration and no fluid loss.
  - b. Plugging depth. A plugging depth less than 3 cm is required.
  - c. Plugging time. Plugging time less than 10 minutes is required.
  - d. Effect of  $\Delta p$ . The greater the  $\Delta p$ , the better the effectiveness. A minimum effective pressure difference of less than 3.0 MPa is required.
  - e. Effect of temperature. No unfavorable effect under reservoir temperature.
  - f. Effect of annular return velocity. The higher the return velocity, the better the effectiveness. An effective shield ring should be formed under the condition of drill collar annulus return velocity.
  - g. Further formation damage by cement slurry. It is required that there is no formation damage by cement slurry after the shield ring is formed.
  - h. Flowback effectiveness. The permeability is required to be recovered to 70% to 80% by flowback.
7. Optimizing the matching perforating technique.
  - a. The underbalanced and deep penetrating perforating is required. The shield zone should be perforated and penetrated through in order to remove the plugging.
  - b. Optimizing the perforating parameters in order to reduce the skin factor to the full extent.
  - c. Perforating fluid compatible with the reservoir is adopted.
 

This technique has been widely applied in onshore and offshore oil fields. The statistical data indicate that more than 10,000 wells adopted this technique by the end of 1998, and obvious results have been obtained. This technique has been used in 60 wells in the Xinjiang Xiazijie oil field, and the individual-well production rate has increased by 45% in comparison with that of wells that have not used this technique. The wells of the low-permeability reservoir of the Tuha Wenmi oil field should be stimulated by using hydraulic fracturing before putting well into production. After drilling-in by using the shield-type temporary plugging technique and perforating, all the 167 wells are flowing, and the individual-well production rate is increased by 20% to 30% in comparison with the designed value.

### Development of Shield-Type Temporary Plugging Technique

The shield-type temporary plugging technique has spread rapidly and become the first choice of reservoir protection technique during drilling and completion due to its good effectiveness. With the increase of technical requirements and the accumulation of practical experience, the research on this technique has been continued, and a signal advance has been made.

#### New Theory and Method of Optimizing Temporary Plugging Agent Particle Size Distribution in Drilling and Completion Fluid.

Research on solid particle selecting and matching and the plugging mechanism in the shield-type temporary plugging technique, especially the Ideal Packing Theory and the  $d_{90}$  rule, have made significant advances.

The Ideal Packing Theory means that in accordance with the reservoir throat size distribution, the corresponding temporary plugging agent particles with continuous particle diameter series distribution are added to the drilling and completion fluid in order to achieve effective bridging in the reservoir throats of various sizes and packing by stages, thus forming a shield ring. On condition that a rational particle diameter series distribution is formed, the formation of a tight cake with a very low permeability can be ensured.

Under normal conditions, the relation between the particle diameter and the cumulative particle volume percentage of a temporary plugging agent in drilling fluid is presented by an S-shaped curve (Figure 4-10). This curve shows the particle diameter distribution range. Kaeuffer applied the research results in the coating industry to the petroleum industry and presented the Ideal Packing Theory or the  $d^{1/2}$  theory<sup>[10]</sup> about temporary plugging agent particles. He supposed that the temporary plugging agent particle distribution accords with the Schuhmann particle size distribution model and observed that the packing efficiency under the model parameter  $n=0.5$  is the highest on the basis of the physical experiments and the computer modeling calculation. It is indicated that the ideal packing of particles can be achieved

when the cumulative particle volume percentage of the temporary plugging agent is directly proportional to the square root of the particle diameter (that is,  $d^{1/2}$ ). In accordance with this theory, if there is a linear relation between the cumulative particle volume percentage of the temporary plugging agent and the  $d^{1/2}$  in the rectangular coordinate system, it is indicated that this temporary plugging agent can meet the necessary condition of ideal packing. The cumulative particle size distribution curves of  $\text{CaCO}_3$  particles (temporary plugging agent) of the four specifications are shown in Figure 4-11. It can be seen that the four curves are close to straight lines within most of the distribution region of each curve. Thus the four specifications of product can all meet the use requirements.

Hands et al. have further presented the  $d_{90}$  rule, which is convenient to perform on site, on the basis of the theory of ideal packing. On condition that the particle diameter distribution of solid particles contained in the drilling fluid system is in accord with normal distribution, when the  $d_{90}$  rule of temporary plugging agent particles (taking effect) on the cumulative particle diameter distribution curve (the particle diameters of 90% particles are lower than this value) is equal to the maximum reservoir throat diameter or the maximum fracture width, an ideal temporary plugging effectiveness can be obtained<sup>[8]</sup>.

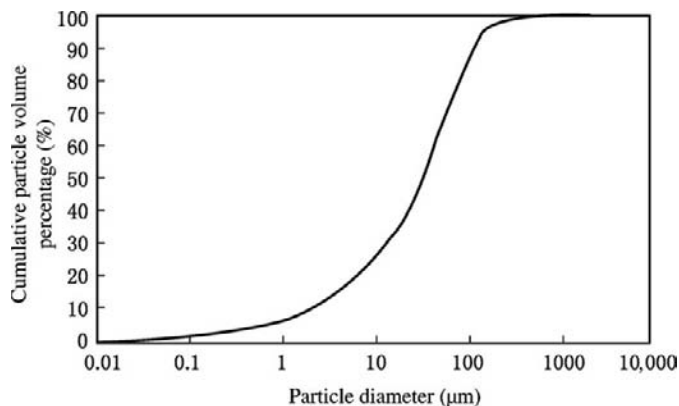


**FIGURE 4-10** The conventional  $\text{CaCO}_3$  particle (temporary plugging agent) size distribution curve of drilling fluid.

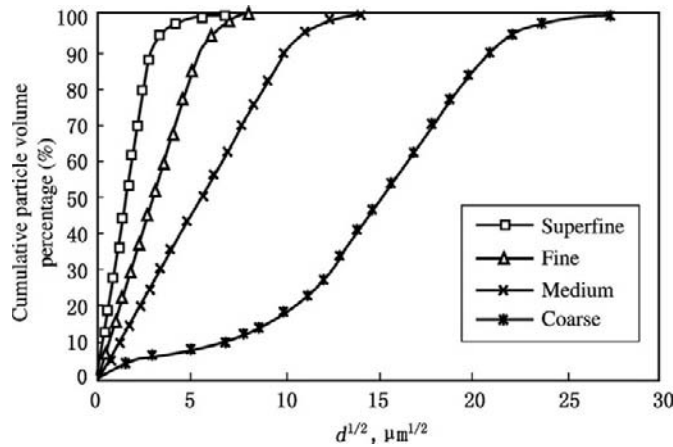


FIGURE 4-11  $\text{CaCO}_3$  particle (temporary plugging agent) size distribution curves of various particle diameters.

The graphical optimization method of temporary plugging agent particle size on the basis of the  $d_{90}$  rule is as follows.

1. Some representative core samples are selected for cast thin section analysis or mercury injection experiment, and the maximum reservoir throat diameter (that is,  $d_{90}$ ) is measured. The  $d_{90}$  rule can also be read out on the cumulative throat size distribution curve.
2. On the cumulative particle volume percentage of temporary plugging agent particles vs.  $\sqrt{d}$  coordinate diagram, the connecting line to the origin is taken as the baseline. For instance, if the maximum throat diameter of a reservoir is  $133 \mu\text{m}$ ,  $\sqrt{d_{90}} = 11.53 \mu\text{m}$ , thus the baseline can be drawn (Figure 4-12). The closer to baseline the optimized cumulative particle diameter distribution curve of temporary plugging agent particles, the higher the packing efficiency of the particles, and the better the temporary plugging effectiveness of formed cake.
3. If the maximum throat diameter cannot be obtained (such as for an exploration well), it can be estimated by using the upper limit value of reservoir permeability, that is:  $(K_{\text{max}})^{1/2} \approx d_{90}$ . If the mean reservoir permeability is given, the  $d_{50}$  is first determined, that is,  $(K_{\text{mean}})^{1/2} \approx d_{50}$ . Then the connecting

line between the point of  $(d_{50})^{1/2}$  and the coordinate origin is extended, and the  $d_{90}$  can be obtained by extrapolation.

Figure 4-12 indicates that with a single temporary plugging agent with some particle distribution characteristics, it is difficult to match the objective line. However, the cumulative particle diameter distribution curve can be basically coincided with the baseline by mixing the temporary plugging particles with two or more than two different particle size distributions in a certain proportion, thus obtaining the ideal temporary plugging program. Experience indicates that because of the shear wear of a temporary plugging agent in annulus, the optimum particle size distribution curve of the compounded temporary plugging agent should be to the right slightly (rather right than to the left). During drilling, the particle size distribution curve of solid particles in drilling fluid may gradually shift to the left. When it is found to be moved over to the left side of the baseline, temporary plugging agent particles of large size should be appropriately added for adjustment.

In order to make the new method more practical, a set of software for optimizing the temporary plugging agent particle size distribution has been developed, and a related database has been established. The field tests have proven that

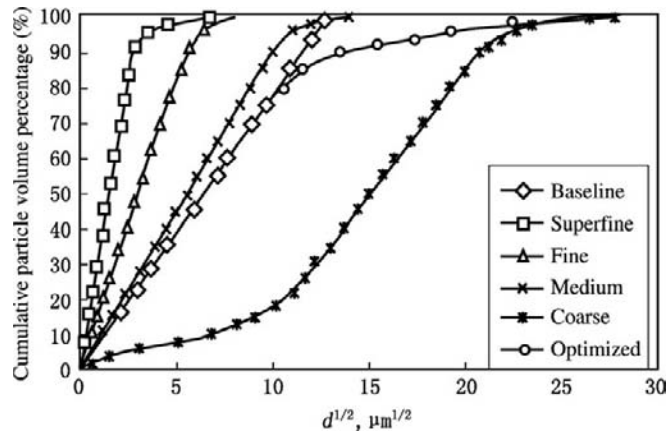


**FIGURE 4-12** Ideal particle size distribution of temporary plugging agent particles in drilling and completion fluid for a reservoir with a maximum throat diameter of 133  $\mu\text{m}$ .

better results can be obtained by using the shield-type temporary plugging technique under the  $d_{90}$  rule.

**Drilling and Completion Fluid for Protecting a Fractured Reservoir.** Formation damage of a fractured reservoir due to drilling and completion fluid will occur after the drilling and completion fluid enters the fracture. In comparison with pore, the fracture can be easy for drilling and completion fluid to enter, and it can be plugged by the solid particles more seriously. Therefore, using solid particles in drilling and completion fluid for effectively plugging the fracture to prevent drilling and completion fluid from going deeper into the fracture is possible, and applying the shield-type temporary plugging technique to a fractured reservoir is feasible. This has been proven in practice.

The bridging particles and bridging process of the shield-type temporary plugging technique that is suitable for a fractured reservoir are different from that for a porous reservoir and are as follows.

1. Irregular particulate material as bridging particle. When the maximum particle size of an irregular solid particle is equal to the narrow seam size in a fracture, the particle may be stuck at the narrow seam, and bridging may be generated. Because the fracture is only sealed by two

faces, the possibility of particles getting stuck in the fracture is much lower than that in pores. Thus the bridging particle to narrow seam size ratio of a fractured reservoir is higher than that of a porous reservoir. The experiments indicate that only when the particle diameter is slightly smaller than the fracture width (about equal to fracture width) can the effective bridging be generated. There are many narrow seams with different widths in a fracture due to the very rough fracture surface. When entering the fracture, this type of particle can bridge the narrow seams. After a large number of bridging particles bridge the narrow seams, the fracture is changed into pores, and the plugging mechanism is similar to that of a porous reservoir.

2. Fibrous material as bridging particle. Special fiber that can be highly dispersed in drilling and completion fluid is used. More than several dozen pieces of fine fiber cross mutually and form flocculated glomerate, which is easily deposited on the fracture surface. This depositing is not a single-point contact, but a multi-point contact, thus forming a reliable bridge and taking a gridding effect. Then the other solid particles in drilling and completion fluid deposit on it. Finally, a very low permeability plugging layer is formed. Furthermore, this type of flocculated glomerate can deform under

pressure difference, enter the fracture, and reach the narrow seam to bridge. In addition, it can pack a fracture of any shape. In comparison with the irregular particulate material, the fibrous material can take plugging effect more effectively.

To sum up, both types of bridging particles can achieve good effectiveness, and the difference is that the fibrous bridging particle is only applicable to fractured reservoirs.

#### **4.4 DRILLING AND COMPLETION FLUID FOR A COMPLICATED RESERVOIR**

The peculiarity of the drilling and completion fluid technique for drilling-in complicated reservoirs is reflected in the following two aspects: first, it should deal with complicated problems for safe and normal drilling (such as lost circulation, blowout, borehole sloughing, and drillpipe sticking) and meet the higher requirements of special drilling technology; second, sensitive reservoir protection problems will further increase the degree of difficulty technically. The complicated drilling problems mingled with reservoir protection problems will become more complicated. Practical experience indicates that the drilling and completion fluid for complicated geological conditions is mostly the modified drilling and completion fluid.

##### **Drilling and Completion Fluid for Wells Prone to Lost Circulation and Borehole Sloughing**

During drilling-in, the drilling and completion fluid should be able to prevent sloughing, lost circulation, blowout, and then formation damage. Thus, the following are required:

1. Determining the rational drilling and completion fluid density. Under this density, the downhole pressure should be able to exceed the lateral stress that causes mechanical instability of the borehole wall (that is, sloughing stress) and should be lower than the formation

breakdown pressure, and the rational rheological property of drilling and completion fluid and the rational drilling parameters (including hydraulic parameters, bottomhole assembly, and tripping speed) should be ensured in order to prevent sloughing and lost circulation due to swabbing and pressure surge.

2. Enhancing the inhibiting ability of drilling and completion fluid. It is required by stabilizing the borehole wall and protecting the sensitive reservoir. The inorganic salt (especially salts that contain  $K^+$ ,  $NH_4^+$ , or  $Ca^{2+}$ ), high molecular polymer (such as non-ionic polymer, cationic polymer, and amphoteric polymer), inorganic polymer, mixed metal hydroxide (MMH), and so on may be used. There are fewer measures for meeting both borehole wall stability and reservoir protection. These two aspects should be considered when the drilling and completion fluid is evaluated and selected.
3. Enhancing wall-building ability and plugging ability. The optimum method is selected for borehole wall stability and reservoir protection in accordance with the reservoir characteristics. The formation breakdown pressure can be increased by using the shield-type temporary plugging technique, thus reducing the possibility of lost circulation.
4. If the reservoir is a lost-circulation zone, the lost circulation problem should be solved first, and then the shield-type temporary plugging is applied. The lost circulation problem and the shield-type temporary plugging are best considered together.
5. Adopting appropriate drilling technology. The modified drilling and completion fluid and the shield-type temporary plugging technique are generally adopted when this type of reservoir is drilled in.

##### **Drilling and Completion Fluid for Adjustment Wells**

The balanced state of the reservoir that will be drilled in by an adjustment well has been upset. As a result, the corresponding measures should

be taken in the light of drilling or reservoir protection.

In general, there are two kinds of cases. First, an oil field is developed by waterflooding, and a flood effectiveness is generated in some single zone that has a pressure much higher than other zones. During the drilling of an adjustment well, lost circulation may be generated if drilling and completion fluid density is too high, and well kick or blowout may be generated if drilling and completion fluid density is too low. Second, an oil field is developed by dissolved gas drive or multiple huff and puff, and the reservoir pressure has been greatly reduced. During the drilling of an adjustment well, the drilling and completion fluid may be lost to a large extent.

In the first case, if the high-pressure zone is at the top, this zone can be suppressed by using high-density drilling and completion fluid, and then the low-pressure zone is plugged, or the shielding and temporary plugging agent is added until the low-pressure zone can bear the liquid column pressure of high-density drilling fluid with no fluid loss. Thus all the reservoirs in the well can be drilled through. If the low-pressure zone is at the top, it can be plugged first, or the shielding and temporary plugging agent is added, the drilling and completion fluid density is gradually increased, and the high-pressure zone is drilled in. In the second case, the shielding and temporary plugging drilling and completion fluid can be used for drilling through the whole section. If there is a high-pressure zone in a thin interbed of a low-pressure zone, a method similar to that in the first case can be adopted.

### **Drilling and Completion Fluid for Deep and Ultra-Deep Wells**

The most important feature of deep and ultra-deep well drilling and completion fluid is that it is used under high-temperature and high-pressure conditions. Drilling and completion fluid with high density (up to  $2.00 \text{ g/cm}^3$  or above) may generate a high overbalance pressure

on the reservoir. The effect of high temperature should first be considered during deep and ultra-deep well drilling. The drilling and completion fluid properties may be changed and damaged under high-temperature conditions.

The complex effect of high temperature makes the downhole high-temperature properties and thermal stability of deep and ultra-deep well drilling and completion fluid very complicated, and a special evaluation method and special temperature-resistant treating agent are needed, thus forming a special technique. Some special completion fluids, such as gas-based completion fluid, clean salt water, and clay-free salt water systems with solids, are inappropriate for high-temperature conditions, and the modified drilling fluid is used instead as the completion fluid. The high temperature, high pressure, high overbalance pressure, and long soak time of a deep well will provide favorable conditions for using the shield-type temporary plugging technique, which needs packing particles that enable generating deformation under high temperature ( $150\text{--}180^\circ\text{C}$ ). The temporary plugging effectiveness under high temperature and overbalance pressure of a deep well should be evaluated in order to apply this technique in practice.

### **Drilling and Completion Fluid for Directional and Horizontal Wells**

During drilling-in the reservoir in a directional or horizontal well, the three difficult technical problems of drilling and completion fluid, including the cuttings-carrying problem (also vertical sinking), borehole stability of the high-angle section and the horizontal section, and friction resistance reducing, should be solved and have been described in the relevant content. The following section only discusses the reservoir protection problem during normal drilling of directional and horizontal wells. The formation damage mechanism of directional and horizontal well drilling is similar to that of straight well drilling, but its evaluation method is different from that of vertical well drilling because

permeabilities in three directions should be considered under the conditions of horizontal well drilling. In addition, the features of formation damage of directional well drilling (especially horizontal well drilling) also include the following in comparison with that of straight well drilling:

1. The area of contact between the reservoir and the drilling fluid is much greater than that of a straight well, and the formation damage may be greater, thus making reservoir protection more difficult.
2. Long soak time of the reservoir. The drilling time of a horizontal well is generally longer than that of a straight well, the duration from drilling-in target to finishing drilling is longer, the range of formation damage is larger, and the radius of formation damage zone is greater (especially for the initial horizontal section).
3. Great pressure difference. During horizontal drilling, with the increase in length of the horizontal section, an additional flow pressure acts on the reservoir, thus gradually increasing the pressure difference.
4. Obvious anisotropy of formation damage. The degree of damage below the borehole is higher than that on both sides of the borehole and that above the borehole due to the action of the drilling tool on borehole wall rock.
5. The plugging removal effectiveness of natural flowback under a certain pressure difference is lower than that of a straight well, and supplementary cake removal methods, such as acid wash, oxidative plugging removal, biological plugging removal, and complex plugging removal, are needed.

### Drilling and Completion Fluid for Tight Sand Gas Reservoir Protection

The drilling and completion technique for gas reservoir protection is similar to that for oil reservoir protection and also has its peculiarity, which is particularly conspicuous in the tight sand gas

reservoir exploration and development. China is a country rich in natural gas resources, and the natural gas resources of tight gas sand account for more than 40%. Tight sand gas reservoir development is an important component part of the natural gas industry (the techniques in this area have been rapidly developed in the United States and Canada), and the tight sand gas reservoir-protecting drilling and completion fluid technique is an essential component part of these techniques. Because the potential formation damage problem of a tight sand gas reservoir is more conspicuous and representative, its settlement is of great theoretical and practical significance for the development of the natural gas industry.

**Features of Formation Damage of Tight Sand Gas Reservoir.** Low-porosity tight gas sand may be under normal pressure or overpressured, and fractures develop. This special pore-fracture configuration and the resulting percolation property aggravate formation damage, and the reservoir is easily affected by external factors. The clay content in tight sand and its distribution in fracture may increase sensitivity to external factors, thus increasing the degree of difficulty of gas reservoir protection.

#### 1. Stress sensitivity and fracture closure

Stress sensitivity means that the reservoir permeability will decrease as the effective stress increases, and formation damage will be caused. The stress sensitivity of a gas reservoir is much more obvious than that of an oil reservoir due to gas compressibility. In the reservoir in which fractures develop, the closing tendency of fracture will be generated under the increased effective stress, thus further aggravating the stress sensitivity. The stress sensitivity of tight sand includes the stress sensitivity of matrix and the stress sensitivity of fracture. Generally, the former is weak while the latter is strong. In practice, the latter is mainly considered. In engineering, the stress sensitivity includes the difference between the measured values of the physical properties of reservoir under

conventional conditions and the physical properties of the reservoir under original reservoir conditions; and the changes in the physical properties of the reservoir, which are induced by the change in effective stress due to various engineering operations under downhole conditions.

On condition that the throat that connects fractures is a slender slit with a width less than 1  $\mu\text{m}$ , and the borehole is communicated with the fracture of the reservoir, when the recovery rate of the gas reservoir is too high or blowout occurs, the pressure difference in the vicinity of the gas reservoir is increased, the effective stress is rapidly increased, the microfractures and slim throats are closed, and the flow conductivity is reduced due to the low reservoir permeability and insufficient gas delivery, thus rapidly causing a low or even zero production rate after a high-yield period or blowout. This is a typical characteristic of a stress-sensitive gas reservoir.

In addition, if there is a mud shale interbed between gas reservoirs, it will be hydrated by the drilling and completion fluid filtrate and will be swelled. The swelling pressure will act on the gas reservoir and increase the effective stress on the gas reservoir, thus causing the fracture of the gas reservoir to close and generating a special formation damage of the gas reservoir.

Too high drilling and completion fluid density may open the fracture to a great extent. If the drilling and completion fluid does not possess an effective plugging ability,

the solid particles and liquid phase of drilling and completion fluid will drive straight in along the fracture, thus causing deep formation damage of the gas reservoir.

- Measures for putting into production should be combined with reservoir protection techniques of drilling and completion.

Many Chinese tight sand gas reservoirs have the common features of continental clastic rock reservoir and engineering geological characteristics, including low porosity and low permeability, fracture, locally ultra-low water saturation, high capillary pressure, abnormal formation pressure, and high formation damage potential. Moreover, in tight sand reservoirs there are very small throats and clay minerals, which are well developed and can easily cause formation damage, including mainly water-sensitive, alkali-sensitive, water phase trap, and stress-sensitive damage. In addition, there is also serious leakage damage in deep fractured tight sand. The related studies and practice indicate that for the tight sand gas reservoir, rational reservoir-protecting measures taken during drilling and completion will greatly favor the effectiveness of stimulation for putting the well into production (Table 4-12).

This is decided by the features of this type of reservoir. For a common porous sandstone, the effects of rate sensitivity, water sensitivity, acid sensitivity, alkali sensitivity, salt sensitivity, water blocking, and so on are themselves

**TABLE 4-12 Reservoir Protection Measures in Tabamao Area since 2002 and Testing Results after Fracturing**

Well No.	Horizon	Open Flow Potential ( $10^4\text{m}^3/\text{d}$ )	Reservoir-Protecting Measure	Hydraulic Fracturing Technique
D7	He 3 member	3.1658	Non-shielding temporary plugging	Sandfrac + liquid nitrogen
D10	He 3 member	4.0350	Initial insertion	Sandfrac + liquid nitrogen
D15	He 3 member	21.0800	Shield-type temporary plugging	Sandfrac + liquid nitrogen
DK2	He 3 member	38.8700	Shield-type temporary plugging	Sandfrac + liquid nitrogen
DK3	He 3 member	13.0000	Shield-type temporary plugging	Sandfrac + liquid nitrogen
DK4	He 3 member	20.3000	Shield-type temporary plugging	Sandfrac + liquid nitrogen
D16	He 3 member	16.4400	Shield-type temporary plugging	Sandfrac + liquid nitrogen

independent of each other. For a fractured carbonatite reservoir, as a result of relatively single sensitive mineral in the throat of the matrix and its lower content, it is traditionally considered that there is no sensitive damage in the matrix, and the formation damage is mainly generated by fracture. However, the conditions are different for tight sand. The various factors of formation damage in the matrix also exist in fracture of tight sand. The composite effects of these factors will complicate the integral damage mechanism of a tight gas reservoir. The damage of drilling and completion fluid to the fracture system will not only cause various types of damage to matrix but also lead the damage into the deep reservoirs (Figure 4-13). Table 4-13 is a conclusion of the damage mechanism of a tight sand reservoir. It should

be noted that the application of the shield-type temporary plugging technique of drilling and completion fluid in the tight sand gas reservoir not only has common merits but also can effectively control the generation of capillary absorption. The shield ring with zero permeability takes a key effect. Therefore, tight sand gas reservoir-protecting measures should be taken during drilling and completion regardless of the stimulation measures before putting the well into production.

**Completion Fluid for Protecting a Tight Sand Gas Reservoir.** In addition to the general requirements for drilling and completion fluid, which should be met, the following points should be noted:

1. Enhancing inhibition of clay hydration caused by completion fluid

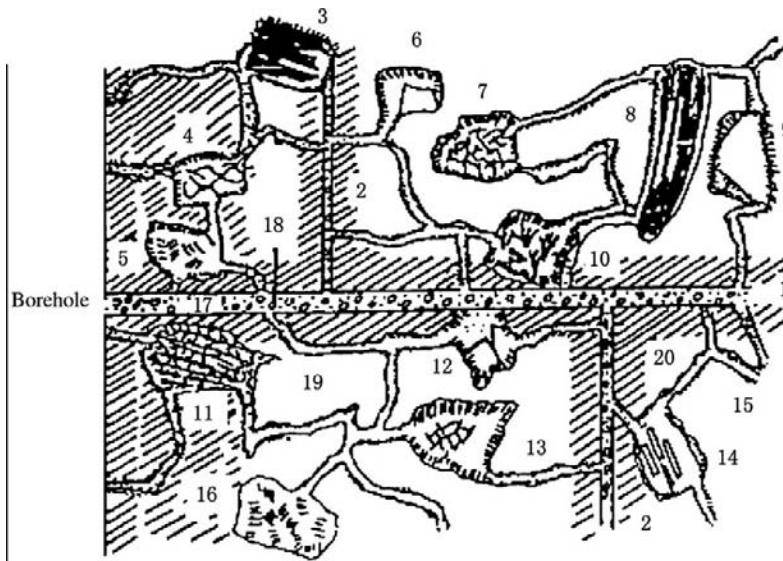


**FIGURE 4-13** Two-dimensional model of storage and percolation media and damage mechanism of tight sand. 1, horizontal principal fracture, unpacked; 2, vertical fracture, open; 3, arkosic dissolved pore; 4, illite and illite-montmorillonite interstratified clay packing in diminutive intergranular pore; 5, kaolin packing in diminutive intergranular pore; 6, quartz plus chlorite coat packing remaining intergranular pore; 7, chlorite packing in intergranular pore; 8, biotite dissolution pore, end face scattering; 9, mold pore, chlorite coat reserved; 10, petal chlorite; 11, intra-cuttings micropore; 12, authigenous quartz packing remaining intergranular pore; 13, remaining intergranular pore, only chlorite on pore wall, illite-montmorillonite interstratification packing at center of pore; 14, arkosic dissolved pore, authigenous feldspar formed in it; 15, throat, chlorite as lining; 16, kaolin packing in arkosic dissolved pore; 17, microfracture, slightly larger than throat; 18, solids that invade fracture; 19, liquid phase that invades through throat; 20, liquid phase that invades through fracture.

TABLE 4-13 Formation Damage Mechanism of Tight Sand Gas Reservoir

Type of Damage	Reason for and Process of Damage	Operation	Precautions and Treatment
Liquid phase trap (liquid blocking)	Water saturation is increased. Capillary percolation (overbalance pressure) Imbibition Displacement leakage	Drilling by using water-based drilling and completion fluid. Cementing Perforating Underbalanced drilling by using water-based working fluid Fracturing, acidizing, workover	Avoiding using water-based working fluid Reducing pressure difference Forming cake with zero permeability Reducing capillary pressure Gas injection Heat treatment Fracturing (N <sub>2</sub> , CO <sub>2</sub> )
	Oil saturation is increased. Capillary percolation Condensation	Drilling by using oil-based drilling fluid Too low flowing pressure during production	Avoiding using oil-based working fluid Controlling pressure difference Gas injection Heat treatment Fracturing
Solids invasion	Particles are deposited in throat of matrix. Particles are deposited in fracture. Packing in fracture Cake in fracture face	Drilling (overbalance pressure, pulsing underbalance pressure) Cementing Well completion (openhole completion) Fracturing Acidizing Well killing Workover, well cleanout	Forming cake with zero permeability Underbalanced drilling Fluid to be used in well should be strictly filtrated Deep penetrating perforating Fracturing, acidizing Heat treatment Ultrasonic treatment
Formation damage of clay minerals	Action of foreign fluid on rock. Alkali sensitivity (pH=9) Water sensitivity Salt sensitivity Rate sensitivity Action of formation fluid on rock. Rate sensitivity	Drilling Cementing Well completion Acidizing Fracturing Well killing Workover, well cleanout Production	Forming cake with zero permeability Underbalanced drilling Potential damage evaluation Adding clay stabilizing agent Reducing pH value Reducing flow rate (using horizontal well) Stable pressure difference, reducing surge Production under flow rate lower than critical flow rate
Chemical adsorption	High-molecular polymer adsorption and retained oil wetting surfactant adsorption Throat surface Fracture face (wall) Emulsification	Drilling Well completion Well killing Fracturing Workover, well cleanout	Laboratory evaluation Gas-based fracturing fluid Using oxidizing agent (enzyme) Microbial degradation polymer

TABLE 4-13 Formation Damage Mechanism of Tight Sand Gas Reservoir—cont'd

Type of Damage	Reason for and Process of Damage	Operation	Precautions and Treatment
Stress sensitivity	Change in throat size of matrix Change in fracture width (open, close)	Overbalanced drilling (lost circulation) Underbalanced drilling Long cemented section cementing Perforating Production	Forming cake with zero permeability Controlling rational pressure difference Horizontal well Inhibiting hydration swell of mud shale of adjacent bed Optimizing perforating parameters
Inorganic scale deposition	Action of foreign fluid on formation fluid. Inorganic salt and water $\text{BaSO}_4$ , $\text{CaCO}_3 \cdot 2\text{H}_2\text{O}$ , $\text{CaCO}_3$ Environmental change of formation fluid Inorganic salt, $\text{CaCO}_3$	Drilling Cementing Well killing Workover, well cleanout Production	Fluid compatibility test Controlling rational pressure difference Prolonging water breakthrough time Using anti-scaling agent Mechanical and chemical scale removed Fracturing, acidizing
Rock face glazing	Tight porcelain layer is formed by rock powder and water under the action of drill bit and drill pipe (high temperature). Plugging throat Plugging fracture	Gas drilling Openhole completion Horizontal well	Increasing lubricity and heat transfer capacity Mist drilling fluid Perforating Cave-in stress completion

This inhibition aims to avoid the formation damage that may be caused by water-, salt-, and alkali-sensitive clay minerals, and so on in the reservoir and aims to avoid the interbedded mud shale hydration and swell, which may generate additional effective stress on the gas reservoir. Thus inorganic salt such as salts that contain  $\text{K}^+$  and  $\text{Ca}^{++}$  and mixed metal hydroxide (MMH) and the inhibitive polymer should be added to the completion fluid, and experimental studies of the inhibition evaluation of interbedded mud shale should be conducted.

2. Particular attention to avoiding water absorption of microfracture

The pore and fracture surfaces of a tight gas reservoir are generally water-wet, and

the water in water-based completion fluid may be automatically absorbed by the surface even if it is under an underbalance pressure. The smaller the fracture width and the lower the original water saturation of the reservoir, the greater the water absorption ability and volume. The water that enters the reservoir is more difficult to displace. For instance, it can be displaced through the throat with a radius of  $0.075 \mu\text{m}$  only under a pressure drop greater than  $\Phi 10 \text{ MPa}$ . The absorption of volumes of water may greatly reduce gas permeability, thus causing reduction of gas well productivity and the gas reservoir gas recovery factor. The peculiar water-phase trap damage of this type of gas reservoir may extend through fracture to deep reservoirs (up to a

depth of several meters or more). The damage results are beyond imagination.

3. Shield-type temporary plugging technique appropriate to tight sand gas reservoir

When the reservoir is drilled-in by drilling and completion fluid under an overbalance pressure, formation damage by solids and liquid phase is avoidable. The formation damage will be very serious due to the characteristics of this type of reservoir. Therefore, the most effective measure to protect a tight sand gas reservoir is to prevent drilling and completion fluid from entering the gas reservoir, and the shield-type temporary plugging technique for protecting a tight sand gas reservoir must be used. In comparison with porous oil and gas reservoirs, the shield-type temporary plugging technique for protecting a tight sand gas reservoir has the following obvious features:

- a. Fracture width prediction. The shield-type temporary plugging of this type of reservoir is mainly aimed at fracture; thus, the borehole wall fracture width of the gas reservoir should be understood in accordance with its plugging mechanism in order to properly select the bridging particle size. Therefore, fracture width and distribution measurement provide a basis for performing this technique. Thin section statistics, mercury injection method, scanning electron microscopy, and so on can be used for measuring. However, the measured data will not truly represent the actual width of the downhole fracture just yet. Therefore, on this basis, the width and distribution range of the downhole fracture should be measured in accordance with the law of stress sensitivity of the reservoir. Well testing, laboratory simulation tests, computerized simulation tests, and so on can be adopted. Even though an accurate prediction has not been achieved yet, the direction and corresponding range of the design of completion fluid to be used are clearly shown conceptually.
- b. Temporary plugging mechanism of a fractured reservoir. This mechanism is not entirely the same as that of a porous reservoir.

It has been proven that the process of plugging fractures by solids includes a series of bridging actions of bridging particles at narrow places of fracture to change fractures to pores and the subsequent pore plugging, similar to the temporary plugging model of a porous reservoir. Thus the key lies in containing the solid particles required in drilling and completion fluid, which can be bridged at narrow seams. Studies have proven that the most effective particles are fibrous particles with a major axis size that is about equal to the fracture width. Recent studies indicate that the highly dispersed flocculated glomeration of fiber has a higher effectiveness. Therefore, as a shield-type temporary plugging agent, a series of fibrous particles with matching sizes are required. At present, this type of product can be provided.

- c. Laboratory evaluation technique of completion fluid effectiveness for fractured reservoir. This technique is quite different from that for a porous reservoir and should reflect the effects of fracture width and stress sensitivity on completion fluid effectiveness at least. At present, in China there have been corresponding methods and standards that can be applied.

In addition, if underbalanced drilling is allowed by the gas reservoir pressure, borehole wall stability, and drilling equipment, an aerated drilling and completion fluid or foam fluid with a relative density lower than 1 can be used as drilling fluid and completion fluid. At present, this technique has been mature and can be provided for selection. During gas drilling, formation damage may be caused by rock face glazing, particularly in the horizontal well drilling process. The completion fluid technique for effectively protecting the reservoir after drilling-in by gas drilling is a problem that has not been fully solved so far and is being speedily studied.

## 4.5 PERFORATING FLUID

Perforated completion is adopted by most oil and gas wells. Perforating fluid design is an important component part of perforating operation design.

Perforating fluid is a working fluid used during a perforating operation and is used for protecting production casing, preventing the perforating gun from deforming, controlling perforating, or testing pressure difference, and providing for performing perforating or combination operation technology. A perforated completion operation will generate channels with certain depth in the reservoir to facilitate the flow between the reservoir and the wellbore. During a perforating operation, perforating fluid will unavoidably contact and enter the reservoir. This shows that rationally designing and selecting perforating fluid is of great significance and will directly affect achieving oil and gas well productivity. Sometimes the unfavorable effects of perforating fluid are even more serious in comparison with drilling fluid. In order to ensure optimum perforating effectiveness, selecting quality perforating fluid appropriate to the reservoir and fluid characteristics is required.

Perforating fluid design and selection should be determined on the basis of the physical properties and fluid properties of the reservoir core, in combination with corresponding perforating technology and laboratory formation damage evaluation experiment results, in accordance with the formation damage mechanism of the perforating fluid.

### Formation Damage Mechanism of the Perforating Fluid

The formation damage mechanism of perforating fluid is the same as that of completion fluid. The potential formation damage will become true damage only due to external causes, and controlling external causes is the only mode of reservoir protection during perforating and formation testing. Current study is aimed at understanding the formation damage mechanism of perforating fluid and avoiding or mitigating induction of potential formation damage. In general, the formation damage of perforating fluid is shown in three aspects.

**Formation Damage of Solid Particles in Perforating Fluid.** When perforating fluid contains solid particles, the solid particles will enter perforation channels or microfractures under overbalance pressure and plug or even fill up the

perforations. The smaller solid particles may enter the reservoir through perforation channel walls, and formation damage may be caused in deep reservoirs. The formation damage in a porous reservoir, a porous fractured reservoir, and a fracture porosity reservoir, which is caused by solid particle migration in a region far from the perforation wall and borehole wall, will possibly lead to wasting all previous efforts during well construction. This formation damage is difficult to remove, and oil and gas well productivity is difficult to restore, if stimulation is not taken. There are many sources of solid particles, such as barite, insoluble lost circulation additive, and clay in modified drilling fluid, which is used as a perforating fluid; clay particle, precipitant, and scale particle in produced water, which is used as perforating fluid; salt crystal, bacteria, and corrosion product; and bullet debris generated during perforating operation.

**Formation Damage Caused by Perforating Fluid Filtration.** Perforating fluid will filtrate and enter the oil and gas reservoir to varying degrees under overbalanced or underbalanced perforating, and various modes of formation damage may be generated. Even if underbalanced perforating is adopted, and the backpressure of wellbore liquid is lower than the reservoir pressure, the energy released during ignition and perforating will generate an obvious water surge in the wellbore, and an overbalance pressure is first generated when a perforation channel is formed. Only after the energy generated by perforating is dissipated, the underbalance pressure environment can be restored in the wellbore, and the perforations can be cleaned by instantaneous backflow. Under an overbalance pressure, the formation damage caused by perforating fluid entering the reservoir includes:

1. Clay mineral swell, dispersion, slabbing, and migration.
2. Chemical precipitation or scaling due to the incompatibility of reservoir minerals or fluid.
3. Decrease in the relative permeability of oil or gas due to the increase in water saturation and the water blocking caused.
4. Viscous emulsion that is formed by perforating fluid and reservoir oil or the wettability

reversal of the reservoir, which will increase oil flow resistance.

5. Long-chain high-molecular polymer in perforating fluid with polymer, which enters the reservoir and decreases the effective radius of the throat due to adsorption by perforation channel surface.
6. Precipitation and plugging generated by the reaction between kill fluid and rock or reservoir fluid due to the irrational use of acid-based perforating fluid in a reservoir with more acid-sensitive minerals.

**Formation Damage of a Rate-Sensitive Reservoir by Perforating Fluid.** The formation damage of a rate-sensitive reservoir by perforating fluid is mainly generated under the following three conditions:

1. The filtration rate of perforating fluid may be increased under an overbalance pressure when the reservoir permeability is higher. A strong interference between the solids in the reservoir and the foreign solids carried by the perforating fluid and the bridging may be generated under a high filtration rate, thus plugging throats. In a seriously rate-sensitive reservoir, the pressure difference should be controlled, or perforating fluid viscosity is increased to reduce filtration.
2. In an unconsolidated or seriously rate-sensitive reservoir, rock grain shedding generated by high-speed backflow under underbalance pressure will also cause throat plugging. Thus the pressure difference should be rationally controlled.
3. Under super-overbalanced or combined perforating, perforating fluid will rapidly enter the reservoir because the wellbore pressure is higher than the reservoir breakdown pressure during operation. Despite the fact that the unclosed fracture may be generated in the vicinity of the wellbore after operation, in the region out of fracture wall face or tip, plugging may be generated due to the high-speed flow of perforating fluid in a seriously rate-sensitive reservoir, thus greatly reducing the effectiveness of super-overbalanced or combined perforating.

The potential formation damage will become true damage only due to external causes, and controlling external causes is the only mode of reservoir protection. Current studies are aimed at avoiding or mitigating induction of potential formation damage during perforating and formation testing. A perforating fluid system should be designed around this key point.

### Design Principle of a Perforating Fluid System

With the increase of attention to reservoir protection and the gradual increase of exploration cost, the application of perforating fluid is becoming wider. In particular, for the exploration and development of a complicated oil and gas field with a high risk and offshore oil and gas field, the most appropriate completion technology and fluid technique are further required in order to minimize formation damage and maximize oil and gas well productivity. With the increase of strictness in environmental protection laws and regulations and the development and application of environmental control techniques, non-toxic or low-toxicity additives and systems with easy biological degradation are required in perforating fluid.

The design principles of perforating fluid are as follows.

1. The system density should be adaptable to the reservoir, and the density should be adjustable.
2. Perforating fluid should be compatible with reservoir rock, that is, it can retain clay stability, does not plug the throat, will not generate wettability reversal, and so on.
3. Perforating fluid should be compatible with the reservoir fluid with no scaling, no crystallization, no hydrate generated, no emulsification, and so on.
4. Perforating fluid can protect tubing, casing, and downhole equipment with low corrosiveness.
5. Perforating fluid should have good thermal stability under surface and downhole conditions.
6. The system can be treated in accordance with conventional safety procedures.

7. Perforating fluid should be favorable to environmental protection and safety (preventing environmental pollution and ensuring operating personnel for safety).
8. Perforating fluid should be adaptable to perforating technology.
9. Perforating fluid has a low cost, and its raw materials have wide sources. In addition, perforating fluid should consider technological complexity and can be used repeatedly.

An ideal perforating fluid system should have appropriate density, crystallization temperature, viscosity and viscosifying ability, stability, corrosion resistance, cleanliness, recovery, and reutilization properties, fluid loss additive effectiveness, compatibility with reservoir rock and fluid, cost and raw material sources, and so on.

### Common Perforating Fluid Systems and Their Features

At present, there are mainly five perforating fluid systems that are commonly used.

#### **Solid-Free Clean Salt-Water Perforating Fluid.**

Solid-free clean salt water perforating fluid was first presented by Conoco in the late 1950s and has been widely used in drilling, completion, and workover operations. Practical experience indicates that it is feasible both technically and economically. Its important effect on the reduction of formation damage has been broadly approved. Field use indicates that solid-free clean salt water perforating fluid can obviously increase oil and gas well production rate by comparison with perforating fluid with solids.

This system is prepared with various salts, clean fresh water, and appropriate additives. The reservoir protection of this perforating fluid is achieved by matching the various inorganic salts and salinity of this system with the various inorganic salts and salinity of formation water. The inorganic salts in liquid may change the ionic environment in the system and reduce ionic activity, thus reducing the adsorptive capacity of clay. After the filtrate invades the reservoir, the clay in the reservoir will still keep stable and will

not easily swell and migrate, thus preventing the sensitive clay minerals in the reservoir from changing. Moreover, there are no foreign solids that will invade the reservoir because there are no solid particles in the perforating fluid. The features of this perforating fluid include low cost, convenience of preparation, and safe use. However, it is inappropriate for fractured reservoirs and reservoirs with high permeability and serious rate sensitivity.

Clean water is used as the base fluid of a solid-free clean salt water perforating fluid system. Appropriate types and concentrations of salts, clay stabilizing agent, demulsifying agent, corrosion inhibitor, and so on should be selected. Solid-free clean salt water perforating fluid systems can be divided into inorganic salt water systems and organic salt water systems.

The types of salts are selected in accordance with clay-inhibiting property, perforating fluid density, economy, and so on. KCl, NH<sub>4</sub>Cl, and CaCl<sub>2</sub> have the most obvious clay-inhibiting effectiveness. The two former salts have a high cost, whereas CaCl<sub>2</sub> is unsuitable for a reservoir in which there is sodium micromontmarillonite. At 21°C, KCl solution density is up to 1.07 g/cm<sup>3</sup> (weight percent 26%), NaCl solution density is up to 1.17 g/cm<sup>3</sup> (weight percent 26%), and CaCl<sub>2</sub> solution density is up to 1.37 g/cm<sup>3</sup> (weight percent 38%). CaCl<sub>2</sub>/CaBr<sub>2</sub>/ZnBr<sub>2</sub> solution density can be up to 23 g/cm<sup>3</sup> (weight percent 77%), however, the cost of bromide is higher. Therefore, when a high perforating fluid density is not required, NaCl, KCl, or NH<sub>4</sub>Cl is generally adopted. The maximum densities of the various salt solutions are shown in Table 4-14.

The salt concentration can be selected and determined by core flow experiments. In many cases, the water analysis data are not the formation water data and possibly the drilling fluid or injected water data, thus the optimum salt concentration selected is not so-called formation water salinity. For a reservoir with serious water sensitivity, a clay-stabilizing agent should be added to the perforating fluid. Despite a certain clay-stabilizing effect, cationic monomers such as K<sup>+</sup>, Na<sup>+</sup>, and NH<sub>4</sub><sup>+</sup> have insufficient effectiveness and

**TABLE 4-14** The Maximum Densities of Various Salt Solutions

Salt Water Solution	Salt Concentration (%)	Maximum Density at 21°C (g/cm <sup>3</sup> )
KCl	26	1.07
NaCl	26	1.17
KBr	39	1.20
HCOONa	45	1.34
CaCl <sub>2</sub>	38	1.37
NaBr	45	1.39
CaCl/CaBr <sub>2</sub>	60	1.50
HCOOK	76	1.69
CaBr <sub>2</sub>	62	1.81
CaCl <sub>2</sub> /CaBr <sub>2</sub> / ZnBr <sub>2</sub>	77	2.30

endurance. Thus, inorganic polymers (such as carboxyl aluminum, chromic hydroxide) and organic polymers (such as polyquaternary ammonium salt, polyquaternary phosphate, polyquaternary sulfate) can be selected. The type and volume of clay-stabilizing agent can be selected by the core or lentil test on the clay swell instrument or the core flow test. Demulsifying agents can be selected by testing under the condition of mixing crude oil and perforating fluid. A corrosion inhibitor should be added when the salt concentration selected is higher, or the reservoir temperature is higher. Its type and volume can be determined by the N80 or P110 steel coupon test. Octadecylamine, dipolyoxyvinyl octadecylamine, quaternary ammonium salt, phosphoric acid, NaSO<sub>4</sub>, and so on are generally used as corrosion inhibitors.

After the various additives and their volumes of this system are selected, compatibility and formation damage tests are required in order to ensure no reaction of the perforating fluid to produced fluid (crude oil, water), that is, no precipitation, no gas bubble, and no residue, and to ensure that the permeability recovery of the final core flow test is higher than 80%.

Bromide salt water can be used as a high-temperature high-density perforating fluid. However, its usage is limited due to its high cost, and it is only used occasionally in offshore oil and gas

field development. The strong corrosiveness of ZnBr<sub>2</sub> salt water may cause serious damage to skin and eyes, and special protection measures are required. A special corrosion inhibitor is needed in order to control the terrible acidic corrosion. The waste fluid that contains ZnBr<sub>2</sub> will seriously damage the local ecologic environment and surface water quality after being drained into the sea.

A high-temperature high-density non-bromide salt water perforating fluid system is mainly prepared by one or several inorganic salts such as CaCl<sub>2</sub>, K<sub>2</sub>CO<sub>3</sub>, Ca(NO<sub>3</sub>)<sub>2</sub>, and Na<sub>2</sub>CO<sub>3</sub>, and has much lower cost, broad raw material sources, and similar or even better performance by comparison with bromide salt water. The non-bromide salt water perforating fluid density can be up to 1.57–2.0 g/cm<sup>3</sup>.

Studies show that organic acid salt water perforating fluid systems in which formate salt water is a representative have better performance than halide salt water but have a cost still higher than that of a bromide salt water perforating fluid system. Advantageous performance includes:

1. High solubility and adjustable density between 1.36–2.4 g/cm<sup>3</sup>. No suspended particles under these conditions.
2. Maintaining particularly low viscosity under high solubility. For instance, sodium formate salt water viscosity is slightly higher than 3 MPa · s at 1.2 g/cm<sup>3</sup>; potassium formate salt water viscosity is only about 3 MPa · s at 1.48 g/cm<sup>3</sup>; and cesium formate salt water viscosity is still lower than 4 MPa · s at 2.36 g/cm<sup>3</sup>. However, halide salt water viscosity is up to 10 MPa · s at 1.72 g/cm<sup>3</sup> and 20°C and up to 23 MPa · s at 2.3 g/cm<sup>3</sup>.
3. Low crystallization point. The crystallization point of cesium formate salt water is –53°C at 1.92 g/cm<sup>3</sup>, whereas the crystallization point of bromide salt water is –28°C at 1.748 g/cm<sup>3</sup>.
4. Favoring environmental protection. Low toxicity. Ease of biological degradation. Low corrosion rate. Favoring protecting tubing, casing, and downhole equipment. No damage to skin and eyes. Cosolvency with polymers commonly used in the oil field. Good

compatibility with the formation water containing  $\text{SO}_4^{2-}$  and  $\text{CO}_3^{2-}$  and good thermal stability (higher than  $130^\circ\text{C}$ ).

To sum up, when a solid-free clean salt water perforating fluid system is used, special attention to the following two aspects should be paid: (1) Cleanliness and filtering should be ensured in order to meet the requirement of no solids. The tank-transport truck, pipeline, and well-bore should be cleaned, and appropriate filtering equipment should be adopted on the basis of reservoir pore conditions and working capacity of treatment. (2) The density adjustment and control should meet the requirement of perforating pressure difference. Attention should be paid to the effect of downhole temperature on salt water density in order to ensure that no salt precipitated at the bottomhole. Salt crystallization inhibitor (such as NAT) is added if necessary.

The advantages of solid-free clean salt water perforating fluid include: (1) There are no solids invading the reservoir, so formation damage can be reduced (core permeability can be recovered by more than 80%). (2) This salt water can inhibit the water-sensitive minerals in the reservoir. (3) Wide adjustable range of density (for example,  $\text{ZnBr}_2/\text{CaBr}_2$  system density can be arbitrarily adjusted between  $1.07\text{ g/cm}^3$  and  $2.33\text{ g/cm}^3$ ). (4) No need to add a weighting admixture. (5) Simple technology, fewer kinds of materials, and convenience of field operation and management. The disadvantages include short clay stabilization time, necessary consideration of corrosion prevention, necessary control of the crystallization point, precision filtering device required during preparation, and high cost.

**Polymer-Type Perforating Fluid.** Polymer-type perforating fluid is mainly used in the wells of oil and gas reservoirs with possible serious leakage (fracture) or filtration (high permeability), greater perforating pressure difference, or serious rate sensitivity. High-molecular polymer with different performance is added to solid-free salt water perforating fluid depending on requirements, in order to adjust rheological properties and control

filtration loss. Solids of different types are sometimes added as a bridging agent in order to achieve further controlling filtration loss. These solids can be acid-soluble (such as  $\text{CaCO}_3$  and  $\text{MgCO}_3$ ), water-soluble (such as salt particles), or oil-soluble (oil-soluble resin). The polymer-type viscosifying agents commonly added to this system include hydroxyethyl cellulose (HEC), modified HEC, biopolymer (XC), polyacrylamide (PAM) and its derivative, calcium lignosulfonate, a synthetic polymer.

The type and concentration of polymer are mainly selected in accordance with filtration loss and damage rate of filtrate, and a low filtration loss and a low degree of formation damage are generally required.

**Oil-Based Perforating Fluid.** Oil-based perforating fluid can be a water-in-oil emulsion or an oil or diesel oil to which a certain quantity of additive is added. Oil-based perforating fluid can avoid the formation damage that may be caused by water sensitivity because the filtrate is oil phase. However, it should be noted that reservoir wettability reversal may be caused (from water wettability to oil wettability) by the action of some additives (such as surfactant), or an emulsion may be caused when the bitumen or paraffin (emulsifying agent) in oil used as perforating fluid enters the reservoir, thus leading to a decrease in permeability. Therefore, the demulsifying experiments are required before use, and an appropriate demulsifying agent is added in light of the specific conditions.

If oil-based perforating fluid is used, the content of bitumen, paraffin, or other solids and the reservoir plugging should be inspected. Attention should be paid to fire prevention and safety during use.

**Acid-Based Perforating Fluid.** Acid-based perforating fluid is prepared with acetic acid or dilute hydrochloric acid to which the additives meeting various requirements are added. Owing to a certain ability of hydrochloric acid or acetic acid to solve rock minerals or impurities, the substance in perforation and in the compacted zone in the vicinity of the perforation wall can be solved to some extent after perforating, thus

preventing the compacted zone permeability from reducing after perforating and preventing the residual particles from plugging the perforation channel. Generally, about 10% acetic acid solution or about 5% hydrochloric acid solution may be used for treating the reservoir.

Acid-based perforating fluid is similar to water-based perforating fluid in that clay-stabilizing agent, demulsifying agent, and corrosion inhibitor should be added to the perforating fluid. In addition, ferric ion stabilizing agent (chelating agent) and acid sludge-resisting additive (acid sludge may form when acid contacts oil) should also be added to acid-based perforating fluid. The type and concentration of acid should be emphatically considered when an acid-based perforating fluid system is selected.

When this type of perforating fluid is used, the following two problems should be noted:

1. It should prevent acid from reacting with rock or reservoir fluid, thus avoiding the generation of precipitation and plugging. Particularly, it should be prudently selected when the reservoir contains more acid-sensitive minerals.
2. Corrosion prevention of equipment and pipeline should be considered. In particular, serious corrosion and embrittlement of steel product may occur when the reservoir has a high  $H_2S$  content.

**Gas-Based Perforating Fluid.** Gas-based perforating fluids developed from underbalanced drilling fluid system means aerated (air, nitrogen, and so on) low-density completion fluids, which are further divided into foam completion fluid, micro-foam completion fluid, and so on in accordance with the gas proportion and the type and density of polymer and additive. Micro-foam completion fluid was first used in the completion operation of a depleted reservoir in the Lake Maracaibo area, in Venezuela. Micro-foam is not single gas bubbles accumulated together, but a micro-bubble network that can resist or mitigate the invasion of liquid into the reservoir. The preparation and maintenance of micro-foam drilling fluid are simple. In general, the micro-foam volume can be up to 8% to 14%.

This type of perforating fluid was developed to meet the requirements of completion and workover of oil and gas wells of low-pressure fractured reservoirs, heavy oil reservoirs, low-pressure strong water-sensitive reservoirs, low-pressure low-permeability reservoirs, reservoirs that easily have serious leakage, depleted reservoirs, and offshore deep-water wells. Its features include low density, low filtration loss, and good effectiveness of oil and gas reservoir protection.

The types, preparation methods, and advantages and disadvantages of various perforating fluids are listed in Table 4-15.

### Requirements of Perforating Technology for Perforating Fluid

The general requirements for perforating fluid include ensuring compatibility between the perforating fluid and the reservoir rock and fluid, preventing further formation damage during and after perforating, and meeting the requirements of perforating technology. Therefore, perforating fluid system selection should be in accordance with the actual reservoir conditions and the type of perforating technology, and the optimum perforating fluid system that can not only protect the reservoir but also smoothly fulfill the operation should be selected.

Controlling formation damage and designing and selecting a perforating fluid system can not only make up a discipline but also become an art. A formulation appropriate to some conditions may not be necessarily appropriate to others. In general, conventional perforating technology such as tubing conveyed perforating (TCP) has no special requirement for a perforating fluid system, and the corresponding perforating fluid system adaptable to reservoir characteristics is selected in light of reservoir protection. However, nonconventional perforating technology has requirements for perforating fluid.

When combined perforating and testing (including TCP+MFE, TCP+HST, TCP+PCT, TCP+APR) are required, the perforating fluid should meet the requirement of testing pressure difference

TABLE 4-15 Main Types of Perforating Fluid

Type	Subtype	Application Range	Preparation	Advantage	Disadvantage
Water-based	Modified drilling fluid	Drilling-in reservoir, perforating, and well killing	Adjusting performance of original drilling fluid, such as adding clay-stabilizing agent, fluid loss additive, and temporary plugging agent, and increasing cationic concentration. Mainly including polymer-type drilling fluid, polymer/lime-type drilling fluid, lignocarbonate drilling fluid, and CaCO <sub>3</sub> -type drilling fluid.	Simplicity, low cost, low degree of formation damage by polymer-type drilling fluid, higher degree of formation damage to high-permeability reservoir than that to low-permeability reservoir	High solids content, possibly higher degree of formation damage
	Solid-free clean salt water	Perforating and well killing	Inorganic salt + clay-stabilizing agent + viscosifying fluid loss additive + pH adjusting agent + corrosion inhibitor	Good reservoir protection effectiveness, adjustable density (1.07–2.3 g/cm <sup>3</sup> )	Slightly poor suspension, filtering required, easily corroded
	Low-solids temporary plugging-type killing fluid	Acid-soluble killing fluid Oil-soluble killing fluid Water-soluble killing fluid	Perforating and well killing	Temporary plugging-type bridging agent + viscosifying agent Acid-soluble bridging agent: carbonate Oil-soluble bridging agent: resin, bitumen Water-soluble bridging agent: salt particle American formulation: CaCO <sub>3</sub> + HEC + temporary plugging agent + XC	Strong inhibiting effect, enabling temporary plugging, core permeability recovery up to 80–90%

Continued

TABLE 4-15 Main Types of Perforating Fluid—cont'd

Type	Subtype	Application Range	Preparation	Advantage	Disadvantage	
	Polymer-type perforating fluid	Polymer + surfactant	High water saturation reservoir and reservoir easily water blocked	Formulation: viscosifying fluid loss additive + surfactant + salt + solids	Backflow of liquid enters reservoir easily	
		Cationic polymer	Water-sensitive reservoir	Viscosifying fluid loss additive + clay-stabilizing agent + surfactant	Inhibiting clay swell, high recovery of permeability	
	Oil-in-water emulsion	Mainly gas reservoir or strong water-sensitive reservoir	Bentonite + CaCl <sub>2</sub> + gas condensate + sulfonyl	Preventing liquid from entering reservoir, easiness of induced flow		
Oil-based	Crude oil or diesel oil	Low-pressure reservoir or reservoir with clear information		No damage to reservoir	Dirty	
	Water-in-oil emulsion and micellar solution	Water-sensitive reservoir	Water + oil + surfactant/alcohol	Solubilizing water	Expensive	
Gas-based	Foam	Low-pressure reservoir or deep-water well	Water + surfactant + water soluble clay-stabilizing agent	Low density, having energizing effectiveness, ease of backflow, no damage to reservoir	Poor stability, matching equipment required	
	Micro-foam		Water + surfactant + water-soluble clay-stabilizing agent + polymer	Having energizing effectiveness, ease of backflow, favoring removal of skin damage	Liquid nitrogen truck and matching equipment required	
	Nitrogen	Super-overbalanced perforating and testing operations	Commonly used in combination with acid-based perforating fluid			
Acid-based	Hydrochloric acid system Acetic acid system	Super-overbalanced perforating, combined perforating and acidizing	Water + hydrochloric acid/acetic acid + clay-stabilizing agent + demulsifying agent + corrosion inhibitor + chelating agent	Enabling removal of damage in perforations and in vicinity of wellbore	Pay attention to flowback	

and should favor packer setting and testing valve switching. Not only can liquid-type perforating fluid be used in light of reservoir conditions, but inert nitrogen can also be used as a testing gas cushion. Not only can this gas cushion play a part in protecting the reservoir and setting packer, but it can also be particularly convenient for regulating backpressure so that reservoir fluid can flow, thus reducing formation damage and avoiding explosion.

When combined perforating and acidizing are required, an acid-based perforating fluid can be used. When combined perforating and fracturing are required, fracturing prepad fluid is selected as the perforating fluid. When a combined perforating and sand control operation (such as gravel packing) is required, the perforating fluid should meet the requirements of reservoir protection and sand control operation.

When super-overbalanced perforating is required, the perforating fluid may be pressurized and enter the reservoir; thus, a rational combined mode of fracturing fluid and liquid nitrogen should be selected in light of the different reservoir conditions. The liquid cushion and liquid nitrogen volumes should be designed in accordance with operational requirements. Regardless of the type of fluid and the size of the fluid's volume, a friction-reducing polymer should be added. The design criteria of perforating fluid for super-overbalanced perforating are shown in Table 4-16.

The fluid volume selected should ensure a certain submergence of the perforating gun and is related to fracture propagation or operation design effectiveness. It can be designed by dynamic simulation analysis and calculation.

When combined perforating and high-energy gas fracturing are required, the perforating fluid may be unavoidably carried into the reservoir; thus, the perforating fluid system should be carefully selected, and a system adaptable to reservoir characteristics should be designed and selected to the full extent.

For a low-pressure low-permeability reservoir, horizontal or multibranch well, and deep-water oil and gas wells, the perforating fluid system should be prudently selected, and low-density

TABLE 4-16

### Selection Criteria of Perforating Fluid for Super-Overbalanced Perforating

Reservoir condition	Type of liquid
Sandstone (specific carbonatite)	2% KCl salt water
Sandstone (water retention)	2% KCl salt water + alcohol
Carbonatite	15–20% HCl
Sandstone (serious water sensitivity)	Crude oil
Sandstone + carbonatite	10% acetic acid
Low-pressure shale gas reservoir	10% acetic acid or 1.5% HF
Heavy oil reservoir (waxy) or drilling with oil-based mud	Xylene
Sandstone gas reservoir (< 7 MPa)	Diesel oil

foam or micro-foam perforating fluid is used to the full extent in order to avoid formation damage that may be caused by perforating fluid and to meet the requirement of underbalance during perforating. For a high-temperature and abnormal high pressure reservoir, a high-temperature high-density clean salt water perforating fluid is required.

Generally, a perforating fluid should be selected in accordance with concrete conditions. For instance, in the Lake Maracaibo area, in Venezuela, in order to prevent perforating fluid and displacement fluid from damaging the reservoir, drilling fluid is displaced by salt water with a density of  $1.02 \text{ g/cm}^3$  during completion, Stable Mul emulsion (oil-in-water emulsion,  $0.89 \text{ g/cm}^3$ , no demulsification at  $160^\circ\text{C}$ ) is used as a perforating fluid, and after perforating, the Stable Mul emulsion is displaced by light oil with a density of  $0.78 \text{ g/cm}^3$  for putting well into production. This indicates that the water-based perforating fluid does not contact the reservoir in the process from the beginning of perforating to putting well into production, thus reducing the formation damage that may be caused by completion fluid. At present, produced water is also used as a perforating fluid, but necessary treatment such as filtering should be implemented before it is used.

## REFERENCES

- [1] Wan Renpu, et al., *Advanced Well Completion Engineering*, second ed, Petroleum Industry Press, Beijing, 2000 (in Chinese).
- [2] Luo Zhetan, et al., *Oil and Gas Reservoir Pore Configuration*, Science Press, Beijing, 1986 (in Chinese).
- [3] M.M. Sharmar, et al., *Release and Deposition of Clay in Sandstones*, SPE 13562, 1985.
- [4] K.E. Porter, *An Overview of Formation Damage*, J. Petroleum Tech. Aug. 1989.
- [5] D.B. Bennion, F.B. Thomas, R.F. Bietz, *Low Permeability Gas Reservoir: Problems, Opportunities and Solutions for Drilling, Completion, Stimulation and Production*, SPE 35577, May 1996.
- [6] D.B. Bennion, *Screening Criteria Help Select Formations for Underbalanced Drilling*, Oil & Gas J. Jan. 1996.
- [7] A. Ghalambor, M.J. Economides, *Formation Damage Abatement: A Quarter-Century Perspective*, SPE 58744, 2000.
- [8] N. Hands, K. Kowbel, S. Maihanz, *Drilling-in Fluid Reduces Formation Damage, Increases Production Rates*, Oil & Gas J. (1998) 28.
- [9] R.F. Krueger, *An Overview of Formation Damage and Well Productivity in Oil Field Operations*, J. Petroleum Tech. Feb. 1986.
- [10] A.W. Layne, A.B. Yost II, *Development of Advanced Drilling, Completion, and Stimulation System for Minimum Formation Damage and Improved Efficiency: A Program Overview*, SPE 27353, 1994.
- [11] D.B. Bennion, F.B. Thom, *Underbalanced Drilling of Horizontal Wells: Does It Really Eliminate Formation Damage?* SPE 27352, 1994.
- [12] Zhang Shaohuai, Luo Pingya, et al., *Reservoir Protection Techniques*, Petroleum Industry Press, Beijing, 1993 (in Chinese).
- [13] Luo Pingya, *CNPC Academician Literature Collection (Luo Pingya's Collection)*, China Encyclopedia Press, Beijing, 1997 (in Chinese).
- [14] Luo Pingya, *Reservoir Protection Techniques*, Petroleum Industry Press, Beijing, 1999 (in Chinese).
- [15] Luo Pingya, Kang Yili, Meng Yingfeng, *Crossing Development of Reservoir Protection in China*, Nat. Gas. Ind. 26 (1) (2006) 84–87 (in Chinese).
- [16] Kang Yili, Luo Pingya, *Effects of Clay Minerals on Sandstone Formation Damage—Review and Prospect, Drilling and Completion Fluids* 17 (5) (2000) 36–40 (in Chinese).
- [17] Kang Yili, Xu Jin, Luo Pingya, *Studies of Protection Techniques of Tight Sands Gas Reservoir in Western Sichuan*, Natural Gas Exploration and Development Symposium, Petroleum Industry Press, Beijing, 2000 (in Chinese).
- [18] Kang Yili, Luo Pingya, Xu Jin, Xu Xinghua, *Employing Both Damage Control and Stimulation: A Way to Successful Development for Tight Gas Sandstone Reservoirs*, SPE 64707, Presented at the SPE International Oil and Gas Conference and Exhibition in China, held in Beijing, China, November 2000.
- [19] Xu Tongtai, Zhao Ming, Xiong Youming, et al., *Oil/Gas Reservoir Protecting Techniques*, second ed, Petroleum Industry Press, Beijing, 2003 (in Chinese).
- [20] Xu Tongtai, Hong Peiyun, Pan Shikui, et al., *Drilling and Completion Fluids of Horizontal Well*, Petroleum Industry Press, Beijing, 1999 (in Chinese).
- [21] Xu Tongtai, et al., *Drilling Fluid and Completion Fluid Techniques Abroad in the Early Part of the Twentieth Century*, Petroleum Industry Press, Beijing, 2004 (in Chinese).
- [22] Fan Shizhong, Yan Jienian, Zhou Dachen, et al., *Drilling Fluid, Completion Fluid, and Oil/Gas Reservoir Protecting Techniques*, Petroleum University Press, Dongying, 1996 (in Chinese).
- [23] Fan Shizhong, *Completion Fluid and Workover Fluid*, China Mining University Press, Xuzhou, 2004 (in Chinese).
- [24] W.F. Foxenberg, *Solid-free Completion Fluids Optimize Rig Operations (Part I: Formation and Selection)*, Pet. Eng. Int. 69 (5) (1996) 32–35.
- [25] C.M. Hudgins, et al., *Heavy Brine Makes Good Fluid for Completion Packer*, Oil and Gas J. (7) (1961) 91–97.
- [26] L.R. Houchin, et al., *Evaluation of Potassium Carbonate as a Non-corrosive, Chloride-free Completion Fluid*, SPE 27392, 1994.
- [27] Xu Tongtai, et al., *New Advances in Drilling Fluid and Completion Fluid Techniques Abroad*, Drilling Fluid & Completion Fluid 21 (2) 2004 (in Chinese).

## Production Casing and Cementing

### OUTLINE

- |   |   |   |
|---|---|---|
| <p><b>5.1 Basic Requirements for Production Casing Design and Integrity Management of Production Casing</b></p> <ul style="list-style-type: none"> <li>Basic Requirements of Production Casing Design <ul style="list-style-type: none"> <li><i>Safety Criteria</i></li> <li><i>Requirements of Well Completion</i></li> <li><i>Requirements of Safe Operation and Working Life</i></li> </ul> </li> <li>Production Casing Integrity Management <ul style="list-style-type: none"> <li><i>Conception of Production Casing Integrity Management</i></li> <li><i>Casing Failure Caused by Corrosion</i></li> <li><i>Initial Failure of Casing in a Perforated Interval</i></li> <li><i>Casing Collapse Mechanism and Potential Risk</i></li> <li><i>Casing Collapse Severity Assessment</i></li> <li><i>Casing Failure of Free Section</i></li> <li><i>Long-Term Service Life of a Cement Sheath</i></li> </ul> </li> </ul> | <p><b>5.2 Hole Structure and Types of Casing</b></p> <ul style="list-style-type: none"> <li>Hole Structure <ul style="list-style-type: none"> <li><i>Hole Structure of Standard Casing Size Series</i></li> <li><i>Hole Structure of Nonstandard Casing Size Series</i></li> <li><i>Expandable Casing Technique and Hole Structure</i></li> </ul> </li> <li>Casing Size and Steel Grade Series <ul style="list-style-type: none"> <li><i>Standard Casing Size Series</i></li> <li><i>Casing Steel Grade Standard and Code</i></li> <li><i>Types of Casing Steel Grade</i></li> <li><i>High Collapsing Strength Casing</i></li> <li><i>Straight Weld Casing</i></li> </ul> </li> <li>Casing Thread and Connection Structure <ul style="list-style-type: none"> <li><i>API/ISO Threads</i></li> <li><i>Gas Sealing Thread of Casing and Connection Structure</i></li> <li><i>Integral Joint Casing</i></li> </ul> </li> <li>Field Make-Up Operation Requirements</li> </ul> | <ul style="list-style-type: none"> <li><i>Make-Up Rotations and Location</i></li> <li><i>Thread Sealant</i></li> </ul> <p><b>5.3 Strength of Casing and Strength Design of Casing String</b></p> <ul style="list-style-type: none"> <li>Casing Strength Calculation in API 5C3 <ul style="list-style-type: none"> <li><i>Collapsing Strength Calculation</i></li> <li><i>Internal Yield Pressure Strength Calculation</i></li> </ul> </li> <li>Collapsing Strength Calculation in ISO 10400 <ul style="list-style-type: none"> <li><i>Basic Supposition and Calculation Principle</i></li> <li><i>Design Collapse Strength of Casing Only under the Action of External Collapsing Pressure</i></li> <li><i>Collapsing Strength under the Action of Axial Tension and Internal Pressure</i></li> <li><i>Calculation Case</i></li> </ul> </li> <li>Internal Pressure Strength Calculation in ISO 10400 <ul style="list-style-type: none"> <li><i>Internal Yield Pressure Strength</i></li> <li><i>Internal Toughness Burst Pressure Strength</i></li> </ul> </li> </ul> |
|---|---|---|

- Internal Crack Destabilization Rupture Pressure Strength Environmental Rupture Failure*
- Other Strength Standards of Casing
  - Tensile Strength Internal Pressure Strength of the Collar ISO/API Thread Seal Pressure*
- Loads Borne by Production Casing String
  - Internal Pressure External Pressure Axial Forces*
- Design Procedure and Design Safety Factor
  - Design Procedure Design Safety Factor of Casing Casing Tension Allowance Design Method*
- 5.4 Cementing**
  - Basic Grounds of Cementing Design
    - Operation Requirements Well Completion Requirements Requirements of Oil and Gas Well Production*
  - Types and Properties of Cement
    - Concept of Oil Well Cement Types and Usable Range of Oil Well Cement Formulation of Oil Well Cement Basic Requirements for Cement Slurry and Set Cement Basic Property Requirements for Cement Slurry*
  - Oil Well Cement Additives
    - Fluid Loss Additive of Oil Well Cement Dispersant of Oil Well Cement Retardant of Oil Well Cement Accelerant of Oil Well Cement Special Function Additives Lightning Admixture Weighting Admixture Thermal Stabilizer*
- Principle of Enhancing Cement Job Quality
  - Measures to Raise Displacement Efficiency of Cementing Cement Slurry Weightlessness and Prevention of Channeling of Oil, Gas, and Water*
- Cement Job Quality Detection and Evaluation
  - Quality Requirements of Cementing Cement Sheath Quality Standards*
- 5.5 Production Casing and Cementing for Complex Type Wells**
  - Superdeep Wells and High-Temperature High-Pressure Gas Wells
    - Main Problems Solving Means*
  - Corrosive Media-Containing Oil and Gas Wells
    - Physico-Chemical Reaction in the Corrosion Process Sulfate Corrosion and Sulfate-Reducing Bacteria Corrosion Corrosion Action of Carbon Dioxide on Set Cement*
- Corrosion Action of Hydrogen Sulfide on Cement Sheath
  - Approaches to Cement Sheath Corrosion Prevention*
- Wells That Absorb Easily
  - Main Problems Approaches to Cementing Leakage Prevention*
- Salt Rock Bed and Salt Paste Bed Wells
  - Main Problems Approaches to Solving Problems*
- Thermal Production Well
  - Main Problems Mechanism of Damage to Material by High Temperature, Thermal Stress and Creep, and Corresponding Games Heat-Resistant Seal Thread for Thermal Production Well High-Temperature-Resistant Cement Mode and Method Selection of Well Completion*
- Horizontal Well
  - Main Problems Approaches to Solving Problems*
- Adjustment Wells
  - Main Problems Approaches to Solving Problems*
- Well Using External Casing Packer
  - Combined External Casing Packer and Screen Completion Without Cementing Combined External Casing Packer and Cementing Completion*

One or more casings are required to be run and set in the process of oil and gas well construction. The casing that is finally used for producing oil and gas is known as production casing. The main functions of production casing include protecting the borehole wall and sealing and separating oil and gas reservoirs in order to achieve safe oil and gas production and separate-zone testing, water injection, and stimulation.

Production casing should be safe and effective throughout the process of oil and gas field development. Production casing bears external collapse pressure, internal pressure, tensile load, and so on during casing running, cementing, and oil and gas producing. During well completion by perforating, production casing is required to bear a large-energy high-temperature transient impact load. In the long-term oil- and gas-producing process, in addition to the external collapse pressure of formation, production casing may bear long-term internal pressure and external load change of multiple stimulation and workover. In addition, production casing is required to withstand corrosion of various fluidic corrosive media, and corrosion has become the main factor in the failure of production casing. Production casing deformation, leaping, breakdown, leakage, and so on may cause oil and gas wells to be unable to produce, cause oil and gas fields to be unable to develop normally, and even lead to underground channeling or underground blowout and serious environmental and safety problems arising therefrom. Therefore, the technical personnel of downhole operations and oil production should master and understand the knowledge of production casing design and present rational technical requirements.

## **5.1 BASIC REQUIREMENTS FOR PRODUCTION CASING DESIGN AND INTEGRITY MANAGEMENT OF PRODUCTION CASING**

### **Basic Requirements of Production Casing Design**

Because the strengths and life of high-temperature high-pressure wells, deep wells, superdeep wells, hydrogen sulfide-containing wells, and steam

thermal production wells are highly related to safety and environment problems, the designer and production management personnel should pay great attention to design, safe operation, and operating life.

**Safety Criteria.** Production casing string should be designed in accordance with the criteria of safety and economy. A balanced relation between casing strength and the pressure borne by casing string should be established on the basis of the downhole working conditions of casing string in order to ensure safety first. However, the external load borne by casing string is different under different engineering and geological conditions. For instance, the external collapse pressure borne by casing string from a downhole halite bed will greatly exceed normal formation pressure; the internal pressure borne by casing string during fracture acidizing is different from the internal pressure during normal oil production; and the external collapse pressure borne by casing string from an oil reservoir that easily sloughs during the early production period is different from that during the middle and late period. Moreover, casing strength will also be changed. For instance, in a downhole corrosive environment, the casing strength is reduced by corrosion, thus causing casing failure; in a thermal production well, the high-temperature steam will lead casing to repeat extending and retracting, thus reducing casing strength; and in a horizontal or high-angle well, the casing strength may be reduced due to wear in the process of long-term downhole operation. Therefore, the application of safety criteria for designing production casing string is difficult to some extent. The typical present solution is mainly that the pressure borne by the production casing string is determined in accordance with the most dangerous downhole working conditions, and then a rational casing string strength design method is used, thus ensuring the safety of casing string.

The basic casing string designs include:

1. Tensile strength design. The tensile strength of casing string is calculated in accordance with the axial tensile force of casing weight during casing running.

2. Collapsing strength design. In general, collapsing strength is calculated in accordance with the internal full-hollowed condition and the external casing collapse pressure determined by using drilling fluid density during casing running. There are several different views including internal partly hollowed and full-hollowed conditions. An external casing collapse pressure based on salt water column pressure in a cementing section and drilling fluid density in a no-cementing section or based on drilling fluid density in a whole section is adopted in practice.
3. Internal pressure strength design. The internal pressure strength is only considered when the well is a gas well, and the internal pressure is calculated in accordance with gas reservoir pressure or the pressure that counts gas column gravity.

A more accurate design for deep wells and high-pressure gas wells should consider the three aforementioned loads combined and the change of casing strength under combined loads. For instance, the reduction of collapsing strength of casing by the action of axial load should be considered in design.

**Requirements of Well Completion.** Most oil and gas wells adopt perforated completion because perforated wells can mitigate the inter-layer interference of a stratified reservoir as much as possible. Perforating may affect the strength and service life of production casing to some extent; therefore, quality casing that may not be broken or deformed after perforating should be selected.

In a gas well that uses a tubing packer during completion, the packer may fail or the sealing of the tubing thread may be damaged in the process of long-term production; thus, gas may enter the tubing-casing annulus, and the production casing will bear high internal pressure and suffer corrosion. Hence a rigorous internal pressure strength check of the production casing is required.

Specific requirements of perforating, sand control, fracturing, and oil pumping for completion

socket length should be considered. In general, socket length should be larger than 10–15 m, and 50–60 m or longer can be selected.

At the same time, some specific conditions should be considered. For instance, if liner completion is adopted, the clearance size between liner and production casing should be considered in order to ensure cement job quality; if gravel pack and slotted liner sand control completion is adopted, a larger casing should be used, and a production casing larger than 7in is selected as far as possible. If the well is a natural gas well or a gas injection well, casing thread and sealing compound should have high sealing performance; if gas is acidic in a gas well, casing material should be corrosion resistant; if the well is a thermal production well by steam, casing thread and sealing compound should be resistant to thermal stress; and a casing with a high collapsing strength should be adopted in a rock salt section.

**Requirements of Safe Operation and Working Life.** The safety and working life of casing and cement sheath are mainly affected by abnormal high external load and corrosion. Integrity of design and management is achieved by requirements of safe operation and working life on the basis of advanced design and management theory.

## Production Casing Integrity Management

**Conception of Production Casing Integrity Management.** A host of cases show that almost all casings that have failed meet the API/ISO standards in designs and operations. This indicates that designing casing only in accordance with API/ISO standards cannot ensure the integrity of casing in the working process. In recent years, the idea of well integrity management has been presented, and the theory and method are still being perfected continuously. Production casing integrity is a key component part of well integrity. Production casing integrity includes the following connotations:

1. Production casing should keep both physical and functional integrities. Physical integrity means no leakage, no deformation, no performance degradation of material, and no wall thickness thinning, while functional integrity means adaptability to pressure and operating during production or downhole operation.
2. Production casing is always in a controlled state. The collapsing loads that can be borne and the limiting working environments in different use periods can be predicted.

Production casing integrity management deals with corrosion, external load estimation, on-line monitoring and casing logging, operating limitation and management, and so on. External load and casing damage or material performance degradation, and so on, are difficult to calculate accurately, and there are no related design standards established. Therefore, the designing and working conditions should be determined by the oil and gas well manager and designer using the risk analysis method.

**Casing Failure Caused by Corrosion.** Corrosion is the most common and serious factor in casing failure. Internal corrosion is predominant in some wells, while external corrosion predominates in others. However, most casing failure may be caused by external corrosion in the no-cementing section. Local corrosion may develop into boring and leaking, thus leading to downhole channeling or downhole blowout and erumpent water block in oil and gas wells. Weight-loss corrosion may lead to wall thickness thinning, thus reducing the strength of casing.

Corrosion may cause performance degradation of steel product or reduction of structural strength. For instance, the toughness of steel product may be reduced by hydrogen sulfide-containing fluid or sulfide or hydrogen atoms generated by chemical reaction, thus generating lagging rupture. This is just performance degradation of material.

The material to be used should be rationally selected, and inappropriate material with low

cost should be avoided in the design stage. Otherwise, the later workover cost may be much higher than the first cost in the design stage. If the production casing cannot be fully sealed by cement, the corrosive components in the reservoir fluid should be examined, and corresponding measures (for example, using casing with external anticorrosive insulation and locally plugging the reservoir that contains corrosive fluid) are designed. The leakage that is caused by corrosion often occurs at an API/ISO standard thread, reducing nipple, stage collar, tie back tool, and casing wall above the drop-out point of condensate water.

Corrosion monitoring or corrosion logging is required by important oil and gas wells in the production stage in order to confine production operation parameters. Corrosion monitoring or corrosion logging can provide grounds for risk assessment.

**Initial Failure of Casing in a Perforated Interval.** Most oil and gas wells adopt perforated completion, and the initial failure of casing in a perforated interval is often generated. The internal cause of initial failure is the reduction of casing strength due to perforating, while the external cause is the complicated downhole loads and corrosion.

When perforations are bored by boring machine with reference to the perforation diameter and distribution of downhole casing perforation, the collapsing strength of the casing is only reduced by about 5%. However, downhole perforating is achieved by deflagrating and boring of perforating charge, the toughness of the material around perforations is reduced by the transient impact, and axial cracking of the casing on the upper and lower edges of perforation is almost unavoidable. During perforating, the dynamic fracture toughness of material controls the cracking tendency. After perforating, the lateral impact toughness of casing controls the extension of longitudinal crack under the action of external collapse pressure or internal pressure. In order to reduce perforating cracking, the lateral impact toughness of the casing should be used as a casing performance index.

In accordance with fracture mechanics theory, a casing that has lateral impact toughness as high as possible and impact toughness and yield strength matchable to the casing wall thickness should be selected. This matching means selecting a high-yield strength steel grade and corresponding higher lateral impact toughness. A thick-wall casing is selected under allowable conditions of well completion and downhole operations in order to obviously increase the structural fracture toughness of the casing. The lateral impact toughness of the casing and collar has been a standard in ISO 11960 and API 5CT, which also specify the requirements of lateral impact toughness of different steel grade and wall thickness. The longitudinal and lateral impact toughness of casing in ISO 11960 and API 5CT are the lowest standards. Practically, the lateral impact toughness of casing in many casing manufacturers has been higher than the ISO/API standards. Due to manufacturing engineering, the lateral impact toughness of casing is only half of the longitudinal impact toughness. In order to prevent casing from cracking due to perforating, the lateral impact toughness of the casing in the reservoir interval should first be increased, and then the perforating parameter design is optimized, and the toughness of cement stone is increased.

**Casing Collapse Mechanism and Potential Risk.** Casing collapse is a generalized denotation and includes the following three failure modes:

1. Symmetric deformation. This is a collapse caused by unequal collapse pressures in both directions of major and minor axes or by a high ovality of the casing.
2. Local sag on the circumference. Local corrosion of the outside wall or local wear of the inside wall leads to reduction of wall thickness, and fluid pressure acts on the thinned surface, thus forming sag.
3. Lateral displacement of casing. Formation rock mass sliding causes lateral displacement of casing.

The casing collapse mechanism and potential risk are as follows.

1. Casing collapse by rock creep

Rock salt bed, cream salt bed, ooze rock, and so on have creep property, which means that these beds will sustainedly generate strain after the borehole is formed. The continuous reducing of these beds may cause casing collapse. The creep of some rock masses can sustain for several months to several years, and the corresponding casing may collapse after several months to several years. In some oil fields, casing collapse is mainly generated in the cementing section. The no-cementing section has not generated casing collapse but has generated boring by external corrosion. In some oil fields, the casing collapsing strength design of the rock salt interval is in accordance with overburden pressure; however, casing collapse is still generated often.

2. Casing collapse by reservoir sloughing and formation sliding

A pressure shortfall of an unconsolidated sandstone reservoir may be generated in the producing period. With the compacting action of the pore structure, the local sloughing of the reservoir interval may be generated, thus generating casing collapse. Sliding at the interface between caprock and reservoir may be generated by various factors during oil and gas production. Caprock sliding may be caused by the effective stress change of reservoir rock during waterflood, reduction of temperature, and water channeling into the interface between caprock and reservoir. In addition, sliding at the interface between caprock and reservoir may also be generated by thermal volumetric expansion in a large range of the reservoir during thermal production of heavy oil. The shearing force of the aforementioned formation sliding is sometimes so great that even with a good cement job it is difficult to prevent sliding and casing collapse or shear deformation. The greater the rock strength difference

between caprock and reservoir rock, the greater the sliding tendency.

Local sliding of formation rock along the formation face or fault surface may generate shearing force acting on the casing, thus causing casing collapse or generating lateral displacement of casing.

3. Casing collapse by unconsolidated sandstone reservoir sand production

An unconsolidated sandstone reservoir may generate sand production during oil production, and with the increase of water saturation, sand production may be aggravated. Cavitation may be generated in the reservoir by continuous sand production and destroy the normal stress distribution around the borehole, thus causing local formation sloughing and sinking. A nonuniform external collapse pressure of the casing may be generated by sand production. Under the combined action of overburden pressure, casing collapse and leap may be generated. The sand production severity can be predicted by using lithomechanical logging data and related software, thus providing grounds for the casing design of reservoir interval and sand control.

4. Casing collapse by high-pressure water injection

Waterflooding is one of the oil field development measures commonly used. When water pressure reaches or exceeds overburden pressure, a large amount of high-pressure water may invade the mud shale interbed, crushed zone of formation interface, and fault surface, thus causing changes in rock properties and geomechanical factors and generating a supernormal external pressure on the production casing. The manifestations are as follows.

- a. A water suction swell of mudstone may generate creep or sliding, thus squeezing the casing. At this time, the casing bears all rock pressure. The dispersed smectite has the highest water content. Mudstone with dispersed smectite content of 50% may have a water content higher than 10%. A bentonite bed contains 95%

smectite, of which the water content can be higher than 50%. Therefore, the higher the smectite content of the mudstone interval, the greater the possibility of squeezing the casing. Obviously, after the high-pressure injected water invades the mudstone, the water content that causes water suction swell of the mudstone may greatly exceed the water content of the mudstone itself. As a result, the various lateral pressures generated by the injected water that invades the mudstone may cause squeezing of the casing to a great extent.

- b. High-pressure injected water enters the primary microfracture of the mudstone bed or generates vertical fracture, which penetrates the interbed, thus generating a squeeze pressure on the casing due to the effect of a water wedge. Thus mudstone may generate creeping and sliding and collapse the casing. This sliding may be more serious in an area with a larger dip angle and an area in which fractures developed, and may also be generated at the top of the structure.
- c. Injected water invades the crushed zone of mudstone or fault interface so that interformational friction resistance is reduced, and rock bed sliding and casing collapse may be caused. When high-pressure water invades the fault surface, a lubricating tendency may be generated at the fault surface, and fault activity may even be activated. The imbalance of formation pressure on both sides of the fault can even reactivate the fault. In an oil field with high-pressure waterflooding, microseism can be measured by using a high-precision seismic monitoring instrument.

**Casing Collapse Severity Assessment.** Under conditions of ample data, the rock-mechanical and geomechanical analyses and studies of caprock, salt rock, cream salt bed, ooze rock, crushed zone, and so on are required in order to quantitatively assess the casing collapse

severity. However, a reliable quantitative calculation is difficult, or decision and design are required to be completed before calculating. Thus a qualitative analysis is valuable. The lateral collapse pressures of rock salt bed, cream salt bed, ooze rock, and unconsolidated reservoir are controlled by an in situ stress state, rock properties, and structural relation.

1. Three-directional in situ stress state assessment based on structural configuration

Suppose that the three principal stresses have  $\sigma_1 > \sigma_2 > \sigma_3$ . Their vertical and horizontal distributions may affect the stress state of the borehole wall. In a normal fault area,  $\sigma_1$  is in the vertical direction, the difference between both horizontal stresses is small, and the lateral collapse is not serious. In a thrust nappe, the intermediate principal stress  $\sigma_2$  is in the vertical direction, while the maximum principal stress and the minimum principal stress are in the horizontal direction. For a straight well, this is a three-directional in situ stress relation, which has the most serious lateral collapse. On both flanks of the anticline, under the conditions of high dip angle, cross-stratification of soft and hard strata, and well-developed bedding, the difference between both horizontal stresses is great, an additional stress may be generated by anisotropy of formation rock, and the lateral collapse is serious. For a straight well, the greater the difference between both horizontal stresses, the higher the reducing rate.

For a long time past, the overburden pressure of the salt bed has been regarded as the lateral collapse pressure on the casing in casing design, but casing collapse has been generated where rock salt bed, cream salt bed, or ooze rock exists.

2. Two types of rheological rock

a. Rheological fluid. Deep-buried or high-temperature rock salt bed, cream salt, or ooze rock may continuously creep until the borehole closes. In some areas, casing deformation or collapse may be generated several years later.

b. Rheological solids. Most rock salt beds, cream salt beds, and ooze rocks are composed of rheological solids. The creep rate reduces with time. After a certain time, the creep may basically stop. In some wells, local reaming and no-cementing measures have been adopted in order to reserve enough space for deforming. After deforming stops, casing collapse will not happen.

c. Qualitative assessment of factors affecting rock creep

In a well that penetrates high-dipping rheological formations (such as rock salt bed, cream salt bed, and ooze rock), the creep rate of rheological rock along formation dip direction is shown in Equation (5-1).

(5-1)

$$S = \frac{ch^2}{12\eta(T)} \rho g \tan\alpha$$

where:  $S$  = areal creep rate, which corresponds to borehole area reducing rate;  $\rho$  = mean overburden density;  $g$  = gravitational acceleration;  $\alpha$  = formation dip angle;  $c$  = coefficient.

Equation (5-1) has the following clear physical and engineering meanings:

1. The thicknesses of rock salt bed, cream salt bed, and ooze rock have a very obvious effect. Creeping formation thickness is a main factor of reducing. Thin salt bed or thin ooze rock formation has a low effect.
2. Formation dip angle  $\alpha$  has an obvious effect. The  $\tan\alpha$  value is obviously increased with the increase of dip angle  $\alpha$ . This means that a rock salt bed, cream salt bed, and ooze rock formation with a high dip angle has a high reducing rate.
3. Temperature affects the coefficient of viscosity of creeping formation, which reflects the degree of ease of creeping of the rock mass and is a function of temperature  $T$ . The higher the temperature, the smaller the coefficient and the higher the reducing rate.

4. Casing collapsing strength design. Rock salt bed, cream salt bed, ooze rock formation, high-pressure waterflooding formation, unconsolidated sandstone reservoir, reservoir sloughing and formation sliding, and so on may collapse the casing. Obviously, the conventional design method cannot solve this casing collapse problem due to the uncertainty of external load character and size. For an interbedded formation of thick salt bed and cream salt bed or rock salt bed or cream salt bed of great difference in elastic modulus with thin mudstone and sandstone, or a rhythmic series of strata of salt lake sedimentation, under the conditions of high formation dip angle or vicinity to fault, the nonuniform creep of rock salt bed and cream salt bed in the lateral plane is the main factor incasing deformation, and a relative interlayer sliding may also be generated. The casing bears a nonuniform squeeze load in these intervals. These are the reasons why casing easily sticks and collapses in most intervals of rock salt, cream salt, and ooze rock of high dipping structure or contorted structure.

The API/ISO thick-wall or nonstandard extra-strong casing is often required to be used in order to solve the aforementioned problems. The thick-wall casing series has been added to the API/ISO standards. For instance, the wall thickness of 10 3/4-in. casing can be increased from 7.09 mm to 20.24 mm, while the wall thickness of 7 5/8-in. casing can be increased from 7.62 mm to 19.05 mm. In a well in which a 7 5/8-in. casing can be set, a 7 3/4-in. casing can also be set. Therefore, 7 3/4-in. casing is added to the API/ISO standards, and each steel grade has only a wall thickness of 15.11 mm. With a constant outside diameter, an increase of wall thickness will decrease the inside diameter, thus affecting subsequent drilling, completion, or downhole operations. In order to solve this problem, the outside diameter can be increased while keeping the inside diameter constant. This will deal with hole structure, safe casing running, close-clearance cement job quality, casing thread,

and so on. The prevention of casing collapse is a composite systems engineering task and should be considered in technical, economic, and risk grade aspects.

The casing collapsing strength formula of API 5C3 cannot be used for calculating the collapsing strength of extra-strong casing, whereas the ISO 10400 standards can be used for calculating the collapsing strength of extra-strong casing.

For a formation at which the casing may be seriously collapsed, the hole structure of concentric casing and concentric cement sheath can be adopted, that is, this formation is sealed by intermediate casing, and liner hanger is set above this formation.

**Casing Failure of Free Section.** The no-cementing section in the annulus is known as the free section. Particular attention should be paid to the casing design and management of this section. The statistical data indicate that the casing failure of the free section is generated more frequently and seriously than that of the cementing section. The following problems should be considered in free section design and management:

1. Free section casing inflexion possibility and effect

Casing inflexion of the free section may be generated when the stability of the free section casing is lost under the action of axial force. For a specific diameter casing, whether the inflexion may be generated depends on increase of temperature, density of drilling fluid retained outside the casing, density of fluid inside the casing, setting force when slip is set in the casinghead, and so on. An appropriate pulling force is needed when slip is set in the casinghead in order to avoid the casing inflexion of the free section during subsequent oil and gas production or downhole operations. Under most conditions the inflexion is restrained by the borehole, and a serious effect may not be generated. However, casing failure may be caused by inflexion when there is a borehole enlargement section. This casing failure may

include thread leak and casing wear during downhole operations, and so on. If inflexion is generated in the former casing, corrosion may be aggravated at the contact point between the two casings.

2. Casing collapse by high pressure of a closed annulus

During two-stage cementing, a closed annulus may occur at the bottom and top of the no-cementing section. If the casing outside of the free section is in the former casing, or some section is at a tight openhole formation interval and another section is in the former casing, a closed annulus can be formed. The temperature and pressure of media retained in the closed annulus may be increased by the returned drilling fluid used for drilling deep formation or the fluid produced through tubing. The high pressure of the annulus may collapse the casing. If corrosion is generated in the free casing section, local pressurized sagging deformation may be generated.

In deep-well and high-temperature high-pressure well designs, the aforementioned downhole closed annulus should be avoided. If some closed annulus is in the openhole section, the high pressure of the closed annulus can be expected to be released and to enter formation.

3. External corrosion of free section casing

The external corrosion of free section casing includes corrosion caused by the drilling fluid retained in the annulus. In addition, the performance of drilling fluid may fail under the long-term action of high temperature, and drilling fluid density may be reduced by forming a water zone due to the separation or precipitation of weighting material and solids, thus leading to the reduction of pressure on formation and the invasion of corrosive fluid in formation. If a micro-annulus is formed due to imperfect cement job quality or downhole operations, the corrosive fluid in the formation sealed by cement may invade

the free section, thus causing serious casing corrosion.

4. Wear and fatigue failure of free section casing

The casing strength of API/ISO standards is calculated on the basis of new casing; however, the strength or fatigue strength may be reduced by free section casing wear and impact, which may generate microcrack. If there is no liner tieback, and the intermediate casing is also used as a production casing, the casing wear and fatigue should be earnestly considered. In addition, casing wear and fatigue during drilling cement plug, workover, or downhole operations must also be considered. When the drill string rotates (especially under high speed) in the casing, the microcrack of free section casing may be generated by impact. If the make-up torque of API/ISO round thread is going too great, fatigue crack may be generated at the complete end thread of the pin thread, and the collar can easily crack longitudinally. The fatigue resistance of a trapezoidal thread is higher than that of a round thread.

**Long-Term Service Life of a Cement Sheath.** At present, the long-term service life of a cement sheath lacks specific standards and reliable monitoring methods in use for cementing design. In high-temperature high-pressure deep wells and H<sub>2</sub>S- and CO<sub>2</sub>-containing wells, the performance and long-term service life of the cement sheath are still faced with a rigorous challenge. The cement job quality detection requirements, which are only met after cementing, cannot ensure the long-term service life of a cement sheath. Cement sheath failure may aggravate casing corrosion and lead to possible blowout. In the integrity management and design of production casing, special attention to the following problems should be paid:

1. Deep-well close-clearance annulus cement job quality. The problems of deep-well

close-clearance annulus cement job quality include cementing circulation loss, which may generate outside-casing local section with no cement; low displacement efficiency, which causes mud channeling; and thin cement sheath, which is easily contaminated by drilling fluid and leads to reduction of strength. Thus the requirement of quality is difficult to meet.

2. High-temperature high-pressure deep well cementing. Overestimation of circulation temperature in consideration of safe cementing may lead to using cement that has an excessively long pumpable time. An overlong cement setting time may cause gas and water to invade the annulus and disrupt cement setting. A high temperature may cause strength retrogression of cement stone or lose the tightness of cement stone.
3. Hydrogen sulfide and carbon dioxide may aggravate the corrosion of the cement sheath under high temperature and pressure. Coexistence or combinations of methane, hydrogen sulfide, carbon dioxide, and formation water may corrode the cement sheath; however, there are no detailed studies and standards about the effects of the coexistence of methane, hydrogen sulfide, carbon dioxide, and formation water on the long-term service life of cement stone. Under high temperature and pressure, hydrogen sulfide and carbon dioxide may first corrode the cement sheath and then proceed to corrode the casing. The corresponding  $H_2S$ - and  $CO_2$ -resisting cement systems and additives need to be researched and developed. Special attention should be paid to the erosion of cement by supercritical carbon dioxide under high temperature and pressure. The corrosion of cement by carbon dioxide and the generation of micro-annulus have been found by casing logging. Laboratory evaluation indicates that for common oil well cement, the set cement may be seriously carbonized and cracked in the environment of 28 MPa

and  $90^\circ C$  supercritical carbon dioxide within one month.

4. The change of pressure or the downhole operations may damage the cement sheath. Cement job quality detection after cementing in many wells shows a good cement job quality; however, further logging after a certain period off production or after downhole operations indicates that micro-annulus has been generated. The colliding and expanding of the casing by downhole operations may damage the cement sheath. The pressure test of the casing has been presented. Hydraulic fracturing with no tubing packer may cause permanent damage to the cement sheath. The improvement in cement properties and the formulation of rational production and downhole operation systems are required in order to ensure the long-term working properties of cement.

## 5.2 HOLE STRUCTURE AND TYPES OF CASING

---

### Hole Structure

In recent years, advances in drilling technology and casing manufacture technology have provided the grounds for the selection of production casing and tubing. Full understanding and application of these technologies are of great importance to the optimization of production casing during well completion. There is a large amount of casing and connection structure of nonstandard size for meeting the requirements of well completion and hole structure. During designing, the ISO 11960 (similar to API SCT) standard casing diameter is first selected, and nonstandard casing size series can be selected if necessary.

**Hole Structure of Standard Casing Size Series.** Figure 5-1 is a casing and bit size selecting and matching path diagram of conventional hole structure. The conventional hole structure is shown by solid lines and is generally as follows.

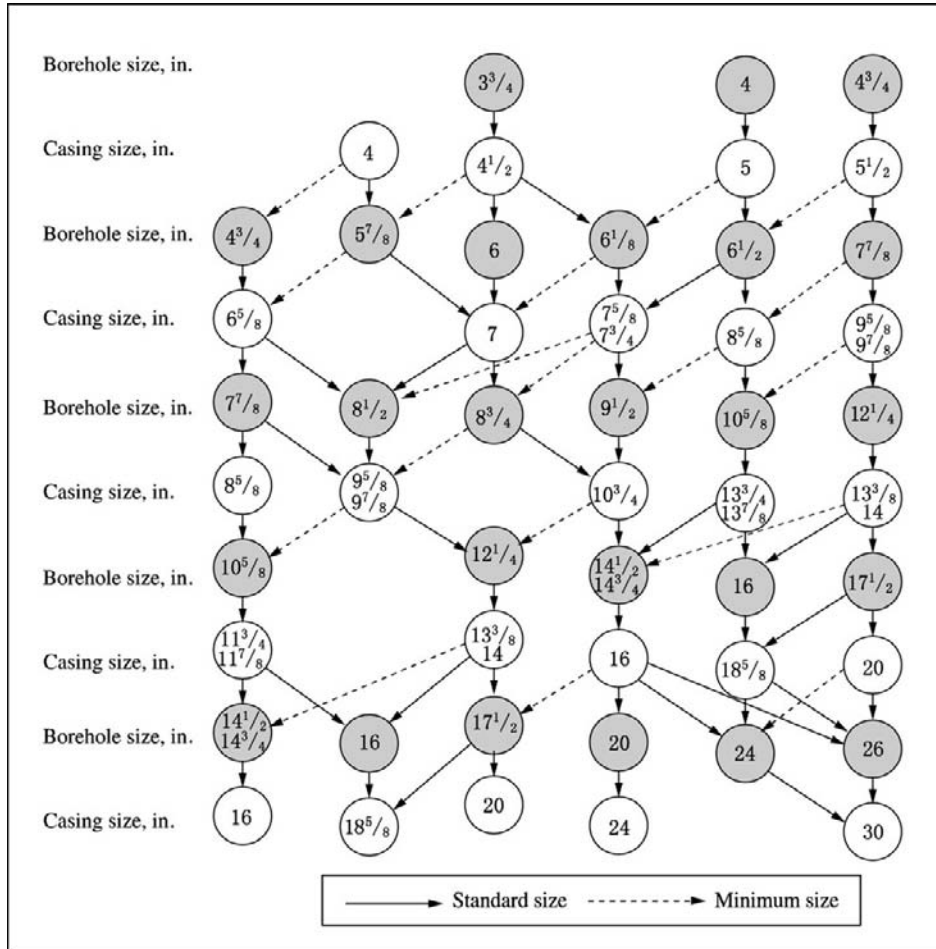


**FIGURE 5-1** Conventional casing program.

Casing: 20 in. + 13 3/8 in. + 9 5/8 in. + 7 in. + 5 in. (4 1/2 in.)

Bit: 26 in. + 17 1/2 in. + 12 1/4 in. + 8 1/2 in. + 5 7/8 in.

This hole structure is generally feasible, and has high matching and standardizing degrees of various tools and accessories.

Long-term production practice has shown problems with this hole structure, such as casing or liner that is too small, which may generate problems of cement job quality, testing, production, downhole operations, safety of string, and so on. Casing sticking may be generated by using a 7-in. or 5-in. casing due to the small clearance

with the borehole, and the cement job quality is difficult to ensure. Enlarging the hole structure by one grade on the basis of present drilling technology may refer to the problems of large borehole size, low drilling rate, high cost, and so on.

A hole structure that has been proven in practice to be comprehensively predominant is 13 3/8 in. + 10 3/4 in. + 7 5/8 in. (or 7 3/4 in.) + 5 in. (or 5 1/2 in., extremeline type). The features of this hole structure are as follows.

1. A 10 3/4-in. casing is set at the former pack-off location of 9 5/8-in. casing. In order

to run the 10 3/4-in. casing smoothly, the previous 12 1/4-in. bit is changed to 12 3/4-in. bit, or the 12 1/4-in. borehole becomes vertical to the full extent with no serious dogleg. The 10 3/4-in. casing with a small diameter collar (or of extremeline type) is used in order to increase the outside casing clearance.

- Under normal conditions, a 7-in. casing is set in a 9 1/2-in. borehole during well completion. A 7-in. casing has a large outside casing clearance, thus enhancing cement job quality.
- Under abnormal conditions, a 7 5/8-in. casing is set in a 9 1/2-in. borehole, and then the well is drilled by using a 6 1/2-in. bit. If necessary, a 5 1/2-in. liner with no collar is set, and even the well is continuously drilled by using a 4 5/8-in. bit, and then open hole completion is adopted.

**Hole Structure of Nonstandard Casing Size Series.** The hole structure of nonstandard casing size series is mainly used under the following conditions:

Deep wells, superdeep wells, high-pressure gas wells, and corrosive gas wells are required to be multicased wells, and the standard casing size series cannot basically meet their requirements. Figure 5-2 shows the hole structure of a sour gas well. It is a stepped structure with a larger upper part and a smaller lower part. A larger casing size is adopted in the upper well section so that a larger casing or liner can be set at the final completion stage. In a high-pressure gas well or acid gas well, a downhole safety valve is generally required to be set at 50 to 100 m below the wellhead. This requires a casing ID large enough to hold the safety valve and control line.

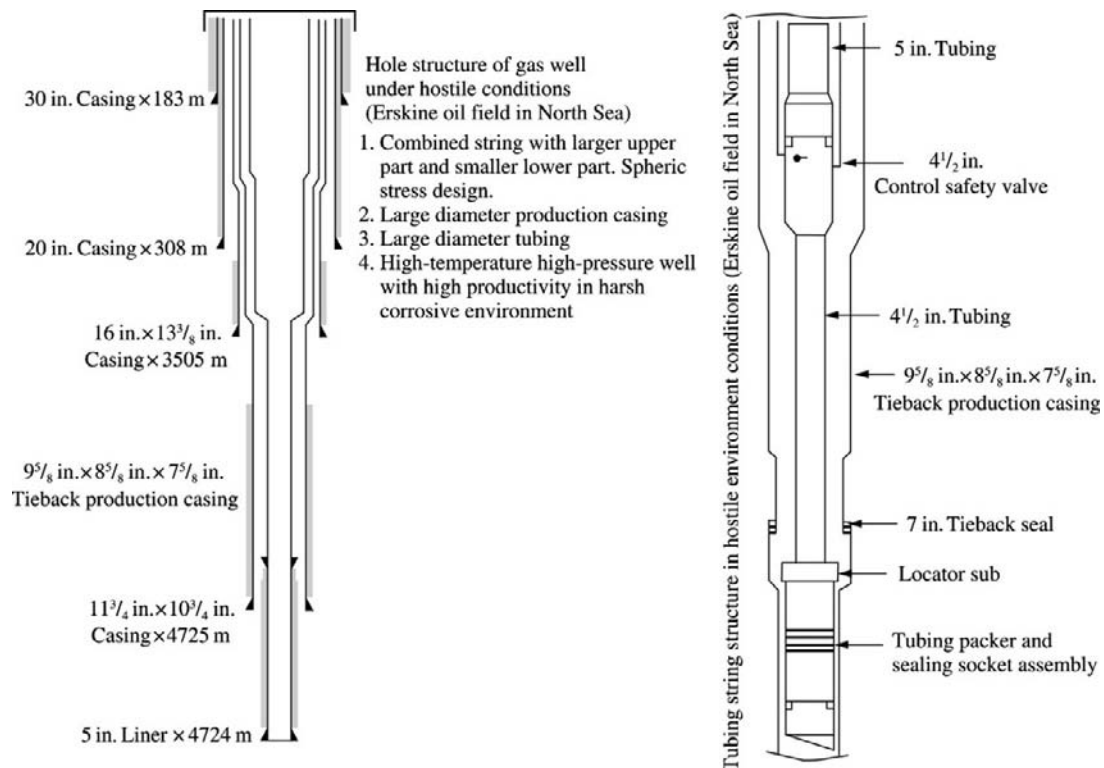


FIGURE 5-2 Hole structure and tubing string structure of gas well in hostile environment.

The nonstandard casing size series is adopted in order to obtain the largest possible production casing diameter. A superstrong casing is sometimes required in order to resist the collapse pressure of rock salt bed or cream salt bed or reduce the stress level of a hydrogen sulfide environment. Therefore, the following measures should be taken:

1. Using special size casing or extremeline casing
2. Using the technique of reaming while drilling
3. Improving the drilling technology and borehole quality, thus favoring running in the casing of small annulus

In a sour gas well, a casing with a yield strength lower than 95ksi and a wall thickness up to 16–25 mm (increasing wall thickness by enlarging OD instead of reducing ID) is required to the full extent. Using a casing program similar to that in Figure 5-2 favors the solving of the annulus clearance problem.

**Expandable Casing Technique and Hole Structure.** The expandable casing of the API standard casing size series is run in the intermediate casing and is expanded to the inner wall of the intermediate casing by using special tools and technology. The openhole part can be cemented, while the overlapping part of the casing has hanging and packing elements. The difference between the two inside diameters of the two casings is only the wall thickness after expansion. This technique is of great importance to deep drilling, drilling under complicated conditions, and hole structure under these conditions. It can increase the casing diameter and the technical and economic benefit during well completion.

## Casing Size and Steel Grade Series

**Standard Casing Size Series.** The casing size series standards have been presented by ISO 11960 and API Spec 5CT and accepted by the international petroleum industry trade. Generally, the casing series are produced in accordance with the API standards. The non-API casing goods are specially ordered.

The casing size series stipulated in the standards include mainly the following:

### 1. Casing OD

There are 14 OD<sub>s</sub> from 114.3 mm (4 1/2 in.) to 508 mm (20 in.). For production casing, the five OD<sub>s</sub> commonly used include 127.0 mm (5 in.), 139.7 mm (5 1/2 in.), 177.8 mm (7 in.), 193.7 mm (7 5/8 in.), and 244.5 mm (9 5/8 in.). The casing OD of 168.3 mm (6 5/8 in.) is rarely used.

### 2. Wall thickness

For the same casing OD, several wall thickness sizes are stipulated by the API standards, thus forming different strength grades for selection. Several wall thickness sizes of heavy wall casing are added to the new wall thickness series in order to meet the requirements of high collapsing strength, high tensile strength, and sufficient corrosion allowance. For example, the casing with 139.7 mm (5 1/2 in.) OD includes 12 wall thickness sizes from 6.20 mm to 22.22 mm in the standards.

### 3. Weight per unit length

The weight per unit length commonly used is a reduced weight that includes collar and thread and is used for calculating the total weight and tensile strength of the casing. Under the conditions of upset end or extremeline casing, the corresponding weight per unit length should be checked.

### 4. Casing ID

The ID can be used for calculating internal volume and strength. It is not a deterministic value and changes with OD and allowance.

### 5. Drift diameter

The diameter of casing through which the standard drift diameter gauge can freely pass is known as drift diameter. The maximum diameter of any casing to be run in the well should be smaller than the drift diameter. This is the final detecting step that should be taken before running the casing in order to determine whether the casing is deformed due to collision or squeeze during transportation. It should be noticed that the drift diameter is not the criterion for checking the ellipticity of

casing, and there are special standards and methods of checking the outside diameter and wall thickness of casing. The diameters and lengths of drift diameter gauge under different casing OD<sub>s</sub> are shown in ISO 10960 and API Spec 5CT.

#### 6. Collar diameter

The standards of common and small diameter collars in smaller casings than 10 3/4 in. are presented by ISO 10960 and API Spec 5CT. A small diameter collar is used when the annulus clearance is smaller. The diameter of a small collar is 9.52 mm to 12.7 mm larger than the diameter of the casing body. Only the buttress thread casing has a small diameter collar. In order to increase the tensile strength and internal pressure strength of small diameter collar, the collar can be made of a steel product of a higher steel grade. The tensile strength of a small diameter collar may be lower than that of the casing body and may also be lower than that of the casing thread of a standard collar. The tensile strength of a round thread casing is higher than that of a small diameter collar casing under the condition of heavy wall casing of the same steel grade and same size. However, under the condition of thin wall casing, the tensile strength of a small diameter collar is still higher than that of standard round thread casing.

**Casing Steel Grade Standard and Code.** The strict quality requirement for steel is due to the harsh working conditions of casing. The steel product should be produced and checked in accordance with special standards or specifications. ISO 11960 and API Spec 5CT have specified the steel product standards of casing. The strength of casing has been calculated by API 5C3 and ISO 10400 in accordance with the material and the specific technical terms stipulated by ISO 11960. The international standard steel grade consists of letter and code. The letter is optional and has no special meaning, while the code shows the minimum tensile yield strength of casing material, which is equal to the code multiplied by 1000 psi (6894.757 kPa).

For instance, the steel grade of N80 has the minimum tensile yield strength of 80,000 psi (551.6 MPa).

The ISO 11960 standards specify in detail the chemical elementary composition, heat treatment status, performance requirement, checking standard, and so on, and the technological requirements of manufacture and quality standard allow for unforeseen circumstances. The specific technical terms can be consulted by buyer and manufacturer. For deep wells and gas wells, and so on, the more rigorous technical terms should be implemented. The strength of the casing is calculated by ISO 10400 in accordance with the material and the specific technical terms of ISO 11960. For instance, different heat treatment statuses may have different internal pressure strengths and collapsing strengths. The internal pressure strengths of casing are respectively calculated under the different defects of wall thickness on the basis of the theory of fracture mechanics. The internal pressure strength of casing under the wall thickness defect of 5% to 12% is lower than that under the wall thickness defect lower than 5%.

**Types of Casing Steel Grade.** The ISO 11960 and API Spec 5CT standards classify the casing steel grades from the angle of manufacture, while this book will briefly explain the classification from the angle of casing selection and design. Casings are classified as common casing, high-strength casing, and corrosion-resistant casing.

#### 1. Steel grades of common casing

Common casing is most commonly used, is technically mature, and is well known by designers and users. The steel grades of common casing include H40, J55, K55, N80-1, N80Q, and P110. The maximum content of sulfur and phosphorus, which are harmful elements, is limited. The elementary composition of other alloying elements is determined by the manufacturer. Common casing may be seamless casing or straight weld casing.

J55 and K55 have the same minimum yield strength value of 375 MPa. However, the ultimate tensile strengths of J55 and K55 are 517 MPa and 655 MPa, respectively. This will give J55 better mechanical and thermal fatigue resistance and crack resistance than K55. For a thermal production well, the heavy wall K55 casing is appropriate instead of J55 casing. The former has a better thermal fatigue resistance property than the latter.

2. N80 is the steel grade most commonly used and most commonly fails. N80-1 and N80Q can be composed of the same alloying elements. During heat treatment, N80-1 steel is treated by normalizing and tempering, while N80Q steel is treated by quenching and tempering. Therefore, the collapsing strength and internal pressure strength of N80Q are higher than that of N80-1. N80-1 or N80Q should be clearly shown by the designer when N80 casing is selected.

3. Steel grades of high-strength casing

Q125 is the only high-strength steel grade in the standards, and others have not been listed. However, 140 ksi and 150 ksi of high steel grade have been used. In a deep well with a depth of 5000–9000 m or the rock salt interval of a deep well, a high steel grade casing is often required. The use performance of high-strength steel is sensitive to the matching of strength with toughness and residual stresses, cracks, and volumetric defects, and so on during manufacture. Be prudent during designing, detection, and use.

The harmful elements (sulfur and phosphorus) in the Q125 steel are restricted more strictly in the standards. Some alloying elements should be limited. For instance, the maximum allowable contents of sulfur and phosphorus in the Q125 steel are 0.010% and 0.020%, respectively. However, the maximum allowable contents of sulfur and phosphorus in common casing steel can be 0.030%. In fact, it is not difficult to control the content of sulfur and phosphorus by using

advanced metallurgical technology, and steel product quality control has been transferred to the rolling process and heat treatment technology. The Q125 steel is sensitive to crack or volumetric defect. The standards stipulate that the defect depth on the internal or external surfaces should not be larger than 5% of wall thickness. However, for common casing steel grade, the defect depth should be smaller than 12.5% of the casing wall thickness, and the casing can still be accepted after proper grinding and repairing. It should be especially noticed to prevent impact, undercut, and any possible corrosion pit during transportation, storage, and downhole operation of high-strength casing.

4. Steel grades of corrosion-resistant casing

The steel grades of corrosion-resistant casing include M65, L80 (L80-1, L80-9C<sub>r</sub>, L80-13C<sub>r</sub>), C90, C95, and T95. In these steel grades (except M65), the harmful elements (sulfur and phosphorus) have been limited more strictly, and some other elements are also limited.

M65 is a new steel grade and has not been widely used. It is a steel grade transitional from J55 to L80. M65 has a limitation of harmful elements (sulfur and phosphorus), which is the same as common casing steel grade. Other alloying elements are not limited. The HCR hardness should not be higher than 22.

In the ISO 11960 standards, L80 includes L80-1, L80-9C<sub>r</sub>, and L80-13C<sub>r</sub> (or API 13C<sub>r</sub>). L80-1 is used in the H<sub>2</sub>S environment, while L80-9C<sub>r</sub> and L80-13C<sub>r</sub> are used in the CO<sub>2</sub> environment. In the corrosive environment in which carbon dioxide predominates, Super 13C<sub>r</sub> has a higher corrosion resistance than L80-13C<sub>r</sub>. This difference should be noticed during designing.

L80-1, C90 (C90-1 and C90-2), C95, and T95 (T95-1 and T95-2) are used in the H<sub>2</sub>S environment. It should be noticed that only L80-1, L90-1, and T95-1 can be used in the H<sub>2</sub>S environment at a temperature lower than 65°C, whereas C95, C90-2, and T95-2 can

only be used in the H<sub>2</sub>S environment at a temperature higher than 65°C. The content control of harmful elements, the contents and matching of alloying elements, and the hardness and deviation range of hardness of the aforementioned typ. 1 are more stringent than those of typ. 2. These differences should be noticed during designing and ordering.

**High Collapsing Strength Casing.** The high collapsing strength casing means casing of which the steel grade and wall thickness accord with the ISO 11960 standards and of which the collapsing strength is higher than the collapsing strength rating of API 5C3. The collapsing strength of high collapsing-strength casing is about 30% higher than that of common casing. This is of great value to deep wells because of the higher collapsing strength under the condition of no increase of wall thickness or casing weight. A high collapse resistance is achieved by reducing ellipticity and wall thickness unevenness and by reducing the generation of residual stress.

At present, high-collapsing-strength casing is of nonstandard casing, and its collapsing strength is provided by the manufacturer. A downhole rock salt bed and a bed that can easily slide may generate nonuniform squeeze pressure or local stress concentration; thus, high-collapsing-strength casing may be inefficient, and heavy wall casing is appropriate under this condition.

**Straight Weld Casing.** Straight weld casing manufactured by using the rolled-plate high-frequency electric resistance welding (ERW) technique is an important technical advance in the steel pipe trade and petroleum pipe engineering. At present, for large-diameter casings (16 in., 18 5/8 in., 20 in., or larger), only the straight weld is gradually adopted. For casings of 5 in. to 13 3/8 in., only the thin wall casing can be manufactured by using straight weld. Because weld is a weak link, in the steel grades that are appropriate to the H<sub>2</sub>S environment, C90 and T95 can only select seamless steel pipe, while C95 can

select straight weld casing (the pipe body is a straight weld pipe, but the collar should be a seamless pipe). In comparison with the common seamless casing, the straight weld casing has the following merits:

1. High accuracy of sizes (including outside diameter, wall thickness, and roundness). Generally, the ellipticity does not exceed 0.5%, and the deviation of wall thickness does not exceed -7.5% of nominal wall thickness.
2. Good toughness. There is a small difference of material property between longitudinal direction and lateral direction.
3. Higher collapsing strength and internal pressure strength. The collapsing strength is 30% to 40% higher than the same type API seamless casing.
4. Low cost and good benefit. In comparison with the same type of seamless casing, the cost of straight weld casing is 5% to 10% lower. Under the condition of the same safety factors, a casing with a smaller wall thickness can be used.

## Casing Thread and Connection Structure

### API/ISO Threads

#### 1. Types of thread

The types of API/ISO threaded casing include short round threaded and coupled (STC) casing, long round threaded and coupled (LTC) casing, buttress threaded and coupled (BTC) casing, and extremeline (XL) casing. Figure 5-3 shows the API/ISO types of thread.

#### 2. API/ISO round thread seal and strength

The API/ISO round thread has a lower manufacture cost and a certain sealing property. The sealing of round thread is achieved by the surplus grip of the thread on the side face. The top clearance of the tooth is 0.152 mm. The filling of sealing compound in the clearance provides a supplementary sealing action.

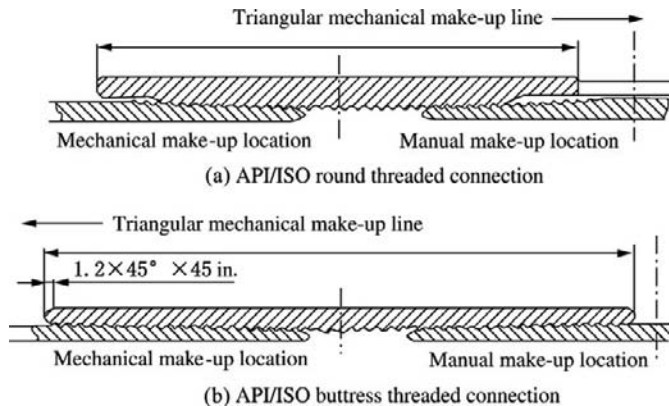


FIGURE 5-3 API/ISO types of thread.

In accordance with the effects of steel grade, wall thickness, and outside diameter on the tensile strength of thread and the matching relation, the API/ISO round thread can be short threaded and coupled (STC) or long threaded and coupled (LTC). The STC and LTC can adopt H40, J55, K55, and K65. Under the condition of thin body wall, it can be STC. The various grade casings of 10 3/4 in. to 18 5/8 in. can only be STC, while the 6 5/8- to 9 5/8-in. casings of steel grades above 80 ksi are mostly LTC (only the casing with thin body wall is STC). The API SC3 or ISO 10400 standard can be consulted to determine which type casing can be STC or LTC.

Round thread casing has been widely used. The following limitations should be noticed when an API/ISO round thread is designed and selected:

- a. Not enough gas tightness inappropriate to high-pressure oil and gas wells;
- b. Low strength of connection, which is only 60% to 80% of the yield strength of the casing body. The statistical data indicate that in the API round thread casing failure cases, the cases of thread connection failure account for more than 75%. The main failure forms include:
  - (1) Thread slipping: External thread reduces and threads off under the action of axial forces.

- (2) Thread galling: Tooth metal seizure makes the thread lose sealing property.
- (3) Thread breaking: Low fatigue strength of round thread. Changes of temperature, pressure, and downhole operations, and so on, may generate alternate load and lead to external round thread root breaking of long no-cementing openhole section casing.
- (4) Thread expanding: Expanding or longitudinal cracking of collar.
- (5) Boring by corrosion: There are various corrosion factors at connection. Boring by corrosion may be from internal wall to external wall or from external wall to internal wall.

### 3. API/ISO round thread and buttress thread with seal ring

In consideration of the inadequate sealing property of API/ISO round thread and buttress thread, the API/ISO standards have specified to make a ring groove at the internal threads of both ends of the collar, and a nonmetallic rectangular sealing ring is inserted into the groove in accordance with the new API/ISO standards. Figure 5-4 shows the collar structure with a sealing ring and the sealing ring. The A, C, and D have different values for round thread, buttress thread, and different casing sizes. The sealing ring width F and thickness E of round thread and buttress thread are 3.96 mm and

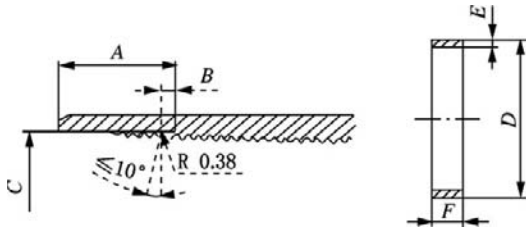


**FIGURE 5-4** The structure of the collar with sealing ring (left) and the sealing ring (right).

2.54 mm, respectively. The material of the sealing ring is the polytetrafluoroethylene (PTFE) resin filled with glass fiber by 25%. The API/ISO round thread and buttress thread with this sealing ring can increase the sealing property and can first be used on production casing that has a high sealing requirement. However, they are not recommended to be used in high-pressure gas wells or gas wells with a high  $H_2S$  or  $CO_2$  content.

#### 4. API/ISO buttress thread seal and strength

The tensile strength of API/ISO buttress thread is higher than that of round thread and is dependent on the strength at the full thread of the end of the pipe body or the strength of the collar. In order to ensure that the cross-sectional area at the body end thread is not smaller than that of the pipe body, the outside diameters of the tubing and casing for making API/ISO buttress thread should be slightly larger than that of the pipe body (that is, a positive allowance is taken). If this requirement can not be met, it is inappropriate to machining buttress thread.

The sealing property of API/ISO buttress thread is lower than that of round thread. API/ISO buttress thread of production casing should be prudently selected, and the API/ISO buttress thread with sealing ring can be selected.

### Gas Sealing Thread of Casing and Connection Structure

#### 1. Gas sealing thread of casing

In order to overcome the aforementioned shortcomings of API/ISO thread, various

casing threads have been developed. They possess higher connecting strength and sealing property. The gas sealing thread means metal-to-metal contact seal and is mainly the metal-to-metal contact seal between the end of the external thread and the internal shoulder of the collar. At present, this connection structure has been widely used but has not entered the API/ISO standards. The gas sealing thread is a customary wording and is also known as premium connection.

The pressure on contact surface and the length of contact are the main decisive factors of gas sealing ability. When the length of contact with the sealing surface is greater, the mean stress on the contact surface may be smaller. Conversely, when the length of contact with the sealing surface is smaller, the mean stress on the contact surface should be greater. In order to achieve better gas sealing ability, it is feasible to increase the pressure on the contact surface and also to increase the length of contact. On the basis of this design concept, the sealing of gas sealing thread structure is generally achieved by the allowance fit of contact between metals.

Gas sealing thread structure can be tapered-face-to-tapered-face, tapered-face-to-spherical-face, and spherical-face-to-spherical-face in the light of sealing surface shape and can be end face seal, radial seal, and multiple seal, which is combined end face seal and radial seal in the light of the sealing surface location. The multiple seal has been widely adopted, and the radial metal-to-metal seal is predominant, while the one-end or multiple-end face seal is supplemental. VAM, NSCC, TM, 3SB, BDS, FOX, and so on, are typical. Figure 5-5 shows several end face seal structures that are commonly used.

The VAM series is the gas sealing thread and connection structure used most widely and is characterized by thick external thread end and rational stress distribution. Figure 5-6 shows a new type of VAM thread.

#### 2. Failure forms of gas sealing thread

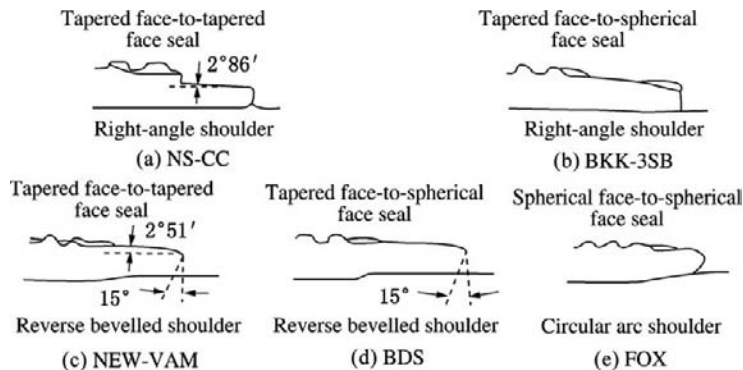


FIGURE 5-5 Several end face seal structures.

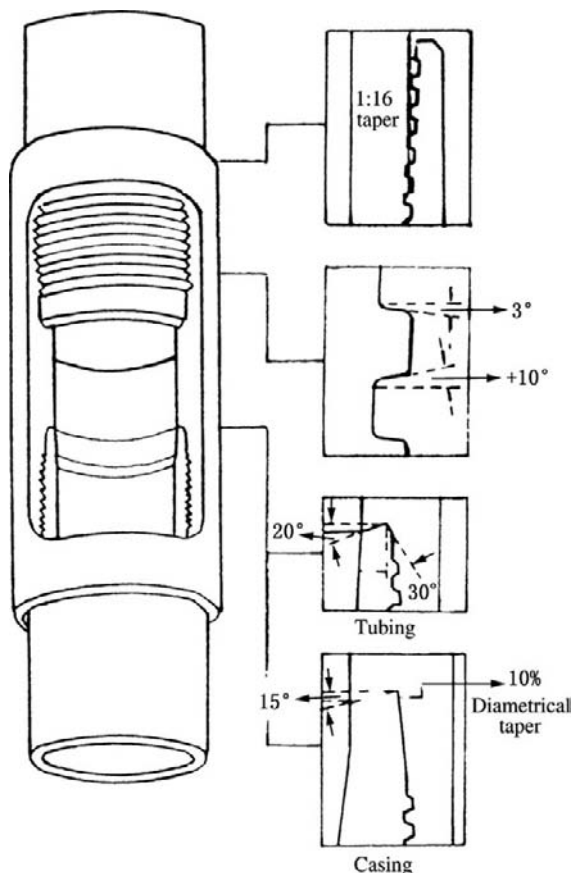


FIGURE 5-6 VAM thread.

There are many types of casing thread of metal-to-metal contact seal. They can be slightly different from each other, but their usabilitys are different. The possible failure forms include:

- Reduction of external thread end. The external thread end is thin and will bear a compressive stress after make-up. Reduction may also be caused by the well-head make-up torque, which is not strictly controlled.
- Boring and leaking at the external thread end by local corrosion. There is a high contact stress at the contact between the external thread end and the internal shoulder of the collar. The excessive compressive stress and contact stress may cause electric potential difference corrosion, stress corrosion, and crevice corrosion. Corrosion pits or holes on the external thread end face can be seen after the tubing is taken out. Serious consequences may be caused by losing the sealing property of tubing thread and leaking of corrosive gas into the tubing-casing annulus. A thick external thread end or a thread structure with a rational stress distribution is selected as much as possible.
- Collar cracking. The collar is under the action of axial, radial, and circumferential stresses. The stress crack of the collar should be considered under the condition of a  $H_2S$  environment or an environment

in which high-strength steel has high chloride content. When it is predicted that the environment may cause collar cracking, in order to reduce stress on the collar, a collar with a diameter as large as possible should be adopted to the full extent on the premise of ensuring that the collar can be run in. At the same time, thread sealant should be strictly selected in accordance with the related standard, and the make-up torque should be strictly controlled.

**Integral Joint Casing.** Under the condition of a smaller annular clearance, internal and external threads can be directly made on the pipe body with no collar. Generally, a pipe end should be upset or expanded, and an internal thread is made. At the other end, an external thread is made after reducing. The API/ISO standards have only specified one type of integral joint casing, which is just the streamline casing and is customarily called extremeline casing. The various integral joint casings developed in recent years have a gas sealing property higher than that of API/ISO streamline casing and have been widely used. During designing and use of other nonstandard integral joint casing, the data provided by the manufacturer can be consulted.

The thread of integral joint casing often adopts inverted trapezoidal thread, that is, the load-bearing face has a negative oblique angle of  $3^\circ$  to  $5^\circ$ . Under the action of axial force, the lateral component force on the load-bearing face will not generate radial component force on the collar, and the collar will not generate radial deformation. Figure 5-7 shows a VAM thread of integral joint casing.

The tensile strength of integral joint casing thread connection is only 65% to 80% of the tensile strength of the pipe body. Integral joint casing is generally used as a liner, and the tensile strength should be able to meet the requirement. The tripping operations of integral joint casing are inconvenient, and special tools are needed. In addition, inappropriate upset and heat treatment may generate residual stress. The stress concentration due to the change of cross-section

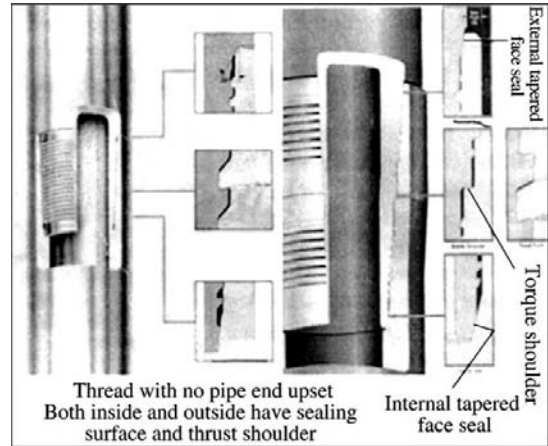


**FIGURE 5-7** Integral joint casing thread used under small annular clearance.

may aggravate stress corrosion. The integral joint casing should not be adopted to the full extent in oil and gas wells that contain hydrogen sulfide.

## Field Make-Up Operation Requirements

**Make-Up Rotations and Location.** Insufficient make-up torque cannot generate sufficient contact stress on the metal contact surface; whereas excessive torque may generate strain and sliding on the metal contact surface, thus leading to seal failure. For a long time, the make-up torque of power tongs was customarily taken as a mark of make-up by field operators. The ISO 11960 and API SCT standards stipulate that this should be based on the make-up rotations and location and that the buttress thread casings of all steel grades and diameters and most round thread casings should be operated in accordance with the following:

A triangle mark has been added to the make-up end of the pipe body by the manufacturer. Each type casing has an initial torque value, on the basis of which certain rotations are required so that the end face of the collar enters the triangle mark area and qualification is achieved at this time. If the triangle mark area is unreach-

or exceeded after making the specified rotations, the make-up operation is unqualified. For the distance between the triangle mark and the pipe end, the initial torque value used for calculating rotations, and the rotations, consult ISO 11960.

The optimum make-up torque value range of gas sealing thread is recommended by the manufacturer on the basis of experimental results.

**Thread Sealant.** Thread sealant is used for lubrication and seal of thread. The lubricant in thread sealant ensures the make-up under the rational torque and prevents thread galling or wearing, while the solids in thread sealant pack the thread backlash and provide sealing. Serious consequences may result from using unqualified thread sealant. Refer to ISO 11960 and ISO 13678. The latter is similar to API RP 5A3. These standards are only the lowest requirements. The thread sealants provided by some manufacturers have higher properties and a more friendly environment than the specified standards.

The thread sealant should meet the following requirements:

1. Appropriate lubricating property. During make-up, an adequate lubricating property is required in order to ensure the rated make-up torque and prevent galling.
2. Thread galling resistivity. Thread galling may affect sealing property and may damage casing.
3. Sealing property. The solids in thread sealant pack the thread backlash and provide sealing. Trapezoidal thread has a low sealing property, and a sealant appropriate to trapezoidal thread should be adopted. The short polytetrafluoroethylene fiber added properly to sealant can obviously enhance the sealing property of trapezoidal thread; however, at the same time, the lubricating property should be adjusted in order to prevent excessive make-up torque.
4. Safety and environmental protection. Lead and organic solvent in the sealant may be harmful to eyes and skin as well as environment. As a result, safety and environmental protection should be taken as a performance index of sealant.
5. Adaptability to environment. It includes:
  - a. High-temperature stability. The lowest standard is that at 148.9°C, the thread sealant may not be excessively liquefied, may not be chemically decomposed, can be oxidation-resistant, may not be dried and hardened, may not absorb water, and has no obvious volumetric change. In oil and gas wells that contain hydrogen sulfide, it should also be corrosion-resistant.
  - b. High-temperature sealing property. The lowest standard is that at 148.9°C the thread sealant should have an adequate sealing property in order to prevent leaking. In wells that have a temperature higher than 148.9°C (such as superdeep wells, thermal production wells, and geothermal wells), a high-temperature thread sealant that has a special formulation should be used.
  - c. In cold weather, it is easy to apply with a brush. In the temperature range of -17.8 to 48.9°C, the sealant can be used for applying and can adhere to metal.

### 5.3 STRENGTH OF CASING AND STRENGTH DESIGN OF CASING STRING

At present, the strength calculation of casing, tubing, and drill pipe is in accordance with the API 5C3 and API 5C5 standards. Both practice and studies indicate that the related standards have some shortcomings, and a new related standard (ISO 10400) has been formulated.

#### Casing Strength Calculation in API 5C3

**Collapsing Strength Calculation.** In the API 5C3 standard, the casing collapse pressure calculation includes four regions, that is, four formulae that include collapse pressure of minimum yield, plastic collapse pressure, elastoplastic collapse pressure, and elastic collapse pressure. The formula of collapse pressure of yield and the formula of elastic collapse pressure are

theoretical derivation formulae, while the formula of plastic collapse pressure is an empirical formula that was obtained by regression analysis of 2888 tests of K55, N80, and P110 test pieces produced before 1968. The formula of elasto-plastic collapse pressure is the transitional region between elastic and plastic collapse pressures.

The meanings of the signs in the formulae are as follows.

D: outside diameter, mm

t: wall thickness, mm

D/t: diameter-to-wall thickness ratio

$p_{YP}$ : minimum yield strength collapse pressure, MPa

$p_p$ : minimum plastic collapse pressure, MPa

$p_T$ : minimum elastoplastic collapse pressure, MPa

$p_E$ : minimum elastic collapse pressure, MPa

$(D/t)_{YP}$ : D/t boundary value between yield strength collapse and plastic collapse

$(D/t)_{PT}$ : D/t boundary value between plastic collapse and elastoplastic collapse

$(D/t)_{TE}$ : D/t boundary value between elasto-plastic collapse and elastic collapse

$Y_p$ : minimum yield strength, MPa

1. Collapse pressure. When the circumferential stress on the inner wall of the casing reaches the minimum yield strength under external collapse pressure, the yield failure of casing is generated, as shown in Equation (5-2):

(5-2)

$$p_{YP} = 2Y_p \left[ \frac{(D/t) - 1}{(D/t)^2} \right]$$

The usable range of Equation (5-2) is  $D/t \leq (D/t)_{YP}$ :

$$(D/t)_{YP} = \frac{\sqrt{(A-2)^2 + 8(B + 6.894757 C/Y_p) + (A-2)}}{2(B + 6.894757 C/Y_p)}$$

2. Plastic collapse pressure. The plastic collapsing formula means that the stress generated by external collapse pressure may cause plastic deformation of the casing, which is a permanent deformation. The plastic collapse pressure formula is an empirical formula that

is based on a large amount of casing collapse test data, as shown in Equation (5-3):

(5-3)

$$p_p = Y_p \left( \frac{A}{D/t} - B \right) - 6.894757 C$$

The usable range of Equation (5-3) is  $(D/t)_{YP} \leq D/t \leq (D/t)_{PT}$ :

$$(D/t)_{PT} = \frac{Y_p(A - F)}{6.894757 C + Y_p(B - G)}$$

3. Elastoplastic collapse pressure. It is appropriate to the transition section between the minimum plastic collapse pressure and the minimum elastic collapse pressure and is also obtained by the regression of the test data, as shown in Equation (5-4):

(5-4)

$$p_T = Y_p \left( \frac{F}{D/t} - G \right)$$

The usable range of Equation (5-4) is  $(D/t)_{PT} \leq D/t \leq (D/t)_{TE}$ :

$$(D/t)_{TE} = \frac{2 + B/A}{3 B/A}$$

4. Elastic collapse pressure. Casing is a cylindrical shell, which may lose its elastic stability under the action of external hydrostatic pressure. The elastic collapse pressure of the casing is only dependent on the elastic modulus of the steel product and the geometry and is independent of the yield strength of the steel product. A large-diameter thin-wall casing is possibly located in the elastic collapse pressure region, thus high-strength steel product is not required.

When  $D/t \geq (D/t)_{TE}$ , as shown in Equation (5-5):

(5-5)

$$p_E = \frac{323.71 \times 10^3}{(D/t)[(D/t) - 1]^2}$$

5. Empirical coefficient values. The D/t boundary values and the coefficients A, B, C, F, and G in the four aforementioned API collapse pressure formulae are shown in Table 5-1.

TABLE 5-1 D/t Boundary Values and Factors in API Collapsing Pressure Formulae

Steel Grade	D/t Range			Plastic Collapse Pressure Factors			Elastoplastic Collapse Pressure Factors	
	(D/t) <sub>YP</sub>	(D/t) <sub>PE</sub>	(D/t) <sub>TE</sub>	A	B	C	F	G
H40	16.40	27.01	42.64	2.950	0.0465	754	2.063	0.0325
JK55	14.81	25.01	37.21	2.991	0.0541	1206	1.989	0.0360
JK60	14.44	24.42	35.73	3.005	0.0566	1356	1.983	0.0373
LN80	13.38	22.47	31.02	3.071	0.0667	1955	1.998	0.0434
C90	13.01	21.69	29.18	3.106	0.0718	2254	2.017	0.0466
CT95	12.85	21.33	28.36	3.124	0.0743	2404	2.029	0.0482
P110	12.44	20.41	26.22	3.181	0.0819	2852	2.066	0.0532
Q125	12.11	19.63	24.46	3.239	0.0895	3301	2.106	0.0582
A140	11.84	18.97	22.98	3.297	0.0971	3751	2.146	0.0632
A150	11.67	18.57	22.11	3.336	0.1021	4053	2.174	0.0666

In practice, the collapsing strength of casing is unnecessarily calculated by using the aforementioned formulae, and the collapsing strength value of specific casing can be found in the API 5C3 standard.

In long-term practice and studies, the following problems have been found in the collapsing strength calculation method of API 5C3:

1. The collapsing strength calculation method of API 5C3 cannot reflect the obvious technical advance in casing manufacture technique in recent years. For a pipe with a D/t value of 10 to 26, the length of the test sample is more than 8 times the pipe diameter. In light of the collapsing test data of the pipes produced by the industry, the measured collapsing strength is higher than the API 5C3 calculation result by more than 30%.
2. The test sample used for API 5C3 casing collapse test at the early stage was too short, and the collapse pressure obtained was on the high side due to the end face effect at both ends. Thus it cannot represent the actual casing collapsing strength. There are many factors that affect collapsing strength; thus, the measured collapsing strength data of production casing and its test piece have a higher discreteness. In order to ensure a lower collapse probability than 5%, the theoretical

formula correction factors and the empirical formulae are on the conservative side.

3. The API 5C3 collapsing strength calculation method cannot reflect the effect of casing manufacture method and quality on collapsing strength. The collapsing strength of casing with a good manufacture quality is higher than that obtained by using API 5C3. In recent years, high collapsing strength casing has been used in the industry. The API 5C3 collapsing strength calculation method cannot reflect the collapsing strength of high collapsing strength casing.

**Internal Yield Pressure Strength Calculation.** The internal pressure strengths of casing, tubing, and drill pipe in the API 5C3 standard are calculated in accordance with the thin wall Barlow's formula, which neglects radial stress. The formula supposes that under the action of internal pressure, pipe may fail when the material of the inner wall of the pipe starts yielding under the action of circumferential stress on the pipe wall. The internal pressure strength calculation formula in API 5C3 is as follows.

$$P_{\text{api}} = 2f_{\text{ymn}}(K_{\text{wall}}t)^2/D$$

where:  $f_{\text{ymn}}$  = minimum yield strength;  $D$  = outside diameter of pipe;  $K_{\text{wall}}$  = pipe wall allowance factor (for example, when the allowance

is  $-12.5\%$ ,  $K_{\text{wall}} = 0.875$ );  $p_{\text{iapi}}$  = internal yield pressure strength in API 5C3;  $t$  = pipe wall thickness.

The API 5C3 internal pressure strength value of casing is higher than that obtained by the formula used in ISO 10400 standard by 1% to 10%.

In effect, the seal integrity is still retained when the inner wall of the pipe starts yielding. The ultimate internal pressure strength of the pipe (pipe rupture and losing seal integrity) has been presented in ISO 10400. The circumferential tensile stress on the pipe wall is generated under the action of internal pressure. Thus the toughness of the material and the potential crack generated during manufacture may obviously affect the ultimate internal pressure strength. The rupture toughness and failure are neglected in the API 5C3 internal pressure strength formula. Therefore, this formula cannot reflect the difference of internal pressure strength between the previous steel pipe manufacture technique and the current advanced technique and cannot give actual internal pressure strength.

## Collapsing Strength Calculation in ISO 10400

### Basic Supposition and Calculation Principle

1. For an ideal thick wall pipe (round pipe with no defect), the ultimate pressure under which whole pipe wall enters the yield stress state is calculated only under the action of external pressure.
2. For an ideal thin wall pipe, the ultimate pressure of geometric elastic destabilization of pipe is calculated only under the action of external pressure.
3. The ultimate external collapsing pressure of pipe is probably between the elastic collapse and the full yield collapse or slightly lower than the full yield collapse value. An intermediate formula between the elastic collapse and the full yield collapse can cover various diameters, wall thicknesses, and steel grades. This formula is aimed at an ideal round pipe and does not take into consideration unavoidable manufacturing defects; thus its result is the ultimate collapsing strength.

4. Steel pipe manufacturing defect and property differences between different manufacturing techniques are hard to avoid. By comparison with the API 5C3 strength formula, the ISO 10400 strength formula contains the correction factors that consider the effects of manufacture defect and different manufacturing techniques on collapsing strength and is known as the formula of design collapse strength on which the design is based. In recent years, in order to meet the requirements of engineering, the non-API thick wall casing and non-API high collapse casing have been manufactured. The ISO 10400 formula of collapsing strength can be used for calculating the collapsing strength of non-API casing and tubing. It is not required to rely fully on the full-scale test sample collapse evaluation, which is only used as a check. The API 5C3 formula cannot be used for calculating the collapsing strengths of non-API thick wall casing and high collapse casing.

### Design Collapse Strength of Casing Only under the Action of External Collapsing Pressure.

In accordance with the aforementioned first supposition the yield collapse strength of ideal thick wall pipe is calculated using Equation (5-6):

$$(5-6) \quad p_{ydes} = k_{ydes} \times 2f_{ymn}(t/D)[1 + t/(2D)]$$

In accordance with the aforementioned second supposition, the ultimate collapsing strength of geometric elastic destabilization of ideal thin wall pipe is calculated using Equation (5-7):

$$(5-7) \quad p_{edes} = 0.825 \times 2E/\{(1 - \nu^2)(D/t)[(D/t) - 1]^2\}$$

The actual collapsing strength of casing can be expressed by using a reverse function. The right side of the formula shows the effect of actual casing ellipticity, wall thickness unevenness, and residual stress on collapsing strength.

$$(p_c - p_e)(p_c - p) = f\left(e, \epsilon, \frac{\sigma_R}{\sigma_Y}\right)$$

This formula is a univariate quadratic equation, and its solution is shown in Equation (5-8):

(5-8)

$$p_{des} = \{(p_{edes} + p_{ydes}) - [(p_{edes} - p_{ydes})^2 + 4p_{edes}p_{ydes}H_{tdes}]^{1/2}\} / [2(1 - H_{tdes})]$$

where: D = outside diameter of pipe; E = Young's modulus,  $206.9 \times 10^9$  N/m<sup>2</sup>;  $f_{ymn}$  = minimum yield strength;  $H_{tdes}$  = influence factor of residual stress during manufacture (Table 5-2);

e = out of roundness of pipe,  $\varepsilon = \frac{2(D_{max} - D_{min})}{D_{max} + D_{min}}$ ;

$\varepsilon$  = wall thickness unevenness of pipe,  $\varepsilon = \frac{2(t_{max} - t_{min})}{t_{max} + t_{min}}$ ;  $k_{ydes}$  = yield strength reduction factor (Table 5-2); t = pipe wall thickness;

$\nu$  = Poisson's ratio, 0.28;  $p_{edes}$  = ultimate collapsing strength of geometric elastic destabilization;  $p_{ydes}$  = collapse yield strength.

**Collapsing Strength under the Action of Axial Tension and Internal Pressure.** In general, the calculation method under the condition

of decrease in collapsing strength due to axial tension is known as the biaxial stress method. The simple biaxial stress method is used by ISO 10400 for calculating collapsing strength under axial tension. Under medium tensile stress ( $0 \leq$  axial stress/yield stress  $\leq 0.4$ ), the error of the simple method is within  $\pm 5\%$  (by comparison with the accurate method). The simple biaxial stress method is a rather safe calculation method and can meet requirements in practice.

1. Equivalent yield stress formula. The decrease of collapsing strength due to axial tension is equivalent to the decrease of yield strength of material under the action of axial tension, as shown in Equation (5-9).

(5-9)

$$f_{ye} = \{[1 - 0.75(\sigma_a/f_{ymn})^2]^{1/2} - 0.5\sigma_a/f_{ymn}\}f_{ymn}$$

where:  $f_{ymn}$  = minimum yield strength of material;  $f_{ye}$  = equivalent yield strength of

**TABLE 5-2 The Residual Stress Influence Factor  $H_{tdes}$  and the Yield Strength Reduction Factor  $K_{ydes}$  for Both Hot Alignment and Cold Alignment**

Steel Grade <sup>1</sup>	Cold Alignment		Hot Alignment	
	$H_{tdes}$	$k_{ydes}$	$H_{tdes}$	$k_{ydes}$
H40	0.22	0.910	Inapplicable <sup>2</sup>	Inapplicable <sup>2</sup>
J55	0.22	0.890	Inapplicable <sup>2</sup>	Inapplicable <sup>2</sup>
K55	0.22	0.890	Inapplicable <sup>2</sup>	Inapplicable <sup>2</sup>
M65	0.22	0.880	Inapplicable <sup>2</sup>	Inapplicable <sup>2</sup>
L80	0.22	0.855	0.20	0.865
L80 9Cr	0.22	0.830	0.20	0.84
L80 13Cr	0.22	0.830	0.20	0.84
N80 (typ 1)	0.22	0.870	0.20	Inapplicable <sup>2</sup>
N80 Q&T	0.22	0.870	0.20	0.870
C90	Inapplicable <sup>3</sup>	Inapplicable <sup>3</sup>	0.20	0.850
C95	0.22	0.840	0.20	0.855
T95	Inapplicable <sup>3</sup>	Inapplicable <sup>3</sup>	0.20	0.855
P110	0.22	0.855	0.20	0.855
Q125	Inapplicable <sup>3</sup>	Inapplicable <sup>3</sup>	0.20	0.850

<sup>1</sup>Only applicable to the nominal yield strengths of various steel grades. It is inadmissible to obtain the residual stress influence factor  $H_{tdes}$  and the yield strength reduction factor  $k_{ydes}$  of actual yield strength by using interpolation method.

<sup>2</sup>Generally, hot alignment is not applied to this steel grade.

<sup>3</sup>The ISO 11960 and API 5CT standards stipulate that cold alignment is inadmissible.

material under the action of axial tension;  $\sigma_a$  = axial stress, which should not be the stress generated by bending.

- By substituting  $f_{ymn}$  with  $f_{ye}$ ,  $p_{ydes}$  is calculated by using Equation (5-6).
- When there is internal pressure, the increase of collapsing strength  $p_{dese}$  is considered by using the linear superposition method, as shown in Equation (5-10):

**(5-10)**

$$p_{dese} = p_{des} + p_i[1 - (2t/D)]$$

where:  $D$  = outside diameter of pipe;  $p_{dese}$  = collapsing strength under axial stress and internal pressure;  $p_i$  = internal pressure;  $t$  = pipe wall thickness.

**Calculation Case.** Calculate the collapsing strength of 9 5/8-in. casing. Steel grade L80. Cole aligning pipe. Weight per unit length 53.5 lb/ft. Wall thickness  $t = 0.545$  in. Using Table 5-2,  $k_{ydes} = 0.855$ ,  $H_{ides} = 0.22$ . The minimum yield strength of L80 is 552 MPa, and the elastic modulus is  $2.07 \times 10^5$  MPa.

The following result is obtained using Equation (5-6):

$$p_{ydes} = 0.855 \times 2 \times 552 \times (0.545/9.625) \{1 + [0.545/(2 \times 9.625)]\} = 54.9 \text{ MPa}$$

The following result is obtained using Equation (5-7):

$$p_{dese} = 0.855 \times 2 \times 2.07 \times 10^5 / \{(1 - 0.28^2) (9.625/0.545)[(9.625/0.545) - 1]^2\} = 75.5 \text{ MPa}$$

The following result is obtained using Equation (5-8):

$$p_{des} = \{(75.5 + 54.9) - [(75.5 - 54.9)^2 + 4 \times 75.5 \times 54.9 \times 0.22]^{1/2}\} / [2(1 - 0.22)] = 43 \text{ MPa}$$

### Internal Pressure Strength Calculation in ISO 10400

Casing and tubing breaking due to internal pressure may have more serious consequences than collapsing. It may lead the borehole to be out of

control and cause an underground blowout, thus generating problems of environment and safety. Casing and tubing breaking due to internal pressure may be generated in a high-temperature high-pressure deep well, a high-pressure gas well, and a gas well that contains hydrogen sulfide, or during some downhole operations.

The ISO 10400 standard has introduced the theory and applicable achievements of advanced material engineering and fracture mechanics. The ISO 10400 internal pressure strength design of tubing, casing, and surface gathering pipeline is different from the API 5C3 internal pressure strength design. The advanced design methods and standards should be understood by oil and gas well engineering design and operation personnel and steel pipe designers and manufacturers.

The internal yield pressure strength based on the ISO 10400 standard is lower than that based on the API 5C3 standard. The internal tough-burst pressure strength under the condition of crack smaller than 5% of wall thickness is higher than the internal yield pressure strength; whereas the internal burst pressure strength under the condition of crack smaller than 12.5% of wall thickness may be lower than the internal yield pressure strength. This indicates that manufacturing quality may greatly affect the calibration of internal pressure strength.

#### Internal Yield Pressure Strength

- Internal yield pressure strength under zero axial load

When axial stress, external pressure, bending moment, and torque are zero, the initial yield strength of thick wall pipe with both open ends under combined radial and circumferential stresses can be calculated by using Equation (5-11):

**(5-11)**

$$p_{iYLO} = f_{ymn}(D^2 - d_{wall}^2)^2 / (3D^4 + d_{wall}^4)^{1/2}$$

where:  $D$  = outside diameter of pipe;  $d$  = inside diameter of pipe,  $d = D - 2t$ ;  $d_{wall}$  = inside diameter of pipe in consideration of wall thickness allowance on the basis of  $k_{wall}$  and  $t$ ,  $d_{wall} = D - 2tk_{wall}$ ;  $f_{ymn}$  = minimum yield strength;

$k_{\text{wall}}$  = wall thickness allowance factor, for example,  $k_{\text{wall}} = 0.875$  when the allowance is  $-12.5\%$ ;  $p_{\text{IYLO}}$  = internal pressure when the thick wall pipe with both open ends is yielded;  $t$  = pipe wall thickness.

- Internal yield pressure strength of pipe with both plugged ends

Internal pressure acts on both pipe ends when both ends are plugged. The pipe is acted on by the axial acting force due to internal pressure. A higher internal pressure strength is required by the axial force.

- Internal yield pressure strength under compound stress

Under the composite action of axial tension and compression, bending moment, and torque, the stresses in an elastic state include radial and circumferential stresses on thick wall cylinder, homogeneous axial stress due to various loads (except bending stress), axial bending stress, and torsional shear stress due to rotation around the axis of pipe string.

The internal yield pressure strength calculation under compound stress has not considered the bending stress generated by longitudinal compression and destabilization.

The initial yielding is defined by the following formula:

$$\sigma_e = f_{\text{ymn}}$$

where:  $f_{\text{ymn}}$  = minimum yield strength;  $\sigma_e$  = equivalent stress.

The equivalent stress  $\sigma_e$  is defined as shown in Equation (5-12)

### (5-12)

$$\sigma_e = [\sigma_r^2 + \sigma_h^2 + (\sigma_a + \sigma_b)^2 - \sigma_r\sigma_h -$$

$$\sigma_r(\sigma_a + \sigma_b) - \sigma_h(\sigma_a + \sigma_b) + 3\tau_{\text{ha}}^2]^{1/2}$$

$$\sigma_r = [(p_i d_{\text{wall}}^2 - p_o D^2) - (p_i - p_o) d_{\text{wall}}^2 D_2 / (4r^2)] / (D^2 - d_{\text{wall}}^2)$$

$$\sigma_h = [(p_i d_{\text{wall}}^2 - p_o D^2) + (p_i - p_o) d_{\text{wall}}^2 D^2 / (4r^2)] / (D^2 - d_{\text{wall}}^2)$$

$$\sigma_a = F_a / A_p$$

$$\sigma_b = \pm M_b / I = \pm E \epsilon$$

$$\tau_{\text{ha}} = T_r / J_p$$

where:  $A_p$  = cross-sectional area of pipe,  $A_p = (D^2 - d^2) \pi / 4$ ;  $c$  = curvature of pipe, that is, reciprocal of curvature radius of central line of pipe;  $D$  = outside diameter of pipe;  $d$  = inside diameter of pipe,  $d = D - 2t$ ;  $d_{\text{wall}}$  = inside diameter based on  $k_{\text{wall}}$ ,  $d_{\text{wall}} = D - 2k_{\text{wall}}t$ ;  $E$  = Young's modulus;  $F_a$  = circumferential stress;  $I$  = rotational inertia of cross section of pipe,  $I = (D^4 - d^4) \pi / 64$ ;  $J_p$  = polar rotational inertia of cross section of pipe,  $J_p = (D^4 - d^4) \pi / 32$ ;  $k_{\text{wall}}$  = wall thickness allowance factor, for example,  $k_{\text{wall}} = 0.875$  when the minimum allowance value is  $12.5\%$ ;  $M_b$  = bending moment;  $p_i$  = internal pressure;  $p_o$  = external pressure;  $T$  = torque exerted;  $r$  = polar coordinates,  $d/2 \leq r \leq D/2$  for  $\sigma_b$  and  $\tau_{\text{ha}}$ ,  $d_{\text{wall}}/2 \leq r \leq D/2$  for  $\sigma_r$  and  $\sigma_h$ ;  $t$  = pipe wall thickness;  $\sigma_a$  = axial stress combination before bending;  $\sigma_b$  = axial stress combination when bending is generated;  $\sigma_e$  = equivalent stress;  $\sigma_h$  = circumferential stress;  $\sigma_r$  = radial stress;  $\tau_{\text{ha}}$  = shear stress.

### Internal Toughness Burst Pressure Strength.

The toughness burst describes the ultimate internal pressure property of the pipe. When the internal pressure reaches the designed toughness rupture value, the pipe cracks and loses the seal integrity. Toughness rupture means that an obvious plastic deformation emerges before material rupture, or it means the work or impact energy that is absorbed by the material before rupture. This toughness rupture is not the property of material that corresponds to brittle rupture. The internal toughness rupture pressure formula in ISO 10400 and the internal pressure strength calculated should meet the following conditions:

- Plastic deformation condition: Material should have sufficient plastic deformation before rupture, and the brittle rupture material should not be used for manufacturing casing.
- Small crack condition. Generating crack is hard to avoid; however, the depth of the crack should be sufficiently small. The present ultrasonic flaw detection technique may leave out cracks with a depth smaller than 5% of wall thickness. Therefore, in

the ISO 10400 standard, the internal pressure value of toughness rupture is calculated on the basis of crack depth smaller than 5% of wall thickness and is marked strength grade 5 in the internal pressure strength table. If the manufacture quality and detection measure of manufacturer can only ensure leaving out the crack with a depth smaller than 12.5% of wall thickness, the strength grade 12.5 is marked in the internal pressure strength table. If the depth of crack left out is limited to a value smaller than 2% of wall thickness after the detection technique is improved in the future, the internal toughness rupture pressure strength value can be further increased.

It can be seen that the ISO 10400 standard is related more closely to manufacturing quality. The toughness rupture design is inappropriate to tubing and casing that has not been tested by rupture toughness detection and crack size detection. In addition, the adaptive working status of toughness burst formula is plugging of both ends.

The minimum toughness burst formula of pipe is shown in Equation (5-13).

**(5-13)**

$$p_{IR} = 2k_{dr} f_{umn} (t k_{wall} - k_a a_N) / [D - (k_{wall} - k_a a_N)]$$

where:  $a_N$  = defect depth (maximum crack-type defect depth), which can be detected by using the detection method and instrument. This depth is known as the threshold value. A crack smaller than the threshold value may be left out. For instance, for a pipe with a wall thickness of 12.70 mm (1/2 in.) under the condition that the instrument can detect the crack with a depth greater than 5% of pipe wall thickness, the defect threshold value  $a_N = 0.05 \times 12.7 = 0.635$  mm (0.025 in.).  $D$  = outside diameter of pipe;  $f_{umn}$  = minimum ultimate tensile strength (it is not the minimum tensile yield strength, which has not appeared in the formula);  $k_a$  = internal pressure strength factor (the  $k_a$  value is 1.0 for quenched or tempered martensite steel or 13Cr while the  $k_a$  value implied is 2.0 for normalized

steel. If there are test data, the  $k_a$  value can be given under the condition of specific tubulars on the basis of test);  $k_{dr}$  = correction factor of strain hardening of material, of which the value is  $[(1/2)^{n+1} + (1/\sqrt{3})^{n+1}]$ ;  $k_{wall}$  = pipe wall allowance factor calculated (for example,  $k_{wall} = 0.875$  when the minimum allowance value is 12.5%. Actual wall thickness allowance can be used if it can be sure that the wall thickness allowance is smaller than 12.5%);  $n$  = dimensionless hardening index (curve fit index of actual stress-strain curve of unilateral stretch test), see Table 5-3;  $p_{IR}$  = internal toughness burst pressure strength;  $t$  = pipe wall thickness.

**Internal Crack Destabilization Rupture Pressure Strength.** When the crack depth is larger than 5% of pipe wall thickness and smaller than 12.5% of pipe wall thickness, the failure is a crack propagation destabilization, the aforementioned internal toughness burst pressure strength formula is inapplicable, and the crack destabilization rupture formula should be adopted. This formula includes a transcendental function based on the fracture mechanics theory and experience, its solution is very complicated, and the related strength table in the ISO 10400 standard can be consulted. It should be noticed that some casings allow crack to have a depth smaller than 5% of pipe wall thickness, while some casings allow crack to

**TABLE 5-3 Material Hardening Index**

API Steel Grade	n
H40	0.14
J55	0.12
K55	0.12
M65	0.12
N80	0.10
L80 type 1	0.10
L80 Cr steel	0.10
C90	0.10
C95	0.09
T95	0.09
P110	0.08
Q125	0.07

have a depth smaller than 12.5% of pipe wall thickness.

**Environmental Rupture Failure.** The rupture failure induced by the working environment will often be generated when the stress level is lower than the yield strength of the material. The rupture failure of tubing and casing, which is induced by the working environment, includes mainly the following types:

1. Stress corrosion cracking

Cracking generated under the combined action of stress and media corrosion is known as stress corrosion cracking, which is more serious than the cracking generated under the sole action of stress or corrosion. The stresses within casing include the stress caused by applied stress, the residual stress during manufacture, and thread connection stress. Sulfide stress corrosion cracking is most serious and should be considered first. When stainless steel is adopted, chloride stress corrosion cracking should also be considered.

2. Fatigue cracking

The vibration induced by oil and gas flow in tubing may lead to fatigue cracking. In addition, the change in temperature or pressure and complicated downhole operations may also generate alternate load.

## Other Strength Standards of Casing

The collapsing and internal pressure strength standards of ISO 10400 are completely different from those of the previous API 5C3; however, the tensile strength and other property calculation is the same as that of the previous API 5C3.

**Tensile Strength.** The tensile strength is on the basis of thread connection strength and includes yield strength, rupture strength, and slippage strength. Once the casing has been run in the well, it is no longer taken out; thus the tensile strength of the casing is calculated on the basis of the ultimate tensile strength of the material. However, tubing needs to be run in and pulled out many times; thus the tensile strength of tubing is calculated on the basis of the yield strength

of the material, that is, only tubing thread yield strength is considered when the tensile strength of tubing is calculated.

When trapezoidal thread is adopted, only the tensile strength of external thread or collar is considered. The weaker one between them is listed in the strength table.

**Internal Pressure Strength of the Collar.** When the ISO/API round thread or buttress thread is adopted, the internal pressure strength of the collar should also be calculated. The smaller one between the internal pressure strengths of collar and pipe body is taken as internal pressure strength.

**ISO/API Thread Seal Pressure.** In the middle of the collar with ISO/API thread, there is a space with a height of about 1 in. (25.4 mm), which is known as the J ring. The internal pressure will act on the contact surface of the thread tooth. The contact pressure on the first contact tooth surface will play a sealing role after power make-up is finished. Then the internal pressure will strive to expand the collar, and the contact pressure of thread tooth will be reduced. The pressure in a balanced state is just the sealing pressure of thread.

The sealing of round thread is achieved by the compression of both side faces of 60° tooth, while the sealing of buttress thread is achieved by the compression between the top of the external thread and the root of the internal thread. Thus the sealing property of buttress thread is lower than that of round thread. Using sealing compound to achieve the sealing property of buttress thread should be prudently considered. The infinite friction coefficient of sealing compound may lead to longitudinal cracking of the collar or stress corrosion boring in the middle of the collar.

The sealing pressure of ISO/API thread is lower than the internal yield pressure strength. Therefore, in the ISO/API thread tubing and casing design, the internal pressure should not be higher than the sealing pressure. The gas-tight thread with metal-to-metal seal should be adopted under the condition of high pressure.

## Loads Borne by Production Casing String

When the production casing string strength is designed, the various forces borne by production casing string in the well should be accurately analyzed, and an appropriate strength design method is selected. Obviously, the more accurate the analysis of forces borne and the more reasonable the design method, the safer and more reliable the production casing string.

At the different stages including production casing string running-in, cementing, and oil and gas well production, the forces borne by the casing string are different. Under different formation conditions and geological settings, the forces borne by the casing string are different. Long-term practice indicates that despite the complicated forces borne by the production casing string, the three basic loads, that is, internal pressure, external squeeze pressure, and axial tension, can still be concluded, except that their acting mechanisms and values are different under different conditions. The states of forces borne by the casing string under various conditions should be comprehensively studied in order to accurately analyze the forces borne by the production casing string. At present the values of forces borne by the production casing string are determined in accordance with the most dangerous working status.

**Internal Pressure.** The internal pressure borne by the production casing is from the formation fluid (oil, gas, and water) pressure and the pressure exerted during special operations (for example, gas injection, water injection, fracturing, acidizing, and cement squeeze). On the premise of no external liquid column pressure, the internal pressure borne by production casing at any well depth can be calculated using Equation (5-14):

(5-14)

$$p_i = p_s + p_b$$

where:  $p_i$  = pressure at any well depth;  $p_s$  = wellhead pressure;  $p_b$  = fluid column pressure at any well depth.

In the interconnected borehole-formation system, the internal pressure  $p_i$  at any well depth not only depends on formation pressure but also is related to fluid properties, well completion mode, special operations, and so on. The working status of the maximum internal pressure, which should be considered during production casing design, includes the following types:

### 1. High-pressure gas well with no packer

Under this working status the gas column pressure is low due to the well, which is fully filled with natural gas; thus the high downhole pressure can be directly transmitted to the wellhead, high wellhead pressure is formed, and then the production casing bears high internal pressure. In accordance with the ideal gas state equation, the relation between wellhead pressure and bottomhole pressure can be approximately expressed by Equation (5-15):

(5-15)

$$p_s = p_b / e^{0.000111554\gamma H}$$

where:  $p_b$  = bottomhole pressure, kPa;  $H$  = well depth, m;  $\gamma$  = relative density of natural gas (0.55 for methane).

In high-temperature high-pressure gas well design, the shut-in wellhead pressure and flowing pressure are required to be predicted on the basis of bottomhole pressure, and the accuracy may affect the tubing and casing designs and the selection and safety of surface equipment. It has previously happened that achieving shut-in wellhead pressure and flowing pressure higher than predicted pressures made the operating of surface equipment unsafe.

Under the condition of correct reservoir pressure prediction, the shut-in wellhead pressure and flowing pressure are just dependent on the accuracy of the calculation model and algorithm. Equation (5-15) is an intrinsically ideal gas law, and the effects of actual natural gas temperature and deviation factor on actual natural gas volume and pressure are not considered. An error up to 30% may be generated in a high-temperature

**TABLE 5-4 Comparison Between Shut-In Wellhead Pressure Values Predicted by Using Ideal Gas Law and PVT Equation**

Downhole Parameter	Normal Pressure Well	High-Temperature High-Pressure Well
Well depth (m)	2881	7520
Static bottomhole pressure (MPa)	32	170
Bottomhole temperature (°C)	74	226
H <sub>2</sub> S weight percentage	0	Trace
CO <sub>2</sub> weight percentage	0	0.02
Shut-in wellhead temperature (°C)	16	16
Relative density of gas	0.68	0.55 (98% CH <sub>4</sub> )
Wellhead pressure based on ideal gas law (MPa)	25.8	107
Wellhead pressure based on actual natural gas PVT equation (MPa)	25.3	145
Actual measurement value (MPa)		145
Difference or error	2%	26%

high-pressure gas well. The aforementioned formula does not have a large error under the condition of wellhead pressure lower than 25 MPa. The shut-in wellhead pressure should be predicted by using the PVT equation of actual natural gas under the condition of high-temperature high-pressure gas well. This is very important to strength design, corrosion prevention, and surface control and treatment equipment. Table 5-4 shows the shut-in wellhead pressures under different working statuses on the basis of different algorithms.

It may be excessively complicated to calculate the shut-in wellhead pressure by using the PVT equation of actual natural gas. In accordance with the Canada IRP1 2007 standard under the condition of well depth more than 1800 m, the wellhead pressure at which 85% of bottomhole pressure is taken is adequately accurate and reliable, regardless of whether the well has high pressure or low pressure.

## 2. High-pressure gas well with packer

The safety of casing cannot be fully ensured during production of a high-pressure gas well with packer. If the tubing thread has leakage in the initial production period of the well, or the packer fails in the late production

period of the well, high-pressure natural gas may enter the tubing-casing annulus through leak position. Under the condition of closed annulus, the gas slips and rises to the wellhead, so that the wellhead annulus pressure is increased, and the deep casing will bear combined wellhead annulus pressure and annulus section liquid-column pressure.

## 3. Hydraulic fracturing or acidizing well with no packer

In the hydraulic fracturing or acidizing well with no packer, the fracture pressure acting on the bottomhole is higher than formation breakdown pressure, so that the wellhead pressure is increased, and the production casing will bear high internal pressure. When this method is used, the maximum internal pressure borne by the casing and the thread connection status should be checked; otherwise, casing failure may be easily caused.

**External Pressure.** The external pressure of casing string includes mainly drilling and completion fluid pressure in sections with no cementing and the oil, gas, and water pressure of the reservoir. The status of external pressure borne by the casing string is complicated due to different conditions of oil and gas wells and different working statuses at different stages.

The effective external pressure of thick-wall casing after balancing internal and external pressures of casing can be calculated by using Equation (5-10).

In general, the most dangerous working status of production casing under the action of external pressure is generated at a late production stage due to the decrease of internal pressure, which may lead to increasing effective external pressure to a value close to or equal to the external casing liquid column pressure. Therefore, in order to ensure the safety of the production casing, the external pressure is calculated in accordance with the empty internal casing and the external casing liquid column of drilling fluid:

$$p_o = 0.981 \rho_m H$$

where:  $H$  = well depth at artificial bottomhole, m;  $\rho_m$  = external casing drilling fluid density,  $g/cm^3$ ;  $p_o$  = external casing drilling fluid column pressure, MPa.

**Axial Forces.** The axial force acting on the casing string is mainly generated by weight and also includes buoyance of drilling fluid in the well and the additional axial force generated under specific conditions.

1. Axial force generated by weight of casing. The axial force generated by the weight of casing increases gradually from bottom to top and reaches the maximum at the wellhead. Suppose the casing string consists of  $n$  sections of casing; then the axial tensile force at the top of the section  $i$  ( $i = 1, 2, \dots, n$ , from bottom to top) of the casing string is shown in Equation (5-16).

(5-16)

$$T_i = \sum T_k = \sum q_k \times L_k$$

where:  $T_i$  = axial tensile force at the top of section  $i$  of casing string, N;  $T_k$  = weight of section  $k$  ( $k = 1, 2, \dots, i$ ) of casing string, N;  $L_k$  = length of section  $k$  of casing string, m;  $q_k$  = weight per meter for section  $k$  of casing string, N/m.

Obviously, at the wellhead  $T_i = T_n = \sum T_k$ , that is, the sum of all casing string

weight. At the top of the lowest section of casing string, it is the weight of this section. The aforementioned formula can be used for calculating the axial tensile force at the top of each section of casing string.

2. Axial force under the action of buoyance. The casing string in the well is under the action of buoyance of drilling fluid, and the axial force distribution may be changed. In accordance with the Archimedes principle, the buoyance value is equal to the product of drilling fluid column pressure at this depth and the bare area of casing in the horizontal direction.

Obviously, the axial tensile force at the wellhead is just the maximum axial tensile force, while the axial compressive force at the bottom of the casing string is just the maximum axial compressive force.

At present, opinion as to whether the buoyance effect should be considered when the axial force is determined has not been unified. Some people think that the buoyance effect should not be considered because the buoyance is counteracted by the additional tensile force generated by friction between the casing string and the borehole wall when the casing is run in or moved. Others think that the buoyance should be considered because the buoyance can be accurately calculated and is related to the drilling fluid density in the well. Some designs adopt different tension safety factor values to differentiate the influence of the buoyance effect.

3. Axial force generated by borehole buckling. Casing may be curved when it is run in the well with a certain deviation angle and curvature change. An uneven axial force is generated by buckling on the cross-section of casing. The increase of axial force, which is caused by an excessive flexural deformation, will reduce casing connection strength and cause thread seal failure. The additional axial tensile force can be calculated simply by using Equation (5-17) on condition that the normal stress of the outside casing

buckling extends to the whole cross-section of casing:

(5-17)

$$T_d = \frac{1}{2} E\theta\pi DA / (180 \times 10^6 L)$$

where:  $T_d$  = additional axial tensile force caused by buckling, kN;  $E$  = elastic modulus of steel,  $E = 2.1 \times 10^8$  kPa;  $L$  = length of buckled section, m;  $\theta$  = whole angle change of deviation space;  $A$  = cross-sectional area of casing,  $\text{cm}^2$ ;  $D$  = outside diameter of casing, cm.

The rate of deviation per 25m is often used for substituting for whole angle change  $\theta$  of deviation space in order to simplify the calculation. Then, the aforementioned formula is changed as shown in Equation (5-18):

(5-18)

$$T_d = 0.0733 DA_\alpha$$

where:  $\alpha$  = rate of deviation, ( $^\circ$ )/25 m.

It is shown that under the same rate of deviation, the additional axial tensile force caused by buckling for a large casing is greater than that for a small casing. Under the same casing size, the greater the rate of deviation, the greater the additional axial tensile force caused by buckling. When a casing string is designed, the effect of flexural stress can be estimated by using the aforementioned formula, and then it is suitable to increase appropriately the tensile safety factor of casing.

Because the outside diameter of the collar is larger than that of the pipe body, the flexural stress of the complete thread at the end of the API round thread or buttress thread casing in a crooked hole is the maximum, and the vulnerable spot of tension resistance is at the external thread.

4. Axial force generated during cementing. During deep or superdeep well cementing, an additional axial tensile force that acts on the casing string will be generated due to a large amount of cement slurry and much higher cement slurry density than drilling fluid density when the cement slurry has not been returned from the casing shoe. It can be

calculated by using the approximate formula shown in Equation (5-19):

(5-19)

$$T_c = h(\rho_c - \rho_m) d^2 \pi / 4000$$

where:  $T_c$  = additional axial tensile force generated by the difference between densities of cement slurry and drilling fluid, kN;  $h$  = cement slurry column height in casing, m;  $\rho_c$  = cement slurry density,  $\text{g/cm}^3$ ;  $\rho_m$  = drilling fluid density,  $\text{g/cm}^3$ ;  $d$  = inside diameter of casing, cm.

When the cement slurry is going to be returned from the casing shoe, this additional tensile force reaches the maximum value. In the casing string design, if the buoyance of drilling fluid is considered, and moving casing is needed by technological requirements, then this additional axial tensile force should be considered. In addition, the hydraulic impact load generated when the top plug bumps the bottom plug during cementing will generate an additional axial tensile force, which acts on the casing. This additional axial tensile force can be calculated using Equation (5-20):

(5-20)

$$T_{ch} = 0.07854 d^2 p_b$$

where:  $T_{ch}$  = additional axial tensile force, kN;  $d$  = inside diameter of casing at plug bump, cm;  $p_b$  = increased value of pump pressure when top plug bumps bottom plug, Pa.

5. Other additional axial forces. Other additional axial forces include the additional axial force generated by impact load during running casing, which is dependent on the change of velocity of casing string putting in well; a large additional axial force due to the friction between casing and borehole wall when casing string is stuck or passes through a sloughing and reducing formation during running casing; a possible large additional axial force due to the reciprocating motion of casing during cementing; the axial force due to pulling casing during installing the wellhead after cementing, and so on. These additional axial forces vary greatly and are generally included in a safety factor.

To sum up, the force-summing status of production casing in a well is complicated. The loads that can be accurately calculated should be meticulously calculated. Under the condition of some loads that cannot be accurately calculated at present, the casing strength selected should allow for unforeseen circumstances, and a rational safety factor should be determined in order to ensure the safety of casing string in the well.

## Design Procedure and Design Safety Factor

**Design Procedure.** The design procedure of production casing includes: selecting the type of steel on the basis of the corrosion environment; selecting the thread on the basis of seal requirement and loads; and making the strength design on the basis of loads, including selection of steel grade and wall thickness.

**Design Safety Factor of Casing.** The safety factor method is a commonly adopted casing string design method.

### 1. Design safety factor of internal pressure strength

In accordance with the Canadian design standard of casing, the safety factor of casing in sour oil and gas wells should be considered respectively under the following conditions:

- a. When there is trace hydrogen sulfide and the partial pressure of hydrogen sulfide is lower than 0.34 kPa, the safety factor is taken to be 1.0.
- b. When the partial pressure of hydrogen sulfide is between 0.34 kPa and 500 kPa, the safety factor is taken to be 1.25. This means that in a hydrogen sulfide environment, the yield strength of material is considered as 80% of the value.
- c. When the partial pressure of hydrogen sulfide is lower than 500 kPa and the partial pressure of carbon dioxide is higher than 2000 kPa, the safety factor is taken to be 1.35.
- d. When the partial pressure of hydrogen sulfide is higher than 500 kPa, the problem

cannot be solved by increasing the safety factor, and stress should be reduced in the range of the whole well during designing.

### 2. Design safety factor of external collapsing strength

It is generally taken to be 1.0–1.1. It has been recommended that the design safety factor of the casing string below the cement top is taken to be 0.85, while the design safety factor of the casing string above cement top is taken to be 1.0, for the following reasons:

- a. Laboratory and field tests indicate that when external casing is cemented, the external casing collapsing strength may be increased due to the support of cement.
- b. The lower parts of the casing string are under a compressive load due to the action of buoyance. The collapsing strength of the casing may be increased under compressive stress.
- c. The API collapsing strength of casing is the minimum value, which may be exceeded by the casings more than 90%.

The biaxial stress design method in which the casing strength may be reduced by the axial tensile force should be considered for adoption in deep wells.

### 3. Design safety factor of tensile strength

It is generally taken to be 1.6. The casing thread connection strength and tensile strength of the casing body should be respectively checked on the basis of different types of thread. In general, round thread casing should be checked for thread connection strength, while buttress thread casing or gas tight thread casing should be checked for the yield strength of casing body and thread strength.

The design safety factor should be determined in accordance with the aforementioned principles and practical experience in the specific area. If the API standard casing strength selected cannot meet the requirement of the design safety factor, a special casing string structure should be adopted, or high-strength casings including high-accuracy casing, extra-strong casing, and special thread casing are specially ordered.

### Casing Tension Allowance Design Method.

The tension allowance value of casing is equal to the tensile strength multiplied by the safety factor minus the weight of the casing in the well. In general, the tension allowance method is used to control the maximum pull-up tension when the casing meets with resistance during running-in. The tension allowance method can also be used to calculate the maximum admissible pull force when the casing is set.

## 5.4 CEMENTING

### Basic Grounds of Cementing Design

**Operation Requirements.** The basic requirements of cement job quality include a complete cement sheath formed after the cementing operation; good consolidation between cement and casing and between cement sheath and borehole wall; a high cement consolidation strength; and good isolation of oil-, gas-, and water-bearing formations with no channeling and no leakage. In order to fulfill these requirements, the various influencing factors should be comprehensively considered, and the designs and operations should be meticulous. The general procedure includes the following:

1. In accordance with the cementing goal and the requirements of geology and engineering, on the basis of the parameters of downhole conditions and the predicted parameters, an elementary project design including selecting the type of cement, determining the formulation of cement slurry, and testing rheology and strength is formulated.
2. The data of borehole diameter, electric logging of oil-, gas-, and water-bearing formations, actual drilling fluid properties, formation pore pressure and breakdown pressure, and so on are acquired; the casing depth and casing components are determined; and cement isolation location and return height are specified. The cementing parameters include actual cement slurry volume injected and displaced, flow regime of drilling fluid used as displacing fluid,

critical displacement rate, change of flowing pressure in the whole process, and time. Cementing pressure equilibrium and the safety of operation time and cement slurry thickening time are checked. Finally, injecting procedure, pumping rate, and pressure are specified.

3. Cementing quality evaluation including acoustic amplitude log, variable density log, temperature log, and pressure test of casing. If there is any cementing quality problem, the corresponding remedial measures (such as a squeeze cement job) should also be taken in order to ensure oil and gas well quality and meet the requirements of performing various stimulation measures.

**Well Completion Requirements.** Cement slurry is a mixed liquid that is composed of cement, water, and various chemical additives and has a certain density. No matter which cementing method is used, cement slurry contacts certainly with the oil and gas reservoir. The cement slurry has a much larger filtration loss than drilling fluid and will unavoidably cause formation damage to various oil and gas reservoirs to a different degree, which includes mainly the mechanical plugging of cement slurry particles, the entering of cement slurry filtrate, the crystallization and precipitation of inorganic matter in cement slurry filtrate, and cement slurry leakage. If a shield-type temporary plugging drilling fluid is adopted during drilling-in, the aforementioned formation damage caused by cement slurry may be obviously reduced.

**Requirements of Oil and Gas Well Production.** In a long-term oil and gas well production process, the environment faced by set cement is very harsh. In order to prolong the production life of oil and gas wells, the cementing design should meet the following requirements:

1. Minimum support strength. The compressive strength of set cement is related to curing time. At least a compressive strength of 3.5 MPa should be achieved by set cement during an effective time in order to conduct the operations of putting the well into production. The measures that can be taken include increasing the tail cement slurry

density, specifying the minimum curing time, and decreasing the internal pressure of casing during curing time.

2. Increasing thermal stability. The strength retrogression of set cement may be generated under a temperature higher than 110°C. Therefore, when the static downhole temperature is higher than 110°C, silica flour or silica sand should be added as a thermal stabilizing agent in order to prevent strength retrogression.
3. Enhancing corrosion resistance. Appropriate additives or special cements are selected in order to reduce corrosion to the full extent.

## Types and Properties of Cement

During cementing of oil and gas wells, it is required to pump cement slurry to a depth of more than several thousand meters, and the properties of cement are closely related to temperature and pressure; thus the properties of the oil well cement and the cement slurry formulated by oil well cement should strictly meet the related requirements.

**Concept of Oil Well Cement.** Oil well cement means the silicate cement (Portland cement) and nonsilicate cement (including modified cement or special cement with additives) which are applied to cementing, workover, squeeze, and so on.

In general, the silicate cements of API grades are known as basic oil well cement, while the other cements such as thixotropic cement, expanding cement, tenacious cement, and corrosion-resistant cement are known as special oil well cement.

**Types and Usable Range of Oil Well Cement.** At present, the commonly used oil well cement is mainly silicate cement, in which hydraulic calcium silicate is the main component and to which a certain quantity of gypsum and grinding aids (or a certain quantity of gypsum or gypsum and water) are added. They form a product after grinding. Dry cement mixed with water (and also additives generally) forms cement slurry. The set cement in the downhole annulus is known as cement sheath.

In order to adapt to requirements of different well depth and prevent the sulfate in formation fluid from corroding the set cement, there are various grades and types of oil well cement that can be selected. The API standard specifies eight grades of oil well cement. The Chinese oil well cement standard has also been formulated with reference to the API standard. The usable range of API oil well cement is shown in Table 5-5.

The chemical and physical indices related to cement and the related test methods are specified in the API standard and Chinese standard.

## Formulation of Oil Well Cement

### 1. Chemical composition

The oxide analysis of typical silicate cement is shown in Table 5-6.

### 2. Mineral composition of cured material

The hydration reaction may be rapidly generated after cement is mixed with water, and various hydrates may be formed. Cement slurry will gradually change from liquid state to solid state. This is just the solidification and hardening process of cement slurry. In oil well cement, the four minerals, tricalcium silicate,  $\beta$ -type dicalcium silicate, tricalcium aluminate, and quadricalcium ferric aluminate, play a leading role in the solidification and hardening process of cement slurry.

- a. Tricalcium:  $3\text{CaO}\cdot\text{SiO}_2$  (that is,  $\text{C}_3\text{S}$ ). This is a main compound that generates the strength of cement. Its silicate makes early strength increase rapidly and generates a high ultimate strength. It accounts for 60% to 65% in a high early strength cement and 40% to 45% in a retarded cement.
- b.  $\beta$ -type dicalcium silicate:  $\beta$ -typ.  $2\text{CaO}\cdot\text{SiO}_2$  (that is,  $\beta\text{-C}_2\text{S}$ ). This has a slow hydration reaction and a slow increase of early strength; however, it plays an important role in raising the ultimate strength of cement.
- c. Tricalcium aluminate:  $3\text{CaO}\cdot\text{Al}_2\text{O}_3$  (that is,  $\text{C}_3\text{A}$ ). This has the most rapid hydration reaction. It plays a main part in deciding the initial setting time and thickening

TABLE 5-5 Usable Range of API Oil Well Cement

Grade	Appropriate Well Depth (m)	Type			Remarks
		Common	Medium Sulfate Resistance	High Sulfate Resistance	
A	0~1830	√	—	—	Common cement
B	0~1830	—	√	√	Sulfate-resisting cement
C	0~1830	√	√	√	High-early-strength cement
D	1830~3050	—	√	√	Medium-temperature medium-pressure conditions
E	3050~4270	—	√	√	High-temperature high-pressure conditions
F	3050~4880	—	√	√	Superhigh-temperature high-pressure conditions
G	0~2440	—	√	√	Basic oil well cement
H	0~2440	—	√	√	Basic oil well cement

Note: "√" means having this type of cement while "—" means not having this type of cement.

The cements of grades G & H are basic oil well cements, can be used under conditions of greater well depth and higher temperature when they are used with curing accelerator or retarding agent, and are the commonly used cements at present.

TABLE 5-6 Oxide Content of Typical Silicate Cement

Oxide	SiO <sub>2</sub>	CaO	Fe <sub>2</sub> O <sub>3</sub>	Al <sub>2</sub> O <sub>3</sub>	MgO	SO <sub>3</sub>	K <sub>2</sub> O	Burning Loss
Content (%)	22.43	64.77	4.10	4.76	1.14	1.67	0.08	0.54

time of cement slurry and also greatly affects the rheology of cement slurry. It is sensitive to the erosion of sulfate, so that its content is limited in sulfate-resistant cement. In a medium sulfate-resistance cement, the content of tricalcium aluminate should not exceed 8%. In a high sulfate-resistance cement, the content of tricalcium aluminate should not be higher than 3%. However, in a high early strength cement, the content of tricalcium aluminate can be up to 15%.

- d. Quadricalcium ferric aluminate:  $4\text{CaO} \cdot \text{Al}_2\text{O}_3 \cdot \text{Fe}_2\text{O}_3$  (that is,  $\text{C}_4\text{AF}$ ). It has a hydration reaction only slower than that of tricalcium aluminate. It makes a rapid increase of early strength but has a small influence on the ultimate strength of cement. The difference between the strength values during hardening for three days and twenty-eight

days is small. In a high-sulfate-resistance cement, the total content of one-share  $\text{C}_4\text{AF}$  and two-share  $\text{C}_3\text{A}$  should not exceed 24%.

**Basic Requirements for Cement Slurry and Set Cement.** The cement slurry and set cement that finally forms should meet specific requirements in order to ensure the safety of operation and enhance cementing quality. The properties required to be measured include cement slurry density, thickening time of cement slurry, rheological property of cement slurry, cement slurry filter loss, free water content of cement slurry (bleeding of cement slurry), compressive strength of set cement, and set cement permeability. The test methods and standards of these properties have been formulated. In the field, the first six items are generally measured, and the set cement permeability is not required to be measured at present.

### 1. Cement slurry density.

Cement slurry density means the cement slurry weight per unit volume. It should be higher than the density of drilling fluid in the well but should not make formation break, and it should also ensure the strength of set cement and the flowability of cement slurry. The other properties of cement slurry and set cement are also related closely to cement slurry density. Under normal conditions, in order to ensure both the strength of set cement and the flowability of cement slurry and to make the other properties easy to regulate, the density of cement slurry is generally  $1.80\text{--}1.90\text{ g/cm}^3$  and much higher than that of drilling fluid.

### 2. Thickening time of cement slurry

With the continuous hydration of cement, the cement slurry thickens continuously until its flowability is lost. In order to ensure safety during the cementing operation and ensure pumping the cement slurry to the desired location in annulus in the well, the cement slurry should keep its flowability during a certain time. The thickening time of cement slurry can be measured by using a pressurized consistometer, which can simulate the downhole temperature and pressure conditions. When the downhole temperature and pressure conditions are simulated by using a pressurized consistometer, the duration from starting warming and pressurizing cement slurry to reaching a cement slurry consistency of 100 Bc (Bearden unit of consistency) is known as the thickening time of cement slurry, which should ensure completion of the cementing operation and has a certain safety factor. Conversely, after the thickening time of cement slurry is determined, the whole cementing operation should be completed within the time specified; otherwise, cement slurry cannot be returned to the predetermined location in the annulus.

### 3. Rheological property of cement slurry

Rheological property of cement slurry means the flow deformation property of cement slurry under the action of applied

shear stress and can be measured by using a rheological parameter that is related to rheological mode. The rheological property of cement slurry should be favorable for enhancing the efficiency of displacing drilling fluid by cement slurry (that is, degree of displacing drilling fluid by cement slurry). In addition, the rheological property of cement slurry is also used for calculating the friction loss of circulation in the cementing process in order to prevent the borehole from leakage and rationally select operational equipment.

### 4. Filter loss of cement slurry

Filter loss of cement slurry means that the free water in cement slurry enters formation through the borehole wall. A large amount of filter loss of cement slurry will cause rapid thickening of cement slurry, reduce the flowability of cement slurry, and even cause the accident of being unable to displace the cement slurry to the predetermined location in the annulus. The filtrate entering the oil and gas reservoir may generate formation damage.

The filter loss of cement slurry is shown by the total filter loss volume within 30 minutes. In principle, the filter loss of cement slurry should be as small as possible; however, the additives used for controlling the filter loss of cement slurry may generally affect the rheological property, thickening time, and compressive strength, and so on; thus, trade-off studies should be made and a compromise is taken. In general, the filter loss of cement slurry should be 100–200 ml/30 min for casing cementing; 50–150 ml/30 min for cement squeeze or liner cementing; 20–40 ml/30 min for gas-channeling prevention; and lower than 50 ml/30 min under the condition of high density cement slurry.

### 5. Bleeding of cement slurry

In a static process, the bleeding of cement slurry means the dropping out of free water in cement slurry and forming a continuous water phase. The volume of free water dropped out per unit volume of cement slurry is just the free-water content of cement slurry

(that is, bleeding of cement slurry). The bleeding of cement slurry reflects the stability of cement slurry settlement to a great extent. An excessive bleeding of cement slurry will lead to an uneven distribution of cement slurry density and an inconsistent strength of set cement. The downhole longitudinal water channel formed by bleeding will affect the sealing property of the annulus. In a directional or horizontal well, if the bleeding of cement slurry is not controlled, a continuous water channel can easily form on the upper side of the annulus and will seriously affect the setting and sealing quality. Therefore, the bleeding of cement slurry should be controlled as much as possible, and a bleeding as low as possible should be selected. A cement slurry with no bleeding should be adopted in a directional or horizontal well.

#### 6. Compressive strength of set cement

The mechanical property of set cement is examined by testing the compressive strength of set cement. The force that the set cement can bear in a unit area under the action of pressure before rupture is known as the compressive strength of set cement.

The strength of set cement should meet the following requirements from the angle of engineering:

- a. Bearing casing. Studies indicate that the compressive strength of set cement, which is required by bearing casing, is low and is only 0.7 MPa, which can generally be met.
- b. Bearing impact load during drilling. The impact load acting on casing and set cement is dependent on drilling technology. Before the pressurizing part of the drill string goes out of the casing shoe, the weight on bit and rotary speed should be controlled in order to reduce the impact load acting on the casing and cement sheath.
- c. Meeting the requirements of acidizing and fracturing. During acidizing or fracturing, the weak link of the cementing section is at the consolidation strengths between the cement sheath and the borehole wall and

between the cement sheath and casing but not at the set cement itself. In general, when the strength of set cement is high, the consolidation strengths between cement sheath and borehole wall and between cement sheath and casing are also high. However, the test method of consolidation strength has not been specified in the related standards. This is possibly due to the difficulty in simulating downhole conditions to test the consolidation strength (especially the consolidation strength between cement sheath and borehole wall).

#### 7. Set cement permeability

Set cement permeability means the ability for fluid passage allowed by set cement. Obviously, the permeability of set cement should be low to the full extent in order to achieve isolation. In practice, the permeability of set cement is mostly lower than  $1 \times 10^{-5} \mu\text{m}^2$ . The analysis indicates that the problem of zonal isolation is not obvious if the permeability of itself is only to be considered; however, the existence of microclearance between set cement and casing or between set cement and borehole wall may seriously affect the effective isolation.

**Basic Property Requirements for Cement Slurry.** A pilot slurry and tail slurry should often be designed and used in order to enhance displacement efficiency. The basic properties of the pilot slurry and tail slurry of production casing cementing and the cement slurry of production liner cementing are shown in Table 5-7.

### Oil Well Cement Additives

The types of oil well cement are limited. In order to meet cementing operation and quality requirements under different conditions, various additives and admixtures are generally required to be added to cement slurry to regulate the cement slurry properties. With the development of the petroleum industry, cementing is faced with conditions that are becoming more and more complicated (such as deep wells, superdeep wells, adjustment wells, horizontal wells, extended reach wells, and slim

TABLE 5-7 Basic Property Requirements for Cement Slurry

Item	Production Casing		
	Pilot Slurry	Tail Slurry	Production Liner
Initial consistency (Bc)	<30		
Thickening time (min)	Cementing operation time + 60 min		
Pumpable time (min)	Difference between thickening time and pumpable time <20 min		
Bleeding (%)	Conventional well	<0.2	<0.2
	Directional well	<0.2	<0.2
	Horizontal well	0	0
Filter loss (6.9 MPa) (ml/30min)	Conventional well	<250	<150
	Directional well	<150	<100
	Horizontal well	<50	<50
Rheological property	Meeting operational requirements		
Compressive strength (MPa)	24h	>8	>14
Permeability ( $10^{-3}\mu\text{m}^2$ )	—	<0.01	<0.01

Note: The test method of cement slurry property is in accordance with GB/T 19139-2003.

For directional and horizontal wells, the measuring cylinder used for testing free liquid level should be placed with a slope of 45°.

For low- or high-density cement slurry, the setting time of compressive strength can be 48 h.

holes), and higher requirements are set on cement slurry. Additives and admixtures are used more widely, and higher requirements are set on additives and admixtures.

In the last 30 years, oil well cement additives have been rapidly developed, and the renewal of products is also rapid. Presently, the additives include fluid loss additive, dispersant, retardant, accelerant, special additives, and supplementary additives. The admixtures include lightening admixture, weighting admixture, and thermal stabilizer.

**Fluid Loss Additive of Oil Well Cement.** During the cementing operation, cement slurry will generate percolation under pressure when it passes through a high-permeability formation. When the filtrate of cement slurry enters formation, filter loss of the cement slurry will be caused, cement slurry flowability will be reduced, and even the operation will fail. In addition, when the filtrate enters formation, formation damage will form in varying degrees.

The API filter loss of raw cement slurry is generally higher than 1500 ml/30 min. In a cementing operation, the filter loss should not exceed 250 ml/30 min in general. Liner cementing and gas-channeling prevention require that the filter

loss should not exceed 50 ml/30 min, so that a fluid loss additive is used in cement slurry.

Fluid loss additive can improve cake structure so that a low-permeability dense cake is formed; thus filter loss is reduced.

Polymer-type fluid loss additive is generally used. It can increase the filtrate viscosity of cement slurry and the resistance to entering formation, thus reducing the filter loss of cement slurry.

At present, the commonly used fluid loss additives include particulate material and high molecular water-soluble material.

1. Particulate material: bentonite, microsilica, asphalt, and thermoplastic resin. Latex is a special material and also has a good filtration-reducing property.
2. Water-soluble high molecular material: natural modified high molecular material and water-soluble polymer. These have become important fluid loss additives of cement slurry. The commonly used water-soluble polymers are as follows.
  - a. Cellulose derivative: hydroxyethyl cellulose (HEC), carboxymethyl cellulose (CMC), carboxymethyl hydroxyethyl cellulose, and

other cellulose derivatives. These are of an important category of fluid loss additives of oil well cement.

- b. Acrylamide-acrylic acid copolymer (AM/AA): acrylamide-sodium acrylate copolymer (AM/AA-Na); binary acrylamide-vinyl imidazole (VI) copolymer; ternary acrylamide-AMPS-imidazole copolymer; N, N-dimethyl acrylamide-AMPS copolymer (NNDMA/AMPS); AA/AMPS copolymer; and vinyl pyrrolidone copolymer.

**Dispersant of Oil Well Cement.** Oil well cement slurry is a high-concentration suspension system in which water is the continuous phase, while cement particles are the dispersed phase. The solid content (weight percent) can be up to 70%. A dispersant is used for providing the suspension system with a good rheological property and thermal stability (that is, not dispersing further at a high temperature but still keeping a strong adsorptivity and dispersity at a high temperature).

Dispersant is generally an anionic, cationic, or nonionic surfactant and is mainly used for adsorption and dispersion.

When cement and water are mixed, positive and negative charges are generated on the surface of cement particles. When solid concentration is high, the cement particles will form a continuous net structure due to the interaction between positive charge and negative charge. When the cement slurry is pumped, the net structure will be broken, thus leading to a reduction of cement slurry viscosity. The types of dispersant include:

1. Polynaphthalene sulfonate;
2. Formaldehyde and acetone (or other ketone) condensation polymer;
3. Lignosulfonate.

**Retardant of Oil Well Cement.** The retardants of oil well cement are used for prolonging the setting time of cement. Commonly used retardants include lignosulfonate, saccharide compound, cellulose derivative, and organic phosphate. In addition, some inorganic salts

(such as borate, phosphate, and chromate) can also act as retardants. The AMPS copolymers developed in recent years are good retardants and have stable property, high effectiveness, wide temperature range, good compatibility with other additives, and no side effect on set cement strength development. They are AMPS-AA and AMPS-itaconic acid copolymers.

**Accelerant of Oil Well Cement.** The accelerants of oil well cement are used for shortening the thickening time and accelerating the cement setting and hardening; or for mitigating the over-retarding caused by adding other additives (such as dispersant and fluid loss additive). The commonly used accelerants may be grouped into two categories: the inorganic accelerant and the organic accelerant.

Chloride is the most common accelerant of oil well cement. Carbonate, silicate, aluminate, nitrate, sulfate, thiosulfate, sodium hydroxide, potassium hydroxide, ammonium hydroxide, and so on are also accelerants of oil well cement. Calcium chloride is the most effective and economic accelerant.

Sodium chloride influences the thickening time and compressive strength development of oil well cement. This is dependent on its concentration and environmental temperature. Sodium chloride is an accelerant when its concentration (weight percent) in cement is lower than 10%. When its concentration is in a range of 10% to 18%, it not only has no accelerating effect but also no retarding effect, and its thickening time is similar to that of fresh cement slurry. When its concentration is increased to more than 18%, a retarding effect will be generated. Obviously, sodium chloride is not a good accelerant and is only used when calcium chloride is in short supply on site or under special conditions.

Sea water is often used for formulating cement slurry in offshore operation. The content of sodium chloride in sea water is about 25 g/L, and an accelerating effect may be generated. The content of magnesium chloride in sea water is about 1.5 g/L and should be simultaneously counted.

Sodium silicate is generally used as a filling material, but it also has an accelerating effect. In the liquid phase of cement slurry, sodium silicate reacts with  $\text{Ca}^{2+}$  and forms a colloidal nucleus of hydrated calcium silicate, thus leading to the ending of the induction period of cement hydration in advance.

Organic accelerants include calcium formate  $\text{Ca}(\text{HCOO})_2$ , ammonium formate, oxalic acid, and triethanolamine.

**Special Function Additives.** In recent years, with the continuous exploration and development of oil and gas fields, the number of wells with complicated conditions has continually increased, and the requirements of special functions for a cement slurry system have also increased, thus developing oil well cement additives with various special functions, such as gas-channeling inhibitor used for preventing gas channeling during setting of cement slurry, toughness promoter used for improving the impact resistance of set cement, expanding agent used for reducing volume contraction during setting of cement slurry, and early strength additive used for enhancing ultra-low and ultra-high density cement strength development.

#### 1. Gas-channeling inhibitor

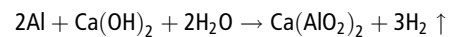
Gas-channeling inhibitors include the inhibitor used for preventing or reducing weight loss during setting of cement slurry and the inhibitor used for increasing resistance to oil, gas, and water to prevent them from entering the cement slurry system.

a. Gas-channeling inhibitor used for preventing or reducing weightlessness. After being added to cement slurry, it can generate minute gas bubbles that disperse evenly in the system and can increase the pore pressure to make up for the decrease of hydrostatic column pressure of cement slurry. This cement is generally known as gas-channeling-resistant compressibility cement.

There are many kinds of gas cement material, such as aluminum powder, zinc powder, oxydol, and bleaching powder.

Aluminum powder is an appropriate material by comprehensive consideration of source and cost (such as Halliburton's Gas Check and the KQ series of Chinese Southwest Petroleum University).

Metal aluminum (Al) has an active chemical property. Hydrogen gas may be generated when aluminum reacts on an acid or alkali. Cement slurry has alkalinity (pH value is about 12 to 13). The chemical reaction that will generate hydrogen gas may be speeded up under the condition of downhole temperature and pressure. Hydrogen gas generated will be evenly distributed in cement slurry (known as gas-charged cement slurry), and an additional pressure may be acted on formation with the aid of slurry column weight, pore resistance, or bridging. This additional pressure will be gradually released when weightlessness is generated during setting of cement slurry, thus making up for the pressure decrease caused by weightlessness. The chemical reaction of aluminum powder in cement slurry is as follows.



b. Gas-channeling inhibitor used for increasing resistance to gas channeling. When it is added to cement slurry, the gas penetration potential of cement slurry and plastic cement slurry permeability can be reduced in the transitional period from liquid state to solid state, and the resistance to gas is increased so that gas channeling is prevented. This cement is generally known as gas-channeling-resistant impermeability cement.

The gas-channeling mechanism of this type of inhibitor is the following: first, the dense cement cake deposited on permeable formation inhibits formation fluid from entering the cement system; second, it makes the formation fluid that enters cement form an impermeable barrier in cement pores,

thus inhibiting gas from continuing to enter the cement system, or superfine material is added for plugging the pore channel and inhibiting gas from entering the cement system. On the basis of this mechanism, polymer emulsion (latex), partially crosslinked polymer, and microsilia, and so on, have been formulated.

Ethylene-butadiene latex is a typical latex used in oil well cement. In addition, the latexes used in oil well cement also include polyvinyl dichloride, polyvinyl acetate (PVA), and styrene-butadiene-ethyl acrylate.

2. Toughness promoter (plasticizing agent)
 

At present, fiber material and latex can be appropriately added to cement slurry in order to improve the impact resistance of set cement.

  - a. Fiber-type toughness promoter: A certain quantity of evenly dispersed fiber material is added to cement slurry, so that the stress concentration at the end of the original defect in set cement is decreased, and the spreading of defect is mitigated (crack-resisting effect). This type of fiber includes fibrous asbestos, carbon fiber, and nylon fiber.
  - b. Latex-type toughness promoter: Latex is evenly distributed in cement slurry. Under normal conditions latex will not react chemically with cement slurry. The water in latex particles may be absorbed during hydration of cement. The latex particles after water loss will agglomerate and form filiform films that are distributed in whole set cement and stretch over the defects and microcracks in set cement. These films have a high tensile strength and deformability, thus mitigating effectively the extension of defect and microcrack of set cement.

**Lightening Admixture.** Lightening admixture is used for decreasing cement slurry density and reducing the hydrostatic column pressure

of cement slurry; thus circulation loss due to the rupture of weak formation can be prevented, and the return height of cement slurry is ensured.

There are three kinds of lightening admixture: bentonite material with its high density, which has high adsorptive capacity and high mud yield and can decrease cement slurry density by increasing the water-cement ratio, such as fly ash, bentonite, soluble silicate, and diatomite; material with lower density than water, such as drift bead and glass microbead; and gases (such as air and nitrogen gas) that can decrease cement slurry density after the cement slurry is aerated with gas, and a foamed cement is formed.

**Weighting Admixture.** When a high-pressure oil and gas well or an adjustment well of an old oil field is cemented, a weighting admixture is often added to cement in order to prevent well blowout and gas channeling and increase cement slurry density. The commonly used weighting admixtures include barite, hematite, titanite iron ore, and silica sand. Sometimes NaCl and some dispersants can also be used for increasing cement slurry density.

**Thermal Stabilizer.** Under the condition of downhole temperature higher than 110°C (such as deep wells, superdeep wells, and thermal production wells), the hydration products (dicalcium silicate and tricalcium silicate) in cement may generate a change of crystal form, so that the strength of set cement will be reduced. When silica flour or silica sand is appropriately added to cement slurry, the strength of set cement can prevent the strength of set cement at high temperature from reducing. The percentage of silica flour or silica sand added is dependent on temperature. Under the condition of downhole static temperature between 110 and 204°C, the percentage is 30% to 40% (the content of silicon oxide is not less than 90%). When the vapor temperature is 240–360°C in the vapor injection well of a heavy oil reservoir, the percentage of silica flour or silica sand added is sometimes up to 60%.

## Principle of Enhancing Cement Job Quality

The purpose in enhancing cement job quality is to isolate oil-, gas-, and water-bearing formations and protect payzones. Thus the two key problems that should be solved include how to fill in the annulus with cement slurry; and how to stably suppress oil-, gas-, and water-bearing formations and isolate these formations fully during the setting time of cement slurry.

**Measures to Raise Displacement Efficiency of Cementing.** The degree of displacement of drilling fluid by cement slurry in the annulus is shown by displacement efficient  $\eta$  as follows:

Cementing section:  $\eta = \text{cement slurry volume} / \text{annulus volume}$ ;

Some cross-section of cementing section:  $\eta = \text{cement slurry area} / \text{annulus area}$ .

When  $\eta$  is equal to 1 (that is, 100%), the drilling fluid is fully displaced by cement slurry. When  $\eta$  is less than 1, the drilling fluid has not been fully displaced by cement slurry, thus leading to a channel.

Measures to raise displacement efficiency include: using a centralizer to reduce the eccentricity of casing in the borehole; moving the casing during cementing; cementing under the condition of turbulent flow or plug flow; using pad fluid, adjusting drilling fluid properties before cementing; and increasing contact time under a turbulent flow regime.

### 1. Using a centralizer for ensuring the eccentricity of casing

In a directional or horizontal well, casing string may be on the lower side of the borehole due to the weight of casing, and an eccentricity is formed. In a straight well, the borehole drilled is also unable to be absolutely vertical, and there is also the eccentricity of casing. The displacement efficiency of cementing is closely related to the eccentricity of the casing in the borehole.

The conditions of flow velocity distribution in a concentric annulus and an eccentric annulus are shown in Figure 5-8.

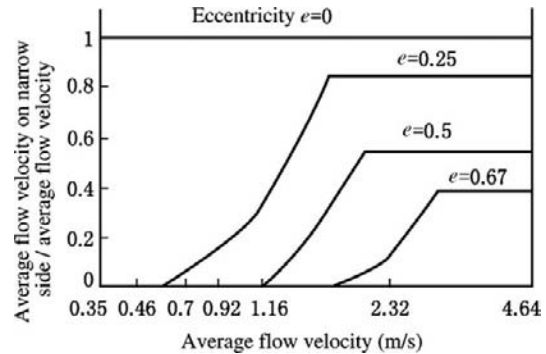
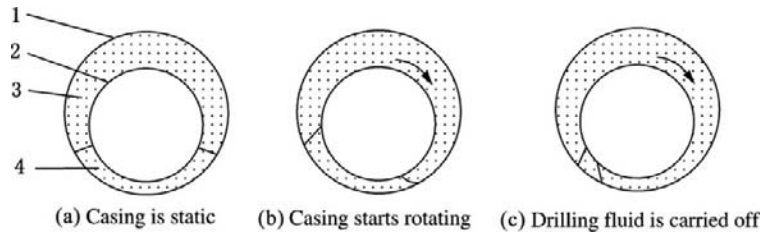


FIGURE 5-8 Flow velocity distributions in a concentric annulus and an eccentric annulus.

In a concentric annulus, the circumferential flow velocity distribution is even due to the equal clearance on the whole circumference of the annulus. In an eccentric annulus, the circumferential flow velocity is uneven due to the unequal clearance on the whole circumference of the annulus, which is due to eccentric casing; the flow velocity in wide clearance is high, and the flow velocity in narrow clearance is low. The more serious the eccentricity of the casing, the more serious the unevenness of flow velocity distribution. The flow velocity distribution of liquid in an eccentric annulus has been measured. When the eccentricity is 69%, the flow velocity in the maximum clearance is 70 times the flow velocity in the minimum clearance.

During the displacement of drilling fluid by cement slurry, a similar condition will also be generated. The speed of displacing drilling fluid by cement slurry in wide clearance is faster than that in narrow clearance, thus leading to different return heights of cement slurry between wide and narrow clearances. Under the condition of serious eccentricity of the casing, the drilling fluid in narrow clearance cannot be displaced and may be left in the original place, thus generating channel.

Therefore, the eccentricity of casing in the borehole should be reduced to the full extent. At present, the measures taken include



**FIGURE 5-9** Rotating the casing to raise displacement efficiency. 1 - borehole; 2 - casing; 3 - flowing cement slurry; 4 - drilling fluid.

attaching a centralizer to the casing string. The casing centralizer spacing calculation method has been recommended in the related Chinese standard.

## 2. Moving casing during cementing

Moving the casing up and down or rotating the casing is an effective measure to raise displacement efficiency. The measure to raise displacement efficiency by rotating casing is shown in Figure 5-9.

When the casing rotates, the drilling fluid held up in narrow annulus clearance or flowing more slowly is carried to wider annulus clearance; on the other hand, casing bending is certainly generated due to the crooked borehole, and casing revolution may be generated by rotating casing, thus generating alternate change between wide and narrow clearances circumferentially. Thus the drilling fluid will be evenly displaced by cement slurry in the whole annulus under the combined action of the two aspects. Rotating may cause the casing to bear an excessive stress. Therefore, a rotating speed of 10 to 20 rotations per minute is appropriate.

It is generally considered that rotating casing may have a better result. Moving the

casing up and down may generate sticking of the casing after pulling up; thus the casing cannot be set to the design location, so that it is difficult to install a wellhead.

## 3. Cementing under the condition of turbulent flow or plug flow

The flow velocity distributions under different flow regimes are shown in Figure 5-10. Turbulent flow regime has a time-average flow velocity distribution. The cross-sectional flow velocity under laminar flow regime is a leptokurtic distribution. The cross-sectional flow velocity distributions under turbulent flow regime and plug flow regime are relatively gentle, thus favoring the uniform advancing of cement slurry to displace drilling fluid. However, in an eccentric annulus, a serious circumferential uneven advancing may be caused under a plug flow regime despite the fact that cement slurry can evenly advance to displace drilling fluid in this clearance.

Displacement under a turbulent flow regime has an even cross-sectional flow velocity distribution. Furthermore, it is more important that the swirl of turbulent flow in turbulent flow displacement fluid can

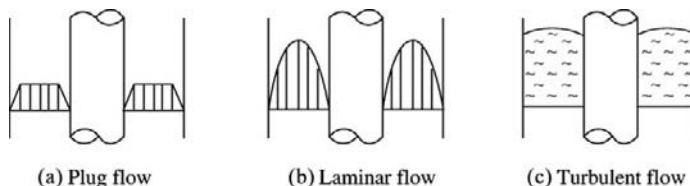


**FIGURE 5-10** Flow velocity distributions under different flow regimes.

generate erosion, disturbance, and carrying effect on the interface between displacement fluid and drilling fluid, thus favoring displacing drilling fluid. In an eccentric annulus, the erosion, disturbance, and carrying effect can gradually displace the drilling fluid in narrow clearance. In an eccentric annulus, the unevenness of circumferential turbulent flow regime is much lower than that under a laminar flow regime (plug flow is intrinsically of laminar flow) and can be reduced by 27% to 76% in accordance with the data obtained by measurement; thus a turbulent flow regime is favorable to displacement in narrow clearance. In addition, the turbulent flow regime has a great friction resistance pressure drop per unit length. This friction resistance pressure drop is a motive force that motivates the retained drilling fluid to flow; thus it favors drilling fluid displacement. Therefore, displacement under turbulent flow regime should first be selected, provided that it is allowed by downhole conditions (that is, it is impossible to cause lost circulation).

#### 4. Using pad fluid

The chemical composition of cement slurry is different from the chemical composition of drilling fluid. When drilling fluid is directly displaced by cement slurry, the drilling fluid and cement slurry in the vicinity of the interface will mix. After mixing of drilling fluid and cement slurry, the cement slurry may be thickened, thus leading to an increase of flow friction resistance in the annulus and even to lost circulation, or the cement slurry cannot be pumped so that the drilling fluid cannot be entirely displaced out of the casing. On the other hand, the mixture of drilling fluid and cement slurry may be very thick and is not easily displaced by the following cement slurry, so that channel of mixture is formed, thus influencing cement job quality. Thus drilling fluid is incompatible with cement slurry, and one or several sections of specially formulated liquid that is simultaneously compatible with drilling fluid and cement slurry

are required to be injected ahead of cement slurry. This liquid is known as pad fluid of cementing.

The pad fluid includes washing fluid and spacer fluid. The washing fluid is used for diluting drilling fluid and washing the borehole wall and casing wall (also isolating drilling fluid from cement slurry) and is mainly used during cementing under turbulent flow regime. The spacer fluid is mainly used for isolating drilling fluid and cement slurry. There are two types of spacer fluid: the thick-type spacer fluid used for cementing under a plug flow regime, and the turbulent flow type spacer fluid used for cementing under a turbulent flow regime.

#### 5. Adjusting drilling fluid properties before cementing

The drilling fluid properties during drilling should meet the requirements of the drilling operation; however, these properties are inappropriate for raising the displacement efficiency of cementing. Therefore, it is generally required to adjust the drilling fluid properties. This is very important. The density, viscosity, and gel strength or thixotropy of drilling fluid should be appropriately reduced on the premise of ensuring downhole safety. Theoretical and experimental studies indicate that reducing the thixotropy is particularly important. The stronger the thixotropy, the greater the internal textural force of drilling fluid and the more unfavorable the displacing of drilling fluid. However, in a deep complicated well, it is difficult to adjust the drilling fluid properties to a great extent in the whole well before cementing. Therefore, under the condition of adjusting drilling fluid properties to the full extent, drilling fluid of about 20 m<sup>3</sup> should be adjusted to have good displacement property and the property of preventing cement slurry from contaminating, and used as a lead fluid before pad fluid in order to raise displacement efficiency.

#### 6. Increasing contact time under turbulent flow regime

As mentioned earlier, displacement under a turbulent flow regime generates mainly erosion, disturbance, and carrying effect. Obviously, the erosion, disturbance, and carrying effect need a certain amount of time. Laboratory simulation studies and statistical analysis of cementing practice indicate that under the condition of casing centricity that is not less than 67%, the drilling fluid can be effectively displaced when the contact time is more than 7 to 10 minutes. Therefore, the pad fluid properties and volume and the cement slurry volume should be rationally designed.

7. Density difference between displacement fluid and drilling fluid

The step-up densities of drilling fluid, pad fluid, and cement slurry (that is, positive density difference) are generally required because the positive density difference will generate a buoyancy effect on drilling fluid, thus favoring displacement. However, the washing fluid can be excepted due to the main effects of washing fluid, which include diluting drilling fluid and washing the borehole wall and casing wall.

**Cement Slurry Weightlessness and Prevention of Channeling of Oil, Gas, and Water.** In the initial stage after cementing, the cement slurry is still in a liquid state, the pressure acting on the reservoir by the annulus liquid is equal to the sum of the hydrostatic pressures of slurry columns above the acting point and can suppress the reservoir due to the density of cement slurry being higher than that of drilling fluid. However, with the setting of cement slurry, the cement slurry column pressure is gradually reduced. This phenomenon is known as cement slurry weightlessness. When the slurry column pressure is lower than reservoir pressure, the oil, gas, and water in the reservoir may enter the annulus and then interzonal cross-flow or channeling to the wellhead along the annulus will be generated. This type of flow or channeling is more possible in wells that have high-pressure formation of oil, gas, and water or great interzonal pressure difference (such as water injection wells).

1. Mechanism of cement slurry weightlessness
 

Cement slurry weightlessness includes gel weightlessness and bridging weightlessness.

  - a. Gelling weightlessness. During hydration and setting of cement slurry, a spatial net texture with a certain gelling strength may be formed between cement particles, between cement particles and the borehole wall, and between cement particles and the casing. When lower slurry volume is decreased due to cement hydration, volume contraction, and fluid loss, the net texture will cause a part of the cement slurry column weight to hang on the borehole wall and casing, and the lower volume decrease cannot be fully compensated, thus reducing the effective stress acting on the lower formation and leading to weightlessness.
  - b. Bridging weightlessness. When cement slurry is static after cementing, the rapid fluid loss of cement slurry at high-permeability formation will cause the cement slurry to thicken rapidly and form plugging (bridging). In addition, the rock blocks and cement particles generated by high-velocity erosion during cementing may sink and form plugging. When a decrease of volume is generated in a lower cement slurry column due to cement hydration, volume contraction, and fluid loss, the upper cement slurry column pressure cannot be effectively transmitted downward due to plugging; thus, the effective pressure acting on lower formation may also be decreased, and weightlessness may be caused.
  - c. Set cement contraction. During the setting of cement slurry, internal contraction of the set cement body due to hydration may form micropores, and the appearance also presents volume contraction, thus reducing the pore pressure and the pressure acting on formation. The shrinkage factor of cement slurry during initial setting time is generally 0.1% to 0.5%; whereas the shrinkage factor during final setting time is higher than 2%.

d. Forming water column by free water separation. The free water separation in cement slurry may form an axial connected water channel, thus reducing the pressure acting on formation. This effect is particularly obvious in a deflecting well, in which an obvious water channel is formed on the upper side of the borehole wall. This is the main channel of channeling of oil, gas, or water.

2. Gas block cement slurry evaluation

The cement slurry weightlessness and gas invasion and the prediction methods have been studied.

a. Gas-channeling potential factor method. The gas-channeling factor of potential (GFP) method was presented by Halliburton in 1984 in accordance with the concept of transient time of cement slurry. The ratio of the maximum reduction  $\Delta p_{max}$  of slurry column pressure when gel strength  $\tau_{cgs}$  of cement slurry equals 240 Pa to the balanced slurry column pressure  $p_{ob}$  in the well is used for describing the hazard level of gas channeling. This is a qualitative estimating method. The formula of GFP is shown in Equation (5-21).

(5-21)

$$GFP = \frac{\Delta p_{max}}{p_{ob}}$$

$$p_{max} = \frac{4L_c \tau_{cgs}}{100(D_h - D_p)}$$

$$p_{ob} = (\rho_c L_c + \rho_{sp} L_{sp} + \rho_m L_m - G_f L) / 100$$

where: L, L<sub>c</sub>, L<sub>sp</sub>, L<sub>m</sub> = well depth, cement slurry section length, pad fluid section length, upper drilling fluid section length,

respectively, m;  $\rho_c, \rho_{sp}, \rho_m$  = densities of cement slurry, pad fluid, drilling fluid in annulus, respectively, g/cm<sup>3</sup>; G<sub>f</sub> = equivalent density of formation pressure at well depth L, g/cm<sup>3</sup>;  $\Delta p_{max}$  = reduction of cement slurry column pressure when  $\tau_{cgs} = 240$  Pa, MPa;  $p_{ob}$  = overbalance pressure acting on reservoir, MPa.

Obviously, the greater the  $p_{ob}$  and the smaller the  $\Delta p_{max}$ , the smaller the GFP and the lower the hazard level of gas channeling. The GFP, possibility of gas channeling, and methods of preventing gas channeling are shown in Table 5-8.

b. Gas-channeling resistance coefficient (E<sub>mig</sub>) method. This method was presented by Southwest Petroleum University in 2002, and a corresponding evaluation instrument was developed. This method is used for comparing the gas-channeling resistances in setting processes of different type or formulation cements so that the cement design may be evaluated or optimized, as shown in Equation (5-22):

(5-22)

$$E_{mig} = \Delta p_{mig} \frac{\sqrt{t_c}}{t}$$

where:  $\Delta p_{mig}$  = gas invasion pressure difference measured at time t of curing, kPa; t = curing time, min; t<sub>c</sub> = initial setting time of cement slurry, t<sub>c</sub> > t, min.

The greater the E<sub>mig</sub>, the greater the gas-channeling resistance of the cement slurry system. The E<sub>mig</sub> value is related to curing time and increases as time increases. The gradation of the gas-channeling resistance coefficient is shown in Table 5-9.

TABLE 5-8 Prediction and Application of Gas Channeling Factor of Potential

GFP	1	2	3	4	5	6	7	8	9	10	∞	
Possibility of gas channeling	Low				Medium				High (high hazard level)			
Recommended cement slurry	High-density cement slurry				Delayed gelling cement slurry				Compressible cement slurry			
	Low fluid-loss cement slurry				Thixotropic cement slurry				Latex-cement slurry			
					Impermeable cement slurry							

**TABLE 5-9 Application of Gas-Channelling Resistance Coefficient**

$E_{mig}$	<8	8–16	16–32	>32
Gas channelling resistance	Low	Medium	High	Very high

c. Main method of preventing gas channelling

A gassing material is added so that the elastic bulging force generated in the setting process of cement can compensate for the cement slurry weightlessness, thus retaining the effective pressure of the cement slurry column. When cement slurry weightlessness is generated, the gassing agent generates gas, thus forming microbubbles that are dispersed in cement slurry. An additional pressure is generated in the gassing cement slurry by using the plug effect formed by hydrostatic pressure and textural force of the slurry column (drilling fluid column or cement slurry column) above gassing cement slurry or the plug effect of bridging section with the aid of microbubbles generated by the gassing agent so that the final pressure of the cement slurry column can be higher than reservoir pressure, thus preventing weightlessness and gas channelling. Aluminum is an active metal. The reaction of treated aluminum powder to caustic water will generate dispersed hydrogen, which can play a part mentioned earlier.

In addition, increasing the drag force of cement slurry during setting, especially for the duration of pressure reduction from cement slurry column pressure to water column pressure, may prevent gas channelling.

## Cement Job Quality Detection and Evaluation

### Quality Requirements of Cementing

1. Specifications of the return height of cement slurry, cement plug length, and artificial borehole bottom. During cementing, the designed return height of cement slurry should exceed 150 m above the top of reservoir, and the actual cement top should exceed 50 m above

the top of reservoir. Natural gas wells and steam injection wells require cement slurry to return to the surface.

2. The double-plug cementing method is adopted in order to ensure the sealing and fixing quality of the casing shoe. The distance between choking ring and casing shoe should not be less than 10 m. It is generally 20 m for intermediate casing or an initial completion well. The casing shoe should be close to the bottom-hole as much as possible. The double-plug method is used for avoiding contaminating cement slurry by liquid film slurry body, which is formed by scraping the internal casing surface during downgoing of a single plug.
3. The distance between the bottom boundary of the reservoir and artificial borehole bottom (cement face in casing) should not be less than 15 m in order to meet the requirements of petroleum production technology.

### Cement Sheath Quality Standards

1. Cement bond log (CBL)

Acoustic amplitude log, which is also known as cement bond log (CBL), is generally taken as the criterion of cement sheath quality assessment, and carried out after curing of 24 to 48 hours; however, the time is determined in accordance with the specific conditions for special wells (liner cementing, cementing by using retarded cement, and so on). The cement sheath quality is determined on the basis of the relative amplitude of acoustic amplitude attenuation on the acoustic amplitude log. The acoustic amplitudes value of the free casing section under the condition of a whole annulus that is fully filled with drilling fluid is taken as a base.

Relative amplitude = acoustic amplitude log amplitude of target section / acoustic amplitude log amplitude of free casing section  $\times 100\%$

**TABLE 5-10 Cement Job Quality Assessment Based on CBL**

Conventional Density Cement	Low-Density Cement	Evaluation Conclusion
CBL ≤ 15%	CBL ≤ 20%	Good
15% < CBL ≤ 30%	20% < CBL ≤ 40%	Medium (qualified)
CBL > 30%	CBL > 40%	Poor (unqualified)

Note Low-density cement means cement slurry with density between 1.30 g/cm<sup>3</sup> and 1.75 g/cm<sup>3</sup>

The relative acoustic amplitude values of cement job quality assessment are shown in Table 5-10.

## 2. Variable density log (VDL)

Variable density log has been commonly used in recent years. It can be used for measuring and recording the formation wave and reflecting the status of the bond between cement and formation (known as second interface). After the results of variable density log are contrasted with the results of acoustic amplitudes log, the cement sheath quality can be comprehensively assessed.

The qualitative quality assessment of the first and second interfaces of cement sheath on the basis of VDL is shown in Table 5-11.

## 3. Segmented cement bond log

Cement bond quality is measured by using a segmented bond tool (SBT) in longitudinal and lateral (circumferential) directions. A segmented bond tool has six slide plates. Two high-frequency oriented transducers are attached to each slide plate and are used for measurement in six sectors of 60° around casing. Six slide plates have six power backup arms. Each arm sticks an emitter-receiver transducer slide plate on the inner wall of the casing. The distance between emitter transducer and receiver transducer is 15.2 cm. Segmented cement bond log is insensitive to gassing in heavy drilling fluid or drilling fluid, the influence of high-speed bed on adopting

**TABLE 5-11 Qualitative Cement Job Quality Assessment Based on VDL**

VDL Characteristics		Qualitative Cement Job Quality Assessment Conclusion	
Casing Wave Characteristic	Formation Wave Characteristic	Bond Status of First Interface	Bond Status of Second Interface
Very weak or no	Clear formation wave; good synchronism of phase line with AC	Good	Good
Very weak or no	No; weak formation by AC; hole not enlarged	Good	Good
Very weak or no	No; weak formation by AC; large hole	Good	Poor
Very weak or no	Weak	Good	Partial bond
Weak	Clear formation wave	Partial bond (or micro-annulus)	Partial to good bond
Weak	No or weak formation wave	Partial bond	Poor
Weak	Unclear formation wave	Medium	Poor
Weak	Weak	Slightly poor	Partial to good bond
Very strong	No	Poor	Unable to determine

Note: AC is compressional wave moveout curve measured in open hole.

short spacing, and the eccentricity of the tool, and so on, are insensitive due to the casing wall contact measurement. These factors have a great influence on conventional cement bond log.

Segmented cement bond log can be used for the following:

- a. Determining the cement bond status on casing-cement interface and formation-cement interface
- b. Showing circumferential, omnidirectional cement bond status around the casing so that the multiple solvability of conventional cement bond log may be overcome
- c. Judging the channeling location
- d. Effective assessment of cement bond status of large-diameter casing (406-mm-dia. casing)
- e. Assessment of the casing bond status of horizontal well

## 5.5 PRODUCTION CASING AND CEMENTING FOR COMPLEX TYPE WELLS

These wells include high-temperature high-pressure deep and superdeep wells, high-temperature high-pressure gas wells, high H<sub>2</sub>S or CO<sub>2</sub> wells, wells that easily lose circulation, thermal production wells, horizontal wells, adjustment wells, and external casing packer wells.

### Superdeep Wells and High-Temperature High-Pressure Gas Wells

**Main Problems.** Production casing and cementing may often be faced with more complicated and special conditions in superdeep wells and high-temperature high-pressure gas wells. The problems include mainly the following:

1. A high-capacity gas well needs to have a large diameter tubing and corresponding large production casing. For instance, production casing diameter is enlarged from 9 5/8 in. to 9 7/8 in. in the KL-2 well. Large diameter production casing under

high pressure may be faced with many technical problems of internal pressure strength and sealing property.

2. A superdeep well needs to have a casing of high-strength steel grade. High-strength steel is sensitive to the failure of cracking. If the reservoir contains hydrogen sulfide, then high-strength steel grade cannot be adopted.
3. Conventional hole structure cannot meet the requirements of a superdeep well, and nonconventional hole structure is required. Nonconventional hole structure requires non-standard size casing and corresponding accessories and tools. If slip-type casinghead is used, the problem of casing collapse and deformation should be considered due to the great casing string weight. Shoulder-type casinghead should be preferentially used for hanging casing string.
4. In a high-temperature high-pressure gas well, tieback is generally required after a liner is run in, and intermediate casing is not generally used as production casing. The tieback sleeve on the liner head and the tubular stinger should be able to bear a high-pressure seal. The failure of the seal may cause a serious result. If lost circulation during cementing is predicted, the tieback technique should be designed to prevent lost circulation during cementing. In a high-temperature high-pressure gas well, cementing by using stage-cementing collar has a low sealing reliability and may generate leakage or breakdown, thus making serious future trouble. At a stage-cementing collar, the setting quality of the external casing cementing is poor, or there is a mixed slurry section, or even there is no cement sheath; thus, external casing corrosion may be caused, and a local compression deformation may be generated at a thinning place due to corrosion on the casing wall.
5. In a superdeep well, liner completion is generally adopted. The cement job quality is difficult to ensure due to the small clearance and long cementing section. Gas channeling after cementing, cementing channel, water invasion of water-bearing permeable interval, lost

circulation during cementing, and excessive pump pressure or even pump bouncing during cement, and so on, may be generated.

### Solving Means

1. Using casing material suitable for superdeep well and high-temperature gas well
  - a. Effect of high temperature on casing strength. The yield strength and elastic modulus of steel may be slightly reduced at high temperature, and the casing strength performance indices calculated in accordance with ISO/API standards may be correspondingly reduced. The safety factor of casing strength design should consider the reduction of steel strength at high temperature. The curves of P110 and Q125 steel grade casing strength reduction with the increase of temperature are shown in Figure 5-11. It is shown that the yield strength is reduced by 8% to 11% at 140°C while the yield strength is reduced by about 11% to 13% at 200°C. The casing strength calculation formula adopts a conservative calculation method or correction factor. For instance, the wall thickness is decreased by 12.5% on the basis of nominal wall

thickness. The actual yield strength of casing produced by the manufacturer is higher than the minimum nominal yield strength in order to ensure fully meeting the requirement of minimum nominal yield strength of 110 ksi or 125 ksi. Thus the material strength reduction at high temperature is only considered when the strength is designed in the critical state.

- b. Performance matching requirements of high-strength steel.

Q125 is a high-strength steel that has been listed in the standard. In addition, the casings of 140 ksi and 150 ksi steel grades are also used by the industrial sector under special conditions. High-strength steel is sensitive to the failure of cracking; thus special attention should be paid to the steel properties that are related to cracking and crack propagation. Charpy impact toughness is a composite index that reflects crack propagation resistance of material and should be matched with the strength and wall thickness. A high-yield strength should correspond to a high Charpy impact toughness. ISO 11960 has specified the

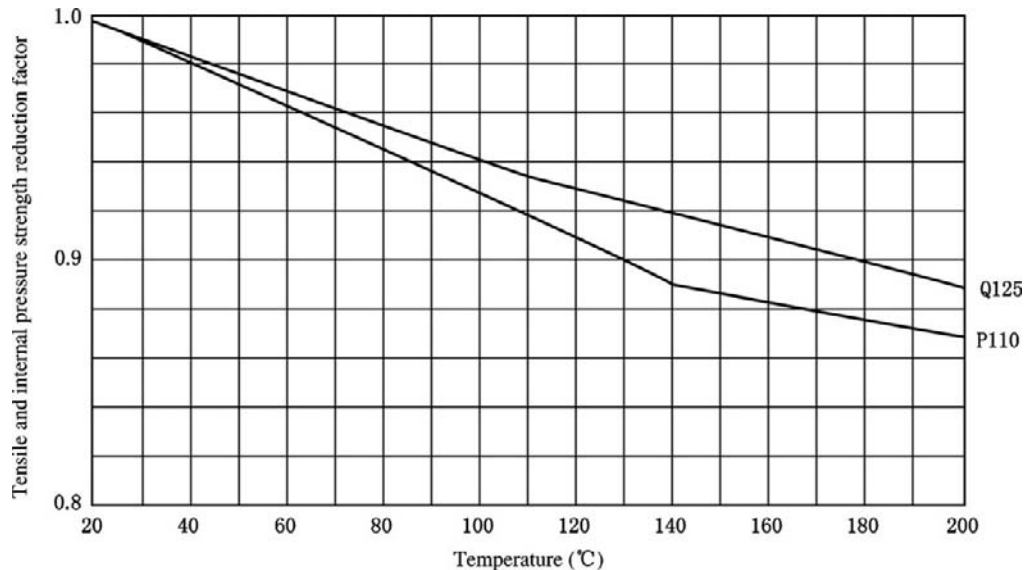


FIGURE 5-11 Casing strength reduction with increase of temperature.

minimum longitudinal and lateral Charpy impact toughness values of different steel grades, which are the minimum standards. Designers should first select casings with high Charpy impact toughness when they are used in high-temperature high-pressure and high-capacity gas wells. The lateral Charpy impact toughness values of collar and casing body play an important part in the longitudinal cracking failure of the collar and disruptive failure of the casing; thus the lateral Charpy impact toughness of casing should be especially emphasized when the casing is used in high-pressure gas wells.

The defect detection of high-strength steel casing above Q125 should be more rigorous. Both the internal and external surfaces of casing should not have a defect that has a crack depth greater than 5% of wall thickness. Scoring should also be avoided during casing running operation and downhole operation.

## 2. Using liner as production casing

Deep and superdeep well completion adopts the same diameter casing. Large diameter production casing when it is run to bottomhole has a great total weight. In addition, the cement job quality of long-section cementing is difficult to ensure. Currently, deep and superdeep well completion mostly adopts liner completion, which is favorable for protecting oil and gas reservoirs and reducing formation damage, can ensure the cement job quality of the reservoir interval and the whole well, and can decrease the usage of large diameter casing and the cement slurry volume. Liner completion has a short cement section and can avoid the cementing channel and the gas invasion or channeling during curing time, thus favoring enhancing cement job quality. After liner cementing, the reservoir has been cemented. The production casing is then run in for tieback (the soak time of drilling fluid is decreased) and cementing. The cementing discharge capacity can be increased just as in conventional cementing, cementing is not disturbed by reservoir oil and gas, and the

cement job quality is also ensured. In addition, a large diameter tubing can be set above the liner. However, the annular clearance of liner completion is generally small, the liner hanger has a complicated structure, the liner completion operation has a complicated procedure, the cementing discharge capacity is limited, and the liner completion should meet high operational requirements.

- a. The annular clearance at the collar should not be less than 5/8 in. (16 mm) in order to ensure a sufficient cement sheath thickness. A reamer bit can be used for reaming. On the basis of experience, a 7 in. (177.8 mm) liner requires a borehole diameter larger than 230 mm, while a 5 1/2 in. (139.3 mm) liner requires a borehole diameter larger than 190 mm in order to ensure annulus cement job quality. However, these requirements have not been achieved in practical operations at present.
- b. During running-in liner, the landing time for each liner should not be less than 1 to 1.5 minutes in order to prevent formation leakoff and prevent hanger spring and slip dog, and so on, from damage.
- c. Sufficient preflush and cement slurry volumes should be ensured in order to ensure that the time of contacting the main isolation interval is not less than 10 minutes.
- d. Attention should be paid to the requirements for cement slurry properties. Cement slurry mobility should be improved, and fluid loss should be decreased. The evenness of the cement slurry should be ensured by using preformulation.
- e. The overlay length of liner and upper casing should be between 50 m and 150 m. Too great overlay length is inappropriate even under special conditions.
- f. When cementing plug impingement is not adopted, a special metering tank should be set up. When cementing plug impingement is adopted, an overdisplacement is also inappropriate if plug impingement has not been achieved yet after displacement volume exceeds compressibility volume.

- g. If allowed by conditions, the liner is appropriately rotated in order to enhance cement job quality. In deep wells, directional wells, and horizontal wells, a liner hanger that can be hydraulically unhung should be adopted in order to prevent mistaken judging of whether back-off operation has been completed.
3. Measures for cementing under small clearances of borehole-casing annulus and intermediate casing-production casing annulus

Deep wells and superdeep wells have a complicated casing program and small clearances of borehole-casing annulus and intermediate casing-production casing annulus, thus causing difficulties in hole structure and cementing.

- a. Using integral joint casing or special clearance collar casing. The casing program of 20 in./13 3/8 in./9 5/8 in./7 in./5 in. and threaded collar joint are adopted in China at present. The casing matching series is affected by collar diameter to a great extent. The collar diameter of standard casing series is 12.7 mm larger than casing body diameter for 4 1/2-in. casing and 25.4 mm larger than casing body diameter for 10 3/4-in. casing. The casing collar-borehole clearances of 7-in. casing in 8 1/2-in. borehole and 5-in. casing in 5 7/8-in. borehole are 10.7 mm and 3.95 mm, respectively (Table 5-12).

A clearance value smaller than 0.5 in. (12.7 mm) may cause difficulty in running casing and cannot ensure cement job quality. An 8 1/2-in. (215.9 mm) bit cannot pass through 9 5/8-in. (244.5 mm) casing with a wall thickness of 13.84 mm and can only pass through 9 5/8-in. high collapsing strength casing with a wall thickness of 11.19 mm, thus requiring an 8 3/8-in. (212.7 mm) bit and causing a further small annular clearance outside 7-in. casing.

One approach to solving this problem is the adoption of integral joint casing or special clearance collar casing.

Integral joint casing has special trapezoidal thread machined directly on the

casing body. There are two types of integral joint casing:

- (1) Casing with upset end. These casings include external upset casing and internal and external upset casing. The OD of the upset end is 2% to 3% larger than the casing body OD.
- (2) Casing with non-upset end. The OD and ID of the non-upset end are the same as that of the casing body. Figure 5-12 shows the integral casing joint structures. Table 5-13 shows the model numbers of threads and specifications of integral joint casings of several manufacturers.

The external collapsing strength and internal pressure strength of integral joint casing are the same as that of common casing, whereas the tensile strength of the thread connection is only 65% to 80% of the tensile strength of the casing body. Integral joint casing is generally used as a liner, and the tensile strength may meet production requirements. Integral joint casing is a non-API casing, and the data provided by the manufacturer can be consulted during design and use.

- b. Special clearance collar casing. The special clearance collar diameter is from 9.52 mm (for 4 1/2-in. special clearance collar casing) to 12.7 mm (for 10 3/4-in. special clearance collar casing) larger than the casing body diameter. Only the buttress thread casing has a special clearance collar and has been listed in the API standard. The collapsing strength and internal pressure strength of a special clearance collar casing are the same as that of a standard collar. The tensile strength of a special collar casing thread is lower than the tensile strength of a standard collar casing thread. For casings with the same steel grade and size, the tensile strength of thick-wall round thread casing is higher than that of special clearance collar

**TABLE 5-12 Clearances Between 7-in. Casing and Bit and Between 5-in. Casing and Bit**

Upper Casing		Lower Casing				Lower Casing OD-Upper Casing Clearance (mm)	Lower Casing Collar-Upper Casing Clearance (mm)	Lower casing OD-Borehole Wall Clearance (mm)	Lower Casing Collar- Borehole Wall Clearance (mm)
OD mm (in.)	Wall Thickness (mm)	ID $a_n$ (mm)	Bit size $b_n$ (mm)	Casing OD $c_n$ (mm)	Collar OD $d_n$ (mm)	$A_n = \frac{a_n - c_n}{2}$	$B_n = \frac{a_n - d_n}{2}$	$C_n = \frac{b_n - c_n}{2}$	$D_n = \frac{b_n - d_n}{2}$
244.5 (9 <sup>5</sup> / <sub>8</sub> )	11.19	$a_1$ :222.12	$b_1$ :215.9	$c_1$ :177.8	$d_1$ :194.5	$A_1$ :22.16	$B_1$ :13.81	$C_1$ :19.05	$D_1$ :10.7
	13.84	$a_2$ :216.12	(8 <sup>1</sup> / <sub>2</sub> )			$A_2$ :19.51	$B_2$ :11.61		
177.8 (7)	10.36	$a_3$ :157.08	$b_2$ :149.2	$c_2$ :127	$d_2$ :141.3	$A_3$ :15.04	$B_3$ :7.89	$C_2$ :11.1	$D_2$ :3.95
	11.51	$a_4$ :154.78	(5 <sup>7</sup> / <sub>8</sub> )			$A_4$ :13.89	$B_4$ :6.74		
	12.65	$a_5$ :152.5				$A_5$ :12.71	$B_5$ :5.60		

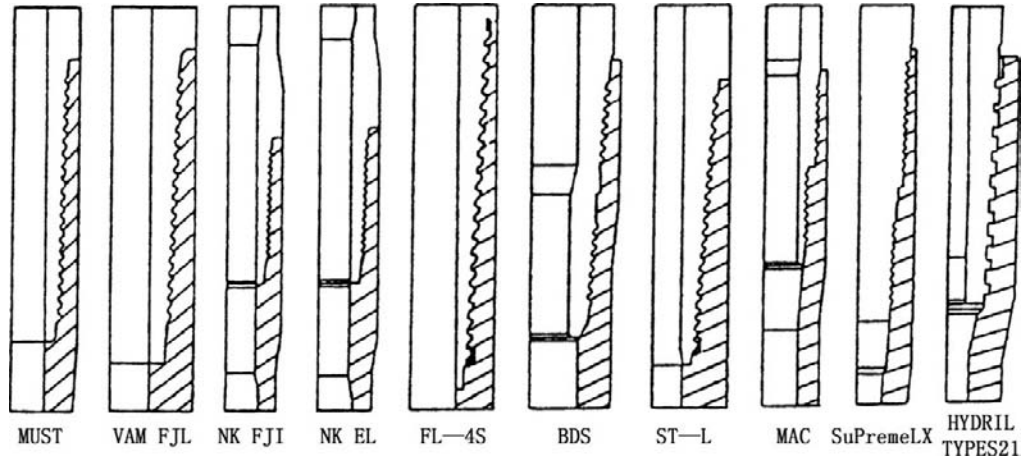


FIGURE 5-12 Integral casing joint structures.

TABLE 5-13 Types of Integral Joint Casing

Manufacturer	Thread Name	Production Casing Specifications		
		Outside Diameter (mm)	Steel Grade	Remarks
Dalmine	FL-4S	101.6~244.475(4~8 <sup>5</sup> / <sub>8</sub> in.)	API series	Full flush type
Siderca	ST-L	101.6~346.075(4~13 <sup>5</sup> / <sub>8</sub> in.)	API series	Internal upset slightly
Tamsa	NJO	101.6~346.075(4~13 <sup>5</sup> / <sub>8</sub> in.)	API series	Upset type
Mannesmann	BDS	114.3~346.075(4 <sup>1</sup> / <sub>2</sub> ~13 <sup>5</sup> / <sub>8</sub> in.)	API series,	Upset type
	MUST	139.7~273.05(5 <sup>1</sup> / <sub>2</sub> ~10 <sup>3</sup> / <sub>4</sub> in.)	API series, MW series	Full flush type
	FLUSH	127.0~323.85(5~12 <sup>3</sup> / <sub>4</sub> in.)	API series, MW series	Full flush type
	OMEGA	114.3~349.75(4 <sup>1</sup> / <sub>2</sub> ~13 <sup>3</sup> / <sub>8</sub> in.)	API series, MW series	Upset type
Hydril	Supreme LX	114.3~346.075(4 <sup>1</sup> / <sub>2</sub> ~13 <sup>5</sup> / <sub>8</sub> in.)	API series, MW series	Upset type
	Typ. 521	114.3~473.075(4 <sup>1</sup> / <sub>2</sub> ~18 <sup>5</sup> / <sub>8</sub> in.)	API series, 140, 150	Upset type
	MAC	127.0~406.4(5~16 in.)	API series, 140, 150	Upset type
NKK	NK-EL	127.0~273.05(5~10 <sup>3</sup> / <sub>4</sub> in.)	API series, NK series	Upset type
	NK FJ1	101.6~196.85(4~7 <sup>3</sup> / <sub>4</sub> in.)	API series, NK series	Upset type
	NK FJ2	101.6~196.85(4~7 <sup>3</sup> / <sub>4</sub> in.)	API series, NK series	Full flush type
	NK HW	127.0~355.6(5~14 in.)	API series, NK series	Upset type
Nippon Steel	BDS	114.3~349.75(4 <sup>1</sup> / <sub>2</sub> ~13 <sup>3</sup> / <sub>8</sub> in.)	API series, NT series	Upset type
	FL-4S	101.6~349.75(4~13 <sup>3</sup> / <sub>8</sub> in.)	API series, NT series	Full flush type
	NSSC-SC		API series, NT series	

casing. However, for thin-wall casing, the tensile strength of a special clearance collar is higher than that of a standard round thread casing. High internal pressure may decrease the slipping strength of a special collar, which, however, has not been introduced into design standards.

#### 4. Reaming and close clearance hole structure

The key technique of solving close clearance hole structure and cement job quality is reaming while drilling. Reaming is used for increasing cement sheath thickness to enhance cement job quality and changing the casing program.

a. Increasing cement sheath thickness. For a deep well, a  $\Phi 127$  mm (5 in.) liner is

often run in a  $\Phi 149.2$  mm (5 7/8 in.) well, and the clearance between collar and borehole is only 3.95 mm (Table 5-12). In addition to running risk, cement job quality cannot be assured. The basic measure is to use a special bicenter bit for reaming while drilling. A 7-in. (177.8 mm) liner requires a borehole diameter larger than 230 mm, while a 5 1/2-in. (139.3 mm) liner requires a borehole diameter larger than 190 mm. The annular clearance of the collar should not be less than 16 mm; however, this is difficult to accomplish in practice.

- b. Changing the casing program. In a deep well, production casing diameter as large as possible is required. When a not too large borehole bit and a production casing as large as possible are required, or the number of casings is required to be increased in order to avoid a complicated downhole condition, it is certain to relate to a close clearance casing program. For instance, a  $\Phi 241.3$  mm (9 1/2 in.) borehole is drilled by using a bicenter bit (reaming while drilling), and a  $\Phi 193.67$  mm (7 5/8 in.) liner or casing is run in. A 5 1/2-in. liner or casing is run in a 7 5/8-in. liner. The standard 7 5/8-in. casing collar OD is 215.9 mm. The collar of this size cannot pass or cannot be sure to pass through 9 5/8-in. casing; thus only a 7 5/8-in. special collar casing (its collar OD is 206.38 mm) can be used. The selection of close clearance casing program is dependent on formation, which is easy to ream while drilling using a bicenter bit. Production casing size is increased in order to favor production and downhole operations, but this is still difficult to perform in practice.
5. Close clearance well cementing

During setting of cement slurry, the smaller the annular clearance, the greater the decline rate of hydrostatic column pressure of cement slurry. This indicates that the weight loss in close clearance annulus is faster than that in normal annulus and large

annulus, and gas channeling may be more likely to be generated during curing; thus a greater gas-channeling inhibiting ability of cement slurry is required, and the following methods can be used:

- a. Decreasing cement slurry weightlessness and increasing gas-channeling resistance. When cement slurry is in a liquid state, or after cement slurry is initially set, gas channeling may be generated in the transitional process from plastic state to solid state, and the structural pores (except the internal defect of slurry body and the defect at the bonding interface) are the weakest spots in the cement body. Therefore, in order to inhibit gas channeling due to cement slurry weightlessness, the following relationship should be met:

Pore pressure (including additional pressure generated by additives) + resistance to flow in pores > gas reservoir pressure

Gas channeling is still possible when common gas-channeling inhibiting cement slurry is used. The supplementary gas-channeling inhibiting measures (such as decreasing cementing section length, using separable setting cement slurry, and increasing annulus backpressure) have a limited effect due to the restriction of downhole conditions. Thus the basic principle of enhancing gas-channeling inhibiting ability is not only compensating for or decreasing cement slurry weightlessness but also increasing gas-channeling resistance when cement slurry is in a plastic state during pore transfer. During setting of this type of cement slurry, the effective pressure can be obviously compensated, and gas-channeling resistance can also be obviously increased and can be increased with the increase of quantity of gas-channeling inhibitor. This indicates that this type of cement slurry can obviously compensate for cement slurry weightlessness and a good gas-channeling inhibiting effect.

- b. Increasing strengths of bonding between cement and casing and between cement

and borehole wall. During cement slurry setting, the micropores form within the set cement body due to hydration, and visual volume contraction is generated. In general, the shrinkage factor of cement slurry during initial setting is 0.1% to 0.5% while the shrinkage factor after final setting is higher than 2%, thus generating micro-annulus and leading to reduction of the formation-isolating ability of cement sheath or causing failure. The method of solving this problem includes adding an expanding agent of appropriate type and quantity to the cement slurry so that there is no volume contraction or there is micro-expansion, thus preventing generation of micro-annulus, which may be formed by hydration and volume contraction, and also enhancing the strength of bonding between cement sheath and formation and between cement sheath and casing.

- c. Decreasing fluid loss and bleeding of cement slurry to the full extent. Under pressure of 6.9 MPa, the fluid loss should be lower than 50 ml/30 min, and the bleeding should be zero or trace.
- d. Using superfine cement or plastic cement system. Using superfine cement or adding fiber material and latex, and so on, to cement can increase cement plasticity and set cement impact toughness, thus favoring preventing the cracking caused by perforating.
- e. Increasing contact time under turbulent flow. The contact time under turbulent flow can only be increased by increasing flush fluid or spacer fluid volume due to lower cement slurry volume of the liner. The liner is rotated during cementing if it is allowed.
- f. Ensuring achieving pressure balance during cementing

In high-temperature high-pressure multi-zone wells, in order to achieve pressure balance and ensure no lost circulation and no blowout, the following basic work should be done:

1. Comprehensively understanding the operational parameters and complicated conditions (especially drilling pump rate and circulation pressure) during drilling and accurately taking the test and predicted data of formation pressure and formation breakdown pressure.
2. Understanding and taking in detail the geological conditions of the sections that are prone to lost circulation and sloughing and the related data of leak-off pressure and location and understanding formation sensitivities to foreign fluids.
3. Rationally designing the densities and service lengths of cement slurry and spacer fluid and checking the annulus pressure.
4. Designing the displacement rate range during cementing in accordance with the most stable condition during drilling.
5. Systematically selecting and designing the cement slurry system and pad fluid system on the basis of formation characteristics and cementing requirement, thus ensuring having good rheological property.
6. Using cementing simulation software for comprehensively analyzing the pressure variation during cementing, and then adjusting and revising the fluid density and volume, pumping rate, and fluid properties; avoiding lost circulation or channeling. The effect of temperature on rheological property, the effect of close clearance on flow calculation, and so on, should be considered in simulation calculation.

### Corrosive Media-Containing Oil and Gas Wells

The corrosive media in formation, which include mainly  $\text{Cl}^-$ ,  $\text{HCO}_3^-$ ,  $\text{Mg}^+$ ,  $\text{CO}_2$ , and  $\text{H}_2\text{S}$ , may corrode the cement sheath and then the casing, thus seriously influencing the service life of an oil and gas well. If a well has an acceptable cementing job quality testified by detection, this does not mean that it has a long-term service life. The problem of the corrosion of the cement sheath by sulfate has been noticed, and sulfate-resistant cement has been correspondingly used;

however, attention has not been paid to the corrosion of cement sheath by carbon dioxide and hydrogen sulfide. In high-temperature high-pressure wells and high-capacity gas wells, the corrosion of the cement sheath by carbon dioxide and hydrogen sulfide may cause casing corrosion boring or interzonal cross-flow, thus generating a potential threat against the safety of this type of well.

**Physico-Chemical Reaction in the Corrosion Process.** The corrosion action of corrosive media on the cement sheath includes dissolution, ion exchange, and crystallization expansion, and which one is predominant depends on cement composition, microstructure of set cement, type of corrosive media, environmental conditions, and so on.

#### 1. Dissolution action

This means mainly the leaching action of media on set cement. The solid  $\text{Ca}(\text{OH})_2$  may be gradually reached under the condition of flowing water, thus causing the failure of the set cement structure. In addition, the hydrated silicate and aluminate may be decomposed due to the decrease of alkaline phase concentration of cement.

#### 2. Ion-exchange erosion action

The carbonic acid (also including  $\text{CO}_2$ ), organic acid, inorganic acid, alkali metal, and alkali earth metal (such as magnesia salt) which are dissolved in water may generate an ion-exchange reaction with set cement. The ion-exchange reaction includes the reaction of carbonic acid to set cement, the reaction of inorganic acid to set cement, and the reaction of alkali metal and alkali earth metal in corrosive media to set cement.

### Sulfate Corrosion and Sulfate-Reducing Bacteria Corrosion

#### 1. Sulfate corrosion

Sulfate corrosion is a typical expansion failure action. The secondary hydration product generated by the reaction of sulfate to set cement may cause the failure of the set cement structure. When the sulfate in

media reacts to  $\text{Ca}(\text{OH})_2$ ,  $\text{C}_3\text{A}$ , and C-S-H, and so on, in set cement, the crystalline (gypsum or calcium aluminate, and so on) may be formed and grows and expands gradually in set cement pores during reaction, thus causing the failure of set cement structure. In addition, sulfate may also compose hydrated silicate and fail the solid structure of cement.

#### 2. Sulfate-reducing bacteria corrosion

Sulfate reducing bacteria (SRB) grow in a specific environment, thus obviously changing the physical and chemical properties of the environment. SRB metabolize by using sulfate, thus reducing  $\text{SO}_4^{2-}$  to  $\text{S}^{2-}$ . The final product, that is,  $\text{H}_2\text{S}$ , which is generated by combining  $\text{S}^{2-}$  and  $\text{HS}^-$  with  $\text{H}^+$ , may aggravate corrosion.

### Corrosion Action of Carbon Dioxide on Set Cement

#### 1. Chemical erosion action of carbon dioxide on set cement

The corrosion action of carbon dioxide on set cement of an oil well is of chemical erosion. The mechanism includes:

- a. Leaching action. Carbon dioxide may enter set cement after dissolving in water, react with  $\text{Ca}(\text{HCO}_3)_2$ , and form  $\text{CaCO}_3$  and water.  $\text{CaCO}_3$  may form  $\text{Ca}(\text{HCO}_3)_2$  under the action of  $\text{CO}_2$ -rich formation water, and then  $\text{Ca}(\text{HCO}_3)_2$  reacts to  $\text{Ca}(\text{OH})_2$  and generates  $\text{CaCO}_3$  and water. The water generated (equivalent to fresh water) continuously dissolves  $\text{Ca}(\text{HCO}_3)_2$ , and this reaction is repeated just as fresh water leaches set cement.
- b. Dissolution action. After  $\text{Ca}(\text{OH})_2$  is consumed, unconsolidated amorphous  $\text{SiO}_2$  is generated by the reaction of  $\text{CO}_2$  with CSH, thus causing the failure of integral consolidation of set cement.
- c. Carbonization contraction action.  $\text{Ca}(\text{OH})_2$  is a main reactant to generate expansive material (calcium aluminate). When  $\text{Ca}(\text{OH})_2$  is consumed by  $\text{CO}_2$ , calcium aluminate cannot exist stably, thus causing the contraction of set cement.

- d. Synergistic action of high-salinity formation water. High-salinity formation water may increase solubility of  $\text{CaCO}_3$ , thus aggravating leaching action.

The aforementioned actions indicate that the main products (that is,  $\text{CaCO}_3$  and amorphous  $\text{SiO}_2$ ) after set cement is corroded by  $\text{CO}_2$  are of unconsolidated material. The theoretical calculation indicates that the 2 mol  $\text{H}^+$  evolution per 1 mol  $\text{CO}_2$  consumption during carbonization may decrease pH value from 12.6 to 8.3. Under this final pH value, almost all the hydration products in set cement may be decomposed.

2. Severity of supercritical carbon dioxide corrosion

Carbon dioxide gas at a temperature above  $31^\circ\text{C}$  under a pressure higher than 7.3 MPa is in a supercritical state. Carbon dioxide in a supercritical state has very high penetrating ability and extractability. Serious strength retrogression of set cement has been observed in laboratory experiments.

### Corrosion Action of Hydrogen Sulfide on Cement Sheath

1. Mechanism of corrosion action of hydrogen sulfide on cement sheath

Hydrogen sulfide will assume acidity after dissolving in water. The components of set cement assume basicity. The reaction of  $\text{H}_2\text{S}$  to set cement will generate  $\text{CaS}$  and  $\text{FeS}$  and will generate  $\text{Ca}(\text{HS})_2$ ,  $\text{CaS}$ , and  $\text{Al}_2\text{S}_3$  (which are unconsolidated products) when the  $\text{H}_2\text{S}$  content is high. After the cement sheath is corroded, the casing will directly expose in the corrosive environment of  $\text{H}_2\text{S}$ .

2. Promotion of corrosive action of hydrogen sulfide on cement by methane gas

It has been observed in laboratory experiments that hydrogen sulfide corrosion will be promoted under the condition of methane.

### Approaches to Cement Sheath Corrosion Prevention

1. Adjusting cement clinker composition

The aforementioned erosion mechanism shows that calcium hydroxide and hydrated

calcium aluminate in set cement is the internal cause leading to set cement failure; thus, the  $\text{C}_3\text{A}$  content should first be controlled for corrosion prevention. The expansion ratio of set cement in  $\text{CaSO}_4$  solution is gradually increased with the increase of  $\text{C}_3\text{A}$  content. The  $\text{C}_4\text{AF}$  in the cement clinker can inhibit expansion reaction to a certain extent. The appropriate increase of  $\text{C}_3\text{AF}$  content (total content of  $\text{C}_3\text{AF}$  and 2  $\text{C}_3\text{A}$  in high-sulfate-resistant cement up to 24%) can enhance sulfate erosion resistance).

2. Decreasing  $\text{Ca}(\text{OH})_2$  crystal content in set cement

The activated  $\text{SiO}_2$ -rich material (such as silica flour or microsilica, volcanic ash, and slag) can react with  $\text{Ca}(\text{OH})_2$  and generate a new hydrated calcium silicate C-S-HIII when added to cement composition, thus increasing erosion resistance of set cement.

3. Enhancing set cement tightness for preventing corrosive media from invading

a. Microsilica is appropriately added to cement composition. Impermeable tight set cement structure is formed due to good size grading between microsilica and cement particles, thus preventing corrosive media from further erosion.

b. A latex cement system is used. Set cement pores are filled with polymer films or gel particles so that set cement permeability is decreased, and erosion resistance is increased. A further satisfactory result can be achieved with the combined use of latex and microsilica or fly ash.

4. Developing a hydrogen sulfide corrosion-resistant oil well cement system

Developing and adopting a hydrogen sulfide corrosion-resistant oil well cement can intrinsically enhance corrosion resistance and are of great significance to sour gas well cementing, cement plug building, sour gas well plugging and abandoning, and so on.

5. Adopting a cement slurry system with high gas-channeling resistance for preventing generating gas channeling during cement slurry setting

This type of cement slurry system includes channeling-resistant compressible cement slurry system (such as KQ series), latex cement slurry system (such as PCR168 and PCR169), slightly expanding latex cement slurry, and so on. Gas-channeling inhibiting measures include rationally using separable setting cement slurry, and acting annulus backpressure during curing.

## Wells That Absorb Easily

### Main Problems

1. Low-pressure wells that absorb easily
 

The typical low-pressure lost-circulation zone includes low-pressure fractured reservoirs and sandstone reservoirs. A drilling fluid column pressure higher than reservoir pressure may cause leakage of a large quantity of drilling fluid during drilling. Cement slurry column pressure higher than reservoir pressure may also cause a leakage of cement slurry during cementing. Lost circulation during cementing may make the reservoir uncemented or imperfectly cemented or cause an insufficient cement slurry return height, which may cause interzone communication, thus causing sloughing because the water in water-bearing formation invades the restraining barrier. In addition, the leakage of cement slurry may plug fractures and cause formation damage.
2. High-pressure leaking wells that easily absorb
 

A high-pressure well that easily absorbs often presents blowout and leaking because there simultaneously are a low-pressure lost-circulation zone and a high-pressure gas reservoir in the same open hole section. In general, there are two situations. One is that a lost-circulation zone is above a high-pressure gas reservoir. During drilling by using low-density drilling fluid or continuous drilling after sealing, a high-pressure gas reservoir is drilled-in. Increasing drilling fluid density may cause an overflow due to the lost-circulation zone, thus inducing blowout. The other situation is that a lost-circulation zone is below a high-pressure gas reservoir. During drilling

the upper part the gas reservoir has been suppressed; however, when the lower lost-circulation zone is drilled in, lost circulation is generated. Thus the whole fluid column pressure in the borehole may be decreased, and an overflow may be caused, or even a blowout may be caused.

In many deep wells, cement slurry is required to be returned to the surface, thus aggravating the risk of lost circulation during cementing.

### Approaches to Cementing Leakage Prevention

1. Improving hole structure and cementing technology
 

The program of improving hole structure, which is to isolate high-pressure or low-pressure reservoirs by using casing, should first be selected. At first the liner is cemented, and then it is tied back to the wellhead. This is the principal approach of enhancing cement job quality and preventing lost circulation during cementing. For high-temperature high-pressure gas wells and sulfur-bearing gas wells, it is appropriate to use this cementing technique predominantly. The two-stage cementing technique with stage-cementing collar can favor solving the lost-circulation problem during cementing; however, it should be prudently considered to use it under the condition of production casing cementing, or it is limited to the oil well. With a stage-cementing collar, it is difficult to meet the requirements of gas tightness, internal pressure strength, and corrosion prevention.

In order to decrease or prevent cementing leakage, the rheology and pressure drop calculations are required under the specific borehole and string conditions, the annulus flow pressure should be reduced to the full extent by adjusting the pumping rate, and the following cement slurry techniques may be used.
2. Using low-density cement system
  - a. Low-density bentonite cement. Bentonite is used as lightening admixture; thus a cement slurry density of 1.50–1.60 g/cm<sup>3</sup> can be obtained. Bentonite cement has good properties except lower strength

and is suitable to low-pressure and lost-circulation reservoir cementing.

- b. Low-density fly ash cement. Fly ash consists mainly of fine glass bead, spongy vitreum, quartz, iron oxide, carbon particles, and sulfate, and so on, in which fine glass bead and spongy vitreum are principal. The cement slurry density may be adjusted by mixing ratio and can be 1.55–1.70 g/cm<sup>3</sup>. The stable low-calcium silicic hydration product that is generated by the reaction of fly ash to the free lime precipitated during cement hydration reaction can increase the strength and tightness of set cement and increase the corrosion resistance.
- c. Low-density fine bead cement. The chemical composition of fine beads includes oxides of silicon, aluminum, and iron. Fine beads have a light weight, little adsorption water, a certain activity, and good compatibility with cement. The fine beads used on site at present are mainly round hollow beads (floating beads), which can be used for formulating a cement slurry with a density of 1.20–1.60 g/cm<sup>3</sup>. The practice indicates that the low-density fine bead cement has a higher compressive strength than other low-density cement and is mainly used in shallow wells with a well depth less than 3000 m.
- d. Low-density foamed cement. A certain quantity of gas is mixed with or generated in cement slurry and evenly distributed in cement slurry, thus reducing cement slurry density. The merits of foamed cement include low density (generally 0.84–1.32 g/cm<sup>3</sup>, down to 0.5–0.6 g/cm<sup>3</sup>); good rheological property (which can fully meet operational requirements); and higher strength than other low-density cements. Under the condition of weight loss, the compressible elastic microbubbles in cement slurry may compensate for the decrease of water volume during hydration, thus restricting the invasion of formation water and avoiding the generation of channeling.

Because of the aforementioned merits, foamed cement is the first selection of cements used in cementing operation of low-pressure low-permeability oil and gas reservoirs.

### 3. Using lost-circulation fiber cement

Inorganic or organic synthetic fiber material is added to cement slurry, and a three-dimensional fiber-bridged cement cake is formed in fracture, vugular pore space, or the vicinity of the borehole wall, thus preventing cement slurry from leaking. In addition, fiber cement can enhance the toughness and impact resistance of the cement sheath. Optimizing fiber material can obviously improve the leak resistance property. The basic requirements for fiber material include appropriate length-to-diameter ratio; good dispersity in cement slurry, not plugging the pipe manifold and downhole casing accessories; inertness of material, not damaging the operational property of cement slurry; and high property of bonding with cement.

### 4. Adopting two-stage cementing

A stage-cementing collar is generally set between main lost-circulation zone and main high-pressure gas reservoirs in accordance with the balanced-pressure cementing principle. When the high-pressure gas reservoir is below the low-pressure lost-circulation zone, the part below the stage-cementing collar can be cemented by using high-strength high-density cement slurry (1.80–1.85 g/cm<sup>3</sup>), while the part above the stage-cementing collar is cemented by using cement slurry with a density lower than that corresponding to the lost-circulation zone pressure gradient. When the high-pressure gas reservoir is above the lost-circulation zone, leakage of the first stage should be noticed when a stage-cementing collar is used for cementing.

### 5. Adopting liner cementing

When liner cementing is adopted, the balanced-pressure calculation should be seriously done so that the high-pressure reservoir is stably suppressed while the low-pressure lost-circulation zone does not generate leaking.

During operation several sections of liquids with different densities (such as low-density cement slurry and high-temperature-resistant high-strength cement slurry) are sometimes required to be injected. If leaking is generated during cementing, cement is squeezed at the top of the liner according to leakage after the cement slurry is set.

## Salt Rock Bed and Salt Paste Bed Wells

**Main Problems.** The plastic creep mechanism generated by salt rock beds or salt paste beds is rather complicated due mainly to the creep property of rock, as shown in Figure 5-13.

Salt rock has a high primary creep rate. Once the borehole is drilled, the primary creep of salt rock will be generated, and the borehole generates a tendency to close. Rational operational measures (such as adjusting drilling fluid properties and multiple redressing) disrupt the primary creep of rock and ensure the safety of the borehole, thus creating favorable conditions for subsequent work (such as cementing and well completion). With the lapse of time, the salt rock enters the secondary creep stage. At this time the creep rate is not high, the external pressure acting on the casing string in the well is not high, and the condition is relatively safe. After the oil and gas well is put into production, salt rock will enter the tertiary creep stage, the creep rate increases rapidly, and a plastic flow is finally

formed. At this time the casing bears high external pressure and is in danger.

Different rocks have different times at which the rocks enter the tertiary creep stage. For hard rocks such as limestone and sandstone, the secondary creep stage can be kept for a long time, and it is difficult to present the plastic flow phenomenon. For soft rocks such as mudstone and shale (especially salt rock), the secondary creep stage is short, they rapidly enter the tertiary creep stage, and the plastic flow that squeezes the casing is generated.

Whether the plastic flow phenomenon will be generated depends also on the in-situ stress at the structure. If the stress relaxation effect is generated (that is, the axial stress at the distance from the maximum triaxial stress point at the borehole wall is above zero) due to the creep in a long geological period, the rock may not generate the plastic flow phenomenon. This is the reason why the casing that penetrates salt rock bed is not supernormally squeezed. Certainly, it is rare to achieve full stress relaxation under normal drilling conditions.

Salt rock beds include potassium salt beds and salt paste beds, which are soluble formations and are also known as plastic formations. Salt rock bed has a large coverage area. The plastic composite salt rock is very unstable and easily causes borehole reduction under the action of overburden pressure, and the borehole wall easily dissolves and erodes. Therefore, accidents, including sticking and borehole sloughing, easily occur during drilling and there will be great difficulty during well completion, which is mainly as follows.

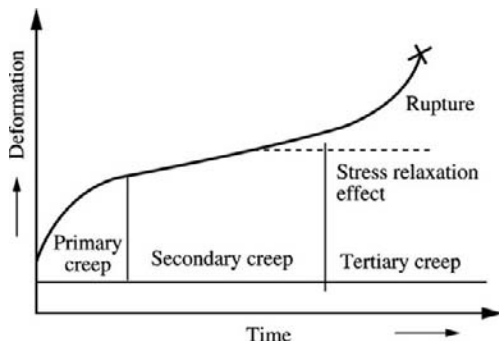


FIGURE 5-13 Generalized creep curve of rock.

1. The creep of salt rock bed or salt paste bed will generate a great external pressure on the casing; thus the casing will be collapsed, and the well will fail. For instance, casing collapse at  $E_{s1}$  salt rock bed is often generated in the Dongpu sag area of the Zhongyuan oil region. The  $E_{s1}$  salt rock bed pressure gradient at 2400 m is up to 0.0217 MPa/m, which is obtained by regression of Schlumberger density logging data, and greatly exceeds the

normal pressure gradient value. In the KL-2 gas well in the Talimu basin, the Paleogene gas reservoir internal includes sandstone, mudstone, salt paste bed, dolomite, paste mudstone, and basal sandstone from top to bottom and has a length of 600 m. The reservoir depth is 3750 m. The depth of dolomite is 4025 m. The salt paste bed and other formations except gas reservoir have a length of 400–500 m. The formation pressure is 74.3 MPa, and pressure coefficient is 2.022. If a casing of API series is used, it may be rapidly collapsed. After study and analysis, the intermediate casing size is increased from 9 5/8 in. to 9 7/8 in. The wall thickness is increased to 15.88 m. The high collapsing strength casing of SM125TT steel grade is adopted. The cement slurry density is 2.0–2.3 g/cm<sup>3</sup>.

2. Cement slurry may be contaminated during cementing due to the solution of salt rock bed, and the flow properties may be changed; thus the displacement efficiency and the strengths of bonding between cement sheath and casing and between the cement sheath and the borehole wall are decreased. The cement job quality is poor, and oil and gas are given off from the wellhead. In effect, the low cementing qualification rate of a salt rock bed is a difficult problem with which the oil and gas fields are faced.

**Approaches to Solving Problems.** Practical experience indicates that the following are effective methods of enhancing the cement job quality of a salt rock bed well:

1. Casing design
  - a. The production casing string strength design is made by using the biaxial stress method; thus the stress loading considered is closer to the complicated downhole stress state. The present method of designing strength in a three-dimensional stress state has also been widely applied to salt rock beds or salt paste beds.
  - b. A high collapsing strength casing is adopted and its length is designed on the basis of overburden pressure gradient. The design section length should ensure more than 50 m above the top and below the bottom of a salt rock bed.
  - c. The intermediate casing depth should be 100 m more than salt rock bed depth as much as possible. During production casing cementing, cement slurry should be returned again to the top of the salt rock bed, and a double-layer casing and cement sheath cementation is formed. Its collapsing strength is higher than the sum of the collapsing strengths of two casings. The casing diameter is sometimes increased in order to increase the wall thickness of the casing.
  - d. Special threaded casing with metal seal is adopted in order to prevent the decrease of the sealing property of the casing connection thread due to bending.
2. Cementing design
  - a. On the basis of the relation between the degree of dissolution of salt rock bed and temperature, supersaturated salt water cement slurry is formulated (supersaturated crystallized salt precipitant generally appears) in order to ensure that the salt water cement slurry is in the state of saturation under the condition of downhole temperature and pressure so that the degree of dissolution of the salt rock bed is decreased.
  - b. The salt-saturated cement slurry density should be 0.05–0.2 g/cm<sup>3</sup> higher than drilling fluid density. The fluid loss of cement slurry should be less than 50 ml.
  - c. Because gas bubbles may be generated during mixing saturated salt water with cement slurry, so that the suction efficiency of pump and the formulated cement slurry density are decreased, weighting admixture, defoamer, and salt dispersant should be added during formulating salt-saturated cement slurry. In addition, fluid loss additive, salt-resisting agent, early strength additive, drag reducer, and so on, are added according to the actual situation in order to improve cement slurry properties.

## Thermal Production Well

At present, steam injection is one of the effective methods of producing heavy oil. The casing and cement in a thermal production well will be seriously damaged due to high temperatures in the production period. The short casing life in a thermal production well restricts the production benefit of a thermal production well. Using some technique cannot solve the problem of casing damage in a thermal production well, and the combined use of the techniques mentioned in the following section is required.

### Main Problems

1. Casing string is in a high-temperature thermal field due to the injected steam, which has a temperature up to 300°C. The casing string will elongate when it is heated, thus generating compressive stress. When the compressive stress exceeds the yield strength of casing material, the casing will break or fail.
2. The string may expand during steam injection, and the normal load is changed from tensile load to compressive load. When steam injection is stopped, the temperature is greatly decreased, and the tensile force will act. The repeated change may lead the collar to leakage and lead the thread to slipping failure.
3. Experiments indicate that the compressive strength of set cement may be greatly decreased when the temperature exceeds 110°C; the set cement will burst when the temperature is increased to 200°C and reaches the critical temperature, thus losing the function of supporting and sealing the casing. In general, the high temperature borne by set cement in a thermal production well has reached or exceeds the critical temperature, and the failure of set cement due to the decrease of strength occurs now and then.

### Mechanism of Damage to Material by High Temperature, Thermal Stress and Creep, and Corresponding Games

1. Mechanism of damage to material by high temperature and thermal stress

The temperature of injected steam in a thermal production well of heavy oil is up to 360°C. The casing is fixed by cement sheath and wellhead equipment. The casing string is in a high-temperature thermal field. It is heated but cannot elongate, thus generating thermal stress in casing material. On the other hand, the yield strength and elastic modulus of material are decreased at high temperature. When the thermal stress exceeds the yield strength of material at high temperature, the casing material will enter a plastic state. The phenomenon of generating a slow plastic deformation of this metal material under a long-term constant-temperature constant-stress condition is known as creep deformation, which may lead to the following problems of damage:

- a. Retained residual stress in material. After the first cycle of huff-and-puff production is ended, the retained residual stress in material due to creep cannot be eliminated. The existence of residual stress means a decrease of strength. After the second and third cycles, residual stress is increased, thus causing a further decrease of strength.
- b. Creep damage of material. The retained residual stress in material is the macroscopic description of damage of material. The essence of the damage is that the creep generates microcrack and microvoid, thus decreasing the effective load-bearing area of the casing. High stress leads to crack propagation until rupture occurs.
- c. Fatigue rupture at high temperature. The casing is in a high-temperature environment for a long time, and the temperature gradient and change of temperature exist; thus the fatigue strength of material may decrease with the increase of environment temperature. The combined action of creep and fatigue loads may hasten the fatigue rupture of casing and decrease obviously the service life at high temperature.
- d. Corrosion in high-temperature environments. Casing is in a high-temperature environment for a long time; thus crystal-boundary oxidation may be generated at

the tip of crack, and the notch effect may cause corrosion crack and lead to early failure.

- e. Decrease of strength of casing steel material due to high temperature. The strengths and properties of various casing materials may be decreased to a different extent at a temperature higher than 120°C. For instance, at a high temperature of 340°C, the yield strength, elastic modulus, and tensile strength of early-stage N80 (N80-1) casing are decreased by 18%, 38%, and 7%, respectively.
2. Game of preventing and decreasing high-temperature thermal stress and creep damage
 

Designing and selecting material properties are the basic technical lines and include:

    - a. Improving alloying design and heat treatment. Improving alloying element design can enhance the high-temperature-resisting property of steel. The casing that will be used in a thermal production well should undergo quenching-tempering treatment. A large amount of former N80 steel had undergone normalizing or normalizing-tempering treatment and had strength higher than that of J55 steel but had still been seriously damaged. ISO/API has specified that the N80 steel of normalizing or normalizing-tempering treatment is Type N80-1 steel, and the N80 steel of quenching-tempering treatment is Type N80Q steel. Rational alloying design and heat treatment can control the microtexture, crystalline grain size, foreign impurity, and low-expansion texture of material and enhance the toughness of material. The properties of material can be used for decreasing the creep damage, that is, the creep does not easily generate microcrack and microvoid and does not easily propagate microcrack that has been generated to form fracture. This means a relatively high critical fracture toughness.
    - b. Reducing yield strength to ultimate tensile strength ratio of steel. J55 and K55 have the same minimum yield strength value of 375 MPa. J55 has an ultimate tensile

strength of 517 MPa; thus the yield strength to ultimate tensile strength is 0.72. The ultimate tensile strength of K55 after heat treatment reaches 655 MPa, and the yield strength to ultimate tensile strength ratio is 0.58. This difference leads K55 to have a thermal residual stress lower than that of J55.

- c. Selecting steel grade with higher yield strength. When the yield strength of the casing is increased, the thermal stress caused by thermal expansion may be lower than the yield strength, so that the casing may be retained in an elastic state. Despite the retained residual stress in material after the first cycle of huff and puff, the remaining effective strength may retain a rather great value to adapt to the second and multiple cycles of huff and puff. At present, the yield strength of the steel used in a thermal production well has reached 100 ksi and 120 ksi (1 ksi = 1000 psi). In addition to high strength, other matching properties are required. It is necessary to formulate the casing material and property standards for a thermal production well.
3. Casing string and cementing of thermal production well
 

The casing load in a thermal production well should consider the effect of the thermal stress cycle. The mechanical properties of casing material are reduced at high temperature, and the API standards related to casing property indices and design safety factor cannot be adopted. The sealing property of casing thread (round thread and buttress thread) is reduced at high temperature, and the connection strength is also reduced at high temperature; thus the multipolar sealing or end face sealing should be adopted.

    - a. Temperature field and thermal stress analysis of thermal production wells. The temperature field calculation of thermal production wells is first dependent on the steam injection parameter design and then dependent on the hole structure. In the steam injection parameter design, the basic steam injection parameters include injection pressure,

temperature, mass flowrate, and steam quality of bottomhole steam, which are not fully independent and are mutually coupled. After the heat loss, pressure loss, and temperature distribution of injected steam in the borehole are considered, the required wellhead steam injection parameters (including pressure, temperature, steam quality, and mass flowrate) are calculated. The thermal stress of the casing is calculated on the basis of the aforementioned steam injection parameters.

In general, the traditional one-dimensional thermal stress calculation method may be used. When the conditions are complicated and the thermal stress of the casing is in a critical state (that is, thermal stress is close to the yield strength of steel), the three-dimensional thermal stress calculation model is appropriate, and the casing thread connection strength should be checked.

- b. Change of the mechanical property of casing material at high temperature. It is important to understand the change of the mechanical property of casing material at high temperature. Improper material selection may cause casing failure in thermal production wells. At normal temperature the strength of N80 steel is higher than that of K55 steel; however, some mechanical properties of N80 steel at high temperature are lower than that of K55.
- (1) Reduction of strength of casing material at high temperature. The strengths and properties of various casing steels (except high-temperature steel) may be reduced at a temperature higher than 120°C to different extents. The changes of strengths and properties of N80 steel at 340°C are shown in Table 5-14.

The data in Table 5-14 reflect only the macroscopic change of property. Different steels have different sensitivities to temperature. L80 has the same minimum yield strength as N80; however, the residual stress of L80 after circulating at high temperature is lower than that of N80.

- (2) Casing collapse. In thermal production wells, the collapsing and biaxial stress effects (collapsing strength will be reduced under the condition of axial tension) of the casing are not negligible. In the collapsing strength design under the condition of biaxial stress, the residual tensile stress and the axial stress caused by casing weight should be stacked. Therefore, it is possible that the collapsing strength under the condition of biaxial stress for low steel grade casing with low residual stress is higher than that of high steel grade casing with high residual stress. For instance, at 354°C, the collapsing strength (under of biaxial stress) of K55 thick-wall casing is higher than that of N80 and C95 thin-wall casings.

**Heat-Resistant Seal Thread for Thermal Production Well.** The related statistical data (especially the multiarm caliper log data) indicate that casing failure in thermal production well is mostly generated at or near the connector of casing; thus the study and selection of casing thread seal in thermal production wells are of great importance.

The Japanese NS-CC special threaded connector, which has good sealing property, high strength, and low circumferential stress, and so on, is shown in Figure 5-14.

**TABLE 5-14 Reduction of Strengths and Properties of N-80 Steel at High Temperature**

Temperature (°C)	Reduction of Yield Strength (%)	Reduction of Elastic Modulus (%)	Reduction of Tensile Strength (%)
340	18	38	7

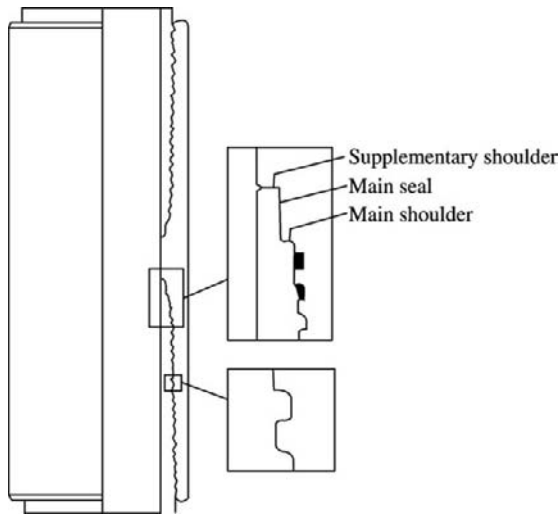


FIGURE 5-14 NS-CC special threaded connector.

The NS-CC connector has two sections of shoulders. A radial seal is between the original torque shoulder and the reversal torque shoulder. The compressive load is borne by the original shoulder; thus the deformation of shoulder may not affect the sealing location. The reversal torque shoulder may bear further compressive load; thus the sealing property can also be ensured under conditions of repeated tension and compression. Comparative tests indicate that the NS-CC thread has certainly a good thermostability.

In the Liaohe oil field, the NS-CC thread, which has good thermostability, has been correspondingly improved and perfected in consideration of the dangerous working status of thermal production casing and the safety requirement for casing connector, and the NS-CC-M special thread, which is suitable to the thermal production wells in this oil field, has been developed. And good results have been obtained.

**High-Temperature-Resistant Cement.** High-temperature-resistant cement is formulated with grade G cement and 30% to 40% quartz sand (80 meshes). Bentonite is not used as an additive in cement to the full extent. If a low-density cement slurry is adopted, it is suitable to use microbeads as lightening admixture. A volcanic

ash-lime series of cement has a better temperature-resisting property (not obvious reduction of strength) and may be adopted if possible.

Practical experience indicates that the annulus in thermal production wells should be fully cemented, that is, cement slurry is returned to the surface. If the hole section is very long, the multistage cementing method can be adopted. During cementing, a certain amount of cement slurry (4–8 m<sup>3</sup>) should be returned out in order to discharge the mixed slurry and ensure the cement sheath cementing quality in the wellhead section. The rational piggyback attaching of casing centralizers on the casing string can enhance displacement efficiency and cement job quality.

#### Mode and Method Selection of Well Completion.

There are two completion modes of thermal production wells, that is, casing perforation completion and openhole wire-wrapped screen or gravel packing slotted liner or metal-fiber sand screen completion. They have their own usable ranges. Openhole wire-wrapped screen or slotted liner or metal-fiber sand screen completion is suitable for massive reservoirs and heavy oil reservoirs with no interbed, gas cap, and bottom water. Simple openhole completion cannot be adopted because a heavy oil well may produce sand and interbeds may generate sloughing, thus plugging the borehole. Casing perforation completion has a wide usable range, that is, it is appropriate for massive reservoirs, stratified reservoirs with interbeds, and oil reservoirs with gas cap and bottom water. In addition, well completion can be pretension prestressed casing cementing completion and non-pretension casing cementing completion. Some problems have been found during pretension of casing. The great pretension is difficult to achieve by existing drilling rig and difficult to bear by casing. Moreover, the existing ground anchor is seated at sandstone or mudstone formation (double ground anchor is sometimes set), and the ground anchor cannot bear such a great tension, so the ground anchor may slide; thus the possibility of generating prestress by pretension may be lost. The existing pretension is only on the basis of existing drilling rig

capability, has not affected the whole casing string, and only straightens the casing string to avoid a bent state. In the Liaohe oil field, the steel grade of the casing has been improved and changed from the previous N80 to TP100H or TP120TH, and a pretension is no longer taken. The effectiveness is being observed.

## Horizontal Well

**Main Problems.** A horizontal well can enlarge the bare area of the reservoir and is an effective measure to develop heavy oil reservoirs, fractured reservoirs in which vertical fracture is predominant, oil and gas reservoirs with gas cap and bottom water, and low-permeability oil and gas reservoirs. Horizontal wells have been widely applied. By comparison with straight wells, horizontal wells have obviously different production casing and cementing designs. The following are characteristic of horizontal wells:

1. Casing bending stress. In the bent section, the casing bears not only the axial tensile force but also the additional axial tensile forces caused by bending, thus requiring further high tensile strength and thread-sealing property.
2. Drilling fluid channel. The results of cementing tests indicate that in almost all deviated sections, there may be drilling fluid channel in the cement sheath in the lower part of the annulus. It is generally considered that the drilling fluid channel may be mainly caused by the deposition of barite and cuttings. The higher cuttings concentration may increase drilling fluid viscosity; thus the drilling fluid is difficult to displace out. The rheological property of drilling fluid and the dip angle of the borehole may also affect the displacement to a certain extent.
3. Free water migration. In high-inclination wells or horizontal wells, free water very easily accumulates on the upper side of the borehole wall due to the short distance of oblique or lateral migration to form continuous water

channel or water belt, which will finally become the passage of oil and gas channeling. Decreasing free water in cement slurry and preventing free water from migrating are always the important factors in enhancing cementing quality. By comparison with vertical wells, the problem of free water migration in horizontal sections should be further noticed.

4. Casing deflection. In a deviated borehole, the casing cannot be at the center of the borehole, thus affecting the debris-carrying capacity and cementing displacement efficiency. In general, the degree of deflection of the casing in the annulus is expressed by using the ratio of minimum clearance. In order to ensure cementing quality, the API 10D standard specifies that the ratio of minimum clearance should be higher than 0.66. This standard is difficult to reach in high-angle wells or horizontal wells.

**Approaches to Solving Problems.** Experiments and practice indicate that in high-angle wells and horizontal wells, the following effective measures should be taken during cementing:

1. Fluid loss additive is added to cement slurry to decrease the free water content to zero to the full extent. It should be noted that in accordance with the API standard, cement slurry with a free water content of 1%, which is measured in a vertical graduated cylinder at normal temperature, will have a free water content of up to 7%, which is measured under the condition of inclination and increased temperature. Therefore, it is recommended to change the existing method of measuring free water content in high-angle wells. Cement slurry is first preheated to the bottomhole circulation temperature, and then the free water content of cement slurry is measured in a graduated cylinder with an inclination angle of at least 45°.
2. Increasing liquid viscosity. For instance, latex is added to cement slurry to increase the liquid viscosity of cement slurry, thus increasing the free water migration resistance.

3. Solid micropowder is added to cement slurry. The recent studies by Norwegian Statoil indicate that the fine silica flour added may be evenly distributed in cement slurry and filled in the channels between cement particles; thus these channels may be partially plugged, and free water flow may be resisted or decreased. The fine silica flour should be evenly dispersed in cement slurry in order to play the role of silica flour.
4. Using spacer fluid. Related studies indicate that in high-angle wells, the turbulent flow state has a good displacement effectiveness. Under low-rate displacement, displacement efficiency may be affected by the difference of density. When the density difference of two fluids is up to a certain degree, wedging will be generated inside and outside the casing; thus, the heavy fluid may pass below the light fluid. This phenomenon may not generate a great effect between drilling fluid and spacer fluid; however, it should be avoided between cement slurry and drilling fluid as much as possible in order to prevent cement slurry from being contaminated or prevent drilling fluid from being partially surrounded and left in cement slurry. Therefore, the spacer fluid density should be close to the cement slurry density, the rheological property of the spacer fluid should be between that of drilling fluid and cement slurry, and the spacer fluid should be sure to fill the annulus length of at least 200–250 m.
5. Using rigid casing centralizer. Tests indicate that in the high-angle wells with a deviation angle of  $70^\circ$  to  $72^\circ$ , the spring leaf of a common spring-type centralizer may be flattened, and serious channel may be caused during cementing. The statistical data indicate that remedial squeeze cementing is required because the spring leaf is out of action. A rigid centralizer can ensure that the ratio of minimum clearance is 67%, thus improving cementing quality. Wells that need remedial squeeze cementing account only for 20%.

## Adjustment Wells

**Main Problems.** With the waterflooding of oil fields, the number of adjustment wells may be gradually increased. Due to long-term water injection (particularly high-pressure water injection in recent years), the reservoir pressure is commonly increased (the water injection pressures of some oil fields have been close to or have exceeded formation breakdown pressures), and in-situ stresses have also been changed. In addition, local superhigh-pressure traps have been formed by reason of poor reservoir connectivity or heterogeneity. All of these changes will generate difficulty in cementing work, such as:

1. Coming of oil, gas, and water from outside of the casing after cementing;
2. Poor setting of cement slurry in waterflooding interval;
3. Longitudinal channel during cementing, unqualified reservoir cementing or interlayer cementing;
4. Leakage during cementing, insufficient return height of cement slurry.

To sum up, the effect of the high-pressure formation formed by water injection and the waterflood channeling on cementing quality is particularly serious and will cause interlayer interference during separate zone production and injection, thus complicating the production technology, decreasing the rate of well utilization, and reducing the service life of the oil well. Therefore, the current testing data should be used as a design basis instead of the original data (including pressure and in-situ stress) of the oil field, thus providing high-quality oil wells for oil production.

### Approaches to Solving Problems

1. Keeping cementing in a static state. After the design section is filled with cement slurry during cementing, a stable environment is required by setting; thus extensive stopping water injection should be performed to the full extent in order to enhance the setting quality of cement slurry.

2. Static-dynamic combination. In some small and medium oil fields, a static state is required during cementing; on the other hand, oil production and water injection are required. The approach to solving this contradiction includes stopping production and injection in a certain radius range during drilling and cementing and keeping continuous production and injection outside this radius range; thus the cement job quality is enhanced and the production is kept.
3. Ending cementing operation before invasion of oil, gas, and water. In some oil fields with shallow oil and water formations (such as Jilin and Yumen oil fields), despite stopping injection, the fluid column pressure is still insufficient to suppress the reservoir due to shallow depth even if the cement slurry density adopted is higher, and the fluid will channel to the wellhead. Under this condition, a separable setting cement slurry can be adopted. The accelerated cement is injected in the lower part (oil and gas reservoir), so that the initial setting time is before the invasion of oil, gas, and water. The conventional cement slurry is injected in the upper part. Thus, the annulus fluid column pressure can still maintain a certain value when the accelerated cement slurry is set and the weightlessness is generated.
4. Local plugging and whole borehole channeling prevention. The external casing isolation of main oil and gas reservoirs is achieved by using an external casing packer. After high-pressure formations of oil, gas, and water are isolated, cement slurry is injected; thus local plugging and whole borehole channeling prevention are achieved.
5. Improving the rheological property of cement slurry to enhance displacement efficiency. The cement slurry density should be appropriately higher than the drilling fluid density. When the cement slurry density is higher than  $2.0 \text{ g/cm}^3$ , the rheological property of cement slurry may be reduced. This is unfavorable to

the increase of displacement efficiency. Using an appropriate water reducer can reduce the precipitation of free water in high-density cement slurry, enhance resistance to water invasion, and improve the rheological property of cement slurry, so that it is easy to reach the turbulent flow displacement state.

6. Using high collapsing strength casing. When the production casing string of an adjustment well is designed, the change of reservoir pressure during waterflooding should be definitely understood and used as the basis of strength design. In addition, measures to prevent casing corrosion should be comprehensively considered in order to prolong the service life of the oil well.

### Well Using External Casing Packer

In some special structure wells, combined external casing packer and cementing may have special efficacy. For instance, an external casing packer is combined with a screen pipe to isolate multiple reservoir or water formation and bare fully fractured system, thus increasing the flow area and the production rate of some reservoirs.

In a multiple-reservoir well, due to different reservoir pressures and different physical properties of various reservoirs, an external casing packer is needed by separate-zone production or downhole operations. At present, several external casing packers may be attached to the slotted liner string. Water formation (especially the interlayer water formation) is isolated by using external casing packers.

**Combined External Casing Packer and Screen Completion Without Cementing.** In the directional or horizontal well with  $\Phi 139.7 \text{ mm}$  or  $\Phi 177.8 \text{ mm}$  casing, cementing quality is difficult to ensure, or cementing cannot be adopted due to the limitations of technology. Under this condition, an external casing packer may have special efficacy.

Typical completion casing string structure: Screen is set in the reservoir section. Casing

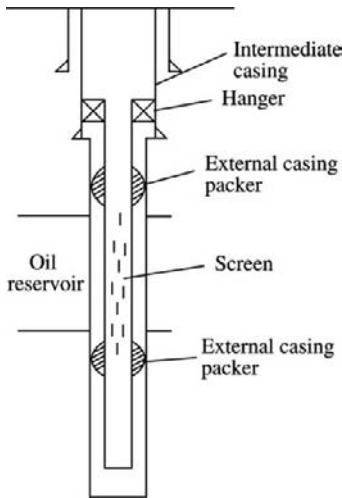


FIGURE 5-15 Combined external casing packer.

is set in the nonreservoir section without cementing. An external casing packer is run in intermediate casing and set at the bottom of the reservoir. An external casing packer is attached to the end of the hanger. The hanger is set at the end of the intermediate casing inside the intermediate casing. Thus the reservoir is isolated from the annulus (Figure 5-15). This completion method is often used in sidetracked directional or horizontal wells.

### Combined External Casing Packer and Cementing Completion

1. The annulus is isolated by using an external casing packer. When the annulus clearance is smaller and the restraining barrier between gas formation and water formation is thin, using only cementing has difficulty in resisting channeling. Thus an external casing packer is set at the barrier and then expanded after cementing is ended. An external casing packer may also be set above the high-pressure gas reservoir to prevent gas channeling after cementing.
2. An external casing packer and cementing collar are set above the screen. After the packer is expanded, the annulus is cemented from a

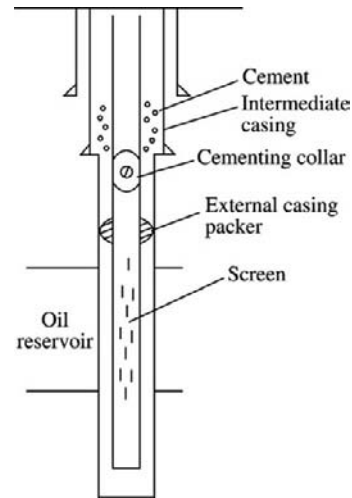


FIGURE 5-16 Combined external casing and screen completion without cementing packer and cementing completion.

cementing collar (Figure 5-16). This completion method is favorable for protecting the reservoir because it avoids contact between the cement slurry in the annulus and reservoir, and the fluid column pressure may not be transmitted to the reservoir.

### REFERENCES

- [1] Liu Chongjian, Xu Tongtai, Huang Bozong, Liu Xiaoliang, et al., *Oil and Gas Well Cementing Theory and Application*, Petroleum Industry Press, Beijing, Sept. 2001 (in Chinese).
- [2] E.B. Nelson, et al., *Advanced Cementing Technology* (Liu Dawei, Tian Xijun, Liao Runkang, Trans.), Liaoning Science and Technology Press, Shenyang, 1994 Feb. (in Chinese).
- [3] Party A Compilation Group, *Drilling Handbook*, Petroleum Industry Press, Beijing, 1991 (in Chinese).
- [4] Chen Ping, et al., *Drilling and Well Completion Engineering*, Petroleum Industry Press, Beijing, Nov. 2005 (in Chinese).
- [5] Concrete and Reinforced Concrete Corrosion and Prevention Methods (Ni Jimiao et al., Trans.), Chemical Industry Press, Beijing, 1988 (in Chinese).
- [6] Gelling Materials Science Compilation Group, *Gelling Materials Science*, China Architectural Industry Press, Beijing, 1980 (in Chinese).

- [7] Yang Yuanguang, et al., Oil Well Cement Corrosion and Prevention Methods, J. SW Petr. Inst. (19) (1997) (in Chinese).
- [8] Tong Manli, et al., Oil Field Chemistry, Petroleum Industry Press, Beijing, 1996 (in Chinese).
- [9] R.A. Bruckdorfer, Carbon Dioxide Corrosion in Oilwell Cement, SPE 15176, 1986.
- [10] N.B. Milestone, et al., Carbonation of Geothermal Grouts—Part 1 CO<sub>2</sub> attack at 150°C, Cement Concrete Reserch 16 (5) (1986) 941–950.
- [11] T. Baird, et al., Morphology and CO<sub>2</sub> Uptake in Tobermorite Gel, J. Colloid Interface Sci. (2) (1975) 87–391.
- [12] А.И. Булатов, Щ.М. Рахибаев, Л.И. Рябова, Коррозия тампонажного камня, Краснодар, 1993.
- [13] Булатов, А.И., Д.Ноохатский, А.К.Рахимов, Коррозия тампонажного шлаковых цементов ташкент, изательство <ФАН> Узбеккой ССР.

## Perforating

**OUTLINE****6.1 Perforating Technology**

Wireline Casing Gun Perforation

- Overbalance Perforating by Wireline Casing Gun
- Underbalance Perforating by Wireline Casing Gun
- Pressurized Wireline Casing Gun Perforation

Tubing-Conveyed Perforation (TCP)

Wireline Modular Gun Perforation Technology

- Operating Principle of Modular Gun Perforation
- Technical Characteristics

Tubing-Conveyed Perforation Combination Technology

- Combined Tubing-Conveyed Perforating and Putting-Into-Production Technology
- Combined Tubing-Conveyed Perforating and Formation-Testing Technology
- Combined Tubing-Conveyed Perforating and Hydraulic Fracturing (Acidizing) Technology
- Combined Perforating and Oil Well Pump Technology

Combined Perforating and High-Energy-Gas Fracturing Technology

Combined Tubing-Conveyed Perforation and Sand Control Technology

Wireline Through-Tubing Perforation (TTP)

- Conventional Through-Tubing Perforation
- Extended-Diameter TTP

Extreme Overbalance Perforating Technology (Forward Shock)

Horizontal Well Perforating Technology

Oriented Perforating Technology

**6.2 Perforated Well****Productivity Influencing Rule Analysis**

Productivity Rule of Perforated Well of Sandstone Reservoir

- Effects of Perforating Parameters on Well Productivity
- Effect of Formation Damage on Perforated Well Productivity

Productivity Rule of Perforated Well of a Fractured Oil Reservoir

- Effects of Various Types of Fracture Network on Oil Well Productivity

Effects of Perforating Parameters on Oil Well Productivity of a Fractured Reservoir

Productivity Rule of a Perforated Horizontal Well

Effects of Location and Degree of Opening by Perforating on Horizontal Well Productivity

Effects of Perforating Parameters on Horizontal Well Productivity of a Sandstone Oil Reservoir

Effects of Perforating Parameters on Horizontal Well Productivity of a Sandstone Gas Reservoir

Effect of Formation Damage on Horizontal Well Productivity

**6.3 Perforating Differential Pressure Design**

Underbalanced Perforating and Extreme Overbalance Perforating

Empirical Relation of W. T. Bell

Empirical Relation of American Core Company

Calculation Method of Conoco	under No Sand Production	Optimizing Perforation Design for a Horizontal Well
Behrmann Method	Rational Perforating Operation Pressure	Optimization of the First Kind of Perforating Parameters
Theoretical Method of Designing Minimum Underbalance Pressure to Ensure Cleanliness of Perforation	Difference Determination Underbalanced Perforating Operation Pressure Difference Design	Optimization of the Second Kind of Perforating Parameters
Tariq Method for Calculating Minimum Underbalance Pressure	Extreme Overbalance Perforating Operation Pressure Design	Optimization of the Third Kind of Perforating Parameters
Minimum Underbalance Pressure Formula for Oil Well Perforating	Safety Constraint of Operating Pressure	Principles of Perforation Designs for Other Special Wells
Minimum Underbalance Pressure Formula for Gas Well Perforating by Southwest Petroleum University	Difference Design	Perforating Parameter Design of a Fractured Well
Theoretical Method of Designing Maximum Underbalance Pressure for Preventing Sand Production	<b>6.4 Optimizing the Perforation Design</b>	Perforating Parameter Design of Sand Control Well
Mohr-Coulomb Yield Criteria	Perforating Parameter Classification	Perforating Parameter Design of Carbonatite Gas Reservoir
Plasticity Zone Stress Model	Optimizing Perforation Design for Sandstone Oil and Gas Wells	Perforating Parameter Design of a Heavy Oil Reservoir
Elasticity Zone Stress Model	Preparation of Perforating Charge Property Data	Perforating Parameter Design of a High-Temperature High-Pressure Deep Well
Critical Equivalent Plastic Strain	Correction to Perforation Penetration Depth and Perforation Diameter of Perforating Charge	Perforating Parameter Design of a High-H <sub>2</sub> S Well
Pressure Distribution around Perforation	Calculation of Drilling Damage Parameters	<b>References</b>
Procedure of Calculating Maximum Perforating Underbalance Pressure	Optimization of Perforating Parameters	
	Rational Selection of Perforating Technology	
	Optimization of Perforating Fluid	

Perforated completion is one of the main modes of oil and gas well completion and has been widely applied by the petroleum industry worldwide. More and more attention has been paid to the importance of perforated completion technology in petroleum exploration and development.

In oil and gas wells completed by using perforating, perforations are the only passages between the reservoir and the wellbore. Formation damage by perforating can be minimized

when rational perforating technology and proper perforating design are adopted and the perforating operation is performed perfectly; thus, a high degree of completeness of well and desired productivity can be achieved.

Over the years, a large number of theoretical, experimental, and field-testing studies of perforating technology, perforating gun and charge and matching equipment, perforating damage mechanism and detection and evaluation methods,

perforating optimization design, and perforating fluid have been performed, thus rapidly developing perforating techniques. It has been known that perforating is a key link of well completion engineering; thus perforated completion is considered to be a form of system engineering, and optimizing perforating design is a necessary basic condition of high-quality completion.

## 6.1 PERFORATING TECHNOLOGY

In accordance with the geological characteristics and fluid properties of the reservoir and the types of oil and gas wells (straight, directional, or horizontal well), the corresponding perforating technologies are selected.

### Wireline Casing Gun Perforation

There are three types of wireline casing gun perforation (WCP) in accordance with perforating pressure difference or wellhead sealing method.

**Overbalance Perforating by Wireline Casing Gun.** The well is killed by using high-density perforating fluid before perforating, so that the bottomhole pressure exceeds the reservoir pressure. A perforating gun is run in by using wireline under the condition of open wellhead. The correlation curve of locating the casing collar is measured by using a magnetic locator attached to the wireline in order to adjust the gun depth and aim at the horizon, and then the oil and gas reservoir is perforated under overbalance pressure. After the perforating gun is pulled out, tubing is run in, the wellhead is installed, and then reservoir fluid flow is induced by displacement, swabbing, or gas lift in order to put the oil and gas well into production.

Overbalance perforating has simple operation, low cost, high perforation density, and deep penetration. However, the solids and liquid phase of perforating fluid may invade the reservoir during overbalance perforating, thus causing serious formation damage. Therefore, quality perforating fluid is required in order to reduce the formation damage that may be caused during overbalanced perforating.

**Underbalance Perforating by Wireline Casing Gun.** This technology is basically the same as overbalance perforating by wireline casing gun, except that before perforating, the wellbore liquid level is dropped to a certain depth in order to establish an appropriate underbalance pressure. This method is mainly applied to low- and medium-pressure thin oil reservoirs.

### Pressurized Wireline Casing Gun Perforation.

This technology adopts a closed wellhead in order to achieve underbalance perforating by large-diameter wireline gun, so that the serious formation damage that may be caused by overbalance perforating is avoided. It is mainly suitable for normal hydrostatic pressure or high-pressure oil reservoirs. The key to this technology lies in the matching of dynamic seals with high-pressure blowout-prevention equipment. In combination with the stage firing technique of wireline perforating, this technology can decrease the disassembling times of the blowout-prevention system, thus reducing labor intensity and enhancing operational efficiency.

### Tubing-Conveyed Perforation (TCP)

The perforating gun is run to the desired perforating depth on tubing. A differential pressure packer, ported nipple, and firing system are attached to the bottom of the tubing. The fluid column existing in partial space of the tubing may cause underbalance pressure. The detonation of perforating charge may be generated by bar dropping, pressure or differential pressure, or wet sub of wireline, and so on, thus perforating the whole reservoir thickness once. The typical TCP operation string is shown in Figure 6-1.

The perforating depth of tubing-conveyed perforator is generally corrected by using a radioactive log. A radioactive isotope is placed in the locator sub of the string assembly. A depth correction instrument is set at a predetermined depth (about 100 m above the locator sub). A radioactivity curve with magnetic location is measured down to about 15 m below the locator sub. The radioactivity curve measured is compared with the radioactivity curve that was previously

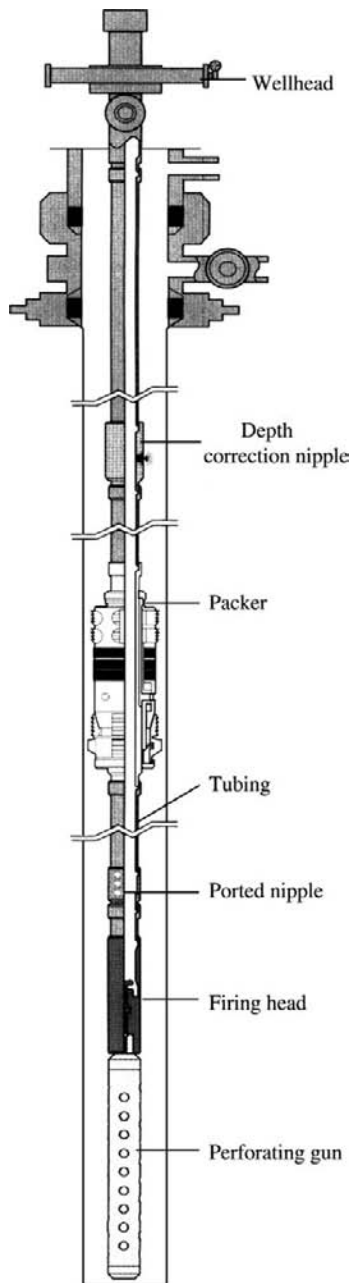


**FIGURE 6-1** TCP operation string.

measured for correction. The depth of the locator sub is obtained by conversion and adjusted at the wellhead by using a tubing pup joint.

There are several detonation methods of tubing-conveyed perforation, of which the

simplest is gravity detonation. A cylindrical metallic bar is placed beforehand in the lubricator at the wellhead and is released during perforating. The bar, which drops at a high velocity, impacts the detonator at the gun head. The usable bars include standard bar, universal joint roller-type bar, series bar, and copper bar. It is required that the tubing string is drifted. Bending of tubing string and excessive borehole deviation are not allowed.

When pressurization in tubing is adopted, nitrogen gas is generally used as a pressure-transmitting medium due to partial liquid column in the tubing. High-pressure nitrogen gas should be released from the wellhead before detonation in order to ensure underbalance pressure at the perforating instant; thus, a longer duration between nitrogen gas pressurization and detonation is required by releasing nitrogen gas. This is known as delay detonation.

When pressurization in the annulus is adopted, annulus and tubing become different pressure systems by using a crossover device in the packer or hydraulic bypass. Pressurization in the annulus may cause an increase of pressure difference between annulus pressure and tubing pressure. When the pressure difference is increased to a preset value, the piston pin is sheared, so that the piston and wire rope clamp bring along the wire rope to rapidly move upward, thus moving the tie rod of the firing head upward, releasing the striker, and detonating the detonator. This is known as pressure difference detonation. At present, high-pressure-resistant metallic conduit is mostly used for transmitting the annulus pressure above the packer to directly shear the shear pin and detonate the detonator, so that the weakness of wire rope, which can easily elongate, slip, and break during dragging by a pressure-firing device, is avoided. Another type of detonation is electric detonation, in which the firing heads include wireline conveyed current firing head and battery bar-dropping firing head.

Because of the poor detonation-transmitting reliability of TCP for long and medium interbeds and the high cost of interbed guns, the

tubing-conveyed multilayer perforating staged detonation technique (staged bar-dropping detonation, combined bar-dropping and pressure detonation, combination pressure-pressure detonation, pressurizing detonation, and so on), multistage simultaneous (underbalance pressure) detonation technique, and baffle detonation transmission technique used mainly for perforating of offshore horizontal wells have been developed and effectively applied, thus solving the various problems induced by long interbeds.

Tubing-conveyed perforation has a high density, deep penetration, and high underbalance pressure, is easy to remove perforating formation damage from, and has a greater once perforating interval thickness. This method is especially suitable for directional wells, horizontal wells, heavy oil wells, and so on, in which wireline is difficult to run. Because a Christmas tree is installed beforehand, the tubing-conveyed perforation method has a good safety property and is very suitable for high-pressure reservoir and gas wells. In addition, after perforating by using this method, the well can just be put into production, and it is convenient to combine perforating with testing, fracturing, acidizing, and so on, thus reducing the times of well killing and string tripping, formation damage, and operation cost.

Tubing-conveyed perforation requires that the sump hole be extended during drilling in order to store the perforating gun, which falls. The perforated interval sometimes is too long, so that the gun is difficult to store at the bottomhole; thus other measures should be taken.

In recent years, a new combined tubing and wireline conveyed perforation system (TWC) has been developed. It has merits of both WCP and TCP. It not only has high perforation density and deep penetration, but also it can meet the special requirements of some high-temperature deep wells. In high-temperature high-pressure deep wells, liner completion may be adopted after intermediate casing or production casing is run in; thus, the perforation interval that is at the liner is far from the tubing, so that it is inconvenient for conventional TCP operation. The high-performance perforating gun of the

TWC system is conveyed to design tubing depth on tubing. When the well is put into production, the wireline is run in and the gun system at the lower end of tubing is unlocked. The gun system is then conveyed on wireline to the interval to be perforated. The gun is anchored to the liner by using a setting tool, and then the wireline and setting tool are retrieved. Pressurization in tubing and delay detonation are applied. The technological process of TWC is shown in Figure 6-2. After automatic releasing of the gun and dropping, the normal production of the well is started.

This system can greatly shorten the duration during which the gun is exposed to a high-temperature high-pressure environment. It has deep penetration and high perforation density and can perforate under the condition of underbalance pressure. It has good safety and reliability. However, the operation is rather complicated.

### Wireline Modular Gun Perforation Technology

The wireline modular gun perforation technique is mainly used in high-pressure oil and gas wells with high reservoir pressure. It can achieve the tubing-conveyed perforation completion process and can prevent blowout. In addition, it can achieve oriented perforating. Modular gun staging running-in is achieved by using wireline. Modular guns are anchored on the casing wall. Modular guns are detonated to perforate the whole perforation interval once. After automatic release, the hanger and modular guns drop to the bottomhole and then are retrieved under pressure (passing a wireline blowout preventer). The most important advantage of this technology is that tubing running is not required and guns are run in by using wireline and anchored at the target horizon. The long perforation interval is perforated once, and guns are freed and drop to the bottomhole, thus achieving a full-bore production completion string. This technology can be performed under the condition of underbalance pressure, thus protecting the reservoir and maximizing oil and gas well productivity.

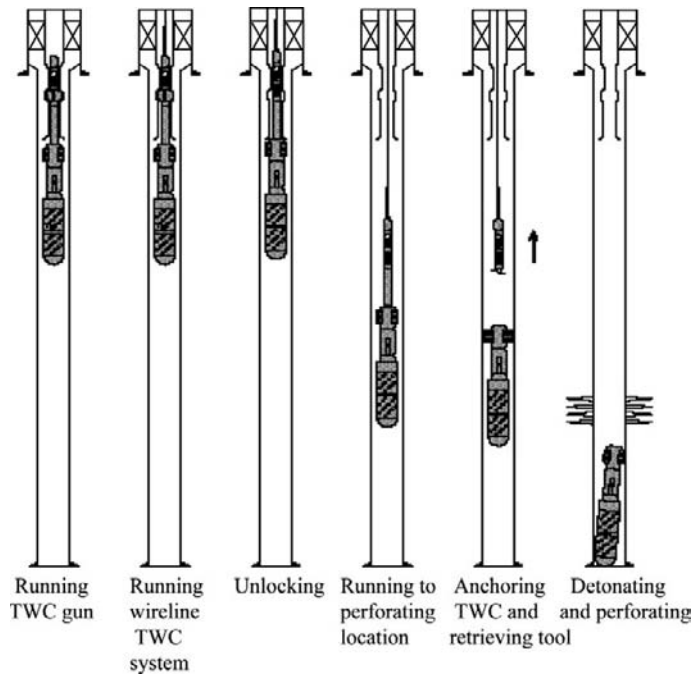


**FIGURE 6-2** Tubing and wireline conveyed perforation system.

For instance, the KL 2-7 gas well has a well depth greater than 4000 m and a bottomhole temperature of about 100°C. It has a massive reservoir with high pressure and ultra-high production rate. The well completion is faced with difficulties, which include: (1) 177.8 mm (7 in.) casing well, perforation interval of up to 200–300 m; (2) formation pressure coefficient of 1.9, bottomhole pressure of 74.5 MPa, wellhead pressure up to 63.5 MPa; (3) gas production rate of  $(300\text{--}700) \times 10^4 \text{ m}^3/\text{d}$ ; (4) 0.2–0.3% CO<sub>2</sub> in fluid, high content of corrosive matter (Cl<sup>-</sup>, and so on) in formation water; (5) water formation below the perforation interval, which makes the sump hole short and the dropping of the gun unsuitable.

The set goals of perforating include: meeting the requirement of gas production engineering, safety and environmental protection, and reliable long-interval perforating. The corresponding modular gun perforating project has been formulated.

### Operating Principle of Modular Gun Perforation.

The downhole string of the KL 2-7 well is shown in Figure 6-3. The drift diameter of the subsurface safety valve is 139.7 mm (5 1/2 in.), which can meet the requirement of through-tubing operation of a modular gun. The main components of a modular gun system include hanger, modular gun, pressure delay detonator, and wellhead blowout preventer.

#### 1. Hanger

The hanger is used for locating the perforating gun. There is a modular plug on it, which is used for connecting to the running tool, magnetic casing collar locator (CCL), and wireline. A slip is set at the predetermined location on the casing after the J-lock of the hanger makes the slip change orbit and open through pulling and dropping by using wireline. After firing, the cone of the hanger is reset, the slip is retrieved, and the hanger and gun series are freed and drop to the bottomhole.

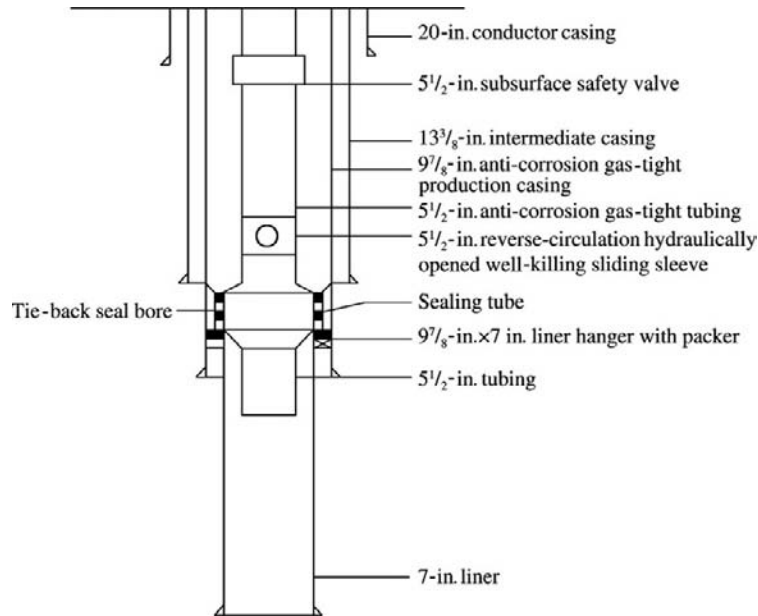


FIGURE 6-3 Downhole string of KL 2-7 well.

## 2. Modular perforating gun

In order to simultaneously perforate a long interval, a perforating gun system consists of independent units. Each unit is just a modular perforating gun. It can achieve the baffle detonation transmitting function in well fluid. The lowest gun is first run in and set on the hanger by using wireline and running tool, and then the other guns are run in and stacked (see Figure 6-4). Finally, the pressure delay detonator is connected with the top modular gun and run in.

The Halliburton modular gun system has an outside diameter of 117.5 mm (4 5/8 in.). The outside diameter of the leaf-spring centralizer is 142.5 mm (5.61 in.). This system can resist a pressure of 138 MPa and has a perforation density of 16 shots/m and a phasing of 60°. The single modular gun has a length of 7.21 m and a weight of 250 kg. The matching perforating charge is Halliburton's 4-in. Millennium HMX Super DP deep-penetrating perforating charge. The concrete target penetrating depth is 1079.5 mm. The perforation diameter is

8.9 mm. The rated temperature is 121°C/1000 h. The recommended usable time is less than 500 hours.

## 3. Pressure delay detonator

The pressure delay detonator has the same structure as the common detonator. It is connected with the modular perforating gun and run in by using a running tool. After it is confirmed that the whole gun series are just trained on the perforation interval, pressure is applied, the detonator is detonated, and perforating is achieved.

## 4. Blowout preventer

A typ. 2FZ 14-70 blowout preventer has a full bore of 140 mm and an operating pressure of 70 MPa. There are three wireline diameters of 5.56 mm, 7.9 mm, and 11.8 mm. Hydraulic sealing lubricator and double ram valve are adopted.

**Technical Characteristics.** The technical characteristics are as follows: (1) the hanger and modular perforating gun can be conveyed by using wireline, wire, or work string; (2) it is not required to use a derrick for tripping the

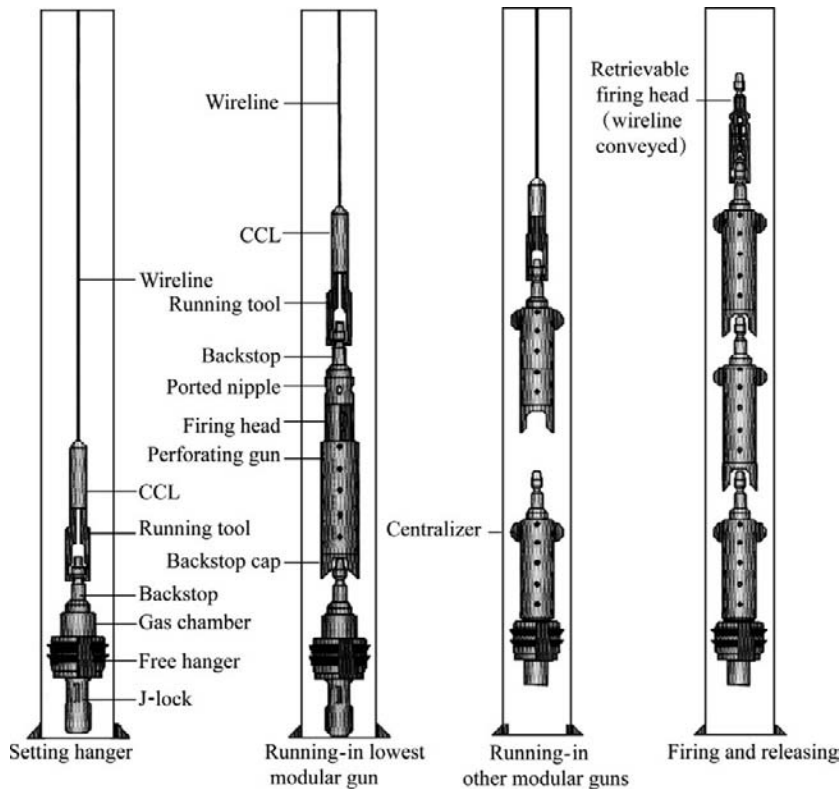


**FIGURE 6-4** Operating principle of modular perforating guns.

modular gun system, and only a special support is needed; (3) the optimum modular guns can be stacked at the bottomhole, and a long interval can be perforated; (4) the desired maximum underbalance or overbalance pressure can be used for perforating; (5) the hanger and modular guns drop automatically to the bottomhole after perforating; (6) the modular guns can be pulled out under pressure; (7) the perforating guns may not be taken out or may be partially taken out; and (8) the production logging, reperforating, bridge plug setting, coiled tubing operations, and so on, can be conducted under the condition of keeping the string from moving.

### Tubing-Conveyed Perforation Combination Technology

**Combined Tubing-Conveyed Perforating and Putting-into-Production Technology.** This

technology has been widely applied in flowing wells. It is safe and economical. Perforating and putting into production can be achieved by running the string once. Different wells adopt different structures of string and different packers. A releasing gun is generally adopted. The Halliburton combined system of tubing-conveyed perforating and putting into production is shown in Figure 6-5. A production packer is first run in on the wireline and set at the production casing, and then a string with a perforating gun is run in. When the guide sub of the string is run to the packer, the string is washed by circulating in order to remove dregs and sludge, and then the string is run further. After the string assembly is set, a bar is dropped from the wellhead in order to impact the detonator at gun head and perforate. After perforating, the perforating gun and residue drop to the bottomhole, and then the well is put into production.

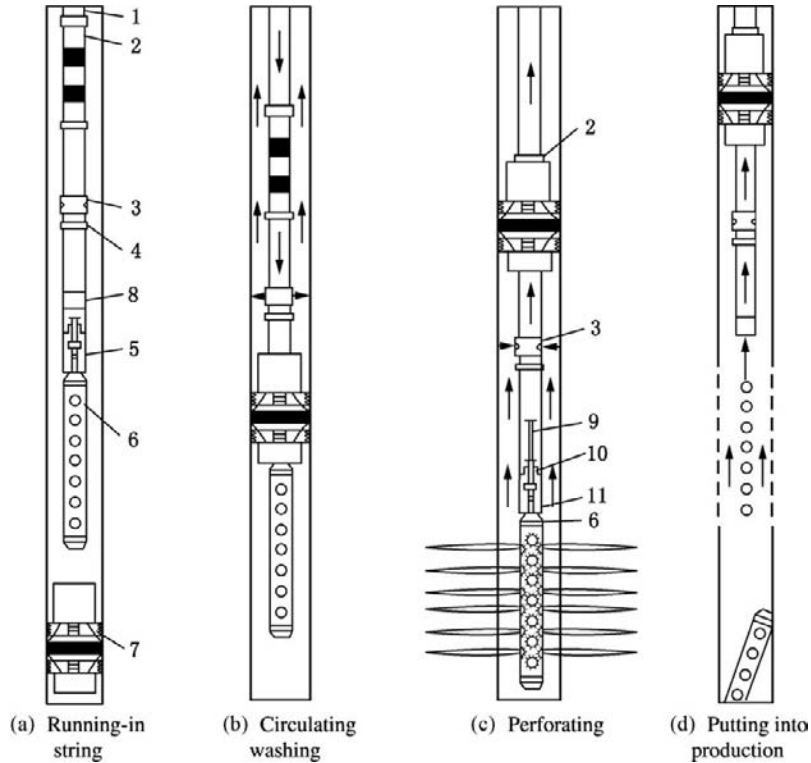


**FIGURE 6-5** Combined technology for tubing-conveyed perforating and putting-into-production. 1, production tubing; 2, production seal assembly; 3, disc-type circulating sub; 4, tubing collar; 5, gravity detonation head and releasing device; 6, perforating gun; 7, production packer; 8, guide sub; 9, bar; 10, impact; 11, detonator.

**Combined Tubing-Conveyed Perforating and Formation-Testing Technology.** The perforating gun, firing head, exciter, and so on of a tubing-conveyed system are attached to the end of a single-packer testing string. After the string is run to the perforating and testing depth, the depth is corrected, the packer is set, and the testing valve is opened. After detonating and perforating, the normal testing procedure is started. The combination TCP test is generally adopted by using the bypass pressure-transmitting technique in China. On the basis of different types of formation testers, the combinations mainly include: TCP + MFE (multiflow evaluator), TCP + PCT (annulus pressure controlled tester), TCP + HST (hydraulic spring tester), and TCP + APR (annulus pressure respondent).

This technology is especially suitable for flowing wells. It can shorten the productivity testing

period, reduce cost, and protect the reservoir. At present, it has been widely used in exploration wells and appraisal wells, especially in deep and superdeep wells, which adopt combined annulus pressure detonation and MFE technology with a success ratio of 90%. The annulus pressure is transmitted to the piston of the detonator through a bypass hole above the packer. The pressurized piston shears the pin and then moves downward, thus impacting detonation primer to detonate and perforate. After perforating, reservoir fluid flows through the annulus and screen pipe into the string, and then the flowsheet may be started. The combined perforating and testing string is shown in Figure 6-6.

In addition, in order to achieve the combined tubing-conveyed perforating and testing technology in a nonflowing well, a jet pump is attached to the work string by Marathon. The string

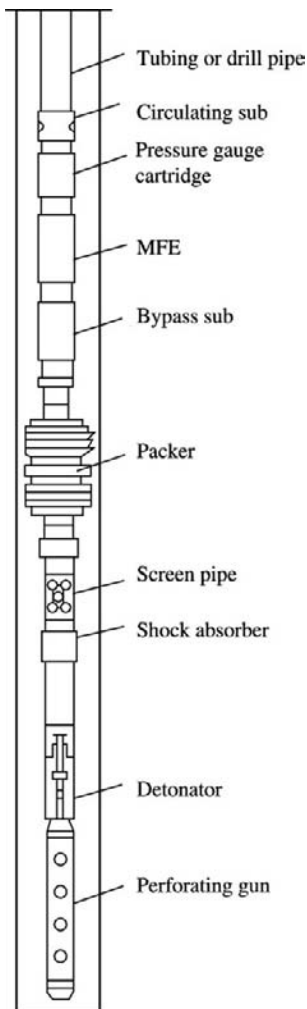


**FIGURE 6-6** Combined perforating and testing string.

consists of perforating gun, packer, underbalance pressure valve, automatic pressure gauge cartridge, standing valve, reverse-flow jet pump with special hollow sleeve, and so on.

The hollow sleeve is closed before perforating. Making the inside of the tubing partially empty may cause an underbalance pressure. After annulus pressurizing, detonating, and perforating, the fluid may enter the work string. As the fluid enters, the bottomhole pressure increases gradually; thus, the production of the oil well may be stopped. Under the action of pressure in the tubing, the safety pin of the

hollow sleeve is sheared, thus making the sleeve rotate and open. At this time, the well starts flowing back by jet pump and the flow test will be conducted. After a stable production rate is obtained, the well is shut in. The pressure build-up test data are obtained. After the pump is stopped, the standing valve is closed off under the action of hydrostatic pressure, thus achieving the downhole shutting-in of the well, eliminating the effect of wellbore storage, and optimizing data acquisition. The combined TCP-MFE jet pump technology has been successfully applied.

#### **Combined Tubing-Conveyed Perforating and Hydraulic Fracturing (Acidizing) Technology.**

This technology has been successfully applied in the Sichuan gas field and Changqing oil field in China. The string is run once during well completion to complete perforating, testing, acidizing, fracturing, well testing, and so on (see Figure 6-7).

#### **Combined Perforating and Oil Well Pump Technology.**

Different oil well pumps adopt different underbalance pressure detonating methods. For instance, a rod insert pump can use bar dropping for detonating, a tubing pump can use pressurizing inside tubing for detonating, whereas a screw pump can only use pressurizing outside tubing for detonating. This technology can avoid the secondary formation damage that may be caused by killing fluid after perforating, can protect the environment, and can enhance productivity to a certain extent. This technology has been successfully applied in the Daqing and Shengli oil fields.

The SRPTCP tubing-conveyed perforation technique developed by Schlumberger, which adopts a separate pressure-difference firing head of sucker rod pumping system, has been widely applied in oil fields more than 500 well-times with a running-in and firing success ratio of 100%. The perforating guns needed in a well are strung together and attached to the end of the tubing string. The auxiliary detonation-transmitting system of the firing head is attached to the top of the perforating gun. A setting sleeve of sucker rod pump is set above the perforating

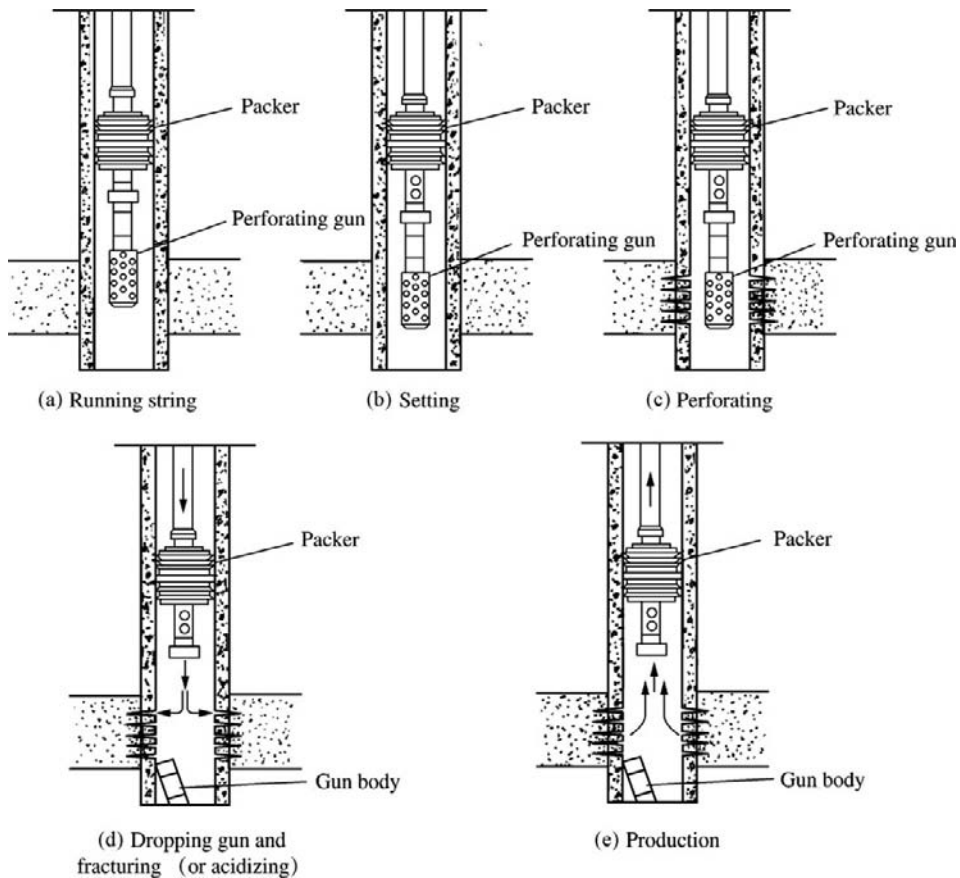


**FIGURE 6-7** Combined tubing-conveyed perforating and hydraulic fracturing (acidizing) technology.

gun. A slotted liner is attached between the setting sleeve and perforating gun. The string is then run in. The depth is corrected by using a radioactivity log or magnetic location curve, which is measured in tubing, and the perforating gun is located at the perforating horizon. A separate firing head detonator is attached to the bottom of the sucker rod pump, and then the firing head detonator and sucker rod pump are run in. After the sucker rod pump is set at the setting sleeve, it starts working. The killing fluid in the annulus can be pumped out of the tubing by the surface power system, and the liquid level in the annulus is lowered, thus generating a pressure difference between the tubing and the annulus, which may excite the pressure-releasing device of the firing head. When the pressure

difference reaches the preset value, the safety pin is sheared, the sliding sleeve moves upward, and the firing head and jar stem are released. When the detonator is impacted, it is detonated, and then the perforated gun is detonated. After perforating, the firing head and sucker rod pump are retrieved together. The whole working process is shown in Figure 6-8.

**Combined Perforating and High-Energy-Gas Fracturing Technology.** The perforating gun with two propellant charges, one on it and the other below it, is run to target horizon on tubing or wireline. Detonation is achieved by dropping or using electricity. One of the propellant charges is ignited. Well pressure rises, then the perforating gun is detonated under overbalance pressure condition. The time interval between propellant

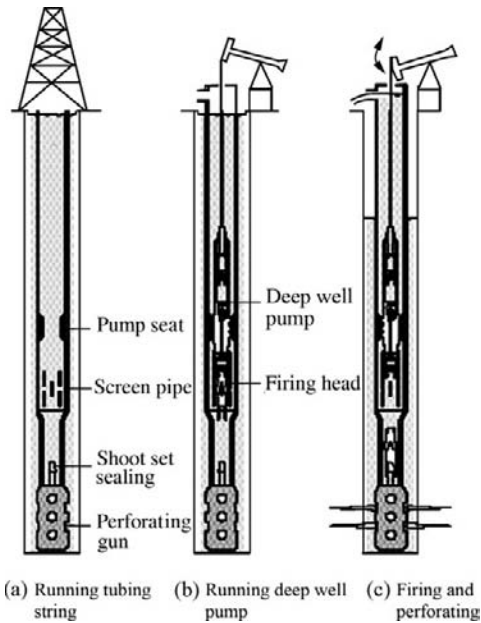


**FIGURE 6-8** Combined perforating and oil well pump technology.

ignition and perforating is controlled by delay cell. After the perforating charge is detonated, the jet flow with high pressure gas produced by propellant burning penetrates casing, and perforations are formed in reservoir. Then the other propellant charge is ignited. The combustion of the second propellant charge subsequently generates high-temperature, high-pressure gas; thus the perforations which are just formed are secured and extended, and the fractures which are not controlled by in situ stress are generated. The fracture length can be 2-8 m. Thus a good bottomhole linking up is formed. The number of fracture is related to the pressure rise rate and peak pressure. In western countries the perforation gun is put into propellant sleeve.

Both perforating and high-energy-gas fracturing operations can be simultaneously performed by running the string once. Separate, symmetric, and sleeve-type perforators have been developed. The integrated perforator can be a perforator with or without a pressure-relief port. The combined perforating and high-energy gas fracturing technology is mainly used for removing plugs

and stimulating in the vicinity of the wellbore and is suitable especially for fractured oil and gas reservoirs, oil and gas reservoirs with serious formation damage, heavy oil reservoirs, and low- or medium-permeability oil and gas reservoirs. In recent years, this technique has been widely applied in many oil fields such as Daqing, Zhongyuan, Dagang, Talimu, Liaohe, Shengli, Changqing, and Qinghai, and a certain effectiveness of stimulation has been obtained.

**Combined Tubing-Conveyed Perforating and Sand Control Technology.** Weakly consolidated or unconsolidated sand formation is very unstable and prone to sand production under the action of extraneous disturbance, and the combined tubing-conveyed perforating and sand control technology can be adopted under this condition. Both perforating and sand control operations are performed by running the string once, thus reducing operation cost and operation time and favoring reservoir protection. Figure 6-9 shows the combination TCP-inside casing gravel pack. A work string with a flight-type perforating gun is adopted. Thus this system is able to circulate under a high pumping rate to remove sand grains in the well and keep the gun from sticking and is also able to effectively pack gravel into perforations. A packer is first set at the bottom of the perforating interval in the casing, the string with a packer in the upper part and a flight-type perforating gun in the lower part (this string can meet the requirement of torque of  $8315 \text{ N} \cdot \text{m}$  by the test at the surface) is run to the bottom of the reservoir, the depth is corrected, the upper packer is set, and then perforating is operated. The upper packer is unset, the wellbore is washed by circulating under a high pumping rate, the carrying fluid is injected through the string and is mixed into the fluid in perforations by rotating the string, and then the pressure and carrying fluid return are observed at the surface. Finally, the string is rotated to a height above the sand surface, and the work string is pulled out after circulating.

A large perforation diameter and a high perforation density should be adopted in order to make the gravel packing operation effective. For instance, in a casing of  $\Phi 114 \text{ mm}$  (4 1/2 in.),

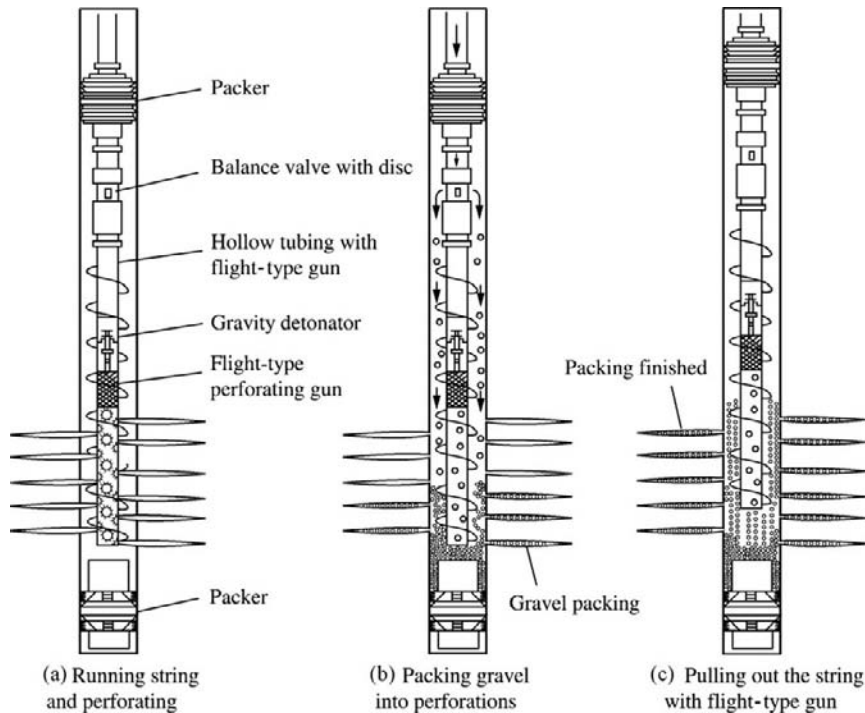


FIGURE 6-9 Combined tubing-conveyed perforation and sand control technology.

a perforating gun of  $\Phi 73$  mm (2 7/8 in.), a perforation density of 18 shots/m, a perforation diameter of 15 mm, and a charge explosive load of 16 g are adopted; in a casing of  $\Phi 139$  mm (5 1/2 in.), a perforating gun of  $\Phi 85.7$  mm (3 3/8 in.), a perforation density of 18 shots/m, a perforation diameter of 17.8 mm, and a charge explosive load of 22.7 g are adopted; in a casing of 244.5 mm (9 5/8 in.), a perforating gun of  $\Phi 177.8$  mm (7 in.), a perforation density of 40 shots/m, a perforation diameter of 25.1 mm, and a charge explosive load of 70 g are adopted.

## Wireline Through-Tubing Perforation (TTP)

### Conventional Through-Tubing Perforation.

This is the earliest used underbalanced perforating technology. A tubing is first run to the top of the reservoir. After a Christmas tree and a lubricator are installed, a perforating gun and wireline adapter are put into the lubricator, and

then the paraffin valve is opened, and the wireline is run in. The perforating gun passes through tubing and runs out of the tubing shoe. The stub casing location is measured by using the magnetic locator at the wireline adapter. The depth is adjusted so that the perforating gun is opposite the reservoir, and then firing and perforating are performed.

The through-tubing perforation has the advantage of underbalanced perforating and reducing formation damage and is particularly suitable for re-perforation and drilling in a new horizon under the condition of not stopping the production of the production well, so that well-killing and tubing-tripping operations can be avoided. The through-tubing perforation gun diameter is limited by the inside diameter of the tubing; thus, a high perforation density and deep penetration (excessive clearance between perforating gun and casing) cannot be achieved. A penetration depth more than 200 mm is difficult to reach. Thus this type of perforation had

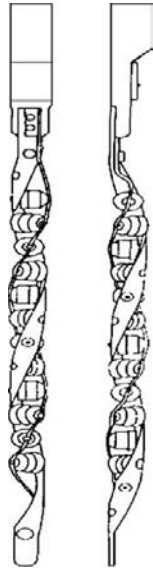


**FIGURE 6-10** Through-tubing perforating guns with phases of 45° and 60°.

been rarely adopted in oil fields for a time. The perforating gun structure has been redesigned by Owen, the gun bodies with 45° and 60° have also been designed (Figure 6-10), and the explosive load is increased, so that the penetration depth can be up to about 600 mm; thus, it has been adopted again in oil fields.

The length of gun run in once during conventional through-tubing perforation is limited by the lubricator height. In a thick oil and gas reservoir, running the gun several times is required, and underbalance pressure cannot be ensured during perforating by later guns. In addition, excessive underbalance pressure is not allowed in order to prevent the wireline from tying a knot, which may be caused by oil and gas channeling upward and may cause accidents after perforating.

**Extended-Diameter TTP.** As mentioned earlier, the through-tubing perforation has the main disadvantage of small gun and small charge, thus limiting the penetration depth. As a result, the extended-diameter TTP system was first developed by Schlumberger in 1992. At present, the through-tubing open-type perforation technology has been widely applied.

The through-tubing open-type perforating gun is run on wireline. After the gun reaches the target, an electric signal is transmitted from the surface for releasing the detonator. After releasing the detonator, detonating and unlocking, the perforating charges are rotated by 90° under the action of the tensile force of the spring, thus making them perpendicular to the axis of the charge carrier. An electric signal is transmitted from the surface for detonating the electric detonator. The primer cord is detonated by the detonator. The perforating charges are detonated by the primer cord, thus achieving through-tubing deep penetration perforating, which corresponds to perforating by using a large-diameter casing perforating gun with a charge explosive load of 23 g. The penetration depth can be more than four times that of an original Typ. 51 gun. Thus oil and gas well productivity can be effectively achieved.

The main features include: (1) reperforating an old well without pulling out the tubing; (2) greatly reducing the sump hole of the well that needs production logging under the condition of releasing gun; (3) achieving deep penetration by using a large perforating charge; (4) the circuit of the main firing system, which is shortened out before releasing the perforating charges, so that it is safer; and (5) reliable mechanical action.

The properties of the open-type through-tubing perforating guns made in China are listed in Table 6-1. The penetration depth in a concrete target is 450 mm. The Owen open-type through-tubing perforating gun can use perforating charges with corresponding explosive load in various tubings (Table 6-2). The explosive load is 11 to 32 g, and the penetration depth is 400 to 800 mm. At present, the through-tubing perforation method can only achieve perforating under a phase of 180° (see Figure 6-11).

### Extreme Overbalance Perforating Technology (Forward Shock)

Extreme overbalance perforating (EOP) technology is a new technology presented first by P. J. Handren et al. of the Oryx Energy Company

**TABLE 6-1 The Properties of Open-Type Through-Tubing Perforating Guns Made in China**

Index	Perforating Gun Made by Sichuan Petroleum Perforation Equipment Co.		Perforating Gun Made by Chuannan Machinery Factory (Detonating after Opening)
Explosive load of perforating charge (g)	23	26	24
Penetration depth in concrete target (mm)	≥450	≥500	450
Inlet bore diameter (mm)	9	10	8.5
Closed gun diameter (mm)	48	54	48
Open gun diameter (mm)	102	105	104
Phase (°)	180	180	180
Perforation density (shots/m)	13	13	14
Gun body length (m)	3	3	/
Resistance to pressure (MPa)	60	80	60

**TABLE 6-2 Parameters of Owen Through-Tubing Perforation Technique**

Gun diameter (closed/open) (m)	$1\frac{3}{8}/3\frac{3}{4}$	$1\frac{11}{16}/3\frac{7}{8}$	$1\frac{11}{16}/4\frac{1}{2}$	$2\frac{1}{8}/5\frac{3}{8}$
OD (tubing/casing) (m)	$2\frac{3}{8}/4\frac{1}{2}$	$2\frac{3}{8}/5\frac{1}{2}$	$2\frac{3}{8}/5\frac{1}{2}$	$2\frac{7}{8}/7$
Perforation density (shots/m)	16	14	13	11
Phase (°)	180	180	180	180
Type of perforating charge	A.P.	A.P.	A.P.	A.P.
Type of explosive	HMX	HMX	HMX	HMX
Explosive load (g)	11.0	15.0	21.7	32.0
Maximum resistance to temperature (°C)	191	191	191	191
Minimum OD (mm)	36.5	45.2	45.2	55.5
Perforation diameter (mm)	7.6	10.7	9.9	12.7
Penetration depth (mm)	406	579	665	886

in the 1990s. It has been applied in more than 900 wells in North America, and good results have been obtained.

The wellbore is pressurized by using a liquid, nitrogen gas, or combined gas and liquid column before perforating so that the bottomhole pressure is at least equal to formation breakdown pressure. The compressed gas energy is directly changed to the pressure acting on the reservoir at the instant of perforating. The pressurized liquid enters the perforations at a very high velocity. The shaped-charge shooting pressure acting on the tip of perforation is up to 10,000 MPa. Such a high pressure greatly exceeds the principal stress and tensile strength of the reservoir rock and causes a high degree of stress concentration on

the perforation wall face, so that a large number of cracks may be generated on the perforation wall face; thus, the shock of following high-velocity fluid may extend the cracks and form effective bottomhole linking. The further injection of liquid nitrogen, acid, or sand-laden fluid after perforating can enhance productivity. The further injection of resin used for consolidating formation sand can control sand.

The EOP technology can be tubing-conveyed EOP technology, through-tubing EOP technology, or wireline casing gun EOP technology in wells that have not been perforated. In addition, there also is independent pumping shock technology after perforating in a well that has been perforated (Figure 6-12).

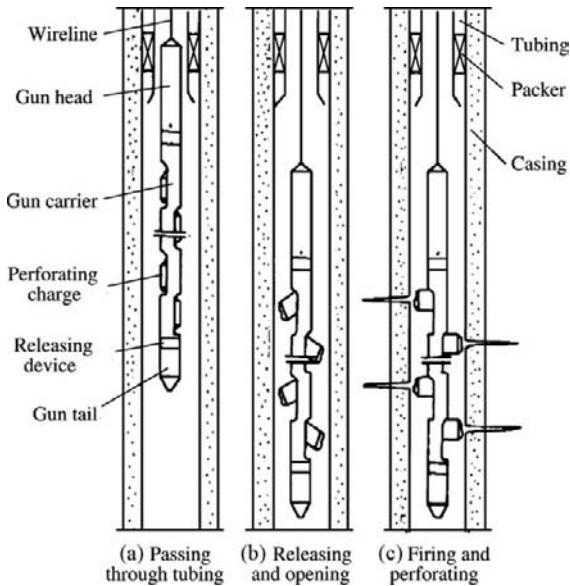


FIGURE 6-11 Open-type through-tubing perforating.

The strings of TCP, WCP, or TTP technology should adopt a perforating gun with gun body as far as possible in order to leave the debris after

perforating in the perforating gun. Tubing-conveyed EOP technology is suitable for complicated or high-pressure reservoirs, whereas wireline EOP technology is suitable for low-pressure reservoirs. Wireline through-tubing EOP technology is appropriate to old wells in which opening a new reservoir or reperforating is required without moving the production tubing string.

Extreme overbalance shock technology is shown in Figure 6-12d. A friable disc (made of glass, ceramics, cast iron, or other friable materials) or a valve is attached to the tail of the tubing. The valve (such as an LPRN or APR valve) can be opened by the tubing-casing annulus pressure difference. The design pressure is achieved by injecting high-pressure nitrogen gas into the tubing. When a friable disc is used, the friable disc may be broken down by releasing the bar at the wellhead lubricator, which drops through tubing and impacts the friable disc. Under the action of high-pressure nitrogen gas, the working fluid rapidly shocks the perforations that have been generated and extends the fractures.

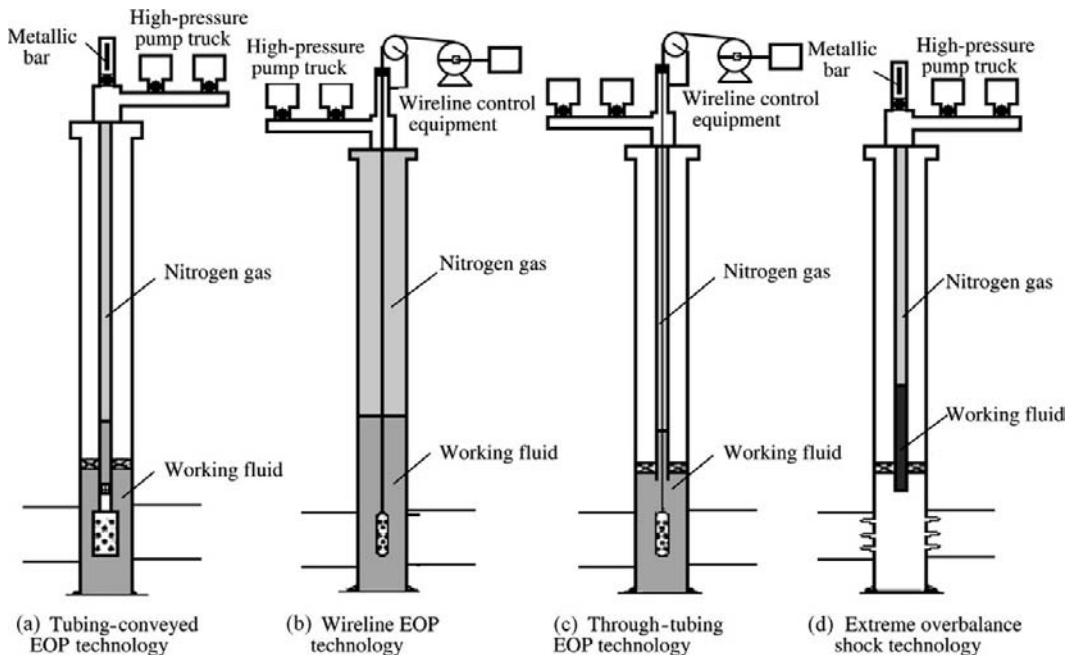


FIGURE 6-12 Strings of extreme overbalance perforating technology.

During tests in the Tuha, Sichuan, and Zhongyuan oil and gas fields, nitrogen gas was injected into wells before perforating so that the pressure exceeds the formation breakdown pressure, and then the wells are perforated. Perforations and microfractures are generated by using a shaped charge. The microfractures are extended by using the expansion energy of high-pressure nitrogen gas so that the near-wellbore permeability is improved. After that, the wellhead is opened, and nitrogen gas is blown down in order to form an underbalance at the bottomhole, thus achieving perforation cleaning and induced flow. In the RN209 well, the reservoir depth is 1298–1303.9 m, the reservoir thickness is 5.9 m, the nitrogen injection pressure is 30 MPa, the overbalance pressure is 22.8 MPa, and the flowing production rate after perforating is 34.5 m<sup>3</sup>/d, which is 1.38 times the production rate of an adjacent well (RN205). The W279 well is a rolling appraisal well and has an estimated reservoir pressure of 32.8 MPa and a breakdown pressure of 52 MPa. The tubing-conveyed super-overbalance perforating technology and tubing pressurization detonation are adopted. The acid volume is 5 m<sup>3</sup>, the liquid nitrogen volume is 2 m<sup>3</sup>, the design wellhead pressure is 40 MPa, the bottomhole pressure is 60 MPa, and the perforating parameters are YD102 gun, 90°, and 16 shots/m. The measured skin factor is about -5, which indicates that this technology has an obvious effectiveness. The analysis indicates that oil well productivity after perforating is four times that of conventional underbalance perforating.

The pressure-bearing abilities of the tubing string, wellhead, and equipment and more effective safety measures should be considered due to the high-pressure operations of EOP technology. In addition, because the liquid may enter the reservoir, good compatibility of completion fluid with the reservoir rock and fluid should be ensured in order to prevent new formation damage.

In general, extreme overbalance perforating technology is suitable for: (1) fracturing pretreatment of low- and medium-permeability oil reservoirs with perforating phase of 120°/180° and low perforation density; (2) plugging removal of

high- and medium-permeability oil reservoirs with high perforation density and low phase (45°/60°); (3) carbonatite oil reservoir (acid liquor required); (4) naturally fractured oil reservoir with high perforation density (phase unrestrained); (5) oil reservoir with serious heterogeneity; and (6) blocking removal by high-pressure shock in the wells that have been perforated.

## Horizontal Well Perforating Technology

The matching techniques and theory that are related to horizontal wells have been greatly advanced since the application of horizontal wells to oil field development began in the early 1980s. At present, long-interval deep-well directional perforating, combined perforating and testing operation of horizontal wells, horizontal well reperforating, limited-entry fracturing perforating of horizontal wells, nitrogen gas extreme overbalance perforating of horizontal wells, and so on, have all been achieved. Horizontal well perforating has become a conventional perforating operation.

Horizontal wells with formations that do not easily slough adopt perforated completion at present in order to effectively prevent gas and water coning and to make separate-zone production and operation convenient. The perforating gun used in a horizontal well is generally conveyed on tubing or coiled tubing. The downhole perforating assembly of a horizontal well includes generally a locator sub, detonating device, underbalance accessories, packer, oriented perforating gun, centralizer, and ball guide shoe.

A horizontal well has a long perforating interval and a large skip distance; thus, the detonation safety of a perforating gun and the detonating quality should be emphatically considered, and several detonators are generally used. Pressure detonation is commonly used for perforating in horizontal wells. On the basis of different goals and usage, it can be tubing pressurization detonation, annulus pressurization detonation, pressure opening device plus pressure difference (delay) detonation, opening gun plus pressure (delay) detonation, integrated pressure (delay) detonation

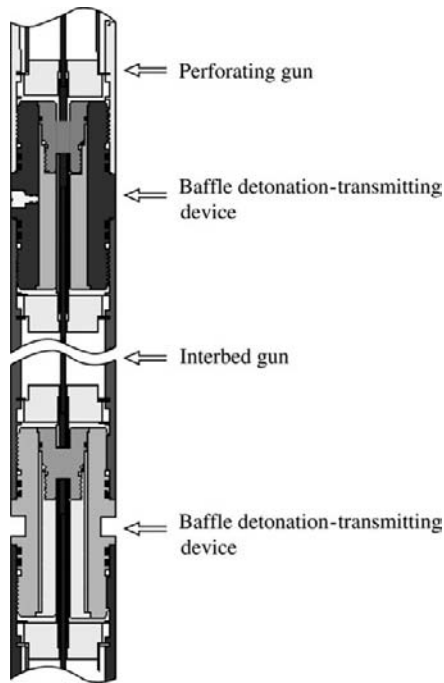


FIGURE 6-13 Baffle detonation-transmitting device.

opening device, or baffle detonation-transmitting device, and so on.

The baffle detonation-transmitting technique is shown in Figure 6-13. Both ends of the interbed gun are plugged by using a baffle fire work-piece. The detonation energy of the perforating gun is reliably transmitted to the perforating gun below the interbed gun through the baffle detonation-transmitting device. Both ends of the interbed gun after explosion are in a sealed state, thus preventing well fluid from entering.

The perforating guns are pulled to the well-head after perforating. The pressure in the interbed gun can be relieved safely and reliably by the pressure relief valve of the baffle detonation-transmitting device. This technique has the following advantages:

1. Suitable for the various perforating operations with gun body
2. Reliable for transmitting detonation energy with stable detonation transmission, resistance to pressure of 100 MPa, and reliable sealing

3. No sillage in the interbed gun, no platform and ocean contamination, and no need for cleaning the interbed gun, which is used repeatedly
4. Reliably releasing the gas in the interbed gun by the pressure relief valve at adapter, safely removing the gun, making gun removal faster, and reducing labor intensity
5. Safe and reliable detonation transmitting from top to bottom or from bottom to top

This technique has been widely applied, and good economic and social benefit has been obtained. Its application will greatly reduce environmental pollution and enhance operational safety and efficiency.

The other key to horizontal well perforating lies in selecting an appropriate perforating gun. The perforating gun should be safely run to target and pulled out safely, which requires no plastic deformation of the perforating gun during passage through the well section of curvature, requires smooth rotating of the charge carrier in the gun body, and requires little deformation of the gun body after perforating without tearing at perforations. Therefore, the perforating gun made of seamless steel pipe, which is processed by using special technology including heat treatment, is selected depending on actual formation conditions. After perforating, the burr height should not exceed 3 mm, and the maximum expansion should not exceed 5 mm.

On the basis of orientation, horizontal well perforating includes circumferential perforating ( $360^\circ$ ) and low-side perforating ( $180^\circ$  and  $120^\circ$ ), as shown in Figure 6-14. The orientation selection is mainly dependent on the degree of hardness of formation. In general, under the condition of unconsolidated reservoir, a perforating orientation of  $120^\circ$  to  $180^\circ$  is adopted in order to avoid wellbore plugging due to dropping of cuttings of the upper part of the horizontal section after perforating.

The horizontal well perforating orientation is dependent on the orientation of the perforating gun of the horizontal well. The gravitational orientation of the perforating gun includes

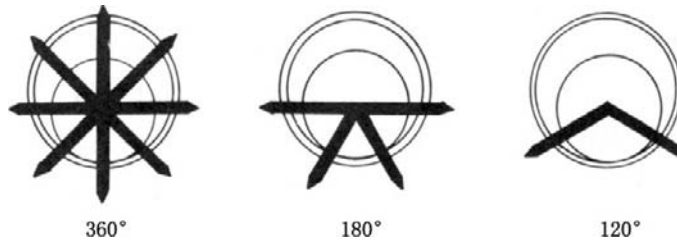


FIGURE 6-14 Perforating orientation for horizontal well.

external orientation and internal orientation. The external orientation adopts the blades melded to the gun body, and the perforating orientation is achieved by the integral rotation of perforating guns under the condition of eccentric gravity under the unbalanced friction resistance between blade and borehole wall in combination with a rotation sub. The internal orientation adopts the eccentric setting of charge carrier in the gun body, and the perforating orientation of each gun is achieved by the rotation of charge carrier under the condition of eccentric gravity in combination with an eccentric support. The internal orientation technique is in common use in China due to its high accuracy, effectiveness, ease of detection, and enabling the installation of a larger perforating gun. The internal orientation includes eccentric rotation type and weight rotation type.

At present, the horizontal well oriented perforating system (HOPS) developed by Baker Hughes also adopts the internal orientation of weight rotation type (Figure 6-15). The orientation of any angle can be achieved by using a rotation sub and has a degree of accuracy of  $\pm 5^\circ$ .

A large-scale horizontal perforating using the HOPS system was achieved in the North Sea in

2002. The well had a horizontal section length of 2246 m and total perforating length of 1490 m. It adopted a casing of  $\Phi 177.8$  mm (7 in.) and a perforation density of 16 shots/m. Tubing-conveyed perforating guns of  $\Phi 114$  mm were adopted. Each gun had a length of 7.11 m (28 ft). The phase of 0 to  $180^\circ$ , which is perpendicular to the minimum principal stress, was adopted in order to achieve sand control (Figure 6-16). A total of 23180 low-debris deep-penetration perforating charges and 188 rotation subs were installed.

Horizontal wells are being increasingly applied in China due to their production effectiveness, which is better than that of straight wells. Thus the perforated completion technology of horizontal wells is also being developed along with the application of horizontal wells and gradually is becoming the main means of horizontal well completion. For instance, wells including TZ 16-7, TZ 16-12, TZ 4-7, H23, and TZ 404 H have all adopted perforated completion. The various perforation strings of a horizontal well have been designed, horizontal well perforating tools that are appropriate to a long horizontal section, deep well, and medium curvature and include a perforating gun made of seamless steel pipe, bidirectional delay pressure detonator, and ball



FIGURE 6-15 Oriented perforating system for horizontal well.

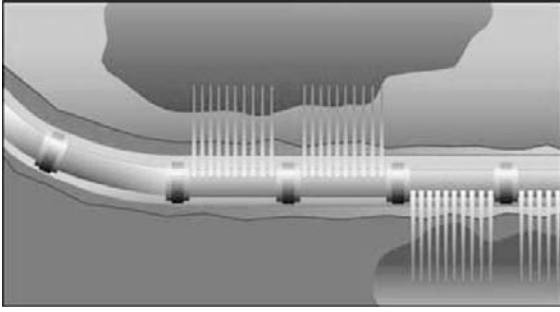


**FIGURE 6-16** Oriented perforating in horizontal well by using HOPS system.

guide shoe have been developed, and the corresponding technological measures have been designed. They have been successfully applied in high-temperature high-pressure horizontal wells, and good technological results have been obtained.

The perforation string of the TZ 16-7 well is shown in Figure 6-17. The combined string of  $\Phi 88.9$  mm drill pipe in the upper part and  $\Phi 73$  mm tubing in the lower part is used for conveying the perforating gun. The string structure includes guide, detonator, perforating gun, bidirectional detonator, perforating gun, detonator, safety gun,  $\Phi 73$  mm tubing, locator sub,  $\Phi 73$  mm tubing, and  $\Phi 88.9$  mm drill pipe to the wellhead.

In recent years, coiled tubing-conveyed perforating technology has been widely applied in horizontal or extended reach wells due to its safe and convenient operation and specific reservoir-protecting action, and so on.

### Oriented Perforating Technology

This technology is mainly used for perforating in the wells of naturally fractured oil reservoirs, horizontal wells, wells to be hydraulically fractured, and wells in which sand control is required. The perforating is generally opposite to the orientation in which the fracture developed or the orientation perpendicular to the minimum horizontal in-situ stress, thus favoring sand control or hydraulic fracturing operation and enhancing the success ratio and effectiveness of operations.

The oriented perforating system of straight or horizontal wells has been widely used. The G-Force system developed by Halliburton has a directional gyroscope, which is located in the protective environment of the gun body, thus avoiding the restrictions that are accepted by the old orientation system. The new orientation system is independent of the special series blades, eccentric sub, and swivel joint. These are affected by the friction and torque generated during the work of the gun, thus leading to a low accuracy of orientation.

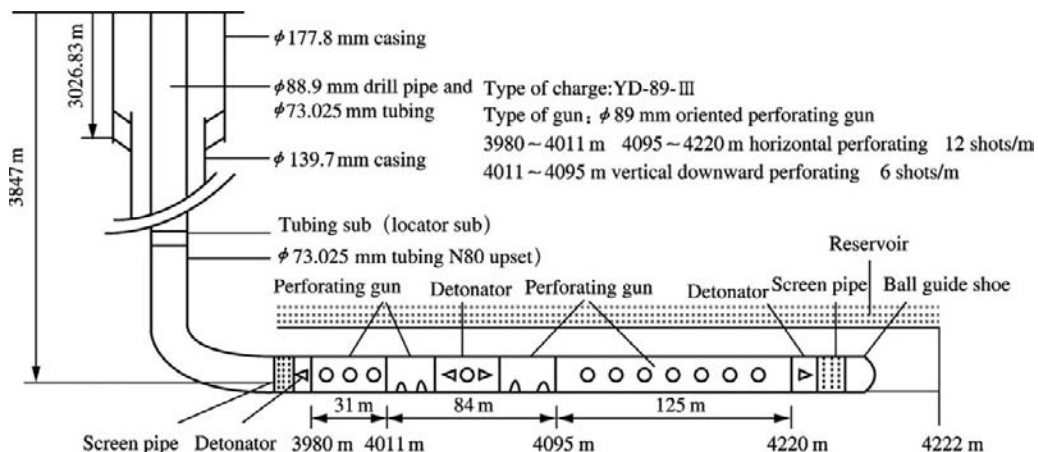


**FIGURE 6-17** TZ 16-7 perforated completion string for horizontal well.

This system is mainly used in wells with a deviation angle higher than  $25^\circ$ . The length of the gun body is 6.7 m (22 ft). There is close seizing each other between guns. This puts the system into alignment, and there is no need of a swivel joint. The internal orientation system is in the gun carrier. This compact configuration makes it possible to place it in a location that other guns cannot reach due to the friction between the gun and casing or obstruction. The system can be conveyed on coiled tubing, wireline, wire, or hinged pipe. There is no need of several orientation subs, and the perforating guns can center in the borehole, thus enhancing perforation efficiency to 90%.

Gravity-oriented perforating technology has had widespread use in horizontal wells in China. The orientation instrument developed by the Sichuan Logging Company uses an accelerometer as an orientation system, and a small-diameter metallic thermos and downhole automatic guide system are used. It is used in wells with a deviation angle larger than or equal to  $2^\circ$  and can be used for orienting in straight wells in combination with a gyro sub. The Liaohe Logging Company has also developed a straight-well oriented perforating system that adopts gyro orientation. The method of determining reservoir fracture or principal stress azimuth, orientation control method and matching tools, the method of acquisition, transmission, and processing of data, and the orientation monitoring and evaluation technique have yet to be improved.

## 6.2 PERFORATED WELL PRODUCTIVITY INFLUENCING RULE ANALYSIS

The effects of the properties of the perforating gun and perforating charge (perforation density, penetration depth, perforation diameter, and compaction damage, and so on) and the parameters of reservoir rock and reservoir fluid on the oil and gas well productivity after perforating are obvious. Formation damage during perforating and perforated well productivities under different perforating conditions should

be predicted and evaluated by laboratory experiments, theoretical studies, and on-site tests of different types of reservoir, fluid, and well in combination with the corresponding perforating technology.

### Productivity Rule of Perforated Well of Sandstone Reservoir

The parameters that influence perforated well productivity include mainly perforation density, penetration depth degree of compaction damage, reservoir heterogeneity, compaction thickness, phase, perforation diameter, degree of drilling damage, drilling fluid contamination thickness, wellbore radius, permeability, producing pressure drawdown, and perforation pattern. The influences of these factors should be comprehensively considered, and the primary should be distinguished from the secondary. The quadrature analysis and significance test should be performed.

The effects of perforating parameters on sandstone reservoir well productivity of sandstone reservoir have been studied by using the electric analogy method and the finite-element numerical simulation method. The studies indicate that the various parameters are of inconsistent importance under the condition of the damage zones having and having not been penetrated through (Table 6-3).

It is shown that the same parameter (especially perforation density, penetration depth, perforation diameter, drilling damage, or compaction damage) has different effects on oil reservoirs and gas reservoirs.

#### Effects of Perforating Parameters on Well Productivity

1. Porous oil reservoir
  - a. Effects of perforation penetration depth and perforation density

The productivity ratio (PR) of an oil well increases with the increase of perforation penetration depth and perforation density, but the rate of increase gradually decreases; that is, the increase of productivity due to the increase of perforation penetration

TABLE 6-3 Order of Significance of Perforating Parameters and Damage

Influencing Parameter	Sandstone Oil Well		Sandstone Gas Well	
	Damage Zone Not Penetrated Through	Damage Zone Penetrated Through	Damage Zone Not Penetrated Through	Damage Zone Penetrated Through
Perforation penetration depth	2	2	2	7
Perforation density	3	1	3	1
Perforation diameter	8	8	4	2
Phase angle	6	6	8	10
Compaction thickness	9	9	11	11
Degree of compaction	5	3	5	9
Damage depth	7	5	10	12
Degree of damage	1	7	1	3
Anisotropy	4	4	7	4
Permeability	No influence	No influence	12	8
Wellbore radius	10	10	6	5
Producing pressure drawdown	No influence	No influence	9	6

Note: The smaller the digit, the more important the parameter.

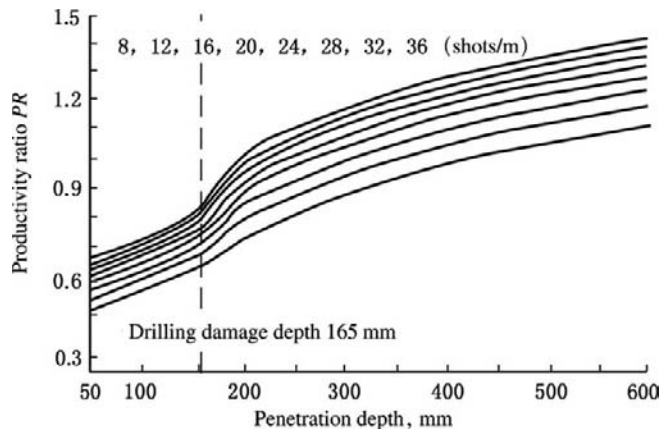


FIGURE 6-18 Effects of perforation penetration depth and perforation density on productivity ratio.

depth and perforation density is limited (Figure 6-18). Economically, the effectiveness of an increase in perforation penetration depth and perforation density when the perforation penetration depth and perforation density are respectively less than 800 mm and 24 shots/m is obvious. At present, the maximum concrete target penetrating depth is about 1080 mm

(corresponding to Berea target penetrating depth of 750 mm) in China; however, for a low- or medium-permeability reservoir, the sandstone penetrating depth is about 500 mm, and the perforation density is mostly 16 shots/m or 20 shots/m. Developing the deep penetrating perforating charge and high perforation density perforation technology is still potential.

The serialization of deep penetrating and high perforation density perforating gun is required. Certainly, the restrictive conditions including cost, damage to casing, technology, and downhole condition should be comprehensively considered in order to rationally select the penetration depth and perforation density.

It is shown that the productivity ratio will obviously increase after the perforations penetrate through the formation damage zone; thus, the drilling fluid damage depth should be controlled as much as possible by using the shield-type temporary plugging technique, and so on.

The studies indicate that when the anisotropy is not serious ( $0.5 \leq K_v/K_h \leq 1.0$ ), perforation penetration depth is of greater importance than perforation density if the damage zone can not be penetrated through (Figure 6-19), and a deep penetration and a medium perforation density (about 16 shots/m) are appropriate, while the perforation density is of greater importance than penetration depth if the damage zone can be penetrated through, and a high perforation density (more than 22 shots/m) should be adopted.

The studies also indicate that when the anisotropy is serious ( $K_v/K_h < 0.5$ ), the effectiveness of high perforation density is obvious. A high perforation density (more than 20 shots/m) should be adopted whether the damage zone can be penetrated through or not (Figure 6-19).

- b. Effect of phase angle. There is an interactive relation between anisotropy and phase angle (Figure 6-20). When the anisotropy is not serious ( $0.7 \leq K_v/K_h \leq 1.0$ ), the phase angle of  $90^\circ$  has the highest productivity ratio, while the phase angle of  $0^\circ$  has the lowest productivity ratio, and the productivity ratio will decrease as the phase angle changes from  $90^\circ$  to  $0^\circ$  though  $120^\circ$ ,  $60^\circ$ ,  $45^\circ$ , and  $180^\circ$ . When the anisotropy is medium ( $0.3 < K_v/K_h < 0.7$ ), the phase angle of  $120^\circ$  has the highest productivity ratio, while the phase angle of  $0^\circ$  has the lowest productivity ratio. When the anisotropy ratio is serious ( $K_v/K_h \leq 0.2$ ), the productivity ratio will decrease as the phase angle changes from  $180^\circ$  to  $0^\circ$  through  $120^\circ$ ,  $90^\circ$ ,  $60^\circ$ , and  $45^\circ$ . Thus  $120^\circ$  and  $180^\circ$  are known as high phase. When the anisotropy is serious, high-phase perforating has a higher productivity ratio

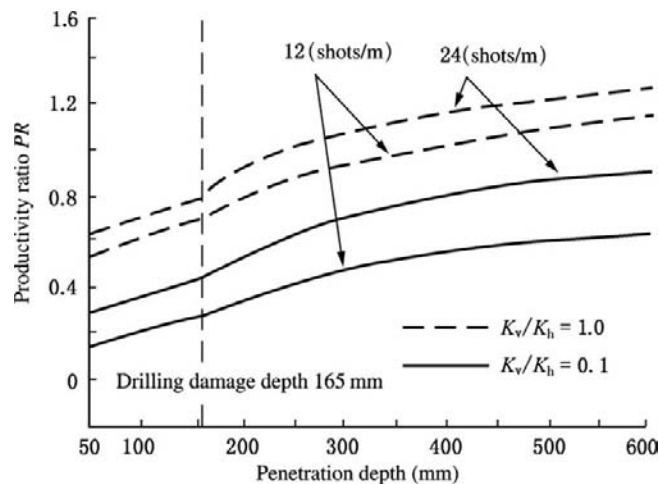
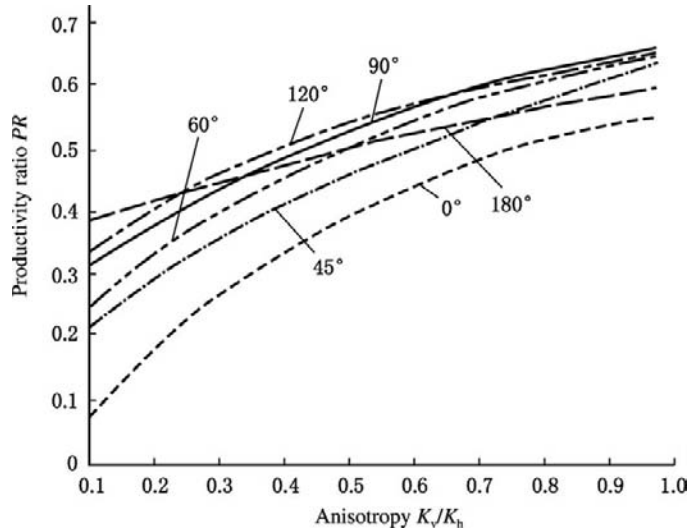


FIGURE 6-19 Effects of anisotropy and perforation density on productivity ratio.



**FIGURE 6-20** Effects of phase angle and anisotropy on productivity ratio.

because the longitudinal distance of two accordant adjacent perforations of high phase will decrease under a certain perforation density so that the influence of anisotropy can be minimized. For a homogeneous formation, not the longitudinal distance of two accordant adjacent perforations but the planar distributary becomes the main problem; thus,  $90^\circ$  and  $60^\circ$  of low phase are superior to  $180^\circ$  under this condition because the low phase can achieve placing of perforations in various directions along the plane. Therefore, the anisotropy has no obvious influence on productivity ratio under the condition of high phase angle, while the anisotropy has a serious influence on productivity ratio under the condition of low phase (such as  $90^\circ$  and  $60^\circ$ ). The anisotropy has an obvious influence on perforated well productivity ratio (Figure 6-20); thus, the perforating phase angle should be optimized on the basis of the degree of anisotropy.

- c. Effect of perforation diameter. The perforation diameter is not a key factor

relatively. A perforation diameter larger than 10 mm is appropriate (Figure 6-21).

The basic parameter values of single-factor analysis are: penetration depth  $L_p = 100$  mm, perforation density  $DEN = 20$  shots/m, perforation diameter  $d_p = 10$  mm, phase angle  $\Phi = 90^\circ$ , compaction thickness  $CZH = 12.5$  mm, degree of compaction  $CZC = 0.2$ , damage depth  $D_H = 165$  mm, degree of damage  $D_c = 0.5$ , anisotropy  $K_v/K_h = 1.0$ . The productivity ratio may change under different parameter values, but the aforementioned rules are unchangeable.

## 2. Porous gas reservoir

The high velocity of gas may generate a non-Darcy effect. The gas flow velocity difference between perforated well and open hole may lead to a different turbulence effect. Thus the factors that may obviously affect the flow velocity (such as permeability and producing pressure drawdown) may affect the productivity ratio of gas well perforating to some extent (Figure 6-22). With the increase of gas reservoir permeability, the turbulence effect of a perforated well becomes increasingly obvious,

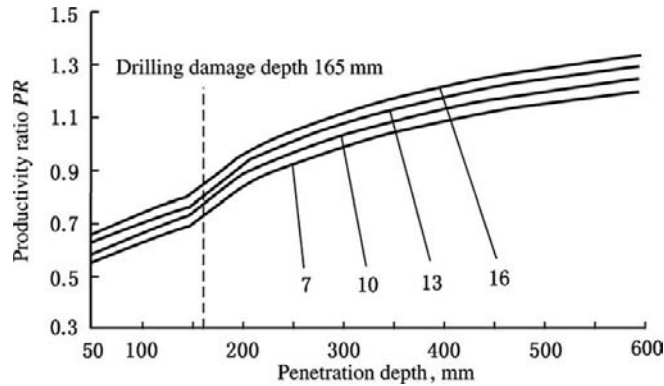


FIGURE 6-21 Effect of perforation diameter on productivity ratio.

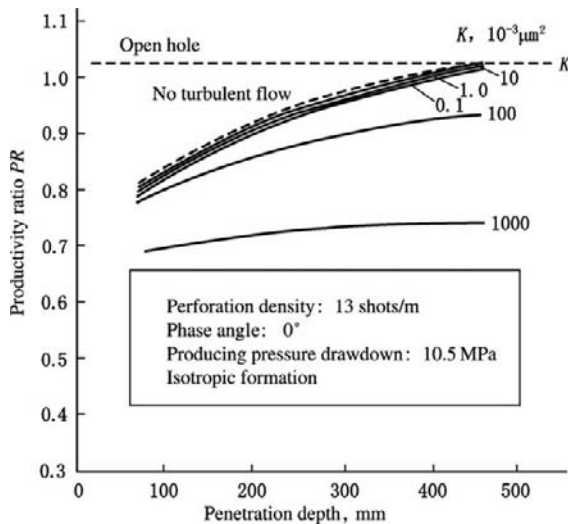


FIGURE 6-22 Relation between gas well productivity ratio and permeability [1].

the productivity ratio is gradually decreased, and the effect of perforation penetration depth is reduced. The increase of producing pressure drawdown may also cause a decrease in productivity ratio.

a. Effects of perforation penetration depth and perforation density. The effects of perforation penetration depth and perforation density on gas well productivity ratio are shown in Figure 6-23. It is indicated that the effect of perforation

penetration depth on the productivity ratio is obvious when the drilling damage zone has not been penetrated through, while the effect of perforation penetration depth on the productivity ratio is not obvious after the drilling damage zone is penetrated through (especially under the condition of low perforation density); however, the effect of perforation density on the productivity ratio is obvious whether the drilling damage zone has been penetrated through or not. In particular, after the drilling damage zone is penetrated through, the increase of productivity ratio due to the increase of perforation density is still obvious even if the perforation density is up to 40 shots/m. Therefore, the high perforation density effectiveness of gas wells is better than that of oil wells.

b. Effect of perforation diameter. Figure 6-24 shows that the effect of perforation diameter on the productivity ratio of gas wells is obvious (especially after the drilling damage zone is penetrated through). This is different from that of oil wells.

c. Effect of producing pressure drawdown. The effect of gas well pressure drawdown on the productivity ratio is obviously different from the effect of oil well pressure drawdown on the productivity

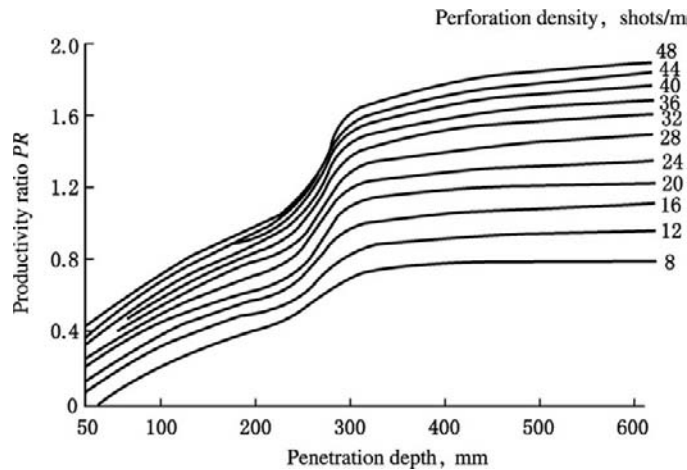


**FIGURE 6-23** Effects of perforation penetration depth and perforation density on gas well productivity ratio.

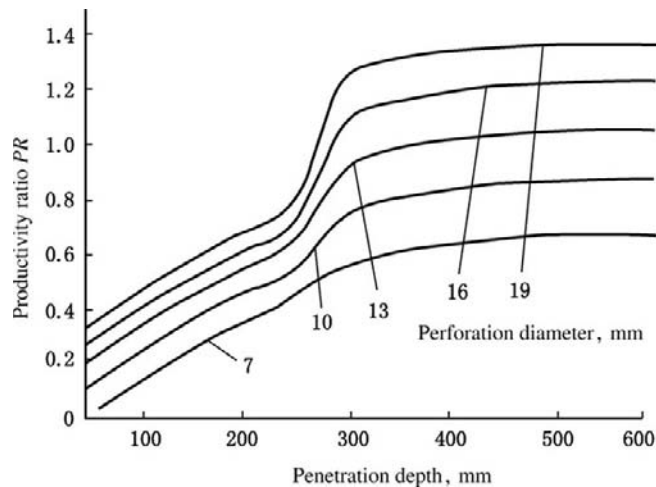


**FIGURE 6-24** Effects of perforation diameter on gas well productivity ratio.

ratio. The gas well productivity ratio is also sensitive to producing pressure drawdown (Figure 6-25). The greater the pressure drawdown, the lower the productivity ratio. The reason is that the non-Darcy turbulence coefficient in the vicinity of the wellbore will be increased; thus, an additional skin will be generated, and the gas well production rate cannot be

doubled and redoubled by increasing the producing pressure drawdown.

- d. Effect of phase angle. The relation between phase angle and productivity ratio is not only related to anisotropy but to producing pressure drawdown and whether damage zone is penetrated through. Table 6-4 shows the relation between phase angle and gas well productivity ratio under different

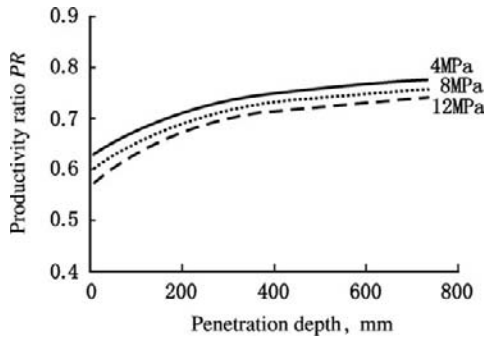


**FIGURE 6-25** Effects of producing pressure drawdown on gas well productivity ratio.

conditions. The parameters given are: perforation diameter  $d_p = 13$  mm, perforation density  $DEN = 20$  shots/m, perforation penetration depth  $L_p = 300$  mm or  $L_p = 200$  mm, damage depth  $D_H = 250$  mm, degree of damage  $D_C = 0.5$ , compaction thickness  $CZH = 12$  mm, and degree of compaction  $CZC = 0.2$ .

**Effect of Formation Damage on Perforated Well Productivity.** The formation damage caused by perforated completion includes compaction damage directly caused by perforating and damage caused by drilling. It has an obvious effect on well productivity.

#### 1. Compaction damage of perforating

A compacted zone may be generated by a high-temperature high-pressure shock wave during shaped-charge perforating around perforation. Figure 6-26 shows the microstructure of the compacted zone around perforation of Berea core target, which is described by R. J. Saucier [4]. The compacted zone consists of crushed zone, grain-fracture zone, and permeability damage zone. The compacted zone permeability ( $K_{cz}$ ) is about 10% of original permeability. This compacted zone with a very low permeability will greatly decrease perforated well productivity. Its effect cannot be entirely eliminated at present.

In 1991, Asadi and Preston [5] discovered that there were small channels around

perforation and large original channels outward in the studies of perforated core; they used a scanning electron microscope and image analyzer (Figure 6-27). The measurement of porosity using the mercury intrusion method also indicated no decrease of porosity around the perforation. However, the pore size distribution curve measured using the mercury intrusion method indicated that the pore size distribution was changed to a great extent despite the fact that the porosity was not changed (Figure 6-28). The large channels had been disrupted and small pores are increased, thus leading to an obvious decrease of permeability.

The studies of the effect of compacted zone on perforated completion well productivity in China indicate that the increase of compacted zone thickness decreases the productivity ratio. Core target testing conducted by the Huabei oil field and Southwest Petroleum Institute indicates that the compaction thickness is between 10 mm and 17 mm. The effect of the degree of compaction damage  $CZC$  ( $K_{cz}/K_o$ ) on productivity is obvious. In particular, after the drilling damage zone is penetrated through by perforation, this effect will obviously increase (Figure 6-29). Therefore, it is necessary to select the perforating charge that has a high core flow efficiency.

#### 2. Drilling damage

Drilling damage has two indices, that is, drilling damage depth and degree of drilling damage  $DC$  ( $K_d/K_o$ ). Figure 6-30 shows the effect of the degree of drilling damage on productivity ratio. When the damage zone is penetrated through by perforation (Line A), the effect of the degree of drilling damage on productivity ratio is small; however, when the damage zone is not penetrated through by perforation (Line B), the effect is much more. Figure 6-31 shows the effect of drilling damage depth on productivity ratio. When the damage zone is not penetrated through by perforation, the effect of damage depth on productivity ratio is small in spite of the fact that the total productivity is low. When the

TABLE 6-4 Relation Between Phase Angle and Gas Well Productivity Ratio under Different Conditions

No.	Producing Pressure Drawdown $\Delta P$ (MPa)	$K_v/K_h$	Whether Drilling Damage Zone Is Penetrated Through or Not	Order of Phase Angle from High to Low (Digit in Bracket Is Productivity Ratio Value)				
1	5	1	No	180°(0.953)	120°(0.807)	90°(0.725)	60°(0.637)	0°(0.433)
2			Yes	180°(1.415)	120°(1.401)	90°(1.336)	60°(1.232)	0°(0.907)
3		0.525	No	180°(0.686)	120°(0.622)	90°(0.599)	60°(0.564)	0°(0.420)
4			Yes	120°(1.175)	90°(1.164)	60°(1.115)	180°(1.080)	0°(0.898)
5		0.1	No	120°(0.463)	90°(0.459)	180°(0.454)	60°(0.449)	0°(0.410)
6			Yes	90°(1.007)	60°(1.006)	120°(0.970)	0°(0.887)	180°(0.777)
7		0.01	No	90°(0.425)	60°(0.423)	120°(0.422)	0°(0.400)	180°(0.397)
8			Yes	60°(0.974)	90°(0.965)	120°(0.917)	0°(0.875)	180°(0.704)
9	10	1	No	180°(0.827)	120°(0.708)	90°(0.640)	60°(0.565)	0°(0.399)
10			Yes	180°(1.351)	120°(1.337)	90°(1.272)	60°(1.168)	0°(0.843)
11		0.525	No	180°(0.656)	120°(0.619)	90°(0.592)	60°(0.559)	0°(0.389)
12			Yes	120°(1.110)	90°(1.099)	60°(1.050)	180°(1.015)	0°(0.833)
13		0.1	No	60°(0.439)	90°(0.436)	0°(0.380)	120°(0.376)	180°(0.355)
14			Yes	90°(0.941)	60°(0.940)	120°(0.904)	0°(0.821)	180°(0.711)
15		0.01	No	0°(0.370)	60°(0.365)	90°(0.354)	120°(0.337)	180°(0.285)
16			Yes	60°(0.910)	90°(0.901)	120°(0.853)	0°(0.810)	180°(0.640)
17	20	1	No	180°(0.669)	120°(0.605)	90°(0.564)	60°(0.517)	0°(0.368)
18			Yes	180°(1.272)	120°(1.259)	90°(1.194)	60°(1.090)	0°(0.765)
19		0.525	No	120°(0.396)	90°(0.396)	60°(0.390)	180°(0.379)	0°(0.360)
20			Yes	120°(1.031)	90°(1.020)	60°(0.970)	180°(0.936)	0°(0.754)
21		0.1	No	0°(0.350)	60°(0.306)	90°(0.276)	120°(0.240)	180°(0.149)
22			Yes	90°(0.864)	60°(0.863)	120°(0.826)	0°(0.744)	180°(0.634)
23		0.01	No	0°(0.340)	60°(0.281)	90°(0.243)	120°(0.199)	180°(0.101)
24			Yes	60°(0.832)	90°(0.823)	120°(0.774)	0°(0.733)	180°(0.562)

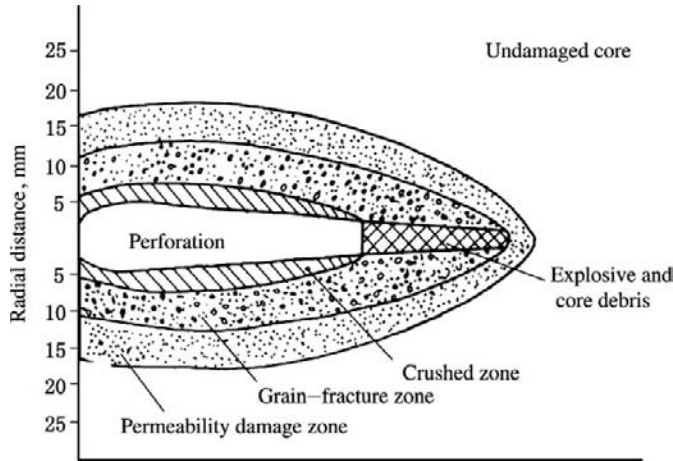
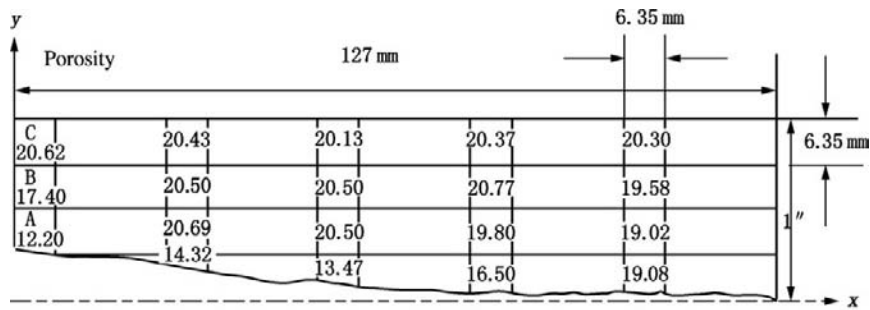
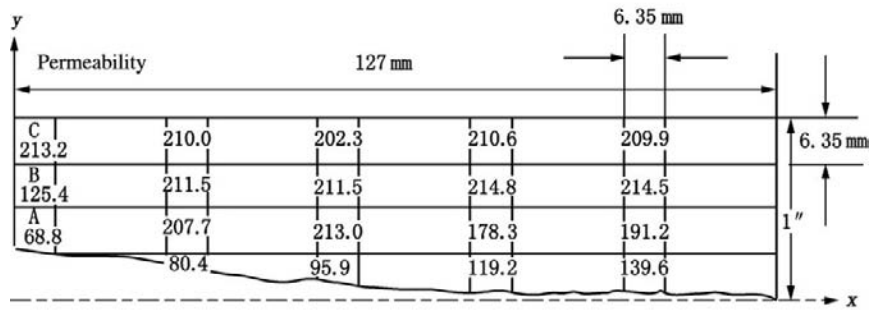


FIGURE 6-26 Microstructure of compacted zone of perforating.



(a) Porosity, %



(b) Permeability,  $10^{-3}\mu\text{m}^2$

FIGURE 6-27 Porosity and permeability distributions around perforation [4].

damage zone is penetrated through by perforation, the total productivity is higher. Therefore, reservoir protection during drilling is of great importance to making full use of oil and

gas well productivity. In addition, a perforating gun and charge that can penetrate through the drilling damage zone should be selected as far as possible.

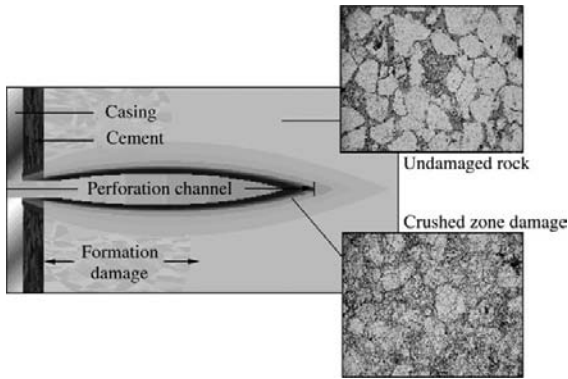


**FIGURE 6-28** Comparison between the channels before and after perforating.

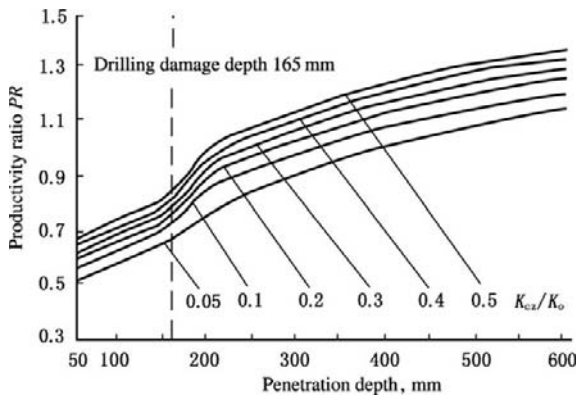


**FIGURE 6-29** Relation between degree of perforating compaction and productivity ratio.

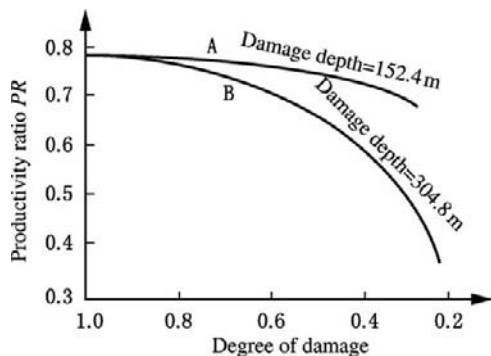


**FIGURE 6-30** Effect of degree of drilling damage on productivity ratio.

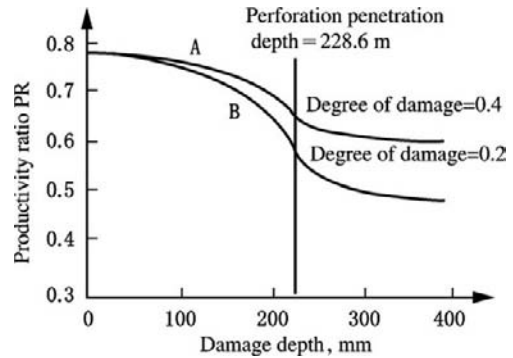


**FIGURE 6-31** Effect of drilling damage depth on productivity ratio.

### Productivity Rule of Perforated Well of a Fractured Oil Reservoir

The perforated well productivity of a natural fracture porosity oil reservoir is fully dependent on the hydraulic communication between perforation and near-wellbore fracture system; that is, the fracture porosity oil reservoir productivity after perforated completion is mainly controlled by the type and distribution density of natural fractures, the penetration depth, diameter and phase of perforation, and so on. In order to understand the relationship between the perforating parameters and the oil well productivity of a fracture porosity oil reservoir, the fracture characteristics of the oil reservoir should be understood, the corresponding physical and mathematical flow models should be established, and the effect of various perforating parameters on the perforated well productivity of a fracture porosity oil reservoir should be studied by using finite element analysis, thus providing theoretical grounds for perforating design.

The fracture network is macroscopically in a disordered state, whereas the fracture system is microscopically ordered. The fracture system consists of the fractures that are parallel to each other in a given range. Such a fracture system in a relatively small near-wellbore area can be considered as a relatively regular system, and the fracture characteristic parameters can be truly obtained by using the data of drilling, coring,

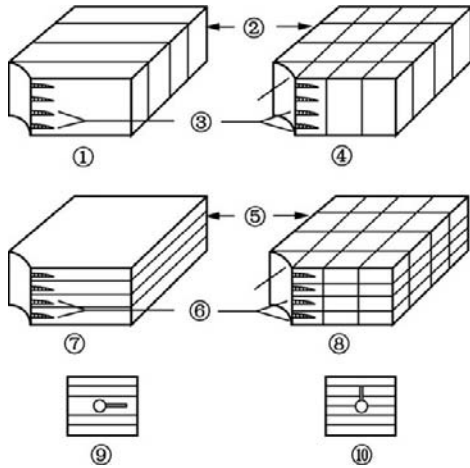


**FIGURE 6-32** Fracture-matrix type [2]. 1, one group of vertical fractures; 2 and 5, fractures; 3 and 6, perforations; 4, two groups of orthogonal vertical fractures; 7, one group of horizontal fractures; 8, orthogonal fractures; 9, perforation parallel to fracture face; 10, perforation perpendicular to fracture face.

and logging. Thus, the fracture system in the vicinity of the wellbore can be divided into four subsystems, that is, one group of vertical fractures, two groups of orthogonal vertical fractures, one group of horizontal fractures, and three groups of orthogonal fractures (Figure 6-32).

The relation between oil well productivity and perforating parameters under the four aforementioned conditions has been studied by S. M. Tariq [2] and the Southwest Petroleum Institute. The characteristic parameters that the model considers include: (1) parameters of formation fracture system, which include type of fracture, fracture density, fracture and matrix permeabilities and porosities; (2) perforating parameters including perforation pattern, phase, perforation penetration depth, perforation density, and perforation diameter; and (3) damage characteristic parameters including the depth and degree of drilling damage and the thickness and degree of the perforating damage zone. These different characteristic parameters make the physical model have different geometric characteristics and will generate different degrees of effect

on fluid flow. The circumferential pressure distribution under the conditions of one group of vertical fractures, 90° phase, and spiral perforation pattern is shown in Figure 6-33. The low-lying place or the place in which the isobars are closer is just the place where the perforation lies.

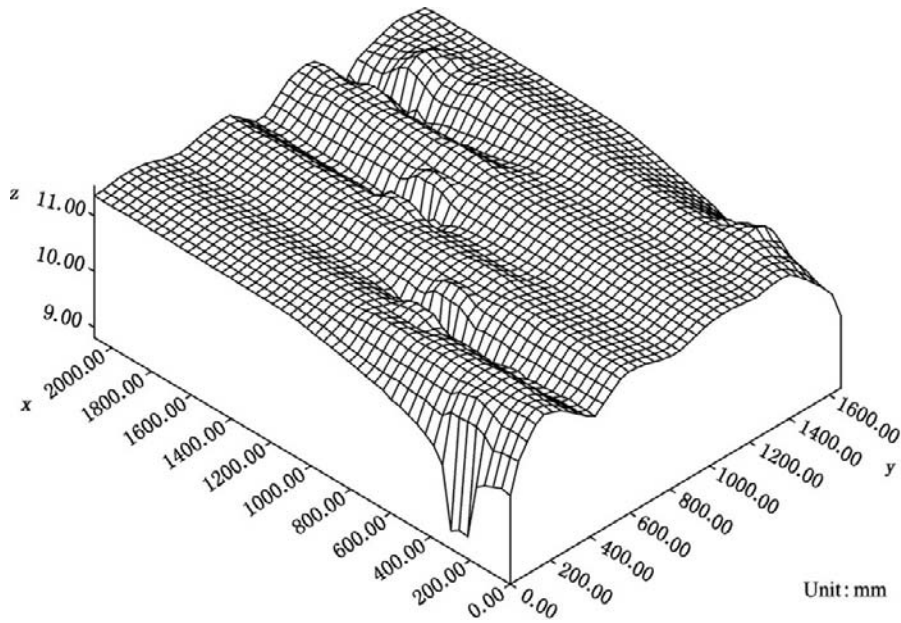
**Effects of Various Types of Fracture Network on Oil Well Productivity.** The different types of physical models of fracture networks have different contributions of the same perforating parameter to oil well productivity. The effects of fracture parameters (such as fracture width and fracture density) of each type of fracture on oil well productivity ratio are also different (Table 6-5).

Table 6-5 shows that under the same perforating parameters, an oil well with two groups of vertical fractures or three groups of orthogonal fractures has a higher productivity ratio than the two others, and an oil well with three groups of orthogonal fractures has the highest flow efficiency. With one group of vertical fractures, the perforation penetration depth is the most important factor and affects oil well productivity in combination with fracture density. With two groups of vertical fractures, the perforation penetration depth and fracture density are still the most sensitive factors, and the effect of perforation density comes second. With one group of horizontal fractures, the combined action of perforation density and fracture density may greatly affect oil well productivity. With three groups of orthogonal fractures, the combined action of perforation penetration depth and fracture density may have an obvious effect, and the effect of perforation density comes second.

### Effects of Perforating Parameters on Oil Well Productivity of a Fractured Reservoir

#### 1. Network model of one group of vertical fractures

With one group of vertical fractures, the best possibility is that the direction of perforation is perpendicular to and penetrates through the fracture, while the worst is that the direction of perforation is parallel to the fracture strike (that is, the perforation cannot



**FIGURE 6-33** Circumferential pressure distribution under the conditions of one group of vertical fractures, 90° phase, and spiral perforation pattern [23].

**TABLE 6-5** Effects of Different Fracture Network Models on Oil Well Productivity Ratio

Type	Perforation Density (Shots/m)			Perforation Penetration Depth (mm)			Fracture Density (Fractures/m)		
	40	24	16	450	300	100	10	5	1
One group of vertical fractures	0.7945	0.7577	0.7364	0.7684	0.7438	0.5201	0.7807	0.7633	0.0723
Two groups of vertical fractures	1.0519	1.0300	1.0162	1.0418	0.9808	0.7789	1.1900	1.069	0.7880
One group of horizontal fractures	0.8918	0.8796	0.7667	0.8787	0.8492	0.6590	0.9350	0.8923	0.8012
Three groups of orthogonal fractures	1.2240	1.2053	1.1932	1.2003	1.1557	0.8182	1.4301	1.2601	0.8652

Note: The basic parameters of perforation density, penetration depth, and fracture density are, respectively, 24,400 and 4.

meet the fracture no matter how deep the penetration is).

If the direction of perforation is parallel to the fracture, the perforation cannot meet the fracture, thus causing perforated well productivity that is on the low side and mainly depends on the conductivity between matrix

and fracture. Figure 6-34 shows the relation between productivity ratio and perforation penetration depth under the condition of the same fracture density and perforation density. The oil well productivity ratio will increase with the increase of perforation penetration depth and then tends to remain constant

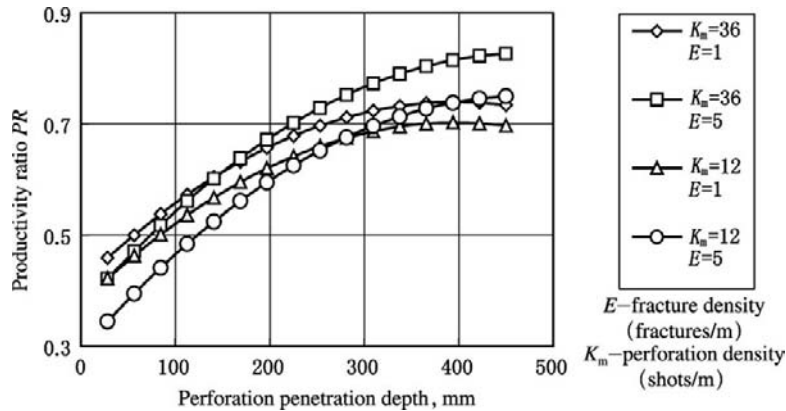


**FIGURE 6-34** Effect of perforation penetration depth on oil well productivity under the condition of one group of vertical fractures.

especially under the condition of lower fracture density  $E$ . And under the condition of smaller perforation penetration depth, the greater the fracture density, the greater the increase of oil well productivity ratio with the increase of perforation penetration depth. Therefore, if the perforation orientation is parallel to the fracture orientation, the oil well productivity ratio is generally low. And the perforation penetration depth has a great effect on oil well productivity ratio, while the perforation density and fracture density have a small effect.

If the direction of the perforation is perpendicular to the fracture, whether the perforation will meet the fracture and a high productivity ratio will be obtained will depend on the perforation penetration depth and fracture density.

## 2. Network model of two groups of vertical fractures

With two groups of vertical fractures, the relation between oil well productivity ratio and perforation phase is not obvious, and the oil well productivity ratio is mainly dependent on whether the perforation connects with the fracture or whether the perforation penetration depth is adaptable to the fracture density. Figure 6-35 shows that oil well productivity increases with the increase of perforation penetration depth; however, if

the fracture density is low and the perforation penetration depth is too small to penetrate through fracture, the oil well productivity ratio is low.

If penetrating through perforation can be achieved by the combination of perforation penetration depth with fracture density, the oil well productivity ratio will be greatly increased. Figure 6-35 shows that oil well productivity ratio increases with the increase of fracture density; however, the effect of perforation density is small, which is similar to that under the condition of one group of vertical fractures and perforation direction perpendicular to fracture direction.

## 3. Network model of one group of horizontal fractures

With one group of horizontal fractures, the oil well productivity ratio is mainly dependent on the perforation density and fracture density. The higher the perforation density and fracture density, the greater the probability of meeting of perforation with fracture. Figure 6-36 shows the curves of the relationship between oil well productivity ratio and perforation density and indicates that the oil well productivity ratio increases with the increase of perforation penetration depth under a given perforation density and fracture density; however, the increase of productivity ratio will greatly reduce with the increase of

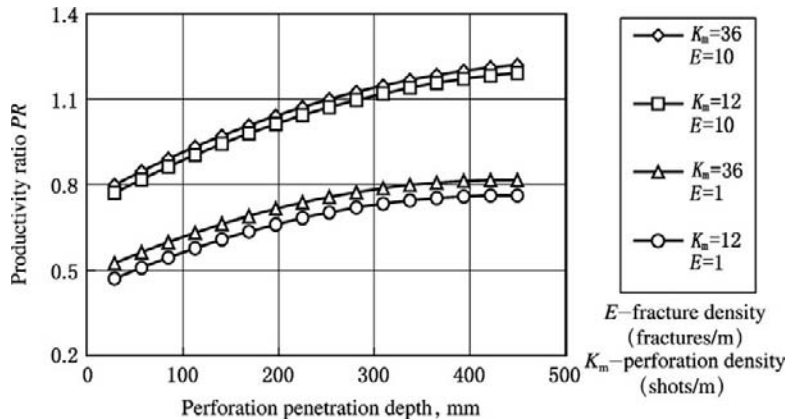


**FIGURE 6-35** Effect of perforation penetration depth on oil well productivity ratio under the condition of two groups of vertical fractures.

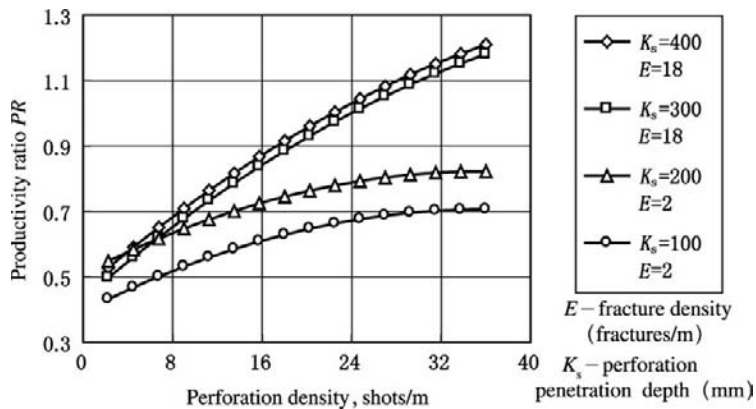


**FIGURE 6-36** Effects of perforation penetration depth and perforation density on productivity ratio under the condition of one group of horizontal fractures.

perforation penetration depth. It also shows that under different perforation densities and fracture densities, there are obvious oil well productivity ratio differences. Figure 6-37 shows that when the perforation penetration depth and fracture density are greater, the oil well productivity ratio will rapidly increase with the increase of perforation density and a higher productivity ratio can be achieved; however, when the perforation penetration depth and fracture density are smaller, the effect of increase of perforation density on oil well productivity ratio is not obvious. Therefore, under the condition of one group of horizontal fractures, the oil well

productivity ratio is mainly affected by perforation density and perforation penetration depth, and it is possible to achieve a higher productivity ratio under high perforation density and deep perforation penetration.

#### 4. Network model of three groups of orthogonal fractures

With three groups of orthogonal fractures, both the horizontal fractures and the vertical fractures have a higher conductivity due to the mutual connectivity of fractures; thus, the oil well will have a higher productivity ratio once the perforation connects with the fracture, and the perforation penetration depth will greatly affect the oil well productivity ratio.

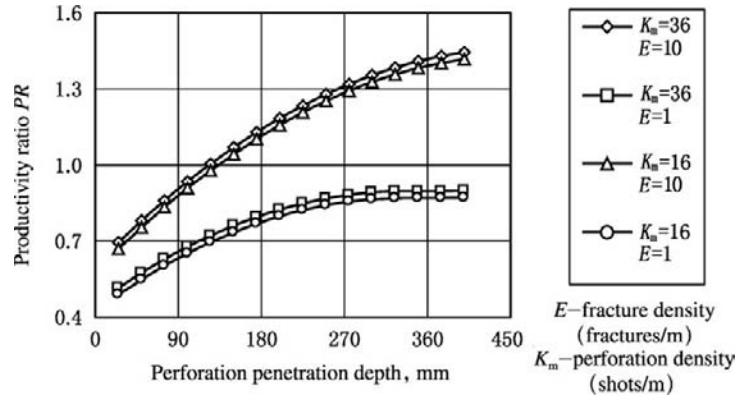


**FIGURE 6-37** Effect of perforation penetration depth on productivity ratio under the condition of one group of horizontal fractures.

Figure 6-38 shows the relation between oil well productivity ratio and perforation depth under different perforation densities and fracture densities. The oil well productivity ratio increases with the increase of perforation penetration depth. Under the condition of a higher fracture density, the oil well will have a very high productivity ratio, and the increase of oil well productivity ratio with the increase of perforation penetration depth is very obvious; however, under the condition of a lower perforation density, the increase of productivity ratio with the increase of perforation penetration depth is small and the productivity ratio is always lower than 1 no matter how dense

the perforations are because no fracture is penetrated through. Only when the perforation penetration is increased to a depth that is sufficient to penetrate through the fracture can the oil well productivity ratio be greatly increased. It is also reflected in Figure 6-38 that the productivity ratio is not sensitive to perforation density whether the fracture is penetrated through by perforation or not.

Figure 6-39 shows the curves of the relationship between oil well productivity ratio and fracture density and indicates that the oil well productivity ratio increases with the increase of fracture density, and the increase of productivity ratio will be greater when the perforation

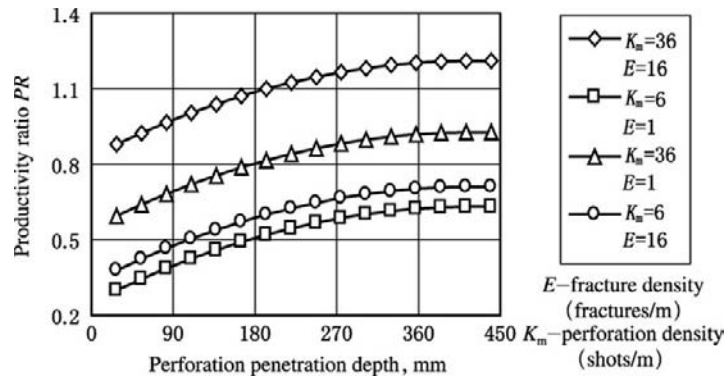


**FIGURE 6-38** Effects of perforation penetration depth and perforation density on productivity ratio under the condition of three groups of orthogonal fractures.

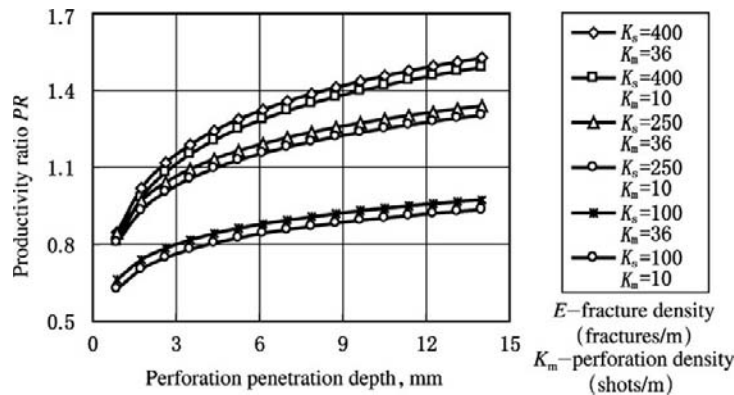


**FIGURE 6-39** Effect of fracture density on productivity ratio under the condition of three groups of orthogonal fractures.

penetration depth is increased; that under the condition of the same fracture density and perforation penetration depth, the higher the perforation density, the greater the oil well productivity ratio, but the difference is not great; and that under the condition of the same fracture density and perforation density, the greater the perforation penetration depth, the higher the productivity ratio, and the difference is greater. Therefore, under the condition of three groups of orthogonal fractures, perforation penetration depth is the most important factor, fracture density is the second, and perforation density is the third.

### Productivity Rule of a Perforated Horizontal Well

Horizontal well completion mainly includes four types: open hole completion, slotted liner completion, external liner (or casing) segregated packer completion, and casing cementing perforated completion. Because of innovations in completion tools, technical advances in horizontal wells, and the practical requirement of payzone control, the casing cementing perforated completion of a horizontal well has gradually become a main well completion method.

A horizontal well is different from a vertical well in that the disturbing effect of wellbore affects not only the near-wellbore area but the whole reservoir [7]. The selection of the degree

of opening and location and distribution of the opened section of perforating and the perforating parameters may affect not only the productivity but also the hydrodynamic condition of a horizontal well. The studies indicate that horizontal well productivity is related to reservoir productivity, the multiphase flow of horizontal wells, the interaction between reservoir and wellbore, and the selection of perforated completion parameters.

### Effects of Location and Degree of Opening by Perforating on Horizontal Well Productivity.

The combined reservoir inflow performance and horizontal wellbore multiphase flow model is used as the simulation method of optimizing the location and degree of opening, and the effect of wellbore pressure drop on horizontal well performance is considered. The effect of perforating parameters of a specific opened section is described using the perforating skin of a local opened section. The effect of location and degree of opening on well productivity ratio is analyzed under the condition of constant perforating parameters.

#### 1. Location of horizontal well perforating

Figure 6-40 shows the simulation result of the effect of perforating section location on well performance under the conditions of horizontal section length of 600 m (only one section 100 m opened) and reservoir permeability of  $300 \times 10^{-3} \mu\text{m}^2$ . The metric labeled

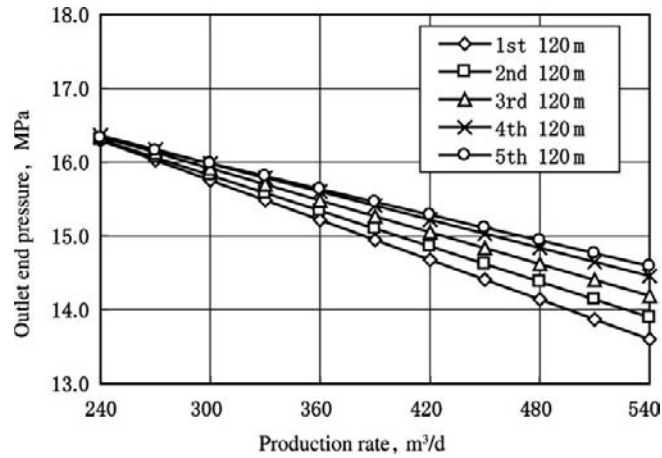


**FIGURE 6-40** Effect of opened section location on horizontal well performance.

“1st” in Figure 6-40 shows that the opened section is located at the toe of the horizontal section, while the 5th shows that the opened section is located at the heel of the horizontal section. It can be indicated that the location of the perforating section may obviously affect the well performance under other given parameters. This effect will become more obvious with the decrease of casing diameter of the horizontal section of a horizontal well. The greater the distance between the opened section of

perforating and the toe of the horizontal well, the better the result. The reason is that the flow in the reservoir is disturbed by the multiphase flow energy loss in the horizontal wellbore.

## 2. Degree of opening of horizontal well perforating

The degree of opening of horizontal well perforating is shown by using the ratio of actual opened length of horizontal section to total horizontal section length. Figures 6-41 and 6-42 show the effects of the degree of opening by perforating on well performance under different

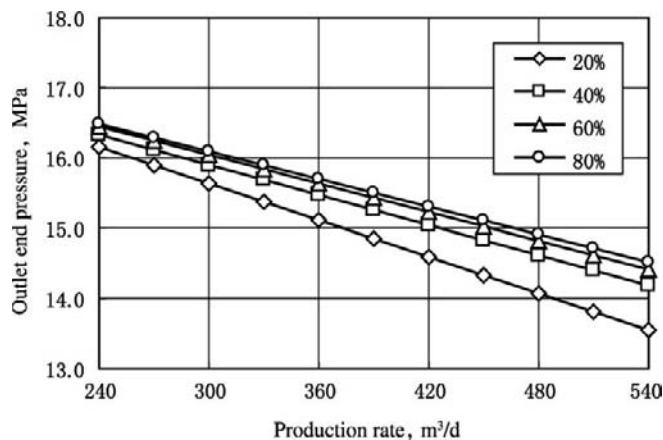


**FIGURE 6-41** Effect of degree of opening by perforating on horizontal well performance (300 m).

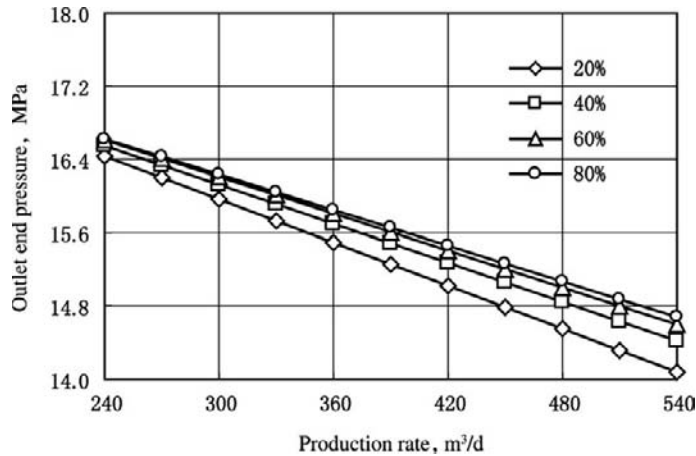


**FIGURE 6-42** Effect of degree of opening by perforating on horizontal well performance (600 m).

simulated wellbore radiuses and horizontal section lengths. The studies indicate a great effect of the degree of opening on oil well productivity under other given parameters. No matter how much the horizontal section length and casing diameter are, the higher the degree of opening, the better the horizontal well performance; however, with the increase of the degree of opening, the increase of horizontal well productivity is obviously reduced. Economically, full opening is inappropriate for a horizontal section and the degree of opening should be optimized on the basis of actual well conditions. It should be noted that these conclusions are only applicable to isotropic reservoirs. If the reservoir permeability obviously changes along the horizontal wellbore, an evaluation is required on the basis of actual well conditions.

The analysis of sensitivity to horizontal section length indicates that oil and gas well productivity cannot be unrestrictedly increased with the increase of horizontal section length, and optimum length exists. The effect of reservoir permeability on horizontal well performance is also obvious.

**Effects of Perforating Parameters on Horizontal Well Productivity of a Sandstone Oil Reservoir.** In order to study the effects of perforation density, phase, perforation penetration

depth, perforating compaction, and drilling damage on the horizontal well productivity of a sandstone oil reservoir, the following are given: horizontal section length = 300 m, reservoir thickness = 20 m, distance between horizontal well and bottom boundary = 7 m, horizontal permeability =  $6 \mu\text{m}^2$ , vertical permeability =  $1.5 \mu\text{m}^2$ , oil viscosity =  $1.5 \text{ MPa} \cdot \text{s}$ , and reservoir pressure = 16 MPa. Productivity and productivity ratio are calculated on the basis of the production rate under pseudoradial flow in reservoir.

#### 1. Perforation density

Figure 6-43 shows that productivity changes with the change of perforation density under the condition of a perforation penetration depth approximate to zero. When perforation density increases to a certain value, the increase of perforation density may not lead to an obvious increase of horizontal well productivity [8]. When perforation density increases to a higher value, the perforated well productivity will reach the open hole productivity. It should especially be noted that under a relatively low perforation density, the productivity ratio of a horizontal well is much higher than that of a vertical well; that is, the perforated completion of a horizontal well can still obtain the desired productivity ratio under a lower perforation density.

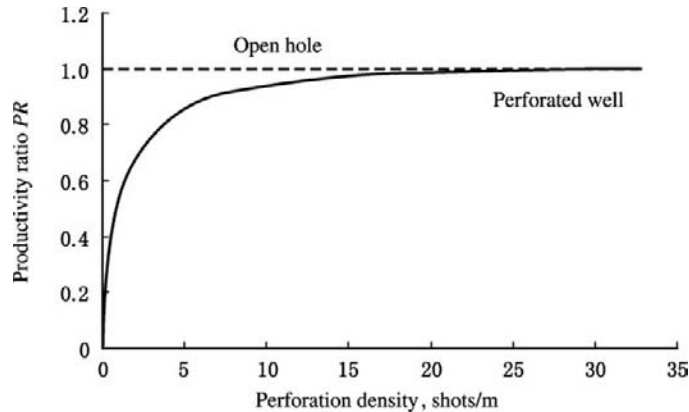


**FIGURE 6-43** Relation between horizontal well productivity ratio and perforation density.

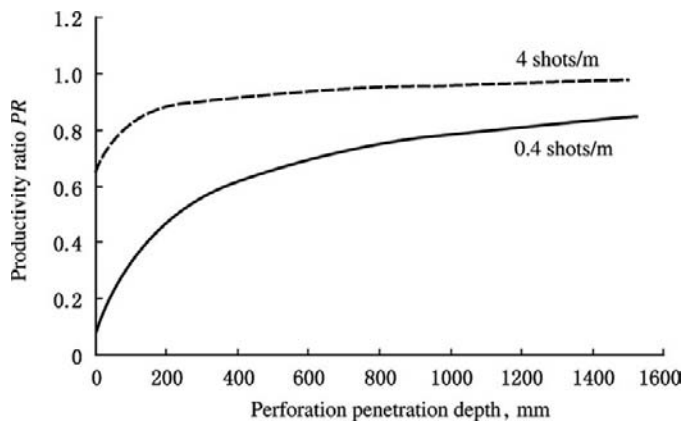
## 2. Perforation penetration depth

Figure 6-44 shows the effects of perforation penetration depth and perforation density on horizontal well productivity ratio [8]. The productivity ratio increases with the increase of perforation penetration depth. When perforation density is low, the effect of perforation penetration depth on the productivity ratio is very obvious. When perforation density is higher, the productivity ratio also increases with the increase of perforation penetration depth; however, when perforation penetration depth is increased to a certain value ( $>200$  mm), the increase of horizontal well productivity ratio is obviously

slowed. Therefore, the effect of perforation penetration depth on productivity ratio is more serious under a low perforation density.

## 3. Phase angle

Figure 6-45 shows the effect of phase angle on horizontal well productivity ratio under the condition of serious anisotropy ( $K_v/K_h = 0.01$ ) [8]. It indicates that the effect of phase angle on productivity ratio is obvious and the phase angle of  $180^\circ$  is most favorable, while the phase angles of  $90^\circ$  and  $45^\circ$  have a lower productivity ratio. This is different from that of the perforated completion of a straight well. The studies indicate that the effect of perforation density on productivity



**FIGURE 6-44** Relation between productivity ratio and perforation penetration depth.

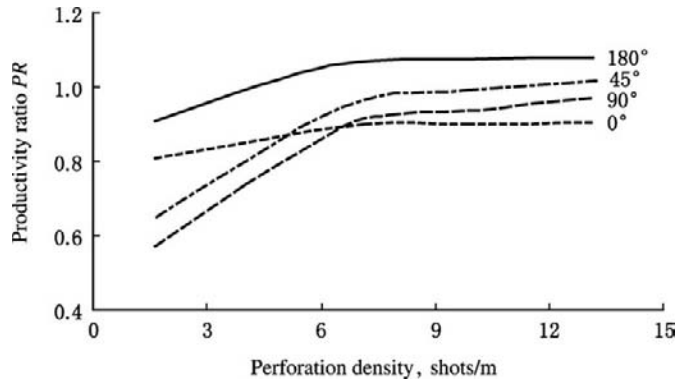


**FIGURE 6-45** Effects of phase angle and perforation density on productivity ratio.

ratio is more serious under the condition of serious anisotropy and smaller perforation penetration depth. The effect of phase angle on productivity ratio is much weaker under the condition of homogeneous reservoir.

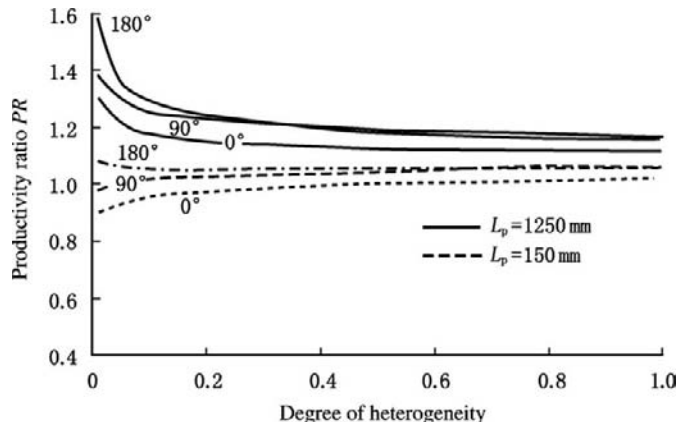
#### 4. Degree of heterogeneity

Figure 6-46 shows the effect of degree of heterogeneity ( $K_v/K_n$ ) on horizontal well productivity ratio [8]. It indicates that under the condition of great perforation penetration depth, the more serious the heterogeneity, the higher the productivity ratio; however, under the condition of small perforation penetration depth, the more serious the heterogeneity, the lower the productivity ratio. It also indicates that under the condition of serious heterogeneity, the effect of phase angle on

productivity ratio is obvious, while under the condition of lower degree of heterogeneity, the effect of phase angle is not obvious and can be neglected. Therefore, under the condition of serious heterogeneity adopting deep perforation penetration, high-medium perforation density and the vertical distribution of perforation with phase angle of  $180^\circ$  will favor enhancing horizontal well productivity.

#### Effects of Perforating Parameters on Horizontal Well Productivity of a Sandstone Gas Reservoir.

The flow rate distribution and pressure drop are mainly generated at the heel of the horizontal section due to gas expansion. For a gas well with a high permeability gas reservoir, the main pressure drop is also generated at



**FIGURE 6-46** Effect of reservoir heterogeneity on productivity ratio.

the heel. The gas expansion and acceleration are generated from the toe to the heel of the horizontal section. The change of momentum may obviously affect the pressure gradient. The effect of wellbore hydrodynamics on gas well productivity should be considered [8].

The following analysis is based on these parameters: perforation penetration depth = 300 mm, perforation diameter = 18 mm, perforation density = 2 shots/m, phase angle =  $180^\circ$ , degree of perforating compaction = 0.2, degree of drilling damage = 0.4, and damage radius = 150 mm.

### 1. Perforation penetration depth

Figure 6-47 shows the effect of perforation penetration depth on gas well productivity ratio. Gas well productivity ratio increases

with the increase of perforation penetration depth. In particular, productivity ratio obviously increases with the increase of perforation penetration depth before the damage zone is penetrated through.

### 2. Perforation density

Figure 6-48 shows the effect of perforation density on gas well productivity ratio. The gas well productivity ratio increases with the increase of perforation density. The desired productivity ratio can still be obtained under a lower perforation density, which is similar to that of a horizontal oil well and different from that of a straight gas well.

### 3. Non-Darcy effect

Figure 6-48 also indicates that the non-Darcy flow and formation damage may decrease the gas well productivity, which is particularly

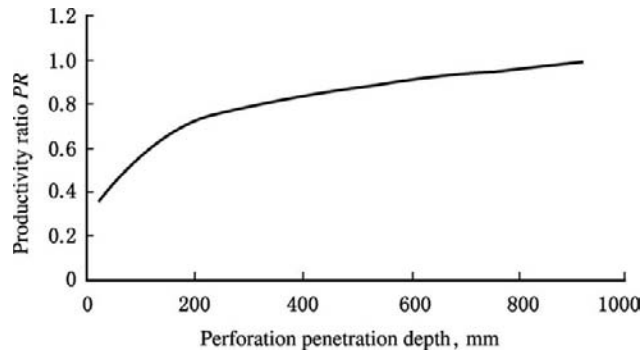


**FIGURE 6-47** Effect of perforation penetration depth on gas well productivity ratio.

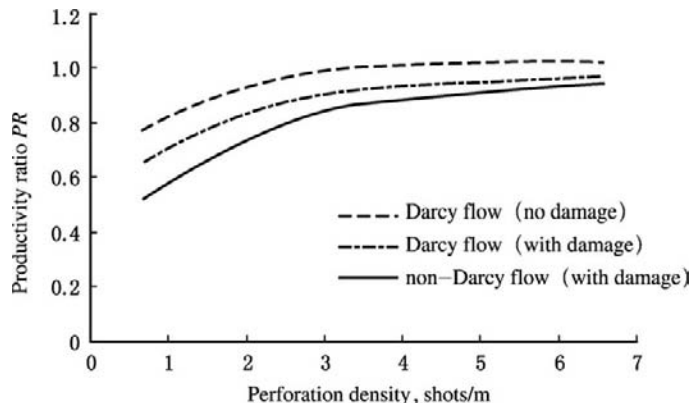


**FIGURE 6-48** Effect of perforation density on gas well productivity ratio.

obvious under the condition of short perforation length and low perforation density [8]. In order to obtain the predicted result, the effect of non-Darcy flow should be considered.

**Effect of Formation Damage on Horizontal Well Productivity.** Formation damage can be expressed by using skin factor. The effect of formation damage on horizontal well productivity ratio is different from the effect of formation damage on vertical well productivity ratio. Under the condition of the formation heterogeneity coefficient of 1, the oil well productivity ratio will decrease with the increase of skin factor whether the well is horizontal or vertical (Figure 6-49). Under the same skin factor, vertical well productivity ratio is lower than horizontal well

productivity ratio. It is more important that under the same skin factor the percentage reduction of horizontal well productivity ratio is much less than that of vertical well productivity ratio; that is, the effect of formation damage on horizontal well productivity ratio is smaller than that on vertical well productivity ratio. It should be particularly noticed that the absolute loss of horizontal well production rate is much greater than that of vertical well production rate because the production rate value of a horizontal well is greater than that of a vertical well.

#### 1. Perforating compaction damage

Figure 6-50 shows the effect of perforating damage on productivity ratio. It is indicated that if  $K_c/K > 0.2$ , the effect of perforating

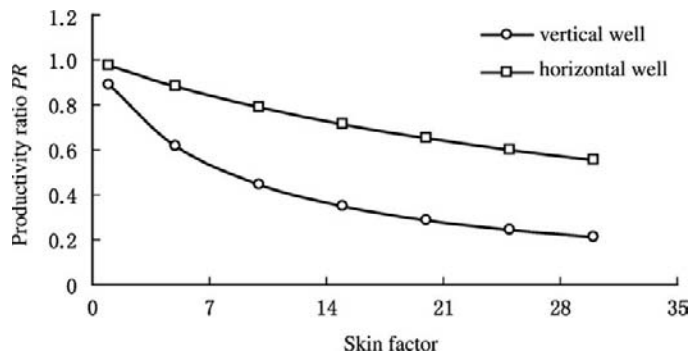


**FIGURE 6-49** Contrast between the effects of formation damage on vertical-well and horizontal-well productivity ratios.

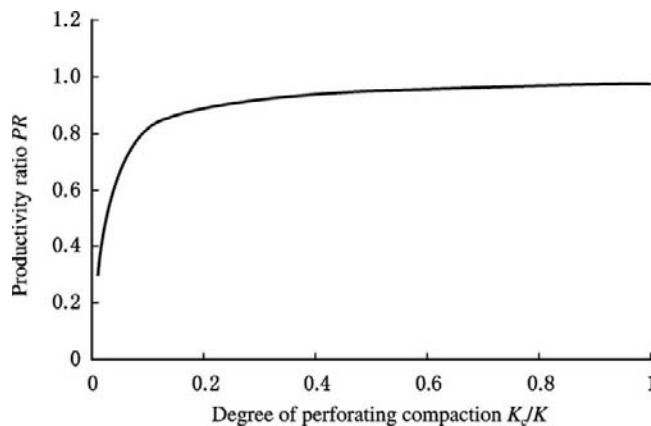


**FIGURE 6-50** Effect of degree of compaction on gas well productivity ratio.

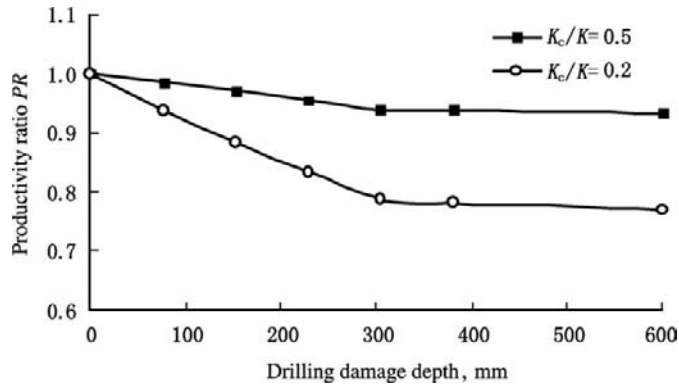


**FIGURE 6-51** Effect of drilling damage on horizontal well productivity ratio.

damage on productivity ratio is not serious. Therefore, the slight permeability reduction caused by perforating is acceptable in a horizontal well. Serious perforating damage can be avoided by using high-quality shaped charge, underbalanced perforating, and rational perforating fluid.

## 2. Drilling damage

Figure 6-51 shows the effect of drilling damage on productivity ratio. It is indicated that the effect of the degree of drilling damage is greater than the effect of damage zone depth. The more serious the drilling damage, the lower the productivity ratio. When damage depth is greater than perforation penetration depth, the decrease of productivity ratio becomes slower with the increase of damage depth. Therefore, it is important to control the drilling damage radius so that perforations can penetrate through the damage zone. This conclusion is the same as that for a vertical well.

## 6.3 PERFORATING DIFFERENTIAL PRESSURE DESIGN

Well completion design requires that the minimum pressure loss of completion interval and the highest production rate should be ensured under the conditions of both safety and economy. Well completion operation can be underbalanced perforating, overbalanced perforating,

and extreme overbalance perforating in accordance with the relation between wellbore pressure and reservoir pressure during perforating. Conventional overbalanced perforating has a very high risk and is rarely used at present due to the chip hold-down effect of perforating fluid during perforating. Both underbalanced perforating and extreme overbalance perforating can improve oil and gas well productivity and have been widely applied worldwide. The former has almost become a industrial standard, while the latter is a beneficial supplement to the former. In order to achieve the desired perforating results on the premise of ensuring oil and gas well safety, perforating differential pressure should be scientifically designed.

### Underbalanced Perforating and Extreme Overbalance Perforating

Underbalanced perforating means that bottom-hole pressure is lower than reservoir pressure during perforating. Underbalanced perforating is to use the high-velocity flowback generated by the underbalance pressure at the instant of perforating to wash perforations and migrate the perforation plugging matter caused by perforating compaction so that perforations with high cleanliness and low damage can be obtained. Therefore, the key to the underbalance pressure design lies in the underbalance pressure value. On the one hand, it is required to ensure

that the fine grains in the crushed and compacted zone around perforation are moved out to obtain clean perforations (the underbalance pressure meeting this requirement is known as minimum underbalance pressure). On the other hand, in order to prevent sand production, sloughing, casing collapse, packer failure, and other problems, the underbalance pressure value should not exceed a specific value, which is critical and is known as maximum underbalance pressure. The rational perforating underbalance pressure value should be between the minimum and maximum underbalance pressures.

Underbalanced perforating can truly enhance oil and gas well productivity effectively and has been widely applied. However, the effectiveness is greatly dependent on perforating technology, underbalance pressure design, and physical properties of the reservoir. In a low-permeability oil and gas reservoir that has not achieved optimized perforating, the underbalance pressure value selected may be on the low side, and the reservoir productivity may not act to the full extent. In a low-permeability oil and gas reservoir with serious damage, full cleaning of the perforations requires a higher underbalance pressure value, which sometimes cannot be achieved. In a reservoir with serious interlayer heterogeneity, the cleanliness of perforation is different if perforating is under the same underbalance pressure. For an underpressured reservoir, sometimes the ideal underbalance pressure value cannot be achieved even if the whole wellbore is emptied. For a weakly consolidated reservoir, underbalance pressure can meet the requirement of cleaning perforations; however, sand production may be caused. Thus it can be seen that although the flowability in the vicinity of the wellbore can be improved by underbalanced perforating under these conditions, the optimum value cannot be achieved, and a more effective method is required.

The aforementioned problems can be avoided by using the extreme overbalance perforating (EOP) method [12]. Firing and perforating are achieved at this instant under a bottomhole pressure higher than formation breakdown pressure.

After perforating, the perforating fluid pad rapidly impacts the perforations on the instant under driving by high-pressure compressed gas expansion energy and rapidly cracks the perforations due to the incompressibility of liquid. The liquid or proppant will erode the formation at the rate of  $16 \text{ m}^3/\text{min}$  and form stable flow channels. In general, when gas reaches the perforations, the fracture propagation will stop at once because the gas will rapidly filtrate and enter the formation.

The wellbore pressure during the EOP operation should be high enough. It should exceed the minimum principal stress of local rock and ensure penetrating through the impermeable debris held in perforation. These debris may often affect operating effectiveness in conventional operations. The studies indicate that the extreme overbalance pressure gradient should be sufficiently high in order to move out these debris and is generally greater than  $30 \text{ kPa/m}$ .

For wells that adopt EOP operation, the decrease of flow conductivity of perforation due to perforation compaction damage is slight because the debris are crushed before hardening and the powder generated is carried to the distal end of the crack. The decrease of permeability due to rock breaking around the perforations is trivial by comparison with the high permeability of fracture generated. When the gas passes the perforation, its velocity approaches acoustic velocity; thus the erosion and friction action on perforation and fracture face may also be generated and permeability is increased.

The effectiveness of extreme overbalance perforating technology is closely related to operating wellhead pressure, liquid nitrogen volume, perforating fluid pad volume, and physical properties of the reservoir, and so on, in which the operating wellhead pressure (or perforating differential pressure) is of great importance. The corresponding bottomhole pressure should be higher than the formation breakdown pressure in the vicinity of the wellbore. Therefore, the accurate prediction of this formation breakdown pressure also directly affects the rational selection of operational parameters.

## Empirical Relation of W. T. Bell

The rule of thumb given by W. T. Bell on the basis of the related data of about 1000 perforated wells shows the corresponding required underbalance pressures determined in accordance with reservoir permeability and type of reservoir (Table 6-6). This method only gives a range, must be used in combination with experience, and can only be used for determining the minimum underbalance pressure.

**Empirical Relation of American Core Company.** The empirical formula for selecting perforating underbalance pressure, which is obtained on the basis of the corrected data of 45 wells, is shown in Equation (6-1).

$$(6-1) \quad \ln \Delta p_{\min} = 5.471 - 0.3688 \ln K$$

where:  $\Delta p_{\min}$  = minimum underbalance pressure of oil well perforating,  $10^{-1}$  MPa;  $K$  = oil reservoir permeability,  $10^{-3} \mu\text{m}^2$ .

**Calculation Method of Conoco.** The method for designing underbalance pressure, which is based on the minimum underbalance pressure formula of G. E. King [13] and the maximum underbalance pressure formula of Colle, was obtained by H. R. Crawford of Conoco in 1989. The empirical formula of the minimum underbalance pressure was obtained by King on the basis of the experience of 90 wells. They indicated that if the increase of productivity is not obvious (<10%) after sandstone oil reservoir perforating and acidizing, the perforations

are clean and the corresponding underbalance pressure is sufficient. Wells with problems of acidizing itself were not included. This empirical formula is shown in Equations (6-2), (6-3), and (6-4).

$$(6-2) \quad \ln \Delta p_{\min(\text{oil})} = 17.24/K^{0.3}$$

$$(6-3) \quad \ln \Delta p_{\min(\text{gas})} = 17.24/K(K < 10^{-3} \mu\text{m}^2)$$

$$(6-4) \quad \ln \Delta p_{\min(\text{gas})} = 17.24/K^{0.18}(K \geq 10^{-3} \mu\text{m}^2)$$

where:  $\Delta p_{\min(\text{oil})}$  = minimum underbalance pressure for oil reservoir, MPa;  $\Delta p_{\min(\text{gas})}$  = minimum underbalance pressure for gas reservoir, MPa;  $K$  = reservoir permeability,  $10^{-3} \mu\text{m}^2$ .

The relation between  $\Delta p_{\max}$  and the interval transit time of adjacent mudstone and the relation between  $\Delta p_{\max}$  and the volume density of adjacent mudstone, which have been established by Colle on the basis of his experience in Venezuela and the Gulf, are as shown in Equations (6-5) through (6-10).

$$(6-5) \quad \Delta p_{\max(\text{oil})} = 24.132 - 0.0399 \Delta T_{\text{as}} (\Delta T_{\text{as}} \geq 300 \mu\text{s}/\text{m})$$

$$(6-6) \quad \Delta p_{\max(\text{gas})} = 33.059 - 0.0524 \Delta T_{\text{as}} (\Delta T_{\text{as}} \geq 300 \mu\text{s}/\text{m})$$

$$(6-7) \quad \Delta p_{\max} = \Delta p_{\text{tub, max}} (\Delta T_{\text{as}} < 300 \mu\text{s}/\text{m})$$

$$(6-8) \quad \Delta p_{\max(\text{oil})} = 16.13 \rho_{\text{as}} - 27.58 (\rho_{\text{as}} \leq 2.4 \text{ g}/\text{cm}^3)$$

$$(6-9) \quad \Delta p_{\max(\text{gas})} = 20 \rho_{\text{as}} - 32.4 (\rho_{\text{as}} \leq 2.4 \text{ g}/\text{cm}^3)$$

$$(6-10) \quad \Delta p_{\max} = \Delta p_{\text{tub, max}} (\rho_{\text{as}} > 2.4 \text{ g}/\text{cm}^3)$$

where:  $\Delta p_{\max}$  = maximum underbalance pressure, MPa;  $\Delta p_{\text{tub, max}}$  = maximum safe underbalance

TABLE 6-6

**W. T. Bell's Rule of Thumb Used for Designing Perforating Underbalance Pressure**

Permeability ( $10^{-3} \mu\text{m}^2$ )	Range of Underbalance Pressure $\Delta p$ (MPa)	
	Oil Reservoir	Gas Reservoir
$K > 100$	1.4~3.5	6.9~13.8
$10 < K \leq 100$	6.9~13.8	13.8~34.5
$K \leq 10$	>13.8	>34.5

pressure of downhole string or cement sheath, MPa;  $\Delta T_{as}$  = interval transit time of adjacent mudstone,  $\mu\text{s}/\text{m}$ ;  $\rho_{as}$  = volume density of adjacent mudstone,  $\text{g}/\text{cm}^3$ ; “oil” and “gas” in formulae mean oil reservoir and gas reservoir, respectively.

**Behrmann Method.** The method of designing the optimum underbalance pressure under the condition of zero compaction skin factor, which was obtained by Behrmann [15] of Schlumberger in 1990s on the basis of experimental data of CT scanning, thin section analysis, mercury intrusion method, and core flow experiment, is shown in Equations (6-11) and (6-12).

(6-11)

$$\text{For } K < 100 \times 10^{-3} \mu\text{m}^2 \Delta p_{\min} = 1.6359 \Phi d_p^{0.3} / K^{0.3333}$$

(6-12)

$$\text{For } K > 100 \times 10^{-3} \mu\text{m}^2 \Delta p = 3.8666 \Phi d_p^{0.3} / K^{0.5}$$

where:  $d_p$  = perforation diameter, mm;  $K$  = reservoir permeability,  $10^{-3} \mu\text{m}^2$ ;  $\Phi$  = porosity, %;  $\Delta p_{\min}$  = minimum underbalance pressure under zero skin factor, MPa.

This method has not provided the maximum underbalance pressure.

### Theoretical Method of Designing Minimum Underbalance Pressure to Ensure Cleanliness of Perforation

The aforementioned methods are simple and convenient; however, only permeability and interval transit time are used for determining the minimum and maximum underbalance pressures. In addition, these methods are only regional, empirical, and statistical and lack theoretical grounds; thus, they may not necessarily be suitable for any oil and gas reservoir. The new methods are described in the following sections.

**Tariq Method for Calculating Minimum Underbalance Pressure.** When the flow in perforation is in the non-Darcy flow state, the drag force for cleaning the plugging matter in perforation is directly proportional to the square of flow velocity, and the perforation compaction zone damage is easy to remove. Thus the finite-element program of unsteady flow under the action of

underbalance pressure after perforating is established. The flow in the model follows the Forchheimer non-Darcy flow rule. The calculation indicates that the pressure and flow velocity are related to location, time, underbalance pressure, perforation size, degree of compaction, reservoir permeability, fluid viscosity, and so on. S. M. Tariq's simulation calculation [14] indicates that when the dimensionless time ( $t_D = \frac{k_t}{\Phi \mu c_t r_{cz}^2}$ ,  $r_{cz}$  = compaction zone radius) is up to 0.1, the effect of underbalance pressure will reach or go beyond the outer boundary of compaction zone. The higher the underbalance pressure and velocity, the more obvious the non-Darcy effect. The Reynolds number  $Re$  at compaction zone boundary at  $t_D = 0.1$  under different compaction zone permeabilities is calculated under different underbalance pressure  $\Delta p$  values, as shown in Equation (6-13).

(6-13)

$$Re = \frac{\beta K_p V_c}{\mu}$$

where:  $\beta$  = non-Darcy turbulence coefficient;  $K$  = reservoir permeability;  $\rho$  = fluid density;  $V_c$  = velocity at outer boundary of compaction zone at  $t_D = 0.1$ ;  $\mu$  = fluid viscosity.

Figure 6-52 shows the relation between permeability, underbalance pressure  $\Delta p$  and  $Re$  under oil viscosity  $\mu = 1 \text{ MPa} \cdot \text{s}$ .

In order to obtain the critical Reynolds number necessary for cleaning perforation, the charts based on G. E. King's statistical data have been drawn by Tariq on the basis of the curves of the relationship between Reynolds number  $Re$ , underbalance pressure  $\Delta p$ , and permeability  $K$ . For an oil well, it has been found that under  $Re = 0.05$ , the relation between  $\Delta p$  and  $K$  is just on the minimum underbalance pressure curve, thus the critical Reynolds number  $Re_c = 0.05$ . For a gas well, the critical Reynolds number is 0.1.

In practical calculation, fluid parameters, reservoir parameters, and perforating and damage parameters are required to be input when the numerical simulation method is used. The values of underbalance pressure  $\Delta p$  repeatedly

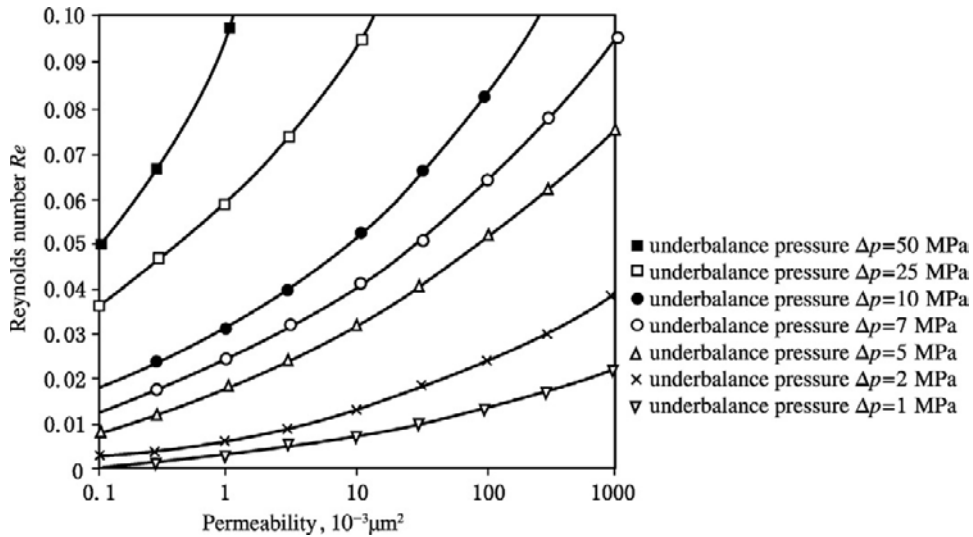


**FIGURE 6-52** Relation between permeability, underbalance pressure, and Reynolds number  $Re$  at compaction zone boundary.

supposed, and the Reynolds number values on the outer boundary of the compaction zone, are calculated under  $t_D = 0.1$ . When the  $\Delta p$  reaches  $Re_c$ , the  $\Delta p$  value supposed is just the minimum underbalance pressure.

This method is based on field data. When the practical physical properties of fluid (such as viscosity  $\mu$ ) and reservoir pressure  $p_r$  are greatly different from the average well values counted by King, error or mistake may result. King’s critical Reynolds number  $Re_c = 0.05$  for oil wells is appropriate to the  $\mu_o$  value in the range 0.7 to 1.2 MPa · s. The  $Re_c$  for gas well changes with permeability. Nevertheless, Tariq’s pioneering work of calculating the minimum underbalance pressure is still of great significance.

**Minimum Underbalance Pressure Formula for Oil Well Perforating.** Tariq considers that the effect of underbalance pressure has exceeded the outer boundary of the compact zone at  $t_D = 0.1$ ; that is, it can be supposed that at this time, the pressure at compaction zone radius is  $p_r$  while the pressure on perforation wall is  $p_{wf}$ . If pressure  $\Delta p$  is sufficient to cause a non-Darcy flow and the Reynolds number at  $r_c$  reaches the critical value  $Re_c$ , this underbalance pressure is just the minimum underbalance pressure  $\Delta p_{min}$ .

The following formula used for calculating  $\Delta p_{min(oil)}$  was obtained by Tariq by using Forchheimer’s binominal and integrating from  $r_p$  to  $r_c$ , as shown in Equation (6-14).

$$(6-14) \quad \Delta p_{min(oil)} = \frac{130.82 \mu_o^2 Re_c r_{cz}}{K_{cz}^{0.4} \rho_o} \left[ \ln \frac{r_{cz}}{r_p} + Re_c r_{cz} \left( \frac{1}{r_p} + \frac{1}{r_{cz}} \right) \right]$$

where: crude oil viscosity, MPa · s;  $Re_c$  = critical Reynolds number necessary for cleaning perforation, taken to be 0.05;  $r_{cz}$  = compaction zone radius, cm;  $r_p$  = perforation radius, cm;  $\rho_o$  = oil density, g/cm<sup>3</sup>;  $K_{cz}$  = compaction zone permeability,  $10^{-3} \mu m^2$ .

The  $Re_c = 0.05$  basically represents the actual condition under a low viscosity because it is obtained by matching King’s field data under  $\mu_o = 0.7-1.2$  MPa · s. For instance, in accordance with Equation (6-14), under  $\mu_o = 2$  MPa · s the underbalance pressure  $\Delta p_{min(oil)}$  will be 4 times the underbalance pressure under  $\mu_o = 1$  MPa · s, while under  $\mu_o = 8$  MPa · s the underbalance pressure will be 64 times the underbalance pressure under  $\mu_o = 1$  MPa · s. This is unreasonable. Therefore, it is recommended that when Tariq’s formula is used,  $\mu_o$  is taken as 1.2 MPa · s if  $\mu_o \gg 1.2$  MPa · s.

It can be seen that the minimum underbalance pressure of oil well perforating is also related to physical properties, perforation size, compaction radius, and degree of compaction damage in addition to reservoir permeability.

**Minimum Underbalance Pressure Formula for Gas Well Perforating by Southwest Petroleum University.** A formula of calculating the gas well  $\Delta p_{\min(\text{gas})}$  has been derived by Tariq in accordance with a formula similar to that for an oil well. However, the calculation indicates that the formula has a different result from that of the curve and cannot be used. The critical Reynolds number of the minimum underbalance pressure for gas well perforating is too small and is a constant, which is incorrect. King's minimum underbalance pressure has been matched by using the typical data, which include: mean reservoir pressure  $p_r = 20$  MPa, gas viscosity  $\mu_g = 0.03$  MPa  $\cdot$  s, mean reservoir temperature  $T_r = 373$  K, gas deviation factor  $Z = 1$ ,  $r_{cz} = 1.78$  cm,  $r_p = 0.51$  cm, and relative gas density  $\gamma_g = 0.6$ . In accordance with Forchheimer's binominal and gas state equation, the following formula of calculating the minimum underbalance pressure for gas well is finally derived, as shown in Equations (6-15) and (6-16)

(6-15)

$$p_r^2 - p_{wf}^2 = 75.088 \frac{\mu_g^2 T_r Z r_{cz}}{\gamma_g CZC^{0.8}} \cdot \frac{Re_{cg}}{K_z^{0.4}} \left[ \ln \frac{r_{cz}}{r_p} + Re_{cg} r_{cz} \left( \frac{1}{r_p} + \frac{1}{r_{cz}} \right) \right]$$

(6-16)

$$Re_{cg} = (0.061 p_r K_r^{0.4} - 0.571)^{0.5} - 0.251$$

where:  $p_r$  = mean reservoir pressure, MPa;  $T_r$  = mean reservoir temperature, K;  $p_{wf}$  = bottomhole pressure during perforating, MPa;  $K_r$  = perforation permeability,  $10^{-3} \mu\text{m}^2$ ;  $\mu_g$  = gas viscosity under mean pressure  $p_r$  and temperature  $T_r$ , MPa  $\cdot$  s;  $Z$  = gas deviation factor under mean pressure  $p_r$  and temperature  $T_r$ ;  $\gamma_g$  = relative gas density;  $CZC$  = degree of compaction damage ( $K_{cz}/K$ ), decimal;  $r_{cz}$  = compaction zone radius, cm;  $r_p$  = perforation radius, cm;  $Re_{cg}$  = critical Reynolds number of minimum underbalance pressure for gas well perforating.

If  $p_r K_r^{0.05} \leq 15$  or the calculated  $p_{wf} < 0$ , it is indicated that the formation energy is insufficient to ensure obtaining the minimum underbalance pressure; thus  $\Delta p_{\min} = p_r$  can be taken.

Equation (6-15) can be used for calculating using programming. Preliminary  $\mu_g$  and  $Z$  values are supposed and  $P_{wf}$  and mean formation pressure  $P_r$  are calculated by using Equation (6-15) (for simplicity, the arithmetic average can be taken). The  $\mu_g$  and  $Z$  values are corrected in accordance with the related formulae and a new  $p_{wf}$  value is calculated. After repeated iterative computation, an accurate  $p_{wf}$  value is obtained; thus the minimum underbalance pressure is shown in Equation (6-17).

(6-17)

$$\Delta p_{\min(\text{gas})} = p_r - p_{wf}$$

### Theoretical Method of Designing Maximum Underbalance Pressure for Preventing Sand Production

In accordance with elastoplasticity mechanics, sand production means that the stability of structure is lost. At the instant of underbalanced perforating, the high-velocity fluid generated by underbalance pressure acts immediately on perforation and neighboring rock, thus causing a rapid change of stress in the vicinity of perforation. Under the action of stress, an elastic deformation is first generated, and then a plastic deformation is subsequently generated. If the stress is sufficient for generating a perforation-neighboring rock deformation that exceeds the critical plastic deformation value, perforation structure failure will be generated, thus leading to a large amount of sand production. The studies indicate that by comparison with the Darcy flow, the non-Darcy flow will greatly increase the instability of perforation; that is, the principle of elastoplasticity mechanics can be applied and the stability of perforation can be appraised by using the equivalent plastic strain. Therefore, pore pressure distribution and perforation stress distribution can be calculated, and perforation stability can be predicted using both the non-Darcy flow

model and the stress strain model in order to determine the maximum allowable underbalance pressure [20].

**Mohr-Coulomb Yield Criteria.** After the oil and gas well is perforated, the perforations are in a complicated three-dimensional stress state. In order to simplify the model, single perforation is taken. Supposing that perforation-neighboring rock has good plasticity, Equation (6-18) can be obtained in accordance with the Mohr-Coulomb yield criteria (the SI unit system is used):

(6-18)

$$f = \sigma_{\theta} - \sigma_r N^2 + (N^2 - 1)p - 2S_0 N = 0$$

$$N = \tan(\pi/4 + \phi/2)$$

where:  $\sigma_r$  = radial stress acting on perforation;  $\sigma_{\theta}$  = tangential stress acting on perforation;  $p$  = pore pressure;  $S_0$  = cohesion force of rock;  $\phi$  = angle of internal friction of rock, rad.

**Plasticity Zone Stress Model.** On the elasto-plastic boundary  $r_c$ , the Mohr-Coulomb yield criterion is also tenable. On the basis of mechanical stability and symmetry, it can be simplified as a plane-strain axi-symmetrical problem; that is, the perforation is considered as cylindrical perforation. The differential equation of force balance is shown in Equation (6-19).

(6-19)

$$r \frac{\partial \sigma_r}{\partial r} + \frac{\sigma_r - \sigma_{\theta}}{r} = 0$$

Substituting Equation (6-18) into Equation (6-19), in accordance with Hook's law of stress strain, the plasticity zone stress distribution is shown in Equations (6-20), (6-21), and (6-22).

(6-20)

$$\sigma_r = (1 - N^2)r^{N^2-1} \int_{r_p}^r pr^{-N^2} dr + \frac{2S_0 N}{1 - N^2} \left( \sigma_{ri} + \frac{2S_0 N}{N^2 - 1} \right) \left( \frac{r}{r_p} \right)^{N^2-1}$$

(6-21)

$$\sigma_{\theta} = N^2(1 - N^2)r^{N^2-1} \int_{r_p}^r pr^{-N^2} dr + \frac{2S_0 N}{1 - N^2} + N^2 \left( \sigma_{ri} + \frac{2S_0 N}{N^2 - 1} \right) \left( \frac{r}{r_p} \right)^{N^2-1} + (1 - N^2)p$$

(6-22)

$$\sigma_{\theta} = (1 - N^2)v r^{N^2-1} \int_{r_p}^r pr^{-N^2} dr + \frac{2S_0 N}{1 - N^2} + (N^2 + 1)v \left( \sigma_{ri} + \frac{2S_0 N}{N^2 - 1} \right) \left( \frac{r}{r_p} \right)^{N^2-1} + (1 - N^2)v p + (1 - 2v)\beta p$$

where:  $r_p$  = perforation radius;  $\sigma_{ri}$  = radial stress on inner wall of perforation;  $v$  = Poisson's ratio;  $\beta$  = formation rock compressibility.

**Elasticity Zone Stress Model.** In consideration of the effect of fluid pressure in porous media, the elastic deformation displacement equation of porous media is shown in Equation (6-23).

(6-23)

$$(\lambda + 2G) \frac{d}{dr} \left( \frac{du}{dr} + \frac{u}{r} \right) + \beta \frac{dp}{dr} = 0$$

where:  $\lambda$ ,  $G$  = Lamé's constants;  $u$  = deformation displacement;  $r$  = radius;  $\beta$  = formation rock compressibility.

In accordance with the relation between stress and strain, in combination with the following boundary condition, shown in Equation (6-24):

(6-24)

$$\sigma_r|_{r=r_p} = \sigma_{ri} \quad \sigma_r|_{r=r_o} = \sigma_{ro}$$

the elasticity zone stress distribution is shown in Equations (6-25), (6-26), and (6-27).

(6-25)

$$\sigma_r = \sigma_{rc} + (\sigma_{ro} - \sigma_{rc}) \frac{1 - (r_c/r)^2}{(r_c/r_o)^2} - \frac{1 - 2v}{1 - v} \frac{\beta}{r_c} \int_{r_c}^r p_r dr + \frac{1 - (r_c/r)^2}{(r_c/r_o)^2} \int_{r_c}^r p_r dr + 2\beta(p - p_c) - 2\beta(p_o - p_c) \frac{1 - (r_c/r)^2}{1 - (r_c/r_o)^2}$$

(6-26)

$$\sigma_{\theta} = \sigma_{rc} + (\sigma_{ro} - \sigma_{rc}) \frac{1 + (r_c/r)^2}{1 + (r_c/r_o)^2} + \frac{1 - 2v}{1 - v} \frac{\beta}{r^2} \int_{r_c}^r p_r dr + \frac{1 + (r_c/r)^2}{1 - (r_c/r_o)^2} \frac{1 - 2v}{1 - v} \times \frac{\beta}{r^2} \int_{r_c}^r p_r dr - 2\beta p_c - 2\beta(p_o - p_c) \frac{1 + (r_c/r)^2}{1 - (r_c/r_o)^2} + \frac{1 - v}{v} \beta p$$

(6-27)

$$\sigma_z = \nu(\sigma_r + \sigma_\theta) - (1 - 2\nu)\beta p$$

where:  $\sigma_{rc}$  = stress at radius of elastoplastic boundary;  $\sigma_{ro}$  = stress at radius of outer boundary of perforation;  $p_c$  = pressure at radius of elastoplastic boundary;  $p_o$  = pressure at radius of outer boundary of perforation.

The radius of elastoplastic boundary ( $r_c$ ) is determined by using Equations (6-18), (6-19), and (6-25).

**Critical Equivalent Plastic Strain.** In order to predict the perforation stability, the concept of equivalent plastic strain  $\epsilon_r^p$  is introduced. Its definition is shown in Equation (6-28).

(6-28)

$$\epsilon_{er}^p = \left(\frac{2}{3}\right)^{\frac{1}{2}} \left[ (\epsilon_{rr}^p)^2 + (\epsilon_{\theta r}^p)^2 \right]^{\frac{1}{2}}$$

The critical equivalent plastic strain is the maximum equivalent strain that can be borne to ensure perforation stability; that is, the perforation will be unstable if the equivalent plastic strain exceeds the critical value. The differential pressure corresponding to the differential plastic strain is just the maximum underbalance pressure of perforating. The critical equivalent plastic strain is defined as shown in Equation (6-29):

(6-29)

$$\epsilon_{ec}^p = B_0 + B_1[2S_0N(1 + \nu)]$$

In order to ensure the perforation stability, Equation (6-30) should be met:

(6-30)

$$\epsilon_e^p \leq \epsilon_{ec}^p$$

**Pressure Distribution around Perforation.** At the instant of underbalanced perforating, the differential pressure that is suddenly exerted makes the fluid flow velocity in the vicinity of perforation very high, and this flow field is in a non-Darcy unstable flow state in a short time. And the pressure wave propagates rapidly. Thus it can be assumed that the flow in the vicinity of perforation is non-Darcy pseudosteady flow. Under the condition of single perforation, the pressure distribution

can be obtained by using the Forchheimer equation, as shown in Equation (6-31).

(6-31)

$$p(r) - p_{wf} = \frac{184.2\mu Q}{KL_p} \ln\left(\frac{r}{r_p}\right) + \frac{3.393 \times 10^{-7} \beta \rho Q^2}{L_p} \left(\frac{1}{r_p} - \frac{1}{r}\right)$$

where:  $p(r)$  = pore pressure at radius  $r$ , MPa;  $\beta$  = turbulence coefficient of fluid, 1/cm;  $\rho$  = fluid density, g/cm<sup>3</sup>;  $\mu$  = fluid viscosity, MPa · s;  $L_p$  = perforation penetration depth, cm;  $Q$  = production rate, cm<sup>3</sup>/s;  $r_p$  = perforation radius, cm.

The parameters including  $r_p$ ,  $L_p$ , and  $K$ , and so on can be obtained by using software for perforating parameter optimization design. It should be pointed out that the  $L_p$  value should be corrected by the Berea target penetration depth of the perforating charge selected and the reservoir porosity. The pore pressure at any radius  $r$  can be obtained by using Equation (6-31).

### Procedure of Calculating Maximum Perforating Underbalance Pressure under No Sand Production

1. The critical equivalent plastic strain is obtained on the basis of the parameters of rock mechanics.
2. The pore pressure distribution  $p(r)$  is calculated using the flow equation. Bottomhole pressure is first assumed, and the pore pressure distribution is then obtained under the underbalance pressure assumed.
3. The equivalent plastic strain under this underbalance pressure assumed is calculated in accordance with the stress strain model. If the equivalent plastic strain is greater than the critical equivalent plastic strain, the underbalance pressure should be decreased. Otherwise the underbalance pressure should be increased.
4. If the given accuracy is met, it is indicated that the maximum perforating underbalance pressure corresponding to the critical equivalent plastic strain has been obtained. Otherwise, steps 2 and 3 are repeated.

5. Or after the equivalent plastic strains under different bottomhole pressures assumed are obtained, the diagram of the relationship between equivalent plastic strain and underbalance pressure is drawn. The maximum underbalance pressure value is obtained by using the intersection of the critical equivalent plastic strain and this curve.

## Rational Perforating Operation Pressure Difference Determination

**Underbalanced Perforating Operation Pressure Difference Design.** After the minimum underbalance pressure  $\Delta p_{\min}$  and the maximum underbalance pressure  $\Delta p_{\max}$  are designed as mentioned earlier, the operating underbalance pressure  $\Delta p_{\text{rec}}$  that should be adopted during the perforating operation should also be designed. After the various factors are comprehensively considered, the method of determining rational perforating underbalance pressure  $\Delta p_{\text{rec}}$  is formulated.

1. Constraint conditions of rational underbalance pressure

The aforementioned  $\Delta p_{\min}$  and  $\Delta p_{\max}$  have not considered the safety factor of downhole casing. Thus Equation (6-32) is required:

(6-32)

$$\Delta p_{\text{rec}} \leq 0.8 \Delta p_{\text{tub, max}}$$

where:  $\Delta p_{\text{tub, max}}$  = maximum safe underbalance pressure that can be borne by the downhole string, MPa.

For a low-pressure oil reservoir, sometimes the underbalance pressure required cannot be achieved even if the whole wellbore is evacuated. Thus Equation (6-33) is required:

(6-33)

$$\Delta p_{\text{rec}} \leq p_r$$

2. Method of selecting optimum underbalance pressure

- a. If  $\Delta p_{\max} \geq \Delta p_{\min}$  and there is no sand production history, then Equation (6-34) applies:

(6-34)

$$\Delta p_{\text{rec}} = 0.8 \Delta p_{\max} + 0.2 \Delta p_{\min}$$

If  $\Delta p_{\max} \geq \Delta p_{\min}$  and there is sand production history or water saturation  $S_w > 50\%$ , then Equation (6-35) applies:

(6-35)

$$\Delta p_{\text{rec}} = 0.2 \Delta p_{\max} + 0.8 \Delta p_{\min}$$

- b.  $\Delta p_{\max} < \Delta p_{\min}$ . This condition sometimes appears because the  $\Delta p_{\max}$  means the maximum allowable underbalance pressure for preventing sand production and may be able to be smaller than the minimum underbalance pressure  $\Delta p_{\min}$  necessary for ensuring perforation cleaning. It cannot be considered in the light of the symbols that the  $\Delta p_{\max}$  value is unquestionably greater than the  $\Delta p_{\min}$  value. At this time the  $\Delta p_{\max}$  value has become the constraint condition of using underbalance pressure in fact. To be on the safe side, Equation (6-36) is adopted:

(6-36)

$$\Delta p_{\text{rec}} = 0.8 \Delta p_{\max}$$

## Extreme Overbalance Perforating Operation Pressure Design.

The operating wellhead pressure of nitrogen pressurizing is one of the key parameters of the extreme overbalance perforating technology under the conditions of maximizing perforating effectiveness, no damage to the wellbore, and no new formation damage. At the instant of perforating, the relation between the pressures in the wellbore is shown in Equation (6-37).

(6-37)

$$P_{\text{wf}} = P_{\text{killing fluid}} + P_{\text{nitrogen column}} + P_{\text{wellhead}}$$

Extreme overbalance perforating technology requires that the bottomhole pressure  $p_{\text{wf}}$  is higher than the formation breakdown pressure and lower than the minimum tubing and casing collapsing pressures, as shown in Equation (6-38).

(6-38)

$$P_{\text{breakdown}} < P_{\text{wf}} < P_{\text{collapsing}}$$

In this range the operating wellhead pressure  $P_{\text{wellhead}}$  can be determined. Practical experience

indicates that the downhole pressure gradient should be in the range 20 to 70 kPa/m depending on practical formation breakdown pressure. The optimizing operating wellhead pressure design should be comprehensively determined by using the dynamic modeling of subsurface fracture propagation under the conditions of different bottomhole pressures, liquid nitrogen volumes, and fluid volumes and the productivity analysis on the basis of desired operating effectiveness.

**Safety Constraint of Operating Pressure Difference Design.** Safety in operating pressure difference is one of the important parameters in the operations of underbalanced perforating, extreme overbalance perforating, and combined perforating and testing. On the premise of meeting the requirements of operating safety and bottomhole structure safety, the operating pressure difference should ensure the optimum result. Different operating purposes have different requirements for operating pressure difference. For instance, under the condition of combined perforating and testing, the operating pressure difference should also meet the requirements of both perforating and testing. Under insufficient pressure difference, the reservoir fluid cannot flow into the well or the production rate is too small to obtain effective testing data that can reflect the reservoir characteristics. An excessive pressure difference may form a water cone or gas cone that damages the reservoir and imperils the safety of testing string, packer, and surface pipeline and equipment. In general, the requirements for pressures during operating are as follows.

#### 1. Tubing safety pressure

It consists of internal pressure, external pressure, and remaining tensile force. Tubing may be acted upon by internal and external medium pressures after it is run into the well. The internal pressure strength, external pressure strength, and tensile strength of tubings of different specifications can be found in the related handbook. The remaining tensile force means the tensile strength of tubing minus the tensile load of pipe string below the tubing and is closely related to the pipe string structure. In

particular, the effect of friction between the packer and casing during packer setting and unsetting operations should be noticed. For some special wells (such as high-pressure deep wells), the compressive strength of string should also be considered.

#### 2. Casing safety pressure

Conceptually, the safety pressure calculation of casing is similar to that of tubing. The difference between them is that the casing is always acted on by the radial squeeze of enclosing rock. The bottomhole casing bears the maximum external and internal pressures and is the most vulnerable spot. The maximum and minimum allowable casing pressures at vulnerable spots should be noted.

#### 3. Effective testing operating pressure

For combined perforating and testing operations, in order to obtain effective data, be convenient for interpretation, and reduce error of interpretation, the testing pressure difference should avoid the multiphase flow and critical flow and should also avoid the damage caused by rate sensitivity during flow.

#### 4. Safety requirements of extreme overbalance perforating

Safety should first be considered during extreme overbalance perforating and stimulation operation. In addition to the aforementioned tubing and casing safety pressures, the pressures borne by the packer, perforating gun system, Christmas tree, isolating tool, lubricator, and blowout control equipment and the safety of used fluid should also be noticed.

## 6.4 OPTIMIZING THE PERFORATION DESIGN

Under specific reservoir characteristics, optimizing the perforation design is required in order to achieve a perfect downhole connectedness. A correct and effective perforation design is dependent on: (1) level of quantitative understanding of the perforated well productivity rule under the condition of various reservoirs and reservoir fluids; (2) accuracies of acquired perforating

parameters, damage parameters, and reservoir and reservoir fluid parameters; (3) degree of serialization of variety and type of perforating gun and charge that can be provided for selecting; and (4) degree of matching of perforating technology and perforating fluid selected with specific reservoir. The perforation design means the perforating parameters and perforating technology that are selected under existing conditions in accordance with the specific reservoir and can ensure maximum well productivity and optimizing perforating fluid combined. Perforation design also relates to the technological requirements for achieving these parameters. The productivity ratio of the well is the objective function.

### Perforating Parameter Classification

Different types of wellbores (vertical well, extended reach well, and horizontal well) have different perforating parameters in perforation design. The perforating parameters are divided into the following three kinds in accordance with the function and usage of perforating parameters:

1. First kind of perforating parameters. The parameters of perforating gun and charge are dependent on the types of perforating gun and charge used for operating perforating operation. Different perforating charges have different geometric parameters of penetration (perforation penetration depth and perforation diameter) and different perforating compaction damage parameters (degree of compaction and compaction thickness). Different perforating guns have different perforation densities, perforation patterns, and phases. The parameters of perforating gun and charge may greatly affect oil and gas well productivity.
2. Second kind of perforating parameters. For a horizontal well, under the same first kind of perforating parameters, different opening locations, degrees of opening, and perforating orientations have different productivity ratios. The parameters of perforation distribution may directly affect the perforated horizontal well productivity. This kind of perforating

parameter includes opening location, degree of opening, and perforating orientation. In accordance with perforating orientation, circumferential perforating ( $360^\circ$ ) or low-side perforating ( $\leq 180^\circ$ ) may be selected.

3. Third kind of perforating parameters. Perforating pressure difference is crucial to achieving perfect bottomhole connectedness. It means to determine the rational underbalance pressure under the condition of underbalanced perforating and to determine the rational operating pressure under the condition of extreme overbalance perforating.

Optimizing perforation design includes mainly the rational design, analysis, and optimization of the three kinds of perforating parameters on the basis of specific reservoir characteristics and the type of wellbore (straight well or horizontal well). For fractured wells, water injection wells, sand control wells, heavy oil and non-Darcy flow wells, and so on, special consideration is further required.

### Optimizing Perforation Design for Sandstone Oil and Gas Wells

The first kind of perforating parameter is discussed in this section. Three problems, that is, productivity ratio, casing damage, and the mechanical stability of borehole under possible parameter combinations, are considered. The productivity ratio of the well is the objective function while the latter two are the constraining conditions.

**Preparation of Perforating Charge Property Data.** During optimizing design, the compaction damage parameters (compaction thickness CZH and degree of compaction CZC) of the perforating charge are required to be known and can be calculated using the perforation penetration depth  $L_p$  of the penetrating core target by perforating charge, perforation diameter  $d_p$ , Berea core target length  $L_c$ , core diameter  $d_c$ , and core flow efficiency CFE.

When compaction thickness CZH is between 10 mm and 17 mm, its effect on design and

prediction is not obvious; thus, the CZH values of various perforating charges can be simply taken to be 12.5 mm. Or CZH = 10 mm is taken for  $d_p = 10$  mm while CZH = 17 mm is taken for  $d_p = 20$  mm. For some  $d_p$  values, the corresponding CZH value can be estimated in accordance with the linear relationship.

Degree of compaction CZC ( $K_{cz}/K_o$ ) may obviously affect the optimizing perforation design and can be calculated by using the finite element analysis software of the perforating core target on the basis of various data (perforation penetration depth, perforation diameter, and flow efficiency, and so on) of penetrating Berea core target by perforating charge.

Optimizing the perforating parameter design should also consider the parameters of the perforating gun, including outside diameter, appropriate perforation density and phase angle, working pressure, outside diameter (including burr) after shooting, and appropriate model number of perforating charge. Matched perforating gun and charges have the best results because a matching perforating gun can ensure that the shot height of the perforating charge is in a rational range.

**Correction to Perforation Penetration Depth and Perforation Diameter of Perforating Charge.** At present, the perforating charge property data provided by the factory are mostly concrete target data and do not represent penetration data under practical subsurface conditions, which are the only data that can be used for evaluating

the perforated well performance. Therefore, the perforating charge property parameters should be corrected during optimizing perforation design in the light of specific reservoir conditions.

The Berea sandstone target correction method has been obtained by a number of tests. In the light of the current situation of using concrete targets in large amounts, the concrete target data correction method should be studied. One is to find a method of converting the concrete target data into the Berea sandstone target data, and the other is to study a method of directly converting the concrete target data into practical formation penetration data.

#### 1. Converting concrete target data into Berea core target data

Some oilfields have established simple concrete targets in order to check the perforating charge properties. Converting the concrete target penetration data into the Berea core target data favors the optimizing design, productivity prediction, and performance analysis. The Daqing oil field data analysis indicates that the penetration data of concrete target and Berea sandstone target are obviously interrelated (which is the same as the conclusion of API RP43 Fifth Edition). Figures 6-53 and 6-54 show the relations calculated in China. The perforation penetration depth and perforation diameter of Berea sandstone can be estimated using these data.

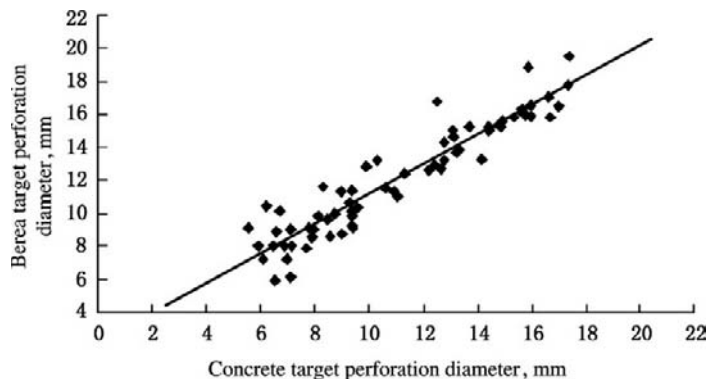


**FIGURE 6-53** Converting concrete target perforation diameter into Berea target perforation diameter.

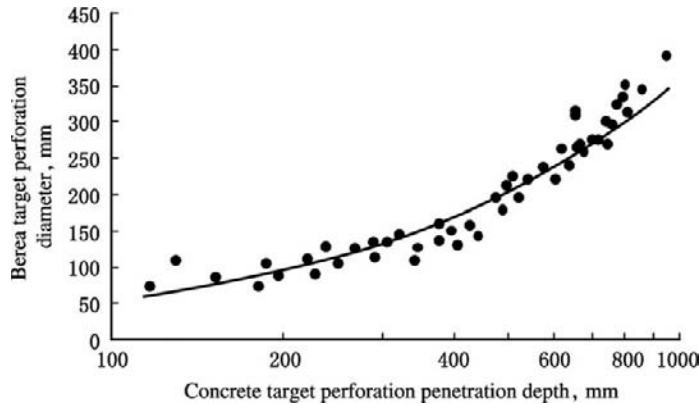


**FIGURE 6-54** Converting concrete target perforation penetration depth into Berea target perforation penetration depth (abscissa is logarithm).

2. Converting Berea target perforation penetration depth and perforation diameter into downhole formation perforation penetration depth and perforation diameter

Despite the fact that the Berea target data can be approximately obtained by using the concrete target data, the practical subsurface perforation penetration depth and perforation diameter are greatly different from the surface Berea sandstone target data. The correction for perforation penetration depth and perforation diameter of perforating charge should include: gun-to-casing clearance, grade and number of production casing, compressive strength of rock, perforating fluid pad pressure, running time, downhole temperature, perforating charge, and perforating charge storage environment and duration. The empirical correction method is as follows.

- a. Correction based on gun-to-casing clearance  $\delta$ . The optimum clearance is 0–13 mm. If  $\delta = 16$ –24 mm, the surface perforation penetration depth and perforation diameter data should be multiplied by 0.95. If  $\delta > 25$  mm, they should be further multiplied by 0.95 on the basis of first multiplication. The effect of gun-to-casing clearance on perforation penetration depth is lower than the effect on perforation diameter. If a perforating charge of large diameter perforation is required,

the effect of gun-to-casing clearance should be determined by experiment. Figure 6-55 shows the effect of gun-to-casing clearance on perforation diameter under the condition of perforating that is not placed in the middle.

- b. Correction based on running duration and downhole temperature. Common explosives have temperature-resisting and time-resisting problems. If the perforating environment exceeds the temperature- and time-resisting limits, the explosive of the perforating charge may be degraded, and the perforating charge property may be seriously affected. If the temperature- and

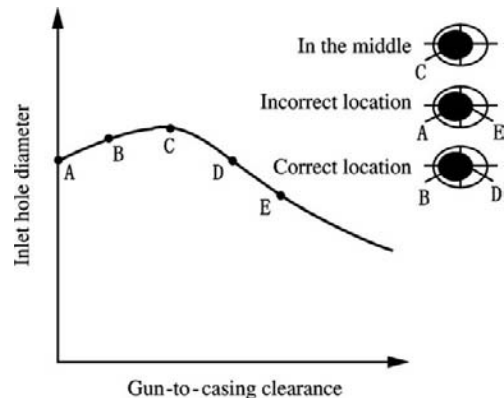


**FIGURE 6-55** Effect of perforating gun location on perforation diameter.

time-resisting ranges may possibly be exceeded, the surface perforation penetration depth should be multiplied by 0.85–0.95. During practical design, the appropriate type of explosive should be selected on the basis of the curves of the relationship between temperature resistance and time resistance for the explosive of the perforating charge in accordance with the practical downhole environment. Figure 6-56 shows the curves of the relationship between temperature resistance and time resistance for common RDX, HMX, HNS, and PYX.

- c. Correction based on the hydrostatic pressure of the perforating fluid. The related studies indicate that the increase of perforating fluid pressure may decrease perforation penetration and perforation diameter. The reason is that the jet flow of shaped-charge shooting may generate cavity in fluid during penetrating the fluid layer. The higher the perforating fluid pressure, the shorter the duration necessary for cavity contracting to original state; thus the penetrating ability is decreased.

At present, the core target testing is conducted under a hole pressure of 10.5 MPa in China. If bottomhole pressure is different from this value, correction to

perforation penetration depth and perforation diameter is required. When bottomhole pressure is lower than 10.5 MPa, the surface perforation penetration depth and perforation diameter should be multiplied by 1.05. If  $p_{wf} = 15\text{--}24$  MPa, they should be multiplied by 0.95. If  $p_{wf} \geq 25$  MPa, they should be further multiplied by 0.95 on the basis of first multiplication.

- d. Correction based on the grade and number of production casing. The strength of the casing may directly affect perforation size. For a high-velocity jet flow deep-penetration perforating charge, the perforation sizes under different casing steel grades can be calculated by using Equation (6-39):

(6-39)

$$\frac{d}{d_r} = \left( \frac{2250 + 4.2\chi_r}{2250 + 4.2\chi} \right)^{0.5}$$

where:  $d$  = perforation diameter of practical downhole casing;  $d_r$  = perforation diameter of surface target casing;  $\chi$  = Brinell hardness of practical downhole casing;  $\chi_r$  = Brinell hardness of surface target casing.

Under the condition of several production casing strings, the change of the perforation diameter of second casing or

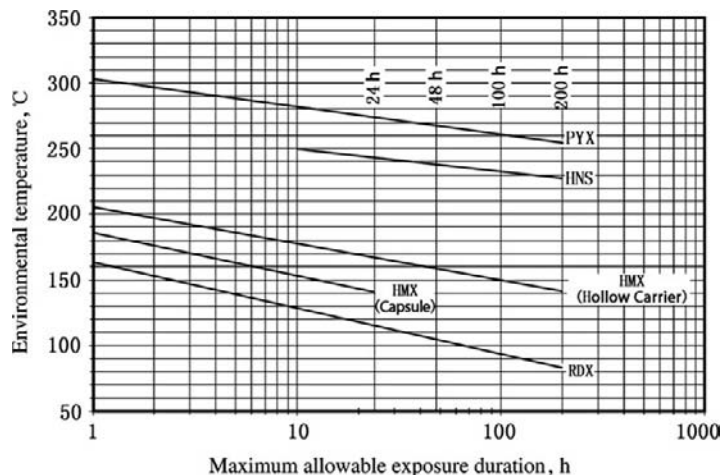


FIGURE 6-56 Curves of the relationship between temperature resistance and time resistance for common explosives.

TABLE 6-7 Casing Grade and Physical Property

Casing Grade	HRB "B"	HRC "C"	HB	Yield Strength (MPa)
J55	81~95		152~209	379
K55	93~102	14~25	203~256	379
C55	93~103	14~26	203~261	517
L80	93~100	14~23	203~243	552
N80	95~102	16~25	209~254	552
C95	96~102	18~25	219~254	655
S95		22~31	238~294	655
P105		25~32	254~303	724
P110		27~35	265~327	758

third casing will change with the type of perforating charge. For a deep-penetration perforating charge, the perforation diameter of the second casing is reduced by 10% to 30% in comparison with the first casing, while the perforation diameter of the third casing is reduced by 10% in comparison with the second casing. Under this condition, the surface target experiment should be adopted, particularly for the large-perforation-diameter shaped charge, which has special usage (such as sand control and gravel packing).

The correction to perforation penetration depth can be determined in accordance with the type of casing. For the N80 casing, the surface perforation penetration depth data should be multiplied by 0.95; for the P110 casing, it should be multiplied by 0.90. For two casings, the surface perforation penetration depth should be multiplied by 0.6. For three casings, the surface perforation penetration depth should be multiplied by 0.4.

- e. Correction based on rock porosity. The decrease of rock porosity may increase the compressive strength of rock, thus decreasing the penetrating ability of perforating charge. Equations (6-40) through (6-42) have been obtained by using regression analysis on the basis of the nomogram in China:

If  $\Phi_f / \Phi_b < 1$ , then

$$(6-40) \quad C = \left(\frac{\Phi_f}{\Phi_b}\right)^{1.5} \left(\frac{19}{\Phi_f}\right)^{1.5}$$

If  $\Phi_f / \Phi_b = 1$ , then  $C = 1$ .

If  $\Phi_f / \Phi_b > 1$  and  $\Phi_b < 19\%$ , then

$$(6-41) \quad C = \left(\frac{\Phi_f}{\Phi_b}\right)^{1.5} \left(\frac{\Phi_b}{19}\right)^{1.5}$$

If  $\Phi_f / \Phi_b > 1$  and  $\Phi_b \geq 19\%$ , then

$$(6-42) \quad C = \left(\frac{\Phi_f}{\Phi_b}\right)^{1.5}$$

where:  $\Phi_f$  = formation porosity, %;  $\Phi_b$  = Berea sandstone target porosity, %;  $C$  = correction coefficient.

If the compressive strength of reservoir rock can be provided, the  $C$  value can be calculated by using Equation (6-43) on the basis of the compressive strength of the Berea target and the compressive strength of the specific formation:

$$(6-43) \quad C = \exp [0.0125 (\sigma_r - \sigma_f)]$$

It should be noted that this formula cannot be directly used for converting from concrete target data to formation data. In addition, the storage duration and environment of the perforating charge may also affect the penetrating property of perforating charge.

### Calculation of Drilling Damage Parameters.

Drilling damage is mainly generated by solids invasion and filtrate invasion, and physical damage and chemical damage are caused, thus reducing reservoir permeability in a certain range of radial depth. The drilling damage parameters (damage depth and degree of damage) are the important parameters that affect the optimizing perforation design. At present, the methods of determining drilling damage parameters include openhole drillstem test method, logging method, reverse calculation method, empirical method, and matching based on practical testing data. The openhole drillstem test method is adopted as far as possible, or the drillstem test data of adjacent wells of the same reservoir under the same drilling conditions are used. Otherwise, the empirical method is adopted on the basis of drilling data. The Chinese optimizing perforation design software has provided the empirical calculation method.

**Optimization of Perforating Parameters.** The optimization of perforating parameters should be based on the correct understanding of the perforating productivity rule under various geological and fluid conditions; that is, the correct model should be established to acquire the quantitative relation. Optimizing perforation design software programs for sandstone oil wells, sandstone gas wells, sandstone water injection wells, and porous fractured oil reservoirs have been provided in China.

When the parameters are optimized under specific reservoir conditions, the various productivity ratios under different possible matches of perforation density, phase, and perforating charge can be calculated by using the aforementioned methods or software, the decreasing coefficients of casing collapsing strength under each matching are calculated, and the perforating parameter matching that has the highest productivity ratio is selected on the premise that the decrease of casing collapsing strength does not exceed 5%.

For a horizontal well, the optimization of the second and third kinds of perforating parameters is also of great importance in addition to the

optimization of the first kind of perforating parameters.

The procedure of optimizing the perforating parameters is as follows.

1. Establishing the mathematical models of perforated well productivity relations under different reservoir and reservoir fluids obtaining the quantitative relations of perforating productivity ratio under various conditions
2. Collecting the related data of local area and adjacent wells, which can be used for correcting the model and optimizing the design
3. Investigating the model number and property testing data of the perforating gun and charge
4. Correcting the perforation penetration depths and perforation diameters of various perforating charges
5. Calculating the compaction damage parameters of various perforating charges
6. Calculating the drilling damage parameters of a designed well
7. Calculating and comparing the productivity ratios and the decreasing coefficient of casing collapsing strength under different possible matching of various parameters, and selecting the optimum perforating parameter matching
8. Calculating the production rate and skin factor under the selected program
9. Calculating the minimum and maximum underbalance pressures and recommending the operating underbalance pressure
10. Selecting appropriate perforating technology and perforating fluid
11. Designing the operating string and compiling an operating design book

The amount of work of the various calculations in this list is great, and the accuracy based on the nomogram is limited. The optimizing perforation design software developed can be used for fast and accurate optimizing perforation design.

### Rational Selection of Perforating Technology.

Each perforating technology has its own merits, demerits, and use conditions. The specific

selection depends on the features of perforating technology, the geological characteristics of the reservoir, the requirements of development and engineering, and so on.

**Optimization of Perforating Fluid.** At present, conventional perforating fluid systems include mainly solid-free clean salt water perforating fluid, polymer perforating fluid, oil-based perforating fluid, and acid-based perforating fluid. The high-density and high-temperature-resistant completion and perforating fluid systems include mainly high-density clean salt-water perforating fluid (bromide brine perforating fluid, non-bromide brine perforating fluid, organic acid salt brine perforating fluid), water-based clay-free perforating fluid, and modified drilling-completion-perforating fluid.

With the change of the focal point of oil and gas exploration and development from shallow reservoir to deep reservoir, the appropriate temperature of perforating fluid changes from low temperature to superhigh temperature, and perforating fluid density is directed toward high density. In addition, a completion and perforating fluid (especially the various additives in it) should be non-toxic or low-toxic and easily degradable biologically due to the strict requirements of environmental protection. A perforating fluid should have: (1) effectiveness of controlling reservoir pressure and adjustable density; (2) good compatibility with reservoir rock and fluid, thus preventing swelling of clay and scaling; (3) low corrosiveness, which favors protecting tubing, casing, and equipment; (4) good stability at the surface and subsurface; (5) good cleanliness and environmental protection; and (6) low cost and broad sources of goods, and so on.

The potential formation damage of the specific reservoir should be considered when a perforating fluid is rationally selected. The perforating fluid formulation should be optimized by using a number of laboratory experiments in order to make the perforating fluid have good compatibility and environmental protection, thus ensuring optimum perforating effectiveness.

## Optimizing Perforation Design for a Horizontal Well

In order to optimize the perforated completion design of a horizontal well and perfect the flow performance of a horizontal well, the main factors affecting the flow performance of perforated horizontal well under different conditions should be understood, and the corresponding technical measures should be taken so that the effects of unfavorable factors can be eliminated. The studies indicate that drilling damage, perforating damage, and the additional skin caused by the fluid flow into perforation are the main factors affecting horizontal well productivity. These are directly related to the selection of the previously mentioned three kinds of parameters.

**Optimization of the First Kind of Perforating Parameters.** The optimization of the first kind of perforating parameters means mainly the optimization of the perforating gun and charge parameters of the section opened by perforating. The data preparation and basic procedure are similar to those of a straight well of sandstone. On the basis of optimization (macroscopic optimization) of the second and third kinds of perforating parameters, the perforating parameters of the section opened are optimized (local optimization), or both are combined to directly optimize the perforating parameters.

The studies indicate that the selection of perforating gun and charge parameters and the evaluation of productivity ratio should be in accordance with the following designing principles:

1. Perforation density may obviously affect the productivity ratio. The perforation density necessary for achieving the optimum productivity ratio is much lower than that of a vertical well; that is, a high perforation density is not required by perforated completion of a horizontal well.
2. The effect of perforation penetration depth on horizontal well productivity ratio is more obvious than that on vertical well productivity ratio. Under low perforation density and high anisotropy ratio, the effect of perforation

penetration depth is even more obvious. Deep penetrating perforation has an obvious effectiveness.

3. For an anisotropic reservoir, the effect of perforating phase angle on productivity ratio is particularly obvious. The phase angle of  $180^\circ$  is more favorable than the phase angle of  $90^\circ$ . For an isotropic reservoir, the effect of phase angle is not obvious and can be neglected.
4. Restricting the drilling damage depth to ensure that the damage zone can be penetrated through by perforating is of great importance to the increase of productivity ratio. If the damage zone may not be penetrated through by perforating, the effect of the ratio of damage zone permeability to reservoir permeability on well productivity is particularly serious. Therefore, serious drilling damage requires deep penetrating perforation.
5. Using high perforation density and deep penetrating perforation can acquire the maximum productivity ratio. Contrarily, in order to control gas-water coning and obtain a consistent flow rate profile, using a lower perforation density at bottomhole is just as appropriate.
6. For an oil well, the effect of non-Darcy flow can be negligible. For a gas well, the effect of non-Darcy flow on productivity is very obvious and should be considered.

### Optimization of the Second Kind of Perforating Parameters

#### 1. Degree of opening and perforated section location

The studies of the horizontal perforated well productivity rule indicate that under the combined action of wellbore flow performance and reservoir fluid flow, the degree of opening and the location and distribution of the perforated section will directly affect horizontal well productivity. The optimization of the perforated section location and the degree of opening of the horizontal well is achieved by using the numerical technique under the combined inflow performance and horizontal wellbore multiphase flow model or by using Green's source function method. The analysis should be based on practical reservoir and wellbore data.

Figure 6-57 shows the flow rate distribution under the sectionalized perforating and full perforating of a horizontal well. It can be seen that the flow rate of a single section under the condition of sectionalized perforating is higher than the flow rate of the corresponding section under the condition of full perforating. If the degree of opening is appropriate, the horizontal well productivity difference between sectionalized perforating and full perforating is

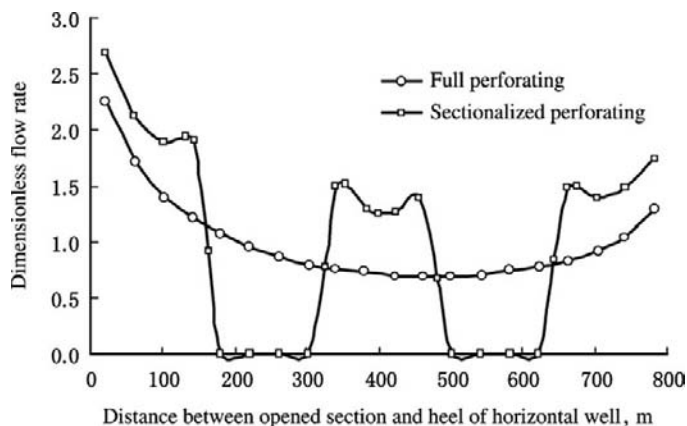


**FIGURE 6-57** Opening mode and flowrate contribution distribution of horizontal well.

not obvious. The rational degree of opening should be determined by corresponding analysis and calculation in combination with the specific reservoir conditions.

It is also shown that the opened section at the horizontal well heel has the maximum flowrate contribution. If sectionalized perforating is adopted, the number and location of sections under a given degree of opening should be simulated and calculated on the basis of specific reservoir conditions, wellbore trajectory, drilling conditions, log interpretation, and so on, and are determined in combination with the implementation of perforating technology. The shorter the distance between the opened section and the heel of the horizontal well, the higher the well productivity.

## 2. Perforation orientation

In addition to the perforated section location and the degree of opening by perforating, the difference between the optimizing perforation designs of horizontal well and straight well also includes the effects of reservoir heterogeneity and perforation orientation. The studies indicate that if the direction of perforation is consistent with the direction of the minimum reservoir permeability, the skin of a perforated well is the minimum; that is, for most anisotropic reservoirs, oriented perforating of  $180^\circ$  is most favorable.

For an anisotropic reservoir, the phases of  $60^\circ$ ,  $90^\circ$ , and  $120^\circ$  are not as effective as  $180^\circ$ ; however, increasing the perforation density can also obtain a result similar to that of  $180^\circ$  and may not require accurate orientation, which is favorable for the operation.

When preventing sand production and perforation sloughing is required, perforating on the low side is more practical.

**Optimization of the Third Kind of Perforating Parameters.** The determination of perforating differential pressure is mainly based on the selection of perforating technology in combination with the methods mentioned earlier.

## Principles of Perforation Designs for Other Special Wells

The optimizing perforation designs for special wells such as wells to be fractured, sand control wells, high-temperature high- $H_2S$  wells, water injection wells, and heavy oil wells, are different from that for conventional straight wells and horizontal wells.

**Perforating Parameter Design of a Fractured Well.** The selection of perforating parameters may have an important effect on the operating qualities of hydraulic fracture, acid fracturing, and matrix acidizing [16]. The optimization of the perforating parameters of a fractured well aims to decrease the pressure loss in the vicinity of the wellbore during fracturing operation and the process of putting the oil and gas well into production to the full extent. The factors of influencing the pressure loss in the vicinity of the wellbore include mainly perforation friction resistance, the micro-annulus local limited-entry pinch point caused by mismatching of shot phasing with the maximum horizontal principal stress plane (Figure 6-58), the generation of many fractures, and the tortuosity of the fracture face.

The perforating parameter design of a fractured well should ensure that the perforating parameters selected are favorable for the fracture initiation and the reduction of sand plug possibility and that the perforating parameters selected have a high proppant-carrying capacity of carrying fluid and low perforation friction resistance, thus ensuring optimum connectedness between perforation and reservoir. Therefore, the starting point of the perforating parameter design of a fractured well is different from that of a conventional perforated well, which concentrates on the highest productivity ratio.

### 1. Perforation penetration depth

Requiring deep perforation penetration is unnecessary because a fracture is generally initiated at the perforation part near the reservoir face and gradually propagated toward the maximum horizontal stress plane, and

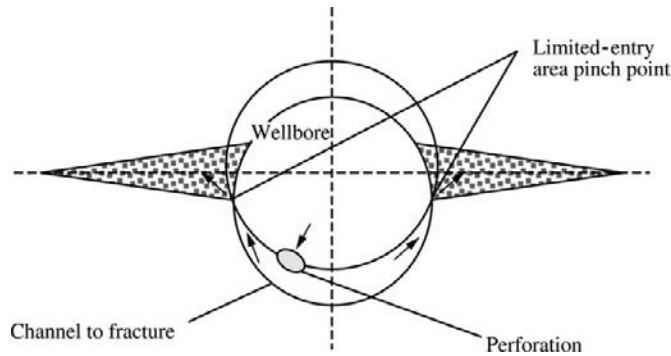


FIGURE 6-58 Fracture initiation limited-entry area [18].

the penetration capacity of the perforating gun and the perforation diameter on the casing condition each other.

## 2. Perforation diameter

When the perforating charges to be used in a well that will be fractured are selected, perforation penetration depth and perforation diameter should be well coordinated. Ensuring sufficient perforation diameter is of great importance to preventing sand fallout and to preventing the bridging of proppant in perforation or in the vicinity of perforation. Premature sand fallout may greatly reduce fracture length and proppant volume.

Cruesbeck and Collins have conducted a series of experiments to determine the minimum allowable ratio of perforation diameter to proppant particle diameter under different proppant concentrations. The studies indicate that when the perforation diameter is more than 6 times the proppant particle diameter, the proppant concentration can be increased and the bridging may not be generated; that is, for a proppant with a high or medium concentration, the perforation diameter should be at least 6 times the mean particle diameter in order to prevent sand fallout. The perforation diameter equal to 8 to 10 times the mean particle diameter may have the best effectiveness and is generally used as an operation standard. At the same time, it should be considered that each product produced by the proppant producer has a range of number of

mesh (such as 16 to 30 mesh). In practice, the actual number of mesh is generally close to the low limit value. When perforation diameter is determined, the effect of the eccentricity of the perforating gun should also be noticed. Perforation diameter will be a function of phase unless the perforating gun is central.

In addition, the friction resistance of perforation may be affected by perforation diameter. Certainly, it is related to the other perforating parameters such as perforation density and perforated thickness. The friction resistance of perforation is a key parameter to fracturing design (especially the limited-entry fracturing design). The calculation formula in which the SI unit system is used is shown in Equation (6-44).

(6-44)

$$p_{\text{pfr}} = C_D Q^2 \frac{\rho}{D_{\text{en}}^2 d^4 C_p^2 h^2}$$

$$C_p = [(1 - e^{-2.2d/\mu 0.1})]^{0.4}$$

where:  $h$  = perforated thickness;  $Q$  = pumping rate;  $\rho$  = fracturing fluid density;  $D_{\text{en}}$  = perforation density;  $d$  = perforation diameter;  $C_p$  = discharge coefficient;  $C_D$  = conversion constant;  $\mu$  = apparent viscosity of fracturing fluid.

When there is no abrasive in the fracturing fluid,  $C_p = 0.6-0.7$ ; however, when a sand-filled fluid is pumped in,  $C_p$  is changed into  $0.6-0.95$  because the perforation is eroded.

The change of  $C_p$  may greatly affect the  $p_{pfr}$  value because  $p_{pfr}$  is inversely proportional to the square of  $C_p$ .

### 3. Perforation density

The surface operating power of hydraulic fracturing may restrict the maximum operating flow rate that can be provided. The mean flow rate passing each perforation is dependent on the number of perforations connecting with fracture. Under the phases of  $0^\circ$  and  $180^\circ$ , each perforation can connect with fracture. Under the phase of  $120^\circ$ , only two-third perforations may connect with fracture; however, under the phase of  $60^\circ$ , only one-third perforations may connect with fracture.

The minimum perforating density is dependent on the injection rate required by each perforation, wellhead pressure restriction, fluid properties, completion casing size, allowable perforation friction pressure loss and perforation inlet diameter, and so on.

For limited-entry fracturing, the perforation density design has a special consideration. Generally, the perforation friction resistance that should be achieved by single perforation is calculated on the basis of the differences of breakdown pressures and in-situ stresses of various intervals, the perforation total is determined on the basis of the geometric parameters of perforation and the operating pumping rate of fracturing, and then the number of perforations for each interval is determined on the basis of the net opened thickness of each interval.

### 4. Perforation phase

The relation between perforation phase and hydraulic fracture propagation has been studied. The ideal operating condition of fracturing is that the direction of perforation is coincident with that of the maximum principal stress, so that the fracture initiated from perforation will propagate along the maximum horizontal principal stress plane that has the minimum resistance.

Under the condition of a given fracture plane, the oriented perforating of the phase of  $180^\circ$  can greatly decrease perforation

friction resistance and increase the treatment effectiveness of fracturing operation. If the accuracy of oriented perforating cannot be ensured, the included angle between perforation and the maximum horizontal principal stress plane should not exceed  $30^\circ$ . If the orientation of the fracture plane is unknown, or the perforating gun is not qualified for orientation, a phase angle of  $60^\circ$  is recommended.

A micro-annulus, that is, the annular path through which carrying fluid passes through around the casing and is also the interface between cement sheath and reservoir face, may be generated after perforation completion or starting pumping the operating fluid. Whether the micro-annulus may be formed or how much the opening of micro-annulus is related to the hydraulic degree of consolidation, the perforating parameters, and the operating parameters of fracturing, and so on. Whether there is a micro-annulus is directly related to the effect of perforating parameters on fracture initiation. If it exists, the fracture initiation is similar to that of openhole fracturing, the effect of perforation phase on the development of initial fracture is not obvious, and the fracture initiation may be generated at perforation only when the included angle between perforation orientation and optimum fracture face (that is, the maximum horizontal principal stress plane) is within  $30^\circ$ .

The rational selection of perforating parameters can not only reduce breakdown pressure and decrease the bending friction resistance of fracture but also increase the success ratio of fracturing.

For a high-inclination well, fracture initiation, the connection of en echelon fractures and the strike of fracture are directly related to the perforating parameters. The selection of perforating parameters is especially important. If the wellbore is just on the maximum horizontal principal stress plane, the oriented perforating of the phase of  $180^\circ$  is the best choice, or the orientation of  $180^\circ$  is in the direction of the minimum circumferential compressive stress. The greater the included angle between wellbore

azimuth and the maximum horizontal principal stress plane, the smaller the intersection between the wellbore and the maximum horizontal principal stress plane (it is the smallest when the included angle is  $90^\circ$ ). At this time, the perforated thickness of the fractured section of a slant well should also be decreased, so that the en echelon fractures initiated at perforation cannot be connected to form many fractures. The perforated thickness of 3 m is sufficient and is recommended.

For a horizontal extended reach well (wellbore deviation angle  $> 75^\circ$ ), if the included angle between wellbore and the maximum horizontal principal stress plane is greater, then sectionalized, concentrated (concentrated in the range of 1 m for each section), high-perforation density and multiphase perforating is recommended; thus, the oil and gas production of a horizontal well can be achieved by using a multifracture system in combination with effective interval isolation tools.

**Perforating Parameter Design of Sand Control Well.** For an unconsolidated or weakly consolidated sandstone formation, sand production is the main obstacle affecting the normal production of oil and gas well. The sand control techniques normally used are divided into sand control without screen and sand control with screen. The former includes mainly fracture pack sand control, chemical sand consolidation, and perforating sand control, while the latter has a bottomhole mechanical sand control device including slotted liner, wire wrapped screen or prepacked screen, inside casing gravel pack, and openhole gravel pack.

#### 1. Perforating sand control

Perforating sand control means to ensure the long-term stability of perforation by the rational selection of perforating parameters and to avoid the risk of a large amount of sand production caused by the change of drawdown pressure, the depletion of reservoir pressure, and the increase of water cut on the premise of the minimum sand production rate that can be borne. Formation sand production

is first due to perforation destabilization and failure, which lead to the falling-off of matrix sand and then due to the migration of sand. The failure of perforation is mainly caused by the change of the stress around perforation, which is generated by the change of drawdown pressure and the depletion of reservoir pressure. The migration of sand is generated by the flow velocity of fluid. The theoretical studies, numerical simulations, and laboratory and field studies indicate that the optimization of perforating parameters (mainly perforation penetration depth, perforation density and phase) is of great importance to achieving perforating sand control.

- a. Perforation penetration depth. The deep penetrating perforating charge should be selected as far as possible because, for the stability of single perforation, the deep penetrating charge has a greater perforation penetration depth and a smaller perforation diameter, so that the mechanical stability of perforation is much higher than that of the perforation generated by larger diameter charge.
- b. Phase and perforation density. In addition to the stability of single perforation, the effect of interactions between perforations on stability should also be considered; that is, the distances between perforations should be sufficient to avoid the mutual overlapping of the elastoplastic stress areas in the vicinity of perforations during oil and gas production and prevent the sloughing and failure of single perforation from leading to a chain reaction, thus avoiding the sloughing and sand production of the whole perforating section.

Perforation spacing may be directly affected by perforation density and phase (Figure 6-59). The lower perforation density (that is, larger perforation spacing) has a smaller mutual interference between perforations; however, the flow rate of single perforation may be increased and the sand migration and production may be generated. Therefore, perforation density

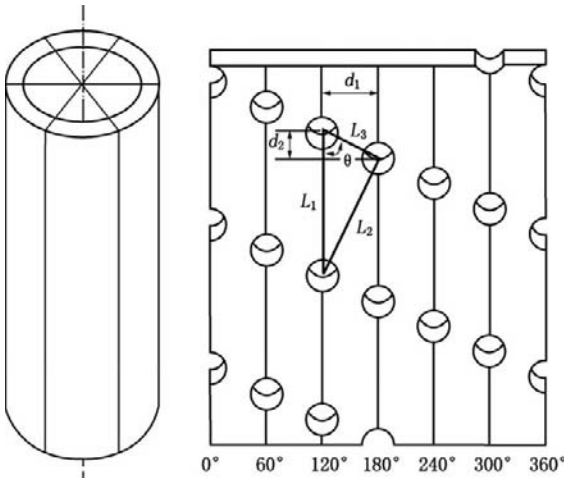


**FIGURE 6-59** Stretch view of perforation spacing under phase of 60°.

should be in a rational range, and the perforation spacing should be maximized by optimizing shot phasing.

In order to obtain the maximum perforation spacing, under a given wellbore diameter and perforation density, the optimum phase is under the condition of  $L_1 = L_2 = L_3$ . However, it is impossible for the three to be equal when the perforations are spirally distributed. Thus the optimum phase is just the phase under which two of the three are equal. Their geometric relation is shown in Equations (6-45) through (6-48) (the SI unit system is used):

(6-45)

$$\begin{cases} d_1 = \frac{1}{k_m} \\ d_2 = \frac{\pi}{180^\circ} \times \alpha \times R_{min} \end{cases}$$

(6-46)

$$L_1 = \frac{360^\circ}{\alpha} \times d_1$$

(6-47)

$$L_2 = \sqrt{L_1 + L_3 - 2L_1L_3 \cos\theta}$$

$$\theta = \arctan(d_2/d_1)$$

(6-48)

$$L_3 \sqrt{d_1^2 + d_2^2}$$

where:  $k_m$  = perforation density;  $\alpha$  = phase angle ( $^\circ$ );  $R_{min}$  = minimum distance between the middle point of perforating gun and reservoir face (it is the wellbore radius when the perforating gun is central).

Given  $R_{min}$  and  $\alpha$ , it follows that it can be achieved by optimizing perforation density.

- c. Oriented perforating. Under the condition of greater differences among vertical reservoir stress, maximum horizontal principal stress, and minimum horizontal principal stress, in order to increase the stability of perforation, oriented perforating should be adopted as far as possible, and the oriented azimuth should be consistent with the direction of the maximum principal stress (the deviation should not exceed 15–20°) [19].

If oriented perforating cannot be achieved, the existing equipment also cannot be used for adjustment to meet the requirement of maximizing perforation spacing. The studies (by N. Morita et al. in 1989) indicate that under low perforation density the phase of 90° has higher critical pressure difference than the phase of 60°, while under high perforation density (>20 shots/m), the perforation stability under the phase of 60° is obviously higher than that of 90°, and the perforation stability may not be decreased even if the perforation density is increased to 40 shots/m (Figure 6-60).

- d. Perforating underbalance pressure. The perforating underbalance pressure should avoid perforation sloughing during cleaning perforation.
2. Inside casing gravel pack (ICGP) sand control  
The sand control action of selecting rational perforating parameters is limited. Sometimes drawdown pressure or production

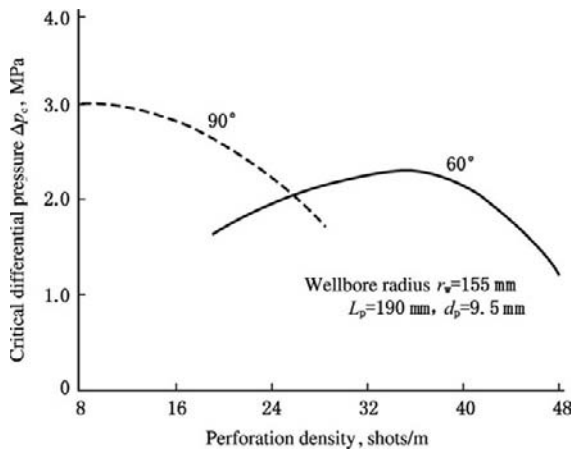


**FIGURE 6-60** Relation between the critical sand production pressure difference and perforation density and phase angle (Morita [3]).

rate has to be reduced to prevent sand production; however, this measure is not taken in general. The inside casing gravel pack sand control has been adopted in many oil and gas wells. It cannot only achieve retaining sand but also can adopt greater draw-down pressure to meet the requirements of practical production.

The perforating parameter selection of inside casing gravel pack aims at favoring gravel packing operation and ensuring a low flowing pressure loss in packed perforation at the casing and cement sheath after gravel packing. If the formation sand that has not been retained and flows into bottomhole along perforations during oil and gas production cannot be removed through the wellbore and is held up in perforation, the flowability of packed perforations will be greatly reduced.

In general, at this time the perforation design should adopt a large diameter perforating charge, increase the wellbore flow area to the full extent, and ensure gravel pack efficiency. A low perforation phase of 60° or 45° and high perforation density (such as 36 shots/m, 48 shots/m, and even up to 64 shots/m) are adopted.

For fracturing packing or high-rate water packing (HRWP), the perforating parameter

selection is similar to that for inside casing gravel packing. For fracturing packing without a gravel pack screen, the reservoir before fracturing packing or the packed fracture after fracturing packing is treated by epoxy resin, thus preventing the backflow of proppant and forming a sand retention barrier. Under this condition there is no gravel in the wellbore and the perforations at casing and cement sheath; thus, the perforating parameter selection is different from that of conventional ICGP or fracturing packing. Similarly, the perforating should ensure the perforation diameter to meet the requirement of frac sand packing. In addition, unnecessary perforations (that is, perforations not connected directly with packed fracture) should be avoided, thus reducing the possibility and risk of sand production. In this kind of well, the phase of 0° or 180° is recommended, the perforating should be oriented to the maximum horizontal principal stress plane as far as possible, and the perforated thickness should also be small as far as possible (such as less than 6 m).

The application in the Bohai oil field indicates that gravel packing requires the perforation diameter to be larger than 18 mm. In order to avoid forming a dead area during gravel packing, multiphase should be adopted, and the clearance between perforating gun and casing should be in the range of 0.5 in.–1.5 in. and is 1 in. as far as possible. For a 9 5/8 in. casing, gravel packing in Malaysia indicates that the perforating guns of 6 in. and 7 1/2 in. have good results; however, underbalanced perforating may possibly generate packed gravel return, so that selecting the perforating gun of 6 in. is safest.

**Perforating Parameter Design of Carbonate Gas Reservoir.** Carbonate includes mainly limestone and dolomite, and most carbonates are of gas reservoirs such as the gas reservoirs in the Sichuan and Changqin gas fields, which has well-developed reservoir fractures and low matrix permeability. The perforation design of this type of reservoir should lay emphasis on the connectedness between perforation and natural fracture network and gas reservoir protection, and the influencing factors include perforation density,

perforation diameter, perforation penetration depth, perforating technology, and perforating fluid.

Medium perforation density, deep penetration, and large perforation diameter are appropriate to carbonatite gas reservoirs in which natural fractures are well developed, while high perforation density and deep penetration are appropriate to carbonatite gas reservoirs in which natural fractures have a low degree of development. There is no special requirement for phase, and  $90^\circ$  is generally selected.

For carbonatite gas reservoirs, on the basis of the perforation parameter selection, the connectiveness between wellbore and fracture can be increased by selecting rational perforating technology. For instance, the combined perforating and high-energy gas fracturing technology and the combined nitrogen-gas extreme overbalance perforating and acid liquor technology can greatly increase the degree of perfection of the bottomhole and fully rouse the productivity of the gas reservoir.

In general, gas reservoirs are sensitive to foreign fluid; thus, the formation damage that may be caused by perforating fluid is not negligible, and a perforating fluid system compatible with the reservoir should be adopted. The compaction damage of perforating fluid and perforating charge can be generally mitigated by underbalanced perforating.

It should be especially stressed that safety in gas well perforating (particularly high-temperature high-pressure carbonatite gas reservoirs that contain corrosive gas) should be noticed and the selection of string structure, conveyance method, and perforating equipment should be especially considered.

**Perforating Parameter Design of a Heavy Oil Reservoir.** At present, heavy oil production methods include the thermal production of heavy oil and the cold flow production of heavy oil.

Thermal production methods include mainly cyclic steam stimulation (CSS), steam drive, and steam-assisted gravity drainage (SAGD). Most heavy oil reservoirs consist of unconsolidated sandstone and have serious sand

production during oil production; thus, sand control completion design is generally adopted and should be used in combination with the specific sand control technology. The perforation design principles of inside casing gravel pack sand control are the same as mentioned earlier; that is, high perforation density, large perforation diameter, and low phase (such as  $60^\circ$ ) should be adopted.

The cold flow production of heavy oil means that formation sand is actuated and produced along with the reservoir fluid and the frothy oil is produced through the highly permeable pore path of sandstone by using the wormhole net mechanism and dissolved gas drive mechanism. This method has low cost and a high production rate. The chief objectives of its perforation design are decreasing perforation plugging, enhancing initial sand production, and stabilizing the late oil production. For the cold flow production of heavy oil, large perforation diameter, high perforation density, low phase, balanced or underbalanced perforating, and whole payzone perforating are generally adopted.

The recent studies indicate that for the cold flow production of heavy oil, attention should be paid to overlying shale exfoliation, overlying shale sloughing, casing damage, difficulty of sand production, the problem of bottom water, and so on. Thus a perforation density that is not too high, a perforation diameter that is not too large, and a medium penetration are recommended. The drawdown pressure should be slowly increased and kept constant during oil production to the full extent (until the wormhole net formed in the vicinity of the wellbore is extended to far from the wellbore), thus favoring keeping the formation sand body stable and enabling it to bear the stress caused by overburden.

**Perforating Parameter Design of a High-Temperature High-Pressure Deep Well.** Perforating parameter selection is similar to that of conventional wells, and safety in the perforating system is stressed.

High temperature is a factor that should be emphatically considered, and the problems generated during the operation under higher

hydrostatic column pressure and wellhead pressure and the condition of rapid increase of wireline load should be simultaneously noticed. The main negative effects of the increase of temperature include the rapid worsening of perforating system component performance, the precipitous reduction of the strength of metal alloy, the increase of corrosion rate, the decrease of the reliability of electrical or electronic equipment, the loss of the performance of elastic rubber, and the degradation of high explosive.

The performance of a perforating system at high temperature is dependent on the exposure duration. Perforating systems generally have the rated values of temperature and exposure time. When the effect of temperature has to be considered, the performance of the system should not be highly estimated because the overall performance of the system is dependent on that of the weakest component of the system.

Better rubber material such as fluoro-elastomer is used to replace conventional standard rubber material such as nitrile-butadiene rubber and chloroprene rubber. The gland should be strengthened in order to prevent collapsing. The electronic component circuit insulation and adapter of the system should be placed in a closed vacuum container in order to prolong service life.

The strengths of perforating gun, fittings, and the outer barrel of electronic equipment may be reduced at high temperature, and these components can easily become corroded. The strength of the perforating gun may be reduced by 15%. A simulation test before running is recommended. A perforating gun that can be used repeatedly should be selected, thus ensuring sustained strength and resistance to pressure.

With the increase of temperature and exposure duration, the performance of high explosive will be rapidly reduced and self-explosion may be even generated. Therefore, the selection of the type of perforating charge explosive, detonating cord, and firing head should meet the requirements of high downhole temperature.

Under the condition of underbalanced perforating, high-temperature high-pressure deep wells often have a higher wellhead pressure; thus a high-pressure wellhead assembly should be used. Overbalanced perforating using the casing perforating gun run on wireline has been applied in many high-temperature deep wells, and the operation is convenient; however, the load acting on wireline should be noticed. A tubing-conveyed perforating gun should be adopted as far as possible.

**Perforating Parameter Design of a High-H<sub>2</sub>S Well.** There is no special requirement. The perforation design is the same as that of a non-H<sub>2</sub>S well. The main problems include personal safety and the potential failure of perforating system equipment. The main harm is the corrosion of the equipment. Under the condition of hydrogen sulfide concentration lower than 2%, a hydrogen sulfide corrosion inhibitor should be coated on the surface of exposed components. Under the condition of hydrogen sulfide concentration higher than 2%, special equipment such as anti-H<sub>2</sub>S alloy wireline, low-strength alloy steel pressure control component, and fluoro-elastomer should be adopted.

## REFERENCES

- [1] M.J. Chara, The Performance of Perforated Completion in Gas Reservoirs, Paper SPE 16384, Presented at the 1987 SPE California Regional Meeting, Ventura, California (April 8–10).
- [2] S.M. Tariq, M.J. Chara, L. Ayestaram, Performance of Perforated Completions in the Presence of Common Heterogeneities: Anisotropy, Laminations, or Natural Fracture, Paper SPE 14320, Presented at the 1985 SPE Annual Technical Conference and Exhibition, Las Vegas, Nevada (Sept. 22–25).
- [3] N. Morita, P.A. Boyd, Typical Sand Production Problems—Case Studies and Strategies for Sand Control, Paper 22739, Presented at the 1991 SPE Annual Technical Conference and Exhibition, Dallas, Texas (Oct. 6–9).
- [4] R.J. Saucier, J.F. Lands, A Laboratory Study of Perforations in Stressed Rocks, *Trans. AIME* (1978) 265.
- [5] M. Asadi, F.W. Preston, Characterization of the Crushed Zone Formed During Jet Perforation by Qualitative Scanning Electron Microscopy and Quantitative Image Analysis, Paper SPE

- 22812, Presented at the 1991 SPE Annual Technical Conference and Exhibition, Dallas, Texas (Oct. 6–9).
- [6] Tang Yula, Pan Yingde, Wang Yongqing, Optimal Design of Perforating Completion for Gas Well, Paper SPE 29274, Presented at the 1995 SPE Asia and Pacific Oil & Gas Conference and Exhibition, Kuala Lumpur, Malaysia (Mar. 20–22).
- [7] B.J. Dikken, Pressure Drop in Horizontal Wells and Its Effect on Production Performance, *J. Petrol. Technol. Nov.* (1990) 1426–1433.
- [8] Y. Tang, E. Ozkan, M. Kelkar, C. Sarica, T. Yildiz, Performance of Horizontal Wells Completed with Slotted-Liners and Perforations, Paper SPE 65516, Presented at the 2000 SPE International Conference on Horizontal Well Technology, Calgary, Canada (Nov. 6–8).
- [9] S. Irvana, Sumaryanto, I.N.H. Kontha, Utilizing Perforation Performance Module (PPM) and Extreme Under-Balance (EUB) Perforating to Maximize Asset Value in Deep Low Porosity—Low Permeability Gas Reservoirs: A Case Study from VICO Indonesia, Paper SPE 88544, Presented at the 2004 SPE Asia Pacific Oil and Gas Conference and Exhibition held in Perth, Australia (Oct. 18–20).
- [10] M. Karakas, S.M. Tariq, Semianalytical Productivity Models for Perforated Completions, *SPE Prod. Eng. Feb.* (1991) 73–82.
- [11] L.A. Behrmann, Underbalance Criteria for Minimum Perforation Damage, *SPE Drilling & Completion Sep.* (1996) 173–177.
- [12] P.J. Handren, T.B. Jupp, J.M. Dees, Overbalance Perforating and Stimulation Methods for Wells, Paper SPE 26515, Presented at the 1993 SPE Annual Technical Conference and Exhibition, Houston, Texas (Oct. 3–6).
- [13] G.E. King, A. Anderson, M. Bingham, A Field Study of Underbalance Pressure Necessary to Obtain Clean Perforations Using Tubing-Conveyed Perforating, Paper SPE 14321, Presented at the 1985 SPE Annual Technical Conference and Exhibition, Las Vegas, Nevada (Sep. 22–25).
- [14] S.M. Tariq, New Generalized Criteria for Determining the Level of Underbalance for Obtaining Clean Perforations, Paper SPE 20636, Presented at the 1990 SPE Annual Technical Conference and Exhibition, New Orleans, Louisiana (Sep. 23–26).
- [15] L.A. Behrmann, Underbalance Criteria for Minimum Perforation Damage, Paper SPE 30081, Presented at the 1995 SPE European Formation Damage Control Conference, The Hague, The Netherlands (May 15–16).
- [16] L.A. Behrmann, K.G. Nolte, Perforating Requirements for Fracture Stimulations, *SPE 59480* (1990), pp. 228–234.
- [17] A.A. Daneshy, Experimental Investigation of Hydraulic Fracturing Through Perforations, *Trans. AIME Oct.* (1973) 1201–1206.
- [18] L.A. Behrmann, J.L. Elbel, Effect of Perforations on Fracture Initiation, *SPE 20661*.
- [19] C.M. Pearson, M.E. Bond, A.J. Eck, Results of Stress-Oriented and Aligned Perforating in Fracturing Deviated Wells, *SPE 22836*.
- [20] Y. Tang, E. Ozkan, et al., Performance of Horizontal Wells Completed with Slotted Liners and Perforations, *SPE 65516-MS*.
- [21] Li Haitao, Wang Yongqing, A Study of the Method of Predicting the Maximum Sand-free Underbalance Pressure of Gas Well Perforating, *Natural Gas Ind.* 3 (1999) (in Chinese).
- [22] Li Haitao, Wang Yongqing, A Study of New Method of Determining the Maximum Underbalance Pressure of Oil Well Perforating, *Petr. Drilling & Prod. Technol.* 4 (1997) (in Chinese).
- [23] Li Haitao, Wang Yongqing, Optimizing Perforation Design Method of Fracturing Operation Well, *Natural Gas Ind.* 3 (1999) (in Chinese).
- [24] Li Haitao, Wang Yongqing, A Finite Element Study of Perforated Well Productivity Rule of Fractured Oil Reservoir, *Petrol. J.* 2 (2002) (in Chinese).
- [25] Zhang Shaohuai, Luo Pingya, et al., Reservoir Protection Techniques, Petroleum Industry Press, Beijing, 1993 (in Chinese).
- [26] Pan Yingde, Tang Yula, Collected Translation of Perforating Techniques, Oil and Gas Well Testing, (Tang Yula, Trans.), 1989 (4) (in Chinese).
- [27] Pan Yingde, Tang Yula, et al., A Finite Element Study of Numerical Stimulation of Perforated Gas Well Non-Darcy Flow, *Petrol. J.* 2 (1992) (in Chinese).
- [28] Pan Yingde, Tang Yula, et al., Evaluation Standards of Perforated Core Target Flow Behavior and Perforation Effectiveness, *Petrol. Drilling & Prod. Technol.* 3 (1990) (in Chinese).
- [29] Song Youwan, Zhao Huaiwen, et al., Perforated Casing Collapse Experiment, *Petrol. J.* 4 (1988) (in Chinese).
- [30] W.T. Bell, R.A. Sukup, S.M. Tariq, Perforating, *SPE Monograph* (1995).
- [31] V. Penmatcha, K. Azia, Comprehensive Reservoir/Wellbore Model for Horizontal Wells, *SPE J. Sep.* (1999) 224–234.
- [32] B.J. Dikken, Pressure Drop in Horizontal Wells and Its Effect on Production Performance, *J. Petrol. Technol. Nov.* (1990) 1426–1433.
- [33] E. Ozkan, C. Sarica, M. Haci, Influence of Pressure Drop along the Wellbore on Horizontal Well Productivity, *SPE J. Sep.* (1999) 288–301.
- [34] T.M.V. Kaiser, S. Wilson, L.A. Venning, Inflow Analysis and Optimization of Slotted Liners, *SPE Drilling & Completion Dec.* (2002) 200–209.

# Well Completion Formation Damage Evaluation

## OUTLINE

### 7.1 Overview

Well Test Analysis:

The Main Method of  
Field Evaluating Well  
Completion Quality

Comparison between  
Field and Laboratory  
Evaluations

Developing a Course of Well  
Test Analysis Technique of  
Evaluating Formation  
Damage

Modern Well Test Analysis  
Method

Requirements of Well  
Completion Formation  
Damage Evaluation  
for Data

### 7.2 Principle of Formation

#### Damage Evaluation by Well Testing

Determination of Degree of  
Formation Damage Using  
Skin Factor  $S$  and

Disintegration of  $S$  Value  
*Determination of Degree  
of Formation Damage*

*Using Skin Factor  $S$*   
*Disintegration of Skin  
Factor  $S$*

Other Parameters for  
Expressing Formation  
Damage

*Flow Efficiency  $FE$*

*Damage Ratio  $DR$*

*Damage Factor  $DF$*

*Completeness Index  $CI$*

*Effective Radius  $r_{we}$*

### 7.3 Formation Damage

#### Diagnosis of Homogeneous Reservoir by Graphic Characteristics

Graphic Characteristics of a  
Homogeneous Reservoir

*Composite Bilogarithmic  
Plot*

*Semilogarithmic Plot*

*Gradation of  $k/\mu$ ,  $S$ ,  
and  $C$*

#### Location Analysis

Method of Well Test

Curves for a Homogeneous  
Reservoir

*Meaning of Location  
Analysis*

*Time Locating*

*Pressure Locating*

*Curve Locating*

*Cases of Location  
Analysis*

*Application of Location  
Analysis*

### 7.4 Graphic Characteristics of a Dual Porosity Reservoir and a Reservoir with a Hydraulically Created Fracture

Graphic Characteristics of a  
Dual Porosity Reservoir

*Two Radial Flow Portions*  
*Radial Flow Portion of*  
*Total System Appears*

*Only*

*Case 1*

*Case 2*

*Case 3*

Graphic Characteristics of a  
Reservoir with

Hydraulically Created  
Fracture

*Mode Charts under*

*Vertical Fractures with*  
*Infinite Flow*

*Conductivity and*

*Uniform Flux*

*Case 4*

*Mode Chart under*

*Vertical Fracture with*

*Finite Flow*

*Conductivity*

Case 5	S Value Using the	Formation Damage
Fracture Skin Factor	Bilogarithmic Type Curve	Evaluation for a Natural
and Its Effect	Match Method	Gas Well
Case 6	Principle of Calculating	Pseudopressure of a Gas
Case 7	Reservoir Parameters	Well
Discussion	Using the Type Curve	Calculating S Using
7.5 Distinguishing	Match Method	Bilogarithmic Type
Effectiveness of Stimulation	Common Type Curves	Curves
by Graphic Characteristics	for Well Test	Calculating S Using
Comparison between Curve	Interpretation	Semilogarithmic
Shapes before and after	Calculating Skin Factor S	Radial-Flow Straight-
Removing Formation	Value Using the	Line Portion
Damage	Semilogarithmic Method	Simplification of
Case 8	Estimating Skin Factor S	Pseudopressure
Change of Curve Shape after	Value of a Homogeneous	Evaluating Formation
Acidizing, Which Improves	Reservoir Using a	Damage Using Systematic
Both Skin Factor and	Bilogarithmic Measured	Well Test Data
Permeability	Pressure Plot	7.7 Well Logging Evaluation
Case 9	Early-Time Portion	of Formation Damage Depth
Change of Curve Shape after	Interpretation Method	Physical Process of
Hydraulic Fracturing by	(Without Radial Flow	Invasion of Drilling Fluid
Which a Large Fracture Is	Portion)	Filtrate into Reservoir
Formed	Empirical Method	Effect of Invasion of
Case 10	Rassel's Method	Drilling Fluid on Log
7.6 Quantitative Interpretation	Other New Methods	Response
of Degree of Formation	of Analyzing	Drilling Fluid Invasion
Damage	Formation Damage	Depth Log Evaluation
Calculating Reservoir	Using Early-Time	Method
Parameters and Skin Factor	Data	References

## 7.1 OVERVIEW

### Well Test Analysis: The Main Method of Field Evaluating Well Completion Quality

Whether formation damage is caused by drilling and well completion and how high the degree of the damage is should be confirmed by field evaluation. If formation damage is generated, powerful measures of removing the formation damage are often required in order to improve the productivity of the oil and gas reservoir. The selection and effectiveness of the measures should also be evaluated on the basis of the field data.

In addition to well test analysis, well log analysis can also be used for field evaluation. However, so far none of the well log analysis

methods can directly measure the degree and depth of formation damage caused by drilling fluid or completion fluid, and there is no method that can be used for making the measured data have a definite relation to the degree of damage.

Micro-electric logging, time-lapse logging, and deep and shallow resistivity logging can all be used to indicate whether the oil and gas reservoir is invaded by drilling fluid filtrate. The amplitude difference on the micro-electric log, the undergauge on the caliper log, the amplitude difference on the time-lapse log, and the amplitude difference on the induction log can all indicate that the reservoir is permeable. Deep and shallow dual laterologs and microspherically focused logs can be used for determining the invasion diameter. However, these are not

sufficient to determine whether formation damage is generated in the oil and gas reservoir.

Well test analysis can directly determine the degree of damage. Using transient well test data, we can obtain the value of skin factor  $S$ . The  $S$  value of a nondamaged well is zero. The  $S$  value of a damaged well is higher than zero; and the higher the  $S$  value, the more serious the damage. The  $S$  value of a well that has been stimulated is lower than zero; and the lower the  $S$  value, the more obvious the effectiveness of the improvement. Thus the value of  $S$  becomes the quantitative evaluation criterion of the degree of formation damage.

In well test analysis, various formation damage parameters are defined. The parameters commonly used include damage factor  $DF$ , flow efficiency  $FE$ , damage ratio  $DR$ , additional bottomhole pressure drop  $\Delta P_s$ , effective bottomhole radius  $r_{we}$ , completion index  $CI$ , condition ratio  $CR$ , and perfection factor  $PF$ . These parameters are substantially consistent with skin factor  $S$  and can all be quantitatively expressed by using the  $S$  value.

To sum up, well test analysis is presently the only effective method for on-site field evaluation of formation damage. In this chapter the methods of evaluating formation damage of various types of oil and gas reservoirs will be introduced and illustrated by field cases.

### Comparison between Field and Laboratory Evaluations

A large amount of evaluation work is completed in the laboratory as viewed from the content of evaluation work. Thus it is necessary to describe the relation between laboratory and field evaluations.

Some laboratory methods of studying formation damage of oil and gas reservoirs have been introduced in Chapter 1.

The following goals can be achieved by applying the laboratory results:

1. Studying the reasons of formation damage, including fluid into well and technological process

2. Selecting rational preventive measures
3. Finding a remedial measure for a damaged reservoir

Laboratory quantitative results, however, can only be used for reference because of the difference between laboratory experimental conditions and practical reservoir conditions, and can only be used for predicting formation damage, analyzing its causes, and determining the degree of damage under simulated downhole conditions; thus, both laboratory and field methods should be adopted when the degree of damage is evaluated. Whether formation damage of the oil and gas reservoir is generated and whether a stimulation treatment should be taken should be determined on the basis of the  $S$  value measured by well test analysis. The effectiveness of the stimulation is determined on the basis of new well test data. Therefore, laboratory and field evaluations support and supplement each other.

### Developing a Course of Well Test Analysis Technique of Evaluating Formation Damage

Using well test analysis for evaluating formation damage was started in the 1930s. Initially, the degree of formation damage was only determined on the basis of the oil and gas well production rate. It gradually became known that reservoirs that are judged to be good oil and gas reservoirs by using core data in some wells have not achieved their proper productivity, which indicates that it is necessary to study the formation damage that may be caused by drilling and that judging drilling damage by using bottomhole pressure is the most effective and convenient method.

The research was advanced by continuous recording pressure gauges such as the Amerada downhole pressure gauge. There were more than 10 types of pressure gauges, which were used until 1993. The Musket method, MDH method, and Horner method used for transient well test analysis have then been presented in succession,

and so-called conventional well test analysis methods have been formed.

In 1953 Van Everdingen and Hurst first presented the concept of skin zone. It was supposed that a permeability reduction zone (called skin zone) may be formed because the borehole wall is damaged to some extent during drilling and well completion. In this zone an additional pressure drop  $\Delta P_s$  is formed due to the skin effect generated by the reduction of permeability. In the Darcy unit system, the additional pressure drop  $\Delta P_s$  is shown in Equation (7-1).

(7-1)

$$\Delta P_s = S \left( \frac{q\mu B}{2\pi Kh} \right)$$

where:  $S$  = skin factor;  $q$  = well production rate,  $\text{cm}^3/\text{s}$ ;  $\mu$  = reservoir fluid viscosity,  $\text{Pa} \cdot \text{s}$ ;  $K$  = reservoir permeability,  $\mu\text{m}^2$ ;  $h$  = reservoir thickness,  $\text{cm}$ ;  $B$  = oil formation volume factor,  $\text{cm}^3/\text{cm}^3$ .

The concept of skin zone has been used so far in well test analysis. The  $S$  value can be obtained by transient well test analysis, that is, pressure drawdown analysis or pressure build-up analysis.

The physical concept of additional pressure drop is shown in Figure 7-1.

The later studies of skin factor  $S$  indicate that the formation damage of the reservoir itself may generate an additional pressure drop and affect

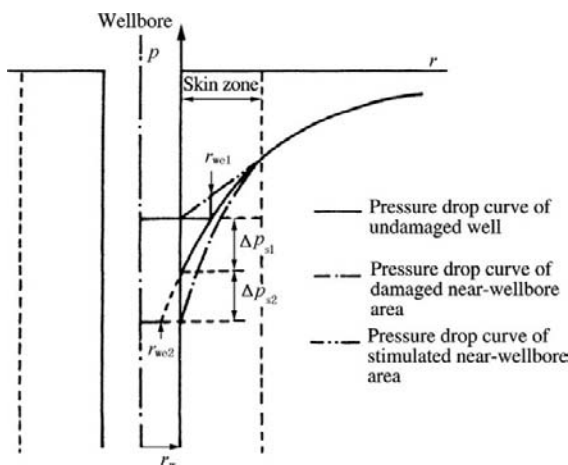


FIGURE 7-1 Additional pressure drop in skin zone.

mainly the value of  $S$ , and also indicate that the partial penetration of the reservoir, the effect of perforating technology, borehole deviation, the turbulent area in the vicinity of the wellbore, the liberation of dissolved gas, and so on may generate an additional pressure drop and affect the value of  $S$ .

In 1970, the type curve analysis method used for transient pressure analysis was first presented. The type curves formulated by Agarwal et al. use wellbore storage coefficient  $C$  and skin factor  $S$  as cross-variables and include several families of curves, thus finding a clear relation between formation damage in the vicinity of the wellbore and the shape of the transient pressure curve (Figure 7-2).

This type of type curve has been improved by Gringarten, and the combined parameter  $C_{De}^{2S}$ , which influences the shape of the curve, has been presented; thus the several families of curves are merged into one family, that is, the type curves commonly adopted at present. In  $C_{De}^{2S}$  the skin factor  $S$  is located at the exponent, thus reflecting more obviously the effect of formation damage on the shape of the curve.

It is shown that the shape of the transient well test curve is dependent on the  $S$  value, which indicates that the degree of formation damage can be determined by the shape characteristics of the transient well test curve clearly and effectively. This is an important component of the key content of the modern well test analysis method.

## Modern Well Test Analysis Method

The modern well test analysis method consists generally of the following:

1. Taking pressure data by using a high-accuracy downhole pressure gauge
2. A complete set of data analysis methods centered around the type curve analysis method
3. Using advanced well test interpretation software

The modern well test analysis method is based on high-precision pressure data because

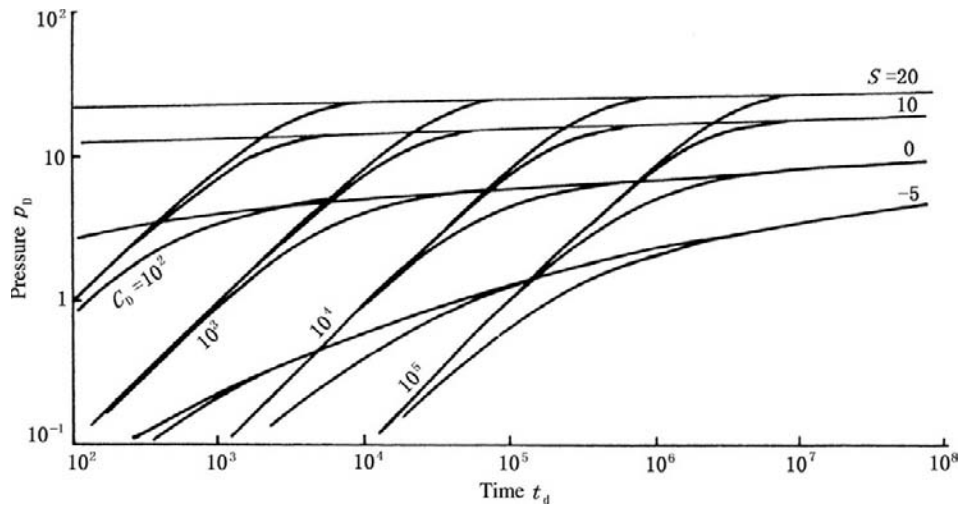


FIGURE 7-2 Agarwal type curves.

the log-log type curve matching method used in well test analysis adopts the Bourdet pressure derivative type curves taken as a core of the analysis method, and the derivative curves that can be used for interpretation cannot be obtained by using low-accuracy pressure data.

The various high-accuracy electronic pressure gauges developed presently have a pressure accuracy up to 0.025% of full scale and a resolution of 0.01 psi (that is, 0.00007 MPa). The measurement range of the gauge is up to 200 MPa and the usable temperature is up to 200°C. This type of gauge can be used in almost any oil and gas well.

In the light of the interpretation method, the log-log type curves suitable for various reservoir conditions have been perfected in succession. So-called conventional well test analysis methods, that is, semilogarithmic methods including the Horner method and MDH method, are still being used, and a complete set of matching and verification methods has been developed in order to avoid the error generated by multisolutions as far as possible.

The whole process of interpreting transient well test data is finally achieved by operating the well test software on computer. The well test software can be used for inputting all the pressure data taken by an electronic pressure gauge and

editing and processing these data for interpretation; providing the various forms of interpretation model type curves of different reservoirs, matching data with type curves in interactive form and evaluating the parameters; and outputting the various resulting diagrams and tables used in the well test report. All testing and interpretation work can be done in the field, and the necessary data can be provided in time.

### Requirements of Well Completion Formation Damage Evaluation for Data

In general, the quality requirements of data for well completion formation damage evaluation consider mainly the reliability of the test target and data interpretation. By reference to the model diagnosis requirement of heterogeneous formation test and the features of parameters, the test duration should also be interactively estimated on the basis of the pressure response curve under constant production rate. The requirements generally include the following:

1. The homogeneous model interpretation requires that the pressure derivative has at least a horizontal portion with 0.5 log periods (easy to see under variable flowrate stacking analysis).

2. The dual-porosity pseudosteady state model and dual-permeability model interpretation require that the pressure derivative has at least a length of one log period after a concave portion or similar late-time radial flow portion.
3. The dual-porosity unsteady-state model interpretation requires that the pressure derivative appears at least in the second horizontal portion with 0.5 log periods.
4. The composite model interpretation requires that the pressure derivative has at least a length of one log period in the influence portion of a composite outside region. Under the condition of both effects of boundary and heterogeneity, the test duration with deterministic boundary is predominantly selected because the appearance of a boundary effect will shield the heterogeneous performance of the reservoir.
5. For fractured wells and horizontal wells (especially long artificial fracture and long horizontal section), the appearance time of the radial flow portion is later, and the test duration before the appearance of the radial flow portion is generally taken.

## 7.2 PRINCIPLE OF FORMATION DAMAGE EVALUATION BY WELL TESTING

### Determination of Degree of Formation Damage Using Skin Factor S and Disintegration of S Value

**Determination of Degree of Formation Damage Using Skin Factor S.** Figure 7-1 and Equation (7-1) show the additional pressure drop caused by the formation damage in the vicinity of the wellbore. Equation (7-1) is in the Darcy unit system and can be changed to the following when the statutory unit system is adopted, as shown in Equation (7-2):

(7-2)

$$\Delta P_s = S \left( \frac{1.842q\mu B}{Kh} \right)$$

where:  $\Delta P_s$  = additional pressure drop, MPa;  $\mu$  = reservoir fluid viscosity, MPa · s;  $q$  = production

rate, cm<sup>3</sup>/d;  $K$  = permeability, 10<sup>-3</sup> μm<sup>2</sup>;  $h$  = reservoir thickness, m;  $B$  = oil formation volume factor, cm<sup>3</sup>/cm<sup>3</sup>.

The permeability from the boundary  $r_s$  of the damage zone to the borehole wall is decreased from normal  $K$  value to  $K_s$  due to formation damage in the vicinity of the wellbore, and the pressure drop is greater than the normal value (Figure 7-1).

Under the condition of no damage, the pressure drop from  $r_s$  to the borehole wall ( $r = r_w$ ) is as follows (in the Darcy unit system).

$$(\Delta P_{wf})_1 = \frac{q\mu B}{2\pi Kh} \ln \frac{r_s}{r_w}$$

The pressure drop under the condition of formation damage is as follows.

$$(\Delta P_{wf})_2 = \frac{q\mu B}{2\pi K_s h} \ln \frac{r_s}{r_w}$$

The additional pressure drop  $\Delta P_s$  is the difference of both and then the following in combination with the formula in Equation (7-1), as shown in Equation (7-3):

(7-3)

$$\Delta P_s = (\Delta P_{wf})_2 - (\Delta P_{wf})_1 = \frac{q\mu B}{2\pi Kh} \left( \frac{K}{K_s} - 1 \right) \ln \frac{r_s}{r_w}$$

By simplification the following result is obtained in Equation (7-4):

(7-4)

$$S = \left( \frac{K}{K_s} - 1 \right) \ln \frac{r_s}{r_w}$$

Equation (7-4) indicates that under the condition of formation damage,  $K_s < K$  and  $S$  is a positive value, while under the condition of a stimulated near-wellbore area,  $K_s > K$  and  $S$  is a negative value. If  $K_s = K$ , then  $S = 0$ .

Equation (7-5) is obtained by Equation (7-3):

(7-5)

$$\Delta P_s = S \left( \frac{1.842q\mu B}{Kh} \right) = 0.8686 \text{ mS}$$

where:  $m$  = semilogarithmic straight slope, MPa/cycle (cycle means log cycle).

Both Equations (7-4) and (7-5) have similar forms in other unit systems.

It should be pointed out that the  $S$  value obtained by well testing is a composite parameter. It is not obtained only by formation damage generated in the process of drilling and well completion, and many factors may generate additional pressure drop. The total skin factor consists of the formula shown in Equation (7-6):

$$(7-6) \quad S_t = S_d + S_\theta + S_{aD} + S_p + S_A + S_{pF} + S_{dp}$$

The actual formation damage skin factor is as follows.

$$S_d = S_t - S_\theta - S_{aD} - S_p - S_A - S_{pF} - S_{dp}$$

where:  $S_t$  = total skin factor;  $S_d$  = formation damage skin factor;  $S_\theta$  = borehole deviation pseudoskin factor;  $S_{aD}$  = non-Darcy pseudoskin factor;  $S_p$  = partial penetration pseudoskin factor;  $S_A$  = reservoir shape skin factor;  $S_{pF}$  = perforating pseudoskin factor;  $S_{dp}$  = perforation geometry pseudoskin factor.

### Disintegration of Skin Factor S

#### 1. Borehole deviation pseudoskin factor

The ideal well should be a vertical well with a zero deviation angle under the condition of horizontal formation. All the real wells have a deviation angle greater than zero, and the resistance to inflow is different from that of a vertical well. The approximate calculation formula for a real well is shown in Equation (7-7).

$$(7-7) \quad S_\theta = -\left(\frac{\theta'}{41}\right)^{2.06} - \left(\frac{\theta'}{56}\right)^{1.865} \lg\left(\frac{h_D}{100}\right)$$

$$h_D = \frac{h}{r_w} \sqrt{\frac{K_H}{K_V}}$$

$$\theta_w' = \arctan\left(\sqrt{\frac{K_V}{K_H}} \tan \theta_w\right)$$

where:  $\theta_w$  = borehole deviation angle, ( $^\circ$ );  $K_H$  = horizontal permeability,  $10^{-3} \mu\text{m}^2$ ;  $K_V$  = vertical permeability,  $10^{-3} \mu\text{m}^2$ ;  $r_w$  = borehole radius, m;  $h$  = effective reservoir thickness, m.

The applicable condition of Equation (7-7) is  $0^\circ \leq \theta \leq 75^\circ$ .

#### 2. Non-Darcy pseudoskin factor, as shown in Equation (7-8):

$$(7-8) \quad S_{aD} = D \cdot q_0$$

where:  $D$  = non-Darcy coefficient, determined by typical well test curve fitting method;  $q_0$  = production rate,  $\text{m}^3/\text{d}$ .

#### 3. Partial penetration pseudoskin factor, as shown in Equation (7-9):

$$(7-9) \quad S_p = \left(\frac{h}{h_p} - 1\right) \left[ \ln\left(\frac{h}{r_w}\right) \left(\frac{K_H}{K_V}\right)^{1/2} - 2 \right]$$

where:  $h_p$  = penetration thickness, m;  $h$  = effective reservoir thickness, m;  $K_H$  = horizontal permeability,  $\mu\text{m}^2$ ;  $K_V$  = vertical permeability,  $\mu\text{m}^2$ ;  $r_w$  = borehole radius, m.

#### 4. Reservoir shape skin factor, as shown in Equation (7-10):

$$(7-10) \quad S_A = 0.5 \ln(31.62/C_A)$$

where:  $C_A$  = reservoir shape coefficient (see Table 7-1), dimensionless.

#### 5. Perforating pseudoskin factor

There are several methods of calculating the pseudoskin factor caused by perforating. The perforating pseudoskin factor under various conditions has been shown in chart form previously. Here the pseudoskin factor caused during perforating is expressed by the sum of the pseudoskin factors in horizontal and vertical directions and the pseudoskin factors caused by the wellbore and compaction zone.

##### a. Pseudoskin factor in horizontal direction, as shown in Equation (7-11):

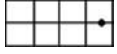
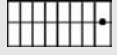
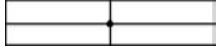
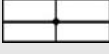
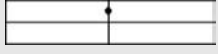
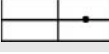
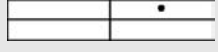
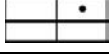
$$(7-11) \quad S_H = \ln\left(\frac{r_w}{r_{we}}\right)$$

$$r_{we}(\theta) = \begin{cases} 1/4L_p & \text{for phase angle} = 0 \\ \alpha_0(r_w + L_p) & \text{for other phase angles} \end{cases}$$

where:  $r_{we}$  = effective borehole diameter, m;  $L_p$  = perforation penetration depth, m;  $r_w$  = borehole radius, m.

The  $\alpha_0$  values are shown in Table 7-2.

**TABLE 7-1 Reservoir Shape Coefficient**

Drainage area shape	$C_A$	Drainage area shape	$C_A$
	30.88		3.16
	12.99		0.581
	4.51		0.111
	3.34		5.38
	21.84		2.69
	10.84		0.232
	4.51		0.116
	2.08		2.36

**TABLE 7-2 The  $\alpha_\theta$  Values**

Perforating Phase Angle (°)	$\alpha_\theta$	Perforating Phase Angle (°)	$\alpha_\theta$
0(360)	0.25	90	0.726
180	0.5	60	0.813
120	0.648	45	0.86

**TABLE 7-3 Relation between Phase Angle,  $c_1(\theta)$ , and  $c_2(\theta)$**

Phase Angle (°)	$c_1(\theta)$	$c_2(\theta)$
0(360)	$1.6 \times 10^{-1}$	2.675
180	$2.6 \times 10^{-2}$	4.532
120	$6.6 \times 10^{-3}$	5.32
90	$1.9 \times 10^{-3}$	6.155
60	$3.0 \times 10^{-4}$	7.509
45	$4.6 \times 10^{-5}$	8.791

- b. Pseudoskin factor caused by the wellbore, as shown in Equation (7-12):

(7-12)

$$S_{wb}(\theta) = c_1(\theta) \exp [c_2(\theta)r_{wD}]$$

$$r_{wD} = r_w (L_p + r_w)$$

The relation between phase angle  $c_1(\theta)$  and  $c_2(\theta)$  is shown in Table 7-3.

- c. Pseudoskin factor in vertical direction, as shown in Equation (7-13):

(7-13)

$$S_v = 10^a h_D^{b-1} r_{pD}^b$$

$$a = a_1 \lg r_{pD} + a_2, \quad b = b_1 r_{pD} + b_2$$

(7-14)

$$h_D = \left( \frac{h_p}{L_p} \right) \sqrt{\frac{K_H}{K_V}}$$

$$r_{pD} = \left( \frac{r_p}{2h_p} \right) \left( 1 + \sqrt{\frac{K_V}{K_H}} \right)$$

$$S_{pF} = S_v + S_H + S_{wb}$$

The values of  $a_1$ ,  $a_2$ ,  $b_1$ , and  $b_2$  are shown in Table 7-4.

After the values of  $S_v$ ,  $S_H$ , and  $S_{wb}$  are determined, the value of the perforating pseudoskin factor can be obtained using Equation (7-14).

**TABLE 7-4** Relation between the Coefficients in Equation of Calculating Pseudoskin Factor in Vertical Direction and Phase Angle

Perforating Phase Angle (°)	a <sub>1</sub>	a <sub>2</sub>	b <sub>1</sub>	B <sub>2</sub>
0(360)	-2.091	0.0453	5.1313	1.8672
180	-2.025	0.953	3.0373	1.8115
120	-20.18	0.0634	1.6136	1.7770
90	-1.905	0.1038	1.5674	1.6935
60	-1.898	0.1023	1.3654	1.6490
45	-1.788	0.2398	1.1915	1.6392

- d. Perforation geometry pseudoskin factor, as shown in Equation (7-15):

(7-15)

$$S_{dp} = \frac{h_p}{L_p N} \left( \frac{K}{K_{dp}} - \frac{K}{K_d} \right) \ln \frac{r_{dp}}{r_p}$$

where: N = number of perforations;  $r_{dp}$  = compaction zone radius, m;  $r_p$  = perforating radius, m; K = reservoir permeability,  $\mu\text{m}^2$ ;  $K_{dp}$  = compaction zone permeability,  $\mu\text{m}^2$ ;  $K_d$  = formation damage zone permeability,  $\mu\text{m}^2$ ;  $h_p$  = spacing of perforations, m;  $L_p$  = perforation penetration depth, m;  $r_{dp} = 0.0125 + r_p$ , m;  $K_{dp} = 0.1K$ ,  $\mu\text{m}^2$ .

### Other Parameters for Expressing Formation Damage

In addition to the S value, there also are some other methods of describing formation damage.

**Flow Efficiency FE.** Flow efficiency is defined as the actual to ideal productivity index ratio, as shown in Equations (7-16), (7-17), and (7-18).

(7-16)

$$FE = \frac{J_{\text{actual}}}{J_{\text{ideal}}}$$

(7-17)

$$J_{\text{actual}} = \frac{q}{p^* - p_{wf}}$$

(7-18)

$$J_{\text{ideal}} = \frac{q}{p^* - p_{wf} - \Delta p_s}$$

where:  $p^*$  = reservoir pressure, calculated by pressure build-up curve or measured;  $J_{\text{actual}}$  = actual productivity index;  $J_{\text{ideal}}$  = productivity index after deducting the additional pressure drop caused by formation damage, that is, the productivity index under the condition of no formation damage.

Thus flow efficiency FE equals the ratio between the pressure drawdowns without and with formation damage, as shown in Equation (7-19):

(7-19)

$$FE = \frac{p^* - p_{wf} - \Delta p_s}{p^* - p_{wf}}$$

Flow efficiency is also called productivity ratio PR, completeness ratio CR, or completion factor PF. These have the same meaning.

**Damage Ratio DR.** The reciprocal of flow efficiency is defined as damage ratio and shown in Equation (7-20).

(7-20)

$$DR = \frac{1}{FE}$$

In combination with Equation (7-19), DR is the ratio of the differential pressure drawdown with formation damage to pressure drawdown without formation damage, as shown in Equation (7-21).

(7-21)

$$DR = \frac{p^* - p_{wf}}{p^* - p_{wf} - \Delta p_s}$$

**Damage Factor DF.** DF is defined as the ratio of the additional pressure drop caused by formation damage to the total drawdown pressure, as shown in Equation (7-22).

(7-22)

$$DF = \frac{\Delta p_s}{p^* - p_{wf}}$$

In combination with Equation (7-19), it is shown in Equation (7-23).

$$(7-23) \quad DF = 1 - FE$$

**Completeness Index CI.** Completeness index CI and the Seven Rule used for diagnosing formation damage are presented by Tong Xianzhang. CI is defined as shown in Equation (7-24).

$$(7-24) \quad CI = \frac{p^* - p_{wf}}{m}$$

where:  $m$  = straight slope of radial flow of pressure build-up curve.

The literature [12] indicates that the  $\frac{0.117A}{r_w^2}$  value can be used as a criterion for diagnosing formation damage. Formation damage of an oil well is generated if  $CI > \frac{0.117A}{r_w^2}$ ; the oil well has good completeness if  $CI = \frac{0.117A}{r_w^2}$ ; and the oil well is nondamaged if  $CI < \frac{0.117A}{r_w^2}$ , where  $A$  means drainage area. On the basis of the drainage area data of the developed oil fields, the author of this literature then determined that the  $\frac{0.117A}{r_w^2}$  value is about 7. Thus the Seven Rule is used as a discriminant criterion of formation damage. The author considers that this rule is suitable for oil reservoirs of which the drainage area is about 0.5 km.

Substituting Equations (7-24) and (7-22) into Equation (7-5), the results in Equations (7-25) and (7-26) are obtained:

$$(7-25) \quad CI = \frac{1}{DF} \cdot \frac{S}{1.1513}$$

$$(7-26) \quad S = 1.1513 DF \cdot CI$$

or the result in Equation (7-27):

$$(7-27) \quad S = 1.1513(1 - FE) CI = 1.1513 \left( \frac{DR - 1}{DR} \right) CI$$

It is indicated that there are certain relations between the parameters mentioned earlier and the skin factor  $S$ .

**Effective Radius  $r_{we}$ .** The effective radius is defined as shown in Equation (7-28).

$$(7-28) \quad r_{we} = r_w \cdot e^{-S}$$

The physical meaning of effective radius is shown in Figure 7-1. When  $S = 0$ ,  $r_{we} = r_w$  (it means actual borehole radius). When  $S > 0$ ,  $r_{we} = r_{we2} < r_w$  (effective radius is smaller than completion borehole radius, which means a reduction of the borehole radius). Conversely, when  $S < 0$ , then  $r_{we} = r_{we1} > r_w$  (this means the increase of borehole radius).

In general, using the  $S$  value is sufficient for evaluating whether a well has formation damage. In general well test reports, the  $S$  value is only provided for indicating the degree of damage. However, the other parameters mentioned earlier can also be applied in order to analyze formation damage from different aspects (Table 7-5).

The formation damage evaluation criteria of homogeneous and fractured reservoirs are shown in Table 7-6. The evaluation criteria of the degree of damage of homogeneous reservoir and fractured reservoir are shown in Table 7-7.

### 7.3 FORMATION DAMAGE DIAGNOSIS OF HOMOGENEOUS RESERVOIR BY GRAPHIC CHARACTERISTICS

The well test data analysis has kept in close contact with the graphic analysis since the self-recording pressure gauge was used for studying the change of transient pressure in the 1940s.

In the 1950s, Horner found that the radial flow in a reservoir corresponds to the linear portion on a semilogarithmic data plot, and he presented the idea that this linear portion can be used for obtaining the value of reservoir permeability. This is a good application of graphic analysis. The bilogarithmic type curve match method was presented by Agarwal et al. in the 1960s and then developed by Gringarten et al., thus forming the current type curve match method of obtaining the values of parameters.

**TABLE 7-5 Formation Damage Evaluation Criteria of Homogeneous Reservoir**

No.	Evaluation Index	Symbol	Damaged	Normal	Stimulated
1	Skin factor	S	>0	=0	<0
2	Additional pressure drop	$\Delta p_s$	>0	=0	<0
3	Damage factor	DF	>0	=0	<0
4	Flow efficiency	FE	<1	=1	>1
5	Productivity ratio	PR	<1	=1	>1
6	Condition ratio	CR	<1	=1	>1
7	Completion coefficient	PF	<1	=1	>1
8	Damage ratio	DR	>1	=1	<1
9	Completeness index	CI	>7	=7	<7
10	Effective radius	$r_{we}$	< $r_w$	= $r_w$	> $r_w$

**TABLE 7-6 Evaluation Criteria of the Skin Factor S of Conventional Homogeneous Reservoir and Fractured Reservoir**

Reservoir	Damaged	Non-Damaged	Stimulated
Homogeneous reservoir	>0	0	<0
Fractured reservoir	>-3	-3	<-3

**TABLE 7-7 Evaluation Criteria of the Degree of Damage of Homogeneous Reservoir**

Homogeneous Reservoir	Most Serious Damage	More Serious Damage	Medium Damage	Slight Damage
Skin factor S	>10	5~10	2~5	0~2

The application of well test software undoubtedly provides a powerful measure for data interpretation. However, the solution method used for well test interpretation is a reverse problem in information theory, and there is a multisolution condition. Thus a graphic diagnosis is first required of well test engineers while using software in combination with the data of geophysics, geology, logging, and so on, to determine the type of reservoir model, and becomes an important part of human-computer interaction.

Graphic diagnosis is also important for reservoir engineers, on-site technical personnel, and management personnel, in addition to well test engineers.

For reasons given earlier, this chapter will place emphasis on the graphic analysis method, and the following goals are required to be achieved as far as possible:

1. Describing the effect of each parameter (especially skin factor S) on the shape characteristics of the well test curve in order to rapidly identify the type of reservoir and the range of parameter value on the basis of graphic characteristics.
2. Characterizing the reservoir using a simple mode chart with typical parameters.
3. Introducing some simple and convenient estimation methods, thus rapidly estimating the approximate ranges of reservoir parameters

(especially the degree of formation damage, that is,  $S$  value) on the basis of graphic characteristics with no need of well test software, which can not only directly guide production, but also can rapidly identify the interpretation results obtained by well test software.

Many types of graphs have been developed with the development of well test analysis methods. For convenience and practical purposes, this book selects only two types of graphs:

1. Composite bilogarithmic plot presented by Gringarten and Bourdet
2. Semilogarithmic plots of pressure, including semilog plot of pressure drop, MDH pressure build-up graph, Horner graph, and superposition function plot

The related literature can be consulted for other types of graphs.

### Graphic Characteristics of a Homogeneous Reservoir

The characteristics of homogeneous formation prevail in most sandstone formations of the

eastern area of China. Some carbonatite and sandstone formations with natural fractures often present the characteristics of homogeneous formation if the fractures are of a single type of uniform fracture. The so-called homogeneous media mean the theoretical models assumed during well test interpretation and indicate that the reservoir has the same permeability at various points and is isotropic in the range that is influenced by well testing. Thus a certain mathematical equation can be used for expressing the flow process.

**Composite Bilogarithmic Plot.** The composite bilogarithmic graph is a typical characteristic graph used for identifying a homogeneous reservoir. It has the shape of a two-tooth fork and can be divided into three portions for analyzing (see Figure 7-3).

1. The first portion has the shape of the handle of the fork. Both pressure and derivative curves join together and become a  $45^\circ$  straight line, which indicates an afterflow effect, that is, the effect of wellbore storage.
2. The second portion is the transition portion. The derivative curve slopes downward after the peak appears. The value of the peak is

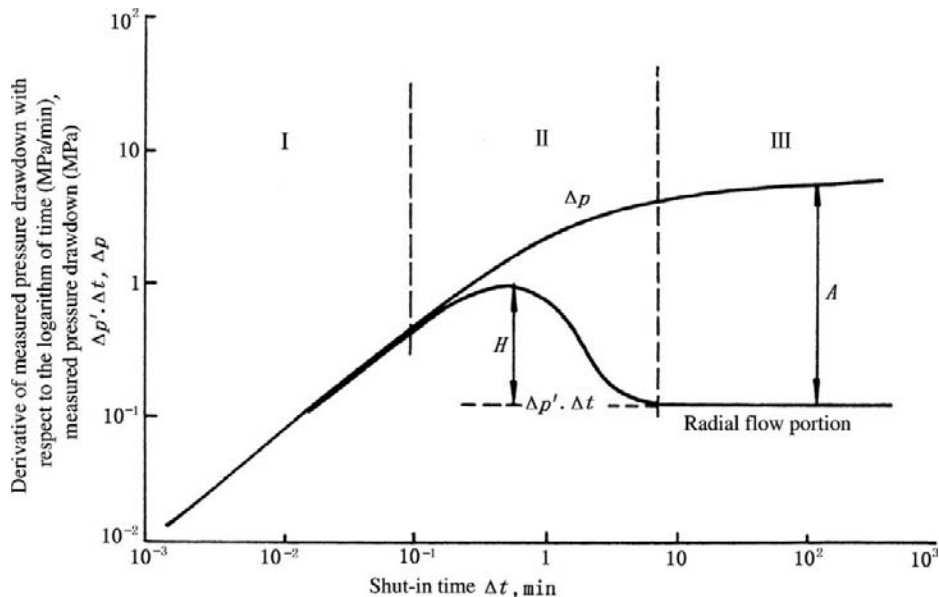


FIGURE 7-3 Composite bilogarithmic plot of homogeneous reservoir.

dependent on the value of parameter  $C_D e^{2S}$  where  $C_D$  is dimensionless wellbore storage coefficient and  $S$  is skin factor. The value of  $S$  has a greater effect due to its exponential position. The greater the  $C_D e^{2S}$  value, the higher the peak value and the steeper the downward slope; furthermore, the peak appears later.

The distance  $H$  between the peak of the derivative curve and the 0.5 horizontal line is related to the  $S$  value as shown in Equation (7-29).

(7-29)

$$S = 10^{(\sqrt{8.65H_D} + 6.14 - 2.75)} - \frac{1}{2} \ln C_D$$

$$H_D = H/Lc$$

where:  $Lc$  = logarithmic period length.

For instance, if the distance between the peak of the derivative curve and the 0.5 horizontal line, which is obtained from the actual measured diagram, is 80 mm and  $Lc$  is equal to 75 mm on log-log paper, then  $H_D = 80/75 = 1.07$ .

In addition,  $C_D = 100$  is obtained on the basis of the  $\Delta p/\Delta t$  data obtained in the early shut-in period and is substituted into Equation (7-29); thus  $S = 12.6$  is obtained.

3. The third portion is a horizontal portion, which is the typical characteristic of radial flow. In the dimensionless coordinate system, the ordinate value of the horizontal line is 0.5, which can be used for confirming the radial-flow straight-line portion on the semilogarithmic plot, such as Horner graph, MDH graph, and superposition function plot.

Before the horizontal portion of the derivative curve appears, both pressure and derivative curves have separated from each other and form a forked shape. The distance  $A$  between the horizontal line of derivative curve and the pressure curve is related to  $C_D e^{2S}$  as shown in Equation (7-30).

(7-30)

$$S = 10^{(\sqrt{5.53A_D} - 3.37 - 1.12)} - \frac{1}{2} \ln C_D$$

$$A_D = A/Lc$$

On the basis of an actual measured diagram, the  $A = 117$  mm can also be obtained. The  $A_D$  value obtained then is substituted into Equation (7-30), and then  $S \approx 12.58$  is also obtained.

The parameter  $C_D$  in Equations (7-29) and (7-30) is known as the dimensionless wellbore storage coefficient and is shown in Equation (7-31).

(7-31)

$$C_D = 0.15916 \frac{C}{\Phi C_t h r_w^2}$$

where:  $C$  = wellbore storage coefficient,  $m^3/MPa$ ;  $\Phi$  = porosity;  $C_t$  = total compressibility coefficient,  $MPa^{-1}$ ;  $h$  = reservoir thickness, m;  $r_w$  = wellbore radius, m.

It can be seen that all the parameters in Equation (7-31) are the parameters given in addition to  $C$ . The method of estimating  $C$  will be described in this chapter.

**Semilogarithmic Plot.** After the homogeneous reservoir is confirmed using a composite bilogarithmic plot and the stages of flow are divided, further analysis will mainly rely on the semilogarithmic plot. There are many types of semilogarithmic plots, and the MDH pressure build-up graph is used for illustration here.

### 1. Shape characteristics

The semilogarithmic plot has the shape of a tablespoon. The afterflow portion (the first portion) and the transition portion (the second portion) make up the spoon head. The radial flow portion (the third portion) is a straight line and is likened to the handle of the spoon. The characteristics of a semilogarithmic plot are shown in Figure 7-4.

The shape characteristics of a semilogarithmic plot include:

- a. Straight-line portion with slope  $m$ ;
- b. Late period afterflow portion with the maximum slope  $m'$ , of which, on the basis of most measured curves, the measurement points form an approximate straight line with slope  $m'$ , which is known as an apparent straight line;
- c. Having intersection  $D$  of the straight lines that have, respectively, the slopes of

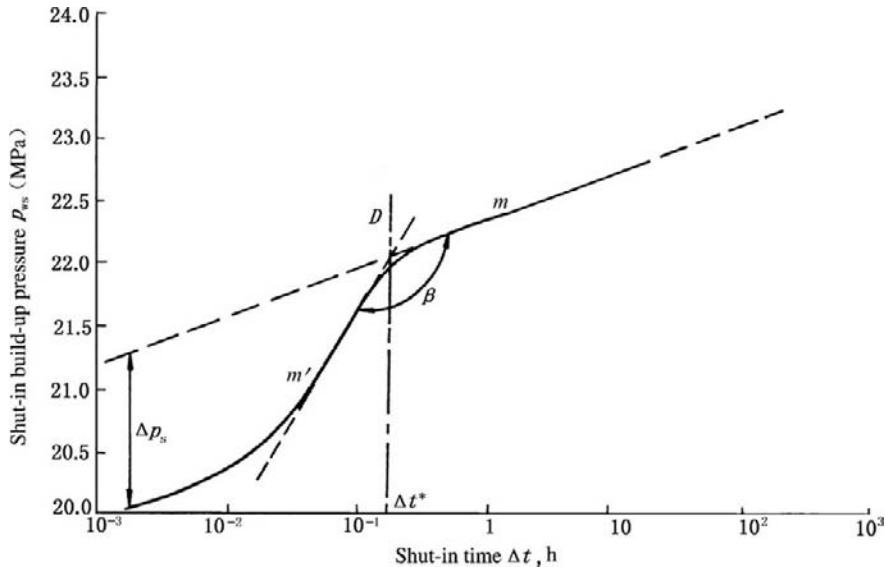


**FIGURE 7-4** Semilogarithmic pressure build-up plot of homogeneous reservoir.

$m$  and  $m'$  and having time coordinate  $\Delta t^*$  of intersection  $D$ ;

- d. Having included angle  $\beta$  between the straight lines with slopes  $m$  and  $m'$ ;
- e. Having a difference between the measured pressure and the bottomhole pressure generated by extending the straight line of radial flow when  $\Delta t$  is small, which represents the pressure difference formed by the effect of skin factor  $S$ .

The effects of the various parameters on the shape characteristics are discussed as follows.

2. Slope  $m$  of the straight-line portion

The  $m$  value and the reservoir parameters meet Equation (7-32):

(7-32)

$$m = 2.121 \times 10^{-3} \frac{qB\mu}{Kh}$$

Equation (7-32) indicates that the  $m$  value is inversely proportional to mobility  $k/\mu$  and is directly proportional to unit-thickness production rate  $qB/h$ .

3. Slope ratio  $m'/m$  and included angle  $\beta$

The  $m'/m$  value and included angle  $\beta$  are mainly affected by the parameter  $C_D e^{2S}$ .

In general, the greater the  $C_D e^{2S}$  value, the greater the  $m'/m$  value and the closer to  $90^\circ$  the  $\beta$  angle. Conversely, if the  $C_D e^{2S}$  value is smaller, then the  $m'/m$  value is close to 1 and the angle  $\beta$  value is close to  $180^\circ$  (Figure 7-5).

If  $C_D e^{2S} > 1$ , then  $1 < m'/m < 20$  and  $90^\circ < \beta < 180^\circ$  in general.

The relation between  $S$  and  $m'/m$  is shown in Equation (7-33).

(7-33)

$$S = 1.417 \left( \frac{m'}{m} - 1 \right) - \frac{1}{2} \ln C_D$$

The  $S$  value can also be calculated by using the  $m'/m$  value in Figure 7-5.

4. Time  $\Delta t^*$  at intersection  $D$

$\Delta t^*$  is approximately advanced by 0.5 log period in comparison with the initial time of the straight-line portion. The  $\Delta t^*$  value is mainly affected by the wellbore storage coefficient  $C$  and is also related to the  $S$  value and other reservoir parameters to a certain extent, as shown in Equation (7-34).

(7-34)

$$\Delta t^* = \frac{\Phi C_t \mu r_w^2}{3.6K} C_D (3.1S + 3.57 \lg C_D + 11.6)$$

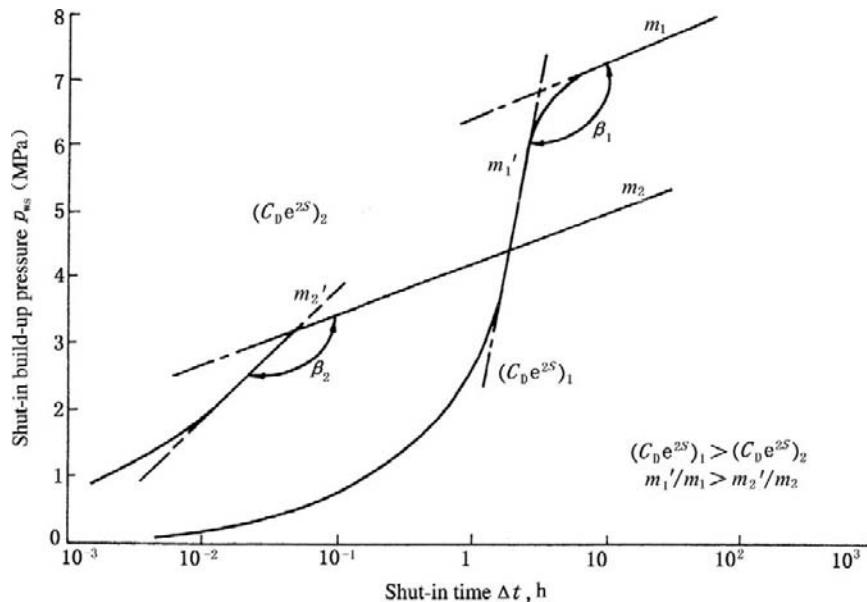


FIGURE 7-5 Effect of  $C_D e^{2S}$  value on the shape of semilogarithmic curve.

Under the conditions of low-permeability reservoir (low  $k/\mu$  value) and shutting-in at the wellhead (high  $C_D$  value),  $\Delta t^*$  may be greater than clock range; thus, only the afterflow portion can be measured. Conversely, when the  $k/\mu$  value is high and the  $C_D$  value is low, the initial testing point may be greater than  $\Delta t^*$  (especially when a mechanical pressure gauge with low resolution is used); thus, only the radial-flow straight-line portion can be measured, and the afterflow portion is not included. This condition has appeared in the well of the Buried Hill reservoir in the Huabei oil field.

5. Pressure drop  $\Delta P_s$  caused by skin factor  $S$

The  $\Delta P_s$  is mainly affected by the  $S$  value. It is inversely proportional to  $k/\mu$  and is directly proportional to  $qB/h$ .

The following points can be summed up:

1. The slope  $m$  of the radial-flow straight-line portion is inversely proportional to the mobility  $\frac{k}{\mu}$  and is directly proportional to the unit-thickness production rate  $\frac{qB}{h}$ .

2. When  $C_D e^{2S} > 1$ , both the ratio  $m'/m$  of the apparent straight-line slope  $m'$  of afterflow to the straight-line slope  $m$  of radial flow and the included angle  $\beta$  are mainly affected by the  $S$  value and are less affected by  $C_D$ .
3. The intersection time  $\Delta t^*$  is mainly affected by the  $C$  and  $k/\mu$  values. It is directly proportional to  $C$ , is inversely proportional to  $k/\mu$ , and is less affected by the  $S$  value.
4. The down-dip amplitude ( $\Delta P_s$  value) of the afterflow portion from the straight-line portion is dependent on the  $S$  value and is directly proportional to  $S$ .

The various combinations of  $k/\mu$ ,  $S$ ,  $C$ , and  $qB/h$  values will form a series of curves with various shapes, which will be introduced later in this chapter in combination with the cases.

### Gradation of $k/\mu$ , $S$ , and $C$

1. Gradation of mobility  $k/\mu$  value

$k/\mu$  is a measure of the flowability of fluid in the reservoir. For convenience, it is divided into seven grades (unit:  $10^{-3} \mu\text{m}^2/\text{MPa} \cdot \text{s}$ ): (1) very high for  $k/\mu > 10^4$ ; (2) high for  $10^4 > k/\mu > 10^3$ ; (3) slightly high for  $10^3 > k/\mu > 10^2$ ; (4) medium for  $10^2 > k/\mu > 10$ ;

(5) slightly low for  $10 > k/\mu > 1$ ; (6) low for  $1 > k/\mu > 0.1$ ; and (7) very low for  $k/\mu < 0.1$ .

## 2. Gradation of C value

The wellbore storage coefficient is affected by various factors such as shut-in valve location, wellbore fluid properties, and free liquid level; thus it is rather difficult to calculate exactly the value of C. However, the value of C can be approximately estimated on the basis of the well condition. This can contribute to the verification and analysis of pressure data and to the well test design (see Table 7-8).

If the C value obtained by well test curve analysis is coincident with the well condition mentioned earlier, the result is correct. If the difference is great, it is possible that an error was generated in the analysis process or some factors such as packer leakage and the gas interbed that have not been known have not been considered. Thus the C value analysis is closely related to identifying the test analysis result and finding new problems in the well and reservoir. As mentioned earlier, the C value may greatly affect the shape of the curve and the duration of radial flow. Therefore, the C value is of great importance.

## 3. Gradation of the S value

The S value shows the degree of formation damage and is also related to the degree of perforation penetration, the turbulent flow generated by high velocity gas, the fractures generated by acid fracturing, and so on. The gradation of the C value is shown in Table 7-9.

**TABLE 7-9** Gradation of the Value of Skin Factor S

Grade	Order of S Value	Approximate Value of $C_D e^{2S}$
Very high	$>20$	$>10^{15}$
High	$5\sim20$	$10^3\sim10^{15}$
Medium	$1\sim5$	$10\sim10^3$
Slight low	$(-1)\sim1$	$5\sim10$
Low	$<-3$	$0.5\sim5$
Very low		$<0.5$

The additional pressure drop caused by blocking is not dependent fully on the S value because  $\Delta P_s$  is directly proportional to S and  $qB/h$  and is inversely proportional to  $k/\mu$ . The  $\Delta P_s$  value may be lower than 1 MPa despite the possible high value of S.

## Location Analysis Method of Well Test Curves for a Homogeneous Reservoir

**Meaning of Location Analysis.** The semilogarithmic plot of measured pressure under the condition of homogeneous reservoir may vary due to different values of  $k/\mu$ , S, C,  $qB$ , and h, thus causing difficulties in identification, analysis, and verification of the data.

The dimensionless semilogarithmic plot of a homogeneous reservoir is shown in Figure 7-6.

**TABLE 7-8** Gradation of Wellbore Storage Coefficient C

Grade	Order of C Value ( $m^3/MPa$ )	Well Condition
Very high	$>10$	Deep gas well, shutting in at wellhead
High	$1\sim10$	High gas content well or simultaneous tubing and casing liquid level build-up well
Slightly high	$0.1\sim1$	Gas column well, shutting in at wellhead, or tubing liquid level build-up well
Medium	$0.05\sim0.1$	Shutting in at tubing head, medium-low gas-oil ratio
Slightly low	$0.01\sim0.05$	Shutting in at tubing head, net oil or water in well, or shutting in by downhole shut-in tool, longer sump hole
Low	$0.001\sim0.01$	Shutting in by downhole shut-in tool
Very low	$<0.001$	Shutting in at downhole, very short sump hole

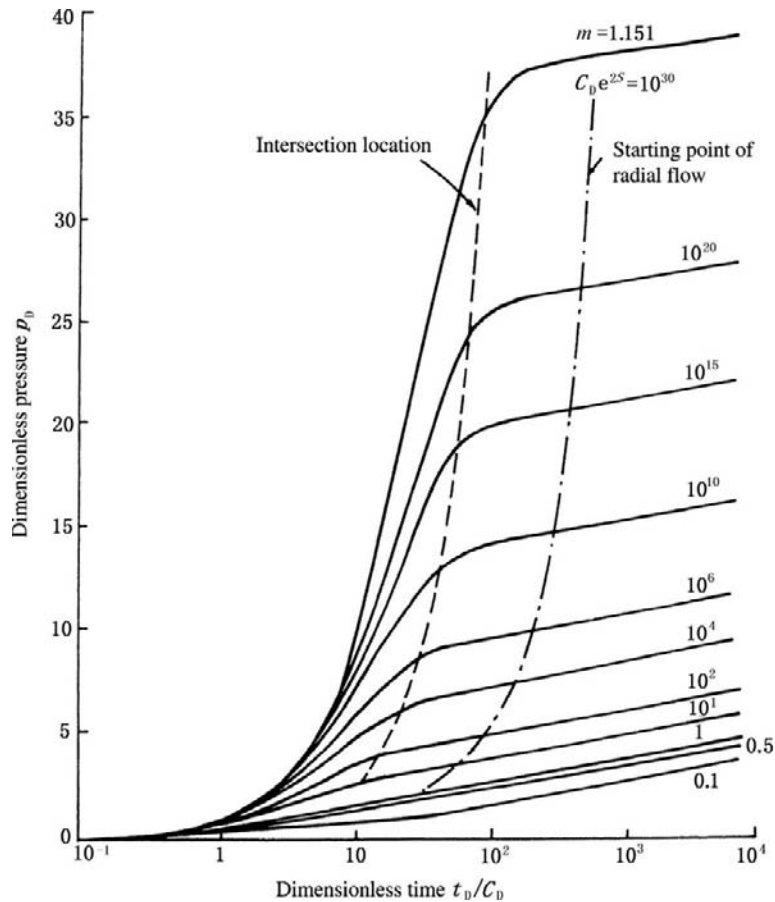


**FIGURE 7-6** Dimensionless semilogarithmic plot of pressure drawdown test of homogeneous reservoir.

In practice, the semilogarithmic plot based on measured data is some specific part of some curve in Figure 7-6. After this part is determined, it can be reconverted into a dimensional coordinate plot on the basis of the measured reservoir parameters.

It should especially be noticed that when the dimensionless coordinates are reconverted to the dimensional coordinates, the location of the curve is restricted. The reasons are as follows.

1. Recording time has a lower limit. Due to the limitation of the point interval of recording pressure data by gauge, the initial or first

point can only be measured by seconds for an electronic pressure gauge or by minutes for a mechanical pressure gauge.

2. Pressure data recording time has an upper limit. The working time of a mechanical pressure gauge can only be several hours or several dozens of hours for running once. The working time of an electronic pressure gauge may be longer. The on-bottom working time of a direct-reading electronic pressure gauge can be infinite in principle; however, the gauge can only work for several hundred hours in practice because of the limitations of on-site working conditions.

3. The pressure value that can be recorded has a lower limit. The measurable minimum value of change in pressure is limited due to the limitation of gauge resolution. It is up to 0.00007–0.00014 MPa for an electronic pressure gauge, while it is only 0.01–0.001 MPa for a mechanical pressure gauge in general.

On the basis of the limitation of the actual recording ability of the downhole gauge, the location of the measured curve in Figure 7-6 is determined and is shown by dimensional coordinate scale, thus confirming the shape of the measured curve. This course of action is known as location analysis.

**Time Locating.** The initial time is first located. In general, the time of the first data point recorded by electronic pressure gauge is 1 to 3 seconds, and the time of 10 seconds is taken as the first point in consideration of a certain course of shut-in operation. The time of the initial point for mechanical pressure gauge is temporarily fixed at 1 minute. Thus for a specific reservoir and well, the dimensionless time at the initial point is calculated as shown in Equation (7-35):

$$(7-35) \quad \left(\frac{t_D}{C_D}\right)_i = 22.62 \frac{Kh}{\mu C} \cdot \Delta t_i$$

where  $i$  means initial. The  $(t_D/C_D)_e$  at the end point ( $e$  means end) has a similar calculation formula but the  $\Delta t_i$  is substituted by  $t_e$ . For instance, if  $k/\mu = 0.1 \mu\text{m}^2/\text{MPa} \cdot \text{s}$ ,  $h = 10 \text{ m}$ ,  $C = 0.1 \text{ m}^3/\text{MPa}$ ,  $q_B = 10 \text{ m}^3/\text{d}$  and  $\Delta t_i = 1 \text{ min}$ , then  $(t_D/C_D)_i = 3.77$ ; if  $t_e = 4 \text{ h}$ , then  $(t_D/C_D)_e = 904.8$ .

**Pressure Locating.** Different types of pressure gauges have different resolution values. When a mechanical pressure gauge with a resolution of 0.01 MPa is used, the initial pressure point is calculated as follows.

$$(p_D)_i := 542.87 \frac{Kh}{\mu} \cdot \frac{1}{q_B} \cdot \Delta p = 542.87 \times \frac{1}{10} \times 10 \times \frac{1}{10} \times 0.01 = 0.543$$

There is no upper limit of pressure generally.

**Curve Locating.**  $S$  and  $C$  values can be estimated on the basis of the well completion data and the hole structure during testing, and then the  $C_{De}^{2S}$  value can be calculated. In combination with the location time and location pressure calculated earlier, the shape of the measured curve can be determined. This location analysis can be used for conducting well test design and also for identifying and verifying the measured data, and the  $S$  and  $C$  values are the parameters of practical well test curve interpretation then.

**Cases of Location Analysis.** Figures 7-7 and 7-8 show the shapes of the curves of various cases after locating. The values of various parameters are listed in Table 7-10.

In Figure 7-7 the b-e portion shows the locating condition in Case 1. It is an integral pressure build-up curve with afterflow portion b-d and radial-flow straight-line portion d-e and can be used for calculating reservoir parameters.

Case 2 corresponds to the condition of a high-permeability reservoir, high gas-oil ratio, and wellhead shut-in testing. The curve is the c-f portion in the location block. It has a longer radial-flow straight-line portion despite the fact that the afterflow portion is absent.

Case 3 corresponds to the condition of medium-mobility reservoir and shutting in at the wellhead. The location curve is the a-d portion in the location block. This curve only has an afterflow portion, and the straight-line portion is absent. The conventional method cannot be used for calculating the parameters.

Case 4 corresponds to the condition of a high-permeability reservoir with a high degree of damage and a high wellbore storage coefficient  $C$ . The curve is in the shape of an inverted L. The curves for some low-medium permeability gas reservoirs are also in this shape due to the low viscosity of gas. These indicate that when the  $\beta$  angle is close to  $90^\circ$ , this type of curve means serious formation damage, and stimulation is required.

#### Application of Location Analysis

1. Verifying and analyzing the results of well test interpretation;

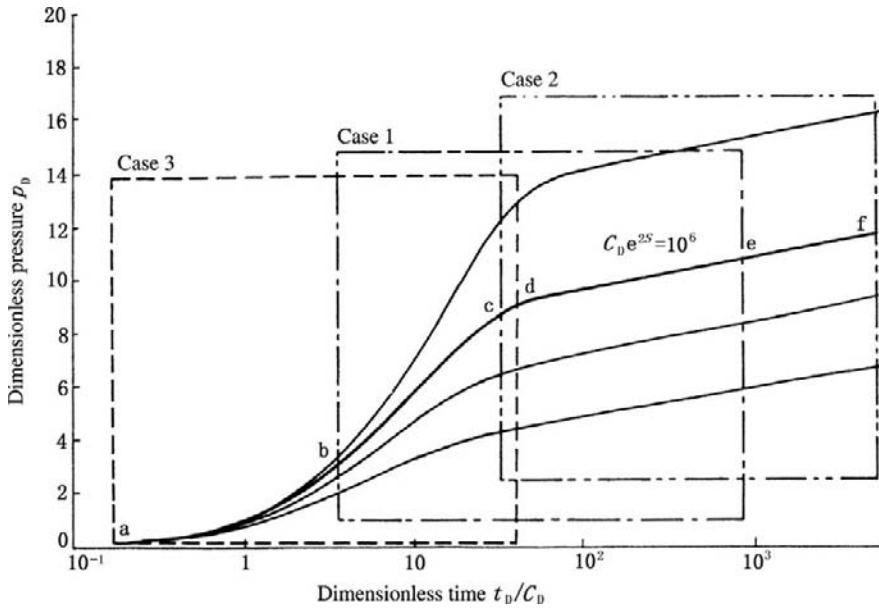


FIGURE 7-7 Location analysis method.

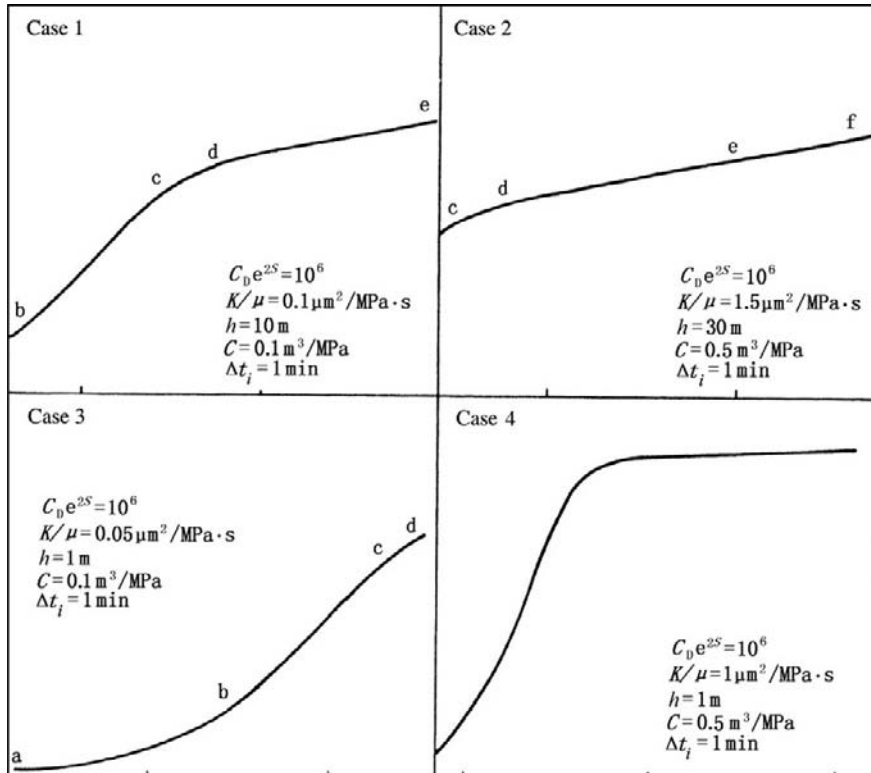


FIGURE 7-8 Cases of location analysis.

TABLE 7-10 Cases of Location Analysis

Case No.	Parameters of Case								Curve Location		
	$C_{De}^{2S}$	$\frac{K/\mu}{\text{MPa} \cdot \text{s}}$	$h$ m	$C$ $\text{m}^3/\text{MPa}$	$\Delta t_i$ min	$\Delta t_e$ h	$\Delta p t_i$ MPa	$qB$ $\text{m}^3$	$\left(\frac{t_D}{C_{De}}\right)$	$\left(\frac{t_D}{C_{Di}}\right)$	$P_{Di}$
1	$10^6$	0.1	10	0.1	1	4	0.01	10	3.77	904.8	0.543
2	$10^6$	1.5	30	0.5	1	4	0.01	100	33.93	$8.14 \times 10^{-3}$	2.44
3	$10^6$	0.05	1	0.1	1	4	0.01	10	0.188	45.24	0.027
4	$10^{30}$	1	1	0.5	1	4	0.01	10	7.5	$1.5 \times 10^3$	0.543

2. Making a well test design by using the location analysis method, that is, making a quantitative simulation for testing after electing parameters and making a semilogarithmic plot, of which the steps include:
  - a. Estimating the values of  $k$  and  $\mu$  on the basis of logging data and the condition of adjacent well and calculating the value of  $k/\mu$ ;
  - b. Obtaining the value of porosity  $\Phi$  from coring and logging data;
  - c. Estimating the values of  $S$  and  $r_w$  by using well completion data;
  - d. Estimating the value of  $C$  in the light of the hole structure of the tested well;
  - e. Calculating the values of  $C_D$  and  $C_{De}^{2S}$  by using Equation (7-31) and  $C_t h r_w^2$ ;
  - f. Calculating the values of  $(t_D/C_D)_i$ ,  $(t_D/C_D)_e$ , and  $(P_D)_i$  by using the location analysis method on the basis of the set value of  $qB/h$ , and then making the simulation curve in the coordinates of  $(t_D/C_D)_e$  and  $P_D$ , as shown in Figure 7-7;
  - g. Transforming the located simulation curve into a dimensional design simulation curve.

If the curve obtained meets the requirements of data analysis (there is no clear radial-flow straight-line portion, for instance), the test is operated in accordance with the original plan. If the simulation curve does not meet the requirements of data analysis, then the test plan should be changed and the test time is adjusted, the test gauge is changed, or the well is shut in another manner in order to meet the desired requirements.

## 7.4 GRAPHIC CHARACTERISTICS OF A DUAL POROSITY RESERVOIR AND A RESERVOIR WITH A HYDRAULICALLY CREATED FRACTURE

### Graphic Characteristics of a Dual Porosity Reservoir

A dual porosity reservoir is also known as a natural fracture porosity reservoir. It means the reticulate fracture storage space formed by the weathering and leaching of the crevices that were generated under in-situ stress or chemical action during the long geological period. In general, a dual porosity reservoir consists of the fracture system, which has fracture width larger than  $10 \mu\text{m}$ , low porosity (1% to 2%), high permeability (Darcy grade), and high oil saturation (up to more than 90%), and the matrix system, which has fracture width of  $1\text{--}10 \mu\text{m}$ , higher porosity (2% to 5%) and low permeability ( $1$  to  $50 \times 10^{-3} \mu\text{m}^2$ ). Thus the oil and gas account for the greater part, which, stored in the matrix, can only flow to the bottomhole through fractures (Figure 7-9).

This type of reservoir was first studied by Bawertlatt and the study results have been improved by many researchers, thus forming a relatively integral theory.

The following parameters are defined:

Graphic parameter of fracture system  $(C_{De}^{2S})_f$

Graphic parameter of total system  $(C_{De}^{2S})_{f+m}$

Storativity ratio:

$$\omega = \frac{(\Phi C_t h)_f}{(\Phi C_t h)_f + (\Phi C_t h)_m}$$

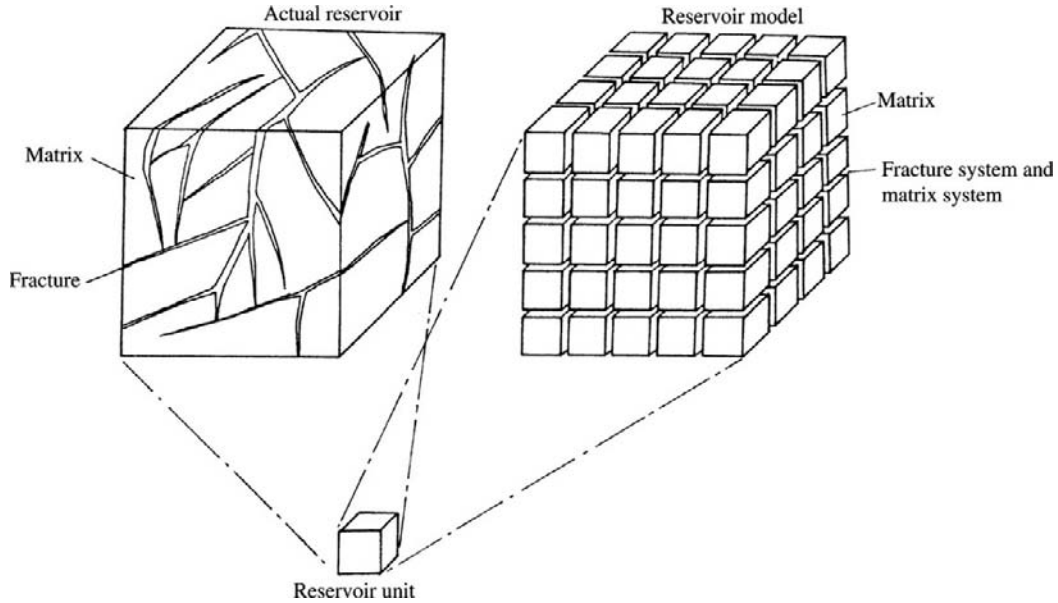


FIGURE 7-9 Dual porosity reservoir unit structure.

Interporosity flow coefficient:

$$\lambda = \frac{\alpha K_m r_w^2}{K_f}$$

Curve location parameter:

$$\frac{K_f h}{\mu c}$$

Interporosity transient flow parameter:

$$\beta = \frac{1.89(C_D e^{2S})_{f+m}}{\lambda e^{-2S}}$$

The aforementioned  $\omega$  and  $\lambda$  can also be as shown in Equations (7-36) and (7-37).

(7-36)

$$\omega = \frac{(C_D e^{2S})_{f+m}}{(C_D e^{2S})_f}$$

(7-37)

$$\lambda = \frac{\lambda e^{-2S}}{e^{-2S}}$$

where  $C_D e^{2S}$  and  $\lambda e^{-2S}$  can be obtained by type curve match.

It is shown that almost all of the parameters affecting the well test curve of a double

porosity reservoir are directly related to the value of skin factor  $S$ , which marks formation damage. However, this effect is more complicated in comparison with that of a homogeneous reservoir.

It should especially be noticed that in a double porosity reservoir, the fractures used as channel connecting with the bottomhole make the vicinity of the wellbore have a better connectedness; thus, the  $S$  value of  $-3$  is used as division criterion when the value of  $S$  is adopted for diagnosing the degree of formation damage in the near-wellbore area. Stimulation has been taken if  $S < -3$ ; formation damage has not been caused if  $S = -3$ ; and formation damage has been generated if  $S > -3$ .

**Two Radial Flow Portions.** Conditions of appearance and typical combination of parameters are as follows.

1. Dual porosity reservoir and interporosity pseudosteady flow with the effects of wellbore storage coefficient  $C$  and skin factor  $S$ ;
2.  $(C_D e^{2S})_t = 10^2$  and  $(C_D e^{2S})_{f+m} = 10$ , which indicate low values of graphic parameters or low value of skin factor  $S$ ;

- $\omega = 0.1$ , which indicates a high storativity ratio or a certain quantity of fluid in fractures;
- $\lambda = 10^{-7}$ , which indicates a low interporosity flow coefficient or great resistance to fluid flow from matrix pores to fractures.

A composite bilogarithmic plot that meets the aforementioned conditions can be divided into the following flow portions (Figure 7-10):

- a-b: Afterflow portion similar to that of a homogeneous reservoir. Curve shape is determined by  $(C_D e^{2S})_f$ .
- b-c: Radial flow portion of fracture. The derivative curve in this portion is a horizontal line with a derivative value of 0.5.
- c-d: Matrix-fracture transition portion. The derivative curve is concave downward and then rises to the horizontal line with a derivative value of 0.5. The dropping and rising of the curve are respectively dependent on

$$\frac{\lambda C_D}{\omega(1-\omega)} \text{ and } \frac{\lambda C_D}{1-\omega}.$$

- d-e: Radial flow portion of total system.

A semilogarithmic plot that meets the aforementioned conditions is shown in Figure 7-11. However, although the existence of this type curve has been theoretically proved, no case has been collected in the field so far.

**Radial Flow Portion of Total System Appears Only.** This is the most common typical condition in oil and gas fields. Conditions of appearance and typical parameters are as follows.

- Interporosity pseudosteady flow with the effects of C and S.
- $(C_D e^{2S})_f = 10^4$  and  $(C_D e^{2S})_{f+m} = 10^2$  with a large  $C_D$  value, which indicate that the effect of afterflow conceals the radial flow portion of fracture and the first radial flow portion cannot be displayed.
- $\omega = 0.01$ , which indicates a low storativity ratio and that fluid is mainly stored in the matrix, so that the portion of flow in fractures is short and easily concealed by the afterflow portion.
- $\lambda = 10^{-6}$ , which indicates a medium interporosity flow coefficient under which not only can the radial flow portion of fracture be concealed, but also the transition flow portion can be retained.

A composite bilogarithmic plot that meets the aforementioned conditions is shown in Figure 7-12. Figure 7-13 is the corresponding semilogarithmic plot.

- a-b-c: This portion is the afterflow portion plus the matrix-fracture transition portion. The former (a-b) portion is mainly affected

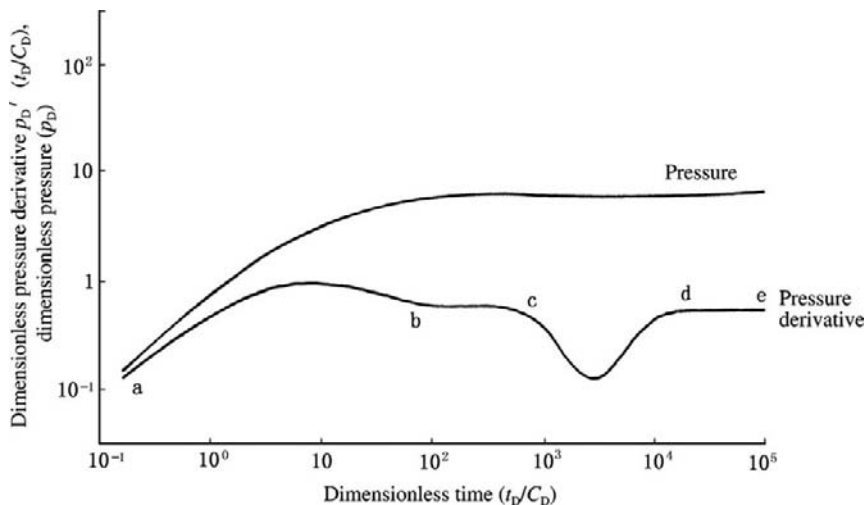


**FIGURE 7-10** Bilogarithmic plot with two radial flow portions under the condition of dual porosity reservoir.

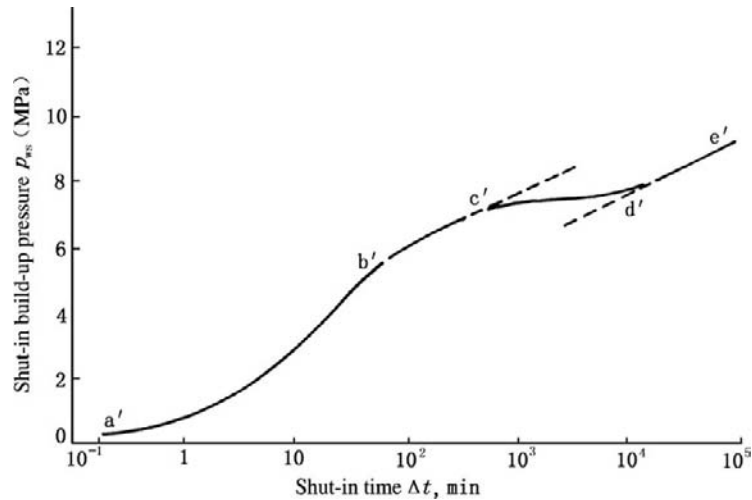


**FIGURE 7-11** Semilogarithmic mode chart with two radial flow portions under the condition of double porosity reservoir.

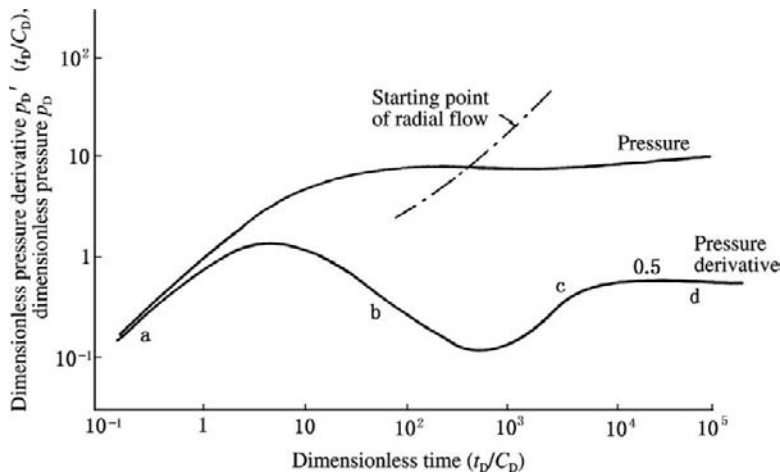


**FIGURE 7-12** Bilogarithmic mode chart having only the radial flow portion of total system under the condition of double porosity reservoir.

- by afterflow, while the latter (b-c) portion is mainly affected by transition flow. The (b-c) portion of the derivative curve is concaved downward and lower than 0.5 horizontal line and is mainly affected by interporosity flow.
2. c-d: This portion is the 0.5 derivative horizontal line, which means that the radial flow of the total system is achieved.
3. a'-b'-c': This portion is the S-shaped transition portion plus the afterflow portion. It is different from that of a homogeneous reservoir in that the b' point is above the extended line of radial-flow straight-line portion c'-d'.
4. c'-d': This portion is the radial flow portion of the total system and can be used for calculating reservoir parameters.

**Case 1**

1. Well test conditions: Sinian dolomite reservoir, 3090 m well depth, 19.5 m reservoir thickness, dry gas produced,  $9.9 \times 10^4 \text{ m}^3/\text{d}$  daily gas production rate.
2. Well test results (see Figure 7-14): The graphic characteristics coincide with that of the mode chart (Figure 7-12). The interpretation

results include: fracture permeability  $K_f = 1.97 \times 10^{-3} \mu\text{m}^2$ , skin factor  $S = -2.3$ , wellbore storage coefficient  $C = 2.5 \text{ m}^3/\text{MPa}$ , graphic parameter  $(C_{DE}^{2S})_f = 30.05$ ,  $(C_{DE}^{2S})_{f+m} = 1.8$ , storativity ratio  $\omega = 0.06$ , and interporosity flow coefficient  $\lambda = 0.96 \times 10^{-6}$ . Skin factor  $S = -2.3$  (close to  $-3$ ) indicates that the dual porosity reservoir is basically undamaged.

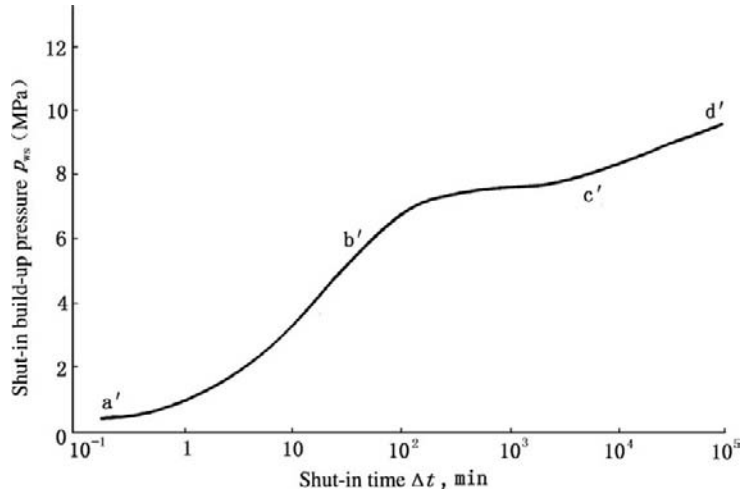


**FIGURE 7-13** Semilogarithmic mode chart having only the radial flow portion of total system under the condition of double porosity reservoir.

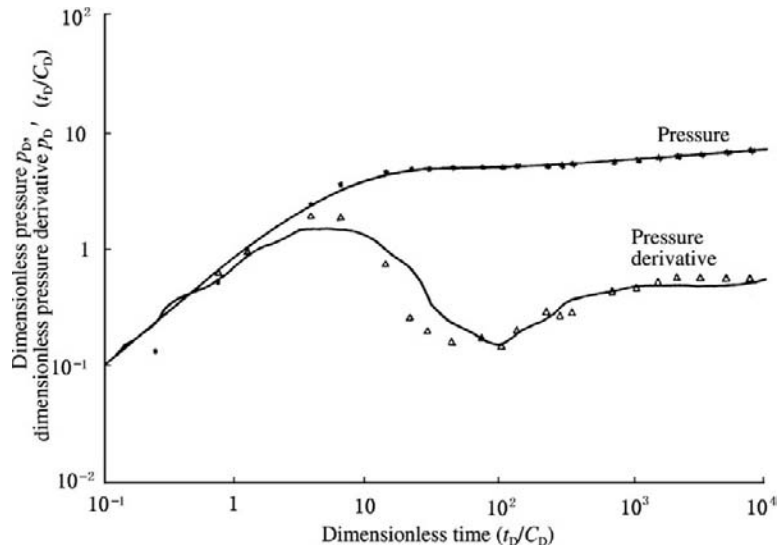


**FIGURE 7-14** Composite bilogarithmic plot of Case 1.

**Case 2**

1. Well test conditions: Carboniferous dolomite reservoir, 4000 m well depth, 19.4 m reservoir thickness, dry gas produced,  $8.3 \times 10^4 \text{ m}^3$  daily gas production rate. Pressure was measured by using a mechanical pressure gauge under the condition of wellhead shut-in and opening.
2. Well test results (see Figure 7-15): The curves measured are basically similar to those in the mode chart (Figure 7-12). A clearer radial flow portion of the total system may be measured if the testing time is further prolonged. The interpretation results include:  $K_f = 4.97 \times 10^{-3} \mu\text{m}^2$ ,  $S = -0.7$ ,  $C = 1.72 \text{ m}^3/\text{MPa}$ ,  $(C_{De}^{2S})_f = 2220$ ,  $(C_{De}^{2S})_{f+m} = 222$ ,  $\omega = 0.01$ , and  $\lambda = 6.57 \times 10^{-6}$ .  $S = -0.7$  indicates that formation damage is generated.

**Case 3**

1. Well test conditions: Ordovician dolomite reservoir, natural fractures (by core observation), 3660 m well depth, 156 m reservoir thickness, and  $340 \text{ m}^3/\text{d}$  daily oil production rate. Bottomhole shut-in was adopted for drillstem testing during drilling, which may only have a slight effect of afterflow.
2. Well test results (see Figure 7-16): The interpretation results include:  $K_f = 0.27 \times 10^{-3} \mu\text{m}^2$ ,  $S = -0.77$ ,  $\omega = 0.08$ ,  $\lambda = 9.4 \times 10^{-4}$ ,  $C = 7.18 \times 10^{-2} \text{ m}^3/\text{MPa}$ ,

$(C_{De}^{2S})_f = 37.5$ , and  $(C_{De}^{2S})_{f+m} = 3$ .  $S = -0.77$  indicates that formation damage of the dual porosity reservoir is generated and may be improved by acidizing.

In addition, under the condition of double porosity reservoir, a method of estimating the value of  $\omega$  by using the bilogarithmic plot is shown in Equation (7-38).

**(7-38)**

$$\omega = 10^{-2L_D}$$

$$L_D = \frac{L_\omega}{L}$$

where:  $L_D$  = dimensionless concave depth of transition portion;  $L_\omega$  = concave depth of derivative curve (Figure 7-12);  $L$  = each logarithmic period length in bilogarithmic coordinates.

For instance, in Case 2 (Figure 7-15),  $L_\omega$  is approximately equal to one logarithmic period length; thus  $L_D = 1$ , and then  $\omega = 10^{-2 \times 1} = 0.01$ . This is coincident with the interpretation results of well test software.

**Graphic Characteristics of a Reservoir with Hydraulically Created Fracture**

A reservoir with a hydraulically created fracture is also known as an artificially fractured reservoir and has a reservoir model that is completely

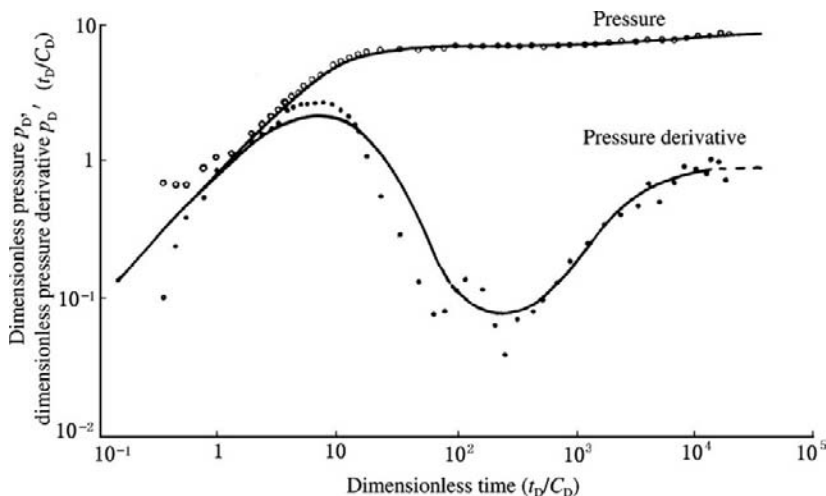


FIGURE 7-15 Composite bilogarithmic plot of Case 2.

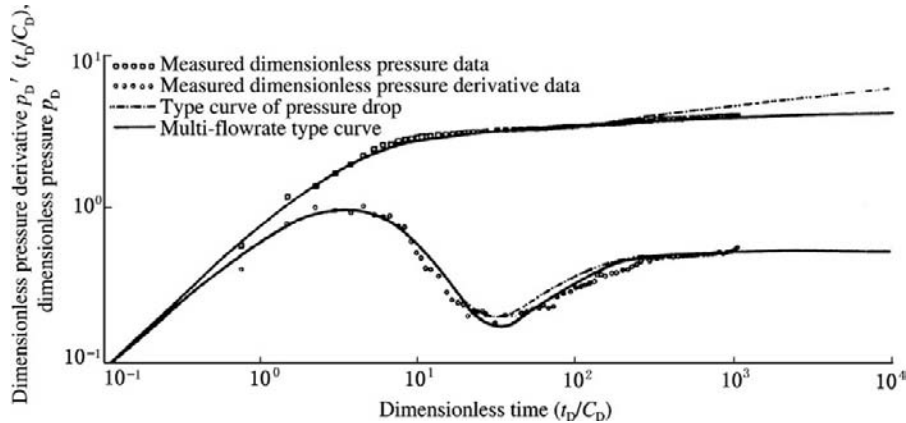


FIGURE 7-16 Composite bilogarithmic plot of Case 3.

different from that of a naturally fractured reservoir. The hydraulically created fracture is a single large fracture formed during hydraulic fracturing and has a high flow conductivity (Figure 7-17).

Hydraulic fracturing can be adopted under the condition of homogeneous reservoir (such as tight sand) or double porosity reservoir (such as dolomite with natural fracture), and a single fracture may often be formed because the high-pressure fluid injected will first move forward in the direction with higher in situ stress; that is, the fracture face is always perpendicular to the direction with lower in situ stress. After having been generated, the fracture may be continuously extended in the initial cracking direction. Under the condition of shallow reservoir, a horizontal fracture may be formed due to a low overburden pressure, while under the condition of

deep reservoir, a vertical fracture, which is often met, may be formed. A homogeneous reservoir cannot be changed to a double porosity reservoir by fracturing. However, in a double porosity reservoir, a large fracture may be formed by fracturing, thus losing the original double-porosity characteristics of a pressure build-up curve. A slope of 1/2 is characteristic of the curve under the condition of hydraulically created fracture.

Such a well, which intersects a single large fracture, has been studied since 1937, and more than 40 types of theoretical models have been created so far. These models can be divided into the following categories:

1. Vertical fracture with infinite flow conductivity, which is formed by hydraulic fracturing
2. Vertical uniform-flux fracture
3. Vertical fracture with finite flow conductivity, which is formed by sand fracturing
4. Horizontal fracture formed in shallow reservoir during fracturing

In addition, an early-stage afterflow portion may be formed due to the effect of wellbore storage under the aforementioned condition.

**Mode Charts under Vertical Fractures with Infinite Flow Conductivity and Uniform Flux.** The mode chart under vertical fracture with infinite flow conductivity is similar to that under vertical uniform-flux fracture except that the time when the linear flow appears is different. The mode charts under these conditions

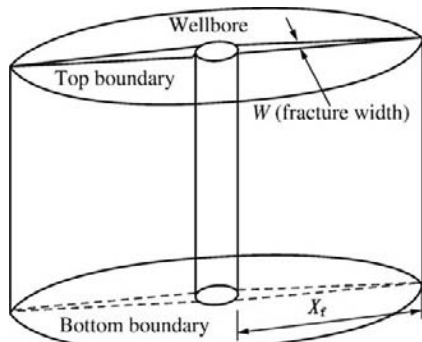
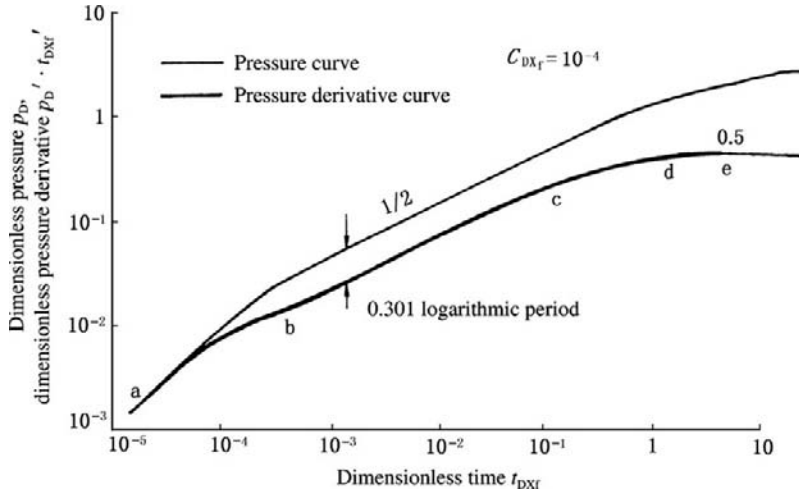


FIGURE 7-17 Hydraulically created fracture shape.



**FIGURE 7-18** Bilogarithmic mode chart of homogeneous reservoir under vertical fractures with infinite flow conductivity and uniform flux.

are greatly different from those under the condition of double porosity reservoir and can be divided into the following portions (Figure 7-18):

1. a-b: Afterflow portion. The curve shape is similar to that of a homogeneous reservoir. The dimensionless wellbore storage coefficient is shown in Equation (7-39).

(7-39)

$$C_{DXf} = 0.15916 \frac{C}{\Phi C_f h X_f^2}$$

where  $X_f$  = vertical fracture half-length. The value of  $C_D$  is about  $1/10^4$  to  $1/10^6$  times that of a homogeneous reservoir.

2. b-c: Linear flow portion. The pressure and pressure derivative curves are parallel lines with a slope of  $1/2$ . The ordinate distance between the two lines is 0.301 logarithmic period. In this portion, the dimensionless pressure is shown in Equation (7-40).

(7-40)

$$P_D = \sqrt{\pi t_{DXf}}$$

that is, as shown in Equation (7-41),

(7-41)

$$\log P_D = \frac{1}{2} \lg t_{DXf} + 0.24857$$

It indicates that in a bilogarithmic plot, it is a straight line with a slope of  $1/2$ . The upper limits of  $t_{DXf}$  under infinite flow conductivity and uniform flux are respectively equal to or less than 0.016 and 0.16. In this portion, the dimensionless pressure derivative is shown in Equation (7-42).

(7-42)

$$\log (P_D' \cdot t_{DXf}') = \frac{1}{2} \lg t_{DXf} - 0.05246$$

It indicates that in a bilogarithmic plot, it is also a straight line with a slope of  $1/2$ . The span between the two straight lines is shown in the following formula:

$$0.24857 + 0.05246 = 0.301$$

This is the most important characteristic of vertically fractured wells under infinite flow conductivity and uniform flux.

3. c-d: Transition portion. The abscissa interval is about  $0.016 \leq t_{DXf} \leq 3$ .
4. d-e: Pseudoradial flow portion. The pressure derivative curve is a horizontal line, and the value of the dimensionless pressure derivative is equal to 0.5.

In the semilogarithmic plot, the curve mentioned earlier is continuously bent upward (Figure 7-19), and the a'-b', b'-c', c'-d', and d'-e' portions correspond to the relevant portions in the bilogarithmic plot.

#### Case 4

1. Well test conditions: Triassic sandstone reservoir, 1900 m reservoir depth, 11.0 m reservoir thickness, 26 m<sup>3</sup>/d daily oil production rate. After producing for 40 days, the pressure build-up curve was measured at the bottomhole by using an electronic pressure gauge under the condition of wellhead shut-in. Hydraulic fracturing had been taken before well testing.
2. Well test results (see Figure 7-20): The graphic characteristics are similar to those of the mode chart (Figure 7-18). Initially, there is an afterflow portion, which is similar to that of a homogeneous reservoir. There is a long 1/2 slope portion after the afterflow portion. The ratio of the distance between the two lines to the ordinate logarithmic period length is approximately 0.3. Such a long portion indicates a long fracture. There is no radial flow portion measured. A semilogarithmic plot cannot be used for calculating reservoir parameters. The values of parameters, which are obtained by bilogarithmic type curve match, include:

$$K = 0.753 \times 10^{-3} \mu\text{m}^2, \frac{Kh}{\mu} = 7.06 \times 10^{-3} \frac{\mu\text{m}^2 \cdot \text{m}}{\text{MPa} \cdot \text{s}}, S = 0.642, C = 2.12 \text{ m}^3/\text{MPa},$$

flow conductivity (as defined by Equation (7-43))  $F_{CD} \geq 100\pi$ , which indicates fracture with infinite flow conductivity, and  $X_f = 339.2 \text{ m}$ .

It is indicated that a good obvious result of hydraulic fracturing has been obtained. A large fracture with a length of 300 m has been formed, thus fully improving the flow condition of the reservoir. If the curves are measured before and after the stimulation, the results can be concretely evaluated.

**Mode Chart under Vertical Fracture with Finite Flow Conductivity.** The flow conductivity of fracture may be a flow conductivity that is comparable to the permeability of the reservoir when a certain particle size distribution of proppant is achieved. There are slightly different definitions of flow conductivity. Flow conductivity is defined by Agarwal as follows.

(7-43)

$$F_{CD} = \frac{K_f W}{K X_f}$$

where:  $K_f$  and  $K$  = fracture permeability and reservoir permeability, respectively;  $W$  = fracture width;  $X_f$  = fracture half-length.

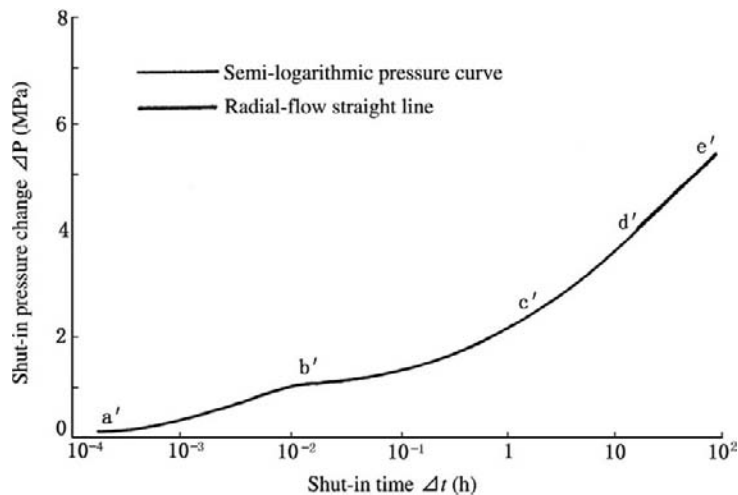


**FIGURE 7-19** Semilogarithmic pressure plot of homogeneous reservoir under vertical fractures with infinite flow conductivity and uniform flux.

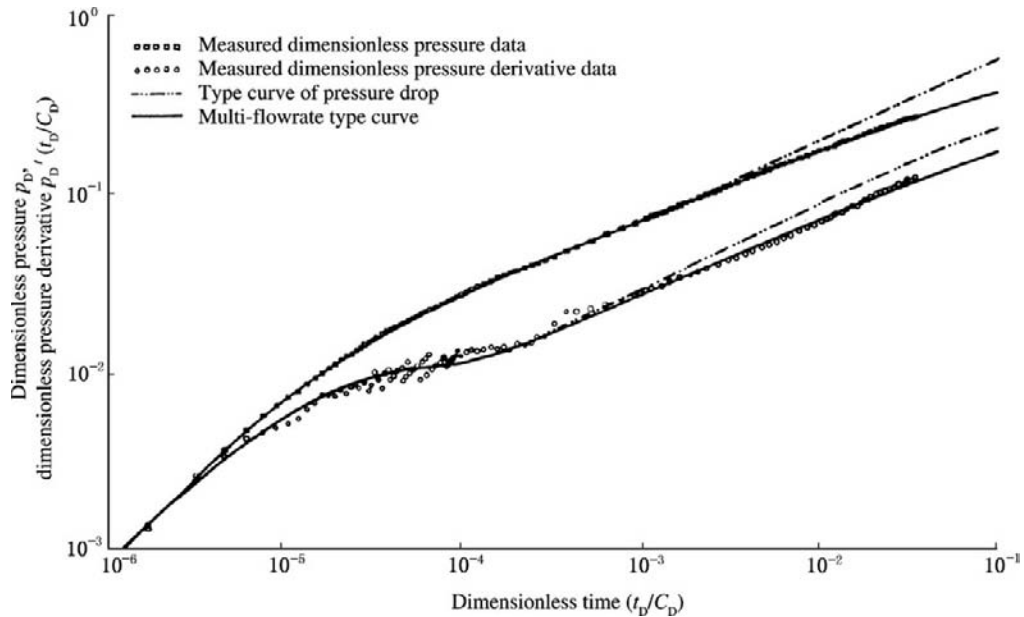


FIGURE 7-20 Composite bilogarithmic plot of Case 4.

Different  $F_{CD}$  values have different pressure curve shapes. When  $F_{CD}$  is low (such as  $F_{CD} = 5$ ), the curve shape is as shown in Figure 7-21.

1. a-b-c: Afterflow portion. The curve shape is similar to that under a low  $C_{Df}^{2S}$  value of homogeneous reservoir.
2. c-d: Bilinear flow portion. The flow along the fracture is a linear transient flow. The pressure and pressure derivative curves are parallel lines with a slope of 1/2. The ordinate distance between the two lines is 0.602 logarithmic period. The representative formula is shown in Equation (7-44).

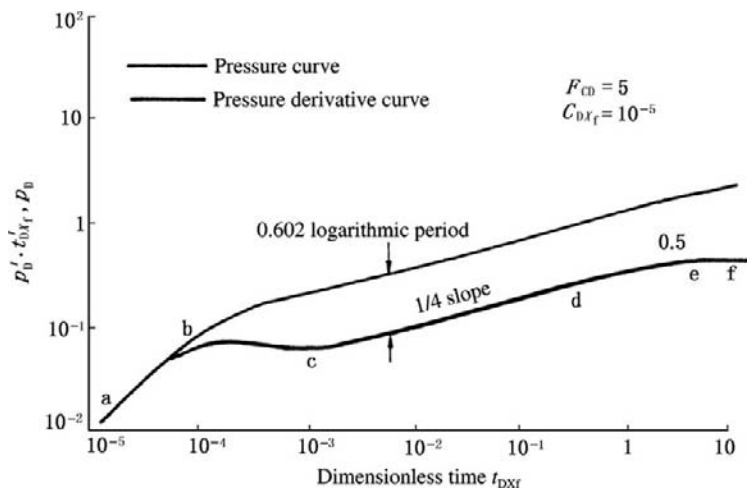


FIGURE 7-21 Bilogarithmic mode chart under vertical fracture with finite flow conductivity and low FCD.

(7-44)

$$P_D = \frac{\pi}{0.906\sqrt{2F_{CD}}} \cdot \sqrt[4]{t_{Dxf}}$$

that is, as shown in Equation (7-45),

(7-45)

$$\log P_D = \frac{1}{4} \lg t_{Dxf} + \lg \frac{\pi}{0.906\sqrt{2F_{CD}}}$$

It is a straight line with a slope of 1/4. After deriving and taking the logarithm, Equation (7-44) can be as shown in Equation (7-46).

(7-46)

$$\log(P_D' \cdot t_{Dxf}) = \frac{1}{4} \lg t_{Dxf} - \lg 4 + \lg \frac{\pi}{0.906\sqrt{2F_{CD}}}$$

It is shown that this line is also a straight line with a slope of 1/4. The difference between Equations (7-45) and (7-46) is 0.602.

- e-f: Pseudoradial flow portion. The derivative curve is a horizontal line. The dimensionless ordinate value is 0.5.

The semilogarithmic mode chart is shown in Figure 7-22.

The flow portions shown in Figure 7-22 correspond to those in Figure 7-21. The curve is continuously bent upward and has no obvious characteristic except the e'-f' pseudoradial-flow straight portion.

**Case 5**

- Well test conditions: Triassic sandstone reservoir, 1370 m reservoir depth, 4.5 m reservoir thickness, 10 m<sup>3</sup>/d daily oil production rate. Hydraulic fracturing with 8 m<sup>3</sup> proppant was adopted after perforating. After producing for 21 days, the pressure build-up curve was measured at the bottomhole by using an electronic pressure gauge under the condition of wellhead shut-in.
- Well test results (see Figure 7-23): The measured curves are similar to those in Figure 7-21 and match the theoretical model well. The interpretation results include:  $k = 9.8 \times 10^{-3} \mu\text{m}^2$ ,  $Kh/\mu = 18.68 \times 10^{-3} \frac{\mu\text{m}^2 \cdot \text{m}}{\text{MPa} \cdot \text{s}}$ ,  $S = 0.28$ ,  $C = 0.30 \text{ m}^3/\text{MPa}$ ,  $X_f = 93.34 \text{ m}$ , and  $F_{CD} = 5$ .

It is known that the stimulation has a good obvious result. The fracture created has a length of 93 m; thus a production rate of 10 m<sup>3</sup>/d can still be obtained under the condition of permeability lower than  $10 \times 10^{-3} \mu\text{m}^2$ . The pressure data had not been taken before stimulation.

**Fracture Skin Factor and Its Effect**

- Mechanism of fracture skin zone damage caused by fracturing

During fracturing operations (particularly massive fracturing), several hundred cubic

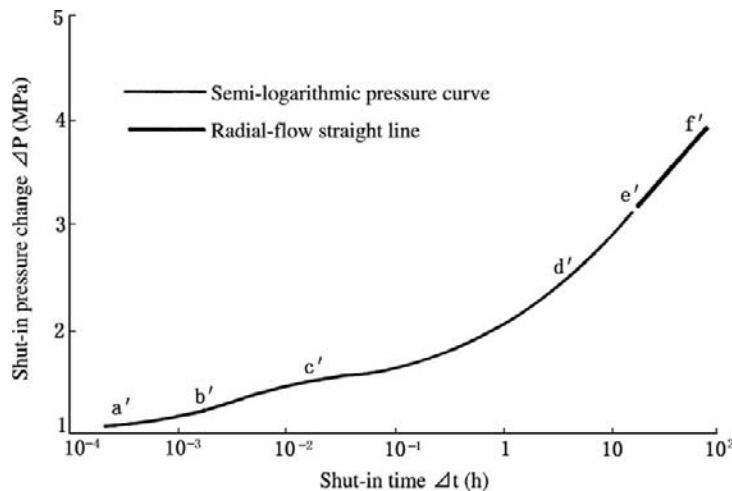


**FIGURE 7-22** Semilogarithmic pressure plot under vertical fracture with finite flow conductivity and low FCD.

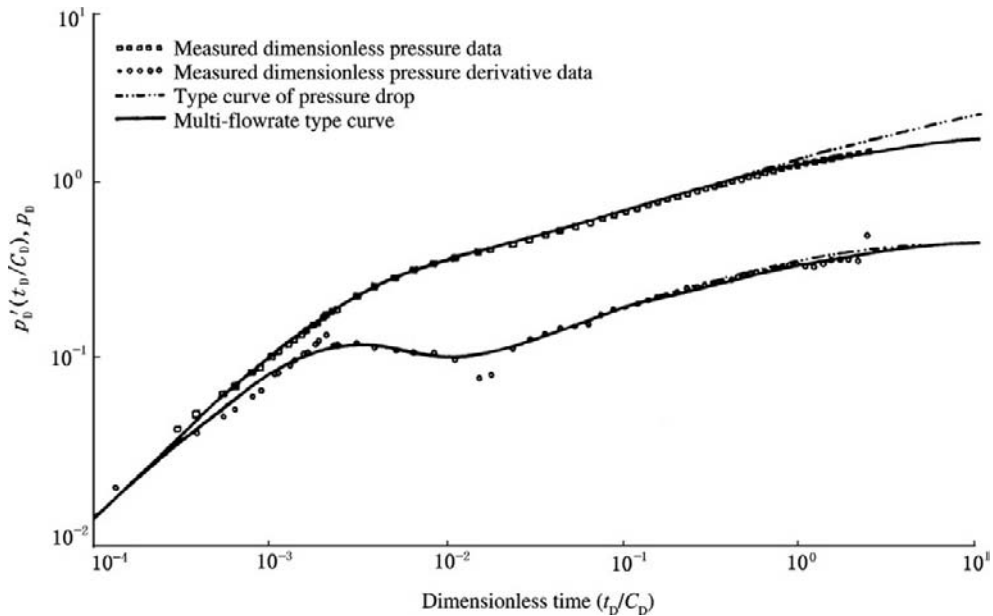


FIGURE 7-23 Composite bilogarithmic plot of Case 5.

meters (even up to a thousand cubic meters) of fracturing fluid are often injected into the reservoir under high pressure and high pumping rate. While cracking the reservoir and generating a large fracture, fracturing fluid may enter the fracture, and formation contaminant and damage may be caused (Figure 7-24).

Fracture skin factor is defined as shown in Equation (7-47).

$$(7-47) \quad S_f = \frac{\pi b_s}{2X_f} \left( \frac{K}{K_s} - 1 \right)$$

where:  $S_f$  = fracture skin factor, dimensionless;  $K$  = reservoir permeability,  $10^{-3} \mu\text{m}^2$ ;

$K_s$  = fracture skin zone permeability,  $10^{-3} \mu\text{m}^2$ ;  $b_s$  = fracture skin zone thickness, m;  $X_f$  = fracture half-length, m.

Equation (7-47) indicates that the  $S_f$  value is mainly affected by the skin zone permeability  $K_s$  and the skin zone thickness  $b_s$ . The more serious the blockage, the lower the  $K_s$  value. Table 7-11 shows the relation between  $K_s$  and  $S_f$  under the conditions of  $b_s = 0.1$  m,  $K = 1 \times 10^{-3} \mu\text{m}^2$ , and  $X_f = 50$  m.

Table 7-11 shows that  $S_f = 0.03$  when  $K_s$  is reduced to 1/10 of original permeability, while  $S_f = 0.3$  when  $K_s$  is reduced to 1/100 of original permeability; thus a slight change

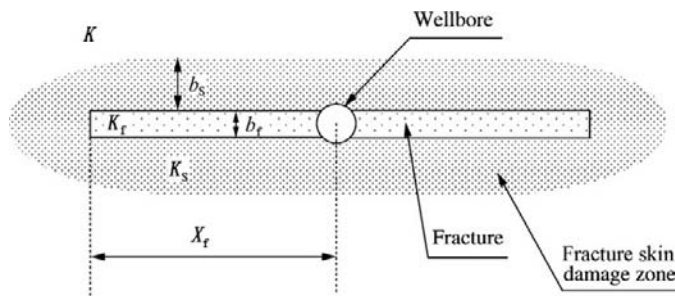


FIGURE 7-24 Mechanism of fracture skin damage caused by fracturing.

**TABLE 7-11** Relation between Fracture Skin Factor  $S_f$  and Fracture Skin Zone Permeability  $K_s$ 

$K_s, 10^{-3} \mu\text{m}^2$	1	0.5	0.2	0.1	0.05	0.01
$S_f$	0	0.003	0.013	0.03	0.06	0.3

of the absolute value of  $S_f$  may reflect very serious fracture skin damage.

## 2. Effect of fracture skin on curve shape

The fracture skin damage may undoubtedly increase resistance to flow and produce pressure drawdown, thus reducing gas well productivity. Despite the fact that the fracture generated by hydraulic fracturing makes the flow at the bottomhole easy and smooth, the total skin effect may be increased due to the existence of fracture skin. The early-time portion of the pressure derivative curve is concave downward due to the increase of the  $S_f$  value, which shows a graphic characteristic different from that of the curve without damage by skin (Figure 7-25).

$$(Kh = 10 \text{ mD} \cdot \text{m}, X_f = 200 \text{ m}, F_{CD} = 15, S_f = 0.3)$$

It is shown that the pressure derivative curve after the afterflow portion becomes concave downward. This is the most obvious characteristic of the existence of fracture skin.

**Case 6.** Figure 7-26 shows the measured pressure build-up curve of the S117 well in the Changbei gas field. The well of the Permian Sanxi-formation

sandstone reservoir was hydraulically fractured during well completion. The gas production rate before shut-in was  $9 \times 10^4 \text{ m}^3/\text{d}$ . The parameter values obtained by well test software analysis include:

1. Reservoir permeability  $K = 0.45 \times 10^{-3} \mu\text{m}^2$ ;
2. Fracture half-length  $X_f = 75.8 \text{ m}$ ;
3. Fracture skin factor  $S_f = 0.90$ ;
4. Non-Darcy flow coefficient  $D = 0$ .

**Case 7.** Figure 7-27 shows the measured pressure build-up curve of the Y27-11 well in the Changbei gas field. The well of the Permian Sanxi-formation sandstone reservoir was hydraulically fractured during well completion. The parameter values obtained by interpretation include:

1. Reservoir permeability  $K = 0.65 \times 10^{-3} \mu\text{m}^2$ ;
2. Fracture half-length  $X_f = 74.1 \text{ m}$ ;
3. Fracture skin factor  $S_f = 1.02$ ;
4. Non-Darcy flow coefficient  $D = 0$ .

## Discussion

1. Under the condition of fracture with finite flow conductivity and a high  $F_{CD}$  value (such as  $F_{CD} = 500$ ), it is theoretically considered

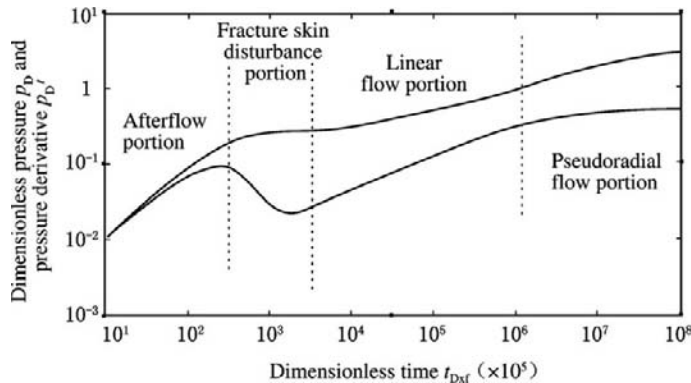


**FIGURE 7-25** Effect of fracture skin factor  $S_f$  on model curve of fractured well.

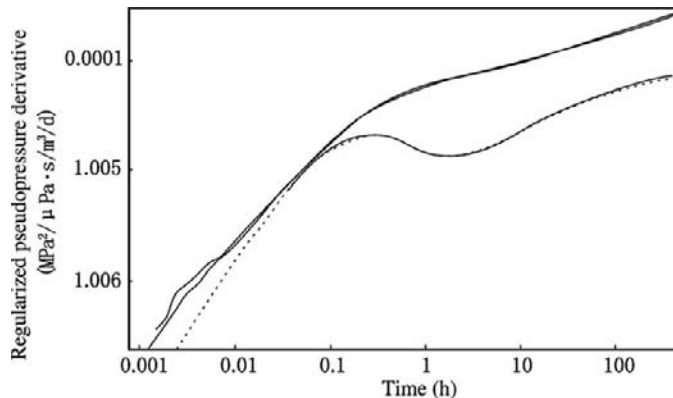


**FIGURE 7-26** Bilogarithmic pressure build-up curve plot of S117 well.

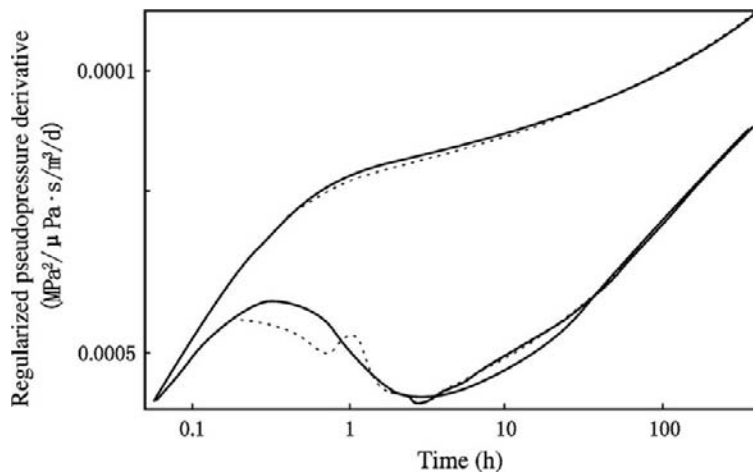


**FIGURE 7-27** Bilogarithmic pressure build-up curve plot of Y27-11 well.

that a linear flow portion with a slope of  $1/2$  may appear when transient flow is converted into steady flow in the fracture after the bilinear flow portion. It is also considered that there is a further early fracture linear-flow portion when the reservoir linear-flow portion has not been presented before the bilinear flow portion under the condition of fracture with finite flow conductivity. Thus under the condition of fracture with finite flow conductivity, there are several flow portions, which include: earlier fracture linear-flow portion, early bilinear-flow portion, reservoir linear-flow portion, pseudoradial

flow portion, and sometimes the possible afterflow portion and late-time boundary response portion.

However, in practice, to measure so many flow portions is difficult; one should use a high-precision electronic pressure gauge and should continuously observe for a long time, which may be several months or years. It is of no practical significance for studying a reservoir and understanding well production.

2. Uniform-flow fracture, if any, may only be formed by penetrating that original natural fracture after stimulation and may not be met often.

3. It is theoretically considered that a horizontal fracture may appear in a shallow well, but typical measured data have not been obtained.

## 7.5 DISTINGUISHING EFFECTIVENESS OF STIMULATION BY GRAPHIC CHARACTERISTICS

At present, various hydraulic fracturing and acidizing treatments have been applied to enhancing the oil and gas well productivity in oil and gas fields. It is necessary to understand the reason for causing low well productivity before designing stimulation in order to make a correct stimulation policy. Pressure build-up curves can be used for obtaining the values of reservoir permeability  $K$  and formation damage skin factor  $S$ , thus judging the reason for causing low well productivity.

There are three circumstances that may follow after stimulation is taken:

1. The degree of formation damage is decreased in the vicinity of the wellbore and the value of  $S$  is decreased.
2. Not only is the degree of formation damage decreased in the near-wellbore area, but the reservoir permeability is also increased.

3. A long fracture that is connected with the wellbore is formed, thus changing the flow regime.

## Comparison between Curve Shapes before and after Removing Formation Damage

After formation damage is removed or partially removed, the value of  $S$  is decreased to zero under the condition of homogeneous reservoir, or the value of  $S$  is decreased to some extent. The changes of curve shape are as follows.

1. In a bilogarithmic composite graph, the pressure derivative peak height  $H$  is reduced.
2. The opening span  $A$  between pressure curve and pressure derivative curve at the radial flow portion in a bilogarithmic plot is decreased.
3. The value of slope ratio  $m'/m$  of semilogarithmic curve is decreased and the turning angle  $\beta$  is increased.

Figure 7-28 shows that the values of  $H$  and  $A$  are decreased to some extent. The value of  $A$  is decreased from 1.25 to 1.0 while the value of  $H$  is decreased from 0.6 to 0.19. Before acidizing,  $S = 3.1$  and  $C_D e^{2S} = 10^4$ , which indicates a slight formation damage. After acidizing,

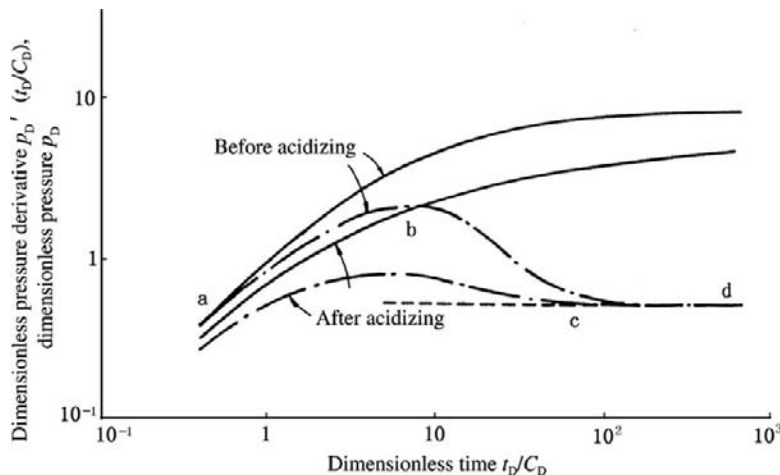


**FIGURE 7-28** Comparison between bilogarithmic curves before and after acidizing, which indicates  $S$  value improved (decreased).

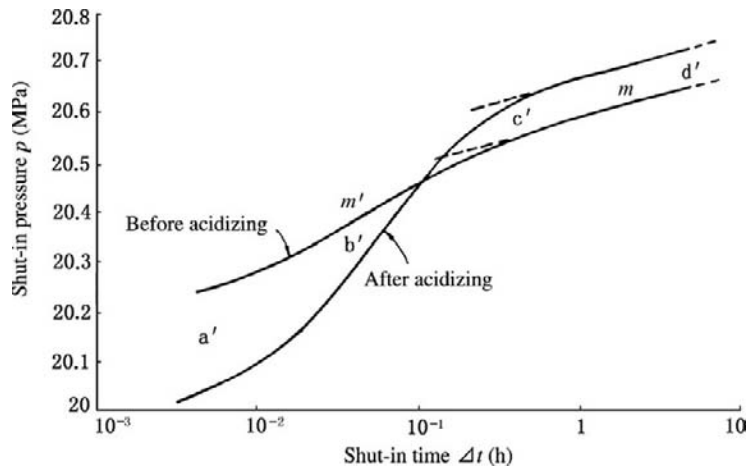


**FIGURE 7-29** Comparison between semilogarithmic curves before and after acidizing, which indicates S value improved (decreased).

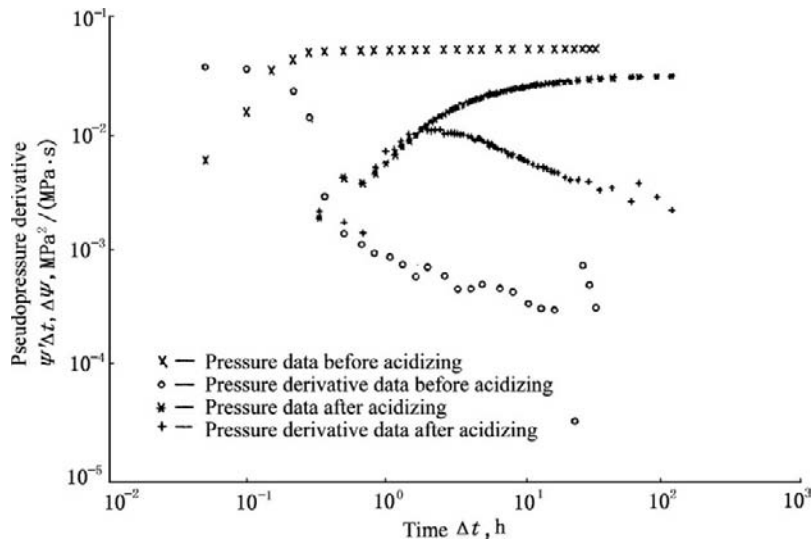
$S = -0.35$  and  $C_D e^{2S} = 10$ , which indicates that the formation damage has been removed. The values of other parameters are unchanged.

Figure 7-29 shows that the turning angle  $\beta$  is obviously increased and the value of  $m'/m$  is decreased.

**Case 8.** A gas well has a depth of 3500 m. The Ordovician mud-siltstone dolomite reservoir has a thickness of 6 m and has net microfractures.

The daily gas production rate was  $1.87 \times 10^4 \text{ m}^3/\text{d}$ , which was obtained by drillstem test and was of no commercial significance; thus acidizing was taken. After acidizing, the gas production rate was increased to  $8.35 \times 10^4 \text{ m}^3/\text{d}$ . This well is important to the evaluation of this area.

The comparison between the bilogarithmic curves before and after acidizing is shown in Figure 7-30. The after-acidizing pressure



**FIGURE 7-30** Comparison between the bilogarithmic curves before and after acidizing in the well of Case 8.

**TABLE 7-12** Comparison between Curve Characteristics before and after Acidizing in the Well of Case 8

Item	Before Acidizing	After Acidizing
$H_D$	2.09	0.5
$A_D$	2.22	1.0
$m'/m$	425	20.1

derivative peak value  $H$  and the opening span  $A$  between curve and pressure derivative curve pressure are much lower than that before acidizing (Table 7-12).

The comparison between the semilogarithmic curves before and after acidizing is shown in Figure 7-31. It can be seen that the  $\beta_2$  angle is much larger than  $\beta_1$  and the  $m'/m$  value is obviously reduced (Table 7-12).

An obvious acidizing effectiveness can be qualitatively determined by Figure 7-30 and Figure 7-31. The specific change of  $S$ , however, should be determined by quantitative interpretation using well test software. Table 7-13 shows the interpretation results.

It is indicated that the permeability measured after acidizing is basically coincident with that measured before acidizing, whereas the value of  $S$  is obviously decreased. The well was seriously damaged before acidizing, whereas the damage was fully removed and good effectiveness was obtained by using acidizing. The gas production rate was obviously increased.  $S$  has no room for improvement. The  $C$  value was low before acidizing because the DST tool was used for testing, while the  $C$  value after acidizing was high because the test was performed under the condition of wellhead shut-in and opening.

### Change of Curve Shape after Acidizing, Which Improves Both Skin Factor and Permeability

In general, acidizing can only reduce the degree of formation damage in the vicinity of the wellbore rather than the whole reservoir. The acid volume injected during acidizing is limited. Hydraulic fracturing can only create a single fracture with a limited length but can increase the near-wellbore reservoir permeability and improve the flow regime to some extent. Massive acidizing

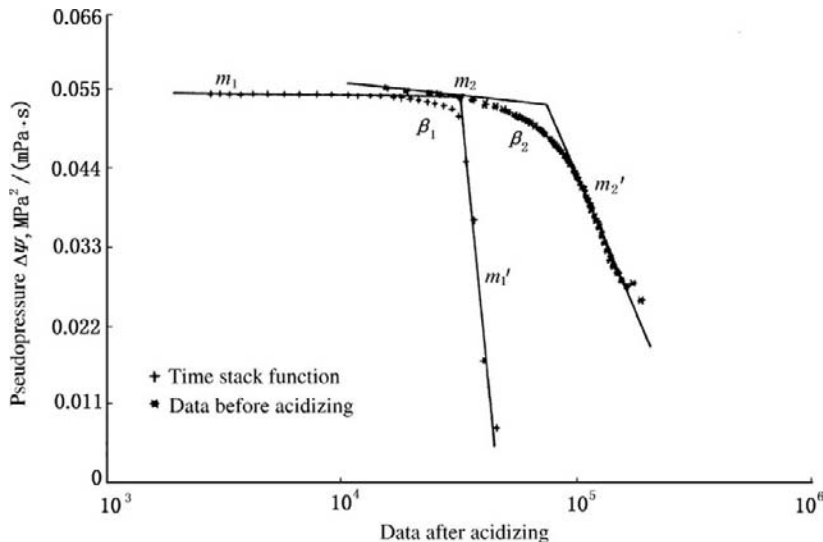


**FIGURE 7-31** Comparison between the semilogarithmic curves before and after acidizing in the well of Case 8.

**TABLE 7-13 Comparison between the Parameter Values before and after Acidizing in the Well of Case 8**

Test time	Permeability K ( $10^{-3} \mu\text{m}^2$ )	Flow coefficient $\text{Kh}/\mu$ ( $\frac{10^{-3} \mu\text{m}^2 \cdot \text{m}}{\text{MP}_a \cdot \text{s}}$ )	Skin factor S	Gas production rate $q_g$ ( $10^4 \text{ m}^3/\text{d}$ )	Wellbore storage coefficient C ( $\frac{\text{m}^3}{\text{MP}_a}$ )
Before acidizing	0.559	418	47	1.87	0.0208
After acidizing	0.420	354	-1.433	8.354	4.9

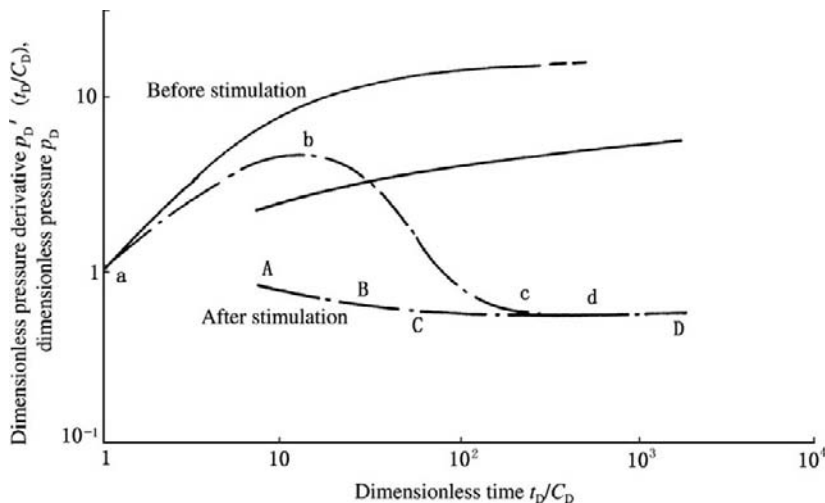
(especially for a reservoir with a net-shaped fracture system) may further dredge the fracture system, thus increasing the measured permeability. Some low-permeability sandstone reservoirs will have an S value decreased and a K value increased after a fracturing operation.

Figure 7-32 indicates that the decrease of S value makes the values of H and A decrease and the increase of K value leads to a curve moving toward the left and losing the early-time portion. Figure 7-33 clearly indicates that the curve from afterflow portion to radial flow portion moves toward the left due to the increase of the K value.

In the mode charts the parameter values before acidizing include:  $S = 10$ ,  $C_{De}^{2S} = 10^{10}$ ,  $K = 10 \times 10^{-3} \mu\text{m}^2$ , and  $qB = 1.7 \text{ m}^3/\text{d}$ , which indicates a low-productivity well with formation

damage; and the parameter values after acidizing include:  $S = 1$ ,  $C_{De}^{2S} = 1.5 \times 10^2$ ,  $K = 50 \times 10^{-3} \mu\text{m}^2$ , and  $qB = 10 \text{ m}^3/\text{d}$ , which indicates that the well is basically a completely penetrating well and the K value is increased by 400%.

**Case 9.** A well is located above a Mesoproterozoic buried hill and has a depth of 3200 m and a limestone reservoir thickness of 45 m. The core observation indicates that fractures are well developed. The production rate measured initially was  $258 \text{ m}^3/\text{d}$ . Despite a high-productivity well, the pressure build-up curve shows obvious formation damage, that is, high  $m/m$  value and a shape of an inverted letter L (Figure 7-34). Thus a massive acidizing was taken.  $60 \text{ m}^3$  of hydrochloric acid with a concentration of



**FIGURE 7-32** Mode chart of bilogarithmic curves under the condition of both K and S values improved.

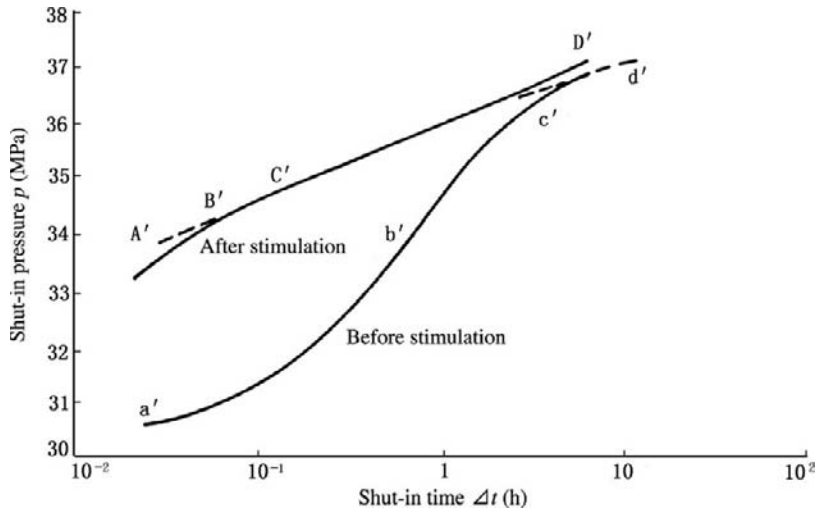


**FIGURE 7-33** Mode chart of semilogarithmic curves under the condition of both  $K$  and  $S$  values improved.

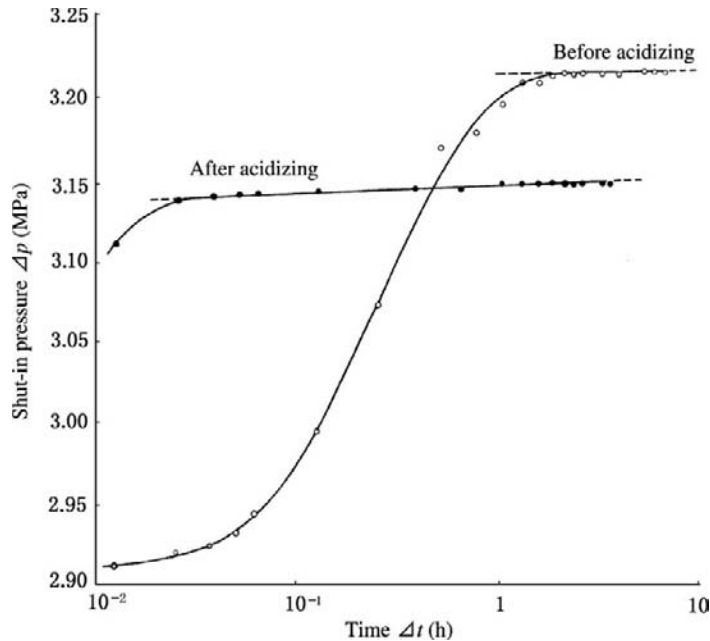


**FIGURE 7-34** Comparison between the semilogarithmic curves before and after acidizing in the well of Case 9.

30% was injected. The increase of production rate was obvious. The test curve is shown in Figure 7-34.

It is shown that the curve is obviously moved downward and the additional differential pressure

$\Delta p_s$ , formed by formation damage in the near-wellbore area, has disappeared. The comparison cannot be done by using  $m'/m$  and  $\beta$  angle, and so on, due to the lack of early data after acidizing.

**TABLE 7-14 Comparison between Parameter Values before and after Acidizing in the Well of Case 9**

Item	Production Rate (m <sup>3</sup> /d)	Producing Pressure Drawdown (MPa)	Skin Factor S	Permeability K (10 <sup>-3</sup> μm <sup>2</sup> )	Productivity Index Jo (m <sup>3</sup> /MPa · d)
Before acidizing	260	3.65	11.9	78	71.23
After acidizing	1215	0.412	3.8	1127	2949

The parameter values obtained by interpretation are listed in Table 7-14.

It is shown that the S value is obviously decreased after acidizing and the damage is removed to a certain degree. The K value is increased by 1300% from  $78 \times 10^{-3} \mu\text{m}^2$  to  $1127 \times 10^{-3} \mu\text{m}^2$ , thus greatly increasing the production rate.

### Change of Curve Shape after Hydraulic Fracturing by Which a Large Fracture Is Formed

When a long fracture is formed during hydraulic fracturing, the well test curve shape may be greatly changed. The curves before hydraulic fracturing have characteristics of homogeneous or double porosity reservoir, while the curves after hydraulic fracturing have a linear flow portion (parallel straight lines with a slope of 1/2 on bilogarithmic plot) or a bilinear flow portion

(parallel straight lines with a slope of 1/4). The longer the fracture, the longer the duration of linear- or bilinear-flow straight-line portion. The mode charts are shown in Figure 7-35 and Figure 7-36.

In the mode charts the parameter values before fracturing under the condition of homogeneous reservoir include  $K = 2 \times 10^{-3} \mu\text{m}^2$ ,  $S = 0.16$ , and  $C_{DE}^{2S} = 10$ , while the values under the condition of dual porosity reservoir include  $K_f = 2 \times 10^{-3} \mu\text{m}^2$ ,  $S = -2$ ,  $\omega = 0.1$ , and  $\lambda = 1 \times 10^{-5}$ ; and the parameter values after fracturing, which forms the vertical fracture with infinite flow conductivity, include  $X_f = 10 \text{ m}$  and  $K = 2 \times 10^{-3} \mu\text{m}^2$ .

**Case 10.** A gas well of the Sinian dolomite reservoir has a depth of 3000 m. During acidizing, which had an action of fracturing, the pump pressure was 30 MPa and the bottomhole pressure was about 60 MPa. The acid volume of  $75.8 \text{ m}^3$  was injected. The gas production rate before

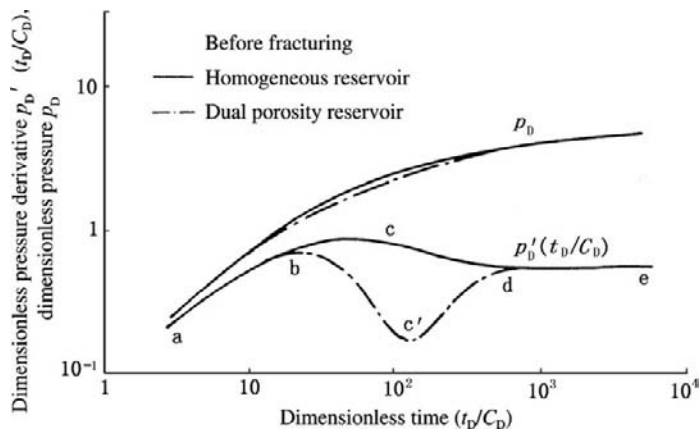


**FIGURE 7-35** The curves which have characteristics of homogeneous or dual porosity reservoir before fracturing.

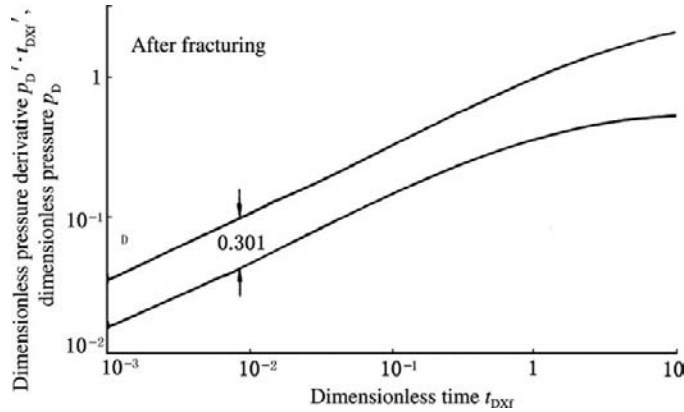


**FIGURE 7-36** The curves which have characteristics of reservoir with fracture created by fracturing.

acidizing was  $9.99 \times 10^4 \text{ m}^3/\text{d}$ , while the gas production rate after acidizing was increased to  $12.8 \times 10^4 \text{ m}^3/\text{d}$  with a water production rate of  $69.3 \text{ m}^3/\text{d}$ .

The bilogarithmic curves before and after acidizing are shown, respectively, in Figure 7-14 and Figure 7-37.

The curves in Figure 7-37 are similar to that in the mode chart, and this method is appropriate to on-site evaluation of stimulation effectiveness.

## 7.6 QUANTITATIVE INTERPRETATION OF DEGREE OF FORMATION DAMAGE

Currently, reservoir parameter calculation on the basis of transient well test data has become a modern well test interpretation method, in which bilogarithmic type curve match analysis and conventional analysis are dominated by semilogarithmic analysis. Well test interpretation

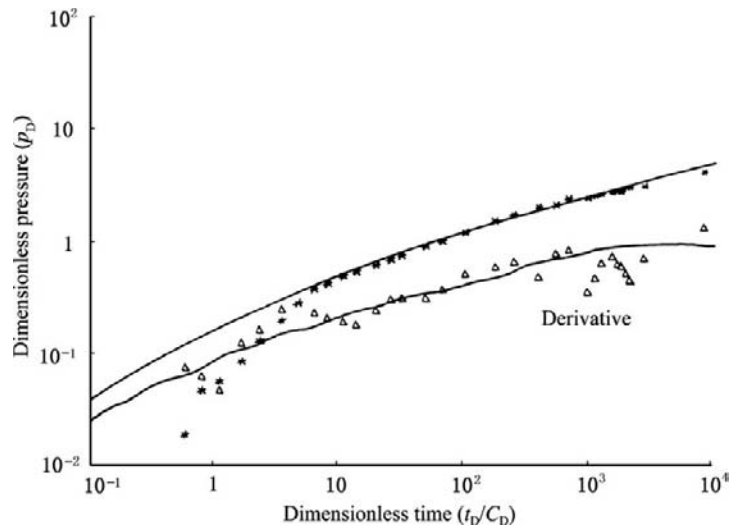


**FIGURE 7-37** Bilogarithmic pressure curve plot after acidizing which formed artificial fracture in the well of Case 10.

software has been formulated by using these methods.

At present, well test interpretation software has been commonly used and quantitative calculation is almost no longer done by manual methods. Well test interpretation software not only can be used for parameter calculation, but it can also be used for checking in order to ensure the reliability of interpretation results. Manual methods cannot be used for checking, and no appropriate type curves can be constantly obtained by the manual method to ensure matching accuracy.

### Calculating Reservoir Parameters and Skin Factor S Value Using the Bilogarithmic Type Curve Match Method

**Principle of Calculating Reservoir Parameters Using the Type Curve Match Method.** The bilogarithmic type curve match method of calculating reservoir parameters is a quantitative well test interpretation method developed recently. Its principles are as follows.

1. Various types of oil and gas reservoirs are simplified into well test interpretation models, which include basic homogeneous, double porosity, and multilayer models with various inner and outer boundary conditions, including also the inner boundary conditions, which consider the formation damage in the vicinity of the wellbore (that is, the S value) and the wellbore storage coefficient C, and so on.
2. The aforementioned well test interpretation models are expressed by mathematical equation, in which pressure p is the unknown variable, time t is the independent variable, and the various parameters such as production rate q, permeability K, skin factor S, wellbore storage coefficient C, fluid viscosity  $\mu$ , volume factor B, compressibility  $C_t$ , reservoir thickness h, and also  $\omega$ ,  $\lambda$ ,  $L_b$ ,  $X_t$ , and  $R_e$ , are cross-variables.

The equation is generally expressed in a dimensionless form. For a homogeneous

reservoir, under the conditions of the wellbore storage coefficient C and skin factor S on the inner boundary and the constant pressure on the infinite outer boundary, the mathematical model is as follows.

$$\frac{\partial^2 P_D}{\partial r_D^2} + \frac{1}{r_D} \cdot \frac{\partial P_D}{\partial r_D} = \frac{\partial P_D}{\partial t_D}$$

The initial condition is:  $P_D(r_D, 0) = 0$ .

The outer boundary condition is:  $P_D(\infty, t_D) = 0$ .

The inner boundary conditions are:

$$C_D \frac{dP_{WD}}{dt_D} - \left( \frac{\partial P_D}{\partial r_D} \right)_{r_D=1} = 1$$

$$P_{WD} = \left[ P_D - S \left( \frac{\partial P_D}{\partial r_D} \right) \right]_{r_D=1}$$

3. The equations are solved by using analytic or numerical methods, the pressure p is expressed as the function of time t and various cross-variables, and then the relational curves are drawn on log-log paper and known as type curves.

Different reservoir models have different type curves.

4. For the convenience of use, dimensionless variables are generally adopted as the coordinates of type curves, as shown in Equations (7-48) and (7-49), that is, ordinate:

(7-48)

$$P_D = 0.54287 \frac{Kh}{\mu qB} \Delta p$$

abscissa:

(7-49)

$$\frac{t_D}{C_D} = 2.262 \times 10^{-2} \frac{Kh}{\mu C} \Delta t$$

Such type curves composed are widely applicable. The Gringarten's type curves for homogeneous reservoir, which have cross-parameter  $C_D e^{2S}$ , are commonly used (Figure 7-38).

1. The data of measured  $\Delta p$  related to  $\Delta t$  are drawn on the log-log paper with the same scales of ordinates, as shown in Figure 7-39, which is generally drawn on cellophane paper in order to be convenient for matching later.

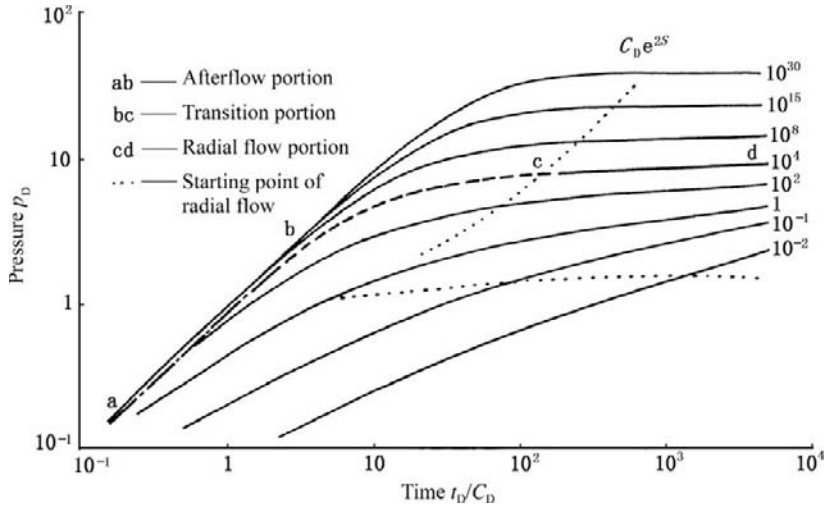


FIGURE 7-38 Gringarten's type curves for homogeneous reservoir.

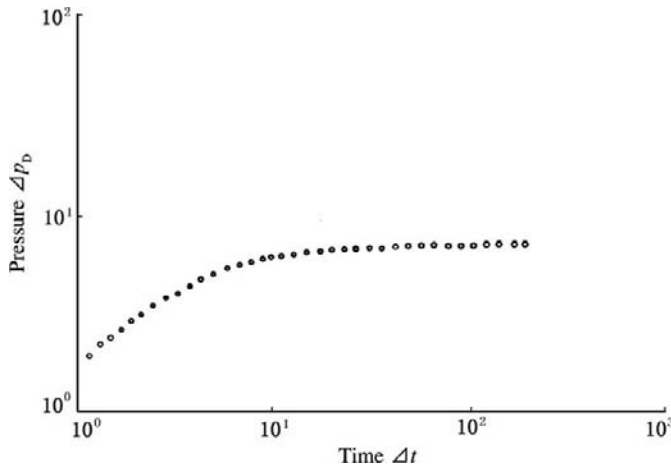


FIGURE 7-39 Bilogarithmic plot of measured pressure data.

2. Figure 7-38 is overlaid with Figure 7-39. If the type curve model is suitable for the reservoir, some type curve may match the measured data points. During matching they are relatively moved under the condition of parallel ordinates and abscissas. The well overlapping and matching curve is shown in Figure 7-40.

A match point M is then selected. The M point has readings  $P_{DM}$  and  $t_D/C_D$  on the type curve plot and has readings  $\Delta P_M$  and  $\Delta t_M$  on

the measured plot, thus obtaining the formula shown in Equations (7-50) and (7-51), in accordance with Equations (7-48) and (7-49):

(7-50)

$$P_{DM} = 0.54287 \frac{Kh}{\mu qB} \cdot \Delta P_M$$

(7-51)

$$\left(\frac{t_D}{C_D}\right)_M = 2.262 \times 10^{-2} \frac{Kh}{\mu C} \Delta t_M$$

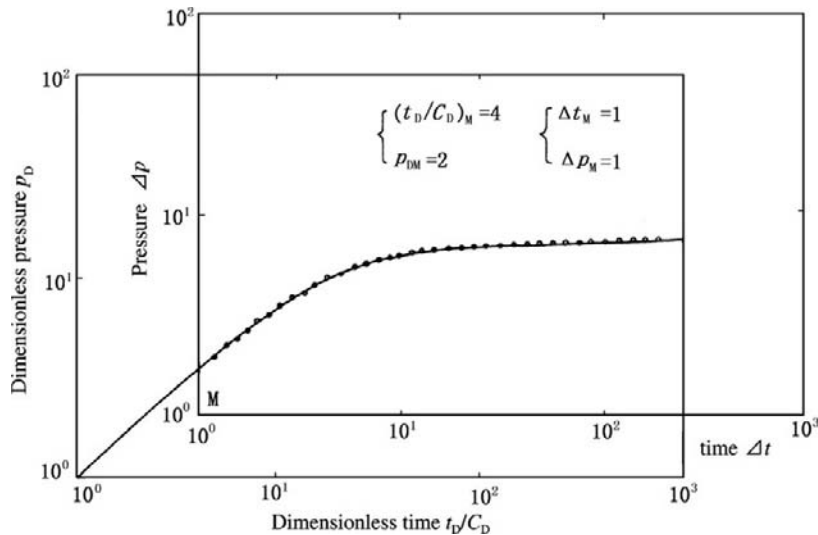


FIGURE 7-40 Bilogarithmic type curve matching.

The reservoir parameters in Equations (7-52) and (7-53) are obtained by Equation (7-50):

(7-52)

$$\frac{Kh}{\mu} = 1.842qB \frac{P_{DM}}{\Delta P_M}$$

(7-53)

$$C = 2.262 \times 10^{-2} \frac{Kh}{\mu} \cdot \frac{\Delta t_M}{(t_D/C_D)_M}$$

It should be noticed that each curve on the type curve plot has cross-parameter  $C_D e^{2S}$  and the only value of  $(C_D e^{2S})_M$  is determined during matching; thus the  $S$  value can be obtained by using  $(C_D e^{2S})_M$  as shown in Equation (7-54).

(7-54)

$$S = \frac{1}{2} \ln \frac{(C_D e^{2S})_M}{C_D}$$

where Equation (7-55) applies:

(7-55)

$$C_D = 0.1592 \frac{C}{\Phi C_f h r_w^2}$$

The  $C$  value can be obtained in combination with Equation (7-53).

This is just the method of determining formation damage ( $S$  value) by using type curves.

**Common Type Curves for Well Test Interpretation.** Since 1970 when Agarwal et al. first gave transient well test interpretation type curves, there have been many type curves under various reservoir conditions and various inner and outer boundary conditions, and many new attempts to take ordinate values have been made.

The pressure derivative type curves were made by Bourdet in 1982 (Figure 7-41). The reservoir characteristics were obviously shown by the pressure derivative curves, which then became the main means of type curve matching. The ordinates of pressure derivative type curves coincide with those of bilogarithmic pressure type curves; thus, composite type curves are often composed of pressure and pressure derivative type curves.

Under the condition of double porosity reservoir, Gringarten et al. adopted separate flow portions of type curve. The homogeneous reservoir type curves are used for the first fracture flow portion and the third fracture-matrix flow portion, while the special transition-flow (steady or unsteady flow) type curves are used for the second transition-flow portion. The matching process is shown in Figure 7-42. The unsteady transition flow portion type curves are shown in Figure 7-43.

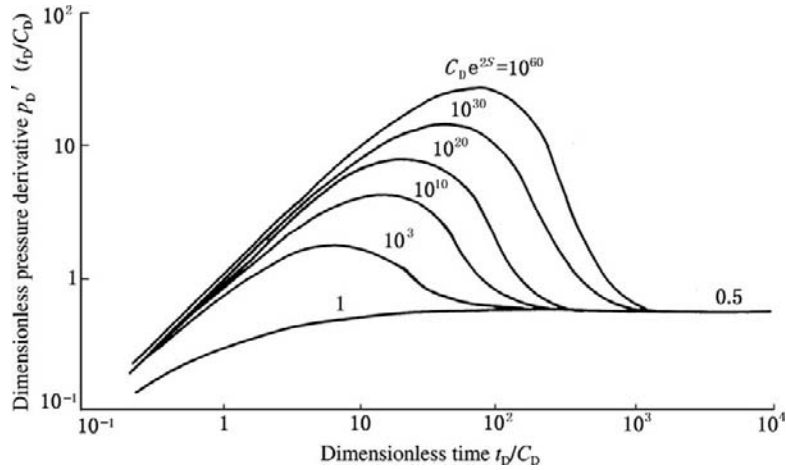


FIGURE 7-41 Pressure derivative type curves for homogeneous reservoir.

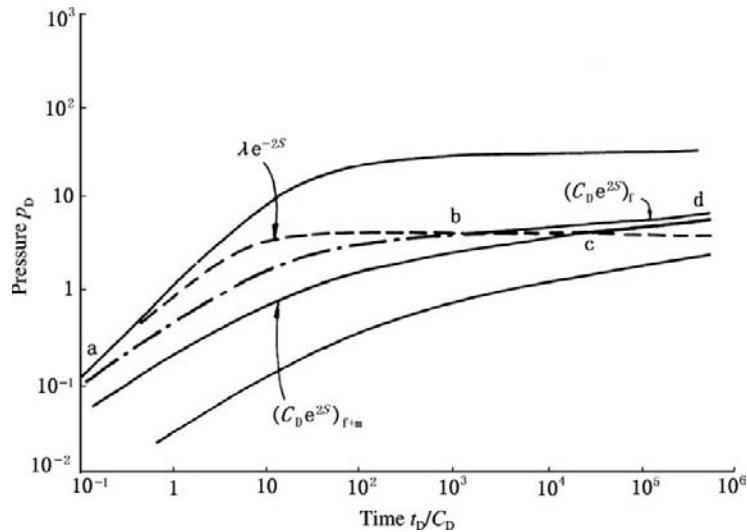


FIGURE 7-42 The matching process for dual porosity reservoir.

The type curves for reservoir with infinite flow-conductivity vertical fracture under the action of  $S$  and  $C$  are shown in Figure 7-44.

### Calculating Skin Factor $S$ Value Using the Semilogarithmic Method

The semilogarithmic method of calculating reservoir parameters is presently known as the

conventional method. The MDH method presented by Miller, Dyes, and Hutchinson in 1950 and the method presented by Horner in 1951 have been applied so far.

The formulae of calculating skin factor  $S$  are introduced as follows.

The radial flow portion is a straight line with a slope of  $m$ , and the reservoir engineering unit is adopted for calculating skin factor  $S$ .

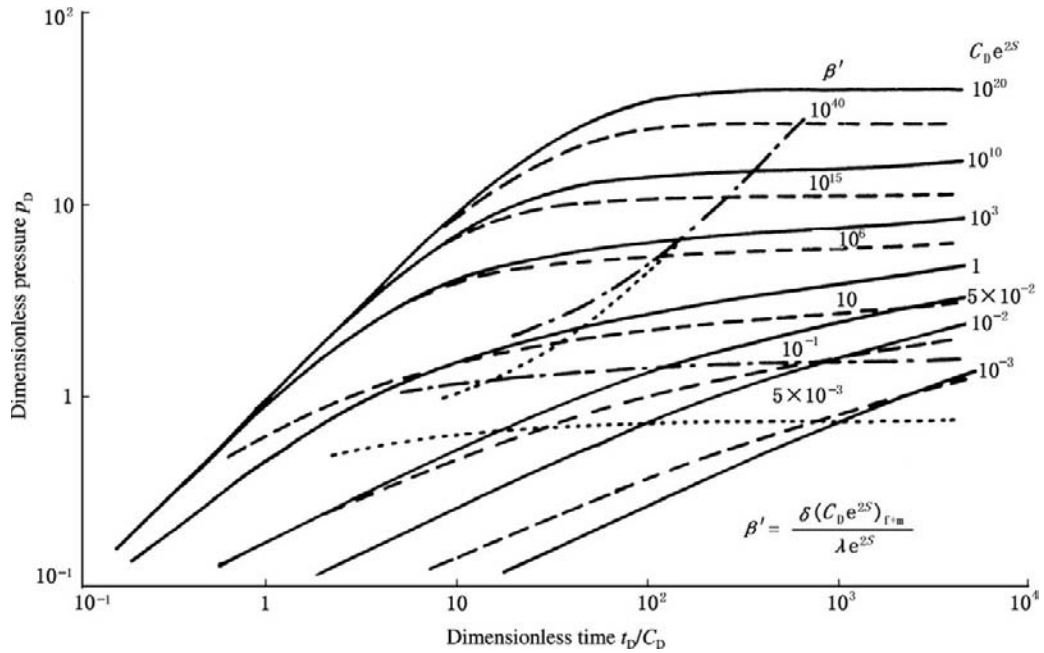


**FIGURE 7-43** Unsteady transition flow portion type curves of dual porosity reservoir.

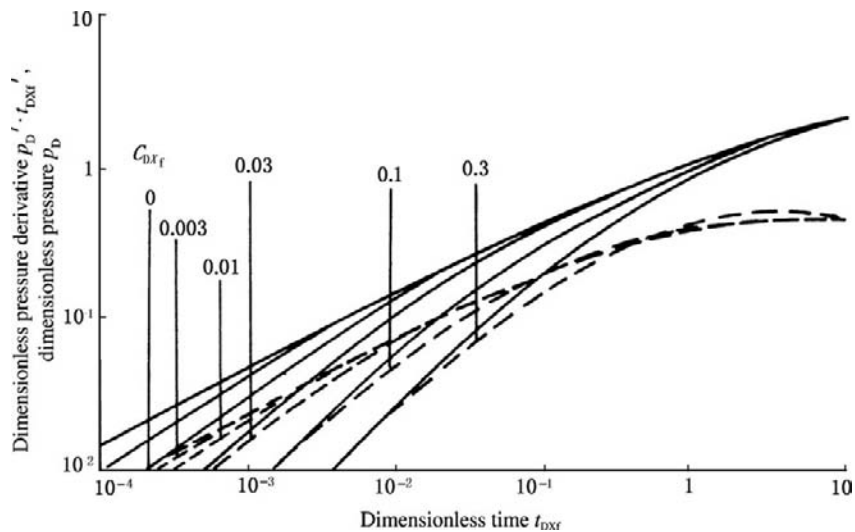


**FIGURE 7-44** The type curves for reservoir with infinite flow-conductivity vertical fracture under the action of  $S$  and  $C$ .

The formula of calculating the  $S$  value on the basis of the pressure drawdown curve is shown in Equation (7-56).

(7-56)

$$S = 1.151 \left[ \frac{P_i - P_{wf}(1h)}{m} - \lg \frac{K}{\Phi \mu C_t r_w^2} - 0.9077 \right]$$

where:  $P_i$  = initial pressure, MPa;  $P_{wf}(1h) = P_{wf}$  value corresponding to 1h on radial-flow straight-line portion or its extended line, MPa;  $m$  = slope of straight line, MPa/cycle.

The formula of calculating the  $S$  value by using the MDH method on the basis of the pressure build-up curve is shown in Equation (7-57).

(7-57)

$$S = 1.151 \left[ \frac{P_{ws}(1h) - P_{ws}(0)}{m} - \lg \frac{K}{\Phi \mu C_t r_w^2} - 0.9077 \right]$$

where:  $P_{ws}(1h) = P_{ws}$  value corresponding to 1h on the straight-line portion or its extended line after shut-in.

Horner's formula on the basis of the pressure build-up curve is shown in Equation (7-58).

(7-58)

$$S = 1.151 \left[ \frac{P_{ws}(1h) - P_{ws}(0)}{m} - \lg \frac{K}{\Phi \mu C_t r_w^2} \cdot \frac{t_p}{t_p + 1} - 0.9077 \right]$$

where:  $t_p$  = flowing time.

### Estimating Skin Factor $S$ Value of a Homogeneous Reservoir Using a Bilogarithmic Measured Pressure Plot

In general, a composite bilogarithmic plot can be drawn during on-site data recording by using a direct-reading electronic pressure gauge. The  $H$  and  $A$  values of measured data points on the plot are substituted into Equations (7-29) and (7-30), thus obtaining the skin factor  $S$  value. In the formulae,  $C_D$  is the dimensionless wellbore storage coefficient, which is an unknown quantity and has an expression, that is, Equation (7-55), where the values of  $\Phi$ ,  $C_t$ ,  $h$ , and  $r_w$  can be obtained from the data of geology and well completion and generally have the following data ranges:

1. Porosity  $\Phi$ : 0.1–0.3 for sandstone reservoir; 0.01–0.1 for carbonatite reservoir. The value

of  $\Phi$  can be obtained from core analysis data for most wells.

2. Composite compressibility  $C_t$ : About  $10^{-3}$   $\text{MPa}^{-1}$  for the oil reservoir; reciprocal of the reservoir pressure approximately. For instance,  $C_t = 0.03 \text{ MPa}^{-1}$  under the reservoir pressure of 30 MPa.
3. Reservoir thickness  $h$ : It can be obtained from completion data.
4. Well radius  $r_w$ :  $r_w = 0.1$  m for 5 1/2-in. casing commonly used.
5. Wellbore storage coefficient  $C$ : It is slightly difficult to determine. There are two methods of estimating the  $C$  value. When the early-time straight-line portion data of the pressure build-up curve is used for calculating the  $C$  value, if the straight-line portion with early slope of 1 appears on the bilogarithmic pressure build-up curve plot, this portion is still a straight line in Cartesian coordinates, and its slope  $m_{ws}$  (unit: MPa/h) can be obtained from the plot, thus obtaining the  $C$  value, as shown in Equation (7-59).

(7-59)

$$C = \frac{qB}{24m_{ws}} (\text{m}^3/\text{MPa})$$

Or Table 7-8 is used for determining the  $C$  value.

After the value of  $C$  is obtained, the value of  $S$  can be obtained by using Equations (7-29) and (7-30).

### Early-Time Portion Interpretation Method (Without Radial Flow Portion)

A pressure build-up or drawdown curve that lacks a radial-flow straight-line portion is inefficient. Despite the fact that formation damage is generated in the vicinity of the wellbore and reflected in early-time data, the degree of formation damage can be determined only if the data of that intermediate radial flow portion, which is comparable to the early-time data, are obtained.

The inapplicability of early-time data is mainly caused by the effect of afterflow.

As shown in Table 7-8, deep wells, oil wells with high gas-oil ratio, or net gas wells have a high C value when pressure is measured under the condition of wellhead shut-in. The high-C well of low-permeability reservoir may have a long afterflow time after shut-in (up to several days or some dozens of days).

For these types of wells, the basic thinking is to find the change of afterflow rate after shut-in, to correct the afterflow portion to radial-flow straight line, and then to calculate the S value by using Equations (7-57) and (7-58). The specific methods are as shown in the following sections.

**Empirical Method.** Suppose the production rate at shutting in ( $\Delta t = 0$ ) is  $Q_0$  and the flow rate at  $\Delta t$  is  $Q$ , as shown in Equations (7-60) and (7-61).

(7-60)

Make

$$\frac{Q_0}{Q} = (1 + \Delta t)^n$$

(7-61)

Then

$$\lg \frac{Q_0}{Q} = n \lg (1 + \Delta t)$$

If only the afterflow rate at  $\Delta t_n$  or the afterflow rate at each  $\Delta t_n$  is found, the value of n can be determined. Simultaneously, the pressure difference  $\Delta p$  of the afterflow portion is corrected to  $\Delta p'$ , and the results shown in Equation (7-62) may be obtained:

(7-62)

$$\Delta p' = \frac{\Delta p}{1 - \frac{Q}{Q_0}}$$

or Equation (7-63):

(7-63)

$$\Delta p' = \frac{\Delta p}{1 - \frac{1}{(1 + \Delta t)^n}}$$

The  $\Delta p'$  versus  $\Delta t$  is made on semilogarithmic paper. Adjust the n value during drawing until a straight line is obtained. It is considered that the straight line after correction is just the radial-flow straight line. Calculate the value of slope m. The value of skin factor S can be calculated in accordance with Equations (7-57) and (7-58).

When the Q value at  $\Delta t$  can be directly measured using instruments, it can be substituted into Equation (7-61) for pressure correction.

**Rassel's Method.** Rassel's method is a cut and trial method, and afterflow rate measurement is not required. Pressure correction coefficient A is defined; thus  $\Delta p'$  revised can be expressed as shown in Equation (7-64).

(7-64)

$$\Delta p' = \frac{\Delta p}{1 - \frac{1}{A \Delta t}}$$

The  $\Delta p' - \lg \Delta t$  plot is made. Adjusting the A value makes the data points become a straight line. It is considered that this A value obtained is just the true value.

After a semilogarithmic plot is made, the slope m of the straight line is calculated and substituted into Equation (7-57) or Equation (7-58), thus obtaining the S value.

**Other New Methods of Analyzing Formation Damage Using Early-Time Data**

1. New instruments that can simultaneously measure the pressure and flow rate at the bottomhole have been developed to simultaneously record the production rate and the pressure of the early-time afterflow portion; thus the data of this portion can be processed by using the deconvolution method, and a straight line is obtained.
2. Grey coefficient method. The A value in Equation (7-64) is defined as the optimum straight-line coefficient. The pressure build-up formula is expressed as shown in Equation (7-65).

(7-65)

$$\frac{\Delta p}{1 - \frac{1}{A \Delta t}} = m \lg \Delta t + D$$

where:  $m = 2.121 \times 10^{-3} \frac{q\mu B}{Kh}$

$$D = m \left[ \lg \left( \frac{K}{\Phi \mu C_r r_w^2} \right) - 0.908 + 0.867S \right]$$

Objective function r is defined as shown in Equation (7-66).

(7-66)

$$r = \min \Sigma \left[ \frac{\frac{\Delta p}{1 - \frac{1}{A \Delta t}} - m \lg \Delta t - D}{1 - \frac{1}{A \Delta t}} \right], A \neq 0, m \neq 0$$

The grey correlation equation of the preceding formula is shown in Equation (7-67).

(7-67)

$$F = \min (1 - R)$$

where R is the grey correlation coefficient. Choose the A value by Equation (7-66) until the R in Equation (7-67) reaches the maximum; thus the A value is determined. The reservoir parameters are obtained as shown in Equations (7-68) and (7-69).

(7-68)

$$K = 2.121 \times 10^{-3} \frac{qB\mu}{mh}$$

(7-69)

$$S = 1.151 \left[ \frac{P_{ws}(1h) - P_{ws}(0)}{m} - \lg \frac{8.1K}{\Phi\mu C_r r_w^2} \right]$$

A computer must be used for calculation due to the complicated calculation process.

### Formation Damage Evaluation for a Natural Gas Well

**Pseudopressure of a Gas Well.** The change of the transient pressure of a gas well is greatly different from that of an oil well due to the obviously different state equation of gas from that of oil and water. When the basic equation of oil and water is derived, it is assumed that the fluid is weakly compressible and the compressibility is constant. This is incorrect under the condition of gas. The viscosity and compressibility of gas are a function of pressure. Due to the real gas, it is related to gas deviation factor Z, which is also a function of pressure.

Thus the concept of pseudopressure is introduced as shown in Equation (7-70).

(7-70)

$$\psi(p) = \int_{p_o}^p \frac{2P}{\mu Z} dp$$

where:  $P_o$  = reference pressure point taken arbitrarily,  $P_o = 0$  often taken.

At this moment the basic equation is expressed as shown in Equation (7-71).

(7-71)

$$\frac{\partial^2 \psi}{\partial r^2} + \frac{1}{r} \cdot \frac{\partial \psi}{\partial r} = \frac{1}{3.6\eta} \cdot \frac{\partial \psi}{\partial t}$$

This coincides entirely with that of oil and water media in form. Thus the data of a gas well can be interpreted like the well test data interpretation of an oil well if the gas pressure is converted into pseudopressure  $\psi$ .

The relation between pseudopressure and pressure is shown in Figure 7-45.

**Calculating S Using Bilogarithmic Type Curves.** The type curves of Gringarten and Bourdet et al. can be used for curve matching and parameter calculation of a gas well like an oil well if only the measured pressure is replaced by pseudopressure  $\psi$  during drawing. The dimensionless pressure is defined as follows.

$$\begin{aligned} P_D &= \frac{0.027143Kh}{q} \cdot \frac{T_{sc}}{T_f P_{sc}} \Delta \psi(p) \\ &= 78.489 \frac{Kh}{qT_f} \Delta \psi(p) \end{aligned}$$

After selecting the match curve, the value of  $C_{DE}^{2S}$  is determined, thus obtaining the following:

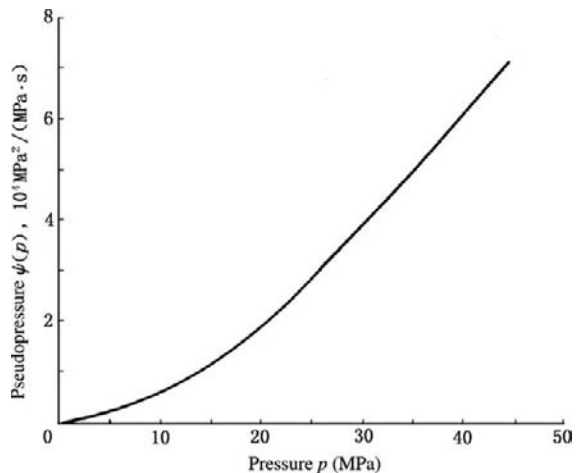


FIGURE 7-45 Relation between pseudopressure and pressure.

$$S = \frac{1}{2} \ln \frac{(C_D e^{2S})_M}{C_D}$$

This skin factor is known as pseudoskin factor  $S_a$  and is the sum of true skin factor  $S$  and the effect of turbulent flow, as shown in Equation (7-72), that is,

(7-72)

$$S_a = S + Dq_g$$

where:  $q_g$  = gas production rate,  $10^4 \text{ m}^3/\text{d}$ ;  $D$  = inertia-turbulent coefficient,  $(10^4 \text{ m}^3/\text{d})^{-1}$ .

The  $D$  value can be determined as follows.

Three different production rates are selected for well testing, and the  $S_a$  and  $q_g$  values obtained are drawn (Figure 7-46).

A straight-line equation is obtained from Figure 7-46; thus  $S = -5.43$  and  $D = 0.0406 (10^4 \text{ m}^3/\text{d})^{-1}$  are determined.

**Calculating  $S$  Using Semilogarithmic Radial-Flow Straight-Line Portion.** The slope  $m$  of the semilogarithmic radial-flow straight-line portion of gas pseudopressure can be used for calculating permeability  $K$  and skin factor  $S$ . Under the condition of pressure build-up,  $S_a$  is as shown in Equation (7-73).

(7-73)

$$S = 1.151 \left[ \frac{\psi[P_{ws}(1h)] - \psi(P_{wf})}{m} - \lg \frac{K}{\Phi \mu C_t r_w^2} - 0.9077 \right]$$

where:  $p_{wf}$  = flowing pressure before shut-in; that is,  $p_{wf} = p_{ws}(0)$ , MPa.

**Simplification of Pseudopressure.** If the pressure of the gas well changes in some range in the whole test process, the pseudopressure  $\psi$  can be generally simplified.

When  $p < 13.8$  MPa,

$$\psi(p) \approx \frac{p^2}{\mu_i Z_i}$$

Thus the so-called pressure square method is formed, and the calculation formula is changed as in Equations (7-74) and (7-75):

(7-74)

$$K = \frac{42.42 \mu Z P_{sc} q T_f}{m T_{sc} h} = \frac{0.01467 \mu Z q T_f}{m h}$$

(7-75)

$$S_a = 1.151 \left[ \frac{P_i^2 - P_{wf}^2(1h)}{m} - \lg \frac{K}{\Phi \mu C_t r_w^2} - 0.9077 \right]$$

for pressure drawdown, and as in Equation (7-76) for pressure build-up:

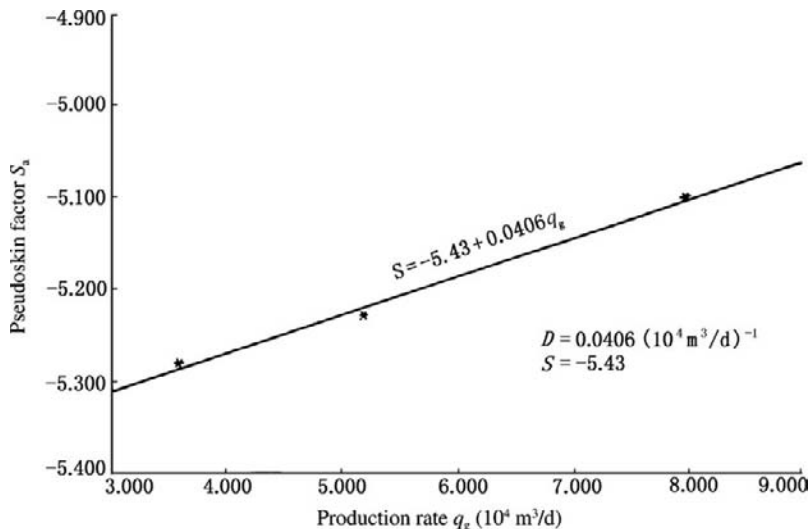


FIGURE 7-46 Determination of inertia-turbulent coefficient  $D$ .

(7-76)

$$S_a = 1.151 \left[ \frac{P_{ws}^2(1h) - P_{wf}^2}{m} - \lg \frac{K}{\Phi \mu C_t r_w^2} - 0.9077 \right]$$

The dimensionless pressure is shown in Equation (7-77).

(7-77)

$$P_D = \frac{0.027143Kh}{q\mu Z} \cdot \frac{T_{SC}}{T_f P_{SC}} \cdot \Delta(p^2) = 78.489 \frac{Kh}{q\mu Z T_f} \Delta(p^2)$$

When  $p > 20.7$  MPa,  $\frac{p}{\mu Z}$  is approximately a constant; thus Equations (7-78), (7-79), and (7-80) for pressure drawdown,

(7-78)

$$\psi(p) = \frac{2p_i}{\mu_i Z_i} p$$

(7-79)

$$K = \frac{21.21\mu_i Z_i P_{SC} q T_f}{P_i T_{SC} m h} = \frac{7.335 \times 10^{-3} \mu_i Z_i q T_f}{P_i m h}$$

(7-80)

$$S_a = 1.151 \left[ \frac{P_i - P_{wf}(1h)}{m} - \lg \frac{K}{\Phi \mu C_t r_w^2} - 0.9077 \right]$$

and Equation (7-81) for pressure build-up.

(7-81)

$$S_a = 1.151 \left[ \frac{P_{ws}(1h) - P_{wf}}{m} - \lg \frac{K}{\Phi \mu C_t r_w^2} - 0.9077 \right]$$

The dimensionless pressure is as follows.

$$P_D = \frac{0.054286Kh}{q} \cdot \frac{T_{SC}}{T_f} \cdot \frac{P_i}{\mu_i Z_i} \cdot \frac{\Delta p}{P_{SC}} = 157 \frac{Kh}{q T_f} \cdot \frac{P_i}{\mu_i Z_i} \Delta p$$

## Evaluating Formation Damage Using Systematic Well Test Data

As mentioned earlier, the systematic well test method can be used for estimating the  $S$  value. It can be used to obtain the productivity index  $J$  under the condition of no formation damage in the vicinity of the wellbore, as shown by Equation (7-18), that is,

$$J_{ideal} = \frac{q}{P^* - P_{wf} - \Delta P_S}$$

The actual productivity index, that is, the ratio of the difference between reservoir pressure

and flowing pressure to production rate, is shown by Equation (7-17), that is,

$$J_{actual} = \frac{q}{P^* - P_{wf}}$$

The ratio between them is flow efficiency FE, as shown by Equation (7-19), that is,

$$FE = \frac{J_{actual}}{J_{ideal}} = \frac{P^* - P_{wf} - \Delta P_S}{P^* - P_{wf}}$$

It can be seen that there is no formation damage if  $FE = 1$ , there is formation damage if  $FE > 1$ , and the well is stimulated if  $FE > 1$ . The degree of formation damage can be qualitatively appraised.

On the basis of Equation (7-27), the following relation between FE and  $S$  is obtained:

$$S = 1.1513 (1 - FE) CI$$

where:

$$CI = \frac{P^* - P_{wf}}{m}$$

which is known as the completeness index.

It can be found that despite the fact that the FE value obtained by systematic well test can be used for calculating the  $S$  value, the  $m$  value should be obtained by transient well test. In addition, the other parameters, such as DR and DF, that are obtained by systematic well test can only be used for qualitative or semiquantitative analysis.

In recent years, many types of well test interpretation software have been developed, and computer-aided well test interpretation has been widely applied in the field [25].

## 7.7 WELL LOGGING EVALUATION OF FORMATION DAMAGE DEPTH

During overbalanced drilling, the reservoir around the borehole will be invaded by drilling fluid filtrate and solids to some extent. If the invasion decreases the reservoir permeability, formation damage is caused by the drilling fluid. Using well logging data can accurately determine whether the drilling fluid filtrate invaded the reservoir, can calculate the invasion depth, and can evaluate the damage depth.

## Physical Process of Invasion of Drilling Fluid Filtrate into Reservoir

The process of the invasion of drilling fluid filtrate into the reservoir is just the process in which the drilling fluid or filtrate displaces the original fluid in the reservoir under overbalance pressure. In this process, water-based drilling fluid or filtrate will also mix with reservoir water, and the ionic diffusion process between fluids with different salinities will be generated. Therefore, the whole process of the invasion of drilling fluid or filtrate includes the process in which drilling fluid or filtrate displaces the original fluid in the reservoir, the process in which the compatible fluids will mix, and the process in which ions will diffuse between the solutions with different concentrations. In a porous reservoir, the invasion depth of drilling fluid filtrate is generally 1–5 m, the inner cake thickness is about 3 cm, and the outer cake thickness is less than 2 cm.

For a porous reservoir, if the process of forming the inner cake is neglected, the process of the invasion of drilling fluid into the reservoir can be regarded as the process in which drilling fluid filtrate displaces the fluid in the reservoir pores. This process follows Darcy's law and multiphase flow equation. The invasion volume is mainly dependent on cake and reservoir permeabilities and also related to the viscosity and compressibility of oil, gas, and water; the difference between drilling fluid column pressure and reservoir pressure; reservoir porosity; oil saturation; residual oil saturation; water saturation; capillary pressure behavior and multiphase flow behavior; and so on.

During the invasion of filtrate into the reservoir, the following three zones with different degrees of displacement will radially form (Figure 7-47):

1. Near-wellbore flushed zone in which a strong displacement is generated
2. Transitional zone (invaded zone) with a weaker displacement outside the flushed zone
3. Virgin zone with no displacement

When the filtrate invades the reservoir and displaces the virgin fluid in the reservoir, fluid

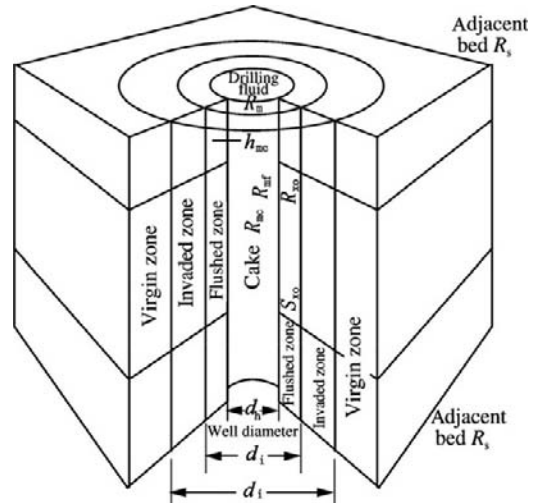


FIGURE 7-47 Invasion of drilling fluid into reservoir.

mixing and ionic diffusion will be generated between filtrate and reservoir water. The mixing process follows the mass transfer equation of single-phase flow and is only generated in the flushed zone and the transitional zone. The ionic diffusion process means the process in which the ions in high-concentration salt solution diffuse into low-concentration salt solution under osmotic pressure when salt solutions with different concentrations contact each other. This process follows diffusion law.

## Effect of Invasion of Drilling Fluid on Log Response

During drilling, the pressure of the drilling fluid column is generally higher or slightly higher than reservoir pressure. Therefore, for a permeable reservoir, the invasion of drilling fluid filtrate into the reservoir is an accustomed situation. However, this invasion is essentially a complicated physical process and is related to the drilling fluid property under the downhole condition, reservoir pressure, reservoir permeability, reservoir porosity, oil saturation, water saturation, oil viscosity, the duration of soaking reservoir by drilling fluid, and so on. After the drilling fluid filtrate invades into the reservoir, the flushed zone, invaded zone and virgin zone are formed (Figure 7-17).

When drilling fluid filtrate that has a salinity much lower than reservoir water salinity invades the reservoir, the oil or gas reservoir and aquifer can be identified by using electrical logging suites with different investigation depths or electrical logging with the same investigation depth at different times due to the radially different water saturations in the invaded zone or the different distributions of different salinities on the basis of the characteristic that the saturation is differently distributed radially in the invaded zone.

The resistivity (approximate to invaded zone resistivity) obtained from the apparent resistivity

curves of shallow investigation laterolog on type curves and the true formation resistivity obtained from the apparent resistivity curves of deep investigation laterolog on type curves (Figure 7-48) are used for analyzing the radial change of reservoir resistivity.

### Drilling Fluid Invasion Depth Log Evaluation Method

The degree of invasion of drilling fluid filtrate into sandstone oil and gas reservoir or aquifer is also related to other factors in addition to drilling fluid properties.

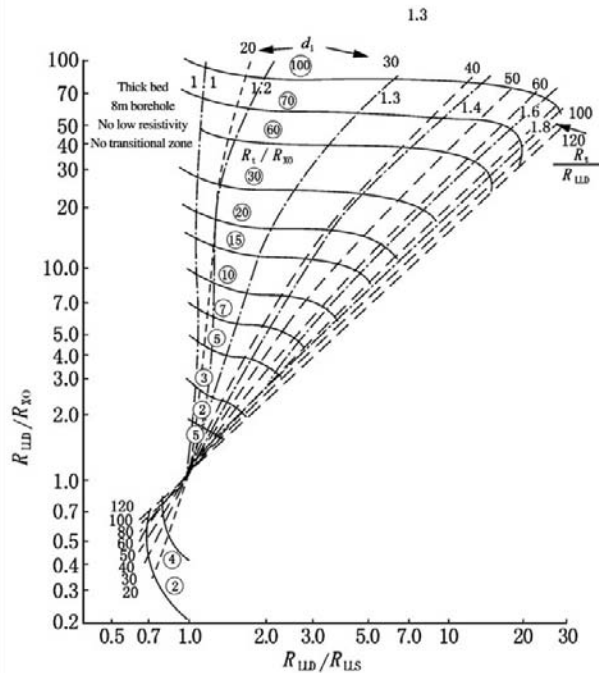
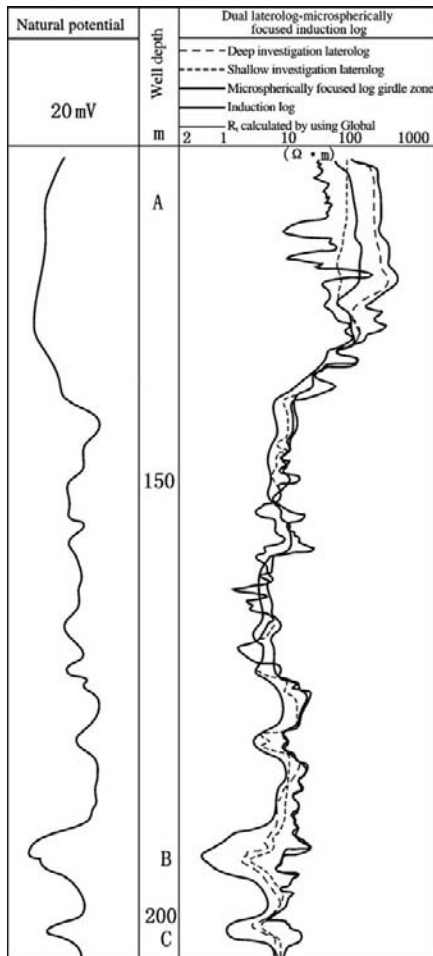


FIGURE 7-48 Deep, medium, and shallow resistivity log of oil and gas well and the type curves of determining filtrate invasion depth.

The radial change of reservoir resistivity by the invasion of drilling fluid filtrate can be reflected on the resistivity logging suite. The commonly used resistivity logging suite includes dual laterolog-microspherically focused log and dual induction-laterolog 8. The values of  $R_{LLD}$ ,  $R_{LLS}$ ,  $R_{XO}$ , and so on are first read on log and then corrected with borehole and shoulder bed. Appropriate cyclone type curves are selected, and filtrate invasion diameter  $d_i$  can be obtained. If borehole diameter  $d$  is given, invasion depth  $d_p$  can be obtained in accordance with Equation (7-82):

(7-82)

$$d_p = \frac{d_i - d}{2}$$

where:  $d_p$  = invasion depth of drilling fluid filtrate into reservoir from borehole wall, cm;  $d_i$  = radial invasion diameter obtained on cyclone type curves, cm;  $d$  = borehole diameter obtained from borehole diameter curve, cm.

## REFERENCES

- [1] C.V. Millikan, C.V. Sidwell, Bottom-hole Pressures in Oil Wells, *Trans. AIME* 92 (1931) 194–205.
- [2] D.G. Hawthorn, Review of Subsurface Pressure Instruments, *Oil Gas J.* 16 (April 20, 1993) 40.
- [3] M. Muskat, Use of Data on the Build-up of Bottom-hole Pressures, *Trans. AIME* 123 (1937) 44–48.
- [4] C.C. Miller, et al., The Estimation of Permeability and Reservoir Pressure from Bottom Hole Pressure Build-up Characteristics, *Trans. AIME* 189 (1950) 91–104.
- [5] D.R. Horner, Pressure Build-up in Wells, in: *Proc. Third World Pet. Cong.*, vol. II, E. J. Brill, Leiden, 1951, p. 503.
- [6] A.F. Van Everdingen, The Skin Effect and Its Influence on the Productive Capacity of a Well, *Trans. AIME* 198 (1953) 171–176.
- [7] W. Hurst, Establishment of the Skin Effect and Its Impediment to Fluid Flow into a Wellbore, *Pet. Eng.* 25 (Oct. 1953) B-6.
- [8] R.G. Agarwal, et al., An Investigation of Wellbore Storage and Skin Effect in Unsteady Liquid Flow: I. Analytical treatment, *Soc. Pet. Eng. J.* (Sept. 1970) 279–290; *Trans. AIME* 249.
- [9] A.C. Gringarten, et al., A Comparison between Different Skin and Wellbore Storage Type-Curves for Early-Time Transient Analysis. Paper SPE 8205, Presented at the 54th Annual Technical Conference and Exhibition of SPE, Las Vegas, Nov., Sept., 23–26 (1979).
- [10] D. Bourdet, et al., A New Set of Type-Curves Simplifies Well Test Analysis, *World Oil* (May 1983) 95–106.
- [11] Tong Xianzhang, Application of Pressure Build-up Curves in Oil and Gas Field Development, Petrochemical Industry Press, Beijing, 1984 (in Chinese).
- [12] Cheng Suimin, Serial Modes of Formation Damage Evaluation Standard, *Gas Industry* (3) (1988) (in Chinese).
- [13] Zhuang Huinong, Graph Analysis Method of Well Test Data, *Buried Hill J.* (4) (1993), (1) 1994, (2) 1994, (4) 1994 (in Chinese).
- [14] G.E. Barenblatt, et al., Basic Conception of the Theory of Homogeneous Liquids in Fissured Rocks, *JAMM (USSR)* 24 (5) (1960) 1286–1303.
- [15] J.E. Warren, P.J. Root, Behavior of Naturally Fractured Reservoirs, *SPEJ* (Sept. 1963) 245.
- [16] H. Kazemi, et al., The Interpretation of Interference Tests in Naturally Fractured Reservoir with Uniform Fracture Distribution, *SPEJ* (Dec. 1969).
- [17] D. Bourdet, A.C. Gringarten, Determination of Fissure Volume and Block Size in Fractured Reservoirs by Type Curve Analysis. *SPE* 9293.
- [18] Zhu Yadong, Well Test Analysis in a Double Porosity Reservoir. *SPE* 14867.
- [19] D. Bourdet, et al., Use of Pressure Derivation in Well Test Interpretation. *SPE* 12777.
- [20] A.C. Gringarten, et al., Unsteady State Pressure Distributions Created by a Well with a Simple Infinite Conductivity Vertical Fracture, *SPEJ* (Aug. 1974) 347–360, *Trans. AIME* 257.
- [21] F. Rodriguiz, et al., Partially Penetrating Vertical Fractures Pressure Transient Behavior of a Finite-conductivity Fracture. *SPE* 13057.
- [22] Liu Nengqiang, Applied Modern Well Test Interpretation Methods, Petroleum Industry Press, Beijing, 1992 (in Chinese).
- [23] Cheng Suimin, New Analysis Methods of Early Time Data of Well Test, *Well Testing* (1) 1992 (in Chinese).
- [24] A.C. Gringarten, Computer-Aided Well Test Analysis. *SPE* 14099.
- [25] Compilation Group of Model Examples of Well Test Interpretation in China, Model Examples of Well Test Interpretation in China, Petroleum Industry Press, Beijing, 1994 (in Chinese).

# Measures for Putting a Well into Production

## OUTLINE

### 8.1 Preparations before Putting a Well into Production

#### Drifting

*Drifting by Using Drift Diameter Gauge*

*Drifting by Using Lead Stamp*

#### Casing Scraping

*Rubber Sleeve Type*

*Casing Scraper*

*Spring-Type Casing Scraper*

#### Well-Flushing

*Properties of Well-Flushing Fluid*

*Well-Flushing Methods  
Technical Requirements for Well-Flushing*

### 8.2 Main Measures for Putting the Well into Production

#### Physical and Chemical

Blocking Removal

#### Acidizing

#### Hydraulic Fracturing

#### Acid Fracturing

#### Acting Mechanisms and

Applicable Ranges of the Main Measures for Putting a Well into Production

### 8.3 Physical and Chemical

#### Blocking Removal

Blocking Removal by Chemicals

*Blocking Removal by Chemical Solvent*

*Blocking Removal by Anti-Swelling and Deswelling Agent*

*Blocking Removal by Viscosity-Reducing Agent*

*Thermo-Chemical*

*Blocking Removal*

*Blocking Removal by Oxidant*

*Blocking Removal by Surface Tension Reducer*

*Blocking Removal by Active Enzyme*

#### Physical Blocking Removal

*Blocking Removal by Ultrasonic Wave*

*Blocking Removal by Microwave*

*Magnetic Treatment Technique*

*Vibration Blocking*

*Removal Technique*

*Low-Frequency Electric Pulse Blocking Removal Technique*

### 8.4 Hydraulic Fracturing for Putting a Well into Production

Hydraulic Fracturing of Sandstone Reservoirs

*Goal and Function of Hydraulic Fracturing*

*Prefrac Appraisal and Analysis*

*Fracturing Fluid*

*Proppant*

*Integral Reservoir (or Block) Frac*

*Optimization Design*

*Hydraulic Fracturing Technology*

*Fracturing Performing and Postfrac*

*Appraisal*

Hydraulic Fracturing for Carbonatite Reservoir

*Difficulties of Hydraulic Fracturing for*

*Carbonatite Reservoir*

*Adaptability Analysis of Carbonatite Reservoir Fracturing*

### 8.5 Acidizing for Putting a Well into Production

Principle and Classification of Acidizing

*Classification of Acidizing Technology*

*Principle of Increasing Productivity by*

*Acidizing*

Matrix Acidizing for Sandstone Reservoir

*Acid Liquor and Additives*  
*Acidizing Technology*  
*Real-Time Monitoring and Effectiveness*  
*Appraisal of Acidizing*  
 Matrix Acidizing for Carbonatite Reservoir  
*Chemical Reaction of Acid Liquor to Carbonatite*  
*Optimization Design Technique for Carbonatite Acidizing*  
 Acid Fracturing for Carbonatite Reservoir  
*Acid-Rock Reaction Kinetics*  
*Acid Liquor Filtration*  
*Loss during Acid Fracturing*  
*Acid-Etched Fracture Flow Conductivity*  
*Commonly Used Acid Liquor Systems and Properties*  
*Acid Fracturing Technology*  
*Acidfrac Design Model in Consideration of Acid-Etched Wormholes*  
*Acidfrac Stimulation Effectiveness Prediction*

**8.6 High-Energy Gas Fracturing for Putting a Well into Production**  
 Mechanism of High-Energy Gas Fracturing  
*Overview*  
*Conditions of Generating Fractures*  
*Cracking Initiation Mechanism*  
*Self-Propping of Fractures*  
*Effects of High-Energy Gas Fracturing*  
 Types of High-Energy Gas Fracturing and Suitabilities  
*Solid Propellant Fracturing*  
*Liquid Propellant Fracturing*  
*Suitabilities of High-Energy Gas Fracturing*  
 High-Energy Gas Fracturing Design  
*Combustion of Propellant*  
*Well Fluid Motion Equation*  
*Relationship between Pressure and Time*  
*Flow Rate of Gas Squeezed into Vertical Fractures*

Combined High-Energy Gas Fracturing and Perforating  
 High-Energy Gas Fracturing Tests  
*Static Test (Peak Pressure Test)*  
*Dynamic Test (Downhole Pressure-Time Process Test)*  
**8.7 Flowing Back**  
 Flowing Back by Displaced Flow  
*Conventional One-Step Displaced Flow Method*  
*Two-Step Displaced Flow Method*  
 Flowing Back by Swabbing  
 Flowing Back by Gas Lift  
*Conventional Gas-Lift Unloading*  
*Multistage Gas-Lift Valve Unloading*  
*Coiled-Tubing Gas-Lift Unloading*  
*Nitrogen Gas Gas-Lift Unloading*  
 Flowing Back by Aerated Water  
 Flowing Back by Foam  
*Foam Composition*  
*Foam Stability*  
*Foam-Generating Equipment*  
**References**

## 8.1 PREPARATIONS BEFORE PUTTING A WELL INTO PRODUCTION

After perforating of a cased well, preparations before putting the well into production are necessary for achieving the desired productivity.

### Drifting

Drifting aims at verifying whether a wellbore is unimpeded. Pipe string or wire rope may be used for drifting. Because most operating units no

longer use bailing drums at present, drifting by using wire rope has been uncommon. Drifting is not only applied in the operation of putting the well into production, but it is also an important procedure before an important pipe string is run in and during well servicing in subsequent production processes. The main tools used for drifting include drift diameter gauge and lead stamp.

**Drifting by Using Drift Diameter Gauge.** Drift diameter gauges are the simple and common tools used for inspecting the drift diameter of casing or tubing to determine whether drift

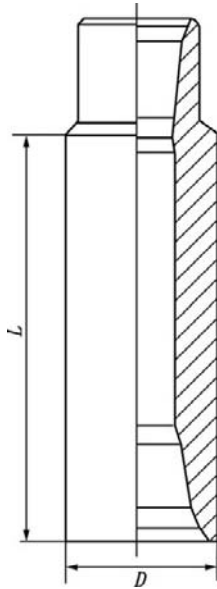


FIGURE 8-1 Drift diameter gauge for casing.

diameter meets the standard (Figure 8-1). The size of the drift diameter gauge is selected in accordance with the minimum casing ID in the well (Table 8-1).

For special usage, the outside diameter  $D$  and length  $L$  of the drift diameter gauge can be determined on the basis of the maximum geometric size of the tool run in. In general, the outside diameter of the drift diameter gauge should be 4 to 6 mm less than the minimum inside diameter of the casing.

If the drift diameter gauge passes smoothly through the wellbore, it indicates that the drift diameter of the wellbore meets the requirement. If the drift diameter gauge meets frontal resistance, there may be sand column, junk, or casing deformation, and further inspection is required.

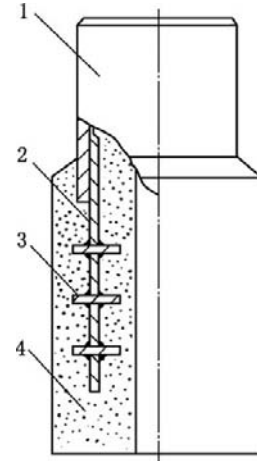


FIGURE 8-2 Lead stamp. 1, collar; 2, nipple; 3, brace; 4, lead body.

**Drifting by Using Lead Stamp.** When the drift diameter gauge meets frontal resistance, it is pulled out and a lead stamp is run for further inspection to determine the condition of junk or downhole casing deformation. The structure of a lead stamp is shown in Figure 8-2. The technical specifications of a lead stamp are listed in Table 8-2.

The lead stamp used for drifting and stamping should not be run too fast, in order to prevent the lead stamp from impacting and deforming midway, which may affect the analysis result. A press exerted can be generally 15–30 kN and is allowed to be increased or decreased appropriately but cannot exceed 50 kN. Impact is not allowable. The lead stamp should just be pulled up after pressing and stamping once. Only one pressing is allowed; a second time of stamping is not allowable.

TABLE 8-1 Sizes of Drift Diameter Gauges of Casing Series

Specifications of casing (in.)	4½	5	5½	5¾	6%	7
Outside diameter $D$ (mm)	92 ~ 95	102 ~ 107	114 ~ 118	119 ~ 128	136 ~ 148	146 ~ 158
Length $L$ (mm)	500	500	500	500	500	500
Connection thread	NC26-12E 2¾ TBG	NC26-12E 2¾ TBG	NC31-22E 2¾ TBG	NC31-22G 2¾ TBG	NC31-22G 2¾ TBG	NC38-32E 3½ TBG

**TABLE 8-2** Technical Specifications of Lead Stamp

Casing size (in.)	4½	5	5½	5¾	6%	7	7%
Outside diameter (mm)	95	105	118	120	145	158	174
Length (mm)	120	120	150	150	180	180	180

After the lead stamp is pulled out, its technical description, photographing, and filing are required.

## Casing Scraping

Casing scraping aims at removing the cement on the inner casing wall and the burrs at perforations in order to ensure the normal working of downhole tools and the successful setting of the packer.

Commonly used casing scrapers include rubber sleeve type casing scraper and spring-type casing scraper.

**Rubber Sleeve Type Casing Scraper.** A rubber sleeve type casing scraper consists mainly of upper connector, housing, rubber sleeve, washing pipe, cutting blade, and lower connector, as shown in Figure 8-3.

There are 18 grooves for cutting blades installed from inside to outside. Cutting blades are arranged into three integral left-hand (or right-hand) helical curves with a helix angle of 30°.

Cutting blades are made of materials with high wear resistance and toughness, using precision casting technology (Figure 8-4).

Rubber sleeve has good elasticity and sufficient hardness. When a cutting blade meets resistance, the rubber sleeve will bear a radial squeeze pressure of the cutting blade and generate a radial feed force acting on the cutting

blade, thus ensuring a sufficient scraping force of the cutting blade.

When the scraper moves downward, the main edge of the cutting blade moves down the casing wall. The dirt on the casing wall can be repeatedly scraped by three cutting blades arranged from top to bottom circumferentially. When the dirt on the casing wall is larger and has a higher hardness, the scraper will meet greater resistance. Under this condition, rotary scraping may be adopted. Scraping is mainly along the helical curve, and the auxiliary edge will take a supplementary scraping effect. The technical specifications of a rubber sleeve type casing scraper are listed in Table 8-3.

**Spring-Type Casing Scraper.** A spring-type casing scraper consists mainly of housing, blade plate, blade plate seat, fixing block, and helical spring, as shown in Figure 8-5.

A spring-type scraper that has been assembled has a maximum diameter larger than the inside diameter of the casing to be scraped. The blade projection on the overhead view encloses a whole circle of 360° and there is a slight overlap. In addition, there is no movement that may loosen the scraper connector thread under the condition of reciprocal scraping up and down or right-hand and reciprocal scraping up and down; thus, the scraper can work safely and reliably. The technical specifications of a spring-type casing scraper are listed in Table 8-4.

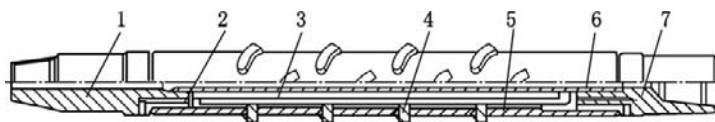


**FIGURE 8-3** Structure of rubber sleeve type casing scraper. 1, upper connector; 2, washing pipe; 3, rubber sleeve; 4, cutting blade; 5, housing; 6, O-ring; 7, lower connector.

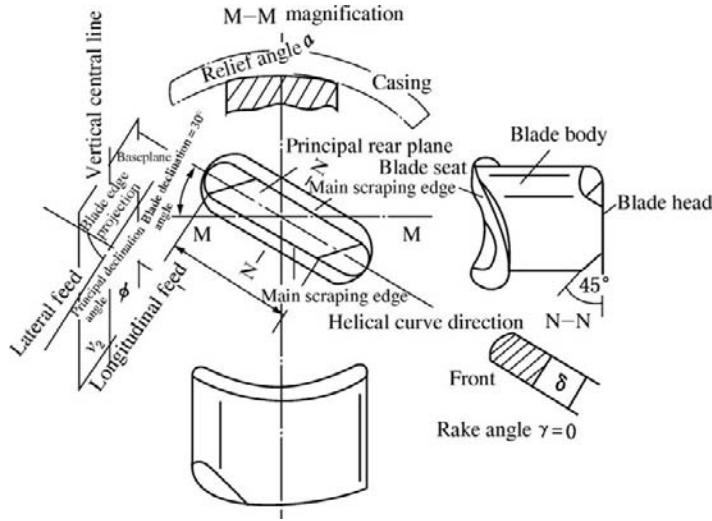


FIGURE 8-4 Structure of cutting blade.

TABLE 8-3 Technical Specifications of Rubber Sleeve Type Casing Scraper

No.	Model Number	Outside Dimensions (mm × mm)	Connector Thread	Use Specification and Performance Parameter	
				Casing Scraped (in.)	Blade Extension (mm)
1	GX-G114	φ112 × 1119	NC26(2A10)	4½	13.5
2	GX-G127	φ119 × 1340	NC26(2A10)	5	12
3	GX-G140	φ129 × 1443	NC31(210)	5½	9
4	GX-G146	φ133 × 1443	NC31(210)	5¾	11
5	GX-G168	φ156 × 1604	330	6⅝	15.5
6	GX-G178	φ166 × 1604	330	7	20.5

## Well-Flushing

Well-flushing aims at flushing the wellbore and carrying the dirt in the well to the surface by flushing fluid in order to prepare for subsequent operations.

**Properties of Well-Flushing Fluid.** Well-flushing fluid should be clean and good quality and should have the same relative density as that of the killing fluid and no formation damage.

### 1. Relative density

The relative densities of commonly used well-flushing fluids are shown in Table 8-5.

### 2. Compatibility

Sodium chloride salt water or the produced formation water after removing oil and solids is commonly adopted as well-flushing fluid. A well-flushing fluid should be compatible with reservoir and formation water, and formation damage should be decreased as much as possible, so that reservoir protection may be achieved. For a sensitive reservoir, the well-flushing fluid formulation can be determined by laboratory compatibility test.

### 3. Suspended solid content, particle diameter, and total iron content

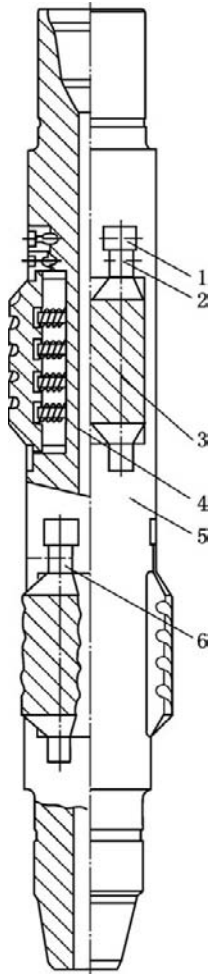


**FIGURE 8-5** Structure of spring-type casing scraper. 1, fixing block; 2, Allen-type socket screw; 3, blade plate; 4, spring; 5, housing; 6, blade plate seat.

Suspended solid content should be less than or equal to 1 mg/l. Suspended solid particle diameter should be less than or equal to 2  $\mu\text{m}$ . Total iron content should be less than 0.5 mg/l.

In order to ensure the quality of well-flushing fluid, a fine filter for well-flushing fluid should be used and well-flushing fluid should be filtrated before entering the well, so that formation damage that may be caused by suspended solid particles and ionic salt colloid precipitate can be prevented.

**Well-Flushing Methods.** Well-flushing methods include direct circulation well-flushing, during which well-flushing fluid is pumped into the well from tubing and returned from the tubing-casing annulus, and reverse circulation well-flushing, during which well-flushing fluid is pumped from the tubing-casing annulus and returned from tubing.

Direct circulation flushing and reverse circulation flushing have different features. When pump pressure and pumping rate are constant, direct circulation flushing has a lower bottomhole backpressure and a lower upward velocity in the tubing-casing annulus, while reverse circulation flushing has a higher bottomhole backpressure and a higher upward velocity in tubing. Therefore, when the pumping rate is sufficiently high, direct circulation flushing should be adopted so that the bottomhole backpressure on the reservoir is lower and formation damage may be avoided; when the pumping rate is lower,

**TABLE 8-4** Technical Specifications of Spring-Type Casing Scraper

No.	Model Number	Outside Dimensions (mm $\times$ mm)	Connector Thread	Use Specification and Performance Parameter	
				Casing Scraped (in.)	Blade Extension (mm)
1	GX-T114	$\phi 112 \times 1119$	NC26(2A10)	4½	13.5
2	GX-T127	$\phi 119 \times 1340$	NC26(2A10)	5	12
3	GX-T140	$\phi 129 \times 1443$	NC31(210)	5½	9
4	GX-T146	$\phi 133 \times 1443$	NC31(210)	5¾	11
5	GX-T168	$\phi 156 \times 1604$	330	6¾	15.5
6	GX-T178	$\phi 166 \times 1604$	330	7	20.5

**TABLE 8-5** Relative Densities of Commonly Used Well-Flushing Fluids

Well-Flushing Fluid	Salt Water		Formation Water
	Common Salt Water	Salt Water with CaCl <sub>2</sub> Added	
Relative density	1 ~ 1.18	1 ~ 1.26	1 ~ 1.03

reverse circulation flushing is appropriate due to the higher upward velocity of well-flushing fluid and higher dirt-carrying ability, but it has a higher backpressure on the reservoir and a possibility of formation damage. Thus direct circulation, high pumping rate, and continuous circulation are adopted for well-flushing.

**Technical Requirements for Well-Flushing.** Blank tubing should be used for well-flushing. During actual tagging of the artificial bottom of a well, the reading on the weight indicator should be decreased by 2–3 t and the error should be less than 0.5 m.

During well-flushing, tubing is run to 2–3 m above the sand surface. The dirt at the bottom-hole should be flushed out. The flushing fluid volume should be larger than two times the wellbore volume. The pumping rate during well-flushing should not be lower than 25 m<sup>3</sup>/h. If any pump bouncing is generated, the tubing should be immediately pulled up, and then the well is flushed by stepwise deepening. Bouncing of the pump under the condition of reverse circulation should be strictly inhibited in order to prevent formation damage.

During well-flushing, a continuous timing sampling at both inlet and outlet is required until the properties of both the samples at inlet and outlet are basically same.

## 8.2 MAIN MEASURES FOR PUTTING THE WELL INTO PRODUCTION

Oil and gas wells will be put into production after perforating. When the natural well productivity cannot meet the requirement of commercial oil and gas stream or the requirement of production tests for productivity, well stimulation is required before putting the well into production.

## Physical and Chemical Blocking Removal

For dozens of years, many new theories and techniques have been introduced into the domain of petroleum production, and physical blocking removal techniques that aim at improving near-wellbore permeability and increasing individual-well production rate have been gradually formed. Physical blocking removal means that the physical fields including thermal field, sound field (broadband), electrostatic field, magnetic field, and alternating electric field are used for exciting the reservoir, removing reservoir blocking, and increasing reservoir fluid flowability, in order to increase the oil and gas well production rate. This type of blocking removal technique has strong adoptability, obvious effects of increasing oil production and decreasing water production, simple technology, low cost and high production, no formation damage, dominance complementarity to chemical drive, and so on, and can have an important effect in oil and gas production.

Chemical blocking removal has been commonly used in recent years. It uses blocking remover chemicals to remove the reservoir flow channel blocking in the vicinity of the wellbore or around perforations.

## Acidizing

Acidizing means that acid (generally hydrochloric acid) is used for removing the contaminant in the vicinity of the wellbore and the blocking matter in pores and fractures or interconnecting and enlarging the original pores or fractures in the reservoir so that reservoir permeability and well productivity are increased. Acid washing

and matrix acidizing are the commonly used acidizing operations of blocking removal. Acid washing is also known as skin blocking removal acidizing and is mainly used for the skin blocking removal of sandstone and carbonatite oil and gas reservoirs and the interconnecting of perforation. Matrix acidizing is also known as conventional acidizing and means that acid liquor is squeezed into the reservoir pore space under a pressure lower than the breakdown pressure of reservoir rock so that the acid liquor can flow radially into the reservoir and dissolve the solids and other blocking matter in the reservoir pore space to enlarge pore space and restore or increase reservoir permeability. Matrix acidizing is mainly used for removing near-wellbore formation damage caused by drilling fluid, completion fluid, or workover fluid. Matrix acidizing technology has a large acid-rock contact area, short acid-rock reaction time, and a treatment range of about 1 m, thus achieving good treatment effectiveness of wells with serious blocking.

## Hydraulic Fracturing

Hydraulic fracturing is a mature stimulation technique that has been applied worldwide. In recent years, its technical level and economic benefit have been obviously enhanced, and hydraulic fracturing has become a main measure for putting wells into production and increasing the well productivity of low-permeability reservoirs.

During hydraulic fracturing of the well, a fracturing fluid is pumped into the well using a high-pressure pump with a pumping rate higher than the absorbing capacity of the reservoir, and a high pressure is formed at the bottomhole to surmount the minimum principal in-situ stress and the tensile strength and fracture toughness of rock so that the formation is cracked and the fracture generated is extended and propped by proppant; thus, a fracture with a specific geometric shape is formed and an increase in well productivity is achieved.

Hydraulic fracturing can be individual-well or integral fracturing in accordance with the point

of view of reservoir engineering. Hydraulic fracturing that takes an individual well as a working cell is known as individual-well hydraulic fracturing and aims mainly at achieving an increase in individual-well productivity using the change of individual-well flow condition and flow resistance. The objective function of economic optimization design is the maximum net present value after individual-well fracturing; that is, the maximum economic benefit obtained by the total economic revenue of cumulative production after individual-well operation minus the cost of fracturing operation. Integral fracturing takes a low-permeability reservoir (or block) as a working cell and uses the flow system, which is the optimal combination of waterflood development pattern and hydraulically created fracture, to achieve an increase in individual-well productivity and sweep efficiency. Both production wells and corresponding water injection wells are generally fractured. The optimization design includes the relationship between oil recovery rate, recovery percent of reserves, and economic benefit to achieve the maximum net present value in the whole development period, that is, the maximum economic benefit obtained by the total economic revenue of cumulative production minus the cost in the whole development period (including drilling cost, production cost, surface construction cost, and fracturing cost).

The hydraulic fracturing technique system includes three basic links: design, operation, and appraisal. Operation is done under the direction of optimization design, and appraisal is the summation of operation and also the examination of whether the design conforms to reservoir and practical operation conditions. The results of the appraisal will also be the important grounds for improving the design. The basic contents of a hydraulic fracturing technique system include a reservoir appraisal before fracturing, optimization and selection of fracturing material, optimizing fracturing design, studies of individual-well and integral fracturing optimization, the operation of fracturing, diagnosis of hydraulically created fracture, and an appraisal after fracturing.

## Acid Fracturing

Acid fracturing is the most commonly used acid treatment technology in carbonatite reservoir stimulation operations. Acid is squeezed into the reservoir under a pressure higher than formation breakdown pressure or natural fracture closure pressure. Thus fracture is formed in the reservoir, and grooving wall or trachydiscontinuity is generated due to the dissolution and etching of acid liquor on wall. After the external pressure is relieved, the fracture generated cannot be fully closed; thus, an artificial fracture with a certain geometric size and flow conductivity is finally formed, so that the condition of flow to the well will be improved and well productivity will be increased. The increase in well productivity by acid fracturing is displayed by the following:

1. Forming fracture, increasing the area of oil and gas flow toward the well, improving oil and gas flow conditions, and increasing near-wellbore flowability
2. Eliminating formation damage in the vicinity of the borehole wall
3. Interconnecting the high-permeability zone, the fracture system in deep reservoirs, and the zone of oil and gas enrichment, which are far from the wellbore

## Acting Mechanisms and Applicable Ranges of the Main Measures for Putting a Well into Production

The present on-site application and testing of measures for putting a well into production indicate that the application effectiveness of physical methods for a low-permeability or extra-low-permeability reservoir is much lower than that for a high-permeability reservoir. This is because the application effectiveness of physical methods is greatly dependent on the physical properties of the reservoir and operational parameters. In particular, for tight oil and gas reservoirs, the removal of contamination in the vicinity of the wellbore is much more difficult than that for

high-permeability oil reservoirs. Chemical blocking removal technology, acidizing, and hydraulic fracturing have been widely applied. The application effectiveness of measures for putting a well into production can only be enhanced by selecting appropriate methods and operational technical parameters on the basis of reservoir characteristics. The acting mechanisms and applicable conditions are listed in Table 8-6.

## 8.3 PHYSICAL AND CHEMICAL BLOCKING REMOVAL

Blocking removal aims at interconnecting the flow channels between reservoir and wellbore and enhancing high well productivity to the full extent. Chemical or physical methods are often used for removing blocking.

### Blocking Removal by Chemicals

Chemical blocking removers have often been used for removing channel blocking in the vicinity of the wellbore or around perforations in recent years. Chemical blocking removers can be divided into acidic blocking remover and nonacidic blocking remover or oxidant blocking remover and nonoxidant blocking remover in accordance with different acting mechanisms. Chemical blocking remover is formulated with organic solvent, water-soluble polymer solvent, clay-swelling inhibitor, viscosity-reducing agent, acid and oxidant in a certain proportion, and the type of chemical blocking remover is optimized in accordance with the type of blocking matter. In addition, under the condition of unidentified blocking matter, a combination system, which consists of organic, inorganic, polar, and nonpolar high-molecular polymer or low-molecular substance and has composite blocking-removing ability, can be used.

### Blocking Removal by Chemical Solvent

1. Mechanism of blocking removal by chemical solvent

The solvent has a strong blocking-matter-dissolving ability. The paraffin, gum, and asphaltine, and so on in oil can mostly be

**TABLE 8-6 Acting Mechanisms and Applicable Conditions of Various Measures for Putting a Well into Production**

Measures for Putting a Well into Production		Acting Mechanism	Applicable Condition and Range
Chemical blocking removal	Chemical solvent	Dissolving blocking matter due to the strong solvability of solvent	Blocking of organic matter precipitated due to change of temperature and pressure, sulfur precipitation blocking for high-sulfur oil and gas wells
	Anti-swelling and deswelling agent	Inhibiting the hydration, swelling, dispersion, and migration of smectite fine, so that crystal sheet may be compressed	Underproduction oil wells and underinjection water injection wells with low acid treatment effectiveness due to clay particle migration and clay mineral swelling
	Viscosity-reducing agent	Wetting and dispersing effect, forming O/W emulsion with heavy oil for visbreaking	Oil wells with high flow resistance due to the deposition of heavy components (gum, asphaltenes, paraffin) in the vicinity of the wellbore
	Heat chemical	Generating a great amount of heat energy and gas by chemical reaction, softening and dissolving blocking matter, reducing heavy oil viscosity	Poor physical properties, complicated relation between oil and water, viscous oil with low flowability, organic matter precipitation, contamination and blocking due to emulsified oil caused by invasion of killing fluid filtrate in the vicinity of the wellbore
	Oxidant	Generating oxidizing and decomposing effects on organic scale blocking matter due to strong oxidizing ability	Oil well and water injection well blocking caused by bacterial slime and the organic matter and organic gel in drilling fluid system
	Surface tension reducer	Obviously reducing the surface tension of water, reducing the starting pressure difference necessary for water phase flow	Water block and emulsion block caused by mud filtrate, water-based well-flushing fluid and killing fluid in reservoir throats and the block caused by oil sillage
	Active enzyme	Releasing reservoir oil adsorbed on rock surface, changing rock surface wettability	When water content in reservoir is less than 50% and formation damage is caused by reservoir rock wettability reversal, active enzyme can be effectively used for removing blocking
Physical blocking removal	Ultrasonic wave	Using the vibration and cavitation effects of ultrasonic wave	Appropriate for oil reservoirs sensitive to water and acid and inappropriate for reservoirs treated by conventional hydraulic fracturing; the lower the reservoir permeability and the higher the oil viscosity, the poorer the effectiveness of ultrasonic treatment
	Blocking removal by microwave	Using the heating effect, fracture-creating effect, and unheating effect of microwave	Appropriate mainly for heavy oil reservoirs, high pour-point oil reservoirs, and low-permeability oil reservoirs

**TABLE 8-6 Acting Mechanisms and Applicable Conditions of Various Measures for Putting a Well into Production—cont'd**

Measures for Putting a Well into Production		Acting Mechanism	Applicable Condition and Range
	Magnetic treatment	Using magnetocolloid effect, hydrogen bond variation, and inner crystal nucleus effect to change the microstructures of paraffin crystal and the crystal with dissolved salt	Appropriate mainly for reservoirs with high viscosity and reservoirs that are easy to paraffin
	Hydraulic vibration	Generating fluid pressure pulse for removing blocking at bottomhole	Appropriate for wells for which conventional stimulation is inefficient and of which the reservoir has a slight sand production
	Mechanical vibration	Generating mechanical wave field for removing blocking by using mechanical device	Appropriate to oil reservoirs that have simple structure, integral tract, good connectedness, medium-viscosity oil, and no or less sand production
	Low-frequency electric pulse	Generating vibration effect, cavitation effect, relative movement effect, twice shock wave effect, and heat effect for removing reservoir blocking	Appropriate for oil and gas reservoirs that have rapid production rate decline and low degree of production and are sensitive to water and acid
Acidizing	Acid cleaning	Generating decomposition and dissolution effect of acid on blocking matter for removing the blocking matter in pores and fracture	Appropriate for skin blocking removal of sandstone and carbonatite oil and gas reservoirs, and interconnection of perforation
	Matrix acidizing	Decomposing and dissolving blocking matter, interconnecting and enlarging original pores and fractures in the reservoir, increasing reservoir permeability	Appropriate for wells that have serious blocking in the vicinity of the wellbore and treatment range of about 1 m
	Acid fracturing	Forming etched channel and etched fracture with a certain geometric size and flow conductivity	The most commonly used treatment technology in carbonatite reservoir stimulation
Fracturing	Hydraulic fracturing	Forming the propped fracture with a certain geometric shape in the reservoir	A mature stimulation technique that which has been widely applied in sandstone reservoirs

dissolved by organic solvent. The organic solvent first permeates to the contact surface between high-molecular substance and solid particles and wets the solid particle surface; thus, the high-molecular substance will fall off and will be rapidly dissolved and dispersed, and the flow channels blocked may then be interconnected.

During production of a high-sulfur oil well, sulfur (free sulfur) may precipitate due

to the change of temperature and pressure and may form blocking along with mechanical admixture. The solvent DMDS and sulfur-dissolving catalyst can be used for removing the blocking. This method has a high sulfur-dissolving rate, low combustibility, safe service, and low corrosiveness; thus, high effectiveness can be achieved.

- Application of blocking removal by chemical solvent

The Chengbei oil field in the Bohai oil region has high-viscosity heavy oil, and paraffin, gum, and asphaltene commonly precipitate in oil wells during production, thus causing blocking. The chemical solvent U-01 has been used for removing blocking. Laboratory and on-site tests indicate that the U-01 blocking remover has a obvious blocking removing effectiveness.

- a. Organic scale solubility in solvent. Downhole organic scale solubility test evaluation results of the Chengbei oil field are listed in Table 8-7.
- b. Core flow test. The blocking removal test results of U-01 blocking remover indicate that core permeability is restored to the level before blocking by using U-01 blocking remover and blocking removal effectiveness is increased with the increase of pressurizing time (Table 8-8).
- c. On-site operation and effectiveness of U-01 blocking remover. In the B9 well of the Chengbei oil field, the designed blocking removal radius of the blocking removal test using U-01 blocking remover is 1 m. The fluid was injected under a pressure lower than formation breakdown pressure. The on-site test results are shown in Table 8-9 and Figure 8-6.

### Blocking Removal by Anti-Swelling and Deswelling Agent

1. Mechanism of blocking removal by anti-swelling and deswelling agent

A unit cell of smectite ( $Al_{1.67}Mg_{0.33}$ )  $[Si_4O_{10}][OH]_2 \cdot nH_2O$  consists of two silica oxygen tetrahedron sheets and one alumina octahedral sheet between them. The tetrahedron and octahedral are connected by a common oxygen atom. The structure of smectite is shown in Figure 8-7. A feature of smectite

crystal structure is that the oxygen layers between overlapping unit cells stand opposite each other and the acting force between them is a weak intermolecular force; thus, the connection between the unit cells is not tight and can easily disperse into fine grains and even separate to the thickness of a unit cell (grains smaller than  $1 \mu m$  are more than 50%). The other feature of smectite crystal structure is that isomorphous replacement is common; that is, the aluminum in alumina octahedral is replaced by magnesium, iron, or zinc, and so on, with a replacement rate of up to 25% to 35%, while the silicon in silica oxygen tetrahedron can also be replaced by aluminum with a lower replacement rate, which is generally less than 5%. Thus the unit cell of smectite carries more negative charges and has greater ion-exchange capacity, which is up to 80–150 meq/ml.

Smectite may swell after meeting water; thus, flow channels will narrow or will be blocked by swelled cementing matter. The swollen smectite has a loose structure, and the fine grains may fall off, migrate, and block the smaller channels. The cation exchange that may be generated between the electropositivity groups of cationic organic polymer molecules in chemical anti-swelling agents and the low-valence cations (such as  $Na^+$ ,  $K^+$ ,  $Ca^{2+}$ , and  $Mg^{2+}$ ) between smectite crystal sheets and on the surface, the strong electrostatic attractive force between the electropositivity ions or groups on macromolecule chains of organic polymer and negative charge centers in smectite, and the Van der Waals force make the macromolecule of organic polymer be firmly adsorbed on the surfaces of smectite and other microcrystal sheets, thus forming a unimolecular film. As a result, the negative charges between

**TABLE 8-7 Downhole Organic Scale Solubilities in Different Solvents in Chengbei Oil Field**

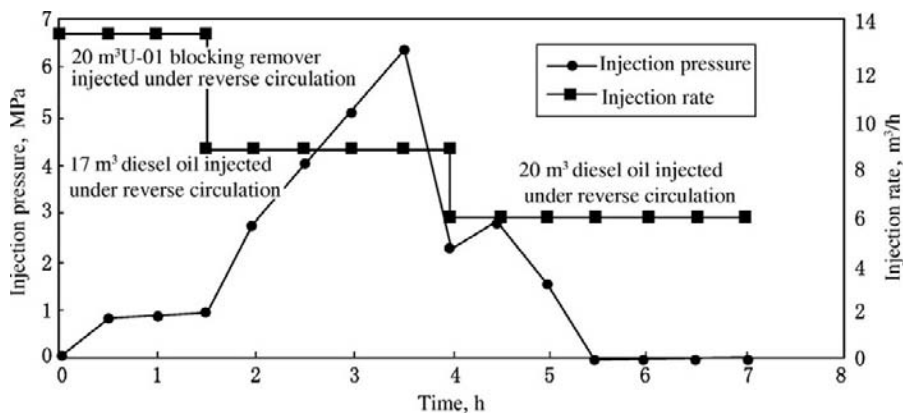
Type of solvent	U-01	Benzene	HL-18	Halohydrocarbon	Pyridine	Diesel
Solubility (%)	100	92	91	61	25	15

**TABLE 8-8 Core Blocking Removal Effectiveness by Using U-01 Blocking Removal under the Condition of Different Pressurizing Times**

Pressurizing Time (h)	Before Blocking			Before Blocking Removal			After Blocking Removal			Blocking Removal Ratio (%)
	Pressure Difference (MPa)	Flow Rate (ml/min)	Mobility ( $\mu\text{m}^{-2}/\text{MPa} \cdot \text{s}$ )	Pressure Difference (MPa)	Flow Rate (ml/min)	Mobility ( $\mu\text{m}^{-2}/\text{MPa} \cdot \text{s}$ )	Pressure Difference (MPa)	Flow Rate (ml/min)	Mobility ( $\mu\text{m}^{-2}/\text{MPa} \cdot \text{s}$ )	
1	0.43	3.9	0.019	>1.7	<0.01	$<2 \times 10^{-5}$	0.39	3.6	0.019	100
0.5	0.44	3.6	0.017	>1.7	<0.01	$<2 \times 10^{-5}$	0.41	3.5	0.016	95

**TABLE 8-9** Change of Production Rate by Blocking Remover in B9 well of Chengbei Oil Field

	Date	Tubing Pressure (MPa)	Liquid-Producing Rate (m <sup>3</sup> /d)	Oil Production Rate (m <sup>3</sup> /d)	Producing Fluid Level (m)
Before blocking removal	1998-10-11	0.85	50.5	7.6	1080
After blocking removal	1998-12	3.2	214.0	21.1	0
	1999-01-02	2.1	156.0	20.6	0
	1999-03-04	1.5	130.0	18.3	0

**FIGURE 8-6** Pressure vs. time for B9 well in Chengbei oil field.

smectite crystal sheets and on the surface are neutralized, electrostatic repulsion between crystal sheets and between grains is decreased, and the crystal sheets shrink and are not easily hydrated, swelled, and dispersed. In addition, the organic polymer molecules can be simultaneously adsorbed on crystal sheets and fine grains due to the long chain, thus inhibiting the dispersion and migration of smectite fines and preventing the hydration and swelling of smectite and the dispersion and migration of its grains. The cationic organic polymer that is adsorbed on smectite crystal sheets and fines is difficult to desorb; thus, it can maintain long-term effectiveness of anti-swelling and blocking removal and may not be affected by acid, alkali, and salt in general.

Clay deswelling agent is a chemically synthesized cationic high molecular polymer and can break the swelled clay lattice and restore reservoir permeability. Under acidic conditions, its cationic group has an oxidizing property, which may break the clay lattice, make the clay after adsorbing water release the adsorbed water, and make the swelled volume contract and restore the blocked capillaries in the reservoir. In general, the hydratability of cations of a clay deswelling agent is lower than that of  $\text{Li}^+$ ,  $\text{Na}^+$ ,  $\text{Mg}^{2+}$ ,  $\text{Ca}^{2+}$ , and so on. Clay may selectively adsorb cations and predominantly adsorb the cations with lower hydratability; thus, the cations of a clay deswelling agent may be predominantly adsorbed by clay in comparison with  $\text{Na}^+$  or  $\text{Ca}^{2+}$ . After they are adsorbed

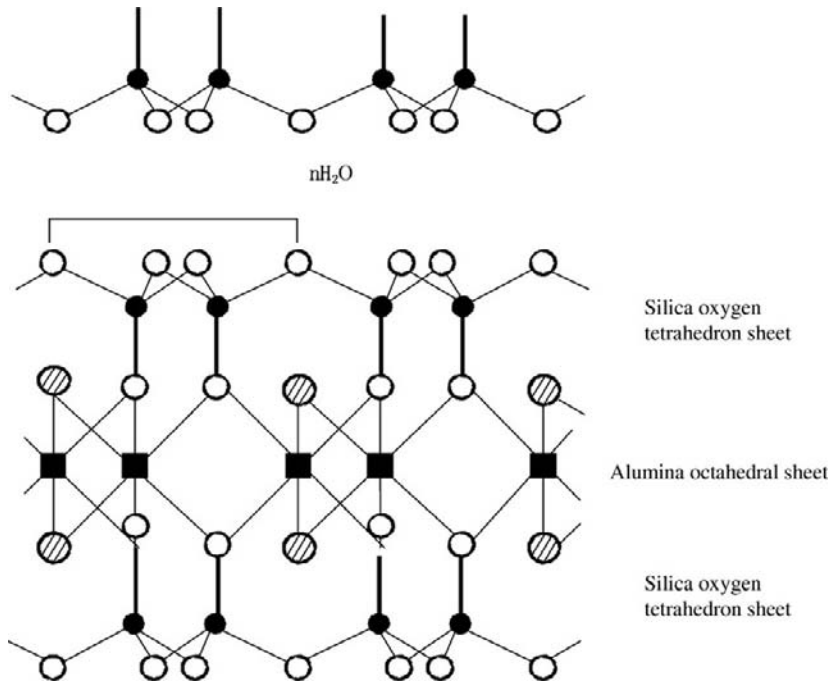


**FIGURE 8-7** Structure of smectite.

by clay, the dehydration between crystal sheets may be impeded, which makes crystal sheets sustain compression; thus, a tight structure is formed and clay hydration is effectively inhibited. The structures of lithium smectite and sodium smectite are shown in Figure 8-8 and Figure 8-9, respectively.

- Application of blocking removal by anti-swelling and deswelling agent

In the Weicheng and Mazhai oil fields of the Zhongyuan oil region, underinjection of water injection wells and underproduction of oil wells has been generated due to fine grain migration and clay mineral swelling. On-site mud acid and hydrochloric acid treatments had low short-term effectiveness. Thus blocking removal technology in which the anti-clay-swelling and deswelling agent

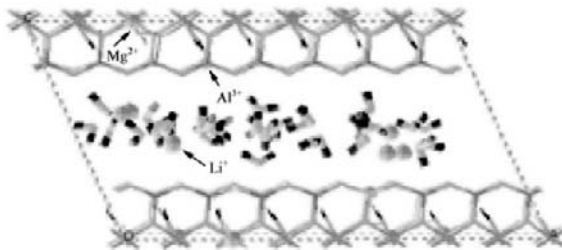


**FIGURE 8-8** The structure of lithium smectite with 32 water molecules.

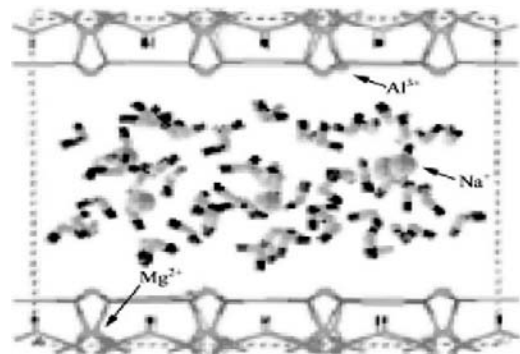


**FIGURE 8-9** The structure of sodium smectite with 64 water molecules.

HDS-01 is predominant has been applied and obvious effectiveness has been obtained. It is especially appropriate for the blocking removal treatment of oil wells and water injection wells in which acidizing treatment has no obvious effectiveness.

This anti-swelling and deswelling agent is a chemically synthesized cationic high molecular polymer and is a slightly orange-colored transparent involatile toxic corrosive liquid that is fully miscible with water. It can prevent clay from swelling, break swelled clay lattice, and restore reservoir permeability.

On the basis of a successful pilot test of water-sensitive reservoir productivity restoration of the Wei 360 well in the Weicheng oil field, the deswelling technology has been applied in the eight oil wells that have water sensitivity. Individual-well daily liquid production rate, daily oil production rate, and cumulative oil production are respectively increased by 5.8 t/d, 3.2 t/d, and 2513 t; thus, good effectiveness has been obtained.

### Blocking Removal by Viscosity-Reducing Agent

#### 1. Mechanism of blocking removal by viscosity-reducing agent

A viscosity-reducing agent contains a certain quantity of surfactant and some basic compounds. A part of the surfactant may be adsorbed onto the rock grain surface to take an oil-displacing action, while the other part of the surfactant may wet and disperse the wax in wax-bearing crude oil to form O/W emulsion and reduce the viscosity of crude oil. After injecting a viscosity-reducing agent, a mixture of the surfactant, the generated surfactant, and the crude oil will be formed and will flow from reservoir to bottomhole and then toward the wellhead. In this process the viscosity-reducing agent makes the heavy oil form oil droplets and disperse in water. Under the effect of the surfactant, the oil-water interfacial tension is greatly reduced, the surface active molecules in the water phase are concentrated at the oil-water

interface and are adsorbed around the oil droplets, the oil droplets are encircled by the films formed by the surfactant, and the O/W emulsion in which heavy oil is a dispersed phase and water is a continuous phase is formed, thus preventing the oil droplets from coagulating. The internal friction of heavy oil is changed to the internal friction of water in flow process due to low water viscosity. During flow in the channel, the friction between the heavy oil and the rock grains around the channel is changed to friction between the water and the rock grains around the channel, thus greatly decreasing the O/W emulsion flow resistance in the vicinity of the wellbore and removing blocking caused by the gum and asphaltene in heavy oil. In deep reservoirs, chemical blocking remover may also mix with heavy oil to form O/W emulsion and decrease heavy oil flow resistance; thus, a heavy production rate can be increased.

#### 2. Application of blocking removal by viscosity-reducing agent

In the production process of the Dalinghe oil reservoir of the Liaohe oil field, reservoir blocking in the vicinity of the wellbore was caused by the precipitation of the heavy components (gum, asphaltene, and wax) in crude oil and matter that easily scales, which is in formation water. The viscosity-reducing blocking remover DLA, which is an aqueous solution of surfactant, dispersant, complexing agent, organic acid, inhibitor, and other aids, has been applied. Twenty-two well-time blocking removal operations were done using DLA in five oil wells of the Dalinghe oil reservoir, and good results were obtained (Table 8-10).

### Thermo-Chemical Blocking Removal

#### 1. Mechanism of thermo-chemical blocking removal

Blocking matter including dead oil, wax, gum, and asphaltene in the reservoir can be rapidly fluxed by a large amount of heat energy and gas, which may be generated during exothermic chemical reactions in

**TABLE 8-10** Blocking Removal Results Using DLA Remover in Dalinghe Oil Reservoir in Liaohe Oil Field

Well No.	DLA Squeezed (t)	Oil Production Rate (t/d)		Liquid Production Rate (t/d)		Valid Period (d)	Cumulative Oil Increased (t)	Cumulative Liquid Increased (t)
		Before Blocking Removal	After Blocking Removal	Before Blocking Removal	After Blocking Removal			
2-8-307	33.22	2.7	6.4	9.1	18.9	91	319.3	842.8
2-7-307	30.18	0.7	5.3	2.8	14.6	86	225.4	578.2
2-8-304	33.01	4.0	5.9	12.5	24.4	105	191.9	1201.9
2-6-313	29.88	6.3	7.9	15.9	24.7	>226	284.8	1566.4
2-08-3	26.20	0.2	2.7	7.8	41.0	>190	497.5	6606.8
2-7-311	29.66	3.3	4.8	14.4	19.7	168	241.5	853.3
2-8-04C	31.21	1.5	3.6	7.1	46.0	116	212.1	3928.9
2-7-209C	28.46	0.3	2.9	6.5	39.4	>90	244.4	3092.6

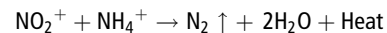
combination with the cleaning action of surfactant on the reservoir, and the gas generated during grains, thus achieving blocking removal and oil flow channel interconnection. In addition, the heat effect of the chemical reaction has the effects of fluxing and visbreaking on the blocking matter.

2. Application of thermo-chemical blocking removal

The Pucheng oil field is a complicated fault-block oil and gas field with poor physical properties, complicated oil-gas relations, heavy oil, low flowability, and organic matter precipitation. The decrease of reservoir permeability in the vicinity of the wellbore and the decrease of production rate (even off production) were caused by near-wellbore contamination and blocking that was caused by the emulsified oil generated by killing fluid filtrate invasion. A heat chemical system that consisted of sodium nitrite, ammonium chloride, and aids was used, and the contamination and blocking in the vicinity of the wellbore was effectively removed, the productivity of the reservoir was brought into full play, and obvious effectiveness was obtained.

a. Composition of thermo-chemical blocking remover and principle of heat generation

This thermo-chemical blocking remover consists of heat-generating agent, retarding agent, and dispersant, in which the heat-generating agent is the principal agent and is used for generating a large amount of heat and nitrogen gas due to the reaction of  $\text{NO}_2^-$  to  $\text{NH}_4^+$ , as shown in the following equation:



The retarding agent is used for controlling the reaction rate of the heat-generating agent, and the pH value of the solution can be regulated in accordance with the requirements of the well to be operated, thus controlling the reaction rate and the exotherm of the system (Figure 8-10). The dispersant is an active substance and is used for dispersing organic matter including wax, gum, and asphaltene into fine grains, so that it can still be in a dispersed state and may not coalesce.

b. On-site application of thermo-chemical blocking removal

A thermo-chemical blocking removal operation was conducted in wells of the Pucheng oil field. Before blocking removal, the near-wellbore areas in a total of 27 wells had serious blocking and low

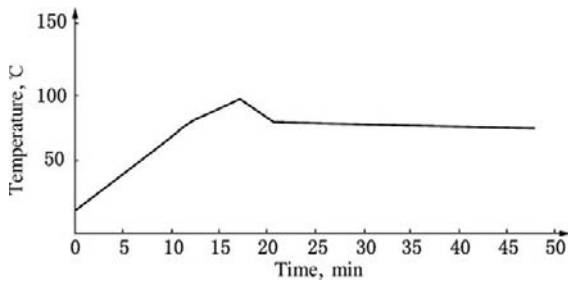


**FIGURE 8-10** Relation between system temperature and reaction time.

permeability and the wells had average individual-well liquid production rate of 5.5 t/d, average individual-well oil production rate of 1.5 t/d, average working fluid level of 1559 m, insufficient liquid supply, low degree of fullness (only 1/4), and low liquid production rate. After blocking removal, a total of 26 wells had obvious effectiveness, average individual-well liquid production rate of 13.5 t/d, average individual-well oil production rate of 4 t/d, and average working fluid level of 1455 m (Table 8-11).

**Blocking Removal by Oxidant.** Acidizing is inefficient to remove blocking caused by bacterial slime, organic matter in the drilling fluid system, and organic gel in oil production wells and water injection wells. However, oxidants such as  $\text{ClO}_2$ ,  $\text{H}_2\text{O}_2$ , and nitric acid have a degradation

action on organic matter and the gel system used for controlling profile and have a bactericidal action on saprophytic bacteria and sulfate-reducing bacteria, and so on.

In the oil production wells and water injection wells of the Huzhan oil field, acidizing was ineffective in removing blocking caused by bacterial slime, organic matter in the drilling fluid system, and organic gel in oil production wells and water injection wells; thus, the  $\text{ClO}_2$  system was used as blocking remover. The degradation action of the  $\text{ClO}_2$  system on organic blocking matter is shown in Table 8-12, and the use effectiveness of the  $\text{ClO}_2$  system in some of the oil wells of the Huzhan oil field is shown in Table 8-13.

**Blocking Removal by Surface Tension Reducer.** Low-pressure tightness of a reservoir easily generates water blocking and emulsion blocking. Water blocking occurs because various working fluid filtrates, formation water, and so on enter and block reservoir pore throats during drilling, well completion, and servicing operations; or the outside casing channeling water enters the reservoir, or formation water is produced. A blocking removal system formulated with surface tension reducer and other aids can obviously reduce the surface tension of water, can generate high ability to clean oil fleck and oil sand, and can greatly decrease the starting pressure drawdown necessary for water phase flow; thus, water phase blocking can be rapidly

**TABLE 8-11** Blocking Removal Results Using Heat Chemical in Pucheng Oil Field

Well No.	Before Blocking Removal			After Blocking Removal			Difference		Cumulative		Valid Period (d) Thermo-chemical
	Liquid (t/d)	Oil (t/d)	Water cut (%)	Liquid (t/d)	Oil (t/d)	Water cut (%)	Liquid (t/d)	Oil (t/d)	Liquid (t/d)	Oil (t/d)	
51-175	3.1	0.5	83.9	18.6	3.3	82.3	15.5	2.8	593	409	147
P2-163	7.2	2.7	62.5	16.7	6.7	60.0	9.5	4.0	873	464	116
6-5911	11.5	1.7	85.2	22.9	2.5	89.1	11.4	0.8	151	80	99
P3-372	3.3	0.8	75.8	5.5	0.7	87.3	2.2	-0.1	38	0	55
Bu 1	11.0	5.4	50.9	18.3	11.4	37.7	7.3	6.0	1501	918	153
Wei 317-4	2.0	1.5	25.0	6.5	3.5	46.2	4.5	2.0	729	324	162
P3-112	112	8.4	92.5	125	12.5	90	13	4.1	2565	832	205

**TABLE 8-12 Degradation Action of  $\text{ClO}_2$  System on Organic Blocking Matter**

Sample	Soak Time, h	Phenomenon
F917 gel (6 g)	2	Gel fully changes into thick solution
PAM gel (6 g)	12	A small amount of flock, which can be carried away. Most of it is oxidized and degraded into solution
PAM expansion body (6 g)	24	Its strength is reduced. It can be broken into small pieces (which can be carried away by water stream) by slight pressurization
PAM crosslinking expansion body (6 g)	24	Swelling by absorbing water. Being fragile by agitating

**TABLE 8-13 Blocking Removal Effectiveness of  $\text{ClO}_2$  System in Some Oil Wells of Huzhan Oil Field**

Well No.	Before Blocking Removal			After Blocking Removal			Cumulative Increase of Oil (t)
	Liquid (t/d)	Oil (t/d)	Water cut (%)	Liquid (t/d)	Oil (t/d)	Water cut (%)	
QC29	Sidetracking	7.0		6.6	5		1386
HC2-28	1.2	1.0	1.7	9.8	5.4	40	704
HCI-88	Sidetracking	18.0		9.2	49		1300

removed. This system is suitable for removing blocking including water blocking, emulsion blocking, oil fleck and oil sand that are generated by drilling fluid filtrate, water-based flushing and killing fluid, and formation water produced.

The CY-3 blocking remover is mainly formulated with organic solvent, special surfactant, penetrant, and anti-swelling agent. It is a water-based solution with medium to weak basicity and effective matter content of 25%, is colorless and transparent, nontoxic and noncombustible, and has high solubility, obvious water surface tension-reducing ability, and strong oil fleck and oil sand-cleaning ability (Table 8-14).

The CY-3 blocking remover is mainly used for removing water blocking, emulsion blocking, and so on caused by working fluid filtrate. It was introduced into on-site application in July 1992 and has been commonly used in the Huabei, Jiling, Xinjiang, Tuha, Jidong, Bohai, and Liaohu oil fields. More than 100 well-times of blocking removal operations in oil wells and

**TABLE 8-14 Surface Tension Values of CY-3 Blocking Remover and Other Surfactants in Sewage and Injection Water in Lunnan Oil Field**

Solution	Surface Tension (mN/m)	
	Sewage	Injection Water
Blank	35.4	63.9
CY-3	22.1	20.7
1% Pingpingjia (O-15)	34.7	34.4
1% OP-10	33.4	32.5
1% Tuwen 80	35.1	35.4

water injection wells have been conducted with a success ratio of 100% and a economic effectiveness of more than 90% (Table 8-15).

**Blocking Removal by Active Enzyme.** An enzyme is a protein with catalytic ability. It is generated by the living body cell of a microorganism and formed by gene grafting. It can release oil that is adsorbed on the rock surface

TABLE 8-15 Blocking Removal Effectiveness of CY-3 Blocking Remover in Oil Wells

Oil Field	Well No.	Daily Liquid Production (m <sup>3</sup> )		Daily Liquid Production (t)		Water cut (%)		Cumulative Oil Increased (t)	Valid Period (d)
		Before Blocking Removal	After Blocking Removal	Before Blocking Removal	After Blocking Removal	Before Blocking Removal	After Blocking Removal		
Jidong	G94-1	0	18.0	0	18.0	—	—	450	35
	L24-1	0	17.0	0	17.0	—	—	2100	235
	L11-1	7.0	11.4	7.0	11.4	0	0	450	160
	G59-35	0	120.0	0	12.0	—	—	2400	>270
Jiling	1-3	15.0	26.8	10.4	16.0	30.5	40.3	128	136
	303	14.2	22.6	6.5	11.4	53.8	54.0	415	180
	A2	9.1	12.6	1.5	2.9	83.4	77.0	259	96

in the reservoir and change the wettability of rock surface. When the reaction is ended, there is no change in chemical property and quantity, that is, no change in itself or breaking. This indicates that its effect can be kept for a long time and means that it can be used repeatedly. When the water cut in reservoir is less than 50% and formation damage is caused by reservoir rock wettability reversal, an active enzyme is effective for blocking removal. At present, concentrated enzyme is used on a trial basis. Packed enzyme is metered by 100% concentration. The operating fluid concentration is generally about 8% to 11%. The on-site tests indicate that under reservoir conditions, the operating fluid is still effective when its concentration is reduced to 5%. The features of enzyme blocking remover include: (1) oil and its attachment can be rapidly separated, catalytic process is a biochemical reaction, and the enzyme can be used repeatedly after reseparation; (2) the remover is pollution-free for the human body and environment; (3) it has a pH value of 7 and is neutral; (4) it can dissolve in oil, but not in water; and (5) the effect of enzyme on basal matter has unicity, and new pollution of the reservoir may not be generated. The dominant ingredients of some blocking remover include Gyeenzyme 280-CAD enzyme, stabilizing agent, and water.

The Qiaokou oil field is an oil field with high temperature, high pressure, high salinity, low

permeability, and serious heterogeneity. The main reservoirs are the sand group. 1–4 of the lower Sha 2 submember and sand group. 2–5 of the upper Sha 3 submember. The lower Sha 2 submember has a buried depth of 2470–2600 m and limy arkose. The reservoir has mean porosity of 20.6%, mean permeability of  $4709 \times 10^3 \mu\text{m}^2$ , original reservoir pressure of 26.65 MPa, saturation pressure of 7.98–12.75 MPa, and formation pressure coefficient of 1.06. It is a medium porosity, medium-low-permeability oil reservoir with heterogeneity.

The active enzyme blocking removal technique has been applied in five wells of the Qiaokou oil field, and good effectiveness has been obtained to varying degrees. Daily oil production and cumulative oil production are respectively increased by 1.0–9.0 t and 2343 t.

### Physical Blocking Removal

Physical blocking removal methods use a heat field, sound field (broadband), electrostatic field, magnetic field, alternating electric field, and so on to excite the oil reservoir, remove reservoir blocking, increase reservoir fluid flowability, and enhance the oil recovery factor. These methods have high adaptability, simple technology, high technical content, less cost, high output, no reservoir contamination, dominance complementarity with the chemical blocking removal

method, and some special properties, and have been widely applied. At present, more than ten physical blocking removal methods, which include the ultrasonic wave method, microwave method, magnetic treatment method, vibration method, and low-frequency electric pulse method, have been put into industrial testing or are being developed.

**Blocking Removal by Ultrasonic Wave.** The vibrating action and cavitation action of ultrasonic waves can be used for removing contamination and blocking in the vicinity of the wellbore to increase oil well productivity, enhance oil recovery factor, prolong the service life of downhole production equipment, and shorten production downtime.

### 1. Mechanism of blocking removal by ultrasonic wave

An ultrasonic wave is a mechanical wave and has the general properties of a wave, that is, vibration and transmitting energy. A high-power ultrasonic transducer is run to reservoir depth. Under mechanical vibrating action, cavitation action, thermal effect, reversed flow action, and sound flow action, the blocking matter loosens and falls off and is carried by fluid to the surface. When a Type CSF-250-3 ultrasonic generator acts on 4 ml of engine oil under insulated conditions, the oil body temperature can be increased from 15°C to 50°C within 18 minutes. The temperature curve measured is shown in Figure 8-11. The vibration generated by the sonic wave in the reservoir may also impel crude oil to flow toward the bottom-hole sonic source along the path of the reflected wave, thus impelling the crude oil in the reservoir to flow and accumulate and increase well productivity (Figure 8-12).

### 2. Technological process of blocking removal by ultrasonic wave

An ultrasonic reservoir-treating system consists of surface equipment and downhole instruments and includes surface sonic and ultrasonic generator, transmitter cable, and high power transmitting electroacoustic transducer (Figure 8-13).

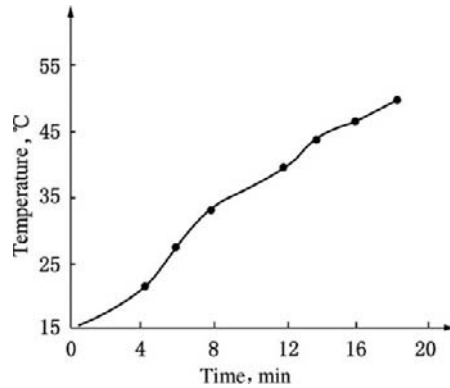


FIGURE 8-11 Thermal effect of ultrasonic wave.

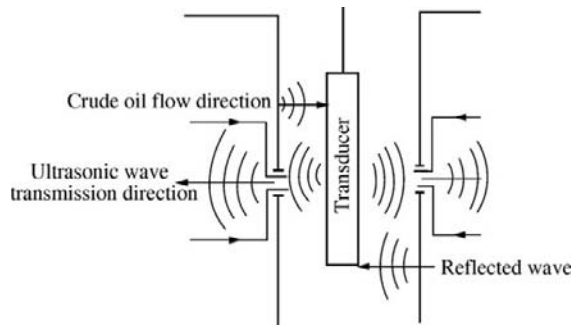


FIGURE 8-12 Effect of ultrasonic wave on the reservoir.

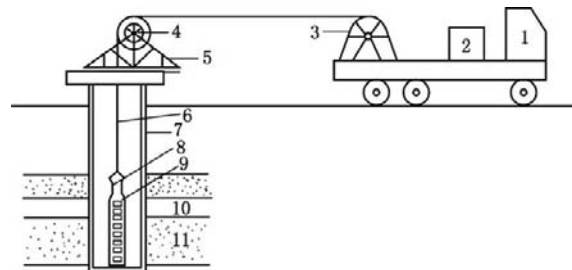


FIGURE 8-13 Technological process of ultrasonic reservoir-treating system. 1, cable measurement truck; 2, ultrasonic generator; 3, cable winch; 4, wellhead pulley; 5, wellhead support; 6, cable; 7, casing; 8, transducer; 9, voltage ceramic ring base array; 10, interbed; 11, oil reservoir.

The following types of wells and reservoirs are appropriate for blocking removal by ultrasonic waves:

1. Oil wells and water injection wells with serious contamination and blocking caused by scaling and wax deposit or wells with contamination generated during the operations of drilling, fracturing, acidizing, chemical sand control, and chemical wax removal, and so on.
2. Oil reservoirs that are sensitive to water or acid.
3. Wells that are unsuitable for fracturing before being put into production due to nearness to aquifer, inferior cement job quality, or ease of channeling, and so on, and reservoirs that are unsuitable for conventional hydraulic fracturing.
4. Oil wells and water injection wells in which other measures cannot be taken for one-trip treatment of some layer under the condition of commingling production.
5. Wells in which conventional measures cannot be taken due to casing leak under the condition of casing deformation and draft diameter larger than 90 mm.
6. Heavy oil wells with high asphaltene content and low productivity under the condition of production by conventional technology.

**Blocking Removal by Microwave.** A microwave is a non-ionizing electromagnetic wave. In the electromagnetic wave spectrum, the microwave region is between the infrared band and the radiowave band. The wavelength of a microwave is 1 cm to 1 m and the frequency of microwave is 300 MHz–300 GHz.

1. Mechanism of blocking removal by microwave  
The microwave blocking removal technique uses a high-power microwave source for radiating microwave on the reservoir to improve permeability in the vicinity of the wellbore by the thermal effect, fracture-creating action, and nonthermal effect of microwave. Microwave has a dielectric thermal effect on matter; that is, when a polar

molecule accepts energy, the molecule affected is instantaneously changed from a relatively static state to a dynamic state. A thermal effect is generated by molecular dipole rotation at a high speed of several billion Hz. An oil reservoir is composed of various types of chemical matter and has an obvious heterogeneity; thus, under the effect of microwaves, different matter components have obviously different increases of temperature and different thermal expansion coefficient values, and differential thermal expansion and shrinkage and great thermal stress are generated, so that many microfractures may be generated or fractures may develop. The generation of secondary microfracture in low-permeability reservoirs may cause an increase in reservoir permeability, thus achieving low-permeability reservoir development under high-permeability conditions. In addition, because the microwave frequency is close to the inherent frequency of the polar molecule of the reservoir fluid, resonance is very easy to generate, so that long-chain molecule compounds, branched-chain molecule compounds, heterocyclic compounds, heterocyclic compounds, and combined gum and loose structure may be broken and cracked, heavy oil may be changed to low-viscosity light oil, setting point may be decreased, and blocking removal can be achieved.

At present, microwave heating techniques include: (1) heating the water or water steam that is injected into the reservoir from the surface using microwave; (2) directly heating the reservoir using microwave to increase reservoir temperature (Figure 8-14); and (3) heating a multibore well reservoir using microwave (Figure 8-15).

2. Microwave blocking removal well completion methods

When heavy oil is produced using microwaves at a low temperature, the reservoir temperature is close to thermal production temperature and a heavy oil reservoir is unconsolidated; thus, the reservoir is prone

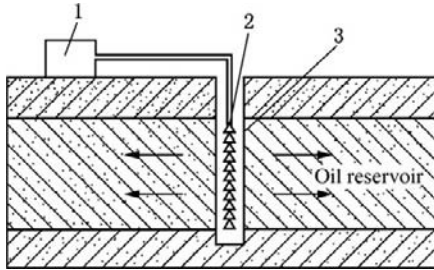


**FIGURE 8-14** Single-well microwave heating. 1, electric power; 2, microwave source and reflector; 3, ceramic (or organic glass) casing.

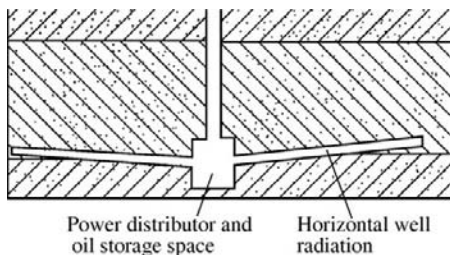


**FIGURE 8-15** Multibore well reservoir heating by microwave.

to sand production during oil production. Hence sand control should be considered in choosing a well completion method. In addition, completion string material and structure should meet the requirements of the microwave blocking removal technique; that is, the completion string should ensure hole stability and sand control and should have a low microwave radiation penetration loss.

a. Ceramic liner completion method. Sand control is achieved by using a special ceramic liner and the natural bridging action of reservoir sand. This method is suitable for sand control under the condition of heavy oil reservoir with no serious sand production. The completion string consists of hook wall packer, telescopic joint, blind pipe, ceramic liner, and ceramic bulkhead. This method has simple structure, convenient operation, and lower sand control ability.

b. Simplified gravel packing ceramic screen completion method. Gravel packing can achieve effective reservoir protection and sand control. It has generally a sand control period of up to 10 to 15 years and is the most effective sand control technology at present. When ceramic screen gravel pack completion is adopted, the simplified gravel pack completion method is appropriate. The completion string consists of hook wall packer, telescopic joint, blind pipe, ceramic screen, and ceramic bulkhead. This method has simple structure and higher sand control effectiveness.

3. Casing string design and cementing design of microwave blocking removal well

During microwave blocking removal, a reservoir is directly heated at the bottomhole, and an insulating casing nipple and a small quantity of telescopic casing joints should be considered to be used under the condition of production at medium and high temperature. The upper part of the casing string has only been slightly affected by temperature, and the effect of temperature on the near-reservoir lower part of the casing string should be emphasized to be considered. In addition, a special cementing design is required in order to ensure the effective sealing property of the annulus between casing and borehole wall.

a. Low-temperature microwave blocking removal. The requirements of low-temperature microwave blocking removal for casing string design and cementing technology are similar to those of conventional thermal production. The lower part of the casing string should adopt high-strength casing to the full extent. Heat-resisting stabilizing agent, thermal insulation additive, and binding additive should be added to cement slurry.

b. Medium- and high-temperature microwave blocking removal. Under the condition of medium- and high-temperature microwave blocking removal, the reservoir is heated to more than 400°C.

In order to prevent casing failure by thermal stress and the failure of sealing between casing string and reservoir, the following special measures should be taken: (1) using special high-temperature-resistant cement for cementing; (2) using special high-temperature-resistant metallic material for blind pipe, hook wall packer, and expansion joint on completion string; (3) using a heat insulation ceramic casing nipple in the lower part of the casing string in order to prevent the casing string from generating casing failure by thermal stress at high temperature; and (4) attaching one or two telescopic glass fiber casing joints to the heat insulation ceramic casing nipple in order to further prevent possible casing deformation.

**Magnetic Treatment Technique.** The effect of a magnetic field on crude oil is used for reducing the interfacial tension, changing the microstructures of wax crystal and salt-solvent crystal, and increasing flowability, so that effectiveness of blocking removal is achieved.

#### 1. Mechanism of blocking removal by magnetic treatment

The magnetic treatment blocking removal technique is mainly based on the magnetic colloidal effect, hydrogen bond variation, and internal crystal nucleus. Magnetic colloidal effect means that an electrical double layer in a metastable state is formed on the surface of particles with a size of nanometer to micrometer under the action of a magnetic field on charged particles, so that the effects including magnetic scale control, magnetic

wax control, and magnetic visbreaking may be generated under a certain condition. Hydrogen bond variation means that the change of hydrogen bond in a polar molecule is only flexural deformation, wrench deformation, and change of strength, but not breaking, so that there is a restoring process after separating from magnetic form; that is, it will be restored to the original stable state again. An internal crystal nucleus may influence the solubility of scale-forming compound in fluid, thus inhibiting the formation of internal crystal nucleus in liquid flow and preventing scale from forming.

#### 2. Magnetic treatment device design

An appropriate magnetic treater is designed using a specific method on the basis of the specific properties of fluid treated and application conditions. In accordance with the installation pattern of magnetic body, the magnetization treatment devices applied in oil fields can be divided into two types, that is, internal magnet-type structure (Figure 8-16) and external magnet-type structure (Figs. 8-17 and 8-18).

**Vibration Blocking Removal Technique.** The wave field established by a vibration source is transmitted to the reservoir using the vibration blocking removal technique in order to remove formation damage generated by liquid emulsification, clay particle migration, precipitant deposition, mechanical impurities, and so on during drilling, thus restoring reservoir permeability in the vicinity of the wellbore. Vibration blocking removal can be blocking removal by hydraulic or mechanical vibration.

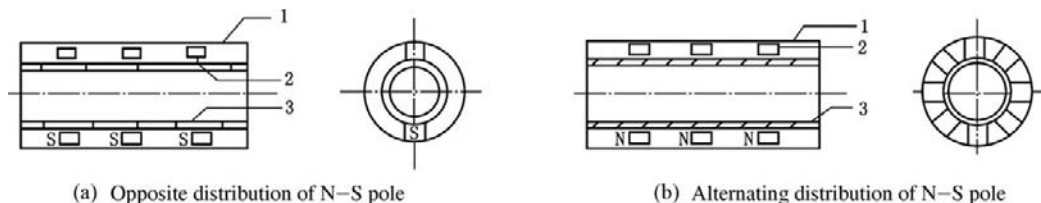


**FIGURE 8-16** Internal magnet-type magnetic treater. 1, housing; 2, permanent magnet; 3, internal steel pipe.

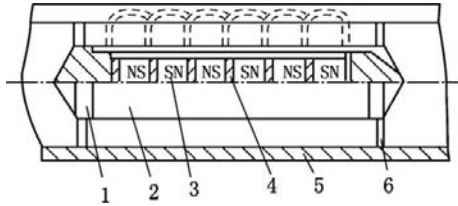


**FIGURE 8-17** Built-in external magnet-type magnetizer. 1, plug; 2, housing; 3, permanent magnet; 4, plate boot; 5, steel wall; 6, support dog.

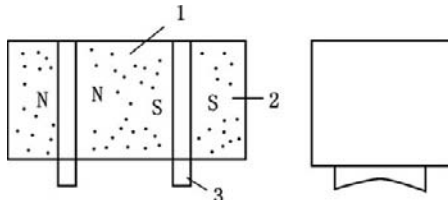


**FIGURE 8-18** External magnet-type magnetic treater. 1, magnet block; 2, housing; 3, magnetic pole.

### 1. Hydraulic vibration blocking removal technique

Hydraulic vibration blocking removal uses fluid movement for generating a vibration wave that acts directly on the reservoir to remove blocking. It can be hydraulic oscillation blocking removal, low-frequency hydraulic pulse blocking removal, and high-pressure water rotation jet flow blocking removal. The common features of this type of treatment technique include high efficiency, high adaptability, good treatment effectiveness, low cost, convenient operation, and ease of spreading.

- a. Hydraulic oscillation blocking removal technique. The hydraulic oscillator that is used as downhole vibration source is run to the well section to be treated. Working fluid is injected from the surface to the oscillator under a certain pumping rate. The oscillator is excited by the fluid flowing through it. Thus a hydraulic pulse wave is generated, acts on the reservoir, and removes the blocking. The oscillator is the core of the hydraulic oscillation blocking removal technique.

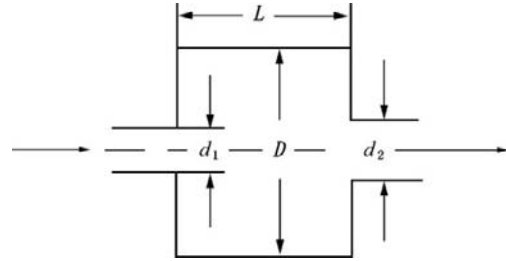


**FIGURE 8-19** Helmholtz chamber-type structure.

The oscillation action of a hydraulic oscillator is generated in the Helmholtz cavity (Figure 8-19). A high-pressure water jet flow enters the nozzle  $d_1$  and leaves the nozzle  $d_2$  through an axi-symmetrical chamber. The chamber has an inside diameter  $D$  much larger than jet flow diameter; thus, the flow velocity of the fluid inside the chamber is much lower than the central jet flow velocity, vigorous shearing movement is generated on the interface of jet flow and in-chamber fluid, and turbulent flow is formed. Under the action of turbulent flow, the flow velocity at the center of jet flow (internal shear layer) will be increased, while the flow velocity in the vicinity of chamber wall (external shear layer) is decreased. The centripetal flow of the fluid on the chamber wall will be generated under the pressure drawdown, and the vortex will move with jet flow down the stream. When the ordered axi-symmetrical vortex ring in the jet flow shear layer collides with the edge of nozzle  $d_2$ , a pressure pulse with a certain frequency may be generated. This pulse will change into a large-amplitude pulse after it passes the outlet nozzle, and the high-pressure water will change into a high-frequency oscillating jet flow, of which the energy can be used for removing reservoir blocking.

A hydraulic vibration blocking removal operation system consists of surface equipment and vibration tubing string. The surface equipment includes pump truck,

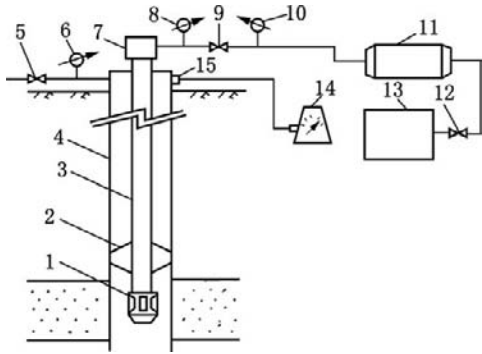


**FIGURE 8-20** On-site operation flowsheet. 1, oscillator; 2, centralizer; 3, tubing; 4, casing; 5, 9, and 12, valve; 6, pressure gauge; 7, wellhead; 10, flowmeter; 11, pump truck; 13, tank truck; 14, test instrument; 15, sensor.

liquid storage truck, and well-servicing unit. The vibration tubing string includes wellhead, tubing, centralizer, and oscillator. The on-site operation flowsheet is shown in Figure 8-20. During operation, sand washover is done after the original tubing string is pulled out, an oscillator is run in on tubing, and high-pressure fluid is pumped to the oscillator by pump truck for treating reservoirs that need removing blocking one by one.

- b. Low-frequency hydraulic pulse blocking removal technique. Water or light oil that has been treated by surfactant is injected into the reservoir, and the pressure is repeatedly increased and decreased, thus generating a surge and forming hydrodynamic pressure under which the static friction between reservoir pore wall and blocking particle is changed to dynamic friction. Under repeated action, the frictional force may be decreased and the blocking particles may be loosened and discharged from the reservoir to the well during decrease of pressure, thus achieving reservoir blocking removal and an increase of well productivity. The principles of water surge, standing wave resonance, and mechanical vibration blocking removal are applied to restore and enhance reservoir flow capacity in the

low-frequency pulse vibration blocking removal technique.

- c. High-pressure water rotation jet flow blocking removal technique. High-pressure water jet flow is generated by using a rotating self-vibration cavitation jet flow blocking removal device that has down-hole controllable speed of rotation to wash perforations directly and generate a high-frequency oscillating hydraulic wave and cavitation noise (ultrasonic wave) for blocking removal.
2. Mechanical vibration blocking removal technique

Mechanical vibration blocking removal techniques include the below-pump damped vibration blocking removal technique and the non-linear wave blocking removal technique.

- a. Below-pump damped vibration blocking removal. The cyclic pulsation of the damper may be generated by the natural telescoping of the end of the tubing string, thus generating a vibration wave that acts directly on the oil reservoir and removes blocking in the vicinity of the wellbore.

Vibration tubing string consists of oil pumping string, oil well pump, damper vibrator, screen pipe, and tailpipe (Figure 8-21). The damper vibrator

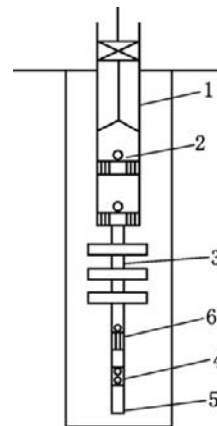


**FIGURE 8-21** Vibration tubing string structure. 1, tubing; 2, oil well pump; 3, damper vibrator; 4, screen pipe; 5, tailpipe; 6, choke valve.

consists of check valve housing, choke valve, center tube, damping discs, and upper connector.

During oil production using an oil well pump, the tubing may bear alternating load, and elastic telescoping of tubing may be generated. The elongation or shortening has a short duration, that is, it is of pulsed type. Thus the pulsed-type reciprocal vibration of below-pump dampener may be generated in the casing when the plunger moves up and down. The choke valve is opened when the damper vibrator moves upward, and interconnecting with the annulus is achieved through the screen pipe. When the damper vibrator moves downward, the choke valve is instantaneously closed under the action of liquid flow resistance below the damping discs, and a higher-pressure pulse is formed below the damping discs. The below-pump dampener is generally located at the oil reservoir, and the vibration wave generated acts directly on the oil reservoir. When the damper vibrator moves downward, the liquid between discs is speeded up, impacts the borehole wall, and effectively flushes the perforations and pore channels, thus removing the blocking in the vicinity of the wellbore.

The main technical parameters of the below-pump damper vibrator that is commonly used in oil fields include: active well pump setting depth > 500 m; active well casing diameter  $\Phi 139$  mm; distance between vibrator and screen pipe = 5–300 m; maximum OD of damper vibrator = 115 mm; vibrator length = 1.21 m; longitudinal pulse amplitude = 15–33 cm; oscillation frequency = 1–10 Hz; and continuous work period.

The applicable conditions include: (1) pump setting depth should be sufficient (about 1000 m) and borehole liquid level should be lower than 500 m in order to ensure that damper vibrator has obvious

vibration amplitude; (2) damper vibrator should be placed at the middle or upper part of the major reservoir and should be as close to the screen pipe as possible; (3) in a shallow well in which the pump setting depth is smaller (400–500 m), the stroke of the damper vibrator can be increased by using a spring; and (4) damper vibrator in the well should have the minimum radial clearance, and it would be best if it vibrates with the pump in a casingless or new well that is selected.

- b. Non-linear wave blocking removal. Several whistle generators are evenly installed in the main body of a non-linear wave generator. Power fluid enters the whistle chamber from the inlet, rotates in the whistle chamber at high speed, and is then ejected from the outlet, thus generating a sonic wave that radiates outward.

In addition to base frequency wave, a non-linear wave is also accompanied by a low-frequency wavelet; thus, it has a stronger penetrating power and larger treatment radius in comparison with other sonic waves. In addition, it is also accompanied by a harmonic wave, which has a higher frequency. A high-frequency wave has concentrated energy. The low-frequency wavelet can be used as the carrier of high-frequency harmonic wave to carry the energy to deep reservoirs. Thus a non-linear wave has a higher energy exchange efficiency in comparison with other types of wave, and blocking removal effectiveness can be enhanced.

In comparison with other vibration blocking removal methods, the non-linear wave blocking removal method can play a role in dissolving organic matter deposition. At the interface between oil flow and reservoir channel, due to the differences of wave field parameters, the energy of a non-linear wave is greatly changed to heat energy by heat transfer and viscous mechanism, so that organic matter in oil flow channels can be dissolved.

**Low-Frequency Electric Pulse Blocking Removal Technique.** The low-frequency electric pulse technique has been used for removing formation damage caused during drilling, well completion, and production since the 1980s.

### 1. Operating principle

Low-frequency electric pulse blocking removal equipment includes a surface control instrument and a downhole electrodischarge instrument. The surface instrument is a small rectification frequency converter. The downhole equipment that is the principal part of the equipment set consists of booster unit, energy storage unit, electrodischarger, and electrodes (Figure 8-22).

The downhole electrodischarger is used for pulse electrodischarge against the oil reservoir. Most energy stored in the capacitor is released in the twinkling of electrodischarge, and a high-pressure plasma area is formed between the two electrodes. The high-energy density may generate a strong shock wave that may break down the oil, water, and mixture in the well and acts on the reservoir through perforations; that is, a large quantity of energy is rapidly released from the small electrodischarge perforations. After multiple pulse electrodischarges, reservoir contamination in the vicinity of the wellbore is removed and near-wellbore permeability is improved, thus achieving blocking removal.

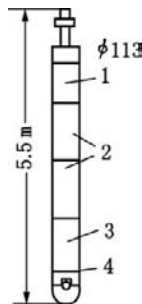


**FIGURE 8-22** Downhole low-frequency electric pulse treatment equipment. 1, booster unit; 2, energy storage unit; 3, electrodischarger; 4, electrode.

### 2. Appropriate geologic conditions of reservoir

The downhole electric pulse blocking removal technique has higher effectiveness under the condition of tight rock (such as limy dolomite and siltstone) with brittle rupture feature, while it has the lowest effectiveness under the condition of rock (such as sandstone) that has irreversible deformation feature. For a longitudinally heterogeneous reservoir, a low-permeability tight reservoir has the highest electrodischarge treatment effectiveness.

### 3. Operational procedure

The downhole low frequency electric pulse blocking removal technology is shown in Figure 8-23. The operational procedure is as follows.

- Killing the well by flushing fluid circulation and pulling out all tubing and sucker rod.
- Running drift diameter gauge, hot washing, and paraffin scraping, for ensuring unimpeded instrument running.
- Tagging sand surface, cleaning out sand to artificial bottom.
- Attaching locator to downhole instrument.
- Connecting cable truck with electric pulse blocking removal instrument, inspecting electric circuit and the sealing property of downhole instrument, and running the instrument to the lowest end of the perforated interval to be treated. Keeping

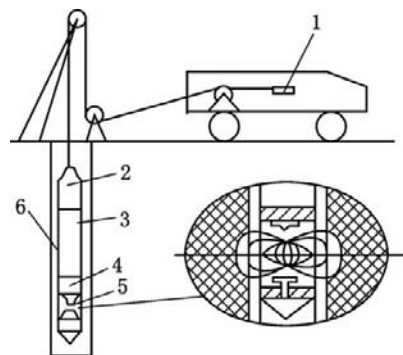


**FIGURE 8-23** Downhole low-frequency electric pulse treatment technology. 1, surface control instrument; 2, transmission part; 3, capacitor; 4, control part; 5, electrodischarger; 6, charger.

an instrument running speed lower than 50 m/min and decreasing the running speed to about 10 m/min when the instrument enters the objective interval.

- f. Connecting electric power supply and emitting electric pulse with a certain frequency. Starting electrodischarge operation from the lowest layer and treating intervals from bottom to top one by one with a treated interval length of 20 cm and 20 to 50 electrodischarges for each interval.
- g. Pulling out downhole instrument after treating and keeping a pulling speed lower than 80 m/min.
- h. Running flushing string, full flushing well, discharging blocking matter that has been loosened and broken, and cleaning the wellbore.
- i. Running in production tubing string.

## 8.4 HYDRAULIC FRACTURING FOR PUTTING A WELL INTO PRODUCTION

### Hydraulic Fracturing of Sandstone Reservoirs

Hydraulic fracturing has been widely used as a well stimulation method for sandstone reservoirs. In recent years, with the renovation of fracturing equipment, the development of fracturing fluid systems, and the raising of the fracturing design standard, the hydraulic fracturing technique has been greatly advanced and developed. At present, hydraulic fracturing has been developed from a single well stimulation to an integral development method of economic and effective production of low-permeability reservoirs. The hydraulic fracturing development technique for low-permeability reservoirs can be used for both solving the contradiction between development cost and gains of low-permeability reservoirs and meeting the requirement of field development for recovery rate. In addition, hydraulic fracturing can also be used as a well stimulation of high-permeability reservoirs in order to enhance well production effectiveness.

### Goal and Function of Hydraulic Fracturing

#### 1. Goal of hydraulic fracturing

Fracturing fluid is pumped into the well by a high-pressure surface pump unit under a pumping rate higher than the fluid-accepting capacity of the reservoir to form high pressure, break down the reservoir, extend the fracture generated, and then pump sand-filled fluid that carries proppant. Sand-packed fracture with a certain length and flow conductivity will be formed in the reservoir after termination of pumping under the action of proppant on fracture. The flowsheet of hydraulic fracturing technology is shown in Figure 8-24. In general, hydraulic fracturing may generate horizontal fracture under the condition of reservoir with a depth shallower than 1000 m and a horizontal bedding that is well developed. In most medium-deep and deep wells, hydraulic fracturing may form vertical fracture. The following discussion will center on vertical fracture, and it is considered that two symmetric wings are formed and wellbore centers.

#### 2. Function of hydraulic fracturing

- a. Improving the flow conditions in the vicinity of the wellbore and achieving an increase of individual-well production rate. In 1986 Lee presented the trilinear flow model of reservoir with finite conductivity fracture (see Figure 8-25). Original radial flow is changed to linear flow by hydraulic fracturing, thus decreasing the flow resistance in the vicinity of the

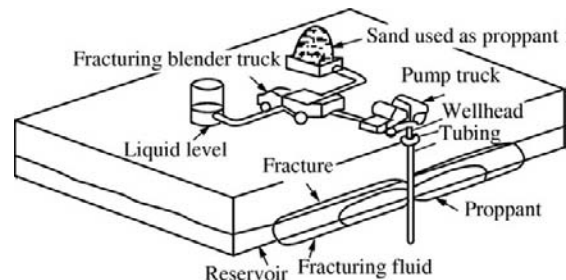


FIGURE 8-24 Hydraulic fracturing technology flowsheet.

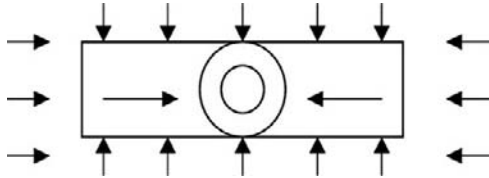


FIGURE 8-25 Trilinear flow model.

wellbore and increasing individual-well production rate under the same pressure drawdown.

- b. Performing the integral fracturing development of the reservoir and enhancing the oil recovery factor of the reservoir. The integral fracturing technology is the direction of fracturing technology application and development. Its meaning is that fracturing stimulation is comprehensively carried out over the development unit in order to fully transform reservoir texture, improve oil and gas flow pattern, and enhance total reservoir productivity.
- c. Interconnecting high-heterogeneity reservoirs, enlarging the drainage area, and increasing individual-well controlled reserves. In high-heterogeneity reservoirs, the well can be interconnected with the oil and gas aggregate far from the wellbore by hydraulically created fracture, thus increasing oil and gas reserves in individual-well controlled drainage areas and favoring long-term stable production with high production rate of oil and gas wells.

### Prefrac Appraisal and Analysis

1. Selection of well and reservoir for fracturing

The selection of well and reservoir for fracturing is an important task before fracturing design and is related to whether fracturing will be successful or not. The selection of wells for fracturing under the condition of exploration well should be especially prudent. For selecting interval, the reservoirs should be comprehensively evaluated using the data of formation test, well test, lithology, electric property, oil-bearing grade, and so on, and an interval with a certain oil-bearing area and thickness is

selected. The interval in which microfractures will be developed should be identified by using core and log data and selected first. Whether a well is appropriate for hydraulic fracturing and how large a scale should be adopted are dependent on the distances to edge water, bottom water, gas cap and fault, barrier bed condition, and the technical condition of the wellbore.

2. Prefrac reservoir appraisal
  - a. General description of geology and reservoir. Understanding the sedimentary setting and geometric shape of the reservoir, the styles of structure and fault, reserves, area, thickness, drainage radius, lithology, reservoir horizon, reservoir pressure and temperature, and so on.
  - b. Log data analysis. Studying the barricading property of the interbed, the profiles of mechanical properties of the reservoir (the elastic modulus, shear modulus, Poisson's ratio, compressibility, and so on), in-situ stress profile, and in-situ stress direction.
  - c. Core analysis. Studying reservoir permeability, reservoir porosity, reservoir rock sensitivity, and the status of natural fracture development, and so on.
  - d. Well and formation testing. Determining effective reservoir permeability, skin factor, reservoir pressure, reservoir temperature, and drainage radius, and so on.
3. Mini-frac analysis
  - a. Near-wellbore friction resistance analysis
    - (1) Causes for generating near-wellbore friction resistance
      - (a) Inconsistency of perforation direction with fracture direction. The cracking direction of fracture is often inconsistent with fracture direction. When fracturing fluid flows from perforation to fracture, it is necessary to pass through a slender channel. If zero-phase perforating is adopted, it is even possible that the direction of perforation is perpendicular to the hydraulically created fracture face.
      - (b) Fracture buckling. It is impossible that fracture is always along some

direction during extending, and it is possible that buckling and deflecting will be generated.

- (c) Perforation pressure drop. A pressure drop is inevitably generated when fluid passes through perforation.
- (2) Features of near-wellbore friction resistance
- (a) Perforation friction resistance is constant under constant discharge capacity before adding sand, while the perforation friction resistance will be decreased after adding sand due to perforation wear effect.
- (b) The pressure drop at the beginning of the operation is greater due to fracture buckling, and then it will be gradually decreased with operation and may be decreased with the increase of liquid viscosity.
- (c) Under the condition of slight perforation wear, the pressure drop generated by the inconsistency of perforation direction with fracture direction will increase with operation. However, the channel from perforation to principal fracture may be eroded by fracturing fluid at both the prepad fluid injection stage and the sand adding stage.
- (3) Solving for near-wellbore friction resistance by reducing discharge capacity

The sum of perforation friction resistance and near-wellbore friction resistance can regress as shown in Equations (8-1) and (8-2).

$$(8-1) \quad \Delta P = k_{pf}Q^2 + k_{near}Q^{1/2}$$

where:  $Q$  = discharge capacity,  $m^3/min$ ;  $k_{pf}$  = perforation friction resistance coefficient,  $\frac{MPa \cdot min^2}{m^6}$ ;  $k_{near}$  = near-wellbore friction resistance coefficient,  $\frac{MPa\sqrt{min}}{m^{3/2}}$ .

(8-2)

$$k_{pf} = \frac{228.88\rho}{n_p^2 d_p^2 c_p^2}$$

where:  $\rho$  = fracturing fluid density,  $g/cm^3$ ;  $n_p$  = number of perforations;  $d_p$  = perforation diameter,  $mm$ ;  $c_p$  = perforation flowrate coefficient.

Equation (8-1) indicates that perforation friction resistance is directly proportional to the square of operational discharge capacity, while the near-wellbore friction resistance is directly proportional to the square root of operational discharge capacity.

On the basis of the discharge capacity reduction test data,  $k_{pf}$  is first calculated using Equation (8-2); that is, the perforation friction resistances under different discharge capacities are obtained. And then  $k_{near}$  is determined by matching Equation (8-1) with the discharge capacity reduction test data, thus obtaining perforation friction resistance and fracture buckling friction resistance.

#### b. Mini-frac technique

The mini-frac technique can be used for determining the breakdown pressure, fracture closure pressure, and fracture closure time of the reservoir and calculating the total filtration coefficient and geometric sizes of fracture. It is an on-site diagnosis technique that has been widely adopted.

##### (1) Step-rate test

Fracturing fluid is injected at the pumping rates from low to high, and the pumping pressure at each pumping rate is recorded and converted into operating bottomhole pressure. The operating bottomhole pressure versus pumping rate is shown in Figure 8-26. Thus the breakdown pressure of the reservoir can be obtained.

##### (2) Pumping and flowing back test

After cracking, a fracturing fluid is injected at a stable pumping rate for 10 minutes, and pumping is stopped.

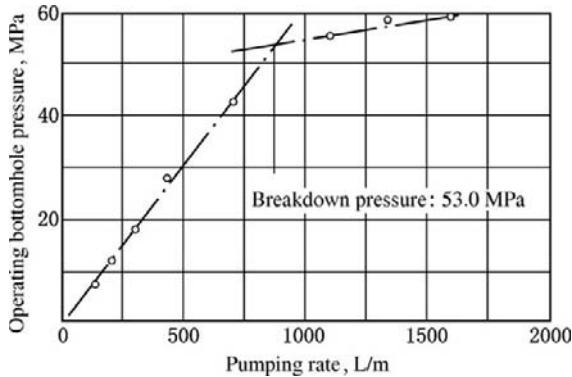


**FIGURE 8-26** Operating bottomhole pressure vs. pumping rate.

Then the well is opened for flowing back at a stable flow rate. The change of pressure is recorded. The operating bottomhole pressure versus fracture closure time is shown in Figure 8-27. Thus the closure stress and close time can be determined.

(3) Pressure fall-off test

After cracking, a fracturing fluid is injected at a stable pumping rate for 10 minutes, pumping is stopped, and the well is shut in. The change of wellhead pressure is recorded, the values of wellhead pressure are converted into bottomhole pressure, the pressure values obtained and corresponding

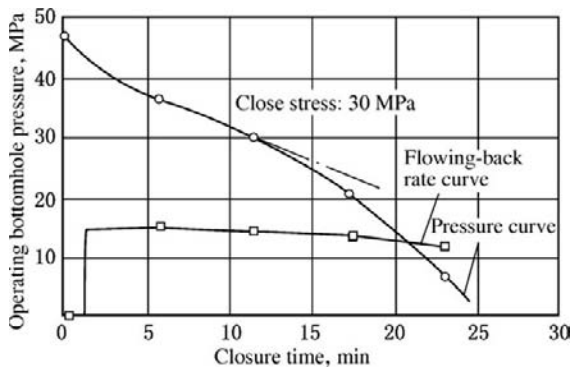


**FIGURE 8-27** Operating bottomhole pressure vs. fracture closure time.

times are input into the computer, and a Nolte matching calculation is performed, and then the obtained values of match pressure  $p^*$  are substituted into various computation models in order to calculate the values of total filtration coefficient, fracturing fluid efficiency, and geometric sizes of fracture under various fracture models.

c. Methods for diagnosing in-situ stress and natural fracture

(1) Core diagnosis technique

(a) Core diameter measurement method. Core size may change due to stress relief after coring. The difference between the two principal stresses in horizontal direction can be judged by measuring the diameters in the X and Y directions. Because the maximum principal stress is generally a vertical stress, the direction of lower principal stress (that is, the direction of smaller diameter measured) of the two principal stresses in horizontal direction is just the direction of the minimum principal stress. The application of this method should have the aid of the orientational coring technology or correct core orientation method. And this method can only judge the minimum principal stress and cannot determine quantitatively the value of in-situ stress; thus, its application is limited.

(b) Acoustic measurement method. The microfractures generated by stress relief will make the propagation of sonic waves have directionality. Measuring the propagation velocity of sonic waves in different directions of the core can determine the direction of microfracture; thus, the minimum principal stress under the condition of stress can be judged.

- (2) Logging diagnosis method
- (a) Caliper log. The change of borehole diameter in the three directions on the horizontal plane of borehole is measured. This change results from formation deformation due to stress relief. Obviously, the direction of the maximum borehole diameter is just the direction of the minimum principal stress.
  - (b) Temperature log. A temperature log can be used for determining the height of hydraulically created fracture and is a widely used logging technique. The well temperature before operation has a normal change while the well temperature after operation has a negative anomaly change because a large quantity of low-temperature fracturing fluid is sucked into fracture. The extension height of hydraulically created fracture can be determined by the range of negative anomaly.
  - (c) Radioactive tracer log. A tracer with a short half-life period is added into the proppant injected before the end of fracturing operation. Natural ray log should be immediately performed after the end of fracturing operation. The extension height of hydraulically created fracture may be displayed by the radioactive tracer added.

**Fracturing Fluid.** Fracturing fluid is the working fluid during hydraulic fracturing stimulation. It is used for transmitting pressure, forming fracture, and carrying proppant into fracture. In general, fracturing fluid should have sufficient viscosity and filtration control property in order to create fracture and carry proppant into fracture, achieve the paving concentration designed, minimize the damage of fracturing fluid to the fracture propped and reservoir, and make it flow back easily. In addition, fracturing fluid should

have good operating property, safety, and low cost. Different types of fracturing fluid are used under different conditions of reservoir and operation (see Table 8-16). At present, the problem to which close attention is paid is how to decrease the damage (especially the damage to the fracture propped) as far as possible. Thus new types of low-polymer fracturing fluid and surfactant fracturing fluid (clean fracturing fluid) are developed. And a weighted fracturing fluid that is appropriate to the reservoir with abnormal breakdown pressure has also been developed.

#### 1. Low polymer fracturing fluid

The fracturing fluid residue remaining in the reservoir is one of the important causes of contamination in the reservoir and fracture. Reducing the residue content in fracturing fluid can mitigate formation damage by fracturing fluid. The performance indices of low-polymer fracturing fluid are determined by laboratory comparative tests and are listed in Table 8-17. The thickening agent, crosslinker, and gel breaker synthesized and selected and the determined basic system composition of low-polymer fracturing fluid should meet the requirements specified in Table 8-17 and should ensure that the broken hydraulic fluid has a small quantity of residue, a low viscosity, and a low surface tension.

##### a. Thickening agent

After breaking, the natural vegetable gum and its derivant have a large quantity of residue and poor temperature tolerance and are easily degraded by bacteria. Thus only synthetic polymer is allowed to be selected as thickening agent. The synthetic polymers that can be provided for selection include PAM (A1, relative molecular mass = 4–6 million), PHPAM (A2, relative molecular mass = 4–6 million, degree of hydrolysis = 10% to 15%), PHPAM (A3, relative molecular mass = 8–10 million, degree of hydrolysis = 20% to 30%), PEO-PHPAM polymer (A4, relative molecular mass = 6 million), and a new

**TABLE 8-16** Types of Fracturing Fluid and Applicable Ranges

No.	Type of Fracturing Fluid	Advantage	Disadvantage	Applicable Range
1	Water-based crosslinked vegetable gum fracturing fluid	Low cost, high safety, strong operability, high overall performance, and wide applicable range	High residue and high damage to fracture propped and reservoir	Normal reservoirs except that with extra-low pressure, oil wettability and strong water sensitivity
2	Oil-based crosslinked gel fracturing fluid	Good compatibility with reservoir, ease of flowing back	Low safety, high cost, poor temperature tolerance, and high filtration loss	Strong water-sensitive and low-pressure reservoirs
3	Emulsified fracturing fluid	Low filtration loss, low residue, high viscosity, and low damage	Low overall performance	Water-sensitive and low-pressure reservoirs, and low- and medium-temperature wells
4	Foamed fracturing fluid	Ease of flowing back, low damage, high proppant-carrying capacity, low friction resistance, and low filtration loss	High operating pressure, requiring special operational equipment and N <sub>2</sub> or CO <sub>2</sub> gas source	Low-pressure water-sensitive reservoirs (especially gas reservoir)
5	Acid-based fracturing fluid	Good dissolution behavior	High filtration loss and high corrosivity	Carbonate reservoir and sandstone reservoir with more lime
6	Alcohol-based fracturing fluid	Low surface tension, enabling to eliminate water blocking	High cost, low safety, and low viscosity	Oil reservoirs with water sensitivity, low pressure, and low permeability

**TABLE 8-17** Performance Indices of Low Polymer Fracturing Fluid

No.	Performance Parameter	Index Required to Be Achieved
1	Shear stability	Apparent viscosity $\geq 50 \text{ MPa} \cdot \text{s}$ under $170 \text{ s}^{-1}$ shear rate for 60 minutes
2	Temperature stability	Apparent viscosity $\geq 50 \text{ MPa} \cdot \text{s}$ at 30-110°C for 60 minutes
3	Temperature tolerance	Apparent viscosity $\geq 50 \text{ MPa} \cdot \text{s}$ at 30-110°C for 60 minutes
4	Broken fracturing fluid viscosity	$\leq 10 \text{ MPa} \cdot \text{s}$
5	Surface tension of broken fracturing fluid	$\leq 26 \text{ mN/m}$
6	Broken fracturing fluid-diesel oil interfacial tension	$\leq 5 \text{ mN/m}$
7	Residue content	$\leq 300 \text{ mg/l}$
8	Crosslinking time	$\leq 180 \text{ s}$

synthetic polymer HM (A5, relative molecular mass = 12 million, degree of hydrolysis = 25%). The corresponding crosslinkers include B1, B2, B3, B4, and B5. Sodium persulfate is selected as gel

breaker. Fracturing fluid can be fully broken by sodium persulfate at 70°C for eight hours. The measured values of residue content of broken fracturing fluid are listed in Table 8-18.

**TABLE 8-18 Comparison between Residue Contents under Different Thickening Agents**

Thickening Agent	Crosslinker	Gel Breaker	Residue Content (mg/l)
A1	B1	Sodium persulfate	343
A2	B2		845
A3	B3		653
A4	B4		204
A5	B5		124

HM is selected as the thickening agent of a new type of low-polymer fracturing fluid in accordance with the residue content of broken fracturing fluid. If only HM is used, the fracturing fluid has low shear resistance; thus, a composite HPG/HM high molecular thickening agent is prepared by the interaction between HPG and HM molecules. The tests indicate that the composite HPG/HM thickening agent has higher viscosity and shear stability of fracturing fluid under the HPG of 30%, while the composite HPG/HM thickening agent may only have a slight increase of viscosity and shear stability if the HPG volume is further increased. Thus the HPG proportion of 30% in HPG/HM thickening agent is adopted.

b. Crosslinker

The reaction product generated by organic matter RA and metallic ion P can control the crosslinking time to be in the range of 40 to 180 s, which meets the requirement of design. Under a certain crosslinker, the crosslinking time of fracturing fluid can be regulated by a crosslinking promoter of different proportions. The crosslinking time will change with

the change of volume of the same crosslinking promoter. Selecting H-1 as crosslinking promoter, selecting the RA/P mole ratio of 1:1, selecting the reaction product (C-2) with crosslinking time of 69 s as crosslinker, and changing H-1 volume can also regulate crosslinking time.

c. Gel breaker

Sodium persulfate (G-1) is used as the gel breaker of low-polymer fracturing fluid. The break properties of low-polymer fracturing fluid at 50°C are listed in Table 8-19.

d. Properties of low-polymer fracturing fluid

The thickening agent (HPG/GM), crosslinker (C-2), and gel breaker (G-1) of low polymer fracturing fluid are selected. On the basis of property evaluation, the following basic low-polymer fracturing fluid formulation, which is appropriate for a reservoir with 50°C, is determined: 0.25%(HM) + 0.07%(HPG) + 0.35%(C-2) + 0.4%(G-1). The properties of the low-polymer fracturing fluid are evaluated. A fracturing fluid viscosity of about 100 MPa · s can still be maintained for 60 minutes under a shear rate of 170 s<sup>-1</sup> at 50°C, thus exceeding the basic index required by conventional fracturing

**TABLE 8-19 Break Properties of Low Polymer Fracturing Fluid at 50°C**

Sample	1	2	3	4	5	6
G-1 proportion (%)	0.1	0.2	0.3	0.4	0.5	0.6
Break time (h)	8	8	8	7.5	7	6.8
Broken fracturing fluid viscosity (Pa · s)	13.4	8.6	5.1	2.6	2.5	2.3
Residue (mg/L)	114	95	74	62.9	43.3	36.8

fluid. The fracturing fluid can be fully broken after 8 hours, the viscosity of broken fracturing fluid is lower than  $5 \text{ MPa} \cdot \text{s}$ , and the residue content of broken fracturing fluid is much lower than  $300 \text{ mg/l}$ , thus meeting the requirements of low damage and fracturing operation.

## 2. Surfactant fracturing fluid

Surfactant fracturing fluid is a new type of fracturing fluid system with no polymer. Its dominant ingredient is a small molecule surfactant. It has no solids and residue and may only have slight formation damage. It can gel and break automatically by the micellar structure of the surfactant. After operation, it can be rapidly flowed back with a high backflow rate, thus preventing the formation damage that may be caused by conventional thickening agents.

### a. Gelling mechanism of surfactant fracturing fluid

In an aqueous solution, surfactant molecules first accumulate and form vermicular micellae. The salt added will equilibrate the electric charges in the system or compress micellar structure to make micellae grow to a certain degree. The organic heterocharge ions added will neutralize micellar charges and will be inserted between surfactant molecules of vermicular aggregate, which makes the aggregate slender. The inorganic homocharge ions added will make the vermicular aggregate be compressed and become more slender. The vermicular micellae that become more slender will tangle with each other, thus forming a spatial net-shaped structure (jelly) like homogeneous floc unit.

### b. Gel-breaking mechanism of surfactant fracturing fluid

There mainly is physical action between surfactant and salt molecules in a surfactant gen system, while the components in polymer (such as guar gum) fracturing fluid are mutually connected by chemical action. Therefore, when the gel in

surfactant fracturing fluid meets with a certain quantity of reservoir water and oil/gas, the acting distance between surfactant and salt molecules may be increased; thus, the mutual tangle of vermicular micellae may be broken, the vermicular micellae may even be dismembered into simple micellae, and the gel system will automatically break.

### c. Properties of surfactant fracturing fluid

(1) Proppant-carrying capacity of surfactant fracturing fluid. For a fracturing fluid system containing 1.25% surfactant and 0.3% organic salt, the elastic and viscous moduli versus oscillation frequency at  $30^\circ\text{C}$  are shown in Figure 8-28. The elastic modulus of this system under low frequency is greater than the viscous modulus and will gradually increase. In conventional guar gum fracturing fluid, despite the fact that it also has viscoelasticity and under high frequency the elastic modulus increases as the oscillation frequency increases, the elastic modulus will be gradually lower than the viscous modulus and the mechanism of proppant carrying is mainly shown as viscous proppant-carrying; however, in surfactant fracturing fluid, which is viscoelastic colloid formed by surfactant micellae under the action of

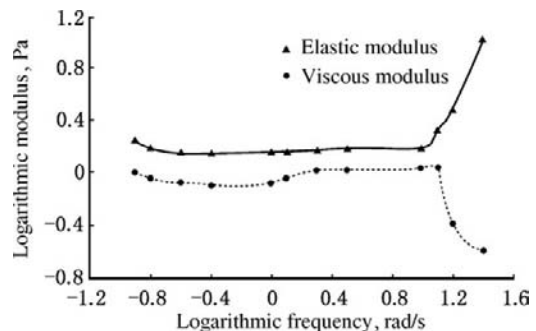


FIGURE 8-28 Elastic modulus and viscous modulus of surfactant fracturing fluid.

electric charges, the mechanism of proppant carrying is mainly shown as elastic proppant carrying. The results of proppant-carrying tests (by Stimlab Co.) of guar gum fracturing fluid and surfactant fracturing fluid using a large-scale proppant-transport model are shown in Table 8-20. It is indicated that under the same conditions, the proppant-carrying viscosity of surfactant fracturing fluid is much lower than that of guar gum fracturing fluid due to different proppant-carrying mechanisms.

- (2) Composite properties of surfactant fracturing fluid. Because surfactant fracturing fluid may not form filter cake on the fracture wall face, the data

measured by using a laboratory test of guar gum fracturing fluid will not actually reflect the filtration property. Fracturing practice indicates that the filtration property of surfactant fracturing fluid is not as high as that measured in the laboratory. Under the pumping rate of  $3 \text{ m}^3/\text{min}$ , the friction resistance is only 25% of clear water. The properties of surfactant fracturing fluid are listed in Table 8-21.

### 3. Weighted fracturing fluid

Under the conditions of deep and super-deep wells, abnormal high pressure, and in-situ stress and tight reservoirs, it is difficult to achieve large-scale sandfrac of low-permeability reservoirs because of high friction resistance, low fluid-accepting ability due to tight reservoir, high operating pressure due to abnormal high pressure, inability to inject under high pumping rate due to limited operational equipment, and difficulty in proppant input and limited proppant concentration under low pumping rate. For a weighted fracturing fluid system in which NaBr–NaCl combination salt is used as weighting admixture, the maximum density is up to  $1.5 \text{ g/cm}^3$ . For a well with a depth of 6000 m, the fluid column pressure can be increased by 30 MPa in comparison with conventional water-based fracturing fluid;

**TABLE 8-20** Comparison Between Proppant-Carrying Viscosities of Surfactant and Guar Gum Fracturing Fluids

Shear Rate ( $\text{S}^{-1}$ )	Surfactant Fracturing Fluid Viscosity ( $\text{MPa} \cdot \text{s}$ )	Guar Gum Fracturing Fluid Viscosity ( $\text{MPa} \cdot \text{s}$ )
100	30	100
170	<30	50

**TABLE 8-21** Properties of Surfactant Fracturing Fluid

No.	Performance Parameter	Performance Index of Surfactant Fracturing Fluid	Performance Index of Guar Gum Fracturing Fluid	
1	Apparent viscosity of broken fluid	at 20–100°C for 60 minutes	$\geq 30 \text{ MPa} \cdot \text{s}$	$\geq 50 \text{ MPa} \cdot \text{s}$
		at 30–110°C for 60 minutes	$\leq 5 \text{ MPa} \cdot \text{s}$	$\leq 10 \text{ MPa} \cdot \text{s}$
2	Surface tension of broken fluid	$\leq 30 \text{ mN/m}$	$\leq 30 \text{ mN/m}$	
3	Broken fluid-diesel oil interfacial tension	$\leq 5 \text{ mN/m}$	$\leq 5 \text{ mN/m}$	
4	Residual cake content	No	$\leq 1400 \text{ mg/l}$	
5	Filter cake	No	Yes	
6	Crosslinking time		20–180s adjustable	
7	Flowing-back time	Enabling rapid flowing back	Enabling rapid flowing back	

thus, operating wellhead pressure is greatly reduced and the fracturing fluid is successfully applied.

a. Basic formulations of weighted fracturing fluid

The base fluid compositions of various weighted fracturing fluid are listed in Table 8-22.

b. Properties of weighted fracturing fluid

The basic fluid viscosity of fracturing fluid is measured under  $170 \text{ S}^{-1}$  at atmospheric temperature, and the change of the pH value of base fluid is observed. The results indicate that a salt with a high concentration can be used for increasing the viscosity of base fluid; GRJ-11 has a high salt resistance; and the weighted fracturing fluid has stable properties after placing for 3 days. The crosslinking time can be controlled under less YC-150 (crosslinking regulator) or no or diluted YP-150, and so on.

This weighted fracturing fluid has a viscosity of  $70\text{--}150 \text{ MPa} \cdot \text{s}$  under  $170 \text{ S}^{-1}$  at  $120^\circ\text{C}$ . It has high temperature tolerance, shear resistance, and rheology property.

Under the condition of pressure difference of  $3.5 \text{ MPa}$ , the static fluid loss coefficients of formulation 1 and 3 (0.45% GRJ-11) systems at  $120^\circ\text{C}$  are respectively  $6.37 \times 10^{-4} \text{ m}/\sqrt{\text{min}}$  and  $7.45 \times 10^{-4} \text{ m}/\sqrt{\text{min}}$ , while the dynamic fluid loss coefficients of formulation 1 and 3 (0.45% GRJ-11) systems at  $100^\circ\text{C}$  are respectively  $5.27 \times 10^{-4} \text{ m}/\sqrt{\text{min}}$  and  $6.037 \times 10^{-4} \text{ m}/\sqrt{\text{min}}$ .

The experiments indicate that weighted fracturing fluid is difficult to break and its rheology property is greatly affected by temperature. Thus micella breaker volume should be appropriately increased and the effect of gel breaker added on the rheology property of fracturing fluid should be avoided, so that the fracturing fluid can be fully broken after fracturing.

The broken fluid of the weighted fracturing fluid formulation 1 or 3 (0.45% GRJ-11) system is mixed with crude oil in the Tazhong 50 well in the proportion of 1:1 under the high speed of 1400 rpm at  $60^\circ\text{C}$  so that it is fully emulsified and is then placed in a thermostatic bath at  $90^\circ\text{C}$  for demulsibility test. The demulsification proportion for 60 minutes is up to more than 90%. It indicates that this weighted fracturing fluid formulation system has a high non-emulsifying and demulsifying property.

The surface tensions of the broken fluid filtrates of formulation 1 and 3 (0.45% GRJ-11) systems are respectively  $1.83 \text{ mN/m}$  and  $1.77 \text{ mN/m}$ , while the interfacial tensions of the broken fluid filtrates of formulation 1 and 3 (0.45% GRJ-11) systems are  $25.4 \text{ mN/m}$  and  $24.8 \text{ mN/m}$  respectively. The corrosion rates of formulations 1 and 2 on a piece of steel are respectively  $0.034 \text{ g/m}^2 \cdot \text{h}$  and  $0.059 \text{ g/m}^2 \cdot \text{h}$ .

4. Environmental protection type low molecular weight fracturing fluid

TABLE 8-22 Base Fluids with Different Densities for Weighted Fracturing Fluid

Formulation	Basic Fluid Composition of Fracturing Fluid	Density (g/cm <sup>3</sup> )
1	26%NaCl + 0.5%GRJ - 11(thickener) + 0.5%DJ - 02(cleanup additive) + 1%DJ - 14(demulsifier) + 0.15%Na <sub>2</sub> CO <sub>3</sub> + 0.04%NaOH	1.2
2	21%NaBr + 15%NaCl + 0.55%GRJ - 11(thickener) + 0.5%DJ - 02(cleanup additive) + 1%DJ - 14(demulsifier) + 0.15%Na <sub>2</sub> CO <sub>3</sub> + 0.04%NaOH	1.34
3	44%NaBr + 4%NaCl + 15%NaCl + 0.4 - 0.5% GRJ - 11(thickener) + 0.5%DJ - 02(cleanup additive) + 1%DJ - 14(demulsifier) + 0.15%Na <sub>2</sub> CO <sub>3</sub> + 0.04%NaOH	1.51

With conventional water-based gel fracturing fluid, it is difficult to prevent drainage after fracturing from a polluting environment, and the volume of its breaker makes it difficult to meet the requirements of both the proppant-carrying and flowing-back properties. Thus low molecular weight fracturing fluid (LMWF) should be adopted.

LMWF uses the chemically modified low molecular compound CJ2-3 as a thickening agent, of which the molecular chain is 25 times smaller than that of traditional guar gum and HPG. Introducing strongly water-wetting groups into a low molecular compound will greatly enhance their water solubility, thus enhancing the solubility of polymer.

LMWF can achieve complex shielding and secondary crosslinking of low molecules, thus increasing the viscosity and effectiveness of crosslinked liquid. The chemical chain structure can be dynamically changed by a temporary chaining reaction, so that the fluid has a higher elasticity and the proppant-carrying capacity is improved. Controlling the pH value of the fluid makes the connection of the chain reversible. Flowing back after fracturing can be achieved by decreasing the pH value of LMWF system.

LMWF combines the advantages of conventional HPGF and clean fracturing fluid. It may maintain a low residue and keep the advantages of polymer fracturing fluid system. It has a low cost and is easy for in situ operation. In particular, the various types of chemical matter in flowback fluid have not been essentially changed because there is no gel breaker, and the flowback fluid treated for recovering can be repeatedly used as fracturing fluid, thus reducing the environmental pollution generated by fracturing fluid drainage and decreasing the composite application cost of fracturing fluid.

5. Fracturing fluid loss calculation

a. Classical method for fluid loss calculation

The composite fluid loss coefficient  $C$  is as shown in Equation (8-3).

(8-3)

$$\frac{1}{C} = \frac{1}{C_1} + \frac{1}{C_2} + \frac{1}{C_3}$$

where  $C_1$ ,  $C_2$ , and  $C_3$  are respectively the fluid loss coefficients controlled by filtrate viscosity, formation fluid compressibility, and wall-building property.

Thus the filtration rate of the fracturing fluid in hydraulically created fracture is calculated as shown in Equation (8-4).

(8-4)

$$v = C\sqrt{t}$$

where:  $t$  = exposure duration of fracturing fluid at some point in fracture.

b. Fluid filtration model for homogeneous reservoir (depending on net pressure)

On the basis of the new fracturing fluid filtration model presented by Fan Y and Economides et al. for homogeneous reservoirs, the fluid filtration rate can be calculated by using the net pressure in fracture and reservoir permeability. The fracturing fluid filtration process is described in Equation (8-5).

(8-5)

$$\begin{cases} \frac{\partial^2 p}{\partial x^2} = \frac{1}{a} \frac{\partial p}{\partial t} \\ p = p_i & (t = 0, x > 0) \\ p = p_{fw}(t) & (x = 0, t > 0) \\ p = p_i & (x \rightarrow \infty, t > 0) \end{cases}$$

where:  $\alpha$  = hydraulic diffusion coefficient,  $m^2/s$ ;  $p_i$  = reservoir pressure, MPa;  $p_{fw}$  = fracture port pressure, MPa;  $t$  = filtration time, s;  $x$  = distance from some point in fracture to fracture port, m.

Fluid filtration rate is shown in Equation (8-6).

(8-6)

$$u = \frac{k}{\sqrt{\pi\alpha\mu_{app}}} \left\{ \sum_{j=1}^{j-1} (p_{f,j} - p_{f,j-1}) \frac{1}{\sqrt{t - t_{j-1}}} - \frac{\bar{s}}{\sqrt{t}} \right\}$$

where:  $\mu_{app}$  = fluid filtration rate, m/s;  $k$  = reservoir permeability,  $m^2$ ;  $p_f$  = pressure

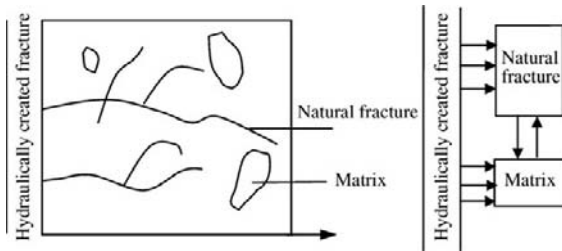


**FIGURE 8-29** Physical model of fracturing fluid loss in naturally fractured reservoir.

in fracture, Pa;  $\bar{s}$  = pressure drop in cake area, Pa;  $j$  = some unit section in fracture.

c. Fracturing fluid loss calculation for naturally fractured reservoirs

The physical model of fracturing fluid loss in a naturally fractured reservoir is shown in Figure 8-29. Suppose that:

- (1) Fracturing fluid flows to natural fracture and matrix and there is fluid exchange between natural fracture and matrix.
- (2) The effect of cake is neglected for the convenience of analysis. Practice indicates that an effective cake is difficult to form during fracturing in naturally fractured reservoirs and the cake area pressure drop, which is much lower than the net fracture pressure, can be neglected. When there is cake, this model is still applicable provided that the net fracture pressure is required to be calculated by iteration.
- (3) Reservoir fluid compressibility is negligible. When the fluid loss in naturally fractured gas reservoir and the dissolved gas content in oil reservoir fluid are high, the compressibility of oil reservoir fluid is negligible.

On the basis of the assumed conditions mentioned in the preceding list, the fracturing fluid flow from hydraulically created fracture to natural fracture and matrix meets Equation (8-7).

(8-7)

$$\left\{ \begin{array}{l} \frac{k_f}{\mu_e} \frac{\partial^2 p_f}{\partial x^2} + \frac{\alpha}{\mu_e} (p_m - p_f) = C_f \Phi_f \frac{\partial p_f}{\partial t} \\ \frac{k_m}{\mu_e} \frac{\partial^2 p_m}{\partial x^2} + \frac{\alpha}{\mu_e} (p_f - p_m) = C_m \Phi_m \frac{\partial p_m}{\partial t} \\ p_f(x, 0) = p_i \quad (0 \leq x \leq L) \\ p_m(x, 0) = p_i \quad (0 \leq x \leq L) \\ p_f(0, t) = p_i + \Delta p \quad \Delta p > 0 \\ p_m(0, t) = p_i + \Delta p \quad \Delta p > 0 \\ p_f(L, t) = p_i \\ p_m(L, t) = p_i \end{array} \right.$$

where:  $p$ ,  $p_i$ , and  $\Delta p$  are respectively fluid pressure, initial reservoir pressure, and net fracture pressure, Pa;  $\mu_e$  = effective viscosity of fracturing fluid, MPa · s;  $\Phi$  = porosity, %;  $k$  = permeability, m<sup>2</sup>;  $C$  = composite compressibility, Pa<sup>-1</sup>;  $t$  = filtration time, s;  $\alpha$  = characteristic coefficient of naturally fractured reservoir rock, dimensionless;  $L$  = distance of external boundary controlled by single well; the subscripts  $f$  and  $m$  show respectively natural fracture system and matrix.

The filtration rate of fracturing fluid is defined as shown in Equation (8-8).

(8-8)

$$v_i = \frac{k_f}{\mu_e} \frac{\partial p_f}{\partial x} \Big|_{x=0} - \frac{k_m}{\mu_e} \frac{\partial p_m}{\partial x} \Big|_{x=0}$$

The filtration loss in natural fracture, the filtration loss in matrix, and the percentage of the filtration loss in natural fracture in total filtration loss of fracturing fluid are shown in Figure 8-30. In the early stage of fracturing fluid filtration, part of the fracturing fluid enters the matrix due to rock compressibility. With the increase of filtration time, the pressure in the vicinity of hydraulically created fracture tends to be stable. Most of the filtrate will flow in the natural fractures, which have a relatively high permeability, and the filtration loss in the matrix will not increase.

For the convenience of comparison with the classic method for filtration loss calculation, the  $V = C \times t^b$  formula is used for matching fracturing fluid filtration rate with filtration time. The least square method is used during matching. The results of matching fracturing fluid filtration rate with filtration time are

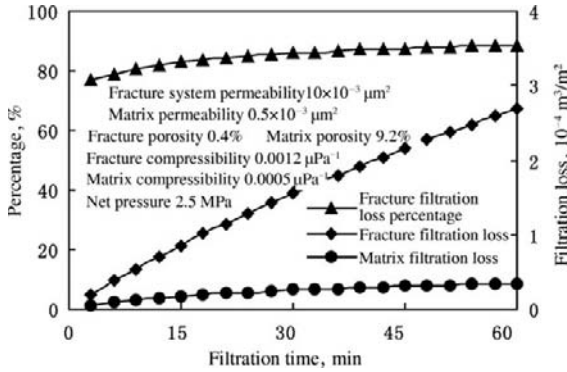


**FIGURE 8-30** Comparison between natural fracture filtration loss and matrix filtration loss.

shown in Table 8-23. Under the various conditions of calculation, the degrees of matching are high, except that there are differences in the coefficient C and the exponent b. Thus the fracturing fluid filtration rate for a naturally fractured reservoir can be characterized by  $V = C \times t^b$ . Table 8-23 shows that the absolute value of negative exponent b is less than 0.5. In accordance with the characteristics of exponential function, when  $t > 1$ , the less the absolute value of negative exponent b, the greater the function value calculated. Thus the fracturing fluid filtration rate for a naturally fractured reservoir is higher than that calculated by  $V = Ct^{-0.5}$ .

**Proppant**

1. Basis for selection of proppant

The selection of proppant is mainly based on the McGuire-Sikora electric analog chart (Figure 8-31) at present. Fracture flow conductivity is determined on the basis of this chart in accordance with the requirement of the increase in reservoir productivity, and proppant is then selected in combination with reservoir closure stress. Figure 8-31 indicates that for a low-permeability reservoir, a higher fracture flow conductivity ratio is easily obtained, and the increase of fracture length should be predominant in order to increase the effectiveness of fracturing. For a high-permeability reservoir, it is not easy to obtain a higher fracture flow conductivity ratio, and increasing fracture flow conductivity is the main approach to increase the effectiveness of fracturing; for a certain fracture length, there is the optimum fracture flow conductivity, above which the effectiveness of increasing fracture flow conductivity is very low; and the maximum stimulation ratio of the oil well under the condition of no damage is 13.6.

The net present value method was used for optimization design in the past. At present, a new design standard has been presented in

**TABLE 8-23** Results Matching Filtration Rate with Filtration Time

Parameter	Matching Relation $V = C \times t^b$		Correlation Coefficient
	C	b	
$\Delta p = 1.5 \text{ MPa}$	11.47	-0.253	0.992
$\Delta p = 2.5 \text{ MPa}$	19.11	-0.252	0.992
$\Delta p = 3.5 \text{ MPa}$	26.76	-0.253	0.992
$K_f = 10 \times 10^{-3} \mu\text{m}^2$	9.00	-0.273	0.983
$K_f = 30 \times 10^{-3} \mu\text{m}^2$	19.11	-0.253	0.992
$K_f = 50 \times 10^{-3} \mu\text{m}^2$	30.88	-0.29	0.971
$\mu_e = 50 \text{ MPa} \cdot \text{s}$	44.92	-0.344	0.962
$\mu_e = 150 \text{ MPa} \cdot \text{s}$	15.91	-0.245	0.995
$\mu_e = 250 \text{ MPa} \cdot \text{s}$	11.13	-0.253	0.986
$\mu_e = 350 \text{ MPa} \cdot \text{s}$	9.14	-0.272	0.983
$\mu_e = 500 \text{ MPa} \cdot \text{s}$	7.56	-0.295	0.987
$\mu_e = 1000 \text{ MPa} \cdot \text{s}$	5.19	-0.334	0.998

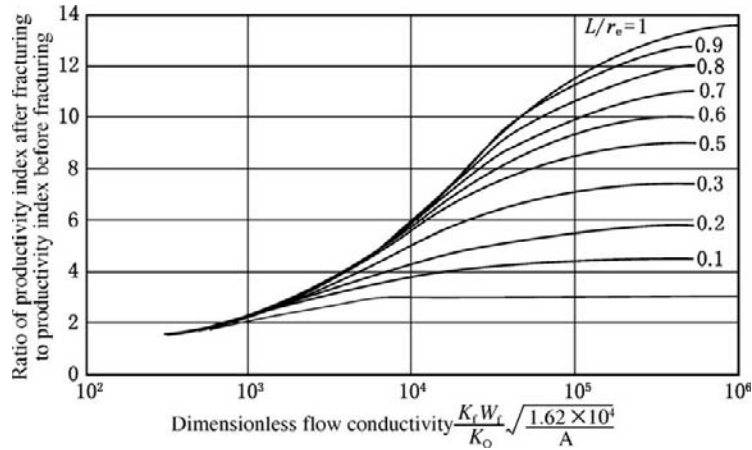


**FIGURE 8-31** McGuire-Sikora stimulation ratio diagram.  $L$ , drainage radius,  $m$ ;  $r_e$ , vertical fracture half-length,  $m$ ;  $k_f w_f$ , fracture flow conductivity,  $10^{-3} \mu m^2 \cdot m$ ;  $k_o$ , oil reservoir permeability,  $10^{-3} \mu m^2 \cdot m$ ;  $A$ , drainage area,  $m^2$ .

order to maximize the productivity index. Thus the dimensionless proppant coefficient is defined as shown in Equation (8-9).

(8-9)

$$N_{prop} = \frac{2k_f v_p}{kv_r}$$

where:  $k_f$  = fracture permeability,  $m^2$ ;  $k$  = reservoir permeability,  $m^2$ ;  $v_p$  = propped fracture volume,  $m^3$ ;  $v_r$  = drainage region volume,  $m^3$ .

Dimensionless productivity index and optimum dimensionless flow conductivity can be shown as the function of the dimensionless

proppant coefficient. Thus the dimensionless productivity index vs. dimensionless flow conductivity is obtained (Figure 8-32).

Given dimensionless proppant coefficient  $N_{prop}$ , there is the optimum dimensionless fracture flow conductivity, which makes the productivity index highest. After the optimum dimensionless fracture flow conductivity is determined, the optimum fracture length and fracture width can be determined. The optimization design procedure includes: (1) determining the type and volume of proppant; (2) determining dimensionless proppant coefficient; (3) determining optimum

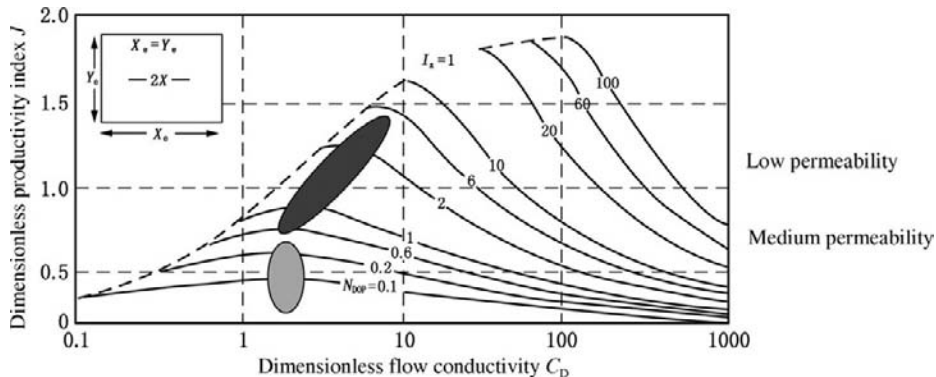


**FIGURE 8-32** Diagram of dimensionless productivity index vs. dimensionless flow conductivity.

dimensionless fracture flow conductivity on the basis of dimensionless proppant coefficient in order to maximize dimensionless productivity index; (4) calculating fracture length and fracture width; and (5) optimizing operational pumping procedure design.

## 2. Natural quartz sand

Natural quartz sand is the proppant used widely (about 55%) during sandfrac. It contains chiefly  $\text{SiO}_2$  and has a small quantity of Al, Fe, Ca, Mg, K, Na, impurities, and so on. Quartz sand is widely distributed in China. Quartz content is an important index for determining the quality of quartz sand. It is generally about 80% in China. In addition to quartz, quartz sand also contains a small quantity of feldspar, chert, and other debris of extrusive or metamorphic rock. The quartz content of quality quartz sand is up to more than 98%.

The main advantages of quartz sand include: (1) quartz sand with high sphericity can still maintain a certain flow conductivity after the quartz sand is crushed; (2) quartz sand has a relatively low density and is convenient to pump; (3) sand of 0.15 mm or silt can be used as fracturing fluid loss additive and can be used for filling a natural fracture that is interconnected with a principal fracture; and (4) it has a low cost and can be drawn from local resources in many areas.

The disadvantages of quartz sand include: (1) quartz sand has a lower strength and an initial crushing pressure of about 20 MPa; thus, it is unsuitable to reservoirs with high closure pressure; (2) quartz sand has a low compressive strength; and the flow conductivity may be reduced to 1/10 of original flow conductivity or lower due to insertion, fine migration, blocking, the damage caused by fracturing fluid, and so on.

## 3. Synthetic ceramsite

Synthetic ceramsite proppant has been developed in order to meet the requirement of fracturing of a deep reservoir with high closure pressure.

### a. Medium-strength ceramsite proppant

It is made of bauxite or siliceous pottery clay (vitriol and aluminum silicate). The aluminum oxide content (weight) is 46% to 77% while the siliceous content is 13% to 55%. In addition, it contains a small quantity of other oxide. Its relative density is 2.7–3.3. The relative density of the low-density medium-strength proppant produced by the manufacturer in Yixin, China is 2.82.

### b. High-strength ceramsite proppant

It is made of bauxite or alumina. The contents of aluminum oxide, silicon oxide, iron oxide, and titanium oxide ( $\text{TiO}_2$ ) are respectively 85% to 90%, 3% to 6%, 4% to 7%, and 3% to 4%.

### c. Advantages and disadvantages of ceramsite

Ceramsite proppant has high strength and can provide high fracture flow conductivity under high closure pressure. It has salt resistance and temperature resistance. The reduction of flow conductivity with the increase of closure pressure and the prolongation of pressure-bearing time is much slower than that of quartz. However, ceramsite has a high density (2700–3600  $\text{kg/m}^3$ ) and is difficult to pump. It has difficult manufacturing technology and high cost. With the increase of aluminum content the compressive strength of ceramsite increases, but the density also increases; thus, a compromise proposal is required.

Table 8-24 shows the test of fracture flow conductivity of some quartz sand and ceramsite in China. Under the action of formation closure stress, the flow conductivities of quartz sand or ceramsite from different sources are different to some degree. The flow conductivity of quartz sand is greatly different from that of ceramsite. In particular, under a higher closure pressure, the flow conductivity of ceramsite is obviously higher than that of quartz sand.

## 4. Resin enclosed proppant

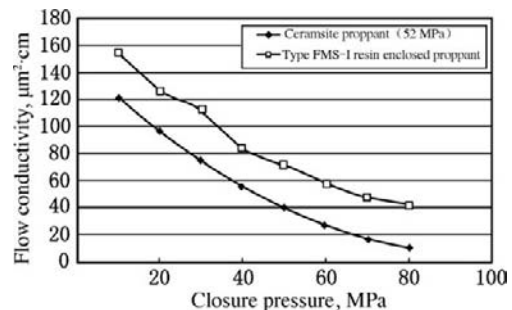
### a. Resin enclosed proppant technique

TABLE 8-24 Flow Conductivities of Some Proppants in China

Closure Pressure (MPa)	Φ0.5-0.80 Quartz Sand				Φ0.8-1.25 Quartz Sand				Φ0.45-0.90 Ceramsite			
	Lanzhou Sand		Yueyang Sand		Lanzhou Sand		Yueyang Sand		Yixin Ceramsite		Chengdu Ceramsite	
	F <sub>RCD</sub> (μm <sup>2</sup> ·cm)	K (μm <sup>2</sup> )	F <sub>RCD</sub> (μm <sup>2</sup> ·cm)	K (μm <sup>2</sup> )	F <sub>RCD</sub> (μm <sup>2</sup> ·cm)	K (μm <sup>2</sup> )	F <sub>RCD</sub> (μm <sup>2</sup> ·cm)	K (μm <sup>2</sup> )	F <sub>RCD</sub> (μm <sup>2</sup> ·cm)	K (μm <sup>2</sup> )	F <sub>RCD</sub> (μm <sup>2</sup> ·cm)	K (μm <sup>2</sup> )
10	88	276	82	260	106	353	179	553	153	462	141	515
20	42	142	48	143	59	211	69	225	111	347	115	421
30	15	62	22	75	24	99	27	93	85	272	92	345
40	6	29							62	205	74	283
50	—								44	148	57	221
60	—								31	108	45	177
70	—								18	65	37	146
80	—								13	46	28	116

Note: API flow guide chamber, 22±3°C; equiquality method; 5.0 kg/m<sup>2</sup> proppant-paving concentration; deionized distilled water as test fluid.

- (1) Resin modification. The feature of the chemical structure of epoxy resin is that there is an epoxy group on a macromolecular chain. Different methods of generating epoxy groups and different materials used have different types of epoxy resin generated. Bisphenol A epoxy resin is not suited to be used as the enclosure of proppant, and modification is required. In order to ensure a firm cohesion of proppant, epoxy resin should have a self-emulsification property; thus, various strong hydrophilic radicals should be introduced on the macromolecule of epoxy resin to modify epoxy resin into a resin that is rich in basic groups, and acid is used for neutralizing it into salt so that it has a certain water affinity and cohesive force is increased.
  - (2) Curing principle of resin enclosure of proppant. Quartz sand and ceramsite are enclosed by synthetic resin using physical and chemical methods, so that quartz sand and ceramsite have a resin enclosure that can be cured. After this type of proppant enters the fracture, the resin layer first softens and will then generate polymerization reaction under the action of an activating agent at reservoir temperature; thus, each particle of proppant has a tough enclosure, and these particles are bonded together by polymerization.
- b. Characteristics of resin-enclosed proppant
- (1) Under a certain closure pressure, the crushing strength of the proppant particle is increased. The mode of contact is changed by the property of resin-enclosed proppant, the contact area is increased, and the pressure acting on proppant particles is dispersed by the enclosure of proppant.
  - (2) Each particle of proppant has a tough resin enclosure. Under a certain closure pressure, the debris of crushed proppant may be coated by resin enclosure,
- so that the migration of debris and fine silt is prevented and fracture has a higher flow conductivity.
- (3) At a certain reservoir temperature, the resin enclosure is first softened. Under the action of reservoir temperature and activating agent, proppant particles are bonded together and bonded with the new fracture surface, thus forming a permeable filtering layer, firming the fracture surface, preventing the proppant from backflowing, decreasing the insertion of proppant into the reservoir, and enabling sand control.
  - (4) Resin enclosure is made in accordance with the specific reservoir temperature and can meet the requirement of specific reservoir temperature conditions.
- c. Flow conductivity test of FMS series resin-enclosed proppant
- (1) Short-term flow conductivity test. The conditions of the short-term flow conductivity test include: testing pressure of 10–80 MPa; testing proppant-paving concentration of 5 kg/m<sup>2</sup>; and testing fluid of 2% KCl solution. The results of the test are shown in Figure 8-33.
  - (2) Long-term flow conductivity test. The conditions of the long-term flow conductivity test include: closure pressure of 60 MPa; testing proppant-paving concentration of 5 kg/m<sup>2</sup>; testing fluid



**FIGURE 8-33** Comparison between flow conductivities of Type FMS-1 resin enclosed proppant and ceramsite proppant.

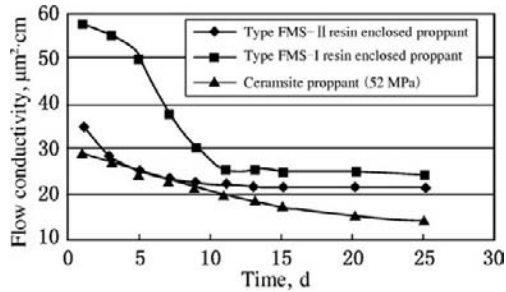


**FIGURE 8-34** Comparison between flow conductivities of resin enclosed proppant and ceramsite proppant.

of 2% KCl solution; and testing time of 25 days. The results of the test are shown in Figure 8-34. It is indicated that with the increase of closure pressure, the flow conductivity of common ceramsite rapidly decreases and the flow conductivities of Type FMS-I and Type FMS-II resin-enclosed proppants slowly decrease despite the fact that they all decrease to some extent.

#### 5. Thermoplastic film proppant

At a temperature lower than 150°C, a soft-surface that interacts with proppant particles will form by thermoplastic film. Despite the fact that its adhesive strength is lower than that of resin enclosure, this surface has a higher friction resistance, and the rolling of proppant in flow string can be mitigated. At a higher temperature, the proppant can be firmed by the thermoplastic film under the action of adhesion and shrinkage. With the increase of temperature, the surface of

the film becomes tough, the proppant may adhere to the surface, and proppant glomerates will form. If the temperature increases further, the film may shrink, and consolidated glomerates that are closer and firmer may form. These glomerates bridged together will form a larger flow space, so that resistance to the flow of broken fluid in the proppant layer during backflow is decreased, thus favoring preventing proppant from backflowing. The advantages of thermoplastic film include: (1) it is compatible with fracturing fluid (including crosslinker and gel breaker), may not react on other additives, and will not affect the chemical properties of fracturing fluid; (2) it is stable in oil, water, and acid liquor; and (3) the thermoplastic material is economical and practical, which means that it can be used in the whole fracturing process.

#### 6. Deformable proppant

Deformable proppant is formed by resin and inertial filling material. It has similar shape and fenestral distribution and is deformable under a certain stress (Figure 8-35). In recent years, it has been used mainly for controlling proppant backflow. This type of proppant is suitable for a reservoir with closure pressure of 5–50 MPa and temperature lower than 185°C. Its volume is generally 10% to 15% of total proppant volume.

After deformable proppant is mixed with ordinary proppant, on the surface of this type of proppant some small cavities or concaves may be formed under a certain closure pressure due to deformation. These cavities or



**FIGURE 8-35** The shapes of deformable proppant before and after exerting force on it.

concaves will be helpful in stabilizing and locking the surrounding proppant. This composite effect will enhance the resistance to flow and compression of the integral proppant filling layer. In addition, this type of proppant has an inner core with a higher pliability and has a larger exterior coating; thus, it has a higher resistance to corrosion and does not easily fail during pumping and under higher in-situ stress. Thus deformable proppant can prevent the backflow of proppant after fracturing and in the production period.

#### 7. Ultra-low-density proppant

Ultra-low-density proppant is an elongation of deformable proppant study. At present, the ultra-low-density proppants recommended include mainly two types, that is, the porous ceramsite resin coating (ULW-1.75) and the resin-soaked and -coated walnut shell (ULW-1.25) modified chemically. The relative densities of their particles are respectively 1.75 and 1.25. Ultra-low-density proppant has incomparable superiority, which other proppants lack, in bulk density, relative density, particle strength analysis, particle settlement, flow conductivity, flow test, and so on.

In general, most proppants with a higher density may rapidly settle below the reservoir in the vicinity of the wellbore to form a settled proppant bank during fracturing; thus, the propped fracture length formed is much less than the hydraulically created fracture length. Practice indicates that the ULW-1.25 proppant can be evenly distributed in fracture to prop better fracture, thus improving flow conductivity both laterally and longitudinally. It can better increase productivity by comparison with ordinary proppant.

### Integral Reservoir (or Block) Frac Optimization Design

#### 1. Working principle of integral frac design software system

The integral frac design software system is a powerful means of integral fracturing

optimization design. Its working principle is as follows.

The parameters required by reservoir simulation are first obtained from the reservoir database and well database that have been established. The rational fracture lengths and flow conductivities are determined by taking optimization aim at recovery percent of reserves on the basis of production performances, recovery percents of reserves, and production indices under various simulated fracture lengths, flow conductivities, and types of fractured wells of predetermined flood pattern system. The optimization results are then stored in a fracture optimization parameter database. Or the types and well spacings of well pattern and the corresponding fracture lengths and flow conductivities are determined by taking optimization aim at recovery percent of reserves on the basis of production performances, recovery percent of reserves, and production indices under various simulated fracture lengths, flow conductivities, and types of fractured wells of various flood patterns for reservoirs undeveloped by fracturing, and the optimization results are then stored in a fracture optimization parameter database.

The frac job program is optimized by using a three-dimensional model, two-dimensional model, or horizontal fracture model in combination with the evaluation results of frac job under the support of fracture optimization parameter database, reservoir parameter database, well parameter database, proppant parameter database, fracturing fluid parameter database, and economic evaluation parameter database.

The frac job is appraised and the parameters of fracture and fracturing fluid are determined on the basis of frac job parameters, reservoir parameters, and real-time data, thus providing information for frac design.

#### 2. Description of integral frac design software system

a. Database management module

The databases of the basic reservoir parameters, proppants, fracturing fluids, rock parameters, phase permeability curves, capillary pressure curves, and so on are established in accordance with the features of integral frac design. The databases are correlated with the data of function modules, thus achieving the full sharing of data resources and reducing the tedious data-in operation.

b. Integral fracturing numerical simulation module

Taking an inverted five-spot well pattern, inverted nine-spot well pattern, and rectangular well pattern as objects of study, the frac development indices of various development well patterns in combination with a hydraulically created fracture system are predicted under the conditions of favorable and unfavorable fracture orientations. Taking recovery percent of reserves or recovery factor as the objective, rational fracture length and flow conductivity are determined. For an arbitrary angle of hydraulically created fracture, the method of interpolation is used for calculating frac development indices. In addition, economic evaluation of integral frac development is performed.

c. Frac simulation design module

The pseudo-three-dimensional fracture model and horizontal fracture model are used for simulating the frac job technology under various pumping rates, various types of proppant, various types of fracturing fluid, and various proppant concentrations in order to determine fracture geometry sizes and flow conductivity distribution, and so on. The optimum frac job program and parameters are designed on the basis of reservoir conditions and the requirements of the fracture length and flow conductivity optimized by reservoir frac simulation. In accordance with the characteristics of foam fracturing, the wellhead control parameters and frac job parameter of foam fracturing are designed

in consideration of foamed fracturing fluid rheology, filtration property, pressure field, flow velocity field, proppant migration and distribution, and so on.

d. Individual-well frac program evaluation module

Post-frac production rates under various lengths of hydraulically created fracture and various flow conductivities of fracture are predicted using the numerical simulation technique and an economic evaluation of the individual-well frac program is performed. The net oil increase and net present value, and so on, on various fracturing scales (combination fracture length and fracture flow conductivity) are obtained in order to provide a basis for individual-well frac program optimization design.

e. Postfrac productivity prediction module

The oil and water flow rules are simulated by using the numerical reservoir simulation technique in order to predict postfrac well production performance and the change of water cut, and the effect of hydraulically created fracture length and flow conductivity on production performance.

f. Postfrac pressure incline analysis module

The values of parameters including fracture length, mean fracture width, fracture closure time, fracture fluid loss coefficient, fracturing fluid efficiency, and the rate of pressure decline are obtained by using a three-dimensional pressure incline analysis model.

3. Integral frac optimization design application

The integral frac optimization design for a tract in the Daqing oil region is taken as an example.

a. Well pattern arrangement under favorable orientation of hydraulically created fracture

The results of study indicate that the included angle of  $0^\circ$  between the orientation of hydraulically created fracture and the well array is most favorable when a five-spot well pattern is adopted, while

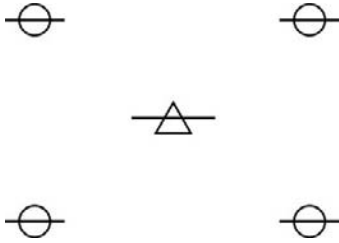


**FIGURE 8-36** Favorable fracture orientation when a five-spot well pattern is adopted.

the included angle of  $45^\circ$  is most favorable when an inverted nine-spot well pattern is adopted (see Figure 8-36 and Figure 8-37).

b. Effect of fracture orientation on production performance under a five-spot well pattern

- (1) In the water-free oil production period or the initial oilfield development period with a water cut lower than 10%, there is no or slight effect of fracture orientation on recovery percent of reserves. With the increase of production time, the water breakthrough of the oil well is becoming faster and sweep efficiency is greatly decreased under the condition of unfavorable fracture orientation.
- (2) Under the condition of unfavorable fracture orientation, the water breakthrough time of a production well is obviously moved up and the water-free recovery factor is greatly decreased.
- (3) Under the condition of favorable fracture orientation, most of the recoverable oil can be produced in the

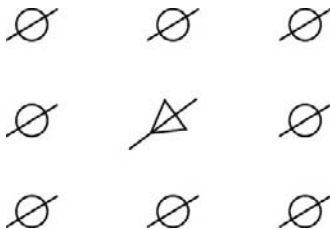


**FIGURE 8-37** Favorable fracture orientation when an inverted nine-spot well pattern is adopted.

water-free production period or low water cut production period; thus, the production effectiveness of a low-permeability oil reservoir is greatly dependent on the length of the water-free production period and the value of water-water recovery factor.

Therefore, for an integral frac vertical-fracture waterflooding low-permeability oil reservoir, the premise of enhancing oil reservoir development effectiveness is the well spacing pattern that makes the fracture have a favorable orientation.

c. Rectangular pattern and inverted nine-spot pattern

Rectangular pattern is an improved well pattern on the basis of an inverted nine-spot pattern in order to improve the development effectiveness of a heterogeneous oil reservoir.

The simulation results indicate that under an inverted nine-spot pattern, the heterogeneity of a reservoir will cause advanced water breakthrough of corner wells, low production rate of central wells, incoordinate production of central wells and corner wells, a great decrease in ultimate recovery factor, a great increase in the water injection pore volumes required under the same recovery percent of reserves, and an unfavorable result for enhancing development effectiveness. They also indicate that under a rectangular pattern and the condition of both homogeneous and heterogeneous reservoirs, the production of both central wells and corner wells can be coordinated, thus increasing oil recovery rate, decreasing water injection pore volumes, and increasing integral ultimate recovery factor. The rectangular pattern of  $L_x/L_y = 2:1$  is favorable for enhancing development effectiveness under the condition of a low degree of heterogeneity, while a rectangular pattern with a higher ratio of length to width can be adopted under the condition of a higher degree of heterogeneity.

d. Parameter optimization of hydraulically created fracture

In order to optimize fracture parameters, factors including oil recovery rate, recovery factor, production effectiveness, equipment capacity, and operation cost, as well as specific conditions of well pattern and reservoir, should be considered. Taking a rectangular pattern with a length-to-width ratio of 2:1 (420 m  $\times$  210 m) and a heterogeneous oil reservoir with  $k_x/k_y = 5$  as an example, the optimization of the fracture penetration coefficients of injection and production wells under a certain fracture flow conductivity ( $30 \mu\text{m}^2 \cdot \text{cm}$ ) is discussed. The step-by-step optimization of fracture penetration coefficients is required. The fracture penetration coefficient of corner well is first optimized under the condition of constant fracture penetration coefficients of injection well and central well. The fracture penetration coefficient of central well is then optimized under the condition of constant fracture penetration coefficients of injection well and corner well. The fracture penetration coefficient of injection well is finally optimized under the condition of constant fracture penetration coefficients of central well and corner well.

- (1) Corner well fracture penetration coefficient optimization. When the fracture penetration coefficients of injection well and central well are respectively 20% and 30%, the simulation results indicate that the optimum fracture penetration coefficient of corner well should be about 10%.
- (2) Center well fracture penetration coefficient optimization. When the fracture penetration coefficients of injection well and corner well are respectively 20% and 10%, the simulation results indicate that the optimum fracture penetration coefficient of central well should be 20%.
- (3) Injection well fracture penetration coefficient optimization. The optimization results of fracture penetration coefficients of corner well and central well are taken, and the effect of injection well fracture penetration coefficient on oil reservoir production performance is simulated and analyzed. The results indicate that the optimum injection well fracture penetration coefficient should be 10%.

### Hydraulic Fracturing Technology

#### 1. Fluid loss reduction technology

For a reservoir in which natural fractures are well developed and serious filtration loss may be generated, realistic measures to reduce filtration loss should be taken in order to ensure a successful frac job and prevent premature sand fallout. At present, the commonly used fluid loss reduction techniques mainly include:

- a. Reducing filtration loss by silt or fine ceramsite. The silt of 100 mesh is added to prepad fluid by a lower proppant concentration in order to plug narrow natural microfractures and open microfractures and force fracturing fluid to extend in artificial principal fracture, thus enhancing fracturing fluid effectiveness and once success ratio.
- b. Reducing filtration loss by slug. There are multiple fractures that extend parallel in the vicinity of the wellbore due to the effect of perforating or natural fracture. In order to solve the problem of multifracture filtration loss, a small quantity of the proppant, which is the same as that in the principal fracture, is added and used as slugs after fracture is generated and before proppant is regularly added. These slugs may plug the natural microfractures, thus increasing the width of artificial principal fracture and attaining the goal of reducing filtration loss.
- c. Reducing filtration loss by combination ceramsite. Ceramsites with different particle diameters are added at different stages

of the operational process and artificial fractures with different widths are respectively packed with the ceramics, thus achieving both filtration loss reduction and rational propping.

- d. Reducing filtration loss by oil-soluble fluid loss additive. Several types of oil-soluble material are mixed in a certain order and a certain proportion, are treated by sulfonation under a certain condition and polymerized, and then form particles with a specific diameter with the aid of specific technology. Appropriate polarity will be generated on the oil-soluble particle surface by using surfactant; thus, the particles can be dispersed in water evenly and stably. The particles are carried to the artificial fracture by water-based prepad fluid, and the temporary plugging of natural fractures is achieved.

## 2. Separate-layer fracturing technology

The separate-layer and selective fracturing techniques are mainly used in multipay oil and gas wells for fracturing of some target or targets. Commonly used techniques include mechanical plugging separate layer fracturing, limited-entry separate-layer fracturing, and ball-sealer selective fracturing.

Ball-sealer selective fracturing has strict demands on the quantity and speed of the ball and the pumping rate during operation and is technologically difficult. Limited-entry fracturing requires achieving the designed proppant distribution on the horizons, which is difficult. Separate layer fracturing with packer is a commonly used fracturing technique at present. It includes the four types: separate layer fracturing with single packer, separate layer fracturing with two packers, separate layer fracturing with bridge plug packer, and separate layer fracturing with sliding sleeves and packers.

A separate layer fracturing with sliding sleeves and packers has no need for moving string, killing, and opening during separate fracturing of multiple layers. It can be used for layer-by-layer fracturing and productivity

testing. It has low formation damage, thus favoring reservoir protection. At most three stages of sliding sleeves are generally used, and four layers are separately fractured once due to the limitation of the inside diameter of the string. If multiple layers are fractured once, the string should be pulled out and changed in order to perform the flowing back and productivity testing of lower horizon.

Separate layer fracturing with sliding sleeves and packers has been widely applied in tight gas reservoirs in western Sichuan, the Daqing Xushen gas field, the coalbed gas reservoir in the Qinshui basin of Shanxi Province, the Bawu gas field of Jiling basin, the Changqin gas field, the Tuba Hongtai gas reservoir, the Zhongyuan Wennan oil field, and so on.

## 3. Fracture height-controlling fracturing technology

At present, fracture height-controlling techniques mainly include:

- a. Artificial restraining barrier technique. An artificial restraining barrier is formed at the top or bottom of the fracture by ascent or sinking type separant, thus increasing the impedance at the tip of fracture, preventing the fluid pressure in fracture from propagating up or down, and controlling the longitudinal extension of fracture.
- b. Variable displacement fracturing technique. The variable displacement fracturing technique can be used for controlling the downward extension of fracture, increasing the length of propped fracture, increasing the proppant-paving concentration in fracture; thus, the effectiveness of stimulation can be effectively increased.
- c. Controlling fracture height by injecting non-proppant slug. Non-proppant liquid slug is injected between prepad fluid and proppant-carrying liquid and plugging particles. Large particles form bridging, while small particles pack the clearance between large particles; thus, an impermeable barrier is formed and fracture height is controlled.

- d. Controlling fracture height by adjusting fracturing fluid density. In order to control the upward extension of fracture, a fracturing fluid with a higher density is adopted, so that fracture is generated downward as far as possible under the action of gravity. Contrarily, if controlling the upward extension of fracture is required, a fracturing fluid with a lower density is used.
  - e. Controlling fracture height by cooling the reservoir. Injecting cold water into a reservoir with a higher temperature makes the reservoir generate thermoelastic stress so that reservoir stress is decreased; thus, fracture height and fracture length are controlled within the range of the reservoir.
4. Formation breakdown condition improving fracturing technology
    - a. Reducing pressure loss during pressure transmission. Reducing the adverse factors that hinder pressure transmission can increase the pressure value that is transmitted to the target, thus increasing the probability of formation breakdown.
    - b. Reducing formation breakdown pressure. The formation breakdown pressure in the vicinity of the wellbore is dependent on in-situ stress and rock properties. In order to reduce formation breakdown pressure, the in-situ stress should be broken. This method is also known as prefrac pretreatment. The relevant measures that are commonly applied at present include acidizing, abrasive perforating, high-energy gas fracturing, and perforating parameter optimization.

used for determining the degree of coincidence between designing and performing and predicting the problems that may be generated. If necessary, the designed parameter values are adjusted. This type of system is an aid to on-site operational decisions.

- b. Fracturing fluid formulation and cross-linking proportion control. Crosslinking proportion should be strictly controlled. An excessively high crosslinker concentration makes gel become brittle or even dehydrated, while an excessively low crosslinker concentration may cause a low proppant-carrying property of fracturing fluid.
- c. Rational proppant concentration change monitoring. The continuity of the change of proppant concentration is very important to the rational distribution of proppant concentration in fracture, that is, the rational distribution of flow conductivity, and should be ensured during operation.
- d. Displacement fluid volume control. The displacement fluid volume near the end of operation should be strictly controlled in accordance with the requirement in design. The displacement fluid is used for displacing the fracture in the vicinity of the wellbore is filled with proppant, thus favoring the flow of oil and gas. Excessive displacement fluid may make proppant enter deep fracture, thus reducing the proppant concentration in the fracture in the vicinity of the wellbore, that is, reducing the flow conductivity of fracture to a great extent.
- e. Flowback time control. The break of fracturing fluid and the closure of fracture should be considered when flowback time is determined. The postfrac flowback of fracturing fluid should be as early as possible. Too long a shut-in time may make the fracture close fully, and the flow may become a pseudoradial flow; thus, production rate may be greatly decreased and the high-yield period may be lost. The forced

### Fracturing Performing and Postfrac Appraisal

1. Frac job quality control
  - a. Real-time monitoring system establishment. A real-time monitoring system is used for on-site real-time monitoring and analysis of operational pressure performance. The measured pressure matching the analog calculation pressure can be

fracture closure technique is often adopted in the field, that is, controlled flowback is promptly taken after fracturing, so that the fracture will rapidly close and effective propping can be achieved to the full extent.

## 2. Postfrac appraisal and analysis

### a. Frac job curve match analysis

The pressure, pumping rate, and proppant concentration vs. time can reflect the real-time extension performance of fracture. The operational net pressure curve can be used for determining the length, width, and height of fracture, fracturing fluid loss coefficient, fracture flow conductivity, and so on, by matching.

### b. Pressure drawdown analysis

Fluid compressibility, fracture extension after closing, three-dimensional fracture extension, and so on are considered for interpreting and analyzing the fracture parameters using fracture pressure at present. The fracture pressure drawdown model of a naturally fractured reservoir is corrected on the basis of the study of a fracturing fluid loss calculation model of a naturally fractured reservoir, thus achieving the fracture pressure drawdown analysis of the naturally fractured reservoir.

### c. Postfrac pressure transient test analysis

The postfrac pressure transient test analysis aims mainly at obtaining the data of propped fracture length, propped fracture flow conductivity, and reservoir permeability; thus, the basic parameters are provided for appraisal of fracturing effectiveness. In accordance with the types of flow, the postfrac pressure transient test of the vertically fractured well with finite flow conductivity after fracturing includes the four flow stages: (1) single linear flow in fracture; and (2) bilinear flow in fracture; (3) single linear flow in formation; (4) pseudoradial flow. A great quantity of software has been developed that can be used for postfrac pressure transient test analysis.

### d. Production history match and inversion by reservoir simulation

On the basis of the related data including the change of postfrac production well production rate with time under a certain static reservoir pressure and a certain flowing pressure, reservoir simulation is used for production history matching; thus, propped fracture flow conductivity or fracture half-length can be obtained by inversion.

## Hydraulic Fracturing for Carbonatite Reservoir

**Difficulties of Hydraulic Fracturing for Carbonatite Reservoir.** In a carbonatite reservoir, natural fractures are well developed. The randomness of natural fracture distribution in the reservoir, the complexity of hydraulically created fracture initiation and extension, and the uncertainty of fracturing fluid loss in pumping operations may seriously affect the effectiveness and aiming of this type of reservoir fracturing design. The difficulties of hydraulic fracturing mainly include:

### 1. Complicated initiation and extension of hydraulically created fracture

In a carbonatite reservoir, fractures and solution cavities often develop, and the reservoir has a high heterogeneity; that is, the distribution of natural fractures and solution cavities is very complicated and spatially random. The existence of natural fractures makes in-situ stress field more complicated. The studies indicate that this type of reservoir can easily generate complicated fractures during fracturing, thus making it difficult to simulate the form in the laboratory and extending the trend of hydraulically created fracture. There has been no perfective simulation software of hydraulically created fracture for naturally fractured reservoirs so far.

### 2. Difficulty in appraising fluid loss during frac job

Due to the existence of inherent natural fractures and fractures that may be opened under the action of external force in a

naturally fractured reservoir, the fluid loss coefficient dynamically changes during operation and is much higher than that of homogeneous media (making an order-of-magnitude increase) under the same conditions, which is an important reason why this type of reservoir has a high proppant plug rate. In addition, the existence of solution cavities in the reservoir may cause an abrupt change of fluid loss during pumping, a great decrease of fracture generation efficiency, and a proppant plug.

3. High proppant plug rate and difficulty in increasing proppant concentration

During fracturing of the reservoir in which natural fractures are well developed, well-head pressure is sensitive to a proppant liquid ratio higher than or equal to 30%. The investigation on the sandfrac of carbonatite reservoirs indicates that the proppant plug rate is generally high and the proppant concentration is difficult to increase.

**Adaptability Analysis of Carbonatite Reservoir Fracturing.** Despite the difficulties of hydraulic fracturing for carbonatite reservoirs, the present fracturing technology has a certain adaptability, and field practice has proven that hydraulic fracturing of carbonatite reservoirs is necessary and feasible.

1. Hydraulic fracturing for carbonatite reservoirs has obvious superiority.

The commonly used acid fracturing technology has played an important promoting part in the effective development of carbonatite oil and gas reservoirs. However, the effective operating distance of acid fracturing in high-temperature carbonatite reservoirs is limited by the rate of reaction between acid and rock and the effective operating distance of fluid loss control; thus, the fractures and solution cavities that are far from the wellbore are difficult to interconnect. Hydraulic fracturing adopts nonreactive working fluid, and the fracture length and proppant distribution are relatively easy to control; thus, propped fracture length, which is much

greater than acid-etched fracture length, can be provided to obtain an obvious increase of productivity.

2. Fracturing practice has proven that sandfrac is feasible for carbonatite reservoirs.

A carbonatite reservoir has fractures that are well developed and high fracturing fluid loss and can easily form multiple fractures during fracturing operation, thus having a higher operating risk. If the difficulties of reservoir stimulation are fully understood and meticulous fracturing design and operation are performed, successful carbonatite reservoir sandfrac can be achieved. Field tests of sandfrac for the Ordovician high-temperature deep reservoir and the Lower Paleozoic dolomite of the Yulin gas field have been done in 20 wells and success has been obtained.

## 8.5 ACIDIZING FOR PUTTING A WELL INTO PRODUCTION

During acidizing, acid liquor is injected into the reservoir to dissolve the mineral components of reservoir rock and the blocking matter caused during drilling, well completion, workover and production, thus improving and increasing reservoir permeability.

### Principle and Classification of Acidizing

#### Classification of Acidizing Technology

1. Acid cleaning

Acid cleaning technology is used for removing acid-soluble scale in wellbore or interconnecting perforations. A small quantity of acid liquor is injected to predetermined sections in order to dissolve the scale on wall or blocking matter in perforations.

2. Matrix acidizing

During matrix acidizing, acid liquor is injected into a near-wellbore reservoir under a pressure lower than formation breakdown pressure to dissolve the particles and blocking matter in pore space, enlarge the pore space, and eliminate the blocking in the

near-wellbore reservoir, thus restoring and increasing reservoir permeability and well productivity.

### 3. Fracture acidizing

During fracture acidizing (also known as acid fracturing), acid liquor is injected into the reservoir under a pressure higher than formation breakdown pressure or natural fracture closure pressure, so that fracture is formed in the reservoir and the rock on the fracture face is unevenly etched by the reaction of acid liquor to the rock on the fracture face, thus forming a groove-shaped or rough fracture. The fracture formed will not be fully closed after the ending of the frac job, and an artificial fracture with a certain size and flow conductivity will be formed; thus, the flow condition of oil and gas will be improved and the productivity of oil and gas wells will be increased.

## Principle of Increasing Productivity by Acidizing

### 1. Principle of increasing productivity by matrix acidizing

The action of matrix acidizing on the increase of productivity mainly includes: (1) acid liquor dissolves the pore wall or natural fracture face, thus increasing pore diameter or extending fracture and increasing the flow capacity of the reservoir; and (2) acid liquor dissolves the blocking matter in perforations and natural fractures, breaks the structure of blocking matter of drilling fluid, cement and rock debris and so on, interconnects flow channels, and removes the effect of blocking matter, thus restoring the original flow capacity of reservoir.

When reservoir fluids (oil, gas, and water) flow radially from the reservoir to the well, the pressure loss is funnel-shaped. During the production of oil and gas, 80% to 90% of the pressure loss is generated in a range of 10 m in the vicinity of the wellbore; thus, increasing near-wellbore flow capacity and decreasing near-wellbore pressure loss can obviously increase oil and gas production

rate under constant producing pressure draw-down. Theoretical analysis indicates that well productivity can be greatly increased by acidizing for a well that is contaminated, whereas it can only be slightly increased by acidizing for a well that has not been contaminated.

### 2. Principle of increasing productivity by fracture acidizing

The fracture face formed by fracturing is unevenly etched by acid liquor during fracture acidizing operations due to the unevenness of the mineral distribution and permeability of reservoir rock. After the fracture acidizing operation is finished, the fracture may not be fully closed under the propping at many points; thus, an artificial fracture with a certain size and flow conductivity is finally formed and reservoir flow capacity.

The principle of increasing productivity by fracture acidizing, which is similar to that of increasing productivity by hydraulic fracturing, mainly includes: (1) increasing the area of oil and gas flow to the well, improving the flow pattern of oil and gas, and increasing the flow capacity in the vicinity of the wellbore; (2) eliminating reservoir contamination in the vicinity of the wellbore; and (3) interconnecting the high-permeability zone, the fracture system at deep reservoirs and the oil and gas zone, which are far from the wellbore.

## Matrix Acidizing for Sandstone Reservoir

Acidizing is one of the main measures for oil and gas well stimulation and water injection well stimulation. Acid liquor can be used for removing contamination in the vicinity of production wells and water injection wells and the blocking matter in pores and fractures or interconnecting and extending the original pores and fractures in the reservoir, thus increasing reservoir permeability and then increasing production well productivity and water injection well injectivity.

### Acid Liquor and Additives

#### 1. Commonly used acid additives

- a. Corrosion inhibitor. It is mainly used for decreasing corroding metallic pipes by acid liquor and decreasing formation damage. The corrosion rate of steel product under the flowing condition of acid liquor is much higher than that under static conditions. It would be best if an appropriate inhibitor could be selected on the basis of the results of a dynamic corrosion test or in full consideration of dynamic corrosion, so that safety may be increased.
- b. Surfactant. It is used for reducing surface tension and interfacial tension and preventing emulsion from forming, leading the reservoir to water wettability and promoting flowing back.
- c. Ferric ion stabilizing agent (chelating agent). It is used for preventing ferric ions and other metallic salts from forming complex ions, thus preventing precipitation from generating.
- d. Cleanup additive. Flowback of spent acid is speeded up with the aid of gas expansion.  $N_2$ , alcohols, and surfactant are commonly used.
- e. Clay stabilizer. It is used for preventing clay minerals from expanding, dispersing, migrating, and blocking pore throats under the action of foreign fluid.
- f. Friction reducer. It is used for reducing the one-way frictional resistance during working fluid flow in wellbore, thus reducing operational pressure.
- g. Temporary plugging agent. It is used for plugging reservoir pores during matrix acidizing and used for plugging perforations or the inlet of fracture during acid fracturing.
- h. Gelling agent. It is the main additive in a gelled acid system.

#### 2. Acid liquor system and adaptability

Sandstone reservoir has a complicated structure and multiple minerals. The acid liquor system that matches reservoir characteristics and the physical properties of rock

should be selected. The commonly used acid liquor systems include:

- a. Conventional mud acid system. It can be used for removing the blocking of sandstone reservoirs in the vicinity of the wellbore.
- b. Retarded fluoboric acid system. It can be used for deep penetration sandstone reservoir acidizing or high-temperature well acidizing. Fluoboric acid has a low hydrolyzing rate, and only the hydrogen fluoride generated by hydrolyzing may react with minerals; thus, it is a retarded acid. The advantages of treating sandstone reservoir by fluoboric acid include:
  - (1) Low rate of reaction of acid to rock, large penetration depth of live acid, and large acid treatment radius.
  - (2) Merging clay into inert particles with other fine particles and consolidating in situ, thus stabilizing clay and preventing formation damage caused by fine particle migration.
  - (3) Inhibiting the swelling of water-sensitive clay minerals.
  - (4) Favoring reservoir protection and keeping a long effective increased productivity period.
- c. Self-generating retarded mud-acid system. Ester is blended with ammonium fluoride at the wellhead and then pumped into reservoir. Ester is decomposed and organic acid is generated. The organic acid then reacts with ammonium fluoride. Theoretically, the acid can be injected into a deep reservoir for acidizing. Different esters can meet the requirements of different reservoir temperatures (40–107°C).
- d. Mud acid system. Hydrochloric acid and ammonium fluorid are injected in sequence. Hydrofluoric acid is generated on clay particle surfaces by using the natural ion exchangeability of clay. Hydrofluoric acid dissolves clay in situ. The essence of the method is that a liquid that can only generate ion exchange with clay is first injected, and a second liquid, which will

react with the first liquid on clay surfaces to generate hydrofluoric acid, is then injected. Multistage repeating may be necessary. The hydrogen fluoride in this system is generated by ion exchange; thus, the relation between reaction rate and reservoir temperature has a lower sensitivity than that of other acid liquor systems. The effective action distance can exceed 2 m. The system can be used for acidizing of the sandstone reservoir with argillaceous cement to remove blocking caused by reservoir clay particle migration and welling or drilling fluid blocking that cannot be fully removed by conventional mud acid.

e. Retarded phosphoric acid system (PPAS). Phosphoric acid has a low ionizability and will have an obvious retarding effectiveness after special additives are added. The combination of PPAS with a high concentration and HCl or HF is particularly suitable for treating a sandstone or limestone reservoir with a high calcic content. This system has good properties, but it has a higher cost than mud acid. It has the following features:

- (1) Retarding the reaction rate of acid, thus increasing the penetration depth of live acid
- (2) Retarding the reaction rate by itself under the calcic condition, ensuring the maximum iron chelating capacity, and having a distinctive siliceous selectivity
- (3) Having a high clay stability and low corrosion rate and water wettability

f. Micella-acid system. It is formulated by adding micella solution into acid. It has properties of both acid and micella solution. Micella and acid will not be mutually dissolved due to the solubilization action of micelle, but micelle is the combination solution, which is necessary for acidizing so that it has a good compatibility with acid and reservoir fluid, thus improving acid liquor property. A micella-acid system is suitable

for removing formation damage caused by inorganic solid blocking including mud, ferrous sulfide, and carbonate, and the organic blocking of hydrocarbons, water block, and drilling fluid. A micella-acid system has the following features:

- (1) Removing organic blocking matter and favoring generating reaction of acid to inorganic blocking matter
  - (2) No emulsification and precipitation when it meets formation water and crude oil, good compatibility
  - (3) The ability to suspend fine particles
  - (4) Low surface tension
- g. Complex acid system. It includes precipitation eliminating acid FD-S and complex acid HBSY. It is suitable for acidizing of oil wells and water injection wells of sandstone and glutenite.

FD-S consists of hydrochloric acid and various additives. It has a strong ability to dissolve calcic, ferruginous, and fluoride precipitation and can eliminate the secondary precipitation formed by acidizing. It has a high corrosion-inhibiting effectiveness and can inhibit clay mineral swelling. It can serve the functions of non-emulsifying, demulsifying, reducing surface tension, preventing ferric ion from precipitating, and so on. It is a new type of anti-contamination dissolvent. The hydrochloric acid in FD-S can be used for removing ferruginous and calcic blocking. The strong water-soluble complex that is formed by FD-S and fluoride ion can eliminate fluoride precipitation.

HBSY consists of hydrochloric acid, hydrofluoric acid, fluoboric acid, and various additives. It has high blocking removing effectiveness and low formation matrix disruption. It not only can remove the blocking in the vicinity of the well and in deep reservoirs, but also can serve the functions of corrosion control, non-emulsifying, demulsifying, reducing surface tension, anti-swelling and stabilizing ferric ion, and so on.

h. Alcoholic mud acid. It is a mixture of mud acid and isopropanol or methanol (up to 50%). It is mainly used for acidizing of low-permeability dry gas reservoir. Alcoholic mud acid diluted with ethanol can reduce the rate of reaction of acid and mineral, thus taking a retarding effect.

This mixture system makes flowback easy when vapor pressure is increased. The reason is that the surface tension of acid is reduced by ethanol and gas permeability is increased due to the decrease in water saturation.

i. Organic mud acid. When mud acid is used, the total acidity may speed up the dissolution of mineral; thus, organic mud acid that can retard the consumption of hydrofluoric acid is adopted. It is prepared by mixing organic acid (generally 9% formic acid used as a substitute for 12% hydrochloric acid) with 3% hydrofluoric acid. Organic mud acid is especially appropriate for high-temperature wells (90–150°C) and can correspondingly decrease the corrosion rate of the pipeline and reduce the risk of forming residue.

### 3. Principles of selecting acid liquor systems

#### a. Mineralogical principle

It mainly includes reservoir sensitivity, reservoir mineral content and distribution, and the diagnosis of formation-damaging matter in accordance with which an acid liquor system is selected. Reservoir sensitivity to acid liquor includes the following various effects that may be generated after rock minerals contact with acid liquor and additives used:

- (1) Disintegration and sloughing of matrix
- (2) Release and migration of fine particles
- (3) Formation of precipitate and blocking
- (4) Change of rock wettability and generation of the Jamin effect
- (5) Removal of blocking of damaging matter

Therefore, when an acid liquor system is selected, laboratory tests and analyses of reservoir compatibility should be

performed in light of the conditions at various operation stages during acidizing. Under the condition of carbonatite reservoir or sandstone reservoir with carbonate mineral content higher than 20%, a hydrochloric acid-based acid liquor system is generally selected in order to avoid the generation of  $\text{CaF}_2$  precipitation due to the reaction of hydrofluoric acid to calcium carbonate. When the carbonate mineral content in the reservoir is lower than 20%, the mud acid that contains hydrofluoric acid or the other systems in which hydrofluoric acid can be generated are adopted.

#### b. Avoiding secondary damage

Because the precipitation of  $\text{CaF}_2$  and  $\text{Fe}^{3+}$  may cause secondary damage, formulation with a low HF content in acidizing fluid with mud acid is stressed. McLeod presented a guide to using acid for sandstone matrix acidizing and recommended special acid liquor formulation for avoiding or retarding precipitation in 1984. On the basis of this, Bertaux presented a decision tree for selecting acid liquor in 1986. The effectiveness of matrix acidizing for undamaged sandstone reservoir is shown in Table 8-25.

#### c. Increasing efficiency of treating fluid

Pre-pad fluid and after-pad fluid can be used for greatly increasing the efficiency of treating fluid; thus, the typical procedure of sandstone acidizing includes pre-pad fluid, host acid liquor, and after-pad fluid.

During sandstone acidizing, hydrochloric acid with a concentration of 8% to 15% is generally used as pre-pad fluid. Aromatic solvent can also be used as pre-pad fluid to remove paraffin and asphalt. In addition, mutual solvent combined with hydrochloric acid or ammonium chloride is often used as pre-pad fluid. After-pad fluid consists of ammonium chloride solution, 5% to 7% hydrochloric acid solution, or diesel oil, and an appropriate quantity of additives including surfactant

**TABLE 8-25 Effectiveness of Matrix Acidizing for Undamaged Sandstone Reservoir**

Effective Action Distance of Acid (m)	Reservoir Productivity after Acidizing		Effective Action Distance of Acid (m)	Reservoir Productivity after Acidizing	
	Undamaged Reservoir Productivity			Undamaged Reservoir Productivity	
0.3048	1.2		0.6096	1.4	
1.2192	1.6		1.8288	1.7	
3.048	1.9		6.096	2.6	
12.192	2.9		18.288	3.3	
30.48	4.1				

(which can reduce interfacial tension and keep reservoir hydrophilicity) or mutual solvent and cleanup additive. In low-pressure wells, nitrogen or liquid nitrogen has been recommended by Gidley for cleaning up.

d. Overcoming shortcomings of conventional mud acid

Conventional mud acid has a short effective action distance during acidizing. In particular, it has a shorter effective action distance at a high temperature, so that restoring productivity by blocking removal using acidizing is difficult to achieve. Mud acid may excessively dissolve the reservoir rock matrix in the vicinity of the wellbore due to its high solvability; thus, formation sloughing and sand production may be caused. During reaction, quartz or clay mineral fines may migrate with acid liquor, so that productivity may be rapidly reduced. Therefore, in addition to appropriate additives, new acid liquor systems such as fluoboric acid, self-generating acid system, organic mud acid, and alcoholic mud acid should be tried.

e. Removing mechanism of damaging

When an acid liquor system is selected, acid-soluble skin damage should be considered (Table 8-26) in the light of different types and degrees of formation damage.

(1) Selecting a mud acid system to dissolve only damaging matter or fine particles

(2) Selecting an acid base suspension system

(3) Selecting a fluoboric acid formulation to dissolve stable damaging matter and mineral fines that are difficult to dissolve. However, the application of this principle presupposes the accurate determination of the type of formation damage

f. Selecting based on reservoir permeability

When an acid liquor system is selected, reservoir permeability should be considered because reservoir permeability affects the type and degree of damage (a high-permeability reservoir can easily be invaded by foreign solid particles or liquid and may have a higher degree of damage) and because reservoir permeability affects the degree of sensitivity of the reservoir to secondary damage (a low-permeability reservoir has small pore throats and has a higher sensitivity to secondary damage). Therefore, the effect of reservoir permeability should be considered when acid liquor and additives are selected.

g. Selecting based on produced fluid

Under some conditions the type of produced fluid may affect the application treating fluid. For gas wells, pure water-based fluid is not used to the full extent and an acid liquor system, which can reduce surface tension, is used. When the physical and chemical properties of formation water or oil are considered, a special

TABLE 8-26 Acid-Soluble Skin Damage

Operation	Mechanism of Damage
Drilling	Invasion of drilling fluid particles Invasion of drilling fluid filtrate
Cementing	Invasion of filtrate (high pH value effect)
Perforating	Perforation zone compaction Formation debris
Production	Organic scale blocking <sup>1</sup> Calcium carbonate Iron scale (change of acid solvability) Fine particle migration
Workover	Invasion of solids Clay swelling and migration
Stimulation	Fine particle release and migration <sup>2</sup> Precipitate generated by reaction of stimulation fluid to formation <sup>3</sup> Damage caused by polymer (fracturing fluid) <sup>4</sup> Change of reservoir wettability <sup>5</sup>

Note:

<sup>1</sup>Only using hydrochloric acid; only using acetic acid; combination formic acid-hydrochloric acid; or substituting hydrochloric acid by EDTA chelating agent.

<sup>2</sup>Alumina silicate mineral (clay, feldspar, smectite); Si (quartz particle).

<sup>3</sup>Including possibly insoluble precipitate.

<sup>4</sup>Using hydrochloric acid.

<sup>5</sup>It is caused by additives, and surfactant is required.

acid liquor compatible with the produced fluid should be adopted.

#### h. Selecting based on well conditions

Reservoir temperature and pressure are the important factors that should be considered during acidizing. High reservoir temperature may reduce the effectiveness of additives including corrosion inhibitor and the rate of reaction of acid to rock, while reservoir pressure may obviously affect the flowback of spent acid. Therefore, an acid liquor system that is appropriate to reservoir temperature and pressure should be selected.

#### 4. Guide to acid liquor selection under conventional sandstone acidizing

The recommended guide to acid liquor selection under conventional sandstone acidizing is shown in Table 8-27.

### Acidizing Technology

#### 1. Temporary plugging acidizing technique

In light of the longitudinal difference in reservoir permeability, the temporary plugging acid first injected into the well enters a high-permeability reservoir, moves to deep reservoirs, and temporarily plugs the reservoir with high oil recovery percent of reserves and high permeability, whereas a reservoir with low permeability still retains fluid entry. This technique is especially appropriate to oil wells with interzonal difference and channels outside casing, or oil wells that cannot adopt mechanical isolation for other reasons. A temporary plugging acid system is oil-soluble and has an automatic plugging removing property.

##### a. Operational procedure

- (1) Displacing a small quantity of standard acid into well
- (2) In light of the fluid receptivity of a high-permeability reservoir, squeezing a certain quantity of standard acid and temporary plugging acid to plug the reservoir with relatively high permeability
- (3) In light of the requirement by a low-permeability reservoir, squeezing a certain quantity of standard acid
- (4) Squeezing displacement fluid under high pressure

##### b. Diverting technique.

- (1) Chemical diverting. Chemicals are used as diverting agent.
- (2) Mechanical diverting. Packer and ball sealer, and so on, are used for plugging high-permeability reservoirs.

##### c. A guide to diverting agent selection is shown in Table 8-28.

#### 2. Foamed acid acidizing technique

Foamed acid is a dispersed system of gas stabilized by a foaming agent in acid solution. The gas phase is air, while the liquid phase can be various acid liquors selected in accordance with the conditions of the oil well.

The two-stage bidirectional foamed acid injection method is adopted. The foamed

TABLE 8-27 Guide to Acid Liquor Selection under Conventional Sandstone Acidizing

Reservoir	Principal Acid	Prepad
HCl solubility > 20%	No HF if possible	5%NH <sub>4</sub> Cl
Calcite or dolomite	15%HCl <sup>1</sup>	5% NH <sub>4</sub> Cl + 3%
Ferric carbonate (magnetite, siderite)	15%HCl + ferric ion stabilizer <sup>1,2</sup>	acetic acid
High-permeability reservoir (>1000 × 10 <sup>-3</sup> μm <sup>2</sup> ) <sup>2,3</sup>	12%HCl + 3%HF	15%HCl
High quartz (>80%), low clay (<5%)	7.5%HCl + 1.5%HF	10%HCl
Medium clay (<5%), low feldspar (<10%)	6.5%HCl + 1%HF	5% ~ 10%HCl
High clay (10%)	13.5%HCl + 1.5%HF	15%HCl
High feldspar (>15%)	9%HCl + 1%HF	10%HCl
High feldspar (>15%), high clay (>10%)	3%HCl + 0.5%HF or 10%	5%HCl or 10%
Ferric chlorite clay (>8%)	acetic acid + 0.5%HF	acetic acid + 0.5%NH <sub>4</sub> Cl
Medium-permeability reservoir (10 × 10 <sup>-3</sup> – 100 × 10 <sup>-3</sup> μm <sup>2</sup> ) <sup>2,3</sup>	6%HCl + 10%HF	10%HCl
High clay (>5% ~ 7%)	9%HCl + 1%HF	10%HCl
Low clay (<5% ~ 7%)	12%HCl + 1.5%HF	10% ~ 15%HCl
High feldspar (>10-15%)	9%HCl + 1%HF	10%HF
High feldspar (10% ~ 15%), high clay (>10%)	3%HCl + 0.5%HF	5%HCl
Ferric chlorite		
Ferric carbonate content (>5% ~ 7%)	10% acetic acid + 0.5%HF	10% acetic acid
	9%HCl + 1%HF	+ 5%NH <sub>4</sub> Cl
	5%HCl + 0.5%HF <sup>6</sup>	10%HCl
		10%HCl
Low-permeability reservoir (1-10 × 10 <sup>-3</sup> μm <sup>2</sup> ) <sup>3,4,5</sup>	First consider hydraulic fracturing	5%HCl
Low clay (<5%), low dissolution by HCl (<10%)	6%HCl + 1.5%HF	5%HCl
High clay (>8% ~ 10%)	3%HCl + 0.5%HF	10% acetic acid
Ferric chlorite (>5%)	10% acetic acid + 0.5%HF	+ 5% NH <sub>4</sub> Cl
High feldspar (>10%)	9%HCl + 1%HF	1%HCl
Very low permeability reservoir (<1 × 10 <sup>-3</sup> μm <sup>2</sup> )	HF should not be used. Matrix acidizing with no HF is used or hydraulic fracture is adopted.	

Note:

<sup>1</sup>The location of carbonate in matrix is very important. The naturally fractured reservoir with high content of calcium carbonate can be treated by HF.

<sup>2</sup>Hydrochloric acid can be partially or fully substituted by acetic acid and formic acid, especially at high temperature (120–150°C).

<sup>3</sup>If there exist Zeotites (>3%), 10% citric acid or other organic acids can be considered to substitute for hydrochloric acid.

<sup>4</sup>Acetic acid or formic acid can be considered to substitute for hydrochloric acid at high temperature (>120°C).

<sup>5</sup>Hydraulic fracturing is preferentially considered to adopt; however, a low-permeability sandstone reservoir with low content of clay mineral can be treated by HF. This is different from conventional thinking.

<sup>6</sup>Permeability < 25 × 10<sup>-3</sup> μm<sup>2</sup>.

fluid is first pumped into the water-bearing formation with a higher permeability to gradually increase fluid flow resistance and generate air-lock effect in throats. Under the superimposed air-lock effect, the foamed acid is then entered in the low-permeability reservoir and reacts with reservoir minerals,

so that more solution channels are formed to remove contamination in the low-permeability reservoir and improve the fluid entry profile. A foamed fluid is finally injected for wellbore unloading and spent acid removing.

a. Principles of selecting wells and reservoirs

**TABLE 8-28** Guide to Diverting Agent Selection

Type	Application	Concentration
Halite (melting point: 800°C)	HCl and non-HF treatment	Perforated completion: 0.7–3 kg/m Openhole completion: 24.4 kg/m <sup>2</sup> reservoir
Benzoic flake (melting point: 122°C)	Gas well, oil well, and water injection well	Perforated completion: 0.7–1.5 kg/m Openhole completion: 12.2 kg/m <sup>2</sup> reservoir
Wax bead (melting point: 66–71°C)	HCl and HF treatment Not used in gas well	Perforated completion: 0.4–1.5 kg/m Openhole completion: 12.2 kg/m <sup>2</sup> reservoir
Oil-soluble resin (melting point: 164°C)	HCl and HF treatment Not used in gas well and salt water injection well	Perforated completion: 2.3–11.4 L 0.5% oil-soluble resin in fluid
Foam	Preferentially used in gas well Higher permeability Increasing viscosity by gelling or emulsifying	Openhole: 5–20 g/t Foam quality: 60% to 80%
Ball sealer	Sinking ball Variable density or floating ball	200% overuse 50% overuse

- (1) Long well section, large thickness, great interzonal difference, and serious heterogeneity
  - (2) Water-sensitive reservoir
  - (3) Contamination and blocking generated during drilling, well completion, and downhole operation
  - (4) Formation pressure coefficient lower than 0.5
  - (5) Deteriorated hole condition by which packer and separate-layer acidizing are not allowed
  - (6) Original permeability higher than  $50 \times 10^{-3} \mu\text{m}^2$
- b. Acid liquor slug formulation
- (1) Foamed prepad fluid. Clean water and foaming agent, and so on.
  - (2) Foamed prepad fluid. 12% to 15% HCl, corrosion inhibitor and foaming agent, and so on.
  - (3) Principal foamed acid. 10% to 12% HCl + 1–3% HF, corrosion inhibitor, chelating agent, clay stabilizing agent, and foaming agent, and so on.
  - (4) After-pad displacing fluid. Hot water and additives.
  - (5) Gasification spent-acid flowback fluid. Hot clean water, sodium carbonate, and corresponding additives.
3. Micellar acid acidizing technique
 

Micellar acid consists of basic acid and micelle agent. Water external micellae can bind the oil phase (insoluble in water) in micellae, thus increasing oil phase solubility. In comparison with conventional acid, micellar acid has merits that include low reaction rate, long effective action time and distance, low surface tension, and high flowback effectiveness. In addition, micellar acid has a high ability to suspend solid particles. The fine particles (insoluble in spent acid) that are released during an acidizing job can be suspended in spent acid by micellar acid under the action of static electricity, thus preventing fine particle migration and settlement that may cause formation damage.
  4. Complex solid acid acidizing technique
 

Inactive nitric acid powder or other solid organic acid is added to conventional acid liquor. After the complex acid system is injected into the reservoir, the nitric acid powder or other solid acid will be gradually

dissolved in reservoir pores; thus, a low pH value can be retained in the reservoir for a longer time and the secondary formation damage caused by acid liquor can be effectively prevented. When oil is used as carrier, the nitric acid powder can be squeezed to a larger radial depth and will be hydrolyzed in a subsequently injected acid solution. The decomposed product ( $\text{HNO}_3^-$ ) will compose an acid mixture together with HCl and HF, and so on. The acid mixture can have a higher ability to dissolve damaging matter, and reservoir permeability can be obviously improved.

When there is blocking matter in deep channels of the reservoir, nitric acid powder is enriched around blocking matter and then dissolved; thus, a higher acid concentration is formed around blocking matter and the ability to dissolve blocking matter is enhanced. For a live acid, its volume should be increased in order to achieve this purpose, whereas using nitric acid powder can reduce live acid volume and then reduce cost.

In addition, inactive nitric acid powder can act as temporary plugging agent or diverting agent during acidizing. During squeezing nitric acid powder, it first enters the high-permeability reservoir, which has low resistance, and piles up to reduce receptivity of the high-permeability reservoir; thus, nitric acid powder can enter a low-permeability reservoir to dissolve the contaminant in a low-permeability reservoir. For a naturally fractured reservoir, this action is even more obvious. Inactive nitric acid powder can be gradually dissolved in the acid solution injected subsequently or in formation water, so that it will not block the flow channels in the reservoir.

#### 5. Heat-gas-acid blocking removal technique

This technique uses acid, heat, gas, and surfactant to generate foamed acid, thus achieving blocking removal.

##### a. Mechanism

- (1) Acidizing action. The active latent acid liquor contained in this system

can remove near-wellbore salt scale blocking to restore reservoir permeability. The complexing agent and the buffer solution with a certain concentration in the system can prevent generating secondary precipitation. The solution rate can be increased by 20% or more in comparison with the mud acid system under the condition of the same concentration.

- (2) Blocking removing action of heat. This system releases a large amount of heat during reaction, thus heating the wellbore and the near-wellbore area and reducing the viscosity of the viscous oil-based matter, including gum, asphaltene, and paraffin, to increase the flowability. In addition, the large amount of high-temperature gas released may enter reservoir pores, shock and disperse bridging matter, and remove flow resistance caused by capillary force. During bleeding, the gas in the reservoir has a high ability to clean up when the gas is migrated toward the wellbore; thus, the oil-based matter dissolves and the spent acid liquor can be carried with foam.
- (3) Action of foam. This system may generate vaporization temperature and form foam by self-reaction. The synergy may increase the penetration depth of live acid in the vicinity of the wellbore, and foam can act as a diverting agent to plug a high-permeability reservoir, thus ensuring uniform acid distribution over all reservoirs.

##### b. Adaptability analysis

- (1) High clay content in the reservoir. This type of reservoir has a high ferric content and is very sensitive to acid and oxygen-containing water. Ferric ion can easily precipitate. This acid liquor system has a complexing agent and a buffering agent with a certain concentration and can retain a certain

- acidity. After reaction time of 4 to 6 hours, the spent acid liquor is flowed back in time. The large amount of gas generated may increase the driving pressure of flowback, thus achieving full flowback. In addition, in order to prevent the rupture of the reservoir pore structure, the latent hydrofluoric acid in the system will be gradually released after the hydrochloric acid pretreating of the reservoir.
- (2) The heat-gas-acid blocking removal injection well stimulation testing of the secondary infill wells in the Taqing Gaotaizi and Xin 13 block indicates that the heat-gas-acid blocking removal adopted after forced flowback can obtain high effectiveness under the conditions of small contamination radius and low degree of damage.
  - (3) For wells that have no or low effectiveness of conventional acidizing but really have formation damage, converted water injection wells, wells in the oil-water transition zone, and wells that may have organic matter blocking, surfactant volume should be increased to increase cleaning efficiency and the volume of additives for generating heat and gas during heat-gas-acid blocking removal should be appropriately increased to further decrease the viscosity of viscous organic matter to increase its flowability. The gas generated can also shock and disperse bridging matter, and the nitrate generated can also take a demulsifying effect to prevent emulsification blocking.
  - (4) For the wells of which water injectivity and water-accepting layers are decreased due to the blocking caused by water pollution during water injection, the requirements of injection allocation can be met by heat-gas-acid blocking removing.
- c. Principles of selecting wells and reservoirs
    - (1) Preferentially selecting high- and mid-permeability reservoirs and wells with high initial water injection rate and rapidly decreased water injection rate
    - (2) Selecting wells and reservoirs that have blocking matter caused during drilling, completion, workover, and production
    - (3) Selecting wells that have low-permeability reservoirs with good connectivity and cannot achieve injection allocation

### Real-Time Monitoring and Effectiveness Appraisal of Acidizing.

Acidizing aims mainly at eliminating near-wellbore contamination and reducing skin factor; thus, the real-time monitoring of acidizing is just tracking the changing process of the simulation well skin factor, understanding and evaluating acid treatment effectiveness in time, and obtaining the optimum final injection-time or real-time steering design during operation.

#### 1. McLeod and Coulter method

McLeod and Coulter considered that during acid treatment, each stage of injection and shutting in is a short well-testing process in 1969. The unsteady pressure response of the reservoir during acid liquor injection is analyzed and explained to determine skin factor and flow conductivity.

Because the changing process during acid treatment cannot be continuously evaluated, skin factor can only be continuously measured during acid treatment (generally before and after acid treatment), and real-time analysis cannot be achieved, this method is rarely applied at present.

#### 2. Paccaloni method

In 1979 Paccaloni presented that the skin factor at a certain time during acid treatment can be calculated by using transient pressure and flow rate values under the condition of single-phase radial horizontal steady-state Darcy flow, as shown in Equation (8-10).

(8-10)

$$p_{wi} - p_e = \frac{141.2q_i B\mu}{Kh} \left( \ln \frac{r_e}{r_w} + S \right)$$

where:  $p_{wi}$  = bottomhole injection pressure, psi;  $p_e$  = reservoir pressure, psi;  $q_i$  = pumping rate, bbl/min;  $B$  = formation volume factor, bbl/bbl;  $\mu$  = viscosity, cp;  $h$  = reservoir thickness, ft;  $r_e$  = reservoir radius, ft;  $r_w$  = wellbore radius, ft;  $S$  = skin factor, dimensionless;  $K$  = permeability,  $10^{-3} \mu\text{m}^2$ .

The damage ratio, which is the ratio of the productivity index under ideal condition ( $S=0$ ) to the actual productivity index under actual condition ( $S \neq 0$ ), is then as shown in Equation (8-11).

(8-11)

$$DR = \frac{PI_{ideal}}{PI_{actual}} = \frac{\ln r_e/r_w + S}{\ln r_e/r_w}$$

Skin factor can be predicted if the formation capacity  $Kh$  is given.

### 3. Prouvost & Economides method

In 1987 Prouvost & Economides presented a method for continuous calculating skin factor during acid treatment, as shown in Equation (8-12). This method is based on the continuous correlation between simulated bottomhole pressure and measured bottomhole pressure.

(8-12)

$$S(t) = S_o + \frac{Kh}{141.2 q(t) B(t) \mu(t)} [p_m(t) - p_s(t, S_o)]$$

where:  $S_o$  = skin factor before acidizing (determined by well test data), dimensionless;  $p_m(t)$ ,  $p_s(t, S_o)$  = measured and simulated bottomhole pressures respectively, psi.

Monitoring procedure: Wellbore fluid is partially or fully displaced into the reservoir by pretreatment fluid under the pumping rate with no fracturing before acidizing.

- a. Pumping off before pretreatment fluid enters the reservoir and recording the change of pressure with time during displacing (duration of 1 hour is generally required) until valuable reservoir data can be obtained by well testing.

- b. Reservoir and well parameters such as formation capacity and skin factor are obtained by pressure drawdown analysis.

### 4. Hill method

The line-source solution of unsteady flow during injection can be obtained using Equation (8-13).

(8-13)

$$\frac{p_e - p_{wf}}{q_N} = m \left[ \sum_{j=1}^N \frac{q_j - q_{j-1}}{q_N} \right] g(t - t_{j-1}) + b$$

where:  $p_{wf}$  = bottomhole flowing pressure, psi;  $q_j$ ,  $q_{j-1}$  = injection rate, bbl/min;  $q_N$  = cumulative injection, bbl;  $t$  = time, min.

Equation (8-13) indicates that when the parameters (especially skin factor) are constant, there is a linear relation between the derivative of injectivity and the stacked time. The slope  $m$  of the straight line is dependent on formation capacity and fluid properties, while the intercept  $b$  of the straight line is dependent on the porosity and permeability of the reservoir, wellbore radius, fluid viscosity, and skin factor. The derivative of injectivity and the stacked time are calculated on the basis of the pressure and pumping rate measured during operation and then graphed in order to determine the skin factors at different times.

### 5. Uses of real-time monitoring technique

In addition to monitoring the change of skin factor during acidizing and judging the effectiveness of acidizing in real time, the uses of the real-time monitoring technique for acidizing also include:

- a. Analyzing the change curve of skin factor and determining the time of pumping off in order to obtain the optimum acidizing effectiveness by the minimum acid volume injected;
- b. Judging the successfulness of the diverting technique when a diverting agent or temporary plugging agent is used in acidizing operation;
- c. Optimizing the acid liquor formulation appropriate to regional features, thus enhancing the directivity of acid liquor;

- d. Analyzing the data obtained during monitoring to optimize acid liquor volume.

The effectiveness of individual-well acidizing is comprehensively evaluated. The effectiveness of an acidized well is predicted and comprehensively evaluated on the basis of the decrease of skin factor. In addition, the flow conductivity of reservoir is analyzed by using pressure draw-down curve, relief time is determined, and the parameters, including valid period, are predicted.

### Matrix Acidizing for Carbonatite Reservoir

During the matrix acidizing of a porous carbonatite reservoir, acid liquor is injected under a pressure lower than formation breakdown pressure to remove formation contaminant and dissolve formation minerals to form solution vugs. During the matrix acidizing of a naturally fractured carbonatite reservoir, acid liquor is injected under a pressure lower than fracture extension pressure to dissolve and interconnect the natural fracture system. Forming solution vugs is characteristic of the matrix acidizing of carbonatite reservoirs. The so-called acid-etched wormhole effect means that the acid liquor as a reactive fluid during flow in porous media dissolves larger pores or natural fractures to form earthworm-shaped holes while extending the principal fracture.

**Chemical Reaction of Acid Liquor to Carbonatite.** Carbonatite is generally classified in accordance with the proportion of calcite to dolomite (Figure 8-38).

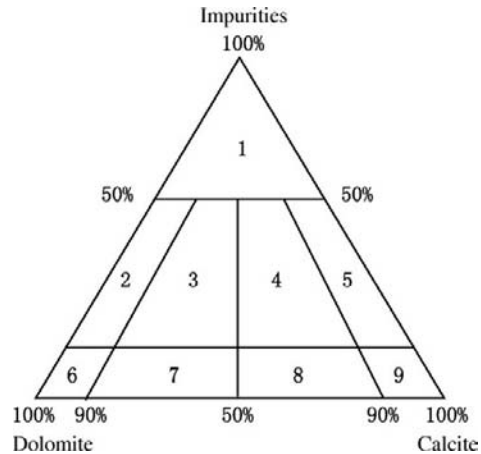


**FIGURE 8-38** Carbonatite mineral classification. 1, non-carbonatite; 2, impure dolomite; 3, impure limy dolomite; 4, impure dolomitic limestone; 5, impure carbonatite; 6, dolomite; 7, limy dolomite; 8, dolomitic limestone; 9, limestone.

1. Properties of reaction of acid liquor to carbonatite
  - a. Reaction of acid liquor to carbonatite

Carbonatite acidizing generally adopts hydrochloric acid. For a well with a temperature higher than 150°C, an organic acid is generally used for reducing the corrosiveness to string and the rate of reaction of acid to rock. The chemical equation of reaction of acid liquor to carbonatite is shown in Table 8-29.

Given the relative molecular masses of reactants and resultants, the acid liquor volume required by dissolving a certain quantity of carbonatite can be determined

**TABLE 8-29** Chemical Equations of Reaction of Acid Liquor to Carbonatite

Acid Liquor	Chemical Reaction Equation
Hydrochloric acid	$\text{CaCO}_3 + 2\text{HCl} \rightarrow \text{CaCl}_2 + \text{H}_2\text{O} + \text{CO}_2\uparrow$
	$\text{CaMg}(\text{CO}_3)_2 + 4\text{HCl} \rightarrow \text{CaCl}_2 + \text{MgCl}_2 + \text{H}_2\text{O} + \text{CO}_2\uparrow$
Formic acid	$\text{CaCO}_3 + 2\text{HCOOH} \rightarrow \text{Ca}(\text{COOH})_2 + \text{H}_2\text{O}\uparrow$
	$\text{CaMg}(\text{CO}_3)_2 + 4\text{COOH} \rightarrow \text{Ca}(\text{HCOOH})_2 + \text{H}_2\text{O} + \text{CO}_2\uparrow$
Acetic acid	$\text{CaCO}_3 + 2\text{CH}(\text{CH}_2\text{COOH}) \rightarrow \text{Ca}(\text{CH}_2\text{COOH})_2 + \text{H}_2\text{O} + \text{CO}_2\uparrow$
	$\text{CaMg}(\text{CO}_3)_2 + 4\text{H}(\text{CH}_2\text{COOH})_2 \rightarrow \text{Ca}(\text{CH}_2\text{COOH})_2 + \text{Mg}(\text{CH}_2\text{COOH})_2 + \text{H}_2\text{O} + \text{CO}_2\uparrow$

**TABLE 8-30** Masses of Components in Reaction of 1 m<sup>3</sup> of Hydrochloric Acid to Carbonatite

Hydrochloric Acid (1 m <sup>3</sup> )	Carbonatite (kg)				Dolomite (kg)			
	CaCO <sub>3</sub>	CaCl <sub>2</sub>	CO <sub>2</sub>	H <sub>2</sub> O	CaCl <sub>2</sub>	MgCl <sub>2</sub>	H <sub>2</sub> O	CO <sub>2</sub>
15%HCl	211	245	97	40	122.4	105.1	35.3	97
20%HCl	437	485	192	79	242.5	208.2	69.9	192.3

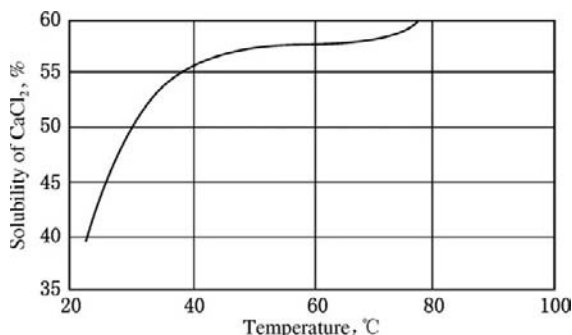
by using the chemical reaction equations shown in Table 8-29. The masses of carbonatite that can be dissolved by 1 m<sup>3</sup> of hydrochloric acid and the masses of resultants are listed in Table 8-30.

- b. Solubilities of resultants of reaction of acid liquor to carbonatite

The main resultants of reaction of acid liquor to carbonatite are CO<sub>2</sub> and CaCl<sub>2</sub>. Under reservoir conditions, CaCl<sub>2</sub> is generally dissolved in spent acid, and CO<sub>2</sub> is generally dissolved in spent acid or appears in spent acid in the form of small bubbles.

- (1) Solubilities of calcium chloride and organic acid salts in water. The curve of solubility of CaCl<sub>2</sub> in water is shown in Figure 8-39. The solubility of organic acid salt in water is shown in Table 8-31.

In addition, the resultants including CaCl<sub>2</sub> will increase the density and viscosity of spent acid. The densities and viscosities of fresh acid are

**FIGURE 8-39** The curve of solubility of CaCl<sub>2</sub> in water.**TABLE 8-31** Solubilities of Organic Acid Salts in Water

Temperature (°C)	Calcium Formate (kg/100 kg H <sub>2</sub> O)	Calcium Acetate (kg/100 kg H <sub>2</sub> O)
10	16.15	37.4
20	—	36.0
30	16.60	34.7
40	—	33.8
50	17.05	33.2
60	17.50	32.7
80	17.95	33.5
90	—	31.1
100	18.40	29.7

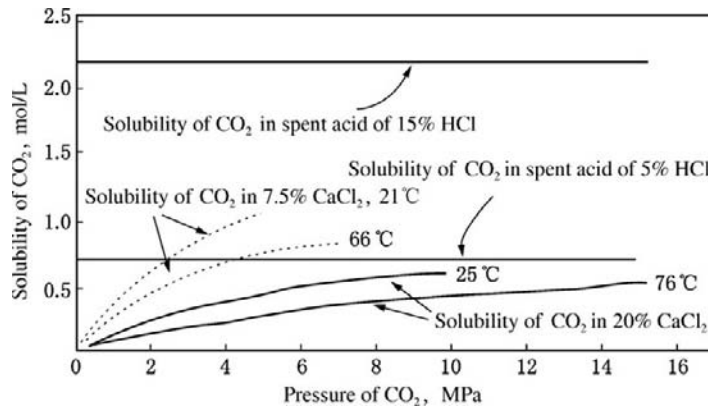
compared with those of spent acid in Table 8-32.

- (2) Solubility of CO<sub>2</sub> in spent acid. The full reaction of 1 m<sup>3</sup> of 15% hydrochloric acid to carbonatite will generate 97 kg of CO<sub>2</sub>, that is, 19.31 m<sup>3</sup> under standard conditions. Obviously, a certain quantity of CO<sub>2</sub> may still be dispersed in spent acid in the form of small bubbles even if it is under the reservoir conditions of 100°C and 50 MPa. This will aid spent acid in flowing back to a certain degree.

The curves of solubilities of CO<sub>2</sub> in the spent acids generated by the reactions of 15% and 5% hydrochloric acids to carbonatite are shown in Figure 8-40. The solid lines are the curves of solubilities of CO<sub>2</sub> in 20%

TABLE 8-32 Physical Properties of Fresh and Spent Acids

Acid Concentration (%)	Acid Density (38°C) ( $10^{-3}$ kg/cm <sup>3</sup> )		Acid Viscosity (25°C) (MPa · s)	
	Fresh Acid	Spent Acid	Fresh Acid	Spent Acid
15	1.07	1.18	1.15	1.7
20	1.10	1.25	1.27	2.4
25	1.12	1.31	1.41	3.8
30	1.15	1.56	1.57	5.9

FIGURE 8-40 Solubilities of CO<sub>2</sub> in spent acid.

CaCl<sub>2</sub> generated by the full reactions of 15% hydrochloric acid to carbonatite at 25°C and 76°C. The dotted lines are the curves of solubilities of CO<sub>2</sub> in 7.5% CaCl<sub>2</sub> generated by the full reactions of 5% hydrochloric acid to carbonatite at 21°C and 66°C.

Obviously, the solubility of CO<sub>2</sub> in spent acid is lower than that in water under the same conditions of temperature and pressure; thus, it is more accurate to adopt the solubility in spent acid.

## 2. Carbonatite acidizing vugular solution forms

The carbonatite acidizing vugular solution forms shown in Figure 8-41 mainly include: (1) surface solution type (acid is consumed on near-wellbore rock wall); (2) conical

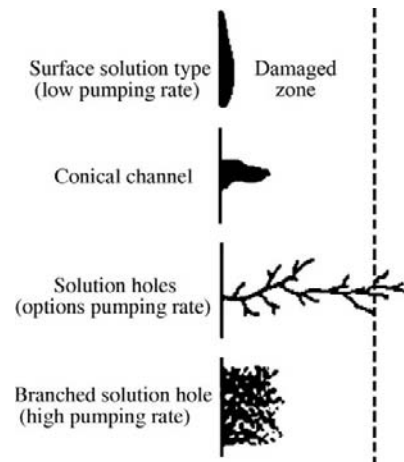


FIGURE 8-41 Carbonatite acidizing solution forms under different pumping rates.

channel (short and larger acid-etched solution hole formed under medium pumping rate); (3) solution holes (one or several main acid-etched solution holes that penetrate into reservoir rock under the condition of uneven reaction of acid to rock are formed, thus breaking through the contaminated zone using less acid volume to obtain a longer acid-etched distance); and (4) branched solution hole (the reaction of acid to rock is relatively even under excessive pumping rate).

Obviously, there is an optimum pumping rate for carbonatite acidizing. Under this condition, the acid liquor volume necessary under a given solution hole penetration depth is minimum. Thus the optimum pumping rate can form a main solution hole and have the maximum acidizing radius.

The skin factors under different solution forms are shown in Figure 8-42. It is indicated that under the same acid liquor volume, the formation of main solution hole will minimize skin factor.

**Optimization Design Technique for Carbonatite Acidizing.** After an acid liquor system is determined, pumping rate and acid liquor volume should be optimized in design and the skin factor and stimulation ratio after acidizing should be predicted.

1. Pumping rate

a. Optimum pumping rate, as shown in Equation (8-14):

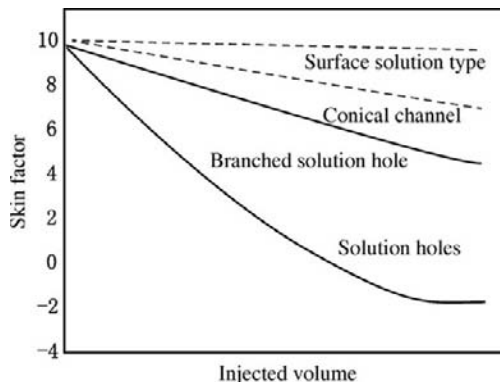


FIGURE 8-42 Skin factors under different solution forms.

(8-14)

$$q_{OP} = 1.29 \times 10^{-3} \frac{\pi r h A_T^{2/3}}{K \cdot K_f C_o^{m-1}}$$

where:  $q_{OP}$  = optimum pumping rate,  $m^3/min$ ;  $A_T$  = maximum primary cross-section area (determined by mercury pore intrusion test),  $cm^2$ ;  $K$  = original permeability,  $10^{-3} \mu m^2$ ;  $K_f$  = reaction rate constant;  $C_o$  = acid liquor concentration,  $mol/L$ ;  $m$  = reaction order;  $r$  = solution hole penetration distance,  $m$ ;  $h$  = treated interval thickness,  $m$ .

b. Maximum pumping rate, as shown in Equation (8-15):

(8-15)

$$q_{max} = \frac{120\pi K h (p_{wf} - p_e)}{\mu_f \left( \ln \frac{r_e}{r_w} - \frac{3}{4} \right)}$$

where:  $q_{max}$  = maximum pumping rate,  $m^3/min$ ;  $K$  = reservoir permeability,  $10^{-3} \mu m^2$ ;  $h$  = treated interval thickness,  $m$ ;  $p_{wf}$  = maximum bottomhole pressure with no formation breakdown,  $Pa$ ;  $p_e$  = reservoir pressure,  $Pa$ ;  $\mu_f$  = reservoir fluid viscosity,  $MPa \cdot s$ ;  $r_w$  = wellbore radius,  $m$ ;  $r_e$  = drainage radius,  $m$ .

Equivalent radius, as follows:

$$r_w' = r_w \exp(-S)$$

2. Solution hole length, as shown in Equations (8-16) and (8-17):

(8-16)

$$r_A = n_f b \frac{V_A X}{2(1 - \Phi)\pi h} N_{pe}^{-1/3} + r_w^{n_f}$$

(8-17)

$$N_{pe} = \frac{q}{D_e h}$$

where:  $n_f$  = fractured dimensions ( $n_f = 1.67$ ;  $b = 1.7 \times 10^4$ );  $V_A$  = injected acid liquor volume,  $m^3$ ;  $X$  = acid liquor solvability;  $D_e$  = acid liquor mass transfer coefficient,  $m^2/s$ ;  $r_w$  = wellbore radius,  $m$ ;  $q$  = pumping rate,  $m^3/s$ ;  $h$  = treated interval thickness,  $m$ .

3. Skin factor, as shown in Equation (8-18):

(8-18)

$$S_a = -\ln \frac{r_A}{r_w}$$

where:  $r_A$  = solution hole radius, m;  $r_w$  = wellbore radius, m.

4. Stimulation ratio after acidizing, as shown in Equation (8-19):

(8-19)

$$\frac{J_s}{J_d} = \frac{\ln \frac{r_e}{r_w} - 0.75}{\ln \frac{r_e}{r_w} - 0.75 + S_a}$$

## Acid Fracturing for Carbonatite Reservoir

### Acid-Rock Reaction Kinetics

1. Acid-rock chemical reaction mechanism

The reaction of acid liquor to carbonatite is a multiphase reaction that is only generated on an acid liquor–rock solid interface (Figure 8-43). The steps of the reaction of acid liquor to carbonatite during acid fracturing include:

- Transferring the  $H^+$  in acid liquor to the carbonatite surface;
- Reacting of  $H^+$  to carbonatite on rock surface;
- Resultants ( $Ca^{2+}$ ,  $Mg^{2+}$ , and  $CO_2$  bubbles) leave the carbonatite surface.

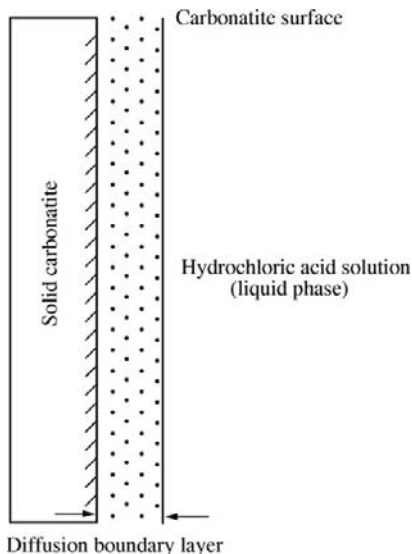


FIGURE 8-43 Acid-rock reaction system.

The reaction of  $H^+$  to carbonatite on rock surface is called surface reaction. A limestone reservoir has a high surface reaction, while a dolomite reservoir has a much lower surface reaction rate.

The slowest step may affect the reaction rate of the system. Limestone has slow transfer of  $H^+$  to carbonatite surface; thus, the acid-rock reaction kinetics of limestone is mass transfer control kinetics. For dolomite, the acid-rock reaction is mainly controlled by surface reaction, and the acid-rock reaction kinetics is surface reaction control kinetics when the fracture wall face temperature is lower than  $65^\circ C$ , while the acid-rock reaction is mainly controlled by mass transfer (the reaction rate is about the same as that of limestone) and the acid-rock reaction kinetics is mass transfer control kinetics when the fracture wall face temperature is higher than  $93^\circ C$ . When the temperature is between  $65^\circ C$  and  $93^\circ C$ , the acid-rock reaction is jointly controlled by both surface reaction and mass transfer.

2. Acid-rock reaction rate

Acid-rock reaction rate is defined as the decrease of acid concentration in unit time and is mainly dependent on  $H^+$  mass transfer rate. The formula of the relationship between the acid-rock reaction rate and the ion concentration gradient in the diffusion boundary layer can be derived by using Fick's law, which shows ion mass transfer rate. The formula is as follows.

(8-20)

$$-\frac{\partial c}{\partial t} = kC^n = D_e \cdot \frac{s}{V} \cdot \frac{\partial c}{\partial y}$$

where:  $\frac{\partial c}{\partial t}$  = transient acid-rock reaction rate, mol/L · s;  $n$  = reaction order;  $k$  = reaction rate constant;  $c$  = acid liquor concentration, mol/L;  $\frac{\partial c}{\partial y}$  = acid liquor concentration gradient in the direction perpendicular to rock face in diffusion boundary layer, mol/L · cm;  $D_e$  =  $H^+$  mass transfer coefficient,  $cm^2$ ;  $s$  = acid-rock reaction contact area,  $cm^2$ ;  $V$  = acid liquor volume that contacts rock face, L.

### 3. Kinetic equations of acid-rock reaction

Kinetic equations of surface reaction and system reaction can be established by using the mass action law, as shown in Equations (8-21), (8-22), and (8-23).

(8-21)

$$J_i = k_s C_s^{n_s} (1 - \Phi)$$

(8-22)

$$J = kC^n$$

(8-23)

$$k = k^0 \exp\left[-\frac{E}{R(T+273)}\right]$$

where:  $J_i$ ,  $J$  = reaction rate,  $\text{mol}/\text{cm}^2 \cdot \text{s}$ ;  $k_s$ ,  $k$  = surface and system acid-rock reaction rate constants;  $k^0$  = frequency factor;  $n_s$ ,  $n$  = surface and system reaction orders, dimensionless;  $\Phi$  = rock porosity, dimensionless;  $T$  = temperature,  $^{\circ}\text{C}$ ;  $E$  = reaction activation energy,  $\text{kcal}/\text{md}$ .

A series of  $C$  and  $T$  values can be measured by using a rotary disc tester and the relation curves are obtained. Acid-rock reaction rate is determined by the differential method. The  $n$  and  $k$  values can be determined by regression analysis. The  $k$  values at different temperatures are measured. The  $E$  and  $k^0$  values can be determined by drawing or regression analysis.

The kinetic equations of reaction of weak acid to carbonate mineral is shown in Equation (8-24).

(8-24)

$$J_{\text{weak acid}} = kK_d^{n/2} C_{\text{weak acid}}^{n/2}$$

where:  $K_d$  = equilibrium constant of weak acid;  $k$  = reaction rate constant.

### 4. Effective $\text{H}^+$ mass transfer coefficient

a. Factors that affect effective  $\text{H}^+$  mass transfer coefficient

The effective  $\text{H}^+$  mass transfer coefficient will decrease with the increase of acid liquor concentration and will increase with the increase of temperature. It is

decreased in consideration of spent acid and common-ion effect. During an acid fracturing operation, the acid liquor flow rate increases and the effective  $\text{H}^+$  mass transfer coefficient also increases. Therefore, a wider fracture is required to be formed during acid fracturing. Lower effective  $\text{H}^+$  mass transfer coefficient, higher pumping rate, and filtration loss as low as possible can obtain a long acid-etched fracture.

b. Method for measuring effective  $\text{H}^+$  mass transfer coefficient  $D_e$

The analytic solution of  $D_e$ , which is obtained by rotary disc testing, is shown in Equations (8-25) and (8-26).

(8-25)

$$D_e = (1.6129 \nu^{1/6} \cdot \omega^{-1/2} \cdot C_t^{-1} \cdot J)^{3/2}$$

(8-26)

$$R_e = \omega \cdot R^2 / \nu$$

where:  $C_t$  = acid liquor concentration at time  $t$ ,  $\text{mol}/\text{L}$ ;  $\omega$  = angular velocity,  $\text{s}^{-1}$ ;  $\nu$  = kinematic viscosity of acid liquor,  $\text{cm}^2/\text{s}$ ;  $J$  = reaction rate coefficient,  $\text{mol}/\text{cm}^2 \cdot \text{s}$ ;  $R_e$  = rotary Reynolds number;  $R$  = disc radius,  $\text{cm}$ .

The values of  $J$ ,  $\nu$ ,  $\omega$ , and  $C$  are measured under given  $R$  during testing.  $R_e$  and  $D_e$  values are calculated and the  $R_e$ - $D_e$  relation curve is drawn.

Because of the complicated surface reaction of hydrochloric acid to dolomite, the  $D_e$  value is determined using the numerical method.

5. Factors that affect the acid-fracturing effectiveness of a carbonatite reservoir

The effectiveness of acid fracturing for a carbonatite reservoir is dependent on the effective length of fracture created by acid fracturing and the flow conductivity of acid-etched fracture after acid fracturing. Effective fracture length depends on the acid liquor filtration property, acid-rock reaction rate, the acid liquor flow velocity in fracture, and the type of acid liquor. The flow conductivity of

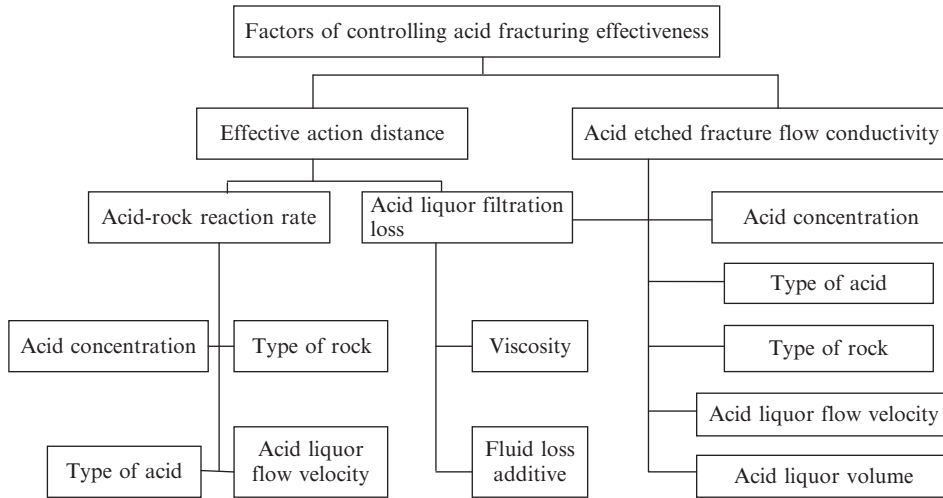


FIGURE 8-44 Main factors of controlling acid fracturing effectiveness.

acid-etched fracture depends on closure, acid solvability, the etched form of acid-rock reaction, the absolute quantity of rock dissolved by acid, and so on. Thus, acid fracturing for carbonatite reservoirs aims mainly at obtaining greater acid-etched fracture length and higher acid-etched fracture flow conductivity. The main factors of controlling acid fracturing effectiveness are shown in Figure 8-44.

**Acid Liquor Filtration Loss during Acid Fracturing.** The classical theory of acid liquor filtration loss during acid fracturing considers that acid liquor may form cake on the fracture wall face and filtration loss is controlled by cake zone, invasion zone, and reservoir fluid compressibility (Figure 8-45).

During acid fracturing, acid liquor may penetrate through the cake zone and act directly on rock to form acid-etched wormholes at the fracture wall face, thus causing a large quantity of acid liquor loss under the common action of both matrix and wormhole filtrations of acid liquor during acid fracturing and thus greatly reducing the effective penetration distance of acid liquor. Therefore, the acid liquor loss during acid fracturing consists of filtration loss from fracture wall face to matrix and fluid loss through acid-etched wormholes (Figure 8-46).

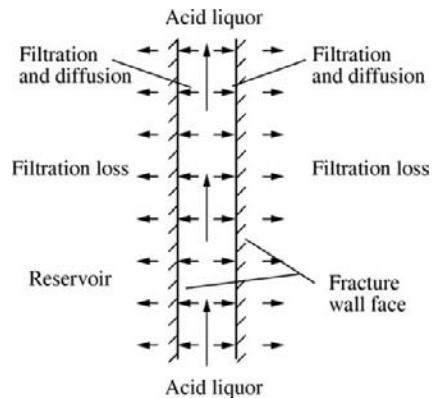


FIGURE 8-45 Classic acidfrac acid liquor filtration loss.

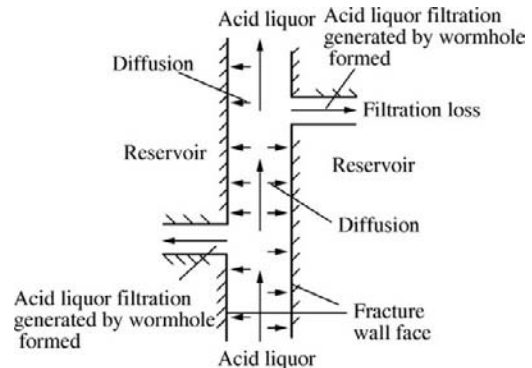
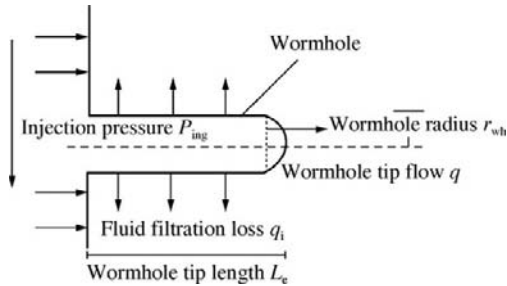


FIGURE 8-46 Actual acid liquor filtration loss during acid fracturing.



**FIGURE 8-47** Acid liquor filtration loss in an acid-etched wormhole.

The fluid loss through acid-etched wormholes consists of the fluid loss generated by the volumetric extension of acid-etched wormholes and the filtration loss through wormhole wall faces and wormhole tips (Figure 8-47).

Acid liquor filtration loss is mainly dependent on acid liquor viscosity and acid-etched wormhole extension velocity. Acid liquor viscosity is mainly affected by the temperatures in fracture and wormholes. Thus the formation of acid-etched wormholes is affected by acid liquor properties, reservoir properties, operational parameters, and so on.

**Acid-Etched Fracture Flow Conductivity.** Acid-etched fracture flow conductivity is the product of acid-etched fracture permeability

and acid-etched fracture width. In an acid-etched fracture flow conductivity test, the change of acid-etched fracture flow conductivity with closure pressure is measured by using a parallel plate core under conditions of simulated reservoir temperature and pressure. Acid-etched fracture flow conductivity is a function of reservoir rock embedment strength, closure pressure, acid etching rate, the irregularity of acid etching along fracture, and acid liquor filtration loss.

1. Effect of closure pressure on acid-etched fracture flow conductivity

With the increase of reservoir closure pressure, the acid-etched fracture flow conductivity will be rapidly decreased. Figure 8-48 shows the results of acid-etched fracture flow conductivity tests for a carbonatite reservoir in China, that is, the results of the multistage acid fracturing closure acidizing tests by using different acid liquor systems under different simulated flow rates. After the closure pressure increases to 40 MPa, the acid-etched fracture flow conductivity can be increased in varying degrees by using closure acidizing.

2. Effect of type of acid liquor on acid-etched fracture flow conductivity

Under reservoir conditions, the acid-etched fracture flow conductivity of conventional

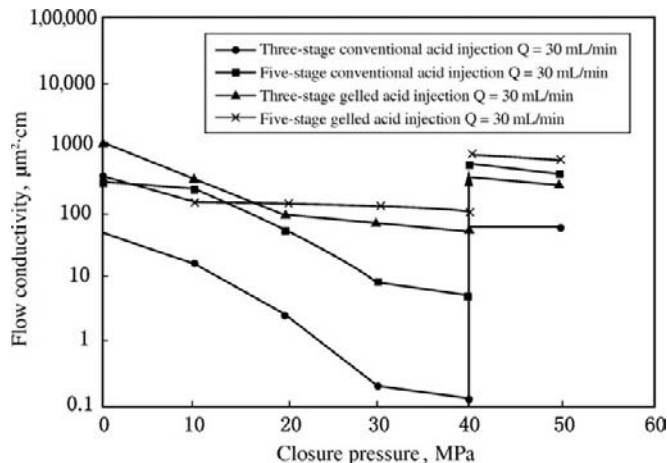


**FIGURE 8-48** Multistage acid-injection acid-etched fracture flow conductivities under acid fracturing.

acid is much lower than that of gelled acid because conventional acid has even etching on fracture wall face while gelled acid has uneven etching.

3. Effect of type of acid fracturing technology on acid-etched fracture flow conductivity

Viscous prepad fluid is injected before acid liquor is injected. The viscous fingering of subsequent acid liquor will increase the degree of uneven etching. The multistage injection acidfrac technology may further intensify the uneven etching at an acid-etched fracture wall face. Thus an acid-etched channel with high flow conductivity may be formed. The test results indicate that multiple stages are more favorable. However, excessive stages may possibly generate operational difficulties.

4. Effect of pumping rate on acid-etched fracture flow conductivity

A high pumping rate may form high-flow conductivity of acid-etched fracture under the conditions of same scale and same stages.

5. Effect of closure acidizing on acid-etched fracture flow conductivity

The acid-etched fracture flow conductivity can be greatly increased by closure acidizing. With the further increase of closure pressure, the acid-etched fracture flow conductivity will decrease by a small margin.

**Commonly Used Acid Liquor Systems and Properties.** The working fluid system during acid fracturing includes prepad fluid and acid liquor. The prepad fluid should have good temperature tolerance and shear-resisting property; good friction-reducing property and filtration-reducing property; low residue content after hydration and good compatibility between reservoir fluid and acid liquor; and low formation damage. Acid liquor should have good filtration-reducing property and retarding property; good corrosion-inhibiting property at high temperature; low friction resistance, low formation damage, and so on.

1. Conventional hydrochloric acid system

A conventional hydrochloric acid system consists of conventional hydrochloric acid and corresponding additives. It has high

solubility and high reaction rate. It is mainly used for carbonatite reservoir matrix acidizing and also used as closure system in the closure acidizing technology. The typical formulation includes: 15% to 28% HCl, 2% to 3% corrosion inhibitor, 0.5% to 1% cleanup additive, 1% to 2% ferric ion stabilizing agent, 0.5% to 1% demulsifying agent, and 0.5% to 1% anti-scum agent.

2. Viscous acid (gelled acid) system

Viscous acid is formulated with conventional acid liquor and a certain quantity of thickening agent which makes viscosity increase to 10–30 MPa · s. The optimum viscosity of viscous acid is generally about 20 MPa · s. The spent acid viscosity for flow-back should be generally between 5 and 10 MPa · s; thus, the spent acid can easily flow back and can also carry solid particles in reservoir fracture after reaction. In addition, viscous acid has a lower friction resistance (generally 30% of clear water friction resistance), thus favoring the increase of pumping rate. The difficulty of on-site application of viscous acid is that it should have a higher thermal stability, low fresh acid visbreaking rate, and low spent acid viscosity. The typical formulation includes: 15% to 28% HCl, 8% to 10% thickening agent (aqueous solution) or 0.6% to 1.0% thickening agent (powder), 2% to 3% corrosion inhibitor, 0.5% to 1.0% cleanup additive, 1% to 2% ferric ion stabilizing agent, 0.5% to 1.0% demulsifying agent, and 0.5% to 1.0% anti-scum agent.

3. Low-polymer high-viscosity gelled acid

A new type of high-temperature-resistant gelling agent and auxiliary additives are added into acid liquor to decrease the polymer content in acid liquor from 0.8% to 0.5%, to increase acid liquor viscosity at high temperature, to decrease acid-rock reaction rate, to decrease acid liquor filtration, and to increase live acid liquor penetration depth.

4. Organic acid system

Formic acid and acetic acid are commonly used organic acids. They have low corrosiveness and low reaction rate and are mainly

suitable for the acid-fracturing treatment of a high-temperature carbonatite reservoir ( $\geq 120^{\circ}\text{C}$ ). The typical formulation includes: 9%  $\text{HCOOH}$  (10%  $\text{CH}_3\text{COOH}$ ), 2% to 3% corrosion inhibitor, 0.5% to 1% cleanup additive, 1% to 2% ferric ion stabilizing agent, 0.5% to 1% demulsifying agent, and 0.5% to 1% anti-scum agent.

#### 5. Foamed acid system

A foamed acid system is appropriate for low-pressure low-permeability carbonatite oil and gas reservoirs and water-sensitive gas reservoirs. A surfactant used as foaming agent and liquid nitrogen are added into acid liquor; thus, the foamed acid system in which acid is continuous phase and gas bubble is dispersed phase is formed. The gas phase volume percentage in total foam volume in the system is known as foam quality. Foamed acid systems can be divided into three types: (1) energized, in which the foam quality is equal to or lower than 52%; (2) foam, in which the foam quality is 52% to 90%; and (3) atomized, in which the foam quality is higher than 90%. The foam quality of the foamed acid used in the field is about 70%; thus, foamed acid has low filtration, good retarding effectiveness, low formation damage, and easy flowback.

#### 6. Emulsified acid system

An emulsified acid system is a dispersed system that consists of two mutually insoluble liquids, that is, crude oil and acid liquor. In order to decrease emulsified acid viscosity, diesel oil, kerosene, and gasoline are added into crude oil, or diesel oil and kerosene are directly used as external phase. The oil-external emulsified acid is predominant. The volumetric ratio of oil phase to acid phase is generally 30:70. The merits of emulsified acid include low reaction rate, long acid-etched fracture, low filtration, and high fracture-generating ability. The demerits of emulsified acid include high friction resistance, which is generally 80% to 150% of that of clear water, a high degree of difficulty to formulate, and low emplacement stability. It is more difficult to use emulsified acid in deep

wells and low-permeability and low-pressure reservoirs. Emulsifying agents that are the main additives of emulsified acid include oil-based and water-based emulsifying agents. Emulsified acid formulated with an emulsifying agent will not be liberated at atmospheric temperature within 48 hours, and the acid liberation rate at  $90^{\circ}\text{C}$  within 1 hour is lower than 3%. The acid liquor viscosity is equal to or higher than  $40\text{ MPa}\cdot\text{S}$  at atmospheric temperature. The typical formulation includes: (1) oil phase: 30% light oil or diesel oil (volumetric ratio), 2% to 3% emulsifying agent and 2% friction reducing agent, and (2) acid phase: 60% to 61%  $\text{HCl}$  (31% industrial hydrochloric acid), 2% to 3% corrosion inhibitor, 2% ferric ion stabilizing agent, and 1% cleanup additive.

#### 7. Surfactant retarded acid

A retarding mechanism includes: (1) adsorption film is formed on rock surface due to the adsorption of surfactant molecules on rock surface, thus decreasing the rate of reaction of  $\text{H}^+$  to rock surface, and (2) an elastic glue crumb diaphragm is formed on the rock-acid liquor interface due to generating acid-rock resultant, thus retaining further the diffusion of  $\text{H}^+$  to rock, decreasing the acid-rock reaction rate, and achieving diverting acidizing. It is also known as surfactant self-diversion acid. This acid liquor system has the following advantages:

- a. No high polymer in acid liquor system, no residue, and low formation damage
- b. High acid liquor viscosity (30–65  $\text{MPa}\cdot\text{S}$  depending on different requirements)
- c. Low reaction rate, good retarding property of acid liquor
- d. Low acid liquor friction resistance, which allows high pumping rate and pressure
- e. Low spent acid viscosity, which makes spent acid easy to flow back

The typical formulation includes: 20%  $\text{HCl}$ , 1.0% surfactant, 2.0% high-temperature corrosion inhibitor, 1.0% high-temperature ferric ion stabilizing agent, and 0.4% to 1.0% extending agent.

### 8. Controlled fluid loss acid (underground crosslinked acid)

Controlled fluid loss acid is crosslinked with  $\text{Fe}^{3+}$  under a lower acid concentration. Crosslinking is started when the pH value is 1.1 and the acid is fully crosslinked when the pH value is 2.5. The viscosity is up to 1000–10,000  $\text{MPa} \cdot \text{S}$  at 100°F.  $\text{Fe}^{3+}$  may be reduced into  $\text{Fe}^{2+}$  by adding activity reductant (pH range of 2.5–3.5).

Underground crosslinked acid has only an initial viscosity of 20  $\text{MPa} \cdot \text{S}$ . After it enters the reservoir, crosslinking is generated with acid-rock reaction and the change of pH value (3–4). After it is crosslinked, the viscosity is greatly increased to about 1000  $\text{MPa} \cdot \text{S}$ . When the pH value is higher than 4, acid liquor viscosity is decreased; thus, the spent acid can be smoothly flowed back.

The merits are that it can prevent acid liquor from filtrating into vugs and natural fractures to form long acid-etched fracture and that the spent acid is easy to flow back, while the demerits include formulating difficulty, high cost, and the unknown conditions of crosslinking and breaking under reservoir conditions.

## Acid Fracturing Technology

### 1. Viscous acid (gelled acid) acidfrac technology

Viscous acid acidfrac technology uses viscous acid to directly fracture the reservoir and form acid-etched fracture with a certain length and flow conductivity. The merits include: low acid liquor friction resistance, which allows injecting at high pumping rate; good retarding effectiveness and long effective action distance greater than that of conventional acid fracturing; and a certain spent acid viscosity, which makes spent acid easily carry solids during flowback. The demerits include high cost and possible secondary formation damage because high molecular material enters the reservoir. It is suitable for high- and medium-permeability (and even low-permeability) reservoirs with natural fractures and is especially suitable for carbonatite in deep and superdeep wells.

### 2. Emulsified acid acidfrac technology

The emulsified acid acidfrac technology uses emulsified acid to directly fracture the reservoir and form acid-etched fracture. The merits include good high-temperature-retarding property of acid liquor, long effective acid-etched fracture, favorable high-temperature corrosion inhibition, and low formation damage. The demerits include: (1) high operational friction resistance, which is generally 80% to 150% of clear water friction resistance and (2) flow conductivity lower than that of viscous acid acidfrac, the problem of spent acid emulsification, and higher cost. It is suitable for the stimulation of a low-permeability carbonatite reservoir. For a superdeep well, this technique is difficult for on-site application due to high friction resistance. It is generally used in combination with viscous acid acidfrac technology.

### 3. Prepad acidfrac technology

A viscous nonreactive prepad is first used to fracture the reservoir and form artificial fracture, and acid liquor is then injected to dissolve and corrode the fracture, thus forming an unevenly etched fracture with a higher flow conductivity. The main function of prepad is to initiate cracking and generate fracture, to decrease fracture temperature and reduce filtration loss. The apparent viscosity of prepad is several dozen to several hundred times that of conventional acid liquor. When acid liquor enters fracture, the acid liquor, which has a lower viscosity in comparison with that of prepad, will form viscous fingering in viscous prepad, thus favoring forming unevenly etched grooves and then forming a longer effective acid-etched fracture.

### 4. Multistage injection acidfrac technology

Prepad is first injected to generate fracture, and then acid liquor and prepad slugs are alternately injected. Acid liquor can be conventional acid, viscous acid, or emulsified acid. Hydrochloric acid with a certain concentration is then injected during the closure of fracture to dissolve the fracture wall face

and form acid-etched fracture with a high flow conductivity, thus achieving an increase in productivity. The merits include: (1) the multistage prepad slugs can effectively plug the acid-etched vugs formed on the fracture wall face to effectively reduce acid liquor filtration loss; (2) viscous fingering due to the viscosity difference may form an unevenly etched shape at the fracture wall face, thus increasing the flow conductivity of acid-etched fracture; and (3) a great quantity of prepad fluid and acid liquor injected can effectively reduce wellbore and reservoir temperatures, thus reducing the acid-rock reaction rate and increasing the effective action distance. This technique is often used in combination with closure acidizing technology. It is suitable for the stimulation of low-permeability reservoirs and reservoirs with high filtration loss.

#### 5. Foamed acid acidfrac technology

Foamed acid is formed by adding a gas ( $N_2$  or  $CO_2$ ) and then a foaming agent into hydrochloric acid. The contents of gas, acid liquor, and surfactant are respectively 65% to 85%, 15% to 35%, and 0.5% to 1%. The merits include: low acid-rock reaction rate; low formation damage to water-sensitive reservoir; high viscosity, which makes insoluble particles easy to suspend; and low acid liquor filtration loss, which may increase effective acid-etched fracture length. The demerits include: high requirements for acidfrac equipment, high operating pressure, high cost, and use limited to shallow and medium-depth wells.

#### 6. Closure acidizing technology

After the closure of the fracture formed during acidfrac, an acid liquor is injected under a low pumping rate and pressure lower than fracture extension pressure in accordance with the minimum resistance principle, which is followed by acid liquor flow, thus further deepening the acid-etched grooves that have been formed and further increasing the flow conductivity of acid-etched fracture in the vicinity of the wellbore. This technology is

often used in combination with other acidfrac technology to form a combined technology such as viscous acid acidfrac fracture closure acidizing technology and multistage injection acidfrac fracture closure acidizing technology, so that long effective acid-etched fracture and high near-wellbore fracture flow conductivity can be obtained and a high effectiveness of increasing productivity can be achieved.

**Acidfrac Design Model in Consideration of Acid-Etched Wormholes.** Acidfrac design models mainly include a wellbore temperature field model, working fluid filtration loss calculation model, fracture geometry calculation model, and acid-rock reaction model, in which acid liquor filtration loss and acid-rock reaction models are the core models for acidfrac design.

#### 1. Calculation of working fluid loss during acidfrac

In practical acidfrac operation, the acid liquor loss includes filtration loss. The latter is predominant and consists of fluid loss generated by volumetric extension of acid-etched wormholes and filtration loss through wormhole wall faces and wormhole tips. The total acid liquor loss during acid fracturing operation is shown in Equation (8-27).

#### (8-27)

$$V_t = V_{af} + V_{aw} + V_{av} + V_{tip}$$

where:  $V_t$  = total acid liquor loss;  $V_{af}$  = acid liquor filtration loss through fracture wall face;  $V_{aw}$  = acid liquor filtration loss through wormhole wall faces;  $V_{av}$  = volume increment of acid-etched wormholes;  $V_{tip}$  = acid liquor filtration loss through wormhole tips.

#### 2. Three-dimensional acid liquor flow reaction model

Supposing that acid liquor is uniform and the effect of free convection on mass transfer can be neglected and that the mass transfer coefficient of hydrogen ion is irrelevant to concentration, the mathematical model of three-dimensional acid liquor flow reaction in consideration of the migration and

convection diffusion in the directions of fracture length and fracture height is shown in Equation (8-28).

(8-28)

$$-\frac{\partial(Cv_x)}{\partial x} - \frac{\partial(Cv_y)}{\partial y} - \frac{\partial(Cv_z)}{\partial z} + \frac{\partial}{\partial y} \left( D_e \frac{\partial C}{\partial y} \right) + \frac{\partial}{\partial z} \left( D_e \frac{\partial C}{\partial z} \right) - \frac{\partial C}{\partial t} = 0$$

Boundary conditions are shown in Equation (8-29):

(8-29)

$$\begin{cases} x=0 & C = C_{inj} \\ y=0 & \frac{\partial C}{\partial y} = 0 \\ y = \pm \frac{w}{2} & (C_1 - C_B)v_1 + D_e \frac{\partial C}{\partial y} + k(1 - \Phi)(C_B - C_{eq})^m = 0 \end{cases}$$

where:  $C$  = acid liquor concentration, mol/L;  $v$  = acid liquor flow velocity, cm/s;  $D_e$  = effective mass transfer coefficient,  $\text{cm}^2/\text{s}$ ;  $m$  = reaction order, dimensionless;  $k$  = reaction rate constant, cm/s;  $C_B$  = wall-face acid concentration, mol/L;  $C_1$  = filtrate acid concentration, mol/L;  $C_{eq}$  = equilibrium acid concentration, mol/L;  $v_1$  = filtration velocity, cm/s.

Resolving the three-dimensional acidfrac model should be in combination with the infraction three-dimensional acid liquor flow velocity field model.

### Acidfrac Stimulation Effectiveness Prediction.

An acid-etched wormhole formed during acidfrac operation may greatly affect the fluid flow. The flow conductivity should be that of acidfrac fracture and acid-etched wormholes combined.

#### 1. Ideal acid-etched fracture width

The ideal fracture width under the condition of acid-etched wormholes generated during acidfrac operation is shown in Equation (8-30).

(8-30)

$$w_i = \frac{x(V - \Delta V_{awh})}{2(1 - \Phi)hL}$$

where:  $w_i$  = ideal acid-etched fracture width, m;  $V$  = total injected acid volume,  $\text{m}^3$ ;  $x$  = volumetric solvability of acid,  $\text{m}^3/\text{m}^3$ ;

$L$  = effective acid liquor action distance, m;  $\Delta V_{awh}$  = acid volume consumed during acid-etched wormhole propagation.

#### 2. Acid-etched fracture flow conductivity

The empirical equation of flow conductivity presented by Nierodo and Kruk's in 1973 is shown in Equation (8-31).

(8-31)

$$(w_k)_{eff} = C_1 \exp(-C_2 \sigma)$$

$$C_1 = 0.256 \text{ wk}_{fi}^{0.822}$$

$$C_2 = \begin{cases} (36.82 - 1.885 \ln S_{RE}) \times 10^{-3} & 0 \text{ MPa} < S_{RE} < 138 \text{ MPa} \\ (9.1 - 0.406 \ln S_{RE}) \times 10^{-3} & 138 \text{ MPa} < S_{RE} < 3450 \text{ MPa} \end{cases}$$

where:  $\sigma$  = effective stress, psi;  $S_{RE}$  = rock insert strength, psi;  $wk_{fi}$  = flow conductivity,  $10^{-3} \mu\text{m}^2/\text{in}$ .

#### 3. Composite acidfrac reservoir permeability in consideration of acid-etched wormhole

a. Fracture permeability calculation, as shown in Equation (8-32):

(8-32)

$$K_f = \Phi_f b^2 \cdot \frac{10^8}{12} = 8.33 \times 10^6 b^2 \Phi_f$$

where:  $b$  = fracture width, m;  $\Phi$  = fracture porosity;  $K_f$  = fracture permeability,  $\mu\text{m}^2$ .

b. Matrix permeability in consideration of acid-etched wormhole effect, as shown in Equation (8-33):

(8-33)

$$K_w = \frac{\pi}{128L_{fe} \cdot H_f} \Sigma D_i^4$$

Fracture-matrix system permeability is the sum of matrix permeability  $K_m$  and fracture permeability  $K_f$ , as shown in Equation (8-34):

(8-34)

$$K_t = K_{mw} + K_f$$

Here  $K_{mw} = K_w$ , that is, the permeability of matrix, which is changed by generating acid-etched wormholes.

### 8.6 HIGH-ENERGY GAS FRACTURING FOR PUTTING A WELL INTO PRODUCTION

#### Mechanism of High-Energy Gas Fracturing

**Overview.** Practice indicates that the stimulation effectiveness of the spike pressure pulse generated by explosion is much lower than that of a stationary pressure pulse; that is, the effectiveness of the detonation of explosive is much lower than that of the combustion of propellant. The combustion rate of an explosive is counted by km/s, and detonation waves may be generated after ignition. The combustion rate of propellant is counted by mm/s and is lower than 10 m/s. The reaction rate of an explosive is independent of environmental conditions, whereas the combustion rate of propellant is affected by environmental temperature and pressure. Despite the fact that the combustion rate of propellant is much lower than that of an explosive, the pressure riserate caused by the combustion of propellant is still much higher than that of hydraulic fracturing. The pressure risetime of hydraulic fracturing is counted by minutes, while the pressure risetime of high-energy gas fracturing (HEGF) is counted by milliseconds

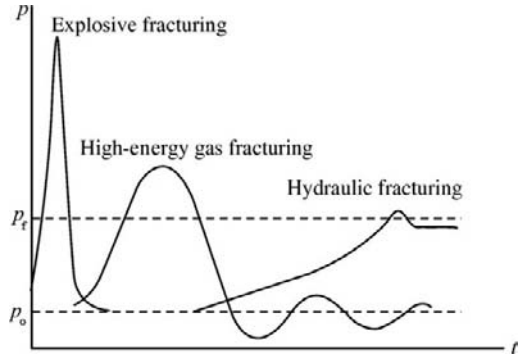


**FIGURE 8-49** Pressure riserates for various types of fracturing.

(Figure 8-49). Theoretical calculations and on-site tests indicate that with the increase of pressure riserate in the wellbore, not only can two fractures be generated in a direction perpendicular to the minimum in-situ stress in the vicinity of the wellbore, but also multiple radial fractures may be generated. In locations farther from the wellbore, these radial fractures will still be extended in the direction of the maximum principal stress. The number of fractures is mainly dependent on the pressure riserate (Figure 8-50).

The results of the tests in gallery by Schmidt in 1980 in the light of cased well are shown in

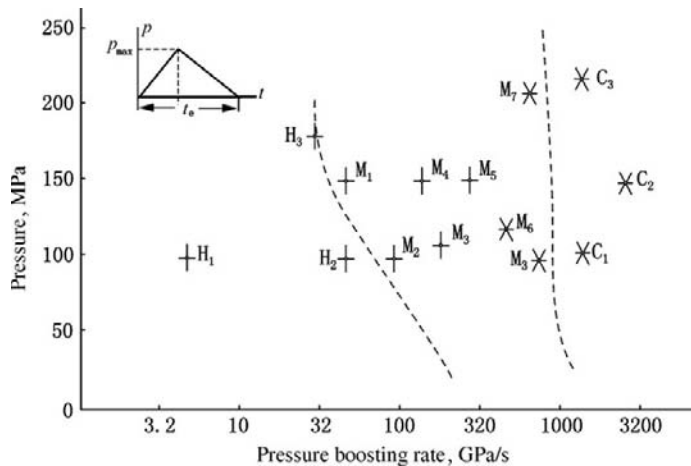


**FIGURE 8-50** Relation between the type of fracture and the pressure riserate.

TABLE 8-33 Relation Between Pressure Load Properties and Fracture Characteristics

Test Name	Peak Pressure ( $10^6$ Pa)	Pressure Riserates ( $10^7$ Pa/s)	Pulse Duration (ms)	Fracture Characteristics
GF1	13	0.6	900	
GF2	95	140	9	
GF3	>200	>10,000	1	
E	250	430		

Table 8-33 and indicate that the number of fractures is dependent on pressure riserate, and downhole explosion may form a crushed zone and compacted zone in the vicinity of the wellbore and obviously cannot increase the near-wellbore permeability.

**Conditions of Generating Fractures.** Provided the downhole pressure in a well is higher than the minimum principal stress in rock formation, fractures may be generated in rock. If the pressure riserate is high so that the fracture generated is insufficient for relieving the downhole pressure, a second fracture may certainly be generated. If the second fracture is still insufficient for relieving the downhole pressure, a third fracture will be generated. However, it is difficult to predict the speed of the growth of fracture for a heterogeneous body such as rock. It is generally considered that the maximum speed of the growth of fracture is about half of the shear wave velocity in rock.

In accordance with elastic statics, it had been considered that the pressure caused by high-energy gas fracturing in a well is higher than that of hydraulic fracturing and may possibly exceed the elastic limit of rock; thus, permanent deformation of rock will be generated during unloading (Figure 8-51) and residual fracture

with a certain fracture width will be generated (Figure 8-52) in the reservoir.

If the Poisson's ratios under loading and unloading, the cracking standard is shown in Equation (8-35).

(8-35)

$$\frac{p - p_f}{\sigma_{\min}} \geq \frac{E_2/E_1}{E_2/E_1 - 1}$$

where:  $p$  = bottomhole pressure, MPa;  $p_f$  = reservoir pressure, MPa;  $\sigma_{\min}$  = minimum principal stress in reservoir, MPa;  $E_2$  = elastic

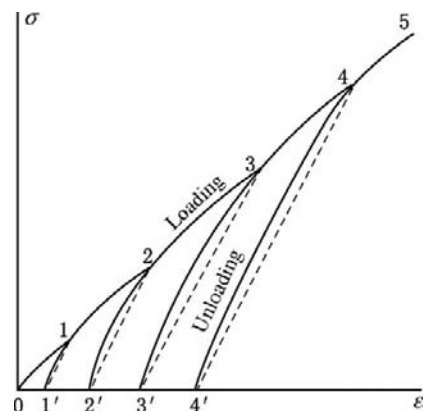


FIGURE 8-51 Relation between rock stress  $\sigma$  and strain  $\epsilon$ .

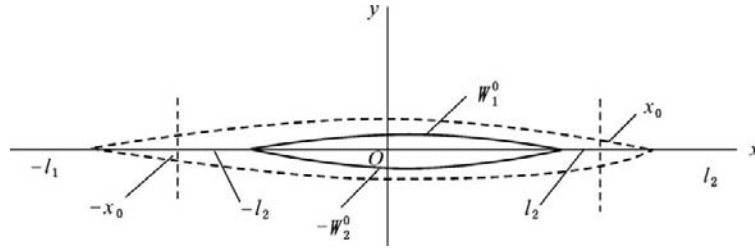


FIGURE 8-52 Residual fracture (shown by solid line).

modulus during unloading, MPa;  $E_1$  = elastic modulus during loading, MPa.

The shortcomings of this model include: (1) it neglects the fact that multiple fractures may be generated in the reservoir under higher pressure riserate; (2) it is not easy to obtain representative  $E_1$  and  $E_2$  data; and (3) because high-energy gas fracturing is performed after perforating, many microfractures have been generated in the reservoir, which is neglected by this model.

**Cracking Initiation Mechanism.** High-energy gas generated by combustion of a propellant has three types of energy: shock energy, expansion energy, and heat energy, in which shock energy and expansion energy are predominant and heat energy has only a low action on the generation of fracture. The effects of shock energy and expansion energy in the five stages of high-energy gas fracturing are as follows (Figure 8-53).

1. Precracking stage. Propellant starts combusting. The gas generated may increase the pressure in the well. The rock around the borehole wall is still in a pressured state.
2. Cracking initiation stage. With the rapid increase of pressure, the cracking of the rock around the borehole wall will be initiated. The first small shoulder appears on pressure-time curve.
3. Shock stage. With the increase of propellant combustion rate, the pressure is rapidly increased. The shock energy and part of the expansion energy will propagate the fracture formed during cracking initiation. The pressure at this time is known as peak pressure.
4. Expansion stage. In this stage the pressure is not increased, but decreased gradually. The fracture is rapidly propagated and branch fractures are generated.

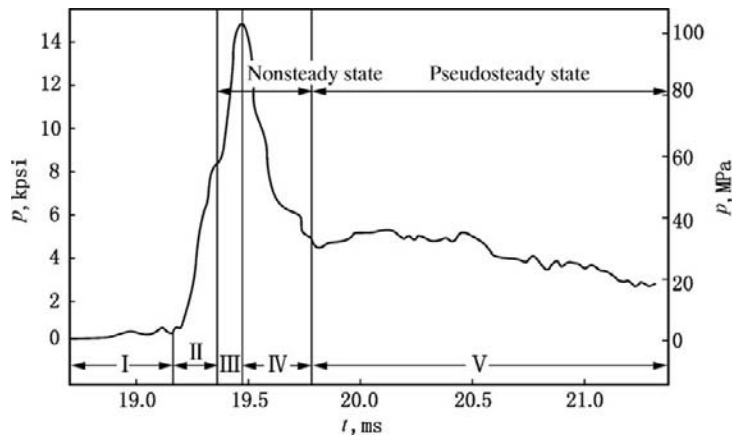


FIGURE 8-53 The change of pressure during downhole combustion of propellant charges in a well filled with water.

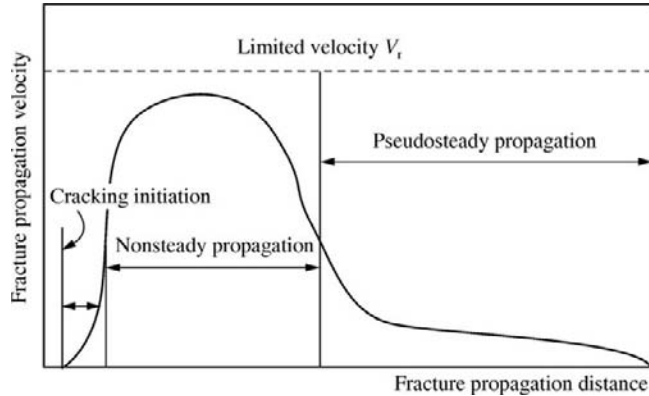


FIGURE 8-54 Fracture propagation.

5. Pseudosteady extension stage. The fracture propagation in unsteady state is changed to the fracture propagation in pseudosteady state. The extending trend of fracture is changed to the orientation of hydraulically created fracture.

The corresponding fracture propagation processes are shown in Figure 8-54.

**Self-Proppping of Fractures.** In a high-energy gas fracturing operation, proppant has not been added. However, practice indicates that fracture will not be closed by itself. In addition to the plastic deformation theory mentioned earlier, there are two points of view, as follows:

1. Shear dislocation propping

As shown in Figure 8-55, the multiple radial fractures formed by high-energy gas fracturing are random, and some fractures are not perpendicular to the minimum principal stress. Under the action of shear stress  $\tau$ , relative movement may be generated on both sides of the fracture. In addition, the fractures are propped by the exfoliated rock grains. Thus self-propped fractures are formed.

2. Rock matrix loosening

This theory considers that the shear stress borne by rock matrix is proportional to the difference between the vertical stress  $\sigma_1$  and horizontal stress  $\sigma_2$  of rock. Under the action of shear stress, the rock grains are dislocated, thus increasing porosity and permeability.

If the shear stress is high, a plastic deformation region is entered and permanent deformation may be generated; thus, fractures will not be closed despite the fact that there is no proppant.

### Effects of High-Energy Gas Fracturing

1. Compression and shock effects

The compression and shock effects of the high-pressure gas generated by the combustion of powder or propellant have been mentioned earlier.

2. Hydraulic oscillation effect

After a fracturing charge is ignited under the condition of fluid column in the well, the fluid column in the well may be pushed

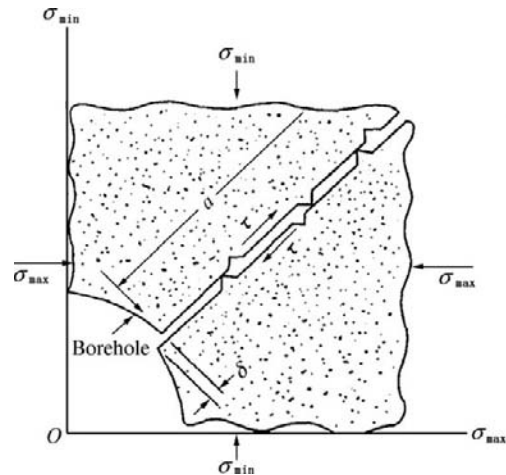


FIGURE 8-55 Self-propping of fracture.

and moved upward by the expansion of high-temperature high-pressure gas, and then the gas pressure may decrease with the increase of volume, thus causing downward movement of the fluid column. The downward movement of the fluid column may compress the gas generated by the combustion of propellant, and the downward movement of the fluid column (except the part that enters the reservoir) may be pushed upward. Thus the periodic attenuation fluctuation of pressure may be generated, which favors the formation of fractures and the cleaning of formation blockage.

### 3. High-temperature heat effect

Well temperature measurements after a high-energy gas fracturing operation indicate that well temperature can be increased to 500–700°C within a certain time after igniting the propellant charge, then rapidly decreases at the beginning and slowly decreases within several hours; thus, the paraffin and asphalt in the vicinity of the wellbore can be melted and the oil viscosity can be decreased (Figure 8-56).

### 4. Chemical action

The products of combustion of propellant are mainly  $\text{CO}_2$ ,  $\text{N}_2$ , and part of  $\text{HCl}$ . These gases may be dissolved in crude oil under high pressure, so that they can reduce oil viscosity and surface tension, thus achieving the increase of productivity.

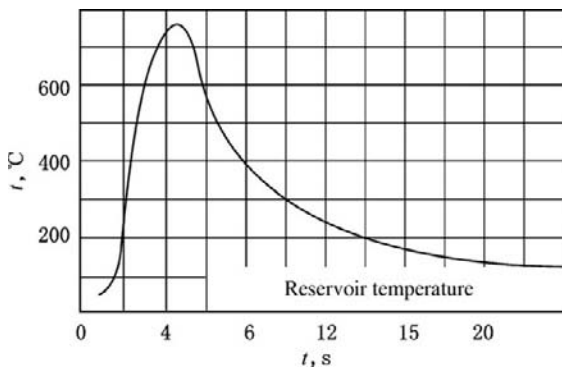


FIGURE 8-56 Well temperature vs. time during high-energy gas fracturing.

## Types of High-Energy Gas Fracturing and Suitabilities

At present, the types of pressure generators used for high-energy gas fracturing include: pressure generator with case, pressure generator with no case, and liquid propellant pressure generator.

### Solid Propellant Fracturing

#### 1. Pressure generator with case

It has a metallic case that can be used repeatedly. The case is a thick-walled cylinder and holds an igniting device and charges in it. An electric cable is used for transmission (Figure 8-57). Ignition location is determined

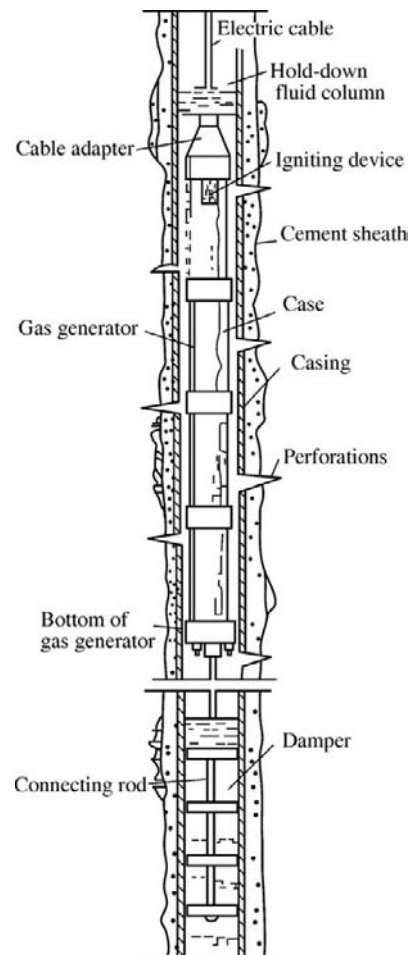


FIGURE 8-57 Pressure generator with case.

by magnetic locator. The merits include safe operation, low cost, short period, and convenient running in. However, it has metallic cases and a small ignition powder weight; thus, it has been rarely applied at present.

## 2. Pressure generator with no case

Each powder (or propellant) charge has a hole of  $\Phi 20\text{--}25$  mm at the center of the charge. The gap between the end faces of aluminum base pipe and charge is sealed with sealing compound. The strength of the aluminum base pipe should bear both the external pressure caused by the hold-down water column and the internal pressure generated by the combustion of ignition powder in the base pipe. The lengths of each charge and aluminum base pipe are respectively 500 mm and 510 mm. Both charges are connected to each other by connecting pipe with a length of 130–150 mm. The total quantity of powder is dependent on formation breakdown pressure, hole-down water column height, number of perforations, and perforation diameter. The ignitor is installed at the top. The auxiliary ignition powder in aluminum base pipe is ignited by the ignitor, so that the base pipe is heated to a temperature higher than  $2800^{\circ}\text{C}$ . At the same time, all the propellant charges are ignited (Figure 8-58).

The surface of the propellant is coated with a waterproof layer. The propellant charge (6) covered by an antiwear protective layer (7) is mounted to the aluminum base pipe (8). Propellant charges are connected to each other by connecting pipe (10) using the threads at the ends of the base pipe. The bottom sub (11) is threaded on to the bottom of the charge. The igniting device is installed in the cablehead. Ignition powder (9) is installed in the base pipe. If the pressure generator is conveyed on tubing, cablehead is replaced by impinging ignitor and cablehead igniting is replaced by bar dropping igniting. Another type of pressure generator with no case uses the axial grooves on the outside surface of the charge and a wireline for connecting. There

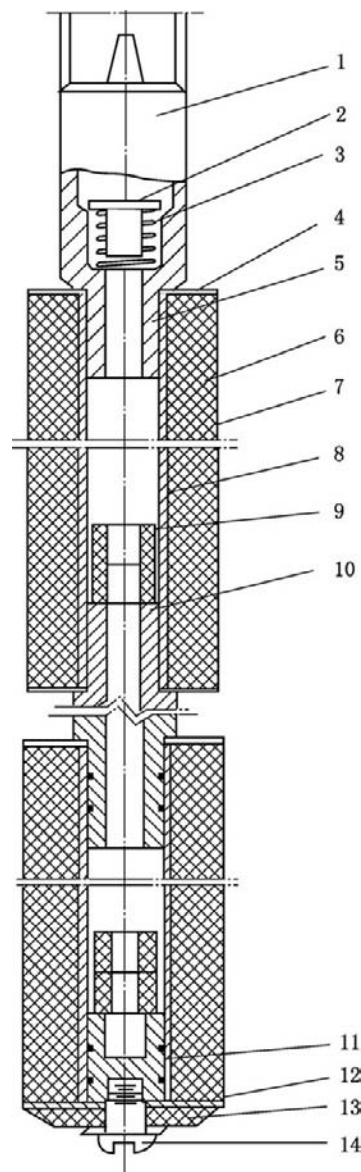


**FIGURE 8-58** Typical structure of pressure generator with no case. 1, seal plug; 2, ignitor; 3, spring; 4, gland; 5, O-ring; 6, propellant charge; 7, protective layer; 8, base pipe; 9, auxiliary ignition ammunition; 10, connecting pipe; 11, tail plug; 12, bottom cover; 13, buffer block; 14, bolt.

is a backing plate at the bottom of the charge (with or without center hole). A sealed resistance wire is used for heating and ignition. The charge with center hole has an ignitor at the

bottom. The combustion of charge is initially generated at the end face, and full-scale combustion is subsequently generated. The propellant charge of this type pressure generator is 20% to 40% higher than that of the case-free pressure generator with center hole. This type of pressure generator has a high pressure riserate and a high temperature of gas generated by propellant; thus it is appropriate for heavy oil reservoirs.

**Liquid Propellant Fracturing.** The case-free pressure generator widely used in high-energy gas fracturing has the following demerits:

1. Increasing charge can only increase pressure-boosting amplitude due to inner combustion. Not only can the action time not be prolonged, but it may be shortened because the increase of pressure may increase the combustion rate.
2. The pressure-boosting process required is actually difficult to generate in directional or cluster wells due to the difficulty of tripping.
3. Using end face combustion may prolong the action time; however, it may reduce the pressure-boosting amplitude, so that the required stimulation effectiveness cannot be achieved.

The solid propellant charge used in high-energy gas fracturing is generally less than 100 kg and the fracture length is smaller than 10 m. Thus liquid propellant has been developed in Russia since 1986. It should meet the following requirements:

1. A case-free pressure generator can be used for ignition.
2. Stable combustion is possible in wide pressure and temperature ranges.
3. Low viscosity and thermal effect on reservoir.
4. Safe and non-toxic raw materials and combustion products.
5. Low cost.
6. Propellant force  $f \geq 4 \times 10^5 \text{ m}^2/\text{s}^2$  ( $T \geq 1300\text{k}$ ) (the solid propellant force is about  $10^6 \text{ m}^2/\text{s}^2$ ).
7. It can form a uniform aqueous solution.

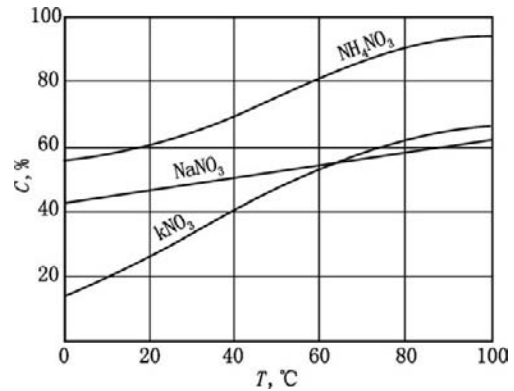


**FIGURE 8-59** Oxidant solubility in water vs. temperature. C = mass concentration; T = temperature.

- a. Oxidant.  $\text{NH}_4\text{NO}_3$  is selected to be the oxidant due to its safety, nontoxic property, and high solubility in water (Figure 8-59). The solubility C in water is 60% to 80% (mass). Thus the mass ratio of  $\text{NH}_4\text{NO}_3$  to water is 60:40.
- b. Comburant. Various combustion additives have been screened under approximate constant volume condition, and the propellants force are measured under different formula ratios. When  $\text{NH}_4\text{NO}_3$  is used as oxidant and glycerin is used as comburant the relation between the combustion temperature, the propellant force generated, and the glycerin concentration is obtained (Figure 8-60). It is shown that a glycerin mass concentration of 9% has the maximum propellant force. The twelve comburants have a propellant force of  $(5-6) \times 10^5 \text{ m}^2/\text{s}^2$  at combustion temperature of 1300–1500 K, which indicates that the combustion property is independent of comburant composition. The comburant selected should have high safety and combustion stability, low cost, and no environmental pollution.

When  $\text{NH}_4\text{NO}_3$  is used as oxidant and glycerin is used as comburant, the combustion products of liquid propellant are gaseous chiefly and nontoxic (Table 8-34).

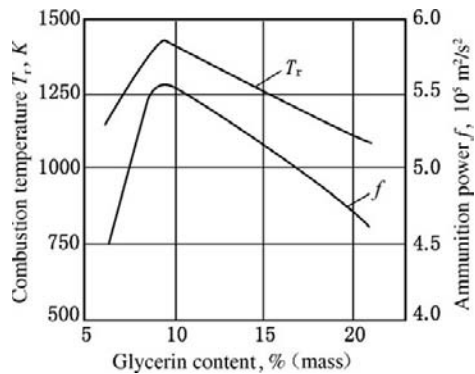


**FIGURE 8-60** Relation between liquid propellant force, combustion temperature, and glycerin content. Note: Propellant force means the energy content per unit mass of propellant, unit: J/kg or  $\text{m}^2/\text{s}^2$ .

The studies indicate that the liquid propellant force is up to  $(6.17\text{--}7.35) \times 10^5 \text{ m}^2/\text{s}^2$ , while the solid propellant force is  $(8.33\text{--}9.31) \times 10^5 \text{ m}^2/\text{s}^2$ , which means the former is 2/3 of the latter. The liquid propellant has a low cost.

The blast cell tests of liquid propellant (oxidant: comburant: water = 6:1:3) indicate that the pressure is obviously increased after igniting liquid propellant, the ignition pressure is high, and the increased value of pressure is high and stable (Table 8-35).

c. Safety

- (1) Twenty comparative tests have proven that liquid propellant is insensitive to friction.
- (2) The tests indicate that the liquid propellant is still not ignited under a

sparkling voltage of 600 kV and energy of 4.2 MJ.

- (3) There was no case of ignition during testing in accordance with the Gost 4545-80 shock sensitivity test standard.
- (4) When the cartridge is heated with resistance wire and ignited, the liquid propellant may only boil and will not be burned.
- (5) The liquid propellant will not be burned by detonating.

d. Reaction mechanism

The high-speed chemical reaction during mingling of water, oxidant, and comburant includes the three steps, that is, the thermal decomposition of oxidant, the thermal decomposition of comburant, and the chemical reaction between the thermal decomposition products of oxidant and comburant, which generates heat.

The decomposition temperature of ammonium nitrate is 290–300°C, while the decomposition temperature of glycerin is 220–230°C; thus, the chemical reaction can only be started by heating the liquid propellant to a temperature higher than 300°C.

The liquid propellant cannot be ignited under surface conditions because water may be vaporized at a temperature higher than 100°C; thus, the initial pressure should be 12–14 Mpa (at this time the boiling point is at 290–300°C) in order to ignite the liquid propellant.

**TABLE 8-34** Composition of Liquid Propellant Combustion Products ( $\text{NH}_4\text{NO}_3/\text{water} = 60/4$ )

Glycerin Content, %	Combustion Product		CO <sub>2</sub>	CO	H <sub>2</sub> O	N <sub>2</sub>	H <sub>2</sub>
9	Molal weight	kg	2.93	0.003	37.74	6.82	0.020
		%	12.89	0.008	67.93	19.10	0.004
10	Molal weight	kg	3.11	0.15	37.11	6.75	0.70
		%	13.68	0.42	66.80	18.90	0.14
12	Molal weight	kg	3.47	0.44	35.86	6.60	2.08
		%	15.27	1.23	64.55	18.48	0.42

TABLE 8-35 Blast Cell Test Results

Propellant No.	Propellant No.	Propellant Density (g/ml)	Propellant $W_B$ (g)	Ignition Pressure $P_B$ (MPa)	Maximum Pressure $P_m$ (MPa)	Time $T_m$ Required to Attain $P_m$ (ms)
No. 1	1	0.20	Nitrocellulose powder 2	21.57	27.56	20.21
	2	0.20	Nitrocellulose powder 2	21.57	26.03	21.30
	3	0.12	Nitrocellulose powder 2	20.40	27.65	64.28
	4	0.12	Nitrocellulose powder 2 Double-base powder 1	50.11	110.82	338.5
No. 3	1	0.20	Nitrocellulose powder 2 Double-base powder 1	52.66	173.09	425.71
	2	0.20	Nitrocellulose powder 2 Double-base powder 1	52.66	91.99	468.12
	3	0.20	Nitrocellulose powder 2 Double-base powder 2	63.25	202.99	195.16
	4	0.20	Nitrocellulose powder 2 Double-base powder 2	63.25	209.37	180.87
	5	0.12	Nitrocellulose powder 1 Double-base powder 2	40.11	90.60	442.35
	6	0.12	Nitrocellulose powder 1 Double-base powder 2	40.11	90.61	442.35
	7	0.12	Nitrocellulose powder 2 Double-base powder 2	50.11	101.79	363.44

In addition, the heat generated should be sufficient for heating water to the boiling point and starting a new chemical reaction in order to ignite the liquid propellant. These have been proven by testing results (Figure 8-61).

e. Ignition of liquid propellant

The tests indicate that the ignition propellant should have energy sufficient for igniting the liquid propellant under semi-closed conditions with ignition pressure of 12–14 MPa. It is indicated that the proportion of ignition propellant and liquid propellant is 1:5, and the energy required to form stable combustion of liquid propellant is 670 kJ/kg.

Supposing that one ton of liquid propellant will be used once, the inside diameter of the casing is 124 mm, and the liquid propellant density is 1.296 g/cm<sup>3</sup>, the liquid propellant length in casing is 62.22 m. A section of standard case-free

pressure generator charge has a length of 500 mm, an outside diameter of 90 mm, and mass of 5 kg. The length and mass of two sections are respectively 1 m and 10 kg. The mass of liquid propellant within a length of 3 m (and around) is 40 kg (the length affected by solid propellant charge is 3 m). The heat generated by the combustion of this liquid propellant can ignite a liquid propellant charge of 60 m within 40 seconds and generate pressure of 60–70 MPa and fractures with a length of 25–50 m.

f. Running-in technology

(1) Tools and equipment. Hoist tractor, tubing, cap tank, or water tanker (3–5 m<sup>3</sup>), the tank (1–3 m<sup>3</sup>) with heating coiled pipe and agitator, steam generator, cementing truck, perforator truck (used for tripping ignitor on wireline), drill-stem tester, casing and cement sheath quality logging instrument, and so on.

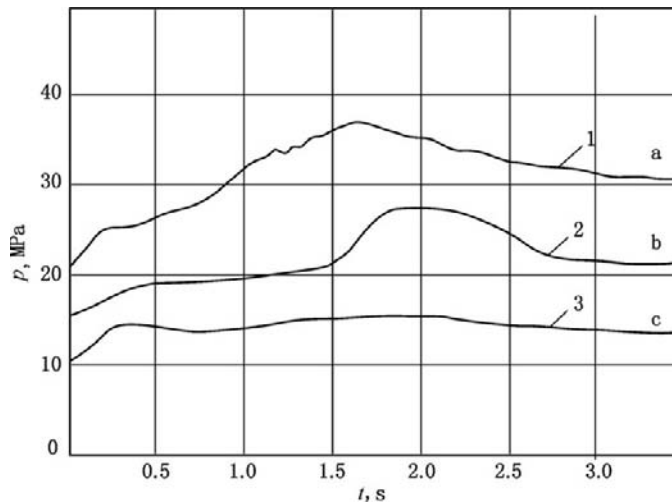


**FIGURE 8-61** Pressure vs. time during liquid propellant combustion in blast cell. 1, initial pressure 20 MPa; 2, initial pressure 15 MPa; 3, initial pressure 12 MPa.

- (2) Spacer fluid. In order to prevent the liquid propellant and the fluid in the well from mingling, which may change performance, both the top and bottom of the liquid propellant should be isolated from the fluid in the well and the ignitor should not be hindered from running. Obviously, the density of the upper spacer fluid should be lower than that of the liquid propellant, and the density of the lower spacer fluid should be higher than that of the liquid propellant. The spacer fluid should not be mutually dissolved with the fluid in the well and the liquid propellant.  $\text{CaCl}_2$  water-diesel oil emulsion can be used as spacer fluid and barite can be used to control the density.
- (3) Running-in procedure
  - (a) Pulling out the previous string, cleaning it, checking it, and changing unqualified tubings
  - (b) Drifting tubing with  $\Phi 59 \text{ mm} \times 500 \text{ mm}$  rabbit
  - (c) Drifting to artificial bottomhole with  $\Phi 118 \text{ mm} \times 1500 \text{ mm}$  drift size gauge tool
  - (d) Flushing to artificial bottomhole with 0.2% active water under a high pumping rate
  - (e) Sand packing in the well to the bottom of perforated interval
  - (f) Running liquid propellant detonation string (on top of the detonator screen that is connected to the bottom of the string, a tubing centralizer is added every 20 m upward)
  - (g) Filling the well with clear water, pumping spacer fluid by cementing truck, pumping the prepared liquid propellant, pumping the remaining spacer fluid, pumping a certain quantity of clear water, and pumping liquid propellant to a designated reservoir location
  - (h) Pulling up string for 11.0 m
  - (i) Opening the wellhead (tubing and casing are opened), dropping a bar for detonation, and then pulling string and accessories
  - (j) Running-in production tubing string

Table 8-36 shows the liquid propellant treatment results in the Huoshaoshan oil field in Xinjiang.

TABLE 8-36 Liquid Ammunition Treatment Results in Huoshaoshan Oil Field in Xinjiang

No.	Well No.	Type of well	Casing Specification (mm)	Perforated Interval (m)	Perforation Thickness (m)/ Number of Layer	Perforation Density Shots/m	Propellant Charge (kg)	Production Rate (t/d)			
								Before Operation		After Operation	
								Liquid	Oil	Liquid	Oil
1	H1141	Oil well	177.8	1633 ~ 1646	13/1	26	800	3.3	2.8	6.6	5.0
2	H1425	Oil well	139.7	1548 ~ 1580.5	27.5/3	16	800	1.7	0.7	8.6	1.6
3	H2442	Oil well	177.8	1566 ~ 1593	9.5/3	16	860	2.9	2.1	4.6	3.4
4	H1421	Oil well	139.7	1598.5 ~ 1630	12/4	26	1080	3.1	3.0	8.6	6.0
5	H1128	Oil well	139.7	1482.5 ~ 1528	11.5/3	20	1000	0	0	3.6	3.1

## Suitabilities of High-Energy Gas Fracturing

### 1. Suitable lithology

High-energy gas fracturing is suitable for brittle formations such as limestone, dolomite, sandstone with a low shale content (<10%), and unsuitable for mudstone, and sandstone may generate serious sand production after fracturing, so that prudence is required.

The concrete conditions of using liquid propellant fracturing include the following:

Porosity	3% to 25%
Permeability	<0.05–0.3 $\mu\text{m}^2$
Oil saturation	$\geq 30\%$
Shale content	$\leq 30\%$
Reservoir thickness	$\leq 150$ m
Reservoir pressure	$\geq 60\%$ of original reservoir pressure
Perforation density	16–30 shots/m
Distance to water formation	$\geq 15$ –20 m

Casing and cementation at perforated interval and 150–200 m above perforated interval are in good condition.

Well depth should be greater than 1000 m, and the liquid propellant in which urea is used as comburant can be used in the well with a depth greater than 500 m.

### 2. High-energy gas fracturing operation

- Before the operation, well flushing, sand washing, and removing the wax on the wall and the cement on the casing wall are required. A well test is also required in order to obtain skin factor, reservoir permeability, production (or injection) profile, and so on.
- Before the operation, acid treatment or acid soak is performed.
- Wellbore fluid within 200 m above the perforated interval is displaced with formation water or an aqueous surfactant solution of NaCl, CaCl<sub>2</sub>, CaBr<sub>2</sub>, or ZnCl<sub>2</sub>.
- If the reservoir is a naturally fractured carbonatite formation, it is recommended that an acid-in-oil emulsion is displaced into the perforated interval. The emulsion volume is 5–6 m<sup>3</sup>. If the reservoir is a sandstone formation, hydrochloric acid

or mud acid can be displaced into the perforated interval.

- Perforation gate (cable ignition) is installed at the wellhead.
- When the perforation diameter is 10 mm, the perforation density should be 20–30 shots/m. Reperforating is required if necessary. When the perforation diameter is 16 mm, the perforation density should be higher than 10 shots/m.
- Theory and practice indicate that the fractures of high-energy gas fracturing are generally formed at 2–4 m below charge near the formation interface or a location with good physical properties; thus, the charges should be distributed at 2–4 m above the treated interval.
- If there is bottom water, on the premise of good cement sheath cementation, the distance between the bottom of charge and the bottom of perforated interval should be more than 5 m.
- The appropriate distance between well fluid level and wellhead is 50–60 m.

## High-Energy Gas Fracturing Design

The working process of fracturing charge in a well can be simulated by a differential equation group consisting of the propellant combustion rule equation, the well fluid motion equation in consideration of compressibility and hydraulic resistance, the perforation flow restriction equation, and the equation of fractures formed and extended when displaced fluid enters the reservoir and propellant gas flows in (Figure 8-62).

**Combustion of Propellant.** The combustion process of a tubular charge can be described by using the concept of relative combustion thickness ( $z = e/e_0$ ) and the powder combustion rule ( $u = A \cdot P$ ), as shown in Equation (8-36):

(8-36)

$$\frac{dz}{dt} = \frac{d(e/e_0)}{dt} = u/e_0 = A \cdot p/e_0$$

where  $z = e/e_0$  is the relative combustion thickness of the tubular charge;  $e_0$  is charge pulp thickness.

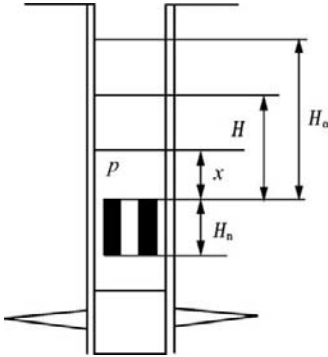


**FIGURE 8-62** Wellbore structure. (a) Missile propellant; (b) Single-base propellant.

The relative mass of the burned part of the charge is as follows.

$$\psi = z[1 + \lambda(z - 1)]$$

where:  $\lambda = e_o / (e_o + d_o)$  if combustion is inside;  $\lambda = -e_o / (e_o + d_o)$  if combustion is outside;  $\lambda = 0$  if combustion is both inside and outside;  $d_o =$  inside hole diameter of tubular charge.

**Well Fluid Motion Equation.** For a gas-liquid interface, Equation (8-37) applies:

$$(8-37) \quad \frac{dx}{dt} = 2v$$

where:  $x =$  gas-liquid interface displacement;  $v =$  liquid column mass center velocity.

The differential equation of liquid motion along the wellbore is shown in Equation (8-38).

$$(8-38) \quad \frac{dv}{dt} = \frac{p - p_o}{\rho_o c_o t} - \frac{v}{t} - \frac{\beta v}{2D}$$

where:  $\beta =$  resistance coefficient;  $\rho_o =$  compressible liquid density;  $p_o =$  hydrostatic pressure at operation section;  $D =$  wellbore diameter;

$c_o = \frac{dH}{dt} =$  slightly compressible wave propagation velocity in well (approximate to acoustic velocity);  $H =$  pressure disturbance propagation distance in well liquid.

**Relationship between Pressure and Time.**

The relationship between pressure and time can be expressed in Equations (8-39) and (8-40):

$$(8-39) \quad \frac{dp}{dt} = \frac{(f - p/\rho_n)m \frac{d\psi}{dt} p^\gamma - (\gamma - 1)q - \gamma p_{Tg} \frac{dV_{Tg}}{dt}}{V_\psi + xS + V_T \frac{(1 - \alpha)P_{Tg} + 2\rho_o \alpha}{2P_{Tg} - (1 - \alpha)p}}$$

$$(8-40) \quad V_\psi = \frac{\pi d_o^2}{4} H_o + m(1/\rho_n - \alpha)\psi$$

where:  $p =$  pressure in gas bubbles formed by combustion products;  $q =$  heat flux of combustion products;  $d_o, H_o =$  inside diameter and height of charge;  $\rho_n, \alpha =$  density and clearance volume of propellant;  $f =$  propellant force;  $m =$  propellant charge mass;  $\gamma =$  polytropic exponent of combustion products;  $V_\psi, V_T =$  the volume released from the burned part of charge and the volume of the liquid squeezed into fractures;  $S =$  cross-sectional area of the well;  $x =$  height of well section held by propellant gas above charge;  $V_{Tg} =$  volume of propellant gas.

The pressure outside the casing, that is, the pressure that presses liquid into fractures, is shown in Equation (8-41).

$$(8-41) \quad p_1 = p - \frac{\rho_o}{2n^2 h^2 S_o^2} \left( \frac{dV_T}{dt} \right)^2 \left( 1 - \frac{n^2 h^2 S_o^2}{S} \right)$$

where:  $n =$  perforation density;  $S_o =$  cross-sectional area of a hole;  $h =$  fracture height.

The length of vertical fracture formed is shown in Equation (8-42).

$$(8-42) \quad L_T = \sqrt{\frac{EV_T}{5.6(1 - \mu_o)(p_1 - 2p_o)h}}$$

The width of vertical fracture formed is shown in Equation (8-43).

$$(8-43) \quad \omega = \frac{4(1 - \mu_o)(p_1 - 2p_o)L_T}{E}$$

where:  $\mu_o =$  Poisson's ratio of rock;  $h =$  fracture height;  $E =$  elastic modulus of rock.

The liquid below the pressure generator is squeezed into fractures, so the downward

displacement of the gas-liquid interface below the pressure generator will be  $H_T = \frac{V_T}{S}$ . If  $H_T \leq y_T$ , only liquid flows into fractures.

The flow rate of the liquid squeezed into vertical fractures is shown in Equation (8-44).

(8-44)

$$\frac{dV_T}{dt} = 22 \left( \frac{p_1 - 2p_o}{E} \right)^{8/7} \left( \frac{p_1 - p_o}{\rho_o} \right)^{4/7} \frac{h^{3/7} V_T^{4/7}}{v^{1/7}}$$

where:  $V_T$  = volume of liquid squeezed into fractures;  $v$  = kinematic viscosity of liquid.

**Flow Rate of Gas Squeezed into Vertical Fractures.** If  $H_T > y_T$ , liquid stops entering fractures and propellant gas starts entering fractures

when  $\frac{dV_T}{dt} = 0$ . When the pressure difference is lower than the critical pressure difference, the flow rate of propellant gas  $P_{Tg}/P > \left( \frac{2}{\gamma + 1} \right)^{\frac{\gamma}{\gamma-1}}$ , and the volumetric is shown in Equation (8-45).

(8-45)

$$\frac{dV_{Tg}}{dt} = nhS_o \left( \frac{P_{Tg}}{\rho} \right)^{1/\gamma} \sqrt{\frac{2\gamma}{\gamma-1} \frac{P_{Tg}}{\rho} \left[ 1 - \left( \frac{P_{Tg}}{P} \right)^{\frac{\gamma}{\gamma-1}} \right]}$$

where:  $V_{Tg}$  = propellant gas volume.

When the critical pressure difference is exceeded,  $P_{Tg}/P < \left( \frac{2}{\gamma + 1} \right)^{\frac{\gamma}{\gamma-1}}$  and the volumetric flow rate of propellant gas is shown in Equations (8-46) and (8-47).

(8-46)

$$\frac{dV_{Tg}}{dt} = nhS_o \left( \frac{P_{Tg}}{\rho} \right)^{1/\gamma} \sqrt{\frac{2\gamma}{\gamma-1} \frac{P}{\rho}}$$

where:  $P_{Tg}$  = propellant gas pressure at fracture inlet outside casing, as in Equation (8-47),

(8-47)

$$\rho = \frac{m\psi f}{V_\psi + Sx + V_T + V_{Tg} \left( \frac{P_{Tg}}{P} \right)^{1-\gamma}}$$

where:  $\rho$  = propellant gas density.

The propellant gas pressure at fracture inlet is shown in Equation (8-48).

(8-48)

$$P_{Tg} = p \frac{(1-a)}{2} \left[ 1 + \sqrt{1 + \frac{4a}{(1-a)^2} \frac{2P_o}{\rho}} \right]$$

$$a = \frac{4W_{Tg}}{\gamma\beta_L \left( L_{TS} - \frac{V_T}{2W_{Tg}h} \right)}$$

where:  $L_{TS}$  = total length of fracture caused by both liquid and gas;  $W_{Tg}$  = fracture width;  $\beta_L$  = coefficient of friction between gas and fracture wall.

The total length of fracture generated is shown in Equation (8-49).

(8-49)

$$L_{TS} = \sqrt{\frac{E(V_T + V_{Tg})}{5.6(P_{Tg} - 2P_o)(1 - v^2)h}}$$

The width of fracture generated is shown in Equation (8-50).

(8-50)

$$W_{TS} = \frac{4(1 - v_o^2)(P_{Tg} - 2P_o)L_{TS}}{E}$$

The heat flux of combustion products is as follows.

$$q(t) = \frac{dQ}{dt} = \alpha S_T (T - T_o)$$

where:  $T_o$  = initial temperature of liquid;  $T$  = propellant gas temperature;  $S_T$  = heat exchange area.

The heat exchange coefficient is shown in Equation (8-51).

(8-51)

$$\alpha = 7.36 \frac{(\rho v)^{0.8}}{D^{0.2}}$$

The heat exchange area between the combustion products and the liquid is shown in Equation (8-52).

(8-52)

$$S_T = \sqrt{\pi(D^2x + D_o^2H)(H_c + x)}$$

where:  $H_c$  = pressure generator height;  $D_o$  = tubular propellant OD;  $D$  = borehole diameter.

The combustion product temperature obtained on the basis of state equation is shown in Equation (8-53).

(8-53)

$$T = \frac{P}{f_p} T_g$$

where:  $T_g$  = propellant combustion temperature (deflagration temperature).

Thus the differential equation group consisting of Equations (8-36), (8-37), (8-38), (8-39), (8-45), and (8-46) has been obtained ( $z$ ,  $x$ ,  $v$ ,  $p$ ,  $V_T$ , and  $V_{Tg}$  are the functions of time). They describe the whole process of the tubular propellant charge combustion in a well filled with liquid.

Using this differential equation group, the rule of the change of well pressure with time and the volume of the fluid squeezed into vertical fractures can be obtained under the initial conditions of  $t = 0$ ,  $x = 0$ ,  $v = 0$ ,  $p = p_o$  ( $p_o = H_o \rho_o g$ , that is, hydrostatic pressure), and  $V_T = 0$ . In addition, the rules of change of the parameters including the pressure of combustion products, the fluid pressure outside the casing, the length of upper gas-liquid interface movement, the speed of upper gas-liquid interface motion, the relative mass of the burned part of the propellant charge, the length and width of fracture, the length of the downward movement of lower gas-liquid interface, and well temperature can also be obtained.

### Combined High-Energy Gas Fracturing and Perforating

The perforating charge carriage in which perforating charges and fracturing propellant charges are rammed is installed in the perforating gun body. The perforating gun is run on tubing, and a bar is dropped for detonating. Perforating charges first form perforations at reservoir interval. The high-temperature high-pressure gas that is generated by delayed combustion of propellant charges will enlarge and deepen the perforations up to 1–2 m, and multiple fractures may be formed along the

perforations. The range of fractures is up to 2–8 m. This technique has the following features:

1. The energy utilization factor of high-temperature high-pressure gas is increased. When high-energy gas fracturing is adopted, the fracturing charges are burned in the casing, and only a small quantity of gas may enter the reservoir through perforations. When combined perforating and high-energy gas fracturing are adopted, the most gas generated by propellant combustion may act on the reservoir through perforations; thus, the energy utilization factor of the gas generated by propellant combustion may be greatly increased.
2. Combined high-energy gas fracturing and perforating simplifies the operations. Perforating (reperforating) and fracturing can be performed once, so that the cost is reduced.
3. When high-temperature high-pressure gas generated by propellant combustion is projected into the reservoir at high speed, the perforations are scoured and deepened. The effectiveness is much higher than that of exclusive high-energy gas fracturing.
4. Simultaneous multi-interval operations can be achieved.

When combined high-energy gas fracturing and perforating is adopted, the propellant selected should be insensitive to explosions, and the surface of propellant should be passivated.

The relationship between combustion rate and pressure for missile propellant and single-base propellant is shown in Figure 8-63. The sensitivity tests indicate that the single-base propellant of nitrocellulose has a lower sensitivity to explosions; thus, nitrocellulose is selected.

### High-Energy Gas Fracturing Tests

The test methods include static test and dynamic test.

**Static Test (Peak Pressure Test).** Peak pressure during fracturing is determined by the plastic deformation of the copper column in the

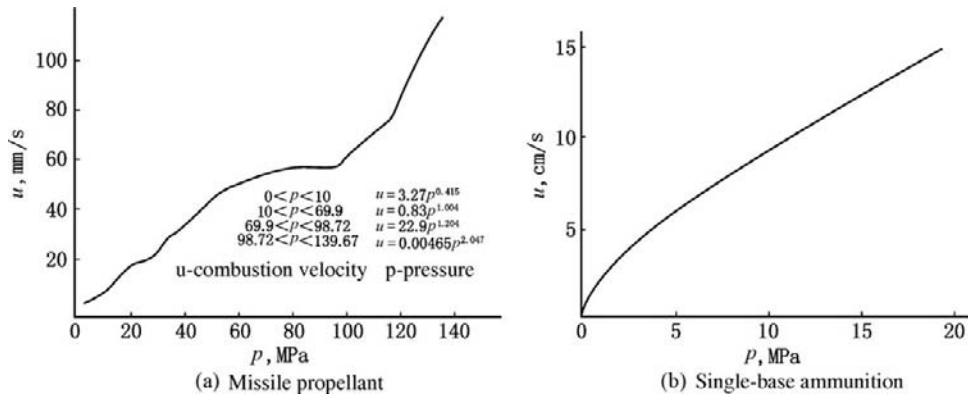


**FIGURE 8-63** Relationship between combustion rate and pressure for missile propellant and single-base propellant.

pressure-measuring unit. The copper-column pressure measurement unit has a simple structure. However, it can only measure approximately the peak pressure of high-energy gas fracturing, and the relationship between pressure and time during fracturing cannot be obtained.

The structure of the pressure-measuring unit is shown in Figure 8-64. Measuring the deformation of the copper column during fracturing can determine the peak pressure; thus, the material, mechanical properties, sizes, and shapes of the copper column should strictly meet the

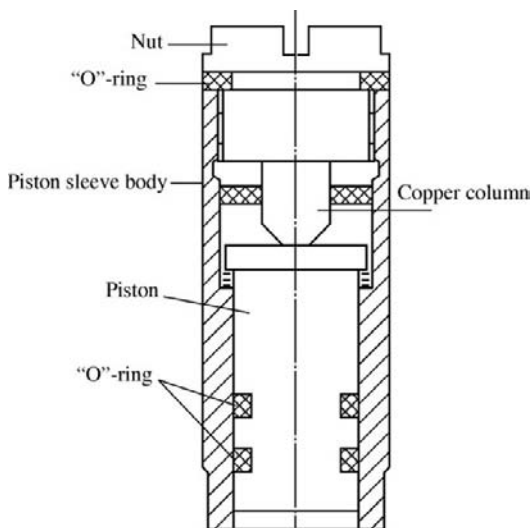


**FIGURE 8-64** Structure of a pressure-measuring unit.

requirements. The specifications of the cylindrical and conical copper columns that are commonly used in oil fields at present are listed in Table 8-37.

On-site experience indicates that a conical copper column of  $\Phi 5 \times 8.1$  should be selected when well depth  $L \leq 2000$  m; a cylindrical copper column of  $\Phi 6 \times 9.8$  should be selected when  $2000 \text{ m} < L \leq 4500$  m; and a cylindrical copper column of  $\Phi 8 \times 13$  should be selected when  $L > 4500$  m.

The relationship between the deformation of the copper column and the pressure is not linear in the full sense; thus, a static pressure (preceding pressure) is generally exerted on the copper column during manufacture, so that the mechanical properties of the copper column may tend to be consistent, and error caused by unevenness of the mechanical properties of the copper column may be avoided. The preceding pressing includes primary preceding pressing and secondary preceding pressing. The fundamental principle of copper-column pressure measurement is used on quasi-static processes; however, high-energy gas fracturing is a dynamic process. Static pressure makes the copper column deform gradually, whereas dynamic pressure may reach the maximum within 1–10 seconds, and the action time is very short.

In order to enhance the accuracy of the peak pressure measurement for high-energy gas

**TABLE 8-37 Copper Column Specifications**

Shape	Diameter × Length (mm)					
Cylindrical	3 × 4.9	4 × 6.5	5 × 8.1	6 × 9.8	8 × 13	10 × 15
Conical	3 × 4.9		5 × 8.1	6 × 9.8	8 × 13	

fracturing, the preceding pressure value of the copper column selected should be slightly lower than the estimated peak pressure of high-energy gas fracturing; thus, only a small deformation will be generated when the peak pressure of high-energy gas fracturing acts on the copper column. For the copper column by primary preceding pressing, the determination of the peak pressure is based on the copper column height after pressing and the corresponding pressure table. The commonly used cylindrical copper columns of  $\Phi 5 \times 8.1$  and  $\Phi 8 \times 13$  are of the copper column by primary preceding pressing. The copper column used in Table 8-38 is the cylindrical copper column of  $\Phi 8 \times 13$ . The table shows the copper column heights after pressing under the condition of primary preceding pressing pressure of 44 MPa and the corresponding peak pressure values.

For the copper column by secondary preceding pressing, the relationship between the plastic deformation of the copper column and the

pressure is approximately linear near the preceding pressure value, and the mechanical properties of the copper column may further tend to be consistent. When the copper column by secondary preceding pressing leaves the factory, a basic parameter, hardness coefficient  $\alpha$ , is given, as shown in Equation (8-54).

(8-54)

$$\alpha = \frac{P_2 - P_1}{H_1 - H_2} \cdot \frac{1}{100}$$

where:  $P_1, P_2$  = primary and secondary preceding pressure values, MPa;  $H_1, H_2$  = heights of copper columns by primary preceding pressing and secondary preceding pressing, mm.

When the copper column height  $H$  after high-energy gas fracturing is measured, the pressure  $P$  of gas generated by burning in the wellbore is shown in Equation (8-55).

(8-55)

$$P = P_2 + \alpha(H_2 - H) \times 100 \quad (\text{MPa})$$

**TABLE 8-38 Relation between Copper Column Height after Pressing and Peak Pressure for Cylindrical Copper Column of  $\Phi 8 \times 13$**

Copper Column Height after Pressing (mm)	P (MPa)									
	0	1	2	3	4	5	6	7	8	9
6.5	196.0	195.5	195.0	194.5	194.0	193.6	193.1	192.6	192.1	191.6
6.6	191.2	190.7	190.2	189.7	189.2	188.7	188.3	187.8	187.3	186.8
6.7	186.4	185.9	185.4	184.9	184.4	184.0	183.6	183.1	182.6	182.1
6.8	181.7	181.2	180.7	180.2	179.7	179.2	178.7	178.3	177.8	177.3
6.9	176.9	176.4	176.0	175.6	175.1	174.7	174.3	173.9	173.5	173.1
7.0	172.6	172.1	171.7	171.3	170.8	170.4	170.0	169.5	169.1	168.8
7.1	168.3	167.8	167.4	167.0	166.6	166.1	165.7	165.5	164.8	164.4
7.2	164.1	163.6	163.2	162.8	162.3	161.9	161.5	161.2	160.6	160.2
7.3	159.7	159.3	158.9	158.5	158.0	157.6	157.2	156.9	156.3	155.9

Note: The numbers of 0–9 in the second line are the second decimal places of the number in the first column. For example, the peak pressure corresponding to the after-press copper column height of 6.52 mm is 195.0 MPa.

**Dynamic Test (Downhole Pressure-Time Process Test).** The optimization of high-energy gas fracturing is based on the data of the downhole pressure-time process, that is, the p-t process test.

At present, the p-t testers mainly include the downhole storage p-t tester and the surface direct-recording p-t tester.

#### 1. Downhole storage p-t tester

It consists of surface instruments and downhole instruments. The surface instruments include a microcomputer and a special interface, which are used for data readback and processing. The downhole instruments include tripped conducting mechanism, electronic circuit, electric battery, ignition system, pressure sensor, and housing. After fracturing charges are run in, the downhole instruments are switched on. The ignition head and ignition powder are connected by a control module in order to detonate fracturing charges and start the acquisition and recording module, so that the change of well-bore pressure with time after propellant ignition can be recorded. The downhole testing instruments are pulled out after fracturing and connected with the special interface of surface instruments, and then the p-t process data in electronic recording module are read out and processed. Figure 8-65 shows the measured curve of a well in the Daqing oil field (1977).

#### 2. Surface direct-recording p-t tester

It consists of a downhole data acquisition part and a surface recording part. The former

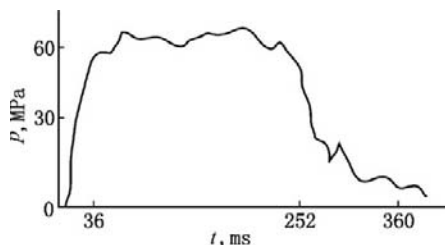


**FIGURE 8-65** The measured p-t curve of a well in Daqing oil field.

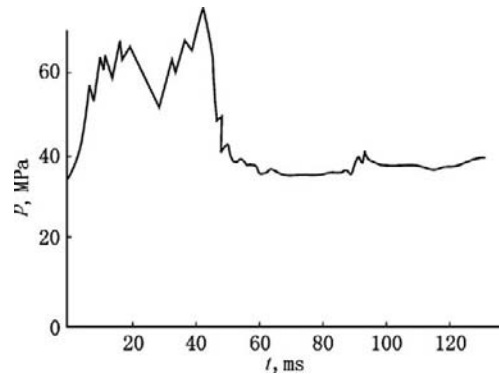


**FIGURE 8-66** The measured p-t curve of a well in Dagang oil field.

includes pressure sensor, pressure transformer, and accessory circuit, while the latter includes input impedance amplifier, converter, chip microprocessor, printer, and ignition high voltage direct current generator.

After fracturing charges and p-t tester are run to the target interval, the ignition system and 8-chip microprocessor are started, and the control system begins data acquisition. Figure 8-66 shows the measured p-t curve of a well in the Dagang oil field.

Making the comparison between the pressure transient testing results before and after operation is the most effective method for evaluating high-energy gas fracturing.

## 8.7 FLOWING BACK

Conventional flowing-back measures include displaced flow, swabbing, gas lift, and foamed flow.

### Flowing Back by Displaced Flow

After oil and gas wells are perforated under overbalance pressure, they will not flow naturally due to the liquid column pressure, which is higher than reservoir pressure. The essence of displaced flow is to decrease the relative density of the liquid in the well to make the backpressure of the liquid column in the well lower than reservoir pressure; thus, an induced flow will be

achieved. The killing fluid is first displaced with a low-density liquid. The commonly used displaced flow methods are as follows.

**Conventional One-Step Displaced Flow Method.** Tubing is run to about 1 m above the artificial bottom of the well, the killing fluid is displaced out with displacement fluid, and then the tubing is pulled up to the middle or upper part of the reservoir. This method is only used in a well that has a low flowing ability and a certain time interval from the finishing of displacement to the flowing of oil to make it possible to pull up the tubing (Figure 8-67).

**Two-Step Displaced Flow Method.** Tubing is run to about 1 m above the artificial bottom of the well, a section of displacement fluid is displaced in and displaced to the top of the reservoir, the tubing is pulled up to the middle of the reservoir, and then all the killing fluid above the top of the reservoir is displaced with displacement fluid; thus, all the killing fluid in the well can be displaced out and the tubing is pulled up to the desired depth (Figure 8-68).

The displaced flow methods have the advantage that the producing pressure drawdown is formed slowly and uniformly, so that borehole wall sloughing and sand production is avoided.

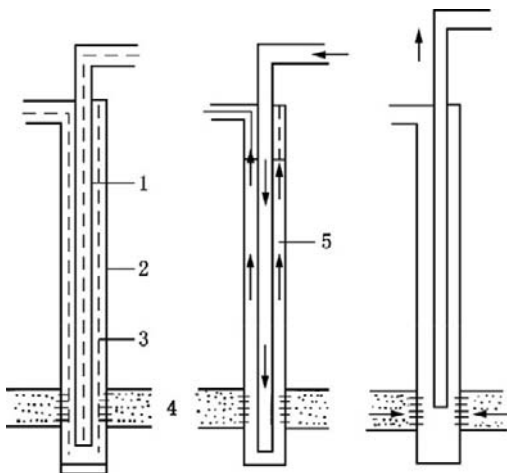


**FIGURE 8-67** One-step displaced flow method. 1, tubing; 2, casing; 3, return fluid; 4, reservoir; 5, displacement fluid.

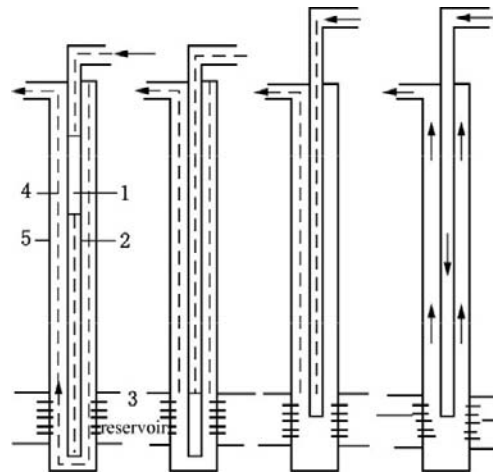


**FIGURE 8-68** Two-step displaced flow method. 1, displacement fluid; 2, tubing; 3, reservoir; 4, return fluid; 5, casing.

The technical requirements of the safety of displaced flow are as follows:

1. The pressure test value of the inlet pipeline should be 1.2–1.5 times the working pressure and a hard pipeline should be used and firmly fixed in order to prevent the pipeline from leaking.
2. Flexible hose and rubber tube should be strictly used as outlet pipeline in order to prevent personnel from injuring themselves due to excessive pressure.
3. In a well with packer, the displacement rate should be controlled in order to prevent drilling fluid from entering the reservoir.
4. In the displaced flow, pumping should be continuously operated and stopping pumping midway is not allowed. If circulation cannot be achieved, pumping should not be held and appropriate measures should be taken.
5. After all the killing fluid in the well is displaced out, the packer should be set in time in order to prevent blowout accidents.
6. For a high-pressure well or gas well with high flowing ability, the two-step displaced flow method should be adopted in order to prevent blowout accidents.

## Flowing Back by Swabbing

The liquid in the well is drawn to the surface in order to lower the liquid level in the well, thus reducing the liquid column backpressure on the reservoir.

The merits include: (1) simple equipment (only a hoist tractor is needed); (2) simple corollary tools, which consist mainly of wire rope, swab assembly, sinker bar, and wellhead saver; (3) convenient operation and a small number of personnel; and (4) no formation damage.

The demerits include: (1) low working efficiency; (2) shallower unloaded depth (swabbed depth < 1200 m); (3) lack of the means of swab wear and leak monitoring; (4) lack of the means of swabbed depth and working fluid level depth monitoring; and (5) serious environmental pollution at the surface.

This method is appropriate for: (1) swabbed depth < 1800 m and (2) wells with produced

liquid including water and thin oil (oil viscosity < 150 MPa · S).

The main swabbing tool is a tubing swab, which can be a valveless swab (that is, two-flapper swab, Figure 8-69) or a swab with valve (Figure 8-70).

The swab connected to wire rope is run in by well serving unit, drilling rig, or electrical hoist through the lower sheave and derrick crown and is moved up and down in tubing. The liquid above the swab is discharged out of the wellhead while pulling the swab up, and a low pressure is caused below the swab; thus, the liquid in the reservoir is gradually drawn to the surface.

Swabbing has not only pressure-reducing action and induction flow action, but it also has reservoir blocking removing action. The swabbing efficiency is dependent on swabbing

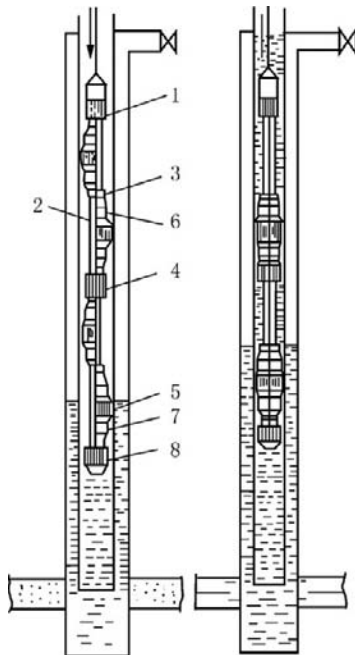


**FIGURE 8-69** Valveless swab. 1, upper sub; 2, rubber slide stem; 3, semiround baffle plate; 4, middle sub; 5, rubber; 6, upper gland of rubber; 7, lower gland of rubber; 8, tail plug.

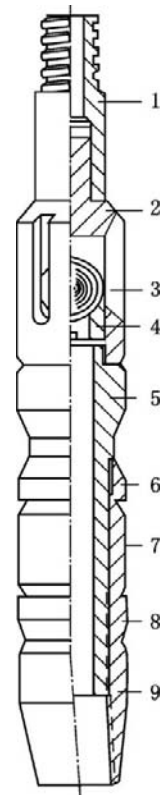


**FIGURE 8-70** Swab with valve. 1, connector; 2, valve housing; 3, valve ball; 4, valve seat; 5, base pipe; 6, upper gland of rubber; 7, rubber; 8, lower gland of rubber; 9, clamp cap.

strength, which is related to swabbing speed, the degree of sealing between swab and tubing wall, and the submergence of swab. Rational swabbing technology parameters should be determined by calculation in accordance with the requirements of flowing back.

For a low-productivity nonflowing well of a low-permeability reservoir with reservoir pressure lower than hydrostatic column pressure, the bailing method is also used for unloading. The main tool is a bailer, which is run to a depth below the liquid level in the well on wire rope. The liquid in the well is bailed to the surface repeatedly in order to reduce the liquid column backpressure on reservoir.

### Flowing Back by Gas Lift

Gas is pressed into the well by a high-pressure gas compressor under a lower wellhead injection pressure to discharge the liquid in the well for a short time by the expansion energy of gas, thus achieving induced flow.

Air is prohibited to be used for gas lift in consideration of safety. If air is used, air may mix with natural gas in the well and an explosion may be generated by open fire when natural gas makes up 5% to 15% of the total mixed gas volume. Therefore, only nitrogen gas and natural gas can be used for gas lift.

This method has the following merits: (1) one trip for unloading; (2) greater unloading depth and high unloading efficiency; (3) short unloading period; (4) low degree of formation damage and high effectiveness of acidizing and fracturing; and (5) relatively low cost.

The demerits include: (1) environmental pollution at the surface; (2) a certain degree of formation damage (formation damage generated by bottomhole backpressure during operation and formation blocking due to the rapid formation of fluid back-disgorging with the rapid decrease of the liquid column pressure when the liquid in the well is discharged); and (3) higher cost.

This method is appropriate for: (1) spent acid flowback by gas lift in an acid-fractured well; (2) unloading of flowing well with bottomhole

liquid storage; (3) causing underbalance in the wellbore for underbalanced perforating; (4) induction flow for putting the well into production, formation test, production test, and so on. The most obvious feature of unloading by gas lift is that the backpressure of the liquid in the well may be rapidly reduced. Thus this method is only appropriate for oil wells of firmly consolidated sandstone and carbonatite. For unconsolidated sandstone, gas lift depth and unloading speed should be appropriately controlled in order to prevent sand production due to the structural failure of the reservoir.

The types of flowing back by gas lift are described in the following section.

**Conventional Gas-Lift Unloading.** Conventional gas-lift unloading can be normal circulation gas-lift unloading or reverse circulation gas-lift unloading. When normal circulation gas-lift unloading is adopted, gas is pressed into the tubing and gas-liquid mixture is lifted to the surface through the tubing-casing annulus. When reverse circulation gas-lift unloading is adopted, gas is injected into the tubing-casing annulus and the gas-liquid mixture is lifted to the surface through the tubing (Figure 8-71).

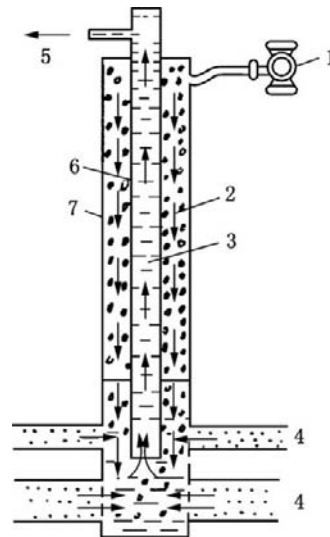


**FIGURE 8-71** Induced flow by gas lift. 1, high-pressure gas injecting pump; 2, injected gas; 3, gas-liquid column; 4, reservoir; 5, oil flowout; 6, tubing; 7, casing.

The conventional gas-lift design is mainly based on the necessary descended depth of the liquid column in the well and the maximum working pressure of the gas compressor. The tubing and other downhole tools should have strengths that should be able to bear the pressure difference. A blank tubing is generally used.

**Multistage Gas-Lift Valve Unloading.** A string with multistage gas-lift valves is designed in accordance with the requirements of unloading. The type of gas-lift valve should be selected, and the setting depths of the valves of stages should be calculated. Refer to the calculation method of gas-lift production design.

The feature of multistage gas-lift valve unloading is that the backpressure of the liquid column in the well is reduced step by step, the reduction of backpressure is more mitigative in comparison with the rapid reduction of the backpressure of conventional gas-lift, and the degree of damage caused is low (Figure 8-72).

**Coiled-Tubing Gas-Lift Unloading.** Coiled tubing is run into production tubing string by a coiled tubing truck and then interconnected with a liquid nitrogen pump truck or nitrogen manufacturing trailer. The low-pressure liquid nitrogen pressure is increased to a high pressure by using a liquid nitrogen pump truck. The high-pressure liquid nitrogen is then vaporized. The nitrogen is injected into the production tubing string from the coiled tubing. The

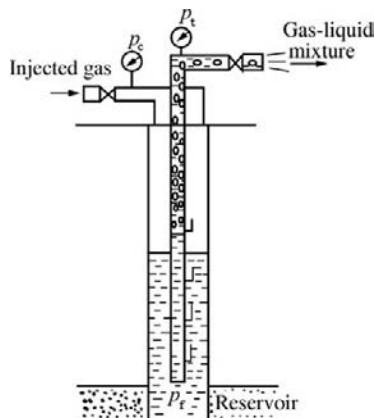


FIGURE 8-72 Induced flow by gas lift valves.

high-pressure nitrogen gas formed lifts the killing fluid in the production tubing string to the surface from the annulus between coiled tubing and production tubing string, thus reducing the backpressure of killing fluid on the reservoir and achieving induced flow.

The features of coiled tubing unloading include: (1) low degree of formation damage due to the gradual reduction of bottomhole backpressure by downward unloading step by step from wellhead and a high unloading speed (discharging the liquid column of 1000 m only takes about 0.5 hour); (2) good pressure tight property (pressure tight grade is up to 35 MPa and 70 MPa); and (3) great unloading depth (the maximum depth is up to 6000 m).

**Nitrogen Gas Gas-Lift Unloading.** A nitrogen manufacturing trailer or liquid nitrogen pump truck can be used for nitrogen gas gas-lift unloading (Table 8-39).

Nitrogen generator trailer unloading uses the advanced molecular film technique to directly separate nitrogen gas from air at atmospheric temperatures. It is an economical and convenient method, and reverse circulation gas lift is generally adopted. Liquid nitrogen pump truck unloading uses liquid nitrogen as gas source, and normal circulation gas lift is generally adopted due to the economical liquid nitrogen volume and the friction resistance that is generated in tubing and causes a low backpressure favorable for reservoir protection. For a complicated well with packer, both liquid nitrogen pump truck and coiled tubing truck are used. This method can be used not only for single-point gas lift but also can be used for gas lift while running to take the effect of a valve. It is mainly used for unloading and induced flow in packer wells and unloading in testing wells, production test and drillstem test wells, and complicated wells.

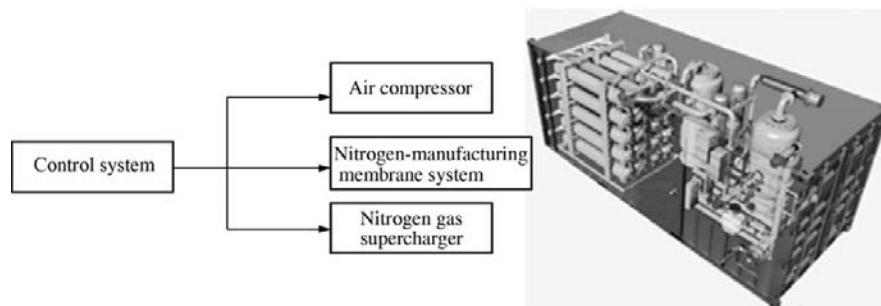
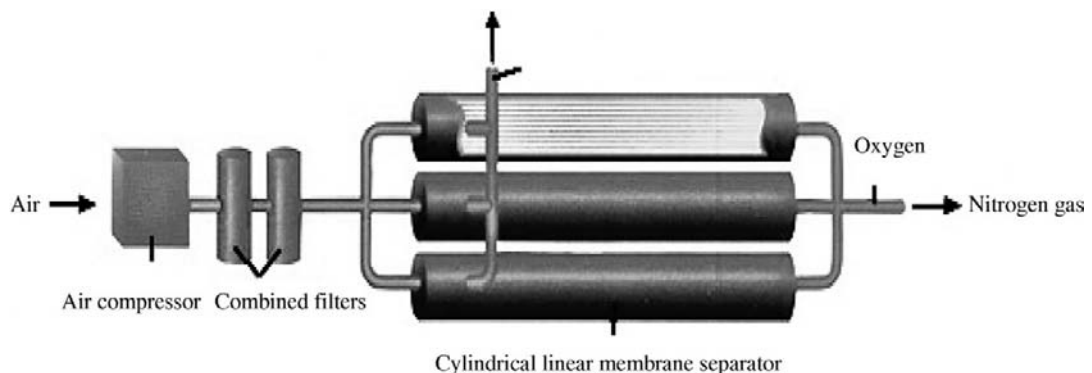
A liquid nitrogen pump truck is a main corollary equipment of coiled tubing truck gas lift. It includes liquid nitrogen tank, high-pressure triplex pump, heat recovery type evaporating pump, control device, and instruments. Its main functions include: storing and transporting

**TABLE 8-39** Property Comparison between Liquid Nitrogen Pump Truck and Nitrogen Generator Trailer

Equipment	Model Number	Nitrogen Gas Pumping Rate (m <sup>3</sup> /min)	Working Pressure (MPa)	Nitrogen Gas Purity (%)	Main Uses
Liquid nitrogen pump truck	NPT 360 HR15	169	103.5	>90	Fracturing, acidizing and gas lift, and so on
Nitrogen generator trailer	500NGU-TL2E	14.16	35	>95	Gas unloading and displacement, and so on

liquid nitrogen, boosting low-pressure liquid nitrogen into high-pressure liquid nitrogen, evaporating high-pressure liquid nitrogen, and injecting it into the well. The basic parameters include: liquid nitrogen tank volume of 7.57 m<sup>3</sup>; maximum operating pressure of 105 MPa; and maximum pumping rate of 10,194.1 m<sup>3</sup>/h.

A nitrogen generator trailer (Figure 8-73) adopts membrane separation technology to separate the air that enters the membrane separator into nitrogen gas and oxygen gas (Figure 8-74). A diesel engine drives the air compressor. The air compressed to a certain pressure passes through an air purification system to remove the oil and water in air. The clean compressed air

**FIGURE 8-73** Nitrogen manufacturing trailer systems.**FIGURE 8-74** Membrane separation principle.

enters the membrane system. Oxygen gas and water steam with high diffusion coefficient pass rapidly through the membrane wall, whereas gas with low diffusion coefficient and low ability of passing through the membrane may generate required nitrogen gas at the end of the membrane. After passing through the supercharger, the nitrogen gas reaches design pressure. This equipment has good performance, high pumping rate, high pumping pressure, and long continuous operation time. The main technical parameters include: maximum pumping rate of 10–15 m<sup>3</sup>/min; maximum operating pressure of 26–35 MPa; and nitrogen gas purity high than 95%.

A nitrogen manufacturing trailer is suitable for conventional gas-lift unloading and has high unloading speed and short operation time. It is appropriate for various reservoir pressures. It is safe and reliable for high-pressure wells, while it can form a greater underbalance favorable for putting a flowing well into production. In combination with a coiled tubing truck, it has high unloading speed and high efficiency in superdeep wells and wells with high liquid column pressure and complicated string structure. The nitrogen gas volumes required are shown in Table 8-40.

### Flowing Back by Aerated Water

The killing fluid in the well is displaced with aerated water, and the backpressure of the liquid column in the well is reduced because the mixture density is lower than the reservoir pressure coefficient. The mixture density can be adjusted by controlling gas pressure and flow rate, so that it can control the reduced degree of bottomhole backpressure. This method is appropriate to oil wells in which both unloading by displaced flow and unloading by gas lift are inappropriate.

When the density  $\rho_1$  of aerated water injected is lower than killing fluid density  $\rho_2$  and the induced flow can still not be achieved by the whole aerated water column with density  $\rho_2$  in the well, the gas rate can be increased in order to reduce aerated water density to  $\rho_2$  or to pure gas density (Figure 8-75).

### Flowing Back by Foam

A surfactant that can form foam when it meets water and is known as a foaming agent is injected from the wellhead to the bottomhole. After bottomhole load water contacts with the foaming agent, a large quantity of water-containing foam may be generated with the aid of the agitation of natural gas flow and carried to the surface by gas flow.

The main factors that affect unloading by foam include the type and concentration of foaming agent, the salt content (total salinity) of bottomhole load water, and condensate content. Salt and condensate are themselves anti-foamers and may affect the foaming effectiveness of the foaming agent, thus reducing foamability to a great extent.

Foam fluid has the following features due to its unique structure: low hydrostatic column pressure; low fluid loss; strong proppant-carrying capacity; low friction loss; strong cleanup ability; low degree of formation damage; and so on. Therefore, foam fluid has widely applied to drilling well completion, well servicing, and stimulation (such as unloading by foam and underbalanced sand washing) of low-pressure, lost-circulation, and water-sensitive reservoirs.

The merits include: (1) high unloading speed and efficiency; (2) ability to select any unloading depth if allowed by casing strength; and (3) suitability for the wellbore of the casing of any size.

The demerits include: (1) high tonnage and low cross-country performance of equipment, which may be inappropriate for remote exploration wells; (2) two types of formation damage (low-temperature damage and surging damage); (3) high operation cost; (4) easy environmental pollution; and (5) unsuitability for wells with packer.

Foam fluid is a dispersed system formed by dispersing insoluble or microsoluble gas in liquid. In a dispersed system, gas is the dispersed phase, while liquid is the dispersed medium.

The first condition of foam generation is the contact between gas and liquid. In addition, some surfactants (foaming agents) should be added in order to stabilize foam.

**TABLE 8-40 Nitrogen Gas Volume (m<sup>3</sup>) Required to Displace the Liquid in Tubing with Nitrogen Gas**

Well Depth (m)	Wellhead Pressure (MPa)													
	5	10	15	20	25	30	35	40	45	50	55	60	65	70
100	5061	10118	15171	20216	25256	30310	35344	40375	45403	50249	55454	60474	65429	70509
200	5121	10237	15342	20450	25539	30620	35687	44074	45805	50856	55906	60946	65982	71016
300	5182	10355	15513	20675	25807	30928	36029	41121	46205	51282	56357	61416	66471	71521
400	5243	10473	15699	20900	26075	31235	36370	41493	46604	51707	56805	61184	66957	72024
500	5304	10592	15873	21124	26343	31542	36710	41863	47002	52130	57252	62351	67442	72526
600	5364	10710	16047	21348	26610	31847	37049	42231	47398	52551	57697	62816	67925	73025
700	5425	10829	16221	21571	26877	32151	37387	42599	47793	52973	58141	63278	68405	73523
800	5486	10947	16395	21749	27143	32455	37722	42965	48187	53390	58582	63740	68884	74018
900	5547	11066	16569	22017	27408	32757	38057	43330	48579	53807	59022	64199	69362	74512
1000	5608	11185	16724	22239	27673	33058	38391	43694	48969	54223	59460	64656	69837	75004
1100	5669	11303	16916	22461	27937	33358	38724	44056	49359	54637	59896	65112	70310	75493
1200	5731	11422	17089	22683	28200	33657	39055	44417	49747	55050	60331	65566	70782	75967
1300	5792	11540	17262	22904	28463	33955	39385	44777	50134	55461	60764	66004	71236	76451
1400	5853	11659	17434	23124	28725	34252	39714	45135	50519	55871	61180	66452	71702	76934
1500	5914	11777	17606	23344	28986	34547	40042	45492	50903	56280	61608	66899	72166	77414
1600	5975	11895	17778	23563	29246	34842	40369	45848	51285	56673	62034	67343	72629	77892
1700	6036	12014	17950	23782	29506	35136	40695	46203	51666	57708	62458	67786	73089	78369
1800	6098	12132	18122	24001	29765	35428	41019	46556	52046	57481	62880	68228	73548	78843
1900	6159	12250	18293	24218	30023	35720	41342	46908	52410	57882	63301	68667	74005	79361
2000	6220	12368	18463	24435	30287	36010	41664	47259	52786	58282	63720	69105	74460	79787
2100	6281	12486	18634	24652	30542	36300	41985	47608	53161	58681	64183	69541	74913	80257
2200	6342	12604	18804	24868	30769	36588	42305	47924	53535	59078	64553	69976	75365	80724
2300	6404	12722	18973	25083	31049	36875	42623	48288	53907	59474	64968	70408	75814	81190
2400	6465	12854	19143	25298	31300	37161	42940	48633	54277	59869	65308	70839	76263	81654
2500	6526	12958	19311	25512	31551	37447	43257	48977	54647	60271	65791	71269	76709	82116
2600	6587	13075	19480	25752	31802	37731	43572	49319	55015	60661	66201	71697	77154	82577
2700	6648	13193	19648	25938	32051	38014	43817	49611	55382	61048	66609	72123	77597	83036
2800	6709	13310	19816	26150	32299	38296	44184	50001	55748	61435	67015	72547	78039	83494
2900	6770	13427	19983	26361	32546	38577	44495	50340	56112	61820	67420	72971	78479	83949
3000	6832	13544	20150	26572	32793	38857	44805	50677	56475	62220	67823	73392	78917	84404
3100	6893	13661	20316	26782	33038	39136	45114	51014	56837	62585	68225	73812	79354	84856
3200	6954	13778	20482	26991	33286	39414	45422	51349	57198	62968	68625	74231	79790	85307
3300	7015	13895	20647	27199	33527	39691	45729	51684	57557	63345	69024	74648	80224	85757
3400	7076	14012	20812	27407	33769	39967	46035	52017	57916	63723	69421	75063	80656	86205
3500	7137	14128	20977	27164	34011	40241	46339	52349	58273	64099	69817	75477	81087	86651

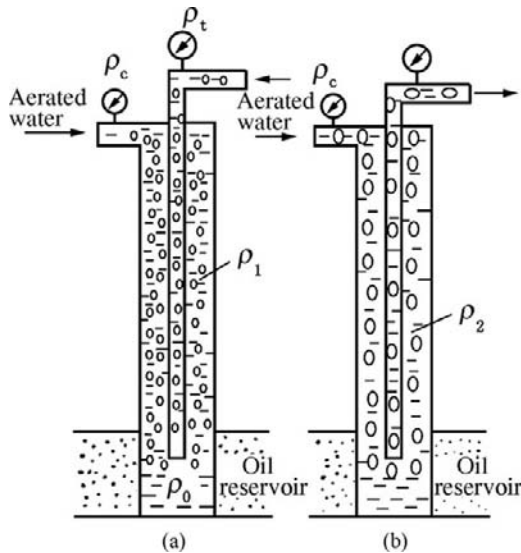


**FIGURE 8-75** Flowing back by aerated water. (a) Injecting the aerated water with density  $\rho_1$  into annulus; (b) then injecting the aerated water with density  $\rho_2$  ( $\rho_2 < \rho_1$ ).

A foaming agent is used for reducing the surface tension of liquid phase, increasing the strength and elasticity of foam liquid film and increasing the surface viscosity of liquid film, thus increasing foam stability.

Foam quality means the ratio of the gas volume in foam fluid to the foam volume under a certain pressure at a certain temperature.

### Foam Composition

#### 1. Gas phase

Air, nitrogen gas, carbon dioxide, or natural gas is adopted.

Nitrogen gas is a colorless, tasteless, non-toxic inert gas under atmospheric pressure at atmospheric temperature. It cannot be burned and may be slightly dissolved in most liquids. Nitrogen gas density is  $1.25 \text{ kg/m}^3$  under atmospheric pressure at the temperature of  $4^\circ\text{C}$  and the solubility in water is about 1/10 of that of carbon dioxide. Thus emulsification and precipitation, which may form blocking in the reservoir, can be avoided. Carbon dioxide has high solubility and reacts easily, so that the foam formed has a low stability. And carbon dioxide has a higher compression ratio,

so the gas-liquid ratio required by nitrogen gas is lower than that required by carbon dioxide under a given foam quality. In addition, the on-site nitrogen gas preparation technique has been rapidly developed in recent years. Therefore, nitrogen gas is applied more widely at present. The advantages of nitrogen gas include: (1) high safety with no explosion and no combustion; (2) inert gas with no corrosion; (3) high liquefaction compression ratio, which favors storage and transportation; (4) high gasification expansion ratio, high expansion energization property, and high cleanup ability in the reservoir and well; and (5) low gas density (in comparison with other common gases), which favors reducing well liquid column pressure, thus favoring flowing back.

#### 2. Liquid phase

There are many types of liquid phases of foam fluid. They can be water-based, alcohol-based, hydrocarbon-based, or acid-based.

#### 3. Foaming agent

Foaming agents mainly include non-ionic and ionic surfactants.

##### a. Requirements for foaming agent

- (1) High foamability. A great quantity of foam can be generated after gas contacts liquid.
- (2) High foam-stabilizing ability. The foam generated has stable performance even if it is under the conditions of pumping and shearing.
- (3) Good compatibility with the rock minerals and fluids of the reservoir. Foaming agent should have stable performance and no formation damage.
- (4) Low pour point, good biodegradability, and low toxicity. Foam should be easy to break when pressure is released.
- (5) Low volume, low cost, and wide source of goods.

##### b. Commonly used foaming agents

Anionic surfactant is predominant in the commonly used foaming agents. The typical anionic surfactants include alkyl

sulfate, alkane sulfonate, and alkyl aryl sulfonate.

Anionic surfactants such as alkyl sulfate, alkane sulfonate, and alkyl aryl sulfonate are generally used during production, formation test, and well servicing of watered oil wells in Russia. The foam formed by alkane sulfonate has the highest stability. The hydrophile-lipophile balance number has been used for rapidly evaluating foaming agents. It is considered that foaming agent (such as dodecyl sulfate) with the hydrophile-lipophile balance number of 9–15 has high foamability.

The commonly used foaming agents in the United States and Canada are respectively shown in Table 8-41 and Table 8-42.

Hydrocarbon base foam is more difficult to foam. Fluorocarbon has often been used as a foaming agent. Because it has high cost and may inhibit crude oil cracking and catalysis, a silicone type (that is, organic siloxane type) foaming agent is substituted for it at present (Table 8-43).

**Foam Stability.** Foam stability is the main property of foam fluid. Foam is a dispersion system composed of gas bubbles and has great free energy. In the thermodynamic sense, foam is an

**TABLE 8-41** Foaming Agents Recommended by Halliburton

No.	Type of Foam	Foaming Agent	Electrical Behavior	Foaming Agent Usage Volume (L/m <sup>3</sup> )	
				Low Temperature	High Temperature
1	Water-based foam	HOWCO-suds	(-)	2 ~ 5/93°C	6 ~ 10/121°C
2		SEM-7	(-)	2 ~ 5/93°C	6 ~ 10/149°C
3		TRI-S	(-)	2 ~ 5/93°C	6 ~ 10/135°C
4		AQF-1	(0)	2 ~ 5/93°C	Not recommended
5		Pen-SE	(0)	5 ~ 10/93°C	Not recommended
6		HC-2	(0)(+)	2 ~ 5/93°C	6 ~ 10/149°C
7	Acid-based foam	Pen-SE	(0)	10/93°C	10/121°C
8		HC-2	(0)(+)	5 ~ 10/93°C	
9	Alcohol + water (alcohol content = 50%)	SEM-7	(-)	4 ~ 6/79°C	Not recommended
10		AQF-1	(0)	5 ~ 7/79°C	Not recommended
11		SEM-7	(-)	4 ~ 6/79°C	10/149°C
12		AQF-1	(0)	4 ~ 5/79°C	Not recommended
13	Hydrocarbon-based foam	OFA-2	(0)	2/88°C	

**TABLE 8-42** Foaming Agents Recommended by Nowsco

No.	Type and Quality of Foam	Foaming Agent	Usage Volume (L/m <sup>3</sup> )
1	Water-based foam (Foam quality = 75%, Gas phase: N <sub>2</sub> )	SF-1	10
2	Oil-based foam (Foam quality = 75%, Gas phase: N <sub>2</sub> )	SF-3	10
3	Acid-based foam (Foam quality = 75%, Gas phase: N <sub>2</sub> )	SF-2	10
4	Compounded foam (Foam quality = 65-90%, Gas phase: CO <sub>2</sub> )	SF-10	10
5	CO <sub>2</sub> foamed acid (Foam quality = 80%)	SF-10	10

Note: SF-1: anionic surfactant (polyoxyethylated alkyl alcohol sodium sulfonate); SF-2: non-ionic surfactant (alkyl, phenyl polyoxyethylene); SF-3: compounded fluorine-containing surfactant (non-ionic-anionic); SF-10: compounded surfactant (non-ionic surfactant is predominant).

TABLE 8-43 Foamability of Silicone-Type Foaming Agent

Base Fluid	Silicone Polymer (1% Volume)	Foam Volume (ml)	Foam Quality (%)	Half-Life Period of Foam (s)
Kerosene	Dow Coming 3011 foaming agent	240	58	92
	Dow Coming 1250 surfactant	225	55	132
Diesel oil No. 2	3011 foaming agent	215	53	132
	1250 surfactant	220	54	152
Condensate	3011 foaming agent	270	63	15
	1250 surfactant	240	58	10
Xylene	3011 foaming agent	275	64	91
	1250 surfactant	310	68	80

unstable system. However, some measures can be taken to change the conditions and prolong the duration of existence, thus meeting the requirements of application.

The factors that affect foam stability mainly include:

1. Surface tension of the foaming solution. With the generation of foam, the surface area of liquid is increased and surface energy is increased. In accordance with the minimum free energy principle of Gibbs, the system always tends to lower surface energy state. Low surface tension may reduce the energy of the foam system, thus favoring the stabilization of foam.
2. Surface viscosity. Surface viscosity is generated by the interaction between hydrophilic groups of surfactant molecules in the unimolecular layer at surface and the hydration. High surface viscosity may form stable foam.
3. Solution viscosity. The addition of water-soluble polymer can increase solution viscosity and prolong the relaxation time of foam gravity unloading, the relaxation time of gas diffusion, and the half-life period of foam.
4. Pressure and bubble size distribution. Foam has different stabilities under different pressures. The higher the pressure, the more stable the foam.
5. Temperature. With the increase of temperature, the stability of foam may reduce.

**Foam-Generating Equipment.** The foam-generating equipment developed in China is the PC-160 foam operating truck, which is also a

data acquisition truck, consisting of foam generator and gas and liquid adjustment and measurement devices. The main parameters of foam operation, which include flow rate and pressure and the flow rate and pressure of liquid, are displayed on the instrument panel. After the base fluid of foam is mixed with gas, qualified foam can be obtained and pumped into the well for various operations such as drilling and well flushing. The liquid supply manifold and gas supply manifold on the operating truck have the regulating valve used for regulating flow rate and the check valve used for preventing gas and liquid from counterflowing. The liquid supply manifold also has a filter and vibration absorber.

This operating truck as a whole can be connected with the pipeline by using a quick coupler during operation, which makes operation quick and convenient. The data can be automatically acquired by the truck during foam operation. The main parameters of the truck include: (1) maximum working pressure (16 MPa); (2) gas flow rate (10–40 m<sup>3</sup>/min); (3) liquid flow rate (200–300 L/min); (4) inside diameter of the main line (50 mm or 2 in.); and (5) weight (2143 kg).

## REFERENCES

- [1] C.V. Millikan, C.V. Sidwell, Bottom-hole Pressures in Oil Wells, *Trans. AIME* 92 (1931) 194–205.
- [2] D.G. Hawthorn, Review of Subsurface Pressure Instruments, *Oil and Gas J.* April 20 16 (1993) 40.
- [3] M. Muskat, Use of Data on the Build-up of Bottom-hole Pressures, *Trans. AIME* 123 (1937) 44–48.

- [4] C.C. Miller, et al., The Estimation of Permeability and Reservoir Pressure from Bottom Hole Pressure Build-up Characteristics, *Trans. AIME* 189 (1950) 91–104.
- [5] D.R. Horner, Pressure Build-up in Wells, in: *Proc. Third World Pet. Cong.*, vol II, E. J. Brill, Leiden, 1951, p. 503.
- [6] A.F. Van Everdingen, The Skin Effect and Its Influence on the Productive Capacity of a Well, *Trans. AIME* 198 (1953) 171–176.
- [7] W. Hurst, Establishment of the Skin Effect and Its Impediment to Fluid Flow into a Wellbore, *Pet. Eng.* 25 (Oct) (1953) B–16.
- [8] R.G. Agarwal et al., An Investigation of Wellbore Storage and Skin Effect in Unsteady Liquid Flow: I. Analytical Treatment, *Soc. Pet. Eng. J. Sept.* (1970) 279–290; *Trans. AIME* 249.
- [9] A.C. Gringarten et al., A Comparison between Different Skin and Wellbore Storage Type-Curves for Early-Time Transient Analysis, Paper SPE 8205, Presented at the 54th Annual Technical Conference and Exhibition, Las Vegas, Nevada, Sept. 1979, pp. 23–26.
- [10] D. Bourdet, et al., A New Set of Type-Curves Simplifies Well Test Analysis, *World Oil*, May (1983) 95–106.
- [11] Tong Xianzhang, Pressure Build-up Curve Application in Oil and Gas Field Development, Petrochemical Industry Press, Beijing, 1984 (in Chinese).
- [12] Cheng Suimin, Serial Types of Formation Damage Evaluation Standard, *Gas Ind.* 3 1988 (in Chinese).
- [13] Zhuang Huinong, Graphic Analysis Method of Well Test Data, *Buried Hill J.* 4 (1993), 1 (1994), 2 (1994), 4 (1994) (in Chinese).
- [14] G.E. Barenblatt, et al., Basic Conception of the Theory of Homogeneous Liquids in Fissured Rocks, *JAMM (USSR)* 24 (5) (1960) 1286–1303.
- [15] J.E. Warren, P.J. Root, Behavior of Naturally Fractured Reservoirs, *SPE J. Sept.* (1963) 245.
- [16] H. Kazemi et al., The Interpretation of Interference Tests in Naturally Fractured Reservoir with Uniform Fracture Distribution, *SPE J. Dec.* 1969.
- [17] D. Bourdet, A.C. Gringarten, Determination of Fracture Volume and Block Size in Fractured Reservoirs by Type Curve Analysis, *SPE* 9293.
- [18] Zhu Yadong, Well Test Analysis in a Double Porosity Reservoir, *SPE* 14867.
- [19] D. Bourdet et al., Use of Pressure Derivation in Well Test Interpretation, *SPE* 12777.
- [20] A.C. Gringarten, Unsteady State Pressure Distributions Created by a Well with a Simple Infinite Conductivity Vertical Fracture, *SPE J. Aug.* (1974) 347–360; *Trans. AIME* 257.
- [21] F. Rodriguiz et al., Partially Penetrating Vertical Fractures Pressure Transient Behavior of a Finite-Conductivity Fracture, *SPE* 13057.
- [22] Liu Nengqiang, Applied Modern Well Test Interpretation Methods, Petroleum Industry Press, Beijing, 1992 (in Chinese).
- [23] Cheng Suimin, New Methods of Well Test Analysis for Early Time Data, *Oil and Gas Well Testing* 1 1992.
- [24] A.C. Gringarten, Computer-Aided Well Test Analysis, *SPE* 14099.
- [25] Compilation Group of Typical Cases of Chinese Oil and Gas Well Test Data Interpretation, Typical Cases of Chinese Oil and Gas Well Test Data Interpretation, Petroleum Industry Press, Beijing, 1994 (in Chinese).

## Well Completion Tubing String

### OUTLINE

#### 9.1 Oil Well Completion

##### Tubing String

- Separate-Layer Production Tubing String
- Sucker-Rod Pumping Well Production Tubing String
- Electrical Submersible Pump Well Production Tubing String
- Downhole Screw Pump Well Production System
- Jet Pump Well Production Tubing String
- Gas Lift Production Tubing String
  - Modes of Gas Lift*
  - Gas-Lift Tubing String*
- Hydraulic Piston Pump Well Production Tubing String
  - Classification*
  - Styles*
  - Tubing String*
- Separate-Layer Production Tubing String with Oil- and Gas-Expandable Openhole Packers and Screens
  - Adaptable Types of Downhole Fluid*
  - On-Site Application Cases*

#### 9.2 Gas Well Completion

- Tubing String
- Gas Production Well Tubing String

- Conventional Gas Well Completion Tubing String*
- High-Pressure High-Rate Gas Well Completion Tubing String*
- Sour Gas Well Completion Tubing String*
- High Acid Content Gas Well Completion Tubing String*
- Sour Gas Well Separate-Layer Production Tubing String*
- Tubing-Conveyed Perforating Gas Production Well Tubing String
- Water-Drainage Gas-Production Tubing String
  - Water-Drainage Gas Production by String Optimization*
  - Water-Drainage Gas Production by Foam*
  - Water-Drainage Gas Production by Pumping Unit*
  - Water-Drainage Gas Production by Gas Lift*
  - Water-Drainage Gas Production by Jet Pump*

- Water-Drainage Gas Production by Electric Submersible Pump*

#### 9.3 Separate-Layer Water Injection String

- Fixed Water Distribution String
  - Hollow Water Distribution Strings
    - Anchored Compensating Separate-Layer Water Injection String*
    - Self-Creeping Compensating Anticreeping Separate-Layer Water Injection String*
    - Other Hollow Water Distribution Strings*
  - Eccentric Water Distribution Strings
- #### 9.4 Heavy Oil Production Tubing String
- Conventional Steam Injection Tubing String
  - Sealing and Separate-Layer Steam Injection String
  - Nitrogen Heat-Insulation Cleanup Tubing String
  - Heavy Oil Huff-and-Puff and Pumping Tubing String
  - Straight Well Production Tubing String*

<i>Slant Well Production Tubing String</i>	<i>Matching of Surface Safety Valve with Subsurface Safety Valve</i>	<i>Deformation of Tubing String Due to Piston Effect</i>
SAGD Production Tubing String	<b>9.6 Tubing String Mechanics</b>	<i>Deformation of the Tubing String Due to Helical Buckling Effect</i>
Heavy-Oil Sand Clean-Out Cold-Flow Production Tubing String	Status Models of Tubing String	Strength Analysis of Tubing String
Hollow-Sucker-Rod Through-Pump Electric Heating Production Tubing String	Helical Inflexion State	String
Production Tubing String of Combined Jet Pump and Oil Well Pump	Analysis of Tubing String	<i>Tension Safety Factor</i>
<b>9.5 Completion Tubing String Safety System</b>	<i>Main Factors Affecting String Inflexion</i>	<i>Internal Pressure Factor and Collapse Safety Factor</i>
Subsurface Safety Valve	<i>Determination of Critical Inflexion Load on Tubing String</i>	<i>Three-Dimensional Combination Stress Analysis</i>
<i>Setting Depth</i>	<i>Contact Load under the Condition of Helical Buckling of Tubing String</i>	<i>Total Safety Factor</i>
<i>Casing Program</i>	Basic Models for Calculating the Deformation of Tubing String	<i>Determination of Ultimate Operational Parameters</i>
Matching Surface Safety Valve System	<i>Deformation of Tubing String Due to Temperature Effect</i>	<b>References</b>
<i>Surface Safety Valve</i>		

Well completion tubing string is an important component part of well completion engineering. It is the only passage during oil and gas production and water and gas injection. The scientific and practical design of well completion tubing string is directly related to the normal production of oil and gas wells, zonal injection, stimulation and water shutoff, and so on. In addition, it may reduce the working capacity of downhole operation and prolong the changeless period (no tripping of string within more than 20 years after the string is run in is required) and ensure the safety of oil and gas wells.

In recent years, well completion tubing string (especially well completion tubing string in high-pressure corrosive-medium-containing oil and gas wells) tends to use one string that can perform various downhole operations without tripping the string. Its functions include:

1. Combined perforating and well completion;
2. Selective staged acidizing, fracturing, and water shutoff;
3. Downhole staged water detection, pressure measurement, and testing;
4. Whole well or staged circulation, which can be achieved by the circulating sliding sleeve on string;
5. Preventing tubing-casing annulus pressure held and injecting corrosion inhibitor by the packers on the tops of reservoirs;
6. Snubbing service and downhole sliding sleeve switching by wire rope, small diameter wire rope, or coiled tubing;
7. Downhole safety valve installed on string and the performable plug dropping at the upper part of the tubing for changing the wellhead assembly or installing a blowout preventer in order to prevent blowout.

## 9.1 OIL WELL COMPLETION TUBING STRING

### Separate-Layer Production Tubing String

Separate-layer production technology can effectively prevent interlayer interference (especially the great interlayer pressure difference), keep

isostatic production of oil reservoirs, and enhance recovery efficiency.

The commonly used separate-layer production tubing strings include single separate-layer string (Figure 9-1) and dual separate-layer string (Figure 9-2). Figure 9-1b shows a tubing-casing separate-layer production tubing string.

### Sucker-Rod Pumping Well Production Tubing String

A sucker-rod pumping well production tubing string should meet the requirements of the type of pump, pump diameter, and well depth. The typical production tubing string is shown in Figure 9-3. A deep-pumping sucker rod pump well tubing string is shown in Figure 9-4. The production tubing string can be lower-reservoir sealing and upper-reservoir producing string,

upper-reservoir sealing and lower-reservoir producing string, middle-reservoir sealing and upper and lower-reservoir producing string, or upper and lower reservoir sealing and middle reservoir producing string, in accordance with the requirements of production (Figure 9-5).

### Electrical Submersible Pump Well Production Tubing String

The electrical submersible pump production system consists mainly of downhole unit, surface equipment, and electrical cable (Figure 9-6).

An electrical submersible pump should be above the top of the perforated interval; thus the liquid flows around the electric motor before it enters the electric submersible pump, and the motor can be cooled and protected from burning due to the failure of insulation material by

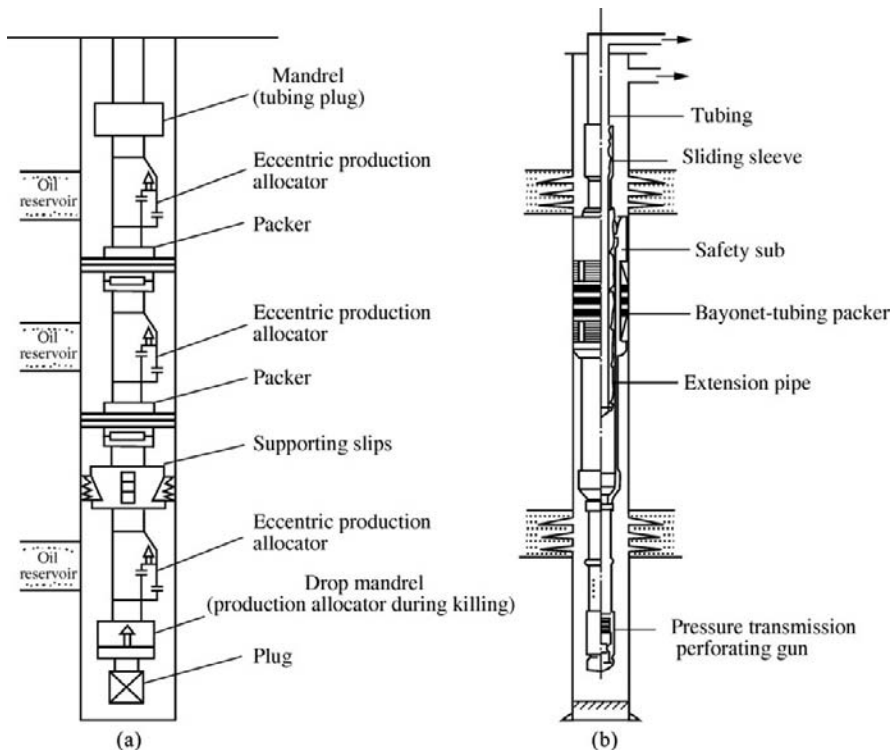


FIGURE 9-1 Single separate-layer string.

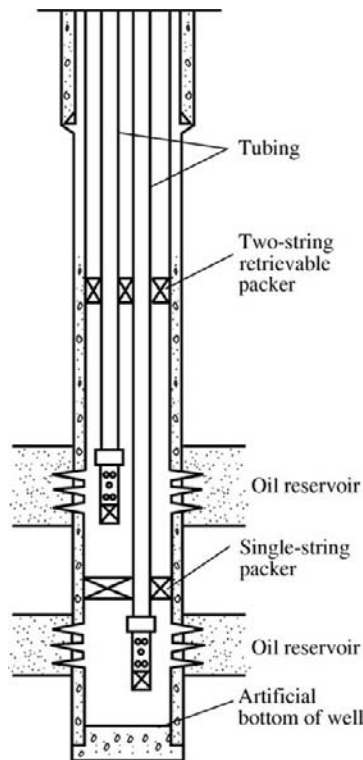


FIGURE 9-2 Dual separate-layer string.

temperature rise. If the electrical submersible pump unit must be below the reservoir, a diverting liner should be used (Figure 9-7).

For a dual-zone well that requires production testing, through-tubing perforating, or coiled tubing operation, the electrical submersible pump with Y-connector can be adopted (Figure 9-8).

A production tubing string can be a single-layer production string, a lower-reservoir sealing and upper-reservoir string, an upper-reservoir sealing and lower-reservoir producing string, or an upper- and lower-reservoir sealing and middle-reservoir producing string, in accordance with the requirements of production (Figure 9-9).

### Downhole Screw Pump Well Production System

The merits of a screw pump oil-production system include: (1) fewer moving components, high suction property, low hydraulic loss, and the

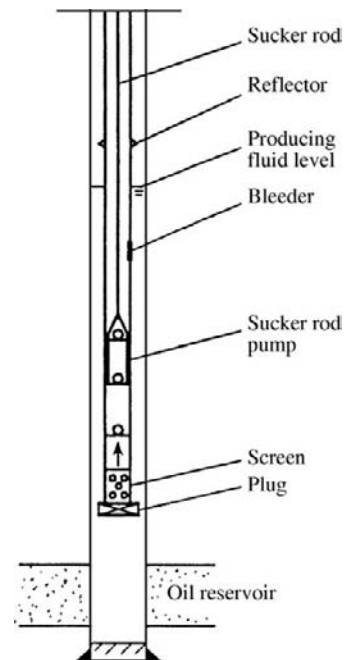


FIGURE 9-3 Typical sucker rod pump well production tubing string.

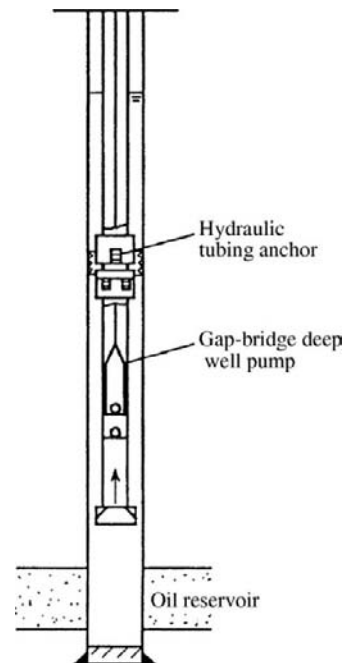
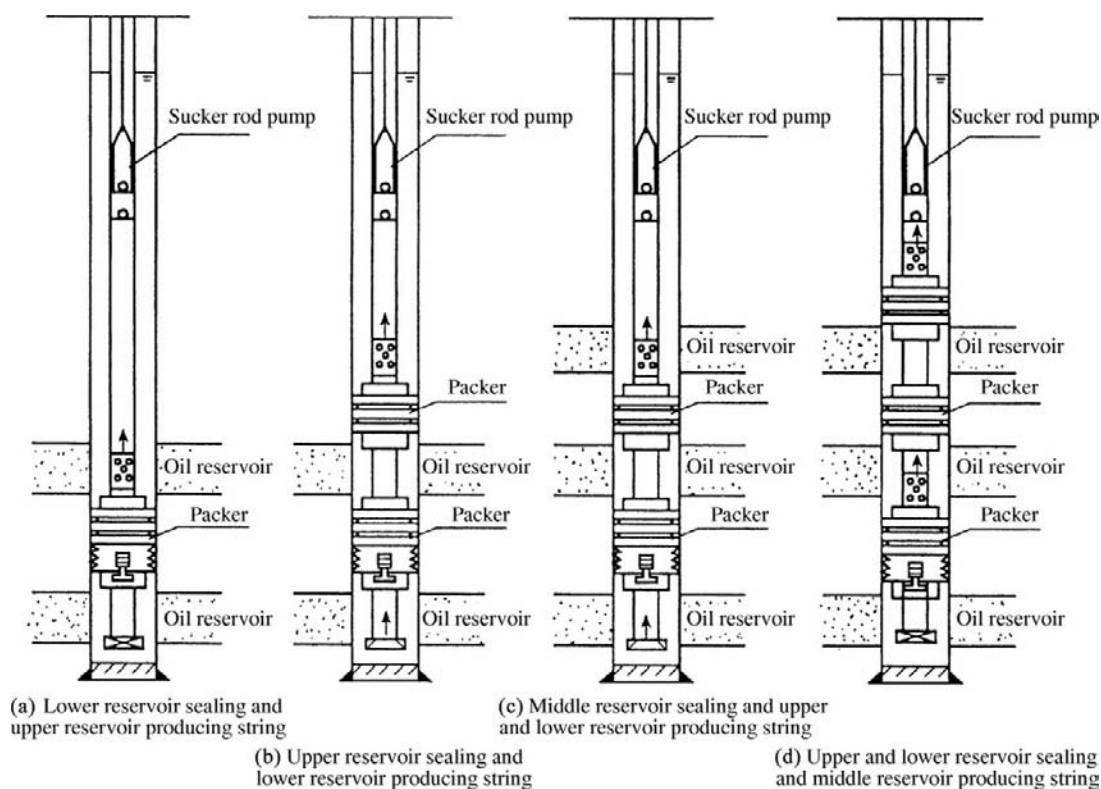


FIGURE 9-4 Deep-pumping sucker rod pump well tubing string.



**FIGURE 9-5** Sucker rod pump well production tubing string structures.

slight wear of flexible stator by sand grains due to the continuous and even suction and discharge of the medium, and (2) no gas lock because there is no suction valve and discharge valve.

A downhole screw pump can be driven by surface power, submersible electric motor, or hydraulic pressure (see Figure 9-10, Figure 9-11, and Figure 9-12).

A screw pump driven by surface power is suitable for heavy oil with higher viscosity, the liquid produced by polymer flooding, and heavy oil with sand (cold flow production of heavy oil). Screw pump oil pumping is achieved by the rotation of the sucker rod. For super-heavy or ultraheavy oil, heavy oil with excessive sand content, or a well with depth greater than 1400 m, sucker rod may bear the torque higher than the limit value

and will thread off or break; thus hollow sucker rod is adopted or a viscous-reducing agent is used to reduce heavy oil viscosity and friction resistance and control sand production. When screw pump well pumping is designed, the type selection and the composition of the sucker rod string and the torque and friction resistance should be calculated, and produced liquid viscosity, sand production, and drive head horsepower should also be considered. For super-heavy or ultraheavy oil wells with depth greater than 1400 m, prudent analyses and comparison are particularly required during the design process.

A downhole screw pump well production string can be a string with tubing or a tubingless string. The three types of tubingless screw pump well production string are shown in Figure 9-13.

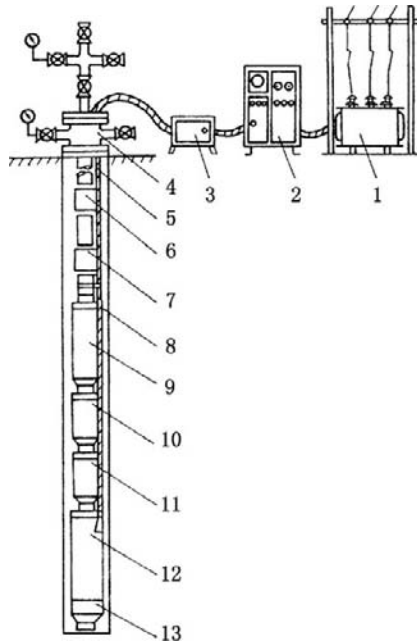


**FIGURE 9-6** Electrical submersible pump production system. 1, transformer; 2, control cabinet; 3, connection box; 4, wellhead assembly; 5, power cable; 6, pressure measurement valve; 7, check valve; 8, small flat cable; 9, multistage centrifugal pump; 10, oil-gas separator; 11, protector; 12, electric motor; 13, test device.

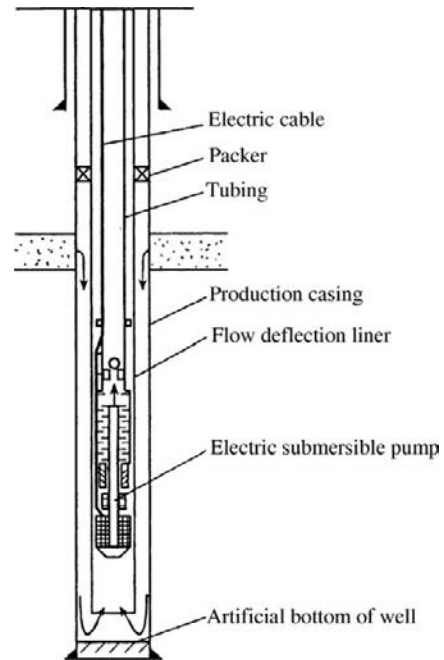


**FIGURE 9-7** Production tubing string for the electric submersible pump unit below the reservoir.

## Jet Pump Well Production Tubing String

The surface equipment and wellbore flow system of a jet pump production system are the same as that of an open hydraulic piston pump production system (see Figure 9-23 later in this chapter). Power fluid mixes with the fluid produced from the reservoir in the well and returns to the surface (Figure 9-14). The jet pump system can be drop-in type or fixed (Figure 9-15).

## Gas Lift Production Tubing String

The density of the liquid column from gas injection depth to the surface is reduced by injecting high-pressure gas into the wellbore, thus causing continuous oil and liquid flow from the reservoir

to the bottomhole and from the bottomhole to the surface.

**Modes of Gas Lift.** Gas lift can be continuous gas lift (Figure 9-16), intermittent gas lift (Figure 9-17), plunger gas lift (Figure 9-18), or chamber gas lift (Figure 9-19). Continuous gas lift is appropriate for oil wells with higher reservoir deliverability and higher production rate. Intermittent gas lift is appropriate for oil wells with low reservoir deliverability and low production rate. Plunger gas lift is a form of intermittent gas lift and appropriate mainly for wells with low bottomhole pressure and low liquid-producing capacity or wells with high bottomhole pressure and low liquid-producing capacity. Chamber gas lift is a closed intermittent gas lift and appropriate particularly for low-productivity wells and low-pressure high-productivity wells.

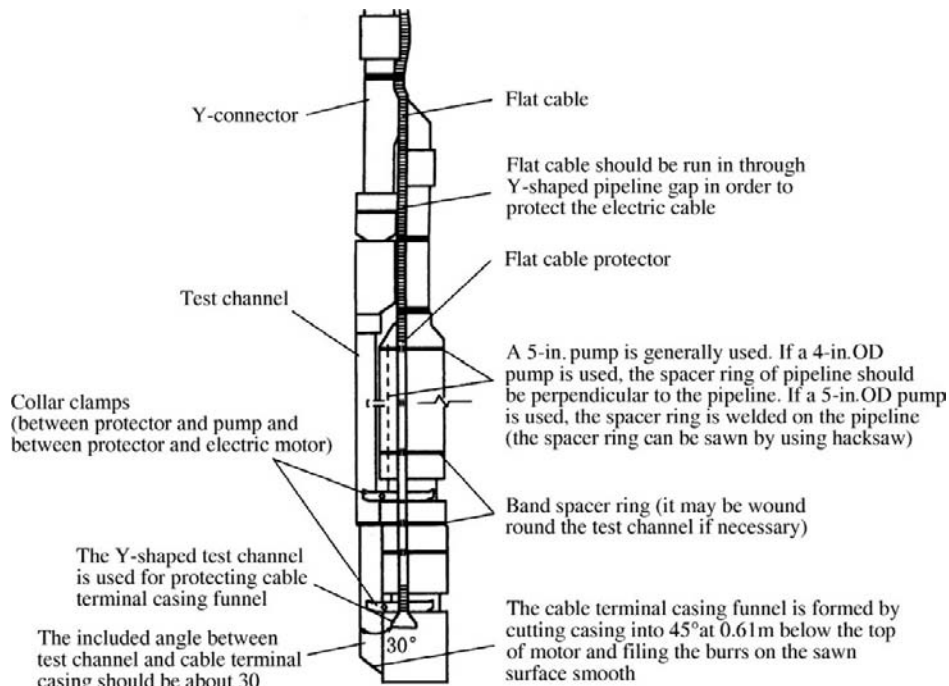


FIGURE 9-8 Y-connector for electric submersible pump.

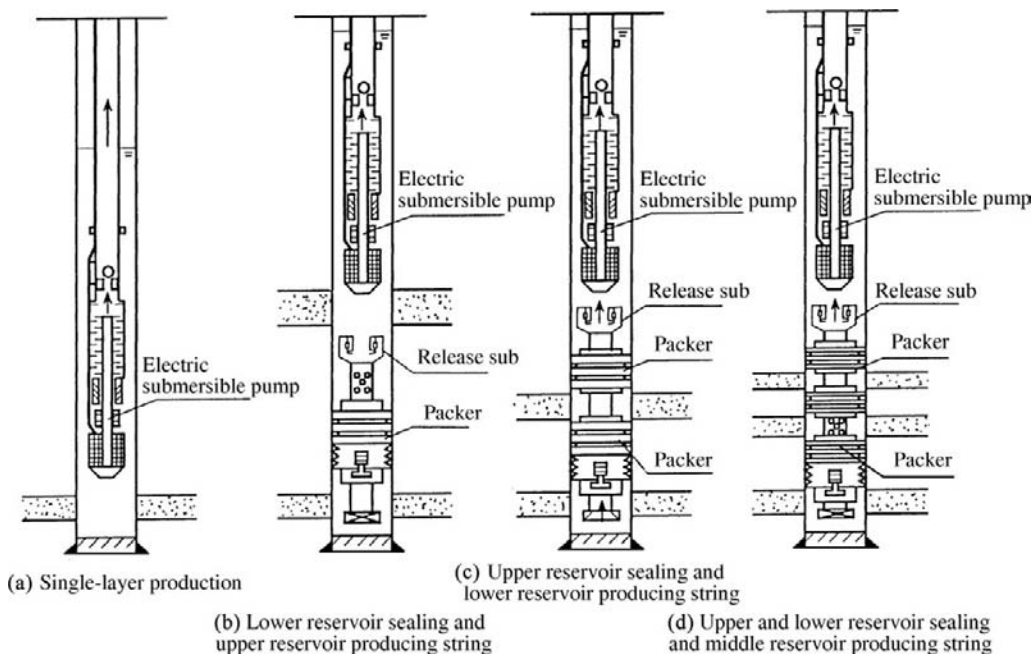
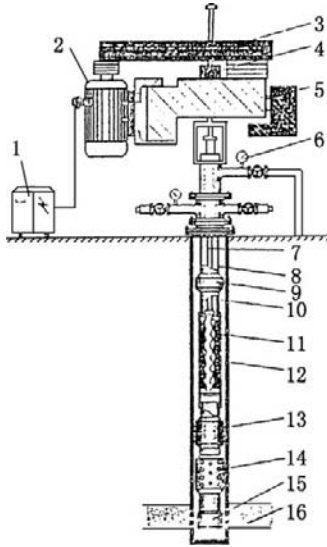
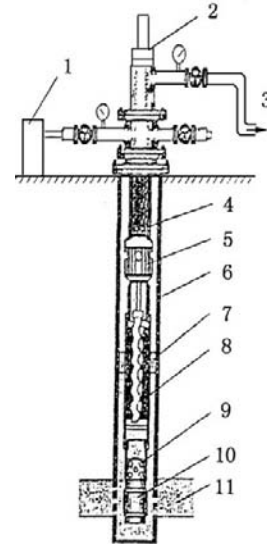


FIGURE 9-9 Electric submersible pump well production tubing string structures.



**FIGURE 9-10** Surface motor-driven screw pump production system. 1, electric control cabinet; 2, electric motor; 3, belt; 4, clamp; 5, counterbalance weight; 6, pressure gauge; 7, sucker rod; 8, tubing; 9, centralizer; 10, producing fluid level; 11, screw pump; 12, casing; 13, rotation-resisting anchor; 14, screen; 15, plug; 16, oil reservoir.



**FIGURE 9-12** Hydraulic drive screw pump production system. 1, power fluid; 2, wellhead assembly; 3, flowline; 4, tubing; 5, hydraulic motor; 6, casing; 7, packer; 8, screw pump; 9, screen; 10, plug; 11, oil reservoir.

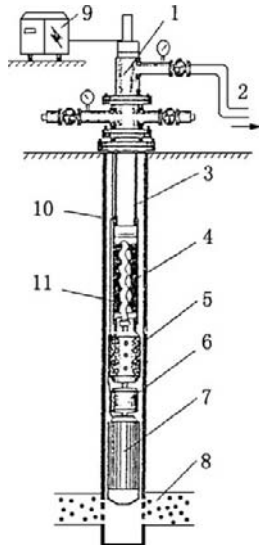


**FIGURE 9-11** Submersible electric motor-driven screw pump production system. 1, wellhead assembly; 2, oil outlet; 3, tubing; 4, screw pump; 5, screen; 6, protector; 7, downhole electric motor; 8, oil reservoir; 9, electric control cabinet; 10, casing; 11, electric cable.

### Gas-Lift Tubing String

#### 1. Single gas-lift string

Single gas-lift string can be chamber type (Figure 9-19) or open, semi-closed, or closed (Figure 9-20) type.

#### 2. Multiple tubing string gas lift

A multiple tubing string structure is used for simultaneous gas lift in the well with more than two reservoirs. This structure is composed of two parallel tubings (Figure 9-21) or concentric tubings (Figure 9-22). The dual-string structure is more commonly used and is generally used in wells with large diameter casing. The concentric string structure is mainly used in oil wells with smaller diameter casing. In comparison with the single-tubing string structure, the multitubing string structure is more complicated and has difficulties in downhole operation and gas lift valve design and configuration, in addition to having a high operating cost; thus, it is less used.

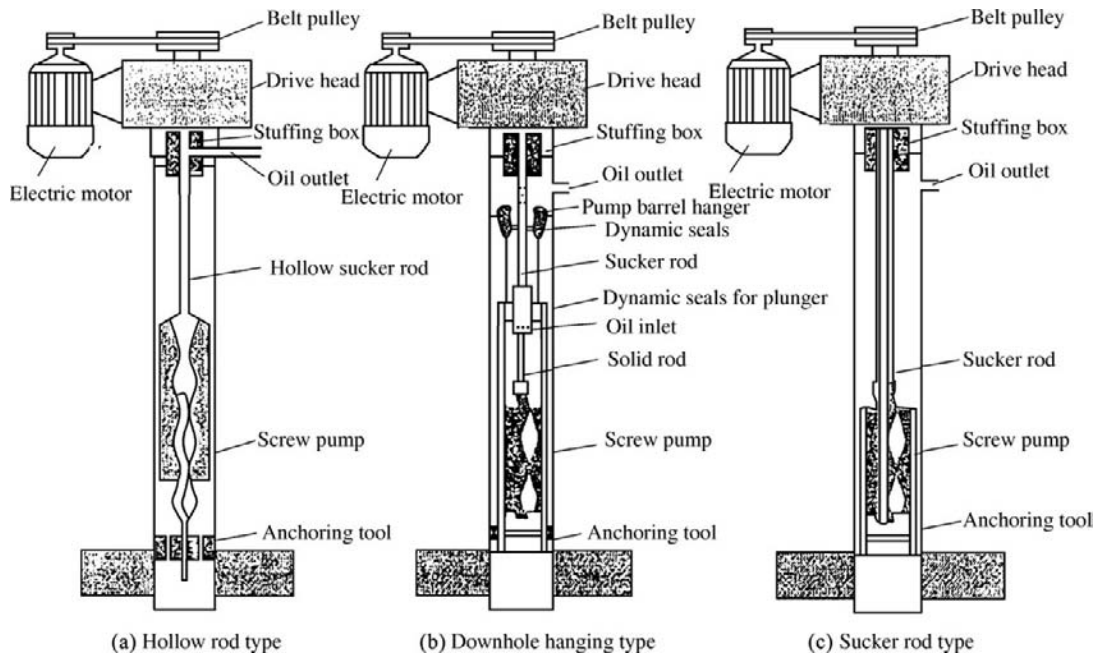


FIGURE 9-13 Tubingless screw pump string structures.

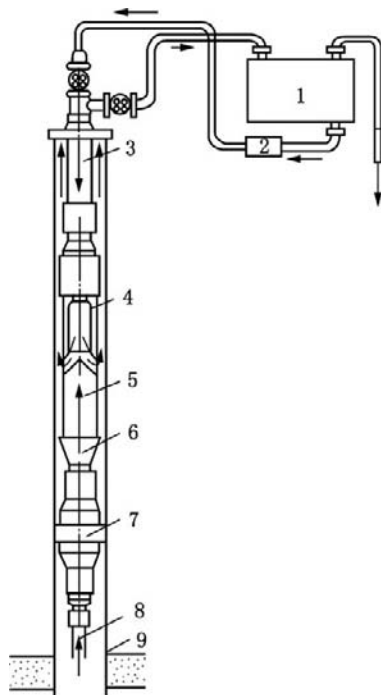


FIGURE 9-14 Jet pump assembly for oil well production. 1, separation equipment; 2, power pump; 3, tubing; 4, jet pump; 5, jet pump shell; 6, left hand threaded funnel; 7, packer; 8, tailpipe; 9, production casing.

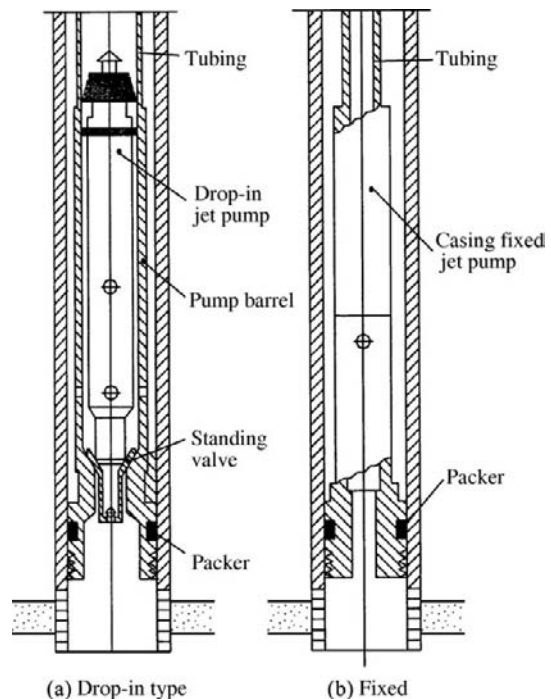


FIGURE 9-15 Jet pump installment.

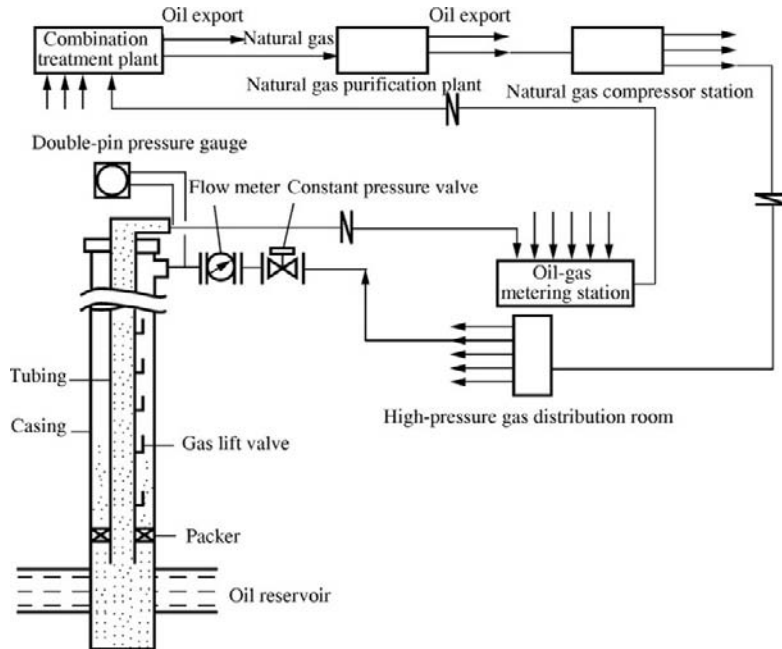


FIGURE 9-16 Continuous gas lift system.

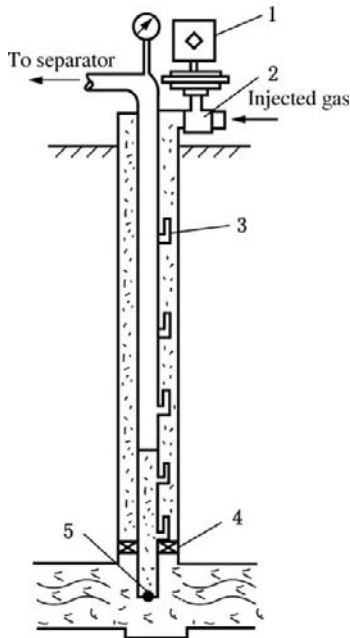


FIGURE 9-17 Intermittent gas lift system. 1, time controller; 2, pneumatic diaphragm control valve; 3, gas lift valve; 4, packer; 5, check valve.

### Hydraulic Piston Pump Well Production Tubing String

Power fluid is pumped into the well and drives the hydraulic motor to move reciprocally up and down. The hydraulic motor drives the plunger of the downhole pump to move reciprocally up and down and lift well fluid to the surface. A hydraulic piston pump is suitable for thin oil, high pour-point oil, conventional heavy oil, and deep well production (Figure 9-23).

**Classification.** The hydraulic piston pump oil-production system can have open power fluid system (Figure 9-24) or closed power fluid system (Figure 9-25).

**Styles.** Hydraulic piston pump oil-production can be fixed, inserted, or drop-in (Figure 9-26).

**Tubing String.** A hydraulic piston pump oil-production system has a downhole full-interval commingled single string (Figure 9-27), a single-interval separated-layer production tubing string (Figure 9-28), a closed parallel dual string (Figure 9-29a), a closed concentric dual string (Figure 9-29b), and so on.

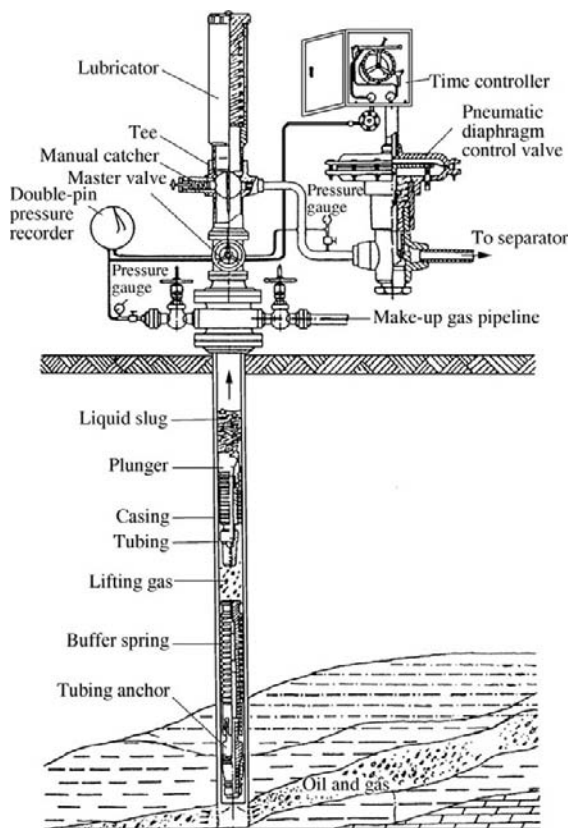


FIGURE 9-18 Plunger gas lift system.

### Separate-Layer Production Tubing String with Oil- and Gas-Expandable Openhole Packers and Screens

This type of string adopts an oil- and gas-expandable packer, which has no slips and no need of pressurization, rotation, pulling up, or setting down. The packing elements may expand and achieve sealing only if they meet oil or gas. If there is no crude oil or gas, light oil can be used for circulation, and the intervals are separated from each other. This type of string can be used for staged straight and horizontal well openhole screen completion and is convenient for operating. The length of interval can be up to 9 m. The occurrence of this type of packer is a great advance in well completion

engineering. Underbalanced drilling can be achieved, and the staged oil- and gas-expandable packer and slotted liner or sliding-sleeve switch completion can be achieved with no well killing, casing running, cementing, or perforating, thus reducing formation damage, favoring the increase of well productivity, simplifying the operating sequence of well completion, and reducing cost.

The packer consists of base pipe, packing element, and end ring (Figure 9-30). The expansion joint comes first out of the end ring and expands with the packing element, thus supporting the packing element and enhancing compressive resistance.

**Adaptable Types of Downhole Fluid.** Downhole fluid is available in four adaptable types:

1. Liquid hydrocarbon. The packer may expand in liquid hydrocarbon.
2. Oil-base drilling fluid, crude oil, condensate, diesel oil, heavy oil, and so on. The packer will expand rapidly in heavy oil and expand slowly in light oil.
3. Natural gas. The packer can expand in natural gas but the effective pressure-bearing ability is limited. After it expands in liquid hydrocarbon, it can keep stable in natural gas.
4. Water. The macromolecules of the packing element may not absorb the molecules of water, can keep stable in water, and can expand in the oil wells with high water content.

**Temperature Tolerance and Producing Pressure Drawdown Resisting Property.** Table 9-1 shows the temperature tolerance of oil- and gas-expandable packers. Figure 9-31 shows the producing pressure drawdown calculated and modified.

#### On-Site Application Cases

1. An oil field in the North Sea: Slim hole, layering, deflecting well, dogleg angle of 18°. A separate-layer production tubing string with 12 sets of oil- and gas-expandable packer plus screen have been run in (Figure 9-32).

The aquifer bed has been sealed off and water production has been obviously reduced.

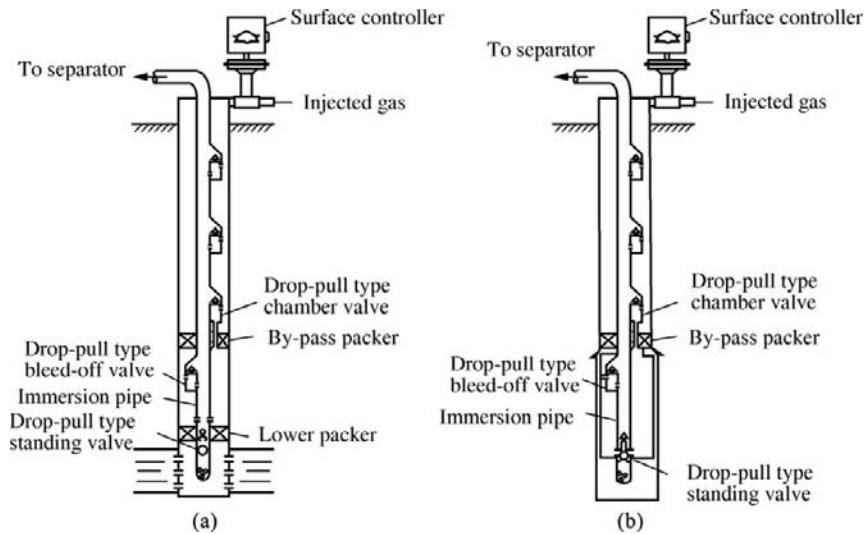


**FIGURE 9-19** Chamber gas lift string structures: (a) Packer type chamber structure; (b) Inserted chamber structure.

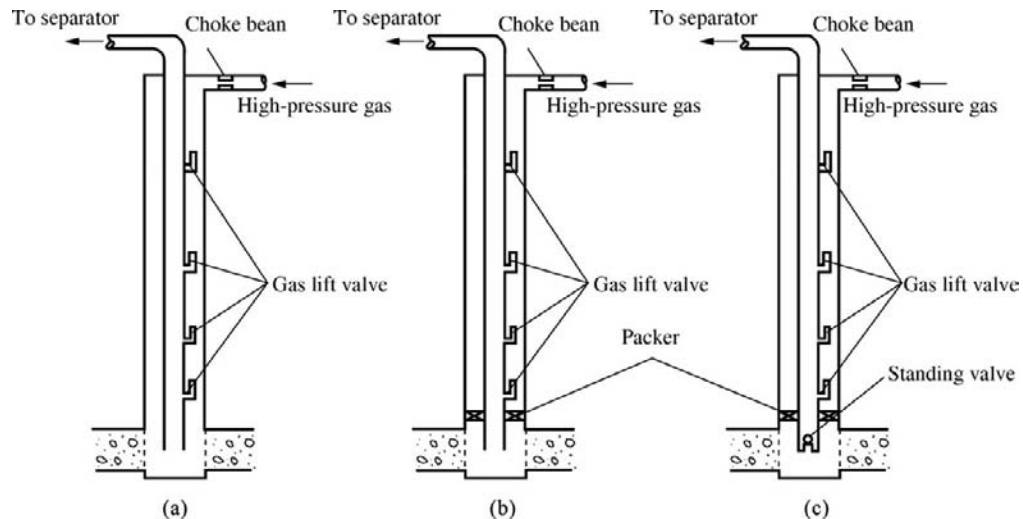


**FIGURE 9-20** Single tubing string structure in gas lift well: (a) open string; (b) semi-closed string; (c) closed string.

The cost has been reduced by 47%. Oil production has been increased.

- An oil field in the Middle East: Openhole horizontal well, layering. The oil- and gas-expandable packer has been run in. Sliding sleeve may be switched through electric cable

(Figure 9-33). The string has been run in for once. The cost has been reduced by 30% to 40%.

- An oil field in Saudi Arabia. A string with oil- and gas-expandable packers and the sliding sleeves for stimulation are shown in

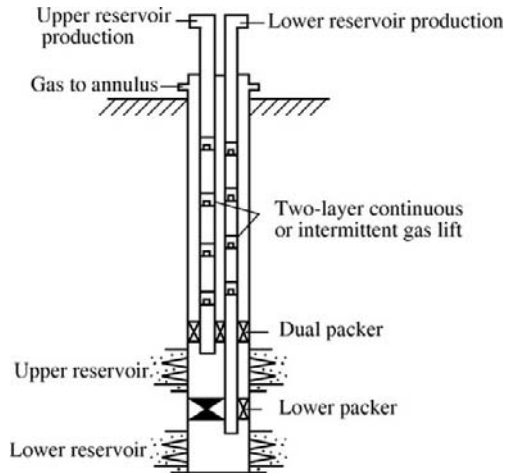


FIGURE 9-21 Dual-tubing string gas lift well structure.

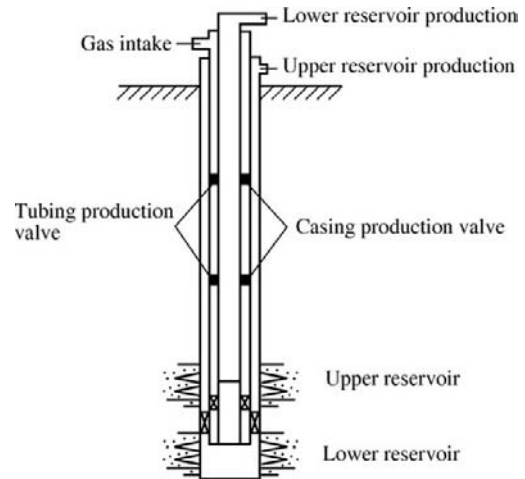


FIGURE 9-22 Concentric string gas lift well structure.

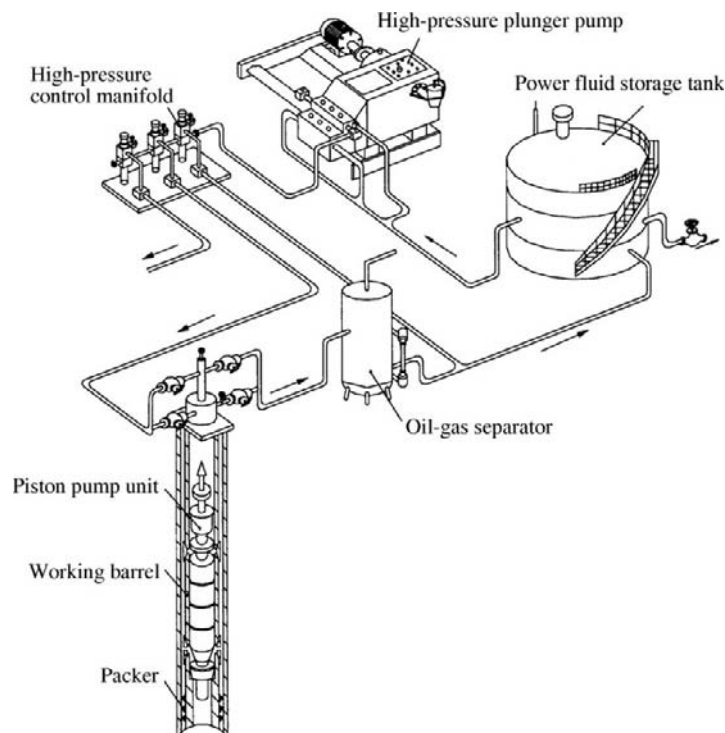
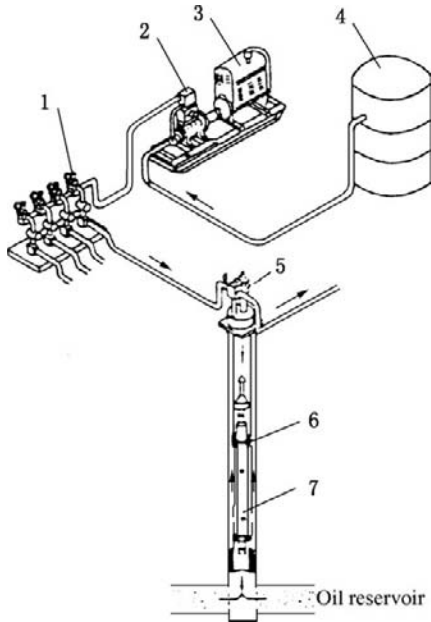
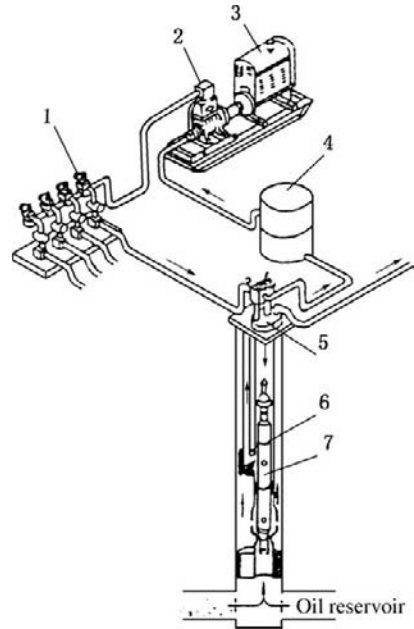


FIGURE 9-23 Hydraulic piston pump production system.



**FIGURE 9-24** Open-circulation hydraulic piston pump oil-production system. 1, high-pressure control manifold; 2, surface pump; 3, engine; 4, power fluid tank; 5, wellhead assembly; 6, pump barrel; 7, immersible pump.



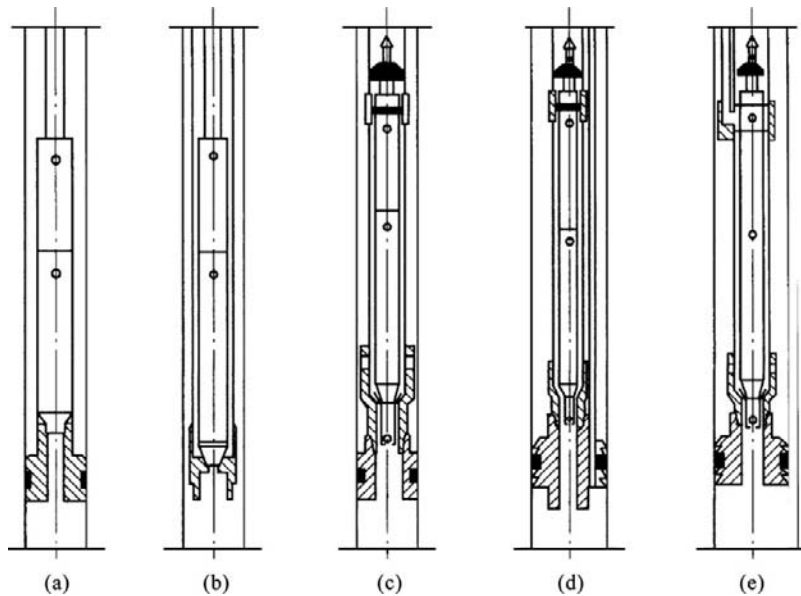
**FIGURE 9-25** Closed-circulation hydraulic piston pump oil-production system. 1, high-pressure control manifold; 2, surface pump; 3, engine; 4, power fluid tank; 5, wellhead assembly; 6, pump barrel; 7, immersible pump.

Figure 9-34. The sliding sleeve can be opened by coiled tubing to perform hydraulic fracturing or other stimulation. Formation with water production can also be closed by a sliding sleeve.

## 9.2 GAS WELL COMPLETION TUBING STRING

The principles of gas well completion tubing string selection are as follows:

1. The well completion tubing string should meet the requirements of both completion operation and gas well production. In addition, the complexity of downhole remedial operation ahead should also be considered.
2. On the premise of meeting the requirements of safety and engineering, the well completion tubing string should be simple and applicable to the full extent and tools and accessories that are unnecessary should not be run in.
3. The well completion tubing string should meet the requirements of nodal analysis to reduce local excessive pressure loss.
4. The well completion tubing string should consider the effects of  $H_2S$ ,  $CO_2$ , and formation water.
5. The quality of casing should be considered when the compressive strength of the well completion tubing string is calculated (especially under the condition of an eccentrically worn casing in deep or superdeep wells). In order to protect the casing, a permanent production packer completion tubing string is recommended.



**FIGURE 9-26** Fixed, inserted, and drop-in type hydraulic piston pumps. (a) Fixed; (b) Inserted; (c) Drop-in (single string); (d) Drop-in (parallel string); (e) Drop-in (parallel dual string).

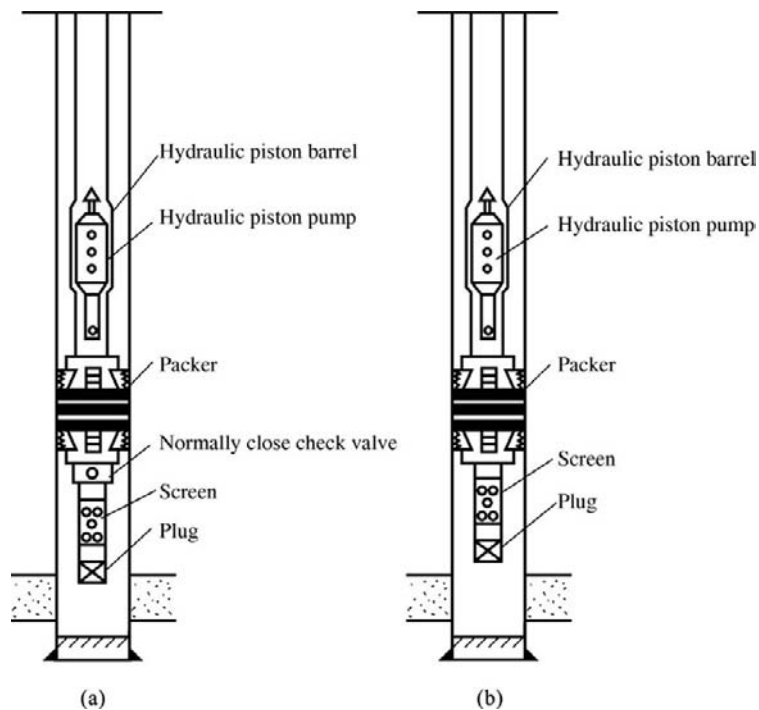


**FIGURE 9-27** Full-interval commingled single string. (a) One-way slip packer and check valve tubing string; (b) One-way slip packer tubing string with no check valve.

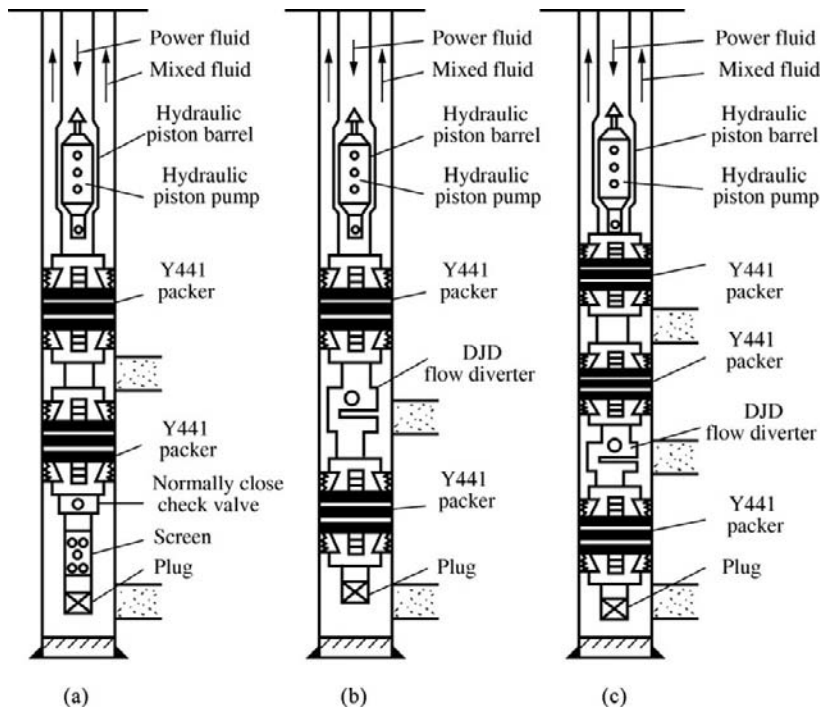


**FIGURE 9-28** Single-interval separate-layer production tubing string. (a) Upper-reservoir sealing and lower-reservoir producing string; (b) Lower-reservoir sealing and upper-reservoir producing string; (c) Upper- and lower-reservoir sealing and middle-reservoir producing string.

## Gas Production Well Tubing String

### Conventional Gas Well Completion Tubing String.

The conventional gas well completion tubing string structure is shown in Figure 9-35.

### High-Pressure High-Rate Gas Well Completion Tubing String.

In order to ensure safe production, the main structure of a high-pressure high-rate gas well completion tubing string includes subsurface safety valve, circulating valve, telescopic joint, and permanent packer. Some gas wells had used 7-in. casing tieback, 4 1/2-in. tubing string (Figure 9-36) and 5 1/2-in. tubing string (Figure 9-37). A 7-in. completion tubing string has been adopted to control gas flow velocity to mitigate the abrasion and erosion of the casing by gas (Figure 9-38).

### Sour Gas Well Completion Tubing String.

A permanent production packer completion tubing string is recommended for sour gas well completion. The 3SB and FOX high gas-tight special thread and tubing with inner wall coating or tubing with inner glassfiber lining are recommended.

#### 1. Conventional sour gas well completion tubing string

The feature of conventional sour gas well completion tubing string is the filling of corrosion inhibitor for preventing corrosion. Corrosion inhibitor film may isolate a steel product surface from a corrosive medium, thus preventing the chemical corrosion of steel product surface by a corrosive medium. The tubing string is shown in Figure 9-39.

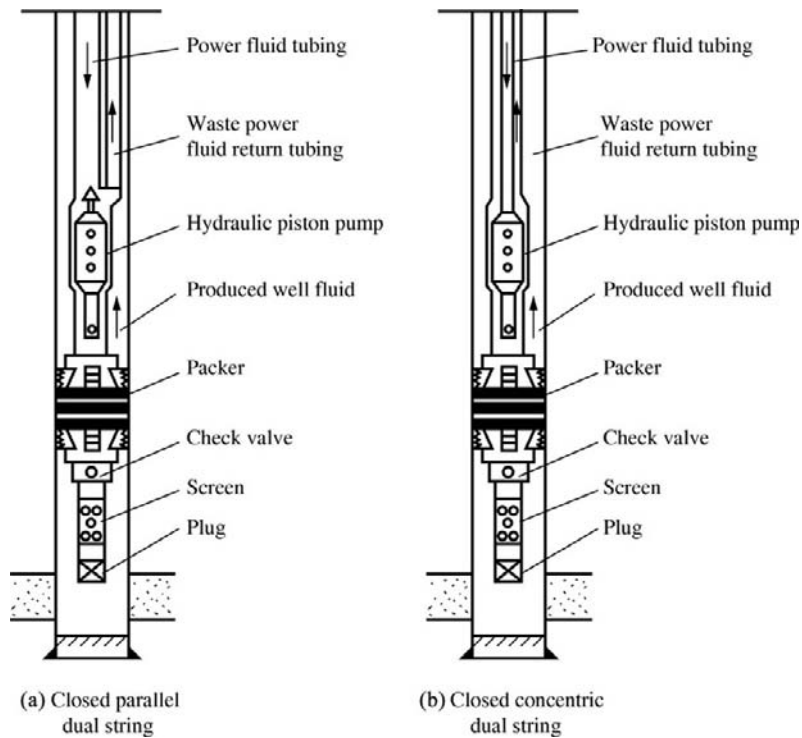


FIGURE 9-29 Dual string for hydraulic piston pump well.

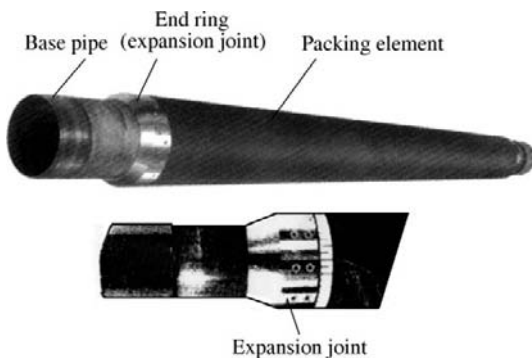


FIGURE 9-30 Oil- and gas-expandable packer.

## 2. One-trip completion tubing string

The merits of one-trip completion tubing string include: sealing tubing-casing annulus and protecting casing; reducing completion cost; shortening the operation period and favoring reducing the degree of formation damage; and matching with approved down-hole tools. The one-trip completion tubing string with Y344 packer is appropriate to wells that have good cement job quality and can achieve gun releasing and formation testing. The one-trip completion tubing string

TABLE 9-1 Temperature Tolerance of Oil- and Gas-Expandable Packer

Item	Tolerated Temperature (°C)	Binding Method
High-temperature system	110–160(230~320°F)	Chemical
Superhigh-temperature system	160–200(320~392°F)	Welding

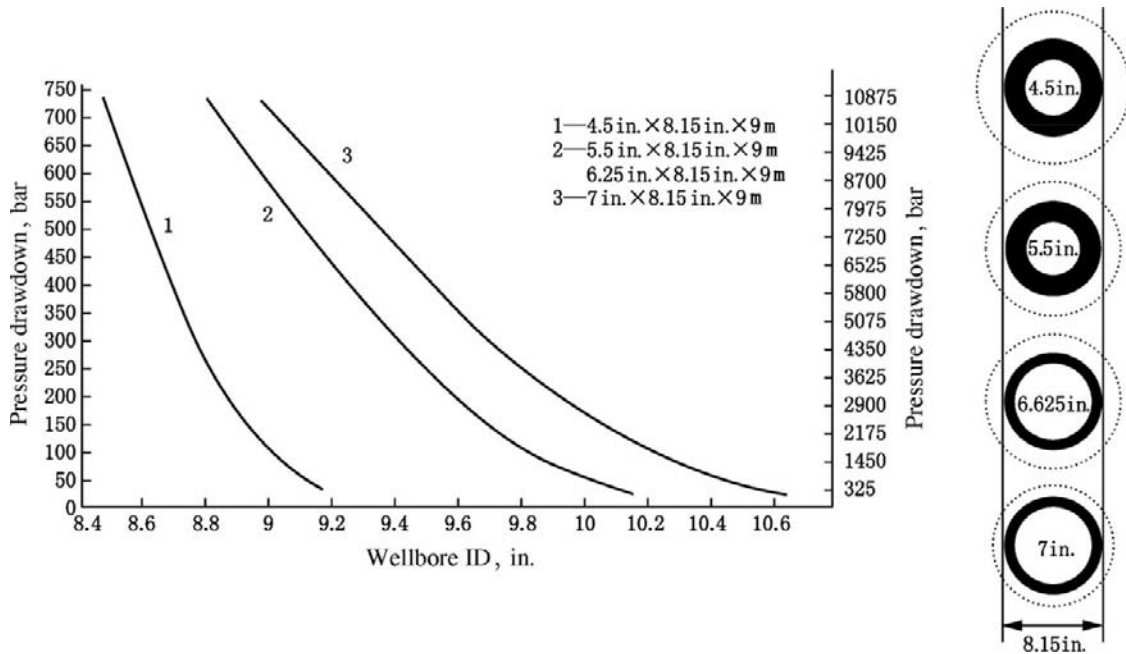


FIGURE 9-31 The producing pressure drawdown calculated and modified.

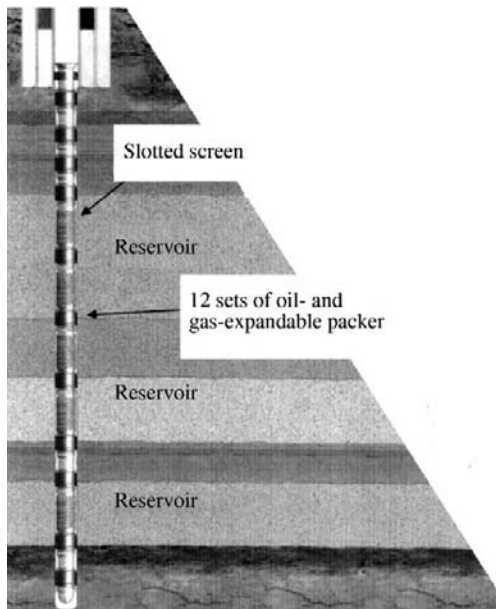


FIGURE 9-32 Separate-layer production tubing string with oil- and gas-expandable packers plus screens in an oil field in the North Sea.

with Y241 packer can be used in wells that have poor cement job quality or low internal pressure strength and can achieve gun releasing and formation testing. Figure 9-40 shows the one-trip formation testing completion tubing string in the Moxi gas field. The process flow chart of formation testing completion is shown in Figure 9-41.

### 3. Horizontal sour gas well glassfiber tubing string

This production tubing string is a compound-wall anticorrosive string. It consists of DST-80SS external upset sulfur-resistant metallic tubing, acid-anhydride type glassfiber tubing, aromatic amine glassfiber tubing, and glassfiber spherical float shoe (Figure 9-42 and Figure 9-43).

**High Acid Content Gas Well Completion Tubing String.** For a high acid content gas well, a subsurface safety valve should be used, and the tubing string should have anticorrosive properties. The subsurface safety valve should

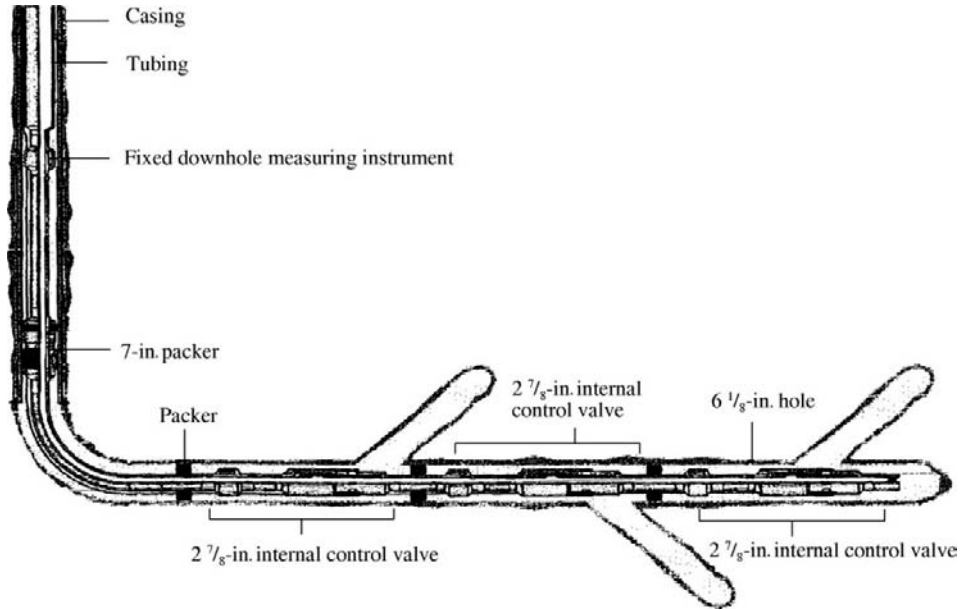


**FIGURE 9-33** Production tubing string with oil- and gas-expandable packer in an oil field in the Middle East.

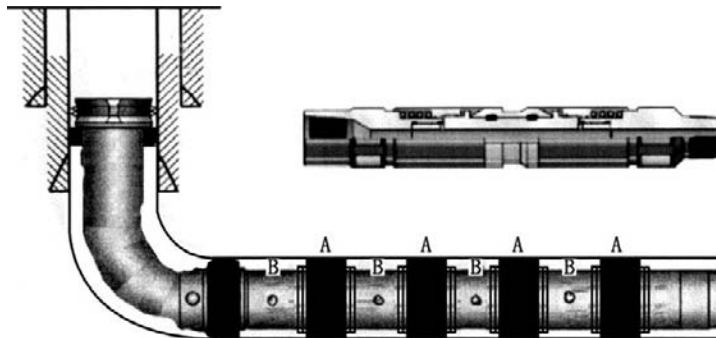


**FIGURE 9-34** String with oil- and gas-expandable packers and sliding sleeves. A: Oil- and gas-expandable packer; B: Sliding sleeve switch.

be 50–100 m apart from the wellhead. Flow nipples are attached to the upper and lower ends of the safety valve in order to mitigate the erosion attachment of the completion tubing string at turbulent flow.

#### 1. Capillary corrosion-inhibitor-filling completion tubing string

The completion tubing string is shown in Figure 9-44.

#### 2. Alloy steel completion tubing string

This string adopts a permanent packer for well completion. Tubing uses high-grade corrosion-resistant alloy Alloy 825 and Alloy G3. Downhole tools adopt the 718 material. For a high-sulfur gas well production tubing

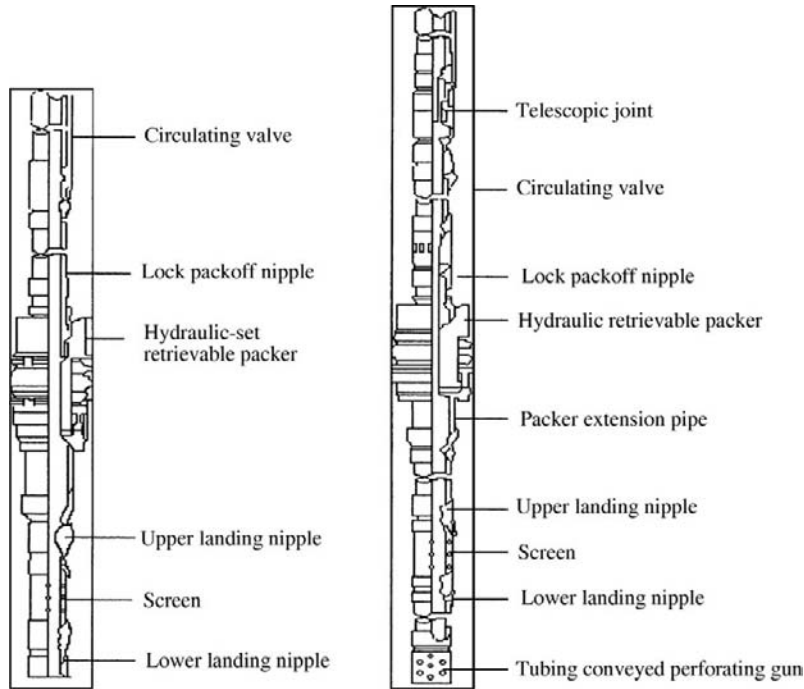


**FIGURE 9-35** Conventional gas well completion tubing string structures.

string, the simplicity of downhole tools is favorable due to the low probability of downhole accidents and remedial operations (Figure 9-45).

### 3. Horizontal high-sulfur gas well completion tubing string

A horizontal high-sulfur gas well completion tubing string is shown in Figure 9-46.

**Sour Gas Well Separate-Layer Production Tubing String.** A sour gas well separate-layer production tubing string is shown in Figure 9-47. The upper and lower reservoirs are separated by a packer. The gas in the lower reservoir is produced from tubing while the gas in the upper reservoir is produced from the tubing-casing annulus. This program is appropriate for a gas well of which the upper reservoir gas has no or very slight  $H_2S$ . Separate-layer production can be achieved by selecting conventional  $H_2S$ -resistant gas production wellhead assembly and packer.

## Tubing-Conveyed Perforating Gas Production Well Tubing String

A tubing-conveyed perforating gas production well tubing string is shown in Figure 9-48.

## Water-Drainage Gas-Production Tubing String

Water-drainage gas production technologies mainly include water-drainage gas production by string optimization, water-drainage gas production by foam, water-drainage gas production by pumping unit, water-drainage gas production by gas lift, water-drainage gas production by jet pump, and water-drainage gas production by electric submersible pump.

**Water-Drainage Gas Production by String Optimization.** The string for water-drainage gas production by string optimization is the same as that of a flowing gas production well.

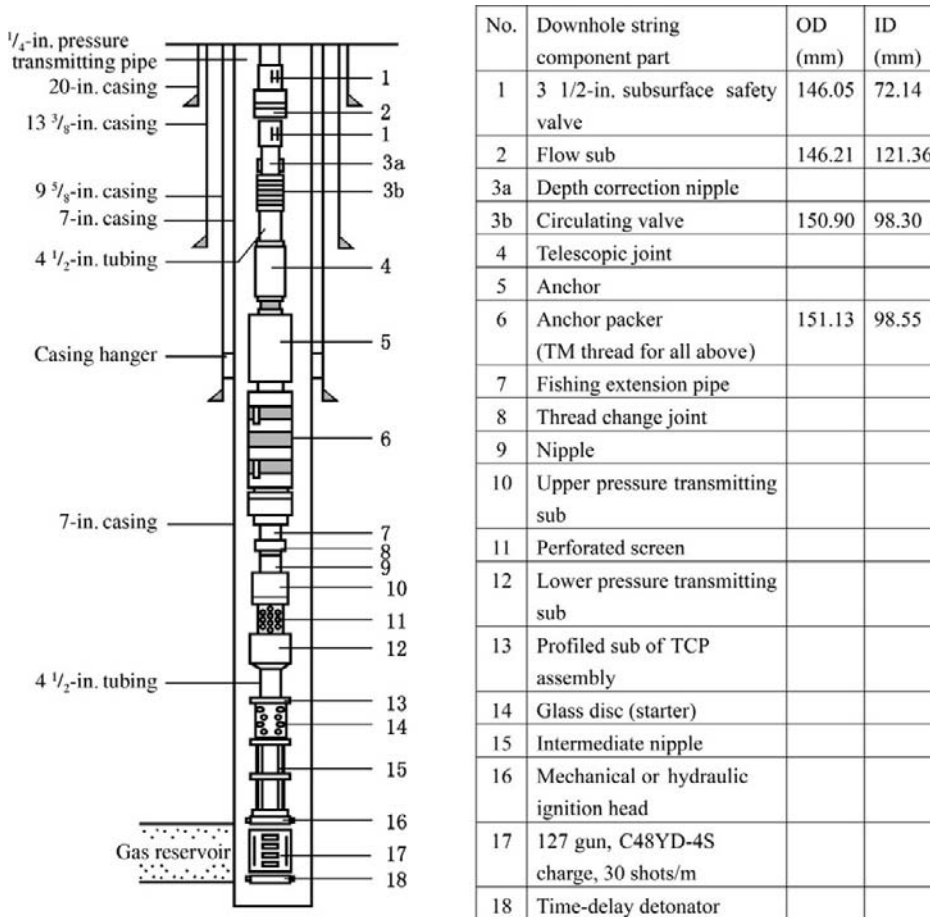


FIGURE 9-36 Well completion tubing string in some wells (7-in. casing and 4 1/2-in. tubing).

**Water-Drainage Gas Production by Foam.** A string for water-drainage gas production by foam is shown in Figure 9-49.

**Water-Drainage Gas Production by Pumping Unit.** A string for water-drainage gas production by pumping unit is shown in Figure 9-50.

**Water-Drainage Gas Production by Gas Lift.** A string for water-drainage gas production by gas lift is shown in Figure 9-51.

**Water-Drainage Gas Production by Jet Pump.** A string for water-drainage gas production by jet pump is shown in Figure 9-52.

**Water-Drainage Gas Production by Electric Submersible Pump.** A string for water-drainage

gas production by electric submersible pump is shown in Figure 9-53.

### 9.3 SEPARATE-LAYER WATER INJECTION STRING

Separate-layer water injection can be single-tubing string water injection or multiple tubing string water injection (Figure 9-54 and Figure 9-55). A single-tubing water injection string can be a fixed water distribution string, a hollow water distribution string, or an eccentric water distribution string.

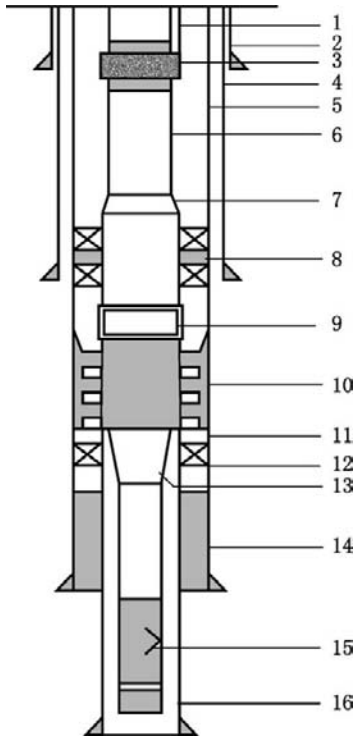


**FIGURE 9-37** Five and one-half-inch completion tubing string. 1, 4 1/2-in. pressure-transmitting pipe; 2, 20-in. conductor; 3, 5 1/2-in. subsurface safety valve and flow nipple; 4, 13 3/8-in. intermediate casing; 5, 9 7/8-in. production casing; 6, 5 1/2-in. tubing; 7, crossover joint (5 1/2-in. internal thread  $\times$  7-in. external thread); 8, 7-in.  $\times$  9 7/8-in. packer + milling extension pipe; 9, ball sealer seat; 10, seal plug-in pipe + tieback seal bore; 11, 7-in.  $\times$  9 7/8-in. combination liner hanger-packer; 12, 9 7/8-in.  $\times$  7-in. liner hanger; 13, 7-in.  $\times$  4 1/2 thread change joint; 14, 4 1/2-in. tubing screen; 15, 114-mm perforating gun assembly; 16, 7-in. liner.

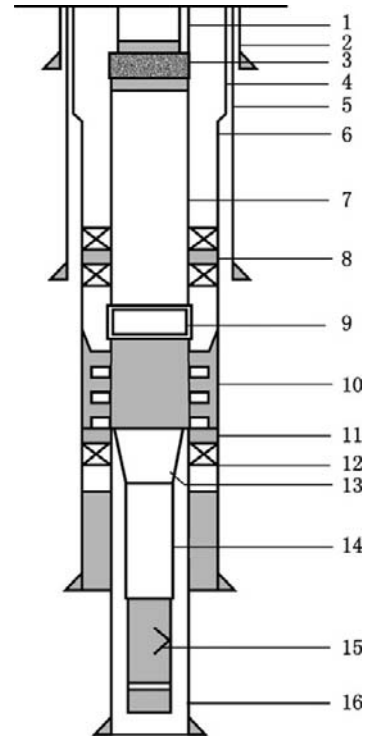


**FIGURE 9-38** Seven-inch completion tubing string. 1, 4 1/2-in. pressure transmitting pipe; 2, 20-in. conductor; 3, 7-in. subsurface safety valve and flow nipple; 4, 10 3/4-in. casing; 5, 13 3/8-in. intermediate casing; 6, 9 5/8-in. production casing; 7, 7-in. tubing; 8, 7-in.  $\times$  9 7/8-in. packer + milling extension pipe; 9, ball sealer seat; 10, seal plug-in pipe + tieback seal bore; 11, 7-in.  $\times$  9 7/8-in. combination liner hanger-packer; 12, 9 7/8-in.  $\times$  7-in. liner hanger; 13, 7-in.  $\times$  5-in. thread change joint; 14, 5-in. tubing screen; 15, 114-mm perforating gun assembly; 16, 7-in. liner.

### Fixed Water Distribution String

A fixed water distribution string is shown in Figure 9-56.

### Hollow Water Distribution Strings

In recent years new types of separate-layer water injection strings including anchored compensating separate-layer water injection string and

self-creeping compensating anticreeping string have been developed, and obvious effectiveness has been obtained in field application.

### Anchored Compensating Separate-Layer Water Injection String

#### 1. Structure

The string consists mainly of compensator, hydraulic anchor, Y341 packer, water flow regulator and hydraulic slips, and so on (Figure 9-57).

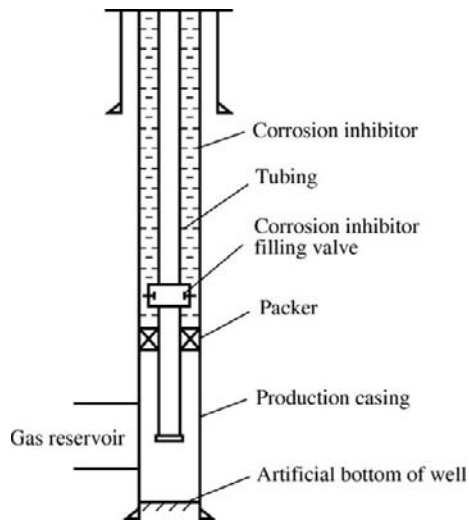


**FIGURE 9-39** Liquid corrosion-inhibitor-filling completion tubing string.

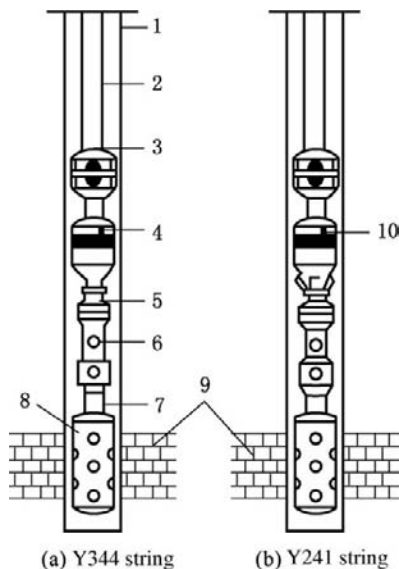


**FIGURE 9-40** One-trip formation testing completion tubing string in the Moxi gas field. 1, casing; 2, tubing; 3, hydraulic anchor; 4, Y344 packer; 5, perforating gun releaser; 6, screen nipple; 7, detonator; 8, perforating gun; 9, gas reservoir; 10, Y241 packer.

## 2. Features

- a. Upper anchoring and lower supporting by hydraulic anchor and slips can effectively prevent the string from creeping, thus

enhancing the reliability of corollary tools including the packer.

- b. The compensator on the string can be used for compensating the string telescoping under the action of temperature and pressure and improving the force-summing condition of the string.
- c. A hollow or eccentric separate-layer water injection string can be formed by selecting different water flow regulators.
- d. The distance between packer setting locations should not be less than 2 m in order to meet the requirement of separate-layer water injection. The fractures in the reservoirs of the Daqing oil field are horizontal fractures, so that the distance between packer setting locations can be appropriately decreased.

## Self-Creeping Compensating Anticreeping Separate-Layer Water Injection String

### 1. Structure

The string consists mainly of anticreeper, packer, water flow regulator, and sump type bottom pressure relief ball (Figure 9-58).

### 2. Features

- a. Long service life of packing elements. The upthrust force of packer makes the anticreeper slips and cone generate displacement. The slip expanding and sticking on the inner wall of casing can form a supporting point, so that packer creeping will not be generated.
- b. Convenient packer-releasing operation. Pulling up the string makes the anticreeper cone move up under the action of pulling-up force and the slips may shrink back, so that the string in the well can be smoothly pulled out.

## Other Hollow Water Distribution Strings.

Other hollow water distribution strings are shown in Figs. 9-59 to 9-64.

## Eccentric Water Distribution Strings

Eccentric water distribution strings are commonly used water distribution strings. The various eccentric water distribution strings are shown in Figs. 9-65 to 9-72.

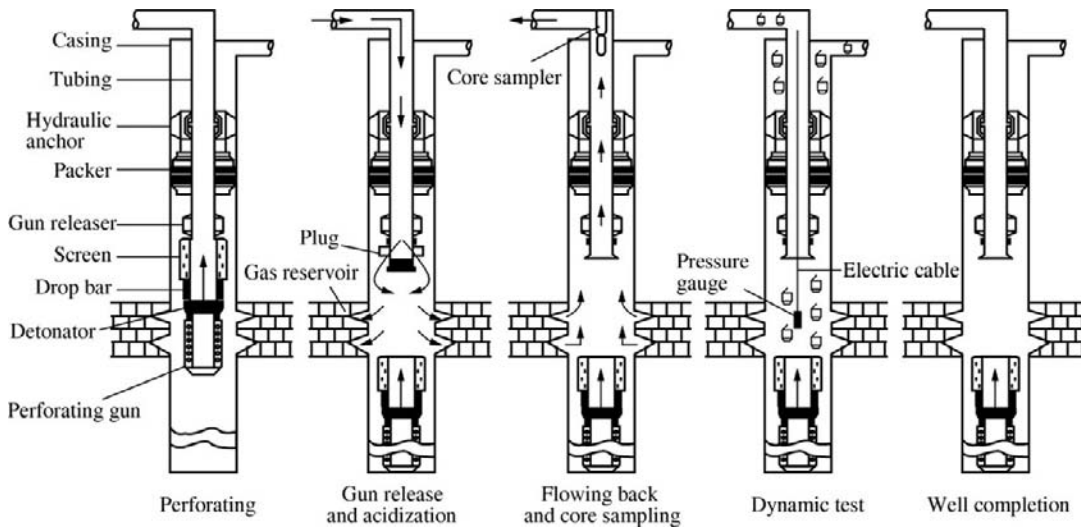


FIGURE 9-41 One-trip completion tubing string formation testing technology in Moxi gas field.

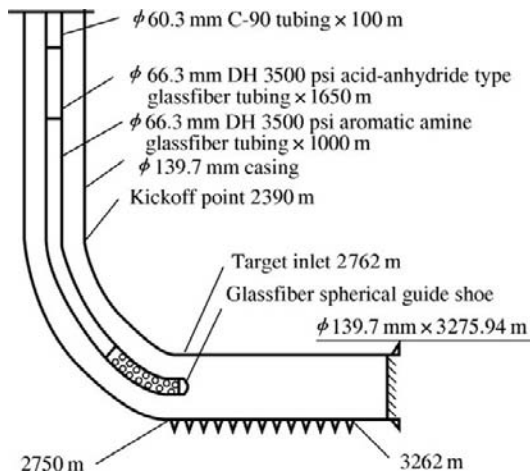


FIGURE 9-42 Perforated horizontal well glassfiber tubing completion string.

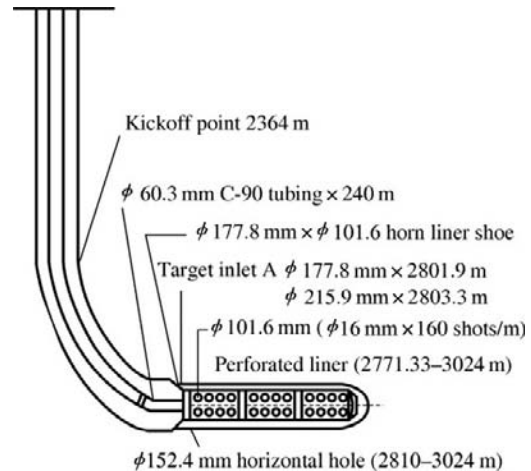


FIGURE 9-43 Horizontal well glassfiber-tubing liner completion string.

## 9.4 HEAVY OIL PRODUCTION TUBING STRING

### Conventional Steam Injection Tubing String

A conventional steam injection tubing string can be a blank-tubing steam-injection string (Figure 9-73), a blank-tubing and heat-insulation-packer steam

injection string (Figure 9-74), or an insulated-tubing steam injection string (Figure 9-75).

### Sealing and Separate-Layer Steam Injection String

A sealing and separate-layer steam injection string is required to be used under the condition of seriously longitudinally heterogeneous heavy

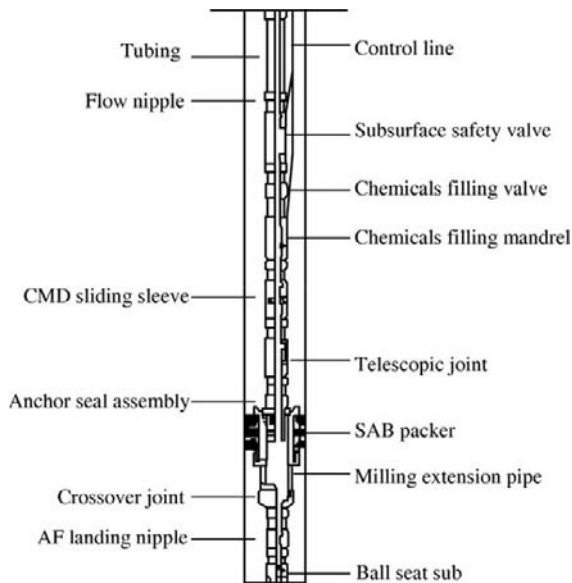


**FIGURE 9-44** Capillary corrosion-inhibitor-filling completion tubing string.

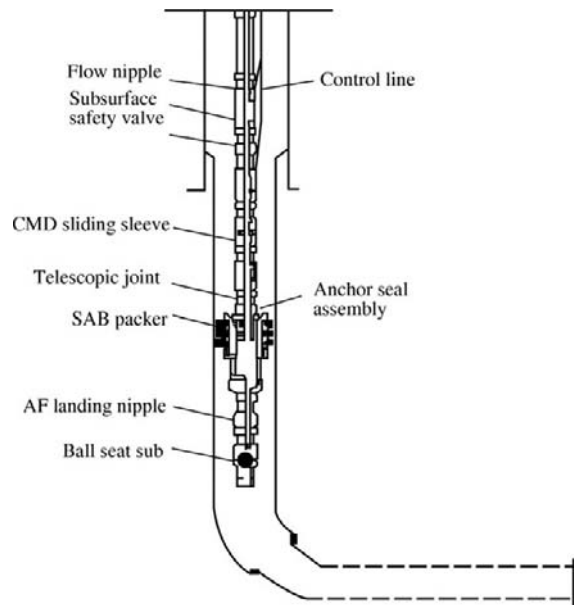


**FIGURE 9-46** Horizontal high-sulfur gas well completion tubing string.

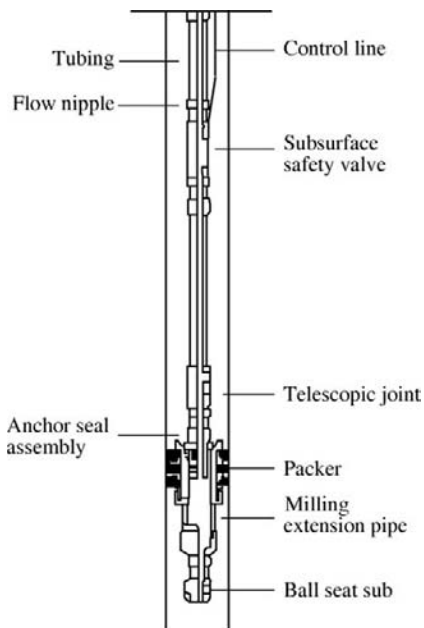


**FIGURE 9-45** Alloy steel completion tubing string.

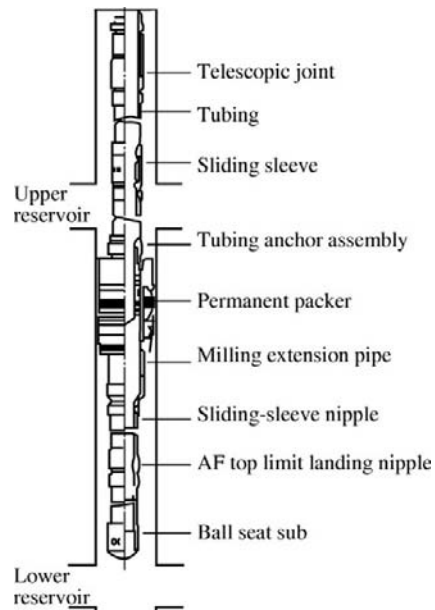


**FIGURE 9-47** Sour gas well separate-layer production tubing string.

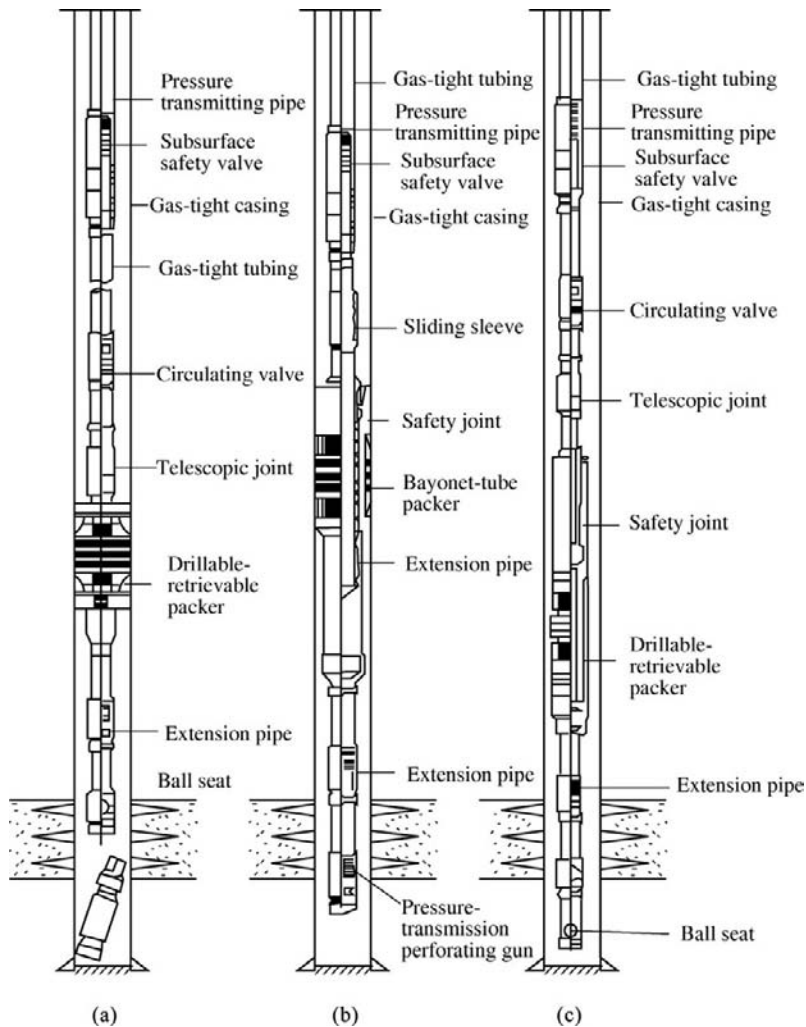


**FIGURE 9-48** Tubing-conveyed perforation gas production well string. (a) Gun release completion string; (b) Completion string with no gun release; (c) Running string.

oil reservoir that has uneven steam injection during huff and puff, low steam conformance efficiency, and low longitudinal producing degree.

Sealing and separate-layer steam injection strings mainly include upper-reservoir sealing and lower-reservoir injection strings (Figure 9-76), lower-reservoir sealing and upper-reservoir

injection strings (Figure 9-77), and separate-layer steam injection strings (Figure 9-78).

### Nitrogen Heat-Insulation Cleanup Tubing String

A nitrogen heat-insulation cleanup tubing string only has insulated tubing used for steam

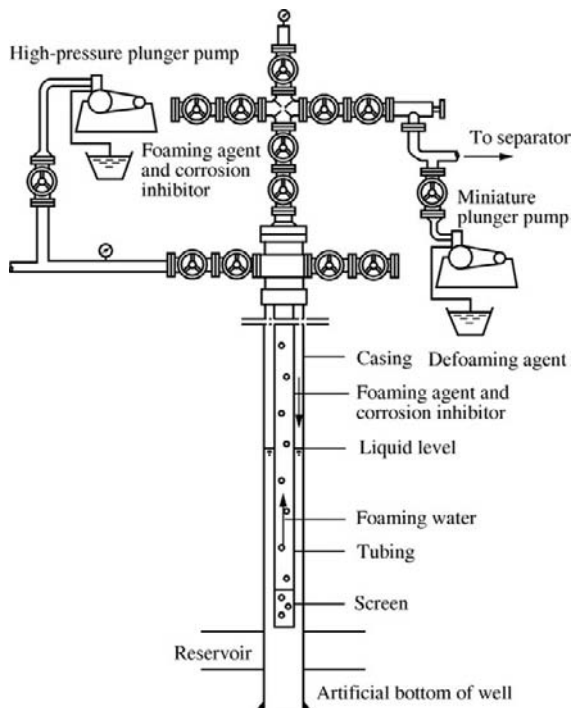


**FIGURE 9-49** The string for water-drainage gas-production by foam.

injection. The nitrogen needed is produced by a nitrogen manufacturing truck (Figure 9-79).

## Heavy Oil Huff-and-Puff and Pumping Tubing String

**Straight Well Production Tubing String.** Straight well production tubing strings include uninsulated blank tubing strings (Figure 9-80) and blank tubing and heat insulation packer heat-proof tubing strings (Figure 9-81).

**Slant Well Production Tubing String.** A slant well production tubing string is similar to a straight well production tubing string only in that a slant well needs a matched slant well pumping unit and a polished rod rotator at the surface and also needs downhole matched sucker rod centralizers and tubing centralizers (Figure 9-82). In addition, a slant well high-viscosity oil pump is required.

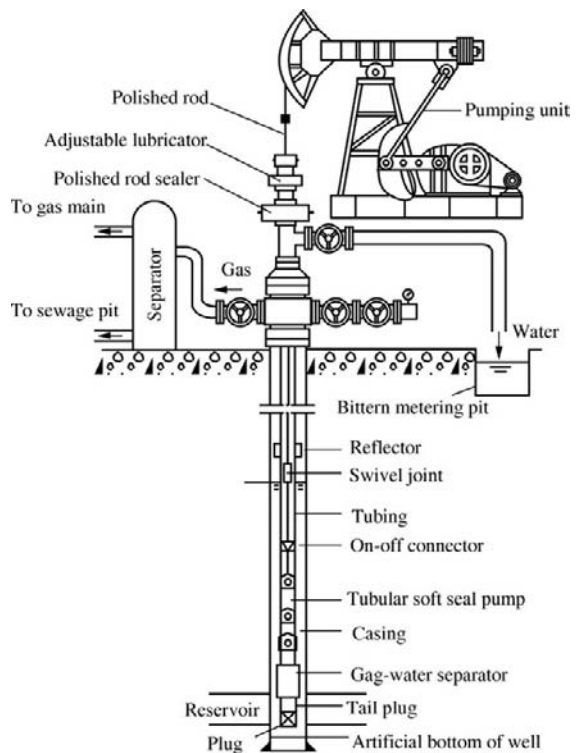


**FIGURE 9-50** The string for water-drainage gas-production by pumping unit.

## SAGD Production Tubing String

The steam-aided gravity drainage (SAGD) production technique is suitable for extra-heavy oil or crude bitumen production, which relies on the action of the gravitational force of bitumen and condensate with the aid of the heat of steam (Figure 9-83).

## Heavy-Oil Sand Clean-Out Cold-Flow Production Tubing String

A heavy oil reservoir is unconsolidated, and sand clean-out is easy. Heavy oil has a high viscosity and a high sand-carrying capacity. It has a certain quantity of dissolved gas under reservoir conditions. Heavy oil can be produced by inducing the reservoir to clean out sand to a considerable degree and forming foam oil. The tubing strings are divided into reverse flushing sand clean-out tubing

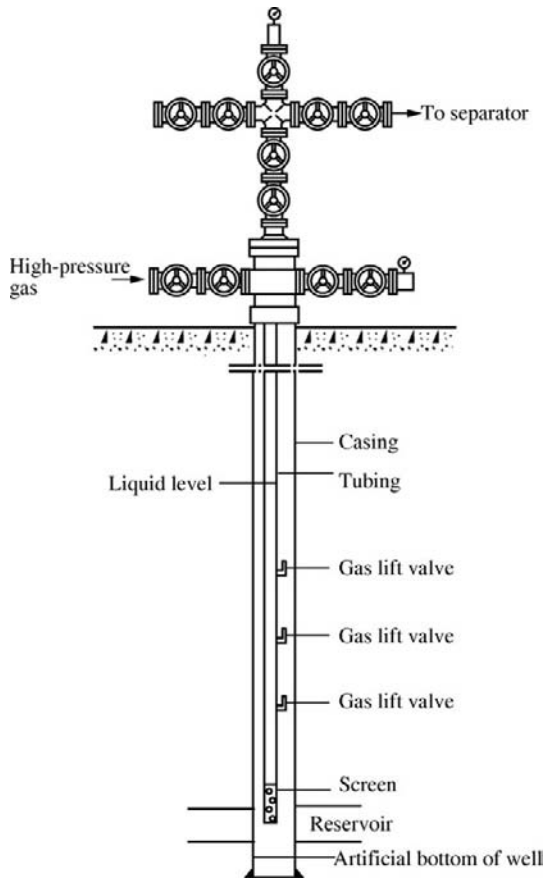


**FIGURE 9-51** The string for water-drainage gas production by gas lift.

strings (Figure 9-84) and hollow-rod staging sand clean-out tubing strings (Figure 9-85).

### Hollow-Sucker-Rod Through-Pump Electric Heating Production Tubing String

An armored heating cable is run in a hollow sucker rod and forms an electric return circuit with the heater below pump, hollow pump and hollow sucker rod by using a circuit connector; thus the transformation of electricity into heat is achieved, crude oil viscosity can be reduced by electric heating, and heavy oil flow resistance in the wellbore can be reduced, which favors pumping heavy oil to the surface (Figure 9-86).

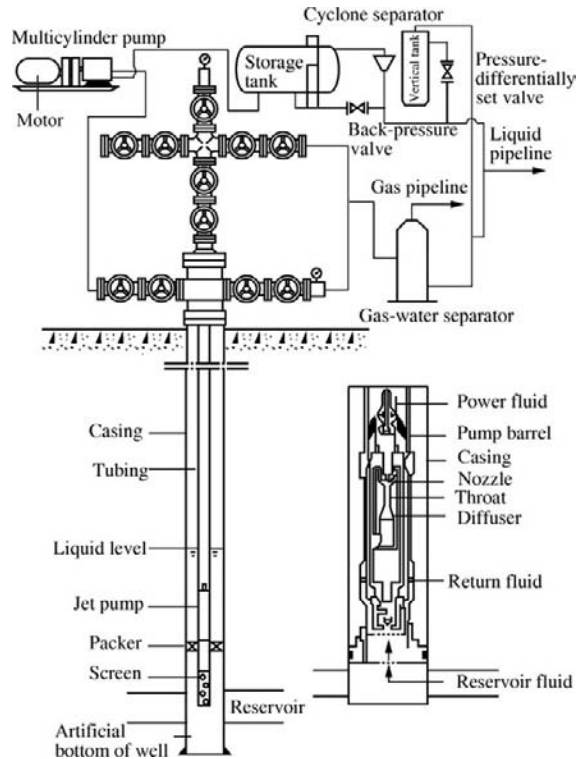


**FIGURE 9-52** The string for water-drainage gas production by jet pump.

### Production Tubing String of Combined Jet Pump and Oil Well Pump

The heavy oil (common heavy oil) of the deep and superdeep wells with a depth greater than 5000 m in the Talimu Tahe oil field can flow from the reservoir to the wellbore, but cannot flow to the wellhead. The pumping unit or electric submersible pump cannot lift it to the surface. A hydraulic piston pump has a complicated technology and high cost despite having enough lifting capacity. A jet pump has a low pump efficiency of less than 25% despite the fact that heavy oil can be produced when active water is used for reducing viscosity. If the lifting

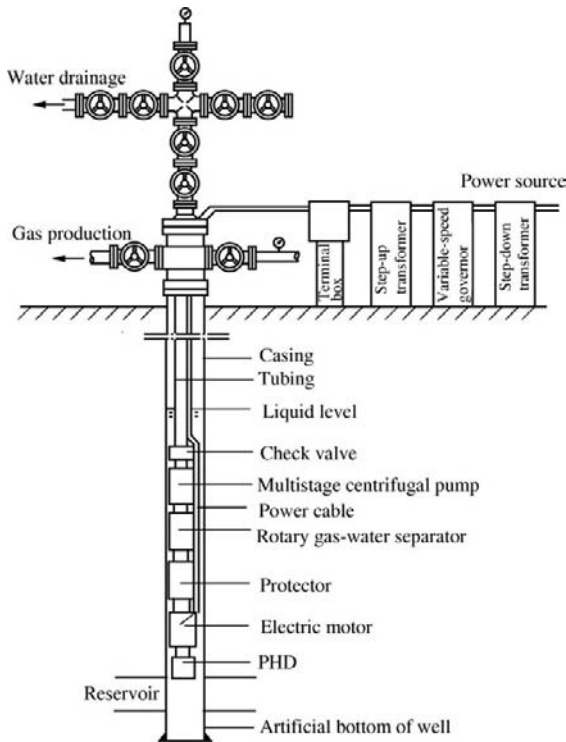


**FIGURE 9-53** Water-drainage gas production by electric submersible pump.

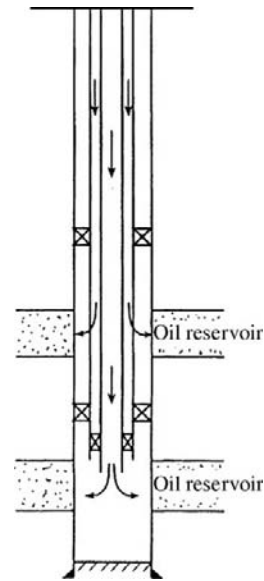


**FIGURE 9-55** Concentric-string separate-layer water injection.

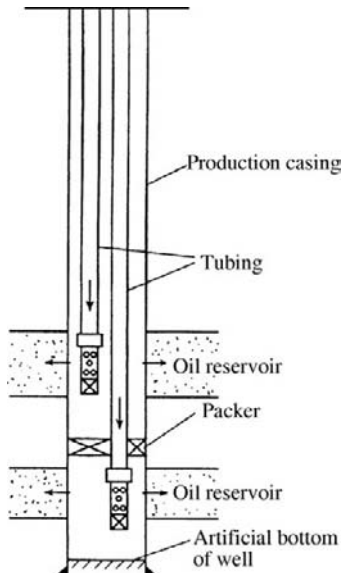


**FIGURE 9-54** Dual-string separate-layer water injection.

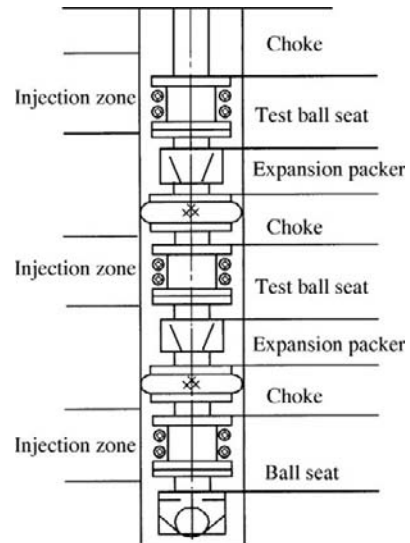


**FIGURE 9-56** Fixed water distribution string.

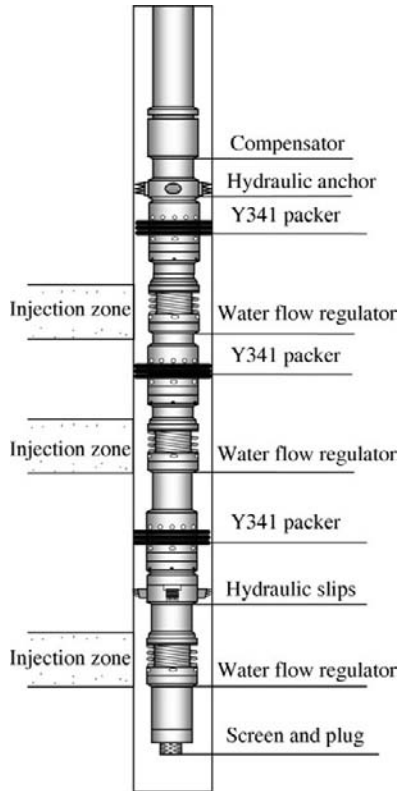


**FIGURE 9-57** Anchored compensating separate-layer water injection string.

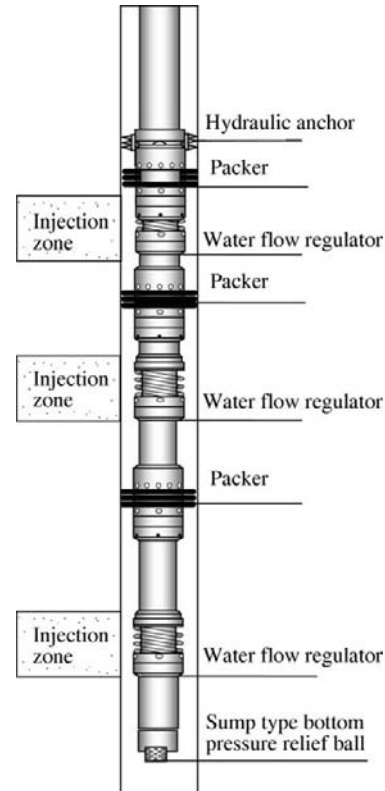


**FIGURE 9-58** Self-creeping compensating anticreeping separate-layer water injection string.

capacity of a jet pump or the pressure draw-down is insufficient, an oil well pump can be run to some depth above the jet pump. The combination of jet pump and oil well pump may have a higher effectiveness (Figure 9-87).

## 9.5 COMPLETION TUBING STRING SAFETY SYSTEM

Completion tubing string is required to be run in after oil and gas well perforating in order to pump oil and gas to the surface. Blowout accidents may often be generated during production due to contingencies such as blowout from high-pressure oil and gas reservoirs, failure of casing or tubing, failure of packer and downhole operational faults, contingencies including natural

calamity, fire hazard and floodwater, and contingencies under lake, river, and sea water. These factors should be considered in the completion tubing string design in order to ensure oil and gas well safety, personal safety, and environmental sanitation.

At present, safety measures for completion tubing string mainly include a packer on the top of the reservoir for isolating tubing-casing annulus, a subsurface safety valve at 100–200 m below the wellhead, and a matching surface safety system. The downhole and surface safety systems are mainly set in the light of the contingencies of high-pressure and high-productivity oil and gas wells. For low-pressure and low-productivity wells, the downhole safety system may be simplified in general.

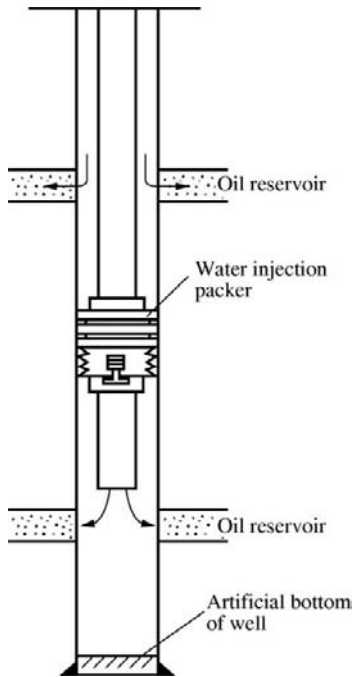


**FIGURE 9-59** Tubing-casing separate-layer water injection string.

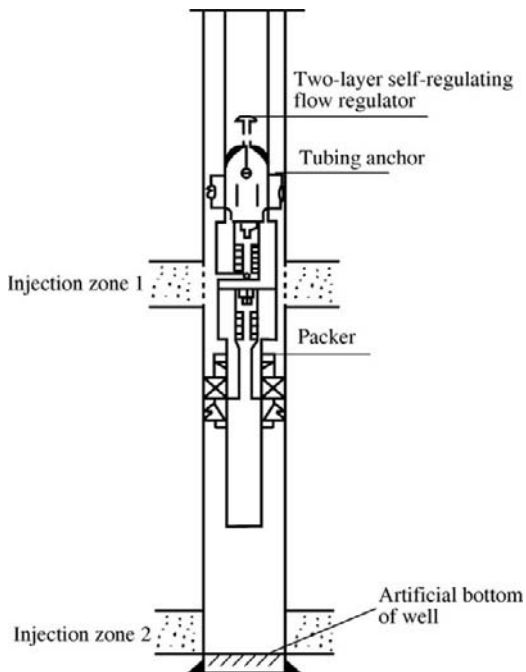


**FIGURE 9-60** Two-layer self-regulating separate-layer water injection string.

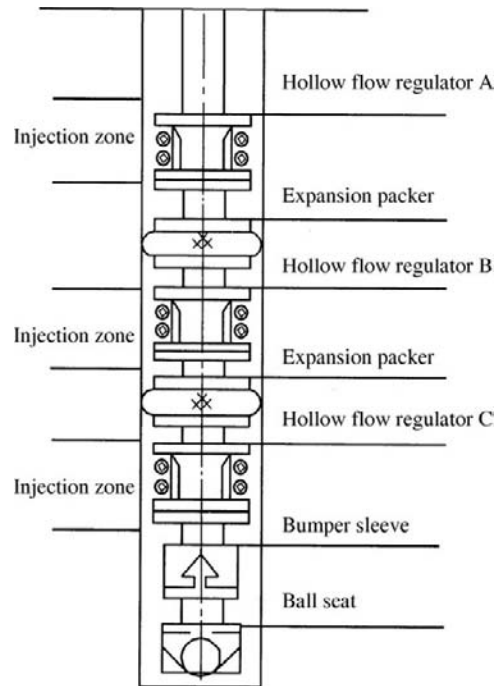


**FIGURE 9-61** Expansion-packer hollow free type water-distribution string.

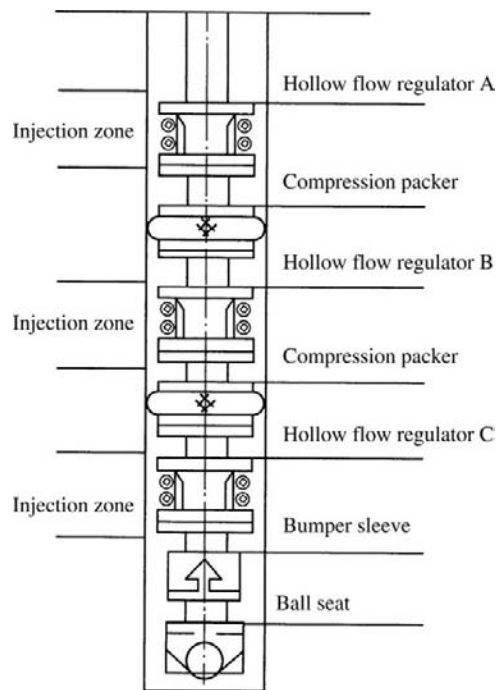


**FIGURE 9-62** Compression-packer hollow free type water-distribution string.

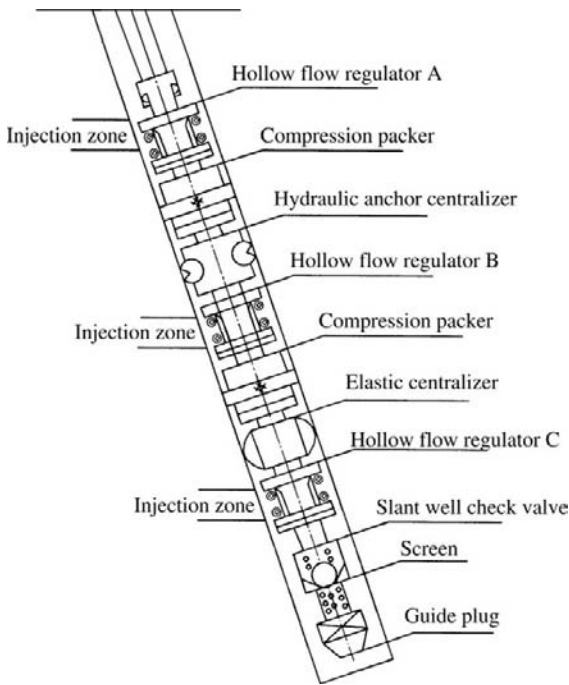


**FIGURE 9-63** Slant well hollow free type water distribution string.

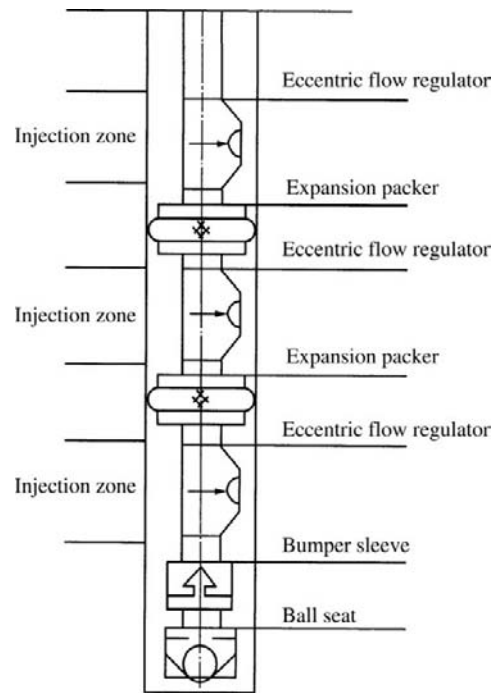


**FIGURE 9-65** Expansion-packer side-pocket water distribution string.

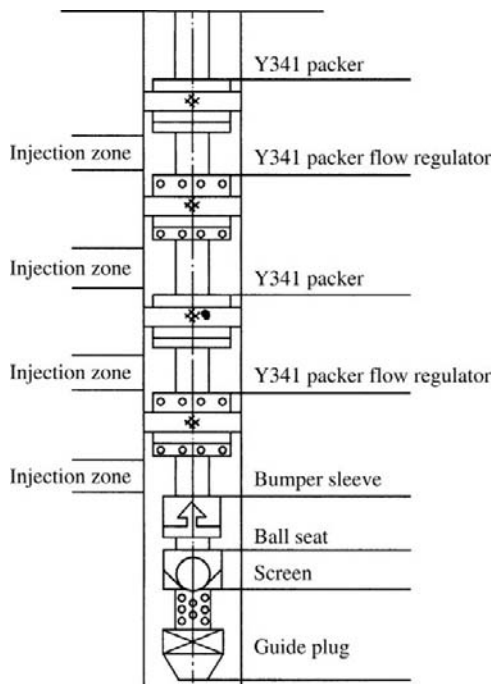


**FIGURE 9-64** Hydraulic drop-pull type separate-layer water distribution string.

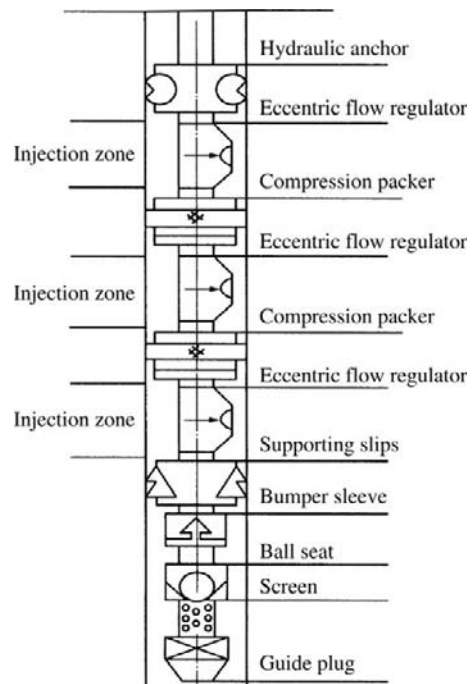


**FIGURE 9-66** Anchor type side-pocket water distribution string.

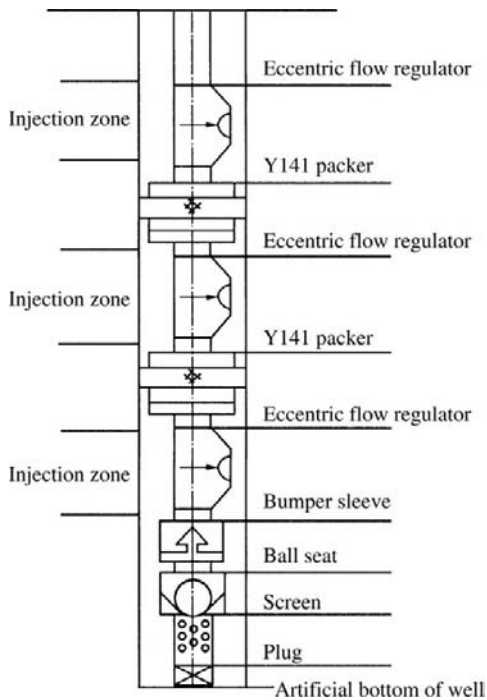


**FIGURE 9-67** Bottomhole support type side-pocket water distribution string.

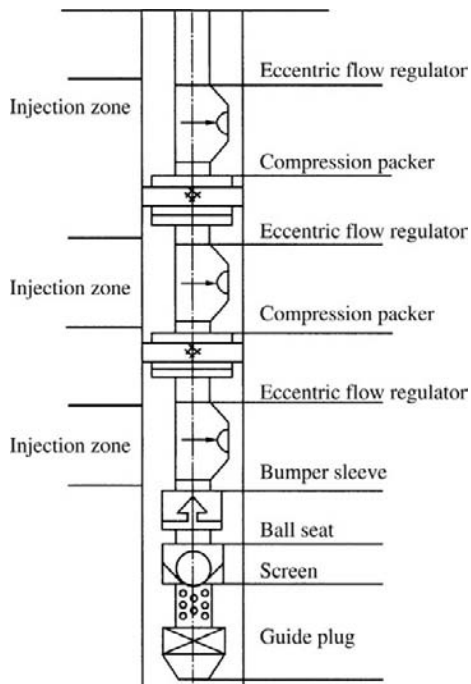


**FIGURE 9-68** Wellhead-hang side-pocket water distribution string.

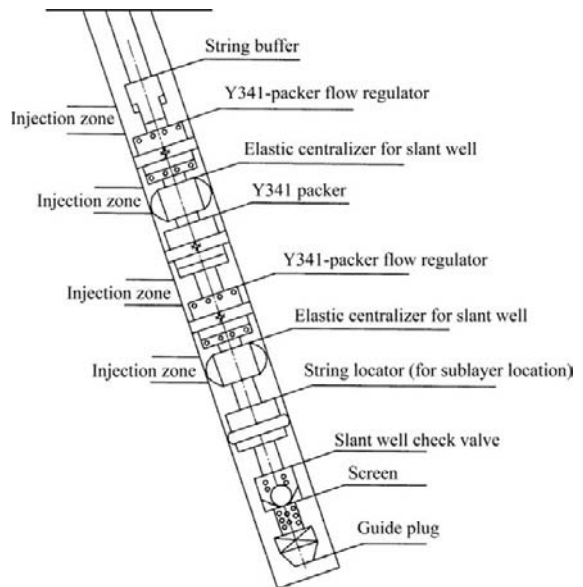


**FIGURE 9-69** Hydraulic dropping-fishing type slant well side-pocket water distribution string.

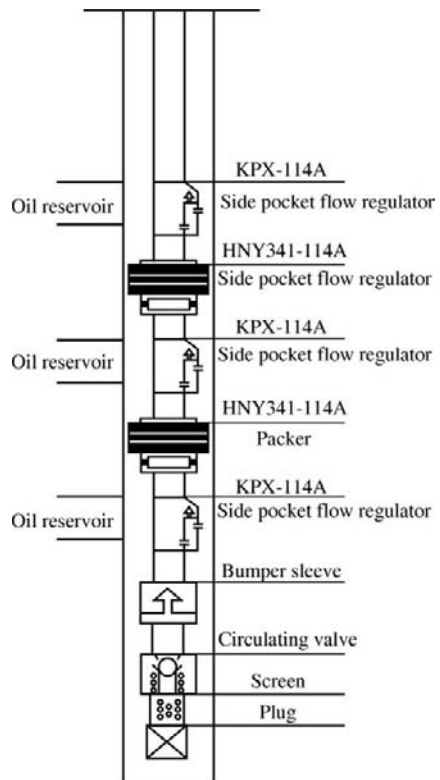


**FIGURE 9-70** No-dropping blind-choke side-pocket water distribution string.

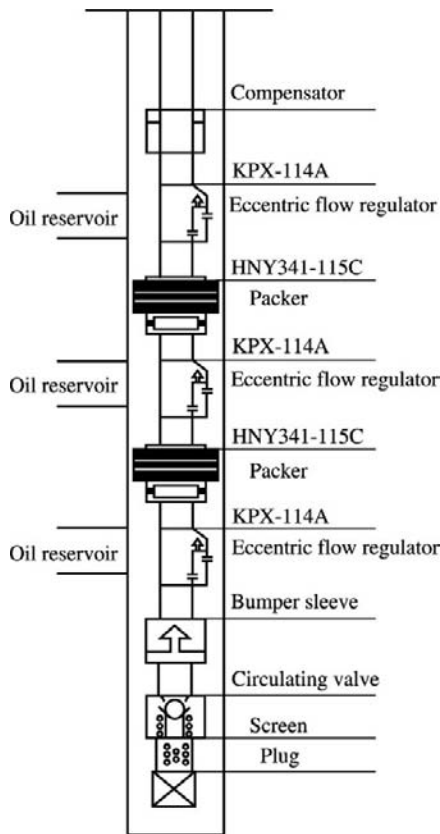


**FIGURE 9-71** Deep- and mid-depth-well side-pocket water distribution string.

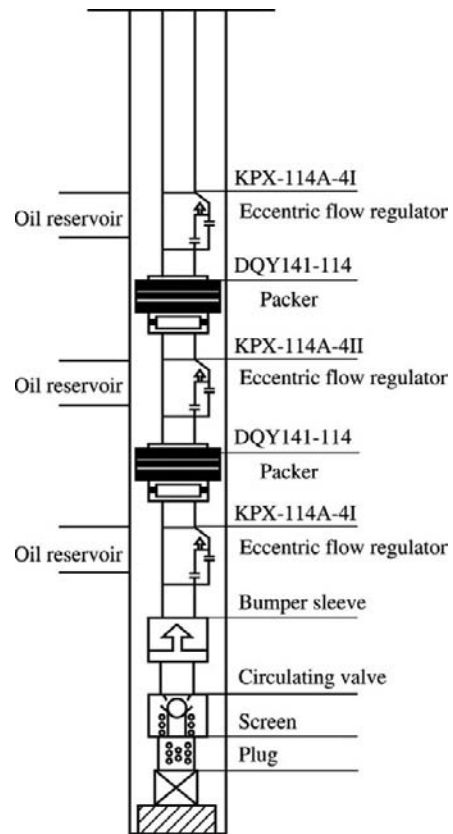


**FIGURE 9-72** Water-injection side-pocket water distribution string.

## Subsurface Safety Valve

A subsurface safety valve is an emergency shut-down valve, which is able to shut down the oil and gas flow passage to the surface when a failure of the well control is generated. A subsurface safety valve can be automatically closed by an abrupt increase in the pressure differential by blowout. It can also be closed by hydraulic pressure. A  $\Phi 1/4$ -in. stainless steel pipe is run in the tubing-casing annulus and connected with the hydraulic set of the subsurface safety valve. The safety valve can be closed by hand gear or automatic device at the surface when blowout is generated. The various subsurface safety valves shown in Figure 9-88 can be selected under different conditions.

**Setting Depth.** The setting depth of a subsurface safety valve is generally about 100–200 m below the surface in onshore oil and gas fields. For oil and gas fields in lakes, rivers, flood-discharge areas, and offshore oil and gas fields, the setting depth of the subsurface safety valve should also be 100–200 m below lake bed, river bed, or wellhead. The reason is that contingencies or blowout will not affect this depth. After the subsurface safety valve is closed, oil and gas well accidents will not extend and the oil and gas field will not be disrupted.

**Casing Program.** The inside diameter of a subsurface safety valve should be the same as that of the tubings connected on the top and underneath in order to be convenient for various tubing

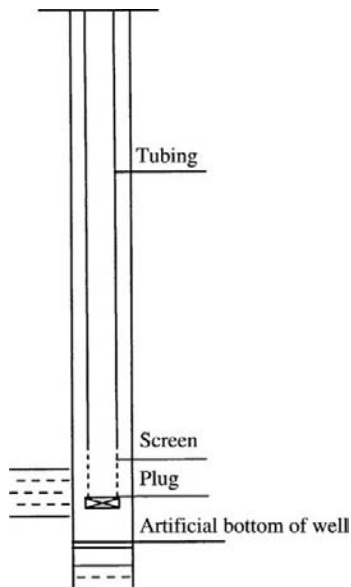


FIGURE 9-73 Blank-tubing steam injection string.

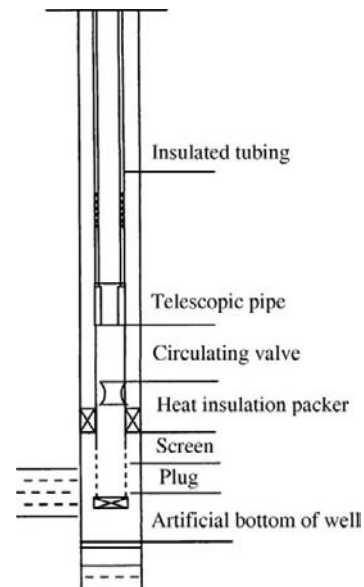


FIGURE 9-75 Insulated-tubing steam injection string.

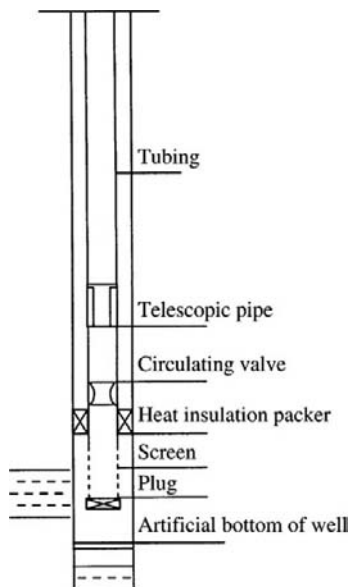


FIGURE 9-74 Blank-tubing and heat-insulation-packer steam injection string.

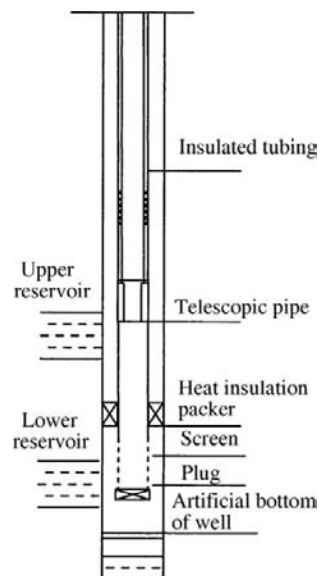
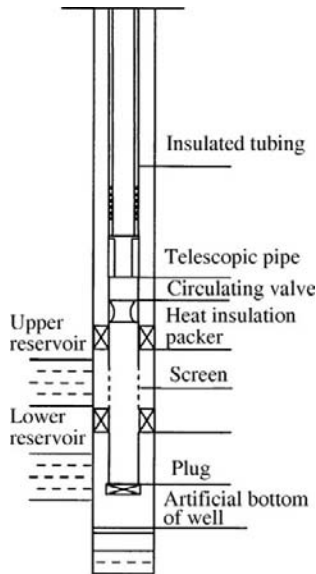
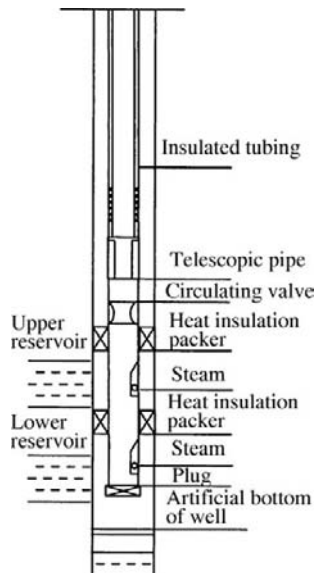


FIGURE 9-76 Upper-reservoir sealing and lower-reservoir steam injecting string.



**FIGURE 9-77** Lower-reservoir sealing and upper-reservoir steam injecting string.



**FIGURE 9-78** Separate-layer steam injecting string.

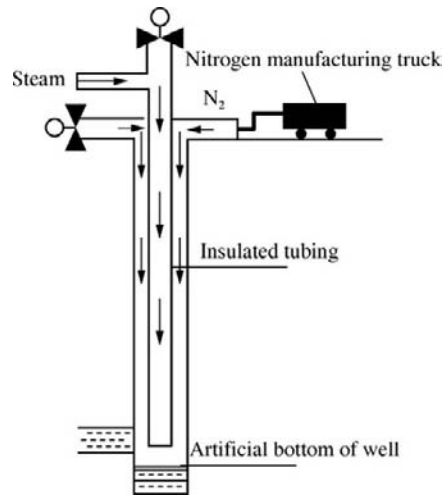


**FIGURE 9-79** Nitrogen heat-insulation steam injection string.

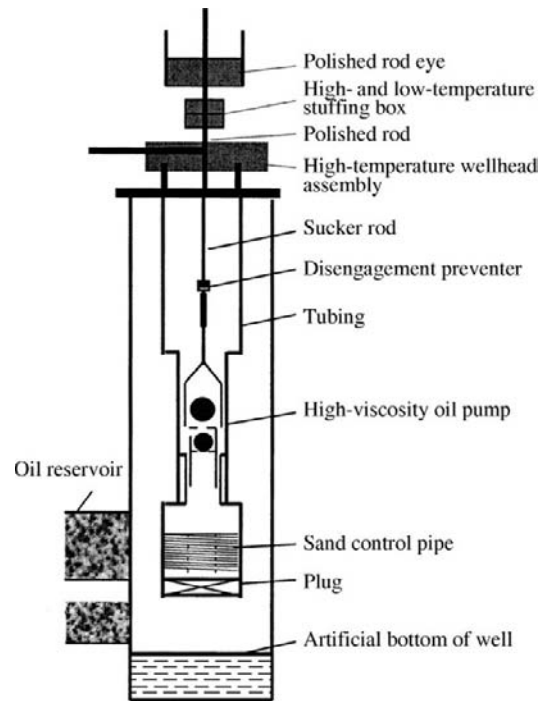


**FIGURE 9-80** Vertical-well blank-tubing uninsulated string.

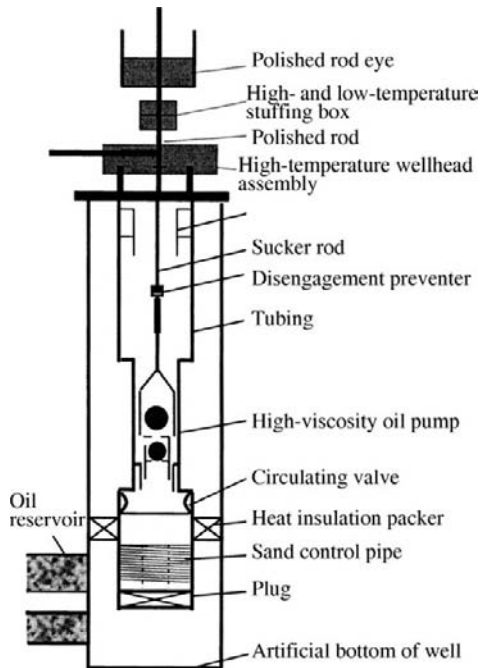


**FIGURE 9-81** Vertical well blank-tubing heat insulation packer insulated string.

operations. In addition, there are various closing components in the subsurface safety valve; thus the outside diameter of the subsurface safety valve should be enlarged, and a subsurface safety valve with an increased outside diameter cannot be run in the originally designed casing. Therefore, the diameters of the casings for oil and gas wells with a subsurface safety valve should be enlarged above the depth of 100–200 m. For instance, the originally designed casing diameter of 7 in. should be increased to 9 5/8 in. the casing of which is connected with the casing of 7 in. by a reducer. The tubing string with a subsurface safety valve should be designed in consideration of the inside diameter of the tubing, the inside and outside diameters of the subsurface safety valve, and the inside diameter of the casing run in. The technical parameters of the subsurface safety valve are listed in Table 9-2.

Selecting a permanent or retrievable packer as the packer on the top of the reservoir is dependent on the pressure drawdown at the packer.

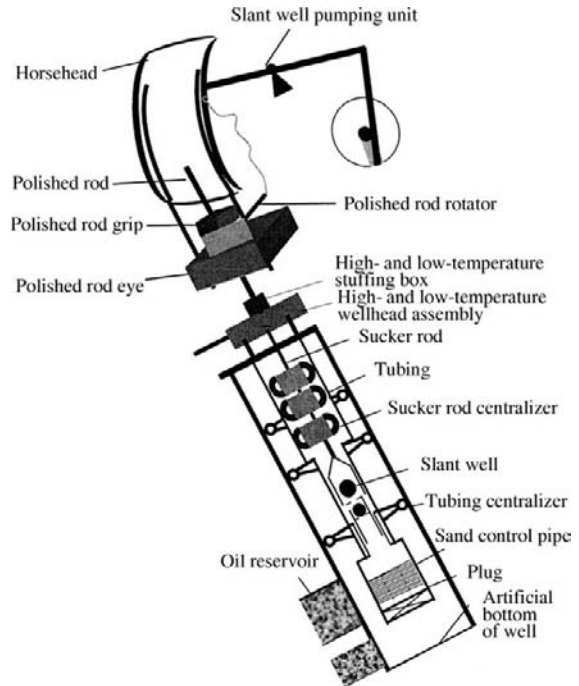


**FIGURE 9-82** Slant well production tubing string.

The packer selected should be able to bear sufficient pressure drawdown and should be corrosion-resistant, so that long-term sealing and effective tubing-casing annulus packing may be achieved.

## Matching Surface Safety Valve System

In order to ensure the safety of onshore and offshore high-pressure high-productivity oil and gas wells, the matching surface safety system is still required in addition to the subsurface safety valve.

**Surface Safety Valve.** Most surface safety valves are reverse gate valves with a piston-type actuating mechanism. The pressure in the valve body may push up the gate to close the valve due to the low pressure borne by the valve stem area. The controlled pressure acting on the piston may push down the gate to open the valve. If the valve body has no pressure, a spring is generally used for closing the valve.

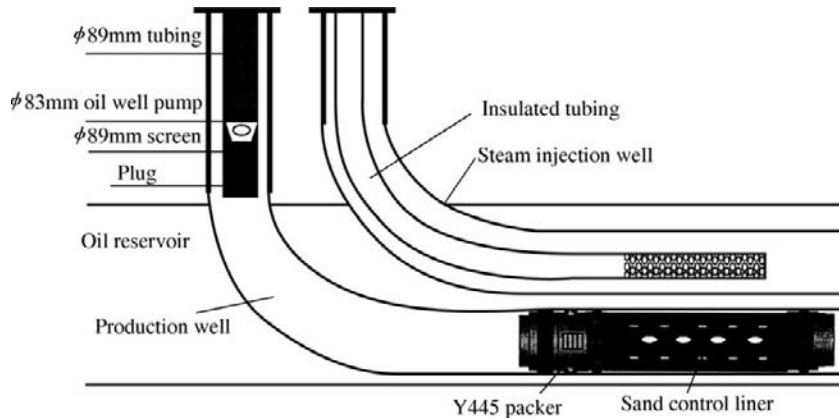


FIGURE 9-83 SAGD production tubing string.

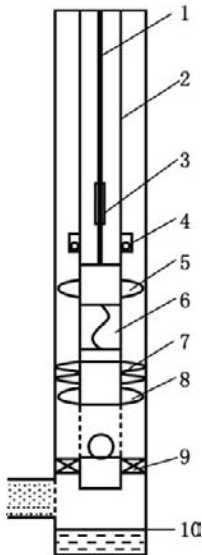


FIGURE 9-84 Reverse-flushing sand washing completion string: 1, polished rod; 2, tubing; 3, sucker rod safety joint; 4, check valve; 5, screw pump; 6, tubing anchor; 7, centralizer; 8, packer; 9, spider; 10, artificial bottom of well.

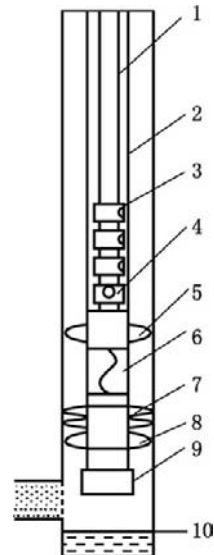
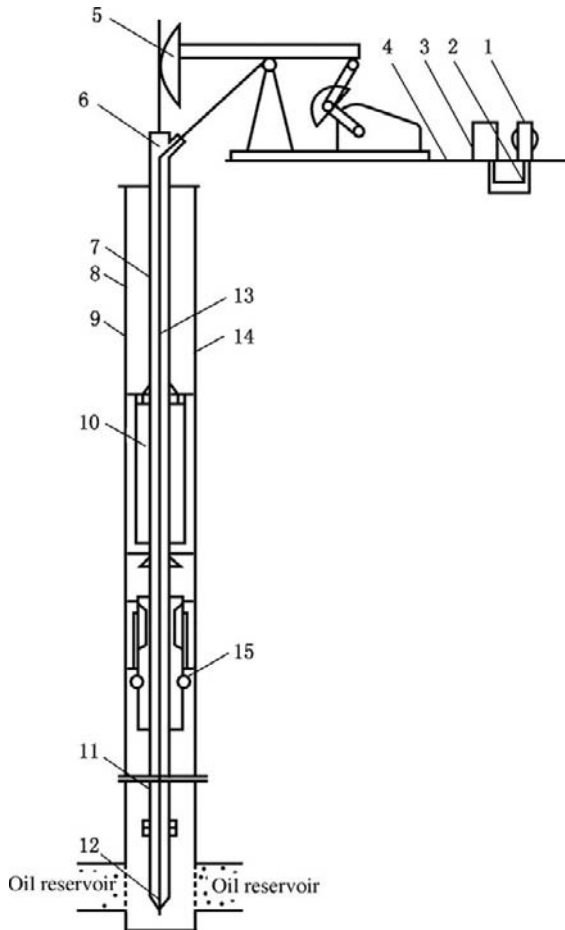


FIGURE 9-85 Hollow-rod stepwise sand washing completion string: 1, hollow rod; 2, tubing; 3, stepwise sand washing tool; 4, check valve; 5, centralizer; 6, screw pump; 7, tubing anchor; 8, centralizer; 9, spider; 10, artificial bottom of well.

**Matching of Surface Safety Valve with Subsurface Safety Valve.** The pressure-differential subsurface safety valve can be automatically closed by pressure differential, while the hydraulic, pneumatic, dual-tubing, or other type of subsurface safety valve is controlled by the surface control system. The surface control

system is controlled by the pressure maintained by the surface device, which is controlled by a servo system. Pressure is transmitted to the subsurface safety valve through a 1/4-in. parallel control line in the annulus or a tubing-casing annulus connected with the packer below the safety valve.



**FIGURE 9-86** Hollow-sucker-rod through-pump electric heating production tubing string. 1, special transformer; 2, power cable; 3, electric control cabinet; 4, service cable; 5, pumping unit; 6, cable guider; 7, hollow sucker rod; 8, tubing; 9, casing; 10, hollow pump; 11, through-pump heater; 12, circuit connector; 13, heating cable; 14, pump housing; 15, snap ring.

The subsurface safety control system is shown in Figure 9-89, and an offshore production platform safety control system is shown in Figure 9-90.

## 9.6 TUBING STRING MECHANICS

The tubing string may be in contact with the borehole wall or the inner wall of the casing after the string inflexes because it is limited by

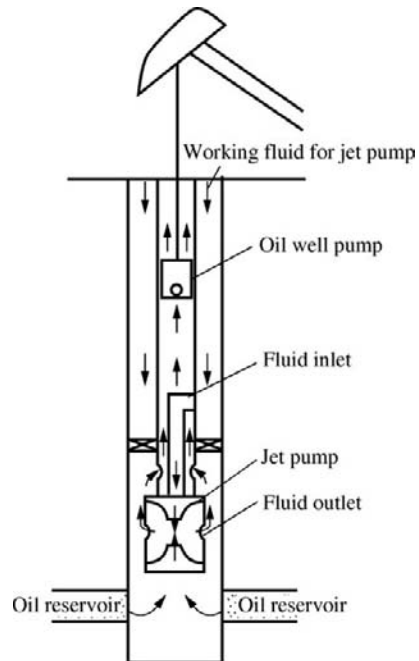


**FIGURE 9-87** Combination jet pump-oil well pump lift string.

the borehole, which makes things complicated. The effects of the fluid friction inside and outside string on the string should be fully considered when the forces borne by the string and the deformation of the string are analyzed.

## Status Models of Tubing String

In light of the relation to the packer, tubing string can be freely movable, restrictedly movable, or immovable (Figure 9-91). Tubing strings can also be divided into tubing strings with hook-wall packer and tubing strings with support-type packer in accordance with tubing string mechanics.

There are the following status models of tubing string during well completion and putting into production:

1. Status before packer setting. The tubing string is used for determining accurate packer setting location.

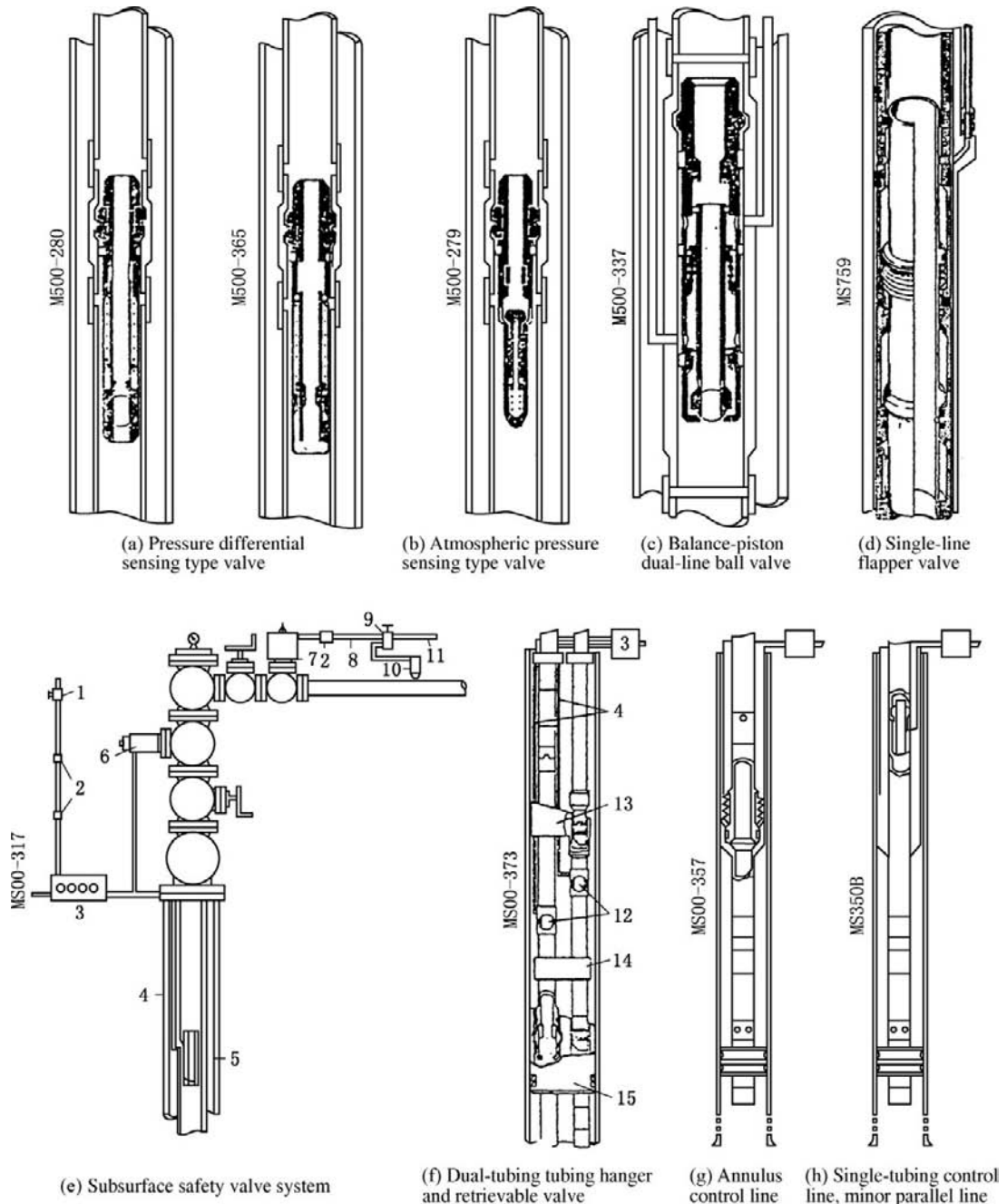


**FIGURE 9-88** Subsurface safety valves and completion forms. 1, emergency shutdown valve; 2, fusible plug; 3, hydraulic control manifold; 4, control line; 5, production casing; 6, hydraulic surface safety valve; 7, pneumatic surface safety valve; 8, low-pressure control line; 9, tee valve; 10, monitor relay; 11, low-pressure air or natural gas source; 12, tubing-retrievable tubing safety valve; 13, head-shaped head; 14, locating head; 15, hydraulic-set hanger.

TABLE 9-2 Technical Parameters of Baker Oil Tools Subsurface Safety Valve

Model Number	Size		Max OD		Min ID		Standard Hole Diameter		Working Pressure		
	in.	mm	in.	mm	in.	mm	in.	mm	psi	bar	
T (E)	2 <sup>3</sup> / <sub>8</sub>	60.33	3.625	92.08	1.906	48.41	1.875	47.63	5000	344.7	
										7500	517.1
	2 <sup>7</sup> / <sub>8</sub>	73.03	4.625	117.8	2.379	60.43	2.312	58.72	5000	344.7	
			5.135	130.43					10,000	689.5	
									5000	344.7	
3 <sup>1</sup> / <sub>2</sub>	88.90	5.380	136.65	2.875	73.03	2.812	71.42				
4 <sup>1</sup> / <sub>2</sub>	114.30	7.125	180.98	3.875	98.43	3.812	96.82				
5 <sup>1</sup> / <sub>2</sub>	139.70	8.375	212.73	4.625	117.48	4.562	115.87				
TM (E)	2 <sup>3</sup> / <sub>8</sub>	60.33	3.625	92.08	1.906	48.41	1.875	47.63	5000	344.7	
										5000	344.7
	2 <sup>7</sup> / <sub>8</sub>	73.03	4.625	117.48	2.379	60.43	2.312	58.72			
			5.135	130.43					10,000	689.5	
									5000	344.7	
	3 <sup>1</sup> / <sub>2</sub>	88.90	5.380	136.65	2.875				5000	344.7	
	4 <sup>1</sup> / <sub>2</sub>	114.30	7.125	180.98	3.875	73.03	2.812	71.42	5000	344.7	
						98.43	3.812	96.82	7500	517.1	
	5 <sup>1</sup> / <sub>2</sub>	139.70	8.375	212.73	4.625	117.48	4.562	115.87	5000	344.7	
									7500	517.1	
								10,000	689.5		
								11,000	758.4		
TSM (E)	2 <sup>3</sup> / <sub>8</sub>	60.33	3.500	88.90	1.906	48.41	1.875	47.63	9000	620.5	
			3.625	92.08						10,000	689.5
	3 <sup>1</sup> / <sub>2</sub>	88.90	5.000	127.00	2.877	73.08	2.812	71.42	5000	344.7	
			5.650	143.51	2.870	72.90			10,000	689.5	
	4 <sup>1</sup> / <sub>2</sub>	114.30	6.550	166.37	3.875	98.43	3.812	96.82	5000	344.7	
									7500	517.1	
									10,000	689.5	
	5 <sup>1</sup> / <sub>2</sub>	139.70	7.500	190.50	3.885	98.68				10,000	689.5
			7.700	195.58	4.625	117.48	4.562	115.87	5000	344.7	
			8.000	203.20	4.580	116.33			7500	551.5	
8.195			208.15	4.375	111.13	4.312	109.52	10,000	689.5		
8.195			208.15	4.550	115.57	θ	θ	11,000	758.4		
7	177.80	8.600	218.44	4.390	111.51	4.312	109.52	13,500	930.7		
		9.200	233.68	6.059	153.90	5.950	151.13	5000	344.7		
								7500	517.1		
								8000	551.5		
		9.300	236.22								
TUSM (E)	4 <sup>1</sup> / <sub>2</sub>	114.30	5.970	151.64	3.875	98.43	3.812	96.82	5000	344.7	
T(E)	Setting depth	ft	4000								
TM(E)		m	1219.5								
TSM(E)	Temperature range	°F	20~300								
TUSM(E)		°C	-6.7~149								

Note: 5 1/2-in. TSM(E) 11,000 psi type has no radial communicating component or valve seat hole.

- Packer setting. Different tubing strings have different appropriate packer-setting methods, which include mechanical press setting, hydraulic setting, and rota-setting.
- Perforating. The high temperature and high pressure generated during perforating may affect the tubing string. However, this status has a short duration.

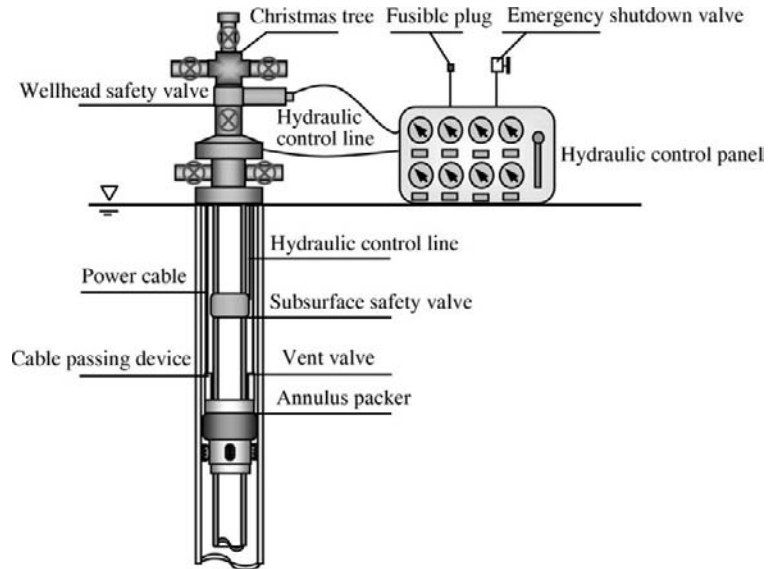


FIGURE 9-89 Subsurface safety control system.

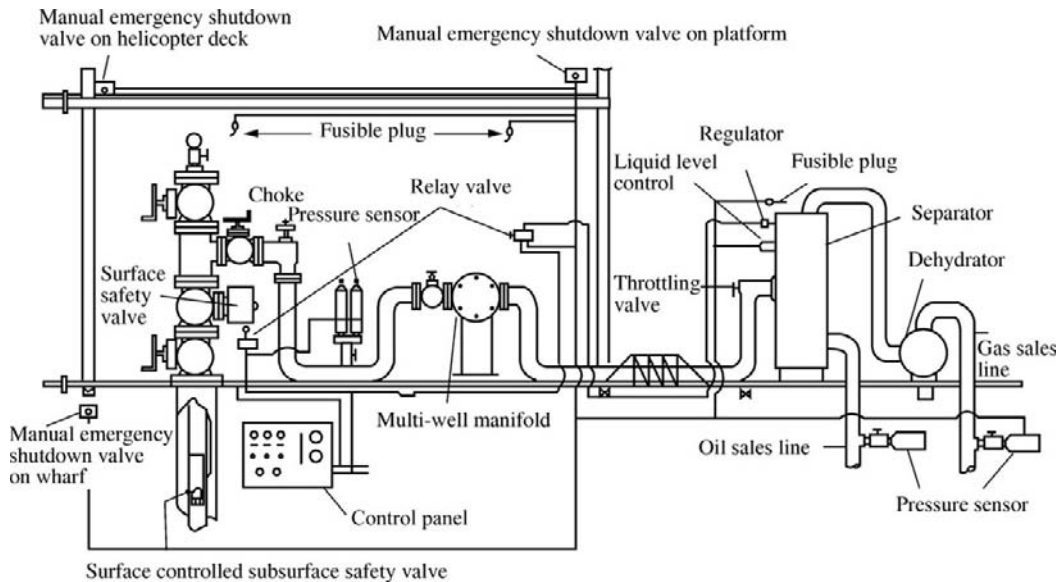


FIGURE 9-90 Offshore production platform safety control system.

4. Open flow, productivity test, or production. There is liquid or gas flowing out from the tubing string.
5. Shut-in pressure survey. The wellhead or testing valve is closed for recording the pressure build-up curve by using a bottomhole

pressure gauge. For a tubing string for combined perforating and testing, the switching of the downhole testing valve is controlled by pulling up and dropping down the string. Several switching times are taken if necessary.

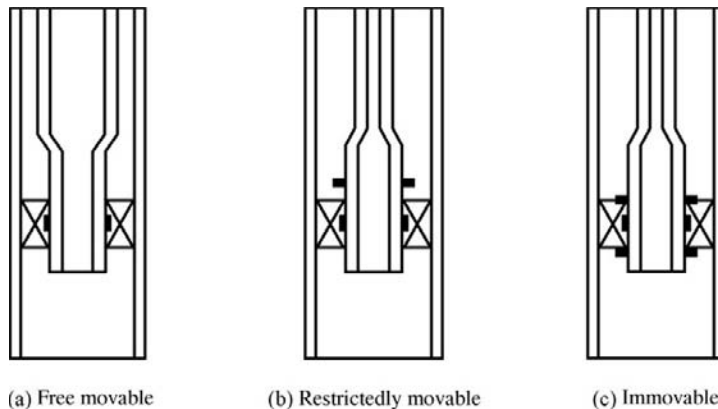


FIGURE 9-91 Relation between tubing string and packer.

6. Acidizing. There is no or low oil and gas production during the productivity test in some wells; thus stimulation is required.
7. Well killing. It can be normal circulation killing, reverse circulation killing, or noncirculatory killing.

### Helical Inflexion State Analysis of Tubing String

Tubing string may be in a straight-line stable state, a sinusoidal buckling state, or a helical buckling state when it bears a pressing load in the well. In practice, tubing string is not in a straight-line state, but in the irregular helical shape with multiple inflexion points and fulcrums. The more irregular the borehole and the longer the tubing string, the more complicated the buckling shape of tubing string.

#### Main Factors Affecting String Inflexion.

Tubing string may inflect under the action of external forces in the borehole, and its deformation may be restricted by the constraining conditions of the borehole wall and end. The affecting factors mainly include: (1) axial force; (2) fluid pressure; (3) bending rigidity of the string cross-section; (4) tubing string length; (5) buoyant weight of the tubing string; (6) borehole or casing size; (7) friction; and (8) constraining condition of the end.

**Determination of Critical Inflexion Load on Tubing String.** Tubing string may generate

helical buckling in a well when it is pressed to a certain degree. The critical buckling load can be derived by using the energy method and is expressed as shown in Equation (9-1).

(9-1)

$$F_{cr} = 5.55 (EIW_e^2)^{1/3}$$

where:  $F_{cr}$  = critical helical buckling load, N;  $E$  = elastic modulus, Pa;  $I$  = cross-sectional inertia moment,  $m^4$ ;  $W_e$  = buoyancy weight of tubing string per unit length, N/m.

In order to consider comprehensively the effect of the axial load on string and the effects of internal and external pressures, equivalent axial force is adopted for analyzing. The expression is shown in Equation (9-2).

(9-2)

$$F_e = F + (p_i + \rho_i v_i^2) A_i - (p_o - \rho_o v_o^2) A_o$$

where:  $F_e$  = equivalent axial force, N;  $F$  = actual axial force, N;  $p_i$ ,  $p_o$  = pressures inside and outside tubing string, Pa;  $v_i$ ,  $v_o$  = fluid velocities inside and outside tubing string, m/s;  $\rho_i$ ,  $\rho_o$  = fluid density inside and outside tubing string,  $kg/m^3$ ;  $A_i$ ,  $A_o$  = inside and outside cross-sectional areas of tubing string,  $m^2$ .

If  $F_e \geq F_{cr}$ , tubing string may generate helical buckling. If  $F_e < F_{cr}$ , tubing string will be approximately in a straight-line stable state.

**Contact Load under the Condition of Helical Buckling of Tubing String.** If  $F_e \geq F_{cr}$ , tubing string will generate helical buckling, of which

the geometric equations are shown in Equation (9-3).

(9-3)

$$U_1 = r \cos\theta, U_2 = r \sin\theta, \theta = 2\pi z/p$$

where:  $U_1, U_2$  = locations of axes of tubing string in the directions of x and y, m;  $\theta$  = helix angle, ( $^\circ$ );  $r$  = radial distance between tubing string and casing wall, m;  $p$  = helix pitch, m;  $z$  = vertical height (above neutral point), m.

The relation between helical pitch and equivalent axial force, which has been obtained by Cheatham, Patillo, and Kwon et al. on the basis of the virtual work principle, is shown in Equation (9-4).

(9-4)

$$p^2 = \frac{8\pi^2 EI}{F_e}$$

The contact load during contact between tubing string per unit length and casing, which has been derived by Mitchell, is shown in Equation (9-5).

(9-5)

$$W_n = \frac{rFe^2}{4EI}$$

where:  $W_n$  = contact load during contact between tubing string per unit length and casing wall, N/m.

### Basic Models for Calculating the Deformation of Tubing String

Temperature effect, piston effect, ballooning effect, and helical buckling effect should be considered when tubing string deformation is calculated.

**Deformation of Tubing String Due to Temperature Effect.** The tubing string length may be greatly changed due to the thermal expansion or shrinkage that is generated by the change of the environmental temperature of the tubing string due to the change of status during running in or working. The change of tubing string length due to temperature effect is calculated as shown in Equation (9-6).

(9-6)

$$\Delta L_w = 3.61 \times 10^{-6} \times L_t \times \Delta \bar{T}$$

where:  $\Delta L_w$  = change of tubing string length due to temperature effect, m;  $L_t$  = tubing string length, m;  $\Delta \bar{T}$  = change of mean temperature,  $^\circ\text{C}$ .

The mean temperature of the tubing string in a given operational mode means the mean value between the temperatures at the top and the bottom of the tubing string. When tubing string movement is restricted, the change in temperature may generate a force on the tubing string. The force due to temperature effect is shown in Equation (9-7).

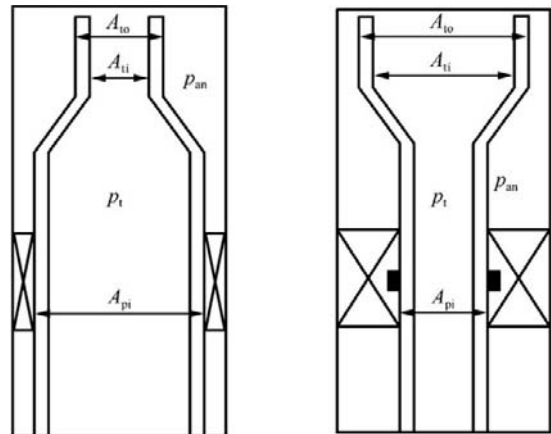
(9-7)

$$F_w = 75.81 \times A_{tw} \times \Delta \bar{T}$$

where:  $F_w$  = force due to temperature effect, N;  $A_{tw}$  = tubing-wall cross-sectional area,  $\text{cm}^2$ .

When the operational mode changes, the temperature effect caused by the difference of mean temperature between two sequent operational modes may generate great change in length and force.

**Deformation of Tubing String Due to Piston Effect.** The changes of the pressure in the annulus at the packer and the pressure in tubing on different areas (Figure 9-92) may generate a force that may change the length due to the piston effect.



(a) Packer with large hole (b) Packer with small hole  
**FIGURE 9-92** Tubing and packer system.

This force and the change of length can be calculated as shown in Equations (9-8) and (9-8).

(9-8)

$$F_h = [\Delta p_t(A_{pi} - A_{ti}) - \Delta p_{an}(A_{pi} - A_{to})] \times 10^{-4}$$

(9-9)

$$\Delta L_h = \frac{L_t}{EA_{tw}} [\Delta p_t(A_{pi} - A_{ti}) - \Delta p_{an}(A_{pi} - A_{to})]$$

where:  $F_h$  = force due to piston effect, N;  $\Delta L_h$  = change of tubing string length due to piston effect, m;  $E$  = elastic modulus ( $2.06 \times 10^{11}$  Pa for steel), Pa;  $A_{pi}$  = area of packer ID,  $\text{cm}^2$ ;  $A_{ti}$  = area of tubing ID,  $\text{cm}^2$ ;  $A_{to}$  = area of tubing OD,  $\text{cm}^2$ ;  $\Delta p_t$  = change of pressure in tubing at packer, Pa;  $\Delta p_{an}$  = change of pressure in annulus at packer, Pa;  $A_{tw}$  = cross-sectional area of tubing steel material,  $\text{cm}^2$ .

A downward force is generated by the pressure in the annulus, and an upward force is generated by the pressure in tubing for the packer with a large hole, which is the opposite of that for the packer with a small hole.

**Deformation of the Tubing String Due to Ballooning and Reverse Ballooning Effect.**

Internal stress may cause tubing to balloon or expand and make it shorten. In addition, annulus pressure may squeeze the tubing string and make it elongate, which is known as reverse ballooning. The change in length and the force are as shown in Equations (9-10) and (9-11).

(9-10)

$$\Delta L_g = \frac{2\nu_t}{E} \times \frac{\Delta \bar{p}_t - R^2 \Delta \bar{p}_{an}}{R^2 - 1}$$

(9-11)

$$F_g = 6.1 \times 10^{-6} (\Delta \bar{p}_t A_{ti} - \Delta \bar{p}_{an} A_{to})$$

where:  $\Delta L_g$  = change of tubing string length due to ballooning effect, m;  $\nu$  = Poisson's ratio ( $\nu = 0.3$  for steel);  $L_t$  = tubing string length, m;  $\Delta \bar{p}_t$  = change of mean pressure in tubing string due to change of operational mode, Pa;  $\Delta \bar{p}_{an}$  = change of mean pressure in annulus due to change of operational mode, Pa;  $R$  = ratio of tubing OD to tubing ID, dimensionless.

**Deformation of the Tubing String Due to Helical Buckling Effect.** For a free tubing

string, it will tend to helical buckling only if  $p_t > p_{an}$ , so that the tubing string is shortened. The force due to helical buckling effect is negligible. The change of tubing string length is shown in Equations (9-12), (9-13), and (9-14).

(9-12)

$$\Delta L_e = \frac{1.25 \times 10^{-3} r^2 A_{pi}^2 (\Delta p_t - \Delta p_{an})^2}{EI (w_t + w_{ft} - w_{fd})}$$

(9-13)

$$r = \frac{d_{ci} - d_{to}}{2}$$

(9-14)

$$I = \frac{\pi (d_{to}^4 - d_{to}^4)}{64}$$

where:  $\Delta L_e$  = change of tubing string length due to helical buckling effect, m;  $r$  = gap radius between tubing OD ( $d_{to}$ ) and casing ID ( $d_{ci}$ ), cm;  $w_t$  = tubing string gravity, N/m;  $w_{ft}$  = tubing string gravity in liquid, N/m;  $w_{fd}$  = gravity of liquid displaced, N/m;  $I$  = inertia moment of tubing string,  $\text{cm}^4$ .

Helical buckling makes tubing string shorten.

The total change of tubing string length (or force) is the sum of the changes of lengths (or forces) due to the piston effect, the ballooning effect, and the temperature effect. The direction of the change of length (or acting force) due to each effect should be considered when these changes in length are totaled. Thus the displacement (or force) due to some effect may be counteracted or augmented by the displacements (or forces) due to other effects when conditions are changed.

The constants of tubing for determining displacement due to helical buckling caused by pressure are listed in Table 9-3 for convenience of calculation.

## Strength Analysis of Tubing String

**Tension Safety Factor.** The tension safety factor is computed as shown in Equation (9-15):

(9-15)

$$K_{RD} = \frac{F_{RD}}{W_e L}$$

where:  $F_{RD}$  = tensile strength of tubing string, N;  $K_{RD}$  = tension safety factor of tubing string, dimensionless;  $L$  = tubing string length, m.

TABLE 9-3 Constants of Tubing for Determining Displacement Due to Helical Buckling Caused by Pressure

Tubing OD (mm)	$W_t$ (N/m)	$A_{to}$ (cm <sup>2</sup> )	$A_{fi}$ (cm <sup>2</sup> )	$A_{fw}$ (cm <sup>2</sup> )	$I$ (cm <sup>2</sup> )	$F_{oi}^2$ (cm <sup>4</sup> )	$W_{ft}$ and $W_{fd}$ (N/m)	Relative Fluid Density											
								0.84	0.96	1.08	1.20	1.32	1.44	1.56	1.68	1.80	1.92	2.04	2.16
42.2	35.12	13.96	9.65	4.31	8.12	1.448	$W_{ft}$	8.1	9.3	10.4	11.6	12.7	14.0	15.0	16.3	17.4	18.6	19.7	20.8
							$W_{fd}$	11.6	13.4	15.0	16.8	18.4	20.0	12.8	23.4	25.0	26.8	28.4	30.2
48.3	42.38	18.29	13.13	5.15	12.90	1.393	$W_{ft}$	11.1	12.5	14.1	15.7	17.4	19.0	20.6	22.0	23.6	25.2	26.8	28.4
							$W_{fd}$	15.4	17.5	19.7	12.0	24.2	26.3	28.4	30.8	32.9	35.1	37.4	39.5
50.8	49.74	20.27	14.13	6.14	16.81	1.434	$W_{ft}$	11.8	13.6	15.2	17.0	18.6	20.4	22.0	23.8	25.4	27.2	28.8	30.6
							$W_{fd}$	17.0	19.5	21.8	24.3	26.8	29.2	31.7	34.0	36.5	39.0	41.3	43.8
52.4	49.74	21.55	15.51	6.04	17.81	1.389	$W_{ft}$	13.1	14.8	16.8	18.6	20.4	22.4	24.2	26.1	27.9	29.9	31.7	33.5
							$W_{fd}$	18.1	20.8	23.3	25.9	28.4	31.1	33.6	36.1	38.8	41.3	44.0	46.5
60.3	68.67	28.57	20.16	8.41	32.63	1.417	$W_{ft}$	17.0	19.3	21.8	24.2	26.7	29.0	31.5	33.8	36.3	38.8	41.1	43.5
							$W_{fd}$	24.0	27.4	30.8	34.3	37.7	41.1	44.5	47.9	51.5	54.9	58.3	61.7
73.0	95.06	41.87	30.19	11.69	64.05	1.387	$W_{ft}$	25.4	29.0	32.6	36.3	39.9	43.5	47.1	50.87	54.4	58.0	61.5	65.1
							$W_{fd}$	35.1	40.3	45.3	50.3	55.3	60.3	65.3	70.3	75.3	80.5	85.5	90.5
88.9	134.50	62.06	45.35	16.71	161.69	1.368	$W_{ft}$	38.1	43.5	49.0	54.4	59.9	65.3	70.7	76.2	81.6	87.1	92.5	98.0
							$W_{fd}$	52.1	59.6	65.3	74.4	81.9	89.5	96.8	104.3	111.8	119.1	126.7	134.0

**Internal Pressure Factor and Collapse Safety**

**Factor.** The internal pressure factor and collapse safety factor are calculated as shown in Equation (9-16).

(9-16)

$$K_{Ri} = \frac{p_{Ri}}{p_i - p_o} \quad K_{Ro} = \frac{p_{ko}}{p_o - p_i}$$

where:  $K_{Ri}$ ,  $K_{Ro}$  = internal pressure factor and collapse safety factor, dimensionless;  $p_{Ri}$ ,  $p_{Ro}$  = internal pressure strength and collapse strength, Pa.

**Three-Dimensional Combination Stress Analysis**

1. Axial stress caused by actual axial force, shown in Equation (9-17)

(9-17)

$$\sigma_{z1} = \frac{F_d}{A_s}$$

where:  $F_d$  = actual axial force of potential dangerous cross-section, N;  $A_s$  = cross-sectional area of dangerous cross-section,  $m^2$ .

2. Axial stress caused by helical buckling, shown in Equation (9-18)

(9-18)

$$\sigma_{z2} = \begin{cases} \frac{F_{ed} r_d}{2I_d}, & Z_d \leq L_{ni}, i = 1, 2, 3 \\ 0 & Z_d > L_{ni}, i = 1, 2, 3 \end{cases}$$

where:  $F_{ed}$  = equivalent axial force of dangerous cross-section, N;  $I_d$  = inertia moment of dangerous cross-section,  $m^4$ ;  $r_d$  = radial distance of arbitrary point on dangerous cross-section, m;  $Z_d$  = location of dangerous cross-section, m.

3. Radial stress and circumferential stress generated by interval and external pressures, shown in Equation (9-19)

(9-19)

$$\sigma_\theta = \frac{p_{id} r_{id}^2 - p_{od} r_{od}^2}{r_{od}^2 - r_{id}^2} - \frac{r_{od}^2 r_{id}^2 - (p_{id} - p_{od})}{(r_{od}^2 - r_{id}^2) r_d^2}$$

$$\sigma_r = \frac{p_{id} r_{id}^2 - p_{od} r_{od}^2}{r_{od}^2 - r_{id}^2} + \frac{r_{od}^2 r_{id}^2 - (p_{id} - p_{od})}{(r_{od}^2 - r_{id}^2) r_d^2}$$

where:  $\sigma_r$  = radial stress, Pa;  $\sigma_\theta$  = axial stress, Pa;  $p_{id}$ ,  $p_{od}$  = internal and external pressures at dangerous cross-section, Pa;  $r_{id}$ ,  $r_{od}$  = inside

and outside radiuses at dangerous cross-section, m.

4. Equivalent stress, shown in Equation (9-20)

(9-20)

$$\sigma_{zd} = \frac{\sqrt{2}}{2} \sqrt{(\sigma_{z1} + \sigma_{z2} - \sigma_r)^2 + (\sigma_{z1} + \sigma_{z2} - \sigma_\theta)^2 + (\sigma_r - \sigma_\theta)^2}$$

5. Safety factor, shown in Equation (9-21)

(9-21)

$$K_{zd} = \frac{[\sigma]}{\sigma_{zd}}$$

where:  $[\sigma]$  = permissible stress, Pa.

**Total Safety Factor.** The total safety factor is computed as shown in Equation (9-22).

(9-22)

$$K_s = \min\{K_{RD}, K_{Ri}, K_{Ro}, K_{zd}\}$$

**Determination of Ultimate Operational Parameters**

1. Residual tensile force, shown in Equation (9-23)

(9-23)

$$F_R = F_{RD} - K_s W_e L = (K_{RD} - K_s) W_e L$$

2. Safe operating pressure difference of tubing string

The maximum operating pressure difference controlled by the inner wall of the tubing string is shown in Equation (9-24).

(9-24)

$$\Delta p_{maxi} = p_{Ri} / K_s$$

The maximum operating pressure difference controlled by the outer wall of the tubing string is shown in Equation (9-25).

(9-25)

$$\Delta p_{maxo} = p_{Ro} / K_s$$

The safe operating pressure difference of the tubing string is shown in Equation (9-26).

(9-26)

$$\Delta p_{max} = \min\{\Delta p_{maxi}, \Delta p_{maxo}\}$$

**REFERENCES**

---

- [1] Wan Renpu, Advanced Well Completion Engineering, second ed., Petroleum Industry Press, Beijing, 2000 (in Chinese).
- [2] Wan Renpu, et al., Petroleum Production Engineering Handbook, Petroleum Industry Press, Beijing, 2000 (in Chinese).
- [3] Zhangqi, Wan Renpu, Petroleum Production Engineering Program Design, Petroleum Industry Press, Beijing, 2002 (in Chinese).
- [4] Chang Zihen, et al., Petroleum Exploration and Development Technology, Petroleum Industry Press, Beijing, 2001 (in Chinese).
- [5] He Shenghou, Zhangqi, Oil and Gas Production Engineering, Petrochemistry Press, Beijing, 2003 (in Chinese).
- [6] Zhangyi, et al., New Progress of Petroleum Production Engineering, Petrochemistry Press, Beijing, 2005 (in Chinese).
- [7] Yand Chuandong, et al., Gas Production Engineering, Petroleum Industry Press, Beijing, 1997 (in Chinese).
- [8] Offshore Oil and Gas Field Well Completion Handbook, Petroleum Industry Press, Beijing, 1998 (in Chinese).
- [9] Liu Yuzhang, Zheng Junde, Progress of Petroleum Production Engineering, Petroleum Industry Press, Beijing, 2006 (in Chinese).
- [10] He Shenghou, Oil and Gas Production Engineer Handbook, Petrochemistry Press, Beijing, 2006 (in Chinese).

# CHAPTER 10

## Wellhead Assembly

### OUTLINE

#### 10.1 Oil-Well Christmas Tree and Tubinghead

- Christmas Tree and Tubinghead for a Flowing Well
  - Common Christmas Tree and Tubinghead for a Flowing Well*
  - Dual-String Christmas Tree and Tubinghead for a Flowing Well*
- Christmas Tree and Tubinghead for an Artificial Lift Well
  - Christmas Tree and Tubinghead for a Sucker Rod Pump Well*
  - Christmas Tree for an Electric Submersible Pump Well*
  - Christmas Tree for a Hydraulic Piston Pump Well*
  - Christmas Tree for a Gas-Lift Production Well*
- Technical Requirements for Christmas Tree and Tubinghead

- Metallic Materials for Main Parts*
- Nonmetallic Packing Element Material*

#### 10.2 Gas-Well Christmas Tree and Tubinghead

- Requirements for Materials Commonly Used Gas-Well Christmas Trees and Tubingheads
  - Gas-Well Christmas Trees*
  - Tubingheads*
- High-Pressure Gas-Well Wellhead Assembly
  - High-Pressure Gas-Well Christmas Tree Tubinghead*
  - Tubing Hanger*
- High-Sulfur Gas-Well Wellhead Assembly
  - CAMERON Wellhead Assembly*
  - Double-Wing Y-Shaped Gas-Well Wellhead Assembly*

#### 10.3 Water Injection and Thermal Production Wellhead Assembly

- Wellhead Assembly for a Water Injection Well
- Wellhead Assembly for a Thermal Production Well
  - Application Range*
  - Notation of Model Numbers*
  - Structures*
  - Basic Parameters*

#### 10.4 Common Components of a Wellhead Assembly

- Casinghead
  - Notation of Model Number*
  - Structures*
  - Basic Parameters*
- Wellhead Valves
- Surface Safety Valves
- Chokes
  - Fixed Choke*
  - Adjustable Choke*
- Tees and Spools
- Seal Gasket Ring and Gasket
- Ring Groove for Flange
  - Application Range*
  - Types and Sizes*
  - Technical Requirements*
- Flanged Connection Nut

#### References

An oil and gas well wellhead assembly is used for hanging downhole tubing string and casing string; sealing tubing-casing and casing-casing annuluses; injecting steam, gas, water, and chemicals; and

acidizing and fracturing. It is a key piece of equipment for safe production. The wellhead assembly consists mainly of casing head, tubing head, and Christmas tree (Figure 10-1).

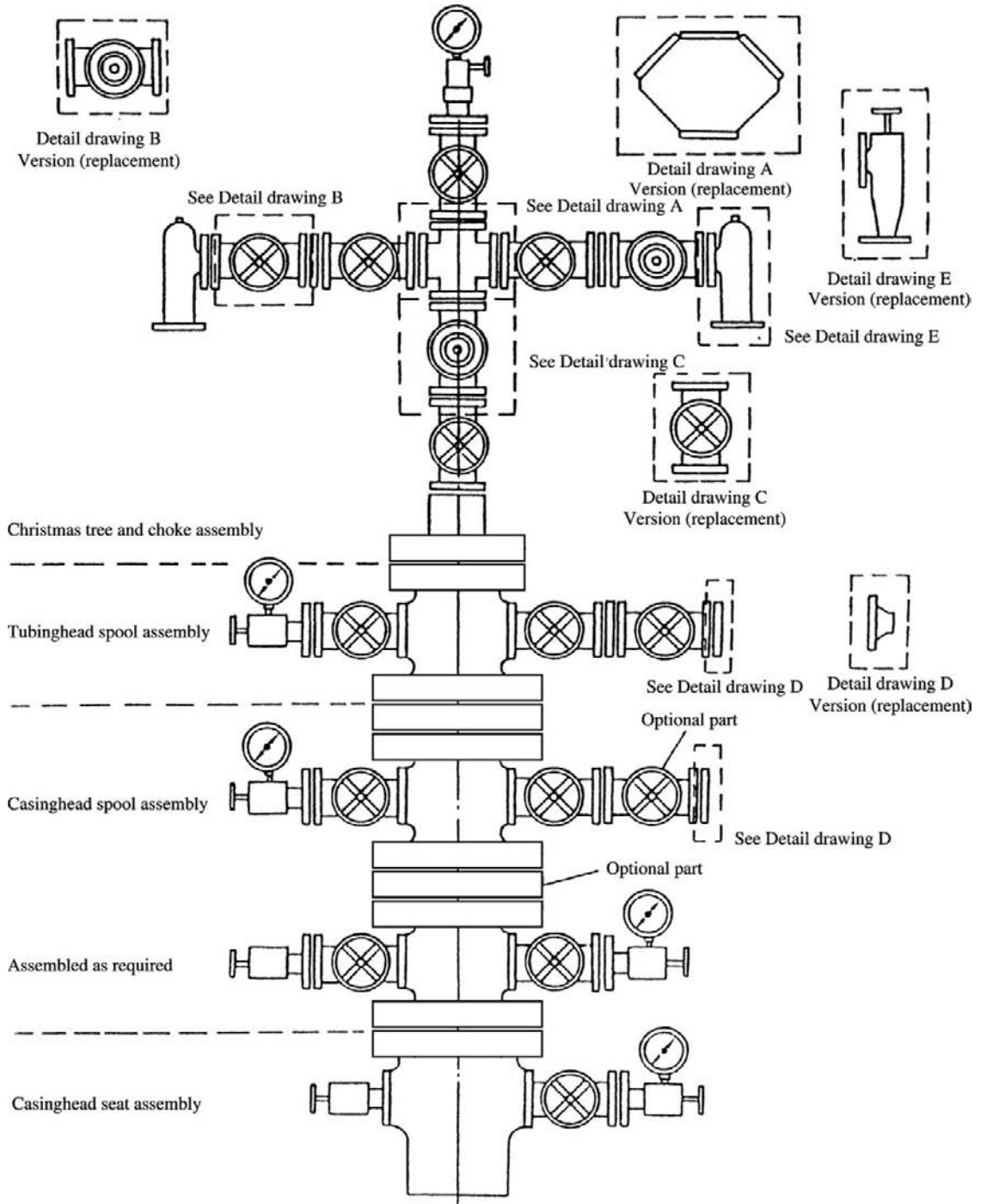


FIGURE 10-1 Oil and gas well wellhead assembly.

A “Christmas tree” is an assembly consisting of valves and fittings and is used for controlling oil- and gas-well fluid and providing outlets and inlets for produced fluid and washing fluid, and so on. It includes all the equipment above the tubinghead spool flange. A Christmas tree assembly can consist of various combinations to meet the requirements of any special usage. Different Christmas trees have different uses including oil production (flowing and artificial lift), gas production (natural gas and various acidic gases), water injection, thermal production, and fracturing and acidizing, and they form a series with different grades of pressures under which they are used.

A tubinghead consists of a tubinghead spool and a tubing hanger. It is mainly used for hanging tubing string and sealing tubing string and tubing-casing annulus. The tubinghead is installed between the Christmas tree and the casinghead. The upper flange plane of the tubinghead spool is the datum level for calculating the distance between the master bushing and the tubing hanger and the well depth data.

The tubinghead spool is installed on the casinghead, which is used for hanging intermediate casing and production casing, sealing casing-casing annulus, and providing a connection for installing upper devices including blowout preventer and tubinghead.

## 10.1 OIL-WELL CHRISTMAS TREE AND TUBINGHEAD

Oil-well Christmas trees include the Christmas tree for a flowing well and the Christmas tree for an artificial lift well. They are connected with the tubingheads, which have corresponding uses.

### Christmas Tree and Tubinghead for a Flowing Well

The Christmas tree for a flowing well is an important component part of the wellhead assembly used for putting into commercial production and controlling the production relying on natural energy. The productive media are

both gas and liquid phases. The Christmas tree and tubinghead for a flowing well have different grades in accordance with wellhead pressure.

**Common Christmas Tree and Tubinghead for a Flowing Well.** The common Christmas trees and tubingheads for a flowing well include KY25-65 Christmas tree and tubinghead and CYb-250S series (Table 10-1 and Figure 10-2).

There are two types of tubinghead: (1) the tubinghead with both upper and lower flanges (Figure 10-3), and (2) the tubinghead with upper flange and lower thread (Figure 10-4). A tubing hanger with a metallic or rubber O-ring is connected with tubing and is seated in the tubinghead spool cone by tubing gravity, which makes operation convenient, makes wellhead assembly easy to change, has high safety, and is the method commonly used in conventional wells.

**Dual-String Christmas Tree and Tubinghead for a Flowing Well.** There are two types of flowing-well Christmas trees and tubingheads used for dual-string separate-layer flowing production: (1) the dual-string Christmas tree, shown in Figure 10-5, and (2) the VG dual-string integral forged Christmas tree, shown in Figure 10-6.

The right side of a dual-string Christmas tree controls main-string production and test, and the tubing pressure gauge only reflects main-string tubing pressure. The left side controls sub-string production and test, and the tubing pressure gauge only reflects sub-string tubing pressure. Casing pressure gauge only reflects sub-string casing pressure.

A parallel dual-string tubinghead is generally used for dual-string production. The tubinghead spool for parallel dual-string completion is basically similar to that for single-string completion, except that a parallel dual-string tubing hanger consists of an overall tubing hanger and both main hanger and sub-hanger. The overall tubing hanger is seated on the spool, and the main hanger and sub-hanger are seated on the overall tubing hanger. The main tubing string, which has a packer, is used for lower-reservoir production, while the sub-string is used for upper-reservoir production.

TABLE 10-1 Technical Parameters for Common Christmas Trees

Model Number	Strength Test Pressure (MPa)	Working Pressure (MPa)	Type of Connection	Weight (kg)	Jackscrew Flange Size (mm)			Valve		Steel ring (mm)		Tubing Hanger O-ring (mm)	Tubing Connected [mm (in.)]	Nominal Drift Diameter (mm)
					Thread OD	Thread Center Distance	Thread Hole OD × number	Type	Number	Valve	Spool			
KYS25-65DG	50	25	Collar clamp	550	380	318	φ30 × 12	Gate	6	88.8	211	1680 × 1480 × 100	73 (2 <sup>7</sup> / <sub>8</sub> )	65
KYS25-65SL	50	25	Collar clamp	380	380	318		Gate	3	92	211	1390 × 1220 × 850	73 (2 <sup>7</sup> / <sub>8</sub> )	65
KYS15-62DG	30	15	Collar clamp	152				Ball valve	3	78	190			
KYS8-65	16	8	Collar clamp	305	380	318	φ30 × 12	Gate	4	88.7	211	168 × 1480 × 100 1390 × 1220 × 8.50	73 (2 <sup>7</sup> / <sub>8</sub> )	65
KYS21-65	42	21	Flange		380	318	φ30 × 12	Gate	6	110	211	1400 × 1200 × 8.5	73 (2 <sup>7</sup> / <sub>8</sub> )	65



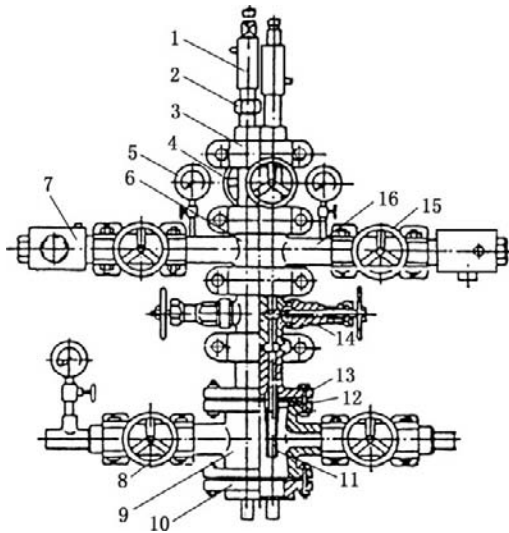


**FIGURE 10-5** Dual-string Christmas tree. 1, lubricator; 2, high-pressure union; 3, collar clamp; 4, paraffin valve; 5, pressure gauge; 6, cross joint; 7, choke nipple; 8, casing valve; 9, tubinghead spool; 10, top flange of casinghead; 11, variable-thread nipple; 12, tubing hanger; 13, Bottom flange of Christmas tree; 14, double-ported valve; 15, production valve; 16, dual tee.

The dual-string tubinghead for a parallel dual-string Christmas tree is shown in Figure 10-7, and the dual-tubing hanger is shown in Figure 10-8.

### Christmas Tree and Tubinghead for an Artificial Lift Well

The Christmas tree for an artificial lift well is used for oil production from a well that has lost flowing capacity and requires artificial lift equipment to be used. Different artificial lift methods require different types of Christmas trees.

#### Christmas Tree and Tubinghead for a Sucker Rod Pump Well

1. Christmas tree for conventional sucker rod pump well.

The Christmas tree and tubinghead for a pumping well are used for hanging tubing, seating tubing-casing annulus, sealing polished rod, and controlling oil well production. The original flowing-well Christmas tree and tubinghead remade can be used due to the low pressure

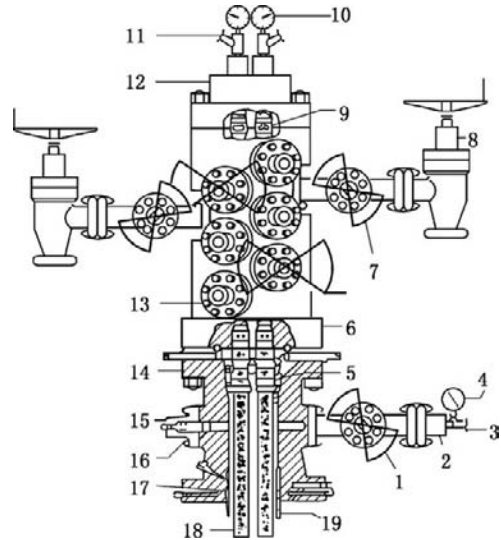


**FIGURE 10-6** Dual-string integral Christmas tree. 1, VG300 valve; 2, blind flange; 3, pressure-gauge needle valve; 4, pressure gauge; 5, tubing hanger; 6, dual-string integral Christmas tree; 7, VG300 valve; 8, variable choke; 9, Type D metallic seal; 10, pressure gauge; 11, pressure-gauge needle valve; 12, top reducing joint; 13, VG300 valve; 14, dual-seal tubinghead; 15, blind flange; 16, VR plug; 17, BT seal; 18, tubing; 19, casing.

borne and the simple structures. The basic components include tubinghead spool, tubing tee, the rubber valve for polished rod sealer, and the related valves (Figure 10-9).

The tubinghead is used for hanging tubing and sealing tubing-casing annulus. The extension pipeline on the side of the spool can be used for measuring the depth of working fluid level, venting casing gas, hot well-flushing, and so on.

The tubing tee is connected with the tubinghead by the upper flange of the tubinghead. Its extension line is connected with the flowline and is the passage of well fluid flow out of the wellhead.

The polished rod sealer is installed at the top end of the tubing tee. Its structure is shown in Figure 10-10. During normal production, the rubber valve is loosened and the polished rod is sealed by the packing element. The rubber valve is closed before the packing element is changed. After the packing element is changed,

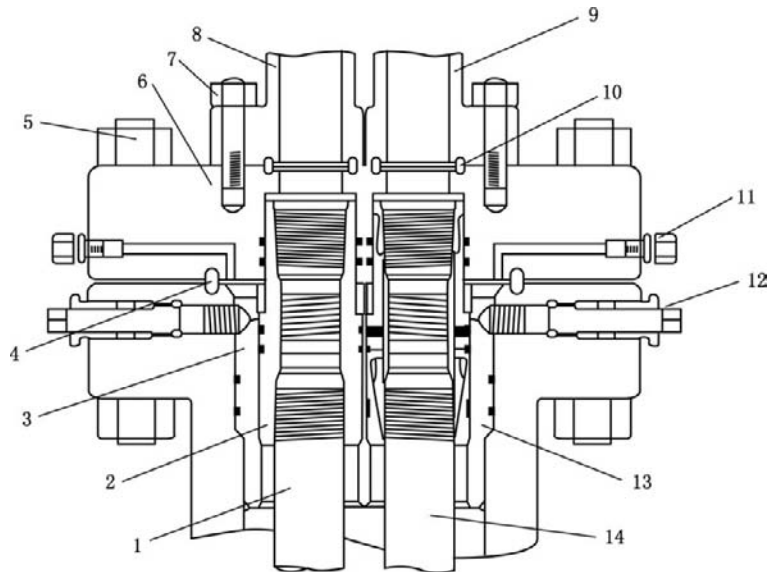


**FIGURE 10-7** Dual-string tubinghead. 1, main tubing; 2, main tubing hanger; 3, overall tubing hanger; 4, larger steel ring; 5, stud bolt; 6, upper flange of tubinghead; 7, bolt; 8, main Christmas tree; 9, sub-tree; 10, small steel ring; 11, seal material filling hole; 12, gib screw; 13, sub-tubing hanger; 14, sub-tubing.

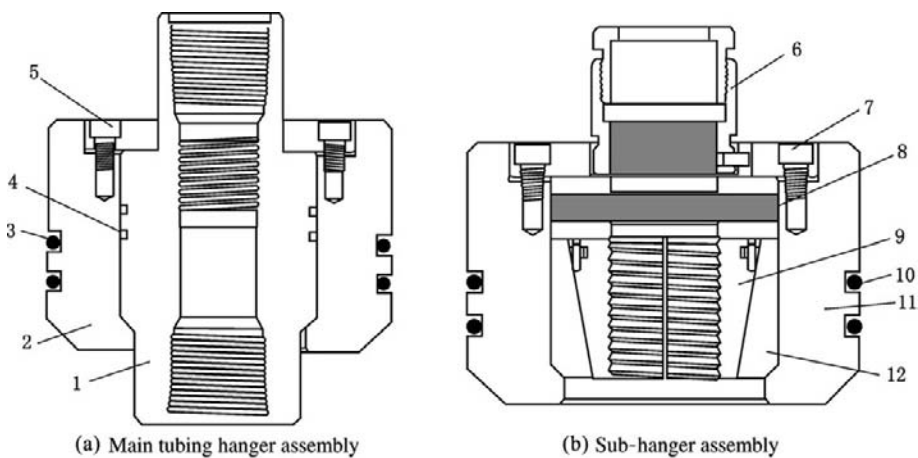


**FIGURE 10-8** Dual-string tubing hanger. 1, main tubing hanger; 2, 11, overall tubing hanger; 3, 10, seal ring of overall tubing hanger; 4, seal ring of main tubing hanger; 5, 7, gib screw; 6, nipple sealer; 8, seal ring of sub-tubing hanger; 9, slips; 12, slip bowl.

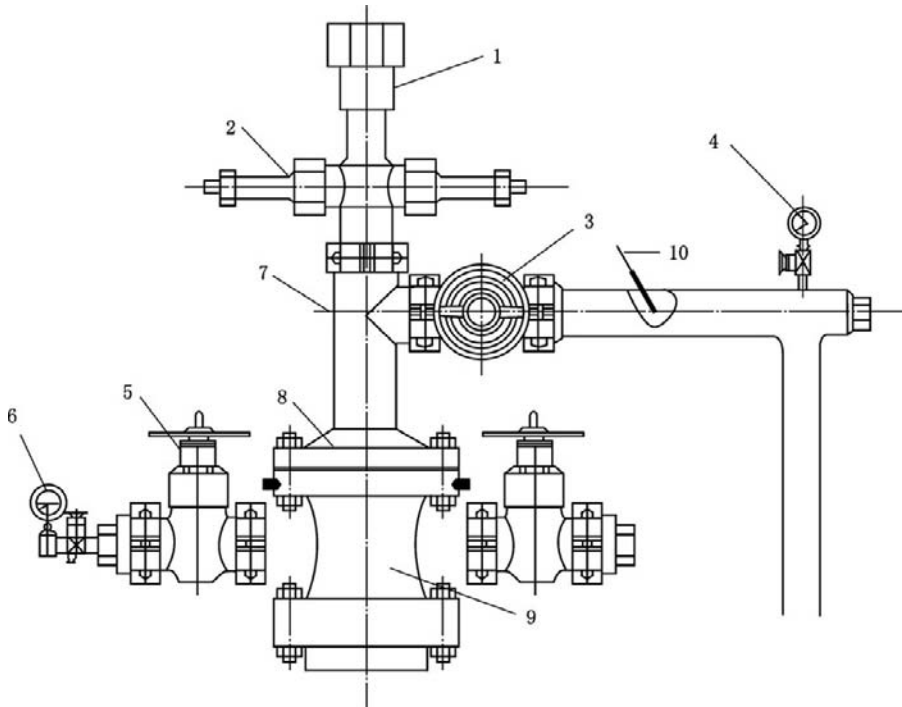


**FIGURE 10-9** Christmas tree and tubinghead for sucker rod pump well. 1, sealing box of polished rod; 2, rubber valve; 3, production valve; 4, tubing pressure gauge; 5, casing valve; 6, casing pressure gauge; 7, tee; 8, upper flange of tubinghead; 9, tubinghead; 10, thermometer.

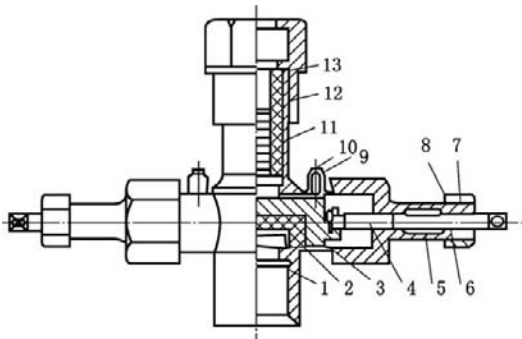


**FIGURE 10-10** Polished rod sealer. 1, main body; 2, sealing rubber; 3, core; 4, screw rod; 5, seal box; 6, 11, sealing rubber; 7, 12, gland; 8, 13, sealing rubber gland; 9, copper washer; 10, guide screw.

the rubber valve is loosened and normal production is resumed.

2. Eccentric tubinghead for testing in annulus.

For a flowing well, a testing instrument can arrive at the reservoir through tubing.

For a pumping well with sucker rod pump, however, the testing instrument cannot pass through tubing due to the sucker rod in the tubing, so testing can only be achieved through annulus. This type of tubinghead can eccentrically hang tubing string and an annulus test passage is formed.

a. Model SPA I single rotating eccentric tubinghead (Figure 10-11). The technical parameters are as follows.

Nominal pressure	16 MPa	Seal pressure	16 MPa
Tester diameter	≤25 mm	Flange diameter	380 mm
Steel ring groove diameter	211 mm	Test hole thread	ZG 1 1/4
Rotation method	Tubing	Tubing hanger thread	2 7/8 NU

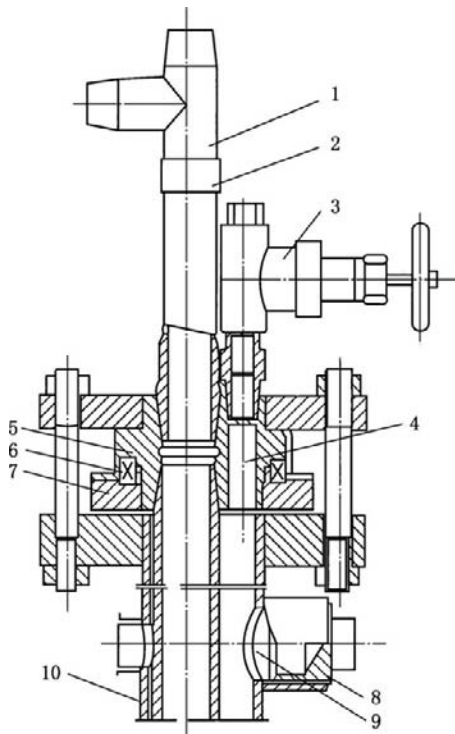


**FIGURE 10-11** Model SPA I single rotating eccentric tubinghead. 1, tee; 2, rotary nipple; 3, blowout preventing valve; 4, test hole; 5, eccentric tubing hanger; 6, planar ball bearing; 7, steel ring cap; 8, sticking releasing head; 9, sight hole; 10, casing nipple.

The eccentric tubinghead and tubing hanger are in an eccentric state in casing. The tubing string in the wellbore is tightly leaned against a side of the inner wall of the casing. The eccentric tubing hanger is seated on the casing flange or the casing spool flange by planar ball bearing; thus the location of the tubing string can change in casing.

When resistance or sticking is generated in the process of downhole instrument pulling or running in annulus or when the problem of electric cable twining around the tubing is generated, turning tubing can change the relative location of the tubing string in the crescent space inside the casing; thus the sticking and twining can be removed.

- b. Model SPA II dual rotating eccentric tubinghead (Figure 10-12). This type of eccentric

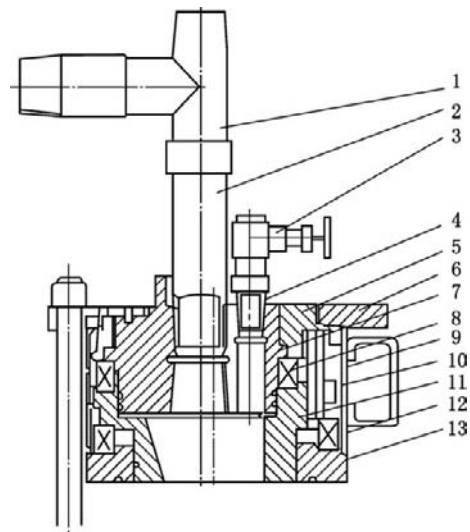


**FIGURE 10-12** Model SPA II dual rotating eccentric tubinghead. 1, tee; 2, rotary nipple; 3, valve; 4, union; 5, upper cap; 6, flange; 7, rotary tubing hanger; 8, bearing; 9, housing; 10, pin; 11, upper bearing seat; 12, bearing; 13, lower bearing seat.

tubinghead has all the functions that the single rotating eccentric tubinghead has. Its distinguishing feature is that the tubinghead can be decomposed into two pieces with different centers and the eccentric shift of tubing in the casing can be achieved, so that the problem of electric cable twining around the tubing may be conveniently removed. The technical parameters are as follows.

Nominal pressure	14 MPa	Seal pressure	14 MPa
Tester diameter	≤25 mm	Flange diameter	380 mm
Steel ring groove diameter	211 mm	Test hole thread	34 mm
Rotation method	Tubing	Tubing hanger	2 7/8 NU thread

**Christmas Tree for an Electric Submersible Pump Well.** The Christmas tree for an electric submersible pump well is similar to that for a conventional flowing well, except that the special wellhead control equipment for sealing the extension line of electric cable and keeping it from

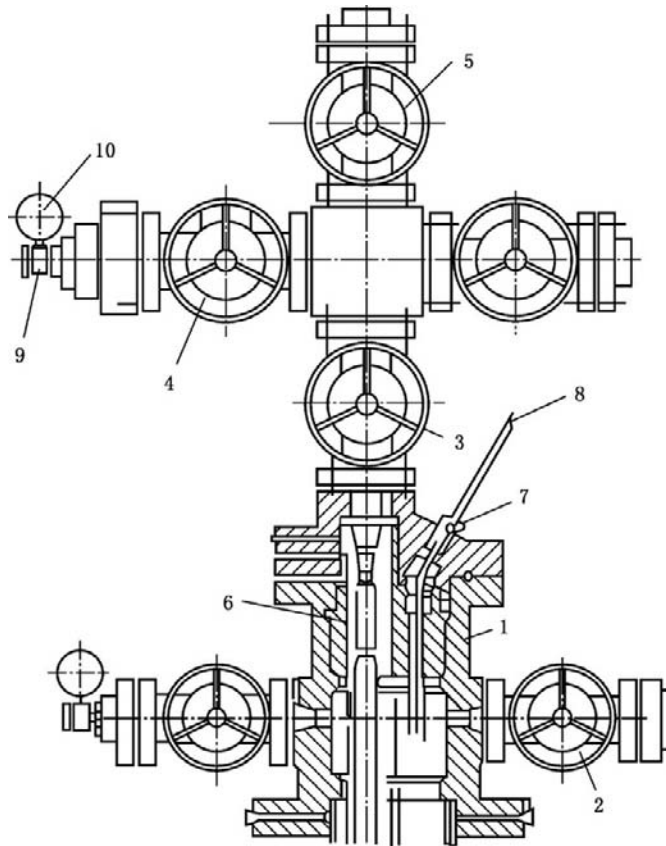


**FIGURE 10-13** Christmas tree and tubinghead with cable penetrator. 1, tubinghead; 2, casing valve; 3, master valve; 4, production valve; 5, paraffin valve; 6, tubing hanger; 7, cable penetrator; 8, electric cable; 9, pressure gauge valve; 10, pressure gauge.

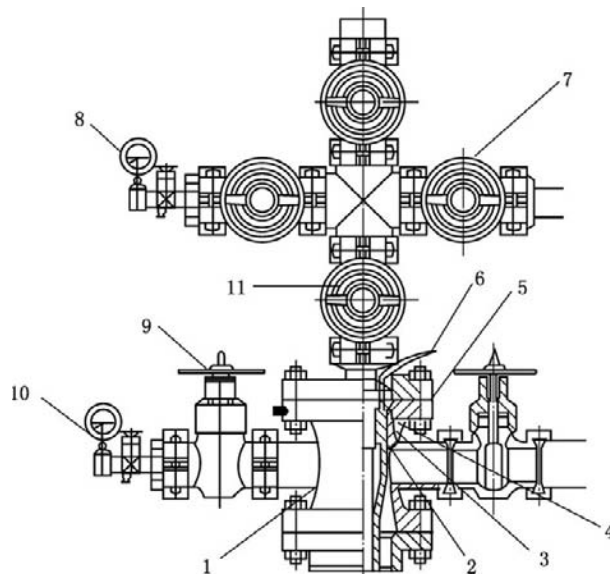
the tubing-casing annulus is added. There are different sealing methods. The wellhead assembly for an electric submersible pump well mainly has through-chamber and side-door types.

The through-chamber type wellhead assembly for an electric submersible pump well is shown in Figure 10-13. The tubing hanger is first connected with tubing. The armored cable is peeled. The cable passes through the saver. Several single-hole and tri-hole sealing rings are pressed into the lubricator. The saver gland is installed and screws are tightened up. The tubing hanger is seated in the tubinghead spool cone. Finally, the flange is installed and screws are tightened up.

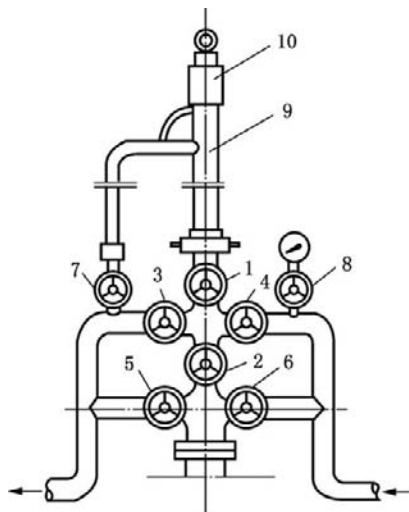
The side-door type wellhead assembly for an electric submersible pump well is shown in

Figure 10-14. The side door is first opened. An armored cable section of 0.5 m in length is peeled. The triple cable is pressed into the hemicycle hole of the rubber sealer. The side door is closed and the screw is tightened up. The tubing hanger is seated in the tubinghead. Finally, the open flange is installed and the flange screws are tightened up.

**Christmas Tree for a Hydraulic Piston Pump Well.** For a hydraulic piston pump well, an open power fluid system is generally adopted in China and a refitted flowing-well Christmas tree is used. The single-string Christmas tree and tubinghead for a hydraulic piston pump well is shown in Figure 10-15. In addition, a special Christmas tree for hydraulic piston pump well is also used. Its distinguishing feature is that all the functions of



**FIGURE 10-14** Side-door type Christmas tree and tubinghead for electric submersible pump well. 1, tubinghead; 2, conical seat; 3, rubber sealer; 4, tubing hanger; 5, bottom flange of Christmas tree; 6, electric cable; 7, production valve; 8, tubing pressure gauge; 9, casing valve; 10, casing pressure gauge; 11, master valve.



**FIGURE 10-15** Christmas tree and tubinghead for a hydraulic piston pump well with an open power fluid system. 1, paraffin removal valve; 2, master valve; 3, 4, production valve; 5, 6, casing valve; 7, release valve; 8, pressure gauge valve; 9, lubricator; 10, catcher.

the single-string Christmas tree and tubinghead for hydraulic piston pump well can be achieved by using a special valve.

The functions of the Christmas tree and tubinghead for a hydraulic piston pump (or jet pump) well include:

1. Injecting power fluid into tubing for normal circulation to run in the hydraulic piston pump and produce reservoir fluid mixed with power fluid;
2. Injecting power fluid into the annulus for reverse circulation to put out the hydraulic piston pump;
3. Holding and catching the hydraulic piston pump during tripping of the pump;
4. Closing the power fluid pipeline, releasing pressure in the tubing, and venting the gas in tubing during dismantling of the pump.

There are two types of closed power fluid circulation systems of a hydraulic piston pump, that is, concentric dual-string system and parallel dual-string system. The separation between

power fluid and produced fluid is characteristic of them. The corresponding Christmas trees are shown in Figure 10-16 and Figure 10-17.

**Christmas Tree for a Gas-Lift Production Well.** During gas-lift production, pressurized natural gas is injected into the well to reduce the liquid column pressure in the tubing and the back-pressure on the reservoir and lift the downhole fluid to the surface. It is one of the main methods of artificial-lift oil production.

The gas lift for oil production can be continuous or intermittent. For an oil well with high reservoir

pressure and high deliverability, continuous gas lift can be adopted. If reservoir pressure or deliverability is low, intermittent gas lift may be adopted.

The Christmas tree and tubinghead for a continuous or intermittent gas-lift well are similar to those for a gas injection well, except that the plunger lift device for intermittent gas lift should be fitted with a lubricator in which there is a buffer spring for absorbing the impact force of the plunger rising to the wellhead, and there also is a time controller for calculating the switching time to control the rate of gas that enters the

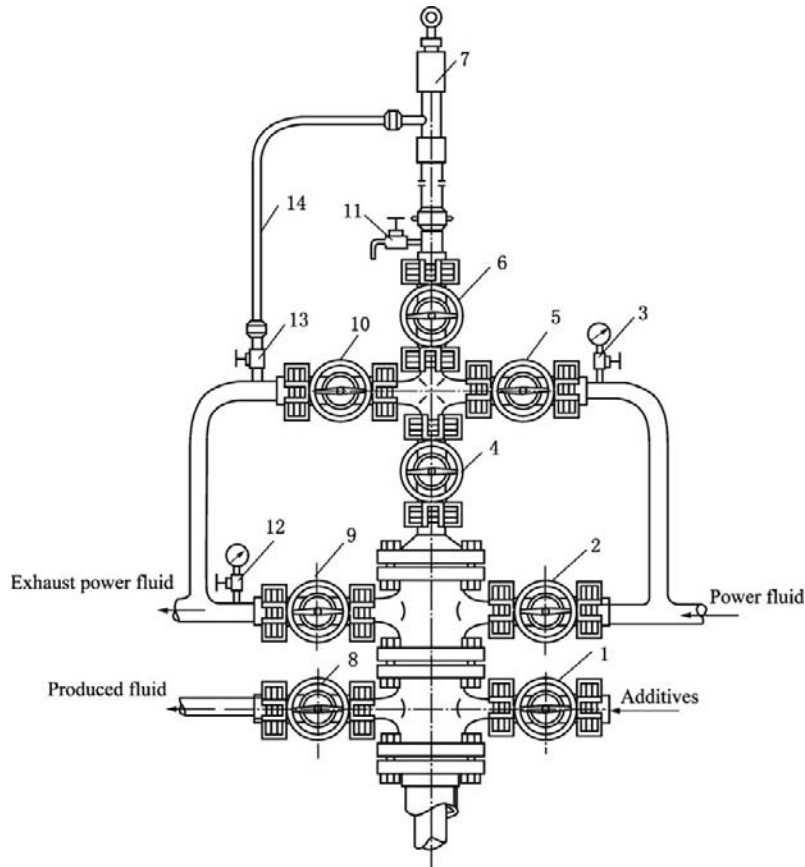


**FIGURE 10-16** Concentric dual-string Christmas tree and tubinghead for a hydraulic piston pump well. 1, 8, casing valve; 2, 9, concentric string valve; 3, pressure gauge valve; 4, master valve; 5, 10, power fluid valve; 6, paraffin removal valve; 7, catcher; 11, pressure release valve; 12, pressure gauge valve; 13, backflow valve; 14, release bypath.

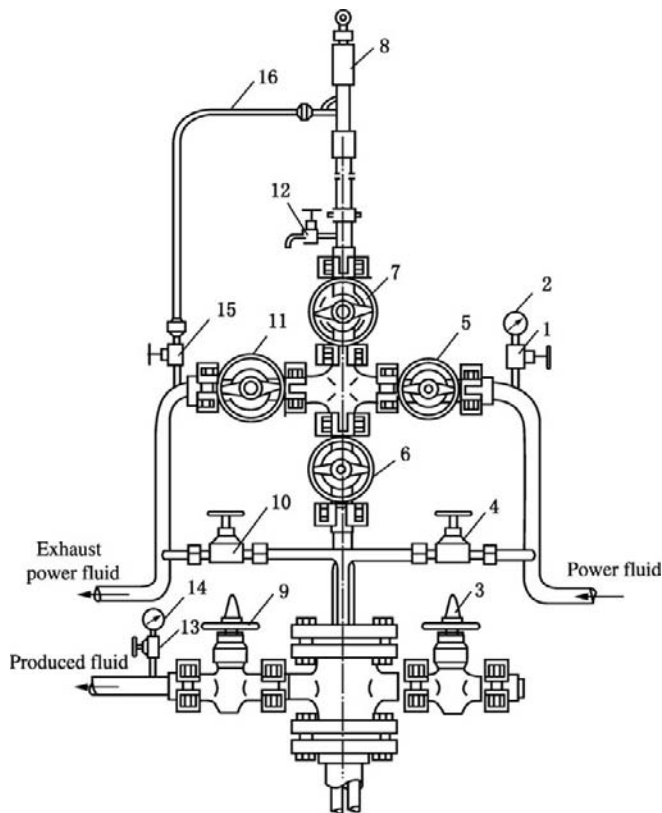


**FIGURE 10-17** Parallel dual-string Christmas tree and tubinghead for hydraulic piston pump well. 1, 13, pressure gauge valve; 2, 14, pressure gauge; 3, 9, casing valve; 4, 10, power fluid balance valve; 5, 11, power fluid valve; 6, master valve; 7, paraffin removal valve; 8, catcher; 12, pressure release valve; 15, backflow valve; 16, release bypath.

tubing to push the liquid above the plunger upward to the wellhead. The Christmas tree and tubinghead for plunger-lift oil production are shown in Figure 10-18.

### Technical Requirements for Christmas Tree and Tubinghead

The Christmas tree and tubinghead should meet the requirements of SY5156 Standard and should be manufactured in accordance with the design and approved technical document.

**Metallic Materials for Main Parts.** The main parts of the Christmas tree and tubinghead

include body, cover, flange, collar clamp, valve stem, valve plate, valve seat, metallic ring gasket, jackscrew, hanger body, bolt, and nut.

1. The mechanical properties of the materials of body, cover, and flange should be in accordance with the prescription in Table 10-2, while the Charpy V-notch impact requirements should be in accordance with the prescription in Table 10-3. When a smaller test sample is used, the values obtained should be multiplied by the corresponding correction factors in Table 10-4. For the parts of PSL 4, smaller test samples are not allowed to be used for impact test. The materials selected

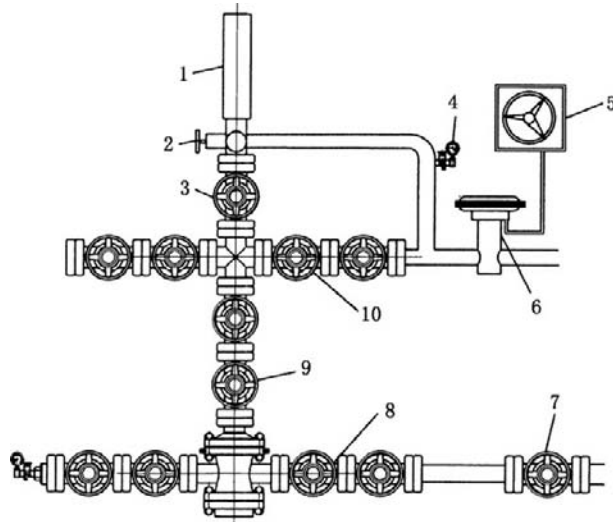


**FIGURE 10-18** Christmas tree and tubinghead for plunger-lift oil production. 1, lubricator; 2, hand catcher; 3, paraffin valve; 4, tubing pressure gauge; 5, time controller; 6, pneumatic membrane valve; 7, gas addition valve; 8, casing valve; 9, master valve; 10, production valve.

**TABLE 10-2** The Mechanical Properties of Materials of Body, Cover, and Flange

Material	Yield Strength, $\sigma_{0.2}$ (MPa)	Tensile Strength, $\sigma_b$ (MPa)	Length Growth Rate, $\sigma_s$ (%)	Cross-Section Shrinkage Factor, $\psi$ (%)
	≥			
36K	248	483	20	—
45K	310	483	17	32
60K	414	586	16	35
75K	517	635	16	35

Note: The K table is the code name in SY 5156 Standard (the same in Table 10-3).

**TABLE 10-3** Charpy V-Notch Impact Requirements

Type of Temperature	Test Temperature (°C)	Test Sample Size (mm)	Minimum Mean Impact Work (J)			Minimum Side Expansion PSL 4 (mm)
			PSL 1	PSL 2	PSL 3	
K	-59	10 × 10	20.3	20.3	20.3	0.38
L	-46					
P	-29		—			
R	-18			—	—	
S						
T						
U						

should accord with the prescription in Table 10-5, and the chemical composition should accord with the prescription in Table 10-6 and Table 10-7.

- The selected materials of tubing hanger body, casing hanger body, valve stem, jackscrew,

valve plate, and valve seat should accord with the prescription in Table 10-6.

- The hardness of the metallic ring gasket material should accord with the prescription in Table 10-8.
- The thickness of the stainless steel of the stainless-steel ring gasket groove bead weld

**TABLE 10-4** Correction Factor of Test Sample

Test Sample Size (mm)	Correction Factor
10 × 7.5	0.833
10 × 5.0	0.667
10 × 2.5	0.333

**TABLE 10-7** Chemical Composition of Material for Impact Test

Element	PSL 1-2 (%)	PSL 3-4 (%)
P	0.040 max	0.025 max
S	0.040 max	0.25 max

**TABLE 10-5** Materials Selected for Impact Test

Name of Parts	Rated Working Pressure (MPa)						
	14	21	35	70	105	140	
Body and cover	36K, 45K, 60K, 75K				45K, 60K, 75K	60K, 75K	
End flange	Integral flange	60K	60K	60K	60K	75K	75K
	Threaded flange				—		
	Clamp-on flange	—	—	—	60K	—	—
Threaded wellhead for oil and gas well	16K, 45K, 60K, 75K						
Unit flange	Welding neck flange	45K	45K	45K	60K	75K	
	Blind flange	60K	60K	60K			
	Threaded flange				—	—	

**TABLE 10-6** Chemical Composition of Materials for Impact Test

Alloy Element	Carbon Steel and Low Alloy Steel (%)	Martensitic Stainless Steel <sup>1</sup> (%)	45K Material for Welding Neck Flange <sup>2</sup> (%)
C	0.45 max	0.15 max	0.35 max
Mn	1.80 max	1.00 max	1.05 max
Si	1.00 max	1.50 max	1.35 max
P	See Table 10-7	See Table 10-7	0.05 max
S			0.05 max
Ni	1.00 max	4.50 max	—
Cr	2.75 max	11.0 ~ 14.0 max	
Al	1.50 max	1.00 max	
V	0.30 max	—	

<sup>1</sup>The nonmartensitic alloy series is not required to accord with the prescription in this table.

<sup>2</sup>When the maximum carbon content is 0.35%, the maximum manganese content is 1.05%. When carbon content is reduced by each 0.01%, the manganese content can be the maximum content of 1.05 plus 0.06%. However, the maximum manganese content should not exceed 1.35%.

**TABLE 10-8** Metallic Ring Gasket Material Hardness Requirements

Material	Maximum Brinell Hardness
Carbon steel or low alloy steel	HB 137
Stainless steel	HB 160

should not be less than 3.2 mm. Welding rod material should be austenitic stainless steel, and heat treatment is required after welding.

- The materials of the bolts and nuts for the wellhead assembly of the production well should accord with the prescription in Table 10-9.
- The material of the collar clamp body and hub and the bolts and nuts of the clamp connector should accord with the prescription of JB 3970.
- When a body, cover, flange, and collar clamp made of carbon steel, low-alloy steel, and martensitic stainless steel are used in a sour environment, their hardnesses should not exceed HRC 22 (HB 237).

**Nonmetallic Packing Element Material.** The nonmetallic packing element material should be able to bear the rated working pressure and working temperature that are borne by the body. In addition, the packing element material should also be able to resist corrosion and sulfide stress cracking correspondingly if the main parts should be able to resist corrosion and sulfide stress cracking.

## 10.2 GAS-WELL CHRISTMAS TREE AND TUBINGHEAD

This type of wellhead assembly is mainly used for gas production and injection. A gas production well or gas injection well has high wellhead pressure and high flow velocity and leaks easily due to the low relative density, low viscosity, and low gas column pressure. In addition, there are special requirements for the material and structure of a wellhead assembly when natural gas contains corrosive media such as H<sub>2</sub>S and CO<sub>2</sub>.

- All components adopt a flanged connection.
- Paired casing gate valves and paired master valves are disposed. One is used for working while the other is used for backing up.
- The choke generally adopts needle valve but not the bean with a constant hole diameter.
- Corrosion-resistant materials of different grades should be adopted in accordance with different concentration values of H<sub>2</sub>S and CO<sub>2</sub> in natural gas.
- In a high-pressure high-productivity gas well, both surface and subsurface safety valves should be installed.

The technical properties of the wellhead assemblies of KQS25/65, KQS35/65, KQS60/65, KQS70/65, and KQS105/65 are listed in Table 10-10. There is the gas-well Christmas tree pressure series of 210 MPa, 185 MPa, and 140 MPa.

**TABLE 10-9** Materials of the Bolts and Nuts of the Wellhead Assembly for a Production Well

Material	Mechanical Property				Hardness	
	$\sigma_{02}$ , MPa $\geq$	$\sigma_{02}$ , MPa	$\sigma_s$ , %	$\psi$ , %		
Bolt	K500	724	860	15	50	<HRC35
	Low alloy steel	724	860	15	50	—
		550 <sup>1</sup>	690 <sup>1</sup>	17 <sup>1</sup>	50 <sup>1</sup>	<HB237 <sup>1</sup>
Nut	Carbon steel	—				HB159 to HB352 HB159 to HB327 <sup>1</sup>

<sup>1</sup>It is suitable for bolts that will be directly exposed to a sour environment.

TABLE 10-10 Technical Parameters of Gas-Well Christmas Trees

Model Number	Strength Test Pressure (MPa)	Working Pressure (MPa)	Type of Connection	Type of Valve	Vertical Drift Diameter of Spool (mm)	Casing Connected [mm (in.)]	Tubing Connected [mm (in.)]
KQS25/65	50	25	Collar clamp and flange	Valve	195	146 ~ 219 (5 <sup>3</sup> / <sub>4</sub> ~ 8 <sup>5</sup> / <sub>8</sub> )	73 (2 <sup>7</sup> / <sub>8</sub> )
KQS35/65	70	35	Collar clamp and flange	Wedge valve	160	146 ~ 168.3 (5 <sup>3</sup> / <sub>4</sub> ~ 6 <sup>5</sup> / <sub>8</sub> )	73 (2 <sup>7</sup> / <sub>8</sub> )
KQS40/67	80	40	Collar clamp and flange	Plate valve	160	146 ~ 219 (5 <sup>3</sup> / <sub>4</sub> ~ 8 <sup>5</sup> / <sub>8</sub> )	73 (2 <sup>7</sup> / <sub>8</sub> )
KWS60/65	90	60	Collar clamp and flange	Wedge valve	160	146 ~ 219 (5 <sup>3</sup> / <sub>4</sub> ~ 8 <sup>5</sup> / <sub>8</sub> )	73 (2 <sup>7</sup> / <sub>8</sub> )
KQS70/65	105	70	Collar clamp and flange	Plate valve	160	177.8 (7)	73 (2 <sup>7</sup> / <sub>8</sub> )
KQS105/65	157.5	105	Collar clamp and flange	Plate valve	230	177.8 (7)	73 (2 <sup>7</sup> / <sub>8</sub> )

## Requirements for Materials

The requirements for materials of a gas-well wellhead assembly are shown in Table 10-11.

The degree of the corrosion of Christmas tree by CO<sub>2</sub> has three grades: (1) no corrosion in general service if CO<sub>2</sub> partial pressure < 0.05 MPa (7 psia); (2) mild corrosion in general

service if 0.05 MPa (7 psia) < CO<sub>2</sub> partial pressure < 0.21 MPa (30 psia); and (3) medium-high corrosion in general service if CO<sub>2</sub> partial pressure > 0.21 MPa (30 psia).

The environment with no H<sub>2</sub>S and with partial pressure lower than 0.000345 MPa (0.05 psi) is defined as general service, and the corresponding grades of materials for a gas-well Christmas tree

TABLE 10-11 Requirements for Materials of Gas-Well Wellhead Assembly

Grade of Material	Working Environment	Body, Cover, End, and Outlet Connection	Pressure Control Parts, Valve Stem Axle, and Hanger
AA	Common environment (no corrosion)	Carbon steel or low alloy steel	Carbon steel or low alloy steel
BB	Common environment (mild corrosion)		Stainless steel
CC	Common environment (medium and high corrosion)	Stainless steel	
DD	Sour environment (no corrosion)	Carbon steel or low alloy steel	Carbon steel or low alloy steel
EE	Sour environment (mild corrosion)		Stainless steel
FF	Sour environment (medium and high corrosion)	Stainless steel	
HH	Sour environment (serious corrosion)	Corrosion-resistant alloy steel	Corrosion-resistant alloy steel

include AA, BB, and CC. An environment with  $H_2S$  and with partial pressure higher than 0.000345 MPa (0.05 psi) is defined as sour service, and corresponding grades of materials for gas-well Christmas tree include DD, EE, and FF. HH grade is a corrosion-resistant alloy and is used in very serious corrosion environments. The components of a Christmas tree are not required to adopt the same grade of corrosion prevention. For the main valve, tubing, and spool of a gas-well Christmas tree, HH grade can be selected. For the other components that connect with corrosive fluid, such as intermediate casing spool and connection (tubing string, safety valve, cross joint and gate valve, throttling valve and production gate valve), the FF grade can be selected. For surface casing spool and connection, the EE grade can be selected.

For casinghead, the DD grade can be adopted. The reference standards for  $H_2S$  and  $CO_2$  corrosion are listed in Table 10-12.

## Commonly Used Gas-Well Christmas Trees and Tubingheads

**Gas-Well Christmas Trees.** Gas-well Christmas trees are used for controlling the normal production of a gas well and doing various operations such as acidizing, fracturing, gas injection, well killing, and well completing test. The gas-well Christmas trees used commonly in a gas field include KQS25/65, KQS60/65, and KQS70/65 (Figure 10-19, Figure 10-20, Figure 10-21, and Figure 10-22).

**Tubingheads.** The tubinghead is installed between the gas-well Christmas tree and the

**TABLE 10-12** Reference Standards for  $H_2S$  and  $CO_2$  Corrosion

Name of Standard	Condition of Corrosion	Useful Range
SY/T 5127-2002	<ol style="list-style-type: none"> <li>1. Sour environment if the following conditions are met:               <ol style="list-style-type: none"> <li>a. Water and <math>H_2S</math>-containing natural gas if total gas pressure <math>\geq 448</math> KPa and <math>H_2S</math> partial pressure <math>\geq 345</math> KPa;</li> <li>b. Water and <math>H_2S</math>-containing natural gas-oil system: gas-oil ratio <math>\geq 1000</math> m<sup>3</sup>/t; total pressure <math>\geq 1.828</math> MPa, <math>H_2S</math> partial pressure <math>\geq 0.345</math> KPa; <math>H_2S</math> partial pressure <math>&gt; 69</math> KPa; or <math>H_2S</math> volumetric content <math>&gt; 15\%</math>;</li> </ol> </li> <li>2. High <math>H_2S</math> concentration:  <math>H_2S</math> concentration of 100 mg/m<sup>3</sup>, distance of explosion radius from wellhead <math>&gt; 15</math> m.</li> </ol>	Wellhead assembly
API SPEC 6A-17 NACE MRO175	<ol style="list-style-type: none"> <li>1. Sour environment: For natural gas, condensate gas and crude oil with <math>H_2S</math>, <math>H_2S</math> partial pressure <math>\geq 0.0003</math> MPa (0.05 psi);</li> <li>2. Corrosion of gas-well Christmas tree by <math>CO_2</math>: No corrosion in general service if <math>CO_2</math> partial pressure <math>&lt; 0.05</math> MPa (7 psia); mild corrosion in general service if <math>0.05</math> MPa (7 psia) <math>&gt; CO_2</math> partial pressure <math>&gt; 0.21</math> MPa (30 psia); and medium-high corrosion in general service if <math>CO_2</math> partial pressure <math>&lt; 0.21</math> MPa (30 psia).</li> </ol>	Wellhead assembly
Petroleum Engineering Handbook by H. Bradley et al.	Corrosion prevention measures should be taken if absolute pressure $> 0.5$ MPa (65 psia) and $H_2S$ partial pressure $> 0.000345$ MPa (0.05 psia)	Wellhead assembly

Note: The definition of sour environment in SY/T 5127-2002 is the same as that in API SPEC 6A-17 and NACE MRO 175.

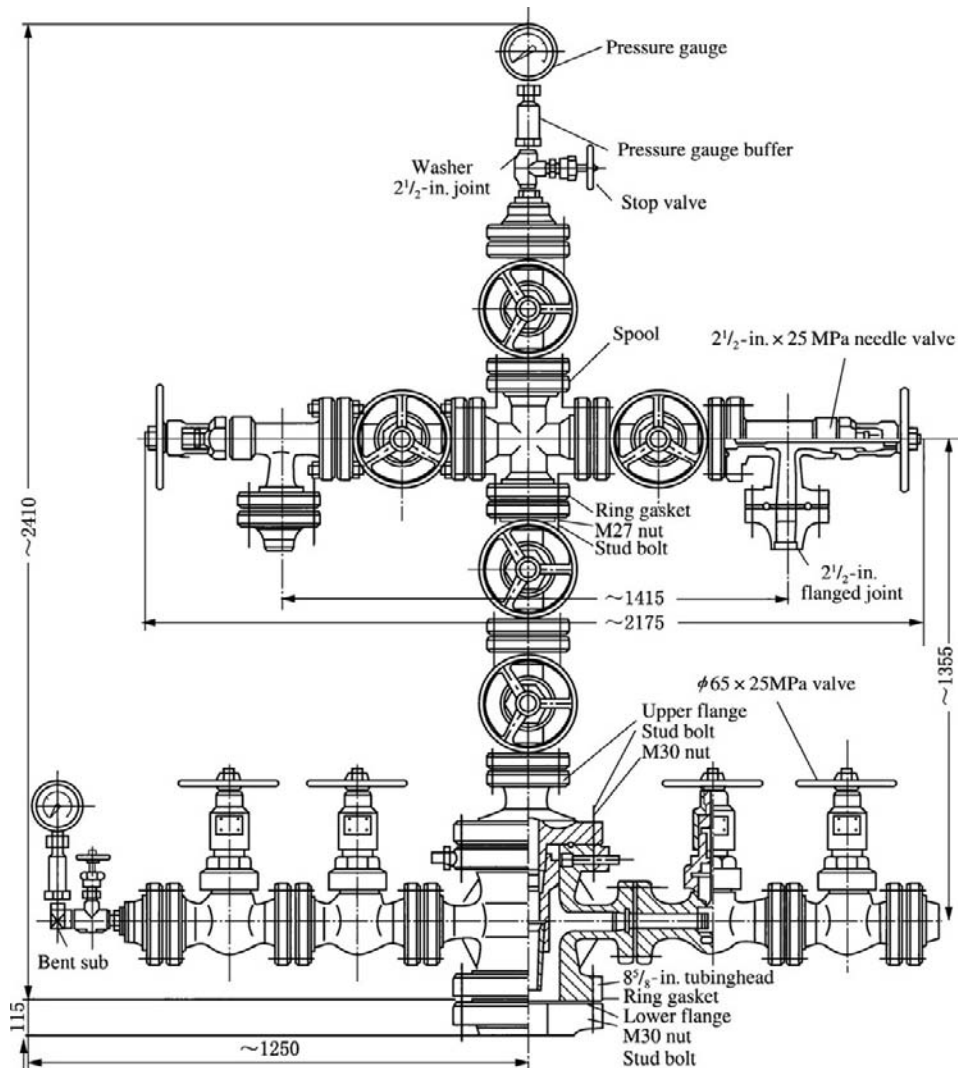
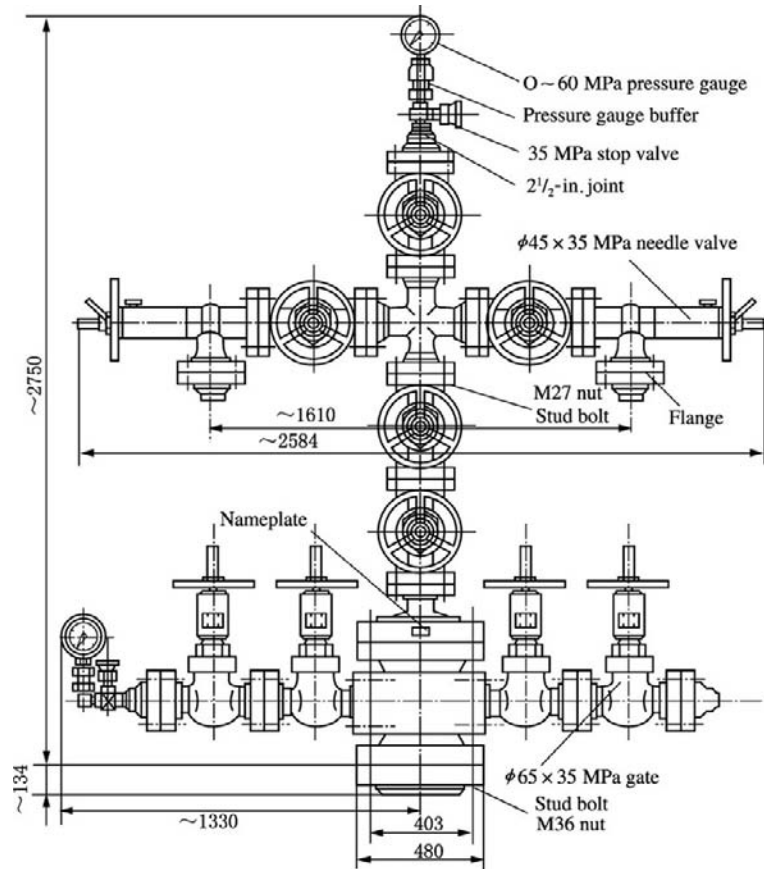


FIGURE 10-19 KQS25/65 sulfur-resistant natural gas production wellhead assembly.

casinghead. The upper flange plane of the tubinghead spool is the datum level for calculating the distance between the master bushing and the tubing hanger and the data of well depth.

1. Functions. The functions of the tubinghead include: (1) hanging the tubing in the well; (2) sealing the tubing-casing annulus in combination with the tubing hanger; (3) connecting with the casinghead at the bottom and
2. Structure. The double-flange tubinghead with a conical face for hanging is shown in Figure 10-23. The 219.1-mm conical seat type tubinghead of DQS 25/65 H<sub>2</sub>S-resistant natural gas production wellhead assembly is

connecting with the Christmas tree at the top; (4) injecting balance fluid and flushing the well by using both the side ports (to casing valve) of the tubinghead spool. The tubing hanger is used for hanging the tubing in the well.



**FIGURE 10-20** KQS35/65 sulfur-resistant natural gas production wellhead assembly.

shown in Figure 10-24. The 152.4-mm conical seat type tubinghead of KQS35/65 or KQS60/65 sulfur-resistant natural gas production wellhead assembly is shown in Figure 10-25. The tubinghead of KQS60/65 sulfur-resistant natural gas production wellhead assembly is shown in Figure 10-26.

## High-Pressure Gas-Well Wellhead Assembly

**High-Pressure Gas-Well Christmas Tree.** The high-pressure gas-well wellhead assembly means generally the wellhead assembly used for the production of a gas well with wellhead shut-in pressure higher than 70 MPa. The 105-MPa

gas-well wellhead assembly has been manufactured in China. In order to ensure safety and reliability under high pressure, all the pressure-bearing components and parts should adopt integral die-forged members. The 140-MPa high-pressure gas-well wellhead assembly used in the Sichuan gas field is shown in Figure 10-27. The technical parameters are the following: (1) drift diameter of 65 mm; (2) resistance to pressure of 140 MPa; and (3) temperature tolerance of  $-20$  to  $350^{\circ}\text{C}$ .

**Tubinghead.** The structure of a tubinghead is shown in Figure 10-28.

1. Tubinghead consists of both left and right valves and spool.

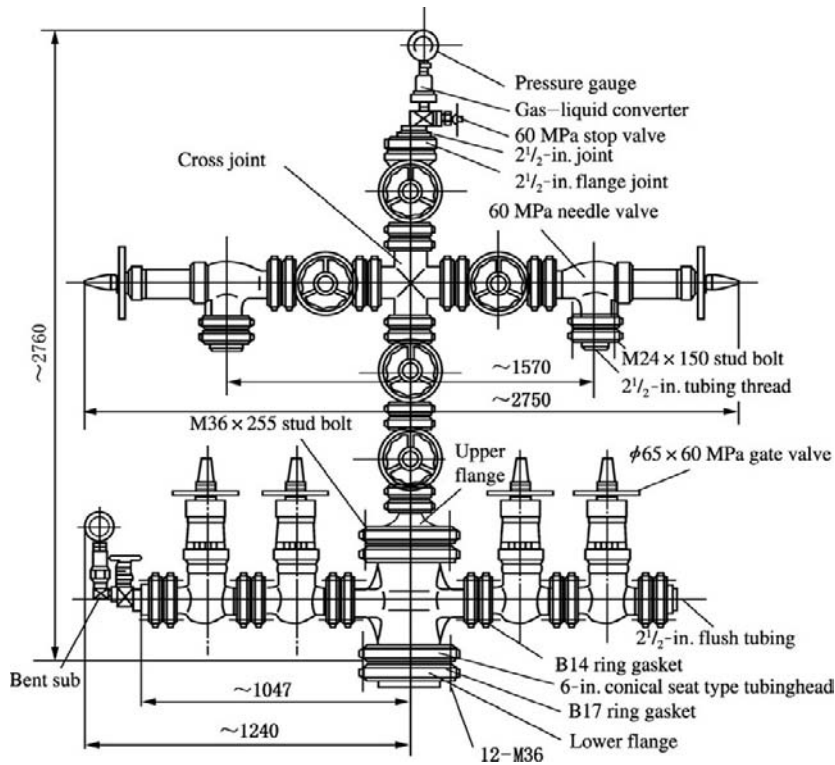


FIGURE 10-21 QQS60/65 natural gas production wellhead assembly.

- Both valves can generate passage for down-hole test tool running, well flushing, and well killing. Valves with working pressure of 140 MPa and size of 65 mm are selected and manual control is adopted. Pulley and sliding rod are required in order to make the opening and closing of valves convenient.
- On both sides the tubinghead is connected with both valves by thread carrying. The lower flange face is connected with 244.5-mm casinghead by using BX 158 steel ring (279.4 mm  $\times$  140 MPa) while the upper flange face is connected with a cover plate flange by using BX 156 steel ring (179.4 mm  $\times$  140 MPa).

### Tubing Hanger

- The seal between the tubing hanger and the inside of the tubinghead is a primary metallic seal. The seal of WOM gas-well Christmas tree is achieved by the V-shaped compression ring. The hardness of this metallic seal

ring is lower than that of the tubing hanger body and that of the inside metallic face of tubinghead. When the tubing hanger is set, the load of string makes the metallic seal ring expand, thus achieving high-pressure sealing.

- The seal between the tubing hanger and cover plate flange is achieved by metallic conical face. The test and production tubing string is run in. The tubing hanger is set. The components above the cover plate flange are set. The screws are tightened up, and both conical faces are pressed together, thus achieving sealing.

### High-Sulfur Gas-Well Wellhead Assembly

For a high-sulfur gas well, the following are specifically required: (1) all the components and parts should be H<sub>2</sub>S- and CO<sub>2</sub>-resistant

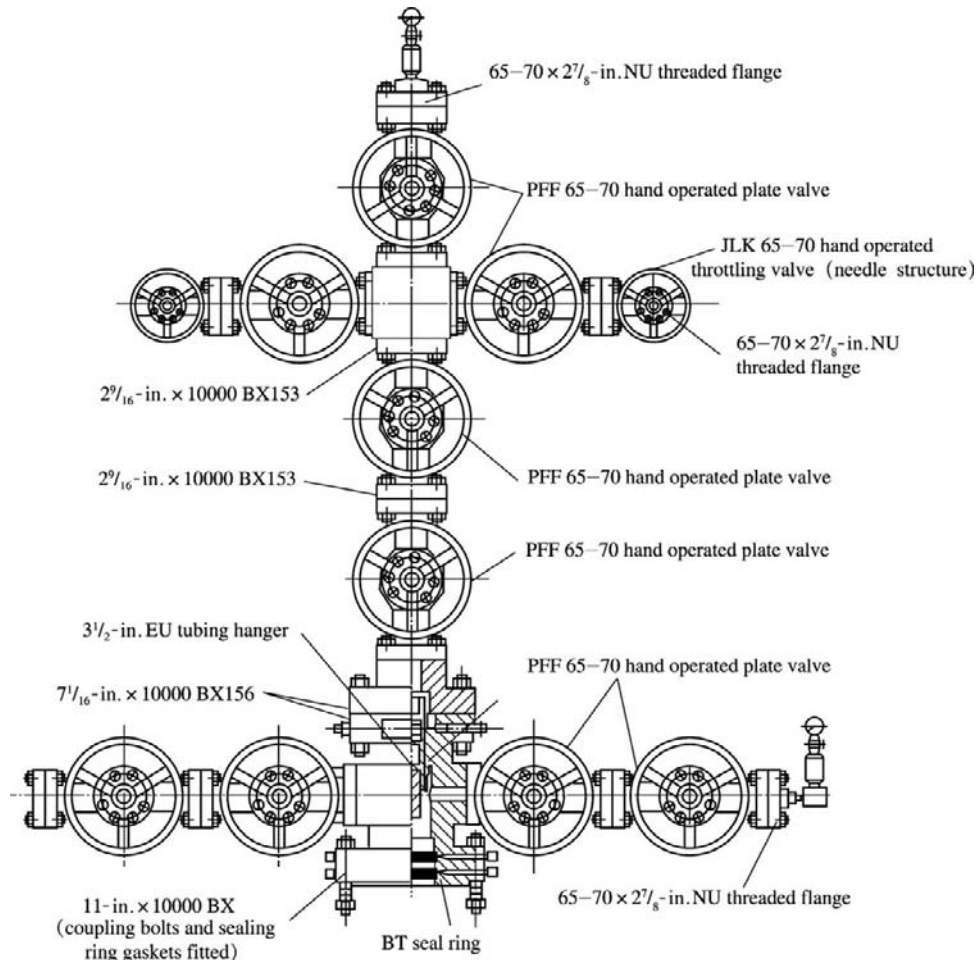


FIGURE 10-22 QQS65/70 natural gas production wellhead assembly.

and (2) subsurface and wellhead safety valves are installed if possible, thus achieving simultaneous subsurface and surface shutting in under emergent condition.

**CAMERON Wellhead Assembly.** The CAMERON wellhead assembly is shown in Figure 10-29. The main valve and wing valves of the Christmas tree are the 103.2-mm FLS hand gate valves (10K), and an integral gate structure is adopted, thus preventing precipitant in the pipeline from entering the valve chamber. Two high-strength thrust bearings are used for absorbing the loads during the opening and closing of the gate, thus minimizing the rotary

torque of the handwheel. The lip seal with a spring made of special inert material, by which the load is borne, not only can protect the metallic seal face but also can enhance the low-pressure sealing property.

The top of an MTBS mandrel type tubing hanger has an SRL seal. There is 114.3-mm VAMTOP thread at the top while there is 114.3-mm EUE thread at the bottom. There are outlets for two 6.35-mm control lines and an outlet for an electric cable.

MTBS tubing hanger is appropriate to working pressure higher than 103 MPa. It has a large drift diameter. Its ring seal is radially squeezed

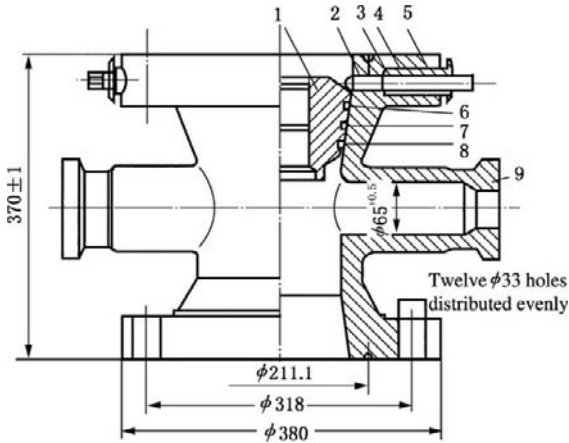


**FIGURE 10-23** Double-flange tubinghead with conical face for hanging. 1, tubing hanger; 2, jackscrew; 3, gasket; 4, jackscrew seal; 5, gland; 6, copper ring; 7, O-ring; 8, copper ring; 9, spool.

into the sealing location. When the tubing hanger is pulled up from the conical seat matched with it, the ring seal will be automatically restored to its original state. The upper seal of the tubing hanger is a pressure-reinforced U-shaped cap type bidirectional metallic seal, and no other additional seal is required. The extended neck of the tubing hanger makes the U-shaped cap type metallic seal reliably centralized during installation.

The wellhead assembly has grade HH material, temperature grade U, and PSL-3 specification, and meets the requirements of the AP 16 A standard. The main merits are as follows.

1. All the pressure-bearing components and parts are of forged alloy steel and can work safely and reliably under high pressure.

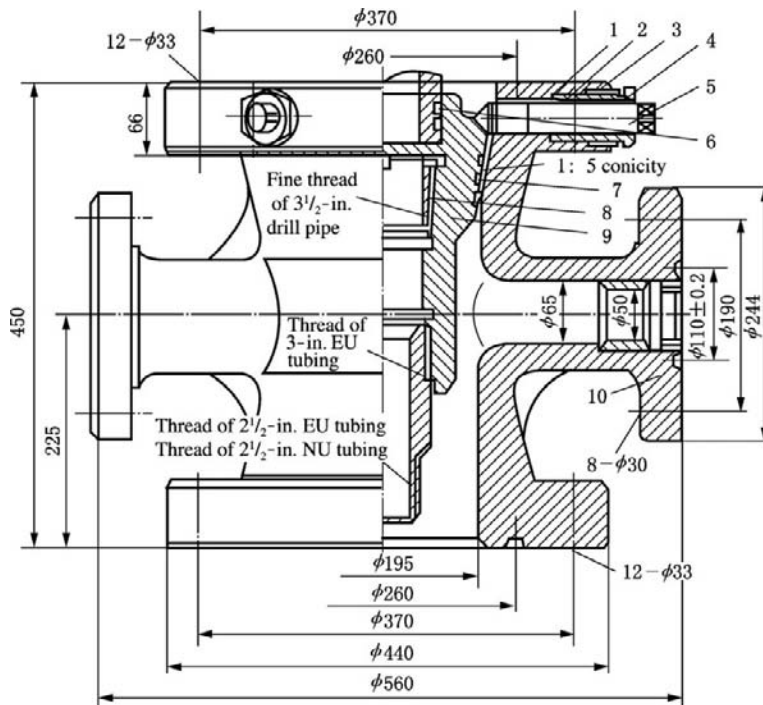


**FIGURE 10-24** A 219.1-mm conical seat type tubinghead. 1, lower seat for seal ring; 2, seal ring; 3, upper seat for seal ring; 4, gland; 5, jackscrew; 6, 7, O-ring; 8, thread protector; 9, tubing hanger with conical face; 10, tubing nipple.

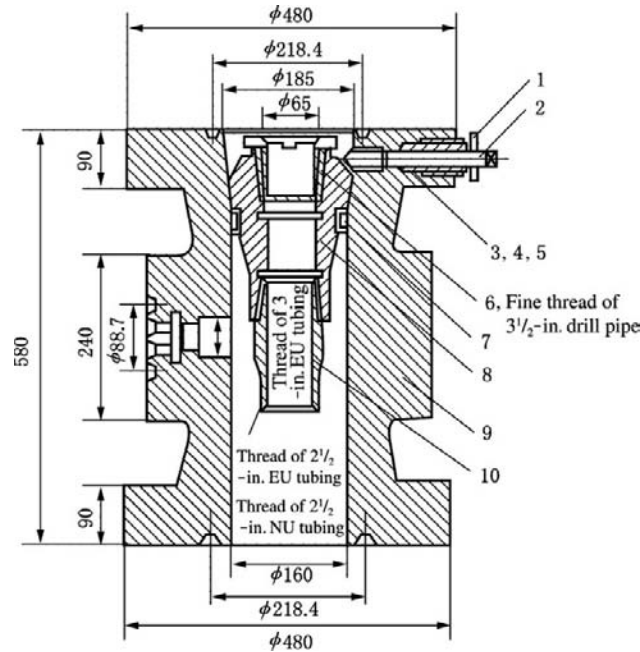


**FIGURE 10-25** The 152.4-mm conical seat type tubinghead. 1, gland; 2, jackscrew; 3, lower seat for seal ring; 4 - V-shaped seal ring; 5, upper seat for seal ring; 6, thread protector; 7, O-ring; 8, tubing hanger; 9, spool; 10, tubing nipple.

2. The main parts adopt H<sub>2</sub>S-resistant material while the other parts also have sufficient corrosion allowance. The heat treatment of these parts are taken. Thus they have a higher resistance to sour corrosion.
3. The seal elements adopt the V-shaped structure, are made of Teflon, may not be corroded by hydrogen sulfide, and have reliable sealing property under high pressure.
4. The metallic seal ring gasket adopts low steel, has good plasticity and toughness, and can be used repeatedly.
5. They have simple structure and low torque during opening and closing.

**Double-Wing Y-Shaped Gas-Well Wellhead Assembly.** The structure of a Y-shaped wellhead assembly is shown in Figure 10-30. The merits are as follows.

1. The Y-shaped structure has higher erosion-resisting property in comparison with the common cross-shaped structure.
2. The Y-shaped wellhead assembly that adopts integral forge has high reliability and safety.
3. The Y-shaped wellhead assembly has a compact structure, reliable seal, and fewer leaks. The on-line maintenance of wing valves can be achieved.

The related performance of the component parts of Y-shaped gas-well wellhead assembly is as follows.

1. The seals of the gas-well spool and pipe sleeve are metallic.
2. The tubing hanger adopts high nickel base alloy steel and metallic seal.

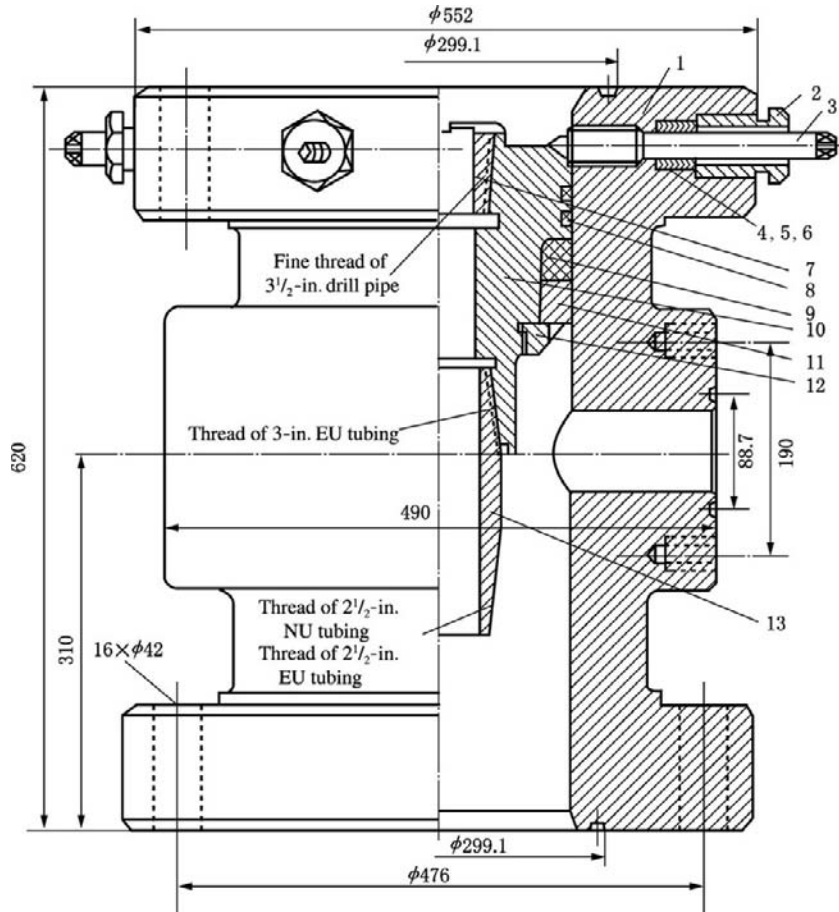


**FIGURE 10-26** The tubinghead of KQS60/65 sulfur-resistant natural gas production wellhead assembly. 1, spool; 2, gland; 3, jackscrew; 4, upper seat for seal ring; 5, seal ring; 6, lower seat for seal ring; 7, thread protector; 8, O-ring; 9, seal ring; 10, tubing hanger; 11, retaining ring; 12, round nut; 13, tubing nipple.

3. The tubing hanger has passages for the control line of the subsurface safety valve and the electric cable of a downhole test instrument.
4. The seals between valve plate, valve seat, and valve body of plate valve are metal-to-metal. The seal packing of valve stem and other parts can be replaced under pressure.
5. The plate valve at the top of a gas-well Christmas tree is used as a testing valve.

### 10.3 WATER INJECTION AND THERMAL PRODUCTION WELLHEAD ASSEMBLY

#### Wellhead Assembly for a Water Injection Well

Wellhead assemblies for water injection wells in onshore oil fields in China are mostly the flowing-well wellhead assemblies derived and

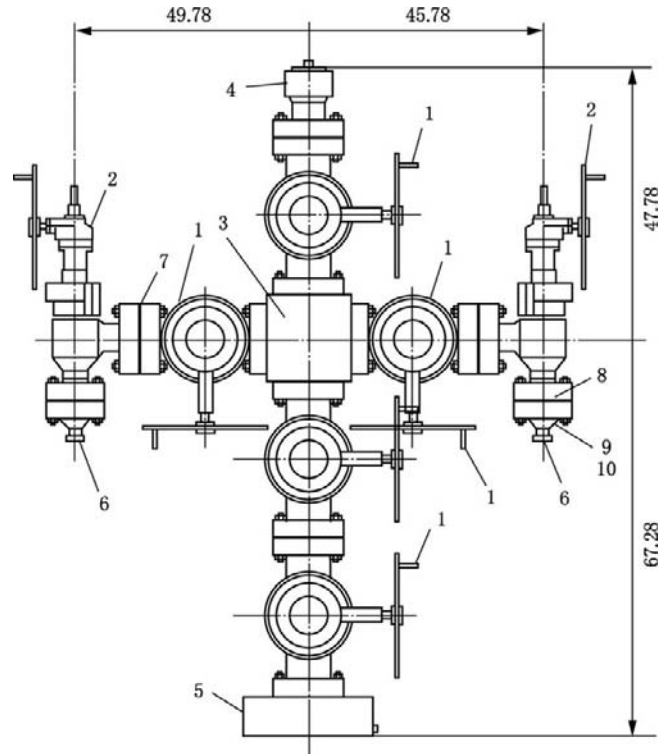


**FIGURE 10-27** High-pressure (140 MPa) gas-well Christmas tree. 1, 140-MPa gate valve; 2, needle-type production valve; 3, cross joint; 4, gas-well Christmas tree cap; 5, bottom flange of gas-well Christmas tree; 6, cross-over joint; 7, flange; 8, washer; 9, bolt; 10, nut.

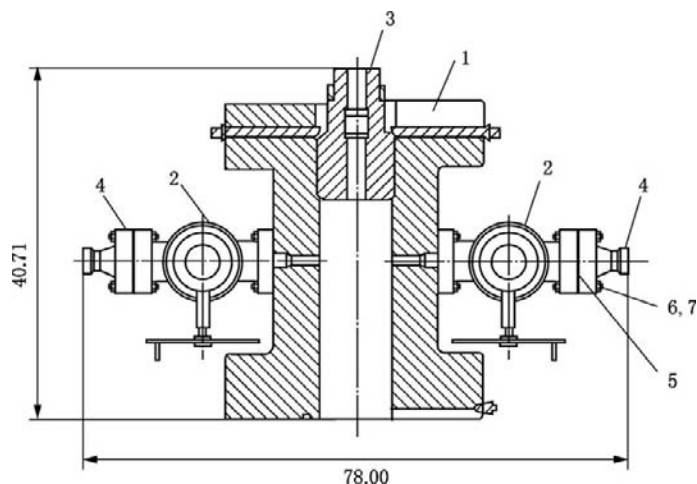


**FIGURE 10-28** Tubinghead of high-pressure gas-well wellhead assembly. 1, tubinghead; 2, gate valve; 3, tubing hanger; 4, crossover flange; 5, washer; 6, bolt; 7, nut.

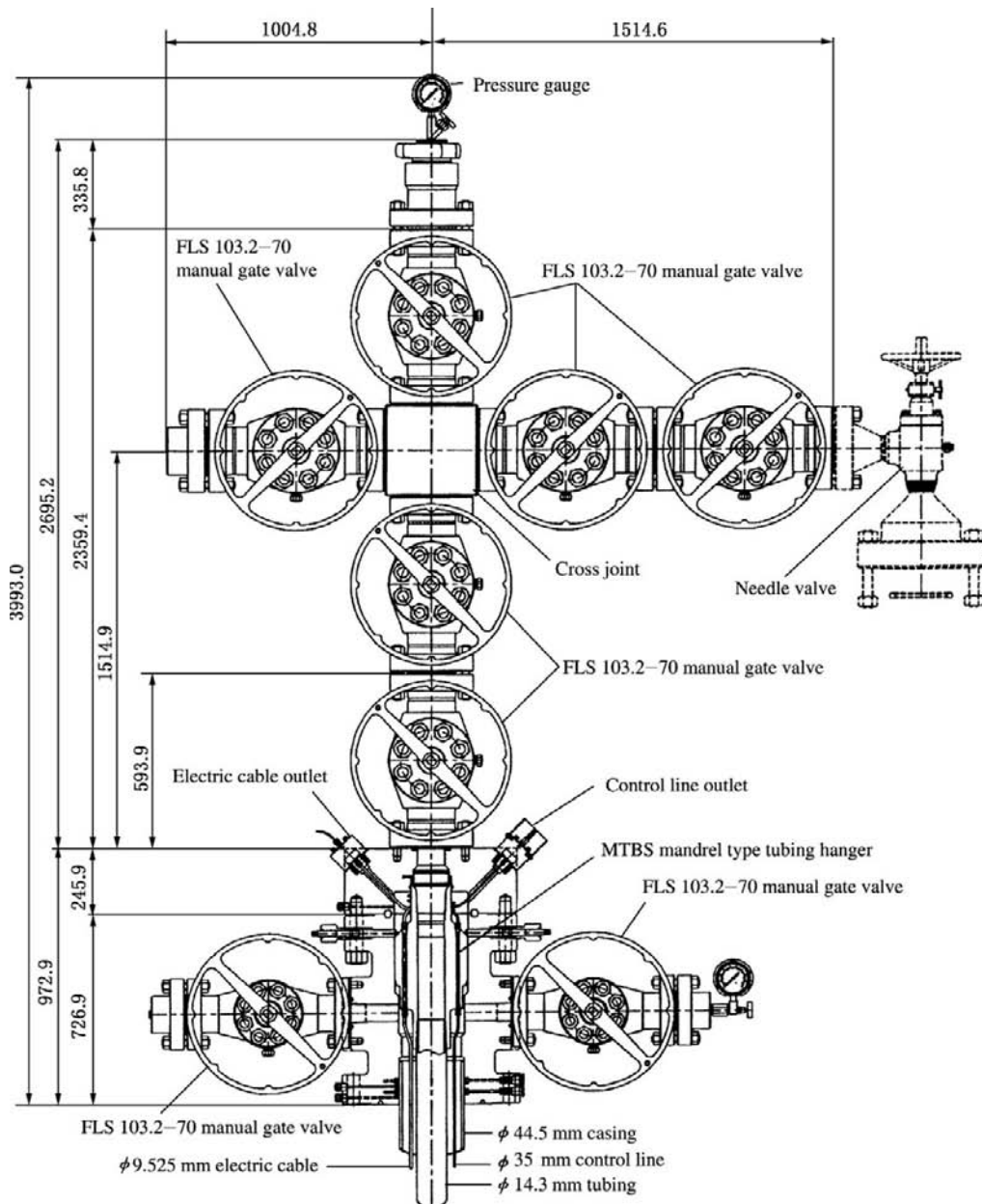


**FIGURE 10-29** CAMERON gas-well wellhead assembly.

reassembled (Figure 10-31). Their functions mainly include:

1. Conventional water injection (by opening the tubing water injection valve and master valve);
2. Annulus water injection (by opening the casing water injection valve);
3. Conventional well-flushing (by opening the tubing water injection valve, master valve, casing well-flushing valve, and return valve);

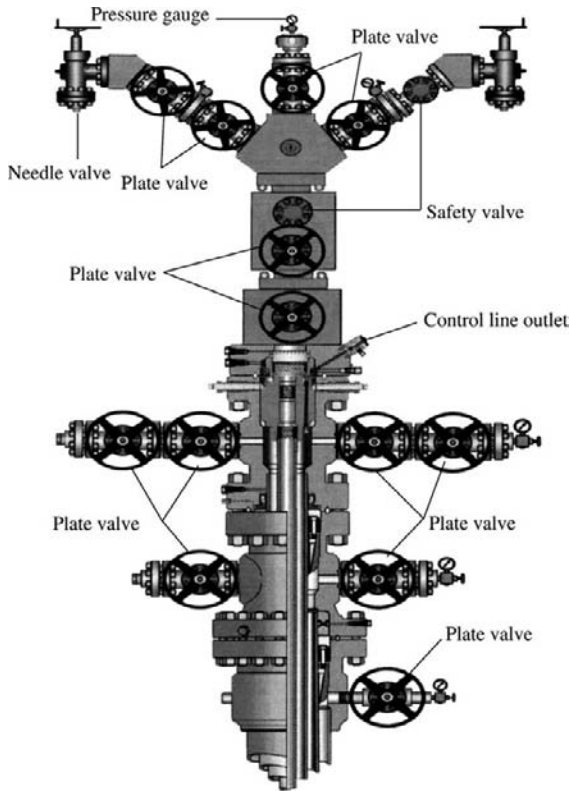


**FIGURE 10-30** Double-wing Y-shaped gas-well wellhead assembly.

4. Reverse well-flushing (by opening the casing water injection valve, master valve, tubing well-flushing valve, and return valve);
5. Water injection testing (by opening the testing valve and master valve).

The installation type of the wellhead assembly depends on the requirements of water injection. The seven-valve type Christmas tree and tubinghead used in the 1960s and the present three-valve type Christmas tree and tubinghead are shown respectively in Figure 10-32 and Figure 10-33.

### Wellhead Assembly for a Thermal Production Well

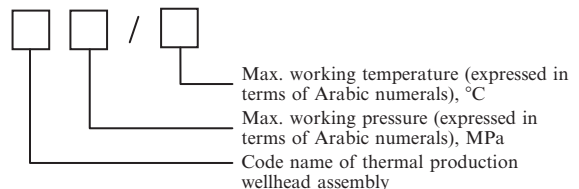
The Christmas tree and tubinghead for thermal production well are special devices for the heavy

oil production by steam injection under high pressure at high temperature. There are three types of Christmas trees and tubingheads for thermal production wells in the heavy oil fields in China at present, that is, KR 21/380 Christmas tree and tubinghead, which are appropriate for various heavy oil wells, and KR 14/340 and KR 14/335 Christmas trees and tubingheads, which are appropriate for heavy oil wells of a shallow reservoir.

The Christmas tree and tubinghead for thermal production well often work under high pressure (21 MPa) at high temperature (about 360°C). For common metal, creepage and strength reduction may be generated. The valves will no longer be sealed after opening and closing several times. Thus the main pressure-bearing components should select heat-resistant stainless steel and heat-resistant low alloy steel (such as ZG20CrMo). At the metal-to-metal seals of Christmas tree and tubinghead for a thermal production well, a double cone steel ring seal is adopted. A graphite-asbestos packing ring, the packing ring woven with metal filament and asbestos, or flexible graphite seal packing, and so on, can be selected as soft seal. A cone seal cannot be used for the seal of the tubing hanger of a thermal production wellhead assembly because the tubing may elongate upward during steam injection and the conical face will not be sealed. Thus the threaded connection can only be adopted between the tubing string and tubing hanger.

**Application Range.** The Christmas tree and tubinghead for thermal production well is suitable for huff and puff, steam flooding, and hot water circulation.

### Notation of Model Numbers



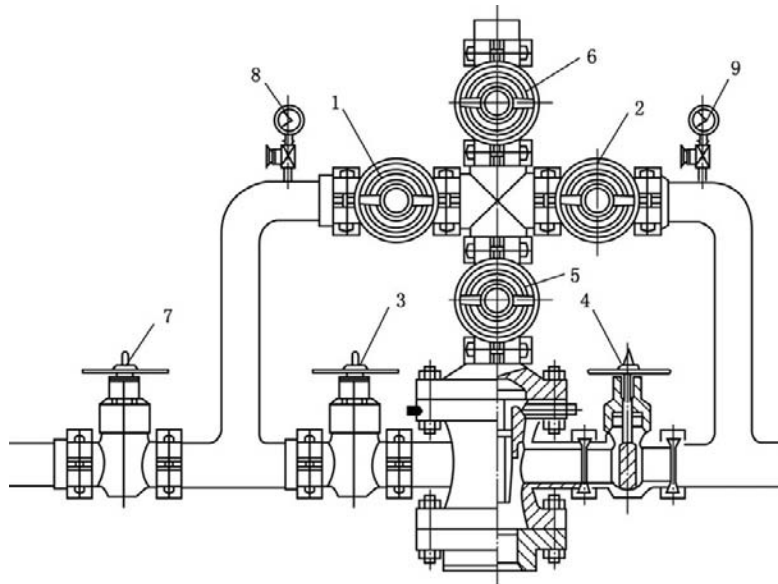


**FIGURE 10-31** Christmas tree and tubinghead for water injection well. 1, tubing well-flushing valve; 2, tubing water injection valve; 3, casing well-flushing valve; 4, casing water injection valve; 5, master valve; 6, testing valve; 7, return valve; 8, casing pressure gauge; 9, water injection pressure gauge.

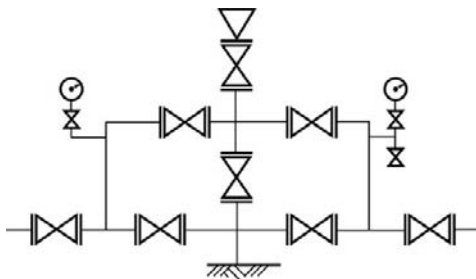


**FIGURE 10-32** Seven-valve type Christmas tree and tubinghead.

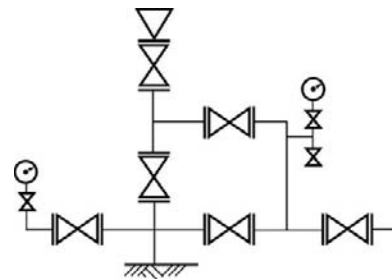


**FIGURE 10-33** Three-valve type Christmas tree and tubinghead.

The model numbers consist of three parts in the following pattern:

AB 11/222

where AB = Code name of thermal production wellhead assembly

11 = Maximum working pressure (expressed in Arabic numerals), MPa

222 = Maximum working temperature (expressed in Arabic numerals), °C

For instance, KR 21/380 means a thermal production wellhead assembly that has a maximum working pressure of 21 MPa and a maximum working temperature of 380°C.

**Structures.** The KR 21/380 structure is shown in Figure 10-34. The KR 14/340 structure is shown in Figure 10-35.

**Basic Parameters.** The basic parameters of a KR 21/380 thermal production Christmas tree and tubinghead are as follows.

Nominal drift dia.	65 mm	Drift dia. of tubinghead (spool)	170 mm
Max. working pressure	21 MPa	Max. working temperature	380°C
Strength test pressure	42 MPa	Connection	Collar clamp or flange
Outside dimensions	1580–1577 mm	Weight	1037 kg

The basic parameters of a KR 14/340 thermal production Christmas tree and tubinghead are as follows.

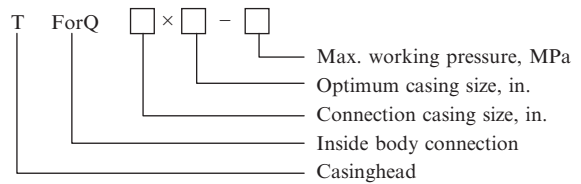
Nominal drift dia.	65 mm	Drift dia. of tubinghead (spool)	170 mm
Max. working pressure	14 MPa	Max. working temperature	340°C
Strength test pressure	35 MPa	Connection	Collar clamp or flange
Outside dimensions	1516–1100 mm	Weight: 467 kg	

## 10.4 COMMON COMPONENTS OF A WELLHEAD ASSEMBLY

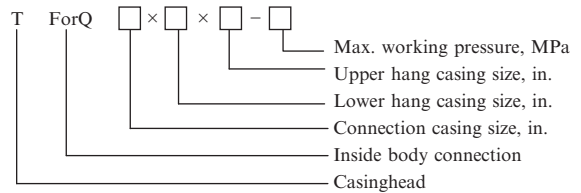
### Casinghead

A casinghead consists of body, casing hanger, and seal assembly. It is used for connecting casing and tubinghead, hanging intermediate casing and production casing, sealing the annulus between these casings, and providing a connection with the upper part of the wellhead assembly (blowout preventer and tubinghead, and so on). The two side ports of the casinghead body are used for remedial cementing and balance fluid injection and so on.

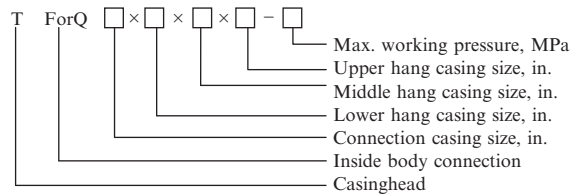
**Notation of Model Number.** The code name of the casinghead size (connection casing and hang casing) means inches of casing OD. The code name of the inside body connection is in the Chinese phonetic alphabet. F means flanged connection and Q means collar clamp connection.



The notation of the model number of a two-stage casinghead is as follows.



The notation of the model number of a three-stage casinghead is as follows.



**Structures.** Casingheads are divided into single-stage casinghead (Figure 10-36), two-stage casinghead (Figure 10-37), and three-stage casinghead (Figure 10-38 and Figure 10-39) in accordance with the number of casings hung.

Casingheads are divided into collar clamp type casinghead (Figure 10-36) and flanged casinghead (Figure 10-37 and Figure 10-38) in accordance with the inside body connection.

Casingheads are divided into the single-type casinghead, which has a single casing hanger in the body (Figure 10-36, Figure 10-37, and Figure 10-38), and the combination-type casinghead, which has multiple casing hangers in the body (Figure 10-39) in accordance with the array configuration of the body.

Casingheads are divided into slip-type casinghead (Figure 10-36, Figure 10-37, and Figure 10-38) and threaded casinghead (Figure 10-40) in accordance with the structure of the casing hanger.

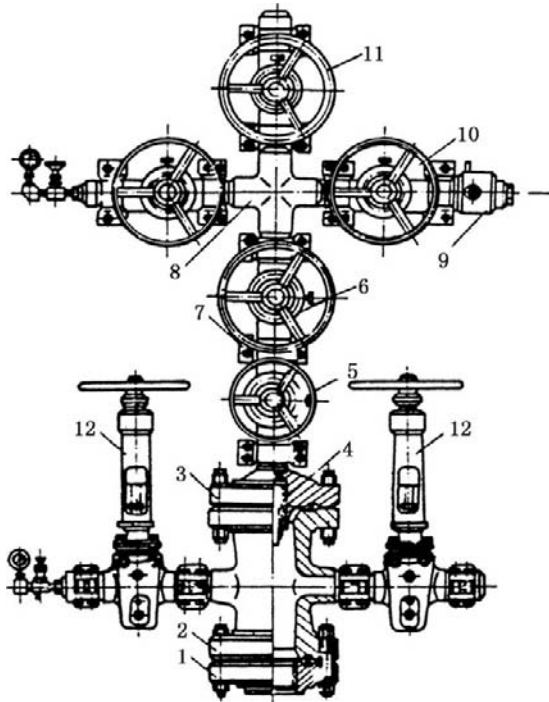


**FIGURE 10-34** KR 21/380 thermal production Christmas tree and tubinghead. 1, upper flange of casinghead; 2, tubinghead; 3, bottom flange of Christmas tree; 4, tubing nipple; 5, valve; 6, master valve; 7, collar clamp. 8, cross joint; 9, choke assembly; 10, production valve; 11, testing valve; 12, casing valve.

A TGA dual-casing casinghead is shown in Figure 10-41.

**Basic Parameters.** The basic parameters of single-stage, two-stage, and three-stage casingheads are listed in Table 10-13, Table 10-14, and Table 10-15, respectively. For a threaded casinghead, the working pressures of 7 MPa and 14 MPa and the corresponding outside diameters of casing and vertical drift diameters of body are only selected.

## Wellhead Valves

Wellhead valves can be parallel-plate valves or chisel-wedge valves. In accordance with the mode of connection, they can be threaded, flanged, or collar clamp type.

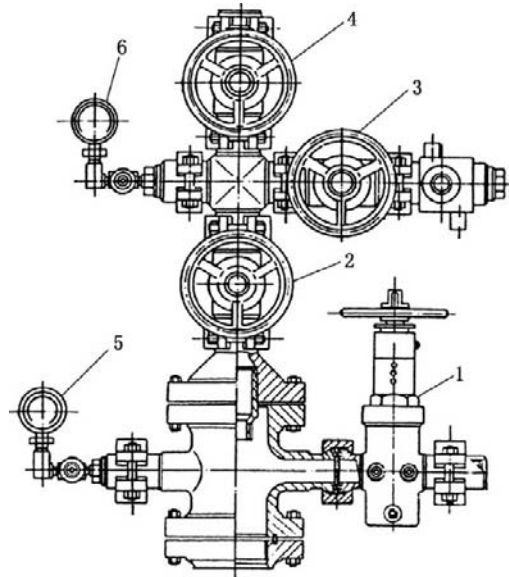


**FIGURE 10-35** KR 14/340 thermal production Christmas tree and tubinghead. 1, casing valve; 2, master valve; 3, production valve; 4, testing valve; 5, 6, casing pressure gauge.

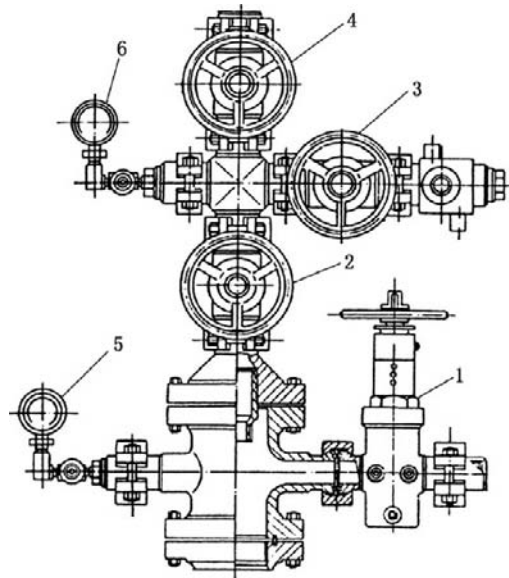


**FIGURE 10-36** Single-stage casinghead. 1, tubinghead; 2, casinghead; 3, casing hanger (slip type); 4, hang casing; 5, surface casing.

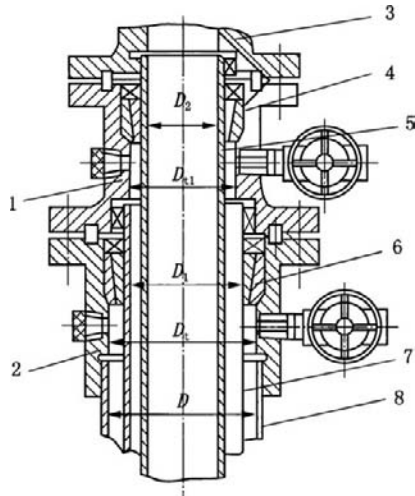


**FIGURE 10-37** Two-stage casinghead. 1, upper casinghead; 2, lower casinghead; 3, tubinghead; 4, upper casing hanger (slip type); 5, upper hang casing; 6, lower casing hanger (slip type); 7, lower hang casing; 8, surface casing.

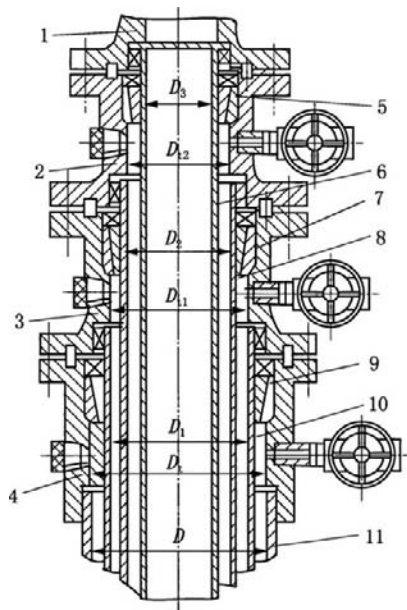


**FIGURE 10-38** Three-stage casinghead. 1, tubinghead; 2, upper casinghead; 3, middle casinghead; 4, lower casinghead; 5, upper casing hanger (slip type); 6, upper hang casing; 7, middle casing hanger (slip type); 8, middle hang casing; 9, lower casing hanger (slip type); 10, lower hang casing; 11, surface casing.

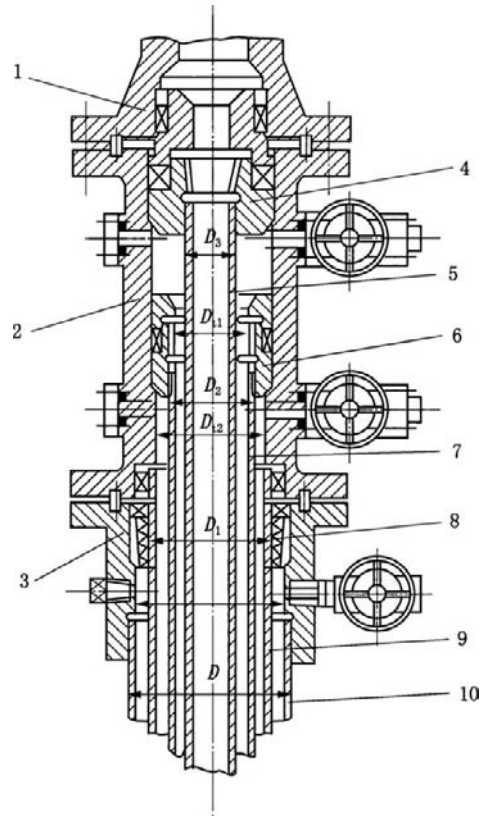


**FIGURE 10-39** Combination-type three-stage casinghead. 1, tubinghead; 2, upper combination-type casinghead; 3, lower casinghead; 4, upper casing hanger (threaded); 5, upper hang casing; 6, middle casing hanger (threaded); 7, middle hang casing; 8, lower casing hanger (slip type); 9, lower hang casing; 10, surface casing.

The technical specifications for chisel-wedge valve (Figure 10-42) and parallel-plate valve (Figure 10-43) are listed in Table 10-16, Table 10-17, and Table 10-18.

### Surface Safety Valves

Because of the serious consequences of blowout of control, particularly for offshore oil and gas wells, gas wells with high sour gas (hydrogen sulfide and carbon dioxide), and high-pressure gas wells, an automated shutdown safety system is very important and is sometimes required by law. The safety system should be able to

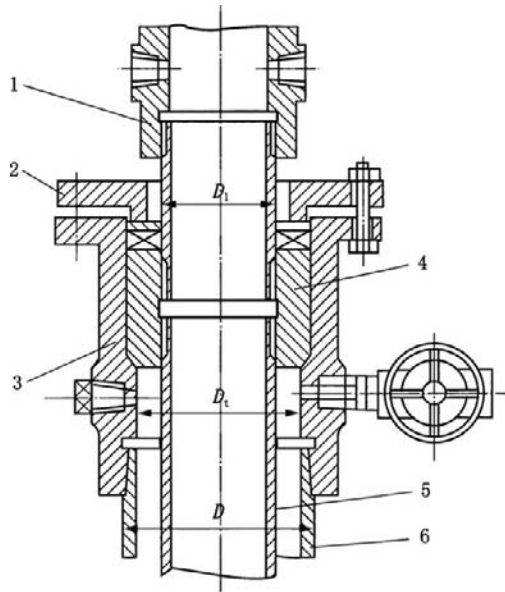


**FIGURE 10-40** Threaded casinghead. 1, tubinghead; 2, stop gland; 3, casinghead; 4, casing hanger (threaded); 5, hang casing; 6, connection casing.

automatically prevent accidents from occurring. The shutdown system should be in a safe state despite the failure of energy source or any link.

Surface safety valves can be installed on symmetric dual-wing dual-valve gas-well Christmas tree or Y-shaped gas-well Christmas tree. Wing valves are installed on the inside of each wing of a gas-well Christmas tree while safety valves are installed on the outside of each wing. On vertical flow passage, the master valve is on the downside of the main full bore while the safety valve is on the upside.

Surface safety valves are reverse-acting gate valves with a piston-type actuating mechanism (Figure 10-44). The pressure in the valve body pushes the gate upward to close the valve due to low pressure borne by the valve stem area. The gate is pushed downward by the control pressure acting on the piston to open the valve. If there is no pressure in the valve body, a spring is used for closing the valve. The control pressure is dependent on the pressure in the valve body and the ratio of the piston area to the valve stem area.

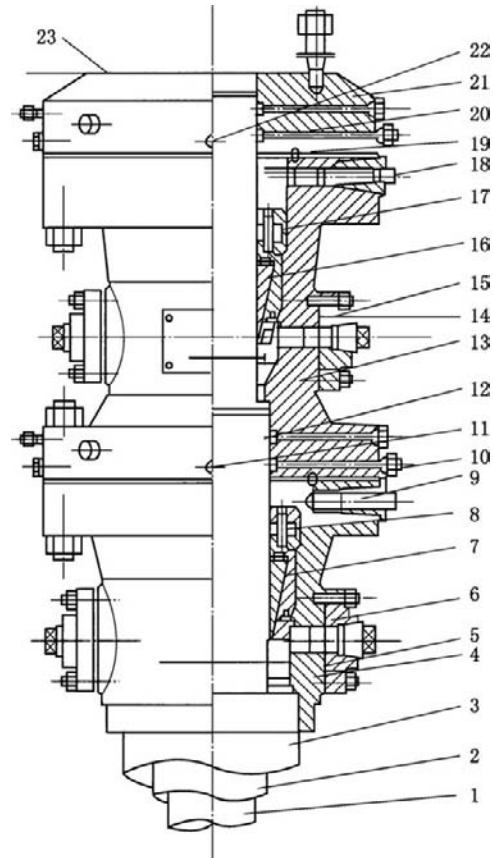


**FIGURE 10-41** TGA dual-casing casinghead. 1, production casing; 2, intermediate casing; 3, surface casing; 4, lower spool; 5, steel ring; 6, side flange; 7, lower hanger; 8, main seal; 9, jackscrew; 10, steel ring; 11, pressure test hole; 12, lower sub-seal; 13, upper spool; 14, steel ring; 15, side flange; 16, upper hanger; 17, main seal; 18, jackscrew; 19, steel ring; 20, upper sub-seal; 21, crossover flange; 22, pressure test hole; 23, connection with tubinghead.

A surface safety valve has a valve stem extending from the threaded sleeve above the cylinder body of the actuating mechanism, which is due to the following:

1. The position of the valve stem can be used as a gate locator.
2. Locator switching may provide a remote feedback signal.
3. Connecting with a mechanically or hydraulically operated pressure cylinder can be

**TABLE 10-13 Basic Parameters of Single-Stage Casinghead**

Connection Casing OD (mm)	Hang Casing OD (mm)	Working Pressure of Casinghead (MPa)	Vertical Drift Dia. of Casinghead (mm)
193.7	114.3	7	178
		14	178
		21	178
244.5	127.0	7	230
		14	230
		21	230
		35	230
273.0	139.7	7	254
		14	254
		21	254
		35	254
298.4	139.7	7	280
		14	280
		21	280
		35	280
325.0	139.7	7	308
		14	308
		21	308
		35	308
339.7	139.7	7	318
		14	318
		21	318
		35	318

**TABLE 10-14 Basic Parameters of Two-Stage Casinghead**

Connection Casing OD (mm)	Hang Casing OD		Working Pressure of Lower Part of Body (MPa)	Vertical Drift Dia. Dt of Lower Part of Body (mm)	Working Pressure of Upper Part of Body (MPa)	Vertical Drift Dia. Dt of Upper Part of Body (mm)
	D <sub>1</sub> (mm)	D <sub>2</sub> (mm)				
339.7	177.8	127.0	14	318	21	162
		139.0	21	318	35	162
			35	318	70	162
339.7	193.7	127.0	14	318	21	178
		139.7	21	318	35	178
			35	318	70	178
339.7	244.5	127.0	14	318	21	230
		139.7	21	318	35	230
		177.8	35	318	70	230

TABLE 10-15 Basic Parameters of Three-Stage Casinghead

Connection Casing OD (mm)	Hang Casing OD			Working Pressure of Lower Part of Body (MPa)	Vertical Drift Dia. Dt of Lower Part of Body (mm)	Working Pressure of Middle Part of Body (MPa)	Vertical Drift Dia. Dt of Middle Part of Body (mm)	Working Pressure of Upper Part of Body (MPa)	Vertical Drift Dia. Dt of Upper Part of Body (mm)
	D <sub>1</sub> (mm)	D <sub>2</sub> (mm)	D <sub>3</sub> (mm)						
339.7	244.5	177.8	127.0	14	318	14	230	21	162
				14	318	21	230	35	162
				21	318	35	230	70	162
406.4	339.7	177.8	127.0	14	390	14	318	21	162
				14	390	21	318	35	162
				14	390	35	318	70	162
406.4	339.7	244.5	139.7	14	390	14	318	21	230
				14	390	21	318	35	230
			177.8	21	390	35	318	70	230
508.0	339.7	177.8	127.0	14	480	14	318	21	162
				14	480	21	318	35	162
				21	480	35	318	70	162
508.0	339.7	244.5	139.7	14	480	14	318	21	230
				14	480	21	318	35	230
			177.8	21	480	35	318	70	230

achieved, so that the safety valve can be opened when control pressure cannot be provided because the control pressure source is downstream from the safety valve or failure is generated in the system.

- When a tripping operation is done on the wire rope through the safety valve or the control system is repaired, control pressure cannot be provided. Under these conditions, a locking valve bonnet or heat-sensitive locking valve bonnet can be connected to keep the safety valve open.

When a safety valve is selected, the valve size is dependent on the flow rate in the place of installation. If the safety valve is installed on the vertical flow passage, its size should be the same as that of the master valve below it. The rated pressure, rated temperature, and other rated parameters should be the same as that of the master valve below it. For actuating mechanism, the pressure that can be provided by the

control system should be considered. The relation between valve body pressure, actuating mechanism ratio, and control pressure is shown in the following equation.

$$p_{cl} = \frac{2p_{vb}}{F_{ac}}$$

where:  $p_{cl}$  = control pressure;  $p_{vb}$  = valve body pressure; and  $F_{ac}$  = actuating mechanism ratio.

The actuating mechanism ratio can be found in the product manual related to various types of surface safety valve.

## Chokes

A choke is a component used for controlling the production rate. It can be a fixed or adjustable choke. The modes of connection include collar clamp, flange, and thread.

**Fixed Choke.** A fixed choke is used for throttling of the oil well. There are two types of fixed

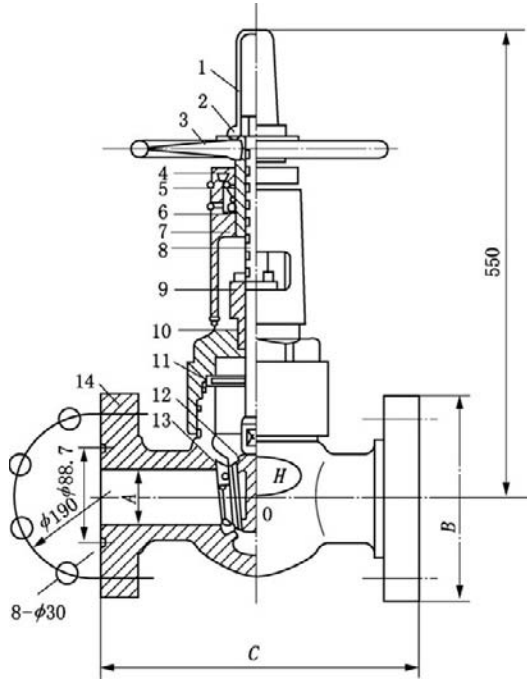


**FIGURE 10-42** Chisel-wedge valve. 1, protecting cap; 2, nut; 3, handwheel; 4, bearing cap; 5, bearing; 6, valve stem nut; 7, bearing seat; 8, valve stem; 9, gland; 10, seal ring; 11, valve bonnet; 12, gate; 13, valve seat; 14, valve body.

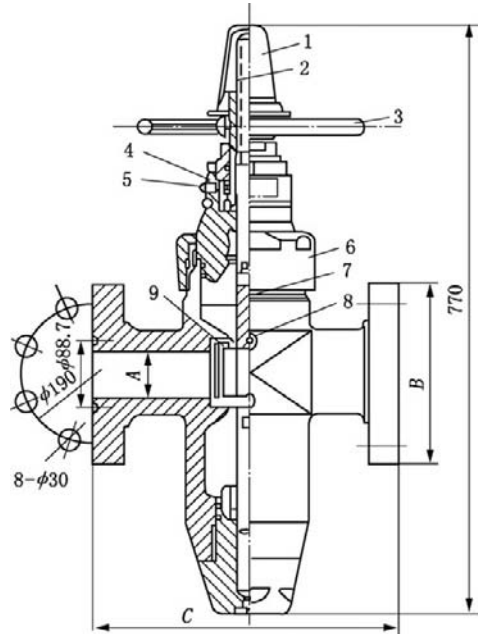


**FIGURE 10-43** Parallel-plate valve. 1, protecting cap; 2, valve stem; 3, handwheel; 4, thrust bearing; 5, grease nipple; 6, valve bonnet; 7, valve plate; 8, valve seat; 9, seal ring.

choke, that is, heated and non-heated chokes. A nonheated choke is shown in Figure 10-45.

A choke bean (Figure 10-46) is a throttling element and is used for controlling the rational producing pressure drawdown of oil wells by replacing bean size (bean hole diameter). Choke bean is made of high carbon alloy steel that is

heat-treated. There are various hole diameters from 2 to 20 mm. The difference of grade is 0.5 mm. Choke beans with a diameter larger than 20 mm are special choke beans.

**Adjustable Choke.** Adjustable choke (needle valve) is generally used for throttling of gas wells and controlling the flow rate by adjusting

**TABLE 10-16** Technical Specifications for 21-MPa Wellhead Valves

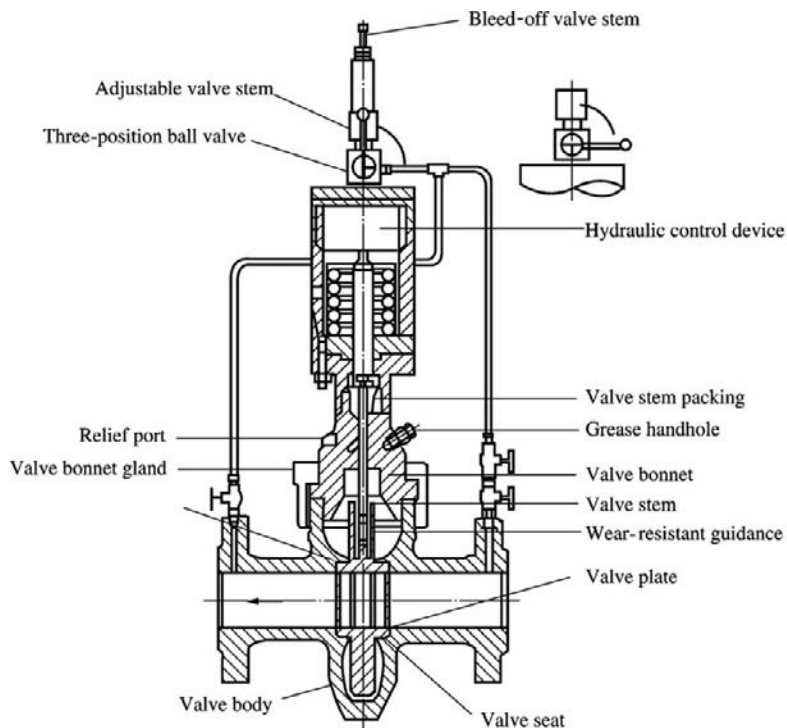
Type	Code Name of Specification	Size or Diameter (mm)				Mode of Connection
Chisel-wedge	A	52.4	65.1	79.4	103.2	Collar clamp Flange
	B		244.1	241		
	C		422.3	435		
Parallel-plate	A	52.4	65.1	79.4	103.2	
	B	216	244.1	241	292.0	
	C	371.5	422.3	435	511.2	

**TABLE 10-17 Technical Specifications for 35-MPa Wellhead Valves**

Type	Code Name of Specification	Size or Diameter (mm)				Mode of Connection
Chisel-wedge	A	52.4	65.1	79.4	103.2	Flange 511.2
	B		244.1	241		
	C		422.3	473.1		
Parallel-plate	A	52.4	65.1	79.4	103.2	
	B	216	244.1	267	311	
	C	371.5	422.3	473.1	549.3	

**TABLE 10-18 Technical Specifications for 70-MPa and 105-MPa Wellhead Valves**

Type	Code Name of Specification	Size or Diameter (mm)				Mode of Connection
Chisel-wedge	A	52.4	65.1	77.8	103.2	Flange
	B	200	232	270	316	
	C	520.7	565.2	619.1	669.9	
Parallel-plate	A	52.4	65.1	77.8	103.2	
	B	232	254	287	360	
	C	482.6	533.4	598.5	736.6	

**FIGURE 10-44** Wellhead safety valve.

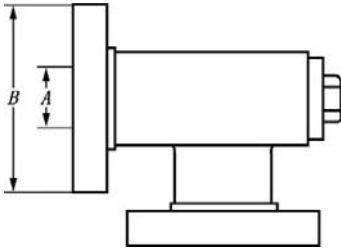


FIGURE 10-45 Nonheated fixed choke.

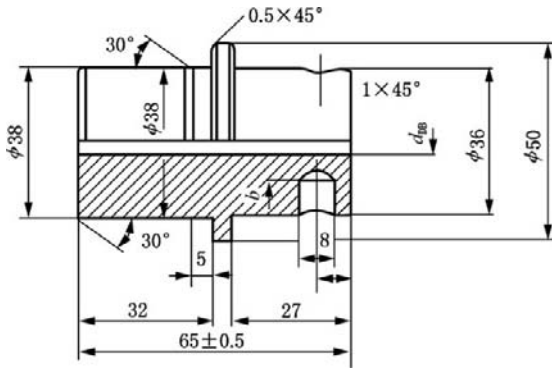


FIGURE 10-46 Choke bean.

the opening. An adjustable choke is a needle valve (Figure 10-47) and can be hand-operated or hydraulically powered.

When the rated working pressure at the inlet end of the choke valve is the same as that at the outlet end, the rated working pressure at the end connection is just the rated working pressure of choke valve.

For the choke valve that has the inlet-end rated working pressure higher than the outlet-end rated working pressure, the rated working pressures at inlet and outlet ends should all be marked.

A fixed choke is used for oil well throttling, while an adjustable choke is generally used for gas well throttling. An adjustable choke is also used for high-GOR oil well throttling.

## Tees and Spools

Tees and spools are shown in Figure 10-48, Figure 10-49, Figure 10-50, and Figure 10-51.

The rated working pressures and nominal drift diameters of flanged tee and spool should meet the requirements in Table 10-19, while the rated working pressures and nominal drift diameters of collar clamp type tee and spool should meet the requirements in Table 10-20.

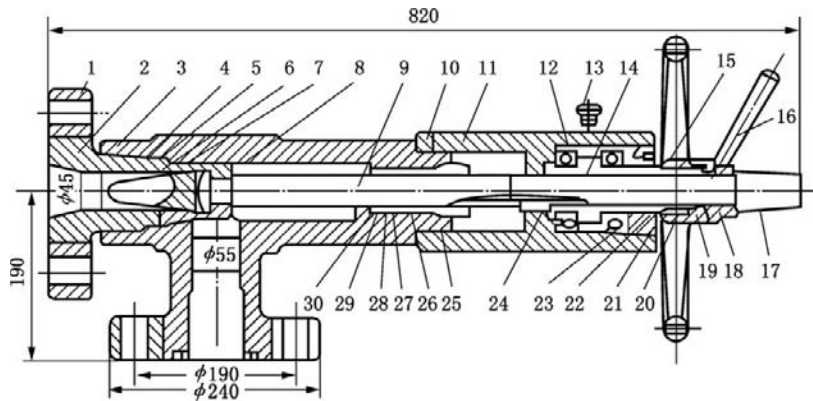


FIGURE 10-47 KQ-700 needle valve (choke). 1, flange; 2, valve seat gland; 3, thread; 4, needle valve body; 5, seal ring; 6, valve seat; 7, seal ring; 8, needle valve; 9, valve stem; 10, screw; 11, valve bonnet; 12, bearing; 13, oil cup; 14, valve stem nut; 15, handwheel; 16, handle; 17, protecting cap; 18, bonnet; 19, nut; 20, key; 21, screw; 22, bearing gland; 23, seal ring; 24, groove key; 25, gland; 26, seal ring; 27, lower groove for seal ring; 28, seal ring; 29, seal ring; 30, gasket.

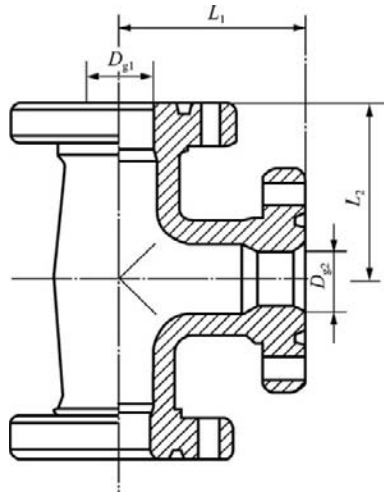


FIGURE 10-48 Flanged tee.

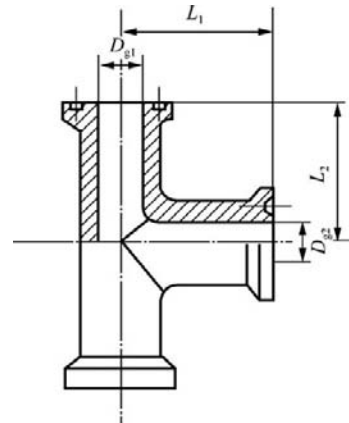


FIGURE 10-50 Collar clamp type tee.

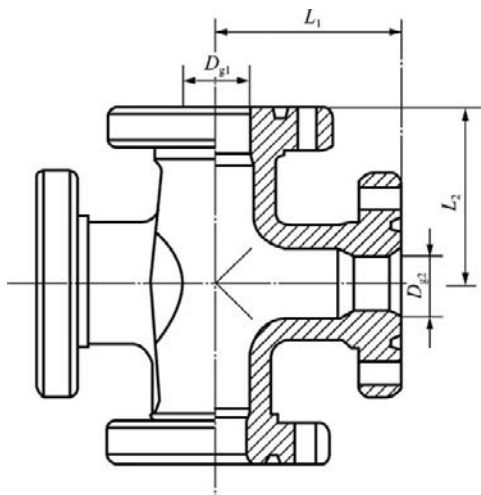


FIGURE 10-49 Flanged spool.

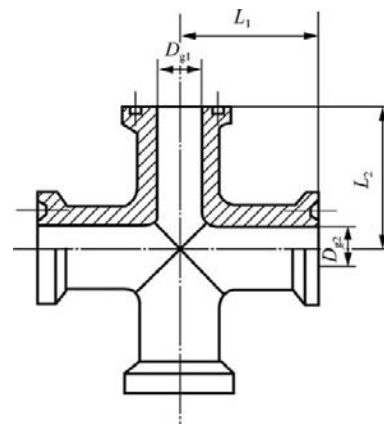


FIGURE 10-51 Collar clamp type spool.

## Seal Gasket Ring and Gasket Ring Groove for Flange

**Application Range.** Seal gasket rings and gasket ring grooves for flanges of wellhead assembly.

### Types and Sizes

1. Seal gasket rings include R mechanical compaction type and RX and BX pressure self-compaction type. The R seal gasket ring is used for 6B flanged connection. The RX seal gasket ring is used for 6B flanged connection

and multistring tubinghead fan-shaped flanged connection. The R and RX seal gasket rings are interchangeable for 6B flanged connection. The BX seal gasket ring is used for 6BX flanged connection.

2. The R seal gasket ring has elliptical or octagonal cross-section and is manufactured in accordance with Figure 10-52 and Table 10-21. The RX seal gasket ring has octagonal cross-section and is manufactured in accordance with Figure 10-53 and Table 10-22. The BX seal

**TABLE 10-19 Parameters of Flanged Tee and Spool**

Rated Working Pressure (MPa)	Nominal Drift Diameter		Distance Between Center and Main Drift Diameter End L <sub>2</sub> (mm) (±0.8)	Distance Between Center and Bypass Diameter End L <sub>1</sub> (mm) (±0.8)
	Main Drift Dia. G <sub>g1</sub> (mm)	Bypass Dia. G <sub>g2</sub> (mm)		
35	52.4 (52)	52.4 (52)	185.7	185.7
	65.1 (65)	52.4 (52)	189	200.2
	79.4 (80)	79.4 (80)	236.5	236.5
	103.2 (103)	52.4 (52)	210.7	244.4
	103.2 (103)	103.2 (103)	274.6	274.6
70	52.4 (52)	46.0 (46)	169.4	173.7
	65.1 (65)	65.1 (65)	198.9	198.9
	77.8 (80)	77.8 (78)	225	225
	103.2 (103)	46.0 (46)	198.4	235
	103.2 (103)	103.2 (103)	262.6	262.6
105	65.1 (65)	52.4 (52)	200.2	209
	65.1 (65)	65.1 (65)	215.9	215.9
	77.8 (78)	65.1 (65)	223	232.7
	77.8 (78)	77.8 (78)	239.8	239.8
	103.2 (103)	77.8 (78)	260.4	279.4
	103.2 (103)	103.2 (103)	296.9	296.9
	52.4 (52)	46.0 (46)	242.8	261.1
	65.1 (65)	65.1 (65)	277.1	277.1
	77.8 (78)	77.8 (78)	302.5	302.5
	103.2 (103)	46.0 (46)	282.5	321.6
103.2 (103)	103.2 (103)	376.9	376.9	

**TABLE 10-20 Parameters of Collar Clamp Type Tee and Spool**

Rated Working Pressure (MPa)	Nominal Drift Diameter		Distance Between Center and Main Drift Diameter End L <sub>2</sub> (mm) (±0.8)	Distance Between Center and Bypass Diameter End L <sub>1</sub> (mm) (±0.8)
	Main Drift Dia. G <sub>g1</sub> (mm)	Bypass Dia. G <sub>g2</sub> (mm)		
14	65.1 (65)	52.4 (52)	183.4	205.5
21	65.1 (65)	65.1 (65)	210.3	210.3
35	79.4 (80)	65.1 (65)	215.1	234.1
	103.2 (103)	65.1 (65)	215.1	251.6
	103.2 (103)	79.4 (79)	238.9	256.4
70	65.1 (65)	52.4 (52)	215	234.1
	65.1 (65)	65.1 (65)	238.9	238.9
	77.8 (78)	65.1 (65)	238.9	256.3
	77.8 (78)	77.8 (78)	256.3	256.3
	103.2 (103)	65.1 (65)	254	300.7
	103.2 (103)	77.8 (78)	271.4	300.7

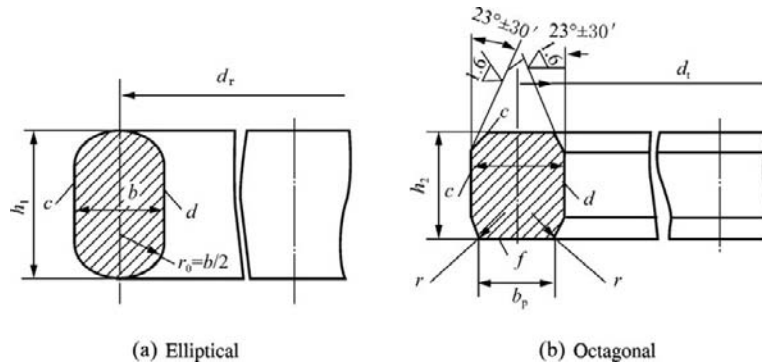


**FIGURE 10-52** R seal gasket ring.

Note:

1. The roundness tolerances of the cylindrical faces  $d$  and  $c$  inside and outside gasket ring are not lower than 10 grades.
2. The perpendicularity tolerances of the octagonal gasket ring end faces  $c$  and  $f$  to the inside and outside cylindrical faces  $d$  and  $c$  are not lower than 10 grades.

**TABLE 10-21** R Seal Gasket Ring (mm)

Gasket Ring Number	Basic Sizes of Gasket Ring (mm)						
	Ring Pitch Diameter (dr) ( $\pm 0.17$ )	Ring Thickness (b) ( $\pm 0.2$ )	Elliptical Ring Height (h <sub>1</sub> ) ( $\pm 0.4$ )	Octagonal Ring Height (h <sub>2</sub> ) ( $\pm 0.4$ )	Plane Width b <sub>p</sub> of Octagonal Ring ( $\pm 0.2$ )	Round Angle Radius r of Octagonal Ring ( $\pm 0.4$ )	Approximate Spacing c <sub>1</sub> of Both Flange End Faces (mm) <sup>1</sup>
R23	82.5	11.11	17.5	16.0	7.75	1.5	4.8
R24	92.25						
R26	101.6						
R27	107.95						
R31	123.83						
R35	136.53						
R37	149.23						
R39	161.93						
R44	193.68						
R41	180.98						
R45	211.14						
R46		12.7	19.0	17.5	8.66		3.3
R49	269.88	11.11	17.5	16.0	7.75		4.8
R50		15.88	22.4	20.6	10.49		4.1
R53	323.85	11.11	17.5	16.0	7.75		4.8
R54		15.88	22.4	20.6	10.49		4.1
R57	381.00	11.11	17.5	16.0	7.75		
R65	469.90						4.8
R66		15.88	22.4	20.6	10.49		4.1
R73	584.20	12.7	19.0	17.5	8.66		3.3
R74		19.05	25.4	23.9	12.32		4.8

<sup>1</sup> c<sub>1</sub> is approximate distance between both flange end faces after seal ring is placed in flange gasket ring and connection is done by stud bolts.

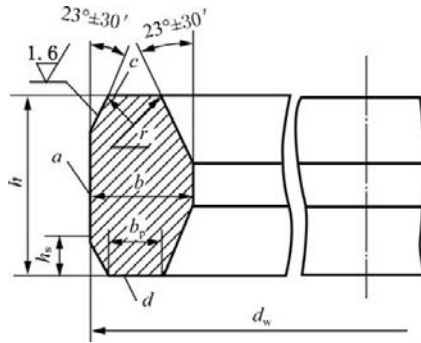
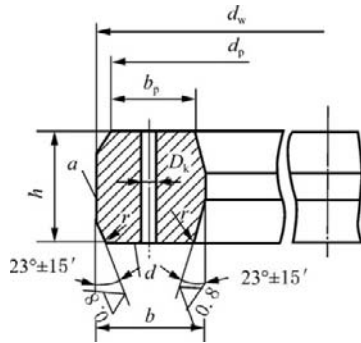


FIGURE 10-53 RX seal gasket ring.

Note: The roundness tolerances of the outside cylindrical face a of gasket ring are not lower than grade 20. The perpendicularity tolerances of gasket ring end faces c and d to the outside cylindrical face a are not lower than grade 10.

TABLE 10-22 RX Seal Gasket Ring (mm)

Gasket Ring Number	Basic Sizes of Gasket Ring (mm)						
	Ring OD $d_w$ +0.50 0	Total Ring Width $b$ +0.20 0	Plane Width $b_p$ +0.15 0	Outside Slope Height $h_s$ 0 0.8	Ring Height $h$ +0.20 0	Round Angle Radius $r$ of Ring $\pm 0.40$	Approximate Spacing $c$ of Both Flange End Faces
RX20	76.2	8.7	4.62	3.2	19.0	1	
RX23	93.27	11.9	6.45	4.2	25.4		11.9
RX24	105.97						
RX25	109.54	8.7	4.62	3.2	19.0		9.7
RX26	111.92	11.9	6.45	4.2	25.4		11.9
RX27	118.27						
RX31	134.54						
RX35	147.24						
RX37	159.94						
RX39	172.64						
RX41	191.69						
RX44	204.39						
RX45	221.85						
RX46	222.25	13.5	6.68	4.8	28.6		
RX49	280.59	11.9	6.45	4.2	25.4	1.5	11.9
RX50	183.37	16.7	8.51	5.3	31.8		
RX53	334.57	11.9	6.45	4.2	25.4		
RX54	337.34	16.7	8.51	5.3	31.8		
RX57	391.72	11.9	6.45	4.2	25.4		
RX65	480.62						
RX66	483.39	16.7	8.51	5.3	31.8		
RX69	544.12	11.9	6.45	4.2	25.4		
RX70	559.07	19.8	10.34	6.9	41.3	2.3	18.3
RX73	596.11	13.5	6.68	5.3	31.8	1.5	15.0
RX74	600.87	19.8	10.34	6.9	41.3	2.3	18.3
RX201	51.46	5.7	3.2	1.4	11.3	0.5	
RX205	62.31	5.6	3.05	1.8	11.1		
RX210	97.63	9.5	5.4	3.1	19.0	0.8	
RX215	140.89	11.9	5.3	4.2	25.4	1.5	



**FIGURE 10-54** BX seal gasket ring.

Note:

1. The round angel radius  $r$  of the ring is 8% to 12% of ring height  $h$ .
2. There is a pressure open-end hole  $D_k$  on ring pitch diameter for each gasket ring.
3. The roundness tolerances of the outside cylindrical face  $a$  of the gasket ring are not lower than grade 10.
4. The perpendicularity tolerances of gasket ring end faces  $c$  and  $d$  to the outside cylindrical face  $a$  are not lower than grade 10.

gasket ring has octagonal cross-section and is manufactured in accordance with Figure 10-54 and Table 10-23.

### Technical Requirements

1. The seal gasket ring material should meet the requirements in Table 10-24.
2. When the seal gasket rings of an oil-well wellhead assembly adopt the steel of Grade 08 or Grade 10, the gasket ring surface should be plated with cadmium or cadmium-titanium alloy that is 0.005–0.013 mm thick.
3. A seal gasket ring should not be used repeatedly.

### Flanged Connection Nut

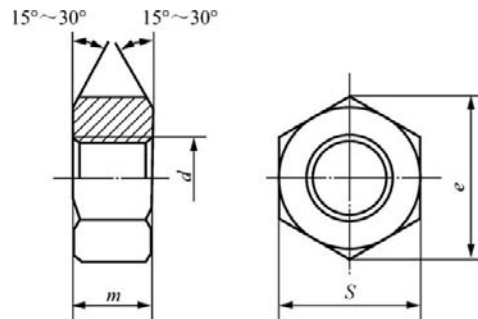
The nominal sizes and allowable tolerances of a flanged connection nut should meet the requirements in Figure 10-55 and Table 10-25.

**TABLE 10-23** BX Seal Gasket Ring (mm)

Gasket Ring Number	Nominal Drift Diameter $D$ (mm)	Basic Sizes of Gasket Ring (mm)					
		Ring OD $d_w$	Ring Height $h$	Total Ring Width $b$	Plane OD $d_p$	Plane Width $b_p$	Hole Diameter $D_k$
		0 -1.5	+0.2 0	+0.2 0	$\pm 0.05$	+ 0.15 0	
BX151	46.0	76.4	9.6	9.6	75.03	8.26	1.5
BX152	52.4	84.68	0.2	10.2	83.24	8.76	
BX153	65.1	100.94	11.4	11.4	99.31	9.78	
BX154	77.8	116.84	12.4	12.4	115.09	10.64	
BX155	103.2	147.96	14.2	14.2	145.95	12.22	
BX156	179.4	237.92	18.6	18.6	235.28	15.98	3.0
BX157	228.6	294.46	21.0	21.0	291.49	18.01	
BX158	279.4	352.04	23.1	23.1	348.77	19.86	
BX159	346.1	426.72	25.7	25.7	423.09	22.0	
BX160		402.59	23.8	13.7	399.21	10.36	
BX162	425.4	475.49	11.2	14.2	473.48	12.24	1.5
BX163	476.2	556.16	30.1	17.4	551.89	13.11	3.0
BX164		570.56		24.6	566.29	20.32	
BX165	539.8	624.71	32.0	18.5	620.19	13.97	
BX166		640.03		26.1	635.51	21.62	
BX167	679.4	759.36	35.9	13.1	754.28	8.03	3.0
BX168		765.25		16.1	760.17	10.97	
BX169	130.2	173.52	15.8	12.9	171.27	10.69	
BX303	762.0	8575	37.9	17.4	847.37	11.61	

**TABLE 10-24 Seal Gasket Ring Material**

Steel Grade	Hardness
08, 10	HB ≤ 137
0Cr18Ni9	HB ≤ 160

**FIGURE 10-55** The nominal sizes and allowable tolerances of a flanged connection nut.**TABLE 10-25 Nominal Sizes and Allowable Tolerances of Flanged Connection Nut (mm)**

d	S		m		e
	Nominal Size	Allowable Tolerance	Nominal Size	Allowable Tolerance	
M12	17	0–0.18	14	±0.35	19.6
M16	22	0–0.21	18		25.4
M20 × 3	27		22	±0.42	31.2
M22 × 3	30		24		34.6
M24 × 3	32	0–0.25	26		36.9
M27 × 3	36		28		41.6
M30 × 3	41		32	±0.50	47.3
M33 × 3	36		35		53.1
M36 × 3	50		38		57.7
M39 × 3	55	0–0.3	41		
M42 × 3			44		63.5
M45 × 3	60		47		69.3
M48 × 3	65		50		75.1
M50 × 3	68		51	±0.60	78.5
M52 × 3	70		52		80.8
M58 × 3	77		58		88.9
M64 × 3	84	0–0.35	63	±0.60	97.0
M70 × 3	92		68		106.2
M76 × 3	100		74		115.4
M80 × 3	105		76		121.2

## REFERENCES

---

- [1] H.B. Bradley et al., Petroleum Engineering Handbook, vol. 1 (Zhang Bainian et al., Trans.), Petroleum Industry Press, Beijing, 1992 (in Chinese).
- [2] Wan Renpu, Luo Yingjun, et al., Petroleum Production Technology Handbook (Book One), Petroleum Industry Press, Beijing, 1994 (in Chinese).
- [3] Wan Renpu, Luo Yingjun, et al., Petroleum Production Technology Handbook (Book Eight), Petroleum Industry Press, Beijing, 1996 (in Chinese).
- [4] Wan Renpu et al., Advanced Well Completion Engineering, first ed., Petroleum Industry Press, Beijing, 1996 (in Chinese).
- [5] Yang Chuandong et al., Gas Production Engineering, Petroleum Industry Press, Beijing, 1997 (in Chinese).

# Oil and Gas Well Corrosion and Corrosion Prevention

## OUTLINE

### 11.1 Related Calculation of Oil and Gas Well Corrosion

Gas Volume Fraction-Mass  
Concentration Conversion

*Example 1*

*Example 2*

Calculation of Partial Pressure  
of Gas under the Condition  
of Having Gas Phase

Calculation of Partial  
Pressure of H<sub>2</sub>S gas in  
Liquid System with No  
Gas Phase

pH Measurement and  
Calculation

### 11.2 Oil and Gas Well Corrosion Mechanisms and Classification

Corrosive Media and  
Corrosion Environment of  
Oil and Gas Wells

*Corrosive Media of Oil  
and Gas Wells*

*Corrosion Environment  
of Oil and Gas Wells*

*Material Selection and  
Structure*

Basic Corrosion

Classification and  
Mechanism

*Electrochemical*

*Corrosion*

*Effects of Environmental  
Factors on*

*Electrochemical  
Corrosion*

Environment-Assisted

Fracture and Stress

Corrosion

*Stress Corrosion*

*Fracture*

*Corrosion Fatigue*

Flow-Induced Corrosion and

Scour Corrosion

*Flow-Induced Corrosion*

*Scour Corrosion*

Corrosion Mechanisms and

Types of Corrosion of

Main Corrosive

Components

*Hydrogen Sulfide*

*Corrosion Mechanism*

*and Types of*

*Corrosion*

*Elemental Sulfur*

*Corrosion*

*Carbon Dioxide*

*Corrosion*

*Brine Corrosion*

*Oxygen Corrosion*

*Bacteria Corrosion*

*Interaction of Corrosive*

*Components and the*

*Effect on Corrosion*

*Acid Corrosion*

### 11.3 Material Selection for Corrosive Environment of Oil and Gas Wells

Overview

*Common Types of  
Material for Corrosive  
Environments of Oil  
and Gas Wells*

*Material Selection under  
Corrosive Conditions of  
Oil and Gas Wells*

*Correlativity of Material  
Selection with Corrosive  
Environments of Oil  
and Gas Wells*

Methods and Criteria for

Evaluating Material

Fracture in Corrosive

Environment of Oil and

Gas Wells

*Criteria*

*NACE Method A*

*(Tension Test)*

*NACE Method B (Beam*

*Bending Test)*

- NACE Method C  
(C-Shaped Ring Test)
- NACE Method D  
(Dual Cantilever  
Beam Test)
- Main Factors That Affect  
Cracking in Corrosive  
Environments
  - Alloy Design, Harmful  
Element Control, and  
Metallurgical Texture  
Strength and Hardness  
Temperature Conditions  
Appropriate for  
Different Steel Grades  
of Casing and Tubing in  
Sour Environments
  - Stress Level and Stress  
State
- Cracking Severity Criteria  
for Carbon Steel and  
Low-Alloy Steel in a Sour  
Environment of Hydrogen  
Sulfide
  - SSC Criteria Diagram  
of Carbon Steel and  
Low-Alloy Steel
  - Selection of Steel  
Material Suitable for  
Zone SSC
  - 0 Environment with  
Low Partial of  
Hydrogen Sulfide  
( $P_{H_2S} < 0.3 \text{ k Pa}$ )
  - Selection of Casing,  
Tubing, and Fittings  
Suitable for Serious  
Sour Environments  
(Zone SSC 3)
  - Selection of Casing,  
Tubing, and Fittings  
Suitable for Medium  
Sour Environments  
(Zone SSC 2)
  - Selection of Casing, Tubing,  
and Fittings Suitable for  
Slight Sour Environments  
(Zone SSC 1)
- Test Requirements of  
Commonly Used Hydrogen  
SSC Resistant Carbon Steel  
and Low-Alloy Steel  
Tubing and Casing
  - J55 and K55 Seamless  
Steel Pipe
  - K55 Electric Resistance  
Welded Pipe Body and  
Collar
  - L80 Type 1, C90 Type 1,  
and T95 Type 1 Casing  
and Collar
- Corrosion-Resistant Alloy  
Steel Tubing and Casing  
Types and Basic  
Compositions of  
Corrosion-Resistant  
Alloys for Tubings and  
Casings in Oil and Gas  
Wells
  - Modes of Corrosion and  
Influence Factors for  
Corrosion-Resistant Alloy  
Service Environment
  - Restriction of Corrosion-  
Resistant Alloy
- Corrosion of Nonmetallic  
Material
- 11.4 Oil and Gas Well  
Corrosion Prevention Design**
  - External Casing Corrosion  
Prevention
    - External Casing  
Corrosion Sources and  
Mechanisms of  
Corrosion
    - External Casing  
Corrosion Prevention  
Design
  - Tubing-Casing Annulus  
(Outside Tubing Wall and  
Inside Casing Wall)  
Corrosion
    - Open Annulus
    - Closed Annulus
  - Flow Velocity Restriction  
Based on Tubing Erosion  
and Corrosion
    - Complexity of Effect of  
Flow Velocity in Tubing  
on Corrosion
    - Calculation of In-Tubing  
Flow Velocity for  
Preventing Erosion and  
Corrosion
  - Tubing and Casing Thread  
Corrosion and Corrosion  
Prevention Design
    - Thread Corrosion  
Mechanism
    - Tubing Thread Selection  
and Anti-Erosion  
and Anti-Corrosion  
Design
    - Optimizing Thread  
Structure and Reducing  
Local Stress
    - Concentration of Thread
  - Design of Preventing  
Galvanic Corrosion
    - Universality of Galvanic  
Corrosion
    - Measures of Preventing  
Galvanic Corrosion
  - Strength Design Safety  
Factor under Corrosive  
Environment Conditions
    - Safety Factor Design Based  
on Critical Stress Percent
    - Safety Factor Design  
Based on Critical  
Environment Fracture  
Toughness  $K_{ISSC}$
  - Design of Reducing Stress  
Level
    - Concept of Stress Level
    - Importance of Reducing  
Working Stress Level
    - Hole Structure Design of  
Reducing the Stress Level
  - Christmas Tree Corrosion
- 11.5 Tubing and Casing  
Corrosion Prevention for  
Sour Gas Reservoirs**
  - Main Types of Tubing and  
Casing Corrosion for Sour  
Gas Reservoirs
    - Hydrogen Sulfide  
Corrosion
    - Carbon Dioxide  
Corrosion
    - Corrosion under  
Coexistence of  $H_2S$  and  
 $CO_2$

<i>Corrosion Due to Water and Other Factors</i>	<i>Glassfiber Reinforced Plastics Liner Tubing</i>	<i>Margins of Comprehensive Tackling and Control of Corrosion Rate in Oil and Gas Fields</i>
Corrosion Prevention	<i>Bimetallic Combination Tubing</i>	<i>Technical Margins of Protective Measures</i>
Technology Selection and Tubing and Casing	Corrosion Inhibitor	<i>Technical Margins of Adding Corrosion Inhibitor</i>
Material Adaptability	Technical Margins of Corrosion Prevention	<i>Technical Margins of Coating Technique Application</i>
Evaluation	Measure	<b>References</b>
<i>Corrosion-Resistant Alloy Steel Tubing</i>	<i>Technical Margins of Sour Oil and Gas Field Facilities' Corrosion Resisting</i>	
<i>High Sulfide-Resistant Steel Tubing</i>	<i>Allowable Corrosion Rates and Technical</i>	
<i>Common Sulfide-Resistant Steel Tubing</i>		
<i>Internal Coating Tubing</i>		

Corrosion in oil and gas well production systems is a serious factor in failures. Corrosion may not only cause economic losses, but may also bring with it problems of safety and protection of resources. Some oil and gas wells have adverse working environments, so their service lives and properties will seriously affect the exploration and development and the operating benefits of oil and gas fields. For sour gas fields, dangerous safety accidents and environmental problems may be generated; thus, understanding the mechanisms and rules of corrosion of oil and gas wells and making rational corrosion prevention design are crucial.

The corrosion in oil and gas well production systems includes internal corrosion and external corrosion, both of which have universality. Internal corrosion means the corrosion of the inner walls of the tubing, casing, Christmas tree system, station and field equipment, and pipeline. External corrosion means the corrosion of the outer wall of the casing and cement sheath that contact with the formation water or reinjected produced water that contains corrosive components (for tubings in the oil and gas wells with no packer, there also is corrosion of the outer wall). The produced oil and gas with high content of CO<sub>2</sub>, H<sub>2</sub>S, and elemental sulfur and the high-salinity formation water, and so on, in some oil and gas wells make the corrosion in

the oil and gas production system and station and field equipment very serious. In addition, the flow passage blocking caused by elemental sulfur sedimentation and hydrate and scale formation, and so on, makes production irregular and downhole operations complicated.

## **11.1 RELATED CALCULATION OF OIL AND GAS WELL CORROSION**

The calculation or conversion of component contents is often required in the analyses and studies of the corrosion of oil and gas wells and in corrosion prevention designs. Different expressions are often adopted on the basis of different customs with different aims.

### **Gas Volume Fraction-Mass Concentration Conversion**

Gas content is often described using the following two methods:

1. Gas mass concentration. It is the grams (mass) per cubic meter volume of some gas under standard conditions (20°C and 101.3 k Pa).
2. Gas volume fraction.

The gas volume fraction-mass concentration conversion is shown in Equation (11-1).

(11-1)

$$X = \frac{GV}{M \times 10}$$

where: X = volume fraction, %; G = mass concentration of some gas, g/m<sup>3</sup>; M = molar weight of some gas, g/mol; V = volume of the gas of 1 mol under standard conditions (20°C and 101.3 k Pa), L/mol.

**Example 1.** Converting the mass concentration of H<sub>2</sub>S gas into volume fraction.

The volume of 1 mol H<sub>2</sub>S gas under standard condition (20°C and 101.3 k Pa) is V = 23.76 L/mol.

The molar weight of H<sub>2</sub>S gas is M = 34.08 g/mol, as shown in Equation (11-2).

(11-2)

$$X_{H_2S} = \frac{G \times 23.76}{34.08 \times 10} = 0.0697 G$$

For H<sub>2</sub>S gas with mass concentration of 75 mg/m<sup>3</sup>, the volume fraction is as follows.

$$X_{H_2S} (\%) = 0.0697 \times 75 \times 10^{-3} = 52 \times 10^{-4} (\%)$$

For ideal gas, the mole fraction is equal to volume fraction.

**Example 2.** CO<sub>2</sub> gas concentration conversion.

The volume of CO<sub>2</sub> gas under standard conditions (20°C and 101.3 k Pa) is V = 23.89 L/mol.

The molar weight of CO<sub>2</sub> gas is M = 44.00 g/mol, as shown in Equation (11-3).

(11-3)

$$X_{CO_2} = \frac{G \times 23.89}{44.00 \times 10} = 0.054 G$$

## Calculation of Partial Pressure of Gas under the Condition of Having Gas Phase

When corrosion is analyzed and studied, the partial pressures of corrosive gases (H<sub>2</sub>S and CO<sub>2</sub>, and so on) are required to be used for indicating the effect of the corrosive gases on the severity of corrosion. In light of volume percent concentration only, an environment with a high concentration of corrosive gas (H<sub>2</sub>S or CO<sub>2</sub>) and a total pressure

that is not high may have an effect that is not more severe than that of the environment with a low concentration of corrosive gas and a high total pressure. In general, the higher the partial pressure of corrosive gas, the more severe the corrosion. A system with low content of H<sub>2</sub>S (or CO<sub>2</sub>) does not mean that the corrosion is not severe. A system with high total pressure may also have partial pressure of H<sub>2</sub>S (or CO<sub>2</sub>); thus, it may generate more severe corrosion than that of a system with high content of H<sub>2</sub>S (or CO<sub>2</sub>) and low total pressure.

The partial pressure of a component in a gas mixture is the pressure of the component if it solely exists in the total volume of the mixture. It is equal to the total absolute pressure multiplied by the mole fraction of the component in the mixture. For ideal gas, the mole fraction is equal to the volume fraction of this component.

The partial pressure of gas is calculated as shown in Equation (11-4).

(11-4)

$$p_x = p_t \times \frac{X}{100}$$

where: p<sub>x</sub> = partial pressure of H<sub>2</sub>S (or CO<sub>2</sub>), MPa; p<sub>t</sub> = total absolute pressure of system, MPa; X = mole fraction of H<sub>2</sub>S (or CO<sub>2</sub>) in gas, %.

For instance, if the total pressure of gas is 70MPa and the mole fraction of H<sub>2</sub>S in gas is 10%, then the partial pressure of H<sub>2</sub>S is 7 MPa. If the total pressure in the system and the H<sub>2</sub>S concentration are given, the partial pressure of H<sub>2</sub>S can be calculated using Figure 11-1.

## Calculation of Partial Pressure of H<sub>2</sub>S Gas in Liquid System with No Gas Phase

For a liquid system with no gas phase, the effective thermodynamic activity of H<sub>2</sub>S can be calculated by using the true partial pressure of H<sub>2</sub>S as follows.

1. Measuring the bubble point pressure (pB) of liquid at some temperature by using an appropriate method (in the pipeline filled with liquid at the downstream of separator, the bubble point pressure can be approximately taken as the total pressure of the last separator);

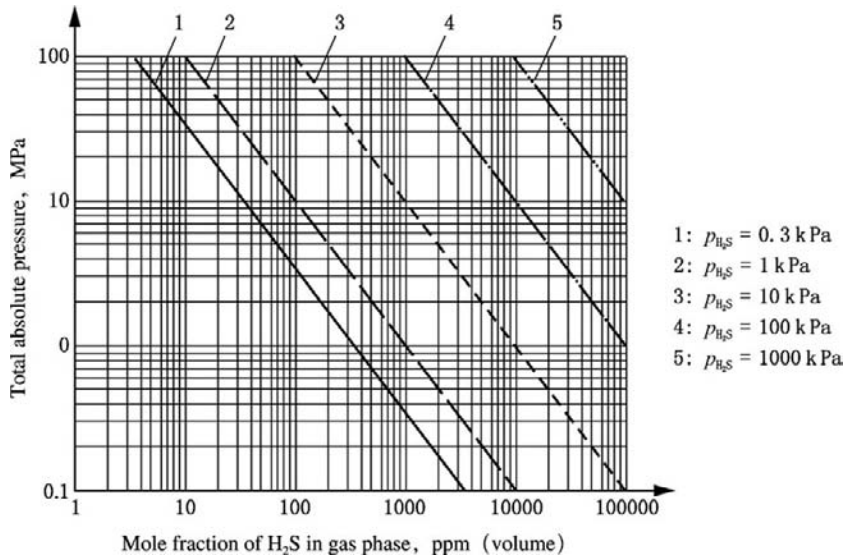


FIGURE 11-1 The pressure contours of partial pressure of  $H_2S$  in a sour gas system.

2. Measuring the mole fraction of  $H_2S$  in gas phase under the condition of bubble point
3. Calculating the partial pressure of  $H_2S$  in natural gas in bubble point state by using Equation (11-5):

(11-5)

$$p_{H_2S} = p_B \times \frac{X_{H_2S}}{100}$$

where:  $p_{H_2S}$  = partial pressure of  $H_2S$ , MPa;  
 $p_B$  = bubble point pressure, MPa;  $X_{H_2S}$  = mole fraction of  $H_2S$  in gas, %.

4. Measuring the partial pressure of  $H_2S$  in liquid system using this method to determine whether the system is in a sour environment.

## pH Measurement and Calculation

The pH value is one of the key factors that affect corrosion. The diagnosis and analysis of field corrosion conditions and corrosion prevention design often involve the pH value, which is affected by the dissolution and escape of components and factors including temperature, pressure, and phase change. Thus there is a pH

value difference between the tubing-casing annulus and the inside of the tubing, and different depths in the well have different pH values. The pH value is also one of the basic grounds of quantitatively describing corrosion severity and selecting material. Therefore, the measurement and calculation of the pH value are of great importance. In general, the pH value measured by using a pressureless water sample taken after separator cannot represent the actual pH value at some point in the well. Thus conversion is required when the pH value obtained at the sampling point is used. The following is a brief method.

The general methods for determining the approximate pH value of water phase under different conditions are shown in Figures 11-2 to 11-6. The error range of pH value is  $\pm 0.5$  pH value. The ordinate is the in-situ pH value, on which the effects of organic acids (such as acetic acid and propionic acid) and acidic salts have not been considered in these figures. The possible organic acids are required to be analyzed in order to revise the calculated pH value at the observation point.

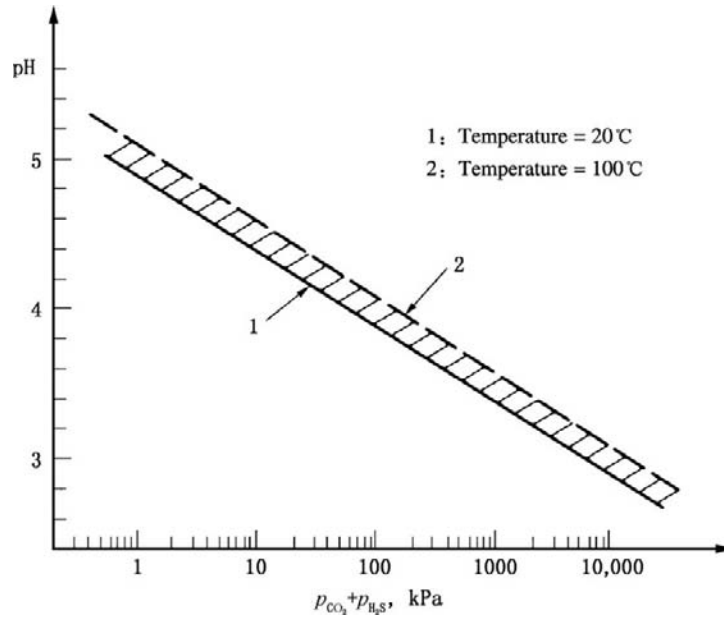


**FIGURE 11-2** Effects of the partial pressures of CO<sub>2</sub> and H<sub>2</sub>S on the pH value of condensate water.

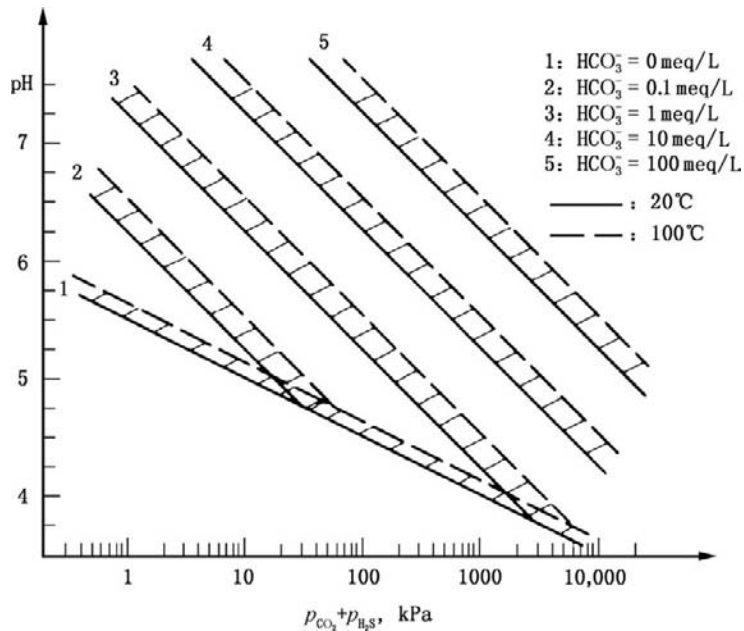


**FIGURE 11-3** Effects of the partial pressures of CO<sub>2</sub> and H<sub>2</sub>S on the pH value of condensate water or formation water that contains bicarbonate.

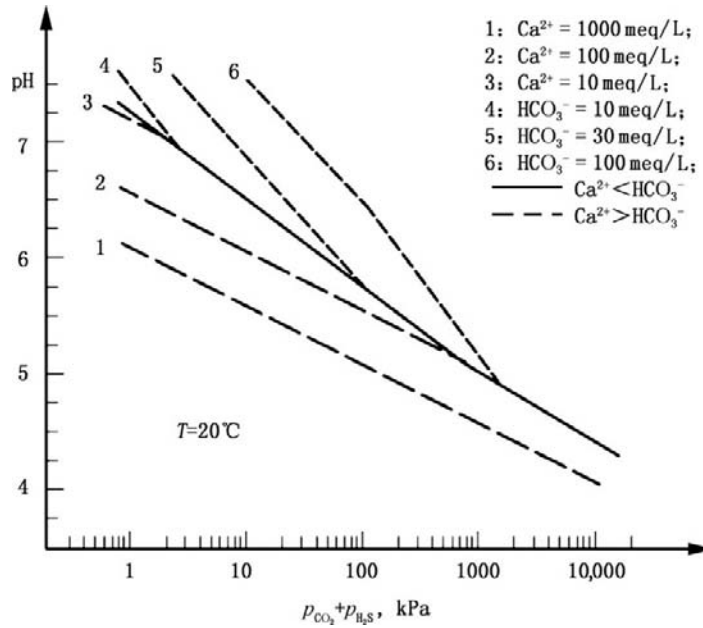


**FIGURE 11-4** The pH value of formation water that is saturated (or supersaturated) with CaCO<sub>3</sub> under the partial pressures of CO<sub>2</sub> and H<sub>2</sub>S at 20°C.

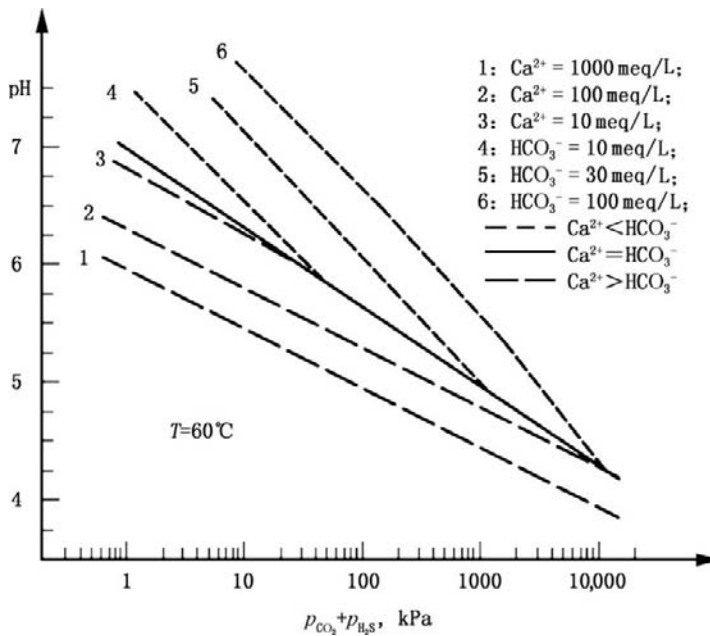


**FIGURE 11-5** The pH value of formation water that is saturated (or supersaturated) with CaCO<sub>3</sub> under the partial pressures of CO<sub>2</sub> and H<sub>2</sub>S at 60°C.

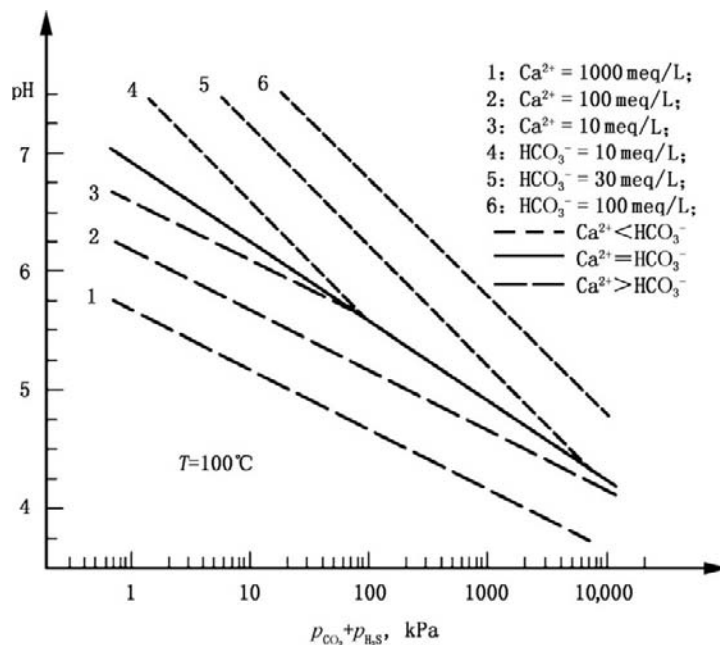


**FIGURE 11-6** The pH value of formation water that is saturated (or supersaturated) with  $\text{CaCO}_3$  under the partial pressures of  $\text{CO}_2$  and  $\text{H}_2\text{S}$  at  $100^\circ\text{C}$ .

The pH value of produced fluid is affected by components and phase changes. The following points should be considered when calculating the pH value:

1. The effect of  $\text{CO}_2$  content on the pH value is obvious. However, the error is obvious if the  $\text{CO}_2$  content is only considered when the pH value is calculated, which is due to some bicarbonate in the system. These figures show the obvious effect of bicarbonate content on the pH value of the system. The effects of the components of oil and gas should also be considered when the downhole corrosion conditions are analyzed.
2. When both  $\text{H}_2\text{S}$  and  $\text{CO}_2$  are contained, the reduction of pH value due to the dissolution of both in water should be considered. However, this is a complicated physical-chemical variation process because of the obvious difference of the solubility of  $\text{H}_2\text{S}$  in solution under different pressures at different temperatures.

3. The effect of temperature on the pH value of system lower than that of pressure.

## 11.2 OIL AND GAS WELL CORROSION MECHANISMS AND CLASSIFICATION

### Corrosive Media and Corrosion Environment of Oil and Gas Wells

Corrosion of oil and gas wells is related to the corrosive media in produced fluid, the corrosion environment, the material selected and structure, and so on, among which there is interaction, thus generating even obvious differences in corrosion severity between wells, in different positions in the same well, and at different producing times for the same well.

In oil and gas production systems, there also are many nonmetallic component parts such as plastic and rubber products, for which attention to corrosion should also be paid.

### Corrosive Media of Oil and Gas Wells

1. Corrosive components in dynamically produced fluid include:
  - a. Carbon dioxide;
  - b. Hydrogen sulfide, elemental sulfur, organic sulfur, and so on;
  - c. Formation water with high-concentration chloride ions, water injected during waterflooding, and condensate water in a gas well;
  - d. Oxygen or other acidic materials that enter the well during well construction and downhole operations (such as acidizing);
  - e. Sulfate, sulfate reducing bacteria and carbonate.
2. Corrosive components that are injected include:
  - a. Injected water;
  - b. Spent acid during acidizing, polymer injected for enhancing recovery factor, carbon dioxide reinjected during enhanced oil recovery, and so on;
  - c. Carbon dioxide injected into condensate gas reservoir and carbon dioxide reinjected during gas recycling;
  - d. High-temperature steam injected during thermal production.
3. Corrosive components in non-productive formations include:
  - a. Acidic gases.  $\text{H}_2\text{S}$ ,  $\text{CO}_2$ , and  $\text{H}^+$ ;
  - b. Dissolved oxygen gas;
  - c. Salt ions.  $\text{HCO}_3^-$ ,  $\text{SO}_4^{2-}$ ,  $\text{Cl}^-$ , and  $\text{OH}^-$ ;
  - d. Bacteria. Sulfate-reducing bacteria, oxyphilous bacteria, and so on;
  - e. Interzonal crossflow due to poor cement job quality or improper downhole operation.

### Corrosion Environment of Oil and Gas Wells.

The corrosion environment of oil and gas wells includes the pressures, temperatures, flow regimes, and flow fields in various positions. These factors may cause a change of the phase state of the system. The change process is accompanied by the dissolution and escape of gas, the disrapture of bubbles, and so on. Shear and cavitation may be generated on the flow passage wall. Corrosion may be aggravated under the action of combined mechanical force and electrochemical corrosion.

The changes of flow passage diameter and flow direction may also generate changes of pressure, temperature, flow regime, and flow field; thus, corrosion may be aggravated.

During oil and gas well production, the contents of corrosive components are changeable. With the prolongation of the production period, the content of formation water will increase and the content of  $\text{H}_2\text{S}$  may also increase.

Contact or connection between different materials may generate an electric potential difference. Some formations or intervals may generate an electric potential difference with casing. Electric potential difference is an important component part of the oil and gas well corrosion environment.

The stress state and stress level of structural members (such as tubing, casing and wellhead assembly) are important in the corrosion environment.

**Material Selection and Structure.** Selecting appropriate material in light of specific corrosive components and corrosion environments is the most important component part of corrosion prevention design. Rational structure design can reduce stress level and reduce corrosion caused by flow field and phase change.

### Basic Corrosion Classification and Mechanism

The deterioration or failure by chemical or electrochemical action generated between metal and its environmental media is known as metallic corrosion. The mechanisms or types of corrosion during oil and gas well production include:

1. Electrochemical corrosion;
2. Chemical corrosion;
3. Environment-assisted fracture and stress corrosion;
4. Flow- and phase change-induced corrosion.

#### Electrochemical Corrosion

1. Electrochemical corrosion mechanism

Tubing, casing, and equipment made of steel are good electric conductors. Various salts or  $\text{CO}_2$  and  $\text{H}_2\text{S}$ , and so on, are dissolved in the

water that oil and gas well fluid produced contains. When steel contacts the aforementioned media, the protective metal-oxide film that has been formed in air may be dissolved in an electrolyte solution. When metal is exposed, the metal as a good electric conductor and the solution as a good ionic conductor form a return circuit. Ferrous ions with positive charges tend to dissolve in electrolyte solution and form ferrous salts. Electrons tend to congregate at the metal end and a certain electric potential difference is formed. Electrons flow toward the solution. This is an oxidation reaction process and is known as anodic reaction. The metal end is known as the anodic area.

In addition, the electrons that enter solution are bound with hydrogen ion, and hydrogen molecules are formed. This is a reduction reaction process and is known as cathodic reaction. The solution end is known as the cathodic area. In an aerobic environment, hydroxide radicals are formed.

Ferric atoms enter solution in the form of ferrous ion and exist there in the forms of  $\text{Fe}_2\text{O}_3 \cdot (\text{H}_2\text{O})_x$ ,  $\text{FeS}_x$ ,  $\text{Fe}_2\text{O}_3$ , and so on. Corrosion products may deposit on the metal surface to form a protective film. Whether the corrosion will be a continued or an electrochemical corrosion process is shown in Figure 11-7.

## 2. Uniform electrochemical corrosion

Electrochemical corrosion that is generated on the whole metal surface is known as uniform corrosion. At present, the corrosion prediction software that has been developed is mainly in light of uniform corrosion, which is easier to predict and prevent by increasing wall thickness, holding corrosion allowance, and so on. Cathodic protection with impressed electric field also is mainly in light of uniform corrosion.

## 3. Local corrosion

There are two boundary conditions that may generate or aggravate electrochemical corrosion.

- If the two metals with a greater electric potential energy level difference have electrolyte solution between them or directly contact each other and are immersed in electrolyte solution, electric potential difference corrosion, which is also known as galvanic corrosion, may be generated.
- When the defect or crevice inside metal exposes in electrolyte solution, local electrochemical corrosion may be generated.

The electrochemical corrosion generated by the aforementioned boundary conditions may cause local corrosion boring or cracking, which is the main form of the corrosion failure of tubing, casing, sucker rod, and equipment.

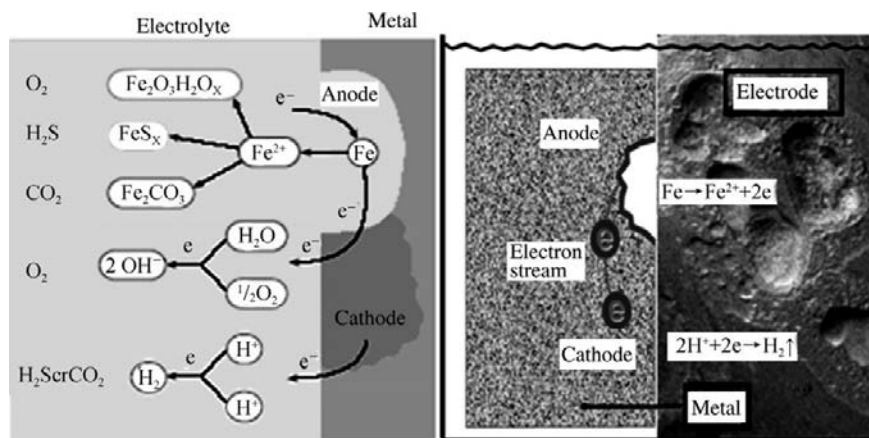


FIGURE 11-7 Electrochemical corrosion.

**Effects of Environmental Factors on Electrochemical Corrosion.** The actual electrochemical reaction is very complicated due to the variety of external environments. Whether the electrochemical reaction will be continued, stopped, mitigated, or aggravated is mainly dependent on the corrosive media and the external environment.

#### 1. Corrosion products and interaction

Corrosion products form a cover film on a metal surface. Cover film is also known as passivating film because cover film can prevent electrochemical corrosion from generating continuously.

- a. Effect of electric conductivity of passivating film. An electrochemical reaction is accompanied by electron streams and ion streams. A low-conductivity conductor can resist both streams and has good protective action. In common industrial products, only metal aluminum oxide and titanium oxide can resist both streams. The iron oxide in steel products may conduct electron streams. A low-conductivity conductor that can resist ion stream can prevent a metal anode from dissolving.
- b. Effect of impressed electric field. Ionic conductivity and electronic conductivity are related to the potential difference between both sides of the cover film. The electric potential difference between two types of metals that have a great electric potential energy level difference between them may still drive electrons or ions to make them penetrate through the film and stream. Electron streams and ion streams can be prevented by using a reverse electric field. This is also the principle of cathodic protection.
- c. Film stability. Iron carbonate film has high stability and adhesion to metal and can resist the course of electrochemical corrosion. When there is hydrogen sulfide, however, the iron sulfide film formed may reduce the stability of iron carbonate film under the coordinated action of iron

carbonate film, except that its concentration is low. Fluid perturbation may cause the ionic concentration to decrease at the metal surface and speed up electrochemical reaction. Local vortex flow and excessive flow velocity may also reduce the stability of film and aggravate corrosion.

#### 2. Stray current corrosion

Stray current corrosion may occur on the outside of the pipeline and oil and gas well casing. Stray current can be electrotelluric current or the stray direct current of cathodic protection. It merits attention that the corrosion caused by direct current may be dozens of times that of alternating current, under the same current strength.

Electrotelluric stray current corrosion may be generated. Different formations that casing passes through have different moistness, and different aquifers have different salinities; thus, different sections of casing have different electrode potentials. Casing can be regarded as anode.

#### 3. Galvanic corrosion

Galvanic corrosion, which is also known as bimetallic contact corrosion, means that a galvanic couple pair is formed when the return circuit is formed by the materials at different electric potential energy levels and the environmental media. Galvanic couple current is generated due to different electric potentials; thus, the dissolution rate of the metal with lower electric potential is increased, and that of the metal with higher electric potential is decreased, which is known as galvanic corrosion because there is a great electric potential difference between two different materials, and the electrolyte solution forms the conductor of electron and ion, thus forming the primary cell of corrosion.

#### 4. Crevice corrosion

Crevice corrosion is also a common local corrosion. Corrosion pits or deep holes with different depths may be formed in crevices after crevice corrosion of metal. They are groove- or seam-shaped. The types of crevices include: (1) crevice at connection between

metallic component parts; (2) metallic crack crevice; and (3) crevice between metal and nonmetal. The following two conditions should be met to form crevice corrosion: (1) having hazardous anions (such as chlorion) and (2) having a crevice that allows corrosive liquid to enter the crevice and makes the liquid stay in the crevice. These crevices are very small and generally 0.025–0.1 mm in width.

For oil and gas wellhead assemblies, crevice corrosion is easy to generate due to the conjugation (riveting, welding, threaded connection, and so on) between metals, the contact between metal and nonmetal (lining, insert, and so on), and a great quantity of chlorions. For instance, crevice corrosion is commonly formed at the drill pipe sub and the threaded connections of tubing and casing. Deposits and adhesions, such as sand and mud, scale and scraps, are commonly generated in some local places on the inner wall of the pipe due to local structure differences.

#### 5. Spot corrosion

Forming many apertures under the condition of almost no corrosion on the surface is characteristic of spot corrosion. The depth of the aperture is often greater than the diameter of the aperture and boring may be generated under serious conditions. The coordinated action of oxygen and chlorion containing corrosive media and defective metallographic texture is the main reason for generating spot corrosion.

### Environment-Assisted Fracture and Stress Corrosion

Environment-assisted fracture may be generated in tubing, casing, and surface assembly because of reduction of the physical and mechanical properties (especially the toughness) of material due to some chemical components or elements. The mutual impelling of structural stress, material selection, corrosive media, and environment parameters may lead to sudden fracture or disrapture, which is generally known as stress corrosion cracking. Environment-assisted fracture

roughly includes stress corrosion and hydrogen embrittlement, both of which can be simultaneously generated, or hydrogen embrittlement is one of the essential factors of stress corrosion. Stress corrosion also includes fatigue corrosion, impingement corrosion, and vacuole corrosion.

**Stress Corrosion Fracture.** The delayed cracking or fracturing of metallic material under the coordinated action of stress and chemical media is known as stress corrosion fracture. Stress corrosion fracture is a brittle fracture and is generated suddenly. It should be predominantly considered in all industrial structure designs. The features of stress corrosion fracturing or cracking include:

1. There is certainly stress, which can be applied stress or residual stress. Tensile stress is the most harmful. When cracking is generated, the tensile stress is lower than the yield strength of the material. There is no obvious plastic deformation before cracking is generated. The greater the stress, the shorter the time before cracking is generated.
2. Whether stress corrosion cracking is generated is mainly dependent on the combination of corrosive media, metallics, temperature, and pH value. For instance, corrosive media that contain chlorion may cause the sudden stress corrosion cracking of 13Cr, super 13Cr, 22Cr, and 25Cr tubing, and pipeline, but will not cause the stress corrosion cracking of low-alloy steel (such as J55, N80, and P110 tubing and casing). In general, the materials that may generate stress corrosion cracking in corrosion environments include: high tensile steel in a hydrogen environment, stainless steel in a high-temperature solution with high chlorion content, and high tensile steel and stainless steel in a wet environment with  $\text{CO}_2 + \text{CO} + \text{H}_2\text{O}$  or  $\text{CO}_2 + \text{HCO}_3^- + \text{H}_2\text{O}$ , and copper alloy in the  $\text{NH}_4^+$ -containing solution.

**Corrosion Fatigue.** When metal bears cyclic stress in a corrosive environment, the cycle index necessary for causing failure under a given stress is reduced. Corrosion may cause fatigue to speed

up; that is, corrosion fatigue is generated. Metal cracking may be generated under the coordinated action of corrosion and fatigue.

The fatigue limit may also be reduced even though metal (especially the metal with protective film) is in an environment with low corrosion severity. The surface film may be repeatedly ruptured under the action of alternate stress, and new metal may be continuously corroded.

When the corrosion fatigue of the structural member metal is generated, macro-cracks may be formed locally. Corrosion fatigue is more harmful in comparison with mechanical fatigue. The reason is that pure mechanical fatigue may generate fatigue failure only under the condition of stress higher than the critical cyclic stress value, known as the fatigue limit. However, corrosion fatigue may generate failure under stress much lower than the critical cyclic stress. The failure of drill pipe or pumping sucker rod under low stress conditions is generally caused by corrosion fatigue. Unsteady-state flow in tubing or high-velocity gas flow at the wellhead throttle manifold and bent tube may induce fluid-solid coupling vibration and lead to corrosion fatigue cracking under the condition of no obvious corrosion failure.

## Flow-Induced Corrosion and Scour Corrosion

The coordinated action of flow, electrochemistry, and mechanical forces may speed up corrosion; that is, flow-induced corrosion and scour corrosion are generated. They are related to each other but different in the type or mechanism of corrosion. The corrosion generated by the flow in tubing and the flow through the control manifold and scour corrosion should be fully considered in oil and gas well control prevention design. If it is considered that fluid-media corrosion and electrochemical corrosion are objectively present, then flow-induced corrosion and scour corrosion can be controlled by rational design to a great extent.

**Flow-Induced Corrosion.** When fluid flows along the wall, a turbulent boundary layer may

be formed in the vicinity of the wall. The formation and evolution of turbulent flow in a boundary layer may cause shock and shear on the wall. This process will speed up the movement of corrosive media toward the metal surface and corrosion products will speed up, leaving the original place, which means that the mass transfer coefficient will be increased and corrosion will be speeded up. Whether flow-induced corrosion will be generated and how high the corrosion severity will be depend on the following:

1. **Multiphase flow regime.** Flow-induced corrosion is mainly dependent on a multiphase flow regime. The water phase in the flow may wet the pipe wall. In addition to corrosive component content, the proportions of oil, water, and gas in multiphase systems and the change of phase state may affect corrosion severity.
2. **Erratic flow.** The change of flow passage, pipe wall tubercles, and bent pipe, and so on, may alter the flow field and lead to erratic flow, which makes the multiphase flow boundary layer off-balance and makes the mass transfer coefficient increase, so that the corrosion in erratic flow areas will be speeded up.

**Scour Corrosion.** Scour corrosion can be roughly considered to be flow corrosion. However, in a strict sense, scour corrosion mainly means that the mechanical force of the flow breaks the protective film on metal. The dissolution of protective film by corrosive media or the low adhesion of protective film to metal body may aggravate corrosion in combination with the scour of the mechanical force of the flow.

The multiphase system of oil, water, gas, and solids may form multiple types of scour corrosion, which mainly include cavitation corrosion (that is, vacuole corrosion), turbulent corrosion, liquid blob shock, gas bubble shock, and solid particle shock.

1. **Cavitation corrosion**

When cavitation corrosion is generated, the liquid phase makes contact with the pipe

wall and there is a certain relative velocity between liquid phase and pipe wall. In the flow process, an abrupt change of flow field is generated and a great disturbance is generated. Gas bubbles or gas vacuoles are formed in a local low-pressure area. The gas bubbles or gas vacuoles are rapidly broken in a high-pressure area to cause local corrosion. When an abrupt change of flow field is generated, vortex flow is generated and a local low-pressure area is formed. In the local low-pressure area, nonsoluble gas bubbles escape from liquid phase.

Cavitation corrosion is caused under the coordinated action of mechanical and chemical factors. Cavitation corrosion is generally accompanied by noise and vibration and also the chemical corrosion process. This corrosion phenomenon often presents at the diameter-changing place of the middle part of an API round-threaded collar, tubing hanger, spool, tee, elbow, and so on.

## 2. Turbulent corrosion

Turbulent corrosion means the steel surface damage caused by the coordinated action of erosion and corrosion, which is greater than the total damage caused by single erosion and single corrosion. In practical production, erosion corrosion may be generated in tubing and at pipeline elbow, valve stem, valve seat, and so on.

Erosion corrosion is mainly caused by high flow velocity. When corrosive liquid contains solid particles (such as insoluble salts, sand grains, and drilling fluid), this type of failing action may be easier to generate. The corrosion products are taken off by the fluid, which directly shocks against them. New metallic face is continuously exposed, and protective film (including corrosion product film and passivating film) is continuously stripped from the metal surface, thus aggravating corrosion. In addition, high-velocity fluid may also rapidly transmit a cathode reactant (such as dissolved oxygen), and corrosion may be speeded up.

## 3. Solid particle shock

Solid particle erosion corrosion may be generated by oil and gas well sand production. The high-velocity fine solid particles impact the metal wall, and metal material is stripped by micro-deformation and micro-cracking.

## Corrosion Mechanisms and Types of Corrosion of Main Corrosive Components

### Hydrogen Sulfide Corrosion Mechanism and Types of Corrosion.

The natural gas of a sulfur-containing gas well and the crude oil and associated gas of a sulfur-containing oil well may contain elemental sulfur, hydrogen sulfide, sulfur alcohol, sulfur ether, disulfide, thiophenic compounds, and more complicated sulfide. The sulfate and sulfate-reducing bacteria in formation may decompose and generate hydrogen sulfide. Sulfonate-containing working fluid for oil and gas wells may decompose at high temperature and generate hydrogen sulfide.

#### 1. Physical properties of hydrogen sulfide

Hydrogen sulfide is a colorless flammable gas with the smell of rotten eggs. It has a relative density of 1.19 and tends to gather in hollow places because its relative density is greater than that of air. Hydrogen sulfide easily dissolves in water and generates hydrosulfuric acid; thus, the solution shows weak acidity. Hydrogen sulfide may burn and explode after blending with air. It is a strong nerve gas and may strongly irritate mucous membranes.

#### 2. Main corrosion types and failure characteristics in hydrogen sulfide environment

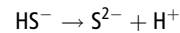
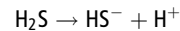
Hydrogen sulfide, when it exists simultaneously with free water, is known as wet hydrogen sulfide, except that it may generate corrosion. When the corrosion of oil and gas wells that contain hydrogen sulfide is appraised in design, it should be considered that the content and partial pressure of hydrogen sulfide are dynamically changeable. In general, with the reduction of reservoir

pressure in the production period, the volume percent concentration of hydrogen sulfide may increase. The main corrosion types and failure characteristics in hydrogen sulfide environment are listed in Table 11-1.

### 3. Electrochemical corrosion

Hydrogen sulfide easily dissolves in water. The solubility is related to partial pressure and temperature (Figure 11-8). The produced water of a sulfide-containing gas well has high acidity, which may cause serious corrosion.

The dissolved hydrogen sulfide may be rapidly ionized. The dissociation reaction is as follows.



Hydrogen ion is a strong depolarizer. After capturing electrons from a steel surface, it is reduced to a hydrogen atom. This process is known as cathodic reaction. The iron that loses an electron reacts with sulfide ion to

**TABLE 11-1 Main Corrosion Types and Failure Characteristics in Hydrogen Sulfide Environments**

Type	Failure Characteristics
Sulfide stress cracking (SSC)	<ol style="list-style-type: none"> <li>(1) Material bears tensile stress of external load or there is residual stress of manufacture. Partial pressure of hydrogen sulfide in environment is higher than 0.0003 MPa.</li> <li>(2) Failure form is brittle fracture of material.</li> <li>(3) Fracturing under low stress. No sign. Short period. High crack propagation velocity.</li> <li>(4) Main crack is perpendicular to force direction in a long crystalline and transcrystalline form. There are branches.</li> <li>(5) Cracking is generated in the location of stress concentration or the location of martensitic structure.</li> <li>(6) High material hardness in general failure position.</li> <li>(7) For low-carbon low-alloy steel, failure is generated at a temperature lower than 80°C.</li> </ol>
Hydrogen-induced cracking (HIC) and stress-oriented hydrogen-induced cracking (SOHIC)	<ol style="list-style-type: none"> <li>(1) Partial pressure of hydrogen sulfide in environment is higher than 0.002 MPa.</li> <li>(2) Hydrogen-induced cracking (HIC) with no external stress or SOHIC under tensile stress.</li> <li>(3) Cracks are generated in belted pearlite within metal. They are step-shaped and parallel to metal rolling direction. Failure is caused after cracks are interconnected.</li> <li>(4) Low crack propagation rate. SOHIC propagation may be promoted under the action of external force.</li> <li>(5) Failure is often generated in low-strength steel and steel with high contents of S, P, and impurities.</li> <li>(6) Surface is often accompanied by hydrogen blisters.</li> <li>(7) Failure is generated at normal temperature.</li> </ol>
Electrochemical corrosion	<ol style="list-style-type: none"> <li>(1) There are black corrosion films (FeS, FeS<sub>2</sub>, and Fe<sub>9</sub>S<sub>8</sub>, etc.) at surface.</li> <li>(2) Metal surface is evenly thinned. There is local pit corrosion (even ulcer-shaped).</li> <li>(3) Corrosion rate is affected by hydrogen sulfide concentration, pH value of solution, temperature, form of corrosion film, and structure, etc.</li> <li>(4) Corrosion may be speeded up by carbon dioxide and chlorion in a corrosive system.</li> <li>(5) Liquid loading in pipe and low gas flow velocity may speed up corrosion. Corrosion may also be speeded up in pipeline sag, elbow section, and gas-liquid erosion section.</li> </ol>

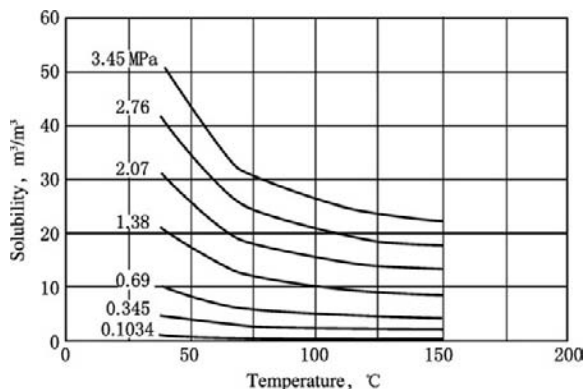
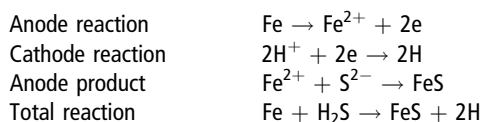


FIGURE 11-8 The solubility of hydrogen sulfide in water.

generate iron sulfide. This process is known as anodic reaction. The iron as anode makes the dissolution reaction speed up. Thus corrosion is caused. The electrochemical equations mentioned earlier are as follows.



The serious results caused by the aforementioned reactions include:

- A hydrogen atom is formed, which causes the hydrogen embrittlement of steel. The existence of  $\text{H}_2\text{S}$  and/or  $\text{HS}^-$  may prevent the hydrogen atom from forming a hydrogen molecule. Excessive hydrogen atoms form hydrogen pressure to permeate and concentrate toward metal defects.
- The higher the partial pressure of hydrogen sulfide, the higher the concentration and the lower the pH value of the solution; thus, the corrosion of the metal may be aggravated.

The anodic products  $\text{FeS}$  and  $\text{FeS}_2$  are tight protective film and will prevent corrosion from continuing. However, due to the differences between corrosion environments, the anodic products also include  $\text{Fe}_3\text{S}_4$  and  $\text{Fe}_9\text{S}_8$ , and so on, which have structural defects and low adhesion to metal and are even as cathode end to form an electric

potential difference with steel surface and generate galvanic corrosion. In an environment where carbon dioxide, chlorion, and oxygen coexist, iron sulfide film may fail, thus speeding up electrochemical corrosion.

- Environment-assisted fracture of steel in hydrogen sulfide

The following environment-assisted fracture phenomena caused by hydrogen sulfide are all related to hydrogen permeation, which makes material brittle (thus they are also known as hydrogen embrittlement):

- Hydrogen-induced cracking (HIC). When atomic hydrogens diffuse into steel and form hydrogen molecules at defects, plane cracks are generated in carbon steel and low-alloy steel by the increase of pressures at the accumulation points of hydrogen, and no external stress is required. These points often have high impurity content in steel and are known as defects. In steel, the areas that have the planar slag inclusion with a higher density or abnormal microscopic texture (such as banded texture) are formed due to the segregation of impurities. The hydrogen atoms that are accumulated in pitfalls are combined into hydrogen molecules. The pressure of hydrogen gas accumulated may be very high (possibly up to 300 MPa). Thus the hydrogen embrittlement of metal, plastic deformation in local areas, and local cracking may be generated.
- Sulfide stress cracking (SSC). This type of cracking of metal is related to corrosion and tensile stress (residual stress and/or working stress) under the condition of existence of water and hydrogen sulfide. It is a form of hydrogen stress cracking (HSC) and is related to the metal brittleness caused by atomic hydrogens, which are generated by acidic corrosion on metal surfaces. When sulfide exists, the absorption of hydrogen may be speeded up. Atomic hydrogen may diffuse into metal, reduce the toughness of metal, and increase sensitivity to cracking. SSC is easy

to generate in high-strength metal material and weld areas with higher hardness.

- c. Hydrogen stress cracking (HSC). This type of cracking of metal is presented under the condition of the existence of hydrogen and tensile stress (residual stress and/or working stress). It is a cracking of the metal that is insensitive to SSC. This type of metal as cathode and the other metal, which is easily corroded, as anode form a galvanic couple. The metal may be brittle under the condition of existence of hydrogen. This type of cracking is also known as galvanic couple-induced hydrogen stress cracking (GHSC). When stainless steel or alloy steel is connected with carbon steel or low-alloy steel, the texture defects in stainless steel or alloy steel may accumulate hydrogen, and the stainless steel or alloy may be brittle under the excitation of galvanic couple.
- d. Stress-oriented hydrogen-induced cracking (SOHIC). It means small staggered cracks that are roughly perpendicular to the direction of the principal stress (residual stress and/or working stress). Existing hydrogen-induced cracks are connected to each other by this type of crack cluster. It is the SSC caused by external stress and local strain around hydrogen-induced cracking. SOHIC may be observed in the heat-affected zones of the base metal of longitudinally welded steel pipe and the weld bead of pressure vessel. It is not a common phenomenon and is generally related to steel for low-strength ferritic steel pipe and pressure vessels.

SOHIC is easy to generate in high-stress positions (such as the positions of high residual stress and stress concentration) of material. Hydrogen may be accumulated in the high-stress areas by stress-induced diffusion under stress gradient. There is a stress concentration phenomenon at defects or crack tips; thus, hydrogen will be accumulated at the front end of the crack by stress-induced diffusion.

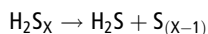
There is a difference between the mechanisms of forming anode dissolution-type cracks and hydrogen-induced cracking type cracks. In practical application, they may transform each other with a change of steel environment or may form and exist simultaneously under appropriate conditions.

- e. Soft zone cracking (SZC). It is a form of SSC. When steel contains local soft zone with a lower yield strength, SZC may be generated. Under the action of operational load, the soft zone may yield and local plastic strain may propagate. This process may aggravate the sensitivity of non-SSC material to SSC. This type of soft zone is closely related to the weld of carbon steel.
- f. Stress corrosion cracking (SSC). This type of metal cracking is related to the anode process of local corrosion and tensile stress (residual stress and/or working stress) under the condition of the existence of water and hydrogen sulfide. Chloride and/or oxidant and high temperature may increase the sensitivity of metal to generating stress corrosion cracking.
- g. Hydrogen-induced blister (HIB). When the pH value shows acidic media, the FeS protective film is dissolved and the material surface is in an active dissolution state due to the existence of a great quantity of anion, thus favoring the permeation of hydrogen atoms generated during reaction toward the inside of the pipe material. After permeating into the inside of metallic pipe material, these hydrogen atoms are accumulated in weak positions (such as caves and nonmetallic impurities) and combined into hydrogen molecules. As accumulation proceeds, the hydrogen pressure is up to about 100 MPa in some positions. In addition, hydrogen atoms may react with the Fe<sub>3</sub>C in material and form CH<sub>4</sub>, which may also be accumulated. The pressure caused by gas may form high internal stress, so that plastic deformation of material may be generated on the

weaker side of the material, and a steel sandwich may bulge to generate blistering, which is cracking caused by stress corrosion gas liberation, and can be generated under the condition of no external load.

**Elemental Sulfur Corrosion.** A high- $\text{H}_2\text{S}$  natural gas reservoir is often accompanied with elemental sulfur, which may be liberated and may cause blocking in the vicinity of the wellbore; thus, formation damage may be caused and the production rate may be reduced. Liberation and blocking in tubing or surface manifold may be a great problem in gas well production. In addition, elemental sulfur precipitation may cause corrosion of the pipeline system. Elemental sulfur is molecular crystal. It is loose, brittle, and water-insoluble and has low electric conductivity. It has several types of isomer. Natural sulfur is a yellow solid and is known as orthorhombic sulfur. The orthorhombic sulfur molecule and monoclinic sulfur molecule consist of eight sulfur atoms and have cyclic structure.

At a temperature higher than  $88^\circ\text{C}$ , hydrogen sulfide reacts with elemental sulfur and generates hydrogen polysulfide. With the reduction of temperature and pressure, polysulfur is decomposed to form elemental sulfur. The reaction equation is as follows.



This is a dynamic chemical equilibrium reaction. High pressure makes reaction leftward while low pressure makes reaction rightward. At the upper part of the well, the cross-section of the flow passage is changed. Particularly in the rear of a throttling valve, the reduction of pressure and the change of flow field make reaction rightward, which means sulfur liberation and precipitation.

For carbon steel and low-alloy steel, when there is elemental sulfur, the reaction is as follows.

Anode reaction	$\text{Fe} \rightarrow \text{Fe}^{2+} + 2\text{e}$
Cathode reaction with no elemental sulfur	$2\text{H}^+ + 2\text{e} \rightarrow 2\text{H} \rightarrow (\rightarrow \text{H}_2)$
Additional cathode reaction which forms sulfur ion	$\text{S} + 2\text{e} \rightarrow \text{S}^{2-}$
Sulfur reacts with hydrogen to form $\text{HS}^-$	$\text{S}^{2-} + \text{H}^+ \rightarrow \text{HS}^-$

Hydrogen is consumed by reduction reaction; thus, hydrogen pressure will not be increased and subsequent sulfide stress cracking and hydrogen-induced cracking will be avoided. However, elemental sulfur may deposit on metal surfaces, and elemental sulfur may speed up the anode reaction process at contact. The corrosion may be mainly speeded up by the reduction of the stability of the protective sulfide passivating film on metal surfaces. If a gas well produces dry gas and also produces formation water in which the chloride content is higher than  $5000 \mu\text{g/g}$ , the existence of chlorion will greatly enhance the corrosiveness of elemental sulfur, and the pitting corrosion boring by elemental sulfur may be serious (boring rate is up to  $30 \text{ mm/a}$ ). On the other hand, for a gas well that contains gas condensate, the gas condensate makes elemental sulfur be in a dissolved state, which prevents elemental sulfur from liberating, thus mitigating the corrosion that is related to elemental sulfur.

Elemental sulfur may make some types of corrosion-resistant alloy generate environment-assisted fracture; thus, whether a specific alloy steel is elemental sulfur-resistant has been especially noted in ISO15156-3. In general, the common and high-alloy austenitic stainless steel cannot resist elemental sulfur at  $25^\circ\text{C}$ ,  $60^\circ\text{C}$ , and  $66^\circ\text{C}$ . The elemental sulfur precipitation study indicates that the flow velocity in tubing or flow passage may be the main control factor. The elemental sulfur precipitation in the flow passage is mainly caused by low production rate and low flow velocity in the flow passage. In addition, the change of flow passage diameter and the change of flow field and phase state through the throttling valve may aggravate the liberation and precipitation of sulfur, which may cause pipe blocking.

**Carbon Dioxide Corrosion.** In the oil and gas industry, carbon dioxide corrosion is known as sweet corrosion, while hydrogen sulfide corrosion is known as sour corrosion. When carbon dioxide is dissolved into water, carbonic acid is formed. Electrochemical corrosion may be generated when metal is in water. Dry carbon

dioxide itself may not corrode metal under the condition of no electrolyte (water). However, with the development of oil and gas fields, the water cut is gradually increased. The carbon dioxide, after being dissolved into water and changed into carbonic acid, may have a stronger corrosiveness.

Carbon dioxide is dissolved into the water phase, thus generating carbonic acid, which may chemically react with the pipe wall. Thus carbon dioxide corrosion is generated. The carbon dioxide content in the water phase is closely related to the partial pressure of carbon dioxide under the condition of gas-liquid equilibrium. If there is no free gas, the carbon dioxide content in water will depend on the gas phase carbon dioxide pressure. Therefore, the carbon dioxide corrosion rate should be predicted as follows on the basis of the partial pressure of the carbon dioxide in gas phase:

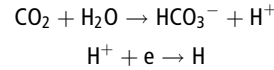
1. Serious corrosion of  $P_{\text{CO}_2} > 0.2$  MPa
2. Corrosion if  $P_{\text{CO}_2} = 0.02\text{--}0.2$  MPa
3. No corrosion if  $P_{\text{CO}_2} < 0.02$  MPa

When  $P_{\text{CO}_2} = 0.05\text{--}0.1$  MPa and formation water exists, the ratio of the molal concentration multiplied by the number of electrovalence for  $\text{Ca}^{2+}$  to that for  $\text{HCO}_3^-$  can be used for determining the corrosion rate as follows.

1. Low corrosion rate if  $\text{Ca}^{2+}/\text{HCO}_3^- < 0.5$
2. Medium corrosion rate if  $\text{Ca}^{2+}/\text{HCO}_3^- > 1000$
3. High corrosion rate if  $0.5 < \text{Ca}^{2+}/\text{HCO}_3^- < 1000$

The carbon dioxide corrosion of pipe includes uniform corrosion and pitting corrosion. The corrosion products are  $\text{FeCO}_3$  and  $\text{Fe}_3\text{O}_4$ .

**Uniform corrosion:** Under certain conditions of temperature and pressure, the water in pipe fluid or the water in natural gas may condense and is adsorbed on the pipe wall to form water film. Carbon dioxide is dissolved into water and a water film with a low pH value is formed, thus generating hydrogen depolarization corrosion. The reaction is as follows.



**Pitting corrosion:** Carbon dioxide may not only cause the uniform corrosion of steel, but it may also cause the local corrosion of steel. Local pitting corrosion, mosslike corrosion, and mesa-like pitting corrosion are typically characteristic of carbon dioxide corrosion, and the mesa-like pitting corrosion is most serious. This corrosion has a high penetrance and may cause serious economic loss. It will lead to stopping production of oil and gas wells or even the abandonment of the wells if maintenance and replacing string, and so on, are not done in time during oil and gas well production. The carbon dioxide corrosion pits may often be hemispherical deep pits with a steep edge (Figure 11-9). The reason the local filmless mesa-like pitting corrosion is generated is that the protective film that is formed on the metal surface by corrosion products ( $\text{FeCO}_3$ ,  $\text{Fe}_3\text{O}_4$ , and so on) during corrosion reaction is often either non-uniformly formed, or failed.

With the increase of pressure, the corrosiveness of corrosive media is enhanced, the partial pressure of carbon dioxide is increased, the solubility is increased, and pipe section that may be slightly corroded originally will be seriously corroded.

In a gas processing device, stress rupture of high-strength steel and stainless steel may be generated in the wet environment of  $\text{CO}_2 + \text{CO} + \text{H}_2\text{O}$  or  $\text{CO}_2 + \text{HCO}_3^- + \text{H}_2\text{O}$ . Under the induction of CO, the hydrogen (corrosion product) absorbing ability of steel is obviously enhanced. Essentially, it is also hydrogen embrittlement cracking. In gas wells that contain carbon dioxide, this type of

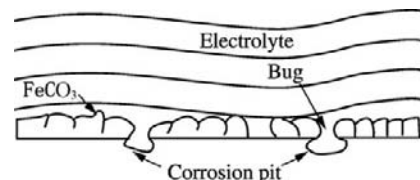


FIGURE 11-9 Mesa-like pitting corrosion.

cracking of logging wire and high-strength low-alloy steel fittings that bear high stress or have residual stress (such as the stress concentration caused by weld bed and structure) may be generated.

Temperature may greatly affect the deformation of corrosion product film; thus, it may greatly affect the carbon dioxide corrosion rate. The following three temperature regions are included in carbon dioxide corrosion process:

1. Region of low temperature lower than 60°C. In this region, the metal surface may form a small quantity of non-protective loose  $\text{FeCO}_3$ , and a maximum corrosion rate of steel is presented (about 40°C for the Mn-containing steel and about 60°C for Cr-containing steel). In this region, uniform corrosion is mainly generated, and the corrosion rate is increased with the increase of temperature.
2. Region of medium temperature of about 100°C. In this region, the distribution of  $\text{FeCO}_3$  film is uneven and loose crystal is formed; thus, serious local corrosion is presented. The corrosion rate reaches a maximum.
3. Region of high temperature higher than 150°C. In this region, the corrosion is inhibited and the corrosion rate is reduced because of the formation of high-adhesion tight  $\text{FeCO}_3$  and  $\text{Fe}_3\text{O}_4$  film.

This complicated situation occurs because the solubility of  $\text{FeCO}_3$  is reduced with the increase of temperature, a corrosion product film is formed on the metal surface, this corrosion product film is from loose to tight, in a certain range of temperature there is a transitional region of corrosion rate and a maximum of corrosion rate is presented, and then the formation and reinforcement of corrosion product film reduce the corrosion rate.

It should be noted that different types of steel and different environment media parameters may have different corrosion temperature rules. It is required to make a concrete analysis of concrete conditions. Corrosion rates under different partial pressures of carbon dioxide are shown in Figure 11-10.

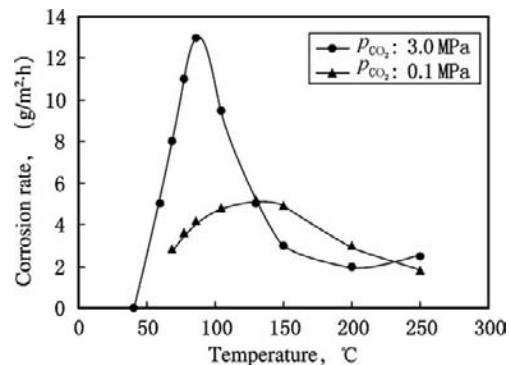


FIGURE 11-10 The relationship between temperature, partial pressure of carbon dioxide, and corrosion rate.

### Brine Corrosion

1. Universality of high-salinity formation water corrosion

The products of most gas and oil wells contain formation water to a certain degree. The universality of this corrosion is greatly higher than that of the previously mentioned hydrogen sulfide and carbon dioxide corrosion. The soluble salts including chloride, sulfate, and carbonate may be dissolved in formation water to varying degrees. In general, the formation water corrosion of tubing, casing, and equipment includes:

- a. Electrochemical corrosion;
  - b. Stress corrosion and stress corrosion cracking of some steels;
  - c. Aggravating corrosion and stress corrosion cracking under the coordinated action of brine, hydrogen sulfide, and/or carbon dioxide;
  - d. Corrosion that is similar to formation water corrosion, including: seawater corrosion, injected water corrosion, high-concentration completion fluid corrosion, injected steam corrosion, and geothermal well production corrosion.
2. Corrosiveness and interaction of dissolution salts

Chlorion may make the protective layer of a steel surface unstable and make the corrosion products on the pipe wall loose. The various types of concentration cell corrosion

(such as salt concentration cell corrosion, hydrogen concentration cell corrosion, oxygen concentration cell corrosion, and crevice corrosion) are formed below the loose scale. A large amount of bacterial activity and the increase of bacterial slime make scaling more serious and will generate a vicious circle. Corrosive products including  $\text{FeS}$ ,  $\text{FeCO}_3$ ,  $\text{Fe}(\text{OH})_2$ , and scale have an electric potential higher than that of iron and become cathode, while iron becomes anode. Thus the corrosion is continued.

Chlorion concentration may affect the corrosion rate of metal to a certain extent. Adding chlorions at normal temperature may reduce the solubility of carbon dioxide in solution and reduce the corrosion rate of carbon steel. Figure 11-11 shows that in high-salinity media, the corrosion of N80 and P110 steel is more serious when chlorion content is about 4%; when chlorion content is 0% to 4%, with the increase of chlorion content, the corrosion rate of steel is increased; and when chlorion content is higher than 4%, with the increase of chlorion content, the corrosion rate of steel is reduced.

In media that contain hydrogen sulfide, chlorions may make the corrosion of metal speed up because chlorions may increase the electric conductivity of the solution, increase the activity of the  $\text{H}^+$  in solution, increase electric conductivity, and prevent tight  $\text{FeS}_2$  and  $\text{Fe}_{(1-x)}\text{S}$  from forming. When chlorion

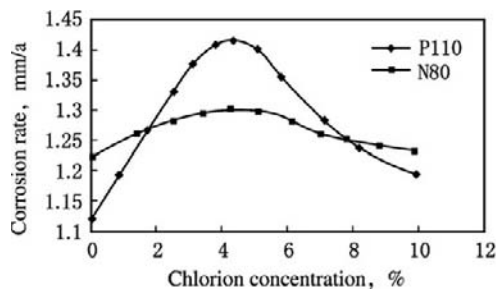


**FIGURE 11-11** The effect of chlorion concentration on corrosion rate.

concentration is high, however, the corrosion of metal is contrarily mitigated due to the high adsorptive capacity of chlorions, which are adsorbed on the metal surface in large quantities and entirely replace the  $\text{H}_2\text{S}$  and  $\text{HS}^-$  adsorbed on metal surfaces.

### 3. Chloride stress cracking

The selective combination of chlorions and some stainless steels or corrosion-resistant alloy steels may generate chloride stress cracking under appropriate conditions of temperature, chlorion concentration, and range of pH value. Pitting corrosion is the main corrosion phenomenon of stainless steel. Under the coordinated action of oxygen and chlorion, crack may be generated at the bottom of the pit; thus, fracturing will be caused. If it is considered that there are chlorions in formation objectively, controlling oxygen entrainment is an important measure that should be taken to prevent or mitigate stress cracking.

Chloride stress corrosion is shown in Figure 11-12. Under the action of working stress and  $\text{Cl}^-$ , local plastic deformation may be generated and a sliding stage is formed. When stress is sufficient to break the surface film, a new base body surface is exposed and crack may be generated on the inside surface of the metal. The electric potential difference between the new surface and the passivation surface may form galvanic corrosion. The new surface as small anode is

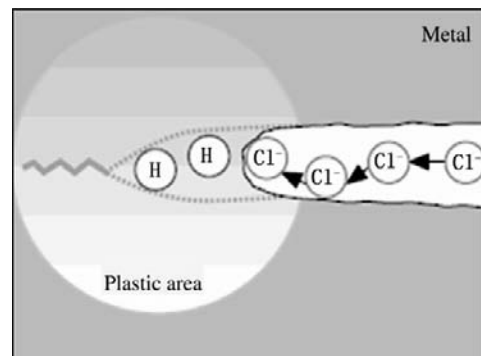


**FIGURE 11-12** Chloride stress corrosion mechanism.

expeditiously corroded and protects the passivation surface. The corrosion groove formed by dissolution extends in a direction perpendicular to tensile stress, thus forming incipient cracks. The unevenness of electrochemical corrosion of a metal surface and surface defects (such as scores, small apertures, and crevices) are the source of crack. The stress concentration area of the crack tip may speed up electrochemical dissolution (corrosion), make stress corrosion crack extend, and cause cracking. Chloride stress corrosion cracking is transcrystalline cracking and may not be affected by the change of the metallographic texture of alloy steel. Cracks are often branched and incipient and extend irregularly in circumference.

The test evaluation indicates that the acidic water solution of any chloride may become the stress corrosion medium of stainless steel. The chlorides that have high sensitivity to stress corrosion include  $MgCl_2$  and the chlorides of Fe, Ca, Na, and Li. The stress corrosion cracking of 22Cr tubing has been found when the 22Cr tubing-casing annulus was filled with CaCl water solution. Due to the high temperature, the wellhead annulus pressure was repeatedly released and air entered the annulus. The coordinated action of oxygen and chlorine causes stress cracking.

In general, tubing or casing of low carbon alloy steel (such as P110, N80, J55, C95, L80, and K55) that has a yield strength lower than 125 ksi will not generate chloride stress corrosion cracking. However, the sensitivity of high-strength steel (yield strength 135 ksi, 140 ksi, 150 ksi above) to chloride stress corrosion cracking should be considered. High-strength steel should be prudently used under the condition of the products with high chloride content in high-temperature high-pressure deep wells, weighted fluid or protective fluid with chloride in the tubing-casing annulus, or killing fluid, which brine is used in order to prevent sudden chloride, sulfide, and hydrogen-induced stress fracturing.

**Oxygen Corrosion.** In injected water or other injected working fluids, oxygen lurking is unavoidable. In addition, underground water that is connected with surface water may also

have oxygen that lurks in it. In an oxygen-containing solution, the oxygen depolarization reaction will be generated on the electrode surface. The reaction mechanism is very complicated. Intermediate particles or oxide may be generally formed. Different solutions have different reaction mechanisms.

The corrosion during which the cathodic process is an oxygen reduction reaction is known as oxygen absorption corrosion. In comparison with a hydrogen reduction reaction, an oxygen reduction reaction can be conducted under positive potential. The corrosion of most metals in neutral or basic solution and the corrosion of a small quantity of metal with positive potential in oxygen-containing weak acid are oxygen absorption corrosion or oxygen depolarization corrosion.

**Bacteria Corrosion.** The corrosive attack of material that is caused or promoted by the life activity of bacteria is known as bacteria corrosion. Formation water may possibly contain sulfate-reducing bacteria (SRB), iron bacteria, sulfur bacteria, and so on, which lurk in formation water and rock. The most common microbiological corrosion in oil fields is sulfate-reducing bacteria corrosion.

**Interaction of Corrosive Components and the Effect on Corrosion.** The produced fluid may include the following corrosive components: (1) acidic gas ( $H_2S$ ,  $CO_2$ , and  $H^+$ ); (2) dissolved oxygen; (3) salt ( $HCO_3^-$ ,  $SO_4^{2-}$ ,  $Cl^-$ , and  $OH^-$ ); and (4) bacteria (sulfate-reducing bacteria, aerophile bacteria, and so on).

The interaction of some components may aggravate or mitigate corrosion.

1. Effect of coexisting hydrogen sulfide and carbon dioxide on corrosion

Sulfide-containing well production practice indicates that when sulfide-resistant carbon steel or low-alloy steel is selected, electrochemical corrosion (metal thinning and pitting corrosion, and so on) will be predominant in comparison with corrosion due to coexisting  $H_2S$  and  $CO_2$ . Electrochemical corrosion is not fully dependent on the contents and partial pressures of  $H_2S$  and  $CO_2$

due to the interaction of corrosive components and is related to the specific dynamic corrosion environment of each gas reservoir. There may be differences between laboratory evaluation and the on-site situation and greater differences between software prediction and the on-site situation. Software prediction may overestimate corrosion severity.

The effect of hydrogen sulfide on carbon dioxide corrosion includes two aspects. Hydrogen sulfide may speed up carbon dioxide corrosion due to cathodic reaction and mitigate corrosion due to FeS precipitation. The change is directly related to temperature and hydrogen sulfide content. In general, at low temperature (30°C), a small quantity of hydrogen sulfide (0.2%) may doubly speed up carbon dioxide corrosion, while high hydrogen sulfide content (such as 21.5%) may reduce the corrosion rate. At high temperature, the corrosion rate is lower than that of pure carbon dioxide when hydrogen sulfide content is higher than 2.1%. When temperature is higher than 150°C, the corrosion rate may not be affected by hydrogen sulfide content. At the same time, low hydrogen sulfide concentration may aggravate corrosion

because hydrogen sulfide may directly attend the cathodic reaction, while high hydrogen sulfide concentration may mitigate corrosion because hydrogen sulfide may react with iron to form FeS film. In addition, hydrogen sulfide may greatly reduce the corrosion resistance of the corrosion-resistant steel, which contains Cr, to cause serious local corrosion and even stress corrosion cracking.

## 2. Effect of coexisting oxygen and carbon dioxide on corrosion

The coexistence of oxygen and carbon dioxide may aggravate corrosion. Oxygen may take a catalytic effect during carbon dioxide corrosion. The higher the oxygen content, the higher the corrosion rate when protective film has not been generated on the steel surface. When protective film has been generated on the steel surface, oxygen content may have a low or almost no effect on corrosion. However, in a solution that is saturated with oxygen, the existence of carbon dioxide may greatly increase the corrosion rate. At this time carbon dioxide takes a catalytic effect in corrosive solution.

Figure 11-13 shows that under the same dissolution gas content, the corrosiveness of

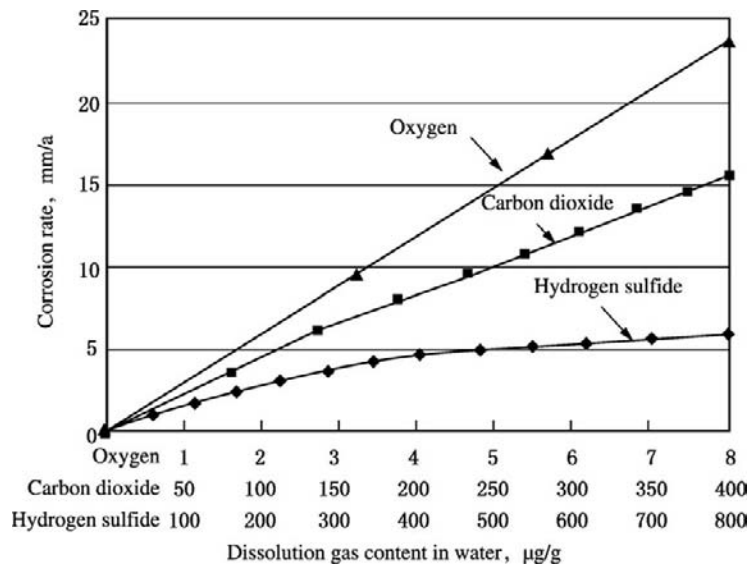


**FIGURE 11-13** Corrosion rate curves for water solutions of different gases (after Schlumberger).

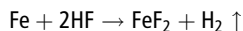
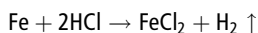
oxygen is 80 times that of carbon dioxide and 400 times that of hydrogen sulfide. With the increase of gas content in the water phase, the corrosion rate is rapidly increased. For a water injection well, if injected water has not been appropriately treated and oxygen content is high, the corrosion rate of the pipe wall is high.

For a high-temperature high-pressure gas well, the effect of oxygen entering on corrosion should be considered when wellhead valves are opened or closed and downhole operations are conducted. Air entering into the wellbore should be prevented, especially when stainless steels of Super 13Cr and 22Cr, and so on, are adopted.

3. Effect of coexisting hydrogen sulfide, carbon dioxide, and chloride on corrosion

For different types of steel, the effects of chlorion are different, and serious local corrosion (pitting corrosion and crevice corrosion, and so on) of steel may be generated. In accordance with the film formation theory, due to small diameter and strong penetrating power, chlorion most easily penetrates the very small pore, reaching the metal surface and interacting with metal to form a soluble compound and change the structure of oxide film and generate corrosion of metal. In addition, chloride may also generate stress corrosion cracking of corrosion-resistant steel.

**Acid Corrosion.** Oil well acidizing generally adopts 13% to 16% hydrochloric acid. The acid corrosion mechanism is as follows.



Under conditions of high temperature and high pressure, iron may vigorously react with acid to cause corrosion failure.

During an acidizing operation, the acid squeezed into the reservoir may not be fully discharged due to incomplete flowing back, bottomhole liquid loading may be formed, the pH value in the lower part of the well may be reduced, and hydrogen ion concentration may be increased, so that the corrosion rate of tubing

may be increased. If hydrogen sulfide exists simultaneously, the pH value of the water solution may be reduced to 3.5–4.5. In a high-acidity environment, sulfide stress corrosion cracking will be a grave problem. In addition, a higher temperature in the lower part of the well may aggravate hydrogen depolarization corrosion.

## 11.3 MATERIAL SELECTION FOR CORROSIVE ENVIRONMENT OF OIL AND GAS WELLS

### Overview

#### Common Types of Material for Corrosive Environments of Oil and Gas Wells

1. Carbon steel and low-alloy steel

Carbon steel is an iron-carbon alloy in which carbon content is lower than 2% and manganese content is lower than 1.65%. It also contains some microelements. A certain quantity of deoxidant (silicon or/and aluminum) may be especially added in order to remove oxygen. The carbon content of the carbon steel used in the petroleum industry is generally lower than 0.8%.

Low-alloy steel is also an iron-carbon alloy in which the total of alloy element is lower than about 5% but is higher than the content prescribed for carbon steel.

In recent years, a new steel grade known as microalloy steel or 3Cr steel has been presented in the carbon steel and low-alloy steel series. After the chromium content in carbon steel is increased to 3% and the alloy is appropriately designed, a stable chromium-rich oxide film may be formed and carbon dioxide corrosion resistance can be obviously increased. In addition, hydrogen sulfide and chloride corrosion resistance may also be obviously improved. The 3Cr steel may accord with the Zone SSC 2 (medium-acidity environment) casing, tubing, and fittings material standard in ISO 15156-2 Standard (Figure 11-14).

ISO 11960 (original API 5CT equal to ISO 11960, 2001) has listed the steel grades of

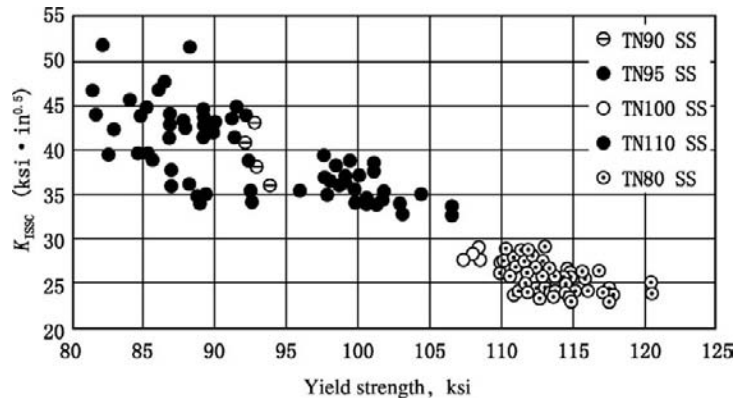


**FIGURE 11-14** The effect of yield strength of common low-alloy steel on the critical stress strength factor  $K_{ISSC}$  of material in a hydrogen sulfide environment (NACE 200511).

common hydrogen sulfide stress cracking resisting carbon steel and low-alloy steel tubings and casings, which include high sulfur-resistance type and finite sulfur-resistance type.

- a. High sulfur-resistance type: Good hydrogen sulfide stress cracking resistance. The steel grades that are predominantly adopted in design include: J55, K55, M65, L80 Type 1, C90 Type 1, and T95 Type 1.
  - b. Finite sulfur-resistance type: Tubing and casing of which the yield strength is equal to or higher than 100 ksi (such as 110 ksi and 125 ksi). Hydrogen sulfide stress cracking resisting tubing and casing of which the yield strength is equal to or higher than 110 ksi are recommended. However, it should be noted that they should meet the operating conditions.
2. Corrosion-resistant alloy material

Corrosion-resistant alloy (CRA) material can resist the general and local corrosion in oil and gas field environments, in which carbon steel and low-alloy steel may be corroded. Stainless steel and alloy steel are known as corrosion-resistant alloy steel in the ISO 15156-3 standard, which gives the detailed technical specifications for corrosion-resistant alloy tubing and casing

and parts made of corrosion-resistant alloy. Corrosion-resistant alloy material includes stainless steel (such as high-alloy austenitic stainless steel, martensitic stainless steel, and diphasic stainless steel) and alloy steel (nickel-based alloy steel, and so on).

### Material Selection under Corrosive Conditions of Oil and Gas Wells

#### 1. Material selection based on standards

Proper selection of the material of tubing, casing, downhole accessories, Christmas tree, and surface equipment is a key problem in corrosion prevention of oil and gas wells. Improper selection of material may not only cause waste, but it may also generate unsafe conditions.

Carbon steel and low-alloy steel are commonly used in sour environments of hydrogen sulfide. Environment-assisted fracture should be predominantly considered when the material is selected in corrosion prevention design that is in light of sour environments of hydrogen sulfide. The ISO 15156-2 standard can be used for selecting the cracking-resistant material in a sour environment.

After sulfide-resistant carbon steel and low-alloy steel are selected, electrochemical corrosion should be emphatically considered. A corrosion inhibitor may be used for

preventing or mitigating electrochemical corrosion. Its feasibility is dependent on technical feasibility, reliability, and risk assessment; medium- and long-term cumulative investments and rate of return; and the cost of replacing tubing during well servicing and the loss assessment.

For a serious corrosive environment (such as high pressure and carbon dioxide; high pressure, carbon dioxide, and hydrogen sulfide), stainless steel, or alloy steel should be adopted in a corrosion-resisting design. Stainless steel or alloy steel is expensive and has a long delivery time. They also have downhole service environment restrictions. Thus test evaluation and technical economical analysis are required.

The strength design should be in accordance with the ISO 10400 standard on the basis of ISO 15156. When carbon steel and low-alloy steel are used under sour environment conditions, corrosion-resistant steel grade with yield strength lower than 95 ksi (655 MPa) should be selected as far as possible. If the strength is insufficient, increasing wall thickness is proper in order to meet the requirement of strength, but not increasing steel grade.

## 2. Fitness design method

Selection of the material suitable for some corrosive environments cannot rely on the ISO 15156 standard. Sometimes the material required is restricted by delivery or technical economical condition. NACE Method A and A solution is a serious sulfide stress cracking evaluation method. Practice indicates that material that is unqualified in accordance with the NACE Method A and A solution has not been cracked during long-term functioning. Therefore, when the source of goods is restricted or technical economical evaluation indicates that higher-grade material is unsuitable, the selection of material on an evaluation based on field environment simulation is admissible. Under normal conditions, corrosive components and temperature are objectively present; however,

optimizing structure design may reduce working stress and make material selection convenient or enhance reliability.

ISO 15156-1 provides a principle of fitness design for determination of material on the basis of on-site empirical data, but the following requirements should be met: (1) the field experience provided should continue for two years at least, and a full inspection after field use is included and (2) environment severity should be lower than that of the field experience provided.

In sulfur-containing high-pressure deep wells, the standard sulfide-resistant tubing and casing with yield strength of 125 ksi are used, and the fitness design method (fit for service, fit for purpose) is adopted. Tubing and casing with yield strength of 125 ksi cannot meet the requirements of a serious sulfide stress cracking evaluation test in accordance with NACE Method of A and A solution. However, the steel material can be adopted, provided that the hydrogen sulfide content of sulfide-containing oil and gas wells and the downhole pH value are lower than the sulfide stress cracking tolerances of this steel material.

**Correlativity of Material Selection with Corrosive Environments of Oil and Gas Wells.** The correlativity of material selection with corrosive environments of oil and gas wells in consideration of both environment-assisted fracture and electrochemical corrosion is as follows.

### 1. Slightly corrosive environment

A slightly corrosive environment includes oil and gas wells of which the products contain formation water, condensate water, micro-hydrogen sulfide and carbon dioxide, and also water injection wells, and so on. Any casing that accords with ISO 11960 can be used. J55, N80, P110, Q125, and so on are commonly used. 3Cr steel may have obvious technical economical effectiveness. In comparison with commonly used N80 steel, the cost may be increased by 120% to

150%, but service life may be increased by 300% to 500%.

2. Sour environment of hydrogen sulfide

In a sour environment of hydrogen sulfide, sulfide stress cracking should be emphatically controlled. The sulfide stress cracking-resisting steel grades corresponding to different temperatures are shown in Table 11-4.

3. Wet carbon dioxide environment

A downhole wet carbon dioxide environment is composed of carbon dioxide and formation water. Electrochemical corrosion is predominant. Martensitic stainless steels with higher chrome content (13Cr, Super 13Cr, or 22Cr) are commonly used.

4. Wet carbon dioxide and micro-hydrogen sulfide environment

22Cr stainless steel can be used in a wet carbon dioxide environment with micro-hydrogen sulfide. When the hydrogen sulfide and chloride content is higher, 25Cr stainless steel can be used.

5. Severe corrosion environment with high hydrogen sulfide and carbon dioxide content

Sulfide stress cracking resisting carbon steel and low-alloy steel may generate serious weight-loss corrosion and pitting corrosion under the condition of unfavorable corrosive media type combination of oil or gas wells and the interaction of content, pressure, and temperature. Thus corrosion-resistant alloy steel should be predominantly adopted. In general, nickel-based alloy material can only be selected under this severe corrosion environment condition.

## Methods and Criteria for Evaluating Material Fracture in Corrosive Environment of Oil and Gas Wells

**Criteria.** The tensile stress value under which the cracking of material may not be generated in the acidic water solution environment of hydrogen sulfide must be evaluated. This stress value is known as critical breaking stress. The NACE TM0177-2005 standard has provided the critical breaking stress test methods and criteria. For

carbon steel and low-alloy steel, atmospheric-temperature atmospheric-pressure breaking resistance testing is only required due to the high sensitivity to sulfide stress cracking at atmospheric temperature. For stainless steel and corrosion-resistant alloy steel, the condition is more complicated. The NACE TM0177-2005 standard has specified the reagents, test samples, equipment, test procedure, and so on, used for testing. This standard includes the following test methods: (1) Method A (tension test, which is a commonly used basic method for evaluating the sulfide stress cracking resistance of material); (2) Method B (beam bending test, which is less often applied); (3) Method C (C-shaped ring test, used mainly for evaluating longitudinally welded pipe); and (4) Method D (dual cantilever beam test, which is used for quantitative calculation in fitting the design method).

In addition to the aforementioned methods, there also is a test method, which is known as the slow strain rate (SSR) method. The coupon is in a very slow tension state (strain rate is reduced to  $10^{-4}$  to  $10^{-7}$  S<sup>-1</sup>). Breaking will be generated within several hours or several days.

**NACE Method A (Tension Test).** The NACE Method A is also known as a constant-load test. A coupon is loaded to a specific stress level and is then immersed in specific corrosive media. The test temperature is controlled at 24°C (75°F) and breaking time is recorded. Experience indicates that the material has breaking resistance under exerted stress if there is no break after 720 hours. In fact, sulfur-nonresistant steel material may be broken within several hours under stress that is 80% of yield strength. For instance, S135 steel is broken within 1 hour and P110 steel is broken within 3 hours.

The solution used for NACE Method A test is known as A solution, which consists of 5% sodium chloride and 0.5% cryogenic acetic acid (mass fraction) and is formulated with distilled water or deionized water and is filled with hydrogen sulfide to the state of saturation. Thus the solution obtained has a pH value of 2.6–2.8 before contacting the coupon.

For tubing and casing, the stress exerted by using the NACE Method A and A solution in

accordance with yield strength for continuous 720 hours is just the critical stress. The ratio of tensile stress to coupon yield strength (%) is often used due to the inconvenient use of the absolute value of stress. For instance, it is specified that the critical stress for sulfide stress cracking of J55 and K55 casing body and collar should be higher than or equal to 80% of yield strength. For L80, C90, and T95, the critical stress value should be 90% of yield strength.

**NACE Method B (Beam Bending Test).** Bore a hole in the coupon, which is then placed in the A solution. Stress concentration may be generated at the hole. This method can be used for determining the sensitivity of stress concentration to sulfide stress cracking. It cannot be used for obtaining the critical stress of cracking and is rarely used for material selection and evaluation.

**NACE Method C (C-Shaped Ring Test).** The ring coupon with a notch is pressed using a bolt to generate circumferential tensile stress. The coupon is placed in the A solution and the sensitivity of material to sulfide stress cracking is measured. The welding seam of longitudinally welded pipe is sensitive to sulfide stress cracking, and this method is suitable for evaluation. The disadvantage of the method is that the breaking time cannot be accurately known. This method is unsuitable for pipes that are too big or too small.

**NACE Method D (Dual Cantilever Beam Test).** In general, structural members may fail if the applied stress reaches the yield strength of material. When a crack exists in a structural member, the criteria of strength may be converted into the relationship between the crack propagation resistance of the material and some mechanical parameter of the crack tip. The motivating force of crack propagation is reflected by using a stress intensity factor, as shown in Equation (11-6).

(11-6)

$$K_I = \sigma Y \sqrt{a}$$

where:  $Y$  = parameter related to the shape of the crack, the mode of loading, and the geometry of coupon;  $\sigma$  = stress, MPa;  $a$  = crack size, m;  $K_I$  = stress intensity factor,  $\text{MPa} \cdot \text{m}^{0.5}$ .

When  $K_I$  is lower than the critical value  $K_{IC}$ , the crack may not be propagated and destabilized. See Equation (11-7).

(11-7)

$$K_{IC} = Y \sigma_c \sqrt{a_c}$$

where:  $\sigma_c$  = breaking stress in critical state, MPa;  $a_c$  = crack size in critical state, m;  $K_{IC}$  = critical stress intensity factor of crack propagation and destabilization, that is, fracture toughness (a self mechanical property of material).

In corrosive media, a motivating force still exists that makes the crack propagate at the crack tip even if the applied stress is much lower than  $K_{IC}$ . After a certain time, the crack may be destabilized and breaking is generated. If the applied stress is reduced to some value and the material works in corrosive media for a sufficient time, the crack may not be destabilized despite the fact that crack propagation is generated to a certain extent. The stress intensity factor in this state is known as the critical stress intensity factor  $K_{IEC}$  under some corrosive media environment conditions, the critical fracture toughness under some corrosive media environment conditions. For a hydrogen sulfide environment, it is shown as  $K_{ISSC}$ .

In sour gas wells, tubing and casing have a tendency to burst due to environmental corrosion under the action of internal pressure; that is, the lateral critical stress intensity factor of tubular goods decides sulfide stress cracking. The general critical stress intensity factor measurement method based on fracture mechanics is unsuitable due to the thin wall of tubing and casing.

The NACE Method D is used for measuring the crack propagation resistance of material of structural members with a crack in corrosive media. The critical stress intensity factor  $K_{ISSC}$  in a sulfide environment is obtained by a test based on fracture mechanics. This method takes only a short time. It can directly give the crack propagation rate value, and evaluation based on the result of fracture or no fracture is no longer required.

The standard dual cantilever beam (DCB) test of the NACE Method D can be used for design

calculation. The critical stress intensity factor  $K_{ISSC}$  is obtained in light of a certain corrosive environment, and applied stress is reduced to a value lower than  $K_{ISSC}$ . This is just the stress reduction design.

The standard dual cantilever beam (DCB) test of the NACE Method D is complicated, and further studies are required in order to obtain reliable results.

## Main Factors That Affect Cracking in Corrosive Environments

The main factors that affect the cracking of steel material include: (1) metallurgical factors (chemical composition, heat treatment, microscopic structure, yield strength, tensile strength, hardness, cold deformation processing, and manufacturing process); (2) stress state (residual stress and applied stress); and (3) critical stress intensity factor  $K_{ISSC}$  of material in hydrogen sulfide environments.

**Alloy Design, Harmful Element Control, and Metallurgical Texture.** The properties of material include chemical composition, manufacture method, shaping mode, strength, hardness, local change of material, cold deformation process load, heat treatment condition, microscopic structure, evenness of microscopic structure, crystalline grain size, material purity, and so on. The evaluation of a single element that affects sulfide stress cracking (SSC) is complicated. Each element and heat treatment should be considered in combination with other elements. The key to ensuring SSC-resistant carbon steel and low-alloy steel casing and tubing quality lies in the content control of harmful elements (sulfur and phosphor). In general, steel with total P and S content lower than 0.008% is considered pure steel. The harmful gas in steel includes hydrogen, oxygen, and nitrogen. The impurities mainly include oxide and carbide. Other harmful elements include As, Sb, Bi, Sn, Pb, and so on, and the content of these elements can be effectively controlled by carefully selecting raw ore. The aforementioned harmful components may reduce steel toughness. In

particular, in sour environments, cracking resistance may be reduced. During heat treatment, the aforementioned harmful components may particularly accumulate at the crystal interface to reduce intercrystalline binding energy; thus, fracturing may be generated along the crystal interface in a sour environment.

When the content of harmful element S of tubing and casing is reduced to a value lower than 0.001%, the SSC resistance can be improved in a constant-load tension test.

The control of P content is related to S content. Under very low S content, the requirement for P content can be slightly relaxed. Due to the action of molybdenum in chrome-molybdenum steel, the P content in 4130 steel, which has a Mo content of 0.20% to 0.80%, can be lower than 0.030% under the condition of low Mn content ( $< 0.75\%$ ).

C, Mn, and Ni are not harmful elements, but their contents should be controlled in an appropriate range. If their contents are not controlled appropriately, the sensitivity of steel material to sulfide stress cracking may be increased. The harmful elements of commonly used sulfur-resistant steels and the control contents of element are listed in Table 11-2. In practice, the level of metallurgical technology is relatively high at present. The contents of sulfur and phosphor of tubing and casing (including sulfide-resistant tubing and casing) are far lower than the contents specified in Table 11-2, which indicates that the standards are not the highest requirements but the compromise between the manufacturers and the users under present conditions. The users have the right to present the supplemental technical conditions higher than that in ISO 15156.

**Strength and Hardness.** Strength and hardness are the important performance parameters of sulfide stress cracking resistance. Too high or too low strength and hardness may cause cracking. Approximately low strength and hardness are the important indices of determining the cracking resistance of carbon steel and low-alloy steel. Restricting strength grade can prevent sulfide stress cracking. Because hardness is related to strength and can be determined by using nondestructive

**TABLE 11-2 Harmful Elements of Commonly Used Sulfur-Resistant Steels and the Control Contents of Elements**

Steel	H40	J55	K55	L80 Typ. 1	C90 Typ. 1	T95 Typ. 1
C	0.35	0.35	0.35	0.35		
Mn	1.40	1.40	1.40	1.40		
P	0.020	0.020	0.020	0.020		
S	0.015	0.015	0.015	0.010		
Ni					0.35	0.35

and convenient methods, hardness has been widely used in sour-environment material selection and quality control specifications.

Figure 11-14 shows that with the increase of strength, the critical stress intensity factor  $K_{ISSC}$  of material in hydrogen sulfide environments is reduced. When yield strength is higher than 100 ksi,  $K_{ISSC}$  is lower than  $33 \text{ MPa} \cdot \text{m}^{0.5}$  (note:  $1 \text{ ksi} \cdot \text{in.}^{0.5} = 1.098 \text{ MPa} \cdot \text{m}^{0.5}$ ). Due to the high effect of yield strength on cracking, material appropriate for a hydrogen sulfide environment should meet the requirement of the minimum yield strength, and it is required to restrict the maximum yield strength.

Material with a hardness lower than HRC22 or HB237 is also sensitive to SSC in very high stress states or severe environments.

The maximum permissible strength and hardness values are related to tensile stress applied and sour environment severity. When the tensile stress borne by material is reduced to some value, the increase of hardness may not generate SSC. The ISO 11960-specified hardness values of commonly used sulfur-resistant steel are listed in Table 11-3.

**Temperature Conditions Appropriate for Different Steel Grades of Casing and Tubing in Sour Environments.** Temperature may greatly affect the hydrogen sulfide stress

corrosion cracking of carbon steel and low-alloy steel. In general, sulfide stress cracking is sensitive to temperatures between room temperature and  $65^\circ\text{C}$ ; thus, the aforementioned test standards are set at  $24^\circ\text{C}$ . If temperature is lower than  $24^\circ\text{C}$ , the cracking tendency may be more serious. Table 11-4 shows that in a sulfur-containing gas well, sulfide-nonresistant tubing and casing with higher strength can be adopted in the well section with a temperature higher than  $65^\circ\text{C}$ . The temperature conditions appropriate for different steel grades of casing and tubing in sour environment are listed in Table 11-4.

There are the following risks when sulfide-nonresistant pipe is adopted in deep sections in the light of the reduction of sulfide stress cracking sensitivity at high temperature:

#### 1. Problem of electrochemical corrosion

With the increase of well temperature, electrochemical corrosion may be aggravated despite the fact that sulfide stress cracking in high-temperature section may not be generated. Therefore, the tubing and casing design for wells with high content of hydrogen sulfide, carbon dioxide, or formation water will be complicated. Appropriate well section design and using appropriate sulfide-resistant steel can only solve

**TABLE 11-3 ISO 11960 Specified Hardness Values of Commonly Used Sulfur-Resistant Steel**

Steel	J55 K55	L80 Typ. 1	C90 Typ. 1	T95 Typ. 1
Maximum hardness	HRC22	HRC23	HRC25	HRC25
Mean hardness	HRC22	HRC22	HRC25	HRC25

Note: Typ. 1 means the maximum yield strength of 1031 MPa (150 ksi), Cr-Mo steel, and Q&T treatment.

**TABLE 11-4 Temperature Conditions Appropriate to Different Steel Grades of Casing and Tubing in a Sour Environment**

Appropriate to All Temperatures	≥65°C (150°F)	≥80°C (175°F)	≥107°C (225°F)
Steel grade	Steel grade	Steel grade	Steel grade
H40	N80 Type Q	N80	Q125 <sup>1</sup>
J55	C95	P110	
K55			
M65			
L80 Type 1			
C90 Type 1			
Y95 Type 1			
Conforming to service condition of Zone 3 in Figure 11-15	Maximum yield strength lower than or equal to 760 MPa (110 ksi) Special Q&T steel	Maximum yield strength lower than or equal to 976 MPa (140 ksi) Special Q&T steel	

<sup>1</sup>Based on maximum yield strength of 1036 MPa (150 ksi). Cr-Mo Q&T steel. C-Mn steel not allowed.

the problem of sulfide stress cracking, but cannot solve the problem of electrochemical corrosion. Electrochemical corrosion may cause a decrease of pipe cross-section or stress concentration at the corrosion pit and heighten the temperature condition appropriate for steel grades of casing and tubing due to stress, so that the problem of cracking may still be generated. Thus it is required to adopt nickel-based corrosion-resistant alloy pipe or to use corrosion inhibitor in order to prevent corrosion.

2. The change from high temperature to low temperature may also generate stress cracking

The reduction of temperature of the sulfide-resistant casing in deep section during cold fluid injection may lead to cracking, which is difficult to avoid during well servicing or downhole operation. The cracking of tubing may also be generated in low-temperature section at the wellhead when tubing is taken out of the well or due to the dynamic load after tubing is pulled out of the well.

**Stress Level and Stress State.** The cracking of metallic material under the coordinated action of stress and chemical media is known as stress corrosion cracking. Stress is the necessary condition of stress corrosion cracking. It can be applied stress or residual stress. Tensile stress is

the most harmful. The tensile stress value when cracking is generated is much lower than the yield strength of material. There is no obvious plastic deformation. The greater the stress, the shorter the time for generating cracking.

If stress is further reduced, some high-strength steels may not generate stress cracking in accordance with the NACE Method A and A solution. For some steel, the maximum stress value under which stress cracking will not be generated can be generally obtained by testing. This stress is just the critical corrosion cracking stress. The NACE Method C can be used to better quantitatively describe the effects of different corrosive media and different stress levels on crack propagation and fracture.

### Cracking Severity Criteria for Carbon Steel and Low-Alloy Steel in a Sour Environment of Hydrogen Sulfide

In environments with hydrogen sulfide, the properties of carbon steel and low-alloy steel may be affected by multiple factors and their interaction, which include:

1. Chemical composition, manufacturing method, forming mode, strength, material hardness and local change, cold process load, heat

treatment condition, microscopic structure of material, microscopic structure homogeneity, crystal grain size, and material purity;

2. Partial pressure of hydrogen sulfide or equivalent concentration in water phase;
3. Chlorion concentration in water phase;
4. The pH value of water phase;
5. Whether elemental sulfur or other oxidant exists;
6. Invasion of non-reservoir fluid or contact with non-reservoir fluid;
7. Temperature;
8. Stress state and total tensile stress (applied stress plus residual stress);
9. Exposure duration.

The most important factors that may affect the properties of carbon steel and low-alloy steel in sour environments include partial pressure and pH value. Thus these two parameters are taken as the criteria of cracking severity in ISO 15156, which only involves the cracking of material and has not involved a general corrosion problem. When material is selected in design, the pH value should be calculated on the basis of component analysis, and cracking severity is determined if the pH value of production system is unknown. It would be best if downhole sample data could be obtained. However, a hydrogen sulfide-containing well is difficult to sample.

**SSC Criteria Diagram of Carbon Steel and Low-Alloy Steel.** The cracking severity criteria diagram of carbon steel and low-alloy steel in a sour environment of hydrogen sulfide is divided into four zones (Figure 11-15).

Figure 11-15 shows that under hydrogen sulfide partial pressure lower than 0.3 kPa, an uncertainty of measurement may be generated. While under partial pressure higher than 1 MPa, steel selection should be based on fitness evaluation; that is, steel material is selected by testing on the basis of downhole working status. When carbon steel and low-alloy steel are selected, evaluation tests based on sour working environment or in accordance with the conditions of Zone SSC1, Zone SSC2, and Zone SSC3 are required.

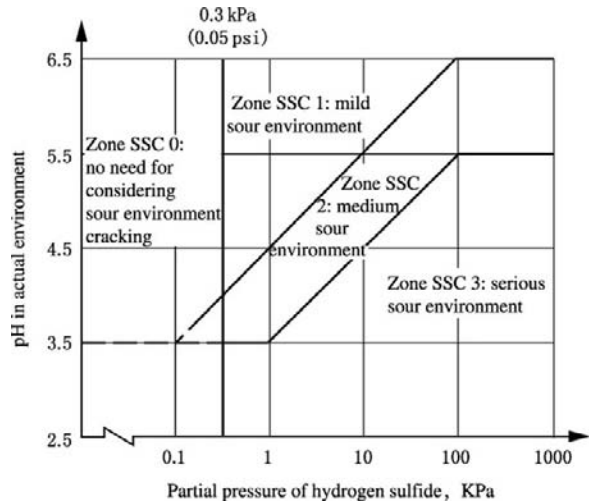


**FIGURE 11-15** The cracking severity criteria diagram of carbon steel and low-alloy steel in a sour environment of hydrogen sulfide.

If there has been field experience about the use of tubing and casing steel to be selected, steel material can also be selected in consideration of the sour working environment. When the severity of the hydrogen sulfide environment is determined, the formation of condensate water due to abnormal operation or production shutdown should be considered. Condensate water may reduce the pH value. In addition, the pH value of acidizing fluid during acidizing should also be considered. The pH value of acidizing fluid may be further reduced after hydrogen sulfide is dissolved in the acidizing fluid. It should be ensured to flow back in time and prevent the spent acid from remaining at the bottomhole.

**Selection of Steel Material Suitable for Zone SSC 0 Environment with Low Partial of Hydrogen Sulfide ( $P_{H_2S} < 0.3$  k Pa).** In general, there is no special requirement for steel material. However, there is hydrogen sulfide after all. Thus the following factors that may lead to cracking should be considered:

1. Steel material that is highly sensitive to sulfide stress cracking (SSC) and hydrogen stress cracking (HSC).

2. The physical and metallurgical properties of steel material affect SSC and HSC resistance.
  3. In a liquid environment with no hydrogen sulfide, superhigh-strength steel material may generate HSC. When yield strength is higher than 965 MPa (140 ksi), the chemical composition of steel material should be especially required, and heat treatment is also required in order to ensure no SSC or HSC in the working environment of Zone SSC 0.
  4. The risk of stress concentration plus cracking.
3. If the pipes and fittings are cold straightened at a temperature equal to or lower than 510°C (950°F), stress should be eliminated at a temperature higher than or equal to 480°C (900°F). If the pipes and fittings are cold shaped (pin thread and/or box thread) and the permanent deformation of outer-layer fiber exceeds 5%, the cold shaped area should be heat treated at a temperature higher than or equal to 595°C (1100°F) in order to eliminate internal stress.

### Selection of Casing, Tubing and Fittings Suitable for Serious Sour Environments (Zone SSC 3).

A pH value of 3.5–5.5 and a  $P_{H_2S}$  value of 0.01–1.0 bar are characteristic of a Zone SSC 3 environment. The environment in which any micro- $H_2S$  can be measured is of Zone SSC 3 provided that the pH value is lower than 3.5. In an environment in which  $H_2S$ ,  $CO_2$ , and water coexist, the pH value may be lower than 3.5.

Casing, tubing, and fittings suitable for a serious sour environment (Zone SSC 3) should meet the following requirements:

1. The pipes and fittings can be made of the Cr-Mo low-alloy steel quenched and tempered. They should have yield strengths of 690 MPa (100 ksi), 720 MPa (105 ksi), and 760 MPa (110 ksi). Hardness should not be higher than HRC30. The deviation of yield strength should be strictly controlled. The difference between actual maximum yield strength and minimum nominal yield strength should not be greater than 103 MPa (15 ksi). The SSC resistance tests of each batch should be recorded. The sulfide stress cracking resistance should be checked by unilateral stretch in accordance with the NACE Method A and A solution.
2. If hardness is not higher than HRC26, pipes and fittings made of Cr-Mo low-alloy steel quenched and tempered can be used. The sulfide stress cracking resistance should be checked by unilateral stretch in accordance with the NACE Method A and A solution.

If a high-strength pipe junction piece that has a hardness higher than HRC22 is cold shaped, the internal stress in junction piece should be eliminated at a temperature higher than or equal to 595°C (1100°F).

The steel grades of casing and tubing that are suitable for Zone SSC 3 include H40, J55, K55, M65, L80 Typ. 1, C90 Typ. 1, and T95 Typ. 1. They are appropriate for any downhole temperature. In addition, for a well section with a temperature higher than 60°C, the steel grades of N80 Type Q and C95 can also be selected. However, the actual maximum yield strength should be lower than or equal to 760 MPa (110 ksi), and special Q&T heat treatment is required.

### Selection of Casing, Tubing and Fittings Suitable for Medium Sour Environments (Zone SSC 2).

Material that is suitable for Zone SSC 3 can be used in Zone SSC 2. In addition, the casing, tubing, and fittings made of Cr-Mo low-alloy steel quenched and tempered can also be used in Zone SSC 2. The actual yield strength of material should not be higher than 760 MPa (110 ksi); that is, the nominal yield strength should not be lower than 550 MPa (80 ksi), which means that the allowable deviation of yield strength of material is 30 ksi. In addition, hardness should not be higher than HRC27. Other technical requirements should accord with the related specifications.

### Selection of Casing, Tubing, and Fittings Suitable for Slight Sour Environments (Zone SSC 1).

The Zone SSC 1 environment characteristics include: (1) pH of 3.5 and  $P_{H_2S}$  of 0.001

bar to pH of 6.5 and  $P_{H_2S}$  of 1.0 bar and (2) pH higher than 6.5 and any  $P_{H_2S}$ .

Material suitable for Zone SSC 3 and Zone SSC 2 can be used for Zone SSC 1. In addition, the casing, tubing, and fittings made of Cr-Mo low-alloy steel quenched and tempered can be used for Zone SSC 1. The actual yield strength should not be higher than 896 MPa (130 ksi); that is, the nominal yield strength should not be lower than 760 MPa (110 ksi), which means that the allowable deviation of yield strength is 20 ksi. In addition, hardness should not be higher than HRC30. Other technical requirements should accord with the related specifications.

### Test Requirements of Commonly Used Hydrogen SSC Resistant Carbon Steel and Low-Alloy Steel Tubing and Casing

**J55 and K55 Seamless Steel Pipe.** Samples should be taken near the inner wall of pipe as far as possible. Testing should be in accordance with the NACE Method A and A solution. The critical stress of the test should not be lower than 80%.

**K55 Electric Resistance Welded Pipe Body and Collar.** For welded seams, the NACE Method A and A solution are used for testing. The critical stress of the test should not be lower than 80%.

**L80 Typ. 1, C90 Typ. 1, and T95 Typ. 1 Casing and Collar.** The NACE Method D and A solution are used for testing. For L80 Typ. 1 and C90 Typ. 1 casing and collar, the NACE Method C should be used for the fatigue test of present fatigue crack. For T95 Typ. 1 casing and collar, the fatigue test of present fatigue crack is not required. For L80 Typ. 1 base metal and welded seam of electric resistance welded pipe, the fatigue test of present fatigue crack is required. For base metals and welded seams of all steel grades, the critical sulfide stress intensity factor  $K_{ISSC}$  should be tested by using a test sample of standard size. The mean value of  $K_{ISSC}$  should not be lower than  $33.0 \text{ MPa} \cdot \text{m}^{0.5}$ , and the  $K_{ISSC}$  value of single sample should not be lower than  $29.7 \text{ MPa} \cdot \text{m}^{0.5}$ .

J55, K55, and ERW L80 Typ. 1 casing and collar are low-strength steel, and stress-oriented hydrogen-induced cracking (SOHIC) or hydrogen-induced cracking (HIC) may be generated depending on manufacturing method and heat treatment.

### Corrosion-Resistant Alloy Steel Tubing and Casing

Corrosion-resistant alloys include stainless steel and alloy steel. Some corrosion-resistant alloys are more sensitive to pitting corrosion and stress corrosion cracking in a corrosive environment. In the petroleum industry history of using corrosion-resistant alloy, severe accidents of stress cracking and pitting corrosion boring of tubing due to improper selection of corrosion-resistant alloy material have been generated.

Local corrosion and fracture are mainly characteristic of the corrosion failure of corrosion-resistant alloy. Selecting corrosion-resistant alloy requires full grounds due to a variety of alloy types, high expense, great difference in price, great difference in fitness for service environment, and less experience in using in oil and gas wells. Appropriate corrosion-resistant alloy material should be selected in light of the specific corrosion environment, and laboratory tests should be done under simulated service conditions as far as possible. In addition, deriving experience in developing similar oil and gas fields is also important.

**Types and Basic Compositions of Corrosion-Resistant Alloys for Tubings and Casings in Oil and Gas Wells.** In corrosion-resistant alloys, Cr, Ni, and Mo are the most important basic alloying elements. Different percentage contents and different manufacturing methods form different types of corrosion-resistant alloys. The aforementioned elements are crucial to the formation of stable protective corrosion product film on structural members. Corrosion will start from the failure of protective corrosion product film.

The main compositions of corrosion-resistant alloys for tubing and casing are listed in Table 11-5. Austenitic stainless steel is used for

TABLE 11-5 Main Composition of Corrosion-Resistant Alloys for Tubing and Casing

Type		UNS	Content of Key Alloy (%)			
			Cr	Ni	Mo	Other
Martensitic stainless steel	ISO 11960		12 ~ 14	0.5		Si = 1, Mn = 0.25 ~ n1, Cu = 0.25
	L80 13Cr					
	13CrS	S41426	11.5 ~ 13.5	4.5 ~ 6.5	1.5 ~ 3	Tu = 0.01 ~ 0.5, V = 0.5
Diphase stainless steel	S/W 13Cr	S41425	12 ~ 15	4 ~ 7	1.5 ~ 2	Cu = 0.3
	22Cr	S31803	21.0 ~ 23.0	4.5 ~ 6.5	2.5 ~ 3.5	Mn, Si, etc.
	25Cr	S32550	24.0 ~ 27.0	4.5 ~ 6.5	2.0 ~ 4.0	Mn, Si, etc.
		S32750	24.0 ~ 26.0	6.0 ~ 8.0	3.0 ~ 4.0	
Nickel base alloy		S32760	24.0 ~ 26.0	6.0 ~ 8.0	3.0 ~ 4.0	
	Alloy C-276	N10276	14.5 ~ 16.5	Rem	15 ~ 17	W = 3.0 ~ 4.5, Co = 2.5
	Alloy 625	N06625	20.0 ~ 23.0	Rem	8.0 ~ 10	Nb = 3.15 ~ 4.15
	Alloy 718	N07718	17.0 ~ 21.0	50.0 ~ 55.0	2.8 ~ 3.3	Nb = 4.75 ~ 5.50
	Alloy 825	N08825	19.5 ~ 23.5	38.0 ~ 46.0	2.5 ~ 3.5	Ti = 0.6 ~ 1.2
	G-2	N06975	23.0 ~ 26.0	47.0 ~ 52.0	5.0 ~ 7.0	
	G-3	N06985	21.0 ~ 23.5	Rem	6.0 ~ 8.0	W = 5.0, Co = 1.5
	G-30	N06030	28.0 ~ 31.5	Rem	4.0 ~ 6.0	W = 5.0, Co = 1.5 ~ 4.0
	028	N08028	26.0 ~ 28.0	29.0 ~ 32.5	3.0 ~ 4.0	Cu = 0.6 ~ 1.4
	2550	N006255	23.0 ~ 26.0	47.0 ~ 52.0	6.0 ~ 9.0	W = 3.0, Cu = 1.2, Ti = 0.69
G-50	N06950	19. ~ 21.0	50.0	8.0 ~ 10.0	W = 1.0, Cu = 0.5, Ti = 0, Co = 2.5	

Note: UNS means unitary numbering system (U.S. metal and alloy numbering system based on SAE-ASTM). Rem means remainder.

manufacturing components and parts and is not used for manufacturing tubing.

**Modes of Corrosion and Influence Factors for Corrosion-Resistant Alloy.** Pitting corrosion or stress corrosion cracking may be generated in the process of using corrosion-resistant alloy. Stress corrosion cracking includes sulfide stress corrosion cracking, chloride stress cracking, and so on.

The following should be considered when corrosion-resistant alloy is selected in accordance with ISO 15156-1:

1. Partial pressure of carbon dioxide in gas phase
2. Partial pressure of hydrogen sulfide in gas phase
3. Temperature during service
4. pH value of water phase
5. Concentration of  $\text{Cl}^-$  or other halide ( $\text{F}^-$ ,  $\text{Br}^-$ )
6. Existence of elemental sulfur

The mechanisms of stress cracking and pitting corrosion of corrosion-resistant alloy are as follows:

1. Stress cracking of corrosion-resistant alloy

The mechanisms of stress cracking of various corrosion-resistant alloys are listed in Table 11-6.

2. Pitting corrosion of corrosion-resistant alloy

The pitting corrosion of corrosion-resistant alloy is a common problem. At the pit the stress level is relatively high and a crack source may be formed. Under the coordinated action of higher working stress and chlorine or oxygen, cracking may be caused. The pitting resistance equivalent number (PREN) is used for evaluating pitting corrosion resistance.

$$\text{PREN} = \% \text{Cr} + 3.3(\% \text{Mo} + 0.5\% \text{W}) + 16\% \text{N}$$

where: %Cr = weight fraction of Cr in alloy, percent of total composition; %Mo = weight fraction of Mo in alloy, percent of total composition; %W = weight fraction of W in alloy, percent of total composition; %N = weight fraction of N in alloy, percent of total composition.

TABLE 11-6 Mechanisms of Stress Cracking of Various Corrosion-Resistant Alloys

Type of Material	Mechanism of Potential Cracking in Hydrogen Sulfide Environment			Remarks
	Sulfide Stress Cracking (SSC)	Sulfide Corrosion Cracking (SCC)	Couple-Induced Hydrogen Stress Cracking	
High-alloy austenitic stainless steel	—	P	—	SSC and HSC may not be generally generated. Low-temperature cracking test is not required.
Martensitic stainless steel	P	S	P	The alloys that contain Ni and Mo may sustain SCC whether or not residual austenite is contained.
Diphase stainless steel	S	P	S	When temperature is higher than the highest use temperature, cracking sensitivity may be high and testing in the range of possible service temperature is required.
Solid-solution nickel-based alloy	S	P	S	Some nickel-based alloys contain a secondary phase in cold forming process and/or ageing state. When an electric couple is formed due to contact with steel, it may be sensitive to HSC.

Note: P means principal mechanism of cracking and S means secondary and possible mechanism of cracking.

PREN has several variables and is used for reflecting and predicting the pitting corrosion resistance of Fe-Cr-Mo stainless steel (CRA) when dissolved chloride and oxygen exist (such as in sea water). Despite the usefulness of this parameter, it cannot directly predict corrosion resistance in a hydrogen sulfide environment.

3. Environmental factors affecting the pitting corrosion and cracking of corrosion-resistant alloy. The factors are complicated, and the following should be considered in design and downhole operations:

- a. Concentration of  $\text{Cl}^-$  or other halide ions ( $\text{F}^-$ ,  $\text{Br}^-$ ).

Sometimes formation water may have a high chloride content, and some wells use high-concentration salt water or natural brine for killing a well. For instance, acidizing fluid contains hydrofluoric acid, and bromide is used as killing fluid and

reservoir-protecting fluid, and so on.  $\text{Cl}^-$  or other halide ion ( $\text{F}^-$ ,  $\text{Br}^-$ ) may fail the passivating film on stainless steel surfaces singly or in combination with oxygen and lead to steel directly adsorbing the hydrogen atom. Stainless steel and alloy are restricted by the concentration of  $\text{Cl}^-$  or other halide ion ( $\text{F}^-$ ,  $\text{Br}^-$ ) to a certain degree in use. If  $\text{CaCl}_2$ ,  $\text{NaCl}$ ,  $\text{ZnCl}_2$ , and  $\text{CaCl}_2$ - $\text{CaBr}_2$  solutions, and so on, are required to be injected in the tubing-casing annulus or well, pitting corrosion and cracking of corrosion-resistant alloy should first be evaluated under simulated downhole conditions and the coordinated action of hydrogen sulfide and carbon dioxide. For martensitic stainless steel and diphase stainless steel, the aforementioned effect of  $\text{Cl}^-$  or other halide ions ( $\text{F}^-$ ,  $\text{Br}^-$ ) should be evaluated.

- b. Effect of the partial pressure of downhole hydrogen sulfide and the pH value of environment on cracking. For nickel-based alloy, the pH value of the environment may not affect the cracking of material in principle. However, for martensitic stainless steel and diphase stainless steel, the potential cracking problem should be considered.
- c. Effect of elemental sulfur on pitting corrosion and environment cracking. Elemental sulfur is a factor that affects the cracking and pitting corrosion of some corrosion-resistant alloys, and an evaluation is required in light of the specific environment.
- d. Effect of oxygen on pitting corrosion and cracking. The reaction of oxygen to hydrogen sulfide may generate sulfuric acid, which has a certain effect on the pitting corrosion and stress cracking of stainless steel. If stainless steel tubing is used, oxygen should be removed, or an oxygen inhibitor should be added when fluid is injected in the well.

### Service Environment Restriction of Corrosion-Resistant Alloy

1. Service environment for martensitic stainless steel

Martensitic stainless steel is stainless steel of such chrome as to maintain martensitic microscopic texture at room temperature. Its mechanical properties including strength, hardness, elasticity, and abrasion resistance can be enhanced and improved by heat treatment. It is widely used as the corrosion-resistant alloy of tubing and casing and is mainly used in corrosive environments in which carbon dioxide is predominant. L80 13Cr as shown in Table 11-5 has been included in the ISO 11960, ISO 15156, and ISO 10400 standards and is basic martensitic stainless steel. S/W 13Cr and S/W 13CrS are the high-performance martensitic stainless steels that are based on L80 and in which the alloying elements including Ni, Mo, and so on are added before the steel is properly heat treated. Thus they are also known as

super 13Cr stainless steel. They have higher mechanical properties, pitting corrosion resistance, sulfide stress corrosion cracking resistance, chloride stress cracking resistance, high-temperature resistance, and so on, than L80 13Cr.

Martensitic stainless steel is used in corrosive environments of carbon dioxide. The L80 13Cr in it cannot be used in an environment with hydrogen sulfide. Super 13Cr stainless steel has a certain sulfide stress cracking resistance when chlorion content is low, and the maximum allowable partial pressure of hydrogen sulfide is 10 k Pa ( $\text{pH} \geq 3.5$ ). High temperature and high sulfide content may generate pitting corrosion or sulfide stress corrosion cracking. The coexistence of high temperature, high sulfide content, and micro-hydrogen sulfide may aggravate pitting corrosion. The electrochemical corrosion and cracking evaluation is required on the basis of specific temperature and the contents of chloride and hydrogen sulfide in order to determine the specific application range.

Limited tests indicate that no pitting corrosion has been observed at temperatures lower than 80°C under  $\text{pH} \geq 3.5$ , partial pressure of hydrogen sulfide lower than 10 k Pa, and sodium chloride content up to 20%, and that pitting corrosion may be caused by micro-hydrogen sulfide at temperatures higher than 120°C. For any martensitic stainless steel, the chloride and micro-hydrogen sulfide pitting corrosion and chloride stress cracking under low pH value in high-temperature environments should be considered, and the sulfide stress corrosion cracking of high-strength steel under low pH value at low temperature should also be considered.

2. Service environment for diphase stainless steel

The solid-solution texture of diphase stainless steel contains ferrite and austenite texture. Diphase stainless steel combines the features of austenite and ferrite. It has the high toughness of austenitic stainless steel

and the high strength and chloride stress corrosion resistance of ferritic stainless steel; thus, it has good corrosion resistance and mechanical properties.

The commonly used diphasic stainless steels include 22Cr and 25Cr steels (especially the 22Cr steel). Diphasic stainless steel has higher resistance to high temperature, higher resistances to corrosion due to high content of carbon dioxide and sulfide, and higher resistance to high-velocity gas flow erosion than martensitic stainless steel. However, it is not certain that the sulfide stress cracking resistance of diphasic 22Cr stainless steel is higher than that of super 13Cr stainless steel. In accordance with ISO 15156-3, the maximum partial pressure of hydrogen sulfide should be lower than 2 kPa if  $30 \leq \text{PREN} \leq 40$  and  $\text{Mo} \geq 1.5\%$  (such as 22Cr), and the maximum partial pressure of hydrogen sulfide is 20 kPa if  $40 < \text{PREN} \leq 45$  (such as diphasic 25Cr stainless steel), but the concentration of chloride should be lower than 120,000 mg/l. The cracking resistance of diphasic stainless steel is related to yield strength and quality control during manufacture to a great extent. The higher the PREN value, the higher the resistance to corrosion. However, PREN may also increase the risk of forming the basic phases of  $\sigma$  and  $\alpha$  in the ferrite phase of material during manufacture.

Diphasic stainless steel is similar to martensitic stainless steel in that chloride and microhydrogen sulfide pitting corrosion and chloride stress cracking under low pH value and high-temperature environment conditions should be considered, and sulfide stress corrosion cracking of high-strength steel under pH value and low-temperature environment conditions should also be considered. The unfavorable combination between the content of chloride and the partial pressure of hydrogen sulfide may cause the stress cracking of diphasic stainless steel. If diphasic stainless steel is connected with carbon steel or low-alloy steel having cathodic protection,

the diphasic stainless steel may generate hydrogen-induced stress cracking (HISC).

### 3. Service environment for nickel-based alloy

Nickel has a high tendency to passivate. At normal temperatures, a nickel surface is covered with an oxide film, which has a high resistance to corrosion. Nickel-based alloy with a content of 25% to 45% has high resistance to corrosion and an environment cracking resistance and also has high strength. Nickel-based alloy for tubing and casing is of nickel-chromium-molybdenum alloy series. The chromium in it is favorable for improving use performance in high-temperature environments, while the molybdenum in it can increase corrosion resistance under low pH value.

Nickel-based alloy that is suitable for manufacturing tubing and casing is a solid-solution nickel-based alloy. It is a single crystalline phase structure composed of two or more than two alloying elements. Solid-solution nickel-based alloy obtains high strength after cold rolling, and the yield strength can be up to 150–180 ksi. The solid-solution nickel-based alloy materials used for manufacturing tubing and casing are listed in Table 11-7. They are divided into three types (4c, 4d, and 4e) on the basis of the contents of nickel and molybdenum. The resistances to pitting corrosion, sulfide stress corrosion cracking, chloride stress cracking, and elemental sulfur corrosion of corrosion-resistant alloy are related to elemental composition, manufacturing method, yield strength, service environment temperature, hydrogen sulfide concentration, and so on.

Table 11-7 shows that 4c and 4d cannot resist elemental sulfur corrosion at high temperatures (higher than 177°C), but 4c can still resist elemental sulfur corrosion at temperatures higher than 204°C. At lower temperatures (lower than 132°C), all the 4c, 4d, and 4e can resist elemental sulfur corrosion. At temperatures higher than 204°C, the partial pressure of hydrogen sulfide under which corrosion can be resisted may also be obviously reduced.

**TABLE 11-7** Types of Solid-Solution Nickel-Based Alloy Material for Tubing and Casing

Types of Material	Minimum Cr Weight Fraction (%)	Minimum Ni + Co Weight Fraction (%)	Minimum Mo Weight Fraction (%)	Minimum Mo + W Weight Fraction (%)	Brand Name and Metallurgical State of Typical Material
Type 4c	19.5	29.5	2.5		0.28 solid-solution tempered or tempered and cold worked
Type 4d	19.0	45		6	825, 625, 2550, 718, and G-2 solid-solution tempered or tempered and cold worked
Type 4e	14.5	52	12		C-276, G-3, and G-30 solid-solution tempered or tempered and cold worked

The corrosion resistances of solid-solution nickel-based alloys that are tempered and cold worked are listed in Table 11-8.

The solid-solution nickel-based products that are forged or cast should be in a tempered and cold worked state and should meet the following requirements:

1. Maximum allowable hardness is HRC40.
2. The maximum yield strength obtained by cold working is
  - a. 1034 MPa (150 ksi) for 4c;
  - b. 1034 MPa (150 ksi) for 4d;
  - c. 1034 MPa (150 ksi) for 4e.

Note: There is overlapping of conditionality of 4c, 4d, and 4e.

The types of solid-solution nickel-based alloy material (4a, 4b, 4c, 4d, and 4e) are listed in Table 11-9. ISO 15156-3 presents the corrosion resistances and limited service environments of corrosion-resistant alloy only in accordance with alloying element composition and manufacturing method. The sequence of corrosion resistances of some alloys is: C-276 > 050 > 625 and G-3 > 825 > 028 > 2550.

Nickel-based alloy is expensive and has a high initial investment; however, it has the highest safety and low long-term operating cost. The aforementioned corrosion resistances and conditionality of nickel-based alloy and ISO 15156-3 can only be used as a guiding basis for selecting material due to the complicated selection and evaluation of nickel-based alloy; thus,

consultation is required in order to properly select material in light of the downhole environment.

### Corrosion of Nonmetallic Material

Some nonmetallic materials are often used as seal elements or parts in downhole tools and wellhead assembly. Corrosion prevention design should consider the corrosion resistance of nonmetallic materials. When the seal material of rubber makes contact with media, the seal material of rubber and the additives may be decomposed due to oxidation, and some media may also make the seal material of rubber swell. Thus fracture and solution of rubber molecules and decomposition and dissolution of additives may be generated.

## 11.4 OIL AND GAS WELL CORROSION PREVENTION DESIGN

### External Casing Corrosion Prevention

**External Casing Corrosion Sources and Mechanisms of Corrosion.** External casing corrosion is mainly generated in free casing sections that have not been cemented. Cement sheath can protect casing to a great extent from corrosion. In a well section that is cemented poorly or a well section in which the cement sheath is damaged by downhole operation, casing may also be corroded. Both uniform corrosion and local corrosion may be present when

**TABLE 11-8** Conditionality of Solid-Solution Nickel Alloy Used for Making Downhole Pipe Fittings, Packer, and Other Downhole Tools

Type of Material	Max. Service Temperature (°C)	Max. Partial Pressure of Hydrogen Sulfide (kPa)	Max. Chloride Concentration (mg/l)	pH	Elemental Sulfur Resistant	Remarks
4c, 4d, and 4e alloys cold worked	232	0.2	See remarks	See remarks	No	Applicable to any combination of chloride concentration and pH value in well
	218	0.7	See remarks	See remarks	No	
	204	1	See remarks	See remarks	No	
	177	1.4	See remarks	See remarks	No	
	132	See remarks	See remarks	See remarks	Yes	Applicable to any combination of hydrogen sulfide, chloride concentration, and pH value in well
4d and 4e alloys cold worked	218	2	See remarks	See remarks	No	Applicable to any combination of chloride concentration and pH value in well
	149	See remarks	See remarks	See remarks	Yes	Applicable to any combination of hydrogen sulfide, chloride concentration, and pH value in well
4e alloy cold worked	232	7	See remarks	See remarks	Yes	Applicable to any combination of chloride concentration and pH value in well
	204	See remarks	See remarks	See remarks	Yes	Applicable to any combination of hydrogen sulfide, chloride concentration, and pH value in well

TABLE 11-9 Types of Solid-Solution Nickel-Based Alloy Material

Type of Material	Cr Weight Fraction Minimum (%)	Ni + Co Weight Fraction Minimum (%)	Mo Weight Fraction Minimum (%)	Mo + W Weight Fraction Minimum (%)	Metallurgical State
4a	19.0	29.5	2.5		Solid-solution tempered or tempered
4b	14.5	52	12		Solid-solution tempered or tempered
4c	19.5	29.5	2.5		Solid-solution tempered or tempered and cold worked
4d	19.0	45		6	Solid-solution tempered or tempered and cold worked
4e	14.5	52	12		Solid-solution tempered or tempered and cold worked

Note: Some chemical components listed may meet one or several restrictions, which are not certain and may be further restricted under some conditions.

external casing corrosion is generated. Pitting corrosion boring is most hazardous and is generated in quite a long well section.

External casing corrosion may be mainly generated if formation water developed in a section that has not been cemented, formation water is in flow state, and the formation water contains corrosive components.

#### 1. Corrosion due to corrosive components in formation water

Formation water may possibly contain the corrosive components including  $H_2S$ ,  $CO_2$ ,  $H^+$ ,  $O_2$ ,  $HCO_3^-$ ,  $SO_4^{2-}$ ,  $Cl^-$ , and  $OH^-$  and bacteria including sulfate-reducing bacteria and aerobic bacteria.

Corrosive components may corrode casing under the following conditions:

- a. Failure of cement sheath is generated during production. For instance, downhole operations cause brittle rupture of cement sheath. The sulfate and sulfate-reducing bacteria in formation water make cement corrode and degrade, thus causing contact between formation fluid and outside casing wall.
- b. In a well section that has not been cemented, the performance of drilling fluid fails under the action of long-term high temperature, thus reducing the pressure

on formation and making formation fluid enter the annulus.

#### 2. Electrotelluric stray current corrosion and local electric potential difference corrosion

Different formations that casing passes through have different moistness, and different aquifers have different salinities; thus, different sections of casing have different electrode potential. In addition, casing that is an anode will be electrochemically corroded when casing is made of carbon steel or low-alloy steel and the packer gas production wellhead, Christmas tree, and tubing are made of stainless steel or have corrosion-resistant metal coating.

#### 3. Remaining annulus drilling fluid corrosion

The drilling fluid remaining in the annulus outside casing and the flushing fluid and spacer fluid for displacing cement slurry may contain some corrosive components such as sulfonate that may decompose and generate hydrogen sulfide. In addition, when the aforementioned fluids are formulated at the surface or pumped into a well, air may be entrained and oxygen corrosion will be caused.

Some drilling fluids and completion fluids are saturated or undersaturated saltwater muds or barite- or ground iron ore-weighted muds. They are good conductors of electric

current and ionic current, thus aggravating electrochemical corrosion. The settling of ground iron ore or barite may lead to spot contact corrosion on the outside casing wall. In addition, the reduction of density of drilling fluid in the annulus outside casing may make formation fluid enter the annulus, and the casing will be corroded.

4. Corrosion due to metallurgical defects of casing steel material, operating damage, and local stress concentration

The API standard and ISO standard emphasize the minimum strength standard of casing and have no particular specifications for long-term corrosion resistance. Casings with different alloy designs and manufacturing techniques and the same mechanical performance have some differences in corrosion resistance. Attention should be paid because the metallurgical defects in the casing manufacturing process (such as alloying defects due to segregation) may cause pitting corrosion in some corrosive media environments. Excessive residual stress during manufacture or tool marks by casing tongs may aggravate local corrosion. Stress corrosion, crevice corrosion, and galvanic corrosion may be generated in casing collar sections and external thread die-out sections, and premature boring or fracturing may be caused in these sections.

### External Casing Corrosion Prevention Design

1. Preventing too long openhole section

Attention to formation water evaluation is not fully paid at present. If the openhole section is too long, a permeable formation that contains high-salinity or corrosive formation water may be met; thus, external casing corrosion may be generated afterward. External corrosion boring of intermediate casing has been generated in some deep wells due to a long drilling cycle when drilling has not been finished.

2. Cementing corrosive section

The problem of lost circulation during cementing should be solved when cement

return height is required to be increased. A stage collar can be used for staged cementing to prevent lost circulation. Formations of 50 m above and below the stage collar should be formations with no circulation loss because cement job quality is difficult to ensure at the stage collar.

3. Using external casing coating or external wrapping protective film

Coating or external wrapping protective film has high resistance to corrosion. Friction resistance is required during running. The film should be resistant to generating tool marks by casing tongs, or it can be patched up on the drill floor in time. The external casing wrapping developed by Tubocote Co. has a very high resistance to corrosion. The brine of the aquifer on the top of oil reservoir in the Changqing oil region has a total salinity of 86,000 mg/l and a pH value of 5.6. It is of acidulous water and is seriously corrosive to casing. The measures taken, including cementing, cathodic protection, and anodic protection, were of no avail. Finally, epoxy resin glass cloth was used to wrap the casing and anode (Zn) protection was also used. No casing corrosion problem has been found for years after the casing was run in.

4. Enhancing cement job quality and using proper sulfate and hydrogen sulfide-resistant cement

Cementing can effectively prevent casing corrosion; however, good cementing job quality is required and the cement should not be corroded by components such as sulfate and hydrogen sulfide in formation fluid. Cement is corroded by formation water in the following two stages:

- a. Cement bond stage. After pumping is finished, formation water may invade cement due to too long a setting time or cement weight loss. The cement invaded by formation water cannot be formed into set cement or has a low consolidation strength. It is often seen that an acoustic amplitude log of mudstone interval shows good cementing job quality, but the

corresponding sandstone interval has a poor cementing job quality due to the failure of cement setting by water invasion.

- b. Later formation water invasion stage. The set cement always has a certain permeability. The set cement invaded by the  $\text{Cl}^-$ ,  $\text{SO}_4^{2-}$ , and  $\text{HCO}_3^-$  in formation water may generate failure such as dissolution, ion exchange, crystallization, and expansion. In addition, the carbon dioxide in formation water may also corrode cement. Formation water percolates through cement and contacts the casing, thus corroding the casing.

Enhancing cement job quality and using proper sulfate-resistant cement are the important approaches to preventing or mitigating external casing corrosion.

### Tubing-Casing Annulus (Outside Tubing Wall and Inside Casing Wall) Corrosion

**Open Annulus.** If there is no packer in the lower part of the tubing, the annulus is known as an open annulus. In an open annulus, the corrosion of the inside casing wall and outside tubing wall are dependent on the changes of phase states of produced fluid and the oil, gas, and water in the annulus. In some oil and gas fields, the corrosion of the outside tubing wall is more serious than that of the inside tubing wall, and local corrosion boring from outside tubing wall to inside can be seen. This may be related to wetting and phase state. Carbon dioxide can be dissolved in condensate water and make the pH value of condensate water reduce to a value lower than 4.0. This condensate water can stably adhere to the outside tubing wall due to no flow in the annulus, thus causing weight loss corrosion or pitting corrosion boring.

The dynamic factor of mass transfer due to the dissolution and precipitation of tubing and casing at the bottom of a gas well near the gas-water interface may aggravate corrosion.

**Closed Annulus.** If there is packer in the lower part of the tubing, the annulus is known as

closed annulus. The protective fluid of closed annulus should have the following properties:

#### 1. Corrosion resistivity

Fresh water is generally used as the protective fluid of the annulus. Sodium hydroxide is added in fresh water in order to increase the pH value to 11; thus, oxygen scavenger and bactericidal agent are not required to be added on the premise of preventing annulus corrosion. In addition, diesel oil is also a good protective fluid for the annulus.

Calcium chloride solution has a good resistance to corrosion under the condition of carbon steel and low-alloy steel. However, if the tubing has leakage, carbon dioxide reacts on calcium chloride to form calcium carbonate, which precipitates on the tubing wall; thus, serious pitting corrosion may be generated. If stainless steel is used as the material of tubing or accessories of tubing, chloride stress corrosion cracking may be generated.

The incomplete displacement of drilling fluid and completion fluid remaining above the packer will be harmful. If weighted drilling fluid contains barite or ground iron ore, drilling fluid may be decomposed under the long-term action of high temperature, and barite or ground iron ore may precipitate and make contact with the outside wall of common low-alloy steel or stainless steel tubing; thus, extensive corrosion pits may be formed and tubing sticking may be caused during downhole operations.

In high-temperature high-pressure corrosive gas wells, the failure of packer, tubing thread leak, and production casing leak, and the improper design of protective fluid of the annulus may also cause tubing-casing annulus corrosion.

#### 2. Stability

A closed annulus should be stable at high temperature or under long-term borehole temperature conditions. A polymer that may not be decomposed and may not generate precipitation is added as weighting material.

### 3. Pressure balance

In some high-temperature high-pressure wells, the protective fluid of the annulus is required to have a certain density in order to balance the high pressure in tubing and exert a certain backpressure on the packer to balance the excessive upward force of the packer.

## Flow Velocity Restriction Based on Tubing Erosion and Corrosion

**Complexity of Effect of Flow Velocity in Tubing on Corrosion.** If tubing erosion has not been fully considered in high-productivity gas-well tubing design or large-diameter tubing cannot be used due to hole structure restrictions, erosion and corrosion may be generated when high-velocity gas flows in the tubing. The flow velocity under which obvious erosion and corrosion are generated is known as erosion flow velocity, critical flow velocity, or ultimate flow velocity. In engineering practice, flow velocity is often the only controllable mechanical index. The tubing wall thickness reduction due to the erosion and corrosion of tubing wall can be controlled by controlling flow velocity.

Flow velocity restriction is related to the following factors: (1) partial pressures, contents, and proportions of carbon dioxide gas and hydrogen sulfide gas; (2) water cut; (3) chlorion content; (4) gas-oil ratios of a condensate gas reservoir in various production periods; (5) temperature distribution; and (6) having or not having elemental sulfur precipitation and reservoir sand production, and so on.

1. Erosion and corrosion problem of in-tubing gas flow velocity higher than erosion flow velocity
  - a. Flow aggravated tubing erosion and corrosion. In particular, when the well contains carbon dioxide, hydrogen sulfide, and formation brine, the initial corrosion product film is continuously scoured and cannot take protection effect. Carbon dioxide corrosion products are loose and easier

to scour. Thus, for a carbon dioxide-containing gas well, the tubing diameter selection and production rate control should be prudent in particular. When corrosion inhibitor is required to be added, too high flow velocity in tubing may make the corrosion inhibitor film on the tubing wall unstable, and the corrosion inhibitor injection cycle is required to be shortened, or even continuous injection is required.

Under the condition of unconsolidated reservoir or excessive testing or producing pressure drawdown, the gas flow that carries sand may aggravate erosion and corrosion. For a reservoir that has higher content of carbon dioxide, chloride, or formation water, correct assessment of sand production is not only valuable for reservoir protection, but it is also important for preventing tubing erosion and corrosion.

- b. Local flow field-induced erosion and corrosion. Any change of diameter or flow direction in tubing may generate flow field-induced erosion and corrosion. Tubing threads and accessories of tubing may be possible erosion and corrosion positions.
- c. High-velocity gas flow-induced fluid-solid coupled vibration. Any change of diameter, flow direction, or flow velocity in the flow channel may generate fluid-solid coupled vibration (that is, flow-induced vibration). When tubing continuously vibrates, mechanical waves may cause dynamic fracturing at cracks in the tubing. For instance, this mechanical wave may lead to the fatigue fracture of thread, speed up the extension and development of body cracks or pits, and finally cause disruption. In practice, cases of tubing fracture and disruption have been generated in high-productivity corrosive gas wells. Some tubings have generated fracturing under the condition of no obvious corrosion mark.

In high-productivity gas wells, the flow channels of the Christmas tree and manifold system acutely change and vigorous

vibration may be generated. The vibration wave may be propagated along the tubing. When the lower part of the tubing is set at the packer, the axial compressed section will be buckled. The high-velocity gas flow in buckled tubing may cause vibration.

The flows in the tubings of gas well and condensate gas well are of unsteady-state flow; that is, the flow velocity is changeable. Changes of temperature and pressure may lead to changes of gas-liquid ratio and gas phase volume; thus, a change of flow velocity may be caused and vibration is induced.

2. Corrosion problem of insufficient gas-flow velocity in tubing

Too low gas flow velocity in tubing may also aggravate corrosion.

a. Condensate water film corrosion. In a carbon dioxide-containing gas well or condensate gas well, condensate water is precipitated when the temperature and pressure in the upper and medium well sections are reduced to lower than dew point. The thickness and distribution of condensate water film adhering to the tubing wall are related to thermodynamics, electrochemistry, and flow velocity. The lower the flow velocity in tubing, the deeper the depth point at which condensate water starts precipitation, and the more stable the water film adsorbed on the tubing wall. Under higher flow velocity, a high temperature of gas flow makes condensate water start precipitation at a shallow depth point, and the water film adhering to the tubing wall is easily flushed away; thus, it is not easy to form a stable water film on the tubing wall.

The condensate water in which carbon dioxide is dissolved has a pH value lower than that of formation water and has more serious corrosiveness. Formation water often contains bicarbonate, which may increase the pH value of water phase and mitigate corrosiveness.

b. Bottomhole load water and working fluid level corrosion. In carbon dioxide- and hydrogen sulfide-containing wells and wells with produced water, if the flow velocity in tubing is insufficient to lift out the bottomhole load water in a timely manner, serious tubing corrosion may be presented in the bottomhole load water section and especially at working fluid level.

c. Elemental sulfur precipitation and in-tubing deposition and blocking. The elemental sulfur in gas flow has no obvious effect. However, the elemental sulfur deposited on the tubing wall may cause pitting corrosion. In a gas well with high content of hydrogen sulfide, flow velocity is the main factor affecting the deposition of elemental sulfur. When flow velocity is high, the sulfur precipitated in tubing may be carried to the surface by gas flow. However, under low flow velocity, elemental sulfur may stably adhere to the tubing wall and in-tubing deposition and blocking may be caused.

3. Multiphase flow erosion and corrosion

The corrosion caused by a multiphase system consisting of oil and gas that contain carbon dioxide, hydrogen sulfide, and formation water or condensate water is known as multiphase flow erosion and corrosion. When water phase is continuous phase or condensate water is precipitated due to pressure and temperature lower than dew point, carbon dioxide is dissolved in condensate water and the water wets the tubing wall, thus aggravating corrosion.

In a gas well, the physical processes including water dissolving in gas and gas dissolving in water, and so on, will affect corrosion. After temperature and pressure are reduced, the water that is dissolved in gas is precipitated, and the effect of condensate water on corrosion will be crucial. The study of mass transfer between water and hydrocarbon phase indicates that when gas phase coexists with water, the carbon dioxide, hydrogen

sulfide, methane, and so on, in the gas phase may be dissolved in the water phase, which may cause a change in gas phase composition and also cause the change of some gas phase properties (such as saturation pressure, gas-oil ratio, and volume factor), thus causing a change of tubing wall corrosion state. During the normal production of a gas well, fluid may generate the change of phase behavior due to the effect of wellbore temperature and pressure. If the dew point line of water is inside the envelope of the condensation phase, no condensate water may be precipitated and the tubing wall may have slight or no corrosion. If the dew point line of water is outside the envelope of the condensed phase, condensate water may be precipitated and the tubing wall may have serious corrosion (Figure 11-16).

When the well product is water-in-oil emulsion, water wetting is prevented, thus greatly reducing the corrosion rate. When water content or other parameter is changed, oil-in-water emulsion may be formed, thus leading to the steel surface being wetted by water. A rule of thumb is that the tubing wall is fully wetted by oil and the corrosion rate is low when water content is lower than 30% (weight fraction), while the tubing wall is wetted by water and corrosion is serious when water content is higher than 50%. When water content is between the two values, the water wetting to tubing is

intermittent. When water content is higher, the water phase may be dispersed in the liquid phase and may also be present in tubing in the form of liquid film or in other form. If the water droplets are not fully carried away even though they are formed, the water phase may also generate liquid film. The existence of water film may greatly increase the corrosion rate. Therefore, local water content, water phase velocity, water film thickness, and water phase wettability on the tubing wall are crucial to the prediction of corrosion rate.

For an oil well, when pressure is higher than bubble point pressure, no gas is released, and flow is single-phase flow and has a low corrosion rate. When pressure is lower than bubble point pressure, the gas that contains hydrogen sulfide and carbon dioxide is separated from oil and dissolved in water; thus, a multiphase-flow corrosion environment is formed and the corrosion rate is greatly increased. In a condensate gas well that contains carbon dioxide, gas condensate is carried by gas flow and adsorbed by the tubing wall, thus preventing or mitigating tubing corrosion to a certain degree.

#### 4. Effects of properties of tubing and equipment material on erosion and corrosion

When the corrosion and erosion pit is shear wafer shaped or rind is made and peeled, material selection should be considered. High-ductility material that can form a

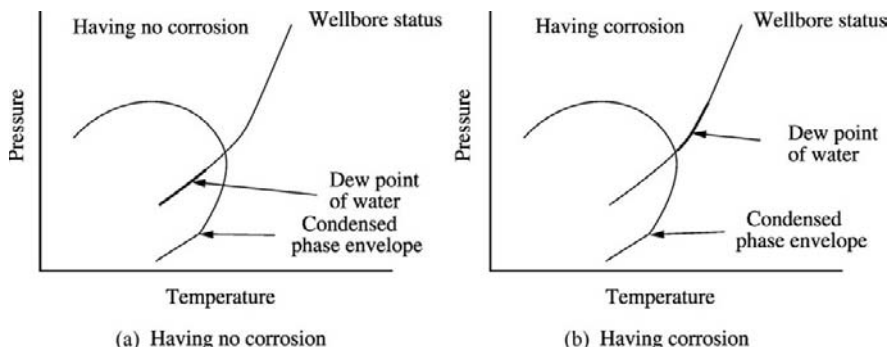


FIGURE 11-16 The effect of gas-well phase behavior on corrosion.

tight corrosion product film with high adhesion on the material surface should be predominantly selected. Increasing chrome content in low-alloy steel can form a tight and smooth protective film, thus increasing resistance to erosion. In high-productivity gas wells with serious corrosiveness, martensitic stainless steel (such as super 13Cr), diphasic stainless steel (such as 22Cr), and up to nickel-based alloy material are respectively selected in accordance with erosion severity. Their corrosion product film and ductility have higher resistance to erosion than that of low-alloy steel. On the basis of long-term practice and studies, a flow velocity restriction for preventing tubing erosion and corrosion failure is presented. Under the condition of dry gas well and common low-alloy carbon steel, the ultimate flow velocity for preventing erosion is 14 m/s. However, for a gas production well that contains carbon dioxide and 13Cr tubing, the ultimate flow velocity for preventing erosion and corrosion is increased to 35 m/s.

**Calculation of In-Tubing Flow Velocity for Preventing Erosion and Corrosion.** On the basis of the ultimate flow velocity, on-line monitoring including ferric ion concentration is recommended. The flow velocity in tubing is required to be adjusted on the basis of on-line monitoring of corrosion severity and evolution.

The ultimate erosion flow velocity in two-phase flow tubing in accordance with API RP14E is shown in Equations (11-8) and (11-9).

$$(11-8) \quad V_e = \frac{C}{\sqrt{\rho_g}}$$

where:  $V_e$  = erosion flow velocity of erosion, m/s;  $C$  = empirical constant (Corrosion rate can be controlled if flow velocity is lower than the critical flow velocity.  $C$  is 116 under the condition of existence of iron sulfide film formed by  $H_2S$  on steel surface.  $C$  is 110 under the condition of existence of iron carbonate film formed by  $CO_2$  on steel surface. For  $Fe_3O_4$  film,  $C$  is 183.);  $\rho_g$  = gas density,  $kg/m^3$ .

(11-9)

$$\rho_g = 3484.4 \frac{\gamma_g P}{ZT}$$

where:  $\gamma_g$  = relative density of mixed gas;  $P$  = flowing tubing (casing) pressure, MPa;  $Z$  = gas deviation factor;  $T$  = absolute gas temperature, K.

If  $C = 120$ , then  $V_e$  is as shown in Equation (11-10):

(11-10)

$$V_e = 2.0329 \left( \frac{ZT}{\gamma_g P} \right)^{0.5}$$

The flowing wellhead pressure is lower than the flowing bottomhole pressure due to gravity and friction resistance. However, the flow velocity gets higher and higher when gas flows from bottomhole to the wellhead. If the gas flow velocity at the wellhead may not generate obvious erosion, the flow velocity at any cross-section in the wellbore may also not generate erosion. The relation between tubing erosion flow velocity at the wellhead, the corresponding gas-well erosion flow rate, and the inner diameter of the tubing is shown in Equation (11-11).

(11-11)

$$V_e = 1.4736 \times 10^5 \frac{q_e}{d^2}$$

where:  $q_e$  = erosion flow rate at wellhead of gas well,  $10^4 m^3/d$ ;  $d$  = inner diameter of tubing, mm.

The formula in Equation (11-12) is obtained from the preceding formulae:

(11-12)

$$q_e = 1.3794 \times 10^{-5} \left( \frac{ZT}{\gamma_g P} \right)^{0.5} d^2$$

The relationship between the erosion flow rate at the wellhead and the volume flow rate under standard surface conditions is shown in Equation (11-13).

(11-13)

$$q_{max} = \frac{Z_{SC} T_{SC} P}{P_{SC} ZT} q_e$$

When standard surface conditions are:  $P_{SC} = 0.101$  MPa,  $T_{SC} = 293$  K, and  $Z_{SC} = 1.0$ , Equation (11-14) is obtained:

(11-14)

$$q_{\max} = 0.04 \left( \frac{P}{ZT\gamma_g} \right)^{0.5} d^2$$

where:  $q_{\max}$  = gas production rate constrained by erosion flow velocity of gas well under standard surface conditions,  $10^4 \text{ m}^3/\text{d}$ .

**Example.** Wellhead tubing pressure and temperature are respectively 5.5 MPa and  $60^\circ\text{C}$ . The relative density of natural gas is 0.65 and gas deviation factor is 0.91. For 2 7/8-in. tubing with wall thickness of 5.51 mm, the gas production rate corresponding to tubing erosion flow velocity is as follows.

$$q_{\max} = 0.04 \left( \frac{5.5}{0.91 \times (273 + 60) \times 0.65} \right)^{0.5} \times (73 - 5.51 \times 2)^2 = 25.7 \times 10^4 \text{ m}^3/\text{d}$$

### Tubing and Casing Thread Corrosion and Corrosion Prevention Design

The threaded connections on tubing and casing strings are the first corroded positions. Under many conditions, tubing bodies can be used repeatedly. However, if the threads become corroded, threads should be made again by lathing, or the whole is abandoned.

### Thread Corrosion Mechanism

1. API round thread and buttress thread corrosion mechanism

When fluid passes through the middle part of the collar of tubing string, fluid flow velocity may be changed due to the increase and reduction of cross-section. Thus the following types of erosion and corrosion may be generated in this region: mechanical force erosion and corrosion (the impact of turbulent flow, suspending liquid droplet, suspending sand grain, and suspending gas bubble on wall face, or empty erosion and subsequent explosion); stress corrosion; crevice corrosion; galvanic corrosion; and phase change-induced corrosion.

The structure of flow channel in thread position is shown in Figure 11-17. The chart on the right shows the flow field obtained by numerical simulation.

2. Metallic-contact gas-tight thread failure mechanism

A gas well often adopts metallic-contact gas-tight thread; however, the problem of corrosion and seal failure in seal position is still presented. The end (nose) of gas-tight external thread is in compression contact with

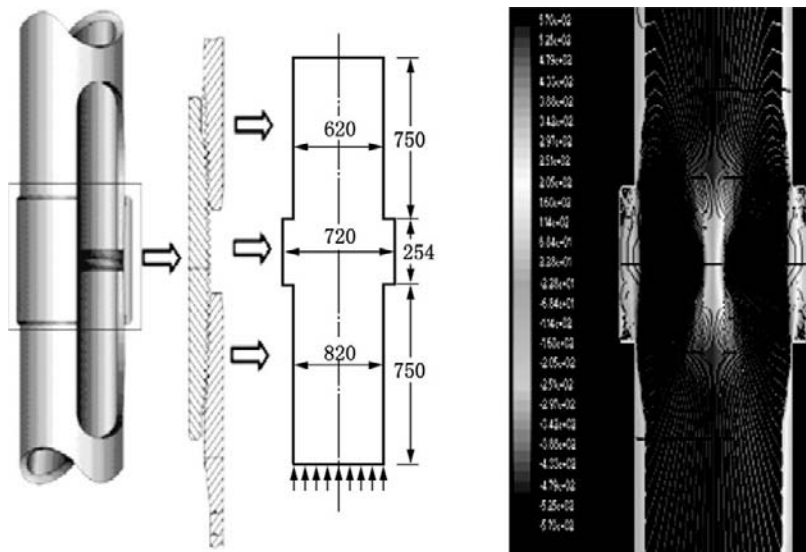


**FIGURE 11-17** The flow channel in the J ring region in the middle part of tubing collar.

the inside step of the collar. Some gas-tight external thread noses have slightly thin walls, and the contact stress levels may be higher than the yield strength of metallics. The local cold-rolled hardened position as the anode of coupled pair may aggravate corrosion. In addition, there is an electric potential difference between collar and pipe body due to different materials and different manufacturing technologies.

The end (nose) of gas-tight external thread after tightening thread is in a multidirectional stress state.

**Tubing Thread Selection and Anti-Erosion and Anti-Corrosion Design.** Thread is a position in which corrosion failure is first generated. Improving its resistance to corrosion can increase the service life of tubing by more than 100%.

#### 1. API standard thread

The modified structure (HUNTING) based on API thread has been obtained in order to prevent the flow and phase change-induced corrosion generated by the flow channel in the J ring region in the middle part of tubing collar, stress corrosion, and crevice corrosion (Figure 11-18).

A thrust ring is added in the J-ring region of API buttress thread, so that turbulent flow may not be generated in channel and excessive make-up torque is prevented (Figure 11-18a). The API round thread collar with inside thrust step may eliminate turbulent flow and prevent excessive make-up (Figure 11-18b). The API round thread collar with inside engineering plastics ring can prevent turbulent flow erosion and galvanic corrosion and reduce crevice corrosion (Figure 11-18c). The engineering plastics ring can have a greater deformation to suit different degrees of compaction. Plastics can be squeezed to pack the gap, thus increasing leakproofness. The engineering plastics ring can protect the inside coating at the end of external thread. For tubing with no inside coating, engineering plastics can be used for preventing turbulent flow erosion and galvanic corrosion. The direct compression at the end of external thread of API buttress thread may eliminate turbulent flow and prevent excessive circumferential stress on collar (Figure 11-18d).

#### 2. Galvanic corrosion spacer ring

Figure 11-19 shows the gas-tight thread and galvanic corrosion spacer ring structure.

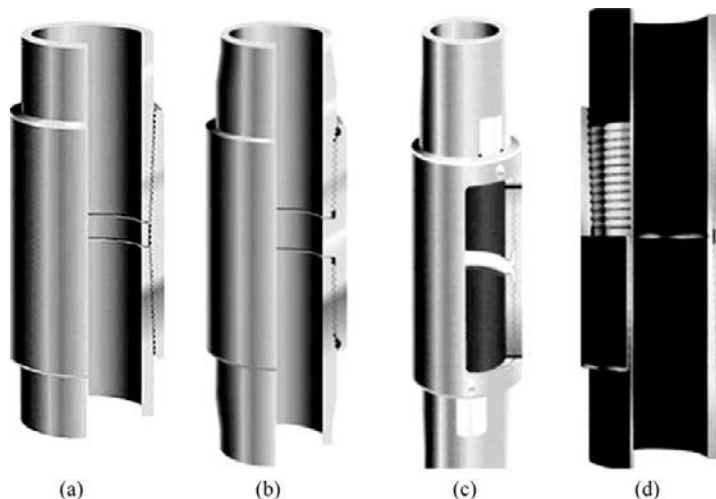
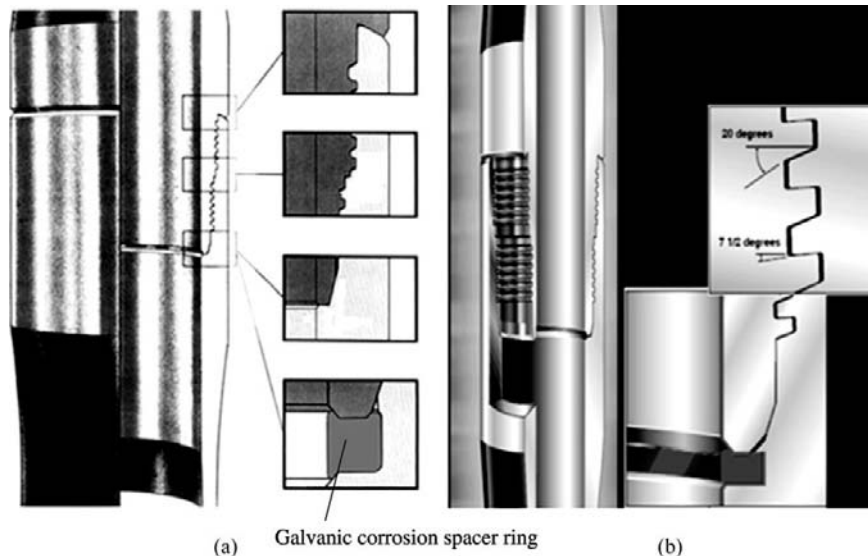


FIGURE 11-18 Modified structure (HUNTING) based on API thread.



**FIGURE 11-19** Gas-tight thread and nonmetallic spacer ring structure. (a) Gas-tight thread and spacer ring for preventing galvanic corrosion; (b) Gas-tight tubing thread with inside coating and nonmetallic spacer ring.

An engineering plastics spacer ring can prevent potential corrosion. The engineering plastics used have temperature resistance, creep resistance, and corrosion resistance. The engineering plastics ring can be replaced each time that tubing tripping is done.

**Optimizing Thread Structure and Reducing Local Stress Concentration of Thread.** The stress concentration and stress state of tubing and casing thread connection should be considered in design in light of sour environments. Excessive local stress concentration or excessive tensile stress value of the principal stress of VME (Von Mises equivalent) stress may increase stress cracking sensitivity.

1. Stress concentration of API standard round thread connection

When API standard round thread is used in sour environments of hydrogen sulfide, the collar may bear higher circumferential tensile stress or excessive local stress concentration; thus, longitudinal cracking may be generated. When API round thread is used, sealing is achieved by tight contact between

both sides of the thread. In order to obtain sufficient sealing pressure, the collar may generate circumferential tensile stress. Therefore, this type of thread is unsuitable for preventing stress corrosion cracking and electrochemical corrosion under sour environment conditions. There is a high stress concentration at the final perfect thread of external thread of API round thread. If the tubing-casing annulus is exposed to corrosive media, this point will be a stress cracking sensitivity point.

2. Thread structure suitable for hydrogen sulfide-containing gas well

Threads and connections are the weak links of tubing and casing. Designed pipe body stress should be lower than the environment fracture stress level. However, the stress level and stress concentration of thread and connection may be much higher than that of the pipe body. Non-API standard gas-tight thread generally adopts buttress thread or other special threads and has low circumferential stress of collar in comparison with API round thread. Reducing the stress

concentration coefficient and preventing excessive local tensile stress should be included in design considerations.

The threads and connections of tubing and casing for a hydrogen sulfide-containing gas well should meet the following requirements:

- a. The end of the external thread should be as thick as possible under the condition of meeting a certain contact stress and sealing. Excessive compressive stress may generate stress corrosion and boring.
- b. Tensile stress level should be reduced as far as possible because the collar bears tensile stress, so that stress cracking can be prevented. If an API standard collar cannot meet the requirement, heavy wall tubing and casing and a heavy wall collar should be adopted.

## Design of Preventing Galvanic Corrosion

**Universality of Galvanic Corrosion.** In oil and gas well production systems, there are various connections and various contacts between structural members. There is an electric potential difference between metals in varying degree. Thus galvanic corrosion has universality. The contact between structural members certainly has a crevice; thus, galvanic corrosion and crevice corrosion are often generated simultaneously and corrosion is then aggravated.

1. Connections that may generate strong galvanic corrosion

The connection between metals that have a great electric potential difference may generate galvanic corrosion, which means corrosion is aggravated on the anode end. In oil and gas well production systems, strong galvanic corrosion may make connections fail. These connections include connections between martensitic stainless steel (such as API 13Cr and Super 13Cr) or diphasic stainless steel (such as 22Cr, 25Cr, and 28Cr) tubing and low-alloy steel tubing. The corrosion of carbon steel or low-alloy steel tubing as galvanic anode is aggravated. When the

external thread at the end of carbon steel or low-alloy steel pipe is connected with the internal thread at the end of stainless steel pipe, the external thread may be seriously corroded due to the external thread cross-section area being less than the internal thread cross-section area.

Austenitic stainless steel (such as 304 and 316) is often used for making components and parts such as electric submersible pump, sucker rod pump, valve, rod, and packer. Their connection with carbon steel or low-alloy steel may also generate strong galvanic corrosion.

2. Connections that may generate weak galvanic corrosion

A high anti-corrosion alloy (such as nickel and titanium) may not generate a corrosion as strong as stainless steel when it is connected with carbon steel or low-alloy steel because of the low electric potential difference between anti-corrosion alloy corrosion product film and carbon steel or low-alloy steel.

Nickel and phosphor-plated, chrome-plated, or other electroplated and chemi-plated tubings should be prudently adopted in order to prevent aggravating the corrosion of other connections despite the fact that the tubing is protected. The connections between strings of different steel grades and the difference in material between pipe body and collar may generate weak galvanic corrosion. When the inner wall of tubing is scaled, steel as anode may generate subscale galvanic corrosion.

There also is an electric potential difference between the stress concentration position or local cold-rolled hardened position (such as tool marks and embossed stamp) of tubing, casing, or equipment and the adjacent metal. The corrosion of the stress concentration position or local cold-rolled hardened position as anode may be aggravated. This is one of the main reasons that the upset transitional zone of external upset tubing may generate corrosion boring.

If welding is used, the electric potential difference between welding seam area and base metal may be generated in electrolytic solution. Corrosion is first started from the welded line of root weld face, corrosion pits are formed, and then the local corrosion pits are developed into lineal corrosion.

### Measures of Preventing Galvanic Corrosion

1. Big anode–small cathode connection design  
For connections in which strong galvanic corrosion may be generated, the volume or mass of the possible corrosion side (anode) should be as big as possible, and the impossible corrosion side (cathode) can be small if structure space allows. The reduction of anode-side current density may mitigate corrosion. In addition, a big anode may reduce assembly stress and applied stress and may also reduce stress corrosion and increase load-bearing capacity and service life. Down-hole tubing and accessories may have connections between stainless steel and low-alloy steel. On the basis of the aforementioned principle, the external thread side should be made of stainless steel and the internal thread side (collar) should be made of low-alloy steel as far as possible. The wall thickness or diameter of the internal thread connection of low-alloy steel should be increased as far as possible if structure space allows.
2. Adding insulation material or seal packing to connection or contact between dissimilar metals  
Adding insulation mat or sleeve or seal packing to connection or contact between dissimilar metals can prevent or mitigate galvanic corrosion and stress corrosion. As long or thick insulation mat or sleeve as possible should be used if structure space allows.
3. Local sacrificial anode protection  
Spray coating, zinc plating, aluminum plating, or magnesium plating of anodes that have a tendency to be corroded can play a role in local protection. The electrons of zinc, aluminum, or magnesium flow to steel, thus reversing the original couple polarity.

This is also a local sacrificial anode protection technique and can only be used after its effectiveness is determined by experiment.

### Strength Design Safety Factor under Corrosive Environment Conditions

**Safety Factor Design Based on Critical Stress Percent.** The strength ratings of tubing and casing mean the strength values obtained in accordance with ISO 10400 or API 5C3. It should be noticed that the valuation of oil and gas well casing and tubing design safety factors under sour environment conditions is different from that under normal well conditions. The strengths of casing and tubing in ISO 10400 and API 5C3 are calculated in accordance with nominal yield strength, and the internal pressure design safety factor can be taken as 1.0. However, the performance of sulfide-resistant tubular goods only ensures the tensile stress value under which cracking may not be generated in a certain sour water solution environment of hydrogen sulfide. This stress value is known as critical environment fracture stress. The ratio of this value to yield strength of material is known as critical stress percent. Different casings have different critical stress percents, but they should not be lower than 80% at least. When the NACE Method A and A solution are used, it is specified that the sulfide stress cracking resistant critical stress of J55 and K55 casing bodies should be 80% of the yield strength of tubular goods. For L80, C90, and T95, the critical stress value should be 90% of yield strength. This is the evaluation criterion of material. For the critical stress percents of tubings and casings of higher steel grades, refer to the performance indices provided by manufacturer.

In order to ensure that the working stress is not higher than the critical stress of environment fracture, the internal pressure strengths of casing and tubing in ISO 10400 or API 5C3 should be multiplied by the critical stress percent (such as 0.8 or 0.9). On this basis the design safety factor is considered. For the steel grades of J55 and K55, if the internal pressure-resisting design

safety factor is 1.0, the actual design safety factor of environment fracture should be  $1.0/0.8 = 1.25$  at least.

The internal pressure-resisting design safety factors of production casing, intermediate casing, and tubing should be taken in accordance with the aforementioned method, and the compensation of external pressure or cement sheath for internal pressure strength should not be considered. In the Canadian hydrogen-sulfide sour oil and gas well casing and tubing design standards, it is specified that the internal pressure-resisting safety factor should be higher than 1.35 under  $\text{CO}_2$  partial pressure higher than 2000 kPa and  $\text{H}_2\text{S}$  partial pressure higher than 0.34 kPa.

### Safety Factor Design Based on Critical Environment Fracture Toughness $K_{\text{ISSC}}$

#### 1. Fracture safety factor

As mentioned earlier, if applied stress is reduced to a certain value, cracks may not be destabilized despite the fact that crack propagation is generated when material has worked for a sufficient time in a corrosive medium. The stress intensity factor in this state is known as the critical environment stress intensity factor in some corrosive media or the critical environment fracture toughness  $K_{\text{ISSC}}$  in some corrosive medium. The ratio of the critical environment fracture toughness  $K_{\text{ISSC}}$  to the stress intensity factor  $K_I$  under external load is just the design safety factor based on critical environment fracture toughness  $K_{\text{ISSC}}$  and is known as the fracture safety factor. The NACE dual cantilever beam (DCB) test provides the method and criterion for evaluating the critical environment fracture toughness  $K_{\text{ISSC}}$  of material. Increasing the environment fracture safety factor requires increasing critical environment fracture toughness  $K_{\text{ISSC}}$  and reducing the stress intensity factor as far as possible. The safety factor design based on critical environment fracture toughness  $K_{\text{ISSC}}$  is complicated and more test data are required. The following qualitative analysis is of a certain value to increasing the fracture safety factor.

#### 2. Measures for increasing environment fracture toughness $K_{\text{ISSC}}$

a. Noticing temperature sensitivity of environment fracture. Table 11-4 shows the temperature condition of cracking resisting of carbon steel and low-alloy steel. It is a material selection criterion based on experience and cannot be used for quantitative calculation of strength. For a low carbon alloy steel with yield strength of 805 MPa (117 ksi) and hardness of HRC 27.2, the effect of temperature on critical environment fracture toughness  $K_{\text{ISSC}}$  is shown in Figure 11-20. When temperature is reduced by  $10^\circ\text{C}$ ,  $K_{\text{ISSC}}$  may be reduced by about  $5 \text{ ksi} \cdot \text{in}^{1/2}$ . For the tubing and casing sections near the wellhead and manifold, it should be especially noted that a reduction of environment fracture toughness  $K_{\text{ISSC}}$  may cause fracturing during shut-in, cold fluid injection, or refrigeration due to the change in phase behavior.

For stainless steel and corrosion-resistant alloy, chloride or other halide ( $\text{F}^-$ ,  $\text{Br}^-$ , and so on) stress cracking is mainly generated in high-temperature environments.

b. Reducing initial surface defects. During manufacture of tubing and casing, there may be initial surface defects such as seams, folds, cracks, and tool marks. The local plastic strain of the crack tip may cause high lattice dislocation density, thus

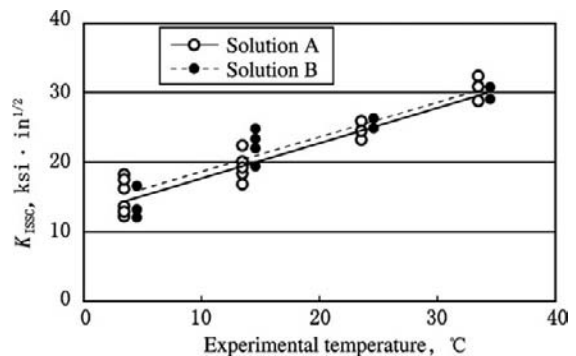


FIGURE 11-20 Cracking resistance of some metallic material.

leading to a high intake of hydrogen and an accumulation of hydrogen. Thus the control of crack is crucial. ISO 11960 divides the maximum allowable depths of these surface defects into the following two groups:

- (1) The maximum allowable depth of surface defect is less than 12.5% of wall thickness. It is suitable for normal service environments, and the appropriate steel grades include H40, J55, K55, 2M65, N80 Type 1, N80Q, L80, C95, and P110.
- (2) The maximum allowable depth of surface defect is less than 5.0% of wall thickness. It is suitable for important service environments, and the appropriate steel grades include C90, T95, P110, and Q125.

This classification standard is a compromise proposal between user and manufacturer. For any steel grade used in gas wells and sour environments, the maximum allowable depth of surface defect should be less than 5.0% of wall thickness. When the maximum allowable depth of surface defect is less than 5.0% of wall thickness, the internal pressure strength can be calculated in accordance with the criteria of yield and toughness fracture. However, when the maximum allowable depth of surface defect is greater than 5% of wall thickness and less than 12.5% of wall thickness, the internal pressure strength is calculated in accordance with crack destabilization and fracture and the internal pressure strength is lower than the internal pressure strength calculated in accordance with the yield criterion. The greater the crack depth, the greater the stress intensity factor and the lower the fracture safety factor.

To reduce the initial defects to the full extent also favors the protection of tubing and casing during downhole

operations. In particular, for deep wells and sour oil and gas wells, the letting-in tool scratching, pipe expanding, impact-induced cracking, and initial crack propagation that may be generated during downhole operations in production casing should be considered.

- c. Adopting thick-wall tubing and casing made of low-strength material. If thin-wall tubing and casing of high-strength steel and thick-wall tubing and casing of low-strength steel have the same strength safety factor, in the sense of environment fracture, thick-wall tubing and casing of low strength steel should be predominantly adopted. Thick-wall tubing and casing of low-strength steel can obviously reduce the sensitivity of material to hydrogen embrittlement and crack propagation; that is, they have higher critical environment fracture toughness  $K_{ISSC}$ .

## Design of Reducing Stress Level

**Concept of Stress Level.** Stress level includes the following three types:

1. Structural VME (Von Mises equivalent) stress, that is, structural equivalent compound stress, such as the equivalent compound stress of tubing or casing body under tensile load, compressive load, bending load, internal pressure, and external pressure, which is calculated in accordance with ISO 10400.
2. Local VME (Von Mises equivalent) stress, which mainly means stress concentration. High stress concentration may be generated at tubing thread and upset vanishing point.
3. Residual tensile stress, which is related to manufacture method. ISO 15156 has specified the requirements of eliminating residual stress under different manufacture methods.

Stress level can also be expressed as a dimensionless number, that is, the ratio of VME stress to the minimum yield strength under the condition of unilateral stretch of steel material.

Reducing the stress level is one of the most important design criteria under the environment condition of sulfide, chloride, and carbon dioxide. High-pressure gas wells may have higher internal pressure, and the tubing and casing in the upper part of the well may bear higher tensile stress.

The upset transitional zone of external upset tubing may often generate corrosion boring due to the stress concentration caused by the change of cross-section in the upset transitional zone. A rational change of geometric cross-section can reduce the stress concentration coefficient to 1.00. However, the local metallographic texture failure generated during end upset cannot be certainly eliminated by heat treatment. Cold compression upset with no subsequent heat treatment may leave serious crystalline granular texture failure zone, stress concentration, and residual stress. Corrosion may be aggravated in this zone, which is as the anode of galvanic corrosion. Hot compression upset and subsequent heat treatment may also leave local crystalline granular texture failure and residual stress due to improper technology or insufficiently strict quality control.

**Importance of Reducing Working Stress Level.** Reducing the stress level of a structure can increase the cracking resistance of material in sour environments or prolong the service life. Under low stress levels, crack propagation velocity is reduced or fracturing time is prolonged. Under low stress levels, material can resist higher partial pressure of hydrogen sulfide; however, under high stress levels, material fracturing may be generated even if the partial pressure of hydrogen sulfide is low. In a hydrogen sulfide environment, under the condition of cracks in the member, fracturing may also be generated even though the applied stress is lower than the yield strength of material. In accordance with NACE MR 0175-88 and ARP (Alberta recommended practices) 1.6 and 2.3 and the related studies, the relations between stress level, hydrogen sulfide content, and steel grade are as follows.

1. Low hydrogen sulfide content and stress level. Under a hydrogen sulfide content lower

than 0.5 mol% and stress level lower than 50%, any API tubular goods lower than 110 ksi can be selected. However, when hydrogen sulfide content is up to 10 mol%, the stress level should be reduced to 30%.

2. Medium hydrogen sulfide content and stress level. When hydrogen sulfide content is up to 2.0 mol%, API sulfide-resistant steel grade should be adopted and stress level is up to 70%. When hydrogen sulfide content is up to 20 mol%, stress level should be reduced to 60%.
3. High hydrogen sulfide content and stress level. When hydrogen sulfide content is up to 5.0 mol%, API sulfide-resistant steel grade should be adopted, and stress level is up to 90%. When hydrogen sulfide content is higher than 20 mol%, the stress level should be reduced to 70%. If the stress level is higher than 90%, the design is unacceptable.

**Hole Structure Design of Reducing the Stress Level.** Improving the hole structure design is the most effective method for reducing stress level. There are the following three approaches to reducing the stress level:

1. Casing tie-back. Running in the whole casing string (especially production casing) in deep wells may generate high axial tensile force near the wellhead, and a casing of high steel grade is required. However, under sour environment conditions, a casing of high steel grade is not allowable and a steel grade with low yield strength should be adopted. When the casing tie-back technique is used, the liner is run in on drill pipe. Running in tie-back casing can reduce the gravity in a part of the section; thus, a thick-wall casing of low steel grade can be used for increasing stress corrosion cracking resistance. For instance, some production casings will not use C125 or above, and C95 or L80 can be used after the casing tie-back technique is adopted. The stress distribution of the whole casing string should be comprehensively considered when liner length is determined.
2. Using ultrathick-walled casing of low steel grade in the upper part to increase sulfide cracking

resistance. Some hydrogen sulfide-containing gas wells should predominantly use this method. For instance, in some gas wells, 6 5/8 in. (168 mm) production casing was run in and high-strength casing was unsuitable due to hydrogen sulfide; thus, ultra-thick-walled casing of which the yield strength is only 586 MPa and the wall thickness is 28.6 mm was adopted.

3. Tapered casing and tubing strings with large diameter in the upper part and small diameter in the lower part may not only be favorable for reducing stress level to use the casing of lower steel grade, but they may also be favorable for running in large-diameter tubing to meet the requirement of the erosion resistance of a high-productivity gas well.

For production casings in hydrogen sulfide-containing gas wells and high-pressure gas wells, stage collar should not be used for cementing due to the following:

1. The casing above the stage collar has a high stress level, and high-strength sulfide-resistant material is difficult to select. A high stress level reduces the safety allowance.
2. The internal pressure strength and seal pressure of the stage collar are much lower than that of the casing. When tubing packer failure or tubing leak or fracture is generated, stage collar may generate leak or rupture.
3. Under most conditions the cement sheath outside the stage collar has a low quality or set cement is not formed; thus, the channeling of corrosive fluid in the annulus may generate external casing corrosion, and leak or rupture may be caused.

If lost circulation may be generated during cementing, a tie-back technique should be designed.

### Christmas Tree Corrosion

A Christmas tree consists of valves, flanges, tubing hanger, spools, adapter bonnets, bent pipes, throttling valve, and so on. They are the

TABLE 11-10

**Christmas Tree Corrosion Grade Division (API SPEC 6A)**

Category of Material	Working Condition
AA	No corrosion in normal environment
BB	Slight corrosion in normal environment
CC	Medium-high corrosion in normal environment
DD	No corrosion in sour environment
EE	Slight corrosion in sour environment
FF	Medium-high corrosion in sour environment
HH	Serious corrosion in sour environment

key components controlled by pressure. For a high-pressure gas well, the erosion and corrosion of high-pressure components may have serious consequences. The key to Christmas tree corrosion control lies in proper lectotype. In light of different corrosion environments, the corresponding categories of Christmas tree should be selected (Table 11-10).

In high-productivity gas wells that contain carbon dioxide, the outstanding problems include flow-induced corrosion and erosion. The Christmas tree and manifold system have bent pipes, changes of flow channel cross-section and throttling device, and so on. A Y-shaped Christmas tree is selected if necessary in order to avoid a right-angle bend. Stainless steel or alloy steel is used in the positions that erode easily.

## 11.5 TUBING AND CASING CORROSION PREVENTION FOR SOUR GAS RESERVOIRS

Tubing and casing corrosion control for sour gas reservoirs is a type of system engineering. Metal material or corrosion inhibitor alone cannot achieve the desired corrosion control effectiveness, and corrosion-resistant material (metal

and nonmetal), chemicals, cathodic protection, and coating should be comprehensively applied. In oil and gas fields, the application of corrosion-resistant metal material has obtained obvious effectiveness in combination with corrosion inhibitor.

## Main Types of Tubing and Casing Corrosion for Sour Gas Reservoirs

### Hydrogen Sulfide Corrosion

1. The dissolution of anode iron in the process of electrochemical reaction may cause comprehensive corrosion or local corrosion including wall thickness reduction and pitting corrosion boring of metallic tubing, casing, facilities, and pipeline.
2. In the process of electrochemical reaction, hydrogen atoms are precipitated from cathode. The hydrogen atoms that cannot be combined into hydrogen molecules due to the existence of  $H_2S$  enter steel and cause hydrogen embattlement and  $H_2S$  environment cracking, including sulfide stress cracking (SSC), hydrogen-induced cracking, hydrogen blistering, and stress-guided hydrogen-induced cracking.

Practice indicates that hydrogen sulfide stress cracking is one of the highest potential risks during oil and gas well production in sour environments. "The sulfide stress cracking resistant metal material of oil field equipment" in NACE MR0175 and "The sulfide stress cracking resistant metal material requirements of natural-gas surface facilities" in SY/T 0599-1998 have specified  $H_2S$ -containing sour oil and gas environments that may generate SSC. In accordance with "The recommended practices of hydrogen sulfide-containing oil and gas production and natural gas treatment plant operations" in API RP55 or NACE MR0175, the following systems are known as sour environments:

- a. Sour natural gas system

Water- and  $H_2S$ -containing natural gas is known as sour natural gas when total absolute gas pressure is higher than or

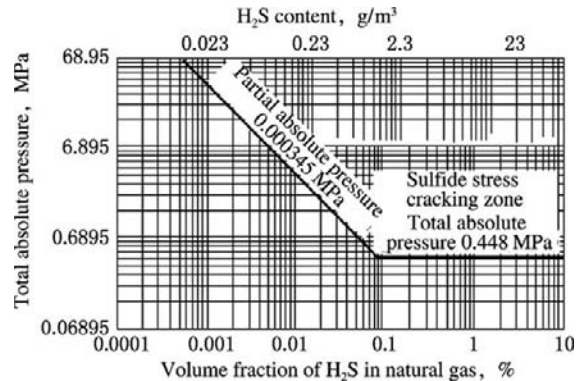


FIGURE 11-21 The sulfide stress cracking zone of sour natural gas system.

equal to 0.4 MPa and the partial absolute pressure of  $H_2S$  in natural gas is higher than or equal to 0.00034 MPa. Sour natural gas may cause the sulfide stress cracking of sensitive natural (Figure 11-21).

- b. Sour natural gas-oil system

When the ratio of natural gas to oil is higher than  $890 \text{ m}^3/\text{m}^3$ , whether sulfide stress cracking may be generated should be determined in accordance with the criterion in (1). When the ratio of natural gas to oil is equal to or lower than  $890 \text{ m}^3/\text{m}^3$  ( $1000 \text{ m}^3/\text{t}$  or  $5000 \text{ ft}^3/\text{bbl}$ ), the sulfide stress cracking of sensitive material may be generated if one of the following conditions is met (Figure 11-22):

- (1) The total absolute pressure of the system is higher than 1.8 MPa and the partial absolute pressure of  $H_2S$  in natural gas is higher than 0.00034 MPa.
- (2) The partial absolute pressure of  $H_2S$  in natural gas is higher than 0.07 MPa.
- (3) Volume fraction of  $H_2S$  in natural gas is greater than 15%.

In the Sichuan basin, the DL 101 well, which produces both oil and gas, has a gas-oil ratio of  $48 \text{ m}^3/\text{m}^3$ , hydrogen sulfide content of 0.0312%, and bottomhole pressure of 12.5 MPa. Thus the partial pressure of  $H_2S$  in the gas phase is  $12.5 \text{ MPa} \times 0.0312\% = 0.0039 \text{ MPa}$ , the gas-oil ratio ( $48 \text{ m}^3/\text{m}^3$ ) is lower than  $890 \text{ m}^3/\text{m}^3$ , the total

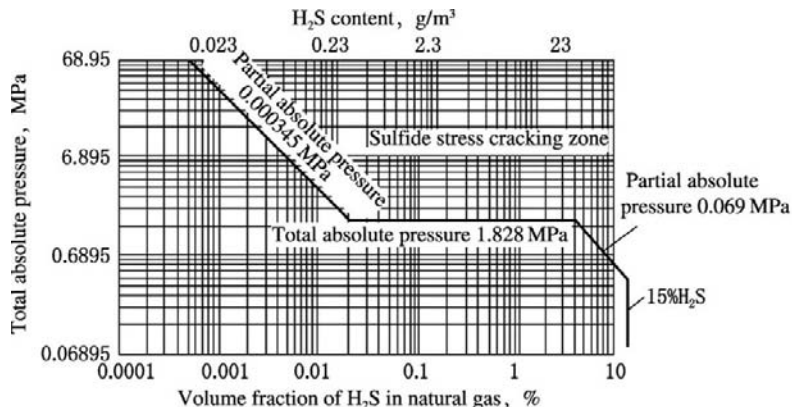


FIGURE 11-22 The sulfide stress cracking zone of sour natural gas-oil systems.

pressure of the system (12.5 MPa) is lower than 1.8 MPa, and the partial pressure of  $H_2S$  (0.0039 MPa) is higher than 0.00034 MPa. On the basis of these data, the following are determined:

1. When the downhole oil-gas system of the well does not contain water, the downhole environment is not a sour environment, the sulfide stress cracking of steel will not be generated, and standard equipment can meet the requirements.
2. When the downhole oil-gas system of the well contains water, the downhole environment is a sour environment and the sulfide stress cracking of material may be generated; thus, the sulfide stress cracking of downhole metal material used in the downhole facilities of the oil-gas system in the well should be considered.

**Carbon Dioxide Corrosion.** Dry carbon dioxide may not cause galvanic corrosion. Galvanic corrosion may be generated when carbon dioxide coexists with water and is dissolved in water to form carbonic acid. The partial pressure of  $CO_2$  may greatly affect the corrosion rate of  $CO_2$ . When the partial pressure of  $CO_2$  is high, the concentration of carbonic acid in water is high and the concentration of hydrogen ions decomposed from carbonic acid is certainly high, thus speeding up corrosion. In accordance with the related standard in NACE  $CO_2$  corrosion environments are divided as follows.

1. When the partial pressure of  $CO_2$  is lower than 0.021 MPa, the environment has no corrosiveness and no measures of  $CO_2$  corrosion prevention are required.
2. When the partial pressure of  $CO_2$  is between 0.021 MPa and 0.21 MPa, the environment has general corrosiveness and corrosion prevention should be considered.
3. When the partial pressure of  $CO_2$  is higher than 0.21 MPa, the environment has serious corrosiveness and special corrosion-resistant material is required.

In the He 100 well of the Sichuan basin, bottomhole pressure  $p = 37.5$  MPa and  $CO_2$  content is 1.143%; thus, the partial pressure of  $CO_2$  is as follows.

$$p_{CO_2} = p \times CO_2\% = 37.5 \text{ MPa} \times 1.143\% = 0.43 \text{ MPa} > 0.21 \text{ MPa}$$

The calculation indicates that serious carbon dioxide corrosion may be generated in the well. The tubing between 1100 m and 1500 m has breakpoints due to serious carbon dioxide corrosion and the corrosion holes have  $CO_2$  precipitation. The first breakpoint is at 1099.5 m. The break opening is irregular. The reduction of wall thickness due to corrosion is about 3 mm. The tubing body has six corrosion holes with the greatest diameter of 20 mm. The inner wall has a quantity of pits and small holes similar to sack holes. In addition, in 1099.5–1189.45 m (length

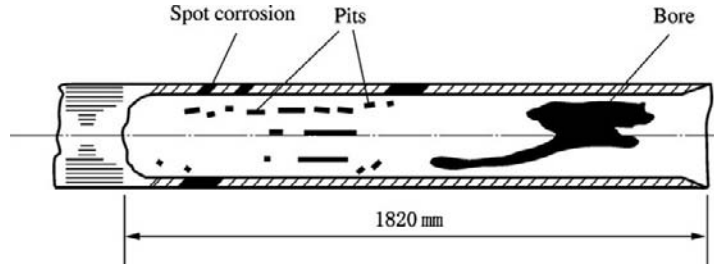


**FIGURE 11-23** Carbon dioxide corrosion boring in the He 100 well of the Sichuan gas field.

is 89.95 m), the breakpoint is at 1189.45 m, the upper break opening is longitudinally split along the tubing (length is 1.8 m), and the end is rusted and is irregular in shape. There are two swollen corrosion holes with thinned wall and a quantity of internal pits, some of which had been bored (Figure 11-23).

**Corrosion under Coexistence of H<sub>2</sub>S and CO<sub>2</sub>.** In general, hydrogen sulfide-containing natural gas also contains a certain quantity of carbon dioxide. For instance, for the Ordovician gas reservoir in the Tazhong I zone, both carbon dioxide and hydrogen sulfide corrosion should be considered, and corrosion-resistant material is required in the light of the partial pressures of hydrogen sulfide and carbon dioxide (Table 11-11).

In recent years, economical H<sub>2</sub>S/CO<sub>2</sub> corrosion-resistant low-alloy steels have been developed. In addition, protective coating and corrosion inhibitor are also required. The H<sub>2</sub>S/CO<sub>2</sub> corrosion control techniques should be

evaluated and optimized. Whether downhole strings and surface equipment and pipelines adopt expensive corrosion-resistant material or coating protection should be determined when the development of oil and gas reservoirs is started. In particular, for offshore oil and gas reservoir development, improper initial measures are difficult to remedy. Therefore, when an oil and gas reservoir development program is formulated, the future corrosion severity should be predicted and economical corrosion-resisting measures should be determined on the basis of the data of one or two wells drilled first.

**Corrosion Due to Water and Other Factors.** Despite the fact that H<sub>2</sub>S/CO<sub>2</sub> is the most severe corrosion factor for the facilities of sour oil and gas fields (especially hydrogen sulfide, which may not only generate abrupt sulfide stress cracking of metal to cause great economic loss but also have toxicity that may threaten personal safety), the corrosion action of mineralized water cannot be underestimated. Water plays a

**TABLE 11-11**

**Partial Pressures of H<sub>2</sub>S and CO<sub>2</sub> in Some Drilled Wells of Ordovician Gas Reservoir in Tazhong I Zone**

Well No.	Reservoir Pressure (MPa)	H <sub>2</sub> S Content (%)	Partial Pressure of H <sub>2</sub> S (MPa)	CO <sub>2</sub> Content (%)	Partial Pressure of CO <sub>2</sub> (MPa)
TZ82	63.164	0.011	0.007	3.42	2.160
TZ622	47.2	0.15	0.071	4.21	1.987
TZ62-1	57.17	0.001	0.0006		
TZ621	57.253	0.034	0.019	2.7	1.546
TZ62-2	55.636	0.230	0.128	2.29	1.274
TZ44	59.4	0.092	0.055		
TZ62	57.835	0.200	0.156	3.14	1.816

leading role in the process of the corrosion of metal material especially under the specific operating conditions of oil and gas fields.

Sour oil and gas field development indicates that in the initial production period of a sour natural gas well, sulfide stress cracking resistant materials based on NACE MR0175 have slight uniform corrosion and spot corrosion due to the low water production rate. With the increase of production time and water production rate, the hydrogen-induced cracks are increased and corrosion is also aggravated. Especially in water accumulation positions, the local reduction of wall thickness and the rate of boring due to the corrosion are sometimes astonishing.

The leading action of water in the process of corrosion includes the following:

1. Water is the necessary and sufficient condition of electrochemical corrosion. The hydrogen sulfide and carbon dioxide corrosion of steel material is essentially electrochemical corrosion. Electrochemical reaction leading to corrosion may be generated only after hydrogen sulfide and carbon dioxide are dissolved in water. Furthermore, hydrogen atoms are released when hydrogen sulfide and carbon dioxide are dissolved in water. The hydrogen atom is a strong depolarizer. It may reduce after catching electrons and promote anode iron to dissolve, thus leading to corrosion.
2. The strong solubility of  $H_2S$  and  $CO_2$  in water may aggravate the severity of corrosion. Hydrogen sulfide and carbon dioxide have high solubility in water. In particular, the saturation concentration of hydrogen sulfide in water is about 3580 mg/l under a

pressure of 760 mmHg at 30°C. The studies indicate that the aqueous solution in which salts, spent acid, hydrogen sulfide, and carbon dioxide are dissolved has a much higher corrosiveness than single hydrogen sulfide or carbon dioxide. The corrosion rate is several dozen or even several hundred times the corrosion rate of hydrogen sulfide or carbon dioxide. In a gas-water diphasic sour system, water is highly harmful.

3. The  $Cl^-$  in formation water may generate serious corrosion of metal. The higher the chlorion concentration, the higher the corrosion rate (especially when chlorion concentration is higher than  $3 \times 10^4$  mg/l). The reason is that the adsorption of chlorion on the metal surface may retard the formation of a  $FeCO_3$  protective film. When chlorion concentration is lower than 50,000 mg/l, common 13Cr can be adopted to prevent carbon dioxide corrosion. When chlorion concentration is higher than 50,000 mg/l, Super 13Cr should be adopted in order to prevent carbon dioxide corrosion.

In most of the wells of the Tazhong 62 and 82 wellblocks, water production has been generated during production tests (Table 11-12). The chlorion concentration is higher than  $4.8 \times 10^4$  mg/l. Water cut is increased with continuous production. In the Tazhong 62-3 well, the daily water production is 11 t. The spot corrosion generated by chlorions in high-salinity formation brine may lead to stress corrosion in various forms.

In the Tazhong 62 and 82 wellblocks, the chlorion concentration in formation water is  $(3.28 \text{ to } 8.49) \times 10^4$  mg/l. The chlorions in

**TABLE 11-12 Formation Water Data of Tazhong 62 and 82 Wellblocks**

Wellblock	Well No.	pH	Relative Density	Cation Concentration (mg/l)			Anion Concentration (mg/l)			Total Salinity (mg/l)	Type of Water
				$K^+ + Na^+$	$Mg^{2+}$	$Ca^{2+}$	$Cl^-$	$SO_4^{2-}$	$HCO_3^-$		
TZ62	TZ622	7.12	1.0646	23000	1695	6176	48900	2779	637	85100	$CaCl_2$
	TZ62	7.05	1.071	36100	439	3029	61900	492	96	110000	$CaCl_2$
TZ82	TZ82	7.18	1.0727	38500	291	3637	65300	1110	941	110000	$CaCl_2$

water have corrosion action on steel and may promote carbon dioxide corrosion; thus, the condition of water production should be considered when the measures of corrosion prevention are formulated, and the effect of chlorion concentration should be considered when carbon dioxide corrosion-resistant material is selected.

It should especially be noticed that in the initial production period, the water steam in natural gas produced from a gas well that has not produced formation water may also speed up the hydrogen sulfide and carbon dioxide corrosion of pipelines and valves. In general, corrosion is more serious at the dew point of water steam. Under reservoir conditions, natural gas often contains a certain quantity of water steam. During the production of natural gas, the water-containing saturated steam in natural gas may be decreased with the reduction of temperature and pressure, and condensate water may be generated when temperature is reduced to dew point. If natural gas contains corrosive components (such as carbon dioxide), corrosion may be generated under appropriate conditions. The Yaxa condensate gas field is a typical example. In addition, during oil and gas production, the acid treatment of low-permeability reservoirs is sometimes required, and the residual downhole inorganic acid may reduce the pH value of produced fluid. In specific positions, strong corrosive hydrogen sulfide may be generated due to the activities of microorganisms (especially sulfate-reducing bacteria). During operations such as well servicing and adding chemicals, oxygen may be entrained to the downhole. These factors may speed up the course of sour oil and gas corrosion.

### Corrosion Prevention Technology Selection and Tubing and Casing Material Adaptability Evaluation

The natural gases of many gas reservoirs contain a certain quantity of hydrogen sulfide and carbon dioxide and there is stress corrosion and electrochemical corrosion generated by sour gas. Therefore, the tubings and casings selected

and used in sour gas-containing gas wells should be made of sour media-resistant steel, or corrosion inhibitor is added (Table 11-13).

#### Corrosion-Resistant Alloy Steel Tubing

1. Advantages of corrosion-resistant alloy steel corrosion control technology

For high-productivity wells in the main position, corrosion-resistant alloy steel tubing should be selected in order to ensure the long-term safety and stable production of the gas well, ensure stable gas supply, avoid well servicing as far as possible, and prolong the workover-free period of gas wells. Using corrosion-resistant alloy steel tubing has the following advantages:

- No need for corrosion inhibitor adding system
- Relatively high strength and thin tubing wall, which make corrosion-resistant alloy steel tubing have a relatively large inside diameter and high throughput capacity in comparison with carbon steel tubing under the same outside diameter
- The tubing life, which is almost same as well life
- High reliability during service time
- Higher quality than that of low-alloy steel tubing
- No need for corrosion monitoring
- No need for corrosion inhibitor adding and transport

2. Corrosion-resistant alloy steel classification

Corrosion-resistant alloy steels mainly include martensitic stainless steel, diphasic martensite-ferrite steel, austenitic stainless steel, and nickel-based alloy steel.

- Martensitic stainless steel. The 13% Cr steel and Super 13% Cr steel are commonly used under the condition of carbon dioxide, under which carbon steel cannot meet the requirement.

Usable conditions:

- $H_2S$  partial pressure  $P_{H_2S} < 0.01$  MPa
- Temperature  $< 150^\circ$  (empirical value)
- No oxygen (pitting corrosion may be generated when corrosion inhibitor is added)

TABLE 11-13 Adaptability Analysis of Various Corrosion Prevention Techniques

Corrosion Control Technique	Advantage	Disadvantage	Adaptability
Corrosion-resistant alloy steel	No need for adding corrosion inhibitor and no need for corrosion monitoring. High reliability and stability during production.	High total investment. Galvanic corrosion during connection with carbon steel pipe.	Appropriate for high-productivity gas wells in harsh corrosive environments.
High sulfide-resistant steel	Low cost. Reliable resistance to SSC.	Need for adding corrosion inhibitor.	Appropriate for harsh corrosive environment.
Common sulfide-resistant steel	Low cost.	Need for adding corrosion inhibitor.	Appropriate for lower productivity gas wells in slightly corrosive environments.
Internal coating tubing	Minimizing corrosion of tubing and casing by both internal coating tubing and packer.	High cost. Imperfect protection at connector. No resistance to impact.	Inappropriate for the condition of no resistance to impact.
Internal glassfiber reinforced plastics liner tubing	High resistance to corrosion.	Used in a certain temperature range. Need for special connector.	Inappropriate for the high-temperature condition of deep gas well.
Bimetallic combination tubing	Minimizing corrosion of tubing and casing by both bimetallic combination tubing and packer.	Complicated technology. Need for special connector.	J55/304 bimetallic combination tubing technique has been proven. P110/825 and SM2535 bimetallic combination tubings are in test stage.
Corrosion inhibitor	Adding a small quantity of corrosion inhibitor in corrosive media to reduce corrosion rate of metal. Low initial investment. No need for continuous adding.	Inability to prevent external casing corrosion. Complicated technology. Obvious influence on production.	Appropriate for low-productivity gas wells in slightly corrosive environment.

13Cr Grade 95 steel is used in more harsh environments. Under the same partial pressure of  $H_2S$  and at a higher temperature, steel that has a higher yield strength can be adopted.

- b. Diphasic martensite-ferrite steel, mainly 22% Cr steel, 25% Cr steel, and Super 25% Cr steel.

Usable range: High-temperature wells that contain carbon dioxide and a small quantity of hydrogen sulfide.

Use conditions: Carbon dioxide corrosion, which martensitic stainless steel cannot deal with.

- (1) Steel with a higher strength can be used and a higher downhole temperature is allowed.
- (2) It should have a higher resistance to  $Cl^-$  and  $O_2$ .

Restriction conditions:

- (1) Partial pressure  $P_{H_2S} < 0.02$  MPa (yield strength should also be considered).

- (2) Temperature < 200°C.
- (3) A small quantity of O<sub>2</sub> or no O<sub>2</sub> and no H<sub>2</sub>S.
- (4) Usable material grade: 448–965 MPa.
- c. Austenitic stainless steel. Only the 28% Cr steel.
  - Use conditions: Coexistence of CO<sub>2</sub>, H<sub>2</sub>S, and Cl<sup>-</sup>, temperature < 204°C.
- d. Nickel-based alloy steel. Incoloy 825 and 925, SM2535, Hastelloy G3, G50, and C276.

Use conditions: Very strong corrosiveness under the combination of H<sub>2</sub>S, Cl<sup>-</sup>, and temperature and also existence of free sulfur.

**High Sulfide-Resistant Steel Tubing.** In the Chuanyu gas field, the SSC resistances of HP13Cr tubing, L80 tubing, and high sulfide-resistant NT80SS tubing have been evaluated in the light of the corrosive environment of the Luojiashai gas field, and the electrochemical weight-loss corrosiveness has been evaluated. The chemical compositions and mechanical properties of these steels are listed in Table 11-14.

In the light of the downhole environments of the Luojiashai and Dukouhe gas fields, it is determined that test pressure is 32 MPa, test temperature is 40–100°C, H<sub>2</sub>S content in natural gas is about 15%, and CO<sub>2</sub> content is about 10%. A distilled water solution of 10% NaCl was formulated for testing on the basis of the water analysis data of the Du 5 well and Luojiashai 8 well. The contents of the main ions are: K<sup>+</sup> = 992 mg/l, Na<sup>+</sup> = 14,811 mg/l, HCO<sub>3</sub><sup>-</sup> = 1665 mg/l, SO<sub>4</sub><sup>-</sup> = 3154 mg/l, Cl<sup>-</sup> = 20,429 mg/l. pH = 8.0. The test data are listed in Tables 11-15 and 11-16.

In accordance with NACE MR 0175, the Sumitomo metal corrosion resistance classification standard (Table 11-17), and SY/T 5329-1994, the corrosion rate of working fluid should be lower than 0.076 mm/a. Tables 11-15 and 11-16 indicate that the SSC resistance of HP13Cr steel tubing cannot meet the use performance requirements of the Luojiashai high sour gas field, while the SSC resistance of L80 and NT80SS steel tubing can meet the use

requirements of the Northeast Sichuan high sour gas field; however, the electrochemical corrosion resistance of L80 steel cannot fully meet the use requirements of the Northeast Sichuan high sour gas field. The corrosion rate in vapor phase is 0.74 mm/a and the corrosion rate in liquid phase is 0.48 mm/a.

The corrosion rates of downhole L80 steel at different temperatures in a corrosive environment that simulates the Luojiashai gas field water are shown in Figures 11-24 and 11-25.

The test data indicate that the liquid-phase corrosion rates of the three types of steel are close. The reason is that in a liquid-phase environment, the coupon surface is enveloped by continuous liquid film and a corrosion product film may be formed, thus protecting the coupon surface.

In a gas-phase environment, with the increase of temperature, NT80SS has the lowest gas-liquid electrochemical corrosion rate, which is related to the chemical composition of NT80SS. NT80SS easily forms a protective film in comparison with the other steels.

The preceding evaluation test results indicate that the Ordovician gas reservoir in the Tazhong I zone can adopt SS steel tubing, but corrosion inhibitor should be added during use.

### Common Sulfide-Resistant Steel Tubing

1. Application of common sulfide-resistant steel tubing to Zhongba Leisan condensate gas reservoirs in the Sichuan basin

The Zhongba Leisan gas reservoir was put into production in March 1982. The buried depth of the gas reservoir is 3140–3510 m. The gas reservoir is an enclosed limited dolomite gas reservoir with edge water and a lower elastic energy. The original reservoir pressure is 35.304 MPa and reservoir temperature is 89°C. The original water saturation is 8% to 25%. This gas reservoir is a condensate gas reservoir with a high hydrogen sulfide content and low gas condensate content. The relative density of natural gas is 0.657–0.686. The content of hydrogen sulfide is 4.90% to 7.75% and the content of carbon dioxide is 4.18% to 5.82%. The edge

TABLE 11-14 Chemical Composition and Mechanical Properties of HP13CR Steel, NT80SS Steel, and L80 Steel

Material Name	Specification	State	Chemical Composition (%)								Mechanical Performance			
			C	Si	Mn	P	S	Cr	Ni	Cu	Mo	$\sigma_s$ MPa	$\sigma_b$ MPa	HRC
HP13Cr	$\phi 73 \times 5.5$	—	0.02 ~0.03	2.21	0.17 ~0.23	0.005 ~0.014	0.001	12.3	4.8		1.6 ~1.7	717	799	25
NT80SS	$\phi 177.8 \times 11.5$	Treated	$\leq 0.30$	$\leq 0.30$	$\leq 1.5$	$\leq 0.02$	$\leq 0.007$					639 (measured)	705 (measured)	$\leq 22$
L80	$\phi 73 \times 5.5$	Treated	0.25	0.23	0.99	0.01	0.005	0.68	0.04	0.1	0.18	625	720	$\leq 22$

Note: The measured mean hardnesses of HP13Cr steel, NT80SS steel, and L80 steel are respectively HRC25.5, HRC18.7, and HRC19.

TABLE 11-15 Sulfide Resistance Evaluation Test Data

Test Material	Test Method and Standard	Test Parameter	Media Solution	Test Results	Common Criteria	Remarks
HP13Cr tubing	NACE0177A method	80% $\sigma_s$ constant load tension, $24 \pm 3^\circ\text{C}$ , normal pressure	NACE0177 standard solution A	Fracture time	1 h 15 h 15 h	Less than 15 h when fracture is generated
L80 tubing		80% $\sigma_s$ constant load tension, normal pressure, 720 h	NACE0177 standard solution A	Fracture time	>720 h	
NT80SS casing		80% $\sigma_s$ constant load tension, normal pressure, 720 h	NACE0177 standard solution A	Fracture time	$\geq 720$ h	
NT80SS casing		85% $\sigma_s$ constant load tension, $24 \pm 3^\circ\text{C}$ , normal pressure, 720 h	NACE0177 standard solution A	Fracture time		
NT80SS casing		90% $\sigma_s$ constant load tension, $24 \pm 3^\circ\text{C}$ , normal pressure	NACE0177 standard solution A	Fracture time	613 h 610 h 417 h	
NT80SS casing	NACE0177B method	$24 \pm 3^\circ\text{C}$ , normal pressure, 72h	NACE0177 standard solution A	Dummy stress S	13 14 15 16 18 20	All coupons not fractured $Sc \geq 10$
NT80SS casing	NACE0177B method (test temperature $40^\circ\text{C}$ )	Test temperature $40^\circ\text{C}$ , $P_{\text{H}_2\text{S}} = 4.0\text{MPa}$ , 72h	NACE0177 standard solution A	Dummy stress S	10 11 14 16 18	All coupons not fractured $Sc \geq 10$

TABLE 11-16 Static Electrochemical Weight-Loss Corrosion Test Data

Test Material	Test Method and Standard	Media Solution	Test Results	Remarks
NT80SS casing	$p_{H_2S} = 4.8$ MPa $p_{CO_2} = 3.2$ MPa $p_{total} = 32$ MPa 100°C, 72 h	Distilled water solution of 10% NaCl	Mean gas-phase corrosion rate = 0.3184 mm/a Mean gas-phase corrosion rate = 0.4690 mm/a	H <sub>2</sub> S 15% CO <sub>2</sub> 10%
L80 tubing	$p_{H_2S} = 3.6$ MPa $p_{CO_2} = 3.2$ MPa $p_{total} = 32\sim 31$ MPa 100°C, 72h	The solution that simulates the gas field water of Luojia 8 well	Mean gas-phase corrosion rate = 1.2311 mm/a Mean gas-phase corrosion rate = 0.4186 mm/a	H <sub>2</sub> S 15% CO <sub>2</sub> 10% Gas-phase coupon has serious local corrosion
NT80SS casing	$p_{H_2S} = 3.6$ MPa $p_{CO_2} = 3.2$ MPa $p_{total} = 32\sim 31$ MPa 100°C, 72h	The solution that simulates the gas field water of Luojia 8 well	Mean gas-phase corrosion rate = 0.2954 mm/a Mean gas-phase corrosion rate = 0.5112 mm/a	H <sub>2</sub> S 11.3% CO <sub>2</sub> 10%
L80 tubing	$p_{H_2S} = 5.6$ MPa $p_{CO_2} = 3.2$ MPa $p_{total} = 32\sim 31$ MPa 80°C, 72h	The solution that simulates the gas field water of Luojia 8 well	Mean gas-phase corrosion rate = 0.4714 mm/a Mean gas-phase corrosion rate = 0.8654 mm/a	H <sub>2</sub> S 15.9% CO <sub>2</sub> 10% Liquid-phase coupon has local corrosion
NT80SS casing	$p_{H_2S} = 5.6$ MPa $p_{CO_2} = 3.2$ MPa $p_{total} = 32\sim 31$ MPa 80°C, 72h	The solution that simulates the gas field water of Luojia 8 well	Mean gas-phase corrosion rate = 0.3239 mm/a Mean gas-phase corrosion rate = 0.4561 mm/a	H <sub>2</sub> S 15.9% CO <sub>2</sub> 10%
NT80SS casing	$p_{H_2S} = 4.8$ MPa $p_{CO_2} = 3.2$ MPa $p_{total} = 32$ MPa 60°C, 72h	The solution that simulates the gas field water of Luojia 8 well	Mean gas-phase corrosion rate = 0.2199 mm/a Mean gas-phase corrosion rate = 0.3343 mm/a	H <sub>2</sub> S 15% CO <sub>2</sub> 10%
L80 tubing	$p_{H_2S} = 4.0$ Mpa $p_{CO_2} = 3.2$ Mpa $p_{total} = 32$ Mpa 40°C, 72h	The solution that simulates the gas field water of Luojia 8 well	Mean gas-phase corrosion rate = 0.7464 mm/a Mean gas-phase corrosion rate = 0.4784 mm/a	H <sub>2</sub> S 12.5% CO <sub>2</sub> 10% Gas-phase coupon has local corrosion
NT80SS casing	$p_{H_2S} = 4.0$ Mpa $p_{CO_2} = 3.2$ Mpa $p_{total} = 32$ Mpa 40°C, 72h	The solution that simulates the gas field water of Luojia 8 well	Mean gas-phase corrosion rate = 0.6224 mm/a Mean gas-phase corrosion rate = 0.3626 mm/a	H <sub>2</sub> S 12.5% CO <sub>2</sub> 10% Gas-phase coupon has local corrosion

**TABLE 11-17** Sumitomo Metal Corrosion Resistance Classification Standard

Corrosion Rate, mm/a	Usable Range
<0.1	Corrosion resistance is strictly required.
0.1–1.0	Corrosion resistance is not strictly required.
>1.0	Low corrosion resistance and low practical value.

water of the gas reservoir is of calcium-chloride type. The total salinity is 117 g/l. The content of  $\text{Cl}^-$  in condensate water is about 400–4500 mg/l. The concentration of gas condensate is about 60 g/m<sup>3</sup>. The partial pressure of hydrogen sulfide is 1.73–2.74 MPa, while the partial pressure of carbon dioxide is 1.48–2.05 MPa.

The gas reservoir is a high-pressure gas reservoir with a high hydrogen sulfide content. In the Zhong 7, Zhong 18, Zhong 42, and Zhong 46 wells of the gas reservoir, packers were used during completion in June 1981–May 1985 and good effectiveness was

obtained. The C75 and SM90S heavy-wall VAM tubings with special threads that have good gas tightness were adopted in the Zhong 42 well ( $\text{H}_2\text{S}$  content 6.86%) and Zhong 18 well ( $\text{H}_2\text{S}$  content 6.75%). This type of tubing has good sealing property, high temperature resistance, high pressure resistance, hydrogen sulfide corrosion resistance, and equal strength of connection and body, does not easily drop out, and has alternating thread. It is especially suitable for tubing string with packers and is appropriate for high-temperature high-pressure sour gas wells (Figures 11-26 and 11-27). For these gas wells, the KQ35 sulfide-resistant well-head assembly was adopted.

Up to the end of 2004, the cumulative gas production of the gas reservoir was  $69.71 \times 10^8 \text{ m}^3$ , cumulative gas condensate production was  $37.72 \times 10^4 \text{ t}$ , and cumulative water production was  $67,566 \text{ m}^3$ . The recovery percent of natural gas reserves was up to 80.78% and gas reservoir development was in the later period. The decline in productivity was started from 2001. The daily gas production of the gas reservoir was  $70 \times 10^4 \text{ m}^3/\text{d}$  early in 2004 and was reduced to  $56 \times 10^4 \text{ m}^3/\text{d}$  by the end of 2004. The

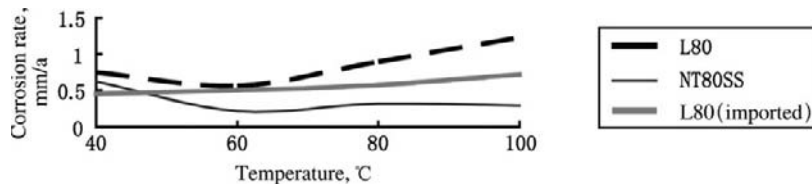


**FIGURE 11-24** Relationship between gas-phase corrosion rate and temperature.

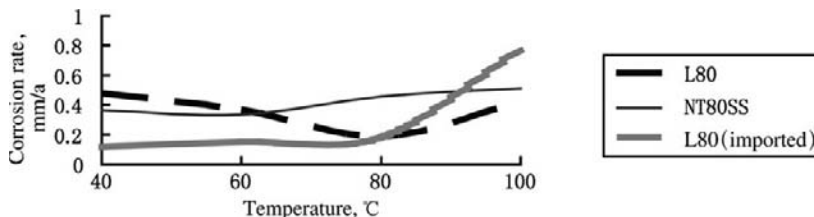


**FIGURE 11-25** Relationship between liquid-phase corrosion rate and temperature.

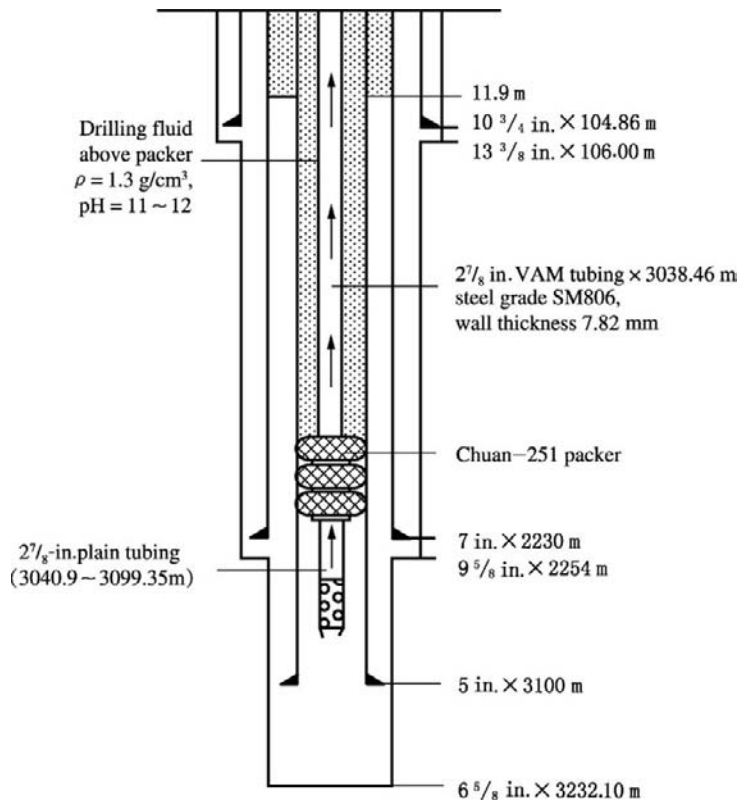


FIGURE 11-26 The hole structure and tubing string in Zhong 42 well.

reservoir pressure measured in 2004 was 7.401 MPa and total reservoir pressure drop was 27.903 MPa.

- Application of common sulfide-resistant steel tubing to Jialingjiang gas reservoir of Wolonghe gas field

The Wo 63 well is a typical sulfide-containing gas well of the Jialingjiang gas reservoir of the Wolonghe gas field. The content of hydrogen sulfide in natural gas is up to 31%. It was spudded in October 1978 and drilling was finished in July 1979. The well depth is 2306.29 m and the reservoirs are Jia5-1 to Jia4-3. The test production of the well was done for about one month in 1994-1995.

API C-75  $\Phi 177.8 \text{ mm}$  sulfide-resistant casing and perforated completion were adopted. Total casing length was 2301.96 m and no

packer was used. A KQ-35 sulfide-resistant wellhead assembly for gas well was adopted. C-75  $\Phi 63.5 \text{ mm}$  sulfide-resistant tubing was run to 2269.29 m. The depth of the middle of the reservoir is 2285.00 m. Two acidizing operations and tests (orifice 9 mm) were done in September 1979. Casing pressure was 5.64 MPa and tubing pressure was 4.27 MPa. Gas production rate was  $4.81 \times 10^4 \text{ m}^3/\text{d}$  and water production rate was 10–20  $\text{m}^3/\text{d}$ . Flowing bottomhole pressure was 7.325 MPa. The maximum shut-in wellhead pressure was 18.849 MPa. The reservoir pressure was 24.862 MPa.

For the Wolonghe gas field, the  $\text{H}_2\text{S}$  content of other gas wells of the Jia5-1 to Jia4-3 gas reservoirs is lower than 5% and the  $\text{CO}_2$  content is lower than 2%. In addition, they produced a small quantity of gas

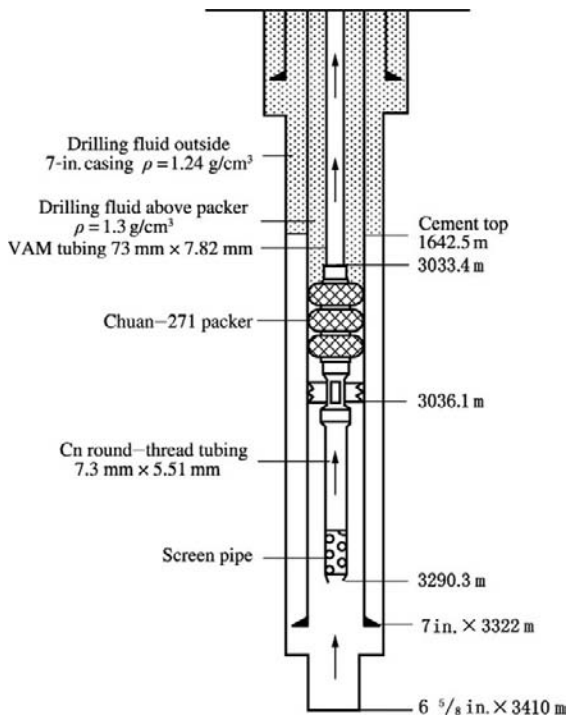


**FIGURE 11-27** The hole structure and tubing string in Zhong 18 well.

condensate, which has a certain protecting action on strings. When high sulfide-resistant and common tubings and the addition of corrosion inhibitor that was appropriate for fluid properties were adopted, the gas wells that had produced for about 10 years could still maintain normal production (Table 11-18).

**Internal Coating Tubing.** In the Talimu oil field, in the light of the serious corrosion of tubing, corrosion-resistant tubing with three composite coatings and corrosion-resistant tubing with AOC-2000T or CK-54 internal coating were used in 2005. These tubings after being coated met the API strength standard of original steel and were required to be suitable for the well condition of the field; that is, they should be resistant to temperature (140°C), acid, alkali, salt,  $\text{Cl}^-$ ,  $\text{CO}_2$ , and  $\text{H}_2\text{S}$  and have full coating in the positions that contact with media inside the body. In 2005, a large number of simulation

and field tests were done in the light of the corrosive environment of the field. A special high molecular MPS coating compound was finally selected and the high-content hydrogen sulfide resistance and the sulfide stress corrosion resistance of the MPS coating were tested under the conditions of pressure of  $32 \pm 1$  MPa,  $P_{\text{CO}_2}$  of 3.2 MPa,  $P_{\text{H}_2\text{S}}$  of 4.0 MPa, temperature of 100°C, time of 72 h, and test media that simulates the Luojiashai gas field water in the Sichuan basin. This gas field has a  $\text{H}_2\text{S}$  content of 7.13% to 13.74% (average 10.44%),  $\text{CO}_2$  content of 5.13% to 10.41% (average 6.79%), and total pressure higher than 40 MPa, and is a high- $\text{H}_2\text{S}$  and medium- $\text{CO}_2$  gas field. The tests indicated that there was no change of color and no corrosion of the metal undercoating, and the coating coupon only had a slight adhesion loss, which was measured using the V-shaped notch method. At present, it is not recommended to substitute MPS coating for sulfide stress cracking resistant steel, despite the fact that the MPS coating has a higher resistance to corrosion to protect steel from galvanic corrosion and sulfide stress cracking.

In sulfide-containing gas wells, sulfide stress cracking resistant steel should be predominantly used. This type of steel after being coated can be used for preventing galvanic corrosion. Only downhole galvanic corrosion may be generated, and disastrous sulfide stress cracking fracture may not be generated even if the coating is damaged. The coating compound has a good resistance to corrosion but has no resistance to abrasion. It can easily drop out. When tubing is expanded or contracted or temperature changes, its effectiveness may be rapidly reduced and failure may even be generated (Figure 11-28). The coating can be thickened to increase its resistance to abrasion, but it can only be used under a lower pressure; otherwise, bubbling or delamination will be generated. In the wells of the Ordovician gas reservoir in the Tazhong I zone, serious corrosion and mechanical friction may be generated. At present, under high-temperature and high-pressure environment conditions, internal coating of tubing is not recommended

TABLE 11-18 Application of Tubing to the Gas Field in Chongqing

No.	Well No.	Productive Horizon	Well Depth (m)	Tubing Steel Grade	Running Date	Pulling Date	H <sub>2</sub> S Concentration (g/m <sup>3</sup> )	CO <sub>2</sub> Concentration (g/m <sup>3</sup> )	Corrosion Description
1	Wo 47	P1m2	3295	BGC90	1978.08	1995.09	11.817	7.849	Pitting, boring
2	Tieshan 12	C2h1	3997.7	C75 C95	1991.05	1994.03	15.2	13.6	Pitting, fracture, and dropout
3	Chi 4	P1m2	3367.26		1979.09	1992.09	6.37	25.6	Weight loss, collapse and deformation, fracture, and dropout
4	Cheng 2	C2h1	2258	KO90S AC80	1978.01	1995.06	3.43	29.51	Multiple fractures and dropouts
5	Qili 43	C2h1	3877.3		1991.04	1997.07	4.591	37.68	Flexural deformation, collar fracturing, dropout
6	Yunhe 3	C2h1	4768	C75	1991.06	1998.06	5.29	44	Pitting, boring
7	Zhang 6	P2ch	3722	NT80SS	1981.02	1999.07	0.005	101.87	Weight loss, fracture, and dropout
8	Tieshan 14	P2ch	3261	Ac80	1991.11	1999.11	11.77	13.7	Weight loss, fracture, and dropout
9	Wo 88	C2h1	4389		1986.01	1999.09	1.478	20.588	Weight loss, fracture, and dropout
10	Qili 25	C2h1	5020	SM90S KO80S	1993.01	2000.07			Dropout
11	Cheng 34	C2h1	4045.6	SM90S KO80S	1987.11	2001.06	3.566	50.724	Weight loss, pitting, fracture, and dropout
12	Cheng 33	C2h1	4021.2	SM80S KO95	1987.06	2001.11	5.458	52.017	Weight loss, pitting, fracture, and dropout
13	Tieshan 12	C2h1	3997.7	BGC90 NT80SS	1994.03	2001.11	15.16	16.501	Weight loss, pitting, fracture, and dropout
14	Wo 93	C2h1	4030	KO80S	1985.03	2002.04	2.735	27.227	Weight loss, pitting

15	Guan 3	C2h1	4652	NY80SS	1984.11	2002.06	6.618	26.395	Pitting, fracture, and dropout
16	Cheng 32	C2h1	3997.43	SM90S	1986.08	2002.08	4.721	52.832	Weight loss, pitting, deformation, fracture, and dropout
17	Cheng 18	C2h1	3945	C75 C95	1982.11	2002.09	3.59	51.199	Pitting, weight loss
18	Guan 2	C2h1	4350		1983.08	2003.05	9.428	23.207	Weight loss, pitting, fracture, and dropout
19	Qili 4	C2h1	4835.71	SM80S	1987.03	2003.05	3.001	48.293	Weight loss, pitting, fracture, and dropout
20	Chi 12	P1m	3461.6	C75	1984.02	2003.05	4.827	15.947	Weight loss, pitting, fracture, and dropout
21	Guan 7	C2h1	4234		1984.05	2003.07	5.467	25.118	Weight loss, pitting, fracture, and dropout
22	Chi 18	C2h1	2689	K095SS	1986.04	2003.07	0.058	15.057	Weight loss, pitting, deformation, fracture, and dropout
23	Qili 9	C2h1	4953	AC90 AC80	1988.12	2004.05	4.453	44.242	Weight loss, pitting, fracture, and dropout

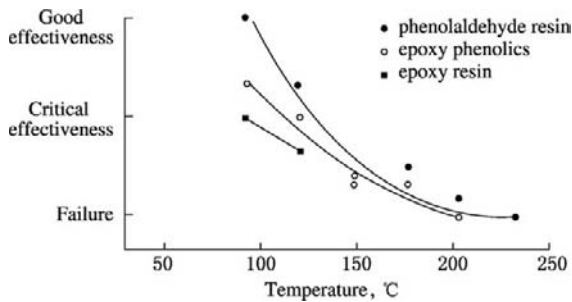


FIGURE 11-28 The effectiveness of coating.

and is rarely used. It is only appropriate for oil and gas wells that require a small quantity of tripping operation and have no need for downhole wireline operation.

**Glassfiber Reinforced Plastics Liner Tubing.** In the Luoja 1, Luoja 6, and Luoja 7 wells, the downhole tools including telescopic joint, sliding sleeve, landing nipple, and ballseat sub use 718 steel; the tubing above the packer uses Maxtube Duoline 20 and Duoline 35 internal liners; the external steel pipe is L80 tubing; and the tubing below the packer is Cr13S-95 tubing (Figure 11-29).

Duoline internal epoxy resin glassfiber reinforced plastics liner is mainly used for protecting the inner wall of the downhole steel pipe in oil and gas wells to increase the resistance to abrasion and corrosion and is also used for repairing the steel pipe that was used in order to prolong the service life of steel pipe.

The internal pressure resistance of Duoline internal liner is mainly achieved by its high circumferential strength and its connection with the inner wall of the steel pipe. Cement slurry is injected into the annulus between the internal liner and the steel pipe wall. A horn-type insert is attached to the pipe end. A corrosion-resisting spacer ring is attached to the connection between two pipes at the collar. Thus an integral continuous protective layer can be formed on the inner wall of the steel pipe, and corrosive media may only make contact with the internal liner, horn-type insert, and corrosion-resisting spacer ring, so that the steel pipe is protected. The portable Duoline internal liner installation

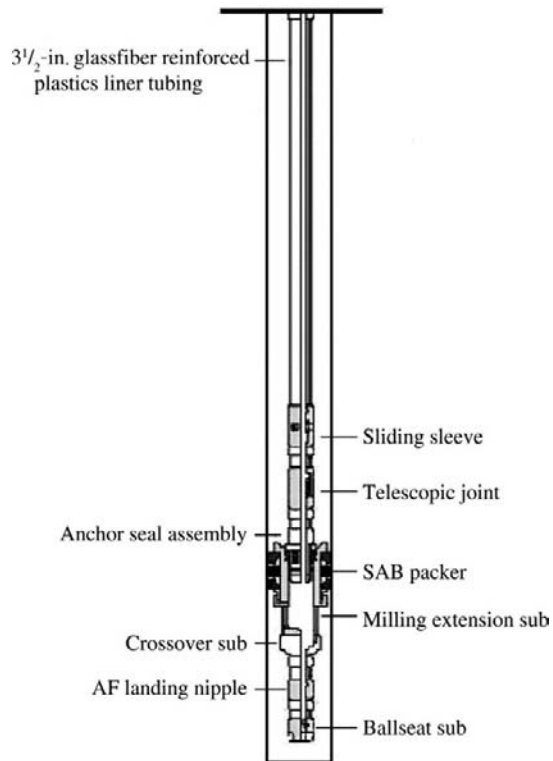


FIGURE 11-29 The tubing string used in the Luoja 1, Luoja 6, and Luoja 7 wells.

equipment can be used for site installation. The types of Duoline internal liners include Duoline 10, Duoline 20, Duoline 30, and Duoline 35. In the Luoja 1 well, Luoja 6 well, and Luoja 7 well, Duoline 20 and Duoline 35 liners are used, and the external steel pipe is of L80.

Duoline 20 internal epoxy resin glassfiber reinforced plastics liner adopts fiber winding and is treated at high temperature. It has a high resistance to corrosion and is used in CO<sub>2</sub> and H<sub>2</sub>S environments of water injection wells, carbon dioxide injection wells, gas production wells, gas-lift oil-producing wells, chemical treatment wells, and so on. The ultimate service temperature is 144°C. Duoline 35 is a more advanced internal liner in comparison with Duoline 30. It has higher resistances to temperature and corrosion. The ultimate service temperature is higher than 180°C. It can be used in a downhole environment that has CO<sub>2</sub> and H<sub>2</sub>S content

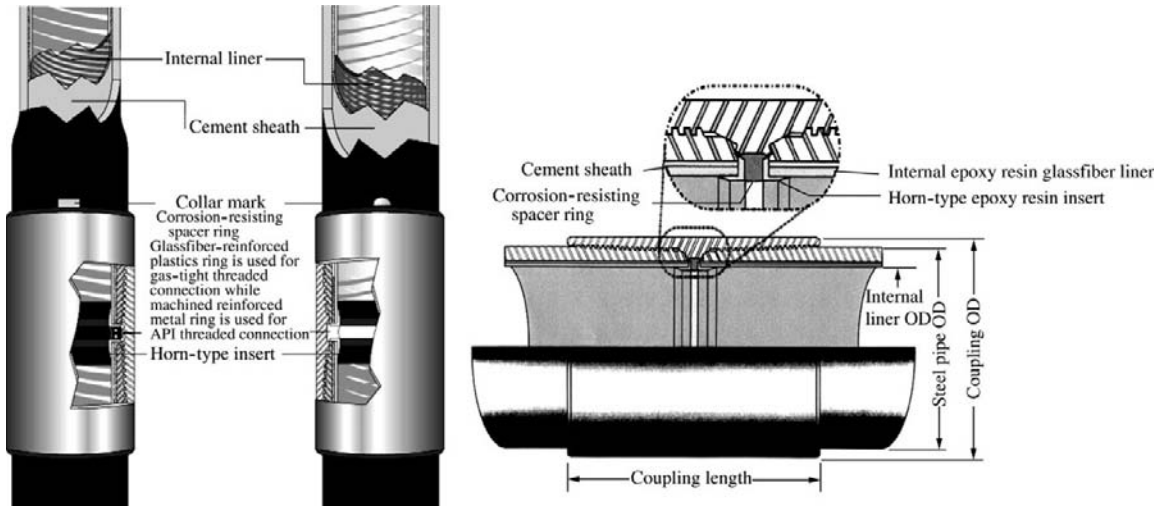


FIGURE 11-30 The structure of the tubing with internal liner.

up to 15%. The structure of the tubing with internal liner is shown in Figure 11-30.

The Luoja 1, Luoja 6, and Luoja 7 wells, which have high sulfide content, were tested after acidizing and drifted before testing. Sticking was generated during drifting (Table 11-19).

When the tubings are pulled out, they show the failure of the glassfiber liner and seal deformation at the collar due to acidizing (Figure 11-31).

At present, tubing with internal glassfiber liner is not recommended due to wireline operations in tubing and the failure of the internal liner or coating.

**Bimetallic Combination Tubing.** Carbon steel pipe is used as the base pipe of bimetallic combination tubing, which has an internal liner made of stainless steel, titanium alloy steel, copper or aluminum, and so on. This type of tubing has

TABLE 11-19 Sticking During Drifting in the LUOJIA 1, LUOJIA 6, and LUOJIA 7 Wells

Well No.	Drifting Time	Max. OD of Drift Size Gauge Tool (mm)	Tubing ID (mm)	Sticking Depth (m)	Location
Luoja 1	2004.6	58	68.6	2061	Close to collar
			68.6	2679	Close to collar
			68.6	2689	Close to collar
			68.6	2699	Close to collar
			68.6	2949	Middle of pipe body
			68.6	2988	Middle of pipe body
			68.6	3007	Middle of pipe body
			68.6	3346	Middle of pipe body
Luoja 6	2003.10	35	68.6	3413	Close to collar
			68.6	3413	Close to collar
Luoja 7	2003.12	56	68.6	1522	Close to collar
			68.6	1758	Close to collar
		35	68.6	1758	Close to collar
			68.6	1633	Pipe body

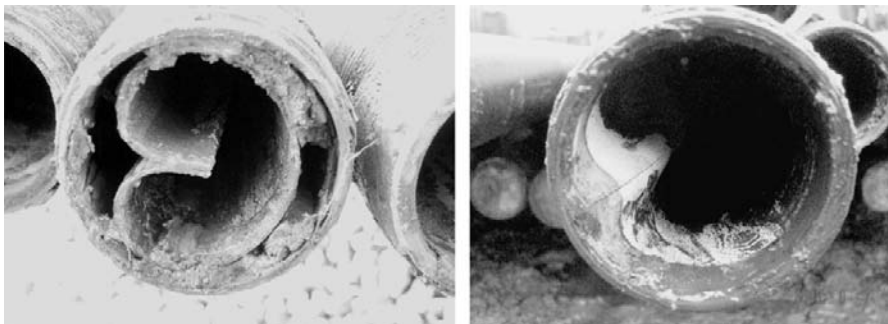


**FIGURE 11-31** The failure of the internal liner of tubing pulled out in Luojiazhai gas field.

high mechanical performance, high corrosion resistance, high weldability, high operational convenience, and high safety. It combines a surface coating technique that has low cost and wide usable range with a corrosion-resisting alloying technique that has complete structure and high tightness (no blowhole) of material; thus, it has high applicability.

#### 1. Application of bimetallic combination tubing

Bimetallic combination tubing has higher resistance to corrosion in comparison with carbon steel pipe and has cost superiority in comparison with diphasic stainless steel and nickel-based alloy steel. Thus it is widely applied in the oil and gas industry and has very high cost performance especially under high chloride corrosion environment conditions. In the light of different corrosion environments, there are SSC-resistant tubing and casing, CO<sub>2</sub>-resistant tubing and casing, and tubing and casing that can resist SSC, chloride, and carbon dioxide.

The studies and experience indicate that the application of nickel-based alloy steel in high sour environments is greatly restricted due to its cost, which is 20 to 25 times the cost of corrosion-resistant steel, despite the fact that it has high resistance to corrosion in high sour environments. The bimetallic combination pipe that has been developed combines the high corrosion resistance of corrosion-resistant alloy with the high

mechanical performance of carbon steel or low-alloy pipe:

- a. In comparison with nickel-based alloy steel, its strength is increased, its weight is reduced, and its cost is reduced by about 100%.
- b. In comparison with carbon steel, its corrosion resistance is obviously increased, thus solving the puzzle of the corrosion problem.
- c. It has very high cost performance and involves the outstanding performances of both carbon steel and corrosion-resistant alloy steel. Its corrosion resistance is the same as that of corrosion-resistant alloy steel. Its cost is reduced by 70% to 80%. Its service life is 10 to 15 times the service life of corrosion-resistant steel.

Super diphasic stainless steel has been applied in oil and gas field development. For instance, UR52N plus S32520 has been used for gathering lines and pipelines in North Sea fields, and SAF2507 steel has been used for oil and gas well production and offshore production platform facilities and oil and gas pipelines in Alaska, the North Sea, and the Gulf of Mexico, and so on. It is generally used under harsh sour environment conditions with no corrosion inhibitor used.

The application of the diphasic combination pipe technique and steel selection technique greatly reduces the application cost of the corrosion-resistant alloy technique and makes its use more convenient, thus

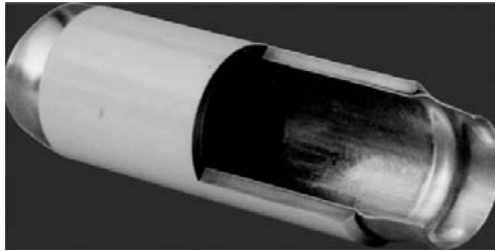


**FIGURE 11-32** The basic structure of bimetallic combination tubing.

promoting the application of the corrosion-resistant alloy technique in the oil and gas industry and enabling corrosion-resistant alloy to be widely applied.

## 2. Basic structure

Base pipe is seamless or welded carbon steel pipe or seamless alloy steel, while liner pipe is common or special stainless steel pipe, titanium-aluminum-copper alloy steel pipe, or other corrosion-resistant alloy steel pipe (Figure 11-32).

Base pipe and liner, which is a thin-wall corrosion-resistant alloy steel pipe, are coaxially assembled at first, and then a hydraulic power pipe is assembled in the liner. The instantaneous chemical energy generated by the hydraulic power pipe is transmitted to the liner through media in the form of detonation waves, so that the liner generates plastic deformation and the base pipe generates elastic deformation. In the moment of deformation, the resilience of base pipe due to deformation is much greater than that of the liner, which makes base pipe and liner nestle together closely and attain an overlapping state.

## 3. Main performance indices

### a. Steel

- (1) Steel for base pipe (mechanical performance). Carbon steel and alloy steel (seamless or welded steel pipe).
- (2) Steel for liner (corrosion resistance). Stainless steel, titanium alloy, aluminum alloy, or copper alloy.
- (3) Environmental temperature  $-35$  to  $300^{\circ}\text{C}$ .

### b. Size indices

- (1) Total wall thickness of combination pipe  $\geq 3$  mm
- (2) Base pipe wall thickness  $\geq 2.5$  mm
- (3) Liner wall thickness  $0.5\text{--}2$  mm
- (4) Combination-pipe OD  $\Phi 20\text{--}1200$  mm
- (5) Combination-pipe length  $\leq 10$  m
- (6) Combination-pipe OD, wall thickness, and allowable deviations (in accordance with international allowable deviations for base pipe)

### c. Mechanical performance indices

- (1) Combination-interface shearing strength  $\geq 0.5$  MPa
- (2) Combination-pipe tensile strength slightly higher than the tensile strength of base pipe
- (3) Combination-pipe internal pressure resistance slightly higher than the internal pressure resistance of base pipe
- (4) Combination-pipe external pressure resistance equal to the external pressure resistance of base pipe

### d. Combination-layer surface performance indices

- (1) Corrosion resistance equal to the corrosion resistance of the liner
- (2) Combination-layer surface roughness  $R_a \leq 0.07$   $\mu\text{m}$
- (3) Combination-layer surface hardness  $\geq$  liner hardness

### e. Connecting form

The connections are the weak links of tubing string; thus, it is required that the connections have strengths and seals that are equal to those of the pipe body. Under poor sealing in the J position of combination tubing collar thread, having an external thread cross-sectional area smaller than that of the internal thread may speed up thread corrosion and boring.

On the basis of the J value range of tubing and the tightening torque range, a special collar seal structure appropriate for different hole conditions has been developed. This structure includes a special adaptive Teflon seal ring and internal

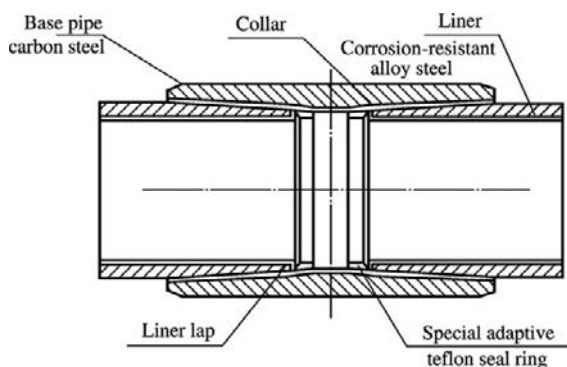


**FIGURE 11-33** Connecting form of bimetallic combination tubing.

corrosion-resistant alloy steel liner (Figure 11-33). The special adaptive Teflon seal ring has high abrasion resistance, tear resistance, oilproofness, leakproofness, and corrosion resistance and is suitable for the matching sealing of combination tubing under different end face treatments. The internal corrosion-resistant alloy steel liner that seals the exposed part of the collar thread can prevent galvanic corrosion in the J position of combination tubing collar thread in combination with the sealing of a special adaptive Teflon seal ring.

## Corrosion Inhibitor

When a corrosion inhibitor is used, a protective film should be rapidly generated on the metal surface as fast as possible; otherwise, a large quantity of corrosive product may be formed to disturb the formation of backwall. If some part of the surface has not been protected, corrosion may be aggravated and pitting corrosion may be generated.

The application of corrosion inhibitors (CT 2-1, CT 2-14, and CT 2-15) in the  $H_2S$ - and  $CO_2$ -containing oil and gas fields in Sichuan has obtained good effectiveness.

In the Qianmiqiao condensate gas field in Dagang, the  $H_2S$  concentration in natural gas is 71.4–188  $mg/m^3$ , the mean  $CO_2$  content is 10%, the  $Cl^-$  concentration is 12,496–73,927  $mg/l$ , bottomhole temperature is 160–170°C, and reservoir pressure is 43 MPa. Gas wells produce gas, oil, and water and have a harsh and complicated corrosive environment. Thus corrosion control is urgent. The CT 2-15 corrosion inhibitor additions of 3.34 L/d, 10 L/d, and 13.3 L/d in the Banshen 6 and Banshen 8 wells can effectively inhibit corrosion (Table 11-20). The test results indicate that the corrosion rate of the coupon after adding corrosion inhibitor is greatly reduced. The inhibitor efficiency is higher than 90%.

**TABLE 11-20** Test Results of Wellhead Coupon for the Banshen 6 and Banshen 8 Wells

Well No.	Corrosion Inhibitor Addition (L/d)	Test Steel	Corrosion Rate (mm/a)	Inhibitor Efficiency (%)	Test Period (d)
Banshen 6	0	NT80SS	0.0215	—	12
		P110	0.0245	—	
	3.34	NT80SS	0.0007	96.7	20
		P110	0.0009	96.3	
Banshen 8	0	NT80SS	0.5684	—	13
		P110	0.7440	—	
	13.3	NT80SS	0.0214	96.2	20
		P110	0.0465	93.8	
	10	NT80SS	0.0115	97.9	34
		P110	0.0918	87.7	

After the ideal corrosion inhibitor is selected, an inappropriate addition method may cause low corrosion-resisting effectiveness. The appropriate addition method can bring corrosion inhibitor into full play and reduce economic loss.

1. Addition by capillary pipe. For oil and gas wells with packer, a capillary pipe from well-head to downhole is installed in the tubing-casing annulus to continuously add corrosion inhibitor (Figure 11-34). Corrosion inhibitor is pumped into the well and returned from tubing. This method requires high cost but

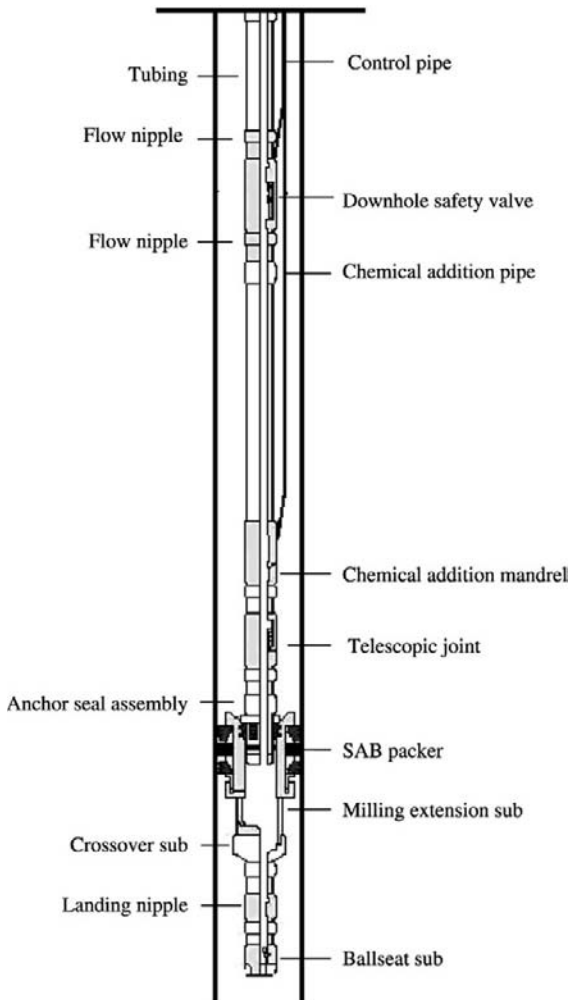


FIGURE 11-34 Chemical addition system.

has high corrosion control effectiveness. It has been commonly adopted.

2. Addition by addition valve. In the wells with packer, a check valve is installed above the tubing packer. When gas reservoir pressure is balanced with the pressure in the tubing-casing annulus or the annulus pressure is lower than gas reservoir pressure, the liquid in the annulus remains. When the annulus pressure is increased by pressurizing and is higher than gas reservoir pressure, the corrosion inhibitor solution will open the check valve and enter tubing at a given rate, and then it will flow upward with gas stream, so that the inner walls of tubing and gas gathering equipment will be protected. The corrosion inhibitor is pressed into the tubing. When tubinghead pressure is relieved, the addition valve is closed and will be opened next time. This method is convenient for use and has a long lifetime.

3. Addition of solid corrosion inhibitor. An addition cylinder that has a diameter similar to the tubing diameter is attached to the well-head tubing. The wellhead relief valve is first closed before adding. Stick or ball corrosion inhibitor is placed into the addition cylinder and the addition cylinder valve is closed. The relief valve is then opened and stick corrosion inhibitor is dropped in the well by gravity (Figure 11-35).

The preceding addition methods can be used respectively or compositely, such as alternate batch addition and continuous addition.

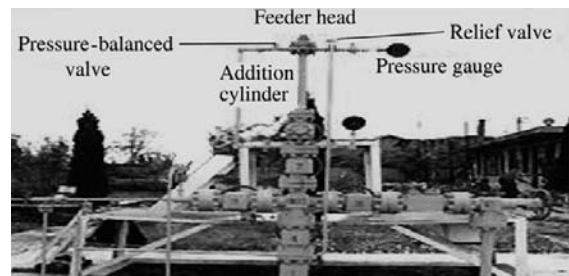


FIGURE 11-35 Stick corrosion inhibitor addition equipment.

**TABLE 11-21 Laboratory Evaluation Results of Three Types of Protective Fluids for Annulus**

Model Number	Addition (%)	Inhibitor Efficiency (%)	Scaling Resisting Efficiency (%)	Bactericidal Efficiency (%)
TZH-1	5	93.1	92	100
TH-1	3	86.07	—	100
XBT-2	3	-687.7	—	0

For the wells with packer, adding protective fluid in the annulus can protect both the outer wall of tubing and the inner wall of casing. It can prevent both corrosion and scaling. Clear water is used as the protective fluid media in the annulus and mainly contains dissolved oxygen; thus, oxygen corrosion may be generated. After perforating, the hydrogen sulfide and carbon dioxide in natural gas are dissolved and enter clear water; thus, hydrogen sulfide corrosion and carbon dioxide corrosion may be generated. Therefore, hydrogen sulfide and carbon dioxide-resisting corrosion inhibitor is required to be added. The protective fluids added in the annulus in the wells of the Ordovician gas reservoir in the Tazhong I zone are listed in Table 11-21.

It is shown that TZH-1 has higher performance; thus, this protective fluid for the annulus and its addition of 5% are recommended.

In the Luojiashai gas reservoir, which contains hydrogen sulfide and carbon dioxide,  $P_{H_2S} = 1.5$  MPa,  $P_{CO_2} = 1.0$  MPa,  $P_{total} = 10.0$  MPa, and temperature is 60°C. The steel used in wells is NT80SS. The corrosion rate of NT80SS in gas phase is 1.02 mm/a and that in liquid phase is 0.936 mm/a. When the CT2-4 of 10% is added, the corrosion rate is 0.0066 mm/a. When the corrosion inhibitor that is used as the protective fluid for annulus and its addition of 10% are recommended, it can be: 10% CT2-4 water-soluble corrosion inhibitor plus 90% clear water or 10% CT2-5 oil-soluble corrosion inhibitor plus 90% diesel oil.

The metered corrosion inhibitor and clear water (or diesel oil) are successively added in the fluid storage tank and evenly mixed to form the corrosion inhibitor type protective fluid.

If there is preparation equipment on site, the protective fluid prepared is displaced into the tubing-casing annulus once. If there is no preparation equipment on site, batch displacement, which is clear water (or diesel oil) + corrosion inhibitor + clear water (or diesel oil), is adopted.

The application of the corrosion inhibitors commonly used in oil and gas fields is shown in Table 11-22.

## Technical Margins of Corrosion Prevention Measure

**Technical Margins of Sour Oil and Gas Field Facilities' Corrosion Resisting.** Hydrogen sulfide and carbon dioxide may generate hazardous corrosion. In particular, hydrogen sulfide may not only generate abrupt sulfide stress cracking of metal to cause great economic loss, but also have toxicity that may threaten personal safety. The classification and determination of sour oil and gas field environments that may generate sulfide stress cracking and carbon dioxide corrosion have been mentioned earlier.

**Allowable Corrosion Rates and Technical Margins of Comprehensive Tackling and Control of Corrosion Rate in Oil and Gas Fields.** It is generally considered that the corrosion rate of surface facilities should not exceed 0.127 mm/a, while the corrosion rate of down-hole facilities should not exceed 0.076 mm/a. Thus comprehensive tackling and control of corrosion rate are required.

Corrosion prediction is the basis of the limited corrosion life design and corrosion catastrophe prevention, while corrosion control is the

TABLE 11-22 Application of Corrosion Inhibitors Commonly Used in Oil and Gas Fields

Corrosion Inhibitor	Main Uses	Oil and Gas Fields
Oil-soluble corrosion inhibitor CT2-1	H <sub>2</sub> S, CO <sub>2</sub> , and chloride corrosion in oil and gas wells and gathering lines	Zhongba, Wolonghe, and Changqin gas fields
Water-soluble corrosion inhibitor CT2-4	H <sub>2</sub> S, CO <sub>2</sub> , and chloride corrosion in oil and gas wells and gathering lines	Zhongba and Datianchi gas fields, Nanhai oil field
Bactericides CT10-1, CT10-2, CT10-3	Sulfate-reducing bacteria corrosion in water reinjection system	Moxi gas field, Huabei, Shengli, and Zhongyuan oil fields
Gas-liquid corrosion inhibitor CT2-15	H <sub>2</sub> S, CO <sub>2</sub> , and chloride corrosion in oil and gas wells and gathering lines	Moxi, Zhongba, and Datianchi gas fields, Dagang oil field
Water-soluble stick corrosion inhibitor CT2-14	H <sub>2</sub> S, CO <sub>2</sub> , and chloride corrosion in wells with high water production	Zhongba and Changqin gas fields, Zhongyuan oil field
Corrosion-resisting corrosion inhibitor CT2-17	CO <sub>2</sub> and chloride corrosion in oil and gas wells and gathering lines	Datianchi gas field, offshore oil fields

necessary means of weakening corrosion. The studies of corrosion mechanisms and rules are the necessary basis of establishing a corrosion prediction model and developing corrosion control means, while corrosion monitoring and detection and corrosion simulation tests are the basis of establishing and correcting the corrosion prediction model. The allowable corrosion rate for oil and gas fields and the comprehensive tackling of corrosion rate can be in accordance with the procedure shown in Figure 11-36.

### Technical Margins of Protective Measures

1. Technical margins of corrosion-resistant material selection

Selecting corrosion-resistant material should be considered first as a corrosion prevention measure. The application of corrosion-resistant material is mainly related to the following:

- Oil and gas well production environments
- Material performance, laboratory test, evaluation data, and on-site use experience

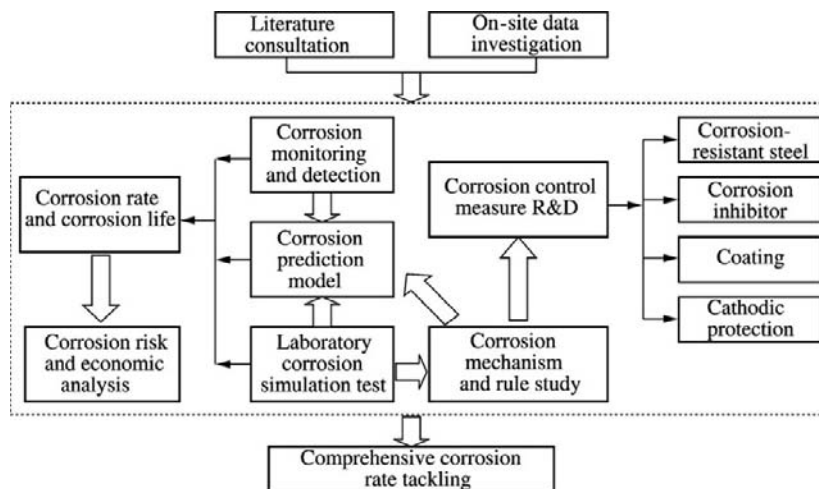


FIGURE 11-36 Comprehensive corrosion rate tackling strategy and procedure for oil and gas field development.

c. Whether corrosion inhibitor, cathodic protection, and comprehensive protective measures are adopted

d. Economic evaluation

To sum up, the selection of material should meet the requirements of rupture protection, strength, weldability, and so on, and should also be economically reasonable.

2. Corrosion-resistant material selection procedure is as follows:

a. Listing the requirements for material

b. Finding and evaluating possible material by using corrosion prevention software or experience

c. Selecting economic material

SOCRATES/OTL is one of the commonly used corrosion-resisting software programs. SOCRATES is the CLI expert system of corrosion prevention simulation and tubing steel selection software. Appropriate steel can be basically determined by using the software formed by the expert system and by inputting necessary parameter data. There is no need for multiple corrosion resistance tests, and there is high accuracy.

When the expert system is used for selecting material, the following appraisals are required: (1) mechanical performance, heat treatment state, and hardness; (2) working pressure, relative density of media, flow velocity, temperature, pH value, partial pressures of  $H_2S$  and  $CO_2$ , sulfide, carbonate, and type of acid; (3) stress-corrosion cracking (SSC), hydrogen-induced cracking (HIC), and sulfide stress cracking (SSC); (4) pitting resistance; and (5) other restrictions related to material. In addition, the necessary data should be input as far as possible in order to ensure the accuracy of material selection.

When WINSOC is used, the necessary basic data required to be input include: highest temperature, lowest temperature,  $CO_2$  content (%),  $H_2S$  content (%), and  $HCO_3^-$  concentration (meq/l).

The pitting indices of high nickel-based alloy steels are calculated under environment

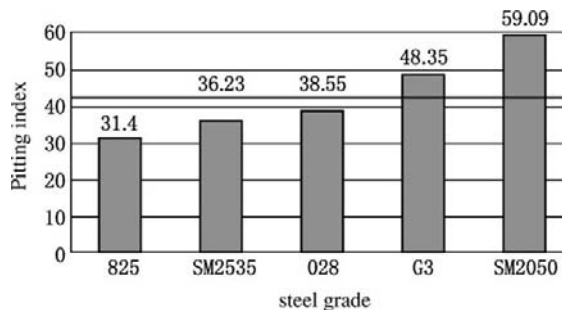


FIGURE 11-37 Pitting index appraisal of high nickel-based alloy steel.

conditions of chloride concentration of 10,000 mg/l, water content of 0.0012%, hydrogen sulfide, carbon dioxide, and elemental sulfur by using the SOCRATES 8.0 software in accordance with the NACE-MR0175 and ISO 15156 standards (Figure 11-37). Under these conditions, the minimum pitting index should be higher than 43 and the pitting index of selected alloy steel should be higher than the minimum pitting index.

It is indicated that G3 and SM2050 can meet the requirement of pitting corrosion resistance; thus, G3 or the same grade of high nickel-based alloy steel as G3 is selected.

For steels that are used under different conditions, the key points that should first be considered are different. For steels of production tubing string, wellhead, valves, and instruments in sulfide-containing gas wells, the hydrogen brittleness resistance and sulfide stress cracking resistance should be predominantly considered.

3. Corrosion prevention measure selection and technical requirements

For high-temperature, high-pressure, high-productivity, and high sour gas wells similar to those of the Feixianguan gas reservoir of the Luojiashai gas field, selecting high-alloy austenitic corrosion-resistant alloy stainless steel or nickel-based corrosion-resistant alloy steel is the main measure of serious hydrogen sulfide and carbon dioxide corrosion prevention to ensure long-term, safe, and stable

production and avoid well servicing and workover as far as possible to ensure stable natural gas supply. This type of corrosion-resistant alloy has a chrome content of 20% to 30% and nickel content of 20% to 35%. High strength is achieved by cold working. It has the highest resistance to corrosion and the highest mechanical performance in all stainless steels. Despite the high cost, the corrosion-resistant alloy has long service life. The service life of corrosion-resistant alloy tubing is similar to the production lives of several gas wells. The corrosion-resistant alloy tubing can be repeatedly used in multiple wells and has no need for adding corrosion inhibitor and replacing tubing, and so on. Thus the total cost is reasonable. For high-pressure and high-productivity oil and gas wells that have strong corrosiveness, this may be an effective and economic corrosion prevention measure.

Hydrogen sulfide and carbon dioxide-resistant steels can be selected by using the steel grade selection diagrams of Sumitomo and NKK in accordance with the partial pressures of hydrogen sulfide and carbon dioxide and downhole temperature (Figure 11-38 and Figure 11-39).

### Technical Margins of Adding Corrosion Inhibitor

#### 1. Applicability of corrosion inhibitor

Different media or steels often require different corrosion inhibitors. Even for the same type

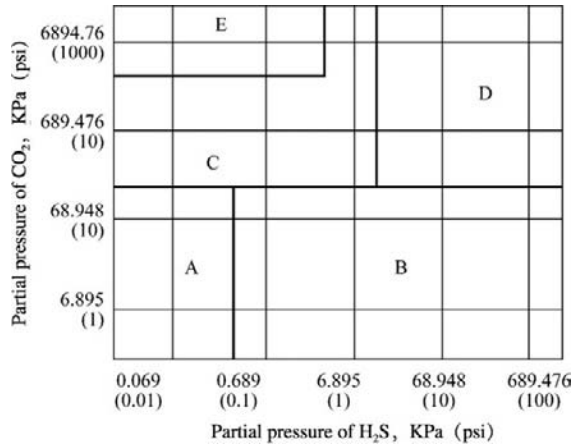


**FIGURE 11-39** Steel grade selection diagram of NKK under CO<sub>2</sub> and H<sub>2</sub>S conditions. Zone A: conventional API steel grade casing; Zone B: AC85, AC85M, AC80, AC90, AC90M, AC80T, AC95, AC95M (AC for H<sub>2</sub>S resisting mainly); Zone C: CR13, CR9 (CR for CO<sub>2</sub> resisting mainly); Zone D: NIC42, NIC62, NIC32, NIC52, NIC25, NIC42M (NIC for H<sub>2</sub>S and CO<sub>2</sub> resisting); Zone E: CR25, CR23 (for high CO<sub>2</sub> resisting).

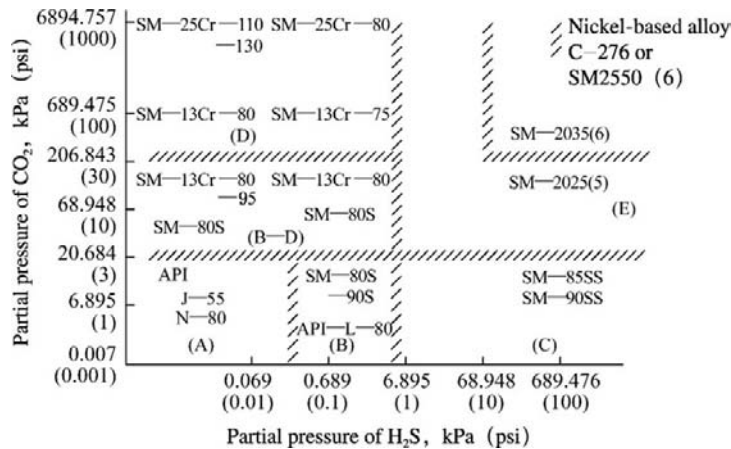


**FIGURE 11-38** Steel grade selection diagram of Sumitomo under CO<sub>2</sub> and H<sub>2</sub>S conditions.

of medium, the corrosion inhibitor used may also be required to be changed when the operating conditions such as temperature, pressure, concentration, velocity, and so on are changed. During oil and gas production from bottomhole to wellhead and then to treatment plant, temperature, pressure, and flow velocity may be greatly changed. Deep gas wells have high bottomhole temperature and pressure. Different production periods of oil and gas wells have different proportions of oil, gas,

and water. In general, with the increase of water production, failure by corrosion may be aggravated. In order to select correctly the corrosion inhibitor that is appropriate for the specific system, not only should the media composition, operational parameters, and possible types of corrosion in the system be considered, but also the necessary evaluation tests of corrosion inhibitor are required in accordance with actual use conditions (Tables 11-23 and 11-24).

**TABLE 11-23 Corrosion Inhibition Effectiveness of CT2-1 Corrosion Inhibitor Under Different H<sub>2</sub>S/CO<sub>2</sub> Values**

H <sub>2</sub> S/CO <sub>2</sub>	Corrosion Rate under No Corrosion Inhibitor (mm/a)	Corrosion Rate after Adding CT2-1 (H <sub>2</sub> S + CO <sub>2</sub> 50 mg/l) (mm/a)	Inhibitor Efficiency (%)
100/0	0.590	0.015	97.3
90/10	0.574	0.017	97.0
85/15	0.574	0.017	97.0
70/30	0.557	0.022	96.0
50/50	0.488	0.020	95.9
30/70	0.421	0.024	94.4
15/85	0.327	0.030	90.7
10/90	0.292	0.042	88.8
0/100	0.285	0.073	74.4

**TABLE 11-24 Static Selection Results of Different Types of Corrosion Inhibitors at 120°C**

Corrosion Inhibitor	Addition (mg/l)	Phase State	Corrosion Rate (mm/a)	Inhibitor Efficiency (%)	Surface State of Coupon
No corrosion inhibitor	0	Gas	0.8382	0	Pitting corrosion
		Liquid	0.4832	0	Pitting corrosion
CT2-1	1000	Gas	0.1610	80.8	Local corrosion
		Liquid	0.3899	11.5	Local corrosion
CT2-4	1000	Gas	0.3670	56.2	Local corrosion
		Liquid	0.2640	45.4	Uniform corrosion
CZ3-1	1000	Gas	0.1624	80.6	Local corrosion
		Liquid	0.0832	82.8	Pitting corrosion
BT-1	1000	Gas	0.1701	79.7	Local corrosion
		Liquid	0.0798	83.5	Pitting corrosion
CZ3-1	1000 (5:1)	Gas	0.2614	62.8	Local corrosion
CZ3-3		Liquid	0.1082	77.6	Pitting corrosion
CT2-15	1000	Gas	0.0422	95.0	Bright
		Liquid	0.0871	82.0	Uniform corrosion

Table 11-23 indicates that in the corrosive environment in which  $H_2S + CO_2$  is 50 mg/l, CT2-1 inhibitor has different efficiencies under different proportions between  $H_2S$  and  $CO_2$ . The lower the  $CO_2$  concentration, the higher the inhibitor efficiency. Table 11-24 indicates that CT2-15 has higher inhibitor efficiency for  $CO_2$  corrosion. Its inhibitor efficiency in gas phase is up to 95%, and the corrosion of tubing and casing can be controlled to a great extent.

The rational and timely addition of corrosion inhibitor can greatly reduce the degree of tubing corrosion. For instance, in the Longhui 2, Tiandong 67, and Tiandong 90 wells in the Sichuan gas field corrosion inhibitor was added when these wells were put into production. The addition period, inhibitor concentration, adding method, and the model number of corrosion inhibitor were based on practical conditions. Tubing protection was achieved and no corrosion has been seen.

## 2. Factors affecting corrosion inhibitor efficiency

In sour oil and gas environments that contain hydrogen sulfide, the factors affecting film-forming-type corrosion inhibitor efficiency include:

- a. Formation of corrosion-inhibiting film. The efficiency of the film-forming-type corrosion inhibitor depends on whether the corrosion product film (iron sulfide) on a metal surface will combine with corrosion inhibitor to form a complete and stable corrosion-inhibiting film.
- b. pH value. The pH values in the range 4 to 9 will have a higher corrosion inhibitor efficiency. The pH values lower than 4 and higher than 9 may reduce corrosion inhibitor efficiency.
- c. Temperature. The film-forming-type corrosion inhibitor may be decomposed and fail when environment temperature exceeds the normal use temperature of film-forming-type corrosion inhibitor. Thus a corrosion inhibitor that will be used in high-temperature high-pressure

deep sour oil and gas wells should have a wide usable temperature range.

- d. Corrosion inhibitor concentration. The lowest corrosion inhibitor concentration should be higher than the allowable value in order to ensure the stability of the corrosion-inhibiting film formed on metal surface.
- ## 3. Technical requirements of corrosion inhibitor selection
- a. Corrosion inhibitor for elemental sulfur, hydrogen sulfide, and carbon dioxide-containing gas wells. High- $H_2S$  natural gas contains a large quantity of elemental sulfur. Corrosion inhibitor and the solvent for sulfur are often used during production in order to prevent tubing plugging. The corrosion inhibitors mainly use long-chain imidazoline acetate, quaternary mixture, long-chain hydroxyethyl aliphatic amine, polyamine, long-chain quaternary aliphatic amine, ammonium salt and alkylphenol, and so on.
  - b. Corrosion inhibitor for high-temperature high-pressure corrosive deep wells. A typical corrosion inhibitor is amine activated dialkyldisulfide. The high molecular amine or fatty amine used is long chain alkylammonium. It is composed of even carbon atoms and is unsaturated. Amine should have a carbon chain that contains 16 to 30 carbon atoms.
  - c. Binary corrosion inhibitor for deep hot gas wells and pumping wells. It consists of epoxy resin and amine, which are mixed within 1 hour before being added into the well. After chemical combination, a reaction is generated on the tubing surface. For a pumping well, corrosion inhibitor is circulated in the tubing and tubing-casing annulus.

**Technical Margins of Coating Technique Application.** The correct amount of corrosion inhibitor is generally required to be added when internal coating is adopted due to possible pinholes, possible damage during production and

maintenance, and the difficult coating at welded joints.

In high-temperature high-pressure gas wells, an internal coating may foam and exfoliate at pinholes, thus leading to pitting corrosion and pinhole corrosion. Therefore, internal coating tubing is inappropriate for hydrogen sulfide-containing sour gas wells and will be replaced by bimetallic combination tubing in this type of gas well. For instance, the 13% Cr/4130 bimetallic material can be used in oil and gas wells that have serious carbon dioxide corrosiveness. This material has both the good mechanical performance of AISI 4130 steel and the corrosion resistance of 13% Cr steel.

## REFERENCES

- [1] Lu Qimin et al., *The Corrosion and Protection in Petroleum Industry*, Chemical Industry Press, Beijing, 2001 (in Chinese).
- [2] Wan Xiping, Zhu Jinchuan, et al., (Trans.), *The Carbon Dioxide Corrosion Control in Oil and Gas Production—Factors Considered in Design*, Petroleum Industry Press, Beijing, 2002 (in Chinese).
- [3] Cen Kefa, Fan Jianren, *Theory and Calculation of Gas-Solid Multiphase Flow in Engineering*, Zhejiang University Press, Hanzhou, 1990 (in Chinese).
- [4] Zhou Lihan, *Numerical Simulation of Two-phase Turbulent Flow and Combustion*, Tsinghua University Press, Beijing, 1991 (in Chinese).
- [5] Oil and Gas Field Corrosion and Protection Handbook Group, *Oil and Gas Field Corrosion and Protection Handbook (Book One)*, Petroleum Industry Press, Beijing, 1999 (in Chinese).
- [6] Chen Caijin, et al., *Advance in Metal Stress Corrosion Cracking Study*, Zhejiang Science and Technology Press, Hanzhou, 1983 (in Chinese).
- [7] Liu Baojun, *Material Corrosion and Control*, Beijing Aviation and Space University Press, Beijing, 1989 (in Chinese).
- [8] Sun Qiuxia et al., *Material Corrosion and Protection*, Metallurgical Industry Press, Beijing, 2001 (in Chinese).
- [9] Zhang Yueyuan et al., *Carbon Dioxide Corrosion and Control*, Chemical Industry Press, Beijing, 2000 (in Chinese).
- [10] Yang Dongchuan et al., *Gas Production Engineering*, Petroleum Industry Press, Beijing, August 1997 (in Chinese).
- [11] Offshore Oil and Gas Field Completion Handbook Group, *Offshore Oil and Gas Field Completion Handbook*, Petroleum Industry Press, Beijing, 2001 (in Chinese).
- [12] API RP68, *Recommended Practice for Oil and Gas Well Servicing and Workover Operations Involving Hydrogen Sulfide*, MOD1998.
- [13] API RP55, *Recommended Practice for Oil and Gas Producing Plant Operations Involving Hydrogen Sulfide*, 1995.
- [14] API RP49, *Recommended Practice for Drilling and Well Servicing Operations Involving Hydrogen Sulfide*, 2001.
- [15] NACE Standard MR 0175-95, *Sulfide Stress Cracking Resistant Metallic Materials for Oil Equipment*.
- [16] *Carbon Dioxide Containing Gas Well Corrosion Resisting Technology Studies and Application*, Nat. Gas Ind. Nov., 27 (2007) 11 (in Chinese).
- [17] SY/T 5327, *Recommended Indices and Analysis Method for Injection Water Quality for Clastic Reservoir*, 1994 (in Chinese).

Note: Page numbers followed by *f* indicate figures and *t* indicate tables.

## A

- Accelerant, oil well cement, 262–263
  - Acid-based perforating fluid, 215–216
  - Acid corrosion, 640
  - Acid fracturing
    - carbonatite reservoir
      - acid liquor
        - filtration loss, 488–489, 488*f*, 489*f*
        - systems and properties, 490–492
      - chemical reactions, 482–485, 482*t*, 483*t*, 484*t*
      - design model in consideration of acid-etched wormholes, 493–494
      - design optimization, 485–486
      - effectiveness prediction, 494
      - fracture flow conductivity, 489–490, 489*f*
      - reaction kinetics, 486–488, 488*f*
      - technology, 492–493
    - classification, 470–471
    - overview, 425
    - productivity increasing mechanism, 471
    - sandstone reservoir
      - acid liquor and additives, 472–476, 477*t*
      - effectiveness, 475*t*, 480–482
      - monitoring, 480–482
      - skin damage, 476*t*
      - technology, 476–480, 478*t*
  - Acidizing
    - curve shape effects in well testing, 399–402, 399*f*, 399*t*, 400*f*, 400*t*, 401*f*, 402*t*
    - overview, 67–68, 423–424
  - Acid sensitivity
    - applications of evaluation, 35*t*
    - evaluation indices, 34*t*
    - experimental procedure and results, 34, 34*t*
    - overview, 33–34
  - Adjustment well
    - overview, 68
    - production casing and cementing problems and solutions, 291–292
  - Aerated drilling and completion fluid, 176
  - Aero-fluid, drilling and completion fluid, 175–176
  - Alkali sensitivity
    - applications of evaluation, 35*t*
    - experimental procedure and results, 31–33, 32*t*, 33*t*
    - overview, 31
  - Ammunition, *see* High-energy gas fracturing
  - Anisotropy, effect on productivity ratio, 317, 317*f*, 318*f*
  - API gravity, equation, 5
  - Artificial lift well
    - adaptability comparison between systems, 140*t*
    - Christmas tree and tubinghead
      - electric submersible pump well, 580–581, 581*f*, 582*f*
      - gas-lift production well, 583–584, 585*f*
      - hydraulic piston pump well, 581–583, 582*f*, 583*f*, 584*f*
      - sucker rod pump well, 577–580, 579*f*, 580*f*
    - daily liquid production rate level in high water-cut period, 138–139
    - lift mode determination
      - chart method, 143–144, 143*f*, 144*f*
      - grade weighted method, 139–143, 142*t*, 143*t*
      - preliminary selection, 139, 140*t*
    - tubing and production casing size determination
      - dual-string production wells, 154, 155*t*, 156*t*
      - electric submersible pump well, 151*t*, 152*t*, 153
      - gas-lift oil well, 150–154, 152*t*, 153*t*
      - hydraulic jet pump well, 148–150, 149*t*
      - hydraulic piston pump well, 146–148, 147*t*, 148*t*
      - overview, 136–156
      - screw pump well, 154, 155*t*
      - sucker rod pump well, 144–146, 145*t*, 146*t*
    - tubing string
      - downhole screw pump well, 527–528, 531*f*
      - electrical submersible pump well, 529*f*, 530*f*, 547–553
      - gas lift well
        - modes of gas lift, 529–530, 533*f*, 534*f*
        - multiple tubing string gas lift, 531, 536*f*
        - single gas-lift string, 531, 535*f*
      - hydraulic piston pump well production tubing string, 533, 536*f*, 537*f*, 538*f*, 539*f*, 540*f*
      - jet pump well, 529, 532*f*
      - sucker-rod pumping well, 526, 527*f*, 528*f*
- Axial force
  - collapse pressure under action of axial tension and internal pressure, 246–247
  - string loads, 253–255

## B

- Backflow, *see* Flowing back
- Bacteria corrosion, 280, 638
- Beam bending test, 644
- Behrmann method, underbalance pressure design, 340
- Bell's relation, underbalance pressure design, 339–340, 339*t*
- Bilogarithmic type curve match method, well testing, 404–406, 405*f*, 406*f*
- Bimetallic combination tubing, 689–692, 691*f*, 692*f*
- Blocking removal
  - chemical blocking removal
    - anti-swelling and deswelling agents, 428–432
    - enzymes, 435–436
    - overview, 423, 425–436, 426*t*
    - oxidants, 434, 435*t*
    - solvents, 425–428, 429*t*, 430*f*, 430*t*
    - surface tension reducers, 434–435, 435*t*, 436*t*

- Blocking removal (*Continued*)  
 thermo-chemical blocking removal, 432–434, 434f, 434t  
 viscosity-reducing agents, 432, 433t  
 physical blocking removal  
 low-frequency electric pulse blocking removal, 444–445, 444f  
 magnetic treatment, 440, 440f, 441f  
 microwave, 438–440, 439f  
 overview, 423, 426t, 436–445  
 ultrasonic wave, 418–420, 437–438, 437f  
 vibration blocking removal, 440–444, 441f, 442f
- Borehole, *in situ* stress  
 firmness, 64–65  
 horizontal principal stress, 63–66  
 mechanical stability, 65–66
- Bottom water, control, 68
- Bridging type, clay mineral analysis, 20
- Brine corrosion, 636–638, 637f
- Broomy scattered type, clay mineral analysis, 3
- C**
- CAMERON wellhead assembly, 593–595, 598f
- Carbonatite, mineral classification, 482f
- Carbonatite reservoir  
 acid fracturing  
 acid liquor  
 filtration loss, 488–489, 488f, 489f  
 systems and properties, 490–492  
 chemical reactions, 482–485, 482t, 483t, 484t  
 design model in consideration of acid-etched wormholes, 493–494  
 design optimization, 485–486  
 effectiveness prediction, 494  
 fracture flow conductivity, 489–490, 489f  
 reaction kinetics, 486–488, 488f  
 technology, 492–493  
 gas reservoir perforating parameter design, 360–361  
 hydraulic fracturing  
 adaptability analysis, 470  
 difficulties, 469–470  
 lithology, 9  
 stress sensitivity analysis  
 Sichuan basin, 52–54, 56t, 57t  
 variation rules, 54, 58f  
 Zhanaruoer oil field, 27t, 52
- Carbon dioxide corrosion  
 overview, 634–636, 635f, 636f  
 set cement, 265–268  
 sour gas well, 674–675, 675f, 675t
- Casing, *see* Production Casing
- Casing gravel pack completion, 84–85, 85f, 85t
- Casinghead  
 model number notation, 601  
 parameters, 602, 605t, 606t  
 structures, 601–602, 602f, 603f, 604f
- Casing perforation completion, 76–77, 77f
- Casing string, *see* Production casing; Wellhead assembly
- CBL, *see* Cement bond log
- Cement bond log (CBL), 270, 271t
- Cementing  
 challenges and solutions  
 absorbing wells  
 problems, 282  
 cement leakage prevention, 282–284  
 adjustment well, 291–292  
 corrosive media-containing wells  
 carbon dioxide corrosion of set cement, 265–268  
 hydrogen sulfide corrosion of cement sheath, 281–282  
 physico-chemical reaction, 280  
 sulfate corrosion, 280  
 sulfate-reducing bacteria corrosion, 280  
 horizontal well, 290–291  
 salt rock bed and salt paste bed wells, 284–285, 284f  
 thermal production well, 286, 289  
 deep wells, 272–279, 273f, 276t, 277t  
 high-temperature high-pressure gas well, 272–279, 273f, 276t, 277t  
 displacement efficiency enhancement, 265–268, 265f, 266f  
 oil well cement  
 additives  
 accelerant, 262–263  
 dispersant, 262  
 fluid loss additive, 261–262  
 gas-channeling inhibitor, 263  
 lightening admixture, 264  
 retardant, 262  
 thermal stabilizer, 264  
 toughness promoter, 264  
 weighting admixture, 264  
 formulation, 257–258  
 overview, 257  
 types and usable range, 257, 258t  
 operation requirements, 256  
 production requirements, 256–257  
 quality  
 cement bond log, 270, 271t  
 requirements, 270  
 segmented bond tool, 271  
 variable density log, 271, 271t  
 set cement requirements, 260  
 slurry  
 requirements, 258–260, 261t  
 weightlessness and prevention of channeling, 268–270, 269t, 270t  
 well completion requirements, 256
- Chemical sand consolidation well completion, 105–106, 107t
- Chloride stress cracking, 637
- Chlorine dioxide, blocking removal, 434, 435t, 436t
- Chlorite, clay mineral analysis, 18
- Chokes, wellhead assembly  
 adjustable chokes, 607–609, 609f, 611t  
 fixed chokes, 606–607, 609f
- Christmas tree, *see* Corrosion; Wellhead assembly
- CI, *see* Completeness index
- Clastic rock, reservoir lithology, 8
- Clay, hydration inhibition by drilling and completion fluid, 174
- Clay mineral analysis, core analysis, 18–21, 19f, 20f, 21f

- Collapse, *see* Production casing integrity; Production casing strength
- Collapse safety factor, 570
- Comb shell type, clay mineral analysis, 19
- Combined tubing and wireline conveyed perforation (TWC), 299, 300*f*
- Completeness index (CI), formation damage, 373
- Conoco method, underbalance pressure design, 339–340
- Core analysis
  - clay mineral analysis, 18–21, 19*f*, 20*f*, 21*f*
  - grain size analysis, 21–22, 22*f*
  - petrographic analysis, 14–15, 16*t*, 17*t*
  - pore configuration analysis, 15–17, 17*t*
  - requirements of well completion engineering, 13–14, 14*t*
- Corrosion
  - acid corrosion, 640
  - alloy steel tubing and casings
    - adaptability analysis, 677–679, 678*t*
    - corrosion modes, 651–653, 652*t*
    - service environment restriction, 653–655, 655*t*, 656*t*, 657*t*
  - types and composition of corrosion-resistant alloys, 650–651, 651*t*
  - bacteria corrosion, 638
  - bimetallic combination tubing, 689–692, 691*f*, 692*f*
  - brine corrosion, 636–638, 637*f*
  - carbon dioxide corrosion, 634–636, 635*f*, 636*f*
  - carbon dioxide corrosion of set cement, 265–268
  - Christmas tree, 672
  - cracking
    - factors affecting
      - alloy design, 645, 646*t*
      - strength and hardness, 645–646, 646*t*
      - stress, 647
      - temperature, 646–647, 647*t*
    - sulfide stress cracking severity criteria and material selection
      - diagram, 648, 648*f*
      - test requirements of commonly used materials, 650
      - Zone SSC 0, 648–649
      - Zone SSC 1, 649–650
      - Zone SSC 2, 649
      - Zone SSC 3, 649
  - electrochemical corrosion
    - environmental influences, 627–628
    - mechanism, 625–626, 626*f*
    - environment of wells, 625
  - flow-induced corrosion, 629
  - fracture evaluation
    - beam bending test, 644
    - C-shaped ring test, 644
    - criteria, 643
    - dual cantilever beam test, 644–645
    - tension test, 643–644
  - gas partial pressure calculation
    - gas phase, 620
    - hydrogen sulfide in liquid system, 620–621, 621*f*
  - gas volume fraction, mass concentration conversion, 619–620
  - glassfiber reinforced plastics liner tubing, 688–689, 688*f*, 689*f*, 689*t*, 690*f*
  - hydrogen sulfide corrosion, 281–282, 630–640, 631*t*, 632*f*
  - inhibitors, 692–694, 692*t*, 693*f*, 694*t*, 695*t*, 697–699
  - interaction of corrosive components, 638–640, 639*f*
  - internal coating tubing, 685–688, 688*f*
  - material selection
    - examples by corrosive environment, 642–643
    - fitness design, 642
    - overview, 640–641
    - standards, 641
  - media of wells, 625
  - non-metallic material corrosion, 655
  - oxygen corrosion, 638
  - pH measurement and calculation, 621–624, 622*f*, 623*f*, 624*f*
  - physico-chemical reaction, 280
  - prevention
    - external casing
      - mechanisms of corrosion, 655–658
      - prevention design, 658–659
    - flow velocity
      - calculation for prevention, 663–664
      - corrosion effects in tubing, 660–663, 662*f*
    - galvanic corrosion
      - prevention, 668
      - universality, 667–668
    - overview, 69
    - technical margins of corrosion prevention measures
      - allowable corrosion rates, 694–695, 695*f*
      - coatings, 699–700
      - corrosion inhibitor, 697–699, 698*t*
      - protective measures, 695–697, 696*f*, 697*f*
      - sour oil and gas field corrosion resisting, 694
    - thread corrosion
      - mechanisms, 664–665, 664*f*
      - prevention, 665–667, 665*f*, 666*f*
    - tubing-casing annulus
      - closed annulus, 659–660
      - open annulus, 659
  - production casing design
    - physico-chemical reaction, 280
    - sulfate corrosion, 280
    - sulfate-reducing bacteria corrosion, 280
    - carbon dioxide corrosion of set cement, 265–268
    - hydrogen sulfide corrosion of cement sheath, 281–282
  - production casing failure, 225
  - reference standards, 589*t*
  - safety factor design
    - critical environment fracture toughness, 669–670
    - critical stress percent, 668–669
  - scour corrosion, 629–630
  - sour gas well
    - carbon dioxide corrosion, 674–675, 675*f*, 675*t*
    - hydrogen sulfide corrosion, 673–674, 673*f*, 674*f*, 675, 675*t*
    - water corrosion, 675–677
  - stress corrosion
    - fatigue, 628–629
    - fracture, 628
  - stress level
    - hole structure design in reduction, 671–672
    - overview, 670–671
    - reducing importance, 671

Corrosion (*Continued*)  
 sulfate corrosion, 280  
 sulfate-reducing bacteria corrosion, 280  
 sulfide-resistant tubing, 679–685, 680*t*, 681*t*, 682*t*, 683*f*, 683*t*, 684*f*  
 sulfur corrosion, 634  
 Critical equivalent plastic strain, maximum underbalance pressure design, 344  
 Crude oil  
   China heavy oil classification, 5*t*  
   reservoir fluid properties, 5–6  
   UNTAR classification standards, 6*t*  
 C-shaped ring test, 644  
 CY3, blocking removal, 434–435, 435*t*

## D

$d_{90}$  rule, 199, 201  
 Damage factor (DF), formation damage, 372–373  
 Damage ratio (DR), formation damage, 372  
 Deep wells  
   drilling and completion fluid, 204  
   perforating parameter design, 361–362  
   production casing and cementing problems and solutions, 272–279, 273*f*, 276*t*, 277*t*  
 Density  
   crude oil properties, 5  
   salt water solutions, 178*t*, 214*t*  
 Depth log evaluation, drilling fluid invasion into reservoir, 415–416  
 DF, *see* Damage factor  
 Dispersant, oil well cement, 262  
 Dispersed particle type, clay mineral analysis, 20  
 Displaced flow, flowing back  
   one-step, 513, 513*f*  
   overview, 512–513  
   two-step, 513, 513*f*  
 Divert pipe gravel pack technique, 90–92, 91*f*, 92*f*  
 DLA, blocking removal, 432, 433*t*  
 Double-wing Y-shaped gas wellhead assembly, 595–596, 599*f*  
 Downhole fluid, adaptable types, 534  
 Downhole pressure gauge, 366–367  
 Downhole tubing string, 574  
 DR, *see* Damage ratio  
 Drifting  
   drift diameter gauge, 418–419, 419*f*, 419*t*  
   lead stamp, 419–420, 420*t*  
 Drilling and completion fluid  
   aero-based fluid  
     aerated drilling and completion fluid, 176  
     aero-fluid, 175–176  
     foam fluid, 176–178  
     fog fluid, 176  
   complicated reservoirs  
     adjustment well, 203–204  
     deep and ultra-deep wells, 204  
     directional and horizontal wells, 204–205  
     tight sand gas reservoir protection, 205–210  
     wells prone to lost circulation and borehole sloughing, 203

formation damage  
   clay hydration inhibition, 174  
   compatibility between filtrate and reservoir fluid, 174  
   particle size, 173–174  
   solids content, 173–174, 174*f*  
   treating agents and damage, 174  
 functions, 172–173  
 oil-based drilling and completion fluid  
   formation damage, 184–185  
   formulation, 185  
   reservoir protection requirements, 174–175  
 shield-type temporary plugging, *see* Shield-type temporary plugging technique  
 water-based drilling and completion fluid  
   clay-free drilling and completion fluid with solids, 182–183  
   density of salt water solutions, 178*t*  
   solid-free clean salt drilling and completion fluid, 178–182, 181*f*  
 Drilling fluid, invasion into reservoir  
   depth log evaluation, 415–416  
   effect on log response, 414–415, 415*f*  
   physical process, 414, 414*f*  
 Dual cantilever beam test, 644–645

## E

Edge water, control, 68  
 Effective radius ( $r_{we}$ ), formation damage, 373  
 Elasticity zone stress model, maximum underbalance pressure design, 343–344  
 Electric submersible pump well, *see* Artificial lift well  
 Electrochemical corrosion  
   environmental influences, 627–628  
   mechanism, 625–626, 626*f*  
 Electron probe analysis, petrographic analysis, 15  
 $E_{mig}$ , *see* Gas channeling resistance coefficient  
 EOP, *see* Extreme overbalance perforating  
 Expandable casing technique, 234  
 External casing packer  
   cementing completion, 293  
   screen completion without cementing, 292–293, 293*f*  
 External guide housing sand filtering screen, 102–105, 104*f*, 105*f*  
 Extreme overbalance perforating (EOP), 308–311, 310*f*, 337–338

## F

Fault block reservoir, 4  
 FE, *see* Flow efficiency  
 Fiber complex silt control  
   application, 109–110  
   overview, 106–110  
   stimulation principle, 106–109, 109*f*  
 Flanged connection nut, wellhead assembly, 614–615, 615*f*, 615*t*  
 Flow efficiency (FE), formation damage, 372, 413  
 Flow-induced corrosion, 629

- Flow velocity
  - calculation for corrosion prevention, 663–664
  - corrosion effects in tubing, 660–663, 662*f*
- Flowing back
  - aerated water, 518, 520*f*
  - displaced flow
    - one-step, 513, 513*f*
    - overview, 512–513
    - two-step, 513, 513*f*
  - foam
    - composition, 520–521, 521*t*, 522*t*
    - generating equipment, 522
    - overview, 518–522
    - stability, 521–522
  - gas lift
    - coiled-tubing gas lift unloading, 516
    - conventional gas lift unloading, 515–516, 515*f*
    - multistage gas lift unloading, 516, 516*f*
    - nitrogen-gas gas lift unloading, 516–518, 517*f*, 517*t*, 519*t*
    - overview, 515–518
    - swabbing, 514–515, 514*f*
- Fluid loss additive, oil well cement, 261–262
- Flushing, *see* Well flushing
- Foam
  - drilling and completion fluid, 176–178
  - flowing back
    - composition, 520–521, 521*t*, 522*t*
    - generating equipment, 522
    - overview, 518–522
    - stability, 521–522
- Fog fluid, drilling and completion fluid, 176
- Formation damage
  - completeness index, 373
  - damage factor, 372–373
  - damage ratio, 372
  - drilling and completion fluid
    - clay hydration inhibition, 174
    - compatibility between filtrate and reservoir fluid, 174
    - oil-based drilling and completion fluid, 184–185
    - particle size, 173–174
    - solids content, 173–174, 174*f*
    - treating agents and damage, 174
  - drilling fluid invasion into reservoir
    - depth log evaluation, 415–416
    - effect on log response, 414–415, 415*f*
    - physical process, 414, 414*f*
  - dynamic damage experiment of drilling and completion fluid, 36, 36*f*, 38*t*, 39*t*, 40*t*
  - effective radius, 373
  - evaluation experiment of drilling and completion fluid
    - invasion depth and degree of damage, 36–37
  - flow efficiency, 372, 413
  - miscellaneous formation damage evaluation techniques, 41, 42*t*
  - overview, 23, 24*t*
  - perforated well productivity effects, 321–323, 323*f*, 324*f*, 336–337, 336*f*, 337*f*
  - perforating fluid mechanisms
    - filtration, 211–212
    - rate-sensitive reservoir damage, 212
    - solid particles, 211
  - sensitivity analysis, *see* Acid sensitivity; Alkali sensitivity; Rate sensitivity; Water sensitivity
  - skin factor
    - disintegration, 370–372, 371*t*, 372*t*
    - formation damage estimation, 369–370
  - static damage experiment of drilling and completion fluid, 35–36, 38*t*, 39*t*, 40*t*
  - tight sand gas reservoir features, 205–207, 207*f*, 208*t*
  - well test analysis
    - acidizing effects on curve shape, 399–402, 399*f*, 399*t*, 400*f*, 400*t*, 401*f*, 402*t*
    - comparison between field and laboratory evaluations, 366
    - curve shape comparison before and after removing formation damage, 397–399, 397*f*, 398*f*
    - dual porosity reservoir graphic characteristics, 383–388, 384*f*, 385*f*, 386*f*, 387*f*, 388*f*, 389*f*
    - fracture reservoir graphic characteristics, 388–397, 389*f*, 390*f*, 391*f*, 392*f*, 393*f*, 394*f*, 395*t*, 396*f*
    - historical perspective, 366–367, 367*f*
    - homogeneous reservoir graphic characteristics
      - composite bilogarithmic plot, 375–376, 375*f*
      - curve locating, 381
      - gradation of  $k/\mu$ ,  $S$ , and  $C$ , 378–379, 379*t*
      - locating analysis overview, 379–383, 380*f*, 382*f*, 383*t*
      - overview, 373–383, 374*t*
      - semilogarithmic plot, 376–378, 377*f*, 378*f*, 380*f*
      - time locating, 381
    - large fracture effect on curve shape, 402–403, 402*f*, 403*f*
    - methodology, 367–368
    - natural gas well evaluation
      - bilogarithmic curves, 411–412, 412*f*
      - pseudopressure, 411, 411*f*, 412–413
      - semilogarithmic radial flow-straight-line portion, 412
    - overview, 365–366
    - quantitative interpretation
      - bilogarithmic measured pressure plot, 409
      - bilogarithmic type curve match method, 404–406, 405*f*, 406*f*
      - common type curves, 406–407, 407*f*, 408*f*
      - early-time portion interpretation method, 409–411
      - semilogarithmic method, 407–409
    - requirements, 368–369
    - systematic well test data, 413
- Formation water
  - pH, 7, 622*f*, 623*f*, 624*f*
  - rate sensitivity evaluation, 25*f*
  - reservoir fluid properties, 6–8, 8*t*
- Fracture packing type, clay mineral analysis, 20
- Fracture porosity reservoir, 3
- Fractured oil reservoir
  - overview, 70–71
  - perforating parameter design, 355–358, 356*f*
  - productivity rule of perforated well
    - fracture network type effects, 325, 326*t*
    - overview, 324–330
    - perforating parameter effects on productivity, 325–330, 327*f*, 328*f*, 329*f*, 330*f*

Fractured oil reservoir (*Continued*)  
 well testing  
   graphic characteristics, 388–397, 389*f*, 390*f*, 391*f*,  
   392*f*, 393*f*, 394*f*, 395*t*, 396*f*  
   large fracture effect on curve shape, 402–403, 402*f*, 403*f*  
 Fracture–vug–pore reservoir, 4  
 Fracturing, 67–68, *see also* Acid fracturing; High-energy gas  
 fracturing; Hydraulic fracturing

## G

Gas-based perforating fluid, 216  
 Gas cap, control, 68  
 Gas channeling factor of potential (GFP), 269, 269*t*  
 Gas-channeling inhibitor, oil well cement, 263  
 Gas channeling resistance coefficient ( $E_{mig}$ ), 269, 270*t*  
 Gas fracturing, *see* High-energy gas fracturing  
 Gas injection, overview, 69  
 Gas lift, flowing back  
   aerated water, 518, 520*f*  
   coiled-tubing gas lift unloading, 516  
   conventional gas lift unloading, 515–516, 515*f*  
   foam  
     composition, 520–521, 521*t*, 522*t*  
     generating equipment, 522  
     overview, 518–522  
     stability, 521–522  
   multistage gas lift unloading, 516, 516*f*  
   nitrogen-gas gas lift unloading, 516–518, 517*f*, 517*t*, 519*t*  
   overview, 515–518  
 Gas lift well, *see* Artificial lift well  
 Gas partial pressure, calculation  
   gas phase, 620  
   hydrogen sulfide in liquid system, 620–621, 621*f*  
 Gas volume fraction, mass concentration  
   conversion, 619–620  
 Gas well, *see* Natural gas well  
 GFP, *see* Gas channeling factor of potential  
 Glassfiber reinforced plastics liner tubing, 688–689, 688*f*,  
 689*f*, 689*t*, 690*f*  
 Grain size analysis, core analysis, 21–22, 22*f*  
 Gravel pack completion  
   casing gravel pack completion, 84–85, 85*f*, 85*t*  
   diverter pipe gravel pack technique, 90–92, 91*f*, 92*f*  
   gravel quality requirements, 86, 86*t*  
   hydraulic fracturing gravel pack technique, 92–94,  
   93*f*, 94*f*  
   multiple gravel pack technology, 86–90, 87*f*, 88*f*, 90*f*, 91*f*  
   open hole gravel pack completion, 84, 84*f*, 85*t*  
   overview, 83–94, 83*f*, 84*f*  
   wire-wrapped screen gap size selection, 86, 87*t*

## H

Heavy oil well  
 perforating parameter design, 361  
 tubing and production casing size determination  
   overview, 161–170  
   steam injection recovery  
     huff and puff, 164–167, 165*f*, 165*t*, 166*f*, 167*t*  
     steam-flooding recovery, 167–168, 167*t*, 168*f*

viscosity versus temperature, 161*f*  
 waterflooding recovery  
   flowing production, 162–163, 162*f*  
   pumping unit and deep well pump, 163–164, 163*f*,  
   164*f*  
 tubing string completion  
   combined jet pump and oil well pump, 551–553, 562*f*  
   conventional steam injection tubing string, 547, 558*f*  
   heavy-oil sand clean-out cold-flow production tubing  
   string, 550–551, 561*f*  
   hollow-sucker-rod through-pump electric heating  
   production tubing string, 551, 562*f*  
   huff-and-puff and pumping tubing string, 550, 559*f*,  
   560*f*  
   nitrogen heat-insulation cleanup tubing string,  
   549–550, 559*f*  
   sealing and separate-layer steam injection string,  
   547–549, 558*f*, 559*f*  
   steam-aided gravity drainage production tubing string,  
   550, 561*f*  
 HIB, *see* Hydrogen-induced blister  
 HIC, *see* Hydrogen-induced cracking  
 High-energy gas fracturing  
   combined fracturing and perforating, 509  
   conditions for generating fractures, 496–497, 497*f*  
   cracking initiation mechanism, 497–498, 497*f*, 498*f*  
   design  
     combustion of ammunition, 506–507  
     flow rate of gas squeezed into vertical fractures,  
     508–509  
     pressure–time relationship, 507–508  
     well fluid motion equation, 507  
   effects, 498–499  
   liquid ammunition fracturing, 501–505, 501*f*, 502*f*, 502*t*,  
   503*t*, 504*f*, 505*t*  
   overview, 495–496, 495*f*, 496*t*  
   self-propping of fractures, 498, 498*f*  
   solid ammunition fracturing, 499–501, 499*f*, 500*f*  
   suitabilities, 506  
   tests  
     dynamic test, 512, 512*f*  
     static test, 509–511, 510*f*, 511*t*  
 High-temperature, high-pressure, long core, multipoint  
   damage evaluation experiment device, 37*f*  
 Hole structure, *see* Production casing size  
 Hook-wall slotted liner completion, 80*f*  
 Horizontal principal stress  
   borehole stress state, 63–66  
   vertical principal stress relationship, 59  
 Horizontal well  
   overview, 72  
   perforating parameter optimization, 353–355, 354*f*  
   perforating technology, 311–314, 312*f*, 313*f*, 314*f*  
   production casing and cementing problems and solutions,  
   290–291  
   productivity rule of perforated well  
     formation damage effect on productivity, 336–337,  
     336*f*, 337*f*  
     location and degree of opening effects on productivity,  
     330–332, 331*f*, 332*f*  
     perforating parameter effects on productivity, 332–336,  
     333*f*, 334*f*, 335*f*

Horner method, well testing, 366–367, 368, 407

HSC, *see* Hydrogen stress cracking

Hydraulic fracturing

carbonatite reservoir

adaptability analysis, 470

difficulties, 469–470

gravel pack technique, 92–94, 93*f*, 94*f*

overview, 424

sandstone reservoir

flowsheet, 445*f*

fracturing fluid, 449–457, 450*t*, 451*t*, 452*f*, 453*t*, 454*t*, 457*t*

function, 445–446

goal, 445–446

integral frac design, 463–466, 465*f*

postfrac appraisal and analysis, 469

prefrac appraisal and analysis, 446–449, 448*f*

proppant, 457–463, 458*f*, 460*t*, 461*f*, 462*f*

quality control, 468

technology

fluid loss reduction, 466

fracture height-controlling techniques, 467

separate-layer fracturing, 467

Hydraulic jet pump well, *see* Artificial lift well

Hydrogen-induced blister (HIB), 633

Hydrogen-induced cracking (HIC), 632

Hydrogen stress cracking (HSC), 633

Hydrogen sulfide, *see also* Sulfide stress cracking

corrosion

cement sheath, 281–282

overview, 630–640, 631*t*, 632*f*

sour gas wells, 673–674, 673*f*, 674*f*, 675, 675*t*

sulfide stress cracking severity criteria and material selection

diagram, 648, 648*f*

test requirements of commonly used materials, 650

Zone SSC 0, 648–649

Zone SSC 1, 649–650

Zone SSC 2, 649

Zone SSC 3, 649

sulfide-resistant tubing, 679–685, 680*t*, 681*t*, 682*t*, 683*f*, 683*t*, 684*f*

gas partial pressure calculation liquid system, 620–621, 621*f*

gas reservoir classification, 6, 7*t*

high-hydrogen sulfide well perforating parameter design, 362

water solubility, 632*f*

## I

Ideal Packing Theory, 199, 200

Illite, clay mineral analysis, 18

Inflow performance relationship (IPR) curve, 122, 125, 128, 132, 139

*In situ* stress

borehole stress state

firmness, 64–65

horizontal principal stress, 63–66

mechanical stability, 65–66

concept, 56–63, 58*f*

types, 58*f*

well completion engineering relationship, 66–67

Integral casing joint

structures, 277*f*

types, 277*t*

Integrity management, *see* Production casing integrity management

Intelligent well completion

functions of system, 111–112, 111*f*

overview, 110–111

Internal coating tubing, 685–688, 688*f*

Internal pressure factor, 570

Internal yield pressure strength, *see* Production casing strength

IPR curve, *see* Inflow performance relationship curve

## K

Kaolin, clay mineral analysis, 18

Kerosene, rate sensitivity evaluation, 25*f*

## L

Lead stamp, drifting, 419–420, 420*t*

Lenticular reservoir, 4

Liner perforation completion, 77, 77*f*

Liner tieback perforation completion, 77–78, 78*f*

Lithology, reservoir, 8–9

LMWF, *see* Low molecular weight fracturing fluid

Locating analysis, *see* Well test analysis

Low molecular weight fracturing fluid (LMWF), 454

Low-frequency electric pulse blocking removal, 444–445, 444*f*

## M

Magnetic treatment, blocking removal, 440, 440*f*, 441*f*

Make-up operation

rotations and location, 241–242

thread sealant, 242

Massive hydraulic fracturing (MHF), 157

Massive reservoir, 4, 70

Material hardening index

ISO/API thread seal pressure, 250

steel grade, 249*t*

MDH method, well testing, 366–367, 368, 407

Metallic fiber sand control screen, 101–102,

104*f*, 104*t*

MHF, *see* Massive hydraulic fracturing

Microwave, blocking removal, 438–440, 439*f*

Mode selection, well completion, 75–76, 108*t*

Mohr-Coloumb yield criteria, maximum underbalance pressure design, 343

Mohr's circle, failure envelope, 62*f*

Monobore well completion

Gulf of Thailand, 113, 113*f*

main features, 113–115, 114*f*, 115*f*

overview, 112–115, 112*f*

Musket method, well testing, 366–367

**N**

- NACE, *see* National Association of Corrosion Engineers  
 National Association of Corrosion Engineers (NACE)  
   beam bending test, 644  
   C-shaped ring test, 644  
   dual cantilever beam test, 644–645  
   fitness design method, 642  
   tension test, 643–644  
 Natural gas well  
   Christmas tree and tubing  
     common types  
       Christmas trees, 589–591, 590*f*, 591*f*, 592*f*, 593*f*  
       tubingheads, 589–591, 594*f*, 595*f*, 596*f*  
       high-pressure gas wellhead assembly, 591–592, 597*f*  
       high-sulfur gas wellhead assembly, 592–596, 598*f*, 599*f*  
       materials, 588–589, 588*t*, 589*t*  
       overview, 587–596  
       technical parameters for Christmas trees, 588*t*  
     formation damage evaluation  
       bilogarithmic curves, 411–412, 412*f*  
       pseudopressure, 411, 411*f*, 412–413  
       semilogarithmic radial flow-straight-line portion, 412  
     production casing and cementing problems and solutions  
       in high-temperature high-pressure wells, 272–279, 273*f*, 276*t*, 277*t*  
     production casing size determination, 136, 137*t*  
     reservoir fluid properties, 6, 7*t*  
     storage well completion, *see* Underground natural gas storage well completion  
     tubing size determination  
       maximum tubing size, 133, 134, 134*f*, 135–136, 135*t*, 136*f*  
       minimum energy consumption of lifting under rational production rate, 130–132, 131*f*, 132*f*  
     tubing string completion  
       conventional tubing string, 539, 543*f*  
       high acid content gas well tubing string, 547  
       high-pressure high-rate tubing string, 539, 544*f*, 545*f*  
       principles, 537–538  
       sour gas well tubing string, 539–541, 546*f*, 547*f*, 548*f*  
       tubing-conveyed perforating gas production well tubing string, 543, 549*f*  
       water-drainage gas-production tubing string, 543–544, 550*f*, 551*f*, 552*f*  
 Nitrogen, gas lift unloading, 516–518, 517*f*, 517*t*, 519*t*  
 Nitrogen heat-insulation cleanup tubing string, 549–550, 559*f*  
 Nodal analysis, overview, 119–121, 120*f*

**O**

- Oil-based drilling and completion fluid  
   formation damage, 184–185  
   formulation, 185  
 Oil-based perforating fluid, 215  
 Oil well cement  
   additives  
     accelerant, 262–263  
     dispersant, 262  
     fluid loss additive, 261–262

- gas-channeling inhibitor, 263  
 lightening admixture, 264  
 retardant, 262  
 thermal stabilizer, 264  
 toughness promoter, 264  
 weighting admixture, 264  
 formulation, 257–258  
 overview, 257  
 types and usable range, 257, 258*t*  
 Open hole completion, 78–80, 78*f*, 79*f*  
 Open hole gravel pack completion, 84, 84*f*, 85*t*  
 OPR curve, *see* Outflow performance relationship curve  
 Outflow performance relationship (OPR) curve, 132  
 Oxygen corrosion, 638

**P**

- Partial pressure, *see* Gas partial pressure  
 Particle metasomatic type, clay mineral analysis, 20  
 Particle size, drilling and completion fluid, 173–174, 199–202  
 Perforated completion  
   casing perforation completion, 76–77, 77*f*  
   combined gas fracturing and perforating, 509  
   combined tubing and wireline conveyed perforation, 299, 300*f*  
   design optimization  
     carbonatite gas reservoir perforating parameter design, 360–361  
     deep well perforating parameter design, 361–362  
     fractured well perforating parameter design, 355–358, 356*f*  
     heavy oil well perforating parameter design, 361  
     high-hydrogen sulfide well perforating parameter design, 362  
     horizontal well perforating parameter optimization, 353–355, 354*f*  
     perforating parameter classification, 347  
     sand control well perforating parameter design, 358–360, 359*f*, 360*f*  
   sandstone reservoirs  
     correction of penetration depth and diameter of perforating charge, 348–351, 348*f*, 349*f*  
     drilling damage parameter calculation, 352  
     perforating charge property data collection, 347–348  
     perforating fluid optimization, 353  
     perforating parameter optimization, 352  
     rational selection of perforating technology, 352–353  
 differential pressure design  
   extreme overbalance perforating, 337–338  
   maximum underbalance pressure design  
     calculation with no sand production, 344–345  
     critical equivalent plastic strain, 344  
     elasticity zone stress model, 343–344  
     Mohr-Colomb yield criteria, 343  
     overview, 342–345  
     plasticity zone stress model, 343  
     pressure distribution around perforation, 344  
   minimum underbalance pressure calculation  
     Southwest Petroleum University formula, 342  
     Tariq method, 340–342

- rational pressure difference determination
  - extreme overbalance perforating operation pressure, 345–346
  - safety constraint, 346
  - underbalanced perforating operation pressure, 345
- underbalance pressure design
  - Behrmann method, 340
  - Bell's relation, 339–340, 339*t*
  - Conoco method, 339–340
- underbalanced perforating overview, 337–338
- extreme overbalance perforating technology, 308–311, 310*f*
- horizontal well, 311–314, 312*f*, 313*f*, 314*f*
- liner perforation completion, 77, 77*f*
- oriented perforating technology, 314–315
- overview, 296–297
- productivity rules of perforated wells
  - fractured oil reservoir
    - fracture network type effects, 325, 326*t*
    - overview, 324–330
    - perforating parameter effects on productivity, 325–330, 327*f*, 328*f*, 329*f*, 330*f*
  - horizontal well
    - formation damage effect on productivity, 336–337, 336*f*, 337*f*
    - location and degree of opening effects on productivity, 330–332, 331*f*, 332*f*
    - perforating parameter effects on productivity, 332–336, 333*f*, 334*f*, 335*f*
  - sandstone reservoir
    - formation damage effect on productivity, 321–323, 323*f*, 324*f*
    - perforating parameter effects on productivity, 315–321, 316*f*, 316*t*, 317*f*, 319*f*, 320*f*, 321*f*, 322*t*, 323*f*
- tubing-conveyed perforation
  - combination technology
    - formation-testing technology, 303–304, 304*f*
    - high-energy-gas fracturing technology, 305–306
    - hydraulic fracturing (acidizing) technology, 304, 305*f*
    - oil well pump technology, 304–305, 306*f*
    - putting-into-production technology, 302
    - sand control technology, 306–307, 307*f*
  - overview, 297–299, 298*f*
  - wireline casing gun perforation
    - overbalance perforating, 297
    - pressurized wireline perforation, 256–257
    - underbalance perforating, 297
  - wireline modular gun perforation
    - operating principle, 300–301, 301*f*, 302*f*
    - overview, 299–302
    - technical characteristics, 301–302
  - wireline through-tubing perforation
    - conventional through-tubing perforation, 307–308
    - extended-diameter through-tubing perforation, 308, 309*t*, 310*f*
- Perforating fluid
  - acid-based perforating fluid, 215–216
  - comparison of types, 217*t*
  - design principles, 212–213
  - formation damage mechanisms
    - filtration, 211–212
    - rate-sensitive reservoir damage, 212
    - solid particles, 211
  - gas-based perforating fluid, 216
  - oil-based perforating fluid, 215
  - optimization for sandstone reservoirs, 353
  - perforating technology requirements, 216–219, 219*t*
  - polymer-type perforating fluid, 215
  - solid-free clean salt water, 213–215
- Permeability
  - acidizing effects on well testing curve shape, 399–402, 399*f*, 399*t*, 400*f*, 400*t*, 401*f*, 402*t*
  - reservoir, 10, 11*t*
- Permeability contrast, 11
- Permeability damage coefficient, versus effective stress, 43*f*
- Permeability variation coefficient, 11
- Petrographic analysis, core analysis, 14–15, 16*t*, 17*t*
- pH
  - formation water, 7, 622*f*, 623*f*, 624*f*
  - measurement and calculation, 621–624, 622*f*, 623*f*, 624*f*
- Phase angle
  - effect on productivity ratio, 317, 318*f*, 322*t*, 333, 334*f*
  - skin factor relations, 371*t*, 372*t*
- Plasticity zone stress model, maximum underbalance pressure design, 343
- Plunger lift well, *see* Artificial lift well
- Polymer-type perforating fluid, 215
- Pore configuration analysis, core analysis, 15–17, 17*t*
- Porosity, reservoir, 10, 10*t*
- Porous fractured reservoir, 3
- Porous reservoir, 3
- Pour point, crude oil properties, 6
- Pour-point oil well, tubing and production casing size determination, 169–170, 169*f*
- Precision Millipore composite sand control screen, 95–96, 95*f*, 96*f*, 96*t*
- Precision punched screen, 96–97, 97*f*, 97*t*, 98*t*
- Prepacked gravel wire-wrapped screen, 101, 103*f*
- Pressure loss
  - sites in production system, 120*f*
  - tubing, 133*t*
- Production casing corrosion, *see* Corrosion
- Production casing design
  - challenges and solutions
    - absorbing wells
      - problems, 282
      - cement leakage prevention, 282–284
    - adjustment well, 291–292
    - corrosive media-containing wells
      - physico-chemical reaction, 280
      - sulfate corrosion, 280
      - sulfate-reducing bacteria corrosion, 280
      - carbon dioxide corrosion of set cement, 265–268
      - hydrogen sulfide corrosion of cement sheath, 281–282
    - deep wells, 272–279, 273*f*, 276*t*, 277*t*
    - external casing packer, 292–293, 293*f*
    - high-temperature high-pressure gas well, 272–279, 273*f*, 276*t*, 277*t*
    - horizontal well, 290–291
    - salt rock bed and salt paste bed wells, 284–285, 284*f*
    - thermal production well, 286, 289
  - procedure, 255

- Production casing design (*Continued*)
    - safe operation and working life requirements, 224
    - safety criteria, 223–224
    - safety factor, 255
    - tension allowance design, 256
    - well completion requirements, 224
  - Production casing integrity management
    - collapse
      - casing failure of free section, 229–230
      - mechanisms and potential risk, 226–227
      - severity assessment, 227–229
    - concept, 224–225
    - failure
      - corrosion, 225
      - perforated interval, 225–226
    - long-term service life of cement sheath, 230–231
  - Production casing scraping
    - rubber sleeve type casing scraper, 420, 421*f*, 421*t*
    - spring-type casing scraper, 420, 422*f*, 422*t*
  - Production casing size
    - determination
      - artificial lift wells
        - dual-string production wells, 154, 155*t*, 156*t*
        - electric submersible pump well, 151*t*, 152*t*, 153
        - gas-lift oil well, 150–154, 152*t*, 153*t*
        - hydraulic jet pump well, 148–150, 149*t*
        - hydraulic piston pump well, 146–148, 147*t*, 148*t*
        - overview, 136–156
        - screw pump well, 154, 155*t*
        - sucker rod pump well, 144–146, 145*t*, 146*t*
      - flowing well, 129
      - natural gas well, 136, 137*t*
    - heavy oil well
      - overview, 161–170
      - steam injection recovery
        - huff and puff, 164–167, 165*f*, 165*t*, 166*f*, 167*t*
        - steam-flooding recovery, 167–168, 167*t*, 168*f*
      - viscosity versus temperature, 161*f*
      - waterflooding recovery
        - flowing production, 162–163, 162*f*
        - pumping unit and deep well pump, 163–164, 163*f*, 164*f*
    - hole structure
      - expandable casing technique, 234
      - nonstandard casing size series, 233–234, 233*f*
      - standard casing size series, 231–233, 232*f*
    - overview, 118–119, 121–129
    - pour-point oil well, 169–170, 169*f*
    - standard casing size series, 234–235
    - stimulation effects, 156–161, 158*t*, 159*f*, 160*f*
  - Production casing steel grade
    - high collapsing strength casing, 237
    - material hardening index by grade, 249*t*
    - physical properties, 351*t*
    - standards, 235
    - straight weld casing, 237
    - types, 235–237
  - Production casing strength
    - collapse strength calculation
      - API 5C3 standard, 242–244, 244*t*
      - ISO 10400 standard
        - casing under action of axial tension and internal pressure, 246–247
        - casing under action of external, 245–246, 246*t*
        - example, 247
        - principles, 245
      - internal pressure strength of collar, 250
    - internal yield pressure strength calculation
      - API 5C3 standard, 244–245
      - ISO 10400 standard
        - environmental rupture failure, 250
        - internal crack destabilization rupture pressure strength, 249–250
        - internal pressure yield strength, 247–248
        - internal toughness burst pressure strength, 248–249
        - overview, 247–250
    - ISO/API thread seal pressure, 250
  - string loads
    - axial forces, 253–255
    - external pressure, 252–253
    - internal pressure, 251–252, 252*t*
    - temperature dependence, 273*f*, 288*t*
    - tensile strength, 250
  - Production casing thread
    - API/ISO threads, 237–239, 238*f*
    - corrosion
      - mechanisms, 664–665, 664*f*
      - prevention, 665–667, 665*f*, 666*f*
    - gas sealing thread of casing and connection
      - structure, 239–241, 240*f*
    - heat-resistant seal thread for thermal production wells, 288–289
    - integral joint casing, 240*f*, 241
    - make-up operation requirements
      - rotations and location, 241–242
    - thread sealant, 242
  - Proppant, hydraulic fracturing, 457–463, 458*f*, 460*t*, 461*f*, 462*f*
  - Pseudopressure, gas well, 411, 411*f*, 412–413
- ## R
- Rassel's method, well testing early-time portion
    - interpretation, 410
  - Rate sensitivity
    - applications of evaluation, 35*t*
    - experimental procedure and results, 23–27, 25*f*, 25*t*
    - overview, 23
  - Reservoir classification
    - development geology types, 4
    - geometric classification, 4
    - reservoir fluid type, 4
    - storage and percolation space systems, 3–4, 3*t*
  - Reservoir protection
    - drilling and completion fluid
      - fractured reservoir protection, 202–203
      - requirements, 174–175
    - shield-type temporary plugging technique, 196–199
    - tight sand gas reservoir completion fluid, 205–210
  - Retardant, oil well cement, 262
  - Rubber sleeve type casing scraper, 420, 421*f*, 421*t*
  - $r_{we}$ , *see* Effective radius

## S

S, *see* Skin factor

Safety factor, *see* Corrosion; Production casing design

Safety valves

well completion tubing string

overview, 553–562

subsurface safety valve

casing program, 557–560, 564*t*

overview, 557–560, 563*f*

setting depth, 557

surface safety valve, 560, 561–562, 565*f*

wellhead assembly

overview, 602–603

technical specifications, 607*f*, 607*t*, 608*t*

surface safety valves, 603–606, 608*f*

SAGD, *see* Steam-aided gravity drainage

Salinity, formation water, 7

Salt sensitivity

applications of evaluation, 35*t*

experimental procedure and results, 28–31, 29*f*,  
30*t*, 31*f*

overview, 28

Sand control

combined tubing-conveyed perforation and sand control  
technology, 306–307, 307*f*

external guide housing sand filtering screen, 102–105,  
104*f*, 105*f*

metallic fiber sand control screen, 101–102, 104*f*, 104*t*  
overview, 69

performance comparison of screens, 99*t*

precision Millipore composite sand control screen, 95–96,  
95*f*, 96*f*, 96*t*

precision punched screen, 96–97, 97*f*, 97*t*, 98*t*

prepacked gravel wire-wrapped screen, 101, 103*f*

STARS composite screen, 98–101, 102*f*, 103*f*

STARS star pore screen, 97–98, 100*f*, 101*f*

Sand control well, perforating parameter design, 358–360,  
359*f*, 360*f*

Sandstone reservoir

acid fracturing

acid liquor and additives, 472–476, 477*t*

effectiveness, 475*t*, 480–482

monitoring, 480–482

skin damage, 476*t*

technology, 476–480, 478*t*

hydraulic fracturing

flowsheet, 445*f*

fracturing fluid, 449–457, 450*t*, 451*t*, 452*f*, 453*t*, 454*t*,  
457*t*

function, 445–446

goal, 445–446

integral frac design, 463–466, 465*f*

postfrac appraisal and analysis, 469

prefrac appraisal and analysis, 446–449, 448*f*

proppant, 457–463, 458*f*, 460*t*, 461*f*, 462*f*

quality control, 468

technology

fluid loss reduction, 466

fracture height-controlling techniques, 467

separate-layer fracturing, 467

perforating design optimization

correction of penetration depth and diameter of

perforating charge, 348–351, 348*f*, 349*f*

drilling damage parameter calculation, 352

perforating charge property data collection, 347–348

perforating fluid optimization, 353

perforating parameter optimization, 352

rational selection of perforating technology, 352–353

productivity rule of perforated well

formation damage effect on productivity, 321–323,  
323*f*, 324*f*

perforating parameter effects on productivity,

315–321, 316*f*, 316*t*, 317*f*, 319*f*, 320*f*, 321*f*,

322*t*, 535*f*

stress sensitivity analysis in low permeability sandstone

oil reservoir, 46–49, 47*t*, 48*f*, 48*t*

Saturation, reservoir, 12

SBT, *see* Segmented bond tool

Scale, control, 69

SCC, *see* Stress corrosion cracking

Scanning electron microscopy (SEM), petrographic analysis,  
15, 16*t*

Scour corrosion, 629–630

Scraping, *see* Production casing scraping

Screw pump well, *see* Artificial lift well

Seal gasket ring, wellhead assembly, 610–614, 612*f*, 612*t*,  
613*f*, 613*t*, 614*f*, 614*t*, 615*t*

Segmented bond tool (SBT), 271

SEM, *see* Scanning electron microscopy

Semilogarithmic method, well testing, 407–409

Sensitivity analysis, tubing size

importance, 122–123

optimization for flowing well

given separator pressure, 123–124, 124*f*, 125*f*

given wellhead tubing pressure and case studies,

124–125, 125*f*, 126*f*, 127*f*, 128*f*

sensitivity affected by inflow performance, 129, 130*f*

Separate-layer production tubing string, 525–526, 526*f*,  
527*f*, 534–537, 543

Separate-layer water injection string

eccentric water distribution strings, 546, 555*f*, 556*f*, 557*f*

fixed water distribution string, 545, 552*f*

hollow water distribution strings, 545–546, 553*f*, 554*f*,  
555*f*

overview, 544–546, 552*f*

Shear strength, 61

Shield-type temporary plugging technique

experimental outcomes, 191*t*, 192*t*, 193*t*, 195*t*, 196*t*,  
197*t*, 198*t*

mechanisms

physical model, 187, 188

single-particle staged plugging model, 188, 189, 189*f*,

190*f*, 191, 192, 193, 194

overview, 185–186

particle size optimization in drilling and completion fluid,  
189*f*, 199–202, 200*f*, 202*f*

rationale, 186–187

reservoir protection

drilling and completion fluid for protecting fractured  
reservoir, 202–203

overview, 196–199

Single-particle staged plugging model, shield-type temporary  
plugging, 188, 189, 189*f*, 190*f*, 191, 192, 193, 194

- Skin factor (S)  
 acidizing effects on well testing curve shape, 399–402, 399*f*, 399*t*, 400*f*, 400*t*, 401*f*, 402*t*  
 determination  
 bilogarithmic measured pressure plot, 409  
 bilogarithmic type curve match method, 404–406, 405*f*, 406*f*  
 natural gas wells  
 bilogarithmic curves, 411–412, 412*f*  
 semilogarithmic radial flow-straight-line portion, 412  
 semilogarithmic method, 407–409  
 disintegration, 370–372, 371*t*, 372*t*  
 formation damage estimation, 369–370, 374*t*, 378–379  
 fracture skin factor, 393–395, 393*f*, 394*f*, 395*t*
- Skin zone, 367, 367*f*
- Slotted liner completion  
 overview, 80–83, 80*f*  
 slot arrangement, 81, 81*f*  
 slot cutting of liner, 83–94  
 slot length, 82  
 slot opening width, 81, 81*f*  
 slot quantity, 82–83  
 slot shape, 81, 81*f*  
 slotted liner size, 81–82, 82*t*
- Slurry, *see* Cementing
- Smectite  
 clay mineral analysis, 18  
 structure, 431*f*
- Soft zone cracking (SZC), 633
- SOHIC, *see* Stress-oriented hydrogen-induced cracking
- Solid-free clean salt water  
 density of salt water solutions, 178*t*, 214*t*  
 drilling and completion fluid, 178–182, 181*f*  
 perforating fluid, 213–215
- Solids content, drilling and completion fluid, 173–174, 174*f*
- Sour gas well  
 corrosion  
 carbon dioxide corrosion, 674–675, 675*f*, 675*t*  
 hydrogen sulfide corrosion, 673–674, 673*f*, 674*f*, 675, 675*t*  
 water corrosion, 675–677  
 tubing string, 527*f*, 539–541, 546*f*, 547*f*
- Southwest Petroleum University formula, minimum underbalance pressure calculation, 342
- Spool, wellhead assembly, 115–116, 610*f*, 611*t*
- Spring-type casing scraper, 420, 422*f*, 422*t*
- SRB, *see* Sulfate-reducing bacteria
- SSC, *see* Sulfide stress cracking
- STARS composite screen, 98–101, 102*f*, 103*f*
- STARS star pore screen, 97–98, 100*f*, 101*f*
- Steam injection, overview, 68
- Steam-aided gravity drainage (SAGD), production tubing string, 550, 561*f*
- Steel grade, *see* Production casing steel grade
- Strain, rock stress relationship, 496*f*
- Stratified oil reservoir, overview, 70
- Stratified reservoir, 4
- Stress corrosion  
 fatigue, 628–629  
 fracture, 628
- Stress sensitivity analysis  
 carbonatite reservoirs  
 Sichuan basin, 52–54, 56*t*, 57*t*  
 variation rules, 54, 58*f*  
 Zhanaruoer oil field, 27*t*, 52  
 comparison of evaluation methods, 45–46, 45*t*, 46*t*  
 evaluation indices, 43–45  
 experimental goals and procedure, 42–43  
 low permeability sandstone oil reservoir, 46–49, 47*t*, 48*f*, 48*t*  
 tight sand gas reservoirs  
 Eerduosi basin, 26*t*, 50–52, 52*f*  
 Rock Mountains, 52, 54*f*  
 Sichuan basin, 49–50, 50*f*, 51*t*
- Stress corrosion cracking (SCC), 633
- Stress-oriented hydrogen-induced cracking (SOHIC), 633
- Subsurface safety valve  
 casing program, 557–560, 564*t*  
 overview, 557–560, 563*f*  
 setting depth, 557
- Sucker rod pump well, *see* Artificial lift well
- Sulfate, corrosion, 280
- Sulfate-reducing bacteria (SRB), corrosion, 280
- Sulfide stress cracking (SSC)  
 cracking severity criteria and material selection  
 diagram, 648, 648*f*  
 test requirements of commonly used materials, 650  
 Zone SSC 0, 648–649  
 Zone SSC 1, 649–650  
 Zone SSC 2, 649  
 Zone SSC 3, 649  
 overview, 632
- Sulfide-resistant tubing, *see* Hydrogen sulfide
- Sulfur corrosion, 634
- Superdeep well, *see* Deep wells
- Surface safety valve  
 well completion tubing string, 560, 561–562, 565*f*  
 wellhead assembly, 603–606, 608*f*
- Swabbing, flowing back, 514–515, 514*f*
- SZC, *see* Soft zone cracking
- T**
- Tariq method, minimum underbalance pressure calculation, 340–342
- TCP, *see* Tubing-conveyed perforation
- Tee, wellhead assembly, 115–116, 610*f*
- Temporary plugging, *see* Shield-type temporary plugging technique
- Tensile strength, 61, 250
- Tension allowance design, production casing design, 256
- Tension test, 643–644
- Thermal production well  
 cement, 289  
 damage mechanisms at high temperature, 286–288  
 heat-resistant seal thread, 288–289  
 problems, 286  
 well completion mode, 289–290
- Thermal production well, wellhead assembly, 599–601
- Thin film type, clay mineral analysis, 19
- Thread, *see* Production casing steel thread

Tight sand gas reservoir  
 completion fluid for protection, 207–210  
 formation damage features, 205–207, 207*f*, 208*t*  
 stress sensitivity analysis  
   Eerduosi basin, 26*t*, 50–52, 52*f*  
   Rock Mountains, 52, 54*f*  
   Sichuan basin, 49–50, 50*f*, 51*t*  
 Total safety factor, 570  
 TPR curve, *see* Tubing performance relationship curve  
 TTP, *see* Wireline through-tubing perforation  
 Tubing-conveyed perforation (TCP)  
   combination technology  
     formation-testing technology, 303–304, 304*f*  
     high-energy-gas fracturing technology, 305–306  
     hydraulic fracturing (acidizing) technology, 304, 305*f*  
     oil well pump technology, 304–305, 306*f*  
     putting-into-production technology, 302  
     sand control technology, 306–307, 307*f*  
   overview, 297–299, 298*f*  
 Tubing corrosion, *see* Corrosion  
 Tubinghead, *see* Wellhead assembly  
 Tubing performance relationship (TPR) curve, 122, 122*f*, 125, 128, 132  
 Tubing size  
   artificial lift well determination  
     dual-string production wells, 154, 155*t*, 156*t*  
     electric submersible pump well, 151*t*, 152*t*, 153  
     gas-lift oil well, 150–154, 152*t*, 153*t*  
     hydraulic jet pump well, 148–150, 149*t*  
     hydraulic piston pump well, 146–148, 147*t*, 148*t*  
     overview, 136–156  
     screw pump well, 154, 155*t*  
     sucker rod pump well, 144–146, 145*t*, 146*t*  
   heavy oil well  
     overview, 161–170  
     steam injection recovery  
       huff and puff, 164–167, 165*f*, 165*t*, 166*f*, 167*t*  
       steam-flooding recovery, 167–168, 167*t*, 168*f*  
     viscosity versus temperature, 161*f*  
     waterflooding recovery  
       flowing production, 162–163, 162*f*  
       pumping unit and deep well pump, 163–164, 163*f*, 164*f*  
   natural gas well determination  
     maximum tubing size, 133, 134, 134*f*, 135–136, 135*t*, 136*f*  
     minimum energy consumption of lifting under rational production rate, 130–132, 131*f*, 132*f*  
   overview, 118–119, 121–129  
   pour-point oil well, 169–170, 169*f*  
   sensitivity analysis  
     importance, 122–123  
     optimization for flowing well  
       given separator pressure, 123–124, 124*f*, 125*f*  
       given wellhead tubing pressure and case studies, 124–125, 125*f*, 126*f*, 127*f*, 128*f*  
     sensitivity affected by inflow performance, 129, 130*f*  
     stimulation effects, 156–161, 158*t*, 159*f*, 160*f*  
 Tubing string, *see* Well completion tubing string  
 TWC, *see* Combined tubing and wireline conveyed perforation  
 Two-string gas lift production, 71*f*

## U

U-01, blocking removal, 425–428, 429*t*  
 Ultradeep well, *see* Deep wells  
 Ultrasonic wave, blocking removal, 418–420, 437–438, 437*f*  
 Underbalanced perforating, *see* Perforated completion  
 Underground natural gas storage well completion  
   depleted oil/gas reservoir and aquifer gas storage well completion, 116  
   overview, 115–116  
 UNTAR, heavy oil and asphalt classification standards, 6*t*

## V

VAM thread, 240*f*, 241  
 Variable density log (VDL), 271, 271*t*  
 VDL, *see* Variable density log  
 Vertical principal stress, gravitational stress, 59  
 Vibration blocking removal, 440–444, 441*f*, 442*f*  
 Viscosity, crude oil properties, 5, 5*t*, 6*t*  
 Von Mises equivalent stress, *see* Stress level

## W

Water, *see* Formation water  
 Water-based drilling and completion fluid  
   clay-free drilling and completion fluid with solids, 182–183  
   density of salt water solutions, 178*t*  
   solid-free clean salt drilling and completion fluid, 178–182, 181*f*  
 Water injection, overview, 67  
 Water injection well, wellhead assembly, 596–599, 600*f*  
 Water sensitivity  
   applications of evaluation, 35*t*  
   evaluation indices, 27*t*  
   experimental procedure and results, 27–28, 28*f*, 28*t*  
   overview, 27  
 WCP, *see* Wireline casing gun perforation  
 Well completion tubing string  
   gas well completion  
     conventional tubing string, 539, 543*f*  
     high acid content gas well tubing string, 547  
     high-pressure high-rate tubing string, 539, 544*f*, 545*f*  
     principles, 537–538  
     sour gas well tubing string, 539–541, 546*f*, 547*f*, 548*f*  
     tubing-conveyed perforating gas production well tubing string, 543, 549*f*  
     water-drainage gas-production tubing string, 543–544, 550*f*, 551*f*, 552*f*  
   heavy oil production  
     combined jet pump and oil well pump, 551–553, 562*f*  
     conventional steam injection tubing string, 547, 558*f*  
     heavy-oil sand clean-out cold-flow production tubing string, 550–551, 561*f*  
     hollow-sucker-rod through-pump electric heating production tubing string, 551, 562*f*

- Well completion tubing string (*Continued*)
- huff-and-puff and pumping tubing string, 550, 559*f*, 560*f*
  - nitrogen heat-insulation cleanup tubing string, 549–550, 559*f*
  - sealing and separate-layer steam injection string, 547–549, 558*f*, 559*f*
  - steam-aided gravity drainage production tubing string, 550, 561*f*
- mechanics
- collapse safety factor, 570
  - deformation calculation
    - ballooning effect, 568
    - helical buckling effect, 568, 569*t*
    - piston effect, 567–568
    - temperature effect, 567
  - helical inflexion state analysis, 566–567
  - internal pressure factor, 570
  - operation parameter determination, 570
  - status models, 562–566, 566*f*
  - three-dimensional combination stress analysis, 570
  - total safety factor, 570
- oil well completion
- downhole screw pump well, 527–528, 531*f*
  - electrical submersible pump well, 529*f*, 530*f*, 547–553
  - gas lift well
    - modes of gas lift, 529–530, 533*f*, 534*f*
    - multiple tubing string gas lift, 531, 536*f*
    - single gas-lift string, 531, 535*f*
  - hydraulic piston pump well production tubing string, 533, 536*f*, 537*f*, 538*f*, 539*f*, 540*f*
  - jet pump well, 529, 532*f*
  - separate-layer production tubing string, 525–526, 526*f*, 527*f*
  - separate-layer production tubing string with oil- and gas-expandable openhole packers and screens, 534–537, 540*f*, 540*t*, 541*f*, 542*f*
  - sucker-rod pumping well, 526, 527*f*, 528*f*
- safety system
- overview, 553–562
  - subsurface safety valve
    - casing program, 557–560, 564*t*
    - overview, 557–560, 563*f*
    - setting depth, 557
  - surface safety valve, 560, 561–562, 565*f*
- separate-layer water injection string
- eccentric water distribution strings, 546, 555*f*, 556*f*, 557*f*
  - fixed water distribution string, 545, 552*f*
  - hollow water distribution strings, 545–546, 553*f*, 554*f*, 555*f*
  - overview, 544–546, 552*f*
- Well corrosion, *see* Corrosion
- Well flushing
- flushing fluid properties, 421–422, 423*t*
  - technical requirements, 424
  - techniques, 422–423
- Wellhead assembly
- casinghead
    - model number notation, 601
    - parameters, 602, 605*t*, 606*t*
    - structures, 601–602, 602*f*, 603*f*, 604*f*
  - gas well Christmas tree and tubing
    - common types
      - Christmas trees, 589–591, 590*f*, 591*f*, 592*f*, 593*f*
      - tubingheads, 589–591, 594*f*, 595*f*, 596*f*
    - high-pressure gas wellhead assembly, 591–592, 597*f*
    - high-sulfur gas wellhead assembly, 592–596, 598*f*, 599*f*
    - materials, 588–589, 588*t*, 589*t*
    - overview, 587–596
    - technical parameters for Christmas trees, 588*t*
  - oil well Christmas tree and tubinghead
    - artificial lift wells
      - electric submersible pump well, 580–581, 581*f*, 582*f*
      - gas-lift production well, 583–584, 585*f*
      - hydraulic piston pump well, 581–583, 582*f*, 583*f*, 584*f*
      - sucker rod pump well, 577–580, 579*f*, 580*f*
    - common types for flowing well, 574, 575*t*, 576*f*
    - dual-string for flowing well, 574–577, 577*f*
    - technical requirements
      - metallic materials, 584–587, 585*t*, 586*t*, 587*t*
      - non-metallic materials, 587
  - overview, 572, 573*f*, 574
  - thermal production well wellhead assembly, 599–601
- valves
- chokes
    - adjustable chokes, 607–609, 609*f*, 611*t*
    - fixed chokes, 606–607, 609*f*
  - flanged connection nut, 614–615, 615*f*, 615*t*
  - overview, 602–603
  - seal gasket ring, 610–614, 612*f*, 612*t*, 613*f*, 613*t*, 614*f*, 614*t*, 615*t*
  - spools, 609, 610*f*, 611*t*
  - surface safety valves, 603–606, 608*f*
  - technical specifications, 607*f*, 607*t*, 608*t*
  - tees, 609, 610*f*
  - water injection well wellhead assembly, 596–599, 600*f*
- Well test analysis
- acidizing effects on curve shape, 399–402, 399*f*, 399*t*, 400*f*, 400*t*, 401*f*, 402*t*
  - comparison between field and laboratory evaluations, 366
  - completeness index, 373
  - curve shape comparison before and after removing
    - formation damage, 397–399, 397*f*, 398*f*
  - damage factor, 372–373
  - damage ratio, 372
  - drilling fluid invasion into reservoir
    - physical process, 414, 414*f*
    - effect on log response, 414–415, 415*f*
    - depth log evaluation, 415–416
  - dual porosity reservoir graphic characteristics, 383–388, 384*f*, 385*f*, 386*f*, 387*f*, 388*f*, 389*f*
  - effective radius, 373
  - flow efficiency, 372, 413
  - fracture reservoir graphic characteristics, 388–397, 389*f*, 390*f*, 391*f*, 392*f*, 393*f*, 394*f*, 395*t*, 396*f*
  - historical perspective, 366–367, 367*f*
  - homogeneous reservoir graphic characteristics
    - composite bilogarithmic plot, 375–376, 375*f*
    - curve locating, 381
    - gradation of  $k/\mu$ ,  $S$ , and  $C$ , 378–379, 379*t*
    - locating analysis overview, 379–383, 380*f*, 382*f*, 383*t*

- overview, 373–383, 374*t*
- semilogarithmic plot, 376–378, 377*f*, 378*f*, 380*f*
- time locating, 381
- interpretation software, 376, 413
- large fracture effect on curve shape, 402–403, 402*f*, 403*f*
- methodology, 367–368
- natural gas well evaluation
  - bilogarithmic curves, 411–412, 412*f*
  - pseudopressure, 411, 411*f*, 412–413
  - semilogarithmic radial flow-straight-line portion, 412
- overview, 365–366
- quantitative interpretation
  - bilogarithmic measured pressure plot, 409
  - bilogarithmic type curve match method, 404–406, 405*f*, 406*f*
  - common type curves, 406–407, 407*f*, 408*f*
  - early-time portion interpretation method, 409–411
  - semilogarithmic method, 407–409
- requirements, 368–369
- skin factor
  - formation damage estimation, 369–370
  - disintegration, 370–372, 371*t*, 372*t*
- systematic well test data, 413

- Wireline casing gun perforation (WCP)
  - overbalance perforating, 297
  - pressurized wireline perforation, 256–257
  - underbalance perforating, 297
- Wireline modular gun perforation
  - operating principle, 300–301, 301*f*, 302*f*
  - overview, 299–302
  - technical characteristics, 301–302
- Wireline through-tubing perforation (TTP)
  - conventional through-tubing perforation, 307–308
  - extended-diameter through-tubing perforation, 308, 309*t*, 310*f*

## X

- X-ray diffraction (XRD), petrographic analysis, 15
- XRD, *see* X-ray diffraction

## Y

- Yield strength, 61

This page intentionally left blank